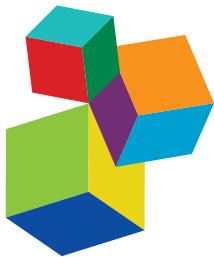




QUALITY OF HORTICULTURAL CROPS: A RECURRENT/NEW CHALLENGE FOR PLANT SCIENTISTS IN A CHANGING WORLD

EDITED BY: Nadia Bertin, Michel Génard and Maarten Hertog
PUBLISHED IN: Frontiers in Plant Science





Frontiers Copyright Statement

© Copyright 2007-2018 Frontiers Media SA. All rights reserved.

All content included on this site, such as text, graphics, logos, button icons, images, video/audio clips, downloads, data compilations and software, is the property of or is licensed to Frontiers Media SA ("Frontiers") or its licensees and/or subcontractors. The copyright in the text of individual articles is the property of their respective authors, subject to a license granted to Frontiers.

The compilation of articles constituting this e-book, wherever published, as well as the compilation of all other content on this site, is the exclusive property of Frontiers. For the conditions for downloading and copying of e-books from Frontiers' website, please see the Terms for Website Use. If purchasing Frontiers e-books from other websites or sources, the conditions of the website concerned apply.

Images and graphics not forming part of user-contributed materials may not be downloaded or copied without permission.

Individual articles may be downloaded and reproduced in accordance with the principles of the CC-BY licence subject to any copyright or other notices. They may not be re-sold as an e-book.

As author or other contributor you grant a CC-BY licence to others to reproduce your articles, including any graphics and third-party materials supplied by you, in accordance with the Conditions for Website Use and subject to any copyright notices which you include in connection with your articles and materials.

All copyright, and all rights therein, are protected by national and international copyright laws.

The above represents a summary only. For the full conditions see the Conditions for Authors and the Conditions for Website Use.

ISSN 1664-8714
ISBN 978-2-88945-597-3
DOI 10.3389/978-2-88945-597-3

About Frontiers

Frontiers is more than just an open-access publisher of scholarly articles: it is a pioneering approach to the world of academia, radically improving the way scholarly research is managed. The grand vision of Frontiers is a world where all people have an equal opportunity to seek, share and generate knowledge. Frontiers provides immediate and permanent online open access to all its publications, but this alone is not enough to realize our grand goals.

Frontiers Journal Series

The Frontiers Journal Series is a multi-tier and interdisciplinary set of open-access, online journals, promising a paradigm shift from the current review, selection and dissemination processes in academic publishing. All Frontiers journals are driven by researchers for researchers; therefore, they constitute a service to the scholarly community. At the same time, the Frontiers Journal Series operates on a revolutionary invention, the tiered publishing system, initially addressing specific communities of scholars, and gradually climbing up to broader public understanding, thus serving the interests of the lay society, too.

Dedication to Quality

Each Frontiers article is a landmark of the highest quality, thanks to genuinely collaborative interactions between authors and review editors, who include some of the world's best academicians. Research must be certified by peers before entering a stream of knowledge that may eventually reach the public - and shape society; therefore, Frontiers only applies the most rigorous and unbiased reviews.

Frontiers revolutionizes research publishing by freely delivering the most outstanding research, evaluated with no bias from both the academic and social point of view. By applying the most advanced information technologies, Frontiers is catapulting scholarly publishing into a new generation.

What are Frontiers Research Topics?

Frontiers Research Topics are very popular trademarks of the Frontiers Journals Series: they are collections of at least ten articles, all centered on a particular subject. With their unique mix of varied contributions from Original Research to Review Articles, Frontiers Research Topics unify the most influential researchers, the latest key findings and historical advances in a hot research area! Find out more on how to host your own Frontiers Research Topic or contribute to one as an author by contacting the Frontiers Editorial Office: researchtopics@frontiersin.org

QUALITY OF HORTICULTURAL CROPS: A RECURRENT/NEW CHALLENGE FOR PLANT SCIENTISTS IN A CHANGING WORLD

Topic Editors:

Nadia Bertin, Plantes et Systèmes de cultures Horticoles, INRA, France

Michel Génard, Plantes et Systèmes de cultures Horticoles, INRA, France

Maarten Hertog, KU Leuven, Belgium



Image: Krzysztof Slusarczyk/Shutterstock.com

Besides increasing crop yield to feed the growing population, improving crop quality is a challenging and key issue. Indeed, quality determines consumer acceptability and increases the attractivity of fresh and processed products. In this respect, fruit and vegetables, which represent a main source of vitamins and other health compounds, play a major role in human diet. This is the case in developing countries where populations are prone to nutritional deficiencies, but this is also a pending issue worldwide, where the growing middle class is increasingly aware and in search of healthy food. So a future challenge for the global horticultural industry will be to answer the demand for better quality food in a changing environment, where many resources will be limited. This e-collection collates state-of-the-art research on the quality of horticultural crops, covering the underlying physiological processes, the genetic and environmental controls during plant and organ development and the postharvest evolution of quality during storage and processing.

Citation: Bertin, N., Génard, M., Hertog, M., eds. (2018). Quality of Horticultural Crops: A Recurrent/New Challenge for Plant Scientists in a Changing World. Lausanne: Frontiers Media. doi: 10.3389/978-2-88945-597-3

Table of Contents

- 06 Editorial: Quality of Horticultural Crops: A Recurrent/New Challenge for Plant Scientists in a Changing World**
Nadia Bertin, Michel Génard and Maarten Hertog

SECTION I

MOLECULAR CONTROLS BEHIND QUALITY TRAITS

- 08 Water Deficit and Salinity Stress Reveal Many Specific QTL for Plant Growth and Fruit Quality Traits in Tomato**
Isidore A. Diouf, Laurent Derivot, Frédérique Bitton, Laura Pascual and Mathilde Causse
- 21 Transcriptome and Metabolome Analyses Provide Insights into the Occurrence of Peel Roughing Disorder on Satsuma Mandarin (*Citrus Unshiu Marc.*) Fruit**
Xiao-Peng Lu, Fei-Fei Li, Jiang Xiong, Xiong-Jun Cao, Xiao-Chuan Ma, Zi-Mu Zhang, Shang-Yin Cao and Shen-Xi Xie
- 37 Soluble Starch Synthase III-1 in Amylopectin Metabolism of Banana Fruit: Characterization, Expression, Enzyme Activity, and Functional Analyses**
Hongxia Miao, Peiguang Sun, Qing Liu, Caihong Jia, Juhua Liu, Wei Hu, Zhiqiang Jin and Biyu Xu
- 49 Insights Into the Molecular Events That Regulate Heat-Induced Chilling Tolerance in Citrus Fruits**
María T. Lafuente, Beatriz Establés-Ortíz and Luis González-Candela

SECTION II

MAIN QUALITY TRAITS

- 63 Coordinated Regulation of Anthocyanin Biosynthesis Genes Confers Varied Phenotypic and Spatial-Temporal Anthocyanin Accumulation in Radish (*Raphanus sativus L.*)**
Everlyne M'mbone Muleke, Lianxue Fan, Yan Wang, Liang Xu, Xianwen Zhu, Wei Zhang, Yang Cao, Benard K. Karanja and Liwang Liu
- 80 Characterization of Genes Encoding key Enzymes Involved in Anthocyanin Metabolism of Kiwifruit During Storage Period**
Boqiang Li, Yongxiu Xia, Yuying Wang, Guozheng Qin and Shiping Tian
- 88 Transcriptome Analysis Reveals Candidate Genes Related to Color Fading of 'Red Bartlett' (*Pyrus communis L.*)**
Zhigang Wang, Hong Du, Rui Zhai, Linyan Song, Fengwang Ma and Lingfei Xu
- 98 Proteomics and SSH Analyses of ALA-Promoted Fruit Coloration and Evidence for the Involvement of a MADS-Box Gene, MdMADS1**
Xinxin Feng, Yuyan An, Jie Zheng, Miao Sun and Liangju Wang

- 117 Comparative Physiological and Proteomic Analysis Reveal Distinct Regulation of Peach Skin Quality Traits by Altitude**
Evangelos Karagiannis, Georgia Tanou, Martina Samiotaki, Michail Michailidis, Grigoris Diamantidis, Ioannis S. Minas and Athanassios Molassiotis
- 131 A FERONIA-Like Receptor Kinase Regulates Strawberry (*Fragaria × ananassa*) Fruit Ripening and Quality Formation**
Meiru Jia, Ning Ding, Qing Zhang, Sinian Xing, Lingzhi Wei, Yaoyao Zhao, Ping Du, Wenwen Mao, Jizheng Li, Bingbing Li and Wensuo Jia
- 145 Exploring Blueberry Aroma Complexity by Chromatographic and Direct-Injection Spectrometric Techniques**
Brian Farneti, Iuliia Khomenko, Marcella Grisenti, Matteo Ajelli, Emanuela Betta, Alberto Alarcon Algarra, Luca Cappellin, Eugenio Aprea, Flavia Gasperi, Franco Biasioli and Lara Giongo
- 164 Insights Into the Sesquiterpenoid Pathway by Metabolic Profiling and De novo Transcriptome Assembly of Stem-Chicory (*Cichorium intybus* Cultigroup "Catalogna")**
Giulio Testone, Giovanni Mele, Elisabetta Di Giacomo, Maria Gonnella, Massimiliano Renna, Gian Carlo Tenore, Chiara Nicolodi, Giovanna Frugis, Maria Adelaide Iannelli, Giuseppe Arnesi, Alessandro Schiappa and Donato Giannino
- 181 Corrigendum: Insights Into the Sesquiterpenoid Pathway by Metabolic Profiling and De novo Transcriptome Assembly of Stem-Chicory (*Cichorium intybus* Cultigroup "Catalogna")**
Giulio Testone, Giovanni Mele, Elisabetta Di Giacomo, Maria Gonnella, Massimiliano Renna, Gian Carlo Tenore, Chiara Nicolodi, Giovanna Frugis, Maria A. Iannelli, Giuseppe Arnesi, Alessandro Schiappa and Donato Giannino
- 183 Mechanisms of Selenium Enrichment and Measurement in Brassicaceous Vegetables, and Their Application to Human Health**
Melanie Wiesner-Reinhold, Monika Schreiner, Susanne Baldermann, Dietmar Schwarz, Franziska S. Hanschen, Anna P. Kipp, Daryl D. Rowan, Kerry L. Bentley-Hewitt and Marian J. McKenzie
- 203 Agronomic Trait Variations and Ploidy Differentiation of Kiwiberrries in Northwest China: Implication for Breeding**
Ying Zhang, Caihong Zhong, Yifei Liu, Qiong Zhang, Xiaorong Sun and Dawei Li
- 215 Grape Composition Under Abiotic Constraints: Water Stress and Salinity**
José M. Mirás-Avalos and Diego S. Intrigliolo
- 223 The Role of Polyphenoloxidase, Peroxidase, and β-Glucosidase in Phenolics Accumulation in *Olea europaea* L. Fruits Under Different Water Regimes**
Marco Cirilli, Giovanni Caruso, Clizia Gennai, Stefania Urbani, Eleonora Frioni, Maurizio Ruzzi, Maurizio Servili, Riccardo Gucci, Elia Poerio and Rosario Muleo
- 236 Evaluating Spatially Resolved Influence of Soil and Tree Water Status on Quality of European Plum Grown in Semi-humid Climate**
Jana Käthner, Alon Ben-Gal, Robin Gebbers, Aviva Peeters, Werner B. Herppich and Manuela Zude-Sasse

246 Vegetable Grafting: The Implications of a Growing Agronomic Imperative for Vegetable Fruit Quality and Nutritive Value

Marios C. Kyriacou, Youssef Rousphael, Giuseppe Colla, Rita Zrenner and Dietmar Schwarz

SECTION III

PREHARVEST IMPACT ON POSTHARVEST QUALITY

269 Assuring Potato Tuber Quality During Storage: A Future Perspective

M. C. Alamar, Roberta Tosetti, Sandra Landahl, Antonio Bermejo and Leon A. Terry

275 Combined Effects of Irrigation Regime, Genotype, and Harvest Stage Determine Tomato Fruit Quality and Aptitude for Processing into Puree

Alexandre Arbex de Castro Vilas Boas, David Page, Robert Giovinazzo, Nadia Bertin and Anne-Laure Fanciullino

291 Firmness at Harvest Impacts Postharvest Fruit Softening and Internal Browning Development in Mechanically Damaged and Non-damaged Highbush Blueberries (*Vaccinium corymbosum L.*)

Claudia Moggia, Jordi Graell, Isabel Lara, Guillermo González and Gustavo A. Lobos

302 Population Modeling Approach to Optimize Crop Harvest Strategy. The Case of Field Tomato

Dinh T. Tran, Maarten L. A. T. M. Hertog, Thi L. H. Tran, Nguyen T. Quyen, Bram Van de Poel, Clara I. Mata and Bart M. Nicolaï



Editorial: Quality of Horticultural Crops: A Recurrent/New Challenge for Plant Scientists in a Changing World

Nadia Bertin^{1*}, Michel Génard¹ and Maarten Hertog²

¹ Plantes et Systèmes de Culture Horticoles, INRA, Avignon, France, ² Department of Biosystems, KU Leuven, Leuven, Belgium

Keywords: quality, horticultural crops, health value, fruit, vegetable, pre- post-harvest links

Editorial on the Research Topic

Quality of Horticultural Crops: A Recurrent/New Challenge for Plant Scientists in a Changing World

Improving crop quality is a challenge in the context of a global horticultural food supply, since the development of sustainable crop production systems inevitably affects many quality traits. Fruit and vegetable quality includes size, visual attractiveness (color, shape), overall flavor (taste and texture), health benefits, shelf life, suitability for processing...etc. At each step of the production chain, specific criteria prevail depending on the product's final destination, either the fresh market or the processing industry. These criteria are not necessarily the same throughout the chain, and likely interact during the product's life. Thus, the management and improvement of postharvest quality requires the integration of knowledge from the field until purchase and consumption of the fresh or processed product. This e-collection collates state-of-the-art research outputs on the quality of fruits and vegetables from seed to fork, covering the underlying physiological processes, the genetic and environmental controls during plant and organ development and the postharvest evolution of quality during storage and processing.

OPEN ACCESS

Edited and reviewed by:

Jose I. Hormaza,
Instituto de Hortofruticultura
Subtropical y Mediterránea La Mayora
(IHSM), Spain

*Correspondence:

Nadia Bertin
nadia.bertin@inra.fr

Specialty section:

This article was submitted to

Plant Breeding,
a section of the journal
Frontiers in Plant Science

Received: 07 June 2018

Accepted: 18 July 2018

Published: 09 August 2018

Citation:

Bertin N, Génard M and Hertog M (2018) Editorial: Quality of Horticultural Crops: A Recurrent/New Challenge for Plant Scientists in a Changing World. *Front. Plant Sci.* 9:1151.
doi: 10.3389/fpls.2018.01151

MOLECULAR CONTROLS BEHIND QUALITY TRAITS

The molecular and genetic controls behind quality build-up are illustrated on different species. Diouf et al. emphasized the complexity of the interaction between genotype and environment in controlling plant growth and fruit quality traits. Based on the MAGIC Tomato population, these authors showed that 33–86% of the phenotypic variation in yield and quality traits is due to the genetics. Among the 54 QTLs detected, 15 revealed significant interactions between genotype and water or salinity stress and 35 QTLs were treatment specific. In citrus, which is an important fruit crop in Mediterranean regions, comparative transcriptome analysis showed that starch and GA metabolisms in peel are involved in roughing disorder induced by severe fruit thinning (Lu et al.). Miao et al. performed a functional analysis of soluble starch synthase genes during banana development and storage and they identified MaSSIII-1 as a key gene responsible for amylopectin biosynthesis. In citrus, molecular events associated with low temperature tolerance induced by heat-conditioning open new perspectives to reduce chilling injury (Lafuente et al.).

MAIN QUALITY TRAITS

Color and pigment accumulation are major criteria of fruit and vegetable quality, which are addressed in several papers. Muleke et al. studied the spatial and temporal regulation of anthocyanin biosynthesis genes in radish taproots and identified five candidate genes that play a major role in phenotypic variations. In red-fleshed kiwi, Li et al. characterized genes involved in the increase of anthocyanin biosynthesis and accumulation during postharvest storage. In pear cultivars differing in color fading, Wang et al. analyzed differentially expressed genes linked to a late decrease in anthocyanin biosynthesis, and which increased during anthocyanin degradation in peel, suggesting the involvement of light signals. Feng et al. evidenced the role of *MdMADS1*, a MADS-Box gene, in *ALA* (a plant growth regulator)-induced anthocyanin accumulation in apple skin. Karagiannis et al. observed higher pigmentation of peach skin grown at high altitude and discussed the altitude effect on protein variations potentially involved in ripening. Jia et al. evidenced the role of FERONIA-like receptor kinase in the control of strawberry ripening by modulating ABA signaling.

Aroma is another important and complex trait of fruit quality. Farneti et al. explored the blueberry volatile organic compounds during ripening by two profiling methods and proposed biomarkers of berry physiology that could be used to phenotype genetic resources. Testone et al. showed that the regulation of sesquiterpene lactone biosynthesis, that confers bitterness to stem chicory, occurs at the transcriptional level.

Regarding the accumulation of health related compounds, Wiesner-Reinhold et al. emphasized the role of selenium and sulfur metabolism in Brassicaceae for human health and reviewed some works on biofortification of this plant family. More generally, Zhang et al. examined the links between ploidy level and agronomical traits and observed some antagonisms among quality traits of kiwi berries, for instance between vitamin C and sugar contents which were, respectively higher and lower in germplasms with high ploidy level, thus questioning the overall advantage of high ploidy.

THE IMPACT OF PREHARVEST STRESSES

Quality variations induced by water and salinity stress are important issues in horticultural crops. At the fruit scale, Miras-Avalos, and Intrigliolo made a meta-analysis of negative and positive effects of these stresses on grape composition and final wine quality, and they proposed a statistical model accounting for the agronomical context. In olive trees, the effects of the watering regime on the molecular and biochemical mechanisms that regulate the accumulation of main phenolic compounds during drupe development, were reported by Cirilli et al., who suggest a differential sensitivity of enzymes involved in phenolic catabolism. At the orchard scale, the study of Käthner et al. based on a thermal imaging approach to evaluate crop water stress index (CWSI) and soil electrical conductivity analysis, revealed that fruit quality could be predicted by interactions between CWSI and cumulative water use efficiency. Grafting is a

key-alternative to adapt to environmental constraints. Kyriacou et al. reviewed how grafting, a practice largely developed for Curcubitaceae and Solanaceae production, influences fruit quality and storability.

PREHARVEST IMPACT ON POSTHARVEST QUALITY

During the postharvest period, as maturation progresses, genetic, chemicals and environmental control can help maintain product quality. Improving shelf life while reducing the use of chemicals is obligatory to meet the consumers' demand and reduce losses along the food chain. Regarding products intended for processing, technological quality traits such as color, texture, viscosity or bio-accessibility impact on the final quality. However, the link between quality build-up in the preharvest period and its impact on the technological quality traits have been largely overlooked and detailed knowledge is still missing to really bridge this gap. Alamar et al. reviewed some alternative methods to control sprouting and diseases to ensure potato tuber quality, stressing the need to better understand interactions between pre- and postharvest factors. As such, Arbex de Castro Vilas Boas et al. evidenced significant interactions among genotype, preharvest interventions and processing methods, affecting major traits of both the fruit and the processed products derived from it, suggesting that managing the quality of processed products starts in the field. The moment of harvest is known to have a clear impact on postharvest quality traits. In blueberry, Moggia et al. observed that soft fruits at harvest exhibited higher softening rate and internal browning as compared to firm fruit cultivars, whereas mechanical damage induced variations in storability of the firm fruit cultivar only.

Finally, modeling the interactions among the factors that control quality in the pre and postharvest fruit life has proven its interest to optimize crop management and understand genetic variability. Tran et al. proposed a model-based optimization approach to optimize harvest date and frequency for field tomato, by predicting fruit-to-fruit variation in ripening and the associated crop economic value.

All these works do contribute in their own right to the complex answer on how to meet the future demand for better quality food in a changing environment, where resources will soon become limited.

AUTHOR CONTRIBUTIONS

All authors listed have made a substantial, direct and intellectual contribution to the work, and approved it for publication.

Conflict of Interest Statement: The authors declare that the research was conducted in the absence of any commercial or financial relationships that could be construed as a potential conflict of interest.

Copyright © 2018 Bertin, Génard and Hertog. This is an open-access article distributed under the terms of the Creative Commons Attribution License (CC BY). The use, distribution or reproduction in other forums is permitted, provided the original author(s) and the copyright owner(s) are credited and that the original publication in this journal is cited, in accordance with accepted academic practice. No use, distribution or reproduction is permitted which does not comply with these terms.



Water Deficit and Salinity Stress Reveal Many Specific QTL for Plant Growth and Fruit Quality Traits in Tomato

Isidore A. Diouf¹, Laurent Derivot², Frédérique Bitton¹, Laura Pascual^{1†} and Mathilde Causse^{1*}

¹ INRA, UR1052, Génétique et Amélioration des Fruits et Légumes, Centre de Recherche PACA, Montfavet, France,

² GAUTIER Semences, Eyragues, France

OPEN ACCESS

Edited by:

Maarten Hertog,
KU Leuven, Belgium

Reviewed by:

Daniela Romano,
Università degli Studi di Catania, Italy
Francisco Perez-Alfocea,
Consejo Superior de Investigaciones
Científicas (CSIC), Spain

*Correspondence:

Mathilde Causse
mathilde.causse@inra.fr

†Present Address:

Laura Pascual,
Department of Biotechnology and
Plant Biology, School of Agronomic
Engineering, Polytechnic University of
Madrid (UPM), Madrid, Spain

Specialty section:

This article was submitted to
Plant Breeding,
a section of the journal
Frontiers in Plant Science

Received: 22 August 2017

Accepted: 19 February 2018

Published: 06 March 2018

Citation:

Diouf IA, Derivot L, Bitton F, Pascual L
and Causse M (2018) Water Deficit
and Salinity Stress Reveal Many
Specific QTL for Plant Growth and
Fruit Quality Traits in Tomato.
Front. Plant Sci. 9:279.
doi: 10.3389/fpls.2018.00279

Quality is a key trait in plant breeding, especially for fruit and vegetables. Quality involves several polygenic components, often influenced by environmental conditions with variable levels of genotype × environment interaction that must be considered in breeding strategies aiming to improve quality. In order to assess the impact of water deficit and salinity on tomato fruit quality, we evaluated a multi-parent advanced generation intercross (MAGIC) tomato population in contrasted environmental conditions over 2 years, one year in control vs. drought condition and the other in control vs. salt condition. Overall 250 individual lines from the MAGIC population—derived from eight parental lines covering a large diversity in cultivated tomato—were used to identify QTL in both experiments for fruit quality and yield component traits (fruit weight, number of fruit, Soluble Solid Content, firmness), phenology traits (time to flower and ripe) and a vegetative trait, leaf length. All the traits showed a large genotype variation (33–86% of total phenotypic variation) in both experiments and high heritability whatever the year or treatment. Significant genotype × treatment interactions were detected for five of the seven traits over the 2 years of experiments. QTL were mapped using 1,345 SNP markers. A total of 54 QTL were found among which 15 revealed genotype × environment interactions and 65% (35 QTL) were treatment specific. Confidence intervals of the QTL were projected on the genome physical map and allowed identifying regions carrying QTL co-localizations, suggesting pleiotropic regulation. We then applied a strategy for candidate gene detection based on the high resolution mapping offered by the MAGIC population, the allelic effect of each parental line at the QTL and the sequence information of the eight parental lines.

Keywords: tomato, fruit quality, MAGIC population, genotype by environment interaction, QTL mapping

INTRODUCTION

Abiotic stress is one of the main factors limiting crop productivity and yield in agriculture. It occurs when plants experience any fluctuation in the growing habitat that alters or disrupts their metabolic homeostasis (de Oliveira et al., 2013). Among the abiotic stresses, drought and salinity are the most common threatening global food demand. Their adverse effect on agriculture is expected

to increase with the predicted climate change (Dai, 2011; Shrivastava and Kumar, 2015). Both drought and salinity stresses drive a series of morphological, physiological, and molecular changes in plants that are overall linked to adaptive mechanisms triggered by the plant to survive, or may simply be pathological consequences of stress injury (Zhu, 2002). Indeed, water deficit has several impacts on plant development due to the decrease of the plant's relative water content and water potential. Osmotic stress and limited nutrient uptake are then observed with stomatal closure, reduced photosynthesis activity, oxidative stress, and leaf growth inhibition. These behaviors are well reviewed by Farooq et al. (2012) and Chaves et al. (2003). For saline soil condition, plants are subjected to stress in two phases: a rapid osmotic stress phase starting immediately (due to the concentration of salt outside the roots) and a second ionic phase that starts when the accumulation of salt in the old leaves reaches a toxic level. The osmotic stress triggered by salinity has almost the same effect as drought with photosynthesis limitation, leaf growth inhibition, and ROS accumulation (Munns and Tester, 2008). Plants deploy a variety of adaptive strategies facing drought and salinity, including osmotic adjustment with the accumulation of osmo-protectants compounds, ROS detoxification, stomatal closure, and cellular signaling.

Drought and salinity arise with other adverse environmental factors threatening crop productivity in many species as a consequence of global climate changes. This has led plant breeders to renew their focus on understanding the molecular basis of plant adaptation to environment, in order to maintain high crop yielding by creating new varieties adapted to limited environmental conditions. As noted by Marais et al. (2013), plant responses to adverse conditions can be viewed as phenotypic plasticity (PP) and may lead to GxE when there is a genetic part shaping these responses. Understanding the molecular mechanism entailing PP and GxE is of great relevance in breeding strategies mainly if different growing areas (or cultural conditions) are targeted. For both PP and GxE, different underpinning models were suggested in the literature. PP can be viewed as additive effect of environmentally sensitive loci meaning that the same loci affect the phenotype in a set of environments at variable degrees, or specific regulatory loci altering differently the gene expression, in the different environments (Via et al., 1995). Non-additive effect such as over-dominance and epistasis or epigenetics can also be at the basis of the occurring GxE. El-Soda et al. (2014) present several statistical models to depict GxE into its individual genetic components through the identification of interactive QTL (QTLxE). Considering plasticity as an individual trait, some studies showed that loci linked to PP are in the vast majority also identified as QTLxE (Ungerer et al., 2003; Gutteling et al., 2007; Tétard-Jones et al., 2011).

Cultivated tomato is a crop moderately sensitive to salinity that can tolerate up to 2.5 dS/m EC, with minor negative impact on yield (Scholberg and Locascio, 1999). Caro et al. (1991) have found that small fruit accessions *S. lycopersicum* var *cerasiforme* are less sensitive to salinity than the large fruit group *S. lycopersicum* var *lycopersicum*. For drought, a negative impact

on yield is observed from a limitation of water supply by 50% compared to control (well irrigated) (Ripoll et al., 2014; Albert et al., 2016a). Under such stresses, tomato yield components as well as fruit quality are greatly affected with different effects depending on the variety, the stage and duration of stress application and also the interaction with other environmental conditions like temperature, light, or relative humidity (Maas and Hoffman, 1977; Scholberg and Locascio, 1999; Ripoll et al., 2014). Furthermore, the genetic background may strongly modify the response to stress conditions (Albert et al., 2016b). This makes selection of genotypes tolerant to water deficit and salinity with high productivity and fruit quality a challenging task.

Several studies revealed that water deficit (WD) and salinity stress (SS) can improve fruit quality through higher accumulation of quality compounds and anti-oxidant (Mitchell et al., 1991; Du et al., 2008; Huang et al., 2009; Albert et al., 2016a; Ripoll et al., 2016). SS also increases inorganic ion content of salinized plants (Mitchell et al., 1991; Navarro et al., 2005). In many species, particularly for fruit and vegetables, quality is a main objective for variety improvement. Breeding for quality arose with the increasing demand of high quality products from consumers these last decades. Accordingly to its definition (Shewfelt, 1999; Causse et al., 2001), quality is complex and involves several chemical, physical, and organoleptic characteristics that can be directly related to consumer preferences or to the requirement of market-oriented production. Many quantitative trait loci (QTL) related to fruit quality traits were identified in several species (Causse et al., 2001; Monforte et al., 2004; Kenis et al., 2008; Eduardo et al., 2011). These studies revealed that most of the quality components are polygenic and based on multiple correlated traits, some of which being regulated by pleiotropic or linked QTLs (Monforte et al., 2004; Kenis et al., 2008).

Multi-parent populations require crosses between more than two inbred parental lines to generate RIL progeny. They include Nested Association Mapping (called NAM, Yu et al., 2008) or Multi-parent Advanced Generation Inter-cross (called MAGIC) populations (Kover et al., 2009; Huang et al., 2012). The interest of multi-parent populations relies on the mating design allowing more genetic diversity to occur in the offspring, which besides undergoes several recombination events. The first MAGIC population was developed in mouse (Threadgill et al., 2002) and expanded to several plant species (Kover et al., 2009; Huang et al., 2012; Bandillo et al., 2013; Milner et al., 2016). The MAGIC populations have some advantages with respect to association panel for GWAS because of the absence of structure and the balanced allelic frequencies. They already demonstrated their capacity to increase length of genetic maps and detect QTL with reduced confidence intervals compared to bi-parental progenies (Pascual et al., 2015; Gardner et al., 2016). Nevertheless, due to the complexity of the mating design, statistical methods used in bi-parental or GWAS populations are not efficient. A regression model estimating all parental effects was proposed by Huang and George (2011).

In the present study we investigated the effect of salinity stress and water deficit on tomato for quality, yield component, vegetative, and phenology traits, using a MAGIC population based on the cultivated tomato and which underwent several

recombination generations. Thus, the objectives were: (1) to assess and compare the impact of both WD and SS at phenotypic level and the trait plasticity, (2) to study the genetic determinants of tomato response to SS and WD and to identify interactive QTL using plasticity and (3) to select candidate genes, based on the parental allelic effect and their genomic sequences.

MATERIALS AND METHODS

Plant Materials

We analyzed the MAGIC tomato population created at INRA center of Avignon (France). It was derived from the cross of eight parental lines, four of them belonging to the small fruit group *S. lycopersicum* var. *cerasiforme* (Cervil, Criolo, Plovdiv24A, and LA1420) and four lines with large fruit from *S. lycopersicum* var. *lycopersicum* group (Levolil, Stupicke Polni Rane, LA0147 and Ferum). Parent's selection was carefully operated within a core collection of 360 cultivated tomatoes to comprise the maximum diversity, notably the genomes of the four *cerasiforme* accessions representing a mosaic between wild and cultivated tomato genomes. A population of 400 families was obtained following the crossing design detailed in Pascual et al. (2015). The genomes of all parental lines were fully sequenced allowing the identification of about 4 millions of single nucleotide polymorphisms (SNP) (Causse et al., 2013).

Greenhouse Trials

The MAGIC population was grown in contrasted conditions in Morocco (Gautier Semences breeding station) over 2 years in greenhouse with similar experimental procedures. Plants were grown in 5L plastic pots filled with loamy substrate (Klasmann 533) and treatments were applied by row. Stressed and control rows were placed side-by-side, each genotype in the stressed row facing its replicate in the control one. The first year of experiment (Exp.1), water deficit and control (well irrigated) treatment were applied, while the second year (Exp.2) was dedicated to salinity stress and its control treatment. The average temperature and relative humidity in the greenhouses were very similar in both experiment with 20.82°C and 60.68 HR for Exp.1 and 21.74°C and 61.60 HR for Exp.2. However, the management of electrical conductivity (EC) differed between the two experiments. In Exp.1, water supply was reduced for WD treatment with respect to the control treatment where plants were subjected to the optimal irrigation. WD treatment consisted in the reduction of irrigation by 25% at the first flowering truss of Cervil (the earliest parent) and by 50% at the second flowering truss. The EC of the loamy substrate was measured in the pots for each plant with a "GroSens HandHeld" instrument, giving an average value of 1.97 dS/m for the two treatments. In Exp.2, both control and salinity treatments were not restricted in the amount of water intake but differed in the EC application. A fertigation solution with a pH of 6.1 and EC of 3 dS/m was used for both treatments at the beginning of the culture until the 2nd truss flowering of at least half of the plants. Then, salt treatment was enriched with NaCl solution and salinity was evaluated by measuring the EC of the substrate every week. On average, the EC of the substrate was 3.76 dS/m in control treatment and 6.50 dS/m in salinity treatment.

The average difference in EC between the controls treatments over the two experiments was thus 1.79 dS/m. First and last rows in the greenhouse were considered as border lines and border genotypes were also placed at the end of rows. The eight parental lines and four F1 hybrids were tested together with 241 MAGIC lines in Exp.1 and 253 MAGIC lines in Exp.2.

Plant Phenotyping

Seven traits were measured in both experiments. For phenology, flowering date (date of first open flower on 4th truss) and maturity date (first ripe fruit on the 4th truss) were recorded. Then time to flower (Flw) and time to ripe (RIP) were recorded as the day number between the sowing date and flowering date for Flw and between the flowering date and maturity date for RIP. Leaf length (Leaf) was measured as vegetative trait for each plant under the 5th truss. Fruits were harvested at maturity every week and for each genotype, fruit number was recorded on plants and fruit weight (FW) measured for at least 10 fruit per genotype on truss 3, 4, 5, and 6. For sugar content in Exp.1, 3 fruits harvested on truss 4 and 5 were pooled and crushed to obtain a fluid on which the soluble solid content (SSC) was measured with an electronic refractometer. In Exp.2 only fruits within each truss were pooled for SSC measurements. A durometer was used to measure fruit firmness (Firm), applying a pressure on the surface of the fruit measuring the strength needed to retract the durometer's tip. Five fruits per genotype were used with two measures per fruit.

For every trait in each experiment, phenotypic plasticity (PP) was measured by the relative difference between the control and stress treatments. For a trait (k) and for a single genotype, we calculated PP as $PP_k = (\text{Stress}_k - \text{Control}_k)/\text{Control}_k$ and used these data to identify interactive QTL between stress and control for each experiment. Considering all the genotypes, the average effect of the stress was evaluated in a single experiment by the mean relative variation as $(\text{Mean Stress}_k - \text{Mean Control}_k)/\text{Mean Control}_k$ and converted in percentage of increase or decrease due to the stress. For convenient comparison between salinity and water deficit effects on phenotypes, the mean variation was also calculated in a second step taking the control in Exp.1 as unique control and all other conditions as stress.

Statistical Analyses

Statistical analyses were performed with the free software R version 3.3.0. Data were firstly checked per trait and per treatment. FW and NFr were log-transformed for normality assumption. Analyses were conducted separately per experiment to allow the comparison of each stress treatment against its control. We tested the fixed effect of genotype and treatment and their interaction by a two way ANOVA following the model: $Y_{ij} = \mu + G_i + T_j + G^*T_{ij} + \varepsilon_{ijk}$, where Y_{ij} represents the phenotype of genotype i (G_i) and treatment j (T_j), G^*T_{ij} the interaction between genotype and treatment and ε_{ijk} the residual error. Pearson's correlations were calculated between the mean trait values per treatment and for each trait between treatments within experiment and between the two control treatments. In each treatment, the broad sense heritability (h^2) was evaluated by means of the following ANOVA model where the genotype

was considered as random: $Y_i = \mu + G_i + \epsilon_{ij}$. G_i and ϵ_{ij} are the random effect of genotype and the residual error respectively. The broad sense heritability was then calculated as $h^2 = \sigma^2_G / (\sigma^2_G + \sigma^2_E/r)$ where σ^2_G and σ^2_E are the genetic and residual variance respectively, and r is the average number of replicates per genotype.

Haplotype Prediction

The MAGIC population is characterized by the complex mating design of the eight parental lines. The parental origin of each allele in the offspring is not intuitive, on the contrary to the bi-parental population. To infer the allelic parental provenance, we estimated the probability of each parent being at the origin of each allele in the MAGIC lines with the function *mpprob* of the mpMap package 2.0 (Huang and George, 2011). We fixed a threshold of 50% above which allelic parental provenance is assigned. These probabilities were further used to perform the QTL identification.

QTL and QTL \times E

The QTL were mapped by interval mapping (IM) procedure with the R package mpMap. Parental probabilities were computed every 2 cM along the genome and at each marker position and then used to estimate parental effects. The regression on the parental allelic effect, at each position where probabilities were computed, allowed the QTL identification. A LOD threshold of 3 was fixed to detect a significant QTL. Confidence interval (CI) of a QTL was estimated with one unit decreasing of the LOD threshold on both sides of a QTL position. Considering one trait, constitutive QTLs were defined when two (or more) QTLs were identified in different conditions (treatments) on the same chromosome with their CI overlapping. They were then considered as a unique QTL expressed in both conditions.

Then, PP was used as single trait for each phenotype, to identify interactive QTL (QTL \times E). Before analysis, plasticity data were checked for normality and log transformed for FW and NFr.

Candidate Genes Identification

We screened for candidate genes under QTL for the QTL \times E and QTL mapped in a CI shorter than 2 Mb. For each QTL, we listed the number of polymorphisms and genes present within the CI region based on the sequence information of all parental lines (Causse et al., 2013) and the reference genome (Tomato Genome Consortium, 2012). We filtered the polymorphisms and genes listed in accordance with the parental allelic effects at the QTL. We focused on QTL that present pronounced divergence in the allelic effect of the eight parents, keeping all polymorphisms and genes commonly shared by the parents varying in the same direction and different from those shared by the parents varying in the opposite direction. The putative function of the remaining genes (when annotated) were then checked on the Sol Genomic Network (solgenomics.net) database in order to identify which candidate's annotated function is correlated to the QTL trait of interest.

RESULTS

Phenotypic Variation in the MAGIC Population

The phenotypic variation observed among the MAGIC lines showed transgressions in both directions in comparison to the eight parental values for every trait (Table 1; Supplemental Figure 1). Except FW in control of Exp.2, the highest value in MAGIC lines always exceeded the best parent in every trait by treatment combination.

The comparison of control treatments between the two experiments showed little mean differences for Firm, RIP and Leaf, which had a relative mean variation below 10%. FW, SSC, and NFr varied considerably between the controls by 38.54, 39.85, and 61.11% respectively (Table 1). Statistical analyses were thus conducted separately for each experiment to assess the impact of WD and SS compared to their specific control treatment.

All traits across treatments exhibited heritability above 0.4 except firmness in Exp.1. Heritability ranged from 0.09 for firmness in WD treatment to 0.92 for flowering time in control of Exp.1. In average, Flw, RIP and FW had the highest heritability. For both experiments, heritability varied between control and stress treatment with the highest variation observed for SSC in Exp.2 where h^2 SSC was 0.69 for the control and 0.48 for the salinity treatment. The heritability of a few traits like RIP was poorly impacted by the stress treatments.

The total sum of square of the two way ANOVAs was partitioned in proportion attributed to genotype, treatment and their interaction. A large part of the phenotypic variation was linked to genotype, accounting from 39 to 86% of the total sum of square in Exp.1 and 33 to 72% in Exp.2 (Table 2). Significant effects of treatment were found for every trait in Exp.1 while Exp.2 showed significant treatment effect only for FW, SSC, and Leaf. Similarly, all traits exhibited significant genotype \times treatment interaction in both experiments except Firm in Exp.1 and NFr in Exp.2.

Significant correlations were observed between traits in each treatment revealing the link between quality, phenology, and vegetative traits. To assess the repeatability of phenotyping measurement, single trait correlations between treatments within each experiment and among control treatments were evaluated. Most of the correlations were significant at $P < 0.001$ (Table 3). The strongest Pearson's correlation was found between FW and leaf in Exp.1, which exhibited a positive correlation. In Exp.2, the correlation between Flw and RIP was the strongest correlation. For both experiments, Flw and RIP were significantly and negatively correlated indicating that the later the truss flowered, the shorter the time to ripe. FW was also negatively correlated to SSC in every treatment. Across experiments, the sign of correlations were conserved for all significant correlations.

Impact of Water Deficit and Salinity Stress at Phenotypic Level

The effect of stress treatment was assessed by the mean relative variation (MV) calculated as detailed in Materials and Methods. In a first step, salinity and water deficit were compared to their relative control treatment in each experiment. In accordance

TABLE 1 | Phenotypic variation among MAGIC lines for all traits and treatments.

Traits	Treatments	P. range	MAGIC lines			MV_WD	MV_Ctrl2	MV_SS	h^2
			Min	Max	Mean				
SSC	Ctrl1	3.50–7.30	2.80	8.20	5.56	11.78	39.85	75.91	0.72
	WD	4.30–10.10	3.10	10.10	6.21				0.80
	Ctrl2	7.50–9.50	4.00	13.00	7.74	25.96			0.69
	SS	8.50–11.00	6.00	12.5	9.75				0.48
Firm	Ctrl1	50.00–72.00	44.00	73.00	59.58	-2.18	2.02	6.92	0.32
	WD	50.00–68.00	45.50	73.00	58.28				0.09
	Ctrl2	38.50–76.00	36.00	82.00	60.60	4.93			0.64
	SS	57.00–70.00	31.00	84.00	63.58				0.57
FW	Ctrl1	6.88–92.00	10.71	110.00	38.75	-23.05	-38.54	-54.62	0.85
	WD	5.35–95.00	10.54	101.67	29.81				0.83
	Ctrl2	5.00–110.00	5.00	95.00	23.84	-26.52			0.77
	SS	5.00–23.84	2.50	74.28	17.52				0.60
NFr	Ctrl1	6.50–45.50	2.50	105.00	15.61	-15.32	-61.11	-59.85	0.75
	WD	3.00–47.00	3.00	50.00	13.22				0.56
	Ctrl2	2.00–12.50	2.00	23.50	6.20	3.70			0.42
	SS	2.00–15.50	2.00	21.00	6.43				0.40
Leaf	Ctrl1	23.50–42.00	18.00	55.00	32.24	-17.97	-7.92	-16.05	0.85
	WD	23.50–35.50	15.00	48.50	26.45				0.69
	Ctrl2	20.50–35.00	11.00	45.50	29.51	-8.66			0.66
	SS	25.00–31.00	11.50	40.00	26.97				0.58
Flw	Ctrl1	77.50–110.00	77.50	117.00	88.76	-0.77	-10.26	-10.74	0.92
	WD	76.50–107.00	75.50	124.00	88.07				0.92
	Ctrl2	80.50–102.00	75.00	102.00	79.74	-0.60			0.85
	SS	79.00–98.00	74.00	105.00	79.26				0.78
RIP	Ctrl1	51.00–71.50	43.50	74.00	57.88	-2.87	-5.30	-6.59	0.87
	WD	46.50–68.00	44.00	70.00	56.22				0.88
	Ctrl2	46.50–72.00	36.00	79.00	55.72	-0.22			0.64
	SS	47.00–66.00	35.50	75.00	55.59				0.75

Min, Max and mean are the minimum, maximum and mean values of MAGIC lines. P. range represents the range of the means of the eight parental lines. MV is the relative mean variation, with respect to control in Exp.1 due to treatments under WD (MV_WD), control in Exp.2 (MV_Ctrl2) and salinity (MV_SS). h^2 is the broad sense heritability calculated for each treatment.

to the results of ANOVA, FW, SSC, and Leaf were the traits most affected by stress treatments. Among all traits, SSC was the only one positively impacted by WD and SS with more than 10% increase compared to controls (**Table 1**). On average, when comparing each stress to its control, WD and SS affected all traits in the same direction except NFr. Indeed, NFr was reduced by WD condition (-15%) but slightly increased when comparing salinity to its control. FW and Leaf were both reduced in stress conditions while stress effects were less obvious for firmness and phenology traits.

For a convenient comparison of WD and SS applied in our study, we considered the control treatment in Exp.1 as reference, taking a subset of 241 lines commonly tested in all treatments. Indeed, the difference between the control in Exp.1

and treatments in Exp.2 lies mainly in the EC application that was 1.7 and 4.5 times higher in control of Exp.2 and SS, respectively. We then calculated the effect of those treatments compared to Ctrl1 and measured the effect of each of them in percentage of increase or decrease (**Supplemental Figure 2**). Using the same control revealed a growing negative effect of salt treatment while control in Exp.2 seemed to be intermediate between WD and SS.

Nevertheless, these average behaviors did not fully reflect the individual variations. FW plasticity was found negatively correlated to FW in control in both experiments, meaning that larger fruits were more affected by the stress. Indeed both stress decreased FW of accessions with fruits larger than 55g (**Figures 1A,B**). The plot of FW plasticity in SS against WD showed clearly that only one genotype had an increased FW

TABLE 2 | Phenotypic variation attributed to the genotype (G), the treatment (T) and the interaction (GxTreat) effects.

Traits	G	SSq G %	Treat	SSq Treat %	GxTreat	SSq GxTreat %	SSq Resid %
EXP.1 (CONTROL vs. WD)							
Firm	***	39.42	***	0.86	ns	18.75	40.97
Flw	***	86.04	***	0.44	***	6.48	7.04
FW	***	54.16	***	9.25	***	4.67	31.92
Leaf	***	47.75	***	14.85	***	23.91	13.48
NFr	***	55.53	*	0.62	*	17.88	25.98
RIP	***	73.27	***	2.77	***	13.62	10.34
SSC	***	61.75	***	6.7	***	15.8	15.75
EXP.2 (CONTROL vs. SS)							
Flw	***	68.76	ns	0.00	***	15.4	15.83
FW	***	47.14	***	6.87	***	26.2	19.78
Leaf	***	52.36	***	3.55	***	18.9	25.19
NFr	***	42.04	ns	0.18	ns	23.59	34.19
RIP	***	59.06	ns	0.01	*	17.56	23.36
SSC	***	33.45	***	27.24	***	23.01	16.29

For each quantitative trait the significance of the explaining factors: G, T and the interaction GxTreat, and their relative proportion of sum of square (SSq G, SSq Treat and SSq GxTreat, respectively) are shown.

***P < 0.001; *P < 0.05; ns = non significant.

TABLE 3 | Correlations among traits in each treatment and experiment.

Ctrl1		Ctrl1-Ctr2		Ctrl2			
Firm	Firm			-0.17	Firm	Firm	
Flw	0.15	Flw		0.61	Flw	ns	Flw
FW	ns	0.24	FW	0.4	FW	ns	FW
Leaf	ns	0.18	0.37	Leaf	0.19	Leaf	ns
NFr	ns	ns	-0.33	ns	NFr	ns	-0.15
RIP	0.17	-0.26	0.22	ns	-0.28	RIP	0.49
SSC	-0.13	ns	-0.17	ns	ns	-0.26	0.23
WD		Ctrl1-WD		Salt		Ctrl2-SS	
Firm	Firm			0.34	Firm	Firm	0.19
Flw	ns	Flw		0.86	Flw	ns	Flw
FW	0.18	0.14	FW	0.84	FW	ns	0.26
Leaf	ns	0.29	0.4	Leaf	0.34	Leaf	ns
NFr	-0.11	ns	-0.38	-0.14	NFr	0.55	NFr
RIP	0.2	-0.31	0.23	ns	-0.12	RIP	0.68
SSC	-0.17	ns	-0.33	-0.17	ns	-0.31	0.6

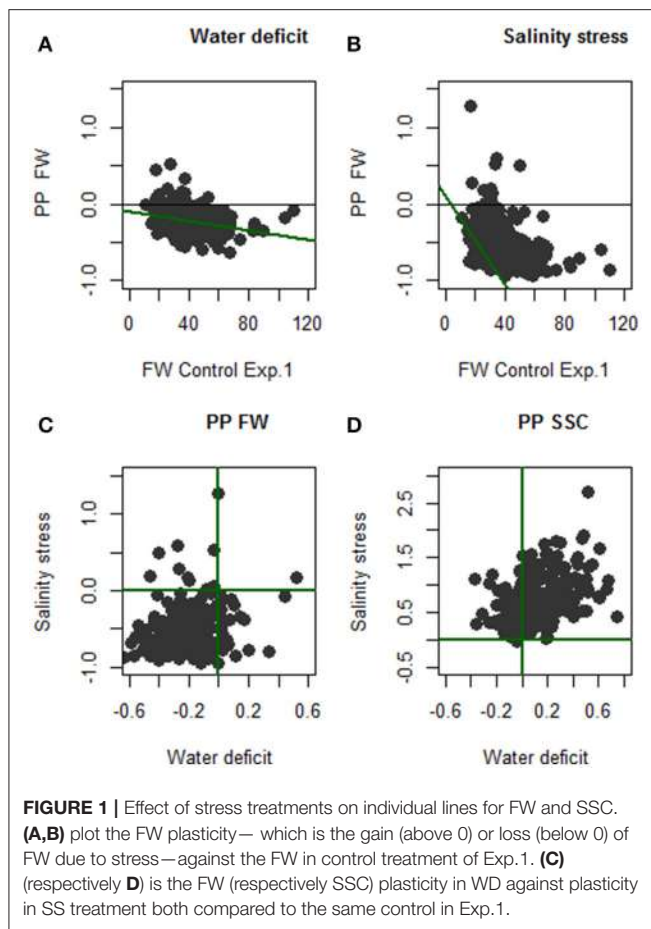
Single trait correlation among controls (Ctrl1-Ctr2) which is a measure of repeatability or between control and stress (Ctrl1-WD and Ctrl2-SS) is presented. Only significant correlations (P < 0.05) are indicated. They are in bold when significance is lower than 0.001. In bold P < 0.001; ns = non significant.

in both conditions while 23 genotypes increased FW under WD and decreased it under SS and 10 genotypes react in the opposite direction (**Figure 1C**). For SSC, all genotypes except H10_84 increased SSC with SS treatment. Altogether, 67% of the genotypes increased SSC under both stresses pointing the possibility to improve sugar content in fruit by irrigation practices. However, as for FW, some genotypes were affected inconsistently by the stress treatments with 55 genotypes (22.8%) that increased SSC only in SS and not under WD (**Figure 1D**).

QTL Detection and Stability

QTL Detection

QTL mapping was performed using a genetic map constructed with 1,345 polymorphic SNP selected from the parental line resequencing data. This genetic map covers more than 84% of the genome and measures 2,156 cM (details in Pascual et al., 2015). With the available information of parental polymorphisms, the offspring haplotype structure was predicted by inferring the parental origin of each allele. On average, 88.7% of founder allele origin was accurately predicted with



only 11% of the alleles that could not be strictly assigned to any parent (**Supplemental Figure 3**). Among the parents, Levovil and LA0147, with <10% of the allelic contribution in the MAGIC lines genome deviated, the most from the expected value of 12.5% of each parental allelic contribution.

Considering all treatments, 54 QTL were identified for the seven traits evaluated and their plasticity. The number of QTL per trait varied from four for Flw to 11 for FW (**Supplemental Table 1**). Among these QTL, 19 were found in at least two treatments and around 65% (35 QTL) were treatment specific. Eleven QTL were common to WD and its control condition, while SS and its control condition shared only four QTL (**Figure 2A**).

Some QTL were specifically detected in one treatment or for plasticity traits (interactive QTL; **Supplemental Table 1**). Indeed, irrespective of interactive QTL, we observed eight and four QTL specific to control treatments for Exp.1 and Exp.2, respectively. Nine and 11 QTL were specific to WD and SS respectively, pointing that stress treatments present higher number of specific QTL. For interactive QTL, six were exclusively identified in Exp.2 and one in Exp.1 and no interactive QTL were shared between the two experiments (**Figure 2B**). This outlined the specificity of the interactive QTL. Confidence intervals (CI) of the QTL ranged from 4 to 60 cM (according to genetic

distance) and 0.43 to 71.49 Mb (according to physical distance; **Supplemental Table 1**). The high number of recombination occurring in the MAGIC population allowed us to map 24 QTL with CI lower than 2Mb. The chromosome 11 presented the largest number of QTL, each trait except Flw presenting at least one QTL on this chromosome, whereas per trait, FW and SSC had the largest number of QTL (11 and 10, respectively).

Identification of Interactive QTL (QTLxE)

We call interactive QTL (QTLxE) those mapped for plasticity traits in each experiment. Thus, for Exp.1, three QTLxE were detected for RIP (two QTL) and SSC. The RIP QTLs (*RIP9.1* and *RIP10.1*) were also mapped in control for Exp.1 and WD treatment, respectively. The QTLxE SSC12.1 was specific to the interaction. Likewise, 12 QTLxE were mapped in Exp.2, among which six were specific to the interaction.

Co-Localization of QTL

Clusters of QTL were localized especially on chromosomes 1, 2, 3, 10, and 11 (**Supplemental Figure 4**). Most of these QTL corresponded to correlated traits. For example, around 45 cM on chromosome 1, QTLs linked to phenology traits, FW, SSC, and NFr clustered and could be related to the pleiotropic effect of one QTL. The same observation was noted on chromosome 2 for quality traits and on chromosome 3 for phenology, quality and vegetative traits.

Candidate Gene Selection

After the identification of constitutive and interactive QTLs, the number of genes and polymorphisms within the CI of any QTL mapped in a region lower than 2Mb was assessed using the sequencing information of all parental lines (Causse et al., 2013). For the 24 QTLs that had a CI shorter than 2 Mb, the number of genes within the CI (potential candidate genes) varied from 75 for *Leaf9.1* to 269 genes for *Firm11.1* with 3,804 and 12,530 polymorphisms associated, respectively (**Table 4**). We attempted to reduce the number of candidate genes (CG) by applying a filter in accordance to parental allelic effects at the QTL as described in Materials and Methods. This procedure was efficient for some QTL and allowed us to reduce the number of CG by nearly 80% of the total number of genes within the CI for *Firm11.1* and *Leaf10.1*. Nevertheless, for *FW11.3* and *RIP4.1* the parental allelic effect filtering wasn't efficient; none of the genes in the CI was discarded as a close haplotype was present in the region (**Supplemental Figure 5**).

The interactive QTL *Firm11.1*, identified in Exp.2 contained the largest number of genes within the CI (269 genes). Regarding the parental allelic effect at this QTL (**Figure 3A**), we filtered the candidates by keeping all polymorphisms that were specific to Cervil parent. This reduced the number of candidates to eight genes and polymorphisms with different effects (**Supplemental Table 2**). For *FW8.1*, we kept all polymorphisms identical between Cervil and Plovdiv and different from Criollo (**Figure 3C**), decreasing the number of CG to 31 genes (**Supplemental Table 2**). Five QTL presented <40 CG after the filtering procedure according to allelic parental effect variation (presented in **Supplemental Table 2** with functional annotation

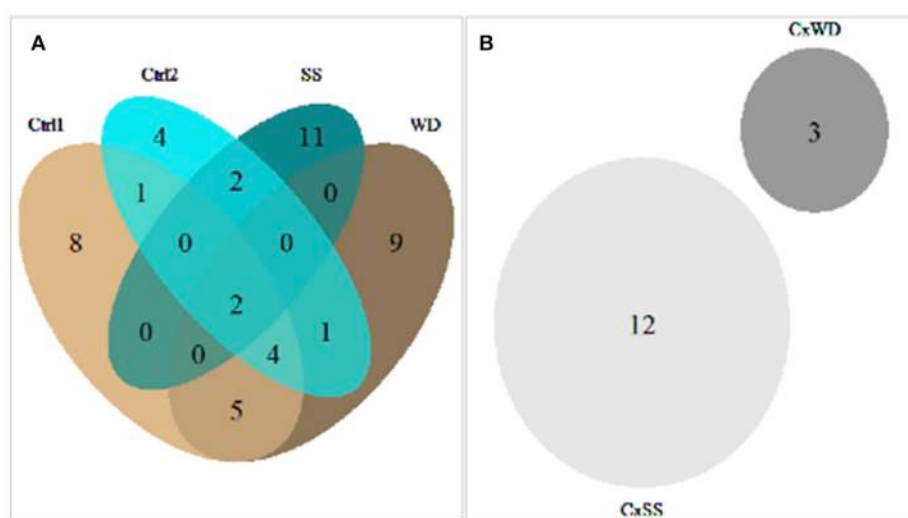


FIGURE 2 | Venn diagram of the number of main effect QTL, detected on mean traits for all treatments (A) and interactive QTL, detected on plasticity traits for the two experiments (B).

of the CG). FW2.2 QTL co-localized with a ripening time QTL *RIP2.1*. These two QTL shared the same CI comprising 1.74 Mb of length and containing 234 genes and 9,957 polymorphisms (Table 4). FW and RIP were highly positively correlated and could be impacted by one pleiotropic QTL. Moreover, *RIP2.1* and FW2.2 presented the same pattern of parental allelic effect, at least for Cervil, Stupicke and LA1420 that had the strongest QTL effect (Figures 3B,D).

DISCUSSION

Parental lines of the MAGIC population did not include any wild accession (from the *S. pimpinellifolium* species) but had sufficient genetic diversity to allow QTL mapping on the offspring. The progeny exhibited a large variability with phenotypic transgressions in both directions in every tested condition (Supplemental Figure 1), suggesting new favorable allelic combinations obtained in the MAGIC population. Besides, the slight impact of WD and SS on the heritability suggests possibility for marker-assisted selection (MAS). Huang et al. (2015) proposed an interesting MAS approach for MAGIC populations called Multi-parent advanced generation recurrent selection (MAGReS) involving the inter-cross of individuals with the best allelic combinations for one (or more) trait(s) of interest to produce highly performant RILs. The MAGIC population tested here is thus a valuable resource to apply such breeding strategy. However, our results showed high level of GxE for the two experiments that affect also the QTL detection, as 35 QTL (65%) were specifically detected on one condition. Furthermore, FW and SSC, the most important agronomic traits, carried ten or more QTL in all condition tested with only one QTL (FW2.2) stable across all treatments. For these traits, MAS may not be of great utility for breeding programs targeting variable cultural areas. Thus, the breeding strategy should take

into account the specificity of the QTL to achieve optimal benefit per environment. Applying the MAGReS strategy by selecting genotypes to inter-cross following the performance per environment in order to achieve rapidly performing crop, is an innovative approach to sustain breeding effort.

On average, WD and SS impacted sugar content, fruit weight and leaf length more than the other traits. They both reduced FW and Leaf while SSC was the only trait positively affected by up to 10% increase with respect to control in Exp.1 (Supplemental Figure 2). Similar results were frequently found in the literature (Villalta et al., 2007; Huang et al., 2009). The higher SSC under WD and SS was assumed to derive from the fruit water content reduction without necessarily involving higher synthesis of soluble sugar. Indeed, several studies reveal a negative correlation between FW and SSC, pointing a physiological link of these two traits making a simultaneous improvement difficult to be achieved. However, Navarro et al. (2005) showed that when SS occurs, the increased concentrations of sugars and acids were probably both due to the decrease in water content in the fruit and additionally to new sugars synthesis, since concentrations calculated on a dry weight basis also increased. Our results showed 20 and 11 genotypes that increased simultaneously FW and SSC under WD and SS respectively. This may be linked to a positive regulation of SSC during drought and salinity. These genotypes are interesting for quality improvement in tomato with minor impact on FW.

The results of the QTL analyses confirmed the polygenic architecture of fruit quality traits. SSC and FW that are among the most important fruit quality traits had the highest number of QTL identified. Besides this polygenic architecture, the positions of these QTL are distributed along the genome. QTLs related to FW and SSC were identified on six and seven chromosomes respectively, considering all treatments but treatment specific QTL were also identified. In optimal growth condition (Control

TABLE 4 | Characteristics of the 24 QTL with a confidence interval (CI) smaller than 2 Mb.

QTL	CI Mb	Cervil	Levoliv	Criollo	Stupicke	Plovdiv	LA1420	Ferum	LA0140	Nb.Genes	Nb.Pol	Filter	Nb.CG	Nb.CP
<i>Firm1.1</i>	1.86	0.608	-1.266	-3.916	2.628	1.655	0.095	-0.629	0.824	245	10991	Criol # Stup	164	620
<i>Firm1.2</i>	1.05	-0.412	-0.539	-0.544	-0.541	-0.372	3.112	-0.428	-0.276	134	5630	LA14 # all	127	1719
<i>Firm11.1</i>	1.87	4.305	-0.651	-0.284	-2.169	-0.821	-0.435	-0.326	0.384	269	11903	Cerv # all	8	3
<i>Firm3.1</i>	1.44	-5.249	4.750	-3.842	3.354	-7.327	0.581	2.679	5.055	171	7051	Plov # (Lev=LA0)	36	29
<i>Firm8.1</i>	1.23	-0.411	-0.421	2.767	-0.815	-0.245	-0.636	-0.009	-0.231	117	7975	Criol # all	27	46
<i>Flw9.1</i>	1.00	0.292	1.523	-0.522	-1.460	3.004	-2.710	3.561	-3.690	119	6375	(Plov=Fer) # LA0	49	35
<i>FW11.2</i>	0.79	-0.131	0.664	-0.043	0.024	0.013	-0.040	0.003	-0.493	91	4478	Lev # LA0	29	32
<i>FW11.3</i>	1.42	-0.155	0.066	-0.049	0.130	-0.001	-0.022	NA	0.033	189	11532	Cerv # (Stup=Lev)	189	6989
<i>FW12.1</i>	0.43	0.008	-0.097	0.048	-0.142	-0.038	0.033	0.171	0.020	79	3407	Fer # (Stup=Lev)	77	562
<i>FW2.2</i>	1.74	-0.138	-0.031	0.050	-0.134	0.031	0.082	0.044	0.093	234	9957	(Cerv=Stup) # (LA14 =LA0)	52	1362
<i>FW3.2</i>	0.97	-0.049	-0.004	-0.087	0.056	0.162	-0.078	-0.005	0.003	122	6490	Criol # Plov	109	3026
<i>FW3.3</i>	1.52	-0.095	-0.007	-0.046	-0.038	0.056	-0.083	0.055	0.157	214	10182	(Cer=LA14) # LA0	142	377
<i>FW8.1</i>	1.63	-0.195	0.019	0.111	0.009	-0.132	0.046	0.097	0.047	180	7959	(Cer=Plov) # Criol	31	738
<i>Leaf10.1</i>	1.86	1.565	-0.622	2.628	-2.586	-0.070	3.058	-2.898	-1.073	264	13108	(Criol=LA14) # (Stup=Fer)	42	52
<i>Leaf11.1</i>	1.55	-2.416	2.005	2.040	3.103	-1.464	-2.799	0.890	-1.356	168	10084	Stup # (Cerv =LA14)	94	524
<i>Leaf3.1</i>	1.46	-2.985	2.944	-2.063	1.403	3.224	-1.286	-0.321	-0.918	193	9944	(Lev=Plov) # Cer	184	5803
<i>Leaf9.1</i>	0.76	0.798	-2.351	-1.744	5.031	-4.669	-2.079	3.154	1.861	75	3804	Plov # Stup	52	963
<i>NFr10.1</i>	1.53	-0.129	-0.021	0.039	0.354	0.063	-0.023	0.042	-0.326	212	5506	Stup # LA0	70	80
<i>RIP2.1</i>	1.74	-4.039	1.956	2.022	-3.948	-0.265	3.585	0.654	0.034	234	9957	(Cer=Stup) # LA14	103	1418
<i>RIP4.1</i>	1.21	-0.053	2.639	1.233	-0.053	1.788	-2.420	-0.653	-2.482	150	10794	(LA14 = LA0) # Lev	150	6629
<i>SSC1.2</i>	1.34	0.156	-0.250	-0.670	-0.207	0.194	-0.290	0.121	0.949	197	10528	LA0 # Criol	68	69
<i>SSC11.2</i>	1.56	0.970	-1.916	0.789	-0.594	0.018	0.398	NA	0.338	203	11813	(Cer = Criol) # Lev	78	681
<i>SSC12.1</i>	1.52	0.047	0.004	-0.007	-0.094	0.122	0.103	-0.153	-0.019	170	8232	(Plov=LA14) # Fer	110	395
<i>SSC4.1</i>	1.93	-0.792	0.363	0.214	0.441	0.811	0.252	-0.682	-0.606	211	15195	(Cerv=Ferum=LA0) # Plov	65	58

The columns of the eight parents present their respective allelic effect for each QTL. Nb.Genes and Nb.Pol count the number of genes and the number of polymorphisms identified—via the Solgenomic database—within the CI. After filtering these genes and polymorphisms according to the allelic effect of parents, the residual numbers of genes are counted as candidate genes (Nb.GC) with the residual number of candidate polymorphisms (N.CP). The parents chosen for the CG filtering are presented in the column "Filter" where the symbols = and # notified respectively parents where identical or divergent polymorphisms were kept.

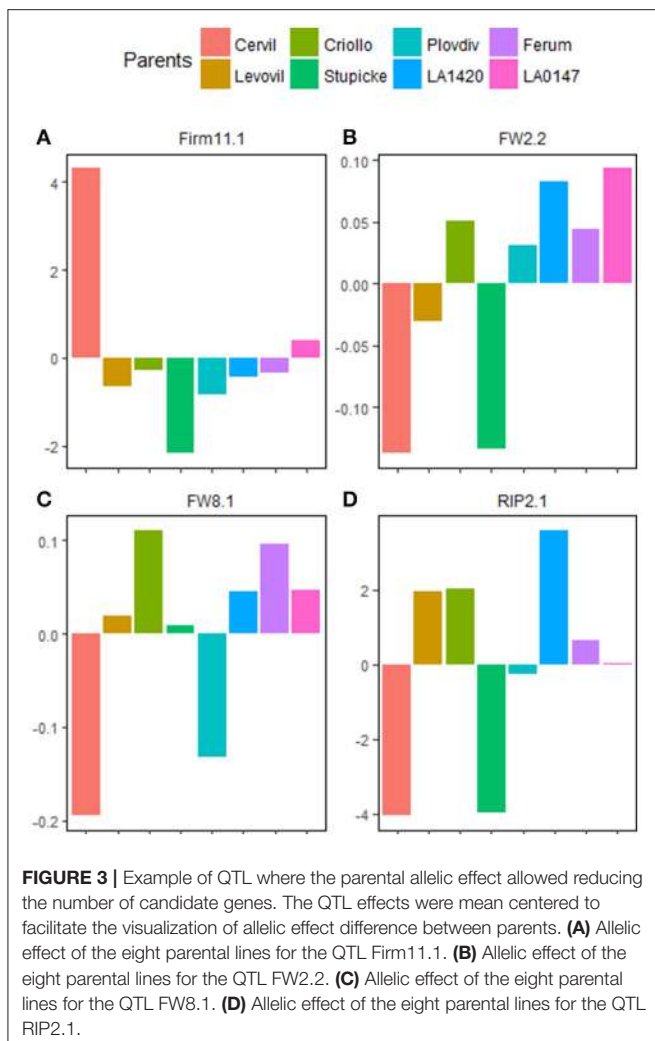
of Exp.1), seven FW QTL (out of the 11 QTL mapped for FW) were identified, explaining additionally 68.68% of the phenotypic variation, while only one SSC QTL (SSC2.1; out of the 10 SSC QTL) was identified, with 6.98% of phenotypic variation. This suggests that SSC QTLs are easier detected in stress than control conditions.

Among all the QTL identified in this study, 35 QTL were treatment specific and only two QTL (*Flw1.1* and *FW2.2*) were stable across every treatment. Depending on the environmental conditions, the main QTL responsible of the observed phenotypic variation are not the same. Only one third of the QTL were detected in at least two treatments. These results reinforce the idea of targeted environment breeding strategy in order to achieve better results per environment.

Fifteen interactive QTL were identified, three in Exp.1 and 12 in Exp.2 but none of them co-localized between the two experiments suggesting different genetic control of the phenotypic plasticity under WD and SS. Two main ideas were developed concerning the genetic control of phenotypic plasticity advocating that: (i) phenotypic plasticity can be caused by environmentally sensitive loci associated with a phenotype, directly influencing the trait value in both environments; (ii) or it can be caused by regulatory genes that simply influence the plasticity of a phenotype. This means that plasticity can be viewed

as the result of the action of alleles that have different effects in different environments or being under the control of regulatory loci (Via et al., 1995). Besides, QTL mapping study can be used to address easily which one of these hypotheses is the most probable (Ungerer et al., 2003; Tétard-Jones et al., 2011). When plasticity QTL co-localized with QTL mapped on mean trait value in at least one of the environment tested, they are assumed to be under the control of allelic sensitivity loci. On the contrary, QTL that are specific to plasticity are mainly linked to regulatory genes. In Exp.1 three QTLxE were identified: *RIP9.1*, *RIP10.1* and *SSC1.2* but only the last one was specific to the interaction. At the same time in Exp.2, among the 12 QTLxE, six were specific to the interaction. One can assume these QTLxE to be under regulation of WD (Exp.1) and SS (Exp.2) response genes, which make them particularly interesting for breeding in stressful environment.

Multi-parental populations offer new insight into fine mapping of quantitative traits (Kover et al., 2009; Milner et al., 2016). The high recombination events occurring in this type of population in addition to the infinite possibility of repeated study are of major interest. One advantage is the high allele segregation compared to bi-parental population and low LD with poor structure compared to GWAS, making them intermediate and complementary between these types of mapping populations (Pascual et al., 2016). Our results were compared to those



of Albert et al. (2016a) and Albert et al. (2016b), that were conducted respectively on bi-parental population and a GWAS panel of tomato grown in similar condition of control and WD treatment than Exp.1. Among the 30 QTL identified in Exp.1, 18 QTL (60%) were also detected in the GWAS or RILs population, but only *Firm11.1* and *SSC11.2* were shared between the three panels. The ability to map QTL considerably depends in the mapping population pointing the relevance of combining different mapping population to identify stable QTL and balanced the advantage and disadvantage of each type of population.

The parental allelic information in the MAGIC population is a real advantage to screen and reduce candidate polymorphisms within the CI of a QTL as first described in Pascual et al. (2015). Indeed, the parents of the MAGIC population present very diverse allelic effects depending on the QTL. Some QTL had very divergent parental allelic effect while some other showed one parent varying differently from others. For example, *Firm1.2*, *Firm8.1*, and *Firm11.1* had all one parent divergent that seem to carry the allele responsible of the phenotypic variation. Besides, those QTL present very strong percentages of variation explained,

that makes them interesting targets for breeding. These effects efficiently facilitate the filtering procedure to reduce CG.

On the chromosome 2, in a nearly 8 Mb region ranging from 44.55 to 52.92 Mb, two FW QTL were identified in our study. However, this region contains at least three already known QTL impacting fruit size and fruit shape, two of them positionally cloned: the fruit weight 2.2 (*Solyc02g090740*) cloned by Frary et al. (2000) and the ovate locus (*Solyc02g085500*) cloned by Liu et al. (2002). A third FW QTL was fine mapped by Muñoz et al. (2011) in this region, corresponding to a locule number (*lc*) locus. The first QTL identified on the chromosome 2 in our study (*FW2.1*) falls in a region of 3.5 Mb covering the *lc* and *ovate* loci. 462 genes and 20,742 polymorphisms were present in this region, and the filtering procedure did not efficiently reduce the CG. The second FW QTL on chromosome 2 (*FW2.2*) fell in a region of 1.74 Mb and covered the QTL *fw2.2* cloned by Frary et al. (2000). However, this QTL was discarded when we attempt to reduce CG according to allelic effect of Cervil and Stupicke (Figure 3B). This suggests a second FW QTL closely linked to *fw2.2*. Nevertheless, Pascual et al. (2015) suggested a possible bias in the estimation of allelic parent's effect in regions where many QTL for a given trait are present. Indeed, in this case, the bias of allelic effect estimation may arise if different allelic combinations control different QTL. The QTL were mapped by interval mapping procedure meaning that each interval was tested for linkage with the phenotype. A whole genome mapping method, as proposed by Verbyla et al. (2014) for MAGIC populations, would better capture all small effect QTL and may limit the bias in QTL effect estimation. Anyhow the region of *FW2.2* is of great interest since several studies conducted on different mapping populations identified FW QTL within (Pascual et al., 2015; Albert et al., 2016a).

The number of candidate genes and polymorphisms was reduced using the parental re-sequencing information that allowed comparison of parental genotypes within CI of any detected QTL. Five QTL presented <40 CG after the filtering procedure (Supplemental Table 2). For these QTL, the putative functions of CG were screened according to the tomato genome annotation (SL2.50). Eight CG were retained for the QTL *Firm11.1* and all the polymorphisms related to these CG were on intergenic regions (Modifier effect in Supplemental Table 2). Among these CG, only *Solyc11g006210* was not annotated. The functional annotation of the seven others highlighted one interesting CG (*Solyc11g005820*) which is a pectinesterase inhibitor. Pectinesterase inhibitors are involved in the rigidification or loosening of the cell wall. Thus, the *Solyc11g005820* gene constitutes a good candidate for firmness variation.

FW8.1 presented 31 CG after the filtering procedure but the number of candidate polymorphisms was very high (Supplemental Table 2). In this region, most of the CG were affected by more than one polymorphism pointing the need of deeper characterization of our candidate regions to confirm the effectiveness of causal polymorphisms. Nevertheless, this region carried three SNP that had a high effect modifying splice site or start/stop codon whereas most of the candidate polymorphisms remaining after the allelic filtering for other QTL were located in intergenic regions. The three SNP with high effect in the CI of

FW8.1 affected the genes Solyc08g075430, Solyc08g075470, and Solyc08g075510.

We showed in this study the presence of high level of genotype \times environment interaction and how these interactions affect the QTL detection according to the environment. Specific and constitutive QTL were identified—in high precision for some—for phenology, vegetative and quality traits and the availability of the parental sequence information was useful for the genetic and genomic characterization of polymorphisms responsible for trait variation. The parental sequences allowed filtering CG and polymorphisms for the QTL mapped on regions carrying divergent parental haplotypes. The transcriptomic response through RNA-sequencing analyses on all parental lines should offer additional information that will be used to improve and support the CG selection. Functional validation could be envisaged afterward in order to detect the exact causal polymorphisms under the QTL of interest.

AUTHOR CONTRIBUTIONS

This work is a part of the Ph.D. project of ID who conducted the statistical analyses and the redaction of the manuscript. LD conducted the experimental trials and phenotyping in Morocco. FB developed the bioinformatics tools to identify the polymorphisms on the MAGIC parental lines. LP reviewed the manuscript and shared a part of the script for QTL mapping analysis. MC supervised all the process of this work, constructed the experimental design and monitored the redaction of the article.

FUNDING

The ANR project ADAPTOM supported this work. ID was supported by the WAAPP (West Africa Agricultural Productivity Project) fellowship and hosted as Ph.D. student in the INRA UR1052, GAFL.

ACKNOWLEDGMENTS

We acknowledge the experimental teams of Gautier SEMENCES for their collaboration in implementing the experimentations and thank the employees of Domaine Margau (Agadir) for the data collection. We thank Christopher Sauvage for proofreading.

REFERENCES

- Albert, E., Gricourt, J., Bertin, N., Bonnefoi, J., Pateyron, S., Tamby, J. P., et al. (2016a). Genotype by watering regime interaction in cultivated tomato: lessons from linkage mapping and gene expression. *Theor. Appl. Genet.* 129, 395–418. doi: 10.1007/s00122-015-2635-5
- Albert, E., Segura, V., Gricourt, J., Bonnefoi, J., Derivot, L., and Causse, M. (2016b). Association mapping reveals the genetic architecture of tomato response to water deficit: focus on major fruit quality traits. *J. Exp. Bot.* 67, 6413–6430. doi: 10.1093/jxb/erw411
- Bandillo, N., Raghavan, C., Muyco, P. A., Sevilla, M. A., Lobina, I. T., Dilla-Ermite, C. J., et al. (2013). Multi-parent Advanced Generation Inter-Cross (MAGIC) populations in rice: progress and potential for genetics research and breeding. *Rice* 6:11. doi: 10.1186/1939-8433-6-11
- Caro, M., Cruz, V., Cuartero, J., Estañ, M. T., and Bolarin, M. C. (1991). Salinity tolerance of normal-fruited and cherry tomato cultivars. *Plant Soil* 136, 249–255.
- Causse, M., Desplat, N., Pascual, L., Le Paslier, M. C., Sauvage, C., Bauchet, G., et al. (2013). Whole genome resequencing in tomato reveals variation associated with introgression and breeding events. *BMC Genomics* 14:791. doi: 10.1186/1471-2164-14-791
- Causse, M., Saliba-Colombani, V., Lesschaeve, I., and Buret, M. (2001). Genetic analysis of organoleptic quality in fresh market tomato. 2. Mapping QTLs for sensory attributes. *Theor. Appl. Genet.* 102, 273–283. doi: 10.1007/s001220051644

SUPPLEMENTARY MATERIAL

The Supplementary Material for this article can be found online at: <https://www.frontiersin.org/articles/10.3389/fpls.2018.00279/full#supplementary-material>

Supplemental Figure 1 | Distribution of mean values across MAGIC lines for each trait in Exp.1 (**A**) and Exp.2 (**B**); For each trait, minimum (dotted lines) and maximum (solid lines) parental values are plotted for control (green) and stress (red) treatment.

Supplemental Figure 2 | Average variation caused by water deficit (WD), salinity (SS) and control in Exp.2 (Ctrl2) relative to control in Exp.1. The effect of each treatment was measured in percentage of increase or decrease against control in Exp.1.

Supplemental Figure 3 | Haplotype prediction. Each of the 12 tomato chromosomes is represented with the percentage of allelic contribution of every parental line. NA represented all positions on the chromosomes where the parental allelic origin could not be assigned.

Supplemental Figure 4 | Mapchart representation of detected QTL on the genetic map for all chromosomes where a QTL was identified. The dashes on the chromosomes barchart represent the centimorgan distances between markers along the chromosomes. Each trait has a color code representation.

Supplemental Figure 5 | Allelic effect of parental lines for QTL that were mapped in a confidence interval smaller than 2Mb.

Supplemental Table 1 | QTL detected in the different conditions. For each trait, all the QTL found are identified by a specific name (QTL name column), the treatment where the QTL was found (Treatment), the chromosome (Chr) and the position (Pos) in cM. The peak region encompassing any QTL is defined by a pair of marker (LeftMrk and RightMrk), corresponding to the lower and upper bound expressed in genetic distances (Lower cM & Upper cM) as well as physical distances (Lower Mb & Upper Mb). The confidence interval in centimorgan (CI cM) and Mega-base (CI Mb) represent the corresponding differences between Upper and Lower. R2 is the percentage of phenotypic variation explained by a QTL. Ctrl 1 and Ctrl2 are the controls treatment for Exp.1 and Exp.2 respectively where the QTL were found. WD and SS are the stress treatment for water deficit and salinity. When interactives QTL are identified in Exp.1 (respectively Exp.2) treatment CxWD (respectively CxSS) are the corresponding treatment designed.

Supplemental Table 2 | Functional annotation of CG retained after the filtering procedure according to allelic parental effect. Only QTL that presented <40 CG were screened. For each QTL, the chromosome and localization (position in pb) were precised. The type of polymorphisms, depending if it is a single nucleotide polymorphism (snP) or insertion deletion (indel) were in the column "Type." The number of snP or indel at a given gene is marked in brackets () when more than one polymorphism affected a given gene. The impact of polymorphisms affecting a gene were defined as MODIFIER when snP or indel are located in upstream or downstream region; MODERATE and LOW when polymorphisms had respectively non-synonymous or synonymous variant effect and HIGH when they affect splice site variant or start/stop codon. The putative function of each CG was checked on the annotation database of the tomato genome assembly (SL2.50).

- Chaves, M. M., Maroco, J. P., and Pereira, J. S. (2003). Understanding plant responses to drought - from genes to the whole plant. *Funct. Plant Biol.* 30, 239–264. doi: 10.1071/FP02076
- Dai, A. (2011). Drought under global warming: a review. *Wiley Interdiscipl. Rev. Clim. Change* 2, 45–65. doi: 10.1002/wcc.81
- de Oliveira, A. B., Alencar, N. L. M., and Gomes-Filho, G. (2013). “Comparison between the water and salt stress effects on plant growth and development,” in *Responses of Organisms to Water Stress*, ed S. Akinci (InTech Publisher), 67–94. doi: 10.5772/54223
- Du, T., Kang, S., Zhang, J., Li, F., and Yan, B. (2008). Water use efficiency and fruit quality of table grape under alternate partial root-zone drip irrigation. *Agric. Water Manage.* 95, 659–668. doi: 10.1016/j.agwat.2008.01.017
- Eduardo, I., Pacheco, I., Chietera, G., Bassi, D., Pozzi, C., Vecchietti, A., et al. (2011). QTL analysis of fruit quality traits in two peach intraspecific populations and importance of maturity date pleiotropic effect. *Tree Genet. Genomes* 7, 323–335. doi: 10.1007/s11295-010-0334-6
- El-Soda, M., Malosetti, M., Zwaan, B. J., Koornneef, M., and Aarts, M. G. M. (2014). Genotype X environment interaction QTL mapping in plants: lessons from arabidopsis. *Trends Plant Sci.* 19, 390–398. doi: 10.1016/j.tplants.2014.01.001
- Farooq, M., Hussain, M., Wahid, A., and Siddique, K. H. M. (2012). “Drought stress in plants: an overview,” in *Plant Responses to Drought Stress*, Vol. 1 (Heidelberg; New York, NY; Dordrecht; London, UK: Springer), 1–33.
- Frary, A., Nesbitt, T. C., Grandillo, S., Knaap, E., Cong, B., Liu, J., et al. (2000). fw2.2: a quantitative trait locus key to the evolution of tomato fruit size. *Science* 289, 85–88. doi: 10.1126/science.289.5476.85
- Gardner, K. A., Wittern, L. M., and Mackay, I. J. (2016). A highly recombinant, high-density, eight-founder wheat MAGIC map reveals extensive segregation distortion and genomic locations of introgression segments. *Plant Biotechnol. J.* 14, 1406–1417. doi: 10.1111/pbi.12504
- Gutteling, E. W., Riksen, J. A., Bakker, J., and Kammenga, J. E. (2007). Mapping phenotypic plasticity and genotype-environment interactions affecting life-history traits in *caenorhabditis elegans*. *Heredity* 98, 28–37. doi: 10.1038/sj.hdy.6800894
- Huang, B. E., and George, A. W. (2011). R/mpMap: a computational platform for the genetic analysis of multiparent recombinant inbred lines. *Bioinformatics* 27, 727–729. doi: 10.1093/bioinformatics/btq719
- Huang, B. E., George, A. W., Forrest, K. L., Kilian, A., Hayden, M. J., Morell, M. K., et al. (2012). A multiparent advanced generation inter-cross population for genetic analysis in wheat. *Plant Biotechnol. J.* 10, 826–839. doi: 10.1111/j.1467-7652.2012.00702.x
- Huang, B. E., Verbyla, K. L., Verbyla, A. P., Raghavan, C., Singh, V. K., Gaur, P., et al. (2015). MAGIC populations in crops: current status and future prospects. *Theor. Appl. Genet.* 128, 999–1017. doi: 10.1007/s00122-015-2506-0
- Huang, Y., Tang, R., Cao, Q., and Bie, Z. (2009). Improving the fruit yield and quality of cucumber by grafting onto the salt tolerant rootstock under NaCl stress. *Sci. Hortic.* 122, 26–31. doi: 10.1016/j.scienta.2009.04.004
- Kenis, K., Keulemans, J., and Davey, M. W. (2008). Identification and stability of QTLs for fruit quality traits in apple. *Tree Genet. Genomes* 4, 647–661. doi: 10.1007/s11295-008-0140-6
- Kover, P. X., Valdar, W., Trakalo, J., Scarcelli, N., Ehrenreich, I. M., Purugganan, M. D., et al. (2009). A multiparent advanced generation inter-cross to fine-map quantitative traits in *Arabidopsis thaliana*. *PLoS Genet.* 5:e1000551. doi: 10.1371/journal.pgen.1000551
- Liu, J., Van Eck, J., Cong, B., and Tanksley, S. D. (2002). A new class of regulatory genes underlying the cause of pear-shaped tomato fruit. *Proc. Natl. Acad. Sci. U.S.A.* 99, 13302–13306. doi: 10.1073/pnas.162485999.c
- Maas, E. V., and Hoffman, G. J. (1977). Crop salt tolerance - current assessment. *J. Irrigat. Drain. Divis.* 103, 115–134.
- Marais, D. L. D., Hernandez, K. M., and Juenger, T. E. (2013). Genotype-by-environment interaction and plasticity: exploring genomic responses of plants to the abiotic environment. *Annu. Rev. Ecol. Evol. Syst.* 44, 5–29. doi: 10.1146/annurev-ecolsys-110512-135806
- Milner, S. G., Maccaferri, M., Huang, B. E., Mantovani, P., Massi, A., Frascarioli, E., et al. (2016). A multiparental cross population for mapping QTL for Agronomic Traits in durum wheat (*Triticum turgidum* ssp. *durum*). *Plant Biotechnol. J.* 14, 735–748. doi: 10.1111/pbi.12424
- Mitchell, J. P., Shennan, C., and Grattan, S. R. (1991). Developmental-changes in tomato fruit composition in response to water deficit and salinity. *Physiol. Plant.* 83, 177–185.
- Monforte, A. J., Oliver, M., Gonzalo, M. J., Alvarez, J. M., and Dolcet-Sanjuan, R. (2004). Identification of quantitative trait loci involved in fruit quality traits in melon (*Cucumis melo* L.). *Theor. Appl. Genet.* 108, 750–758. doi: 10.1007/s00122-003-1483-x
- Munns, R., and Tester, M. (2008). Mechanisms of salinity tolerance. *Annu. Rev. Plant Biol.* 59, 651–681. doi: 10.1146/annurev.arplant.59.032607.092911
- Muñoz, S., Ranc, N., Botton, E., Bérard, A., Rolland, S., Duffé, P., et al. (2011). Increase in tomato locule number is controlled by two single-nucleotide polymorphisms located near WUSCHEL. *Plant Physiol.* 156, 2244–2254. doi: 10.1104/pp.111.173997
- Navarro, J. M., Flores, P., Carvajal, M., and Martinez, V. (2005). Changes in quality and yield of tomato fruit with ammonium, bicarbonate and calcium fertilisation under saline conditions. *J. Hortic. Sci. Biotechnol.* 80, 351–357. doi: 10.1080/14620316.2005.11511943
- Pascual, L., Albert, E., Sauvage, C., Duangjit, J., Bouchet, J.-P., Bitton, F., et al. (2016). Plant science dissecting quantitative trait variation in the resequencing era : complementarity of bi-parental, multi-parental and association panels. *Plant Sci.* 242, 120–130. doi: 10.1016/j.plantsci.2015.06.017
- Pascual, L., Desplat, N., Huang, B. E., Desgroux, A., Bruguier, L., Bouchet, J. P., et al. (2015). Potential of a tomato MAGIC population to decipher the genetic control of quantitative traits and detect causal variants in the resequencing era. *Plant Biotechnol. J.* 13, 565–577. doi: 10.1111/pbi.12282
- Ripoll, J., Urban, L., and Bertin, N. (2016). The potential of the MAGIC TOM parental accessions to explore the genetic variability in tomato acclimation to repeated cycles of water deficit and recovery. *Front. Plant Sci.* 6:1172. doi: 10.3389/fpls.2015.01172
- Ripoll, J., Urban, L., Staudt, M., Lopez-Lauri, F., Bidel, L. P., and Bertin, N. (2014). Water shortage and quality of fleshy fruits—making the most of the unavoidable. *J. Exp. Bot.* 65, 4097–4117. doi: 10.1093/jxb/eru197
- Scholberg, J. M. S., and Locascio, S. J. (1999). Growth response of snap bean and tomato as affected by salinity and irrigation method. *HortScience* 34, 259–264.
- Shewfelt, R. L. (1999). What is quality? *Postharvest Biol. Technol.* 15, 197–200.
- Shrivastava, P., and Kumar, R. (2015). Soil salinity: a serious environmental issue and plant growth promoting bacteria as one of the tools for its alleviation. *Saudi J. Biol. Sci.* 22, 123–131. doi: 10.1016/j.sjbs.2014.12.001
- Tétard-Jones, C., Kertesz, M. A., and Preziosi, R. F. (2011). Quantitative trait loci mapping of phenotypic plasticity and genotype-environment interactions in plant and insect performance. *Philos. Trans. R. Soc. Lond. B Biol. Sci.* 366, 1368–1379. doi: 10.1098/rstb.2010.0356
- Threadgill, D. W., Hunter, K. W., and Williams, R. W. (2002). Genetic dissection of complex and quantitative traits: from fantasy to reality via a community effort. *Mamm. Genome* 13, 175–178. doi: 10.1007/s00335-001-4001-y
- Tomato Genome Consortium (2012). The tomato genome sequence provides insights into fleshy fruit evolution. *Nature* 485, 635–641. doi: 10.1038/nature11119
- Ungerer, M. C., Halldorsdottir, S. S., Purugganan, M. D., and Mackay, T. F. C. (2003). Genotype-environment interactions at quantitative trait loci affecting inflorescence development in *Arabidopsis thaliana*. *Genetics* 165, 353–365.
- Verbyla, A. P., Cavanagh, C. R., and Verbyla, K. L. (2014). Whole-genome analysis of multienvironment or multtrait QTL in MAGIC. *G3* 4, 1569–1584. doi: 10.1534/g3.114.012971
- Via, S., Gomulkiewicz, R., De Jong, G., Scheiner, S. M., Schlichting, C. D., and Van Tienderen, P. H. (1995). Adaptive phenotypic plasticity: consensus and controversy. *Trends Ecol. Evol.* 10, 212–217.

- Villalta, I., Bernet, G. P., Carbonell, E. A., and Asins, M. J. (2007). Comparative QTL analysis of salinity tolerance in terms of fruit yield using two solanum populations of F7 lines. *Theor. Appl. Genet.* 114, 1001–1017. doi: 10.1007/s00122-006-0494-9
- Yu, J., Holland, J. B., McMullen, M. D., and Buckler, E. S. (2008). Genetic design and statistical power of nested association mapping in maize. *Genetics* 178, 539–551. doi: 10.1534/genetics.107.074245
- Zhu, J. K. (2002). Salt and drought stress signal transduction in plants. *Annu. Rev. Plant Biol.* 53, 247–273. doi: 10.1146/annurev.arplant.53.091401.143329

Conflict of Interest Statement: The authors declare that the research was conducted in the absence of any commercial or financial relationships that could be construed as a potential conflict of interest.

Copyright © 2018 Diouf, Derivot, Bitton, Pascual and Causse. This is an open-access article distributed under the terms of the Creative Commons Attribution License (CC BY). The use, distribution or reproduction in other forums is permitted, provided the original author(s) and the copyright owner are credited and that the original publication in this journal is cited, in accordance with accepted academic practice. No use, distribution or reproduction is permitted which does not comply with these terms.



Transcriptome and Metabolome Analyses Provide Insights into the Occurrence of Peel Roughing Disorder on Satsuma Mandarin (*Citrus unshiu* Marc.) Fruit

Xiao-Peng Lu^{1,2}, Fei-Fei Li^{1,2,3}, Jiang Xiong^{1,2}, Xiong-Jun Cao^{1,2}, Xiao-Chuan Ma^{1,2}, Zi-Mu Zhang^{1,2}, Shang-Yin Cao⁴ and Shen-Xi Xie^{1,2*}

¹ Horticulture Department, College of Horticulture and Landscape, Hunan Agricultural University, Changsha, China, ² National Centre for Citrus Improvement, Changsha, China, ³ Institute of Horticulture, Hunan Academy of Agricultural Science, Changsha, China, ⁴ Zhengzhou Fruit Research Institute, Chinese Academy of Agricultural Sciences, Zhengzhou, China

OPEN ACCESS

Edited by:

Nadia Bertin,
Plantes et Système de cultures
Horticoles (INRA), France

Reviewed by:

Olivier Pailly,
INRA Centre Corse, France

Stefano La Malfa,

Università degli Studi di Catania, Italy

*Correspondence:

Shen-Xi Xie
shenxie@163.com

Specialty section:

This article was submitted to
Plant Breeding,
a section of the journal
Frontiers in Plant Science

Received: 28 June 2017

Accepted: 23 October 2017

Published: 07 November 2017

Citation:

Lu X-P, Li F-F, Xiong J, Cao X-J, Ma X-C, Zhang Z-M, Cao S-Y and Xie S-X (2017) Transcriptome and Metabolome Analyses Provide Insights into the Occurrence of Peel Roughing Disorder on Satsuma Mandarin (*Citrus unshiu* Marc.) Fruit. *Front. Plant Sci.* 8:1907.
doi: 10.3389/fpls.2017.01907

Roughing disorder (RD) is a significant quality barrier in citrus fruit, prevalent on easy-peeling mandarins. As RD is not yet well-understood, this study aimed to examine the changes and synergic molecular processes involved in peel RD. Peel with RD was induced by severely defruiting Satsuma mandarin trees. Morphology observations, RNA-sequencing, and targeted and untargeted metabolic analyses were conducted. The results showed that the primary metabolites of sugars, organic acids and amino acids are dramatically changed in RD peel. The RD peel was always characterized by higher magnesium content during development. Comparative transcriptome profiling was performed for CK and RD peels at 30, 80, and 170 days after full bloom (DAFB) which represented fruit at cell division stage, cell enlargement stage and fruit maturity stage, respectively. Physiological and molecular biological evidence suggested that the month after full bloom is a crucial stage for RD initiation. A total of 4,855 differentially expressed genes (DEGs) in RD peel, relative to CK peel were detected at cell division stage, about 2 to 4-fold more than other stages had. Among the differentially expressed transcription factors, the bHLH family were affected most by RD, and six bHLH transcription factors functionally involved in GA metabolism were assessed to associate with RD occurrence. Gene set enrichment analysis suggested that RD significantly altered starch and GA metabolism in peel. Higher starch content and hydrolysed chain status were found in RD peel at cell division stage. RD occurrence on the peel was influenced significantly by GA, especially abundant GA before July. These changes may mean a significant alteration in sink strength of RD peel. The findings of this study provide insights into the emergence, development and molecular mechanisms of RD.

Keywords: satsuma mandarin, roughing disorder, GA, starch, mineral nutrients, RNA-sequencing, metabolome

INTRODUCTION

The Satsuma mandarin (*Citrus unshiu* Marc.) is an important easy-peeling mandarin around the world, and Asian countries including China, Japan and Korea are the largest producers. In China, the Satsuma mandarin is one of two important easy-peeling mandarins, and makes up more than thirty per cent of total citrus production each year. Although the Satsuma mandarin is popular among world consumers, farmers in traditional growing areas are facing serious pressures, such as low prices due to large yields, fruit quality decline, and faster cultivar renewal. Of these, fruit quality problems are the most significant and receive more attention from producers and consumers. Roughing disorder (RD), also termed rough fruit, rough peel disorder (Erner et al., 1975, 1976; Liu, 2012), peel roughness (Liu et al., 1988), and rind roughness (Kubo and Hiratsuka, 1998, 1999) is a common and typical quality barrier in Satsuma mandarin fruit. RD is characterized by excessively thick, rough peel and large fruit size (Erner et al., 1976). It significantly impairs the commodity value of Satsuma mandarin fruit, but the molecular mechanisms involved are still not clear.

RD of Satsuma mandarin fruit occurs through a complicated process, and is influenced by hormones, soil, air humidity, and rootstock (Erner et al., 1976). Two major factors often lead to RD in Satsuma mandarin plants. The first factor is low fruit load. Citrus trees in the primary fruiting stage usually produce few fruit, most of which are characterized by RD. In addition, a heavy fruit load (ON-Crop) in 1 year inhibits the return bloom in the following year (Monselise and Goldschmidt, 1982; Shalom et al., 2014). The second year is characterized by a low yield (OFF-Crop) in which fruit with RD are predominant. The second factor that induces RD is the bearing angle. On a Satsuma mandarin tree, upward fruit frequently develop RD, but sideward fruit are smoother. A marked difference between them can be observed from mid-July (Kubo and Hiratsuka, 1998). The growth condition of the bearing basal shoot is also associated with RD. Generally, the bearing basal shoot is a spring and leafy shoot, usually shorter than 6 cm and thicker than 0.4–0.6 cm (Liu, 2012). Unlike fruit puffiness, which appears near or during the maturity stage, RD could be commonly observed during Satsuma mandarin fruit development. Satsuma mandarin fruit on low-crop-load trees exhibit RD symptoms in mid-June, showing higher fruit weight, bigger epidermal size, and hypodermal and parenchymal cells in the peel (Kubo and Hiratsuka, 1999). Because there is an increase in cell layer and cell diameter 7–28 days after full bloom (DAFB), this period has been identified as key in RD development (Liu, 2012).

A histological comparison of normal and RD fruit suggested that vigorous oil gland and hypodermal tissues contribute to RD in Satsuma mandarin fruit (Kubo and Hiratsuka, 1999). Another histological comparison of two peel types showed that peel thickness increment in RD fruit depended on the number of cell layers but not cell size (Liu, 2012). Hormones are believed to be another important factor behind RD in Satsuma mandarin. It is believed that exogenous GA₃ application at an early fruit development stage induces RD (Liu et al., 1987). Upward fruit on “Okitsu wase” mandarin (*C. unshiu* Marc.) trees tending to

have RD had higher GA content than sideward fruit with smooth peel. Exogenous applications of different hormones suggested that GA₃ and BA treatments in late June significantly induced RD whereas others did not (Kubo and Hiratsuka, 1998, 2000). “Owari” mandarin (*C. unshiu* Marc.) fruit enlarged significantly with 2,4-DP, but fruit peel thickness did not (Agusti et al., 1994).

RD probably occurs in situations where source/sink ratio is excessive, but the mechanism of initial RD occurrence in Satsuma mandarin is still unclear. RD involves changes to fruit size, peel, segment membrane, juice sac, juice and so on, among which peel RD is the most obvious and typical phenotype. Although morphological changes have been documented, metabolic profiling of RD peel has not been investigated. The untargeted metabolome is appropriate to this study because metabolic fluxes might be directly related to peel RD. Thus, in this study we first aimed to reveal the overall mechanism of peel RD occurrence through comprehensive exterior and interior phenotypic characterization, along with genome-wide gene expression throughout RD peel development. Finally, metabolites, mineral nutrients, synergic pathways and genes correlated with the development of peel RD were identified. The results presented help clarify previously fragmentary knowledge, and provide further insight into the genetic and physiological basis of peel roughing, an important *Citrus* disorder.

MATERIALS AND METHODS

Plant Materials and Sampling

Eight-year-old “Yamashitabeni wase” Satsuma mandarin (*C. unshiu* Marc.) grafted on trifoliolate orange [*Poncirus trifoliata* (L.) Raf.] rootstocks were used in this study. Fifteen healthy and approximately uniform trees were selected for the experiment and fruit with RD were induced via severe fruit removal. At fruit set stage in spring, 10 trees were defruited, with 15 upward fruits left on each tree, while the other five trees without fruit removal served as the control (CK). For CK and treatment, fruit was randomly harvested at 20, 30, 40, 50, 60, 80, 110, 140, and 170 DAFB. For each CK sampling, 30 fruits from three CK trees with 10 for each tree were sampled. For treatment sampling, 21 fruits from three treated trees with seven fruits for each tree were sampled at 20, 30, and 40 DAFB, 15 fruits from three treated trees with five fruits for each tree at 50, 60, and 80 DAFB and nine fruits from at least three treated trees at 110, 140, and 170 DAFB were collected. At each sampling date, fruit growth was estimated by measuring transverse diameter of 30 fruits growing on the trees for CK and 30 fruits growing on the trees or all the remaining fruits if there were <30 for treatment. Peel thickness was measured on all fruits individually. For each of the triplicate fruit groups mentioned above, the peel was isolated, immediately frozen in liquid nitrogen, and stored at -80°C for further analyses; the fruit pulp was stored at -40°C for targeted metabolites analyses.

Morphological Observation for the Peel Using SEM

CK and RD peels isolated from fruit at 30, 80, and 170 DAFB, representing fruit at cell division stage, cell enlargement stage

and fruit maturity stage, respectively were used for SEM. At each of three sampling dates, six 5×5 mm peel squares from three fruits were collected from CK peel and RD peel, respectively. The samples were dehydrated using a graded ethanol series (50, 70, and 100%), critical-point dried, mounted on copper stubs and gold sputtered. The samples were examined under a JSM-6380LV scanning electron microscope (SEM, Jeol, Tokyo, Japan). Both peel surface and cross section were observed by SEM and representative images were selected.

Untargeted and Targeted Metabolites Analyses

To analyse untargeted metabolites in RD peel, another five “Yamashitabeni wase” Satsuma mandarin trees, each of which typically had both smooth (CK) fruits and RD fruits were chosen. In each of five trees, three downward CK fruits and three upward RD fruits were collected and had peel isolated at 170 DAFB. Peel samples from three fruits on one tree were mixed as a replicate with a total of five replicates for both CK and RD. The untargeted metabolic profiling was performed according to published methods with minor modification (Osorio et al., 2012). An Agilent 5975C MSD mass spectrometer (MS, Agilent Technologies, Palo Alto, CA, USA) coupled to an Agilent 7890A gas chromatograph (GC) system was used. Ten micrograms of ground and freeze-dried samples were used for metabolite extraction with 1 mL pre-chilled solvent mixture (Acetonitrile: Isopropanol: Water, 3: 3: 2), and underwent ultrasonication for 32s in ice-water mixture. Samples were then centrifuged for 10 min at 13,000 rpm and 4°C and supernatant was collected. Eight hundred microliter aliquots of supernatant plus 8 μL of 3 mg/mL Myristic acid- d_{27} were concentrated to complete dryness with nitrogen blowing. The residue was dissolved in 20 μL of 40 mg/mL methoxyamine hydrochloride/pyridine, and incubated for 90 min at 30°C. Samples were then treated with 90 μL N-methyl-N-(trimethylsilyl) trifluoroacetamide (1% trimethylchlorosilane) for 30 min at 37°C. After a second centrifugation at 12,000 rpm for 2 min, the supernatant was analyzed. Relative concentrations of the metabolites were determined by peak area (mm^2) and the mass spectra were then compared to known and commercially available mass spectral libraries.

For targeted amino acid determination in CK and RD peels, triplicate samples out of five used in GC-MS were chosen for analysis. Peels were dried at 75°C for 3 days and ground immediately in a disintegrator (FW100, TAISITE, Tianjin, China). One gram powder samples were analyzed using the published method with a HITACHIL-8900 amino acid analyser (Hitachi, Wako, Japan) (Lu et al., 2016). To measure the targeted starch, organic acids and sugars, the isolated and frozen CK and RD peels at 40, 80, 110, 140, and 170 DAFB were used. The starch content was determined according to the published method with slight modification (Xu et al., 1998). One hundred milligram peel samples were ground in 80% alcohol and centrifuged at 4,000 rpm for 2 min. The suspension was collected and the residue was extracted another three times with 80% (m/v) $\text{Ca}(\text{NO}_3)_2$ at 100°C (5 mL each, 10 min per extraction). The extract was added to a

final volume of 20 mL with 80% $\text{Ca}(\text{NO}_3)_2$. One milliliter extract solution was diluted using 1 mL 80% $\text{Ca}(\text{NO}_3)_2$, colored with 100 μL 0.1 M $\text{I}_2\text{-KI}$ and then absorption determined at 620 nm using a spectrophotometer (UV-1800, Shimadzu, Kyoto, Japan). The absolute amount of starch was determined by comparison with calibration standard curve and calculated based on peel fresh weight. Organic acid and sugar components were measured using high-performance liquid chromatography (HPLC) (LC-20A, Shimadzu, Kyoto, Japan) according to the published method (Lu et al., 2016). Organic acid and sugar were also determined in pulp using samples stored at -40°C. Triplicate tissue samples were analyzed for the above assays.

Mineral Nutrient Analyses

For difference-screening analyses of macro- and micro-minerals between CK and RD peels, the same samples from targeted amino acid analyses were used. For targeted mineral nutrient, peel samples collected at 30, 80, and 110 DAFB, as described in the Plant Materials and Sampling section, were chosen to test the reliable content-difference between CK and RD peels. The peel samples were dried at 75°C for 3 days and ground immediately in a disintegrator (FW100, TAISITE, Tianjin, China). In assay, N and P were extracted and measured according to published methods (Bao, 2000). Peel K, Ca, Mg, Mn, Cu, and Zn were extracted with 1 M HCl and assayed using atomic absorption spectrophotometry. B was measured using the curcumin method after ashing the sample at 500°C for 5 h and dissolving in 0.1 M HCl (Li et al., 2015).

Transcriptome Sequencing and Analyses

According to citrus fruit size and peel thickness development, 30, 80, and 170 DAFB were chosen to represent the fruit cell division stage, cell enlargement stage and fruit maturity stages respectively. Six libraries were constructed for transcriptome sequencing and named peel for control at 30 DAFB (CK30), peel for control at 80 DAFB (CK80), peel for control at 170 DAFB (CK170), peel with RD at 30 DAFB (RD30), peel with RD at 80 DAFB (RD80), and peel with RD at 170 DAFB (RD170). For each library construction, peels subsampled from triplicate peel samples described in Plant Materials and Sampling were mixed to produce a pool. One gram of peel was used for total RNA isolation using TRIzol reagent (TaKaRa, Dalian, China) according to the manufacturer's instructions, and the mRNA was enriched using magnetic oligo (dT) beads. Preparation of the paired-end libraries and sequencing was performed following standard Illumina methods and protocols. The cDNA libraries were sequenced on an Illumina Hiseq2000 platform and 100 bp single-end reads were generated.

Clean reads were obtained by removing reads containing adapter, ploy-N and low quality sequence from raw data, and were aligned to the *Citrus sinensis* genome (Xu et al., 2013) using Bowtie (Langmead et al., 2009) and BWA (Mortazavi et al., 2008). To estimate gene expression levels, fragments per kilobase per million mapped reads (FPKM) of each gene were calculated (Li and Dewey, 2011). Differentially expressed genes (DEGs) in pairwise comparisons were then identified (Audic and Claverie, 1997). All the statistical results for multiple testing were corrected

with the Benjamini-Hochberg false discovery rate ($FDR < 0.001$) (Benjamini and Yekutieli, 2001). Sequence expressions were deemed to be significantly different if $FDR < 0.001$ and there was at least a 2-fold change (>1 or <-1 in \log^2 ratio value) in FPKM between two libraries. Gene Ontology (GO) annotation was performed using Blast2 GO software (Conesa et al., 2005). Finally, DEGs were enriched in GO and Kyoto Encyclopedia of Genes and Genomes (KEGG) databases so as to identify the changes in biological functions and metabolism pathways. In addition, all DEGs were aligned in a plant transcription factor database (Pérezrodríguez et al., 2009) using HMMER (Finn et al., 2015) to screen the transcription factors.

Quantitative Real-Time PCR Analyses

Total RNA was isolated from the frozen peel following the method described above. Roughly $1.0 \mu\text{g}$ total RNA was used for first-strand cDNA synthesis using the iSCRIPT cDNA synthesis kit (Bio-Rad) following the manufacturer's instructions. Specific primers were designed from the selected gene sequences using Primer Express Version 3.0 (Applied Biosystems, CA, USA) and the primer sequences are given in Table S1. Quantitative RT-PCR was performed according to previous reports (Yan et al., 2012; Lu et al., 2016). Samples for qRT-PCR were run in three biological replicates with three technical replicates.

Hormone Treatment Experiment

In the same plot described in plant material, six healthy and approximately uniform "Yamashitabeni wase" trees were chosen for the hormone treatment experiment. Three trees grown normally served as the control (CK). For IAA, CTK, GA₃ and mixture (IAA+CTK+GA₃) treatments, 20 representative fruits on each of another three trees were treated with the corresponding solutions. Aqueous solutions for IAA, CTK, GA₃, and mixture treatments contained 50 mg L^{-1} IAA, 3 mg L^{-1} CTK, 50 mg L^{-1} GA₃, and the mixture with their own concentration respectively. Triton X-100 (0.05%) was added to

each solution as a surfactant. At 40 DAFB, 20 representative fruit on each tree were soaked in treatment solution for 1 min. This was repeated again at 50 DAFB. At 85 and 115 DAFB in CK and treatments, 10 fruit from each treated tree for a total of 30 fruit per phenotype were collected. The collection of fruit size and peel thickness data, isolation of peel and pulp, determination of organic acid and sugar were all identical to the methods described above.

Statistical Analyses

Five individual biological replicates were used for GC-MS analyses and data were statistically analyzed using Student's *t*-test ($P < 0.05$). Three biological replicates were used in the organic acid, sugar, amino acid, and mineral nutrient determination and data were analyzed statistically using Duncan's multiple range test in an ANOVA program of SAS (Cary, NC, USA) at $P < 0.05$. Due to 30 fruits for CK in each sampling but 9 to 21 fruits for RD depending on sampling, Duncan's multiple range test for unequal replication in an ANOVA program at $P < 0.05$ was employed for the statistical analyses of data in fruit size and peel thickness.

RESULTS

Characteristics of Satsuma Mandarin Fruit with RD

Relative to CK fruit, RD fruit have significantly different interior and exterior characteristics. Rough fruit surfaces, bigger fruit sizes and delayed fruit degreening are noticeable in RD fruit. Furthermore, thicker peels, enlarged fruit segments, and bigger juice sacs all contribute to the increased size of RD fruit. In RD fruit, the segment membrane and the tail of juice sacs are whiter and more indistinct, suggesting severe lignification (Figure 1A). RD fruit showed significant differences in development patterns compared to CK fruit. Although both types of fruit shared similar characteristics at 20 DAFB, RD fruit were larger than CK fruit at 30DAFB and had a rough surface. At 170 DAFB, RD fruit

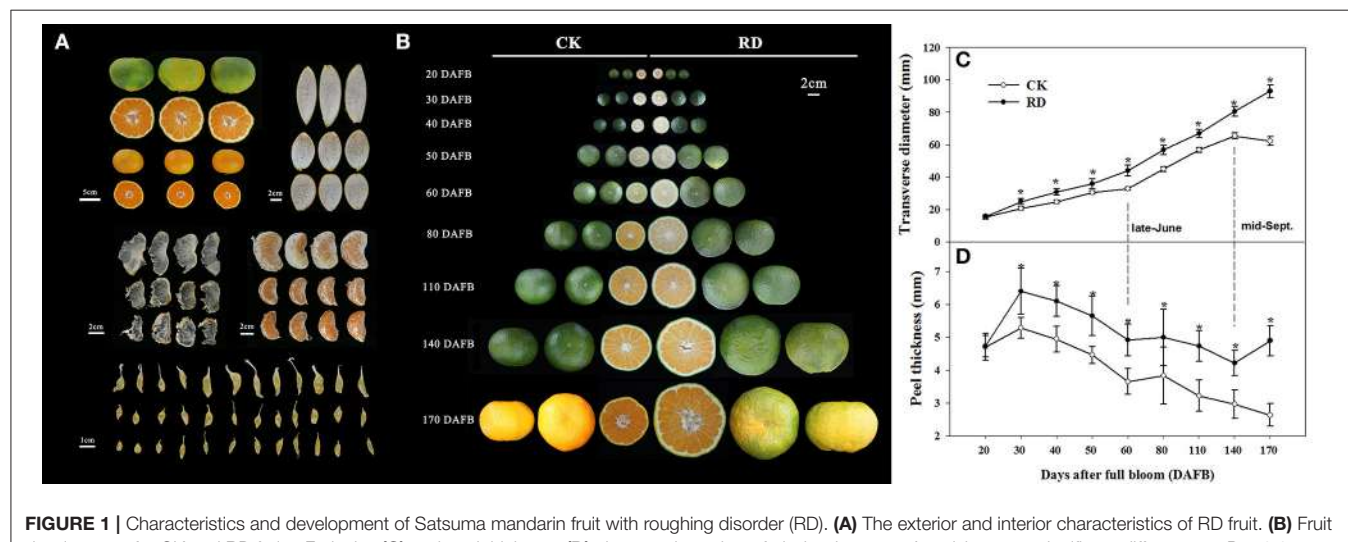


FIGURE 1 | Characteristics and development of Satsuma mandarin fruit with roughing disorder (RD). **(A)** The exterior and interior characteristics of RD fruit. **(B)** Fruit development for CK and RD fruits. **(C)** Fruit size and **(D)** peel thickness changes throughout fruit development. Asterisk means significant difference at $P < 0.05$.

was developing color whereas CK fruit had colored completely (**Figure 1B**). Satsuma mandarin fruit develop through cell division, cell enlargement, and maturity stages, during which fruit size changes in distinct patterns (Bain, 1958; Kubo and Hiratsuka, 1998). In this study, CK fruit clearly followed that process: cell division occurred from flowering to 60 DAFB (late-June), cell enlargement from 60 to 140 DAFB (mid-September), and fruit maturation from 140 to 170 DAFB (mid-October). In contrast, RD fruit size constantly increased throughout fruit development, differing from the classical development pattern. RD fruit always had thicker peel than CK fruit, but both followed the three-stage growth pattern (**Figure 1C**). Peel thickness of CK and RD fruit rapidly peaked at 30 DAFB and then decreased until 60 DAFB. A plateau phase in peel thickness growth occurred from 60 to 80 DAFB. After that, peel thickness continued to decrease in CK fruit, but RD peel thickness was stable from 140 to 170 DAFB (**Figure 1D**).

Ultrastructure Alterations of RD Peel during Development

Due to the significant changes in RD peel, scanning electron microscopy was used to study the ultrastructure alterations. Both peels were examined at 30, 80, and 170 DAFB (representing fruit at cell division, cell enlargement and maturity stage) to provide insights into the development of RD peel. At 30 DAFB, flavedo and albedo (which compose citrus peel) could not be clearly distinguished. At this stage the peels mainly comprised parenchymatic cells and few oil cells. Compared to CK, RD, peel had much greater thickness, more cells and lower oil cell density (**Figures 2A,D**). Furthermore, at this stage RD peel had bigger cell sizes, more clearly shaped parenchymatic cells, bigger intercellular spaces and thinner cell arrangement than CK peel (**Figure 2B,C,E,F**). Greater polysaccharide effluence was observed in CK peel than in RD peel (**Figures 2C,F**). At 80 DAFB, the flavedo and albedo of RD peel were thicker than those of CK peel and vascular bundles were observed. CK peel clearly had regular oil cells while flavedo was irregular in RD peel (**Figures 2G,J**). CK flavedo had spherical oil cells with smooth inner walls, but the oil cells in RD flavedo took non-identical sizes and had rough inner walls. In addition, normal parenchymatic cells layered regularly in CK flavedo, but the cell wall of these cells were significantly thickened in RD flavedo (**Figures 2H,K**). Lower cell density and larger intercellular space increased in RD albedo at 80 DAFB, consistent with the increase in RD peel (**Figures 2I,L**). CK and RD fruit exhibited relatively thin peel at 170 DAFB, although RD peel was still thicker than CK. CK flavedo remained spherical and featured small oil cells still characterized by smooth inner walls, but in the bigger oil cells in RD flavedo, a laminated structure on the rough inner-wall was found. Moreover, flavedo in RD peel had more epidermal cell layers and bigger cell size relative to CK (**Figures 2N,Q**). Vascular bundles in albedo were clearer in both peels at 170 DAFB, but the amount appeared greater in RD albedo (**Figures 2M,P**). At fruit maturation, flocculent structures filled albedo instead of regular cells. However, flocculent structures were much more loosely arranged and had thicker cell walls in RD albedo than in CK albedo (**Figures 2O,R**).

Changes of Metabolites and Mineral Nutrients in RD Peel

Using GC-MS, an untargeted metabolomic analyses was conducted to identify the metabolites associated with peel RD. Because the typical and complete RD occurs at fruit maturity stage, the peels at 170DAFB were chosen for comparison. As the relative concentrations of the metabolites were estimated by peak area, 855 metabolites were identified in both CK and RD peels. According to >1.2 or <0.8 in RD/CK ratio and statistical analyses, 30 metabolites were significantly different across CK and RD peels. These metabolites were classified as sugars, organic acids, amino acids and derivatives, alcohols, heterocyclic compounds, amines, and two other compounds (**Table 1**). Of these classifications, the main differences were found in sugars, organic acids, amino acids, and derivatives. Notably, most amino acids and derivatives were significantly higher in RD peel than in CK peel, and citrulline, beta-homoserine, and glutamine were 4.80-, 5.51-, and 8.43-folds higher in RD peel, respectively. In further targeted amino acid analyses, 13 of 17 amino acids were significantly higher in RD peel (**Table 2**). Three amino acids were lower in RD peel and Arg was not different across the two peel types. Asp, Glu, and Pro had the highest levels but Cys, Met, and Tyr had the lowest levels in mandarin peel. Some mineral nutrients also had significant changes in RD peel. Analyses revealed that higher N, Mg and Cu levels occurred in mature peel, while other mineral nutrients showed no differences (**Table 3**). To further characterize the mineral nutrient changes in RD peel, four candidate mineral nutrients were determined during fruit development. Analyses over the developmental course suggested that Mg content was constantly higher in RD peel relative to CK (**Figure 3**).

Changes in Global Gene Expression Responding to Peel RD

During fruit development, CK peel at 30 DAFB, RD peel at 30 DAFB, CK peel at 80 DAFB, RD peel at 80 DAFB, CK peel at 170 DAFB, and RD peel at 170 DAFB were chosen to construct sequencing libraries, named CK30, RD30, CK80, RD80, CK170, and RD170, respectively. After filtering, more than 65.5 million clean sequence reads for each library were generated, for a total of 39.83 GB of sequence data (Table S2). Of the total clean reads from the samples, 70.5–72.2% were unique matches with the sweet orange (*Citrus sinensis*) genome (<http://citrus.hzau.edu.cn/orange/>) while multi-position match reads were 4.0–5.1%. Finally, 20,339 expressed genes in CK30, 20,997 expressed genes in RD30, 20,659 expressed genes in CK80, 20,711 expressed genes in RD80, 20,554 expressed genes in CK170 and 20,501 expressed genes in RD170 were detected based on the reference genome. Gene-expression levels were determined using the fragments per kilobase of transcript per million mapped reads (FPKM) method. A total of 4,855, 1,164, and 2,526 DEGs were detected at 30, 80, and 170 DAFB, respectively (Table S3). Of these, two peels at 30 DAFB exhibited the most DEGs with 3,863 (79.6%) upregulated and 992 (20.4%) down-regulated. The differentially expressed transcription factors between CK and RD peels were also analyzed. A total of 43 differentially expressed transcription factor families were found during RD development. Of these,

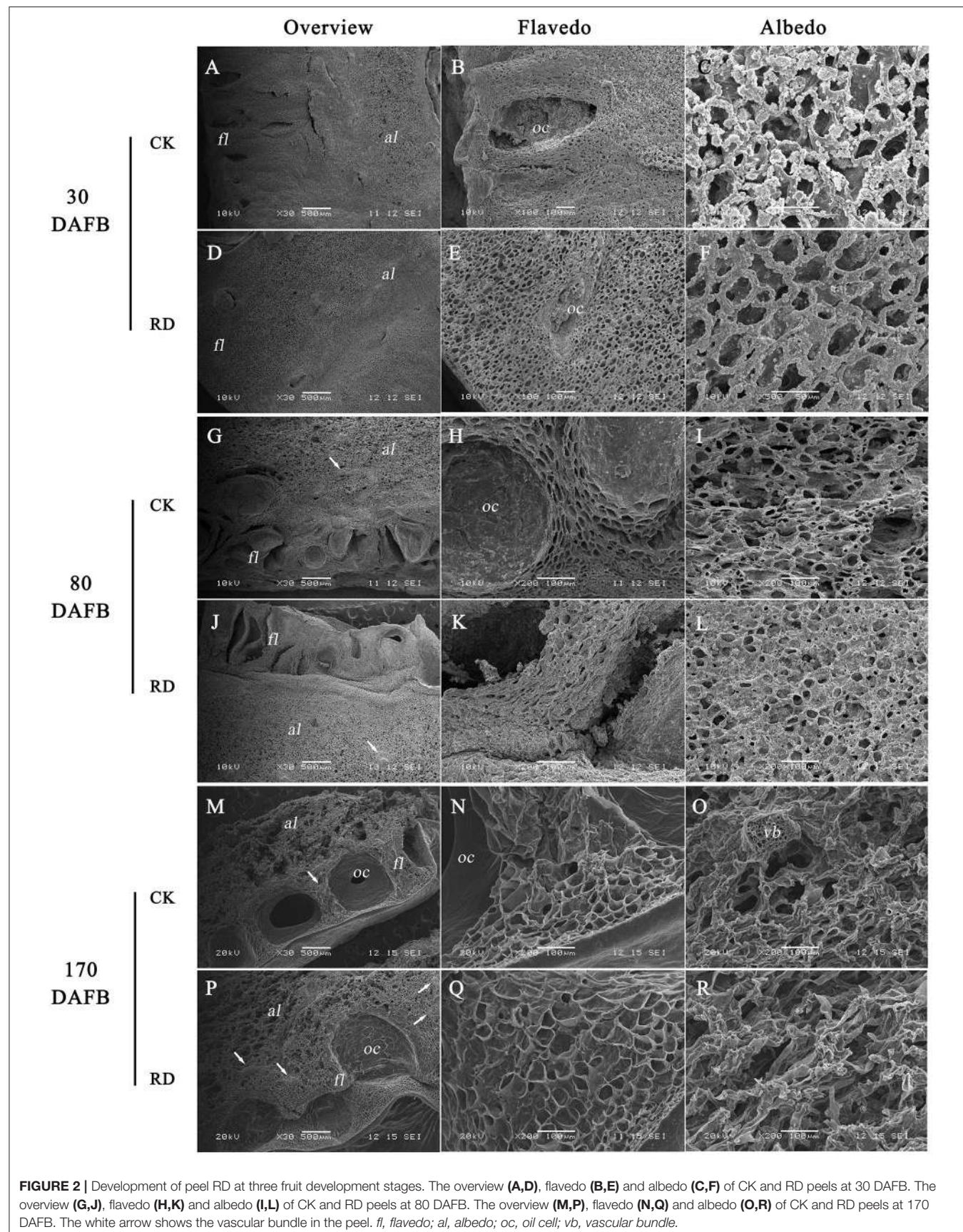


TABLE 1 | Classification of metabolites with significant difference between CK and RD peels.

Classification	Putative Name	Fold change (PD/CK ratio)	t-test
Sugars	1-Kestose	0.54	0.036
	1,6-anhydro-beta-Glucose	0.57	0.022
	Raffinose	0.65	0.043
	Galactose	1.54	0.015
	Psicose	2.02	0.036
	Sorbose	2.19	0.003
	Galactonic acid	0.77	0.049
Organic acids	Glyoxylic acid	0.57	0.020
	Benzoic acid	0.58	0.045
	Shikimic acid	0.60	0.002
	methyl-Malonic acid	0.64	0.004
	1-Pyrroline-3-hydroxy-5-carboxylic-acid	1.62	0.001
	2-oxo-Gulonic acid	2.59	0.013
	Lactic acid	4.06	<0.0001
	Glyceric acid	4.54	0.004
Amino acids and derivatives	Phenylalanine	0.52	0.036
	3-cyano-Alanine	1.71	0.021
	Threonine	1.83	0.019
	Glycine	2.16	<0.0001
	Norvaline	2.60	0.000
	Citrulline	4.80	0.000
	beta-Homoserine	5.51	<0.0001
	Glutamine	8.43	0.01
	Indole-3-lactic acid	3.21	0.004
Alcohols	Viburnitol	0.69	0.005
Heterocyclic compound	Similar to Lumichrome	5.91	<0.0001
Amines	Butyro-1,4-lactam	1.31	0.027
	Propylamine-2,3-diol	1.56	0.019
Others	2-hydroxy-Pyridine	0.62	0.042
	Epinephrine	1.72	0.031

The relative concentrations of metabolites are based on peak areas, and five individually biological replicates were conducted for a t-test. The RD/CK ratio was calculated on the mean values.

42 families were expressed differently at 30 DAFB, with 241 up-regulated and 55 down-regulated transcription factors. MYB and bHLH families predominated, with 40 and 32 transcription factors differentially expressed, respectively (Table S4).

Hierarchical cluster analyses was performed using the log-[FPKM (RD/CK)] values of samples at three stages. Results showed that during the three stages, the DEGs in peel were divided into more than five groups (Figure 4A). Of these groups, four were predominant: in group I, genes downregulated at all three development stages; in group II, genes upregulated at all

TABLE 2 | Amino acids in CK and RD peels. Values are mean \pm SD of three biological replicates.

	CK (mg/100g DW)	PD (mg/100g DW)
Asp	0.69 \pm 0.02	0.78 \pm 0.02**
Thr	0.15 \pm 0.005	0.18 \pm 0.003**
Ser	0.19 \pm 0.02	0.22 \pm 0.02**
Glu	0.48 \pm 0.02	0.56 \pm 0.01**
Pro	0.52 \pm 0.02	0.49 \pm 0.01*
Gly	0.20 \pm 0.006	0.23 \pm 0.004**
Ala	0.27 \pm 0.02	0.30 \pm 0.005**
Cys	0.07 \pm 0.02	0.04 \pm 0.003**
Val	0.19 \pm 0.009	0.20 \pm 0.004**
Met	0.03 \pm 0.008	0.02 \pm 0.004*
Ile	0.13 \pm 0.004	0.14 \pm 0.0103**
Leu	0.25 \pm 0.005	0.28 \pm 0.005**
Tyr	0.02 \pm 0.03	0.07 \pm 0.005**
Phe	0.18 \pm 0.01	0.23 \pm 0.005**
Lys	0.21 \pm 0.02	0.27 \pm 0.02**
His	0.09 \pm 0.003	0.12 \pm 0.004**
Arg	0.20 \pm 0.003	0.21 \pm 0.10N

Asterisk and double asterisk mean significant difference at $P < 0.05$ and $P < 0.01$, respectively. N means no significant difference.

three development stages; in group III, genes upregulated at cell division stage and downregulated at cell enlargement and maturity stage and in group IV, genes upregulated at cell division and enlargement stages and then downregulated at maturity stage. This supported the notion that different genes worked during fruit puffing development. To analyse the metabolic and regulatory pathways involved in peel RD, a comparison of DEGs at three development stages was made. In RD peel, 3,863 genes at 30 DAFB, 544 genes at 80 DAFB and 1,105 genes at 170 DAFB were up-regulated relative to CK peel, with three groups sharing 43 genes (Figure 4B up). In contrast, 992 genes at 30 DAFB, 620 genes at 80 DAFB and 1,421 genes at 170 DAFB were down-regulated, with 94 genes common to the three groups (Figure 4B down). To identify DEGs that showed alternation in their expression during peel development and common or different pathways that altered developmentally, they were clustered according to their expression patterns. Three patterned DEGs with up-up-regulation, up-down-regulation and down-down-regulation during peel development were identified. In these three patterns, down-down-regulation had the most genes (237) while up-up-regulation contained the least genes (63) (Figure 4C). All DEGs were assigned to metabolism pathways (Table S5). At 30 DAFB, plant hormone signal transduction with 173 DEGs and starch and sucrose metabolism with 130 DEGs were altered most significantly in RD peels. Subsequently, pathways involved in plant circadian rhythms, amino sugar, and nucleotide sugar metabolism and stilbenoid, diarylheptanoid, and gingerol biosynthesis were also affected. At 80 and 170 DAFB, the metabolic pathway and biosynthesis of secondary metabolites possessed the most DEGs that accorded with fruit development and carotenoid biosynthesis (Figure 5).

TABLE 3 | Mineral nutrients in mature CK and RD peels.

	N (%)	P (%)	K (%)	Ca (%)	Mg (%)	Zn (ug/g)
CK	0.79 ± 0.02	0.04 ± 0.01	1.13 ± 0.04	0.50 ± 0.02	0.07 ± 0.01	4.40 ± 0.23
RD	0.88 ± 0.03*	0.05 ± 0.001	1.00 ± 0.11	0.51 ± 0.05	0.19 ± 0.01*	4.81 ± 0.06
	Cu (ug/g)	Mn (ug/g)	Fe (ug/g)	B (ug/g)	Mo (ug/g)	
CK	1.87 ± 0.13	7.58 ± 2.09	28.99 ± 12.23	17.91 ± 0.13	0.04 ± 0.00	
RD	2.96 ± 0.44*	9.71 ± 0.45	29.15 ± 9.59	18.60 ± 0.63	0.05 ± 0.02	

Values are mean ± SD of three biological replicates. Asterisk means significant difference at $P < 0.05$.

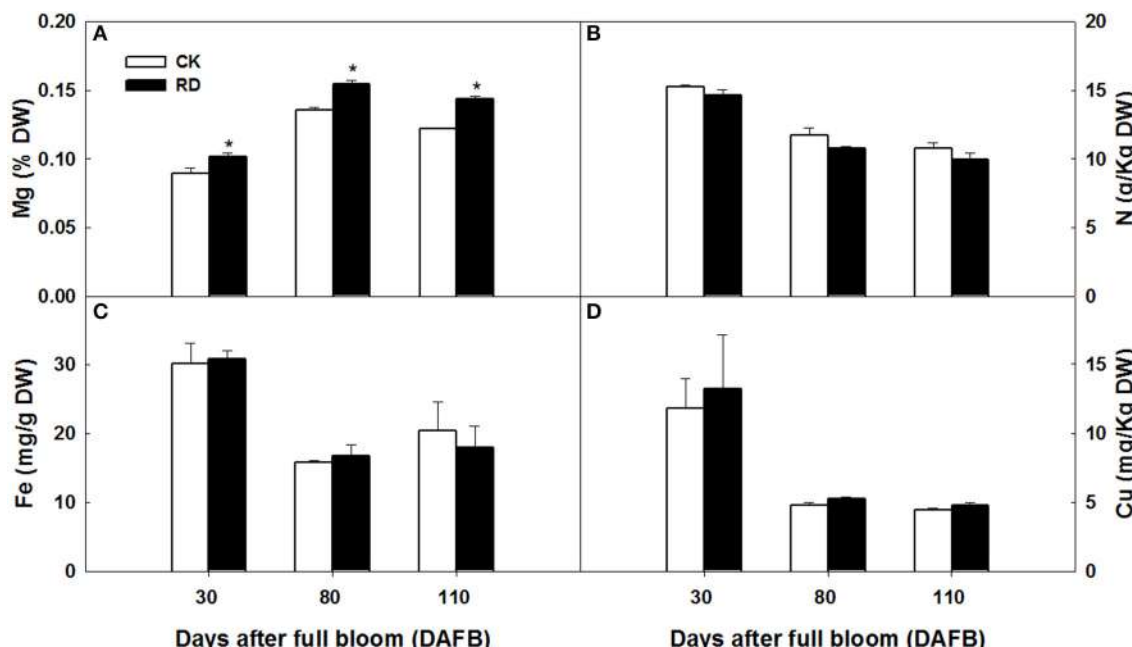


FIGURE 3 | Mg (A), N (B), Fe (C) and Cu (D) content in CK and RD peels during development. Asterisk means significant difference at $P < 0.05$.

Starch, Sugar, and Acid Accumulation in RD Peel of Satsuma Mandarin Fruit

Transcriptome analyses showed that gene expression in starch and sucrose pathways alternated significantly at different stages, indicating the important roles of the pathways in RD peel formation. Therefore, starch and sucrose contents in the peel during fruit development were measured. The results showed that starch was up to 10 mg/gFW in RD peel at 30 DAFB, significantly higher than 5 mg/gFW in CK peel. Subsequently, starch content in both peels decreased quickly and remained at 6–9% until fruit maturity (Figure 6A). Starch difference between the two peels was evident in content as well as in morphology. Due to the abundant starch in citrus fruitlet, starch overflow after cutting could be observed easily. *In situ* observation under SEM, starch in CK peel had longer chains than starch in RD peel, and starch accumulation was much denser in RD peel than in CK peel (Figure 7).

During peel development, two or three sampling dates out of five indicated significantly higher sucrose, glucose and fructose

levels in CK peel than in RD peel. Three sugars all had lower levels in RD peel at 170 DAFB (Figures 6B–D). Between the two peels, there was no difference in citrate at most sampling dates. Malate was higher in RD peel than in CK peel between 40 and 140 DAFB, but the difference disappeared at 170 DAFB (Figures 6E,F). Because peel is the media tissue for leaf photosynthate transporting to fruit pulp, there should be links in sugars and acids between peel and pulp. Analyses showed that pulp of RD fruit had lower sucrose, glucose, and fructose content at 170 DAFB but showed no difference in organic acids, similar to patterns in RD peel (Figure S1).

Hormone Signal Transduction in RD Peel of Satsuma Mandarin Fruit

Of the pathways revealed by RNA-sequencing, plant hormone signal transduction was clearly and significantly affected in RD peel, especially at 30 DAFB. Based on the observations and previous reports, effects of auxin, cytokinin, and gibberellin, which are likely associated with peel RD, were further studied.

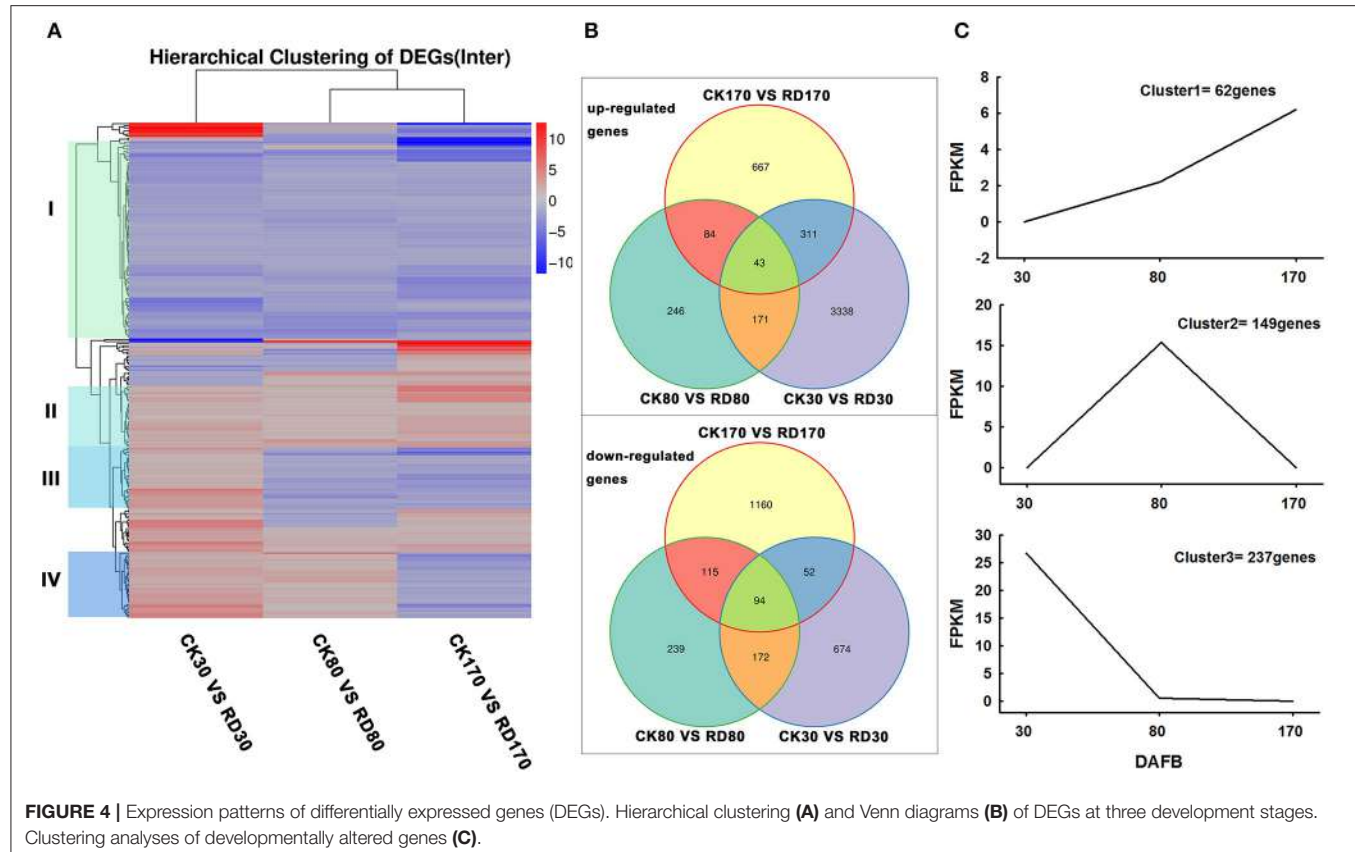


FIGURE 4 | Expression patterns of differentially expressed genes (DEGs). Hierarchical clustering (A) and Venn diagrams (B) of DEGs at three development stages. Clustering analyses of developmentally altered genes (C).

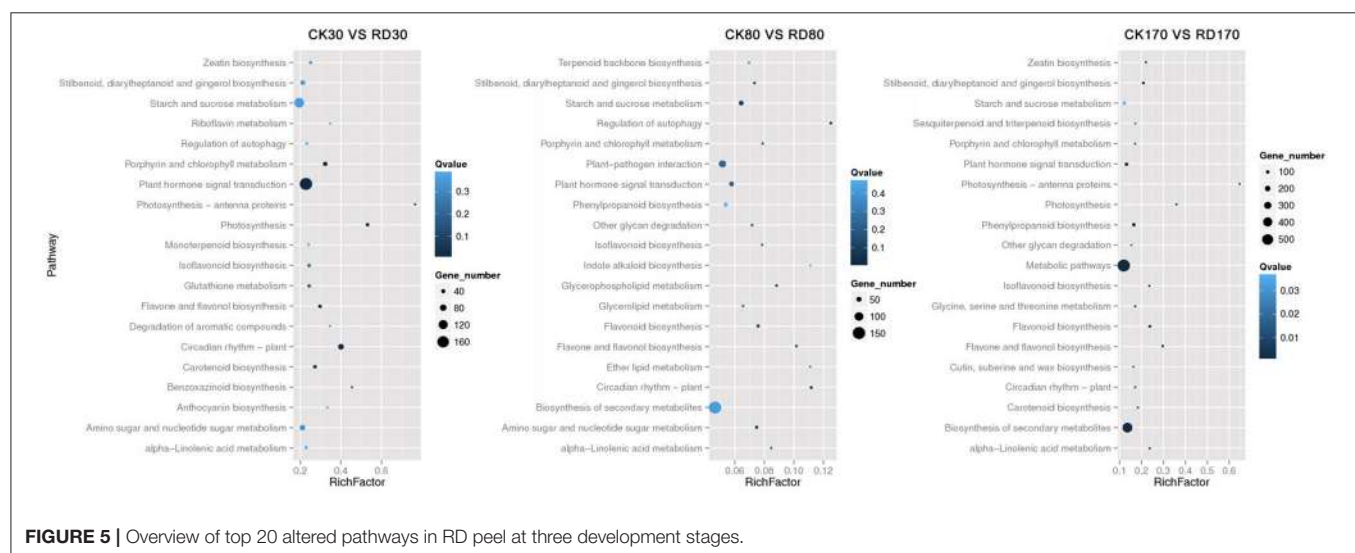


FIGURE 5 | Overview of top 20 altered pathways in RD peel at three development stages.

Exogenous applications of auxin (IAA), gibberellin (GA₃), cytokinin (CTK) or a mixture (IAA+GA₃+CTK), were used to soak the normal fruit to identify their roles in RD. After twice soaking at 40 and 50 DAFB, fruits of all treatments enlarged significantly at 85 and 115 DAFB compared to CK, while mixture treatment drove the largest fruit enlargement at 85 DAFB. However, there was no fruit size difference between

IAA, GA₃, CTK, and mixture treatments except a slightly larger fruit in mixture treatment at 85 DAFB. Along with fruit enlargement, fruit peel thickness changed significantly depending on hormones (Table 4). Compared to CK, thickened peel was found at 85 DAFB, a month after treating, and peel thickness was 3.56, 3.27, and 3.78 mm in IAA, GA₃, and mixture treatments, respectively. CTK and CK treatments were thinner, <2.9 mm.

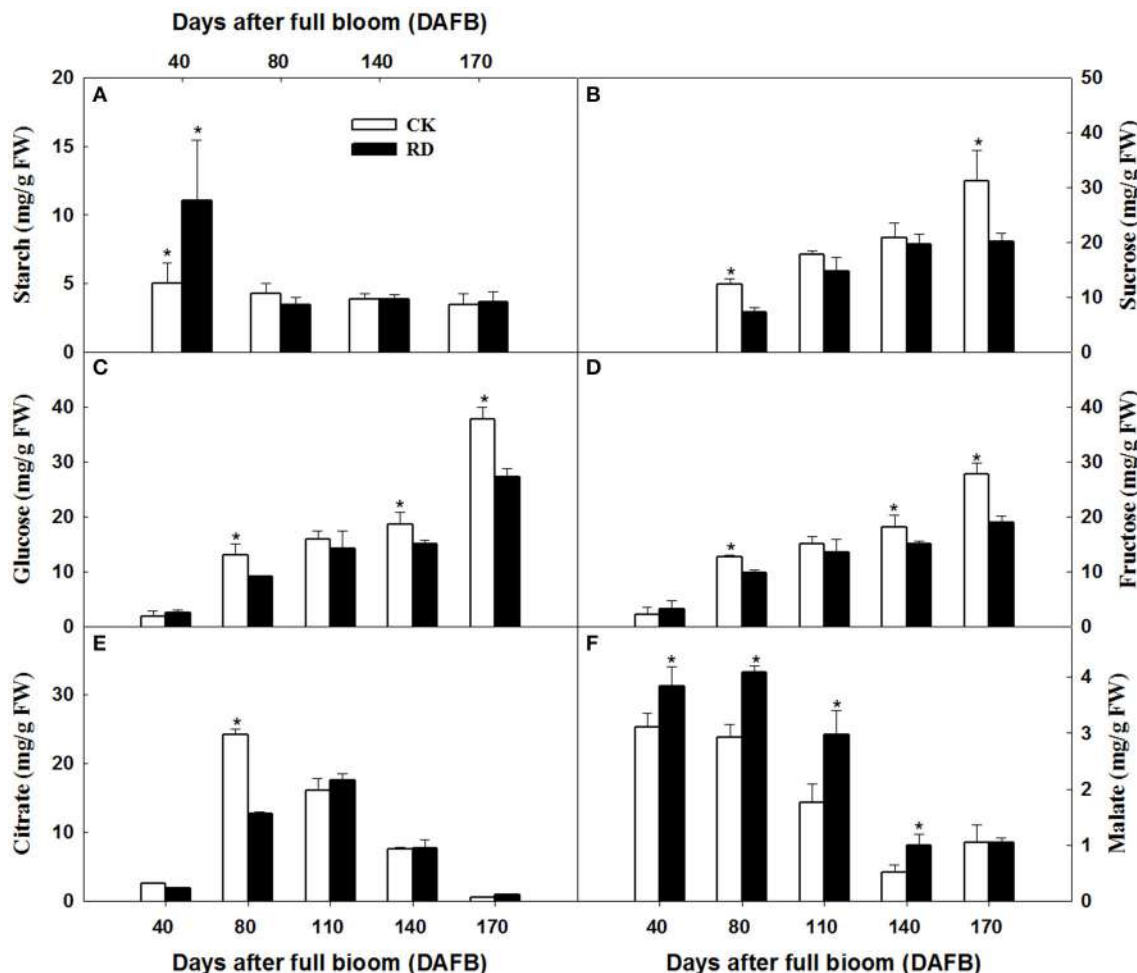


FIGURE 6 | Starch (A), sucrose (B), glucose (C), fructose (D), citrate (E), and malate (F) accumulation in CK and RD peel during fruit development. Asterisk means significant difference at $P < 0.05$.

Subsequently at 115 DAFB, with RD appearing, the peel thickness in IAA, CTK, and mixture treating fruit showed a slight decrease, but in GA₃ treated fruit the thickness increased, contributing to peel RD (**Figure 8, Table 4**). In the bigger fruit after hormone treatment, larger steles at 85 DAFB and hollow steles at 115 DAFB were observed (**Figure 8**).

Accumulation of sugars and organic acids in fruit were altered after hormone treatment. From June to September, sugars in peel accumulated constantly and significantly whether treated by hormones or not, with an exception of GA₃ on sucrose (**Figures 9A–C**). Peel sucrose and glucose contents showed no difference between hormone treatments at 40 days after treatment (DAT) while these in IAA, GA₃, and mixture treatments were lower than that in CK and CTK treatment at 100 DAT (**Figures 9A,B**). Peel fructose was lower stably in GA₃ treatment since 40DAT (**Figure 9C**). Citrate increased significantly from 0 to 40 DAT and then decreased sharply in all peels, while malate decreased slightly from 0 to 40 DAT and increased after that. Peel citrate decreased after all hormone treatments except CTK at 40 DAT. In peel at 100 DAT, CTK,

and mixture induced the lowest citrate (**Figure 9D**). Malate in peel declined after hormone treatments and that occurred 100 DAT mainly (**Figure 9E**). In pulp, total soluble solids (TSS) also decreased after IAA, GA₃, and mixture treatments at 100 DAT (**Figure S2A**). Sucrose showed slight decrease in IAA and mixture treatments at 100 DAT (**Figure S2B**). Consistent with the TSS pattern, fructose and glucose were also lower in IAA, GA₃, and mixture treatments than in CK and CTK treatments (**Figures S2C,D**). Pulp in CTK treated fruit exhibited lower citrate levels than CK and other hormone treated fruit from 40 to 100 DAT. Malate in the pulp of IAA, GA₃, and CTK treated fruit was higher than in CK and mixture treated fruit at 100 DAT (**Figures S2E,F**).

Genes Initially Responsible for Peel RD

The genes potentially associated with initial RD were assessed in this study. Because gibberellin works on both tissue growth and starch metabolism, genes involved in gibberellin signal transduction at 30 DAFB were most probably associated with peel RD. Of 4,857 DEGs at 30 DAFB, 243 DEGs were assigned to

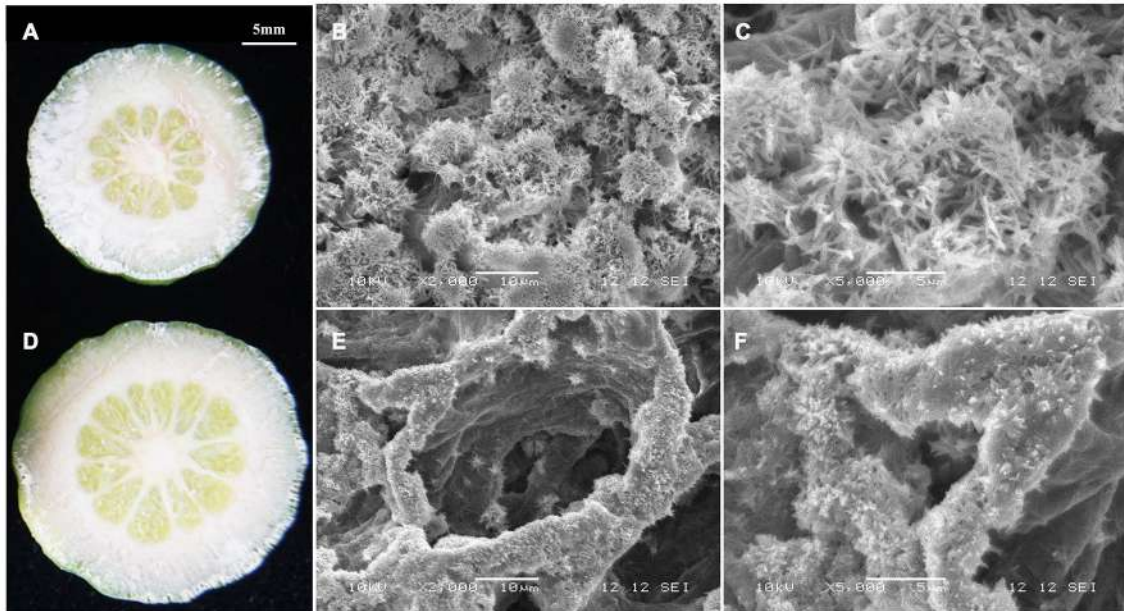


FIGURE 7 | Morphology of starch in CK peel (**A–C**) and RD peel (**D–F**) at 30 DAFB.

TABLE 4 | Changes of fruit size and peel thickness after hormone treatment.

	DAFB	CK	IAA	CTK	GA3	IAA+CTK+GA3
Fruit diameter (mm)	85	42.80 ± 1.47c	51.20 ± 3.25b	50.27 ± 3.12b	51.13 ± 3.86b	53.35 ± 2.73a
	115	60.20 ± 2.90b	67.50 ± 5.55a	67.43 ± 11.60a	68.45 ± 5.94a	68.30 ± 5.11a
Peel thickness (mm)	85	2.41 ± 0.42d	3.56 ± 0.36ab	2.89 ± 0.39c	3.27 ± 0.43b	3.78 ± 0.55a
	115	2.29 ± 0.48d	2.49 ± 0.68cd	2.87 ± 0.21bc	3.38 ± 0.43a	3.07 ± 0.75ab

Values are mean ± SD of thirty individual replicates. Different letters mean significant difference at $P < 0.05$.

the plant hormone signal transduction pathway. Among these, 49 genes belonged to gibberellin signal transduction, and contained 19 GA insensitive dwarf (GID) genes, 14 DELLA genes and 16 transcription factors. In the gibberellin signal transduction pathway, *GID* and transcription factors positively regulate tissue growth, but DELLA negatively regulates it. As such, 15 out of 49 genes were further screened. The expression levels of 13 genes were higher in RD30 than in CK30, but two DELLA genes, *DELA7* and *DELA8*, had downregulated expression in RD30 (Table 5). To confirm this gene expression pattern in the gibberellin signal transduction pathway, 21 DEGs containing 15 potentially crucial genes and 6 *bHLH* transcription factors were selected for expression profile analyses using quantitative RT-PCR. The results showed similar expression patterns to RNA-sequencing results, despite some quantitative differences (Figure S3).

DISCUSSION

RD is a physiological fruit disorder in Satsuma mandarins, occurring in most production areas. Although Satsuma mandarin

RD has been described in previous studies, it has not been comprehensively examined and interpreted. In the present study, the exterior and interior characteristics of RD fruit were observed, with particular emphasis on peel RD. Unlike puffing disorder, which is characterized by a split between peel and pulp and the production of aerial spaces through dissolution of albedo (Kuraoka, 1962; Martinelli et al., 2015), RD is mainly characterized by a rough fruit surface, enlarged fruit size and thicker peel. Apart from the rough appearance, it also exhibits other quality barriers such as delayed degreening, enlarged segments, thickened flavedo and albedo, and lignified segment membranes and juice sacs (Figures 1A,B). RD fruit follows an altered development pattern involved in both fruit size and peel. It appears that the imbalance of source/sink ratio originating from some physiological factors causes the constant and vigorous growth pattern of RD fruit (Figures 1C,D).

At fruit maturity stage, more than 850 metabolites were found in CK and RD peels. Most differences (and the largest differences) were in the intermediates of primary metabolism involved in sugar, organic acid, and amino acid metabolism (Table 1). In particular, both targeted and untargeted

measurements revealed significantly higher amino acid contents in RD peel, suggesting upregulated amino acid metabolism (**Table 2**). Meanwhile, the higher Glu content might contribute

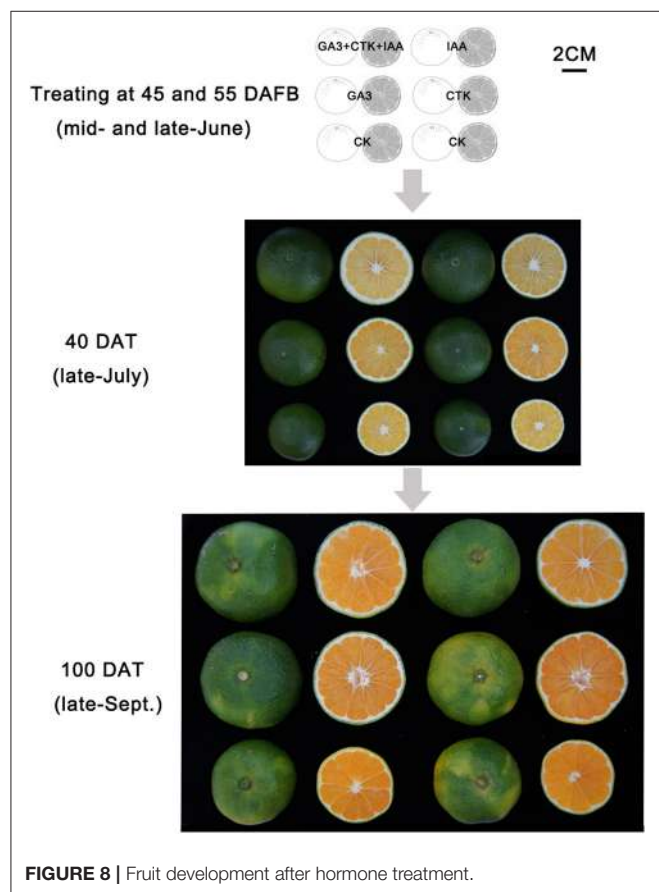


FIGURE 8 | Fruit development after hormone treatment.

to the chlorophyll precursor, which is associated with delayed degreening of RD peel. Magnesium and nitrogen play important roles in citrus chlorophyll accumulation (Yin et al., 1998; Huang et al., 2014). Mineral nutrient analyses showed that RD peel contained more magnesium and nitrogen than CK peel throughout fruit development, which could be responsible for the delayed degreening (**Figure 3, Table 3**). The month after full bloom is a key period for RD development. Following the three developmental stages for Satsuma mandarins (Kubo and Hiratsuka, 1998), cell division occurred before 60 DAFB in this work when the cell amount and thickness of the peel changed. Upward fruit of “Okitsu wase” mandarin exhibited significant RD at the end of cell division stage (Kubo and Hiratsuka, 1998). In “Guoqing No. 1” mandarins, where defruiting induces RD, histological analyses showed that loose cell arrangement in albedo occurred after 21 DAFB and rough cell arrangement in flavedo appeared after 28 DAFB (Liu, 2012). In this study, SEM analyses showed that increased cell layers, enlarged cell volume and looser cell arrangements in RD peel were present at 30 DAFB, and these differences remained during subsequent development stages (**Figure 2**). All the above results indicate that vigorous cell division supplied a basis for disorder development at subsequent stages and was an early symptom of peel RD, which generally happened within a month after full bloom.

Citrus fruit set needs sufficient carbohydrate support (Mehouachi et al., 2000). In Satsuma mandarin, source–sink imbalance assays through defoliation and sucrose stem injection demonstrated that fruit set and fruitlet growth are highly dependent on carbohydrate availability (Iglesias et al., 2003, 2006). The major carbohydrates in citrus fruit are starch at early development stage and sugars and acids at middle and late development stages. Branch girdling on “Okitsu wase” mandarins performed at anthesis temporarily delayed the initial process of natural fruitlet drop, while higher carbohydrates

TABLE 5 | List of important DEGs initially responding to peel roughing disorder.

Gene name	Transcript ID	Log ₂ (FPKM ratio)			RD FPKM		
		RD30/ CK30	RD80/ CK80	RD170/ CK170	30 DAFB	80 DAFB	170 DAFB
GID1e1	Cs5g34000	4.13	–	–	4.73	1.83	0.19
GID1b1	Cs8g05610	3.46	–	–	15	10.15	2.6
GID1b2	Cs7g05330	2.92	–	–	5.59	4.61	3.66
GID1	Cs8g05590	2.85	–	–	6.47	3.2	0.65
GID1e2	Cs5g34010	2.38	–	–	21.71	16.26	3.34
GID1c	Cs5g19100	1.83	–	–	18.54	11.1	7.62
GID2	Cs3g23040	1.03	–	–	60.99	60.06	40.68
DELLA7	Cs2g01990	-1.74	–	–	150.59	116.09	148.67
DELLA8	Cs4g12130	-2.20	-1.68	-1.14	88.12	59.84	35.24
bHLH51	Cs7g30860	4.20	–	–	6.63	3.37	1.76
bHLH 30	Cs3g17300	3.34	–	–	5.78	4.21	7.9
bHLH 122	orange1.1t03173	2.06	1.12	–	11.44	10.61	4.9
bHLH 56	Cs3g23320	1.97	–	–	3.37	1.8	0.61
bHLH 7	Cs9g13980	1.53	–	–	22.69	17.04	18.46
bHLH 122.1	Cs7g02010	1.08	-1.10	–	33.59	15.24	11.38

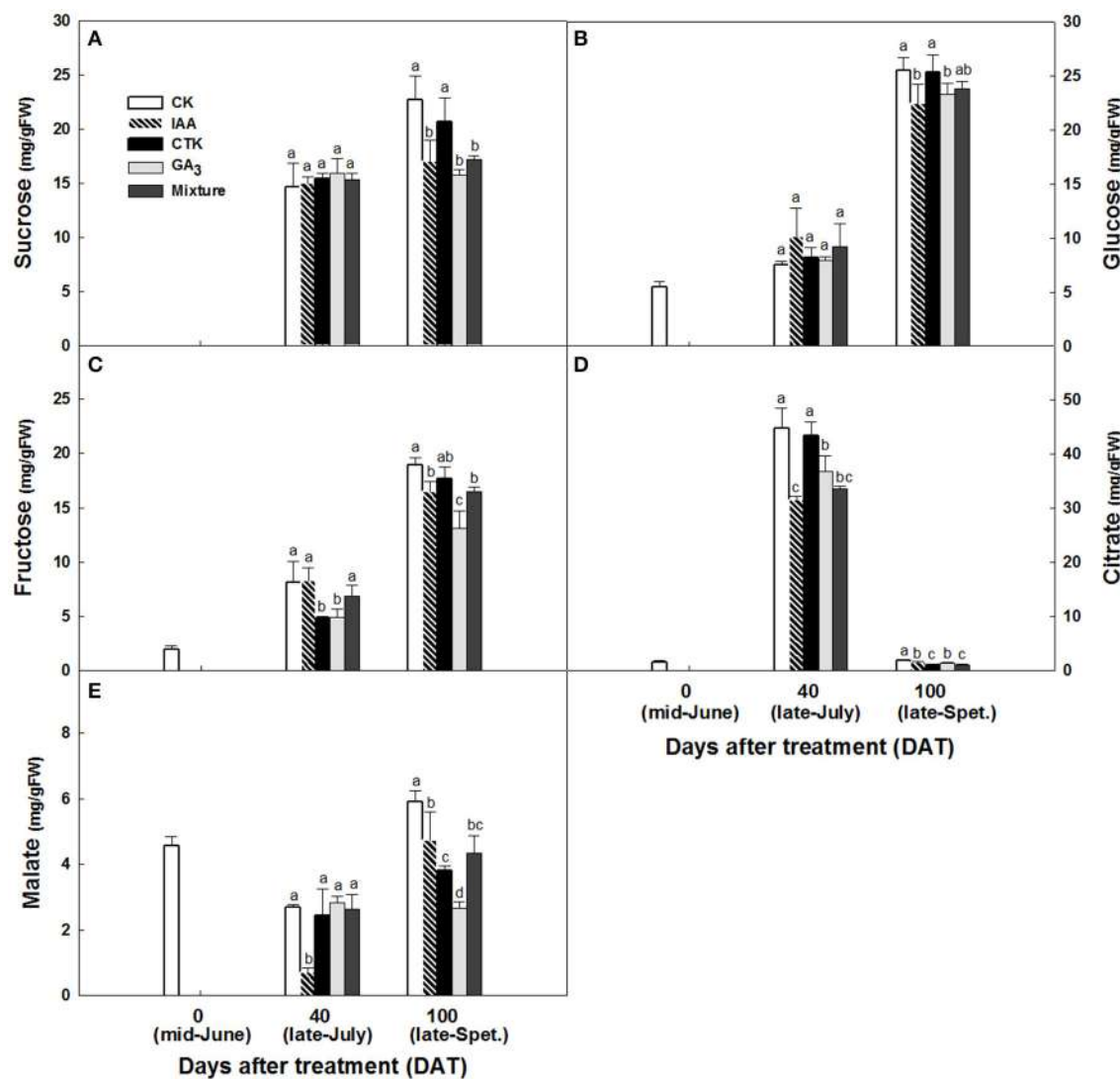
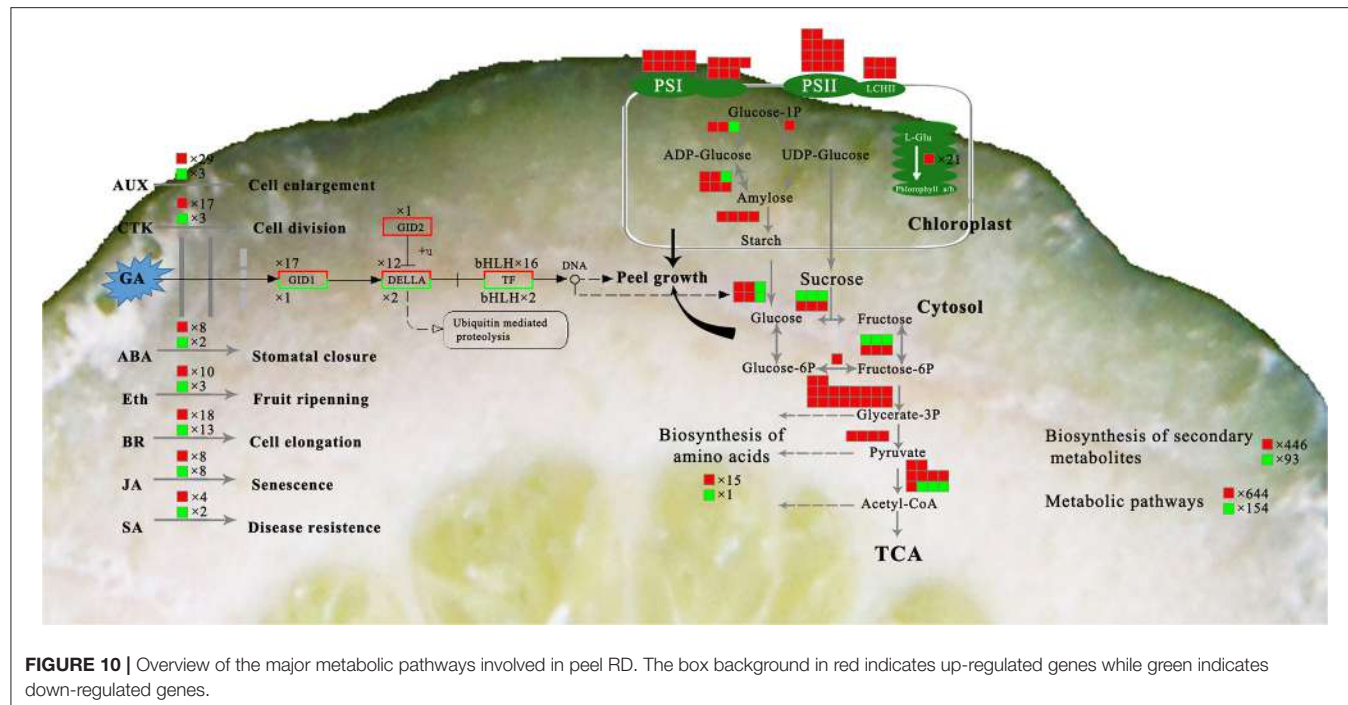


FIGURE 9 | Sucrose (A), glucose (B), fructose (C), citrate (D) and malate (E) accumulation in peel after hormone treatment. Different letters mean significant difference at $P < 0.05$.

(hexose and starch) and GAs contributed to the delay of fruitlet abscission (Mahouachi et al., 2009). In this work, defruiting at fruit set caused significantly more starch accumulation in RD peel, a similar effect to branch girdling at anthesis. These results indicated that the strategies enhancing carbohydrate accumulation in fruitlets were beneficial to fruit set and fruitlet growth. Furthermore, the starch chain was affected in RD peel in addition to an increase in starch content (Figures 6A, 7). This is probably associated with gibberellin signal activity in RD peel, which is an important accelerator for starch hydrolysis. Gibberellin-mediated starch hydrolysis had been identified in avocados (Leshem et al., 1973), maize (Cao and Shannon, 1997), *Medicago sativa* L. and other crops (Kepczynska and Zielinska, 2006). Thus, increased gibberellin signal transduction likely promotes fruitlet development and drives starch hydrolysis in RD peel.

As the other major carbohydrates in Satsuma mandarins, sugars and acids determine fruit flavor. In Satsuma mandarin pulp, sugars increase from early September until fruit maturity, and acids increase until mid-August and then decrease until fruit maturity (Zhao, 2008). In the juice of Satsuma mandarin fruit with RD, total sugar and its components were all lower in RD fruit than CK fruit from mid-August to early December. Total acid and citrate levels were higher in RD fruit than CK fruit from early August to mid-September but malate displayed the reverse pattern. However, all the acid differences between CK and RD fruit disappeared after late September (Kubo and Hiratsuka, 1998). Low fruit load, possibly inducing RD, led to lower sucrose in Satsuma mandarin pulp (Kubo et al., 2001). Results in this study indicated that there is less sugar in RD peel and pulp, especially at fruit maturity stage (Figure 6 and Figure S1); IAA, CTK, GA₃ and mixture treatments could lead to lower sugars



and acids in both peel and pulp, with GA₃ working efficiently and stably (**Figure 9** and **Figure S2**). Together, these results suggest that RD negatively affects sugar and acid accumulation in Satsuma mandarin fruit through GA₃ playing an important role.

It is generally accepted that GA operates in fruit set in citrus (Talon, 1992; Ben-Cheikh et al., 1997; Mahouachi et al., 2009). GA is an activator of cell division and cell enlargement processes, and its presence is generally associated with the initiation of both phases. In Tankan (*Citrus tankan Hayata*), exogenous GA₃ induced RD due to increased flavedo thickness and a prolonged cell division stage (Liu et al., 1988). A similar effect of exogenous GA₃ was also found in "Okitsu wase" mandarin, but IAA, BA and ABA had no effect on RD (Kubo and Hiratsuka, 2000). In addition, application at early development stage also means that GA results in RD. GA₃ application in late June led to peel RD but did not do so in mid-July. GA content was higher in RD peel in late June but the difference disappeared in mid-July (Kubo and Hiratsuka, 2000). Similarly, the effect of GA on biological function depending on application time was also found in citrus flowering induction (Guardiola et al., 1982; Lord and Eckard, 1987; Goldberg-Moeller et al., 2013). Together with our tests of GA₃, IAA, and CTK on RD, these findings indicate that GA plays a crucial role in peel RD, and the early development stage is a key period for GA-induced RD in Satsuma mandarin. In the gibberellin signal transduction pathway, expression of *CsGIDs*, *CsDELAs*, and *bHLH* families were affected at 30 DAFB in response to peel RD. Of these genes, transcription factors were involved in both peel growth and starch hydrolysis in peel, indicating their crucial roles in initiating RD (**Figure 10**). In fruit, the *bHLH* family is associated with peel pigment metabolism. The *bHLH* family regulates anthocyanin metabolism in apples (An et al., 2012; Xie et al., 2012; Meng

et al., 2016), Chinese bayberry (Liu et al., 2013), and blood oranges (Sun et al., 2014). The *bHLH* family is also involved in fruit development in model plants (Groszmann et al., 2008, 2011). In Satsuma mandarins, *CubHLH1* modulates carotenoid metabolism in the peel, which can be accelerated or slowed by ethylene or gibberellin, respectively (Fujii et al., 2007, 2008; Endo et al., 2016). In this study, expression of all six *bHLHs* involved in gibberellin transduction (*bHLH51*, *bHLH 30*, *bHLH 122*, *bHLH 56*, *bHLH 7*, and *bHLH 122.1*) were upregulated, indicating their roles in peel RD development.

CONCLUSION

Satsuma mandarin fruit RD could be initiated at the month after full bloom. Metabolome analysis of RD peel showed that content of Mg and many carbohydrates were significantly affected. RNA-sequencing suggested there were many more DEGs responding to RD at early fruit development stage than at subsequent stages. This study revealed starch metabolism and GA signal transduction pathways were changed significantly. Several aspects might account for peel RD, including: (a) The RD peel had more vigorous carbohydrate metabolism at early fruit development stage relative to CK peel; (b) GA played a crucial role in RD peel initiation through cell division, peel growth and carbohydrate metabolism; (c) The higher Mg content might contribute to the chlorophyll biosynthesis, carbohydrate accumulation and delayed degreening in RD peel.

DATA ACCESS

RNA-sequencing data are submitted to Gene Expression Omnibus (GEO) repository under accession No. GSE100512

(<http://www.ncbi.nlm.nih.gov/geo/query/acc.cgi?acc=GSE100512>).

AUTHOR CONTRIBUTIONS

X-PL, S-YC, and S-XX conceived and designed research. X-PL, JX, and F-FL conducted experiments. Z-MZ and X-CM contributed new reagents and analytical tools. X-PL and F-FL analyzed data. X-PL wrote the manuscript and S-XX revised the manuscript. All authors read and approved the manuscript.

ACKNOWLEDGMENTS

This research was supported by the National Natural Science Foundation of China (31401824), A Project Supported by Scientific Research Fund of Hunan Provincial Education Department (17B127), Hunan Provincial Natural Science Foundation of China (2017JJ3168), the National Modern Agro-industry (Citrus) Technology Systems of China (CARS-27)

and the Priority Major of Horticulture in Hunan Province. The authors thank Dr. Benjamin Bryant Orcheski of Cornell University, USA, for the critical suggestion and language correction.

SUPPLEMENTARY MATERIAL

The Supplementary Material for this article can be found online at: <https://www.frontiersin.org/articles/10.3389/fpls.2017.01907/full#supplementary-material>

Figure S1 | Sucrose (**A**), fructose (**B**), glucose (**C**), citrate (**D**), and malate (**E**) accumulation in CK and RD pulp during fruit development. Asterisk means significant difference at $P < 0.05$.

Figure S2 | TSS (**A**), sucrose (**B**), fructose (**C**), glucose (**D**), citrate (**E**), and malate (**F**) accumulation in pulp after hormone treatments. Different letters mean significant difference at $P < 0.05$.

Figure S3 | Relative expression of genes involved in GA signal transduction. Values are mean \pm SD of three biological replicates calibrated against the amount of β -actin control expression. Numbers at the top of the columns represent the FPKM values calculated from sequencing data.

REFERENCES

- Agusti, M., Almela, V., Aznar, M., El-Otmani, M., and Pons, J. (1994). Satsuma mandarin fruit size increased by 2,4-DP. *Hortscience* 29, 279–281.
- An, X. H., Tian, Y., Chen, K. Q., Wang, X. F., and Hao, Y. J. (2012). The apple WD40 protein MdTTG1 interacts with bHLH but not MYB proteins to regulate anthocyanin accumulation. *J. Plant Physiol.* 169, 710–717. doi: 10.1016/j.jplph.2012.01.015
- Audic, S., and Claverie, J. M. (1997). The significance of digital gene expression profiles. *Genome Res.* 7, 986–995. doi: 10.1101/gr.7.10.986
- Bain, J. M. (1958). Morphological, anatomical, and physiological changes in the developing fruit of the Valencia orange, *Citrus sinensis* (L.) Osbeck. *Aust. J. Bot.* 6, 1–23. doi: 10.1071/BT9580001
- Bao, S. (2000). *Agrochemical Soil Analysis*. Beijing: China Agriculture Press.
- Ben-Cheikh, W., Perez-Botella, J., Tadeo, F. R., Talon, M., and Primo-Millo, E. (1997). Pollination increases gibberellin levels in developing ovaries of seeded varieties of citrus. *Plant Physiol.* 114, 557–564. doi: 10.1104/pp.114.2.557
- Benjamini, Y., and Yekutieli, D. (2001). The control of the false discovery rate in multiple testing under dependency. *Ann. Stat.* 29, 1165–1188. Available online at: <http://www.jstor.org/stable/2674075>
- Cao, H., and Shannon, J. C. (1997). Effect of gibberellin on growth, protein secretion, and starch accumulation in maize endosperm suspension cells. *J. Plant Growth Regul.* 16, 137–140. doi: 10.1007/PL00006987
- Conesa, B. A., Götz, S., García-Gómez, J., Terol, J., Talón, M., and Robles, M. (2005). Blast2GO: a universal tool for annotation, visualization and analysis in functional genomics research. *Bioinformatics* 21, 3674–3676. doi: 10.1093/bioinformatics/bti610
- Endo, T., Fujii, H., Sugiyama, A., Nakano, M., Nakajima, N., Ikoma, Y., et al. (2016). Overexpression of a citrus basic helix-loop-helix transcription factor (CubHLH1), which is homologous to *Arabidopsis* activation-tagged bri1 suppressor 1 interacting factor genes, modulates carotenoid metabolism in transgenic tomato. *Plant Sci.* 243, 35–48. doi: 10.1016/j.plantsci.2015.11.005
- Erner, Y., Goren, R., and Monselise, S. P. (1976). The rough fruit condition of the Shamouti orange—connections with the endogenous hormonal balance. *J. Hortic. Sci.* 51, 367–374. doi: 10.1080/00221589.1976.11514700
- Erner, Y., Monselise, S. P., and Goren, R. (1975). Rough fruit condition of the Shamouti orange: occurrence and patterns of development. *Physiol. Vége.* 13, 435–443.
- Finn, R. D., Clements, J., Arndt, W., Miller, B. L., Wheeler, T. J., Schreiber, F., et al. (2015). HMMER web server: 2015 update. *Nucleic Acids Res.* 43, 30–38. doi: 10.1093/nar/gkv397
- Fujii, H., Shimada, T., Sugiyama, A., Endo, T., Nishikawa, F., Nakano, M., et al. (2008). Profiling gibberellin (GA 3)-responsive genes in mature mandarin fruit using a citrus 22K oligoarray. *Sci. Hortic. Amsterdam* 116, 291–298. doi: 10.1016/j.scienta.2008.01.010
- Fujii, H., Shimada, T., Sugiyama, A., Nishikawa, F., Endo, T., Nakano, M., et al. (2007). Profiling ethylene-responsive genes in mature mandarin fruit using a citrus 22K oligoarray. *Plant Sci.* 173, 340–348. doi: 10.1016/j.plantsci.2007.06.006
- Goldberg-Moeller, R., Shalom, L., Shlizerman, L., Samuels, S., Zur, N., Ophir, R., et al. (2013). Effects of gibberellin treatment during flowering induction period on global gene expression and the transcription of flowering-control genes in Citrus buds. *Plant Sci.* 198, 46–57. doi: 10.1016/j.plantsci.2012.09.012
- Groszmann, M., Paicu, T., Alvarez, J. P., Swain, S. M., and Smyth, D. R. (2011). SPATULA and ALCATRAZ, are partially redundant, functionally diverging bHLH genes required for *Arabidopsis* gynoecium and fruit development. *Plant J.* 68, 816–829. doi: 10.1111/j.1365-313X.2011.04732.x
- Groszmann, M., Paicu, T., and Smyth, D. R. (2008). Functional domains of SPATULA, a bHLH transcription factor involved in carpel and fruit development in *Arabidopsis*. *Plant J.* 55, 40–52. doi: 10.1111/j.1365-313X.2008.03469.x
- Guardiola, J. L., Monerri, C., and Agusti, M. (1982). The inhibitory effect of gibberellic acid on flowering in Citrus. *Physiol. Plant.* 55, 136–142. doi: 10.1111/j.1399-3054.1982.tb02276.x
- Huang, C. N., Xiao-Peng, L. U., Xiao, Y. M., Jing, L. I., Cao, X. J., Sun, M. H., et al. (2014). Effect of nitrogen application on expression of key enzyme genes in pathway of Ponkan leaf nitrogen assimilation and chlorophyll biosynthesis. *J. Fruit Sci.* 31, 7–12. doi: 10.1038/srep25698
- Iglesias, D. J., Tadeo, F. R. M., and Talon, M. (2006). Carbohydrate and ethylene levels related to fruitlet drop through abscission zone A in citrus. *Trees* 20, 348–355. doi: 10.1007/s00468-005-0047-x
- Iglesias, D. J., Tadeo, F. R., Primo-Millo, E., Talon, M., Iglesias, D. J., Primo-Millo, E., et al. (2003). Fruit set dependence on carbohydrate availability in citrus trees. *Tree Physiol.* 23, 199–204. doi: 10.1093/treephys/23.3.199
- Kepczynska, E., and Zielinska, S. (2006). Regulation of *Medicago sativa* L. somatic embryos regeneration by gibberellin A3 and abscisic acid in relation to starch content and α -amylase activity. *Plant Growth Regul.* 49, 209–217. doi: 10.1007/s10725-006-9106-6
- Kubo, T., and Hiratsuka, S. (1998). Effect of bearing angle of Satsuma mandarin fruit on rind roughness, pigmentation, and sugar and organic acid concentrations in the juice. *J. Jpn. Soc. Hortic. Sci.* 67, 51–58. doi: 10.2503/jjshs.67.51

- Kubo, T., and Hiratsuka, S. (1999). Histological study on rind roughness of Satsuma mandarin fruit. *Engei Gakkai Zasshi* 68, 101–107. doi: 10.2503/jjshs.68.101
- Kubo, T., and Hiratsuka, S. (2000). Relationship between rind roughness and gibberellins in Satsuma mandarin fruit. *Engei Gakkai Zasshi* 69, 718–723. doi: 10.2503/jjshs.69.718
- Kubo, T., Hohjo, I., and Hiratsuka, S. (2001). Sucrose accumulation and its related enzyme activities in the juice sacs of Satsuma mandarin fruit from trees with different crop loads. *Sci. Hortic. Amsterdam* 91, 215–225. doi: 10.1016/S0304-4238(01)00262-X
- Kuraoka, T. (1962). *Histological Studies on the Fruit Development of the Satsuma Orange with Special Reference to Peel-Puffing*. Dissertation, Memoirs of Ehime University, Matsuyama.
- Langmead, B., Trapnell, C., Pop, M., and Salzberg, S. L. (2009). Ultrafast and memory-efficient alignment of short DNA sequences to the human genome. *Genome Biol.* 10:R25. doi: 10.1186/gb-2009-10-3-r25
- Leshem, Y., Seifer, H., and Segal, N. (1973). On the function of seedcoats in gibberellin-induced hydrolysis of starch reserves during Avocado (*Persea americana*) germination. *Ann. Bot. Lond.* 37, 383–388. doi: 10.1093/oxfordjournals.aob.a084703
- Li, B., and Dewey, C. N. (2011). RSEM: accurate transcript quantification from RNA-Seq data with or without a reference genome. *BMC Bioinformatics* 12:323. doi: 10.1186/1471-2105-12-323
- Li, Y., Han, M. Q., Lin, F., Ten, Y., Lin, J., Zhu, D. H., et al. (2015). Soil chemical properties, 'Guanximiyou' pummelo leaf mineral nutrient status and fruit quality in the southern region of Fujian province, China. *J. Soil Sci. Plant Nut.* 15, 263–269. doi: 10.4067/S0718-9516201500500029
- Liu, F. (2012). *Study on the Anatomical Morphology and Quality Changes of Rough of Satsuma*. Dissertation, Huazhong Agricultural University, Wuhan.
- Liu, J., Huang, C., and Chen, D. (1987). The effects of some plant growth regulators on fruit coloring and quality of Tankan (*Citrus tankan* Hayata). *Guangdong Agric. Sci.* 4, 17–19
- Liu, J., Huang, C., and Chen, D. (1988). Effects of plant growth regulators on the development of flavedo and its relationship with peel roughness in *Citrus reticulata* Cv. Tankan. *Acta Hortic. Sci.* 15, 165–168.
- Liu, X. F., Yin, X. R., Allan, A. C., Lin-Wang, K., Shi, Y. N., Huang, Y. J., et al. (2013). The role of MrbHLH1 and MrMYB1 in regulating anthocyanin biosynthetic genes in tobacco and Chinese bayberry (*Myrica rubra*) during anthocyanin biosynthesis. *Plant Cell Tiss. Org.* 115, 285–298. doi: 10.1007/s11240-013-0361-8
- Lord, E. M., and Eckard, K. J. (1987). Shoot development in *Citrus sinensis* L. (Washington Navel Orange). II. alteration of developmental fate of flowering shoots after GA3 treatment. *Int. J. Plant Sci.* 148, 17–22.
- Lu, X., Cao, X., Li, F., Li, J., Xiong, J., Long, G., et al. (2016). Comparative transcriptome analysis reveals a global insight into molecular processes regulating citrate accumulation in sweet orange (*Citrus sinensis*). *Physiol. Plant.* 158, 463–482. doi: 10.1111/ppl.12484
- Mahouachi, J., Iglesias, D. J., Agustí, M., and Talon, M. (2009). Delay of early fruitlet abscission by branch girdling in citrus coincides with previous increases in carbohydrate and gibberellin concentrations. *Plant Growth Regul.* 58, 15–23. doi: 10.1007/s10725-008-9348-6
- Martinelli, F., Ibanez, A. M., Reagan, R. L., Davino, S., and Dandekar, A. M. (2015). Stress responses in citrus peel: comparative analysis of host responses to Huanglongbing disease and puffing disorder. *Sci. Hortic. Amsterdam* 192, 409–420. doi: 10.1016/j.scienta.2015.06.037
- Mehouachi, J., Iglesias, D. J., Tadeo, F. R., Agustí, M., Primomillo, E., and Talon, M. (2000). The role of leaves in citrus fruitlet abscission: effects on endogenous gibberellin levels and carbohydrate content. *J. Hortic. Sci. Biotech.* 75, 79–85. doi: 10.1080/14620316.2000.11511204
- Meng, R., Zhang, J., An, L., Zhang, B., Jiang, X., Yang, Y., et al. (2016). Expression profiling of several gene families involved in anthocyanin biosynthesis in apple (*Malus domestica* Borkh.) skin during fruit development. *J. Plant Growth Regul.* 35, 449–464. doi: 10.1007/s00344-015-9552-3
- Monselise, S. P., and Goldschmidt, E. E. (1982). Alternate bearing in fruit trees. *Hortic. Rev.* 4, 128–173.
- Mortazavi, A., Williams, B. A., McCue, K., Schaeffer, L., and Wold, B. (2008). Mapping and quantifying mammalian transcriptomes by RNA-Seq. *Nat. Methods* 5, 621–628. doi: 10.1038/nmeth.1226
- Osorio, S., Do, P. T., and Fernie, A. R. (2012). Profiling primary metabolites of tomato fruit with gas chromatography/mass spectrometry. *Methods Mol. Biol.* 860, 101–109. doi: 10.1007/978-1-61779-594-7_7
- Pérezrodríguez, P., Corrêa, L. G. G., Rensing, S. A., Kersten, B., and Muellerroeben, B. (2009). PlnTFDB: updated content and new features of the plant transcription factor database. *Nucleic Acids Res.* 38, D822–D827. doi: 10.1093/nar/gkp805
- Shalom, L., Samuels, S., Zur, N., Shlizerman, L., Doron-Faigenboim, A., Blumwald, E. (2014). Fruit load induces changes in global gene expression and in abscisic acid (ABA) and indole acetic acid (IAA) homeostasis in citrus buds. *J. Exp. Bot.* 65, 3029. doi: 10.1093/jxb/eru148
- Sun, Q., Zheng, L., Xi, W. P., He, S. L., Yi, S. L., Qiang, L., et al. (2014). Transcriptome analysis of blood orange (*Citrus sinensis*) following fruit bagging treatment by digital gene expression profiling. *J. Hortic. Sci. Biotech.* 89, 397–407. doi: 10.1080/14620316.2014.11513098
- Talon, M. (1992). Gibberellins and parthenocarpic ability in developing ovaries of seedless mandarins. *Plant Physiol.* 99, 1575–1581. doi: 10.1104/pp.99.4.1575
- Xie, X. B., Li, S., Zhang, R. F., Zhao, J., Chen, Y. C., Zhao, Q., et al. (2012). The bHLH transcription factor MdbHLH3 promotes anthocyanin accumulation and fruit colouration in response to low temperature in apples. *Plant Cell Environ.* 35, 1884–1897. doi: 10.1111/j.1365-3040.2012.02523.x
- Xu, C., Chen, W., Chen, K., and Zhang, S. (1998). A simple method for determining the content of starch-iodine colorimetry. *Biotechnology* 8, 41–43
- Xu, Q., Chen, L. L., Ruan, X., Chen, D., Zhu, A., Chen, C., et al. (2013). The draft genome of sweet orange (*Citrus sinensis*). *Nat. Genet.* 45, 59. doi: 10.1038/ng.2472
- Yan, J., Yuan, F., Long, G., Qin, L., and Deng, Z. (2012). Selection of reference genes for quantitative real-time RT-PCR analysis in citrus. *Mol. Biol. Rep.* 39, 1831–1838. doi: 10.1007/s11033-011-0925-9
- Yin, K., Li, Y., Wang, C., and Wang, S. (1998). Studies on the correlations among foliar nutrition of Mg, Fe, Zn and chlorophyll content in citrus cultivated in calcareous purple soil. *J. Southwest Agric. Univ.* 20, 283–287.
- Zhao, M. (2008). *Study on the Metabolism of Organic Acid and Regulation in Citrus Fruits*. Dissertation, Anhui Agricultural University, Hefei.
- Conflict of Interest Statement:** The authors declare that the research was conducted in the absence of any commercial or financial relationships that could be construed as a potential conflict of interest.
- Copyright © 2017 Lu, Li, Xiong, Cao, Ma, Zhang, Cao and Xie. This is an open-access article distributed under the terms of the Creative Commons Attribution License (CC BY). The use, distribution or reproduction in other forums is permitted, provided the original author(s) or licensor are credited and that the original publication in this journal is cited, in accordance with accepted academic practice. No use, distribution or reproduction is permitted which does not comply with these terms.



Soluble Starch Synthase III-1 in Amylopectin Metabolism of Banana Fruit: Characterization, Expression, Enzyme Activity, and Functional Analyses

Hongxia Miao^{1*†}, Peiguang Sun^{2†}, Qing Liu³, Caihong Jia¹, Juhua Liu¹, Wei Hu¹, Zhiqiang Jin^{1,2*} and Biyu Xu^{1*}

¹ Key Laboratory of Tropical Crop Biotechnology, Ministry of Agriculture, Institute of Tropical Bioscience and Biotechnology, Chinese Academy of Tropical Agricultural Sciences, Haikou, China; ² Key Laboratory of Genetic Improvement of Bananas, Hainan Province, Haikou Experimental Station, Chinese Academy of Tropical Agricultural Sciences, Haikou, China,

³ Commonwealth Scientific and Industrial Research Organization Agriculture and Food, Canberra, ACT, Australia

OPEN ACCESS

Edited by:

Nadia Bertin,

Plantes et Système de cultures
Horticoles (INRA), France

Reviewed by:

Massimiliano Corso,

Université libre de Bruxelles, Belgium

Diane Maria Beckles,

University of California, Davis, USA

*Correspondence:

Zhiqiang Jin

jinzhiqiang@itbb.org.cn

Biyu Xu

bixyuxu@126.com

Hongxia Miao

hxmain@163.com

[†]These authors have contributed
equally to this work.

Specialty section:

This article was submitted to

Crop Science and Horticulture,

a section of the journal

Frontiers in Plant Science

Received: 25 August 2016

Accepted: 15 March 2017

Published: 30 March 2017

Citation:

Miao H, Sun P, Liu Q, Jia C, Liu J, Hu W, Jin Z and Xu B (2017) Soluble Starch Synthase III-1 in Amylopectin Metabolism of Banana Fruit: Characterization, Expression, Enzyme Activity, and Functional Analyses. *Front. Plant Sci.* 8:454. doi: 10.3389/fpls.2017.00454

Soluble starch synthase (SS) is one of the key enzymes involved in amylopectin biosynthesis in plants. However, no information is currently available about this gene family in the important fruit crop banana. Herein, we characterized the function of MaSSIII-1 in amylopectin metabolism of banana fruit and described the putative role of the other MaSS family members. Firstly, starch granules, starch and amylopectin content were found to increase during banana fruit development, but decline during storage. The SS activity started to increase later than amylopectin and starch content. Secondly, four putative SS genes were cloned and characterized from banana fruit. Among them, MaSSIII-1 showed the highest expression in banana pulp during fruit development at transcriptional levels. Further Western blot analysis suggested that the protein was gradually increased during banana fruit development, but drastically reduced during storage. This expression pattern was highly consistent with changes in starch granules, amylopectin content, and SS activity at the late phase of banana fruit development. Lastly, overexpression of MaSSIII-1 in tomato plants distinctly changed the morphology of starch granules and significantly increased the total starch accumulation, amylopectin content, and SS activity at mature-green stage in comparison to wild-type. The findings demonstrated that MaSSIII-1 is a key gene expressed in banana fruit and responsible for the active amylopectin biosynthesis, this is the first report in a fresh fruit species. Such a finding may enable the development of molecular markers for banana breeding and genetic improvement of nutritional value and functional properties of banana fruit.

Keywords: banana (*Musa acuminata* L.), soluble starch synthase, amylopectin metabolism, expression analysis, SSIII-1 function

INTRODUCTION

Starch is the most widespread carbohydrate storage molecule in plants and plays a vital role in human nutrition, food industry and chemical manufacturing. The physicochemical properties of starch are strongly affected by its two key components, amylose and amylopectin (Zeeman et al., 2010; Bischof et al., 2013). In higher plants, there are at least six classes of enzymes that are involved in amylose and amylopectin biosynthesis: ADP-Glc

pyrophosphorylase (AGPase), granule-bound starch synthase (GBSS), soluble starch synthase (SS), starch branching enzyme (SBE), starch debranching enzyme (DBE), and starch phosphorylase (SP) (Fujita et al., 2008; Szydlowski et al., 2009; Jeon et al., 2010; Subasinghe et al., 2014).

Starch synthase uses ADP-glucose for chain elongation via α -1,4-glycosidic linkages, and directly catalyzes the amylopectin biosynthesis (Szydlowski et al., 2009, 2011). A plant typically carries at least four SS subfamilies, termed as SSI, II, III, and IV, respectively (Dian et al., 2005). Comparison of the deduced amino acid sequences showed that these four subfamilies are highly similar in a span of approximately 450 amino acid residues in the C-terminus that comprises the catalytic and starch-binding domains (Schwarze et al., 2013). The sizes of SSI, II, and III proteins were estimated to be approximately 67, 81, and 112 kDa, respectively, in *Arabidopsis* leaves (Delvalle et al., 2005; Zhang et al., 2008; Gámez-Arjona et al., 2014). SS gene expression was recently profiled in a numbers of plants including rice (Crofts et al., 2015), maize (Liu et al., 2015; Huang et al., 2016), potato (Edwards et al., 1999), *Arabidopsis* (Schwarze et al., 2013), wheat and taro (Li et al., 2000; Lin and Jeang, 2005). However, different SSs may predominate in storage organs of different species e.g., SSI in rice endosperm, SSII in wheat (Li et al., 2000; Crofts et al., 2015). In common wheat, SSIII expression was detected from very early to the middle stages of endosperm development (Li et al., 2000). Rice SSIII-2 and SSIV-1 showed the highest expression level at the middle and late development stages of rice endosperm, respectively (Dian et al., 2005).

Amylopectin chain length distribution and amylopectin/amylase ratio affected starch functionality (Dian et al., 2005; Zhang et al., 2005). Biochemical and gene overexpression experiments revealed that SSI, II, and III are involved in the elongation of short (dp 8–12) (Fujita et al., 2008), medium (dp 13–25), and long (dp > 30) starch chains (Szydlowski et al., 2011; Zhu et al., 2014), respectively. SSIV is closely related to SSIII; both have similar structures (Leterrier et al., 2008). Further reverse genetic studies showed that impaired SSI expression was reported to result in structurally altered amylopectin in *Arabidopsis* leaves (Delvalle et al., 2005) and rice endosperm (Takemoto-Kuno et al., 2006; Fujita et al., 2008). Inhibition of SSII gene expression gave rise to lower pasting temperature as the result of alterations in amylopectin structure (Edwards et al., 1999). Loss of SSIII expression reduced the proportion of amylopectin with very long chains and affected the amylopectin/amylase ratio in maize (Zhu et al., 2014), *Arabidopsis* (Zhang et al., 2005), and rice (Dian et al., 2005). A defective mutant of SSIV displayed a severely compromised growth phenotype with fewer but larger starch granules within the plastid in *Arabidopsis* (Roldán et al., 2007). However, Zhang et al. (2008) reported that some SSs, such as SSII and SSIII, may overlap in amylopectin biosynthesis in *Arabidopsis*. In addition, GBSSI from other SS isoforms also contributed to amylopectin synthesis in rice and *Chlamydomonas reinhardtii* (Ral et al., 2006; Hanashiro et al., 2008). These evidences suggested the important roles of the SS genes in regulating plant amylopectin metabolism.

Banana (*Musa* spp.) is not only one of the most highly consumed fruits in the world but also widely used as a staple

food in the tropical and subtropical regions (D'Hont et al., 2012). The typical starch content of a green dessert banana fruit accounts for 20~25% of fresh weight or 60~75% of dry weight (DW), and the starch granules are relatively large (8~48 μm in diameter) compared to those of cereals (Hubbard et al., 1990; de Barros Mesquita et al., 2016). Hence banana is also a potential excellent model plant for studying fresh fruit starch metabolism. Current research on banana starch has mainly focused on granule structure (Low et al., 2015) and antioxidant capacities (Sarawong et al., 2014), as well as physicochemical properties of starch (Zhang and Hamaker, 2012; Utrilla-Coello et al., 2014). Several key genes involved in starch biosynthesis or conversion of starch to sucrose have been isolated and characterized in banana, including *MaGBSSI* (Miao et al., 2014), *DBE* (Bierhals et al., 2004), *SUCROSE PHOSPHATE SYNTHASE (SPS)*, *SUCROSE SYNTHASE (SuSy)*, and *INVERTASE* (Hubbard et al., 1990). However, to our knowledge, the function of SS genes has not been characterized in banana.

Amylopectin is the major component of immature banana fruit (Torre-Gutiérrez et al., 2008), which has a number of remarkable features, including higher retrogradation and lower pasting temperature (Sarawong et al., 2014), relative to those in rice (Syahariza et al., 2013), maize (Huang et al., 2016), and potato (Wikman et al., 2014). Due to the important role of SS in amylopectin metabolism, there is a need to investigate the function of SS in banana. In this study, we revealed that *MaSSIII-1* is a key gene expressed in banana fruit and responsible for the active amylopectin biosynthesis by expression, enzyme activity, and functional analyses. This result could be used in the genetic manipulation of banana fruit for genetic improvement of its nutritional values as well as value-added industrial applications, such as high starch foods, higher retrogradation and lower pasting temperature raw processing materials.

MATERIALS AND METHODS

Plant Materials and Treatments

Banana (*M. acuminata* L. AAA group, cv. 'Dwarf Cavendish'; ITC 0002) seedlings were obtained from the banana tissue culture center (Chinese Academy of Tropical Agricultural Sciences, Danzhou, China) and were grown at 28°C with 70% humidity, 200 $\mu\text{mol}\cdot\text{m}^{-2}\cdot\text{s}^{-1}$ light intensity, and long day condition (16 h light/8 h dark cycle). When banana seedlings produced five leaves, they were planted in the Institute of Tropical Bioscience and Biotechnology banana plantation (Chengmai, Hainan, 20N, 110E) until harvest. Roots, stems, leaves, bracts, flowers, peels, and pulps at 60 days after emergence from the pseudostem (DAF) were collected separately using tweezers, frozen immediately in liquid nitrogen, and stored at -80°C until expression analysis in different tissues. For each biological replicate, two banana hands having a similar developmental stage from two plants were selected and six fingers from the hands were obtained. Banana pulps at 0, 10, 20, 30, 40, 50, and 60 DAF were collected, immediately frozen in liquid nitrogen, and stored at -80°C until starch/amyopectin quantification, mRNA and protein expression analysis.

Banana hands (60 DAF) were separated into individual fingers representing the same developmental stage. For natural ripening treatment, banana samples were kept at 22°C and allowed to ripen in open air. In accordance with the previously published banana ripening stages (Miao et al., 2014), fruits stored for 0, 5, 10, 15, 20, 25, and 30 days period of post-harvest (DPH) were frozen in liquid nitrogen and stored at -80°C until starch/amyopectin quantification, mRNA and protein expression analysis.

Scanning Electron Microscopy (SEM) Observation

Pulp samples were fixed in stubs using double-faced tape and coated with a 10 nm thick platinum layer using a Bal-tec MED 020 Coating system (Kettleshulme, UK) before analysis with a FEI Quanta 600 FEG Scanning Electron Microscope (FEI Company, Hillsboro, OR, USA). SEM observations were performed using the secondary electron mode operating at 15 kV.

Determination of Total Starch Content, Amylopectin Content, and SS Activity

Banana pulp was immersed in 0.5% (w/v) sodium bisulfite solution for 10 min to prevent browning, and then dried at 40°C for 20~24 h. The dried pulp was milled to powder and suspended in 5 mL 80% (w/v) $\text{Ca}(\text{NO}_3)_2$, placed in a boiling water bath for 10 min, and centrifuged for 4 min at low speed (3,800 g). The supernatant was then transferred to a 20 mL volumetric flask. The total starch, amylose, and amylopectin contents of the extract were determined following Yang et al. (1992) and Miao et al. (2014). The amylopectin content was calculated by subtracting the amylose content from the total starch content. Enzymatic analysis of SS activity was carried out following Nakamura et al. (1989). A unit represents increasing 0.01 OD value per min at 340 nm.

Cloning and Sequence Analysis of Genes Encoding SS in Banana Fruit

RNA purification and cDNA synthesis were performed as previously described by Li et al. (2015). To obtain full-length cDNAs, sequences of four SS family members, including SSI (GSMUA_Achr3G03290_00), SSII (GSMUA_Achr6G23190_001), SSIII-1 (GSMUA_Achr11G18570_001), and SSIII-2 (GSMUA_Achr5G00700_001), were retrieved from the banana DH-Pang (AA group) genome sequence database¹. Four primer pairs (Supplementary Table S1) were designed based on these sequences. The SS coding sequences were submitted to BLAST analysis to recover their corresponding genomic DNA sequences. Exon lengths were calculated by alignment of genomic DNA sequences with cDNA sequences, and introns were determined according to the “GC-AG” rule (Miao et al., 2014). The deduced amino acid sequences were aligned using Clustal W, and a phylogenetic tree was constructed based on the neighbor-joining (NJ) method with a Kimura 2-parameter model using MEGA5.0 software (Arizona State University, Tempe, AZ, USA). The

numerical value for each interior branch is the percent bootstrap value calculated from 1,000 replicates.

Quantitative Real-Time PCR (qRT-PCR) Analysis

Specific primer pairs were designed using Primer 5.0 software. Primers that had high specificity and efficiency on the basis of melting curve analysis were used to conduct quantification analysis (Supplementary Table S1). Moreover, PCR products were sequenced to confirm the specificity of primer pairs. Amplification efficiencies of primer pairs ranged from 0.9 to 1.1. The levels of *MaSS* and *SISSIII-1* expression were quantified by qRT-PCR using an iQ5 real-time PCR detection system (Bio-Rad, Hercules, CA, USA) with the SYBR *ExScript* RT-PCR Kit (TaKaRa, Dalian, China). *ACTIN* or *GAPDH* that were verified to be constitutive in expression and hence suitable to be used as internal controls were used as reference genes to normalize transcriptional levels of each *MaSS* gene and *SISSIII-1* (Supplementary Table S1). Relative expression levels of four *MaSS* genes were analyzed in three technical replicates and calculated using the $2^{-\Delta\Delta CT}$ method (Livak and Schmittgen, 2001). Each sample contains three biological replicates.

Detection of MaSSIII-1 Protein Levels by Western Blot Analysis

Pulp samples (0.5 g) were homogenized with a set of mortar and pestle on ice in an equal volume of solution, which consisted of 50 mM HEPES-NaOH (pH 7.4), 2 mM MgCl_2 , 50 mM β -mercaptoethanol, and 12.5% (v/v) glycerol (Nishi et al., 2001). A 20 μL aliquot of the supernatant was incubated with 36 μL of solution I consisting of 50 mM HEPES-NaOH (pH 7.4), 1.6 mM adenosine diphosphate glucose (ADPG), 0.7 mg amylopectin, and 15 mM DL-dithiothreitol (DTT) for 20 min at 30°C. Following the reaction termination at 100°C for 30 s, 20 μL solution II was added, which consisted of 50 mM HEPES-NaOH, 4 mM phosphoenolpyruvate (PEP), 200 mM KCl, 10 mM MgCl_2 , and 1.2 U pyruvate kinase, and incubation on ice for 5 min. The reaction was incubated at 30°C for 20 min before it was terminated at 100°C for 30 s. A 60 μL aliquot of the supernatant was mixed with 43 μL of solution III (50 mM HEPES-NaOH, 10 mM glucose, 20 mM MgCl_2 , 2 mM nicotinamide adenine dinucleotide phosphate, 1.4 U hexokinase, 0.35 U glucose-6-phosphate dehydrogenase) and incubated at 30°C for 10 min. The supernatant (SS enzyme solution) was used to Western blot analysis.

For Western blot analysis, 30 μL of the SS enzyme solution from banana pulps at different developmental stages extracted by the above methods was loaded on each lane and separated on a 12% polyacrylamide gel. Proteins were then transferred onto Hybond™-N⁺ membranes (Amersham Biosciences, Buckinghamshire, UK). Membranes were probed with rabbit anti-MaSSIII-1 polyclonal antibody (Abmart, Shanghai, China) and banana actin antibody (control) in 1:1,000 dilution in PBS-Tween 20 plus 3% BSA, respectively, followed by alkaline

¹<http://banana-genome.cirad.fr/>

phosphatase-conjugated anti-rabbit IgG secondary antibody (Sigma, St. Louis, MO, USA) in 1:1,000 dilution. Positive signals on the membranes were detected with a 5-bromo-4-chloro-3-indolyl-phosphate/nitro blue tetrazolium (BCIP/NBT) solution (Amresco, Solon, OH, USA).

Plant Transformation, Generation and Southern Blot Analysis of *MaSSIII-1* Transgenic Plants

The entire *MaSSIII-1* coding region was inserted into the pCAMBIA-1302 vector under the transcriptional control of CaMV 35S promoter following a double digestion with *Nco* I and *Spe* I. The pCAMBIA-1302-*MaSSIII-1* was transferred into *A. tumefaciens* strain LBA4404. Transgenic tomato (*Solanum lycopersicum* L.) plants were generated using the Agrobacterium-mediated transformation as previously described (Arshad et al., 2014). Kanamycin-resistant transgenic tomato lines were selected and the transgene integration was determined by Southern blot analysis. Genomic DNA (10 µg per sample) from transgenic tomato leaves was isolated using a CTAB method (Li et al., 2015) and digested with *Eco*R I overnight at 37°C, separated on a 0.8% (w/v) agarose gel and transferred onto Hybond-N⁺ nylon membranes (Hybond N⁺, Amersham, UK) (Li et al., 2015). Probes were prepared from the PCR product amplified using the primers (5'-gagagagaagatggtaatctat-3' and 5'-aggagactagaccagtcatgac-3') and labeled with DIG-dUTP according to the manufacturer's instructions (Roche Applied Science, Mannheim, Germany). Fruits from two single-copy transgenic plants L4 and L11 were used for expression analysis and functional investigation of *MaSSIII-1* in comparison to wild-type.

Statistical Analysis

Three biological replicates were performed for each sample, unless specified otherwise. Statistical analyses were performed using Microsoft Excel and SPSS (Chicago, IL, USA). Analysis of variance was used to compare the statistical difference based on Student's *t*-tests, at significant levels of *p* < 0.05 (*), and *p* < 0.01 (**).

RESULTS

Change in Starch Granules, Total Starch Content, Amylopectin Content, and SS Enzyme Activity at Different Developmental and Storage Stages of Banana Fruit

During banana fruit development the fruit size gradually increases and it becomes curled in a crescent shape as fruit develops (Figure 1A). As observed using SEM, starch granules in banana pulp were barely detectable at the initial sampling time, i.e., 0 DAF, but the oval-shaped starch granules become clearly visible and were significantly increased in size as the fruit developed from 10 (6.0~8.2 µm) to 60 DAF (28.0~35.7 µm).

Morphological comparison of starch granules during this period of time indicated that the shape and number of starch granules remained consistent, but the size was significantly increased and maximized at 60 DAF (Figure 1B).

Starch granules in mature banana pulp were also observed using SEM at the 30 DPH during storage at 22°C, at 5 days' intervals. Compared to the first time point (0 DPH), the quantity of starch granules per unit volume decreased rapidly over time. After 15 DPH of storage, starch granules were hardly detectable (Figure 1C).

The total starch content and amylopectin content in pulp increased as fruit developed and peaked at 50 DAF (these two polymers reached to 67 and 44% DW, respectively) before decline at the 60 DAF time point and continued to decrease gradually during storage (Figures 1D,E), implying that after maturity starch and amylopectin may have experienced a rapid degradation process. However, the SS enzyme activity increased later than starch and amylopectin accumulation at maturity and had an abrupt decline at the very beginning of storage (Figure 1F).

Nucleotide Sequence Characteristics, Chromosomal Localization, and Phylogenetic Analysis of Banana MaSS Genes

Full-length cDNAs encoding *MaSSI*, *MaSSII*, *MaSSIII-1*, and *MaSSIII-2* were 2,076 bp, 1,851 bp, 2,397 bp, and 3,267 bp, respectively. All these sequences were deposited at GenBank and their accession numbers were listed in Figure 2. BLAST analysis against the banana DH-Pang (AA group) genome sequence database² revealed that *MaSSI*, *MaSSII*, *MaSSIII-1*, and *MaSSIII-2* are located on chromosome 3, 6, 11, and 5, respectively (Supplementary Figure S1). The sequence analysis also revealed markedly different primary structures as *MaSSI*, *MaSSII*, *MaSSIII-1*, and *MaSSIII-2* contain 25, 6, 5, and 9 exons, respectively. The stop codon usage is also different as TAA was used by *MaSSI* and *MaSSIII-1*, but TGA was used by *MaSSII* and *MaSSIII-2* (Supplementary Figure S1).

The deduced amino acid sequences of the *MaSSI* and *MaSSII* shared three conserved regions, referred to as Domain I, II, and III (Supplementary Table S2), as previously identified in SS enzymes from amaranth (Park et al., 2012). The *MaSSIII-1* and *MaSSIII-2* amino acid sequences contained four distinct regions: a transit peptide region, a variable repeat region, a SSIII specific region, and a C-terminal catalytic domain (Supplementary Table S3), as previously identified in SSIII enzymes from wheat (Li et al., 2000). According to PI/MW software analysis³, the predicted molecular weights of the *MaSSI*, *MaSSII*, *MaSSIII-1*, and *MaSSIII-2* proteins were 76.69, 69.85, 90.69, and 119.26 kDa, respectively, and their theoretical pIs were 5.24, 5.36, 6.44, and 8.21, respectively.

To elucidate phylogenetic relationship of banana MaSS genes, the four deduced polypeptide sequences were aligned

²<http://banana-genome.cirad.fr/>

³<http://expasy.org/computepi/>

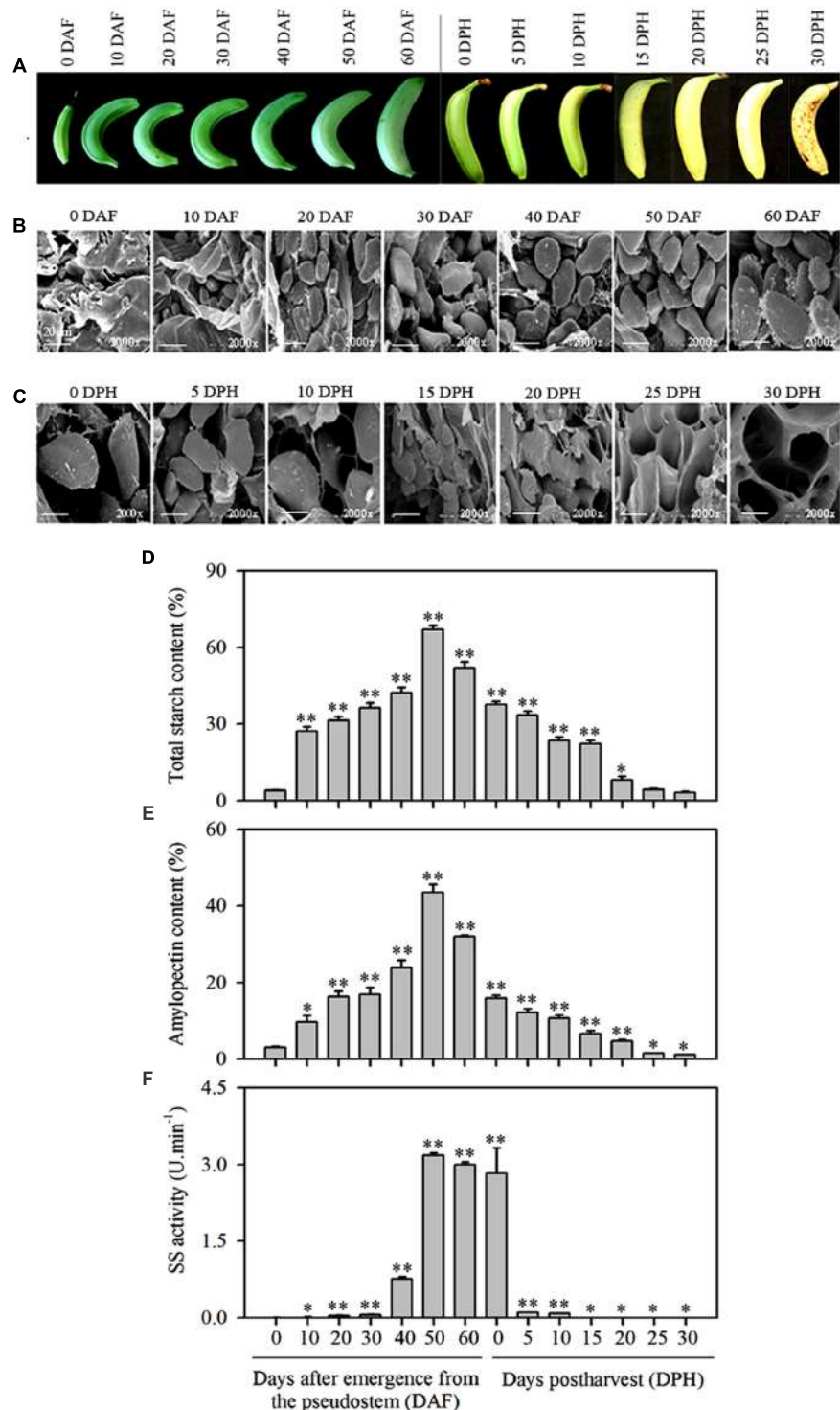


FIGURE 1 | Changes in starch granules, total starch content, amylopectin content, and SS activity in banana pulp at different stages of development and during storage. (A) Banana fruit at different development stages (0, 10, 20, 30, 40, 50, and 60 DAF) and following storage for varying amounts of time (0, 5, 10, 15, 20, 25, and 30 DPH). **(B)** SEM of starch granules in pulp during banana fruit development. **(C)** SEM of starch granules in pulp during banana fruit storage. **(D)** Total starch content in banana pulp at different stages of development and during storage. **(E)** Amylopectin content in banana pulp at different stages of development and during storage. **(F)** SS activity in banana pulp at different stages of development and during storage. DAF: days after emergence from the pseudostem; DPH: days of post-harvest. The vertical bars represent the mean \pm SD of three replicates. Asterisks indicate significant difference from 0 DAF and 0 DPH vs. the following days (* $p < 0.05$; ** $p < 0.01$). Scale bar = 20 μm .

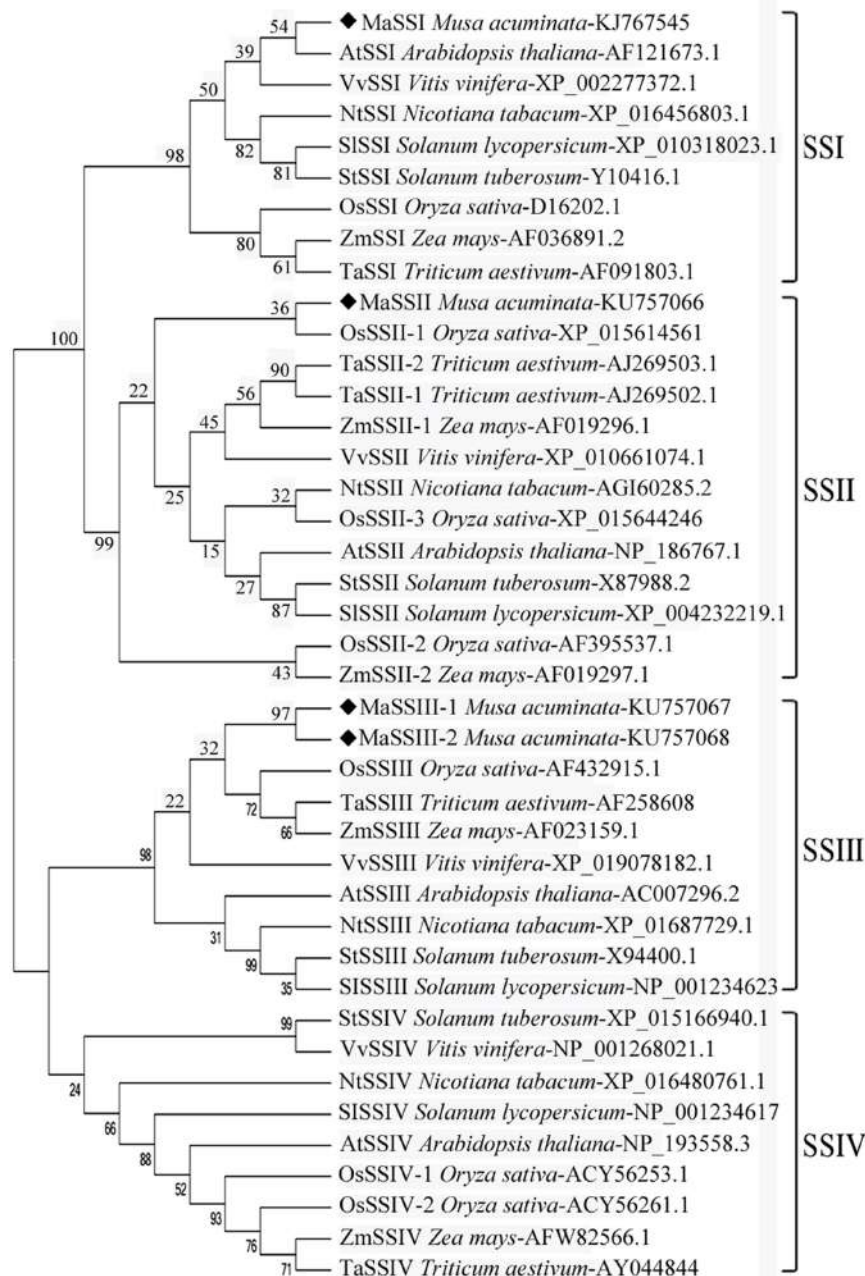


FIGURE 2 | Phylogeny of MaSSI, MaSSII, MaSSIII-1, and MaSSIII-2 amino acid sequences in relation to other known SS sequences. Bootstrapping was performed with 1000 replicates. The numbers indicated for each clade represent bootstrap support values given as percentages. Scale bar represents 0.2 substitutions per amino acid position.

with orthologous SS sequences and a NJ tree was constructed (Figure 2). MaSSIII-1 and MaSSIII-2 are aligned next to each other, forming a side branch in association with other SSIII sequences from monocot species. Similarly, MaSSI and MaSSII are clustered together with their respective orthologs from other species. This may also indicate that the divergence of the SSI, SSII and SSIII occurred prior to the speciation of these plant species, but the separation of SSIII-1 and SSIII-2 might be of a more

recent history likely through a gene duplication and subsequent divergence.

Spatially and Temporally Differential Expression of Four MaSS Genes

The spatial expression patterns of the four MaSS genes were analyzed by qRT-PCR in seven different tissues, including

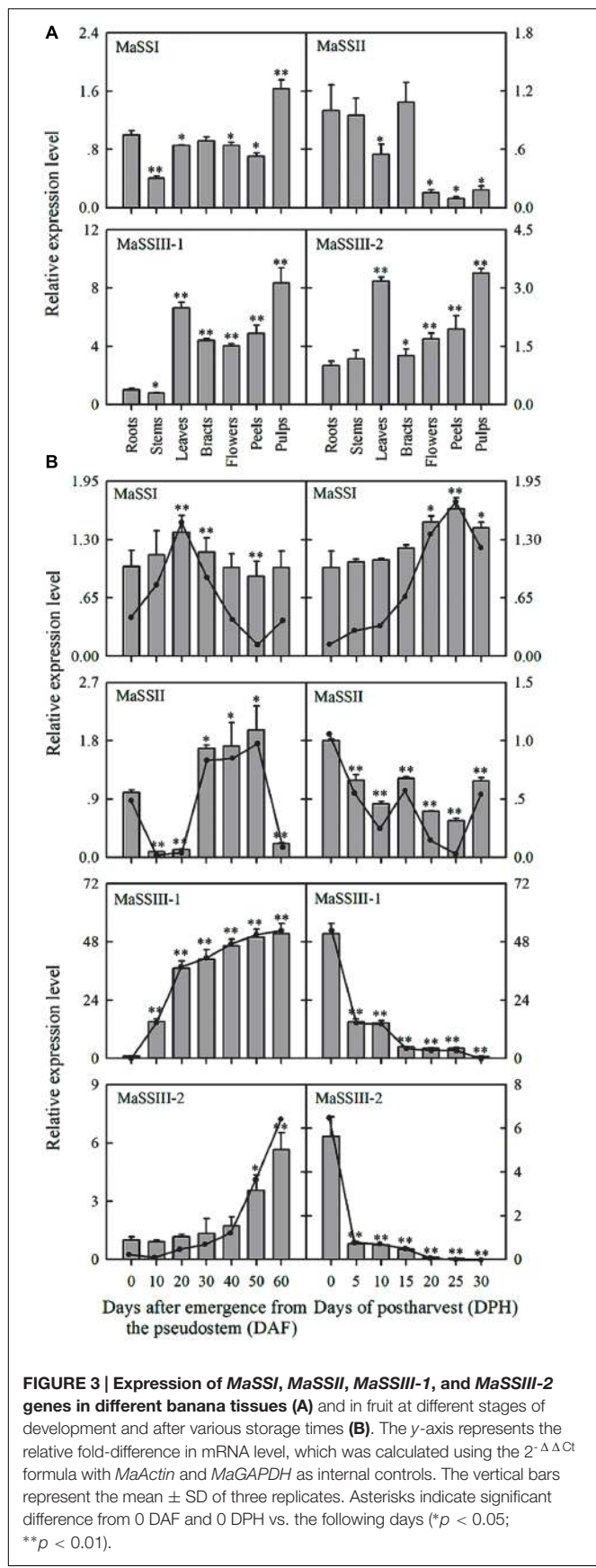


FIGURE 3 | Expression of *MaSSI*, *MaSSII*, *MaSSIII-1*, and *MaSSIII-2* genes in different banana tissues (A) and in fruit at different stages of development and after various storage times (B). The y-axis represents the relative fold-difference in mRNA level, which was calculated using the $2^{-\Delta\Delta Ct}$ formula with *MaActin* and *MaGAPDH* as internal controls. The vertical bars represent the mean \pm SD of three replicates. Asterisks indicate significant difference from 0 DAF and 0 DPH vs. the following days (* $p < 0.05$; ** $p < 0.01$).

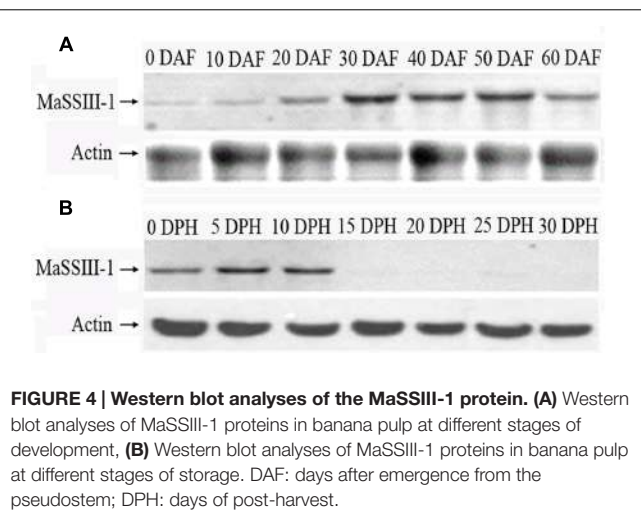


FIGURE 4 | Western blot analyses of the *MaSSIII-1* protein. (A) Western blot analyses of *MaSSIII-1* proteins in banana pulp at different stages of development. **(B)** Western blot analyses of *MaSSIII-1* proteins in banana pulp at different stages of storage. DAF: days after emergence from the pseudostem; DPH: days of post-harvest.

roots, stems, leaves, bracts, flowers, peels, and pulp (60 DAF) (**Figure 3A**). *MaSSI* was expressed at low levels in all tissues examined with the highest expression in pulps. *MaSSII* was also found to express low in all the vegetative tissues, including roots, stems, leaves, and bracts, and particularly low in flowers and fruit tissues. The expression patterns of *MaSSIII-1* and *MaSSIII-2* were very similar, with highest expression in pulps and leaves (starch content in leaves was approximately $22.67 \pm 1.32\%$), but that *MaSSIII-1* had the highest levels of expression.

The temporal expression of *MaSSI*, *MaSSII*, *MaSSIII-1*, and *MaSSIII-2* during banana fruit development was also determined by qRT-PCR (**Figure 3B**). Despite of being highly variable, the expression levels of *MaSSI* and *MaSSII* genes were found to be generally low throughout the entire banana pulp development. Both *MaSSIII-1* and *MaSSIII-2* showed a sharp increase of expression during the fruit development, the increase in expression occurred earlier in *MaSSIII-1* than in *MaSSIII-2*, with the highest expression detected at the last sampling stage when banana had reached its maturity. However, the expression of *MaSSIII-1* was about 10~20-fold higher than that of *MaSSIII-2* during the fruit development.

When the naturally ripen banana fruits were subjected to varying period of storage, the *MaSS* genes were also found to be differentially expressed (**Figure 3B**). *MaSSII* showed consistently low levels of expression throughout the storage period, but the *MaSSI* expression was slightly increased during storage. The seemingly negative association between *MaSSI* expression and starch degradation needs to be further investigated. Although there can be a lack of congruency between transcript and activity, it is possible that there can be some starch biosynthesis occurring even during net degradation (Luengwilai and Beckles, 2009). In contrast, a drastic reduction of expression was detected at 5 days after storage, as observed in both *MaSSIII-1* and *MaSSIII-2*.

Western Blot Analyses of *MaSSIII-1* Protein

Western blot analysis with rabbit anti-*MaSSIII-1* polyclonal antibody as a probe indicated that the size of *MaSSIII-1*

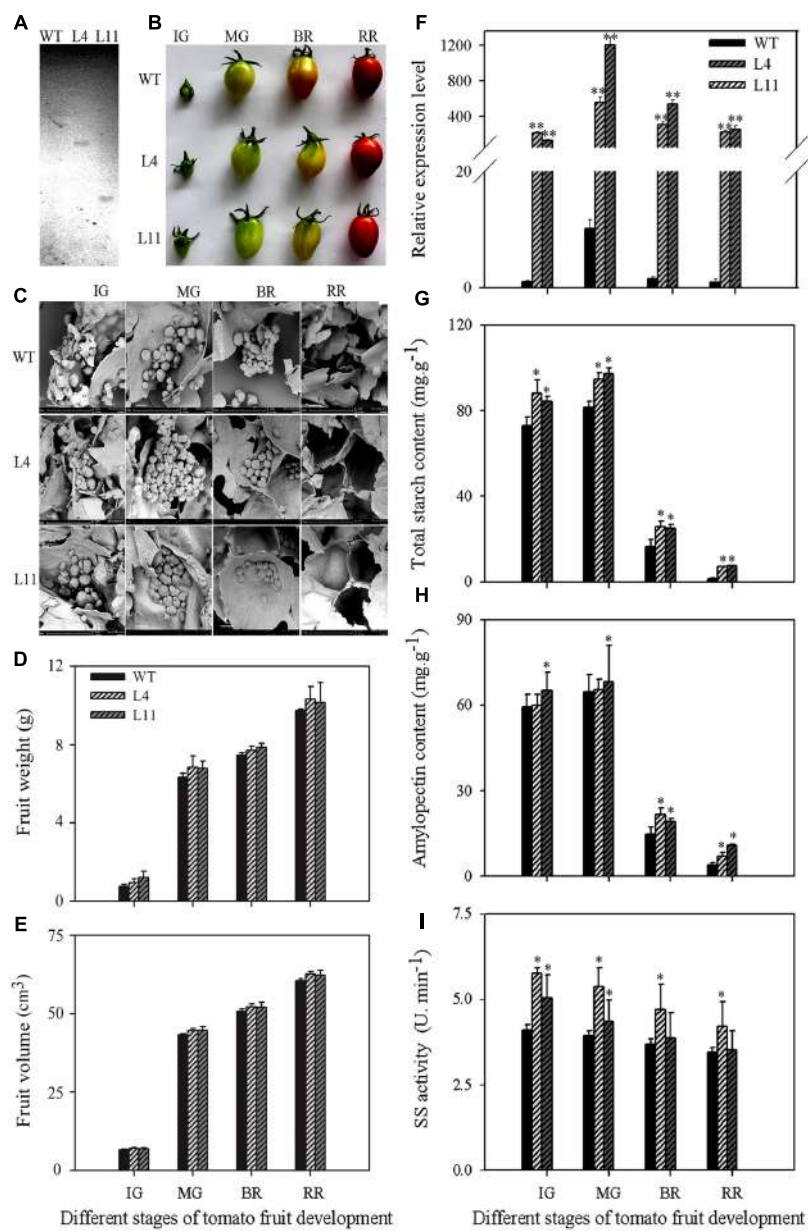


FIGURE 5 | Southern blot analysis (**A**) and change of fruit shape (**B**), starch granule (**C**), fruit weight (**D**), fruit volume (**E**), gene expression (**F**), total starch content (**G**), amylopectin content (**H**), and SS enzyme activity (**I**) at different developmental stages of *MaSSIII-1* transgenic plants in tomato. WT: wild-type; L4, L11: *MaSSIII-1* transgenic plants; IG: immature green; MG: mature-green; BR: orange-breaker; RR: red ripening stage. Asterisks indicate significant difference between the WT and *MaSSIII-1* transgenic plants (* $p < 0.05$; ** $p < 0.01$). Three biological experiments were performed, which produced similar results. Scale bar = 15 μ m.

is approximately 90.0 kDa, which is consistent with the molecular weight (90.69 kDa) as predicted by the PeptideMass program. The expression of *MaSSIII-1* protein was gradually increased during banana fruit development, but drastically reduced from 0 to 30 DPH of storage (Figures 4A,B). The Western blot results was consistent with changes in starch granules (Figures 1B,C), amylopectin content (Figure 1E) and SS activity (Figure 1F) during banana development and ripening, suggesting the expression of *MaSSIII-1* protein might play an important role in regulating amylopectin

metabolism in banana fruit during development and ripening.

Overexpression of *MaSSIII-1* in Tomato Changes the Morphology of Starch Granules and Increases the Amylopectin Content and SS Activity

To further examine the function of *MaSSIII-1* during fruit development and ripening, *MaSSIII-1* was introduced into a

pCAMBIA-1302 vector under the transcriptional control of the CaMV 35S promoter. Two single-copy transgenic plants (named L4 and L11) were identified by Southern blot analysis (**Figure 5A**). The fruit shape, starch granule morphology, gene expression, total starch content, amylopectin content, and SS activity were investigated in the wild-type (WT) and the *MaSSIII-1* overexpressing transgenic plants.

Compared to WT, the fruit shape of *MaSSIII-1* transgenic plants did not change (**Figure 5B**), but the morphology of starch granules was significantly altered from immature green (IG) to orange-breaker (BR) in transgenic tomato plants, severe cracks in the surface of starch granules were observed (**Figure 5C**). For fruit weight and volume, there are no significant differences between *MaSSIII-1* transgenic plants and WT (**Figures 5D,E**). Overexpression of *MaSSIII-1* in tomato plants significantly increased the gene expression (**Figure 5F**), *SISSIII-1* (NP_001234623; *MaSSIII-1* orthologs) expression in tomato fruit was lower than that of *MaSSIII-1* transgenic plants (**Figure 5F** and **Supplementary Figure S2**). At IG and mature-green (MG) stages, total starch content, amylopectin content, and SS activity showed significant differences between transgenic plants and WT (**Figures 5G–I**). Especially at the MG stage, the gene expression, total starch content, amylopectin content, and SS activity significantly increased 55~120-fold, 13.47~15.83 mg·g⁻¹, 6.36~9.17 mg·g⁻¹, and 0.54~0.80 U·min⁻¹ in the transgenic fruits compared to WT, respectively.

DISCUSSION

Despite of the extensive studies on cereal starch, little information is available regarding the dynamics of starch accumulation (net result of starch synthesis and degradation), SS activity, and amylopectin metabolism during fruit development and storage in fresh starchy fruits, such as banana. In tomato, starch is transiently accumulated during fruit development and degraded within the lifecycle of that organ, while starch synthesis and degradation are occurring simultaneously (Luengwilai and Beckles, 2009). However, change characteristics of SS activity are unclear. In this study, a temporal modulation in starch content was found concomitant to banana fruit development and storage. The result was consistent with the report of tomato (Luengwilai and Beckles, 2009). SS activity increased as the starch granule expanded in size and amylopectin content increased during fruit development, but decreased significantly along with the degradation of amylopectin and starch granule during storage. Moreover, we found that SS activity increased later than starch and amylopectin accumulation, the same was true for transcript and protein analyses, implying SS act at later stages of fruit development while other enzymes may act in the early phases.

The SS isoforms comprise at least four families (namely SSI, SSII, SSIII, and SSIV) in plants and play important roles in amylopectin biosynthesis (Park et al., 2012). GBSS as a separate from the other SS isoforms also influences biosynthesis of extra-long unit chains of amylopectin in rice (Hanashiro et al., 2008).

Six GBSS genes have been cloned and identified in banana (Miao et al., 2014). In this report, we characterized the function of *MaSSIII-1* in amylopectin metabolism of banana fruit and described the putative role of the other MaSS family members. Four MaSSs could be categorized into three classes, including *MaSSI*, *MaSSII*, and *MaSSIII*s (*MaSSIII-1* and *MaSSIII-2*). This scenario seems to apply in some lower green algae species where the gene distribution of SSIV is patchy (Deschamps et al., 2008). Moreover, in Arabidopsis the role of SSIV in starch granule seeding can be replaced, in part, by the phylogenetically related SSIII (Szydlowski et al., 2011). Sequence analysis indicated that the *MaSSI*, *II*, *III-1*, and *III-2* genes showed characteristics of a typical plant SS gene (Li et al., 2000; Park et al., 2012). The *MaSSI* and *MaSSII* amino acid sequences shared three conserved regions encoding Domain I, II, and III, respectively (Park et al., 2012). Domain I is a putative N-terminal transit peptide, Domains II and III are the C-terminal catalytic domain (Park et al., 2012). The amino acid sequences of *MaSSIII-1* and *MaSSIII-2* contained four distinct regions: a transit peptide region, a variable repeat region, a SSIII specific region, and a C-terminal catalytic domain. The SSIII domain organization was reported in wheat (Li et al., 2000).

Starch synthase paralogs show varying spatial-temporal expression (Senoura et al., 2004; Dian et al., 2005). *MaSSI* and *MaSSII* were found to express in low levels in vegetative organs, flower and banana fruits, similar to their homologs in kidney bean (Senoura et al., 2004) and rice (Jiang et al., 2004). In comparison, *MaSSIII-1* and *MaSSIII-2* were abundantly expressed in the late phase of developing fruit pulp, with the expression level of *MaSSIII-1* being significantly higher (**Figure 3A**). Such an observation is consistent with previous studies in rice, wheat, and Arabidopsis (Li et al., 2000; Dian et al., 2005; Busi et al., 2008; Valdez et al., 2008). Taken together, it is proposed that the four MaSS genes cloned from banana fruit may play divergent roles, with *MaSSI* and *MaSSII* being house-keeping, but *MaSSIII-1* and *MaSSIII-2* expression at transcription level clearly occurs at later stages of fruit development, they're not involved in amylopectin synthesis during early phase of fruit development.

SSIII protein as a catalytic factor plays an important role in amylopectin metabolism (Zhu et al., 2014; Huang et al., 2016). SSIII contributes the major activity (80% of the total) in potato tubers (Abel et al., 1996). In Arabidopsis, loss of both SSII and SSIII caused slower plant growth and dramatically reduced starch content (Zhang et al., 2008). Defective SSIII mutations resulted in change of starch structure into large clusters with more singly branched building blocks in amylopectin in maize (Zhu et al., 2014). Inhibition of SSIII expression resulted in a drastic drop in the overall rate of starch accumulation and the proportion of amylopectin with very long chains in potato (Abel et al., 1996; Edwards et al., 1999). SSIII activity was found to affect starch phosphorylation in potato tubers (Carpenter et al., 2015). In fresh fruits, whether starch metabolism was affected by SS, as far as we know there has not been reported. In this study, *MaSSIII-1* transcript in both transgenic lines was 100-fold higher than WT. SS activity, total starch content, and amylopectin content

were enhanced significantly by overexpressing *MaSSIII-1* gene in tomato transgenic plants at MG stage (**Figure 5**), suggesting these parameter increases may be attributed to MaSSIII because of increased transcript and polypeptide. Similar results were reported in wheat (Li et al., 2000) and rice (Dian et al., 2005), but this is the first report in a fresh fruit species. In addition, we found that overexpression of *MaSSIII-1* in tomato fruit showed severe cracks in the surface of starch granules and changed the starch granules morphology. This study suggests that *MaSSIII-1* is a key gene in the amylopectin biosynthesis and therefore it could be used as a useful tool for marker assisted molecular breeding in banana.

CONCLUSION

Starch synthase activity increased along with the amylopectin accumulation at later stages of banana fruit development, but declined during storage. Four SS genes encoding *MaSSI*, *MaSSII*, *MaSSIII-1*, and *MaSSIII-2* were cloned and characterized. Expression pattern of only *MaSSIII-1* was highly consistent with dynamic changes in starch granules, amylopectin content, and SS activity. *MaSSIII-1* transgenic lines distinctly changed the morphology of starch granules. Overexpression of *MaSSIII-1* in tomato plants significantly increased the amylopectin accumulation and SS activity in comparison to WT. This is the first report about the *MaSSIII-1* gene involved in amylopectin metabolism in a fresh fruit species. These findings establish a solid foundation to further regulate the amylopectin metabolism in banana fruits or other fresh fruits using the *MaSSIII-1* or its homologous genes.

AUTHOR CONTRIBUTIONS

ZJ and BX conceived and designed the experiments. HM, PS, QL, CJ, JL, and WH performed the experiments and carried

REFERENCES

- Abel, G. J., Springer, F., Willmitzer, L., and Kossmann, J. (1996). Cloning and functional analysis of a cDNA encoding a novel 139 kDa starch synthase from potato (*Solanum tuberosum* L.). *Plant J.* 10, 981–991. doi: 10.1046/j.1365-313X.1996.10060981.x
- Arshad, W., Haq, I. U., Waheed, M. T., Mysore, K. S., and Mirza, B. (2014). Agrobacterium-mediated transformation of tomato with rolB gene result in enhancement of fruit quality and foliar resistance against fungal pathogens. *PLoS ONE* 9:e96979. doi: 10.1371/journal.pone.0096979
- Bierhals, J. D., Lajolo, F. M., Cordenunsi, B. R., and Oliveira do Nascimento, J. R. (2004). Activity, cloning, and expression of an isoamylase-type starch-debranching enzyme from banana fruit. *J. Agric. Food Chem.* 52, 7412–7418. doi: 10.1021/jf049300g
- Bischof, S., Umhang, M., Eicke, S., Streb, S., Qi, W., and Zeeman, S. C. (2013). *Cecropia peltata* accumulates starch or soluble glycogen by differentially regulating starch biosynthesis genes. *Plant Cell* 25, 1400–1415. doi: 10.1105/tpc.113.109793
- Busi, M. V., Palopoli, N., Valdez, H. A., Formasari, M. S., Wayllace, N. Z., Gomez-Casati, D. F., et al. (2008). Functional and structural characterization of the out the analysis. HM, PS, and QL designed the experiments and wrote the manuscript. All authors read and approved the final manuscript.

ACKNOWLEDGMENTS

This work was supported by the National Natural Science Foundation of China (31401843 and 31071788), the Modern Agro-industry Technology Research System (CARS-32), the 973 Projects (2014CB160314), and the Natural Science Foundation of Hainan Province (314100).

SUPPLEMENTARY MATERIAL

The Supplementary Material for this article can be found online at: <http://journal.frontiersin.org/article/10.3389/fpls.2017.00454/full#supplementary-material>

FIGURE S1 | Sequence motifs and chromosomal localization of four MaSS genes in banana. (A) Structural organization of banana MaSS genes, solid boxes indicate exons, and bold lines represent introns, (B) Chromosomal localization of banana MaSS genes.

FIGURE S2 | Expression of SiSSIII-1 at different stages of development in tomato fruit. IG: immature green; MG: mature-green; BR: orange-breaker; RR: red ripening stage. The y-axis represents the relative fold-difference in mRNA level, which was calculated using the $2^{-\Delta\Delta Ct}$ formula. The vertical bars represent the mean \pm SD of three replicates. Asterisks indicate significant difference from IG stage vs. the following stages (* $p < 0.05$; ** $p < 0.01$).

TABLE S1 | Primers used in this study.

TABLE S2 | Comparison of the deduced amino acid sequences of banana fruit MaSSI and MaSSII. The three consensus regions (Domain I, II, and III) for both starch synthases are highlighted in bold and box.

TABLE S3 | Comparison of the deduced amino acid sequences of banana fruit MaSSIII-1 and MaSSIII-2. The four consensus regions (Transit peptide region, Variable repeat region, SSIII specific region, and Catalytic domain) for both starch synthases are highlighted in bold and box.

catalytic domain of the starch synthase III from *Arabidopsis thaliana*. *Proteins* 70, 31–40. doi: 10.1002/prot.21469

Carpenter, M. A., Joyce, N. I., Genet, R. A., Cooper, R. D., Murray, S. R., Noble, A. D., et al. (2015). Starch phosphorylation in potato tubers is influenced by allelic variation in the genes encoding glucan water dikinase, starch branching enzymes I and II, and starch synthase III. *Front. Plant Sci.* 6:143. doi: 10.3389/fpls.2015.00143

Crofts, N., Abe, N., Oitome, N. F., Matsushima, R., Hayashi, M., Tetlow, I. J., et al. (2015). Amylopectin biosynthetic enzymes from developing rice seed form enzymatically active protein complexes. *J. Exp. Bot.* 66, 4469–4482. doi: 10.1093/jxb/erv122

de Barros Mesquita, C., Leonel, M., Franco, C. M., Leonel, S., Garcia, E. L., and Dos Santos, T. P. (2016). Characterization of banana starches obtained from cultivars growth in Brazil. *Int. J. Biol. Macromol.* 89, 632–639. doi: 10.1016/j.ijbiomac.2016.05.040

Delvallé, D., Dumez, S., Wattebled, F., Roldán, I., Planchot, V., Berbezzy, P., et al. (2005). Soluble starch synthase I: a major determinant for the synthesis of amylopectin in *Arabidopsis thaliana* leaves. *Plant J.* 43, 398–412. doi: 10.1111/j.1365-313X.2005.02462.x

Deschamps, P., Moreau, H., Worden, A. Z., Dauvillée, D., and Ball, S. G. (2008). Early gene duplication within chloroplastida and its correspondence with

- relocation of starch metabolism to chloroplasts. *Genetics* 178, 2373–2387. doi: 10.1534/genetics.108.087205
- D'Hont, A., Denoeud, F., Aury, J. M., Baurens, F. C., Carreel, F., Garsmeur, O., et al. (2012). The banana (*Musa acuminata*) genome and the evolution of monocotyledonous plants. *Nature* 488, 213–217. doi: 10.1038/nature11241
- Dian, W., Jiang, H. W., and Wu, P. (2005). Evolution and expression analysis of starch synthase III and IV in rice. *J. Exp. Bot.* 56, 623–632. doi: 10.1093/jxb/eri065
- Edwards, A., Fulton, D. C., Hylton, C. M., Jobling, S. A., Gidley, M., Rössner, U., et al. (1999). A combined reduction in activity of starch synthases II and III of potato has novel effects on the starch of tubers. *Plant J.* 17, 251–261. doi: 10.1046/j.1365-313X.1999.00371.x
- Fujita, N., Goto, S., Yoshida, M., Suzuki, E., and Nakamura, Y. (2008). The function of rice starch synthase I expressed in *E. coli*. *J. Appl. Glycosci.* 55, 167–172. doi: 10.1093/jxb/eri065
- Gámez-Arjona, F. M., Raynaud, S., Ragel, P., and Mérida, A. (2014). Starch synthase 4 is located in the thylakoid membrane and interacts with plastoglobule-associated proteins in *Arabidopsis*. *Plant J.* 80, 305–316. doi: 10.1111/tpj.12633
- Hanashiro, I., Itoh, K., Kuratomi, Y., Yamazaki, M., Igarashi, T., Matsugasako, J., et al. (2008). Granule-bound starch synthase I is responsible for biosynthesis of extra-long unit chains of amylopectin in rice. *Plant Cell Physiol.* 49, 925–933. doi: 10.1093/pcp/pcn066
- Huang, B., Keeling, P. L., Hennen-Bierwagen, T. A., and Myers, A. M. (2016). Comparative in vitro analyses of recombinant maize starch synthases SSII, SSIIa, and SSIII reveal direct regulatory interactions and thermosensitivity. *Arch. Biochem. Biophys.* 16, 30051–30060. doi: 10.1016/j.abb.2016.02.032
- Hubbard, N. L., Pharr, D. M., and Huber, S. C. (1990). Role of sucrose phosphate synthase in sucrose biosynthesis in ripening bananas and its relationship to the respiratory climacteric. *Plant Physiol.* 94, 201–208.
- Jeon, J. S., Ryoo, N., Hahn, T. R., Walia, H., and Nakamura, Y. (2010). Starch biosynthesis in cereal endosperm. *Plant Physiol. Biochem.* 48, 383–392. doi: 10.1016/j.plaphy.2010.03.006
- Jiang, H., Dian, W., Liu, F., and Wu, P. (2004). Molecular cloning and expression analysis of three genes encoding starch synthase II in rice. *Planta* 218, 1062–1070. doi: 10.1007/s00425-003-1189-y
- Leterrier, M., Holappa, L. D., Broglie, K. E., and Beckles, D. M. (2008). Cloning, characterization and comparative analysis of a starch synthase IV gene in wheat: functional and evolutionary implications. *BMC Plant Biol.* 8:98. doi: 10.1186/1471-2229-8-98
- Li, P., Miao, H. X., Ma, Y. W., Wang, L., Hu, G. B., Ye, Z. X., et al. (2015). *CrWSKP1*, an *SKP1-like* gene, is involved in the self-incompatibility reaction of "Wuzishatangu" (*Citrus reticulate* Blanco). *Int. J. Mol. Sci.* 16, 21695–21710. doi: 10.3390/ijms160921695
- Li, Z., Mouille, G., Kosar-Hashemi, B., Rahman, S., Clarke, B., Gale, K. R., et al. (2000). The structure and expression of the wheat starch synthase III gene. Motifs in the expressed gene define the lineage of the starch synthase III gene family. *Plant Physiol.* 123, 613–624.
- Lin, D. G., and Jeang, C. L. (2005). Cloning, expression, and characterization of soluble starch synthase I cDNA from taro (*Colocasia esculenta* Var. *esculenta*). *J. Agric. Food Chem.* 53, 7985–7990. doi: 10.1021/jf0504566
- Liu, H., Yu, G., Wei, B., Wang, Y., Zhang, J., Hu, Y., et al. (2015). Identification and phylogenetic analysis of a novel starch synthase in maize. *Front. Plant Sci.* 6:1013. doi: 10.3389/fpls.2015.01013
- Livak, K. J., and Schmittgen, T. D. (2001). Analysis of relative gene expression data using real-time quantitative PCR and the $2^{-\Delta\Delta CT}$ Method. *Methods* 25, 402–408. doi: 10.1006/meth.2001.1262
- Low, D. Y., Williams, B. A., D'Arcy, B. R., Flanagan, B. M., and Gidley, M. J. (2015). In vitro fermentation of chewed mango and banana: particle size, starch and vascular fibre effects. *Food Funct.* 6, 2464–2474. doi: 10.1039/c5fo00363f
- Luengwilai, K., and Beckles, D. M. (2009). Starch granules in tomato fruit show a complex pattern of degradation. *J. Agric. Food Chem.* 57, 8480–8487. doi: 10.1021/jf901593m
- Miao, H. X., Sun, P. G., Liu, W. X., Xu, B. Y., and Jin, Z. Q. (2014). Identification of genes encoding granule-bound starch synthase involved in amylose metabolism in banana fruit. *PLoS ONE* 9:e88077. doi: 10.1371/journal.pone.0088077
- Nakamura, Y., Yuki, K., Park, S. Y., and Ohya, T. (1989). Carbohydrate metabolism in the developing endosperm of rice grains. *Plant Cell Physiol.* 30, 833–839. doi: 10.1104/pp.108.125633
- Nishi, A., Nakamura, Y., Tanaka, N., and Satoh, H. (2001). Biochemical and genetic analysis of the effects of amylose-extender mutation in rice endosperm. *Plant Physiol.* 127, 459–472.
- Park, Y. J., Nishikawa, T., Tomooka, N., and Nemoto, K. (2012). Molecular cloning and expression analysis of a gene encoding soluble starch synthase I from grain amaranth. *Mol. Breed.* 30, 1065–1076.
- Ral, J. P., Colleoni, C., Wattebled, F., Dauvillée, D., Nempon, C., Deschamps, P., et al. (2006). Circadian clock regulation of starch metabolism establishes GBSSI as a major contributor to amylopectin synthesis in *Chlamydomonas reinhardtii*. *Plant Physiol.* 142, 305–317. doi: 10.1104/pp.106.081885
- Roldán, I., Wattebled, F., Lucas, M. M., Delvalle, D., Planchot, V., Jiménez, S., et al. (2007). The phenotype of soluble starch synthase IV defective mutant of *Arabidopsis thaliana* suggests a novel function of elongation enzyme in the control of starch granule formation. *Plant J.* 49, 492–504. doi: 10.1111/j.1365-313X.2006.02968.x
- Sarawong, C., Schoenlechner, R., Sekiguchi, K., Berghofer, E., and Ng, P. K. (2014). Effect of extrusion cooking on the physicochemical properties, resistant starch, phenolic content and antioxidant capacities of green banana flour. *Food Chem.* 143, 33–39. doi: 10.1016/j.foodchem.2013.07.081
- Schwarte, S., Brust, H., Steup, M., and Tiedemann, R. (2013). Intraspecific sequence variation and differential expression in starch synthase genes of *Arabidopsis thaliana*. *BMC Res. Notes* 6:84. doi: 10.1186/1756-0500-6-84
- Senoura, T., Isono, N., Yoshikawa, M., Asao, A., Hamada, S., Watanabe, K., et al. (2004). Characterization of starch synthase I and II expressed in early developing seeds of kidney bean (*Phaseolus vulgaris* L.). *Biosci. Biotechnol. Biochem.* 68, 1949–1960.
- Subasinghe, R. M., Liu, F., Polack, U. C., Lee, E. A., Emes, M. J., and Tetlow, I. J. (2014). Multimeric states of starch phosphorylase determine protein-protein interactions with starch biosynthetic enzymes in amyloplasts. *Plant Physiol. Biochem.* 83, 168–179. doi: 10.1016/j.plaphy.2014.07.016
- Syahariza, Z. A., Sar, S., Hasjim, J., Tizzotti, M. J., and Gilbert, R. G. (2013). The importance of amylose and amylopectin fine structures for starch digestibility in cooked rice grains. *Food Chem.* 136, 742–749. doi: 10.1016/j.foodchem.2012.08.053
- Szydlowski, N., Ragel, P., Hennen-Bierwagen, T. A., Planchot, V., Myers, A. M., Mérida, A., et al. (2011). Integrated functions among multiple starch synthases determine both amylopectin chain length and branch linkage location in *Arabidopsis* leaf starch. *J. Exp. Bot.* 62, 4547–4559. doi: 10.1093/jxb/err172
- Szydlowski, N., Ragel, P., Raynaud, S., Lucas, M. M., Roldán, I., Montero, M., et al. (2009). Starch granule initiation in *Arabidopsis* requires the presence of either class IV or class III starch synthases. *Plant Cell* 21, 2443–2457. doi: 10.1101/tpc.109.066522
- Takemoto-Kuno, Y., Suzuki, K., Nakamura, S., Satoh, H., and Ohtsubo, K. (2006). Soluble starch synthase I effects differences in amylopectin structure between indica and japonica rice varieties. *J. Agric. Food Chem.* 54, 9234–9240. doi: 10.1021/jf061200i
- Torre-Gutiérrez, L., Chel-Guerrero, L. A., and Betancur-Ancona, D. (2008). Functional properties of square banana (*Musa balbisiana*) starch. *Food Chem.* 106, 1138–1144. doi: 10.1016/j.foodchem.2007.07044
- Utrilla-Coello, R. G., Rodríguez-Huezo, M. E., Carrillo-Navia, H., Hernández-Jaimes, C., Vernon-Carter, E. J., and Alvarez-Ramirez, J. (2014). In vitro digestibility, physicochemical, thermal and rheological properties of banana starches. *Carbohydr. Polym.* 101, 154–162. doi: 10.1016/j.carbpol.2013.09.019
- Valdez, H. A., Busi, M. V., Wayllace, N. Z., Parisi, G., Ugalde, R. A., and Gomez-Casati, D. F. (2008). Role of the N-terminal starch-binding domains in the kinetic properties of starch synthase III from *Arabidopsis thaliana*. *Biochemistry* 47, 3026–3032. doi: 10.1021/bi702418h
- Wikman, J., Blennow, A., Buléon, A., Putaux, J., Pérez, S., Seetharaman, K., et al. (2014). Influence of amylopectin structure and degree of phosphorylation on the molecular composition of potato starch linters. *Biopolymers* 101, 257–271. doi: 10.1002/bip.22344
- Yang, J. H., Bi, C. G., and Song, W. C. (1992). A half-grain method for analyzing the amylose content in rice grains and its application. *Acta Agron. Sin.* 18, 366–372.

- Zeeman, S. C., Kossmann, J., and Smith, A. M. (2010). Starch: its metabolism, evolution, and biotechnological modification in plants. *Annu. Rev. Plant Biol.* 61, 209–234. doi: 10.1146/annurev-arplant-042809-112301
- Zhang, P., and Hamaker, B. R. (2012). Banana starch structure and digestibility. *Carbohydr. Polym.* 87, 1552–1558. doi: 10.1016/j.carbpol.2011.09.053
- Zhang, X., Szydlowski, N., Delvallé, D., D'Hulst, C., James, M. G., and Myers, A. M. (2008). Overlapping functions of the starch synthases SSII and SSIII in amylopectin biosynthesis in *Arabidopsis*. *BMC Plant Biol.* 8:96. doi: 10.1186/1471-2229-8-96
- Zhang, X. L., Myers, A. M., and James, M. G. (2005). Mutations affecting starch synthase III in *Arabidopsis* alter leaf starch structure and increase the rate of starch synthesis. *Plant Physiol.* 138, 663–674. doi: 10.1104/pp.105.060319
- Zhu, F., Bertoft, E., and Seetharaman, K. (2014). Distribution of branches in whole starches from maize mutants deficient in starch synthase III. *J. Agric. Food Chem.* 62, 4577–4583. doi: 10.1021/jf500697g

Conflict of Interest Statement: The authors declare that the research was conducted in the absence of any commercial or financial relationships that could be construed as a potential conflict of interest.

Copyright © 2017 Miao, Sun, Liu, Jia, Liu, Hu, Jin and Xu. This is an open-access article distributed under the terms of the Creative Commons Attribution License (CC BY). The use, distribution or reproduction in other forums is permitted, provided the original author(s) or licensor are credited and that the original publication in this journal is cited, in accordance with accepted academic practice. No use, distribution or reproduction is permitted which does not comply with these terms.



Insights into the Molecular Events That Regulate Heat-Induced Chilling Tolerance in Citrus Fruits

Maria T. Lafuente *, **Beatriz Establés-Ortíz** and **Luis González-Candelas**

Department of Biotechnology, Instituto de Agroquímica y Tecnología de Alimentos (CSIC), Valencia, Spain

OPEN ACCESS

Edited by:

Maarten Hertog,
KU Leuven, Belgium

Reviewed by:

George A. Manganaris,
Cyprus University of Technology,
Cyprus
Ioannis S. Minas,
Colorado State University,
United States

*Correspondence:

Maria T. Lafuente
mtlafuente@iata.csic.es

Specialty section:

This article was submitted to
Crop Science and Horticulture,
a section of the journal
Frontiers in Plant Science

Received: 24 February 2017

Accepted: 08 June 2017

Published: 26 June 2017

Citation:

Lafuente MT, Establés-Ortíz B and González-Candelas L (2017) Insights into the Molecular Events That Regulate Heat-Induced Chilling Tolerance in Citrus Fruits. *Front. Plant Sci.* 8:1113.
doi: 10.3389/fpls.2017.01113

Low non-freezing temperature may cause chilling injury (CI), which is responsible for external quality deterioration in many chilling-sensitive horticultural crops. Exposure of chilling-sensitive citrus cultivars to non-lethal high-temperature conditioning may increase their chilling tolerance. Very little information is available about the molecular events involved in such tolerance. In this work, the molecular events associated with the low temperature tolerance induced by heating Fortune mandarin, which is very sensitive to chilling, for 3 days at 37°C prior to cold storage is presented. A transcriptomic analysis reveals that heat-conditioning has an important impact favoring the repression of genes in cold-stored fruit, and that long-term heat-induced chilling tolerance is an active process that requires activation of transcription factors involved in transcription initiation and of the WRKY family. The analysis also shows that chilling favors degradation processes, which affect lipids and proteins, and that the protective effect of the heat-conditioning treatment is more likely to be related to the repression of the genes involved in lipid degradation than to the modification of fatty acids unsaturation, which affects membrane permeability. Another major factor associated with the beneficial effect of the heat treatment on reducing CI is the regulation of stress-related proteins. Many of the genes that encoded such proteins are involved in secondary metabolism and in oxidative stress-related processes.

Keywords: cold stress, fruit physiology, gene expression, heat-conditioning, oxidative stress, physiological disorder, transcriptome, WRKY

INTRODUCTION

Storage at low non-freezing temperature is necessary to extend the postharvest life of horticultural crops because it delays senescence and reduces water loss and decay. Moreover, low-temperature treatments are required for pest control in quarantine treatments. Nevertheless, storage at temperatures below 12°C may cause injury in many chilling-sensitive crops of tropical and subtropical origin (Sevillano et al., 2009).

Abbreviations: ABA, abscisic acid; CI, chilling injury; CFGP, citrus functional genomic project; DEGs, differentially expressed genes; GST, glutathione transferase; HA, hot humid air; HICT, heat-induced chilling tolerance; HSP, heat-shock protein; HWD, hot water dip; SAM, significant analysis of microarrays; 1-MCP, 1-methylcyclopropene; OMTs, oxygen methyl transferases; ROS, reactive oxygen species; PAL, phenylalanine ammonia-lyase; SOD, superoxide dismutase; SSH, suppression subtractive hybridization; TFs, transcription factors.

Fruits of many citrus cultivars are very prone to develop chilling injury (CI) (Mulas and Schirra, 2007). Susceptibility to CI vastly differs among species. The incidence of this physiological disorder in citrus fruit also depends on pre-harvest factors, including maturation stage and environmental conditions during fruit growth (Lafuente et al., 1997), and on field temperatures prior to cold storage (Gonzalez-Aguilar et al., 2000). This might partly explain variations in the seasonal development of CI among chilling-susceptible citrus fruits, such as grapefruits and mandarins harvested in different geographical regions (Purvis et al., 1979; Lafuente et al., 1997).

Citrus fruits are the highest value fruit crop in terms of international trade. Current annual worldwide citrus production is estimated at over 137 million tons (www.fao.org/faostat) and about two-third of citrus fruit production goes for fresh consumption. Important economic losses can occur in citrus fruit because of the manifestation of CI that affects external fruit quality due to the appearance of aesthetic defects, manifested as peel pitting (Sanchez-Ballesta et al., 2003) and superficial scald (Alférez et al., 2005) on the outer colored part of the peel (flavedo).

Considerable efforts have been made to develop strategies that reduce the incidence of CI in horticultural crops (Saltveit, 1991; Wang, 1993; Lurie, 1998; Sevillano et al., 2009). Understanding the mechanisms that underlie the beneficial effects of these strategies, and the influence of pre-harvest factors (Ferguson et al., 1999; Pedreschi and Lurie, 2015), would help to develop more feasible methods to extend the postharvest storage of citrus fruits. Pre-storage temperature conditioning is the most important means of increasing chilling tolerance in citrus fruits. Temperature-conditioning methods include using: (a) intermittent warming, i.e., periodic warming above the chilling temperature; (b) application of intermediate temperatures between growing and chilling temperatures (hardening); (c) non-lethal high temperatures (Saltveit, 1991; Wang, 1993; Lurie, 1998; Schirra and Cohen, 1999). High temperature conditioning is applied by using hot humid air (HA) (Martinez-Tellez and Lafuente, 1997; Ferguson et al., 2000) or hot water dip (HWD) treatments (Wild, 1993; Rodov et al., 1995; Schirra et al., 1997). Conditioning citrus fruits with HA for 3 days at about 37°C has been consistently found to be very effective in increasing chilling tolerance without inducing heat damage. This has been demonstrated for different citrus seasons and in fruits harvested at all maturity stages, despite the variable susceptibility of fruit throughout the season (Lafuente et al., 1997; Holland et al., 1999; Gonzalez-Aguilar et al., 2000). The excellent efficacy and reproducibility of the 3-day treatment at 37°C, named curing, has been shown with Fortune mandarins (hybrid of “Dancy” mandarin x “Clementine” mandarin) as a model of study because of its high susceptibility to chilling. Therefore, this cultivar and the availability of this HA treatment have provided a very valuable tool to study the physiological mechanisms that underlie long-term heat-induced chilling tolerance in citrus fruits, and also the influence of pre-harvest factors.

Physiological studies have provided very valuable information about the involvement of hormones, oxidative stress, lipids, carbohydrates, and phenolics metabolism in the susceptibility

of citrus fruits to chilling and also in the heat-induced chilling tolerance (Lafuente et al., 2005). Moreover, physiological studies have demonstrated that pre-harvest conditions have a strong effect on the heat-induced responses in cold-stored citrus fruits. Thus, for a similar CI index, the more mature the fruit, the greater the cold-induced shift in the activity of the enzyme PAL, at the entry point of phenylpropanoids metabolism (Lafuente et al., 2003). Maturity or pre-harvest environmental conditions may also influence other chilling- or heat-induced responses as changes that occur in abscisic acid (ABA) (Lafuente et al., 1997), polyamines (Gonzalez-Aguilar et al., 1998, 2000), or in carbohydrates metabolism (Holland et al., 2002). These results envisage that the CI problem is not a simple one and indicate that heat-induced chilling tolerance in citrus fruit appears to be an active process that requires the activation of complex mechanisms, which can vary with fruit maturity stage or other pre-harvest factors.

Studies on molecular events related to citrus fruit tolerance to chilling began at the beginning of the twenty-first century. Different stress-related genes, induced by cold stress or by temperature-conditioning treatments that favor chilling tolerance, were identified in mandarins and grapefruits (Lafuente et al., 2005; Sanchez-Ballesta et al., 2006; Sapitnitskaya et al., 2006). Comparison of the results found in different citrus fruit cultivars suggested that the various temperature-conditioning treatments may induce distinct molecular mechanisms related to citrus fruit tolerance to chilling, regardless of whether they involved heat or not (Sanchez-Ballesta et al., 2003, 2004; Sapitnitskaya et al., 2006).

Information about the global mechanisms associated with cross-adaptation induced by heat to cold stress in citrus fruits is very scarce. In an early genomic approach, a suppression subtractive hybridization (SSH) cDNA library was constructed. This library was enriched in the genes induced in the flavedo of Fortune mandarins conditioned for 3 days at 37°C with HA, whose expression persisted when fruits were transferred to low temperature, and also in the genes induced by a heat+cold combination (Sanchez-Ballesta et al., 2003). About 38% of the genes in this library showed a homology with proteins of known functions. Among them, the most abundant encoded proteins involved in metabolism, plant defense responses, and transcription and signal transduction (Sanchez-Ballesta et al., 2003).

Very little information is available about the global mechanisms induced by heat or cold in the flavedo of citrus fruit that develop injury in response to chilling. Transcriptomic, proteomic, and metabolomic analyses have been performed on the pericarp and juice sacs of citrus fruit, exposed or not to heat treatments, and stored at low temperatures that did not cause CI (Perotti et al., 2011, 2015; Yun et al., 2012, 2013). As far as we are aware, only one report has compared the transcriptome profiling of the flavedo of grapefruits stored at a temperature that causes CI after being conditioned, or not, at a temperature treatment that reduces CI (Maul et al., 2008). This treatment was performed at 16°C for 7 days, so the acclimation mechanisms induced by this hardening treatment should differ, at least in part, from those related to cross-adaptation induced by heat to cold stress.

Therefore, the aim of this study has been to determine global changes in gene expression that occur in Fortune mandarins, either exposed or not to a heat-conditioning treatment (HA 37°C for 3 days, curing) and stored at low temperature. Emphasis has been placed on the changes that occur in response to the heat+cold combination because the genes in this category are the best candidates to be involved in heat-induced tolerance to chilling. These genes have been named HICT, from heat-induced chilling tolerance. With this approach we will add knowledge about cross-adaptation in plants whereby exposure to one stress, like heat, provides tolerance to another, like chilling.

MATERIALS AND METHODS

Fruit and Heat-Conditioning and Storage Temperatures

Full mature fruits of the hybrid mandarin Fortune (*Citrus clementina* Hort. Ex Tanaka x *Citrus reticulata*, Blanco) were harvested in March during three citrus seasons from a commercial orchard at Castellón, Spain. By this month, Fortune mandarins had a maturity index (°Brix/acid content) higher than 12 and the fruits have reached the maximum orange peel color (h° lower than 40) (Holland et al., 1999). Fruits were selected for homogeneous size, free from defects, and immediately delivered to the laboratory. For each experiment, fruits were randomly divided in two lots per temperature assayed. The first lot was sorted into three replicates of 10 fruits each to estimate chilling damage along fruit storage. The second lot, made up of three replicates of 10 fruits per temperature and storage period, was used to evaluate changes in gene expression. Periodically, flavedo samples were collected from the total surface of fruits, frozen and homogenized in liquid nitrogen. The homogenized tissue was stored at -80°C for later analysis.

For transcriptomic analysis, Fortune mandarins were conditioned at 37°C and 90–95% RH for up to 3 days and then were stored at 2°C and 80–85% relative humidity (RH) for 60 days. Control non-conditioned fruits were stored immediately after harvest under the same storage conditions (2°C and 80–85% RH). In addition, to determine changes in the expression of genes encoding transcription factors (TFs), another group of fruits, which were not conditioned at 37°C, were stored at a non-chilling temperature (12°C) and 80–85% RH for the same storage period.

Estimation of CI Index

Brown pit like depressions in the flavedo were the main CI symptoms in Fortune mandarins. The effect of the heat treatment on the severity of cold-induced damage was evaluated on a rating scale that ranged from 0 (no injury) to 3 (severe injury) (Figure 1A), and the CI index was calculated as previously described (Lafuente et al., 1997) by summing the products of the number of fruits in each category by the value assigned to each category in the rating scale, and dividing the sum by the total number of fruits evaluated. The results are the means of three replicate samples containing 10 fruit samples ± SE.

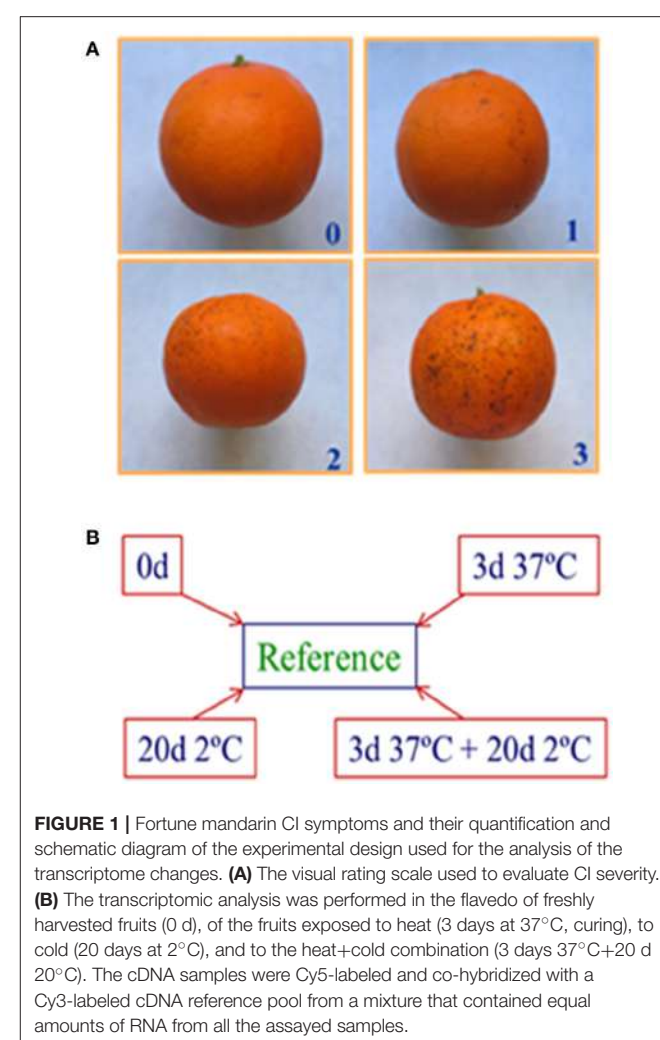


FIGURE 1 | Fortune mandarin CI symptoms and their quantification and schematic diagram of the experimental design used for the analysis of the transcriptome changes. **(A)** The visual rating scale used to evaluate CI severity. **(B)** The transcriptomic analysis was performed in the flavedo of freshly harvested fruits (0 d), of the fruits exposed to heat (3 days at 37°C, curing), to cold (20 days at 2°C), and to the heat+cold combination (3 days 37°C+20 d 20°C). The cDNA samples were Cy5-labeled and co-hybridized with a Cy3-labeled cDNA reference pool from a mixture that contained equal amounts of RNA from all the assayed samples.

RNA Isolation and cDNA Labeling and Microarray Hybridization

Total RNA was extracted from frozen flavedo as previously described by Ballester et al. (2011). Possible genomic DNA contaminations were removed by treating total RNA with Ribonuclease-free DNase (Ambion/Applied Biosystems, Austin, TX, USA) following the manufacturer's instructions and RNA concentration was measured spectrophotometrically (Nanodrop, Thermo Fisher Scientific, Madrid, Spain). RNA integrity was verified by agarose gel electrophoresis and ethidium-bromide staining (Ballester et al., 2011). cDNA synthesis and purification, dye coupling, and labeled-cDNA purification were performed according to Forment et al. (2005). Three biological replicates from samples harvested during the same citrus season or during three different seasons were used for RNA isolation and the subsequent microarray hybridization.

Microarray Hybridization, Data Acquisition, and Analysis

The analysis of the transcriptome changes that take place in the flavedo of Fortune mandarins during fruit exposure to heat

(3 d 37°C), cold (20 d 2°C), and the heat+cold combination (3 d 37°C+20 d 2°C) was done to know the molecular events associated with long-term heat-induced chilling tolerance (**Figure 1B**). Our previous data have shown that the chilling- and the heat-induced physiological responses of citrus fruits are strongly influenced by pre-harvest factors. Therefore, a transcriptomic analysis was first performed with three biological replicate samples harvested at the same maturity stage during only one citrus season and the results were compared with those obtained by using biological replicates from fruits harvested during three different seasons at the same maturity stage.

Two microarrays were used, which were developed as part of the citrus functional genomics project (CFGp) (<http://bioinfo.ibmcn.upv.es/genomics/cfgpDB/>) (Forment et al., 2005), and contained about 7,000 (7 K) and 12,000 (12 K) unigenes. The samples from different citrus seasons were analyzed with the 12 K microarray (Ballester et al., 2011), which includes all the genes of the 7 K microarray. All the genes were isolated from 52 cDNA libraries of citrus that cover different tissues, a wide range of fruit varieties, developmental and fruit ripening stages, and also distinct stress conditions (Forment et al., 2005). These microarrays include the genes isolated from a cDNA library, named FlavCurFr1, from the flavedo of Fortune mandarins fruits exposed to 37°C for periods that ranged from 4 h to 3 days, and also from fruits preconditioned for 3 days at this temperature and held from 1 to 10 days at a chilling temperature (Forment et al., 2005). The cDNA samples were Cy5-labeled and co-hybridized with a Cy3-labeled cDNA reference pool from a mixture that contained equal amounts of RNA from all the assayed samples (**Figure 1B**). This reference sample allowed to lower the number of hybridizations to make all the possible pairwise comparisons between samples (Ballester et al., 2011). Hybridized microarrays were scanned by using a GenePix 4000A scanner (Axon Instruments, Sunnyvale, CA, USA) and only spots with a background-subtracted intensity greater than 2-fold the mean of background intensity were used for normalization and further analysis (Romero et al., 2012). A significant analysis of microarrays (SAM), included in the TM4 Microarray Software Suite, was performed to identify differentially expressed genes for all possible pairwise comparisons using a False Discovery Rate threshold *p*-value < 0.01 as previously described (Ballester et al., 2011). The identification of biological processes that were significantly under- or over-represented in a set of differentially expressed genes respect to a reference group composed of all genes in the microarray with an *Arabidopsis thaliana* homolog was carried out using the program FatiGO+ (Babelomics, <http://babelomics.bioinfo.cipf.es>) (Ballester et al., 2011). A Fisher two-tailed test (*p*-value < 0.05) was independently performed for gene ontology analysis of induced and repressed genes.

Northern Analysis of Selected Transcription Factors (TFs)

Special attention was paid to transcription factors (TFs) given their relevance in modulating the expression of specific groups of genes, and also because of previous results that have highlighted the relevance of TFs in heat-induced chilling tolerance (Sanchez-Ballesta et al., 2003). A detailed study of the

expression of a group of TFs (21 TFs) selected from the 50 TFs present in the FlavCurFr1 cDNA library was performed. Changes in expression levels were analyzed by Northern blot hybridization in fruits exposed for different periods at 37°C, and in the non-conditioned and conditioned (3 days at 37°C) fruits stored for up 60 days at 2°C. Moreover, changes in their expression in non-conditioned fruits stored at a non-chilling temperature (12°C) were compared with those taking place in the non-conditioned fruits stored at the chilling temperature.

Samples of denatured total RNA (10 µg) were separated on 1.2% (w/v) agarose-formaldehyde gel, transferred to a nylon Hybond-N+ membrane (Amersham Biosciences) using 20X SSC (3 M sodium chloride, 0.3 M sodium citrate, pH 7.0) as the transfer medium and cross-linked using a UV Crosslinker UVC 500 (Hoefer, Inc.). Membranes were stained with methylene blue 0.03% in 0.3 M sodium acetate pH 5.2 to measure loading variation and pre-hybridized for 2 h at 42°C in UltrahybTM Hybridization Buffer (Ambion, Inc.). Selected probes were labeled with $\alpha^{32}\text{P}$ -dATP by linear amplification using a Strip-EZTM PCR Kit (Ambion, Inc.). Hybridization with selected probes was carried out overnight at 42°C (Ballester et al., 2006) and membranes washed and exposed to “Imaging Plate” (Fujifilm) film with intensifying screens. Quantification of the hybridization signals was performed with the Image Gauge Program V 4.0 (Fuji). The filters were stripped off and re-hybridized to the 26S rDNA *C. sinensis* probe as described by Ballester et al. (2006) to normalize the hybridization of the TFs genes. The ratio between the hybridization signal of each TF mRNA and that obtained using the 26S rDNA *C. sinensis* probe was calculated and transcript accumulations were normalized respect to the values found in freshly harvested fruits. A value of 100 was assigned to this sample.

RESULTS AND DISCUSSION

Effect of Heat-Conditioning on CI Injury of Fortune Mandarins

The effect of conditioning Fortune mandarins for 3 days at 37°C was examined in fruits harvested during three different citrus seasons. As shown in **Figure 2A**, CI developed in the non-conditioned fruit after 10 days of cold storage (2°C). The severity of the disorder was low by day 20 (CI index of about 1 in a rating scale from 0 to 3) and by day 60 all the non-conditioned fruits showed severe damage (CI index 3). Results also showed that the susceptibility of the fruits harvested during the three citrus seasons was very similar since CI damage changed similarly during cold storage in the non-conditioned fruits. As expected, conditioning the fruits at 37°C for 3 days was always very effective reducing CI. As shown in **Figures 2A,B**, Fortune mandarins from the three citrus seasons did not develop CI for at least 60 days if previously cured. On the basis of these results, samples taken from the three seasons can be very useful to compare molecular responses induced by heat conditioning and cold stress in fruits showing similar chilling susceptibility but exposed to different pre-harvest conditions.

Heat-Induced Transcriptomic Changes in Cold Stored Citrus Fruits

The heat-conditioning treatment selected to study changes in the transcriptome was one that lasted 3 days at 37°C. The treatment was selected because of its high efficacy in reducing CI has been proven to be very reproducible throughout different citrus seasons, and it is independent of pre-harvest factors (Lafuente et al., 1997; Gonzalez-Aguilar et al., 2000). Moreover, previous physiological data have shown that shortening the duration of the conditioning period would reduce the treatment's efficacy in Fortune mandarins (Gonzalez-Aguilar et al., 1998; Lafuente et al., 2011), which suggests that the heat-induced chilling tolerance is not limited only to the transient responses induced at 37°C. The treatment allowed to extend cold storage for at least 60 days. Therefore, we focused in the molecular events associated with long-term heat-induced chilling tolerance and examined changes occurring in fruits heated for 3 days at 37°C and in conditioned and non-conditioned fruits held for

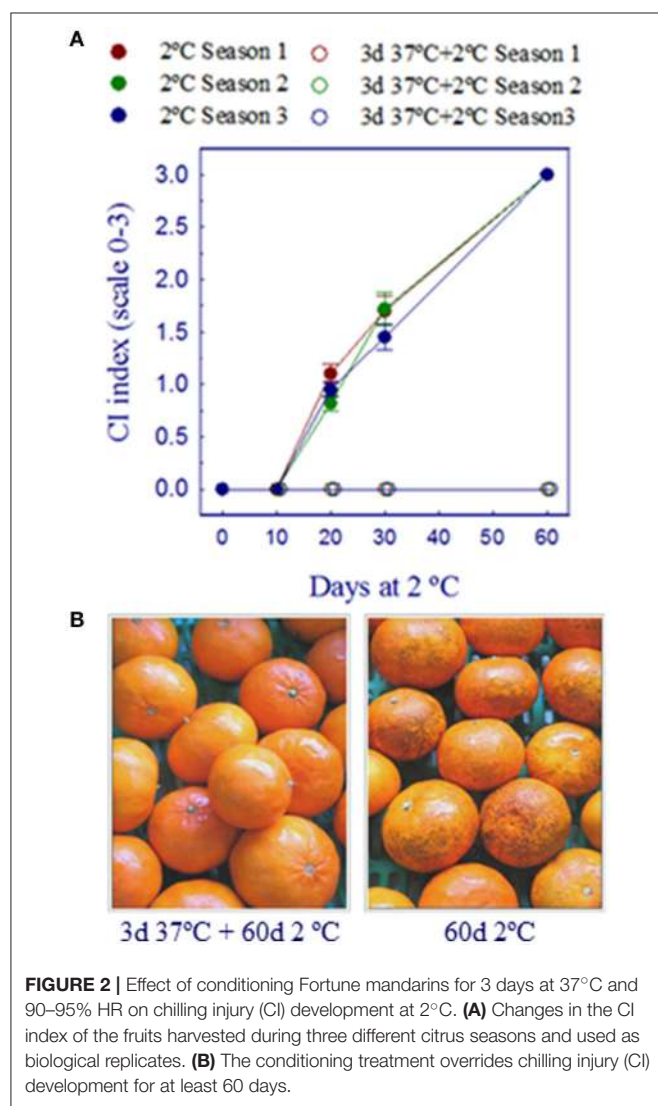


FIGURE 2 | Effect of conditioning Fortune mandarins for 3 days at 37°C and 90–95% HR on chilling injury (CI) development at 2°C. **(A)** Changes in the CI index of the fruits harvested during three different citrus seasons and used as biological replicates. **(B)** The conditioning treatment overrides chilling injury (CI) development for at least 60 days.

20 days at the chilling temperature (2°C) (**Figure 1B**). The 20 days period was selected to determine molecular responses that were induced by the heat treatment, whose expression persisted after prolonged cold storage, and that were induced by the combination of heat plus long-term storage. By this period, chilling damage started only in non-conditioned fruits. It is well-known that pre-harvest factors have a marked effect on the chilling- and the heat-induced physiological responses of citrus fruits (Lafuente et al., 1997, 2003; Gonzalez-Aguilar et al., 2000; Holland et al., 2002). Therefore, the transcriptomic analysis was first performed with three biological replicate samples harvested during one citrus season and the results were compared with those obtained by using biological replicates from three different citrus seasons. Fruits from these replicates were harvested in the same maturity stage, and showed the same susceptibility to CI (**Figure 2A**). In this way, our analysis is more restrictive, but the level of confidence in the molecular changes that are associated with heat-induced chilling tolerance is higher. The microarray includes genes isolated from 52 cDNA libraries of citrus, including the genes isolated from the FlavCurFr1 cDNA library. This library covers the genes induced by the heat-conditioning treatment, whose expression could persist or not when mandarins are subsequently transferred to chilling. Moreover, it covers genes that were not induced by the heat-conditioning treatment alone, but conditioning enhanced or accelerated their induction in chilled fruit (Forment et al., 2005).

The transcriptomic changes that occur in response to heat and cold, and the heat+cold combination, were studied. A significant analysis of microarrays (SAM) showed that 38% of the differentially expressed genes (DEGs) corresponded to the HICT category, as they responded to the heat+cold combination (**Figure 3**). Transcriptomic analysis also showed that repression prevailed in heat-conditioned fruits as there

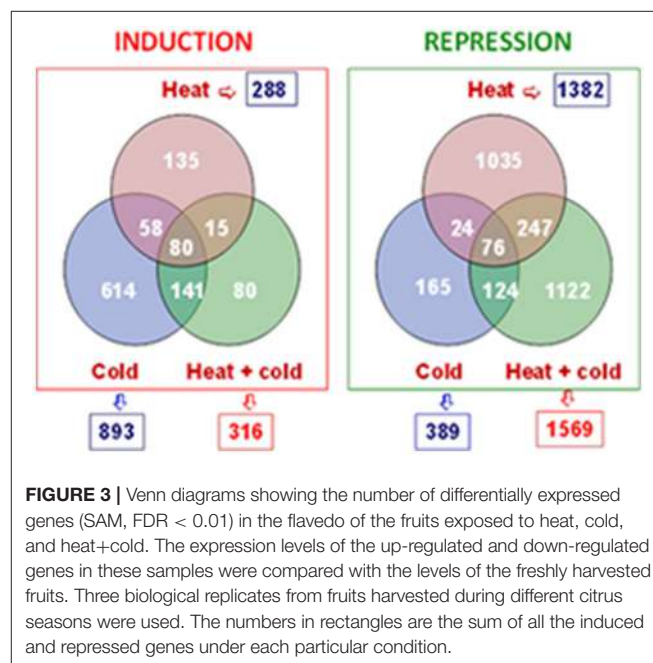


FIGURE 3 | Venn diagrams showing the number of differentially expressed genes (SAM, FDR < 0.01) in the flavedo of the fruits exposed to heat, cold, and heat+cold. The expression levels of the up-regulated and down-regulated genes in these samples were compared with the levels of the freshly harvested fruits. Three biological replicates from fruits harvested during different citrus seasons were used. The numbers in rectangles are the sum of all the induced and repressed genes under each particular condition.

were many more genes repressed under this condition (1569), and also in response to heat (1382), than induced (316 and 288, respectively). In contrast, induction prevailed in the flavedo of the chilled fruits that had not been previously conditioned at 37°C (893 induced genes and repressed 389 ones).

The gene ontology analysis of DEGs in the fruits exposed to the heat treatment in non-conditioned cold-stored fruits and in fruits exposed to the heat+cold combination allowed to group DEGs in biological processes, which were over- or under-represented in response to different treatments (**Table 1**). The number of over- or under-represented biological processes was much lower when biological replicates from fruits harvested during three different seasons, rather than harvested the same day in one citrus season, were included in the transcriptomic analysis. This effect reflects a higher dispersion of the results as a consequence of the influence of pre-harvest factors. However, as mentioned above, the level of confidence in the processes that would be associated with heat-induced chilling tolerance would be higher. As shown in **Table 1**, the only common differentially expressed processes in both analysis were the lipid biosynthetic process, which was repressed by heat in cold-stored fruits compared to freshly harvested fruit, and translation, which was significantly repressed by cold stress, but only when the effect of cold was compared with the induced by heating the fruits at 37°C for 3 days (**Table 1**).

TABLE 1 | Significant non-redundant biological processes over- or under-represented in the flavedo of Fortune mandarins exposed to heat (H), cold (C), or to the heat+cold combination (HC).

Biological process (FatiGO+)	1 Citrus season	3 Citrus season
LEVEL GO 5		
Amino acid derivative metabolic process	HC > FH	
	HC > C	
Macromolecule biosynthetic process	C&HC < FH	
Carboxylic acid metabolic process		HC < FH
LEVEL GO 6		
Lipid biosynthetic process	H < FH	
	HC < FH	HC < FH
	C > HC	
Translation	HC < FH	
	C < H	C < H
	C < FH	
LEVEL GO 7		
Isoprenoid biosynthetic process		HC < FH
LEVEL GO 8		
Regulation of transcription, DNA-dependent	HC > FH	
	C > FH	

A gene ontology (GO) analysis was performed by the program FatiGO+ (FatiGO+, $P < 0.05$) Lower GO levels represent general biological processes, whereas higher ones denote more precise information. Symbols > and < indicate that the process was over- or under-represented under the first storage condition indicated in the comparison. The results obtained by using samples harvested from one and three citrus seasons showing the same susceptibility to CI (**Figure 2A**) were compared.

Genes Involved in Lipid Metabolism

Many authors agree with the theory proposed by Lyons (1973), which indicates that changes in membrane fluidity induced by cold stress is the primary event related to CI in plants, and that fluidity depends on both the degree of fatty acid unsaturation and the fatty acid composition of phospholipids. This idea has been supported by the results found in different plant systems, including transgenic plants, but has also failed in numerous species (Parkin et al., 1989). Considering the relevance of lipids in membrane permeability, and our above mentioned results in heat-conditioned Fortune mandarins, special attention has been paid to changes in the expression of genes belonging to the lipid biosynthetic process.

The genes related to carotenoid and epicuticular wax (CUT 1, CER) biosynthesis, and also to lipid biosynthesis or elongation, and encoding several desaturases, were found mainly among the genes included in the lipid biosynthetic biological processes repressed by the heat-conditioning treatment in cold-stressed fruit (**Table S1**). Carmona et al. (2006) have shown that curing treatment may affect carotenoid content and composition in sweet oranges. Likewise, Matsumoto et al. (2009) have demonstrated in Satsuma mandarins that carotenoid composition and accumulation is highly dependent on postharvest temperature, and that the synthesis of various carotenoids decreases in fruits treated at high temperature

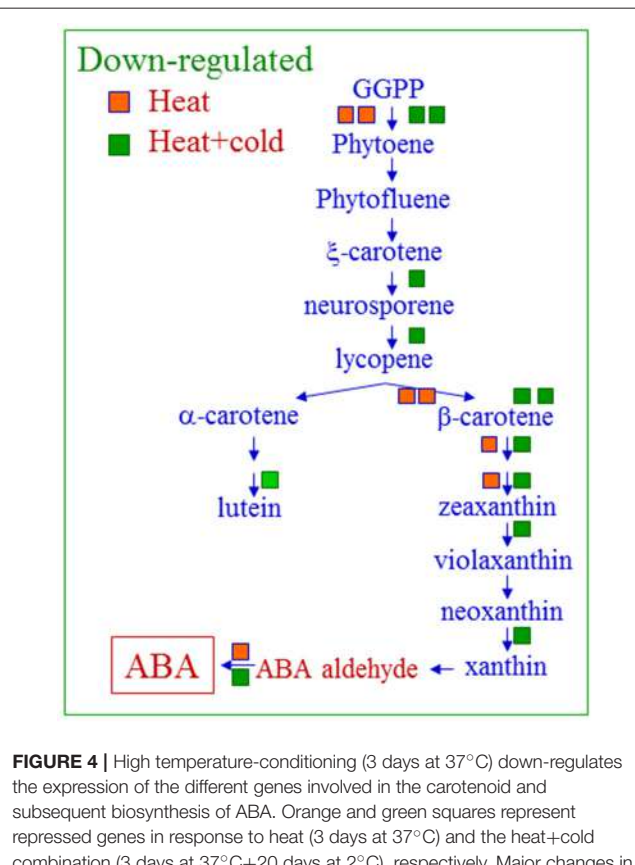


FIGURE 4 | High temperature-conditioning (3 days at 37°C) down-regulates the expression of the different genes involved in the carotenoid and subsequent biosynthesis of ABA. Orange and green squares represent repressed genes in response to heat (3 days at 37°C) and the heat+cold combination (3 days at 37°C + 20 days at 2°C), respectively. Major changes in gene expression levels are indicated by using two squares.

(30°C). These results agree with those found in the present work (**Table S1**) and summarized in **Figure 4**. As shown in this figure, the heat-conditioning treatment had a strong impact and down-regulated a set of genes involved in the biosynthesis of carotenoids which, in turn, are precursors of ABA (orange squares in **Figure 4**). This effect was enhanced after holding the previously heat-conditioned fruit at low temperature (green squares in **Figure 4**). These results could explain our previous data, which showed that ABA levels lowered after exposing fruits for 3 days at 37°C, and remained lower in conditioned fruits than in non-conditioned ones during storage at 2°C (Lafuente et al., 1997). Data on grapefruits have indicated that a hardening treatment of 16°C increases fruit chilling tolerance and up-regulates some genes involved in ABA biosynthesis (Maul et al., 2008). So, it is feasible to think that ABA might be involved in the efficacy of this hardening treatment in grapefruits, but not in that of the heat-conditioning treatment at 37°C in Fortune mandarins. Thus, previous physiological data, which indicate that ABA may even enhance CI in citrus, should be considered (Lafuente et al., 1997; Gosalbes et al., 2004; Alférez et al., 2005). This is in line with the findings that have indicated that ABA is not involved in low-temperature stress response in the juice sacs of cold-stored citrus fruits (Yun et al., 2012).

The study of the genes included in the lipid biosynthetic process also revealed that the expression levels of three desaturases in cold-stressed fruits were lower in the fruits previously exposed to heat treatment than in non-conditioned fruits (**Figure 5A**). Only the expression level of a sphingolipid desaturase (SLD2), which responds to cold stress, increased when the previous heat treatment was applied. This was a relevant effect, as heat-conditioned chilled fruit exhibited an 8-fold accumulation of this desaturase (**Figure 5A**). By using an *Arabidopsis* mutant, the *AtSLD2* gene has been found to play a key role in protecting plants against chilling (Chen et al., 2012). It is noteworthy that sphingolipids are required for the normal activity and stability of the plasma membrane, and they may act as second messengers in regulating defense responses, and are linked to redox signaling (Gechev et al., 2006). These results suggest that the degree of fatty acid unsaturation is not a limiting factor in the heat-induced chilling tolerance of Fortune mandarins. This agrees with previous physiological data, which have shown that exposing citrus fruit to high temperature, by applying the same HA (37°C for 3 days) treatment, or to an intermittent warming treatment, barely affects the degree of lipid unsaturation in cold-stored citrus fruits (Mulas et al., 1997; Schirra and Cohen, 1999). Therefore, it would seem that the degree of lipid unsaturation is not likely a critical factor in the chilling tolerance of citrus fruits. In contrast, the HA-conditioning treatment had a clear effect repressing chilling-induced increases in the expression levels of different phospholipases, especially type D phospholipases, and the expression of an acylglycerol lipase (α/β hydrolase), which is involved in lipid degradation (**Figure 5B**). Although phospholipases may produce signaling molecules that play a defensive role in plants against stress cues, they also cause membrane damage if plant systems are exposed to severe or continuous stress. So, the protective effect of the heat-conditioned treatment appears to be more

likely related to the repression of the genes involved in lipid degradation than to the modification of fatty acids unsaturation that affects membrane permeability. Interestingly, changes in the expression of the genes that encode desaturases are up-regulated in grapefruits exposed to the hardening treatment (7 days at 16°C), which also reduces CI, while the expression of a lipase 3 induced by chilling in this fruit barely varies by treatment (Maul et al., 2008). This further confirms that the cross-adaptive mechanism, which operates in the chilling tolerance induced by treatments that involve heat, may differ from those associated with acclimation to cold induced by a hardening process.

Transcription Factors

Special attention was also paid to TFs given their relevance in modulating the expression of specific groups of genes, and also because of results found by Sanchez-Ballesta et al. (2003) that highlighted the relevance of transcription initiation factor IIB (TFIIB) and two WRKY TFs in heat-induced chilling tolerance. **Table 2** shows the results obtained from the study of changes in the expression of the TFs selected from the FlavCurFr1cDNA library (Forment et al., 2005). Changes in expression levels were analyzed by Northern blot hybridization in Fortune mandarins treated from 4 h to 3 days at 37°C, and in the conditioned (3 days at 37°C) and non-conditioned fruits kept from 1 to 60 days at 2°C, to know early and late responses to cold stress, to heat during the conditioning treatment, and to the heat+cold combination. A gene expression analysis allowed TFs to be clustered in three groups. The TFs with a higher or lower expression in heat-conditioned than in non-conditioned fruits when stored at the chilling temperature were clustered in pattern 1 and pattern 2, respectively. Therefore, the TFs in these patterns might participate in heat-induced chilling tolerance. Other genes repressed by cold stress in both the heat-conditioned and the control non-conditioned fruits, or that did not respond to either cold or heat+cold, were included in pattern 3 (**Table 2**).

Within the expression pattern 1, which included the HICT genes, three WRKY TFs were identified. Two presented a similar expression pattern, with maximum mRNA accumulation in the heated fruit maintained at 2°C for 20–30 days, when CI became evident in the non-conditioned fruits, but not in the heat-pretreated fruits (**Table 2**). Their expression pattern was especially interesting as their relative accumulation increased by the heat+cold combination despite transcripts levels not rising in response to cold or heat. WRKY TFs are one of the largest families of transcriptional regulators found only in plants. Nowadays, diverse biological functions have been described for these TFs, including cold and heat tolerance (Bakshi and Oelmüller, 2014). Although very little is known about the participation of the WRKY family in the tolerance of plants to chilling (Bakshi and Oelmüller, 2014), these results reinforce our previous idea and highlight the relevance of WRKY TFs in the cross-protection induced by heat against chilling in citrus fruits (Sanchez-Ballesta et al., 2003). In line with this, it should be pointed out that the WRKY TFs shown in **Table 2** differed from those previously reported as HICT TFs (Sanchez-Ballesta et al., 2003), and that all the selected TFs that encoded WRKYS were included in the same expression pattern. Moreover, the three WRKYS within pattern 1 were found only in the library

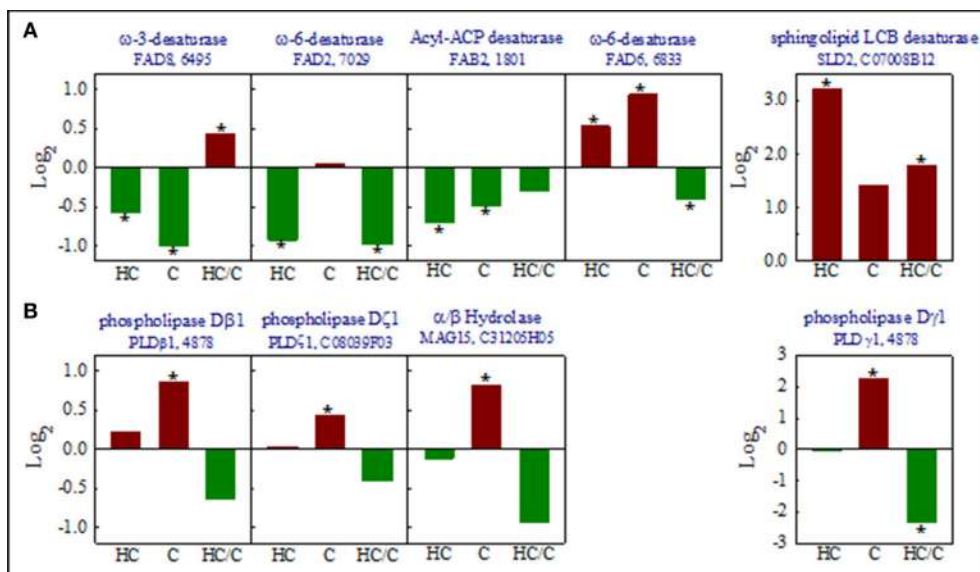


FIGURE 5 | Changes in the expression levels of the genes that encode lipid desaturases (A) and the lipases (B) that occur in response to heat (H, 3 days at 37°C), cold (C, 20 days at 2°C), and the heat+cold combination (3 days at 37°C + 20 days at 2°C). Values were obtained by comparing the changes in expression levels that occurred in response to heat plus cold (HC) or cold (C) to the expression levels of the freshly harvested (FH) fruits, and by also comparing the expression levels between the heat-conditioned cold-stored fruits (HC) and the cold-stored non-conditioned fruits (C). Unigenes are indicated at the top of each graph. The asterisk indicates statistically differences in each comparison according to SAM (FDR-adjusted p -value < 0.01).

FlavCurFr among the 52 cDNA libraries constructed in the CFGP, which covers a wide range of tissues, varieties, developmental, and fruit ripening stages and stress conditions (Forment et al., 2005). Heat-conditioning also favored the cold induction of two components of the RNA polymerase II transcription machinery in the eukaryotes that belong to the TFIID complex (initiation complex TFIID), which is required for transcription initiation and activated transcription in plant cells (Pan et al., 2000), a TATA-binding protein and a TFIIA factor. As shown in Table 2, the expression of these genes was higher in the conditioned fruits after 20 and 60 days of cold storage, respectively. Moreover, the transcriptome analysis revealed that a gene that encodes a TFIE factor was expressed only in the fruits exposed to the heat+cold combination. These results are in line with the idea that the TFs that are relevant for the transcriptional and translational apparatus of plant cells are also important in heat-induced chilling tolerance. The transcriptomic analysis also showed that the HA-conditioning treatment favored the up-regulation of genes involved in ethylene signaling, of ethylene-responsive transcription factors (EIN4, EIN 3, EREBT), and of TFs that belong to the zinc finger, NAC/NAM and Myb/Myc families in fruits stored at low temperature (Table S1). However, only relevant differences were found in expression levels of a gene of the NAC family protein. The participation of the above mentioned HICT genes in inducing tolerance against chilling appears to be specifically associated with heat treatment since genes from these families are not related to acquiring the chilling tolerance induced at 16°C in grapefruits (Maul et al., 2008). Therefore, protection strategies induced by both temperature-conditioning treatments to cope with citrus fruit

tolerance to chilling are likely to differ. The cultivar effect should also be considered. In fact, in non-conditioned grapefruits, cold stress favors the repression of some WRKYs (Maul et al., 2008), with minor changes occurring in response to cold stress in the Fortune mandarins that were not previously conditioned (Table 2).

Other TFs were induced in response to low temperature in non-conditioned fruits and the mRNA accumulation of these genes was totally, or to some extent, repressed if fruits were preconditioned at 37°C (pattern 2, Table 2). The expression of these genes generally increased with CI development for up to 30 days. This behavior may indicate that their up-regulation is not necessary in heat-conditioned fruit to cope with cell damage since the HA treatment avoids development of CI. However, we cannot rule out that heat-induced damage reduction may be associated with the repression of these genes in cold-stored citrus fruits. They encode proteins of different families, including zing finger proteins, MYB, a co-regulator transcriptional SEUSS, and an auxine response factor (ARF), whose expression only increases in non-conditioned fruits. The role of this hormone in the chilling tolerance of citrus fruits is unknown, but auxines may play a protecting role against oxidative stress (Kovtun et al., 2000), which has been associated with CI in Fortune mandarin (Sala and Lafuente, 1999; Sanchez-Ballesta et al., 2003) and other citrus cultivars (Sala et al., 2005; Rivera et al., 2007; Ghasemnezhad et al., 2008; Maul et al., 2008; Lado et al., 2016). The transcriptomic analysis also showed slight differences in the expression of two TFs from the YABBY and two from the HSTF families, which showed a higher expression in cold-stored fruits if they had not been previously conditioned at 37°C.

TABLE 2 | Relative expression level of the genes that encode transcription factors (TFs) isolated from the cDNA library FlavOurFr1 in the flavedo of the fruits exposed to different temperature regimes.

Tair10define	Transcript		37°C (H)						3 d 37°C + 2°C (H+C)						2°C (C)						12°C						
	ID	FH	4 h	12 h	1 d	3 d	1 d	3 d	10 d	20 d	30 d	60 d	1 d	3 d	10 d	20 d	30 d	60 d	1 d	3 d	10 d	20 d	30 d	60 d			
Pattern 1: H+C > C																											
TATA binding protein 2	19256625	100	73	92	126	85	75	85	150	241	125	122	55	64	114	92	116	102	138	148	135	114	116	102	103	103	
WRKY DNA-binding protein 48	19260860	100	91	112	83	74	89	86	109	165	125	119	114	116	117	105	111	115	103	109	107	100	100	94	94	94	
WRKY DNA-binding protein 28	19279147	100	94	113	71	65	96	132	205	260	111	82	66	93	55	72	73	122	123	175	144	179	152	152	152	152	
WRKY transcription factor 40	19232004	100	124	93	92	77	106	124	102	44	40	68	65	81	43	70	65	107	41	46	59	43	55	55	167	167	
Transcription factor II A, alpha/beta subunit	19282074	100	69	90	79	69	92	84	95	160	199	259	147	126	138	168	184	177	112	143	136	120	126	105	105	105	
Pattern 2: H+C ≤ C																											
Transcriptional corepressor SEUSS	19272965	100	95	79	77	67	87	86	94	101	120	135	147	162	148	148	141	106	109	108	117	98	98	94	94	94	
Auxin response factor 19	19262959	100	81	95	69	71	93	66	71	167	263	284	259	141	147	171	186	101	146	132	139	107	107	151	151	151	
Zinc finger protein, LSD1-type	19266170	100	131	106	97	101	117	128	167	28	136	280	144	143	125	261	440	245	280	177	126	114	110	94	93	93	
Telomere repeat-binding protein 1	19283888	100	47	40	35	28	38	58	58	31	44	58	108	231	295	191	327	224	319	246	146	128	102	80	87	88	63
RING-U-box superfamily protein	19262758	100	65	63	30	31	44	58	89	103	80	66	63	107	123	126	139	132	170	183	141	140	106	109	114	105	105
RING-H2 finger protein RHCl1a	19270794	100	98	110	153	94	89	133	124	105	68	44	49	56	129	111	66	73	74	91	58	52	65	66	68	64	
Transcription factor bHLH113	19276300	100	116	145	145	133	124	105	68	44	49	56	149	56	129	111	66	73	74	91	58	52	65	66	68	64	
Pattern 3: H+C = C																											
DREB subfamily A-4 of ERF/AP2 transcription factor family (ERF026)	19275624	100	103	94	79	92	48	32	36	39	44	37	42	41	30	50	64	98	50	52	83	52	67	365	365	365	
Heat Stress Transcription Factor (Hsf) family	19276116	100	59	64	38	37	44	41	47	44	37	35	67	65	57	52	56	60	52	48	52	43	43	43	75	75	
Knotted1-like homeobox gene 3	19261948	100	76	85	64	62	68	59	63	56	52	47	99	87	63	53	54	72	96	107	119	108	93	109	109	109	
Calcium-binding transcription factor involved in salt stress signaling	19276886	100	108	94	68	60	55	50	51	45	57	81	74	73	62	56	75	98	77	59	51	63	61	61	109	109	
Transcription factor, MADS-box	19279286	100	82	71	50	39	42	42	35	25	21	27	97	84	67	54	61	63	119	128	119	132	130	119	119	119	
Component of the Facilitates Chromatin Transcription (FACT) complex	19285547	100	83	66	78	45	33	37	37	35	33	45	81	74	66	54	65	77	108	75	66	71	60	109	109	109	
B-box containing transcriptional regulator	19280828	100	69	85	70	71	62	70	67	117	85	79	70	63	86	58	65	85	100	103	105	102	82	82	82	82	
RING-U-box superfamily protein	19259847	100	81	89	66	60	70	66	72	89	92	82	80	86	76	86	92	108	101	96	109	87	128	128	128	128	
Multiprotein bridging factor 1	19288326	100	120	144	172	96	88	91	87	73	66	72	88	97	99	82	89	74	196	178	163	150	139	147	147	147	
Chilling injury index (scale 0-3)																											
	0.0	0.0	0.0	0.0	0.0	0.0	0.0	0.0	0.0	0.0	0.0	0.0	0.0	0.0	0.0	0.0	0.0	0.0	0.0	0.0	0.0	0.0	0.0	0.0	0.0	0.0	

Transcript accumulations were normalized respect to values found in the freshly harvested fruits (FH), and a value of 100 was assigned to this sample. Changes in expression were analyzed in fruits exposed to heat (H_1 , 37°C) from 4 h till 3 days; in the non-conditioned (C) and in heat-conditioned fruits (3 days at 37°C) (H+C) maintained from 1 to 60 days at 2°C, and in the fruits maintained at a non-chilling temperature (12°C) for the same storage periods. Changes in CI index are shown at the end of the Table. Inductions are marked in red (\bullet > 140–200; \bullet > 201) and repression in green (\bullet < 60). Genes were grouped in three patterns of expression. Pattern 1 and 2 group the genes whose expression was higher (>) or lower (<), respectively, in cold-stored fruits that were previously heat-conditioned (H+C) at 37°C for 3 days. Pattern 3 groups the genes repressed by cold stress in both the heat-conditioned and the control non-conditioned fruits, or that did not respond either to cold or heat plus cold.

The TFs within pattern 3 (**Table 2**) do not appear relevant for the cold acclimation of Fortune mandarins to chilling, although some genes from these TFs families may play important roles in the defense of plants and fruits against various stresses (Sevillano et al., 2009). Most of these genes are down-regulated by cold stress in both heat-conditioned and non-conditioned fruits, despite the fact that some including CBF1, MADS-box, MYC, or HSFs, belong to the gene families related to cold-stress acclimation in grapefruits or other chilling-sensitive crops (Maul et al., 2008; Sevillano et al., 2009; Peng et al., 2015).

These results thus reinforce the idea that the molecular mechanisms that operate in the defense of citrus fruits against chilling differ with the conditioning treatment type. Moreover, they agree with the idea raised by Wang et al. (2001) from their research in apple fruit cells that suggests that the protective effect of heat treatments may be related to an increased transcription capacity in cold-stressed cells (Wang et al., 2001). The global results from changes in expression of TFs also reflect that long-term heat-induced chilling tolerance in citrus fruit is an active process that requires new transcription factors in cold-stored fruits from the WRKY family. Many genes from this family can be induced by cold and heat stress in *Arabidopsis* (Bakshi and Oelmüller, 2014) and, interestingly, the WRKY HICT identified in citrus fruits were up-regulated only by the heat+cold combination. Therefore, these genes could be good candidates to be involved in heat-induced tolerance against chilling in citrus fruits, and further research should be conducted to decipher their regulatory role in this process.

Major Changes in Gene Expression in Miscellaneous Categories

The transcriptomic analysis also provided very valuable information about other genes that may be related to the tolerance or susceptibility of citrus fruits to chilling. Changes in the expression levels of these genes were relevant, although the number of genes within a specific category was not high enough to reveal the over-representation of a specific biological process. Such information is shown in **Table S1** and summarized in **Figure 6**. From such data, it can be pointed out that cold stress in non-conditioned chilled citrus fruit favors membrane integrity loss as it promotes degradation processes that affect both lipids and proteins, as we identified rises in lipases (**Figure 5**), and also in some proteases, from which the most relevant changes took place in cysteine proteases. Furthermore, cold stress induced marked increases in the expression levels of genes that encode cell wall-degrading enzymes, like a β -polygalacturonase encoding genes and a β -xylosidase, whose expression was at least 4-fold higher in cold-stored non-conditioned fruits. Interestingly, it has been recently shown that cell wall-derived oligomers reduce CI in citrus fruits (Vera-Guzman et al., 2017).

Chilling also had a strong effect by up-regulating a set of genes related to stress responses, many of which are involved in oxidative stress. It induced relevant changes in the expression levels of not only several ABC transporters, whose expression increased by up to 9-fold, but also of cold responsive (COR) genes and dehydrins, which could help fruit to cope with chilling stress. Among them, the expression of *cor15* genes was higher

in non-conditioned fruits, which reinforces the idea exposed by Sanchez-Ballesta et al. (2004) that these proteins are not related to heat-induced chilling tolerance in citrus fruits. Likewise, the expression of different genes that encode LEA proteins increased in response to cold stress, and most of them were repressed by heat in cold stored fruits. Although these proteins have been linked mainly to water stress, they are induced in response to diverse stresses, including cold and oxidative stress (Mowla et al., 2006). Chilling also up-regulated the expression of different genes belonging to the phenylpropanoid metabolism, which is in agreement with findings in cold-stressed mango indicating that chilling stress activates phenylpropanoid pathway (Sivankalyani et al., 2016). Moreover, it had an important impact increasing expression level of oxidative-stress related genes in non-conditioned fruits. Among them, we found a high representation of genes encoding FAD-dependent oxidoreductases and of cytochrome P450 (monooxygenase-1electron) related-proteins, which were down-regulated by the heat-conditioning treatment. Among the FAD-dependent oxidoreductases, the marked rises in nectarin 5 (NEC5) and CPRD2 were noteworthy, whose expression increased by more than 8-fold in response to cold stress. These genes are involved in the accumulation of ROS and membrane damage. Likewise, a very high increase (9–16-fold) was observed in various cytochrome P450-encoding CYP79A2 proteins. These proteins lead to the synthesis of glycosylated compounds that contain sulfur and display antioxidant activity. These genes were among the most induced in non-conditioned cold-stored mandarins and its expression was down-regulated if the fruits were previously treated for 3 days at 37°C. Genes encoding hemoglobin were also among the most cold-induced genes in non-conditioned mandarins. A 25-fold increase in expression levels of two hemoglobins was found. While these proteins are widespread in the plant kingdom, their function is still not well-understood. However, it has been suggested that they may provide an alternative type of respiration to mitochondrial electron transport under limiting oxygen concentrations and also modulate nitric oxide levels in stressed plants (Dordas, 2009).

On the other hand, from the results obtained with the transcriptomic analysis, it can be pointed out that heat-induced chilling tolerance in citrus fruit seems to be an active process requiring, besides new transcription factors, the activation of stress-related proteins and the repression of genes favoring tissue damage (**Figure 6**). Many of the genes that encode stress-related proteins were involved in the prevention or elimination of ROS and in secondary metabolism. Within oxidative stress, major increases (10-fold) in the expression levels of a gene that encodes a ferritin, which could sequester ferrous ions, were observed. Therefore, the HA treatment could reduce oxidative stress by preventing the Fenton effect and the subsequent formation of hydroxyl radicals (Gechev et al., 2006). This highly toxic species may cause severe oxidative damage to lipids, but also to DNA and proteins. The analysis has also shown that high-temperature conditioning might protect citrus fruit against CI by scavenging ROS through enzymes like SOD, glutathione transferase (GST), glutaredoxin, tioredoxin, as well as different metalloproteins (**Table S1**). These results add further knowledge about the

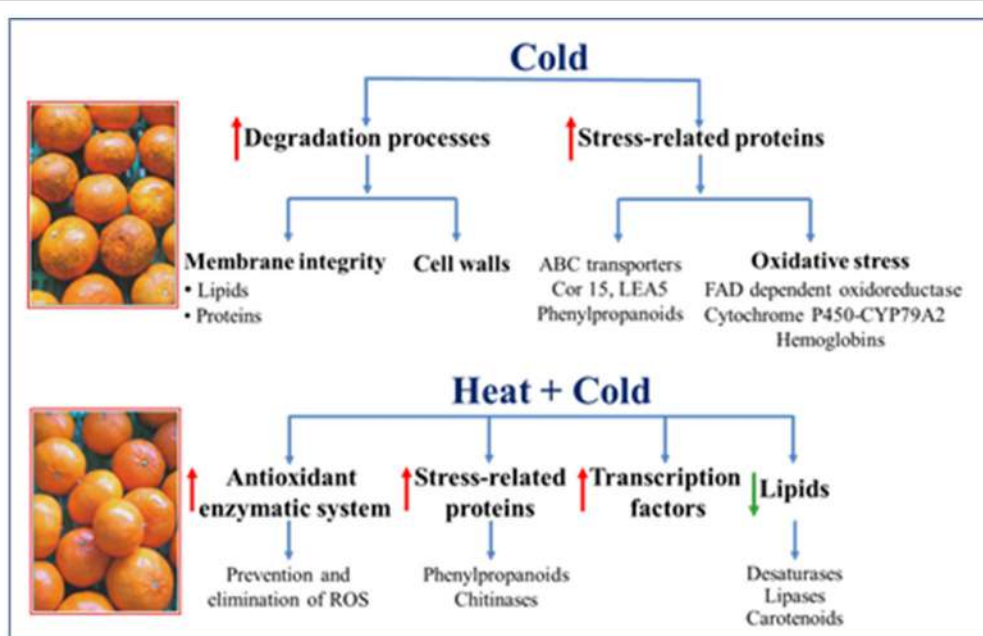


FIGURE 6 | Summary of the cold-activated (\uparrow) or repressed (\downarrow) responses in the non-conditioned (Cold) and heat-conditioned (Heat+cold) Fortune mandarins.

enzymes that protect cold-stored citrus fruit from oxidative stress, and demonstrate that such protection in citrus fruits is not limited only to the traditional SOD, catalase, peroxidase, and Halliwell-Asada cycle antioxidant enzymatic system (Sala and Lafuente, 2000; Sanchez-Ballesta et al., 2003; Rivera et al., 2007; Ghasemnezhad et al., 2008; Siboa et al., 2014; Lado et al., 2016). Likewise, the heat-conditioning treatment repressed lipases and hydrolases in cold-stressed fruits and could, therefore, reduce ROS formation associated with membrane damage. The effect of the heat-conditioning treatment on inducing chitinases was also remarkable since the expression of different genes of this multigene family increased in response to both heat and the heat+cold combination. The induction of these genes in response to heat, and persistence during fruit cold storage, support previous data obtained by an SSH approach. With this approach, an acidic chitinase class II was identified as a HICT gene (Sanchez-Ballesta et al., 2003); and a high correlation has been found between the induction of this gene and the chilling tolerance induced by different temperature-conditioning treatments that display diverse efficacy against chilling (Lluch, 2006). That chitinase shows high homology with one of those identified herein by means of a transcriptomic analysis. The role of chitinases in the defense of citrus fruits against chilling remains unknown. By using an *Arabidopsis* mutant, it has been shown that they may play a role against different stresses like heat, dehydration, and salt stress (Kwon et al., 2007). This effect has been related to the participation of chitinases in the formation of cell walls and in adhesion between cell membranes and the cell wall. Moreover, Gao and Showalter (1999) have reported that the alteration of these glycoproteins leads to cell death in *Arabidopsis* cells. After considering these results, and

that membranes are the first cell component affected by cold stress, the study of the role of chitinases in the chilling tolerance of citrus fruits and other horticultural crops deserves further attention. Within the secondary metabolism, the effect of the heat-conditioning treatment increasing the expression levels of diverse genes of the phenylpropanoids metabolism in cold-stored fruits was remarkable. The genes that encode cinnamate 4-hydroxylase and isoflavone reductase proteins, and four oxygen methyl transferases (OMTs), showed higher expressions in heat-conditioned fruits than in the non-conditioned ones stored at low temperatures. Conversely, the expression of a gene that encodes PAL, which catalyzes the first phenylpropanoid biosynthesis step, remained unaltered in the heat-conditioned fruits maintained under chilling conditions, but increased in response to cold stress in the non-conditioned fruits (Table S1). Therefore, the beneficial effect of curing treatment is more likely to be related to the metabolic shifts of phenylpropanoids by leading to the synthesis of both flavonoids and methylated phenylpropanoid compounds than to increasing phenolics content. OMTs perform diverse functions in plants. In the present work, it should be mentioned that they are the principal enzymes in the complex network of reactions that occur as part of lignin biosynthesis, but OMTs may also lead to the synthesis of coumarins, which display antioxidant activity (Lee and Jang, 2015). Therefore, heat-conditioning could have an effect on cell wall fortification, but also on increasing levels of the natural compounds in the flavedo with antioxidant activity. Accordingly, Yun et al. (2013) found that a HWD treatment performed at 52°C for 2 min up-regulated stress response proteins that belong to the secondary metabolism in the citrus pericarp. Although these authors did not examine the maintenance of these responses after transferring fruits to

cold stress, it is interesting to note that the short heat treatment was able to increase lignin content in the pericarp.

Chilling increases ethylene production in citrus fruits (Martinez-Tellez and Lafuente, 1997). Previous reports have indicated that this phytohormone plays a protective role against chilling in Shamouti oranges and Fortune mandarins, since applying inhibitors of ethylene action, such as 1-methylcyclopropene (1-MCP), and synthesis increase chilling-induced damage (Porat et al., 1999; Lafuente et al., 2001). However, low 1-MCP levels may reduce the incidence of the disorder in other citrus cultivars (Salvador et al., 2006). Other results have shown that ethylene production transiently increases at 37°C during the 3-day conditioning treatment (Holland et al., 2012), which markedly reduces CI. However, the conditioning treatment prevented the rise in ethylene that occurs in non-conditioned fruits in response to chilling, which was much higher than that induced at 37°C (Holland et al., 2012). This result might suggest that during the 3 days that the conditioning treatment at 37°C lasts, some defense mechanism against chilling is initiated and, therefore, the cold-induced increase in ethylene is not necessary to cope with stress or to contain lesion propagation in tissues that present CI. Global results thus suggested that ethylene may participate in the defense of citrus fruits against chilling, but does not play a critical role in reducing CI. In the present work, we found very marked changes in the genes that encode FAD-dependent oxidoreductases, in abundant GSTs, ABC transporters, and also in different transcription factors, which were only induced in non-conditioned fruits in response to cold stress (**Table S1**). These genes are regulated in citrus fruits by ethylene (Establés-Ortiz et al., 2016). However, the comparison of the changes in the transcriptome of the flavedo of chilling-exposed fruits with those previously identified in our laboratory when studying the effect of exogenous ethylene (Establés-Ortiz et al., 2016) have shown that the percentage of genes regulated by both chilling and ethylene did not exceed 15% (Establés-Ortiz, 2008). Therefore, this is in line with our previous idea that most protective mechanisms of citrus fruits against chilling do not depend on ethylene.

CONCLUSION

Heat conditioning is a very effective reproducible method to reduce CI in citrus fruits. Transcriptomic data has revealed that although some responses to heat and cold temperatures in citrus fruits are common, specific responses toward each condition prevail. Moreover, data highlight that the heat+cold combination induces a high proportion of specific responses. Hence, these responses should be the best candidates to be involved in the heat-induced chilling tolerance in citrus fruits. Inhibition of cold-induced responses may play an important role in the events that control heat-induced chilling tolerance.

REFERENCES

- Alférez, F., Sala, J. M., Sánchez-Ballesta, M. T., Mulas, M., Lafuente, M. T., and Zacarias, L. (2005). A comparative study of the postharvest performance

In fact, gene repression prevails in heat-conditioned chilled fruits, while induction prevails in non-conditioned cold-stored fruits. The study also highlights the importance of pre-harvest environmental conditions on heat and/or cold-induced responses. Moreover, comparison of results from this study with previously reported data in citrus fruits shows the importance of varietal differences, and that the events that control the chilling tolerance induced by distinct temperature-conditioning treatments, may differ. These results envisage that the CI problem is not a simple one and that the primary CI event in citrus fruits remains unknown. Three major factors seem to correlate with the chilling tolerance induced by preconditioning citrus fruit at high temperature: (1) repression of genes involved in membrane degradation; (2) activation of the responses that aim to prevent oxidative damage; (3) activation of the HICT TFs of the WRKY family involved in transcription initiation.

AUTHOR CONTRIBUTIONS

ML reviewed the literature and wrote the paper and designed the experiments leading to data shown. BE carried out such experiments and participated in data analysis. LG contributed to drafting the manuscript as well as to the design of the experiments and to data analysis. All authors read and approved the final manuscript.

FUNDING

This work was supported by the Spanish Ministry of Economy and Competitiveness (Research Grants AGL2002-01727 and AGL2014-55802-R) and the Generalitat Valenciana, Spain (Grant PROMETEOII/2014/027). We also acknowledge support of the publication fee by the CSIC Open Access Publication Support Initiative through its Unit of Information Resources for Research (URICI).

ACKNOWLEDGMENTS

Special thanks go to Dr. J. Gadea and Dr. J. Forment (CFGP) for their help in microarray generation and for bioinformatics assistance and to Dr. A. R. Ballester for bioinformatics assistance.

SUPPLEMENTARY MATERIAL

The Supplementary Material for this article can be found online at: <http://journal.frontiersin.org/article/10.3389/fpls.2017.01113/full#supplementary-material>

Table S1 | Fortune mandarin transcript expression profile in heat-conditioned (3 days at 37°C) and non-conditioned fruits stored for 20 days at 2°C. Sheets 7 and 12 k show the results of the hybridizations with the 7 and 12 k microarrays, respectively. The sheet "readme" explains data shown in both sheets.

of an ABA-deficient mutant of oranges: I. Physiological and quality aspects. *Postharvest Biol. Technol.* 37, 222–231. doi: 10.1016/j.postharvbio.2005.05.010
Bakshi, M., and Oelmüller, R. (2014). WRKY transcription factors jack of many trades in plants. *Plant Signal. Behav.* 9:e27700. doi: 10.4161/psb.27700

- Ballester, A.-R., Lafuente, M. T., and González-Candelas, L. (2006). Spatial study of antioxidant enzymes, peroxidase and phenylalanine ammonia-lyase in the citrus fruit–*Penicillium digitatum* interaction. *Postharvest Biol. Technol.* 39, 115–124. doi: 10.1016/j.postharvbio.2005.10.002
- Ballester, A.-R., Lafuente, M. T., Forment, J., Gadea, J., de Vos, R. C. H., Bovy, A. G., et al. (2011). Transcriptomic profiling of citrus fruit peel tissues reveals fundamental effects of phenylpropanoids and ethylene on induced resistance. *Mol. Plant Pathol.* 12, 879–897. doi: 10.1111/j.1364-3703.2011.00721.x
- Carmona, L., Zacarias, L., and Rodrigo, M. J. (2006). “Efecto del acondicionamiento térmico en el color y acumulación de carotenoides en la piel de los frutos cítricos” in *Innovaciones Fisiológicas y Tecnológicas de la Maduración y Post-Recolección De Frutas y Hortalizas*, eds D. Valero and M. Serrano (Elche: CEE Limencop, S.L.), 49–52.
- Chen, M., Markham, J. E., and Cahoon, E. B. (2012). Sphingolipid Δ8 unsaturation is important for glucosylceramide biosynthesis and low-temperature performance in *Arabidopsis*. *Plant J.* 69, 769–781. doi: 10.1111/j.1365-313X.2011.04829.x
- Dordas, C. (2009). Nonsymbiotic hemoglobins and stress tolerance in plants. *Plant Sci.* 176, 433–440. doi: 10.1016/j.plantsci.2009.01.003
- Establés-Ortiz, B. (2008). *Estudio Transcriptómico de los Mecanismos Implicados en la Tolerancia Inducida por el Curado al Daño de Frio y por el Etileno al Colapso de la Corteza en los Frutos Cítricos*. Ph.D. dissertation. University of Valencia, Valencia.
- Establés-Ortiz, B., Romero, P., Ballester, A.-R., González-Candelas, L., and Lafuente, M. T. (2016). Inhibiting ethylene perception with 1-methylcyclopropene triggers molecular responses aimed to cope with cell toxicity and increased respiration in citrus fruits. *Plant Physiol. Biochem.* 103, 154–166. doi: 10.1016/j.plaphy.2016.02.036
- Ferguson, I. B., Ben-Yehoshua, S., Mitcham, E. J., McDonald, R. E., and Lurie, S. (2000). Postharvest heat treatments: introduction and workshop summary. *Postharvest Biol. Technol.* 21, 1–6. doi: 10.1016/S0925-5214(00)00160-5
- Ferguson, I., Volz, R., and Woolf, A. (1999). Preharvest factors affecting physiological disorders of fruit. *Postharvest Biol. Technol.* 15, 255–262. doi: 10.1016/S0925-5214(98)00089-1
- Forment, J., Gadea, J., Huerta, L., Abizanda, L., Agusti, J., Alamar, S., et al. (2005). Development of a citrus genome-wide EST collection and cDNA microarray as resources for genomic studies. *Plant Mol. Biol.* 57, 375–391. doi: 10.1007/s11103-004-7926-1
- Gao, M., and Showalter, A. M. (1999). Yariv reagent treatment induces programmed cell death in *Arabidopsis* cell cultures and implicates arabinogalactan protein involvement. *Plant J.* 19, 321–331. doi: 10.1046/j.1365-313X.1999.00544.x
- Gechev, T. S., Van Breusegem, F., Stone, J. M., Denev, I., and Laloi, C. H. (2006). Reactive oxygen species as signals that modulate plant stress responses and programmed cell death. *Bioessays* 28, 1091–1101. doi: 10.1002/bies.20493
- Ghasemnezhad, M., Marsh, K., Shilton, R., Babalar, M., and Woolf, A. (2008). Effect of hot water treatments on chilling injury and heat damage in ‘satsuma’ mandarins: Antioxidant enzymes and vacuolar ATPase, and pyrophosphatase. *Postharvest Biol. Technol.* 48, 364–371. doi: 10.1016/j.postharvbio.2007.09.014
- Gonzalez-Aguilar, G. A., Zacarias, L., and Lafuente, M. T. (1998). Ripening affects high-temperature induced polyamines and their changes during cold storage of ‘Fortune’ mandarins. *J. Agric. Food Chem.* 46, 3503–3508. doi: 10.1021/jf980173w
- Gonzalez-Aguilar, G. A., Zacarias, L., Perez-Amador, M. A., Carbonell, J., and Lafuente, M. T. (2000). Polyamine content and chilling susceptibility are affected by seasonal changes in temperature and by conditioning temperature in cold-stored ‘Fortune’ mandarin fruit. *Physiol. Plant.* 108, 140–146. doi: 10.1034/j.1399-3054.2000.108002140.x
- Gosalbes, M. J., Zacarias, L., and Lafuente, M. T. (2004). Characterization of the expression of an oxygenase involved in chilling-induced damage in citrus fruit. *Postharvest Biol. Technol.* 33, 219–228. doi: 10.1016/j.postharvbio.2004.04.001
- Holland, N., Menezes, H. C., and Lafuente, M. T. (2002). Carbohydrates as related to the heat-induced chilling tolerance and respiratory rate of ‘Fortune’ mandarin fruit harvested at different maturity stages. *Postharvest Biol. Technol.* 25, 181–191. doi: 10.1016/S0925-5214(01)00182-X
- Holland, N., Nunes, F. L. S., de Medeiros, I. U. D., and Lafuente, M. T. (2012). High-temperature conditioning induces chilling tolerance in mandarin fruit: a cell wall approach. *J. Sci. Food Agric.* 92, 3039–3045. doi: 10.1002/jsfa.5721
- Holland, N., Sala, J. M., Menezes, H. C., and Lafuente, M. T. (1999). Carbohydrate content and metabolism as related to maturity and chilling sensitivity of cv. Fortune mandarins. *J. Agric. Food Chem.* 47, 2513–2518. doi: 10.1021/jf981402h
- Kovtun, Y., Chiu, W.-L., Tena, G., and Sheen, J. (2000). Functional analysis of oxidative stress-activated mitogen-activated protein kinase cascade in plants. *Proc. Natl. Acad. Sci. U.S.A.* 97, 2940–2945. doi: 10.1073/pnas.97.6.2940
- Kwon, Y., Kim, S.-H., Jung, M.-S., Kim, M.-S., Oh, J.-E., Ju, H.-W., et al. (2007). *Arabidopsis hot2* encodes an endochitinase-like protein that is essential for tolerance to heat, salt and drought stresses. *Plant J.* 49, 184–193. doi: 10.1111/j.1365-313X.2006.02950.x
- Lado, J., Rodrigo, M. J., López-Climent, M., Gómez-Cadenas, A., and Zacarías, L. (2016). Implication of the antioxidant system in chilling injury tolerance in the red peel of grapefruit. *Postharvest Biol. Technol.* 111, 214–223. doi: 10.1016/j.postharvbio.2015.09.013
- Lafuente, M. T., Ballester, A. R., Calejero, J., and González-Candelas, L. (2011). Effect of high-temperature-conditioning treatments on quality, flavonoid composition and vitamin C of cold stored ‘Fortune’ mandarins. *Food Chem.* 128, 1080–1086. doi: 10.1016/j.foodchem.2011.03.129
- Lafuente, M. T., Martínez-Téllez, M. A., and Zacarías, L. (1997). Abscisic acid in the response of ‘Fortune’ mandarins to chilling. Effect of maturity and high-temperature conditioning. *J. Sci. Food Agric.* 73, 494–502. doi: 10.1002/(SICI)1097-0010(199704)73:4<494::AID-JSFA761>3.0.CO;2-B
- Lafuente, M. T., Zacarias, L., Martínez-Téllez, M. A., Sanchez-Ballesta, M. T., and Dupille, E. (2001). Phenylalanine ammonia-lyase as related to ethylene in the development of chilling symptoms during cold storage of citrus fruits. *J. Agric. Food Chem.* 49, 6020–6025. doi: 10.1021/jf010790b
- Lafuente, M. T., Zacarias, L., Martínez-Téllez, M. A., Sanchez-Ballesta, M. T., and Granell, A. (2003). Phenylalanine ammonia-lyase and ethylene in relation to chilling injury as affected by fruit age in citrus. *Postharvest Biol. Technol.* 29, 308–317. doi: 10.1016/S0925-5214(03)00047-4
- Lafuente, M. T., Zacarias, L., Sala, J. M., Sanchez-Ballesta, M. T., Gosálbez, M. J., Marcos, J. F., et al. (2005). Understanding the basis of chilling injury in citrus fruit. *Acta Hortic.* 682, 831–842. doi: 10.17660/ActaHortic.2005.682.108
- Lee, S.-H., and Jang, H.-D. (2015). Scoparone attenuates RANKL-induced osteoclastic differentiation through controlling reactive oxygen species production and scavenging. *Exp. Cell Res.* 331, 267–277. doi: 10.1016/j.yexcr.2014.12.018
- Lluch, Y. (2006). *Bases Moleculares del Mecanismo de Tolerancia al Frio Inducido por Tratamientos de Acondicionamiento a Altas Temperaturas en Frutos Cítricos*. Ph.D. dissertation. University of Valencia, Valencia.
- Lurie, S. (1998). Postharvest heat treatments. *Postharvest Biol. Technol.* 14, 257–269. doi: 10.1016/S0925-5214(98)00045-3
- Lyons, J. M. (1973). Chilling injury in plants. *Annu. Rev. Plant Physiol.* 24, 445–466. doi: 10.1146/annurev.pp.24.060173.002305
- Martinez-Téllez, M. A., and Lafuente, M. T. (1997). Effect of high temperature conditioning on ethylene, phenylalanine ammonia-lyase, peroxidase and polyphenol oxidase activities in flavedo of chilled fortune mandarin fruit. *J. Plant Physiol.* 150, 674–678. doi: 10.1016/S0176-1617(97)80282-9
- Matsumoto, H., Ikoma, Y., Kato, M., Nakajima, N., and Hasegawa, Y. (2009). Effect of postharvest temperature and ethylene on carotenoid accumulation in the flavedo and juice sacs of satsuma mandarin (*Citrus unshiu* Marc.). *J. Agric. Food Chem.* 57, 4724–4732. doi: 10.1021/jf9005998
- Maul, P., McCollum, G. T., Popp, M., Guy, C. L., and Porat, R. (2008). Transcriptome profiling of grapefruit flavedo following exposure to low temperature and conditioning treatments uncovers principal molecular components involved in chilling tolerance and susceptibility. *Plant Cell Environ.* 31, 752–768. doi: 10.1111/j.1365-3040.2008.01793.x
- Mowla, S. B., Cuypers, A., Driscoll, S. P., Kiddle, G., Thomson, J., Foyer, C. H., et al. (2006). Yeast complementation reveals a role for an *Arabidopsis thaliana* late embryogenesis abundant (LEA)-like protein in oxidative stress tolerance. *Plant J.* 48, 743–756. doi: 10.1111/j.1365-313X.2006.02911.x
- Mulas, M., Lafuente, M. T., and Zacarias, L. (1997). Postharvest temperature conditioning and chilling effects on flavedo lipid composition of ‘Fortune’ mandarin. *Proc. Int. Soc. Citricult.* 2, 1132–1135.

- Mulas, M., and Schirra, M. (2007). The effect of heat conditioning treatments on the postharvest quality of horticultural crops. *Stewart Postharvest Rev.* 3, 1–6. doi: 10.2212/spr.2007.1.2
- Pan, S., Czarnecka-Verner, E., and Gurley, W. B. (2000). Role of the TATA binding protein-transcription factor IIB interaction in supporting basal and activated transcription in plant cells. *Plant Cell* 12, 125–135. doi: 10.1105/tpc.12.1.125
- Parkin, K. L., Marangoni, A., Jackman, R. L., Yada, R. Y., and Stanley, D. W. (1989). Chilling injury. A review of possible mechanisms. *J. Food Biochem.* 13, 127–153. doi: 10.1111/j.1745-4514.1989.tb00389.x
- Pedreschi, R., and Lurie, S. (2015). Advances and current challenges in understanding postharvest abiotic stresses in perishables. *Postharvest Biol. Technol.* 107, 77–89. doi: 10.1016/j.postharvbio.2015.05.004
- Peng, X., Wu, Q., Teng, L., Tang, F., Pi, Z., and Shen, S. (2015). Transcriptional regulation of the paper mulberry under cold stress as revealed by a comprehensive analysis of transcription factors. *BMC Plant Biol.* 15:108. doi: 10.1186/s12870-015-0489-2
- Perotti, V. E., Del Vecchio, H. A., Sansevich, A., Meier, G., Bello, F., Cocco, M., et al. (2011). Proteomic, metabolomic, and biochemical analysis of heat treated Valencia oranges during storage. *Postharvest Biol. Technol.* 62, 97–114. doi: 10.1016/j.postharvbio.2011.05.015
- Perotti, V. E., Moreno, A. S., Tripodi, K., Del Vecchio, H. A., Meier, G., Bello, F., et al. (2015). Biochemical characterization of the flavedo of heat-treated Valencia orange during postharvest cold storage. *Postharvest Biol. Technol.* 99, 80–87. doi: 10.1016/j.postharvbio.2014.08.007
- Porat, R., Weiss, B., Cohen, L., Daus, A., Goren, R., and Droby, S. (1999). Effects of ethylene and 1-methylcyclopropene on the postharvest qualities of 'Shamouti' oranges. *Postharvest Biol. Technol.* 15, 155–163. doi: 10.1016/S0925-5214(98)00079-9
- Purvis, A. C., Kawada, K., and Grierson, W. (1979). Relationship between mid-season resistance to chilling injury and reducing sugar level in grapefruit peel. *Hortscience* 14, 227–229.
- Rivera, F., Pelayo-Zaldivar, C., De Leon, F. D., Buentello, B., Castillo-Rivera, M., and Pérez-Flores, L. J. (2007). Cold-conditioning treatment reduces chilling injury in Mexican limes (*Citrus aurantiifolia* S.) stored at different temperatures. *J. Food Biochem.* 30, 121–134. doi: 10.1111/j.1745-4557.2007.00110.x
- Rodov, V., Ben-Yehoshua, S., Albagli, R., and Fang, D. Q. (1995). Reducing chilling injury and decay of stored citrus fruit by hot water dips. *Postharvest Biol. Technol.* 5, 119–127. doi: 10.1016/0925-5214(94)00011-G
- Romero, P., Rodrigo, M. J., Alférez, F., Ballester, A. R., González-Candelas, L., Zacarias, L., et al. (2012). Unravelling molecular responses to moderate water stress in sweet orange (*Citrus sinensis* L. Osbeck) by using a fruit-specific ABA-deficient mutant. *J. Exp. Bot.* 63, 2753–2767. doi: 10.1093/jxb/err461
- Sala, J. M., and Lafuente, M. T. (1999). Catalase in the heat-induced chilling tolerance of cold-stored hybrid Fortune mandarin fruits. *J. Agric. Food Chem.* 47, 2410–2414. doi: 10.1021/jf980805e
- Sala, J. M., and Lafuente, M. T. (2000). Catalase enzyme activity is related to tolerance of mandarin fruits to chilling. *Postharvest Biol. Technol.* 20, 81–89. doi: 10.1016/S0925-5214(00)00115-0
- Sala, J. M., Sanchez-Ballesta, M. T., Alférez, F., Mulas, M., Zacarias, L., and Lafuente, M. T. (2005). A comparative study of the postharvest performance of an ABA-deficient mutant of oranges. II. Antioxidant enzymatic system and phenylalanine ammonia-lyase in non-chilling and chilling peel disorders of citrus fruit. *Postharvest Biol. Technol.* 37, 232–240. doi: 10.1016/j.postharvbio.2005.05.006
- Saltveit, M. E. (1991). Prior temperature exposure affects subsequent chilling sensitivity. *Physiol. Plant.* 82, 529–536. doi: 10.1111/j.1399-3054.1991.tb02943.x
- Salvador, A., Carvalho, C. P., Monterde, A., and Martinez-Jávega, J. M. (2006). Note. 1-MCP effect on chilling injury development in 'Nova' and 'Ortanique' mandarins. *Food Sci. Technol. Int.* 12, 165–170. doi: 10.1177/1082013206063736
- Sanchez-Ballesta, M. T., Gosalbes, M. J., Rodrigo, M. J., Granell, A., Zacarias, L., and Lafuente, M. T. (2006). Characterization of a β-1,3-glucanase from citrus as related to chilling-induced injury and ethylene production. *Postharvest Biol. Technol.* 40, 133–140. doi: 10.1016/j.postharvbio.2006.01.002
- Sanchez-Ballesta, M. T., Lluch, Y., Gosalbes, M. J., Zacarias, L., Granell, A., and Lafuente, M. T. (2003). A survey of genes differentially expressed during long-term heat-induced chilling tolerance in citrus fruit. *Planta* 218, 65–70. doi: 10.1007/s00425-003-1086-4
- Sanchez-Ballesta, M. T., Rodrigo, M. J., Lafuente, M. T., Granell, A., and Zacarias, L. (2004). Dehydrin from Citrus, which confers *in vitro* dehydration and freezing protection activity, is constitutive and highly expressed in the flavedo of fruit but responsive to cold and water stress in leaves. *J. Agric. Food Chem.* 52, 1950–1957. doi: 10.1021/jf035216+
- Sapintskaya, M., Maul, P., McCollum, G. T., Guy, C. L., Weiss, B., Samach, A., et al. (2006). Postharvest heat and conditioning treatments activate different molecular responses and reduce chilling injuries in grapefruit. *J. Exp. Bot.* 57, 2943–2953. doi: 10.1093/jxb/erl055
- Schirra, M., Agabbio, M., D'Hallewin, G., Pala, M., and Ruggiu, R. (1997). Response of Tarocco oranges to picking date, postharvest hot water dips, and chilling storage temperature. *J. Agric. Food Chem.* 45, 3216–3220. doi: 10.1021/jf970273m
- Schirra, M., and Cohen, E. (1999). Long-term storage of 'Olinda' oranges under chilling and intermittent warming temperatures. *Postharvest Biol. Technol.* 16, 63–69. doi: 10.1016/S0925-5214(98)00097-0
- Sevillano, L., Sanchez-Ballesta, M. T., Romojaro, F., and Flores, F. B. (2009). Physiological, hormonal and molecular mechanisms regulating chilling injury in horticultural species. Postharvest technologies applied to reduce its impact. *J. Sci. Food Agric.* 89, 555–573. doi: 10.1002/jsfa.3468
- Sibouza, X. I., Bertling, I., and Odindo, A. O. (2014). Salicylic acid and methyl jasmonate improve chilling tolerance in cold-stored lemon fruit (*Citrus limon*). *J. Plant Physiol.* 171, 1722–1731. doi: 10.1016/j.jplph.2014.05.012
- Sivankalyani, V., Sela, N., Feygenberg, O., Zemach, H., Maurer, D., and Alkan, N. (2016). Transcriptome dynamics in mango fruit peel reveals mechanisms of chilling stress. *Front. Plant Sci.* 7:1579. doi: 10.3389/fpls.2016.01579
- Vera-Guzman, A. M., Lafuente, M. T., Aispuro-Hernandez, E., Vargas-Arispuro, I., and Martinez-Tellez, M. T. (2017). Pectic and galacturonic acid oligosaccharides on the postharvest performance of Citrus fruits. *Hortscience* 52, 1–7. doi: 10.21273/HORTSCI11466-16
- Wang, C. Y. (1993). "Approaches to reduce chilling injury of fruits and vegetables," in *Horticultural Reviews*, Vol. 15, ed J. Janick (Oxford, UK: Wiley Online Library), 63–95.
- Wang, C. Y., Bowen, J. H., Weir, I. E., Allan, A. C., and Ferguson, I. B. (2001). Heat-induced protection against death of suspension-cultured apple fruit cells exposed to low temperature. *Plant Cell Environ.* 24, 1199–1207. doi: 10.1046/j.1365-3040.2001.00770.x
- Wild, B. L. (1993). Reduction of chilling injury in grapefruit and oranges stored at 1°C by prestorage hot dip treatments, curing, and wax application. *Aust. J. Exp. Agric.* 33, 495–498. doi: 10.1071/EA9930495
- Yun, Z., Gao, H., Liu, P., Liu, S., Luo, T., Jin, S., et al. (2013). Comparative proteomic and metabolomic profiling of citrus fruit with enhancement of disease resistance by postharvest heat treatment. *BMC Plant Biol.* 13:44. doi: 10.1186/1471-2229-13-44
- Yun, Z., Jin, S., Ding, Y., Wang, Z., Gao, H., Pan, Z., et al. (2012). Comparative transcriptomics and proteomics analysis of citrus fruit, to improve understanding of the effect of low temperature on maintaining fruit quality during lengthy post-harvest storage. *J. Exp. Bot.* 63, 2873–2893. doi: 10.1093/jxb/err390
- Conflict of Interest Statement:** The authors declare that the research was conducted in the absence of any commercial or financial relationships that could be construed as a potential conflict of interest.
- Copyright © 2017 Lafuente, Establés-Ortíz and González-Candelas. This is an open-access article distributed under the terms of the Creative Commons Attribution License (CC BY). The use, distribution or reproduction in other forums is permitted, provided the original author(s) or licensor are credited and that the original publication in this journal is cited, in accordance with accepted academic practice. No use, distribution or reproduction is permitted which does not comply with these terms.



Coordinated Regulation of Anthocyanin Biosynthesis Genes Confers Varied Phenotypic and Spatial-Temporal Anthocyanin Accumulation in Radish (*Raphanus sativus* L.)

Everlyne M'mbone Muleke¹, Lianxue Fan¹, Yan Wang¹, Liang Xu¹, Xianwen Zhu², Wei Zhang¹, Yang Cao¹, Benard K. Karanja¹ and Liwang Liu^{1*}

¹ National Key Laboratory of Crop Genetics and Germplasm Enhancement, Key Laboratory of Horticultural Crop Biology and Genetic Improvement (East China) of MOA, College of Horticulture, Nanjing Agricultural University, Nanjing, China,

² Department of Plant Sciences, North Dakota State University, Fargo, ND, United States

OPEN ACCESS

Edited by:

Maarten Hertog,
KU Leuven, Belgium

Reviewed by:

Rosario Muleo,

Università degli Studi della Tuscia, Italy

Antonio Ferrante,

Università degli Studi di Milano, Italy

*Correspondence:

Liwang Liu
nauliulw@njau.edu.cn

Specialty section:

This article was submitted to
Crop Science and Horticulture,
a section of the journal
Frontiers in Plant Science

Received: 25 March 2017

Accepted: 30 June 2017

Published: 19 July 2017

Citation:

Muleke EM, Fan L, Wang Y, Xu L, Zhu X, Zhang W, Cao Y, Karanja BK and Liu L (2017) Coordinated Regulation of Anthocyanin Biosynthesis Genes Confers Varied Phenotypic and Spatial-Temporal Anthocyanin Accumulation in Radish (*Raphanus sativus* L.). *Front. Plant Sci.* 8:1243.
doi: 10.3389/fpls.2017.01243

Anthocyanins are natural pigments that have important functions in plant growth and development. Radish taproots are rich in anthocyanins which confer different taproot colors and are potentially beneficial to human health. The crop differentially accumulates anthocyanin during various stages of growth, yet molecular mechanisms underlying this differential anthocyanin accumulation remains unknown. In the present study, transcriptome analysis was used to concisely identify putative genes involved in anthocyanin biosynthesis in radish. Spatial-temporal transcript expressions were then profiled in four color variant radish cultivars. From the total transcript sequences obtained through illumina sequencing, 102 assembled unigenes, and 20 candidate genes were identified to be involved in anthocyanin biosynthesis. Fifteen genomic sequences were isolated and sequenced from radish taproot. The length of these sequences was between 900 and 1,579 bp, and the unigene coverage to all of the corresponding cloned sequences was more than 93%. Gene structure analysis revealed that *RsF3'H* is intronless and anthocyanin biosynthesis genes (ABGs) bear asymmetrical exons, except *RsSAM*. Anthocyanin accumulation showed a gradual increase in the leaf of the red radish and the taproot of colored cultivars during development, with a rapid increase at 30 days after sowing (DAS), and the highest content at maturity. Spatial-temporal transcriptional analysis of 14 genes revealed detectable expressions of 12 ABGs in various tissues at different growth levels. The investigation of anthocyanin accumulation and gene expression in four color variant radish cultivars, at different stages of development, indicated that total anthocyanin correlated with transcript levels of ABGs, particularly *RsUGT*, *RsF3H*, *RsANS*, *RsCHS3* and *RsF3'H1*. Our results suggest that these candidate genes play key roles in phenotypic and spatial-temporal anthocyanin accumulation in radish through coordinated regulation and the major control point in anthocyanin biosynthesis in radish is *RsUGT*. The present findings lend invaluable insights into anthocyanin biosynthesis and may facilitate genetic manipulation for enhanced anthocyanin content in radish.

Keywords: anthocyanin, color variation, coordinated regulation, gene expression, *Raphanus sativus*, spatial-temporal, transcriptome

INTRODUCTION

Anthocyanins are a big group of naturally occurring water-soluble pigments that belong to a larger group of ubiquitous secondary metabolites referred to as flavonoids (Rodriguez-Saona et al., 1999). They play integral biological functions in plants by protecting plant tissues or senescent leaves against extreme temperatures, photo-oxidative injury and irradiation (Nhukarume et al., 2010). They also contribute in pollination and facilitating seed distribution (Harborne and Williams, 2000). Besides being directly beneficial to plants, anthocyanins have also been shown to display vital nutraceutical properties that prevent heart disease and cancer in humans (Lamy et al., 2007; Nhukarume et al., 2010). Additionally, red radish derived anthocyanins continue to be largely used in food industries as coloring agents because they are highly stable and exhibit properties similar to those of synthetic food Red No.40 (Rodriguez-Saona et al., 1999).

Anthocyanins are synthesized from the phenylpropanoid pathway comprised of multienzymes that catalyze several key biosynthetic steps (Figure S1; Park et al., 2011; Wei et al., 2011). The synthesis of anthocyanins is dependent on the enzymes of the general flavonoid pathway as well as those of the specific anthocyanin pathway. The enzymes which catalyze specific steps of the anthocyanin biosynthesis pathway are encoded by structural genes which are in-turn under the control of regulatory genes (transcription factors). In addition, substrate specificity for the genes between different leucoanthocyanidins with regard to the hydroxylation ring is a mechanism that explains the variation in anthocyanin aglycons in different genotypes. The anthocyanin biosynthetic pathway is one of the earliest studied pathways since 1980 (Holton and Cornish, 1995). In various plant species most enzymes of the anthocyanin biosynthetic pathway are already identified (He et al., 2010; Park et al., 2011; Jaakola, 2013). The first stage of the general phenylpropanoid pathway is where phenylalanine is converted to coumarate-CoA by phenylalanine ammonia lyase gene (*PAL*), cinnamate 4-hydroxylase gene (*C4H*), and 4-coumarate CoA ligase gene (*4CL*). The anthocyanin pathway branches from the general phenylpropanoid pathway when enzymes chalcone synthase (*CHS*), chalcone isomerase (*CHI*), flavanone 3-hydroxylase (*F3H*) and flavonoid 3'-hydroxylase (*F3'H*), catalyze the synthesis of tetrahydroxychalcone (THC) from the combination of a 4-coumaroyl CoA molecule and three of malonyl-CoA (Tanaka et al., 2008). When *CHS* gene was modulated through RNA interference, the blue color of the flower changed from blue to white (Fukusaki et al., 2004). The flavonoid genes were also found to exhibit up-regulation with advance toward ripening stage, resulting in color development in strawberry (*F. ananassa*), which establishes

a positive correlation between transcript levels of flavonoid genes and anthocyanin accumulation (Carbone et al., 2009). The immediate step is the generation of various anthocyanidins by dihydroflavonols, catalyzed by anthocyanidin synthase gene (*ANS*) and dihydroflavonol 4-reductase gene (*DFR*) which uses NADPH as a cofactor (Lepiniec et al., 2006). In *Pyrus pyrifolia* the *DFR* and *ANS* genes have been considered the limiting factors for the skin color of the mildly colored pears (Zhang et al., 2011). Over 20 types of, anthocyanidins/ aglycons, of anthocyanins are known (Jaakola, 2013), and are clustered into six major classes: cyanidin, delphinidins, malvidin, pelargonidin, peonidin and petunidin; the major anthocyanin aglycons in radish being cyanidin and pelargonidin (Park et al., 2011). The synthesized anthocyanidins then undergo modification through a series of methylation and glycosylation steps to form stable anthocyanidins. These steps are catalyzed by glucosyltransferases, glycosyltransferases and methyltransferases, which are encoded by a large number of genes depending on the anthocyanin aglycon and the genotype. In grape berry, it was reported that loss of color in white grapes was due to the absence of *UDP-glucose: flavonoid 3-O-glucosyltransferase (UFGT)* gene which is deemed critical for anthocyanin biosynthesis (Kobayashi et al., 2001). The downstream steps involve the mutual sequestration of the anthocyanins into the vacuoles, which involve the non-covalent activity of *glutathione S-transferase (GST)* genes. Several GSTs involved in the sequestration of anthocyanins have been isolated in several plants including apple (*Malus domestica*), Arabidopsis (*A. thaliana*) and grape (*V. vinifera*) (Cutanda-Perez et al., 2009; Li et al., 2011; Ahn and Yun, 2016). Although different genes may encode different families of GSTs, they are all necessary for the sequestration of anthocyanins into the vacuoles.

Radish (*Raphanus sativus*) is a member of the Brassicaceae family and among the most economically important root vegetable crops grown globally. The color of the taproots varies from white to red, to purple-pink, to green, to bicolor, due to its accumulation of large amounts of anthocyanins (Chen et al., 2016). Studies on anthocyanin and the underlying molecular mechanism in radish dwell on single-tissue analysis and mostly at maturity stage (Park et al., 2011; Bae et al., 2012; Chen et al., 2016). A growing body of research provides evidence that as growth advances, anthocyanin accumulation is not localized in the plant but rather, discriminatively accumulates in specific clusters of cells located in different plant tissues (Zuluaga et al., 2008; Zhang et al., 2014). Radish is rich in anthocyanin and a very versatile crop with regards to anthocyanin accumulation and distribution; while some varieties concentrate anthocyanins in the flesh, some accumulate in the skin, stems, leaves or both, depending on the genotype and developmental stage. These presents radish as an appropriate model organism for deciphering the mechanisms that contribute to differential anthocyanin accumulation.

Recently, several studies tried to elucidate the mechanisms that contribute to color variation in intra-tissues during different levels of growth. These include cherry (Liu et al., 2013), dendrobium (Kriangphan et al., 2015), mulberry (Li et al., 2014), grape (Xie et al., 2015) and yam (Yin et al., 2015). It was suggested that patterns of anthocyanin biosynthesis in different grape berry tissues are discontinuous, implying that ABGs are regulated

Abbreviations: 4CL, Courmarate 4-ligase; ANR, Anthocyanidin reductase; ANS, Anthocyanidin synthase; CHI, Chalcone isomerase; CHS, Chalcone synthase; DAS, Days after sowing; DFR, Dihydroflavonol reductase; F3'H, Flavonoid 3'-hydroxylase; F3H, Flavanone 3-hydroxylase; GST, Glutathione-S-transferase; OMT, Methyl O-transferase; PAL, Phenylalanine ammonia lyase; SAM, S-Adenosylmethyl Transferase; TT12, Transparent Testa12; UFGT, UDP glucose:flavonoid 3-O-glucosyltransferase.

spatially and temporally (Fagginella et al., 2012; Xie et al., 2015). Transcript levels of anthocyanin biosynthetic genes in strawberry fruits were also found to be increased during fruit ripening with the expression levels being much higher in red colored tissues than white tissues (Salvaterra et al., 2010). In purple yam, anthocyanin biosynthesis genes were highly expressed at the early stages of growth in leaves and stems, but peaked at growth stages: the middle and later stages of growth (Yin et al., 2015). Radish differentially accumulates anthocyanin during various stages of growth, yet, molecular mechanisms underlying this differential anthocyanin accumulation remained unknown.

In this study, high-throughput sequencing data was employed to concisely identify key ABGs in radish. Secondly, four different radish cultivars were utilized to provide a comprehensive comparative spatial-temporal transcript analysis of candidate ABGs. Profiling at different growth stages also aimed at determining the stage at which the anthocyanin biosynthetic pathway switches off leading to the loss of anthocyanin in the non-colored radish. These findings could provide additional vital fundamental knowledge to dissect molecular mechanisms underlying differential anthocyanin accumulation and contribute to the ultimate genetic improvement of anthocyanin in radish taproots.

MATERIALS AND METHODS

Plant Materials

Four advanced inbred radish lines “NAU-YH”, “NAU-XLM”, “NAU-XBC”, and “NAU-YZH” were used. The cultivars exhibit red skin-white flesh, green skin-pink-purple flesh, white skin-white flesh and red skin-red flesh, respectively (Figure 1). Seeds were selected and surface sterilized before being germinated

on moist filter paper in darkness for 3 days. They were then transplanted into plastic pots containing 1:1 mixture of sterilized soil and peat substrate, and cultured in the greenhouse. The growth conditions included a 14 h light/10 h darkness photoperiod with an average temperature of 18°C. The inability of radish cortex cells to undergo division and expansion results in splitting, an occurrence that is vital for the initiation of taproot thickening. The development of cortex splitting is an important signal of the initiation of taproot thickening growth in radish due to the inability of the cortex cells to undergo division and expansion (Wang et al., 2013). Cortex splitting has been found to begin at around 12 days after sowing (DAS), thus 10 DAS is the pre-cortex splitting, while the peak of root cortex splitting is at 30 DAS. The maximum taproot thickening is achieved at 50 DAS. Subsamples of leaf and taproot issues were collected at 10 DAS (pre-cortex splitting stage), 30 DAS (cortex splitting stage) and 50 DAS (taproot thickening stage). At maturity stage, prior to experiments, radishes were briefly, manually peeled to separate the skin and the flesh, which were then cut into small cubes. Samples in three biological replicates were separated into different batches for anthocyanin and total RNA extraction. Samples for anthocyanin were used immediately, while those for RNA extraction were frozen in liquid nitrogen and stored at -80°C until use.

Determination of Total Anthocyanin Accumulation

Individual samples were ground into fine powder in the presence of liquid nitrogen before anthocyanin extraction. The anthocyanin content was measured with the modified method (Mehrtens et al., 2005; Yin et al., 2015). Totally, 2.00 g of

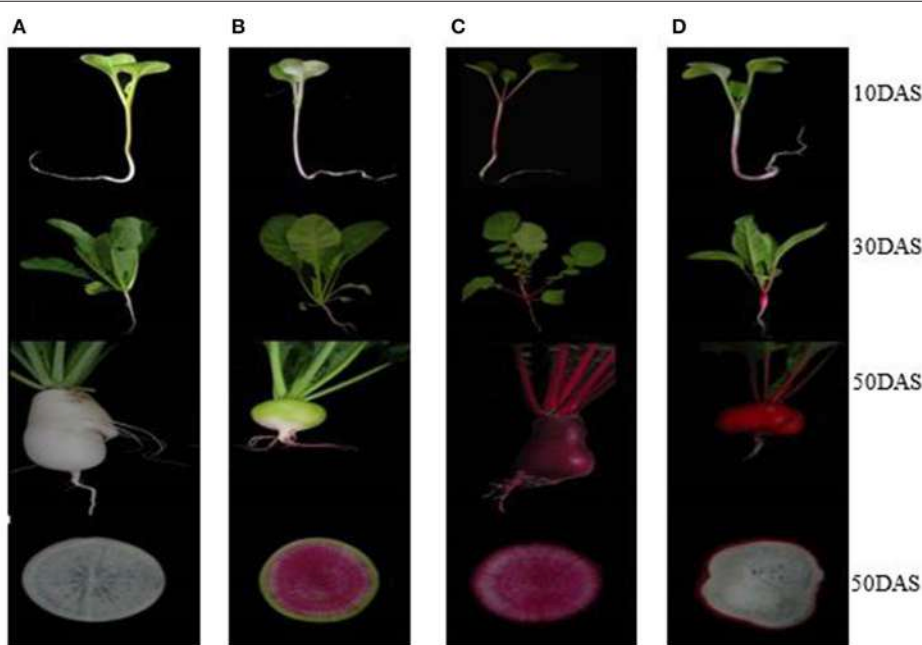


FIGURE 1 | Four different colored radish genotypes at different developmental stages. **(A)** “NAU-XBC”, **(B)** “NAU-XLM”, **(C)** “NAU-YZH”, **(D)** “NAU-YH”.

the ground powder were dissolved in 6 mL of an extraction solution [concentrated HCl + 80% (v/v) ethanol, 1:99], then extracted by shaking on a mechanical shaker at 110 rpm at room temperature, while shielding from light for 24 h. Then 1 mL of the mature radish extract or 2 mL of seedling (10 DAS) extract was filtered and diluted to 10 mL with 0.4 M sodium acetate (pH 4.5) and 0.025 M hydrochloric acid (pH 1.0) buffers. The absorbance was then observed at 530 and 657 nm on a UV-VIS spectrophotometer (ND752, SPSIC, Shanghai, China). The anthocyanin content (Q) detected was calculated as $Q = \frac{A_{530} - (0.25 \times A_{657})}{g\text{ FW}}$, where g FW is the fresh mass of the sample in grams. Values, representing means from three independent experiments were subjected to analysis of variance (ANOVA) using PROC GLM code of SAS version 9 (2005). Significant means were separated using the Tukey's Honestly Significant Difference Test at $P \leq 0.05$, while Microsoft Office Excel version 2013 was used to generate figures.

Genomic DNA, Total RNA Extraction and Reverse Transcription

The cetyltrimethylammonium bromide CTAB method (Liu et al., 2003) was used for extraction of genomic DNA from mature leaf and root tissues of "NAU-YH". After being digested with RNase, it was re-extracted with phenol/chloroform/isoamyl alcohol (25:24:1) and chloroform/isoamyl alcohol (24:1). Total RNA from the leaf and root tissues of all the four cultivars at the three previously mentioned developmental stages was extracted according to the previous protocol (Xu et al., 2013). Integrity analysis of DNA and RNA was performed by electrophoresis on a 1% ethidium bromide stained agarose gel. cDNA was synthesized from 2 μ g of RNA using a PrimeScriptTM RT reagent Kit with gDNA Eraser (TaKaRa Bio Inc., Dalian, China). Prior to reverse transcription, DNase was used to remove contaminating DNA according to the manufacturer's instructions. Total RNA was reverse-transcribed using M-MLV reverse transcriptase (Promega, Madison, WI, USA) and an oligo d (T) 18 primer.

Identification, Isolation, and Sequence Analysis of Candidate Anthocyanin Biosynthesis Genes (ABGs)

For RNA Sequencing Library Construction and Illumina Sequencing, radish (*Raphanus sativus* L.) advanced inbred line "NAU-YH" was used. Sequencing was done on Illumina HiSeqTM 2500 platform at the Beijing Genomics Institute (BGI, Shenzhen, China). The construction of the library and Illumina sequencing were performed according to a method previously described (Cheng et al., 2013). Radish unigene sequences from the *de novo* transcriptome data, deposited in the NCBI Sequence Read Archive repository: SRX707630 (Yu et al., 2016) were analyzed to identify and isolate the genes associated with anthocyanin biosynthesis. Using nucleotide sequences from these genes as queries, BLASTx was done against the NCBI Gene Bank (<http://www.ncbi.nlm.nih.gov/genbank>), radish genome (<http://www.nodai-genome-d.org/>)

(Kitashiba et al., 2014) and "NAU-YH" transcriptome databases. For validation of the transcriptome data, fifteen candidate genes including *RsPAL1*, *Rs4CL3*, *RsCHS3*, *RsCHI*, *RsF3H*, *RsF3'H1*, *RsDFR*, *RsANS*, *RsANR*, *RsUGT*, *RsTT12*, *RsSAM*, *RsOMT*, *RsGSTU5*, and *RsGSTF10* were isolated from "NAU-YH". Gene-specific primers (GSPs) were designed based on the genomic nucleotides and used to amplify the ABGs using mixed root and leaf DNA as the template. Primers used for cloning are shown in Table S1. Each PCR reaction was carried out in a total volume of 20 μ L containing 2.0 mM Mg²⁺, 0.2 mM dNTP, 1.0 μ M of gene specific primer, 0.8 μ L Taq DNA polymerase (TaKaRa Bio Inc., Dalian, China) and 20 ng of diluted DNA template. The conditions for PCR were as follows: 94°C for 3 min; 35 cycles of 50 s at 94°C, 50 s at annealing temperature (Tm) and 90 s at 72°C, and finally extension at 72°C for 10 min. PCR products were purified and cloned into a pMD19-T vector (TaKaRa Bio Inc., Dalian, China). Three independent positive clones from each isolated gene were sequenced on an ABI3730 sequencer (Applied Bio systems, USA). These cloned sequences were aligned with the corresponding unigenes from the transcriptome (<https://www.ncbi.nlm.nih.gov/sra/SRX707630/>), to access the coverage. The chromosomal location and related predicted sequences were obtained through a manual search from (<http://www.nodai-genome-d.org/>). ORF Finder and the BLAST (<https://www.ncbi.nlm.nih.gov/orffinder/>) programs were employed to analyze the cDNA and amino acid sequences. Pfam (<http://www.pfam.xfam.org/>) was used to identify conserved domains. Coding sequences (CDS) were aligned to DNA sequences and schematics generated using Gene Structure Display Server (<http://gsds.cbi.pku.edu.cn/>).

Transcript Profiling of Anthocyanin Biosynthetic Genes (ABGs)

Following gene validation, a spatiotemporal analysis of the respective anthocyanin biosynthetic genes' transcript levels, was performed using quantitative real time PCR (RT-qPCR). Sequence-specific primers used for RT-qPCR were designed using Beacon Designer v7.0 (Premier Biosoft International, USA; Table S2). An iQTM 5 Multicolor Real-Time PCR Detection System (Bio-Rad Laboratories, Berkeley, CA, USA) was used to perform PCR. Each reaction (20 μ L) contained 10 μ L of SYBR[®] Premix Ex Taq (Takara), 2.0 μ L of cDNA and 0.2 μ M of each primer. PCR was carried out under the program of 95°C for 3 min, 40 cycles of 95°C for 5 s, 58°C for 30 s, and 72°C for 10 s. The data were analyzed using iQTM 5 Optical System Software (version 2.1, Bio-Rad) and expression levels of the gene normalized to *RsActin* gene (Xu et al., 2012). Relative fold expression changes were calculated using the $2^{-\Delta\Delta C_T}$ method (Livak and Schmittgen, 2001). The ANOVA was performed using PROC GLM code of SAS version 9 (2005) and means separated using Tukey's Honestly Significant Difference Test at $P \leq 0.05$, while Microsoft Office Excel version 2013 was used to generate figures. Specifically, point analysis was done, depicting the significant variations between the leaf and

root tissue, within each gene. Pearson's correlation coefficient, MetaboAnalyst 3.0 (<http://www.metaboanalyst.ca/faces/Secure/upload/StatUploadView.xhtml>) was used for correlation analysis between gene expression levels and accumulation of total anthocyanin.

RESULTS

Profiling of Total Anthocyanin in Radish

Differences in the quantity of anthocyanin were observed in the leaf, young root, flesh and skin of different radish genotypes at different growth stages (Figure 2). At all sampling points, there were no detectable amounts of anthocyanin in the leaf and root tissues of "NAU-XBC". At 10 DAS significant anthocyanin amounts were only detected in the leaf and root of "NAU-YZH". There was a steady global increase in anthocyanin content at 30 DAS, wherein, anthocyanin was detected in the leaves of "NAU-YH" and "NAU-YZH", being highest in "NAU-YZH" while insignificant in "NAU-XLM". In the root tissues at 30 DAS, anthocyanin was detected in "NAU-YZH", "NAU-YH", and "NAU-XLM" with consistently high levels in "NAU-YZH" and lower but equally significant amounts recorded in "NAU-YH" and "NAU-XLM".

Among the three developmental stages, the maximum value of anthocyanin content was recorded at 50 DAS. At this stage, the root and the skin were separated into the respective skin and flesh components. Consistent with other stages, "NAU-YZH" accumulated considerable amounts of anthocyanin in both tissues. Anthocyanin was only detected in the leaf of "NAU-YZH" and "NAU-YH" being significantly high in the latter cultivar. Sufficiently high amount of anthocyanin was recorded in the flesh of "NAU-YZH" closely followed by "NAU-XLM" but barely detectable in the "NAU-YH" flesh. In the skin at 50 DAS, significant anthocyanin amounts were detected in "NAU-YZH" and "NAU-YH" (NAU-YZH>NAU-YH) (Figure 2).

Identification and Isolation of Anthocyanin Biosynthetic Genes (ABGs)

To identify the genes associated with anthocyanin biosynthesis, the anthocyanin biosynthetic pathway was analyzed based on the Kyoto Encyclopedia of Genes and Genomes (KEGG), which divided this pathway into three distinct phases: the general phenylpropanoid biosynthesis pathway (ko00940), the flavonoid biosynthesis pathway (ko00941) and later the specific anthocyanin biosynthetic pathway (ko00942). According to de novo assembled transcriptome (SRX707630), using local blast search and sequences functionally annotated by the KEGG pathway analysis, 20 genes encoding enzymes of the anthocyanin biosynthesis pathway were identified. These included three *PAL* (K10775, EC: 4.3.1.24) syntenic genes (14 unigenes), five *4CL* (K01904, EC: 6.2.1.12) syntenic genes (17 unigenes), four *CHS* (K00660, EC:2.3.1.74) syntenic genes (10 unigenes), two *F3'H* (K00475, EC:1.14.11.9) syntenic genes (11 unigenes) and one gene each for *C4H*, *CHI* (K01859, EC:5.5.1.6), *DFR* (K13082, EC: 1.1.1.219 1.1.1.234), *ANS* (K05277, EC: 1.14.11.19), *F3H* (K05280, EC 1.14.13.21) (8, 6, 6, 11 and 11 unigenes, respectively), and 129 unigenes were found to correspond to genes involved in methylation, glucosylation and glycosylation: *UGFT* (K12338, EC: 2.4.1.298), *UGAT* (K12937, EC: 2.3.1.254), *AT* (K12930, EC: 2.4.1.115), *MT* (K12931, EC: 2.3.1.171), *GT1* (K12938, EC: 2.4.1.-) (Table 1).

A total of 102 assembled unigenes were annotated as those that correspond to enzymes involved in the upstream anthocyanin biosynthesis pathway. Specifically, 39 assembled unigenes were found to correspond to the genes in the general phenylpropanoid pathway. From malonyl-CoA to the colored unstable flavonoids, 55 unigene sequences related to six enzymes involved in the flavonoid biosynthetic pathways were isolated. One-twenty nine unigenes were found to be associated with the glycosylation of different anthocyanin aglycons in the specific pathway (Table S4). In the downstream steps of the anthocyanin biosynthesis pathway,

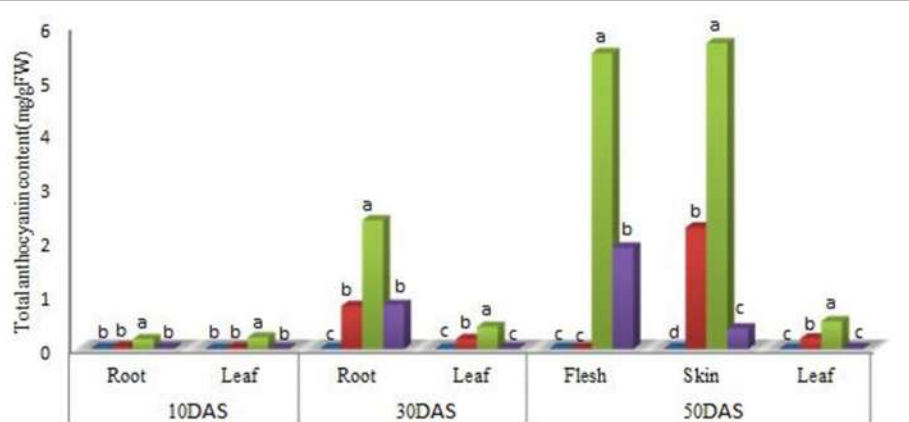


FIGURE 2 | Changes in the concentration of anthocyanin (mg/g Fw) in the leaf and root of four radish cultivars during different stages of growth. XB, YH, YZ and XL represents "NAU-XBC", "NAU-YH", "NAU-YZH", and "NAU-XLM", respectively. Values are means of three independent replicates. Values not connected by the same letter within the same data point are significantly different according to Tukey's HSD test ($P \geq 0.5$).

TABLE 1 | Transcriptome-based identification of genes involved in anthocyanin biosynthesis in radish.

Enzyme	Full gene name	EC number	Number of Unigenes	Gene Annotation	Unigene ID
PAL	<i>Phenylalanine ammonia lyase</i>	EC:4.3.1.24	14	PAL1	CL2858.Contig3_NAU-YH, Unigene13215_NAU-YH, Unigene29856_NAU-YH, Unigene29857_NAU-YH, Unigene3029_NAU-YH
				PAL2	CL2858.Contig2_NAU-YH, CL2858.Contig4_NAU-YH, CL2858.Contig5_NAU-YH, Unigene29855_NAU-YH, CL2858.Contig1_NAU-YH
				PAL4	Unigene17724_NAU-YH, Unigene17857_NAU-YH, Unigene17723_NAU-YH
C4H	<i>Cinnamate 4-hydroxylase</i>	EC:1.14.13.11	8	C4H	CL3932.Contig4_NAU-YH, CL3932.Contig5_NAU-YH, Unigene10552_NAU-YH, Unigene11266_NAU-YH, CL3932.Contig1_NAU-YH, CL3932.Contig2_NAU-YH, CL3932.Contig3_NAU-YH, Unigene29684_NAU-YH
4CL	<i>4-coumarate–CoA</i>	EC:6.2.1.12	17	4CL1	Unigene28587_NAU-YH, Unigene28588_NAU-YH
				4CL4	Unigene26090_NAU-YH, Unigene11346_NAU-YH, Unigene1876_NAU-YH
				4CL3	Unigene24485_NAU-YH, Unigene24486_NAU-YH, Unigene24487_NAU-YH, Unigene24488_NAU-YH, CL6005.Contig1_NAU-YH, CL6005.Contig2_NAU-YH
				4CL10	CL10957.Contig1_NAU-YH, CL2343.Contig1_NAU-YH
				4CL-LIKE	CL5789.Contig1_NAU-YH, CL5789.Contig2_NAU-YH, CL11872.Contig1_NAU-YH, CL11872.Contig2_NAU-YH
				CHS1	CL14029.Contig2_NAU-YH, Unigene4661_NAU-YH, Unigene9761_NAU-YH, CL14029.Contig1_NAU-YH, CL2470.Contig2_NAU-YH, Unigene5006_NAU-YH
				CHS3	CL2470.Contig1_NAU-YH, Unigene37218_NAU-YH
CHS	<i>Chalcone synthase</i>	EC:2.3.1.74	10	CHS8	Unigene3641_NAU-YH
				CHS5	Unigene5900_NAU-YH
				CHI	CL12905.Contig1_NAU-YH, CL12905.Contig2_NAU-YH, CL4842.Contig1_NAU-YH, CL4842.Contig2_NAU-YH, Unigene12692_NAU-YH, Unigene14025_NAU-YH
CHI	<i>Chalcone–flavonone isomerase</i>	EC:5.5.1.6	6		

(Continued)

TABLE 1 | Continued

Enzyme	Full gene name	EC number	Number of Unigenes	Gene Annotation	Unigene ID
F3H	<i>Flavanone 3-hydroxylase/Flavonol synthase</i>	EC:1.14.11.23	11	<i>F3H</i>	Unigene17936_NAU-YH, Unigene17937_NAU-YH, CL6897.Contig2_NAU-YH, CL7327.Contig5_NAU-YH, Unigene10168_NAU-YH, Unigene10580_NAU-YH, Unigene11483_NAU-YH, Unigene13117_NAU-YH, Unigene22378_NAU-YH, Unigene34749_NAU-YH, Unigene3501_NAU-YH
F3'H	<i>Flavonoid 3' hydroxylase</i>	EC:1.14.13.21	11	<i>F3'H1</i>	Unigene8907_NAU-YH, Unigene8883_NAU-YH, Unigene8884_NAU-YH, CL1992.Contig1_NAU-YH, CL2046.Contig3_NAU-YH
				<i>F3'H2</i>	CL2785.Contig1_NAU-YH, Unigene1076_NAU-YH, Unigene1361_NAU-YH, Unigene210_NAU-YH, Unigene2815_NAU-YH, Unigene8885_NAU-YH
DFR	<i>Dihydroflavonol 4-reductase</i>	EC:1.1.1.219 1.1.1.234	6	<i>DFR</i>	CL1858.Contig1_NAU-YH, CL1858.Contig2_NAU-YH, CL1858.Contig3_NAU-YH, Unigene20944_NAU-YH, Unigene34696_NAU-YH
				<i>DFR-LIKE</i>	Unigene5033_NAU-YH
ANS	<i>Anthocyanidin synthase/leucoanthocyanidin dioxygenase</i>	EC:1.14.11.19	11	ANS	CL12532.Contig1_NAU-YH, CL12532.Contig2_NAU-YH, CL6245.Contig1_NAU-YH, CL6593.Contig1_NAU-YH, CL6593.Contig2_NAU-YH, CL8001.Contig1_NAU-YH, Unigene13296_NAU-YH, CL13551.Contig1_NAU-YH, CL6549.Contig1_NAU-YH, Unigene4289_NAU-YH, Unigene4558_NAU-YH
ANR	<i>Anthocyanidin reductase</i>	EC:1.3.1.77	1	ANR	Unigene4158_NAU-YH
UGT	<i>UDP-glucosyl transferase</i>	EC:2.4.1.-	147	UGT	CL1797.Contig1_NAU-YH, CL1797.Contig2_NAU-YH, Unigene3464_NAU-YH, Unigene12158_NAU-YH, Unigene17156_NAU-YH, Unigene11916_NAU-YH, CL8206.Contig1_NAU-YH, CL7501.Contig1_NAU-YH, CL5504.Contig1_NAU-YH
GST	<i>Glutathione S-transferase</i>	EC:2.5.1.18	61	GST	CL1126.Contig1_NAU-YH, CL1126.Contig2_NAU-YH, CL11539.Contig1_NAU-YH, CL11539.Contig2_NAU-YH, CL12204.Contig1_NAU-YH, CL12204.Contig2_NAU-YH, CL1696.Contig1_NAU-YH,

(Continued)

TABLE 1 | Continued

Enzyme	Full gene name	EC number	Number of Unigenes	Gene Annotation	Unigene ID
OMT	<i>Flavone 3'-O-methyl transferase</i>	EC:2.1.1.76	24	OMT	CL1696.Contig2_NAU-YH, CL1696.Contig3_NAU-YH, CL1696.Contig4_NAU-YH, CL1696.Contig5_NAU-YH

stable anthocyanins are trafficked to the anthocyanin vacuole via the non-covalent activity of glutathione S-transferase (GST, EC: 2.5.1.18); 61 unigenes were found to correspond to different GSTs.

Cloning and Sequence Analysis of Genes Involved in Anthocyanin Biosynthesis of Radish

Partial DNA fragments or full-length sequences of 15 genes encoding anthocyanin biosynthesis-related enzymes were isolated through cloning. Full length genomic fragments of nine genes (*RsCHS3*, *RsCHI*, *RsF3H*, *RsF3'H1*, *RsANS*, *RsANR*, *RsUGT78D2*, *RsGSTU5*, and *RsGSTU10*), and partial fragments of six genes (*RsPAL1*, *Rs4CL3*, *RsSAM*, *RsOMT*, *RsTT12*, and *RsDFR*), were isolated. The sequences of these genes were submitted to the National Center for Biotechnology Information (NCBI)/GenBank database under the following accession numbers: *RsCHS3* (MF182893), *RsCHI* (MF182892), *RsF3H* (MF182895), *RsF3'H1* (MF182896), *RsANS* (MF182899), *RsANR* (MF182891), *RsUGT78D2* (MF183115), *RsTT12* (MF182901), *RsGSTU5* (MF182897), *RsGSTU17* (MF182898), *RsPAL1* (MF285801), *Rs4CL3* (MF285800), *RsSAM* (MF182902), *RsOMT* (MF182900), and *RsDFR* (MF182894). The length of these gene sequences varied from 900 to 1,579 bp, and the unigene coverage to corresponding genomic sequences was above 93% (Table 2).

Genomic sequence analysis depicted the different domains of each of the ABGs, which bear the catalytic sites that enable the unique reactions performed by each gene. Intron classification revealed that most of the anthocyanin biosynthetic genes bear phase one introns with predominantly asymmetrical exons, except *RsSAM* which has one symmetrical (1-1) exon (Figure S2). The analysis also revealed unique features in the flavanone hydroxylase genes; the *RsF3'H1* gene located on scaffold 45 is intronless, while *RsF3H* bears exclusively phase 0

TABLE 2 | Sequence validation of genes involved in anthocyanin biosynthesis in radish.

Gene	Length	Unigenes	Coverage (%)	Accession number	ORF similarity (%)	Gap (%)
<i>RsPAL1</i>	1,228	6	97	MF285801	96	3
<i>Rs4CL3</i>	1,049	6	99	MF285800	96	1
<i>RsCHS3</i>	1,303	2	93	MF182893	98	7
<i>RsCHI</i>	1,269	6	100	MF182892	98	0
<i>RsF3H</i>	1,356	11	100	MF182895	94	0
<i>RsF3'H1</i>	1,579	5	99	MF182896	99	1
<i>RsDFR</i>	1,054	5	99	MF182894	100	1
<i>RsANS</i>	1,191	11	98	MF182899	99	2
<i>RsANR</i>	1,048	1	99	MF182891	100	1
<i>RsUGT78D2</i>	1,240	2	100	MF183115	100	0
<i>RsOMT</i>	1,102	1	100	MF182900	100	0
<i>RsSAM</i>	1,170	2	100	MF182902	89	0
<i>RsTT12</i>	1,146	3	100	MF182901	98	0
<i>RsGSTU5</i>	900	1	99	MF182897	99	1
<i>RsGSTF17</i>	1,223	2	99	MF182898	99	1

introns. The *RsSAM* ABG has the highest number of introns (10) and the isoelectric points of radish ABGs are between 4.589 (*RsCHI*) and 11.87 (*RsPAL1*), which categorizes the radish ABGs as stable (Table 3).

Transcript Profiling of ABGs in Four Radish Genotypes

RT-qPCR was utilized to analyze transcript levels of 14 radish genes associated with anthocyanin biosynthesis, relative to the cultivar, developmental stage and plant tissue. Four color variant radish genotypes ("NAU-YZH", "NAU-YH", "NAU-XBC" and "NAU-XLM") at three developmental stages (10, 30, and 50

TABLE 3 | Characteristics of anthocyanin biosynthesis genes in radish.

Gene	Scaffold	Strand	Start-end	CDS length ^a	Number of exons ^b	Protein size	Theoretical MW(kDa)	Theoretical PI
<i>RsPAL1</i>	Rs_scaf92	(+)	243886-247511	2,400	3	756	85,897.42	11.874
<i>RsPAL2</i>	Rs_scaf801	(-)	53717-56216	2,175	1	724	78,601.91	6.194
<i>RsPAL4</i>	Rs_scaf132	(-)	77225-80788	2,125	2	702	76,795.77	5.865
<i>Rs4CL1</i>	Rs_scaf707	(-)	80817-83472	1,659	3	552	60,216.51	5.263
<i>Rs4CL4</i>	Rs_scaf34	(-)	351971-356525	1,782	5	593	65,050.21	5.039
<i>Rs4CL3</i>	Rs_scaf424	(-)	13415-20270	1,677	10	558	60,552.82	6.117
<i>Rs4CL10</i>	Rs_scaf4963	(-)	3583-5666	1,545	4	514	55,334.04	6.183
<i>RsCHS1</i>	Rs_scaf14	(+)	335667-337099	1,191	1	396	43,052.88	6.671
<i>RsCHS3</i>	Rs_scaf11	(-)	1269822-1271094	1,188	1	395	42,982.62	6.145
<i>RsCHS5</i>	Rs_scaf119	(-)	138269-139725	1,991	1	396	43,094.76	6.277
<i>RsCHS8</i>	Rs_scaf217	(-)	277834-279184	1,101	1	366	39,757.1	5.948
<i>RsCHI</i>	Rs_scaf7714	(-)	522-2902	618	3	206	26,620.36	4.589
<i>RsF3H</i>	Rs_scaf58	(+)	29065-30370	1,077	2	358	40,087.57	5.465
<i>RsF3'H1</i>	Rs_scaf45	(+)	58827-60401	1,575	0	524	59,512.06	6.622
<i>RsF3'H2</i>	Rs_scaf62	(-)	524013-524884	871	2	156	37,572.63	10.858
<i>RsDFR</i>	Rs_scaf2809	(-)	21463-23363	924	5	306	33,883.97	5.627
<i>RsANS</i>	Rs_scaf190	(-)	249786-250944	1,074	1	357	40,810.16	5.747
<i>RsUGT</i>	Rs_scaf749	(-)	40726-42222	1,383	1	460	50,932.69	4.983
<i>RsANR</i>	Rs_scaf197	(-)	78407-79919	1,017	5	338	37,799.2	5.016
<i>RsGSTF11</i>	Rs_scaf1076	(-)	945-2916	987	4	328	37,159.2	6.273
<i>RsGSTU10</i>	Rs_scaf648	(+)	14594-15478	642	1	213	24,185.78	7.041
<i>RsGSTU5</i>	Rs_scaf10	(-)	594776-595590	621	1	207	24,273.96	7.685
<i>RsOMT</i>	Rs_scaf464	(-)	133367-135867	1,495	3	364	39,906.35	5.76
<i>RsSAM</i>	Rs_scaf 831	(+)	88381-91197	930	10	309	34,158	6.373

^aThe CDS length was based on predicted sequences.^bThe number of exons was based on the genomic data.

DAS) and the leaf, young root, taproot flesh and skin were used. The initial steps of the flavonoid pathway from 4-coumaroyl CoA through chalcone and naringenin to dihydroflavonol are catalyzed by CHS, CHI, F3H, and F3'H (Tanaka et al., 2008). *RsCHS3* and *RsCHI* abundantly expressed in the leaf and root tissues of all genotypes under study, with the highest expression in "NAU-YZH" leaf and "NAU-XLM" root at 10 DAS (**Figure 3**). The latter gene was 12-folds up regulated at 30 DAS characterized by high levels in "NAU-YZH" leaf and "NAU-YH" root, and non-traceable in all tissues of "NAU-XBC" while there was a general dramatic decline of *RsCHI* in the root (**Figure 3**). At 50 DAS, however, the expression levels of *RsCHS3* increased by 2-folds with consistent high expression in "NAU-YZH" and "NAU-YH" leaf, flesh and skin, respectively (**Figure 3**). *RsCHI* on the other hand generally showed no change in transcript levels with significant high expression in the leaf of "NAU-YH" and the skin and root of "NAU-YZH". Notably, while the lowest transcripts of *RsCHI* significantly were expressed in "NAU-XLM" leaf, this gene was increased by 4-folds in the flesh at 50 DAS (**Figure 3**).

The transcripts of *RsF3H* were equally expressed in both leaf and root but with significantly higher expression of *RsF3'H1* in "NAU-YZH" and "Nau-YH" at 10 DAS (**Figure 3**). However, *RsF3'H* peaked in the leaf and was barely detected in the root at 30 DAS, while *RsF3H* remained consistently up regulated with high expression in "NAU-YZH" leaf and "NAU-YH" root

(**Figure 3**). There was no change in transcript levels of *RsF3H* but *RsF3'H1* globally increased by 10-folds, and both genes showed a consistent high expression in the leaf and skin of "NAU-YZH" and "NAU-YH" respectively, at 50 DAS (**Figure 3**). Transcripts of *RsF3H* were notably significantly repressed in the leaf and skin but increased by 5-folds in the flesh of "NAU-XLM".

In the synthesis of dihydroflavanols, which are intermediates in anthocyanin biosynthesis, the genes *RsDFR* and *RsANS* play critical synthesis functions, while *RsANR* acts as an inhibitory gene to *RsANS*. The *RsANS* gene was down-regulated in the leaf of "NAU-XBC", and up-regulated in "NAU-YZH" and "NAU-YH" with no significant variation in the root tissues at 10 DAS (**Figure 3**). Transcript levels increased in the leaves, against traceable levels in the root at 30 DAS and continued to increase at 50 DAS while remaining highly expressed in "NAU-YZH" leaf, flesh and skin, "NAU-XLM" flesh and "NAU-YH" skin (**Figure 3**). In all genotypes under study, transcript levels of *RsDFR* were not variable in the 10 DAS and 30 DAS leaves and 10 DAS root but with the exception of "NAU-XBC", decreased in the root at 30 DAS (**Figure 3**). However, *RsDFR* expression steadily increased at 50 DAS with the highest levels depicted in the "NAU-YZH" and "NAU-XLM" flesh and "NAU-YZH" and "NAU-YH" skin (**Figure 3**). There was a high expression of *RsANR* in "NAU-YH" leaf and over 10-fold expression in "NAU-XBC" leaves. Over

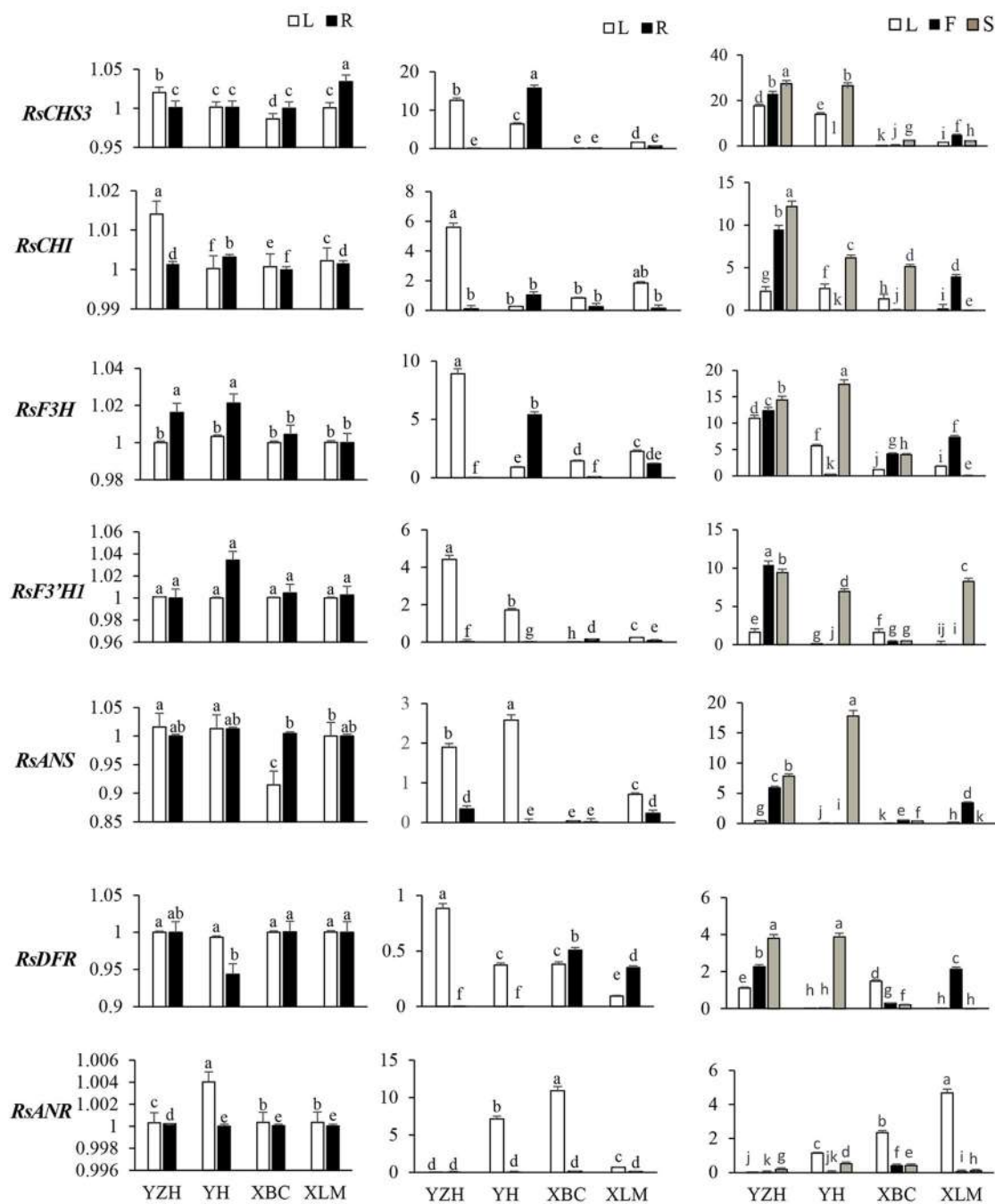
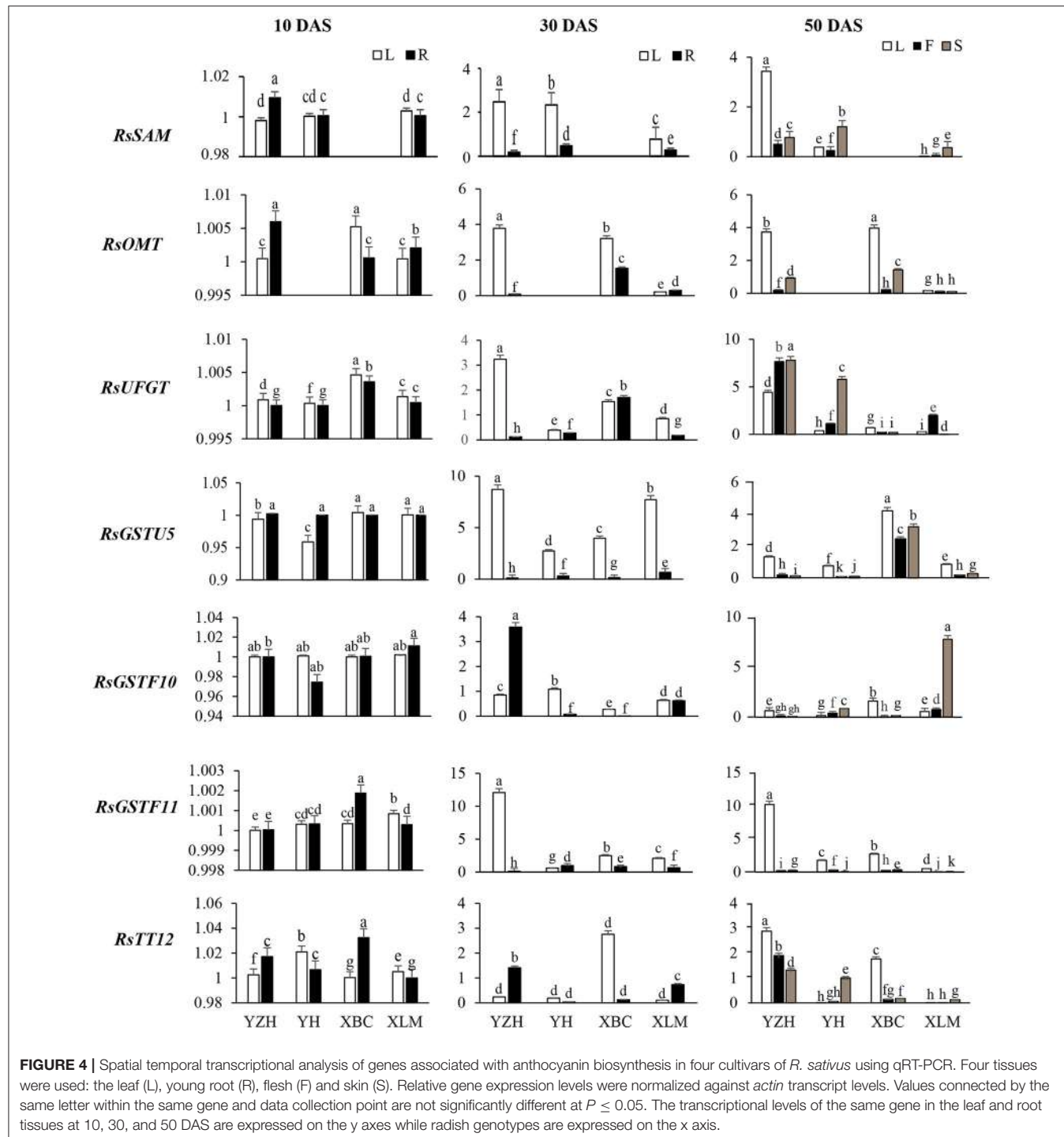


FIGURE 3 | Spatial temporal transcriptional analysis of genes associated with anthocyanin biosynthesis in four cultivars of *R. sativus* using qRT-PCR. Four tissues were used: the leaf (L), young root (R), flesh (F) and skin (S). Relative gene expression levels were normalized against *actin* transcript levels. Values connected by the same letter within the same gene and data collection point are not significantly different at $P \leq 0.05$. The transcriptional levels of the same gene in the leaf and root tissues at 10, 30, and 50 DAS are expressed on the y axes while radish genotypes are expressed on the x axis.

6-fold increased expression was recorded in the leaf of “NAU-XLM” but silenced in the root tissues at 50 DAS (Figure 3).

RsSAM, *RsOMT*, and *RsUGT* are involved in glucosylation and methylation of anthocyanidins, resulting in stable compounds. Transcripts of *RsSAM* were highly expressed

in tissues of “NAU-YZH” and the colored tissues of “NAU-YH” and “NAU-XLM”, and undetectable in all tissues of “NAU-XBC” at 30 and 50 DAS (Figure 4). *RsOMT* on the other hand was significantly expressed in the “NAU-YZH” and “NAU-XLM” with higher expression in the root and the leaf at 10 and 30 DAS,



respectively. Notably, transcripts of *RsOMT* were significantly elevated at 50 DAS in the white colored “NAU-XBC” (**Figure 4**). Nevertheless, *RsUGT* consistently increased across the three developmental stages, with consistent high expression in the colored radish cultivars, although the expression dramatically decreased in the root of “NAU-YH” at 30 DAS (**Figure 4**). Generally, the transcripts of *RsSAM*, *RsOMT*, and *RsUGT* were upgraded in tissues expressing high anthocyanin content.

There was no distinct variation in the glutathione transferase transcripts at 10 DAS, but their levels heightened at 30 DAS in the leaf and were barely detectable in the root at this stage (**Figure 4**). However, *RsGSTF11* was over 15-folds up-regulated in the leaf, with a constant up-regulation in all tissues of the “NAU-YZH” at 50 DAS. On the other hand, *RsGSTU5* and *RsGSTF10* transcript levels increased in the skin with an up-regulation in the “NAU-XBC” and “NAU-YH” flesh and skin, respectively (**Figure 4**).

Correlation between Gene Expression and Total Anthocyanin

The genotype “NAU-YZH” was used to analyze the relationship between transcript levels and total anthocyanin content. Three sampling points, three biological replicates and the leaf, young root (10 and 30 DAS), leaf, taproot skin and flesh tissues (50 DAS) were regarded as independent factors in the transcript pairwise comparisons of total anthocyanin, yielding 21 transcriptional data points for each gene (**Figure 5**). Pearson’s correlation coefficient was used for the correlation analysis.

Transcripts of *RsF3H*, *RsUGT*, *RsANS*, and *RsF3'H1*, showed a significant correlation ($r > 0.85$) with total anthocyanin content (**Table S3**). The co-expression patterns between the gene expression and anthocyanin contents were generated and are depicted in a heat map of clustered correlations (**Figure 5**). The set of genes from number 8–11 had the strongest positive correlation with total anthocyanin, including *RsF3H* ($r = 0.92$), *RsUGT* ($r = 0.92$), *RsF3'H1* ($r = 0.84$), and *RsANS* ($r =$

0.89) while those in lines 1–4 exhibited the strongest negative correlation: *RsGSTU5* ($r = 0.62$), *RsSAM* ($r = 0.5$), *RsGSTF10* ($r = -0.47$), and *RsANR* ($r = -0.47$) (**Table S3**). Linear regressions performed between the cumulative transcription of each of the 14 genes and the corresponding anthocyanin contents were shown in **Figure S3**. These data indicated that *RsF3H*, *RsUGT*, *RsANS*, and *RsF3'H1* might be candidate genes ascribed to the red pigment of the “NAU-YZH” root.

DISCUSSION

Total Anthocyanin Content in Tissues of Four Radish Genotypes

The anthocyanin concentrations of radish under study increased with increase in days after sowing, resulting in higher concentrations in mature taproots than sprouts of colored tissues. There were variations in the levels of anthocyanin in the skin and flesh organs of the four different radish cultivars. The

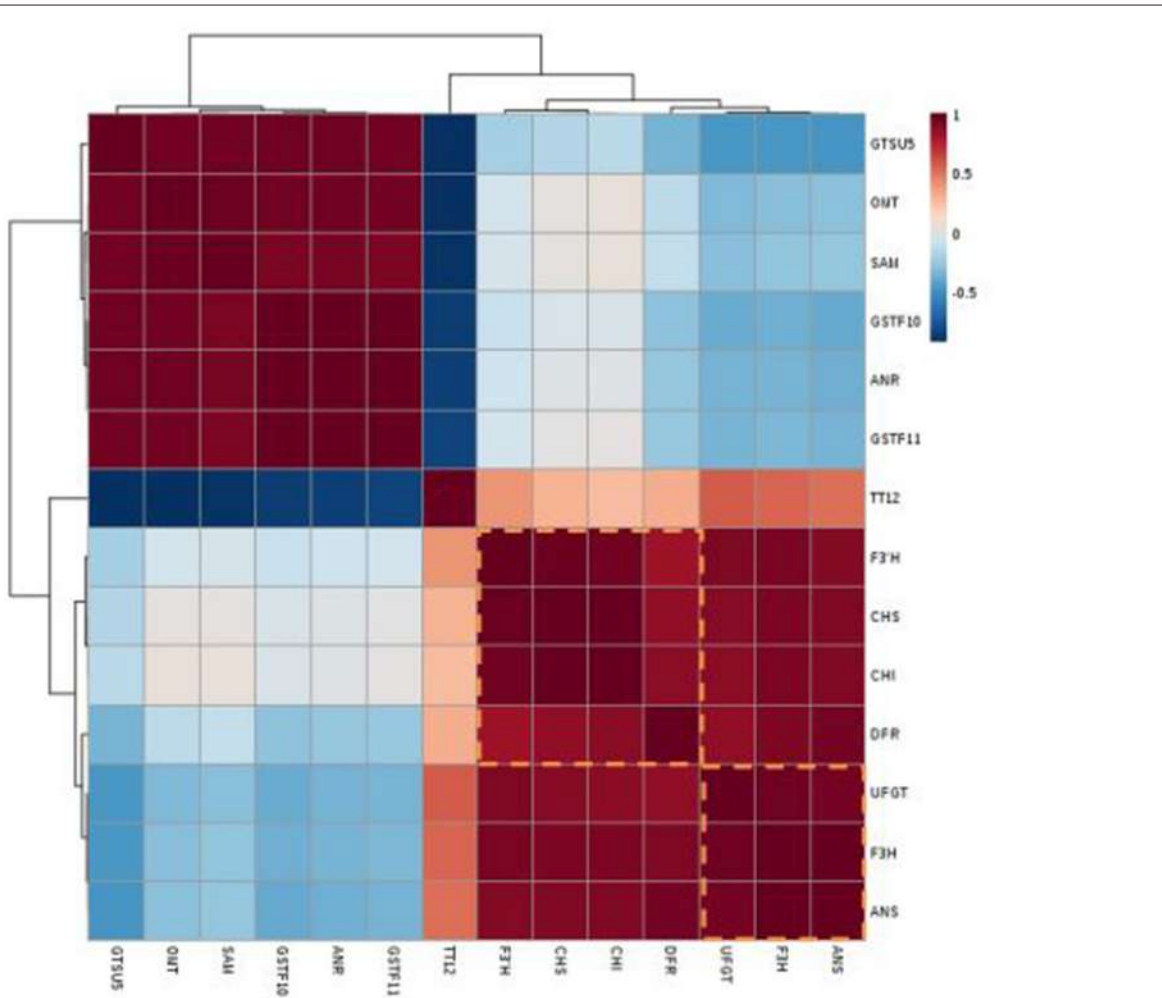


FIGURE 5 | Heat map of the clustered correlations between anthocyanin accumulation patterns and gene expressions in red radish. Three sampling stages, three biological replicates, skin and flesh tissues were treated as independent factors in anthocyanin-transcript pairwise comparisons, which were carried out for 21 transcriptional data points for each gene.

increase in anthocyanin accumulation as the crop advances in growth could be due to increased accumulation of anthocyanin content in tissues, resulting from increase in size and hence the capacity of the plant's biosynthetic machinery. It is speculated that this occurrence is associated with the coordination of plant metabolism because of the ability of plants to regulate the metabolism in respective organs at various developmental stages (Majdi et al., 2014). These results concur with those found in yam, cherry, grape, and chili (Aza-Gonzalez et al., 2013; Liu et al., 2013; Xie et al., 2015; Yin et al., 2015). There was also a difference in the accumulation of anthocyanin in tissues of different radish at each developmental stage. For instance in "NAU-YH" anthocyanin in the skin was higher than in the flesh, while "NAU-XLM" recorded higher anthocyanin content in the flesh and significantly low amounts in its skin, but these contents increased progressively with growth, though at varying rates.

Characterization and Expression of ABGs in Radish

The length of cloned gene sequences from our study varied from 900 to 1,579 bp, and the unigene coverage to corresponding genomic sequences was above 93%, indicating that the radish anthocyanin unigenes from RNA-seq were successfully assembled and were viable for further investigation.

Gene structure analysis predicted the significant domains in each gene, which help to explain their mechanism of action. For instance, the distinct substrate specificity of the NAD_binding _4 domain of *RsDFR* with ASN-active catalytic site explains the preferential accumulation of pelargonidin and cyanidin derivatives instead of malvidin or petunidin (Shimada et al., 2005). The analysis also revealed that *RsF3'H* is intronless and that most of the ABGs bear phase one introns with predominantly asymmetrical exons, except *RsSAM* which has one symmetrical (1-1) exon. Transcript abundance of *RsF3'H* was found to be consistently lower when compared to *RsF3H*. Introns have been found to contribute to increased protein abundance while elimination of introns renders protein product undetectable. This impeccable intronic function is referred to as intron-mediated enhancement (Akua et al., 2010). Extensive analyses further confirmed these inferences where genes bearing introns in yeast were found to have enhanced mRNA and protein levels than intronless genes (Juneau et al., 2006). The pattern of spliceosomal introns has a significant relationship with the conservation of splice signals sequence of exons, therefore, the relatively dominated phase 1 introns in the ABGs in radish indicates a relative reduction in conservation of these genes (Long and Deutsch, 1999).

Despite the consistent occurrence of all ABGs in any studied variety, a species-specific control of the genes of the basic pathway and at key branching points is assumed to contribute to the differences in anthocyanin content and the shift from lighter to darker hues as the crop develops (Ageorges et al., 2006). In the present study, variations in anthocyanin coloration across tissues of four radish genotypes are ascribable to alterations in the unique expression patterns of the overall set of anthocyanin genes.

The transcripts of ABGs portrayed a commensurate expression for most of the genes in the leaf and root tissues of the four radish cultivars at 10 DAS, revealing that ABGs are coordinately expressed at early stages of development. However, the expression of anthocyanin pathway genes is consistent with the accumulation of anthocyanins: as the plant begins to pigment, the expression of key anthocyanin biosynthesis genes is detected to obviously increase.

Expression of ABGs Involved in Primary Flavonoid Upstream Pathway

Chalcone synthase (CHS) and *Chalcone isomerase (CHI)* are the first genes in the flavonoid branch of the anthocyanin biosynthesis pathway. *RsCHS3* recorded the highest level of transcripts when compared to all the other genes and consistently increased throughout plant development. Its transcript abundance correlated positively with total anthocyanin, signifying that it is a key gene for anthocyanin synthesis, findings that echo previous research (Park et al., 2011; Chen et al., 2016). The loss of the *RsCHS3* gene from the 30 DAS stage, through 50 DAS, in the "NAU-XBC" could perhaps be the single most factor contributing to the loss of color in this cultivar. A knockout mutation of the gene impeded anthocyanin accumulation in seeds resulting in a transparent testa in *Arabidopsis* (Shirley et al., 1995). Although *RsCHI* correlated positively with anthocyanin content, its transcription levels were markedly down-regulated in the root at 50 DAS, being non-consistent with previous reports (Xu et al., 2014). This result indicates that a single gene is not responsible for anthocyanin accumulation and that anthocyanin biosynthesis involves the coordinated mechanism of many genes (Walker et al., 2007; Yu et al., 2012).

The transcription of *RsF3'H1* seems to have been developmentally activated after pre-cortex splitting (30 DAS) in "NAU-YZH", "NAU-YH" skin, and "NAU-XLM" flesh, but with lower transcript levels than *RsF3H* and was barely transcribed in "NAU-XBC", which is white colored. However, the expression of *RsF3H* and *RsF3'H1* greatly increased in all cultivars at maturity except for the non-pigmented, taproot skin of "NAU-XLM", taproot flesh of "NAU-YH" and tissues of "NAU-XBC". In the latter cultivar, the levels of transcripts remained low but detectable. Striking variations were also observed in the regulation of the flavonoid hydroxylase genes. The expression profile of *RsF3H* was relatively high even before 50 DAS and transcripts of this gene were present at maturity in all cultivars, including the white cultivar "NAU-XBC".

The reciprocal expression levels of these flavonoid hydroxylase genes most likely contribute to different color hues in radish. Previous studies also proposed a plausible cause of color transition from pelargonidin type in "NAU-YZH" to cyanidin type in "NAU-XLM" which could be due to a reduced *RsF3'H1* mRNA level (Mudalige-Jaywickrama et al., 2005) resulting in the inefficient production of dihydroquercitin and increased dihydrokaempferol and subsequently, pink-purple coloration. Differential expression of transcripts encoding flavonoid-hydroxylase was also reported in mulberry (*Morus alba L.*), cauliflower (*Brassica oleracea* var *botrytis*), and

Chinese bayberry (*Myrica rubra*) (Chiu et al., 2010; Niu et al., 2010; Li et al., 2014). Notably, *RsF3H* and *RsCHI* were clearly expressed in the white-flesh radish “NAU-XBC”, but anthocyanin accumulation was not detected. These findings suggest that *RsF3H* and *RsCHI* are likely more highly regulated than the other anthocyanin biosynthesis structural genes. Additionally, findings from other studies indicate that *CHI* and *F3H* are early genes in the anthocyanin biosynthetic pathway and are coordinately expressed, with increased transcript levels toward plant maturity (Ravaglia et al., 2013).

Expression of ABGs Involved in Anthocyanin Modification Specific Pathway

Dihydroflavonol 4-Reductase (DFR) encoded by a single gene (*DFR*) converts dihydroflavonols to leucoanthocyanidins. Besides the high expression in colored tissues, this gene was also found to be well expressed in the white tissues of “NAU-XBC”, and is, therefore, likely to participate in the synthesis of other secondary metabolites like free-auxins (Shen et al., 2013). These results relate to those obtained in litchi and kiwifruit (Montefiori et al., 2011; Wei et al., 2011).

Anthocyanidin synthase/leucoanthocyanidin oxidase (LDOX) catalyzes the conversion reaction of leucoanthocyanidins to colored anthocyanidins. However in this study, in spite of the high expression of *RsANS* in the early developing stage, the leaf color of three colored radishes is green. This could result from the catalysis of Anthocyanidin synthase (ANS) substrate into flavonol or/and the inhibitory role of the *RsANR*, which converts the colored anthocyanidins to epicatechin, resulting in redirection of anthocyanin pathway into proanthocyanidin pathway (Jaakola et al., 2002). Our study is consistent with findings from bilberry (Jaakola, 2013). However in the later stages ANS is highly expressed in colored tissues and at stages coinciding with elevated anthocyanin amounts, consistent with previous findings (Zhang et al., 2015).

Down-stream genes such as glucosyltransferases greatly influence the direction of anthocyanin synthesis through the regulation of anthocyanidin glucosyltransferase in thickening radish taproot.

It was found that the transcription level of *RsUFGT* was much lower in the white-flesh cultivar “NAU-XBC” than in the red and pink colored radishes. Similar to *RsCHS3*, our results also showed that the mRNA levels encoding *RsUFGT*, the specific gene for anthocyanin biosynthesis, increased proportionally to the anthocyanin content across all the three developmental stages, suggesting that these two genes are under a different regulatory regime, in comparison to the other ABGs in radish, and that the biosynthesis of anthocyanin is controlled at an earlier stage as reported in previous studies (Kobayashi et al., 2001). The expression of O-Methyltransferase (*RsOMT*) in the red colored “NAU-YZH” was higher than that of *RsUFGT*, which was also well expressed in all genotypes, unlike *RsOMT*. The purple-pinkish colored “NAU-XLM” expressed comparatively lower levels of *OMT* when compared to *RsUFGT*. It has been

proposed that the methylation of B-ring hydroxyl groups causes a shift toward deeper red colors (Tanaka et al., 2008). Therefore, it can be inferred that the relative abundance of *RsF3H* to *RsF3'H1* and *RsOMT* to *RsUFGT* could *per se* explain to a greater extent the phenotypic variation of anthocyanin content, color hue and color intensity in radish. Secondly, the key regulation point for quantitative anthocyanin variation is in the downstream pathway at the *RsUFGT* level, but the qualitative differences are precisely controlled upstream of *RsUFGT* at the flavonoid hydroxylases’ level and at *RsOMT* which is downstream of *RsUFGT*.

ABGs Involved in Transportation and Localization of Anthocyanins

The sequestration of anthocyanin from the cytoplasm to the vacuole is poorly understood, and various mechanisms have been put across to explain the process, including transport proteins like GSTs and MATE transporters. The GSTs encoded by a group of *Glutathione-S-transferase* genes, whose specific functions remain to be elucidated in radish, have been implicated in the transport of anthocyanin in other crops (He et al., 2010; Gomez et al., 2011). In this study, the featured GSTs were found to positively coincide with total anthocyanin and exhibit similar expression patterns to the *RsUFGT*, although the correlation between cumulative transcription and total anthocyanin throughout crop development was lower. The abundance of GST transcripts in the present study exhibited genotypic specificity, as *RsGSTF10* was found to correlate with elevated anthocyanin in “NAU-XLM”, *RsGSTU5* with “NAU-YZH” and *RsGSTF11* with “NAU-YZH”, “NAU-YH” and “NAU-XLM”. *RsGSTU5* may contribute to spatial differential accumulation in red radish, owing to its elevated transcript levels in the root against the suppressed transcript levels of key ABGs at 30 DAS. In anthocyanin transport, it has been suggested through mutant analysis that the anthocyanin defective mutants were unable to accumulate anthocyanins into the vacuoles (Conn et al., 2008) implying that glutathione transferases are possible anthocyanin transporters.

At 30 DAS, the red colored radish accumulated significant amounts of anthocyanin in the root despite the down regulation of major ABGs in this tissue. It was also found that *TT12*, a MATE transporter was consistently up-regulated in the red colored radish but low amounts in the white colored tissues. *TT12* was reported to mediate anthocyanin transportation in *Arabidopsis* (Marinova et al., 2007).

To our knowledge, this is the first report describing the spatial-temporal expression patterns of anthocyanin biosynthetic genes (ABGs) in radish. Our results demonstrate the coordinated expression of ABGs in relation to anthocyanin accumulation in radish tissues and that there may be a common regulatory mechanism governing the coordinated expression of related genes. Furthermore, it appears that the major control point to anthocyanin biosynthesis in radish is *UFGT*. Globally, the correlation of anthocyanin content with coordinated gene regulation would be the key contributing factor to phenotypic and spatial-temporal anthocyanin accumulation in radish.

AUTHOR CONTRIBUTIONS

MM and LL designed the experiments and wrote the manuscript. MM, LF, YC and WZ performed validation experiments. YW contributed powerful analytical tools. XZ and KK contributed to proofreading of this manuscript. XL and LL conceived the study and managed the experiments. All authors read and approved the final manuscript.

ACKNOWLEDGMENTS

This work was in part supported by grants from National Key Technology Research and Development Program of China (2016YFD0100204; 2017YFD0101803), Key Technology R & D Program of Jiangsu Province (BE2016379) and Jiangsu Agricultural Science and Technology Innovation Fund (CX (16) 1012).

SUPPLEMENTARY MATERIAL

The Supplementary Material for this article can be found online at: <http://journal.frontiersin.org/article/10.3389/fpls.2017.01243/full#supplementary-material>

REFERENCES

- Ageorges, A., Fernandez, L., Vialet, S., Merdinoglu, D., Terrier, N., and Romieu, C. (2006). Four specific isogenes of the anthocyanin metabolic pathway are systematically co-expressed with the red colour of grape berries. *Plant Sci.* 170, 372–383. doi: 10.1016/j.plantsci.2005.09.007
- Ahn, S. Y., and Yun, H. K. (2016). Glutathione S-transferase genes differently expressed by pathogen-infection in *Vitis flexuosa*. *Plant Breed. Biotechnol.* 4, 61–70. doi: 10.9787/PBB.2016.4.1.061
- Akua, T., Berezin, I., and Shaul, O. (2010). The leader intron of *AtMHX* can elicit, in the absence of splicing, low-level intron-mediated enhancement that depends on the internal intron sequence. *BMC Plant Biol.* 10:93. doi: 10.1186/1471-2229-10-93
- Aza-Gonzalez, C., Herrera-Isidró, L., Núñez-Paleni, H., De La Vega, O. M., and Ochoa-Alejo, N. (2013). Anthocyanin accumulation and expression analysis of biosynthesis-related genes during chili pepper fruit development. *Biol. Plant.* 57, 49–55. doi: 10.1007/s10535-012-0265-1
- Bae, H., Kim, Y. B., Park, N. I., Kim, H. H., Kim, Y. S., Lee, M. Y., et al. (2012). Agrobacterium rhizogenes-mediated genetic transformation of radish (*Raphanus sativus* L. cv. Valentine) for accumulation of anthocyanin. *Plant Omics* 5:381. doi: 10.2478/johr-2014-0019
- Carbone, F., Preuss, A., Vos, R. C. H. D., D'Amico, E., Perrotta, G., Bovy, A. G., et al. (2009). Developmental, genetic and environmental factors affect the expression of flavonoid genes, enzymes and metabolites in strawberry fruits. *Plant Cell Environ.* 32, 1117–1131. doi: 10.1111/j.1365-3040.2009.01994.x
- Chen, F., Xing, C., Huo, S., Cao, C., Yao, Q., and Fang, P. (2016). Red pigment content and expression of genes related to anthocyanin biosynthesis in radishes (*Raphanus sativus* L.) with different colored flesh. *J. Agric. Sci.* 8:126. doi: 10.5539/jas.v8n8p126
- Cheng, L., Li, S., Yin, J., Li, L., and Chen, X. (2013). Genome-wide analysis of differentially expressed genes relevant to rhizome formation in lotus root (*Nelumbo nucifera* Gaertn.). *PLoS ONE* 8:e67116. doi: 10.1371/journal.pone.0067116
- Chiu, L.-W., Zhou, X., Burke, S., Wu, X., Prior, R. L., and Li, L. (2010). The purple cauliflower arises from activation of a MYB transcription factor. *Plant Physiol.* 154, 1470–1480. doi: 10.1104/pp.110.164160
- Conn, S., Curtin, C., Bézier, A., Franco, C., and Zhang, W. (2008). Purification, molecular cloning, and characterization of glutathione S-transferases (GSTs) from pigmented *Vitis vinifera* L. cell suspension cultures as putative anthocyanin transport proteins. *J. Exp. Bot.* 59, 3621–3634. doi: 10.1093/jxb/ern217
- Cutanda-Perez, M.-C., Ageorges, A., Gomez, C., Vialet, S., Terrier, N., Romieu, C., et al. (2009). Ectopic expression of VlmybA1 in grapevine activates a narrow set of genes involved in anthocyanin synthesis and transport. *Plant Mol. Biol.* 69, 633–648. doi: 10.1104/pp.109.140376
- Falginella, L., Di Gaspero, G., and Castellarin, S. D. (2012). Expression of flavonoid genes in the red grape berry of 'Alicante Bouschet' varies with the histological distribution of anthocyanins and their chemical composition. *Planta* 236, 1037–1051. doi: 10.1007/s00425-012-1658-2
- Fukusaki, E., Kawasaki, K., Kajiyama, S., Ana, C., Suzuki, K., Tanaka, Y., et al. (2004). Flower color modulations of *Torenia hybrida* by downregulation of chalcone synthase genes with RNA interference. *J. Biotechnol.* 111:229–240. doi: 10.1016/j.jbiotec.2004.02.019
- Gomez, C., Conejero, G., Torregrosa, L., Cheynier, V., Terrier, N., and Ageorges, A. (2011). *In vivo* grapevine anthocyanin transport involves vesicle-mediated trafficking and the contribution of anthoMATE transporters and GST. *Plant J.* 67, 960–970. doi: 10.1111/j.1365-313X.2011.04648
- Harborne, J. B., and Williams, C. A. (2000). Advances in flavonoid research since 1992. *Phytochemistry* 55, 481–504. doi: 10.1016/S0031-9422(00)00235-1
- He, F., Mu, L., Yan, G.-L., Liang, N.-N., Pan, Q.-H., Wang, J., et al. (2010). Biosynthesis of anthocyanins and their regulation in colored grapes. *Molecules* 15, 9057–9091. doi: 10.3390/molecules15129057
- Holton, T. A., and Cornish, E. C. (1995). Genetics and biochemistry of anthocyanin biosynthesis. *Plant Cell* 7:1071. doi: 10.1105/tpc.7.7.1071
- Jaakola, L., Määttä, K., Pirttilä, A. M., Törrönen, R., Kärenlampi, S., and Hohtola, A. (2002). Expression of genes involved in anthocyanin biosynthesis in relation to anthocyanin, proanthocyanidin, and flavonol levels during bilberry fruit development. *Plant Physiol.* 130, 729–739. doi: 10.1104/pp.006957
- Jaakola, L. (2013). New insights into the regulation of anthocyanin biosynthesis in fruits. *Trends Plant Sci.* 18, 477–483. doi: 10.1016/j.tplants.2013.06.003

Figure S1 | The proposed anthocyanin biosynthesis pathway. Anthocyanins are synthesized by a multienzyme complex loosely associated to the endoplasmic reticulum in the plant cytosol (PAL, phenylalanine ammonia lyase; C4H, cinnamate 4-hydroxylase; CHS, chalcone synthase; CHI, chalcone isomerase; F3H, flavanone 3-hydroxylase; F3'H, flavonoid 3'-hydroxylase; DFR, dihydroflavonol reductase; ANS, anthocyanidin synthase; UFGT, UDP-glucose flavonoid 3-O-glucosyltransferase; MT, methyltransferase; GST, glutathione S-transferase). Proanthocyanidins (PAs) are synthesized when the pathway branches off the anthocyanin pathway, catalyzed by enzymes such as ANR, anthocyanidin reductase. The numbers in the brackets are unigenes corresponding to the genes in the radish transcriptome.

Figure S2 | Gene structure and predicted functional domains of radish anthocyanin biosynthetic genes. Functional domains were predicted in SMART (http://smart.embl-heidelberg.de/smart/set_mode.cgi?) NORMAL = 1. Gene structures were displayed by Gene Structure Display Server (<http://gsds.cbi.pku.edu.cn/>).

Figure S3 | Linear regression between the cumulative gene transcription and total anthocyanin content in "NAU-YZH".

Table S1 | Gene specific primers used for cloning.

Table S2 | Primers used for RT-qPCR.

Table S3 | The r and p values of the correlations between anthocyanin accumulation patterns and gene expression in "NAU-YZH".

Table S4 | List of unigenes involved in anthocyanin biosynthesis pathway of radish in the transcriptome database.

- Juneau, K., Miranda, M., Hillenmeyer, M. E., Nislow, C., and Davis, R. W. (2006). Introns regulate RNA and protein abundance in yeast. *Genetics* 174, 511–518. doi: 10.3410/f.1047669.497662
- Kitashiba, H., Li, F., Hirakawa, H., Kawanabe, T., Zou, Z., Hasegawa, Y., et al. (2014). Draft sequences of the radish (*Raphanus sativus L.*) genome. *DNA Res.* 21, 481–490. doi: 10.1093/dnares/dsu014
- Kobayashi, S., Ishimaru, M., Ding, C., Yakushiji, H., and Goto, N. (2001). Comparison of UDP-glucose: flavonoid 3-O-glucosyltransferase (UFGT) gene sequences between white grapes (*Vitis vinifera*) and their sports with red skin. *Plant Sci.* 160, 543–550. doi: 10.1016/S0168-9452(00)00425-8
- Kriangphan, N., Vuttipongchaikij, S., Kittiwongwattana, C., Suttangkakul, A., Pinmanee, P., Sakulsathaporn, A., et al. (2015). Effects of sequence and expression of eight anthocyanin biosynthesis genes on floral coloration in four dendrobium hybrids. *J. Jpn. Soc. Hortic. Sci.* 84, 83–92. doi: 10.2503/hortj.mi-020
- Lamy, S., Lafleur, R., Bédard, V., Moghrabi, A., Barrette, S., Gingras, D., et al. (2007). Anthocyanidins inhibit migration of glioblastoma cells: structure-activity relationship and involvement of the plasminolytic system. *J. Cell. Biochem.* 100, 100–111. doi: 10.1002/jcb.21023
- Lepiniec, L., Debeaujon, I., Routaboul, J. M., Baudry, A., Pourcel, L., Nesi, N., et al. (2006). Genetics and biochemistry of seed flavonoids. *Annu. Rev. Plant Biol.* 57, 405–430. doi: 10.1146/annurev.arplant.57.032905.105252
- Li, J., Lü, R.-H., Zhao, A. C., Wang, X. L., Liu, C. Y., Zhang, Q. Y., et al. (2014). Isolation and expression analysis of anthocyanin biosynthetic genes in *Morus alba L.* *Biol. Plant.* 58, 618–626. doi: 10.1007/s10535-014-450-5
- Li, X., Gao, P., Cui, D., Wu, L., Parkin, I., Saberianfar, R., et al. (2011). The *Arabidopsis* tt19-4 mutant differentially accumulates proanthocyanidin and anthocyanin through a 3' amino acid substitution in glutathione S-transferase. *Plant Cell Environ.* 34, 374–388. doi: 10.1111/j.1365-3040.2010.02249
- Liu, L., Guo, W., Zhu, X., and Zhang, T. (2003). Inheritance and fine mapping of fertility restoration for cytoplasmic male sterility in *Gossypium hirsutum L.* *Theor. Appld. Genet.* 106, 461–469. doi: 10.1007/s00122-002-1084-0
- Liu, Y., Shen, X., Zhao, K., Ben, Y., Guo, X., Zhang, X., et al. (2013). Expression analysis of anthocyanin biosynthetic genes in different colored sweet cherries (*Prunus avium L.*) during fruit development. *J. Plant Growth Regul.* 32, 901–907. doi: 10.1371/journal.pone.0126991
- Livak, K. J., and Schmittgen, T. D. (2001). Analysis of relative gene expression data using real-time quantitative PCR and the $2^{-\Delta\Delta CT}$ method. *Methods* 25, 402–408. doi: 10.1006/meth.2001.1262
- Long, M., and Deutsch, M. (1999). Association of intron phases with conservation at splice site sequences and evolution of spliceosomal introns. *Mol. Biol. Evol.* 16, 1528–1534. doi: 10.116/1471-2148-14-50
- Majdi, M., Karimzadeh, G., and Malboobi, M. (2014). Spatial and developmental expression of key genes of terpene biosynthesis in *Tanacetum parthenium*. *Biol. Plant.* 58, 379–384. doi: 10.1007/s10535-014-0398-5
- Marinova, K., Pourcel, L., Weder, B., Schwarz, M., Barron, D., Routaboul, J. M., et al. (2007). The *Arabidopsis* MATE transporter TT12 acts as a vacuolar flavonoid/H⁺-antiporter active in proanthocyanidin-accumulating cells of the seed coat. *Plant Cell* 19, 2023–2038. doi: 10.1105/tpc.106.046029
- Mehrtens, F., Kranz, H., Bednarek, P., and Weisshaar, B. (2005). The *Arabidopsis* transcription factor MYB12 is a flavonol-specific regulator of phenylpropanoid biosynthesis. *Plant Physiol.* 138, 1083–1096. doi: 10.1104/pp.104.058032
- Montefiori, M., Esplay, R. V., Stevenson, D., Cooney, J., Datson, P. M., Saiz, A., et al. (2011). Identification and characterisation of F3GT1 and F3GGT1, two glycosyltransferases responsible for anthocyanin biosynthesis in red-fleshed kiwifruit (*Actinidia chinensis*). *Plant J.* 65, 106–118. doi: 10.1111/j.1365-313X.2010.04409.x
- Mudalige-Jaywickrama, R. G., Champagne, M. M., Hieber, A. D., and Kuehnle, A. R. (2005). Cloning and characterization of two anthocyanin biosynthetic genes from *Dendrobium* orchid. *J. Am. Soc. Hortic. Sci.* 130, 611–618. doi: 10.1186/s12870-015-0577-3
- Nhukarume, L., Chikwambi, Z., Muchuweti, M., and Chipurura, B. (2010). Phenolic content and antioxidant capacities of *Parinari curatellifolia*, *Strychnos spinosa* and *Adansonia digitata*. *J. Food Biochem.* 34, 207–221. doi: 10.1111/j.1745-4514.2009.00325.x
- Niu, S.-S., Xu, C.-J., Zhang, W.-S., Zhang, B., Li, X., Lin-Wang, K., et al. (2010). Coordinated regulation of anthocyanin biosynthesis in Chinese bayberry (*Myrica rubra*) fruit by a R2R3-MYB transcription factor. *Planta* 231, 887–899. doi: 10.1007/s00425-009-1095-z
- Park, N. I., Xu, H., Li, X., Jang, J. H., Park, S., Ahn, G. H., et al. (2011). Anthocyanin accumulation and expression of anthocyanin biosynthetic genes in radish (*Raphanus sativus*). *J. Agric. Food Chem.* 59, 6034–6039. doi: 10.1021/jf200824c
- Ravaglia, D., Esplay, R. V., Henry-Kirk, R., Andreotti, C., Ziosi, V., Hellens, R. P., et al. (2013). Transcriptional regulation of flavonoid biosynthesis in nectarine (*Prunus persica*) by a set of R2R3-MYB transcription factors. *BMC Plant Biol.* 13:68. doi: 10.1111/tpj.13487
- Rodriguez-Saona, L., Giusti, M., and Wrolstad, R. (1999). Color and pigment stability of red radish and red-fleshed potato anthocyanins in juice model systems. *J. Food Sci.* 64, 451–456. doi: 10.1111/j.1365-2621.1999.tb15061.x
- Salvaterra, A., Pimentel, P., Moya-Leon, M. A., Caligari, P. D., and Herrera, R. (2010). Comparison of transcriptional profiles of flavonoid genes and anthocyanin contents during fruit development of two botanical forms of *Fragaria chiloensis* ssp. *chiloensis*. *Phytochemistry* 71, 1839–1847. doi: 10.1016/j.phytochem.2010.08.005
- Shen, Z., Confolent, C., Lambert, P., Poëssel, J. L., Quilot-Turion, B., Yu, M., et al. (2013). Characterization and genetic mapping of a new blood-flesh trait controlled by the single dominant locus DBF in peach. *Tree Genet. Genomes* 9, 1435–1446. doi: 10.1007/s11295-013-0649-1
- Shimada, N., Sasaki, R., Sato, S., Kaneko, T., Tabata, S., Aoki, T., et al. (2005). A comprehensive analysis of six dihydroflavonol 4-reductases encoded by a gene cluster of the *Lotus japonicus* genome. *J. Exp. Bot.* 56, 2573–2585. doi: 10.1093/jxb/eri251
- Shirley, B. W., Kubasek, W. L., Storz, G., Bruggemann, E., Koornneef, M., Ausubel, F. M., et al. (1995). Analysis of *Arabidopsis* mutants deficient in flavonoid biosynthesis. *Plant J.* 8, 659–671.
- Tanaka, Y., Sasaki, N., and Ohmiya, A. (2008). Biosynthesis of plant pigments: anthocyanins, betalains and carotenoids. *Plant J.* 54, 733–749. doi: 10.1111/j.1365-313X.2008.03447.x
- Walker, A. R., Lee, E., Bogs, J., McDavid, D. A., Thomas, M. R., and Robinson, S. P. (2007). White grapes arose through the mutation of two similar and adjacent regulatory genes. *Plant J.* 49, 772–785. doi: 10.1007/s00122-008-0840-1
- Wang, Y., Pan, Y., Liu, Z., Zhu, X., Zhai, L., Xu, L., et al. (2013). *In vivo* transcriptome sequencing of radish (*Raphanus sativus L.*) and analysis of major genes involved in glucosinolate metabolism. *BMC Genomics* 14:836. doi: 10.1186/1471-2164-14-836
- Wei, Y. Z., Hu, F.-C., Hu, G.-B., Li, X. J., Huang, X. M., and Wang, H. C. (2011). Differential expression of anthocyanin biosynthetic genes in relation to anthocyanin accumulation in the pericarp of *Litchi chinensis* Sonn. *PLoS ONE* 6:e19455. doi: 10.1371/journal.pone.0019455
- Xie, S., Song, C., Wang, X., Liu, M., Zhang, Z., and Xi, Z. (2015). Tissue-specific expression analysis of anthocyanin biosynthetic genes in white-and red-fleshed grape cultivars. *Molecules* 20, 22767–22780. doi: 10.3390/molecules201219883
- Xu, L., Wang, Y., Zhai, L., Xu, Y., Wang, L., Zhu, X., et al. (2013). Genome-wide identification and characterization of cadmium-responsive microRNAs and their target genes in radish (*Raphanus sativus L.*) roots. *J. Exp. Bot.* 64, 4271–4287. doi: 10.1093/jxb/ert240
- Xu, Y., Zhu, X., Gong, Y., Xu, L., Wang, Y., and Liu, L. (2012). Evaluation of reference genes for gene expression studies in radish (*Raphanus sativus L.*) using quantitative real-time PCR. *Biochem. Biophys. Res. Commun.* 424, 398–403. doi: 10.1016/j.bbrc.2012.06.119
- Xu, Z. S., Huang, Y., Wang, F., Song, X., Wang, G. L., and Xiong, A.-S. (2014). Transcript profiling of structural genes involved in cyanidin-based anthocyanin biosynthesis between purple and non-purple carrot (*Daucus carota L.*) cultivars reveals distinct patterns. *BMC Plant Biol.* 14:262. doi: 10.1186/s12870-014-0262-y
- Yin, J., Yan, R., Zhang, P., Han, X., and Wang, L. (2015). Anthocyanin accumulation rate and the biosynthesis related gene expression in *Dioscorea alata*. *Biol. Plant.* 59, 325–330. doi: 10.1007/s10535-015-0502-5
- Yu, B., Zhang, D., Huang, C., Qian, M., Zheng, X., Teng, Y., et al. (2012). Isolation of anthocyanin biosynthetic genes in red Chinese sand pear (*Pyrus pyrifolia*

- Nakai*) and their expression as affected by organ/tissue, cultivar, bagging and fruit side. *Sci. Hortic.* 136, 29–37. doi: 10.1007/s11105-013-0652-6
- Yu, R., Wang, J., Xu, L., Wang, Y., Wang, R., Zhu, X., et al. (2016). Transcriptome profiling of taproot reveals complex regulatory networks during taproot thickening in radish (*Raphanus sativus* L.). *Front. Plant Sci.* 7:1210. doi: 10.3389/fpls.2016.01210
- Zhang, H., Jordheim, M., Lewis, D. H., Arathoon, S., Andersen, M., and Davies, K. M. (2014). Anthocyanins and their differential accumulation in the floral and vegetative tissues of a shrub species (*Rhabdothamnus solandri* A. Cunn.). *Sci. Hortic.* 165, 29–35. doi: 10.1016/j.scienta.2013.10.032
- Zhang, J., Han, Z., Tian, J., Zhang, X., Song, T., and Yao, Y. (2015). The expression level of anthocyanidin synthase determines the anthocyanin content of crabapple (*Malus* sp.) petals. *Acta Physiol. Plant.* 37, 1–10. doi: 10.1007/s11738-015-1857-0
- Zhang, X., C., Allan, A., Yi, Q., Chen, L., Li, K., Shu, Q., et al. (2011). Differential gene expression analysis of Yunnan red pear, *Pyrus Pyrifolia*, during fruit skin coloration. *Plant Mol. Biol. Rep.* 29, 305–314. doi: 10.1007/s11105-010-0231-z
- Zuluaga, D. L., Gonzali, S., Loretí, E., Pucciariello, C., Degl’Innocenti, E., Guidi, L., et al. (2008). *Arabidopsis thaliana* MYB75/PAP1 transcription factor induces anthocyanin production in transgenic tomato plants. *Funct. Plant Biol.* 35, 606–618. doi: 10.1071/FP08021

Conflict of Interest Statement: The authors declare that the research was conducted in the absence of any commercial or financial relationships that could be construed as a potential conflict of interest.

Copyright © 2017 Muleke, Fan, Wang, Xu, Zhu, Zhang, Cao, Karanja and Liu. This is an open-access article distributed under the terms of the Creative Commons Attribution License (CC BY). The use, distribution or reproduction in other forums is permitted, provided the original author(s) or licensor are credited and that the original publication in this journal is cited, in accordance with accepted academic practice. No use, distribution or reproduction is permitted which does not comply with these terms.



Characterization of Genes Encoding Key Enzymes Involved in Anthocyanin Metabolism of Kiwifruit during Storage Period

Boqiang Li¹, Yongxiu Xia^{1,2}, Yuying Wang¹, Guozheng Qin¹ and Shiping Tian^{1,2*}

¹ Key Laboratory of Plant Resources, Institute of Botany, Chinese Academy of Sciences, Beijing, China, ² College of Life Sciences, University of Chinese Academy of Sciences, Beijing, China

OPEN ACCESS

Edited by:

Nadia Bertin,
PSH Research Unit (INRA), France

Reviewed by:

Alon Samach,
Hebrew University of Jerusalem, Israel
Massimiliano Corso,
Université Libre de Bruxelles, Belgium

*Correspondence:

Shiping Tian
tsp@ibcas.ac.cn

Specialty section:

This article was submitted to
Crop Science and Horticulture,
a section of the journal
Frontiers in Plant Science

Received: 24 October 2016

Accepted: 27 February 2017

Published: 10 March 2017

Citation:

Li B, Xia Y, Wang Y, Qin G and
Tian S (2017) Characterization of
Genes Encoding Key Enzymes
Involved in Anthocyanin Metabolism
of Kiwifruit during Storage Period.
Front. Plant Sci. 8:341.
doi: 10.3389/fpls.2017.00341

'Hongyang' is a red fleshed kiwifruit with high anthocyanin content. In this study, we mainly investigated effects of different temperatures (25 and 0°C) on anthocyanin biosynthesis in harvested kiwifruit, and characterized the genes encoding key enzymes involved in anthocyanin metabolism, as well as evaluated the mode of the action, by which low temperature regulates anthocyanin accumulation in 'Hongyang' kiwifruit during storage period. The results showed that low temperature could effectively enhance the anthocyanin accumulation of kiwifruit in the end of storage period (90 days), which related to the increase in mRNA levels of *ANS1*, *ANS2*, *DRF1*, *DRF2*, and *UGFT2*. Moreover, the transcript abundance of *MYBA1-1* and *MYB5-1*, the genes encoding an important component of MYB-bHLH-WD40 (MBW) complex, was up-regulated, possibly contributing to the induction of specific anthocyanin biosynthesis genes under the low temperature. To further investigate the roles of AcMYB5-1/5-2/A1-1 in regulation of anthocyanin biosynthesis, genes encoding the three transcription factors were transiently transformed in *Nicotiana benthamiana* leaves. Overexpression of AcMYB5-1/5-2/A1-1 activated the gene expression of *NtANS* and *NtDFR* in tobacco. Our results suggested that low temperature storage could stimulate the anthocyanin accumulation in harvested kiwifruit via regulating several structural and regulatory genes involved in anthocyanin biosynthesis.

Keywords: red fleshed kiwifruit, anthocyanin, low temperature, molecular basis, MYB transcription factor

INTRODUCTION

Anthocyanins are one of the most important plant pigments and usually accumulate in specific plant tissues, such as leaves, roots, fruits, and flowers, contributing to their red, blue, purple and dark color. As an important secondary plant metabolite, anthocyanins have many functions in plants, ranging from the resistance to UV, light and pathogen to the attraction of pollinators and seed dispersers for reproduction (Ubi et al., 2006; Jaakola, 2013). Moreover, anthocyanins have been extensively used in food to improve human health because of their specific function in antioxidant activity, such as prevention of heart disease and anticancer activity (He and Giusti, 2010). Fruits and vegetables are still the common food source of anthocyanins due to the low stability of anthocyanins during processing in food system (Giusti and Wrolstad, 2003). However,

poor ripening quality along with less accumulation of anthocyanins is always accompanied with fruit that were commercially harvested at 'mature' stage. In addition, some fruits, such as apple and pears, easily lose pre-harvest colors during inappropriate storage condition due to decreased ability to accumulate anthocyanin (Steyn et al., 2004). Therefore, exploring the regulating mechanism of anthocyanins biosynthesis in fruits has biologically interesting and economically significance.

Some genes involved in the anthocyanin pathway have been cloned and characterized in fruits (Montefiori et al., 2011; Tang et al., 2016). Among them, three key enzymes, dihydroflavonol 4-reductase (DFR), anthocyanidin synthase (ANS) and UDP-glucose:flavonoid 3-O-glucosyltransferase (UFGT or F3GT), contribute to the last step of anthocyanin biosynthesis, from the anthocyanidins to the anthocyanin (Jaakola, 2013). And these genes usually show different expression patterns in different fruits during the process of anthocyanin biosynthesis. For example, UFGT has been reported to be one of the mayor control points of anthocyanin biosynthesis in grape and litchi (Boss et al., 1996; Zhao et al., 2012), while the expression of DFR was found to be closely correlated with anthocyanin content in different genotypes of pomegranate (Wang et al., 2012). Moreover, anthocyanin pigment is also regulated by developmental factors and various environmental factors in plants. MYB-bHLH-WD40 (MBW) complex plays important role in regulation of anthocyanin synthesis in plants (Petroni and Tonelli, 2011). Among the three components, the R2R3 MYBs, which are the main secondary metabolism regulators, determine the patterning and spatial localization of anthocyanins (Liu et al., 2015). Many MYB genes involved in anthocyanin regulation are characterized in various fruits and flowers, such as apple, grape, blueberry, strawberry, cherry, and petunia (Jaakola, 2013; Cavallini et al., 2014). Additionally, light and temperature, serve as important environmental factors, have been reported to control anthocyanin biosynthesis in plant, particularly low temperature (Jaakola, 2013; Liu et al., 2015).

'Hongyang' kiwifruit is one of the most popular cultivars in China because of its special quality, including unique anthocyanin accumulation, high sugar and vitamin C (Wu et al., 2013). 'Hongyang' kiwifruit grown in high altitude with low temperature usually have the higher accumulation of anthocyanin during fruit development, than that grown in low altitude area (Man et al., 2015b). In the previous study, we compared the expression profiles of 25 oxidative stress-related genes in 'Hongyang' kiwifruit stored in air and CA by quantitative real-time polymerase chain reaction (qRT-PCR), and proved expression of *SOD3*, *CAT1*, *APX1*, *APX2* and *GR3* may predominantly contribute to the maintaining of antioxidative systems (Xia et al., 2016). In this study, we determined the changes of anthocyanin content in kiwifruit stored at room- and low-temperature, then cloned and characterized several structural and regulatory genes involved in anthocyanin biosynthesis in 'Hongyang' kiwifruit. Our findings provide evidence for understanding the effect of low temperature on anthocyanin biosynthesis in kiwifruit during post-harvest storage periods.

MATERIALS AND METHODS

Fruit Material

Kiwifruit (*Actinidia chinensis* cv. Hongyang) were harvested from a commercial orchard in Duijiangyan City (Sichuan, China) at a commercial mature stage. Fruits of similar size and the absence of physical injuries or decays were selected, and randomly divided into 6 lots with 100 fruits each. Three lots were stored at low temperature (0°C) for 3 months (90 days), and other three were kept at room temperature (25°C) for 9 days. All fruits were enclosed with polyethylene film bag (0.02-mm thickness) to maintain relative humidity of about 95%. As replicates for each treatment (room- and cold-storage), three lots of 15 fruits were sampled in every interval of 3 or 30 days storage at room- or low-temperature, respectively. Fruit firmness and the soluble solids content (SSC) were measured as described (Xia et al., 2016). The kiwifruit sampled at the paired time points (3 days at 25°C vs. 30 days at 0°C, 6 days at 25°C vs. 60 days at 0°C, 9 days at 25°C vs. 90 days at 0°C) showed similar SSC and firmness. For further molecular and biochemical analysis, inner pericarp tissue collected from the equatorial region (1.5-cm thickness) of each fruit was cut into pieces, frozen in liquid nitrogen and stored at -80°C.

LC-MS Analysis of Anthocyanin

Anthocyanin was extracted and analyzed according to the following procedure. Briefly, 10 g of frozen samples were ground and extracted in 30 ml of methanol containing 2% (v/v) formic acid. After vortex, the homogenates were sonic-treated in ice-cold water for 20 min and then inoculated at 4°C overnight, followed by centrifugation at 3000g for 10 min. The extract was then filtered through 0.22 μm polytetrafluoroethylene filters and retained for component analysis. The anthocyanin analysis was performed on an Agilent 1290 Infinity UHPLC system coupled to Agilent 6540 UHD Accurate-Mass Q-TOF mass spectrometer (Agilent Technologies, USA). A 10 μl aliquot of sample was injected on C18 (150 mm × 4.6 mm) column and separations were carried out using a binary solvent system of Solvent A (water +0.1% formic acid) and Solvent B (acetonitrile +0.1% formic acid) at a flow of 300 μl min⁻¹. The initial mobile phase was 95%A 5%B, increased linearly to 30%A 70% B in 20 min, and held for 5 min before resetting to 95%A 5%B ready for the next injection. The column temperature was set to 30°C and anthocyanins were monitored at 520 nm. Quantification of anthocyanins was conducted by comparison with authenticated standard solution of cyanidin 3-O-galactoside (Sigma). Anthocyanin peaks were further identified by ESI-MS and the spectral data were obtained in positive ion mode over the range m/z 100–1000. The ESI voltage, capillary temperature, and capillary voltages was 39 V, 300°C and 7 μV, respectively.

Gene Identification and Alignment

Dihydroflavonol 4-reductase, *ANS*, and *UDP-flavonoid 3-O-galactosyl transferase* (UFGT) genes from *A. chinensis* 'Hongyang' were initially cloned using gene specific primers (Supplementary Table S1) designed on *DFR* (EST FG410069.1), *ANS* (EST

FG407400.1) and *UFGT* (EST FG405592.1) sequences from an available kiwifruit EST library (Crowhurst et al., 2008). Full-length cDNA were cloned using a Rapid-amplification of cDNA Ends (RACE) kit (Takara). Putative MYB transcription factors were identified from the kiwifruit genome database (Huang et al., 2013), and four full-length *MYB* genes highly expressed in fruit tissue were selected. The open reading frames (ORFs) were predicted using GENSCAN, and protein sequences were aligned using ClustalX2.1. Phylogenetic tree of *MYB* proteins were constructed by neighbor-joining matrix with 1,000 bootstrap replicates using MEGA6. Names of all cloned genes in this study were according to the previous report by Li et al. (2015), except *MYB4a* which was named according to the phylogenetic analysis.

RNA Extraction and Gene Expression Analysis

Total RNA was extracted according to the methods reported by Zhu et al. (2013) from 1 g of kiwifruit tissues. Using a Takara PrimeScript[®] RT reagent kit with gDNA eraser, the first strand cDNA was synthesized by reverse transcription following manufacturer's instruction. Quantitative real-time PCR was performed on StepOnePlus Real-Time PCR System (Applied Biosystems) using SYBR[®] Premix Ex TaqTM (TliRNaseH Plus) (Takara, Japan). Gene-specific primers were designed with Primer Express software 3.0 and presented in Supplementary Table S2. The PCR program was conducted as follows: 15 s at 95°C; 40 cycles of 5 s at 95°C, and 30 s at 60°C; followed by an automatic melting curve analysis. Three independent biological replicates were measured for each sample. The relative expression level for each gene was calculated using the comparative Ct method ($2^{-\Delta Ct}$ method) with a kiwifruit *actin* as a reference.

Transient Expression in *Nicotiana benthamiana*

The CDS of *AcMYB5-1*, *AcMYB5-2*, and *AcMYBA1-1* were amplified using specific primers (Supplementary Table S3) containing *KpnI* and *BamHI* restriction enzymatic site, respectively. The PCR product was recombined with the linearized vector pCAMBIA2300 (In-Fusion HD Cloning Kit; Clontech). The resulting construct were sequenced and introduced into *Agrobacterium tumefaciens* strain GV3101. *Agrobacterium* were cultured on LB agar plates with kanamycin and incubated at 28°C. The freshly grown *Agrobacterium* were sedimented by centrifugation for 5 min at 6000 g, resuspended in infiltration buffer, and incubated at room temperature for 2 h before infiltration. Tobacco plants were grown for five to six weeks and the young leaves were syringe-infiltrated with *A. tumefaciens* suspension in abaxial side of the leaf. Control was infiltrated with *Agrobacterium* containing pCAMBIA2300 (empty vector) at the same time and the transient expression was assayed 5 days after infiltration.

Statistical Analysis

All statistical analyses were carried out using SPSS 13.0 software (SPSS Inc., USA). Data from assay of anthocyanin content

or gene expression were analyzed by one-way analysis of variance (ANOVA), and the mean comparison was performed by Duncan's multiple range tests. Differences at $P < 0.05$ were considered as significant.

RESULTS

Anthocyanin Profile

Red-flesh is the distinguishing feature of 'Hongyang' kiwifruit due to the accumulation of anthocyanin in its inner pericarp during ripening. To identify the main anthocyanin in kiwifruit during storage, UHPLC Q-TOF-MS was applied to analyze the anthocyanin composition from the extract of fruit. Our results showed that all samples of 'Hongyang' kiwifruit presented two peaks that were identified as cyanidin 3-O-xylo(1-2)-galactoside and 3-O-galactoside by comparing both retention times and ESI-MS data (Supplementary Figure S1). The dominant anthocyanin peak had a molecular ion of m/z 581, while another peak had a molecular ion of m/z 499. The results indicated that cyanidin 3-O-xylo(1-2)-galactoside was the major anthocyanin present in 'Hongyang' fruit during storage, which is consistent with previous report in pre-harvest 'Hongyang' fruit (Man et al., 2015b).

Effect of Low Temperature Storage on Fruit Color, Anthocyanin Content, and Fruit Quality

As shown in **Figure 1A**, after 90 days of storage at low temperature, the red coloration of fruit inner pericarp was more notable than that of fruit at room temperature for 9 days. To investigate the influence of low temperature on anthocyanin content in 'Hongyang' fruit, the accumulation of major anthocyanin during the storage was investigated. The 3-O-xylo(1-2)-galactoside content in inner pericarp increased gradually with prolonged storage time (**Figure 1B**). In room temperature-stored fruit, it increased rapidly from 11.88 at 0 day to 18.87 $\mu\text{g}\cdot\text{g}^{-1}$ FW at 9 days. By contrast, in low temperature-stored fruit, it accumulated gradually and reached a peak value of 23.87 $\mu\text{g}\cdot\text{g}^{-1}$ FW after 90 days. At the same time, fruit firmness decreased obviously with storage time prolonging (**Figure 1C**), and SSC increased gradually (**Figure 1D**) in kiwifruit both stored at 25 and 0°C. The firmness and SSC of fruit stored at room temperature for 9 days and low temperature for 90 days showed no significant difference.

Effect of Low Temperature Storage on the Expression of Anthocyanin Biosynthesis Genes

Full-length cDNA sequence of genes involved in the anthocyanin biosynthesis pathway, were cloned from ripe 'Hongyang' kiwifruit using RT-PCR and RACE, annotated as *DFR1* (*Achn014341*), *DFR2* (*Achn0135311*), *ANS1* (*Achn002561*), *ANS2* (*Achn361621*), *UFGT1* (*Achn209671*), *UFGT2* (*Achn017071*) and *UFGT3* (*Achn321621*) according to previous description by Li et al. (2015). Expression level of those genes, i.e., *DFR*,

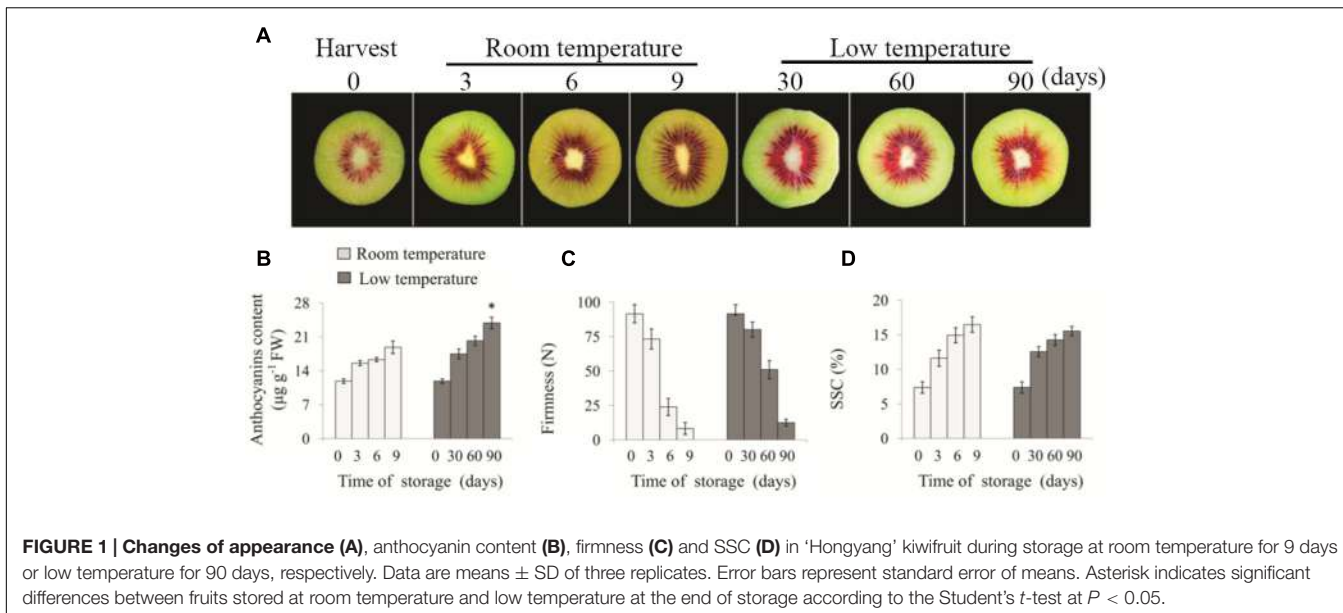


FIGURE 1 | Changes of appearance (A), anthocyanin content (B), firmness (C) and SSC (D) in 'Hongyang' kiwifruit during storage at room temperature for 9 days or low temperature for 90 days, respectively. Data are means \pm SD of three replicates. Error bars represent standard error of means. Asterisk indicates significant differences between fruits stored at room temperature and low temperature at the end of storage according to the Student's *t*-test at $P < 0.05$.

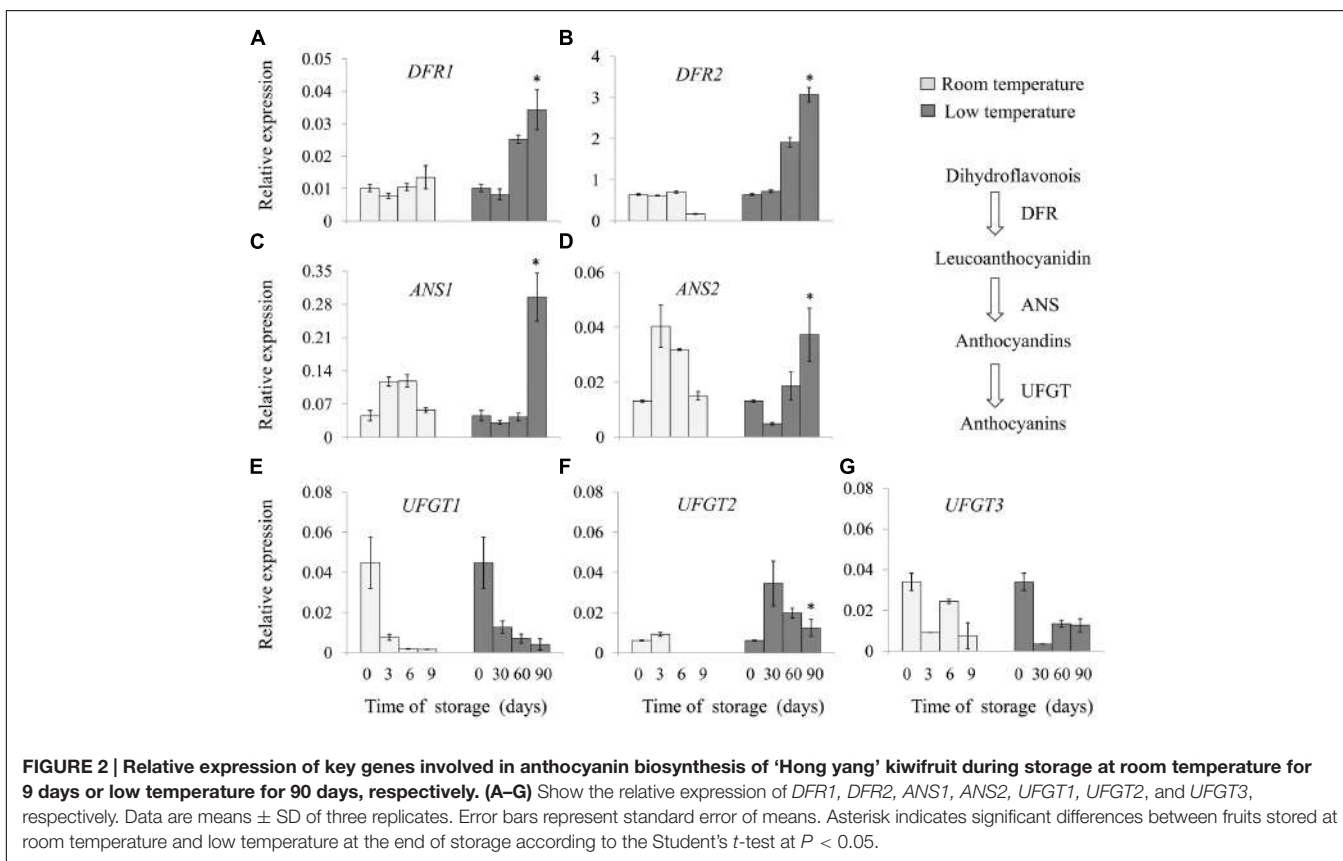


FIGURE 2 | Relative expression of key genes involved in anthocyanin biosynthesis of 'Hong yang' kiwifruit during storage at room temperature for 9 days or low temperature for 90 days, respectively. (A–G) Show the relative expression of *DFR1*, *DFR2*, *ANS1*, *ANS2*, *UFGT1*, *UFGT2*, and *UFGT3*, respectively. Data are means \pm SD of three replicates. Error bars represent standard error of means. Asterisk indicates significant differences between fruits stored at room temperature and low temperature at the end of storage according to the Student's *t*-test at $P < 0.05$.

ANS, and *UFGT*, were analyzed in fruit stored at room- and low-temperature (Figure 2).

Significant differences in the expression pattern of these genes were revealed during storage. The transcript abundance of *DFR1* and *DFR2* was not changed in fruit stored at room temperature, whereas it was obviously increased in fruit stored

at low temperature, with a higher level after 90 days, about 3.4 and 4.8 times that of the initial storage, respectively. *ANS* expression gradually increased in the early stage of storage, with the maximum value at 3 and 6 days, respectively, and then declined in room temperature-stored fruit. By contrast, fruits stored at low temperature remained a lower level of the

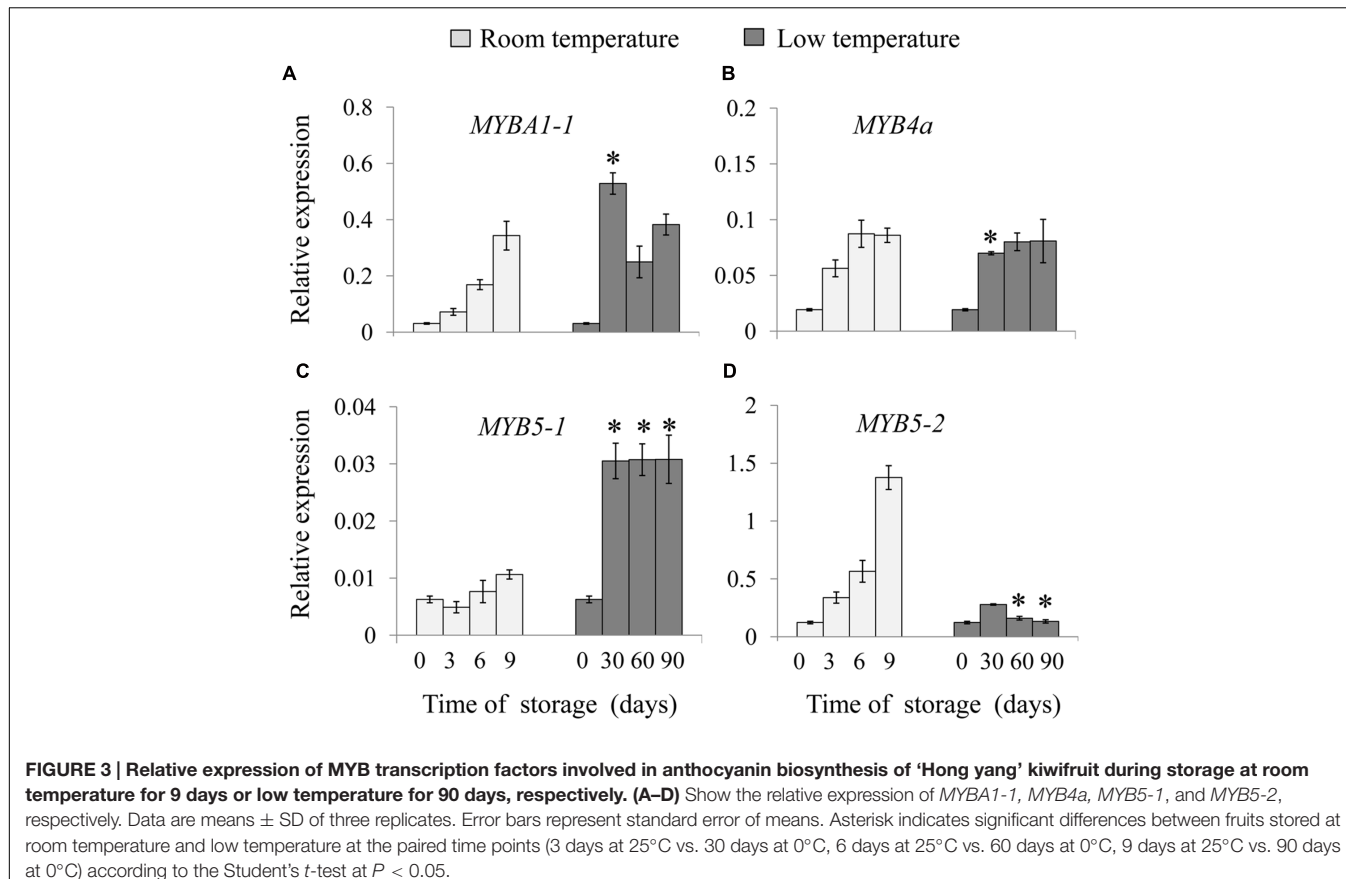


FIGURE 3 | Relative expression of MYB transcription factors involved in anthocyanin biosynthesis of 'Hong yang' kiwifruit during storage at room temperature for 9 days or low temperature for 90 days, respectively. (A–D) Show the relative expression of *MYBA1-1*, *MYB4a*, *MYB5-1*, and *MYB5-2*, respectively. Data are means \pm SD of three replicates. Error bars represent standard error of means. Asterisk indicates significant differences between fruits stored at room temperature and low temperature at the paired time points (3 days at 25°C vs. 30 days at 0°C, 6 days at 25°C vs. 60 days at 0°C, 9 days at 25°C vs. 90 days at 0°C) according to the Student's *t*-test at $P < 0.05$.

expression of *ANS1* and *ANS2* in the first 60 days of storage, but exhibited a higher level after 90 days. The expression of *UFGT1* and *UFGT3* decreased in fruit stored either at room temperature or low temperature; however, *UFGT2* expression firstly increased and then declined. Low temperature storage enhanced the *UFGT2* expression from 30 to 90 days. These results indicated that the mRNA levels of specific anthocyanin biosynthesis genes were induced by low temperature.

Effect of Low Temperature Storage on the Expression of MYB Family Genes

From the draft kiwifruit genome, four full-length MYB-related sequences were cloned from the 'Hongyang' kiwifruit, annotated as *MYBA1-1* (*Achn104391*), *MYB4a* (*Achn020361*), *MYB5-1* (*Achn148821*) and *MYB5-2* (*Achn366791*). Phylogenetic analysis using the predicted protein sequences of the four kiwifruit MYBs and other published MYBs sequences suggested that *MYB1-1* was most closely related to *VvMYBPA1*, and *MYB4a* was clustered with *AtMYB4*. Moreover, *MYB5-1* and *MYB5-2* were included in a small group with *VvMYB5a* and *VvMYB5b* (Supplementary Figure S2).

Expression levels of the four *MYBs* were analyzed in room and low temperature-stored fruit, respectively. As shown from Figure 3A, mRNA levels of *MYBA1-1* increased gradually in room temperature-stored fruit, while its level rapidly increased in low temperature-stored fruit. There was no significant difference

in the expression of *MYB4a* during low temperature storage (Figure 3B). Interestingly, the most significant differences were observed in the expression patterns of *MYB5-1* and *MYB5-2* in kiwifruit. The expression of *MYB5-1* had a constantly lower level in fruit stored at room temperature throughout the storage time; however, it was sharply increased in low temperature-stored fruit, being a five times higher than that of initial time point, after 90 days of storage (Figure 3C). On the contrary, the *MYB5-2* expression in room temperature-stored fruits increased gradually and peaked at 9 days, however, it remained at a basal level till the end of storage in low temperature-stored fruit (Figure 3D). The results indicated that low temperature storage could induce and enhance the expression of certain members of *MYBs* gene family.

Transient Expression in *N. benthamiana*

To further investigate the roles of *AcMYB5-1/5-2/A1-1* in regulation of anthocyanin biosynthesis, transient transformation of genes encoding the three transcription factors was carried out in *Nicotiana benthamiana* leaves. The expression levels of *NtANS*, *NtDFR*, and *NtUFGT* were analyzed in transiently transformed tobacco leaves (Figure 4). Transiently overexpression of *AcMYB5-1/5-2/A1-1* up-regulated expression levels of *NtANS* and *NtDFR*, but did not alter the expression of *NtUFGT* in tobacco leaves. A strong induction of the *NtANS* and the *NtDFR* genes was found in *AcMYB5-2* agro-infiltrated leaves, about 7 and 13 times higher, respectively, than that in control leaves. The

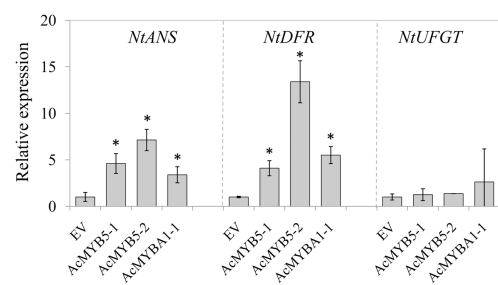


FIGURE 4 | Gene expression of *NtANS*, *NtDFR*, and *NtUGT* in tobacco leaves transiently overexpressing AcMYB5-1/5-2/A1-1. Data are means \pm SD of three replicates. Error bars represent standard error of means. Asterisk indicates significant difference at $P < 0.05$.

results suggested that overexpression of AcMYB5-1/5-2/A1-1 could activate the gene expression of *NtANS* and *NtDFR* in tobacco.

DISCUSSION

Anthocyanin is preferentially accumulated in the center of 'Hongyang' fruit (Figure 1A), which makes it more attractive for customers. Ripening is considered to be related to anthocyanin production in fruits. A number of reports suggested that there was a positive relation between soluble sugar and anthocyanin contents in fruits, such as bayberry (Shi et al., 2014) and grape berry (Dai et al., 2014). Shi and Xie (2014) considered that glycosylation could modify the stability of anthocyanin in aqueous solution. In the present study, we found that anthocyanin content gradually increased in 'Hongyang' kiwifruit along with the increase in SSC and decrease in firmness during storage under both room and low temperatures (Figure 1). Comparing with fruit at 0 day, anthocyanin content improved 60 and 100% at the end of storage at 25 and 0°C, respectively. These results indicate that maturity and sugar content are positively related to anthocyanin production in harvested 'Hongyang' kiwifruit. Further, we noticed that kiwifruit with similar SSC showed different level of anthocyanin, when they were separately stored at different temperature. For example, anthocyanin content of kiwifruit stored at 0°C (90 days) was significantly higher than those stored at 25°C (9 days), indicating that low temperature can enhance anthocyanin accumulation in 'Hongyang' kiwifruit. The similar results were also reported in pear (Zhang et al., 2012) and red orange (Lo Piero et al., 2005).

Low temperature stimulating anthocyanin biosynthesis may contribute to induce the expression of some genes involved in anthocyanin biosynthesis. Lo Piero et al. (2005) considered that long cold-storage strongly induced the expression of 'late gene' (i.e., *DFR* and *UGT*) rather than the 'early gene' of the anthocyanin biosynthesis in the red orange fruit. Zhang et al. (2012) showed that low temperature treatment enhanced the expression of the anthocyanin biosynthetic genes, especially *ANS* and *UGT* in the skin of pear fruit, but did not affect the transcript level of *DFR* gene. Hasegawa et al. (2001) reported

that the mRNA level of *DFR* was significantly increased under low temperature condition, indicating the important role of *DFR* in the regulation of anthocyanin biosynthesis. In recent, Man et al. (2015b) found that both 'early' and 'late' structure genes, including *CHS*, *CHI*, *F3H*, *DFR1*, *LDOX*, and *F3GT2* showed higher expression in 'Hongyang' kiwifruit grown in high altitude with lower temperature compared to low altitude area. Moreover, they also found that expressions of *CHS*, *CHI*, *F3H*, *DFR*, *LDOX*, *ANR*, and *FLS* were inhibited at 40°C compared with that at 25°C in harvested 'Hongyang' kiwifruit (Man et al., 2015a). These results suggested that temperature might affect both anthocyanin and other branches of flavonoid metabolism in kiwifruit. However, the effect of low temperature on anthocyanin accumulation and involving mechanisms are rarely reported in harvested 'Hongyang' kiwifruit. In this study, we found that low temperature enhances anthocyanin accumulation in 'Hongyang' kiwifruit via stimulating the expression of *ANS1*, *ANS2*, *DFR1*, *DFR2*, and *UGT2* genes involved in anthocyanin biosynthesis (Figure 2).

It has been widely reported that anthocyanin biosynthesis is regulated by MBW complex (Petroni and Tonelli, 2011). All the three components of MBW complex are important for activating anthocyanin synthesis. Among them, MYBs encoded by multi-gene families with diverse spatial expression domains. The MYBs are often more specific in the genes and pathways they target compared with the bHLH and WD40 components, which may be shared with MBW complexes regulating processes (Albert et al., 2014). Recently, Li et al. (2015) have identified 9 R2R3 MYBs potentially participated in anthocyanin metabolism during fruit development using the transcriptome analysis in 'Hongyang' kiwifruit. Among them, MYB5 and MYBA have been proved to be positive activators in the early development of 'Hongyang' fruit (7 days after anthesis, DAA), where kiwifruit undergo a temporary accumulation of anthocyanin, as well as later during the fruit development (Li et al., 2015; Man et al., 2015b). The fact that the mRNA abundance of *MYB5* and *MYBA1* in 'Hongyang' kiwifruit increased along with anthocyanin accumulation during storage time both at room- and low-temperature, further indicates that the two genes are positively related to anthocyanin production. Moreover, MYB regulators might be a critical factor related to anthocyanin biosynthesis under low temperature (Lai et al., 2011). Some results indicated that *VvMYB5a* and *VvMYB5b* in grape, along with *MdMYBA* in apple, could be induced by low-temperature, then activated the expression of *ANS*, leading to the anthocyanin accumulation in fruit (Ban et al., 2007; Deluc et al., 2008). Our results demonstrated that low temperature enhanced the expression of *MYBA1-1* and *MYB5-1*, but not *MYB5-2* (Figure 3), possibly resulting in the induction of specific *ANS*, *DFR* and *UGT* expression and thereby the increase of anthocyanin accumulation in 'Hongyang' kiwifruit during storage. We also found that the mRNA levels of *MYB5-1* and *MYB5-2* exhibited opposite trends during storage at different temperatures. It is possible that both *MYB5-1* and *MYB5-2* have similar function in anthocyanin biosynthesis, but appear to be responsible for different environment factors. Transiently overexpression of AcMYB5-1/5-2/A1-1 in *N. benthamiana* leaves up-regulated expression levels of *NtANS* and *NtDFR*, which

further indicate that those MYB transcription factors may participate in anthocyanin biosynthetic pathway. However, we did not observe the changes in leaf color and accumulation of anthocyanins. Transient transformation of MYBs may be not enough to activate the whole biosynthetic pathway of anthocyanins in *N. benthamiana* leaves.

In summary, in the present study, we found that anthocyanins gradually increased in 'Hongyang' kiwifruit during post-harvest storage under both room and low temperatures. Low temperature storage could enhance anthocyanin accumulation, and induce the expression of several structural and regulatory genes related to anthocyanin biosynthesis. Other regulators (such as bHLHs and WD40) and involved molecular mechanisms need to be further addressed.

AUTHOR CONTRIBUTIONS

ST conceived and designed the experiments. BL and YX performed the experiments. BL, YX, YW, and GQ analyzed the

data. BL, YW, and ST drafted the manuscript. All authors read and approved the final manuscript.

FUNDING

This work was supported by National Nature Science Foundation of China (31530057), Ministry of Science and Technology of China (2016YFD0400902), Youth Innovation Promotion Association CAS (2015063), and Open Fund of Key Laboratory of Biotechnology and Bioresources Utilization (Dalian Minzu University), State Ethnic Affairs Commission & Ministry of Education, China.

SUPPLEMENTARY MATERIAL

The Supplementary Material for this article can be found online at: <http://journal.frontiersin.org/article/10.3389/fpls.2017.00341/full#supplementary-material>

REFERENCES

- Albert, N. W., Davies, K. M., and Schwinn, K. E. (2014). Gene regulation networks generate diverse pigmentation patterns in plants. *Plant Signal. Behav.* 9:e29526. doi: 10.4161/psb.29526
- Ban, Y., Honda, C., Hatsuyama, Y., Igarashi, M., Bessho, H., and Moriguchi, T. (2007). Isolation and functional analysis of a MYB transcription factor gene that is a key regulator for the development of red coloration in apple skin. *Plant Cell Physiol.* 48, 958–970. doi: 10.1093/pcp/pcm066
- Boss, P. K., Davies, C., and Robinson, S. P. (1996). Expression of anthocyanin biosynthesis pathway genes in red and white grapes. *Plant Mol. Biol.* 32, 565–569. doi: 10.1007/BF00019111
- Cavallini, E., Zenoni, S., Finezzo, L., Guzzo, F., Zamboni, A., Avesani, L., et al. (2014). Functional diversification of grapevine MYB5a and MYB5b in the control of flavonoid biosynthesis in a petunia anthocyanin regulatory mutant. *Plant Cell Physiol.* 55, 517–534. doi: 10.1093/pcp/pct190
- Crowhurst, R. N., Gleave, A. P., MacRae, E. A., Ampomah-Dwamena, C., Atkinson, R. G., Beuning, L. L., et al. (2008). Analysis of expressed sequence tags from *Actinidia*: applications of a cross species EST database for gene discovery in the areas of flavor, health, color and ripening. *BMC Genomics* 9:1. doi: 10.1186/1471-2161-9-351
- Dai, Z., Meddar, M., Renaud, C., Renaud, C., Merlin, I., Hilbert, G., et al. (2014). Long-term in vitro culture of grape berries and its application to assess the effects of sugar supply on anthocyanin accumulation. *J. Exp. Bot.* 65, 4665–4677. doi: 10.1093/jxb/ert489
- Deluc, L., Bogs, J., Walker, A. R., Ferrier, T., Decendit, A., Merillon, J., et al. (2008). The transcription factor VvMYB5b contributes to the regulation of anthocyanin and proanthocyanidin biosynthesis in developing grape berries. *Plant Physiol.* 147, 2041–2053. doi: 10.1104/pp.108.118919
- Giusti, M. M., and Wrolstad, R. E. (2003). Acylated anthocyanins from edible sources and their applications in food systems. *Biochem. Eng. J.* 14, 217–225. doi: 10.1016/S1369-703X(02)00221-8
- Hasegawa, H., Fukasawa-Akada, T., Okuno, T., Niizeki, M., and Suzuki, M. (2001). Anthocyanin accumulation and related gene expression in Japanese parsley (*Oenanthe stolonifera*, DC.) induced by low temperature. *J. Plant Physiol.* 158, 71–78. doi: 10.1078/0176-1617-00038
- He, J., and Giusti, M. M. (2010). Anthocyanins: natural colorants with health-promoting properties. *Annu. Rev. Food Sci. Technol.* 1, 163–187. doi: 10.1146/annurev.food.080708.100754
- Huang, S., Ding, J., Deng, D., Tang, W., Sun, H., Liu, D., et al. (2013). Draft genome of the kiwifruit *Actinidia chinensis*. *Nat. Commun.* 4, 2640. doi: 10.1038/ncomms3640
- Jaakola, L. (2013). New insights into the regulation of anthocyanin biosynthesis in fruits. *Trends Plant Sci.* 18, 477–483. doi: 10.1016/j.tplants.2013.06.003
- Lai, Y., Yamagishi, M., and Suzuki, T. (2011). Elevated temperature inhibits anthocyanin biosynthesis in the tepals of an Oriental hybrid lily via the suppression of LhMYB12 transcription. *Sci. Hortic.* 132, 59–65. doi: 10.1016/j.scientia.2011.09.030
- Li, W., Liu, Y., Zeng, S., Xiao, G., Wang, G., Wang, Y., et al. (2015). Gene expression profiling of development and anthocyanin accumulation in kiwifruit (*Actinidia chinensis*) based on transcriptome sequencing. *PLoS ONE* 10:e0136439. doi: 10.1371/journal.pone.0136439
- Liu, J., Osbourn, A., and Ma, P. (2015). MYB transcription factors as regulators of phenylpropanoid metabolism in plants. *Mol. Plant* 8, 689–708. doi: 10.1016/j.molp.2015.03.012
- Lo Piero, A. R., Puglisi, I., Rapisarda, P., and Petrone, G. (2005). Anthocyanins accumulation and related gene expression in red orange fruit induced by low temperature storage. *J. Agric. Food Chem.* 53, 9083–9088. doi: 10.1021/jf051609s
- Man, Y., Wang, Y., Jiang, Z., and Gong, J. (2015a). Transcriptomic analysis of pigmented inner pericarp of red-fleshed kiwifruit in response to high temperature. *Acta Hortic.* 1096, 215–220. doi: 10.17660/ActaHortic.2015.1096.23
- Man, Y., Wang, Y., Li, Z., Jiang, Z., Yang, H., Gong, J., et al. (2015b). High-temperature inhibition of biosynthesis and transportation of anthocyanins results in the poor red coloration in red-fleshed *Actinidia chinensis*. *Physiol. Plant.* 153, 565–583. doi: 10.1111/ppl.12263
- Montefiori, M., Espley, R. V., Stevenson, D., Cooney, J., Datson, P. M., Saiz, A., et al. (2011). Identification and characterisation of F3GT1 and F3GGT1, two glycosyltransferases responsible for anthocyanin biosynthesis in red-fleshed kiwifruit (*Actinidia chinensis*). *Plant J.* 65, 106–118. doi: 10.1111/j.1365-313X.2010.04409.x
- Petroni, K., and Tonelli, C. (2011). Recent advances on the regulation of anthocyanin synthesis in reproductive organs. *Plant Sci.* 181, 219–229. doi: 10.1016/j.plantsci.2011.05.009
- Shi, L., Cao, S., Shao, J., Chen, W., Zheng, Y., Jiang, Y., et al. (2014). Relationship between sucrose metabolism and anthocyanin biosynthesis during ripening in chinese bayberry fruit. *J. Agric. Food Chem.* 62, 10522–10528. doi: 10.1021/jf503317k
- Shi, M., and Xie, D. (2014). Biosynthesis and metabolic engineering of anthocyanins in *Arabidopsis thaliana*. *Recent Pat. Biotechnol.* 8, 47–60. doi: 10.2174/1872208307666131218123538
- Steyn, W. J., Holcroft, D. M., Wand, S. J. E., and Jacobs, G. (2004). Anthocyanin degradation in detached pome fruit with reference to preharvest red color loss

- and pigmentation patterns of blushed and fully red pears. *J. Am. Soc. Hortic. Sci.* 129, 13–19.
- Tang, W., Zheng, Y., Dong, J., Yu, J., Yue, J., Liu, F., et al. (2016). Comprehensive transcriptome profiling reveals long noncoding RNA expression and alternative splicing regulation during fruit development and ripening in kiwifruit (*Actinidia chinensis*). *Front. Plant Sci.* 7:335. doi: 10.3389/fpls.2016.00335
- Ubi, B. E., Honda, C., Bessho, H., Kondo, S., Wada, M., Kobayashi, S., et al. (2006). Expression analysis of anthocyanin biosynthetic genes in apple skin: effect of UV-B and temperature. *Plant Sci.* 170, 571–578. doi: 10.1016/j.plantsci.2005.10.009
- Wang, Y., Zhang, L., Man, Y., Li, Z., and Qin, R. (2012). Phenotypic characterization and simple sequence repeat identification of red-fleshed kiwifruit germplasm accessions. *HortScience* 47, 992–999.
- Wu, J., Ferguson, A. R., Murray, B. G., Duffy, A. M., Jia, Y., Cheng, C., et al. (2013). Fruit quality in induced polyploids of *Actinidia chinensis*. *HortScience* 48, 701–707.
- Xia, Y. X., Chen, T., Qin, G. Z., Li, B. Q., and Tian, S. P. (2016). Synergistic action of antioxidative systems contributes to the alleviation of senescence in kiwifruit. *Postharvest Biol. Technol.* 111, 15–24. doi: 10.1016/j.postharvbio.2015.07.026
- Zhang, D., Yu, B., Bai, J., Qian, M., Shu, Q., Su, J., et al. (2012). Effects of high temperatures on UV-B/visible irradiation induced postharvest anthocyanin accumulation in 'Yunhongli No. 1' (*Pyrus pyrifolia Nakai*) pears. *Sci. Hortic.* 134, 53–59. doi: 10.1016/j.scienta.2011.10.025
- Zhao, Z., Hu, G., Hu, F., Wang, H., Yang, Z., and Lai, B. (2012). The UDP glucose:flavonoid-3-O-glucosyltransferase (UFGT) gene regulates anthocyanin biosynthesis in litchi (*Litchi chinensis Sonn.*) during fruit coloration. *Mol. Biol. Rep.* 39, 6409–6415. doi: 10.1007/s11033-011-1303-3
- Zhu, Z., Liu, R. L., Li, B. Q., and Tian, S. P. (2013). Characterization of genes encoding key enzymes involved in sugar metabolism of apple fruit in controlled atmosphere storage. *Food Chem.* 141, 3323–3328. doi: 10.1016/j.foodchem.2013.06.025

Conflict of Interest Statement: The authors declare that the research was conducted in the absence of any commercial or financial relationships that could be construed as a potential conflict of interest.

Copyright © 2017 Li, Xia, Wang, Qin and Tian. This is an open-access article distributed under the terms of the Creative Commons Attribution License (CC BY). The use, distribution or reproduction in other forums is permitted, provided the original author(s) or licensor are credited and that the original publication in this journal is cited, in accordance with accepted academic practice. No use, distribution or reproduction is permitted which does not comply with these terms.



Transcriptome Analysis Reveals Candidate Genes Related to Color Fading of 'Red Bartlett' (*Pyrus communis* L.)

Zhigang Wang[†], Hong Du[†], Rui Zhai, Linyan Song, Fengwang Ma and Lingfei Xu*

College of Horticulture, Northwest A&F University, Yangling, China

OPEN ACCESS

Edited by:

Nadia Bertin,
Plantes et Système de Cultures
Horticoles (INRA), France

Reviewed by:

Henryk Flachowsky,
Julius Kühn-Institut, Germany
Benedetto Ruperti,
University of Padova, Italy

*Correspondence:

Lingfei Xu
lingfxu2013@sina.com

[†]These authors have contributed equally to this work.

Specialty section:

This article was submitted to
Crop Science and Horticulture,
a section of the journal
Frontiers in Plant Science

Received: 08 November 2016

Accepted: 15 March 2017

Published: 31 March 2017

Citation:

Wang Z, Du H, Zhai R, Song L, Ma F and Xu L (2017) Transcriptome Analysis Reveals Candidate Genes Related to Color Fading of 'Red Bartlett' (*Pyrus communis* L.). *Front. Plant Sci.* 8:455.
doi: 10.3389/fpls.2017.00455

The red color of fruit is an attractive plant trait for consumers. Plants with color-faded fruit have a lower commercial value, such as 'Red Bartlett' pears (*Pyrus communis* L.) that have dark-red fruit in the early stages of fruit development that subsequently fade to red-green at maturity. To identify the reason for color fading, we first analyzed the anthocyanin content of peel from 'Red Bartlett,' which displays the color fading phenomenon, and 'Starkrimson,' which has no color fading. Results showed that the anthocyanin content of 'Red Bartlett' peel decreased significantly late in fruit development, while in 'Starkrimson' there was no significant decrease. Next, RNA-Sequencing was used to identify 947 differentially expressed genes (DEGs) between 'Red Bartlett' and 'Starkrimson.' Among them, 471 genes were upregulated and 476 genes were downregulated in 'Red Bartlett' at the late development stage relative to 'Starkrimson.' During 'Red Bartlett' color fading, the structural gene *LDOX* and six GST family genes were downregulated, while *FLS*, *LAC*, *POD*, and five light-responding genes were significantly upregulated. Additionally, 45 genes encoding transcription factors *MYB*, *bHLH*, *WRKY*, *NAC*, *ERF*, and zinc finger were identified among 947 DEGs. Changes in the expression of these genes may be responsible for the decrease in anthocyanin accumulation in 'Red Bartlett' fruit. Taken together, this study demonstrated that color fading of 'Red Bartlett' was closely linked to reduced anthocyanin biosynthesis, increased anthocyanin degradation and suppression of anthocyanin transport. It also provided novel evidence for the involvement of light signals in the color fading of red-skinned pears.

Keywords: 'Red Bartlett' pear, transcriptome, color fading, anthocyanin, differentially expressed genes

INTRODUCTION

Fruit peel color is a key trait for fruit quality. In red fruit, the key factor affecting fruit peel coloration is the plant pigment anthocyanin. Anthocyanin is a water-soluble flavonoid and a natural colorant that accumulates widely in many plant tissues such as the flesh (Boss et al., 1996), peel (Honda et al., 2002), and petal (Vaknin et al., 2005).

The anthocyanin biosynthetic pathway has been described in a number of model plants (Winkel-shirley, 2001) and also in many fruit trees such as apple (Espley et al., 2007), grape (Kobayashi et al., 2002), and pear (*Pyrus communis* L.) (Fischer et al., 2007). In pear, the structural

genes involved in anthocyanin biosynthesis have been isolated and are coordinately regulated by a MBW complex of MYB, basic helix-loop-helix proteins (bHLH), and WD40 proteins. For example, MYB10 and PyMYB10.1 Interact with bHLH, Enhance Anthocyanin Accumulation in Pears (Feng et al., 2015). By regulating transcript levels of PcuUGT, the methylation level of the PcmYB10 promoter affected the formation of the green-skinned sport of ‘Red Bartlett’ (Wang et al., 2013). PbMYB9, a TRANSPARENT TESTA 2-type MYB transcription factor (TF) regulating the flavonol branch, has also been identified in pear fruit (Zhai et al., 2015). In apple, the cold-induced bHLH TF gene MdbHLH3 promoted fruit coloration (Xie et al., 2012). Recently, it has been reported that anthocyanin biosynthesis was also regulated by other TFs such as WRKY and NAC family members (Johnson et al., 2002; Zhou et al., 2015). In addition to the effects of endogenous genes, anthocyanin synthesis was also modulated and affected by environmental factors, in particular by light (Cutuli et al., 1999). When dark-grown fruit were exposed to sunlight, MdMYB1 transcript levels increased over several days, correlating with anthocyanin synthesis in red apple (Takos et al., 2006). Furthermore, the associated MBW complex could be decreased under low light intensity and dark conditions, leading to the downregulation of structural genes and a resulting decrease in anthocyanin content (Azuma et al., 2012). In addition, AP2 and WARK regulated the anthocyanin biosynthesis in red skinned ‘Starkrimson,’ and ANR and LAR promote PA biosynthesis and contribute to the green skinned variant (Yang et al., 2015a). Recently, reports of anthocyanin degradation and color fading have received much attention. Three common enzyme families, polyphenol oxidases (PPOs), class III peroxidases, and β -glucosidases, were reported to be involved in anthocyanin degradation (Oren-Shamir, 2009). To date, BcPrx01, a basic vacuolar peroxidase, was shown to be responsible for anthocyanin degradation in Brunfelsia calycina flowers (Zipor et al., 2015) while laccase, a novel anthocyanin degradation enzyme, was identified in litchi pericarp (Fang et al., 2015).

However, anthocyanin content was not only associated with anthocyanin metabolism but also with anthocyanin transport. Anthocyanins were synthesized at the cytoplasmic face of the endoplasmic reticulum before being transported to the vacuole for anthocyanin accumulation (Marrs et al., 1995). Moreover, it was described that in addition to the glutathione S-transferase (GST) family, the ATP-binding cassette (ABC) and multidrug and toxic compound extrusion (MATE) families were also involved in anthocyanin transport (Mueller et al., 2000; Klein et al., 2006; Gomez et al., 2009). In maize, the *Bronze2* (*bz2*) gene, a GST family member, was confirmed to be involved in vacuolar transfer of anthocyanins by conjugating with glutathione (Marrs et al., 1995). TRANSPARENT TESTA 19 (*TT19*), a member of the *Arabidopsis thaliana* GST gene family, was also found to be required for the transportation of anthocyanins into vacuoles (Kitamura et al., 2004). MdGST (MDP0000252292) from apple has been shown to be the most suppressed gene in a yellow-skin somatic mutant apple line with corresponding reductions in anthocyanin content (Elsharkawy

et al., 2015). Nevertheless, to date, no direct evidence for the role of GSTs in conjugating anthocyanins in pear has been found.

In this study, utilizing RNA-sequencing (RNA-Seq) technology, we sequenced the transcriptome of two red-skinned European pears: ‘Red Bartlett,’ the fruit of which were red in the early stages of development before obviously fading into red-green during the later development period, and ‘Starkrimson,’ the fruit of which lacked clear color deviation and maintained a purplish-red color throughout whole development. Also, we identified a set of differentially expressed genes (DEGs) potentially involved in fruit coloration.

MATERIALS AND METHODS

Plant Materials and Fruit Treatment

In this study, the fruit of ‘Red Bartlett’ and ‘Starkrimson’ were selected as plant materials and were obtained from the orchard of Mei County, Shanxi Province, China, in 2015. The fruits of pear were harvested at 15, 35, 55, 75, and 95 days after full bloom (DAFB) (as showed in Figure 1). The peel of each pears was pared at a thickness of approximately 1 mm, frozen immediately in liquid nitrogen, and then stored at -80°C for further study.

Extraction and Determination of Anthocyanins

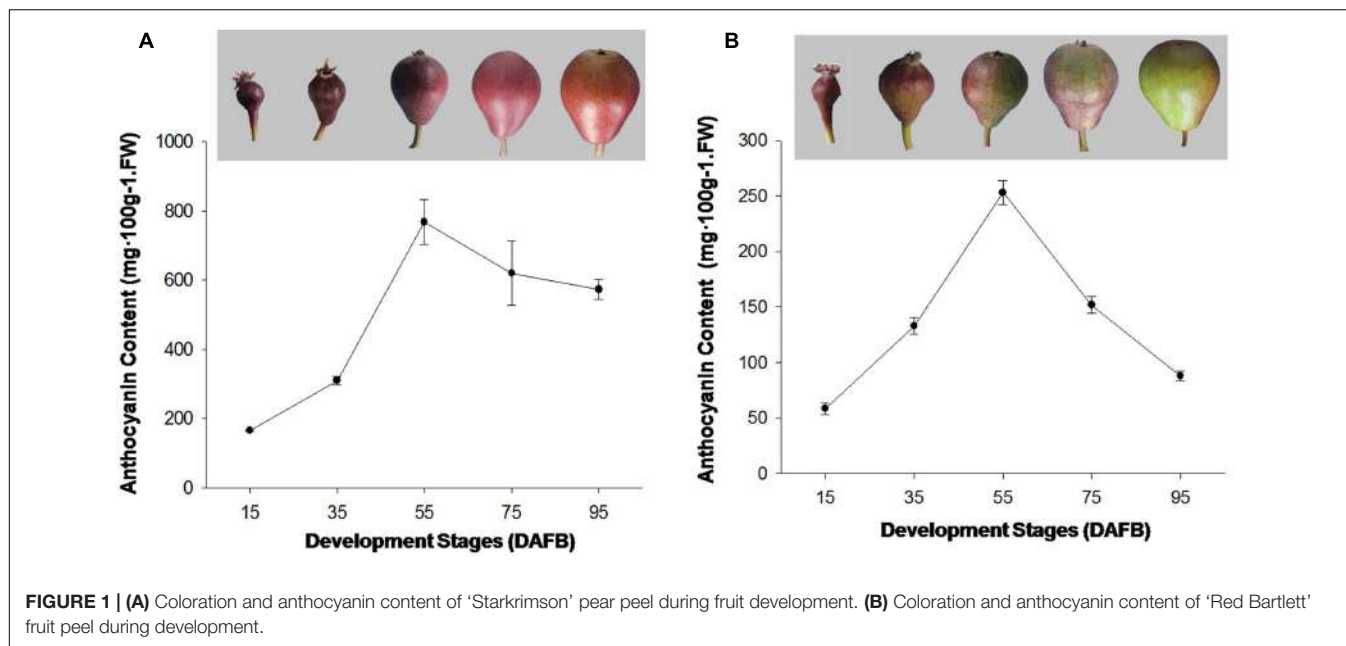
Anthocyanin extraction was conducted according to the method of Giusti and Wrolstad (2001), with slight modifications. Approximately, 1 g of skin tissue was collected and quickly ground into powder in liquid nitrogen before 5 ml of 1% HCl-methanol solution was added and the sample was incubated in the dark at 4°C for 12 h. After centrifugation at $12,000 \times g$ for 20 min, the supernatant was transferred to a clean tube and used for two dilutions, one with 0.025 M potassium chloride buffer ($\text{pH} = 1.0$) and the other with 0.4 M sodium acetate buffer ($\text{pH} = 4.5$). These dilutions were left to equilibrate for 15 min before the absorbance of each dilution was measured at 530 and 700 nm with a UV-Visible spectrophotometer (UV-1700, Kyoto, Japan), using a blank cell filled with distilled water for calibration. The anthocyanin content was calculated using the following formula:

$$C = A \times V \times n \times MW \times 100 / (\epsilon \times m),$$

where C stood for anthocyanin content ($\text{mg} \cdot 100 \text{ g}^{-1} \text{ FW}$), V for extraction solution volume, n for dilution factor, MW for the molecular weight of cyanidin-3-glucoside: 449.2, ϵ for molar absorptivity: 30200, m for the weight of fruit skin, and A = (A₅₃₀–A₇₀₀ nm) pH_{1.0} (A₅₃₀–A₇₀₀ nm) pH_{4.5}. The value for each sample represented the mean of three independent biological replicates.

RNA Extraction and cDNA Synthesis

Owing to anthocyanin levels are peaked at 55 DAFB in both of ‘Red Bartlett’ and ‘Starkrimson,’ five fruit peels of ‘Red Bartlett’



and 'Starkrimson' at 35 and 75 DAFB were mixed respectively and used for RNA-sequencing, with two biological replicates used for each cultivar at each time point. The total RNA was extracted and purified using an RNAPrep Pure Plant Kit (TIANGEN, Beijing, China), according to the manufacturer's instructions. RNA quality was checked using a NanoDrop Spectrophotometer (NanoDrop 2000C, Wilmington, DE, USA) and 5 μ l of RNA was used in 1–1.5% agarose gel electrophoresis to examine its integrity and purity. First strand cDNA synthesis was performed using a PrimeScript RT-PCR Kit (TaKaRa, Dalian, China) according to the manufacturer's instructions and stored at -20°C for RT-qPCR assays.

Library Construction and Transcriptome Sequencing

The Agilent 2100 Bioanalyzer was used to further examine the RNA quality of all samples. Samples with an RNA integrity number ≥ 7 , RNA content of $\geq 4 \mu\text{g}$, an RNA concentration of $\geq 50 \text{ ng}/\mu\text{l}$, and 28S:18S RNA ratio of ≥ 2 were used to construct RNA-Seq libraries for Illumina sequencing. Library generation involved five steps: the first step was to purify and fragment the mRNA; next, double stranded cDNA was synthesized using the fragmented mRNA, third, the sticky end of short fragments was repaired with end repair reagents to avoid self-connection; fourthly, sequencing adaptors were added to the cDNA fragments that were then enriched by PCR amplification; and finally, quality control analysis of the constructed libraries was carried out. The libraries were constructed using an Illumina HiSeqTM 2500 by the Millennium Corporation (Shenzhen, China). Including the two developmental stages of the two European pears, four RNA-Seq libraries were constructed and labeled as follows: Starkrimson-35 (35 DAFB of 'Starkrimson'), Red Bartlett-35 (35 DAFB of 'Red Bartlett'), Starkrimson-75 (75 DAFB of 'Starkrimson'), and Red Bartlett-75 (75 DAFB of 'Red Bartlett').

RNA-Sequencing Data Analysis

To ensure the accuracy and reliability of RNA-sequencing data, some poor quality reads were eliminated from the raw reads and only the remaining high-quality reads (clean reads) were used for statistics analysis. The level of gene expression was determined according to the number of fragments per kilobase of exon per million fragments mapped. The genes with a false discovery rate of <0.001 and an absolute value of the \log_2 (Fold Change) ≥ 1 were defined as DEGs. The functional annotation information for these DEGs was obtained using Batch Entrez¹. Additionally, Gene Ontology (GO) annotations and Kyoto Encyclopedia of Genes and Genomes (KEGG) pathway analyses were conducted using Blast2GO software (Conesa et al., 2005), and provided a comprehensive set of evidenced-based associations between the genes and UniProtKB proteins or the significantly enriched pathways (Mao et al., 2005; Dimmer et al., 2011).

RT-qPCR Validation

In order to verify the reliability of the RNA-Seq results, eight important DEGs were selected and measured by RT-qPCR on an iQ5 (Bio-Rad, Berkeley, CA, USA) using the SYBR Premix Ex Taq II (TaKaRa) according to the manufacturer's instructions. ACTIN was used as the reference gene, and the relative gene expression levels were determined using the $2^{-\Delta\Delta CT}$ approach. Each sample (including three biological repetitions) was quantified in triplicate. The reaction system included 100 ng cDNA, 0.8 μl forward and reverse primers (10 μM), respectively, and 10 μl SYBR Premix Ex Taq II, adjusted to 20 μl with sterile water. A two-step program was used, with an initial hot start at 95°C for 30 s followed by 40 cycles of 95°C for 5 s and 60°C for 34 s. Melting curves were generated using the following program: 95°C for 15 s, 60°C for 1 min, and 95°C for 15 s. A list

¹<https://www.ncbi.nlm.nih.gov/sites/batchentrez>

of RT-qPCR primers for *ACTIN* and the 12 selected genes is displayed in **Supplementary Table S1**.

Statistical Analysis

Statistical analysis was performed using Microsoft Excel 2010 and SigmaPlot 10.0 (Systat Software, Inc., San Jose, CA, USA). Each value represented mean \pm SD of three independent biological replicates.

RESULTS

Changes in the Anthocyanin Content and ACS1 Gene Expression of the Two Cultivars

The red color appeared on fruit at the early development stages in ‘Red Bartlett.’ The coloration reduced from the middle stages (DAFB 55) as the fruit matured before finally most of the fruit surface turned green. The anthocyanin content of ‘Red Bartlett’ fruit increased significantly at the early stage, reached $253 \text{ mg} \cdot 100 \text{ g}^{-1}$ FW at 55 DAFB before subsequently declining to $88 \text{ mg} \cdot 100 \text{ g}^{-1}$ FW at 95 DAFB, in accordance with the color fading of ‘Red Bartlett’ (**Figure 1A**). However, in ‘Starkrimson’ fruit, the coloration progressively changed from red to dark-red until 55 DAFB and then appeared bright red after 55 DAFB. Furthermore, the anthocyanin content of ‘Red Bartlett’ increased sharply and significantly during the early stages of development, before decreasing after 55 DAFB. This differed from ‘Starkrimson’ where the anthocyanin levels did not change significantly after 55 DAFB (**Figure 1B**). Moreover, the anthocyanin level of ‘Starkrimson’ was always higher than ‘Red Bartlett’ in whole development stage.

The expression of ACS1 gene in both cultivars were similar and showed the same change trend (**Supplementary Figure S1**), indicating that the developmental stages under comparison were homogeneous between the two cultivars.

The RNA-Seq Data Analysis

To ensure the validity of transcriptome results, the data obtained from RNA-Seq was used for statistical analysis. In the present study, the high-quality libraries (with a mapping rate higher than 56% and Q20 and Q30 values higher than 90%), were constructed using the fruit skin of Starkrimson-35 (35 DAFB of ‘Starkrimson’), Red Bartlett-35 (35 DAFB of ‘Red Bartlett’), Starkrimson-75 (75 DAFB of ‘Starkrimson’), and Red Bartlett-75 (75 DAFB of ‘Red Bartlett’), respectively (**Supplementary Table S7**). Additionally, the gene coverage coincided with the results of the library construction (**Supplementary Figure S2**). These results indicate that the RNA-Seq data we obtained was useable for this study.

Identification of DEGs between ‘Red Bartlett’ and ‘Starkrimson’

To find candidate genes, pairwise comparison analysis was conducted. In the two cultivars, 3154 redundant DEGs (with an absolute value of \log_2 (Fold Change) ≥ 1 and a false discovery

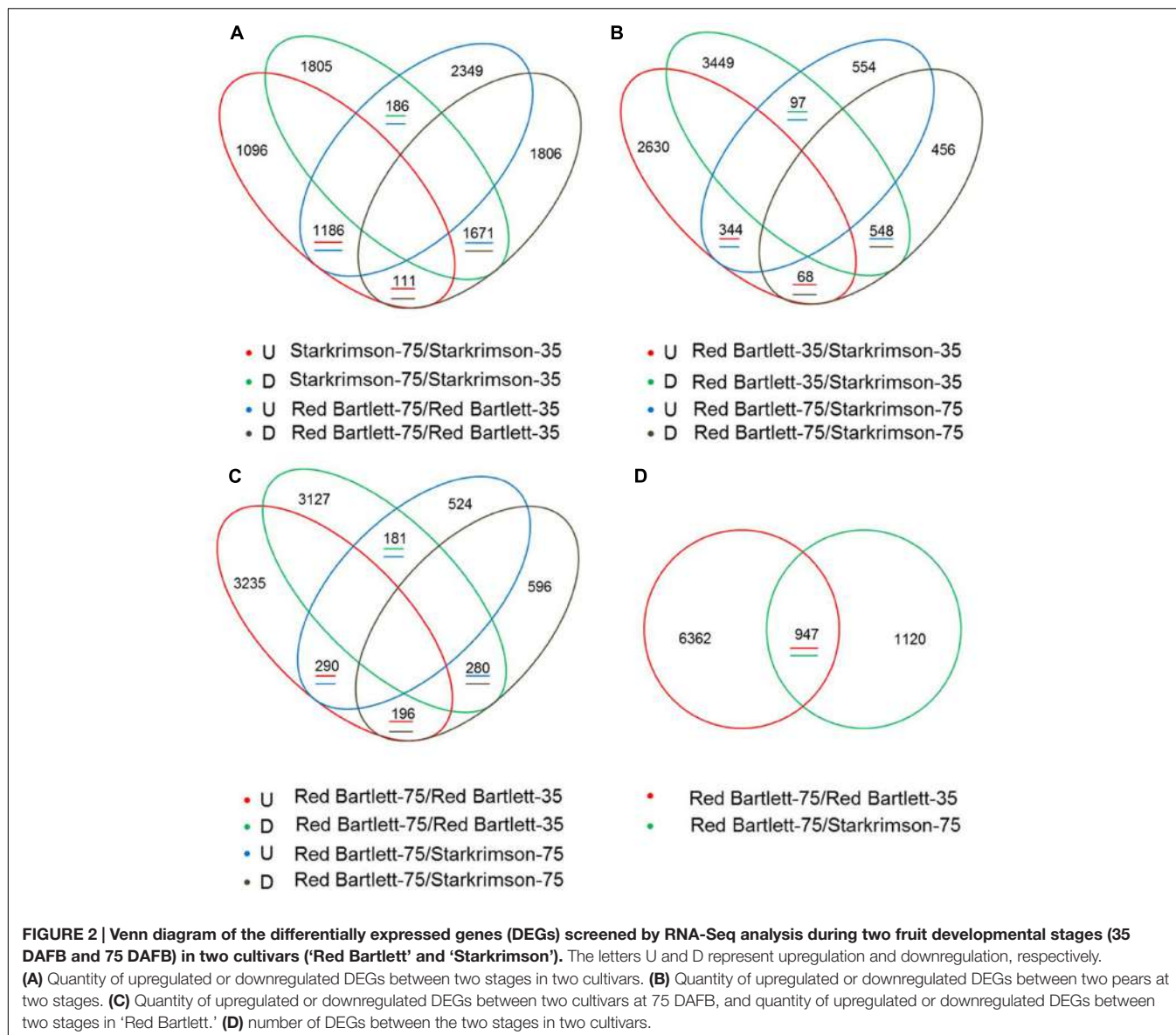
rate of <0.001) were identified between 75 DAFB and 35 DAFB (**Figure 2A**). At the two developmental stages, 1057 redundant DEGs were also found between the two cultivars (**Figure 2B**). Overall, by pairwise comparison, 947 DEGs were redundant between ‘Red Bartlett-75/Red Bartlett-35’ (DEGs between the two development stages in ‘Red Bartlett’) and ‘Red Bartlett-75/Starkrimson-75’ (DEGs between the two cultivars at 75 DAFB) (**Figure 2D**). Compared with ‘Starkrimson,’ 471 DEGs were significantly upregulated at 75 DAFB in ‘Red Bartlett,’ while 476 were significantly downregulated (**Figure 2C**). These 947 DEGs were, therefore, selected as candidate genes potentially associated with the color fading of ‘Red Bartlett’ (**Supplementary Table S2**), and were subjected to further functional analysis.

GO Annotation, KEGG Pathway, and Enrichment Analyses

In the present study, the predicted functions of 947 DEGs were obtained by GO annotation, KEGG pathway, and enrichment analyses. According to GO annotation, these DEGs were distributed into 40 functional terms as follows: 16 terms for biological process; 18 terms for molecular function, and six terms for cellular component. The genes in the biological process group were mainly involved in photosynthesis and regulation of defense response. The molecular function terms related to beta-amylase, flavonol synthase (FLS), and isoflavone 2'-hydroxylase. Most of the cellular component genes were located in the chloroplast thylakoid membrane, photosystem II, magnesium chelatase complex, and vacuole (**Figure 3**). Meanwhile, KEGG pathway and enrichment analysis showed that DEGs were significantly enriched in the pathways of circadian rhythm, photosynthesis, and peroxisome (**Supplementary Table S3**).

Analysis of Genes Involved in the Anthocyanin Synthesis, Degradation, and Transport

Structural genes involved in anthocyanin synthesis were identified (**Figure 4A** and **Supplementary Table S4**). The predicted proteins encoded by upstream genes included one phenylalanine ammonia lyase (LOC103962533), one chalcone synthase (LOC103959489), one chalcone isomerase (LOC103940646), and one flavanone-3-hydroxylase (LOC103953484). The predicted proteins encoded by downstream genes included two dihydroflavonol-4-reductase (LOC103928717 and LOC103954960), two leucoanthocyanidin dioxygenase (LDOX) (LOC103958614 and LOC103966324) and one UDP-glucose:flavonoid 3-O-glucosyltransferase (LOC103951514). In ‘Red Bartlett,’ the predicted coding genes of the phenylalanine ammonia lyase (LOC103962533), chalcone synthase (LOC103959489), and dihydroflavonol-4-reductase (LOC103928717 and LOC103954960) were significantly upregulated at 75 DAFB, while two LDOX-predicted coding genes (LOC103958614 and LOC103966324) were significantly downregulated. Moreover, the UFGT-predicted coding gene (LOC103951514), a key anthocyanin synthetic gene, decreased in expression during both development stages in ‘Red Bartlett’ but did not change in expression in ‘Starkrimson.’ Genes related to



other flavonoid metabolic pathways showed a significant increase in mature 'Red Bartlett' fruit, especially the FLS-predicted coding gene (LOC103933697).

In the present study, one LAC-predicted coding gene (LOC103946137) and two POD-predicted coding genes (LOC103945527 and LOC103961180) were identified (**Figure 4A** and **Supplementary Table S4**). In 'Red Bartlett,' expression levels of these three genes at 75 DAFB were all higher than at 35 DAFB. This result suggests that these genes involved in anthocyanin degradation may take part in the color fading phenotype of 'Red Bartlett.'

Ten predicted coding genes involved in anthocyanin transport were identified (**Figure 4A** and **Supplementary Table S4**), including six GST (LOC103955362, LOC103945951, LOC103945952, LOC103955337, LOC103960192, and LOC103960208), two MATE (LOC103933301 and LOC103955660), and

two ABC (LOC103928557 and LOC103947696). Moreover, two genes predicted to encode ABCs were significantly downregulated in expression in the late fruit development stage of 'Red Bartlett.' However, expression of these two genes did not significantly differ [the absolute value of \log_2 (Fold Change) < 1] between the two cultivars at 75 DAFB. Therefore, six GSTs and two MATEs, but not the two ABCs, were candidate key genes for anthocyanin transport.

Anthocyanin synthesis was regulated by a series of TFs and in the present study, 45 DEGs predicted to encode TFs were identified (**Figure 4B** and **Supplementary Table S5**). These genes were divided into six categories: MYB, bHLH, WRKY, NAC, ethylene response factor (ERF), and zinc finger. Among these 45 genes, 20 have significantly increased transcript levels at 75 DAFB in 'Red Bartlett' relative to 35 DAFB, while expression of the remainder decreased significantly. Genes annotated as

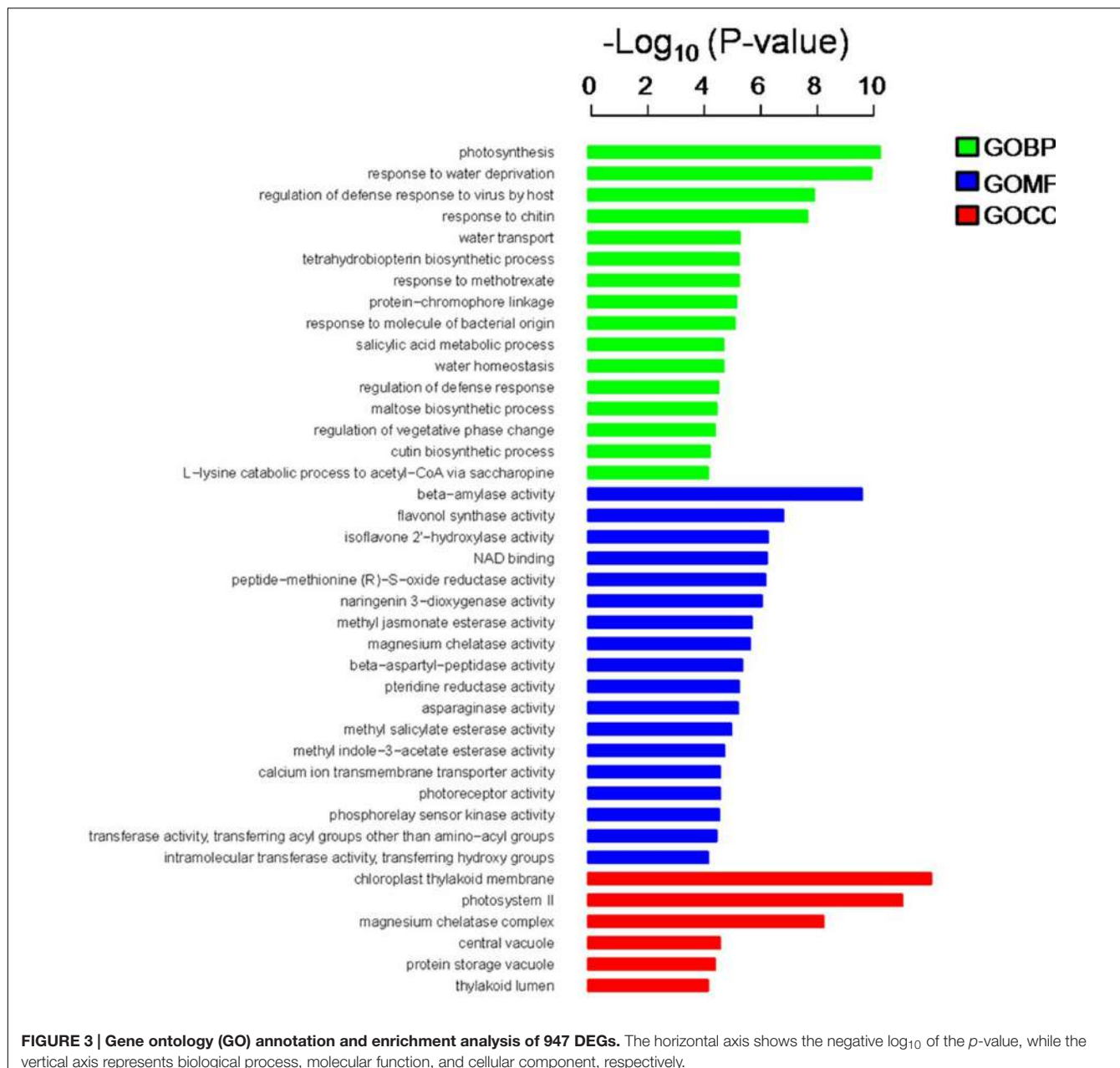


FIGURE 3 | Gene ontology (GO) annotation and enrichment analysis of 947 DEGs. The horizontal axis shows the negative log₁₀ of the p-value, while the vertical axis represents biological process, molecular function, and cellular component, respectively.

MYB 108 (LOC103961264), MYB 108-like (LOC103956865), Myb-like (LOC103959532 and LOC103957053), bHLH149 (LOC103962349), bHLH041 (LOC103944005), and bHLH35-like (LOC103939710) were downregulated in the mature fruit of ‘Red Bartlett’ while the rest of genes predicted to encode MYB and bHLH TFs were upregulated (Figure 4B). Additionally, TFs annotated as WRKY, NAC, ERF, and zinc finger family members also changed significantly in expression during fruit development in ‘Red Bartlett’ (Supplementary Table S5). Finally, seven DEGs involved in the light signal transduction pathway and photomorphogenesis were also identified. These genes were annotated as UV RESISTANCE LOCUS8 (LOC103954102 and LOC103962736), phytochrome B

(LOC103961302 and LOC103928909), Phytochrome-interacting factors 3 (LOC103955304), CONSTITUTIVELY PHOTOMORPHOGENIC 1-like (COP1) (LOC103960466) and SUPPRESSOR OF PHYA105 (SPA; LOC103965891). In ‘Red Bartlett’, the transcript level of these seven genes increased significantly at the late development stage (Supplementary Table S6).

Therefore, these results demonstrate that the color fading phenotype of ‘Red Bartlett’ was induced by anthocyanin synthesis, degradation, and transport, as well as by TF regulation. They also indicate that the light signal was involved in color fading of ‘Red Bartlett’ pears. To verify the reliability of the RNA-Seq data, 12 candidate DEGs were selected for RT-qPCR

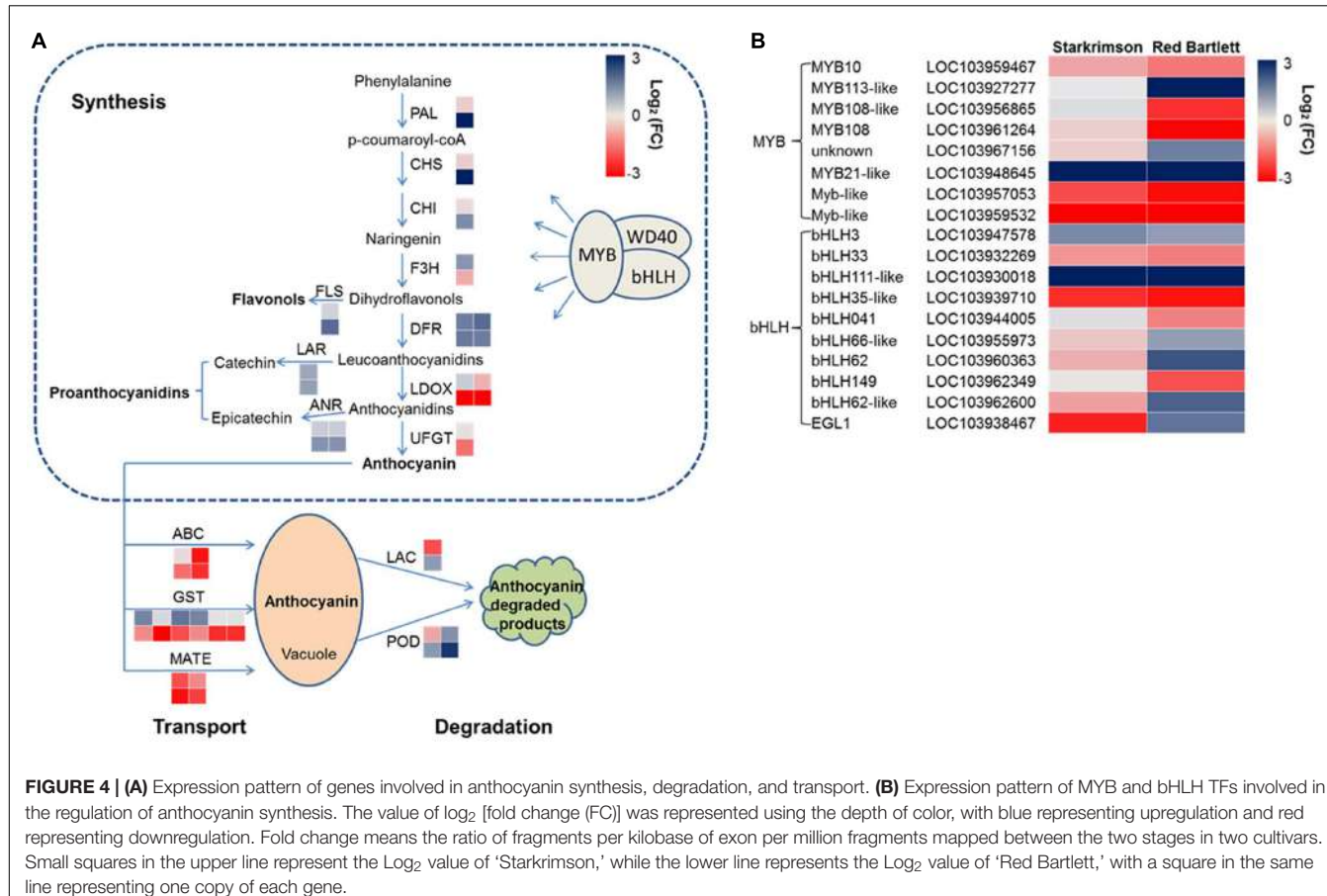


FIGURE 4 | (A) Expression pattern of genes involved in anthocyanin synthesis, degradation, and transport. **(B)** Expression pattern of MYB and bHLH TFs involved in the regulation of anthocyanin synthesis. The value of \log_2 [fold change (FC)] was represented using the depth of color, with blue representing upregulation and red representing downregulation. Fold change means the ratio of fragments per kilobase of exon per million fragments mapped between the two stages in two cultivars. Small squares in the upper line represent the \log_2 value of 'Starkrimson,' while the lower line represents the \log_2 value of 'Red Bartlett,' with a square in the same line representing one copy of each gene.

assays. The results of RT-qPCR were consistent with those of the transcriptome analysis (Supplementary Figure S3).

DISCUSSION

The Anthocyanin Content and Color Variation between 'Red Bartlett' and 'Starkrimson'

The formation of red-skinned pears is dependent on the level of anthocyanin in the fruit and its differing accumulation patterns. In some European pears, the peak of red fruit coloration appeared in the middle development stage and faded at harvest (Steyn et al., 2004). In 'Red Bartlett,' anthocyanin levels peaked at 56 DAFB before fading gradually from 63 DAFB to maturation (Wang et al., 2013). In this study, 'Red Bartlett' and 'Starkrimson' had similar pigmentation patterns and showed higher anthocyanin levels early in fruit development that then peaked in the middle of the development stage. The anthocyanin level then significantly decreased in 'Red Bartlett' fruit after 55 DAFB but did not change significantly in 'Starkrimson,' consistent with the observed changes in fruit color of 'Red Bartlett' and 'Starkrimson' during development (Figure 1). These results indicate that the color fading of fruit skin late in the development of 'Red Bartlett' pears is induced by decreasing anthocyanin levels.

DEGs Involved in the Anthocyanin Biosynthesis Pathway

Anthocyanin biosynthesis relies on the transcript levels of a series of encoding structural genes, most of which have been isolated and cloned in pear (Zhang et al., 2011; Yang et al., 2015b). In this study, transcriptome analysis showed that the expression level of two LDOX genes significantly decreased in the later stages of fruit development in 'Red Bartlett.' UFGT, a key anthocyanin biosynthesis gene, decreased in expression level at 75 DAFB in 'Red Bartlett' (Figure 4A). This gene was not one of the 947 DEGs selected for further analysis, and may not be a determinant of the color variation of the two pears. Therefore, we speculated that LDOX was closely related to color fading of 'Red Bartlett' and that UFGT was not. FLS may be involved in the flavonol pathway (Holton et al., 1994) and its expression was found here to be significantly upregulated in the later stages of 'Red Bartlett' fruit development. FLS expression levels were negatively associated with anthocyanin accumulation. These results demonstrate that the reduced anthocyanin levels in 'Red Bartlett' may be associated with decreased anthocyanin synthesis and increased FLS.

Anthocyanin biosynthesis is usually regulated by various TFs and in particular the MBW complex (Gonzalez et al., 2008). By analyzing RNA-Seq data, many genes encoding TFs were identified, including seven MYBs (Figure 4B), four of which were significantly downregulated in transcription in the

late development stage of 'Red Bartlett' while the others were upregulated. Previously, genes like MYB10 and its homolog MdMYB110a (Lee and Choo, 2013) were found to be key activators of the anthocyanin biosynthetic pathway in Rosaceae (Lin-Wang et al., 2010). In this study an MYB10 homolog (LOC103959467) showed a significant decrease in transcription from the early to late stages in 'Red Bartlett,' suggesting that MYB10 expression correlates with anthocyanin levels. However, LOC103959467 was not significantly differentially expressed between the two cultivars at 75 DAFB and, therefore, did not belong to the group of 947 redundant DEGs. This suggests that the most important factor responsible for the color fading of 'Red Bartlett' pears could not be MYB10. Transcript levels of other MYBs were significantly reduced during color fading in 'Red Bartlett' indicating a positive correlation with anthocyanin accumulation. Additionally, The co-expression of MYB10 and bHLH3 activated expression of dihydroflavonol-4-reductase and UFGT, leading to anthocyanin accumulation (Xie et al., 2012; Ravaglia et al., 2013). In our study, five bHLHs were upregulated and three were downregulated during the later development stage of 'Red Bartlett' (**Figure 4B**). Furthermore, in the late development stage of 'Red Bartlett,' expression of bHLH3 (LOC103947578) was significantly upregulated, while expression of bHLH33 (LOC103932269) was significantly downregulated. These results suggest that the bHLH family is involved in the regulation of anthocyanins synthesis by the different expression pattern.

Recently, the connections between other TFs and anthocyanin synthesis have attracted much attention. A gene encoding an NAC protein was found to be highly upregulated in blood-fleshed peach (Zhou et al., 2015). The overexpression of *zinc finger* of *Arabidopsis* 6 inhibited root growth and increased anthocyanin accumulation (Devaiah et al., 2007). In the present study, eight WRKY, nine ERF, four NAC, and nine zinc finger TFs were also screened from the 947 DEGs, with 12 found to be upregulated and 18 downregulated during the color fading stages of 'Red Bartlett' (**Supplementary Table S5**). These genes may be involved in the regulation of anthocyanin accumulation. Also, these genes point out the direction for further study on coloration of fruit.

DEGs Involved in Anthocyanin Transport and Degradation

In plants, GSTs were involved in the transfer of anthocyanins from the endoplasmic reticulum to the vacuole and were required for anthocyanin sequestration (Marrs et al., 1995; Mueller et al., 2000). Previously, GST showed a positive correlation with anthocyanin accumulation, such as TT19 (Kitamura et al., 2004). According to our results, transcription of six GST genes decreased significantly in the late development stages of 'Red Bartlett' fruit (**Figure 4A**), corresponding to the reduction in anthocyanin levels. So down-regulated GSTs may play a negative role in anthocyanin transport and led to a decrease in vacuolar anthocyanin levels. In addition, the ABC-C transporter and MATE family were also involved in the transport and accumulation of anthocyanins (Goodman et al., 2004; Gomez et al., 2011). In this study, two MATE genes

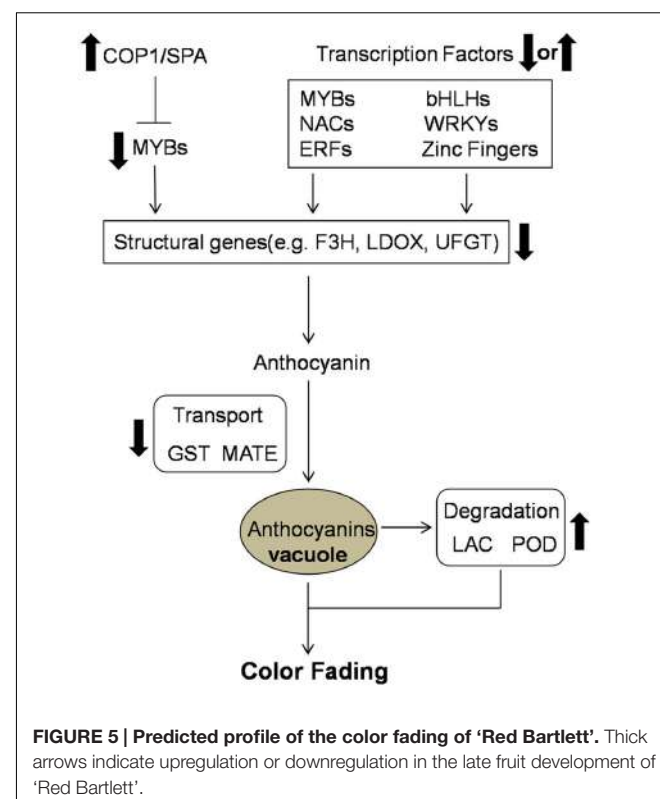


FIGURE 5 | Predicted profile of the color fading of 'Red Bartlett'. Thick arrows indicate upregulation or downregulation in the late fruit development of 'Red Bartlett'.

were significantly downregulated at the later stages of 'Red Bartlett' fruit development. These results suggest that expression of the two MATE genes correlated positively with anthocyanin accumulation. Thus, anthocyanin transport is closely linked to color fading of 'Red Bartlett' pears.

Vacuolar peroxidases, a class III peroxidase family, were more likely candidates for anthocyanin degradation in plants (Ferreres et al., 2011), with this relationship confirmed in Brunfelsia (Vaknin et al., 2005; Zipor et al., 2015). Later, an intracellular laccase, an anthocyanin degradation enzyme, was found to be responsible for epicatechin-mediated anthocyanin degradation in litchi fruit pericarp (Fang et al., 2015). In the present study, one LAC gene and two POD genes were identified among the 947 DEGs (**Figure 4A**). The expression of the three genes increased significantly at 75 DAFB in 'Red Bartlett' as the anthocyanin content of the fruit peel decreased significantly. This suggests that increased anthocyanin degradation was likely to contribute to the color fading of 'Red Bartlett' pears.

DEGs Related to Light Signal

The light signal usually activated a series of anthocyanin-associated structural and regulatory genes that control anthocyanin synthesis (Cominelli et al., 2008; Guan et al., 2015). In our study, GO annotation and KEGG pathway enrichment analysis determined that the 947 DEGs were significantly enriched in the 'Photosynthesis' and 'Circadian rhythm' pathways (**Figure 3** and **Supplementary Table S3**). In particular, the module 'Circadian rhythm' included several genes responding to light signals, such as phytochrome B,

Phytochrome-interacting factors 3, SPA, and COP1. These genes significantly increased in expression during the color fading stage of 'Red Bartlett' and negatively correlated with anthocyanin accumulation (**Supplementary Table S6**). In darkness, by the way of ubiquitination, the COP1/SPA complex was responsible for degradation of light-induced TFs involved in the regulation of anthocyanin synthesis, such as R2R3-MYBs (Zhu et al., 2008; Li et al., 2012; Maier et al., 2013). In our study, the COP1/SPA complex was upregulated significantly in the later development stage of 'Red Bartlett' pears. This results in decreased anthocyanin biosynthesis through the action of anthocyanin degrading regulatory factors and leads to a reduction in the level of anthocyanin in 'Red Bartlett.' These data suggest that the light signal may played a crucial role in the regulation of anthocyanin synthesis, confirming that the light signal was closely related to color fading in the fruit skin of 'Red Bartlett' pears.

CONCLUSION

Candidate genes involved in the color fading of 'Red Bartlett' pears were identified using transcriptome analysis. Based on our results, the color fading of 'Red Bartlett' was a complex process regulated by a series of metabolic pathways (**Figure 5**). The light signal was perceived by the light receptor and maybe involved in anthocyanin synthesis by regulating TFs. Furthermore, MYB, bHLH, WRKY, NAC, ERF, and zinc finger TFs were more likely to have a tight connection with anthocyanin accumulation. In anthocyanin transport, GST and MATE were significantly down-regulated in 75 DAFB of 'Red Bartlett,' indicating a decrease in anthocyanin accumulation in the vacuole. Finally, anthocyanin degradation enzymes

REFERENCES

- Azuma, A., Yakushiji, H., Koshita, Y., and Kobayashi, S. (2012). Flavonoid biosynthesis-related genes in grape skin are differentially regulated by temperature and light conditions. *Planta* 236, 1067–1080. doi: 10.1007/s00425-012-1650-x
- Boss, P. K., Davies, C., and Robinson, S. P. (1996). Analysis of the expression of anthocyanin pathway genes in developing *Vitis vinifera* L. cv Shiraz grape berries and the implications for pathway regulation. *Plant Physiol.* 111, 1059–1066.
- Cominelli, E., Gusmaroli, G., Allegra, D., Galbiati, M., Wade, H. K., Jenkins, G. I., et al. (2008). Expression analysis of anthocyanin regulatory genes in response to different light qualities in *Arabidopsis thaliana*. *J. Plant Physiol.* 165, 886–894. doi: 10.1016/j.jplph.2007.06.010
- Conesa, A., Götz, S., García-Gómez, J. M., Terol, J., Talón, M., and Robles, M. (2005). Blast2GO: a universal tool for annotation, visualization and analysis in functional genomics research. *Bioinformatics* 21, 3674–3676. doi: 10.1093/bioinformatics/bti610
- Cutuli, B., Lemanski, C., Fourquet, A., Lafontan, B. D., Giard, S., Lancrenon, S., et al. (1999). Environmental significance of anthocyanins in plant stress responses. *Photochem. Photobiol.* 70, 1–9. doi: 10.1111/j.1751-1097.1999.tb01944.x
- Devaiah, B. N., Karthikeyan, A. S., and Raghothama, K. G. (2007). WRKY75 transcription factor is a modulator of phosphate acquisition and root development in *Arabidopsis*. *Plant Physiol.* 143, 1789–1801. doi: 10.1104/pp.106.093971
- Dimmer, E. C., Huntley, R. P., Alam-Faruque, Y., Sawford, T., O'Donovan, C., Martin, M. J., et al. (2011). The UniProt-GO annotation database in 2011. *Nucleic Acids Res.* 40, D570–D570. doi: 10.1093/nar/gkr1048
- Elsharkawy, I., Liang, D., and Xu, K. (2015). Transcriptome analysis of an apple (*Malus × domestica*) yellow fruit somatic mutation identifies a gene network module highly associated with anthocyanin and epigenetic regulation. *J. Exp. Bot.* 47(Suppl. 1), 218–225. doi: 10.1093/jxb/erv433
- Espley, R. V., Hellens, R. P., Putterill, J., Stevenson, D. E., Kutty-Amma, S., and Allan, A. C. (2007). Red colouration in apple fruit is due to the activity of the MYB transcription factor, MdMYB10. *Plant J.* 49, 414–427. doi: 10.1111/j.1365-313X.2006.02964.x
- Fang, F., Zhang, X., Luo, H., Zhou, J., Gong, Y., Li, W., et al. (2015). An intracellular laccase is responsible for the epicatechin mediated anthocyanin degradation in litchi fruit pericarp. *Plant Physiol.* 169, 2391–2408. doi: 10.1104/pp.15.00359
- Feng, S., Sun, S., Chen, X., Wu, S., Wang, D., and Chen, X. (2015). PyMYB10 and PPyMYB10.1 interact with bHLH to enhance anthocyanin accumulation in pears. *PLoS ONE* 10:e0142112. doi: 10.1371/journal.pone.0142112
- Ferrer, F., Figueiredo, R., Bettencourt, S., Carqueijeiro, I., Oliveira, J., Gilizquierdo, A., et al. (2011). Identification of phenolic compounds in isolated vacuoles of the medicinal plant *Catharanthus roseus* and their interaction with vacuolar class III peroxidase: an H2O2 affair? *J. Exp. Bot.* 62, 2841–2854. doi: 10.1093/jxb/erq458
- Fischer, T. C., Gosch, C., Pfeiffer, J., Halbwirth, H., Halle, C., Stich, K., et al. (2007). Flavonoid genes of pear (*Pyrus communis*). *Trees* 21, 521–529. doi: 10.1007/s00468-007-0145-z

like LAC and POD might play a critical role in degrading anthocyanin.

AUTHOR CONTRIBUTIONS

ZW and LX: conceived the project; RZ and LS: carried out experiments; ZW, RZ, and HD: analyzed the data; ZW, HD, FM, LX: manuscript preparation and editing.

FUNDING

This work is supported by the National Natural Science Foundation of China (31401845, 31572086).

SUPPLEMENTARY MATERIAL

The Supplementary Material for this article can be found online at: <http://journal.frontiersin.org/article/10.3389/fpls.2017.00455/full#supplementary-material>

TABLE S1 | List of RT-qPCR primers.

TABLE S2 | Summary of 947 DEGs in RNA-Seq.

TABLE S3 | KEGG pathways of 947 DEGs in RNA-Seq.

TABLE S4 | Differentially expressed genes involved in the anthocyanin anthocyanin synthesis, degradation, and transport.

TABLE S5 | Differentially expressed genes involved in the anthocyanin regulation.

TABLE S6 | Differentially expressed genes response to light signal.

TABLE S7 | Statistics of RNA-Seq data.

- Giusti, M., and Wrolstad, R. E. (eds). (2001). "Characterization and measurement of anthocyanins by UV-visible spectroscopy," in *Current Protocols in Food Analytical Chemistry* (New York, NY: John Wiley & Sons). doi: 10.1002/0471142913.faf0102s00
- Gomez, C., Conejero, G., Torregrosa, L., Cheynier, V., Terrier, N., and Ageorges, A. (2011). In vivo grapevine anthocyanin transport involves vesicle-mediated trafficking and the contribution of anthoMATE transporters and GST. *Plant J.* 67, 960–970. doi: 10.1111/j.1365-313X.2011.04648.x
- Gomez, C., Terrier, N., Torregrosa, L., Vialet, S., Fournierlevel, A., Verriès, C., et al. (2009). Grapevine MATE-type proteins act as vacuolar H⁺-dependent acylated anthocyanin transporters. *Plant Physiol.* 150, 402–415. doi: 10.1104/ pp.109.135624
- Gonzalez, A., Zhao, M., Leavitt, J. M., and Lloyd, A. M. (2008). Regulation of the anthocyanin biosynthetic pathway by the TTG1/bHLH/Myb transcriptional complex in *Arabidopsis* seedlings. *Plant J.* 53, 814–827. doi: 10.1111/j.1365-313X.2007.03373.x
- Goodman, C. D., Casati, P., and Walbot, V. (2004). A multidrug resistance-associated protein involved in anthocyanin transport in *Zea mays*. *Plant Cell* 16, 1812–1826. doi: 10.1105/tpc.022574
- Guan, L., Dai, Z., Wu, B. H., Wu, J., Merlin, I., Hilbert, G., et al. (2015). Anthocyanin biosynthesis is differentially regulated by light in the skin and flesh of white-fleshed and teinturier grape berries. *Planta* 243, 23–41. doi: 10.1007/s00425-015-2391-4
- Holton, T. A., Brugliera, F., and Tanaka, Y. (1994). Cloning and expression of flavonol synthase from *Petunia hybrida*. *Plant J. Cell Mol. Biol.* 4, 1003–1010. doi: 10.1046/j.1365-313X.1993.04061003.x
- Honda, C., Kotoda, N., Wada, M., Kondo, S., Kobayashi, S., Soejima, J., et al. (2002). Anthocyanin biosynthetic genes are coordinately expressed during red coloration in apple skin. *Plant Physiol. Biochem.* 40, 955–962. doi: 10.1016/S0981-9428(02)01454-7
- Johnson, C. S., Kolevski, B., and Smyth, D. R. (2002). TRANSPARENT TESTA GLABRA2, a trichome and seed coat development gene of *Arabidopsis*, encodes a WRKY transcription factor. *Plant Cell* 14, 1359–1375. doi: 10.1105/tpc.001404
- Kitamura, S., Shikazono, N., and Tanaka, A. (2004). TRANSPARENT TESTA 19 is involved in the accumulation of both anthocyanins and proanthocyanidins in *Arabidopsis*. *Plant J.* 37, 104–114. doi: 10.1046/j.1365-313X.2003.01943.x
- Klein, M., Bo, B., and Martinoia, E. (2006). The multidrug resistance-associated protein (MRP/ABCC) subfamily of ATP-binding cassette transporters in plants. *FEBS Lett.* 580, 1112–1122. doi: 10.1016/j.febslet.2005.11.056
- Kobayashi, S., Ishimaru, M., Hiraoka, K., and Honda, C. (2002). Myb-related genes of the Kyoho grape (*Vitis labruscana*) regulate anthocyanin biosynthesis. *Planta* 215, 924–933. doi: 10.1007/s00425-002-0830-5
- Lee, K. C., and Choo, K. H. (2013). An ancient duplication of apple MYB transcription factors is responsible for novel red fruit-flesh phenotypes. *Plant Physiol.* 161, 225–239. doi: 10.1104/pp.112.206771
- Li, Y. Y., Mao, K., Zhao, C., Zhao, X. Y., Zhang, H. L., Shu, H. R., et al. (2012). MdCOP1 ubiquitin E3 ligases interact with MdMYB1 to regulate light-induced anthocyanin biosynthesis and red fruit coloration in apple. *Plant Physiol.* 160, 1011–1022. doi: 10.1104/pp.112.199703
- Lin-Wang, K., Bolitho, K., Grafton, K., Kortstee, A., Karunairetnam, S., Mcghee, T. K., et al. (2010). An R2R3 MYB transcription factor associated with regulation of the anthocyanin biosynthetic pathway in Rosaceae. *BMC Plant Biol.* 10:50. doi: 10.1186/1471-2229-10-50
- Maier, A., Schrader, A., Kokkelink, L., Falke, C., Welter, B., Iniesto, E., et al. (2013). Light and the E3 ubiquitin ligase COP1/SPA control the protein stability of the MYB transcription factors PAP1 and PAP2 involved in anthocyanin accumulation in *Arabidopsis*. *Plant J.* 74, 638–651. doi: 10.1111/tpj.12153
- Mao, X., Cai, T., Olyarchuk, J. G., and Wei, L. (2005). Automated genome annotation and pathway identification using the KEGG Orthology (KO) as a controlled vocabulary. *Bioinformatics* 21, 3787–3793. doi: 10.1093/bioinformatics/bti430
- Marrs, K. A., Alfenito, M. R., Lloyd, A. M., and Walbot, V. (1995). A glutathione S-transferase involved in vacuolar transfer encoded by the maize gene Bronze-2. *Nature* 375, 397–400. doi: 10.1038/375397a0
- Mueller, L. A., Goodman, C. D., Silady, R. A., and Walbot, V. (2000). AN9, a petunia glutathione S-transferase required for anthocyanin sequestration, is a flavonoid-binding protein. *Plant Physiol.* 123, 1561–1570. doi: 10.1104/pp.123.4.1561
- Oren-Shamir, M. (2009). Does anthocyanin degradation play a significant role in determining pigment concentration in plants? *Plant Sci.* 177, 310–316. doi: 10.1016/j.plantsci.2009.06.015
- Ravaglia, D., Esplay, R. V., Henry-Kirk, R. A., Andreotti, C., Ziosi, V., Hellens, R. P., et al. (2013). Transcriptional regulation of flavonoid biosynthesis in nectarine (*Prunus persica*) by a set of R2R3 MYB transcription factors. *BMC Plant Biol.* 13:53. doi: 10.1186/1471-2229-13-68
- Steyn, W. J., Holcroft, D. M., Wand, S. J. E., and Jacobs, G. (2004). Anthocyanin degradation in detached pome fruit with reference to preharvest red color loss and pigmentation patterns of blushed and fully red pears. *J. Am. Soc. Hortic. Sci.* 129, 13–19.
- Takos, A. M., Jaffé, F. W., Jacob, S. R., Bogs, J., Robinson, S. P., and Walker, A. R. (2006). Light-induced expression of a MYB gene regulates anthocyanin biosynthesis in red apples. *Plant Physiol.* 142, 1216–1232. doi: 10.1104/pp.106.088104
- Vaknin, H., Bar-Akiva, A., Ovadia, R., Nissim-Levi, A., Forer, I., Weiss, D., et al. (2005). Active anthocyanin degradation in *Brunfelsia calycina* (yesterday-tomorrow) flowers. *Planta* 222, 19–26. doi: 10.1007/s00425-005-1509-5
- Wang, Z., Meng, D., Wang, A., Li, T., Jiang, S., Cong, P., et al. (2013). The methylation of the PcMYB10 promoter is associated with green-skinned sport in Max Red Bartlett pear. *Plant Physiol.* 162, 885–896. doi: 10.1104/pp.113.214700
- Winkel-shirley, B. (2001). Flavonoid biosynthesis. A colorful model for genetics, biochemistry, cell biology, and biotechnology. *Plant Physiol.* 126, 485–493. doi: 10.1104/pp.126.2.485
- Xie, X. B., Shen, L. I., Zhang, R. F., Zhao, J., Chen, Y. C., Zhao, Q., et al. (2012). The bHLH transcription factor MdbHLH3 promotes anthocyanin accumulation and fruit colouration in response to low temperature in apples. *Plant Cell Environ.* 35, 1884–1897. doi: 10.1111/j.1365-3040.2012.02523.x
- Yang, Y., Yao, G., Yue, W., Zhang, S., and Wu, J. (2015a). Transcriptome profiling reveals differential gene expression in proanthocyanidin biosynthesis associated with red/green skin color mutant of pear (*Pyrus communis* L.). *Front. Plant Sci.* 6:795. doi: 10.3389/fpls.2015.00795
- Yang, Y., Yao, G. F., Zheng, D., Zhang, S. L., Wang, C., Zhang, M. Y., et al. (2015b). Expression differences of anthocyanin biosynthesis genes reveal regulation patterns for red pear coloration. *Plant Cell Rep.* 34, 189–198. doi: 10.1007/s00299-014-1698-0
- Zhai, R., Wang, Z., Zhang, S., Meng, G., Song, L., Wang, Z., et al. (2015). Two MYB transcription factors regulate flavonoid biosynthesis in pear fruit (*Pyrus bretschneideri* Rehd.). *J. Exp. Bot.* 67, 1275–1284. doi: 10.1093/jxb/erv524
- Zhang, X., Allan, A. C., Yi, Q., Chen, L., Li, K., Shu, Q., et al. (2011). Differential gene expression analysis of yunnan red pear, *Pyrus pyrifolia*, during fruit skin coloration. *Plant Mol. Biol. Rep.* 29, 305–314. doi: 10.1007/s11105-010-0231-z
- Zhou, H., Lin-Wang, K., Wang, H., Gu, C., Dare, A. P., Esplay, R. V., et al. (2015). Molecular genetics of blood-fleshed peach reveals activation of anthocyanin biosynthesis by NAC transcription factors. *Plant J. Cell Mol. Biol.* 82, 105–121. doi: 10.1111/tpj.12792
- Zhu, D., Maier, A., Lee, J. H., Laubinger, S., Saijo, Y., Wang, H., et al. (2008). Biochemical characterization of *Arabidopsis* complexes containing CONSTITUTIVELY PHOTOMORPHOGENIC1 and SUPPRESSOR OF PHYA proteins in light control of plant development. *Plant Cell* 20, 2307–2323. doi: 10.1105/tpc.107.056580
- Zipor, G., Duarte, P., Carqueijeiro, I., Shahar, L., Ovadia, R., Teper-Bamnolker, P., et al. (2015). *In planta* anthocyanin degradation by a vacuolar class III peroxidase in *Brunfelsia calycina* flowers. *New Phytol.* 205, 653–665. doi: 10.1111/nph.13038

Conflict of Interest Statement: The authors declare that the research was conducted in the absence of any commercial or financial relationships that could be construed as a potential conflict of interest.

Copyright © 2017 Wang, Du, Zhai, Song, Ma and Xu. This is an open-access article distributed under the terms of the Creative Commons Attribution License (CC BY). The use, distribution or reproduction in other forums is permitted, provided the original author(s) or licensor are credited and that the original publication in this journal is cited, in accordance with accepted academic practice. No use, distribution or reproduction is permitted which does not comply with these terms.



Proteomics and SSH Analyses of ALA-Promoted Fruit Coloration and Evidence for the Involvement of a MADS-Box Gene, *MdMADS1*

Xinxin Feng [†], Yuyan An [†], Jie Zheng, Miao Sun and Liangju Wang ^{*}

College of Horticulture, Nanjing Agricultural University, Nanjing, China

OPEN ACCESS

Edited by:

Maarten Hertog,
KU Leuven, Belgium

Reviewed by:

Panagiotis Kalaitzis,
Mediterranean Agronomic Institute of
Chania, Greece
Luca Espen,
University of Milan, Italy

*Correspondence:

Liangju Wang
wj@njau.edu.cn

[†]These authors have contributed
equally to this work.

Specialty section:

This article was submitted to
Crop Science and Horticulture,
a section of the journal
Frontiers in Plant Science

Received: 29 June 2016

Accepted: 12 October 2016

Published: 07 November 2016

Citation:

Feng X, An Y, Zheng J, Sun M and
Wang L (2016) Proteomics and SSH
Analyses of ALA-Promoted Fruit
Coloration and Evidence for the
Involvement of a MADS-Box Gene,
MdMADS1. *Front. Plant Sci.* 7:1615.
doi: 10.3389/fpls.2016.01615

Skin color is a key quality attribute of fruits and how to improve fruit coloration has long been a major concern. 5-Aminolevulinic acid (ALA), a natural plant growth regulator, can significantly increase anthocyanin accumulation in fruit skin and therefore effectively improve coloration of many fruits, including apple. However, the molecular mechanism how ALA stimulates anthocyanin accumulation in fruit skin remains unknown. Here, we investigated the impact of ALA on apple skin at the protein and mRNA levels. A total of 85 differentially expressed proteins in apple skins between ALA and water treatment (control) were identified by complementary gel-based and gel-free separation techniques. Most of these differentially expressed proteins were up-regulated by ALA. Function analysis suggested that 87.06% of the ALA-responsive proteins were associated with fruit ripening. To further screen ALA-responsive regulators, we constructed a subtracted cDNA library (tester: ALA treatment; driver: control) and obtained 104 differentially expressed unigenes, of which 38 unigenes were indicators for the fruit ripening-related genes. The differentially changed proteins and transcripts did not correspond well at an individual level, but showed similar regulated direction in function at the pathway level. Among the identified fruit ripening-related genes, the expression of *MdMADS1*, a developmental transcription regulator of fruit ripening, was positively correlated with expression of anthocyanin biosynthetic genes (*MdCHS*, *MdDFR*, *MdLDOX*, and *MdUFGT*) in apple skin under ALA treatment. Moreover, overexpression of *MdMADS1* enhanced anthocyanin content in transformed apple calli, which was further enhanced by ALA. The anthocyanin content in *MdMADS1*-silenced calli was less than that in the control with ALA treatment, but higher than that without ALA treatment. These results indicated that *MdMADS1* is involved in ALA-induced anthocyanin accumulation. In addition, anthocyanin-related verification in apple calli suggested that the regulation of *MdMADS1* on anthocyanin biosynthesis was partially independent of fruit ripening process. Taken together, our findings provide insight into the mechanism how ALA regulates anthocyanin accumulation and add new information on transcriptase regulators of fruit coloration.

Keywords: anthocyanin, apple, 5-aminolevulinic acid (ALA), proteomics, suppression subtractive hybridization (SSH), *MdMADS1*

INTRODUCTION

Skin color is a key quality attribute of apple fruit, and hence one of the most important factors determining apple market acceptance. Generally, well-colored red cultivars are preferred because consumers always associate the red color with some indication of fruit quality, such as maturity, nutrition, taste, and flavor. At commercial apple orchards of southern China, poor red coloration has been an important limiting factor of apple commodity value. Thus, how to promote apple fruit coloration has become a major concern.

Many attempts have been applied to improve red coloration in apple fruits. The traditional fruit production practices contain paper bagging (Ju, 1998) and covering the orchard floor with reflecting films (Meinholt et al., 2010). However, these methods demand a mass of manpower, material resources, and time, or even bring orchard pollution. By contrast, the application of plant growth substances has been proposed as an economically viable alternative. 5-Aminolevulinic acid (ALA), an essential biosynthetic precursor of tetrapyrrole molecules, acts as a new-type plant growth regulator. ALA has gained increasing attention because of its multiple physiological roles in plants, such as increasing plant resistance to various stresses, and improving plant photosynthesis (Akram and Ashraf, 2013; Murooka and Tanaka, 2014). In fruit production, ALA has been demonstrated to be effective for the promotion of fruit coloration in several fruit crops, including apple (Xie et al., 2013; Zhang L. Y. et al., 2015), peach (Guo et al., 2013), pear (Xiao et al., 2012), and litchi (Feng et al., 2015). Importantly, it was also reported that ALA significantly increased fruit interior quality (Gao et al., 2013; Zhang L. Y. et al., 2015). Furthermore, ALA is readily biodegradable and has no adverse effects on animals and humans (Perez et al., 2013). Therefore, ALA can simultaneously improve fruit coloration and fruit interior quality without any detrimental effects, suggesting great application prospect in fruit production.

Red coloration in various plant tissues is predominantly caused by anthocyanin, which accumulates as granules in the vacuole (Bae et al., 2006). This pigment belongs to the diverse group of ubiquitous secondary metabolites collectively known as flavonoids. In plants, two categories of genetic control relate to anthocyanin accumulation. One category is the biosynthetic genes that encode enzymes required for anthocyanin biosynthesis, including chalcone synthase (CHS), chalcone isomerase (CHI), flavanone-3-hydroxylase (F3H), dihydroflavonol-4-reductase (DFR), leucoanthocyanidin dioxygenase (LDOX), and UDP-glycose: flavonoid 3-O-glucosyltransferase (UFGT) (An et al., 2015). All of these six genes have been isolated in various plants and their transcription levels are positively correlated with anthocyanin concentration (Han et al., 2010; Feng et al., 2013). Another category is regulatory genes that influence the intensity and pattern of anthocyanin biosynthetic genes. In this category, most studies on the regulation of anthocyanins have focused on transcription factors of R2R3-MYB, basic helix-loop-helix (bHLH), and WD40 classes. These three regulators can form a MYB-bHLH-WD40 protein complex that binds to promoters and then induces transcription of anthocyanin biosynthetic pathway genes. In recent two decades, additional potential regulators

have also been reported in model plant *Arabidopsis thaliana* to affect anthocyanin synthesis, including PHYTOCHROME-INTERACTING FACTOR 3 (PIF3), LONG HYPOCOTYL 5 (HY5), CONSTITUTIVELY PHOTOMORPHOGENIC 1 (COP1), WRKY, WIP domain, MADS-box domain, NAC (NAM, ATAF, CUC), Jasmonate ZIM-domain (JAZ), and the SQUAMOSA promoter-binding protein-like (SPL) (Zhou et al., 2015).

Several studies have been conducted to investigate the regulatory mechanisms behind anthocyanin accumulation in apple. Conserved *MYB*, *bHLH*, and *WD40* genes in the apple that are homologs of *Arabidopsis* MYB-bHLH-WD40 protein complex have been demonstrated to be responsible for the accumulation of anthocyanins (Takos et al., 2006; An et al., 2012; Xie et al., 2012). Likewise, new regulators involved in anthocyanin biosynthesis were identified in apple fruits. For example, *MdCOP1* has been demonstrated to be involved in the ubiquitination and degradation of the *MdMYB1* protein under dark conditions (Li et al., 2012) and *MdJAZ2* has been proposed to be involved in the regulation of anthocyanin accumulation during the response of apple fruits to jasmonate (An et al., 2015). Since the regulatory mechanism modulates anthocyanin biosynthesis is highly conserved in higher plants, more research is necessary to develop the anthocyanin regulation network in apple. Research on ALA promoting anthocyanin accumulation in apple fruits has been linked to up-regulating anthocyanin biosynthetic genes and regulatory genes *MYB*, *bHLH*, and *WD40* (Xie et al., 2013). However, little information is available regarding special regulative effects of ALA on fruit skin and its regulatory mechanisms remain unknown. Current knowledge about the function of ALA on fruit is derived from research on some physiological aspects of fruit growth and ripening. Therefore, an overall molecular framework is needed for better understanding the ALA-associated fruit coloration.

Proteomic and transcriptomic techniques are often used to investigate the molecular mechanisms involved in complex traits. To make a comprehensive understanding of ALA-stimulated fruit coloration, integrated proteomic, and transcriptomic techniques were employed in this study. We identified and analyzed ALA-induced various changes at protein and mRNA levels using gel-free and two-dimensional gel electrophoresis (2-DE) gel-based proteomic techniques and suppression subtractive hybridization (SSH). Based on the results of proteomics and SSH, a candidate biomarker *MdMADS1* was selected to explore the molecular mechanism underlying ALA-induced anthocyanin accumulation. Our data offers new molecular evidence elucidating the regulatory mechanism of fruit coloration by ALA, and provides a valuable reference for further research on anthocyanin accumulation in apple fruits.

MATERIALS AND METHODS

Fruit Source and Apple Flesh Calli Induction

Fruits were collected from apple (*Malus × domestica* Borkh. cv. Fuji) trees at commercial apple orchards of eastern China, Fengxian County in Jiangsu Province. All fruits were bagged

with paper-bags in late May, debagged in early October, and the fruits were commercially harvested in late October. In this study, the debagged fruits which were collected from eight trees were harvested in early October (at onset of fruit coloration) and immediately transported to the laboratory for two different treatments. Solutions containing 0.01% Tween-20 alone (control), or with 200 mg/L ALA (treatment) were sprayed to the surface of debagged fruits. The fruits were then transferred into growth chamber with $150 \mu\text{mol m}^{-2} \text{s}^{-1}$ photon flux density (PFD) at 22°C and sampled at 0, 6, 12, 24, 36, 48, and 72 h of light exposure. At each of the sampling points, skins from 15 different fruits were collected and divided randomly into two groups. One group of skin samples was used for measurements of anthocyanin content, and the other was stored at -80°C for RNA and protein isolation after being frozen in liquid nitrogen. Since the time course of anthocyanin accumulation in apple skin showed that the promotion of ALA on anthocyanin accumulation initiated after 24 h light irradiation (See the "Results"), to identify the early upstream regulators of anthocyanin biosynthesis induced by ALA, we chose skins of apples that exposed to light for 24 h for the proteomics and SSH analysis.

Calli from "Fuji" fruit flesh were induced on Murashige and Skoog medium containing 1 mg/L 6-benzylaminopurine (BAP) and 1 mg/L 2,4-dichlorophenoxyacetic acid (2,4-D) at 25°C in the dark, and subcultured at 14-day intervals. For ALA treatment, the calli were transferred to medium containing 100 mg/L ALA. To induce anthocyanin accumulation, transgenic calli were cultured in a culture room under $100 \mu\text{mol m}^{-2} \text{s}^{-1}$ PFD at 25°C for 4 days, and then collected for determination of anthocyanin content and RNA isolation.

Measurement of Anthocyanin Content

Anthocyanin content was extracted using 1% (v/v) HCl-methanol for 24 h at room temperature in the dark. The extracts were centrifuged at 15,000 g for 15 min, and the absorbance at 530 nm was then measured with a spectrophotometer. The amount of anthocyanin was expressed as nmol of cyanidin-3-galactoside per g of the sample using a molar extinction coefficient of 3.43×10^4 (Ubi et al., 2006). Mean values were obtained from five independent replicates.

Proteomic Analysis by 2-DE

Protein extraction of apple skin was performed using phenol-based method (Deytieux et al., 2007). The final pellet was dissolved in a solution containing 7 M urea, 2 M thiourea, 4% (w/v) 3-[3-cholamidopropyl] dimethylammonio]-1-propanesulfonate (CHAPS), 1% (w/v) dithiothreitol (DTT), and 0.5% (v/v) immobilized pH gradient (IPG) buffer (pH 4–7; GE Healthcare, USA). The protein concentration was quantified according to the method suggested by Bradford (1976), using bovine serum albumin as standard.

For 2-DE, protein samples (1 mg) were brought to 450 μL of isoelectric focusing (IEF) rehydration solution (7 M urea, 2 M thiourea, 4% (w/v) CHAPS, 1% (w/v) DTT, 0.5% (v/v) IPG buffer, and 0.01% bromophenol blue). The whole volume was transferred into a well of the Immobiline DryStrip Reswelling Tray and IPG strips (24 cm, pH 4–7; GE Healthcare) were rehydrated

overnight at 20°C. The strips were then loaded onto an Ettan IPGphor 3 instrument (GE Healthcare), and IEF was performed according to the following steps: 100 V for 1 h, 500 V for 1 h, followed by 8 h gradient from 1000 to 10000 V, and finally focused for 65,000 Vh at 10,000 V. The maximum current per strip was set at 50 μA. After two-step equilibration, the IPG strips were loaded on a 12% w/v sodium dodecyl sulfate-polyacrylamide gel electrophoresis (SDS-PAGE) gels using the Ettan Daltsix system (GE Healthcare). The gels were run at 150 V until the dye front reached the bottom of the gel. The gels were visualized using the Coomassie Brilliant Blue G-250 stain and scanned using Image Scanner software (GE Healthcare). Afterward, gel images were processed using the PDQuest 2-DE analysis software (Version 8.0.1, Bio-Rad, USA) in a three-step manner: spot detection, volumetric quantification, and matching. Differences in protein content were analyzed using a *t*-test and calculated as the fold ratio in three biological replicates with two technical replicates. A threshold of $P < 0.05$ and fold change of >1.5 or <0.67 was used to identify significant differentially expressed protein spots.

Spots from 2-DE were excised from the gel and digested with trypsin. Then, samples were re-suspended with 5 μL 0.1% TFA followed by mixing in 1:1 ratio with a matrix consisting of a saturated solution of α-cyano-4-hydroxy-trans-cinnamic acid in 50% ACN containing 0.1% TFA. One microliter mixture was spotted on a stainless steel sample target plate. Peptide mass spectrometry (MS) and MS/MS were performed on an ABI 5800 MALDI-TOF/TOF Plus mass spectrometer (Applied Biosystems, USA). Data were acquired in the positive MS reflector using a CalMix5 standard to calibrate the instrument (ABI5800 Calibration Mixture). Both the MS and MS/MS data were integrated and processed using GPS Explorer V3.6 software (Applied Biosystems, USA) with default parameters. Based on the combined MS and MS/MS spectra, proteins were successfully identified based on 95% or higher confidence interval of their scores in MASCOT V2.3 search engine (Matrix Science Ltd, London, U.K.), using the following search parameters: the apple expressed sequence tag (EST) database (32,768 entries, Jan. 14th 2014) downloaded from the Genome Database for Rosaceae (GDR) (https://www.rosaceae.org/species/malus/malus_x_domestica/genome_v1.0); trypsin as the digestion enzyme; one missed cleavage site; fixed modifications of Carbamidomethyl (C); partial modifications of Acetyl (Protein N-term), Deamidated (NQ), Dioxidation (W), Oxidation (M); 100 ppm for precursor ion tolerance, and 0.5 Da for fragment ion tolerance.

The functional annotation of the identified proteins was based on UniProt, GDR, NCBI protein database, and the literature.

Proteomic Analysis by Label-Free

For shotgun analysis, apple skin proteins (100 μg) dissolved in 6 M urea and 50 mM Tris-HCl (pH 8.0) were reduced by added 1 M DTT until at final concentration of 4 mM for 1 h at 60°C, and then added with 1 M iodoacetamide until at a final concentration of 25 mM for 45 min at 25°C in the dark. The 6 M urea was removed by ultrafiltration in case it influenced digestion. Proteins were dissolved in 50 mM NH₄HCO₃ (pH 7.8) and then treated with trypsin (2 μg,

Promega, USA) at 37°C for 12 h. Finally, protein desalting using a C18 column (Empore) and freeze-dried before sample injection.

A liquid chromatography-MS (LC-MS) system consisting of a Dionex Ultimate 3000 nano-LC system (nano UHPLC, Sunnyvale, CA, USA), connected to a linear quadrupole ion trap Orbitrap (LTQ Orbitrap XL) mass spectrometer (Thermo Electron, Bremen, Germany), and equipped with a nanoelectrospray ion source. For LC separation, an Acclaim PepMap 100 column (C18, 3 μm, 100 Å) (Dionex, Sunnyvale, CA, USA) capillary with a 15 cm bed length was used with a flow rate of 300 nL/min. Two solvents, A (0.1% formic acid) and B (aqueous 80% acetonitrile in 0.08% formic acid), were used to elute the peptides from the nanocolumn. The gradient went from 5 to 40% B in 32 min and from 40 to 95% B in 1 min, with a total run time of 60 min. The mass spectrometer was operated in the data-dependent mode so as to automatically switch between Orbitrap-MS and LTQ-MS/MS acquisition. Electrospray voltage and the temperature of the ion transfer capillary were 2.2 kV and 200°C, respectively. Survey full scan MS spectra (from m/z 350 to 1800) were acquired in the Orbitrap with a resolution $r = 60,000$ at m/z 400, allowing the sequential isolation of the top ten signal intensity ions for collision-induced dissociation at a collision energy of 35 V. A dynamic exclusion mode was enabled to exclude the previously selected ions during the repeated cycle of 60 s. The external mass calibration of the Orbitrap was performed once every 3 days to ensure a working mass accuracy < 5 ppm. For each run, 1.5 μg of the digest was injected on a reverse-phase C18 column.

The obtained MS/MS spectra were searched against the apple EST database using SEQUEST algorithm in Proteome Discoverer 1.3 software (Thermo Scientific, San Jose, CA, USA). Search results were filtered for a False Discovery rate of 1% employing a decoy search strategy utilizing a reverse database.

For quantitative proteome analysis, four MS raw files from each group were analyzed using SIEVE software (Version 2.0, Thermo Scientific, USA). Eight MS raw files were performed the SIEVE experimental workflow of “two sample differential analysis,” where ALA-treated samples were compared to control samples. For the alignment step, the chromatographic peaks detected by Orbitrap were aligned by their retention time (\pm 2.5 min) and mass (\pm 0.02 unit) among all sample runs. After alignment, the feature detection and integration (or framing) process were performed using the MS level data with a feature called “Frames from MS2 Scans” only. The parameters consisted of a frame m/z width of 10 ppm and a retention time width of 2.5 min. Then, the peak integration was performed for each frame and these values were used for statistical analysis. Next, peptide sequences obtained from the database search were imported into SIEVE. A frame filter rule which was defined as “PRRoot > 0 and GoodID > 0 and CV_ALA treatment < 25 and CV_control < 25” was applied to obtain confident overall protein ratio. Peptides were grouped into proteins and a protein ratio and P-value were calculated. Only proteins observed in all two groups were quantified. The quantified proteins were considered as significantly different expressed proteins if they matched at least

two peptides, and changed over 1.5-fold cutoff (ratio above 1.5 or below 1/1.5) with P -value < 0.05.

Suppression Subtractive Hybridization (SSH)

Total RNA was isolated from apple skins by CTAB-LiCl methods (Jaakola et al., 2001). Isolation of poly A⁺ RNA from total RNA was performed by PolyATtract mRNA Isolation Systems Kit (Promega, USA) according to the manufacturer's instructions. The integrity of RNA was ascertained by electrophoresis on 1% agarose gel. The concentration of total RNA and poly A⁺ RNA was measured by Nanodrop 2000 spectrophotometer (Thermo Scientific, USA).

The SSH library was carried out using the PCR-Select™ cDNA Subtraction Kit (Clontech, USA) according to the manufacturer's instructions, starting with 2 μg poly A⁺ RNA from the tester (ALA) and driver (control) samples. After checking subtraction efficiency, subtracted second PCR products were cloned into the pMD-19T vector (Takara, Dalian, China) and then transformed into Trans1-T1 phage resistant chemically competent cells (TransGen Biotech, China). Subsequently, white colonies from Luria-Bertani (LB) solid medium plates containing ampicillin, 5-bromo-4-chloro-3-indolyl-β-D-galacto-pyranoside (X-Gal), and isopropyl-β-D-1-thiogalactopyranoside (IPTG) were selected for colony polymerase chain reaction (PCR). The PCR amplification used the primer set of Nested PCR primer 1 and Nested PCR primer 2R provided along the SSH kit. Then, clones which PCR products were single inserts and longer than 100 bp insertion fragment size were sequenced with the universal M13 sequencing primer. After removing vector and adaptor sequences from the raw EST sequences, the resulting ESTs were assembled into unigenes using iAssembler (Zheng et al., 2011). Annotation and function analysis of the resulting unigenes were compared against the apple EST database.

Transfection of Apple Fruit Calli by Agroinfiltration

In order to overexpress *MdMADS1* (Accession No. U78947), the open reading frame was amplified by PCR from cDNA of Fuji apple fruits skin with primers *MdMADS1(OE)-F* and *MdMADS1(OE)-R* (Supplementary Table S1), followed by ligation to the linearized plant transformation vector pBI121 based on homologous recombination method using the NovoRec® PCR Seamless Cloning Kit (Novoprotein Scientific Inc, China).

To silence *MdMADS1*, a 259 base pair (bp) fragment including 58 bp sequence homologous to the RNA-interference (RNAi) vector pHELLSGATE2 and 201 bp of *MdMADS1* coding sequence was amplified by RT-PCR using primers *MdMADS1(i)-F* and *MdMADS1(i)-R* (Supplementary Table S1). Amplified fragments were transferred to the RNAi vector through Gateway BP reaction generating RNAi construct in which the sense and antisense *MdMADS1* RNA sequences would be linked in tandem separated by the PDK intron.

The resulting recombinant plasmids and empty plasmids were transformed into *Agrobacterium* strain EHA105. One single

separated colony containing the target gene was grown at 28°C in LB broth supplemented with appropriate antibiotics. When the optical density at 600 nm (OD600) of the culture liquid reached approximately 0.5, *Agrobacterium* cells were harvested and resuspended in a modified MacConkey agar (MMA) medium (Murashige and Shoog salts, 10 mM morpholine ethane sulphonate acid pH 5.6, 20 g/L sucrose). The fresh calli were soaked into the *Agrobacterium* solution for 15 min. The calli were co-cultured on Murashige and Skoog medium containing 1 mg/L 2, 4-D and 1 mg/L BAP for 2 d at 25°C in the dark. Subsequently, the calli were washed 5 times with sterile water and transferred to MS medium supplemented with 250 mg/L of carbenicillin and 30 mg/L kanamycin for transgenic selection.

Quantitative Real-Time Reverse Transcription-PCR

The cDNA synthesis was performed using the PrimeScript First-Strand cDNA Synthesis Kit (TaKaRa Bio, China). Quantitative real-time reverse transcription-PCR (qRT-PCR) was performed with SYBR® Premix Ex Taq™ (TaKaRa Bio, China) as described by the manufacturer's instructions. Using specific primers (Supplementary Table S1), the transcript levels were calculated using the $2^{-\Delta\Delta CT}$ method (Livak and Schmittgen, 2001), where *MdACTIN* gene was used as an internal reference. In this study, the relative expression levels of corresponding genes were presented as values relative to corresponding indicated samples. Data were derived from 3 independent replicates.

Statistical Analysis

All data were obtained from at least three independent experiments. Statistical and correlation analysis was performed using SPSS statistical computer package (version 19.0 SPSS Inc. Chicago, IL). Data was compared with the control or among treatments by analysis of variance (ANOVA) to discriminate significant differences at $P < 0.05$ followed by least significant difference tests (LSD).

RESULTS

ALA Promoted Anthocyanin Accumulation in the Skin of Debagged Apple Fruits

To confirm the effect of ALA on apple fruit coloration and provide more detailed information on this process, we investigated the time course of anthocyanin accumulation in apple skin after ALA treatment. Results showed that ALA treatment notably promoted fruit coloration within 72 h of light irradiation (Figure 1A). Anthocyanin determination showed that ALA did not stimulate anthocyanin accumulation within 24 h, but significantly increased anthocyanin content after 24 h, compared with the control (Figure 1B). Anthocyanin content in ALA-treated apple skin was about 23, 50, and 45%, respectively, higher than that in control at 36, 48, and 72 h. These results indicated that ALA-induced upstream regulatory factors of anthocyanin accumulation probably function before 36 h. Therefore, to identify the early upstream regulators of anthocyanin biosynthesis induced by ALA, skins of apples that

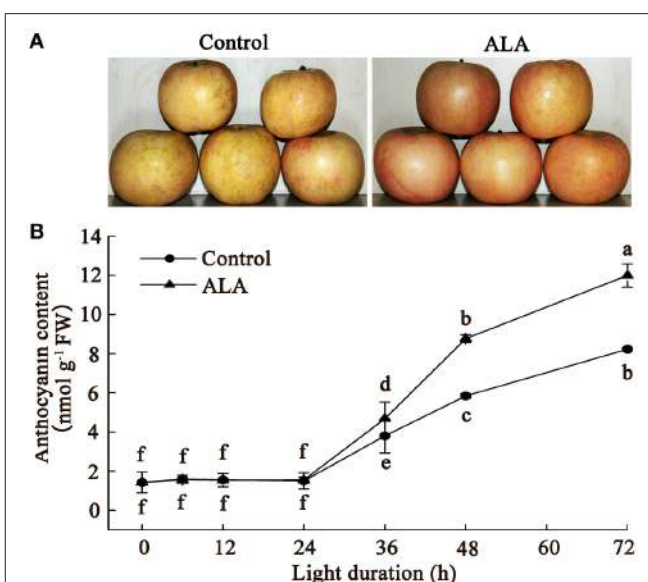


FIGURE 1 | ALA induces anthocyanin accumulation in apple skin. The bagged fruits from Fuji apple trees were collected in early October and immediately transported to the laboratory for 200 mg/L ALA treatment and water treatment (control). Then, fruits coloration was induced in a growth chamber with $150 \mu\text{mol m}^{-2} \text{ s}^{-1}$ photon flux density at 22°C. (A) A photo displays the color difference between ALA treatment and the control in apple skin at 72 h light duration. (B) Time courses of anthocyanin accumulation after ALA application. The different small letters represent significant differences at $P = 0.05$ level.

exposed to light for 24 h were used for the following proteomics and SSH analysis.

Protein Identification Using Gel-Based and Gel-Free Proteomics

To explore the mechanism how ALA regulated anthocyanin accumulation, we measured changes in the abundance of proteins and compared them between control and ALA-treated fruit skin using 2-DE gel-based proteomics. Analysis of the 2-DE pattern revealed that nearly 500 resolved spots were detected after ignoring very faint spots and spots with undefined shapes and areas (Figure 2). To analyze ALA-responsive proteins, the changes in spot intensity between ALA-treated and control were quantified by PDQuest software. Quantitative analysis of spot intensity by integration of the staining signal for each gel revealed that levels of 57 proteins changed in an ALA-dependent manner (ratio > 1.5 or ratio < 0.67) in three independent replications. Using MALDI-TOF/TOF MS/MS, 56 protein spots representing 50 differently expressed proteins were then successfully identified according to the GDR database (Supplementary Table S2).

To obtain a more comprehensive understanding of proteins affected by ALA, we further performed label-free shotgun proteomics of apple skin. Data acquired by nano-ESI-MS/MS on a Q-Exactive spectrometer were processed with SIEVE software to reveal up- or down-regulated proteins by ALA. A total of four runs per group were analyzed and the quality of the alignment of

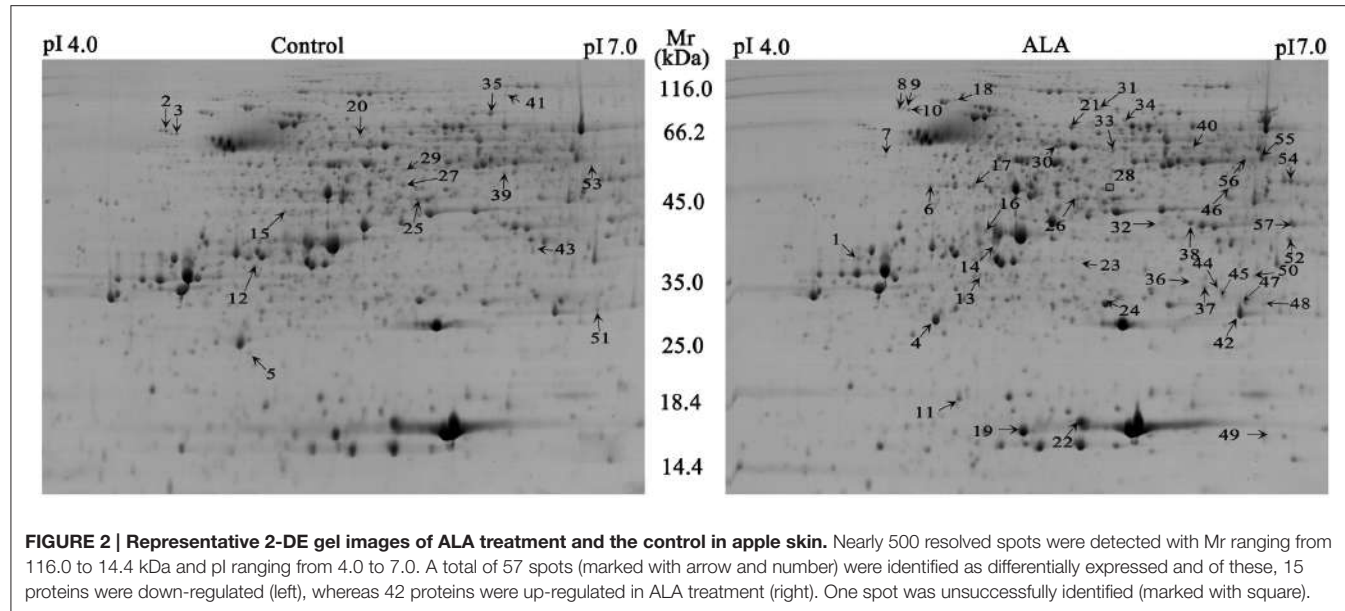


FIGURE 2 | Representative 2-DE gel images of ALA treatment and the control in apple skin. Nearly 500 resolved spots were detected with Mr ranging from 116.0 to 14.4 kDa and pI ranging from 4.0 to 7.0. A total of 57 spots (marked with arrow and number) were identified as differentially expressed and of these, 15 proteins were down-regulated (left), whereas 42 proteins were up-regulated in ALA treatment (right). One spot was unsuccessfully identified (marked with square).

the chromatographic peaks between ALA treatment group and control group was high (Supplementary Figure S1). Significant differences in protein abundance were considered with a ratio of ALA-treated/control higher than 1.5 or lower than 0.67 ($P < 0.05$). As a result, a total of 47 proteins were identified (Supplementary Table S3).

The identified proteins by gel-based and gel-free proteomics were further categorized into different classes (Figure 3A), where the 50 proteins identified using gel-based proteomics were mainly involved in stress response and defense, carbohydrate metabolism and energy, amino acid metabolism, nucleotide metabolism, lipid metabolism, nucleotide metabolism, and secondary metabolism. Similarly, the 47 proteins identified using gel-free proteomics were predominantly related to stress response and defense, carbohydrate metabolism and energy, amino acid metabolism and secondary metabolism.

Combined the results of gel-based and gel-free proteomics, a total of 85 differently expressed proteins were identified (Table 1, Figure 3B). Among these proteins, 72.82% of changed proteins were up-regulated by ALA, and 12 proteins were commonly identified by the two proteomics techniques (Supplementary Table S4). Moreover, among the total ALA-responsive proteins, about 87.06% of changed proteins are related to orthologous fruit ripening associated genes (Figure 3C), indicating that ALA might increase anthocyanin accumulation by regulating fruit ripening process.

Screening of ALA-Induced Genes from Apple Skins by Suppression Subtractive Hybridization

To further determine how ALA stimulates fruit coloration, a forward SSH library was constructed with mRNA isolated from ALA-treated to water-treated (control) apple peel (Figure 4A). Subtraction was performed between ALA-treated cDNA (tester) and the control cDNA (driver). Positive clones were selected for

sequencing, and the vector and other uninformative sequences were removed. A total of 125 ESTs were successfully sequenced and identified in the apple database and then these ESTs were further assembled into 104 unigenes (Supplementary Table S5). The unigenes present in the forward SSH library were classified into 13 major functional groups, using information from various sources (Figure 4B). Among that, 10 out of 12 functional groups (not including unknown category) were regulated at both protein and mRNA levels. Genes involved in structural component and transcription factor were only detected at mRNA levels. In addition, 1-aminocyclopropane-1-carboxylate oxidase 1 (MDP0000195885), abscisic acid stress ripening protein (MDP0000253074), universal stress protein (MDP0000452572), glutamine amidotransferase-like class I superfamily protein (MDP0000668552), and an uncharacterized protein (MDP0000170439), were detected at both mRNA and protein levels.

Thirty-eight unigenes have been reported to be relevant to fruit ripening (Table 2). The largest category, consisting of 9 genes, was associated with stress response and defense, such as major allergen Mal d 1, a universal stress protein, acidic endochitinase, and dehydrin family protein. Eleven genes were predicted to be associated with primary metabolism, including amino acid metabolism, carbohydrate metabolism and energy, lipid metabolism. Four genes were predicted to be associated with protein synthesis and degradation. In secondary metabolism group, two pigments biosynthesis genes (phytoene dehydrogenase and UFGT) and two aroma production gene (α -farnesene synthase and farnesyl pyrophosphate synthase) were identified. Among the differentially expressed genes, five genes associated with hormonal metabolism and signal transduction. Interestingly, a transcription factor *MADS1*, also referred to as *MADS8* and *SEPALLATA1* (Ireland et al., 2013) was identified from the SSH libraries, which accounted for ripening-related genes.

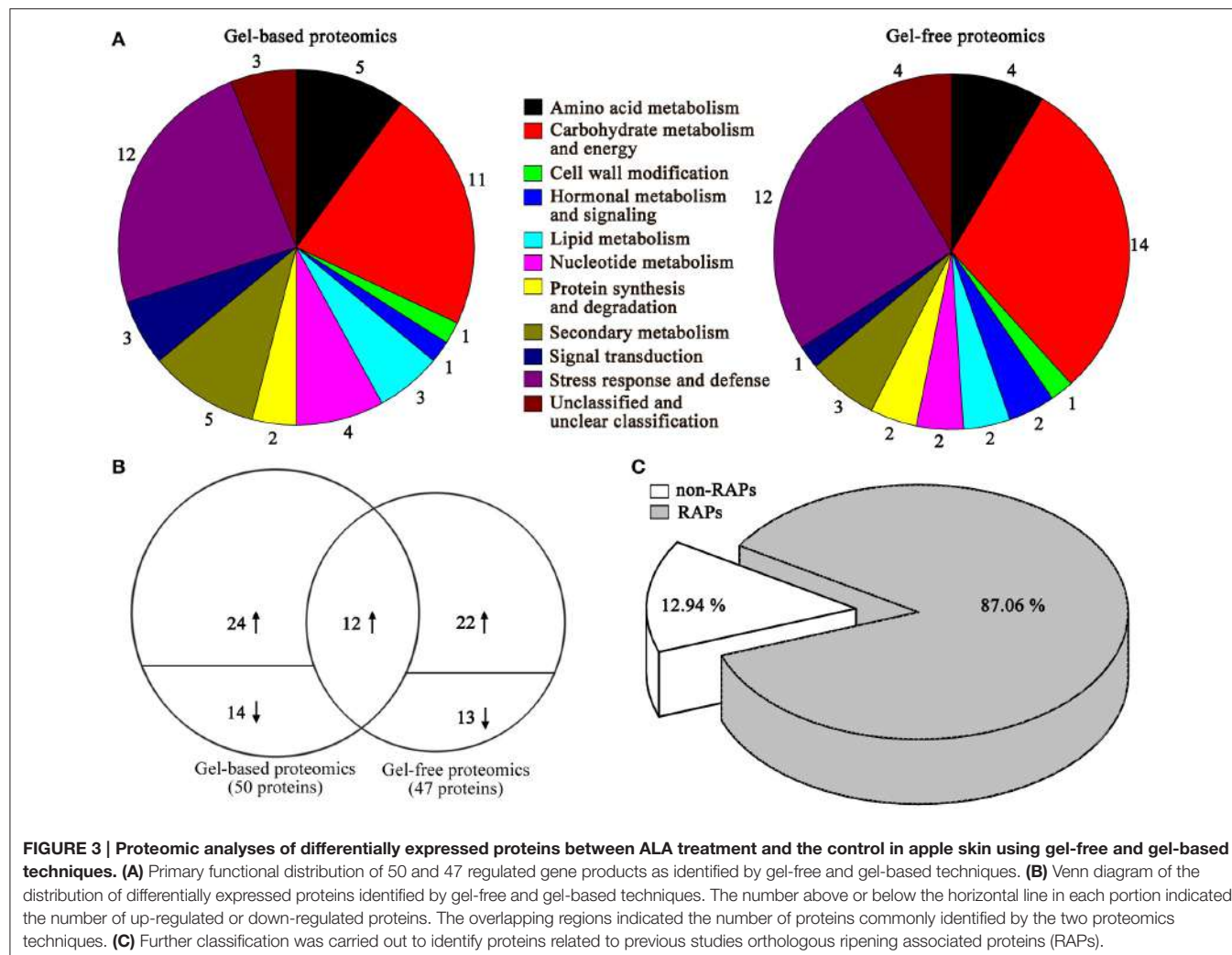


FIGURE 3 | Proteomic analyses of differentially expressed proteins between ALA treatment and the control in apple skin using gel-free and gel-based techniques. (A) Primary functional distribution of 50 and 47 regulated gene products as identified by gel-free and gel-based techniques. **(B)** Venn diagram of the distribution of differentially expressed proteins identified by gel-free and gel-based techniques. The number above or below the horizontal line in each portion indicated the number of up-regulated or down-regulated proteins. The overlapping regions indicated the number of proteins commonly identified by the two proteomics techniques. **(C)** Further classification was carried out to identify proteins related to previous studies orthologous ripening associated proteins (RAPs).

***MdMADS1* Expression Is Positively Correlated with Anthocyanin Biosynthesis-Related Genes in ALA Treatment**

The above results indicated that ALA-induced anthocyanin accumulation was probably associated with its regulation of fruit ripening process. Recently, *MdMADS1* was reported to be involved in regulation of apple fruit ripening and *MdMADS1*-antisense lines showed inhibited fruit coloration (Ireland et al., 2013). Therefore, we speculated that the up-regulation of *MdMADS1* expression might play an important role in ALA-induced anthocyanin accumulation. We confirmed by qRT-PCR that ALA indeed enhanced the expression of *MdMADS1* at 12, 24, and 48 h of light irradiation (Figure 5), but decreased it at 72 h. These results indicated that *MdMADS1* was induced by ALA application.

To show the potential role of *MdMADS1* in ALA-induced anthocyanin accumulation, we simultaneously measured the expression of anthocyanin biosynthetic genes (*MdCHS*, *MdCHI*, *MdF3H*, *MdDFR*, *MdLDOX*, and *MdUFGT*) in response to ALA and investigated the relationship between the expression

of *MdMADS1* and anthocyanin biosynthetic genes. We found that the expression of *MdMADS1* showed similar changing pattern to that of anthocyanin biosynthetic genes (*MdCHS*, *MdDFR*, *MdLDOX*, and *MdUFGT*) at different light duration (Figure 5). Correlation analysis further showed that the expression of *MdMADS1* was significantly positively correlated with anthocyanin biosynthetic genes, except *MdCHI* and *MdF3H* (Table 3). These results suggested a positive role of *MdMADS1* in ALA-induced improvement of anthocyanin biosynthesis in apple skin.

***MdMADS1* Is Involved in Anthocyanin Regulation in Apple Calli**

Callus was a reliable material for anthocyanin-related research (Lalusin et al., 2006; Xie et al., 2012; An et al., 2015). To confirm the role of *MdMADS1* in ALA-induced anthocyanin accumulation, the gene was overexpressed and silenced in apple fruit calli, respectively. In overexpression lines (OE), the expression of *MdMADS1* was significantly increased compared with the corresponding empty plasmids control [control(OE)],

TABLE 1 | Differently expressed proteins obtained by 2-DE and label-free analysis in ALA-treated apple skin.

No.	Regulated ^a	Accession No.	Annotation	Method	Ripening associated references
AMINO ACID METABOLISM					
1	-	MDP0000663130	Acireductone dioxygenase	2-DE	n/a
2	-	MDP0000806502	4-hydroxyphenylpyruvate dioxygenase	2-DE	Apple (Zhang Z. et al., 2015)
3	-	MDP0000188304	Aminoacylase-1	2-DE	Grape (Fraige et al., 2014)
4	+	MDP0000301987	Ketol-acid reductoisomerase	2-DE	Peach (Prinsi et al., 2011)
5	+	MDP0000148984	Methylthioribose kinase	2-DE	Tomato (Kushad et al., 1985)
6	+	MDP0000668552	Glutamine amidotransferase-like Class I superfamily protein	label-free	n/a
7	-	MDP0000284588	Glutamate decarboxylase	label-free	Tomato (Gallego et al., 1995) Citrus (Liu et al., 2014)
8	-	MDP0000239328	Methylmalonate-semialdehyde dehydrogenase	label-free	Apple (Zhang Z. et al., 2015)
9	-	MDP0000147916	Serine acetyltransferase	label-free	n/a
CARBOHYDRATE METABOLISM AND ENERGY					
10	+	MDP0000234480	Transaldolase	2-DE	Kiwifruit (Minas et al., 2012)
11	+	MDP0000147610	F-type ATPases	2-DE label-free	Apricot (D'Ambrosio et al., 2013) Grape (Giribaldi et al., 2007; Martínez-Esteso et al., 2013)
12	+	MDP0000769597	Pyruvate dehydrogenase E1 subunit-β	2-DE	Date palm (Marondedze et al., 2014)
13	+	MDP0000316685	Transaldolase	2-DE	Kiwifruit (Minas et al., 2012)
14	+	MDP0000248012	Vacuolar proton pump subunit A	2-DE	Papaya (Huerta-Ocampo et al., 2012) Grape (Giribaldi et al., 2007; Martínez-Esteso et al., 2013)
15	+	MDP0000300513	Vacuolar proton ATPase subunit C	2-DE	Grape (Giribaldi et al., 2007; Martínez-Esteso et al., 2013; Fraige et al., 2014)
16	+	MDP0000198482	Glyceraldehyde-3-phosphate dehydrogenase	2-DE	Apple (Zheng et al., 2013)
17	+	MDP0000249227	Soluble inorganic pyrophosphatase	2-DE label-free	Apricot (D'Ambrosio et al., 2013) Grape (Martínez-Esteso et al., 2013)
18	+	MDP0000755275	Aldose 1-epimerase	2-DE	Grape (Martínez-Esteso et al., 2013)
19	+	MDP0000273688	Fructose-bisphosphate aldolase	2-DE label-free	Kiwifruit (Minas et al., 2012) Grape (Martínez-Esteso et al., 2013; Fraige et al., 2014)
20	+	MDP0000179036	Enolase	2-DE	Kiwifruit (Minas et al., 2012) Grape (Negri et al., 2008; Martínez-Esteso et al., 2013)
21	+	MDP0000297664	Putative mitochondrial 2-oxoglutarate/malate carrier protein	label-free	n/a
22	+	MDP0000298613	Ubiquinol-cytochrome c reductase complex 14 kDa protein	label-free	n/a
23	+	MDP0000442105	LYR family of Fe/S cluster biogenesis protein	label-free	n/a
24	+	MDP0000321341	Pyrophosphate: fructose 6-phosphate 1-phosphotransferase	label-free	Tomato (Wong et al., 1990)
25	+	MDP0000796883	Adenine nucleotide translocator	label-free	Tomato (Kumar et al., 2015)
26	+	MDP0000217005	Transketolase	label-free	Kiwifruit (Minas et al., 2012)
27	+	MDP0000527995	Glyceraldehyde-3-phosphate dehydrogenase	label-free	Apple (Zheng et al., 2013)
28	-	MDP0000153379	L-arabinokinase	label-free	n/a
29	-	MDP0000183725	Pyruvate kinase	label-free	Apple and tomato (Janssen et al., 2008)
30	-	MDP0000597996	Ribulose-1,5-bisphosphate carboxylase	label-free	Apple (Zheng et al., 2013)
31	-	MDP0000268037	NADP-dependent malic enzyme	label-free	Apple (Shi et al., 2014)
CELL WALL MODIFICATION					
32	+	MDP0000416548	β-Galactosidase	2-DE	Apple (Shi et al., 2014)
33	+	MDP0000269483	Xyloglucan endotransglucosylase/hydrolase protein 6	label-free	Grape (Negri et al., 2008)
HORMONAL METABOLISM AND SIGNALING					
34	+	MDP0000195885	1-aminocyclopropane-1-carboxylate oxidase 1	2-DE label-free	Apple (Shi et al., 2014)
35	+	MDP0000219737	Ethylene receptor 2	label-free	Apple (Li and Yuan, 2008)
LIPID METABOLISM					
36	+	MDP0000333058	Acetyl-CoA carboxyltransferase β-subunit	2-DE	n/a
37	-	MDP0000764262	3,4-dihydroxy-2-butanone kinase	2-DE	n/a

(Continued)

TABLE 1 | Continued

No.	Regulated ^a	Accession No.	Annotation	Method	Ripening associated references
38	–	MDP0000300217	Phospholipase D alpha	2-DE	Strawberry (Yuan et al., 2006)
39	–	MDP0000450991	Lipoxygenase	label-free	Tomato (Qin et al., 2012)
40	+	MDP0000940078	Plant lipid transfer protein	label-free	Apple and tomato (Janssen et al., 2008)
NUCLEOTIDE METABOLISM					
41	+	MDP0000121897	Adenine phosphoribosyltransferase	2-DE label-free	Apple (Shi et al., 2014)
42	–	MDP0000225318	Adenosine kinase	2-DE	Grape (Negri et al., 2008)
43	+	MDP0000322880	Nucleoside diphosphate kinase	2-DE label-free	Kiwifruit (Minas et al., 2012) Papaya (Huerta-Ocampo et al., 2012)
44	–	MDP0000165865	Uridine 5'-monophosphate synthase	2-DE	n/a
PROTEIN SYNTHESIS AND DEGRADATION					
45	–	MDP0000146975	Glycyl-tRNA synthetase 1	2-DE	n/a
46	–	MDP000014145	Proteasome subunit β type-7	2-DE	Apple (Shi et al., 2014)
47	–	MDP0000256937	40S ribosomal protein S3-3-like	label-free	Apple (Zhang Z. et al., 2015)
48	–	MDP0000616695	60S ribosomal protein L11 isoform X1	label-free	Tomato (Kumar et al., 2015)
SECONDARY METABOLISM					
49	+	MDP0000609966	Polyphenol oxidase	2-DE label-free	Apricot (D'Ambrosio et al., 2013) Grape (Negri et al., 2008; Fraige et al., 2014)
50	+	MDP000052862	UDP-glucose: anthocyanidin 3-O-glucosyltransferase	2-DE label-free	Apricot (D'Ambrosio et al., 2013) Tomato (Kumar et al., 2015)
51	+	MDP0000221498	Polyphenol oxidase	2-DE	Apricot (D'Ambrosio et al., 2013) Grape (Negri et al., 2008; Fraige et al., 2014)
52	–	MDP0000269612	Cinnamoyl-CoA reductase	2-DE	n/a
53	+	MDP0000699845	Polyphenol oxidase	2-DE	Apricot (D'Ambrosio et al., 2013) Grape (Negri et al., 2008; Fraige et al., 2014)
54	+	MDP0000615956	4-coumarate-CoA ligase	label-free	Apple (Zhang Z. et al., 2015)
SIGNAL TRANSDUCTION					
55	+	MDP0000270640	14-3-3 protein 7-like	2-DE	Apple (Shi et al., 2014)
56	+	MDP0000376563	Protein phosphatase 2c-like protein	2-DE	Citrus (Wu et al., 2014)
57	+	MDP0000166687	14-3-3 protein	2-DE	Apple (Shi et al., 2014)
58	+	MDP0000325949	14-3-3 protein family	label-free	Apple (Shi et al., 2014)
STRESS RESPONSE AND DEFENSE					
59	+	MDP0000298502	Heat shock protein 70	2-DE	Kiwifruit (Minas et al., 2012) Papaya (Huerta-Ocampo et al., 2012; Nogueira et al., 2012)
60	+	MDP0000416706	Heat shock protein 70	2-DE	Kiwifruit (Minas et al., 2012) Papaya (Huerta-Ocampo et al., 2012; Nogueira et al., 2012)
61	+	MDP0000303430	Heat shock protein 90	2-DE	Apricot (D'Ambrosio et al., 2013) Grape (Negri et al., 2008)
62	+	MDP0000246775	Thaumatin-like protein 1a	2-DE label-free	Apple (Shi et al., 2014)
63	+	MDP0000277802	MLP-like protein 329	2-DE label-free	Apple (Shi et al., 2014)
64	+	MDP0000103621	Major allergen mal d 1	2-DE	Apple (Shi et al., 2014)
65	+	MDP0000199034	L-ascorbate peroxidase	2-DE label-free	Apple (Shi et al., 2014)
66	+	MDP0000248823	L-aascorbate peroxidase 6	2-DE	Apple (Shi et al., 2014)
67	–	MDP0000287459	Aldo/keto reductase	2-DE	Papaya (Huerta-Ocampo et al., 2012) Grape (Martínez-Esteso et al., 2013)
68	+	MDP0000096349	Glutathione S-transferase	2-DE label-free	Apple (Shi et al., 2014)
69	+	MDP0000868045	Abscisic acid response protein	2-DE	Apple (Shi et al., 2014)
70	+	MDP0000261821	Monodehydroascorbate reductase	2-DE	Tomato (Kumar et al., 2015)
71	+	MDP0000519575	Peroxiredoxin	label-free	Apple (Zhang Z. et al., 2015)
72	+	MDP0000913598	Glutathione peroxidase	label-free	Apricot (D'Ambrosio et al., 2013) Tomato (Qin et al., 2012)
73	+	MDP0000320612	Peroxiredoxin	label-free	Apple (Shi et al., 2014)
74	+	MDP0000253074	Abscisic acid stress ripening protein homolog	label-free	Apple (Shi et al., 2014)
75	+	MDP0000280265	Acidic endochitinase	label-free	Apricot (D'Ambrosio et al., 2013)

(Continued)

TABLE 1 | Continued

No.	Regulated ^a	Accession No.	Annotation	Method	Ripening associated references
76	+	MDP0000452572	Universal stress protein	label-free	Apple (Shi et al., 2014)
77	+	MDP0000288293	Major allergen Pru ar 1	label-free	Apple (Shi et al., 2014)
78	-	MDP0000770493	Dehydrin-like protein	label-free	Peach (Prinsi et al., 2011)
UNCLASSIFIED AND UNCLEAR CLASSIFICATION					
79	-	MDP0000201559	Plasma membrane-associated cation-binding protein 1-like isoform 2	2-DE	n/a
80	-	MDP0000296243	NAD(P)-binding Rossmann-fold superfamily protein	2-DE	n/a
81	-	MDP0000170439	Uncharacterized protein	2-DE	n/a
82	-	MDP0000543784	Uncharacterized protein	label-free	n/a
83	+	MDP0000279955	Uncharacterized protein	label-free	n/a
84	+	MDP0000251031	Uncharacterized protein	label-free	n/a
85	-	MDP0000250284	Uncharacterized protein	label-free	n/a

^aProteins were up-regulated (+) or down-regulated (-) in ALA-treated apple skin compared to control.

The detailed information on the fold ratio (ALA/control) and P-value were exhibited in Supplementary Tables S2 and S3.

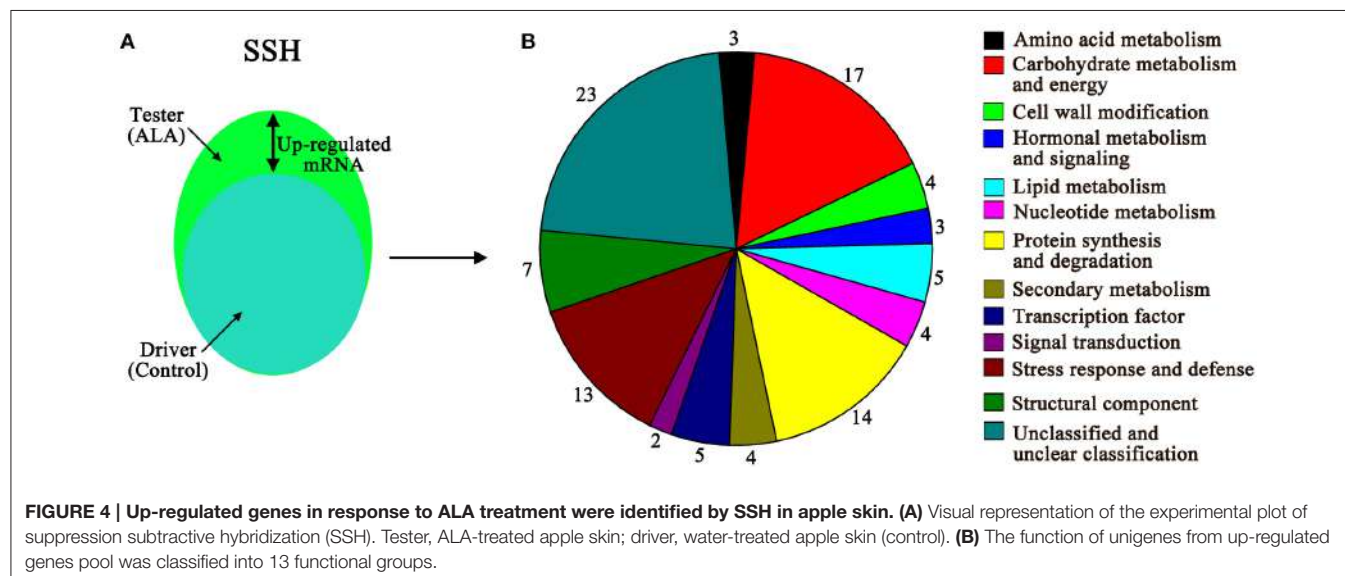


FIGURE 4 | Up-regulated genes in response to ALA treatment were identified by SSH in apple skin. (A) Visual representation of the experimental plot of suppression subtractive hybridization (SSH). Tester, ALA-treated apple skin; driver, water-treated apple skin (control). **(B)** The function of unigenes from up-regulated genes pool was classified into 13 functional groups.

and in the silenced lines (RNAi), the expression was drastically reduced compared with the corresponding empty plasmids control [control(i)] (**Figure 6A**). Under light condition, the appearance revealed that OE calli looked redder in color than the control and RNAi calli (**Figure 6B**), suggesting that *MdMADS1* overexpression increased anthocyanin accumulation. Spectrophotometric analysis further confirmed that OE calli contained significantly higher content of anthocyanin than the control and RNAi calli (**Figure 6C**), suggesting that *MdMADS1* play a positive role in anthocyanin accumulation. The expression of the anthocyanin biosynthetic genes were significantly up-regulated and down-regulated in OE and RNAi calli than the control (**Figures 6D,E**), respectively, indicating that *MdMADS1* regulates anthocyanin accumulation by modulating expression of anthocyanin biosynthesis-related genes.

To determine whether *MdMADS1* functioned in ALA-induced anthocyanin accumulation, we compared the anthocyanin content in transgenic calli which were treated with or without ALA. In **Figure 6B**, results showed that OE calli looked redder and accumulated the markedly higher level of anthocyanin after ALA treatment; ALA-treated RNAi calli were less red than ALA-treated control but much redder than the control without ALA. Spectrophotometric assay showed that ALA significantly promoted the anthocyanin accumulation in OE and RNAi calli (**Figure 6C**). In addition, we found that the expression levels of anthocyanin biosynthetic genes were higher in OE calli with ALA treatment than that in control(OE) calli with ALA treatment and OE calli, except *MdLDOX* (**Figure 6D**). Interestingly, ALA reversed the expression levels of three anthocyanin biosynthetic genes (*MdF3H*, *MdLDOX*, and *MdUFGT*) in RNAi transgenic calli (**Figure 6E**). These

TABLE 2 | Selected fruit ripening-related genes differentially expressed in ALA-treated apple skin.

Unigene No.	Accession No.	Annotation	Ripening associated references
AMINO ACID METABOLISM			
UN070	MDP0000621545	Acetolactate synthase	Citrus (Burns et al., 1999)
CARBOHYDRATE METABOLISM AND ENERGY			
UN042	MDP0000196182	NADH dehydrogenase [ubiquinone] iron-sulfur protein 6, mitochondrial	Apple (Janssen et al., 2008)
UN062	MDP0000789873	Glycoside hydrolase	Tomato (Kumar et al., 2015)
UN068	MDP0000253390	Phosphoenolpyruvate carboxylase-related kinase 2	Banana (Law and Plaxton, 1997)
UN076	MDP0000164592	NADH dehydrogenase [ubiquinone] iron-sulfur protein 8	Apple (Janssen et al., 2008)
UN088	MDP0000925483	Transaldolase	Kiwifruit (Minas et al., 2012)
UN092	MDP0000267248	6-Phosphofructokinase	Banana (Turner and Plaxton, 2003)
LIPID METABOLISM			
UN005	MDP0000251991	Lipid transport superfamily protein	Apple (Janssen et al., 2008)
UN057	MDP0000262512	lipases; hydrolases, acting on ester bonds	Apple (Sunchung et al., 2006)
UN101	MDP0000305778	Acyl-CoA-binding protein 6	Apple (Sunchung et al., 2006)
CELL WALL MODIFICATION			
UN013	MDP0000184228	Pectinesterase-like	Apple (Zhang Z. et al., 2015)
UN014	MDP0000236092	COBRA-like protein 10	Tomato (Cao et al., 2012)
UN020	MDP0000127542	β -Galactosidase	Apple (Zhang Z. et al., 2015)
UN055	MDP0000570395	Glucan endo-1,3- β -glucosidase	Apple (Zhang Z. et al., 2015)
UN079	MDP0000130449	Cytochrome P450 monooxygenase	Apple (Zhang Z. et al., 2015)
HORMONAL METABOLISM AND SIGNALING			
UN044	MDP0000171041	S-Adenosylmethionine decarboxylase	Peach (Bregoli et al., 2002)
UN054	MDP0000231245	Probable indole-3-acetic acid-amido synthetase GH3.6	Apple (Schaffer et al., 2013)
UN095	MDP0000195885	1-Aminocyclopropane-1-carboxylate oxidase 1	Apple (Shi et al., 2014)
SECONDARY METABOLISM			
UN007	MDP0000170162	UDP-glucose: anthocyanidin 3-O-glucosyltransferase	Apricot (D'Ambrosio et al., 2013) Tomato (Kumar et al., 2015)
UN056	MDP0000148978	Phytoene dehydrogenase	Tomato (Kumar et al., 2015)
UN043	MDP0000199152	α -Farnesene synthase	Apple (Ju and Curry, 2000)
UN096	MDP0000198736	Farnesy pyrophosphate synthase	Apple (Ju and Curry, 2000)
PROTEIN SYNTHESIS AND DEGRADATION			
UN028	MDP0000294774	Proteasome subunit β type 2A	Apple (Shi et al., 2014)
UN071	MDP0000263908	40S ribosomal protein S27	Apple (Zhang Z. et al., 2015)
UN082	MDP0000674266	40s ribosomal protein S25	Apple (Zhang Z. et al., 2015)
UN085	MDP0000222113	Ubiquitin-protein ligase 10/12	Tomato (Kumar et al., 2015)
SIGNAL TRANSDUCTION			
UN060	MDP0000258968	Probable protein phosphatase 2C 60	Citrus (Wu et al., 2014)
UN089	MDP0000325949	14-3-3 protein family	Apple (Shi et al., 2014)
STRESS RESPONSE AND DEFENSE			
UN001	MDP0000864747	Major allergen mal d 1	Apple (Shi et al., 2014)
UN022	MDP0000770493	Dehydrin family	Tomato (Weiss and Egea-Cortines, 2009)
UN027	MDP0000940313	Acidic endochitinase	Banana (Liu et al., 2012)
UN037	MDP0000452572	Universal stress protein A-like protein	Apple (Shi et al., 2014)
UN039	MDP0000942516	Major allergen mal d 1	Apple (Shi et al., 2014)
UN040	MDP0000295542	Major allergen Mal d 1	Apple (Shi et al., 2014)
UN069	MDP0000153123	Metallothionein-like protein	Strawberry (Aguilar et al., 1997)
UN077	MDP0000103627	Major allergen Mal d 1	Apple (Shi et al., 2014)
UN093	MDP0000253074	Abscisic acid stress ripening protein homolog	Apple (Shi et al., 2014)
TRANSCRIPTION FACTOR			
UN038	MDP0000366022	MADS1	Apple (Ireland et al., 2013)

results indicated that *MdMADS1* was involved in ALA-induced anthocyanin accumulation, but the latter was not completely dependent on the former.

DISCUSSION

ALA has shown to be effective in promoting fruit coloration, yield and quality, so that it has great application potential in horticulture. However, little information is available on regulatory mechanisms behind ALA-induced fruit coloration. Here, two proteomic techniques and SSH were employed to identify the early responses of apple skin coloration to ALA treatment at protein and mRNA levels.

The difference in pretreatment, depth of proteome coverage, analyses of isoforms and quantification statistical power often result in poor correspondence between the proteins identified by different proteomic techniques (Scherp et al., 2011). For example, Yin et al. (2014) found only 9 of 115 in soybean root tips were commonly detected by gel-based and gel-free proteomics under flooding stress. Majeran et al. (2005) reported

that among the 125 chloroplast proteins quantified in the three methods (2-DE, ICAT, and label-free), only 20 proteins were quantified in common. Moreover, the SDS-PAGE-based and gel-free-based proteomic techniques were combined to explore the molecular mechanism responsible for low silk production, a total of 17 of 174 changed proteins were common between the two techniques (Wang et al., 2014). Similarly, here, we identified 85 changed proteins using gel-based and gel-free techniques, among which only 12 proteins were commonly identified by two methods. Although most of the proteins were not identified simultaneously by different proteomic techniques, they showed similar altered trends in biological function (Figure 3A, Yin et al., 2014). Our data together with the above previous studies indicate that utilization of different proteomic approaches can lead to a more comprehensive proteome profiling, providing complementary information and hence a better understanding of the mechanisms.

Only five ALA-responsive genes were identified at both protein and mRNA levels, indicating that the expression levels of individual proteins were not strictly correlated with the up-regulated transcripts. Similar results have been reported in several previous studies (Lan et al., 2012; Arcondéguy et al., 2013; Wang et al., 2014). The regulation of mRNA synthesis, the post-transcriptional regulation of mRNA splicing and supervision mechanism, and the post-translational modification of the mRNA translated product can all result in altered protein levels (Arcondéguy et al., 2013). In addition, the different expression time course between mRNA and proteins also can lead to the divergence of mRNA and protein expression levels (Lan et al., 2012; Wang et al., 2014). Although the differentially changed proteins and transcripts did not correspond well at an individual level, the pathway analysis showed that proteome and transcriptome in the present study were well-matched. A total of 10 out of 12 transcriptome-involved pathways were found in the proteome-involved pathways, suggesting that the changed direction of proteins and transcripts were coordinated. Therefore, the proteomics and SSH techniques were mutually complementary and verified in this study, and provide valuable information on mechanisms involved in ALA-regulated apple skin.

Higher levels of anthocyanins are closely related to higher expression of anthocyanin biosynthetic genes. Previous studies have reported that exogenous ALA up-regulated the expression level of key genes in the pathway of anthocyanin biosynthesis (Xie et al., 2013; Feng et al., 2015). At protein level, a 4-coumarate-CoA ligase (No. 54 in Table 1), which catalyses the

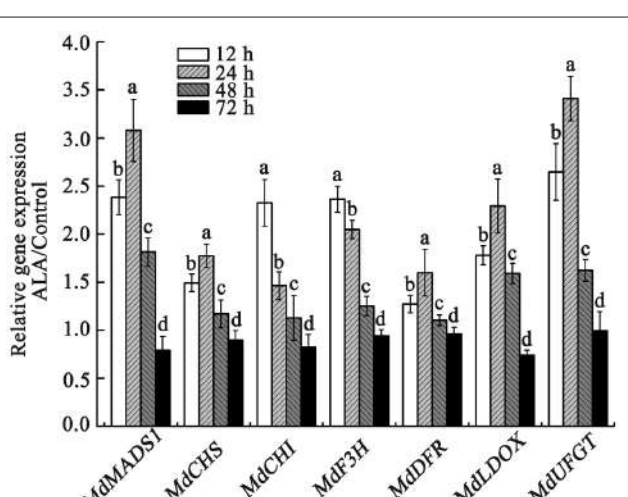


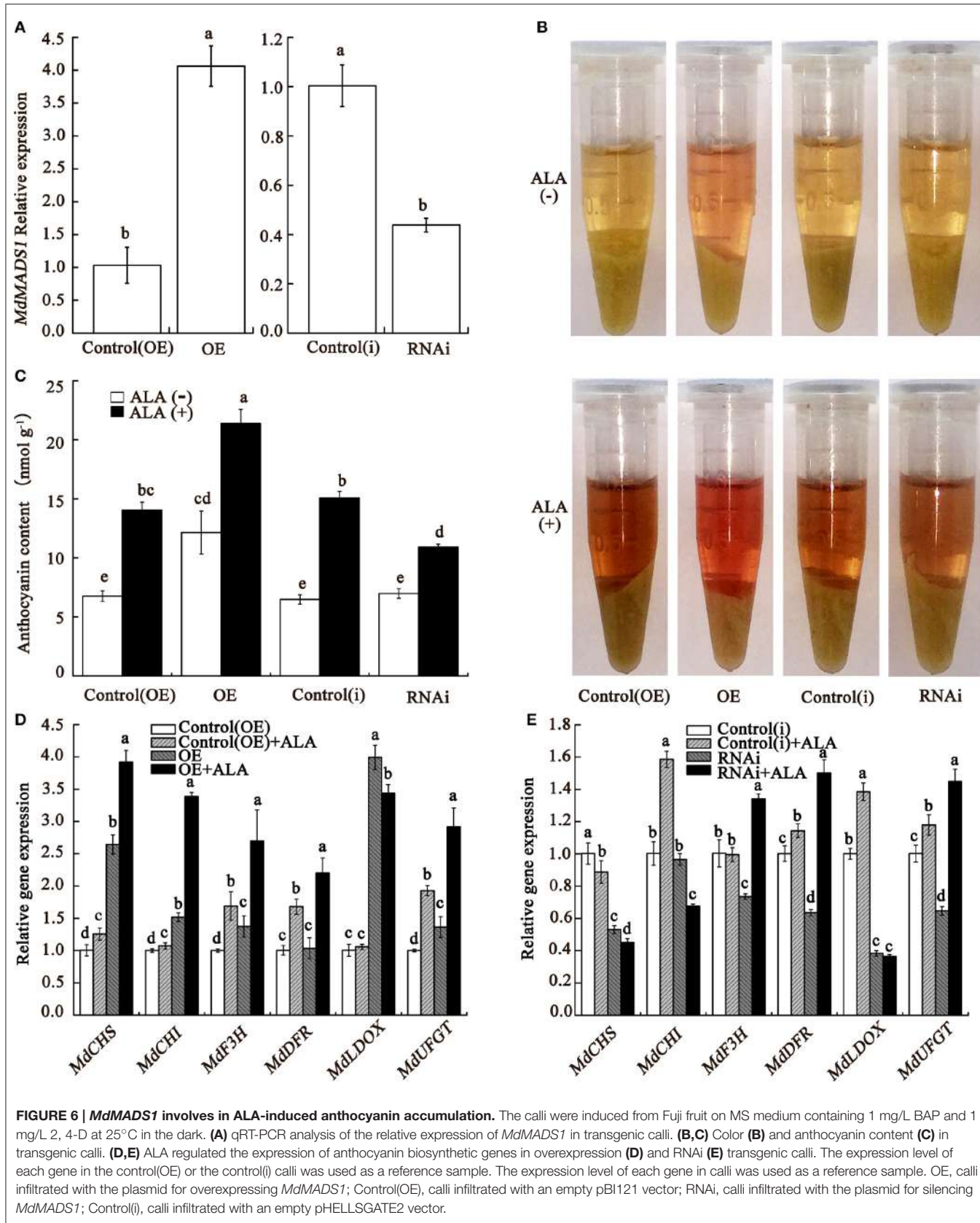
FIGURE 5 | qRT-PCR analysis of the expression of *MdMADS1* and anthocyanin biosynthetic genes in apple skin under ALA treatment. The relative expression of *MdMADS1* and anthocyanin biosynthetic genes (*MdCHS*, *MdCHI*, *MdF3H*, *MdDFR*, *MdLDOX*, *MdUFGT*) were simultaneously analyzed in apple skin with ALA treatment at 12, 24, 48, and 72 h light duration. The expression level of each gene in control was used as a reference sample at each time point.

TABLE 3 | Correlations between the relative expressions of *MdMADS1* and anthocyanin biosynthetic genes under ALA treatment.

	<i>MdCHS</i>	<i>MdCHI</i>	<i>MdF3H</i>	<i>MdDFR</i>	<i>MdLDOX</i>	<i>MdUFGT</i>
<i>MdMADS1</i>	Pearson correlation	0.98*	0.62	0.85	0.96*	0.99**
	Significance (2-tailed)	0.02	0.38	0.15	0.04	0.00
	N	4	4	4	4	4

*Correlation is significant at the 0.05 level (2-tailed).

**Correlation is significant at the 0.01 level (2-tailed).



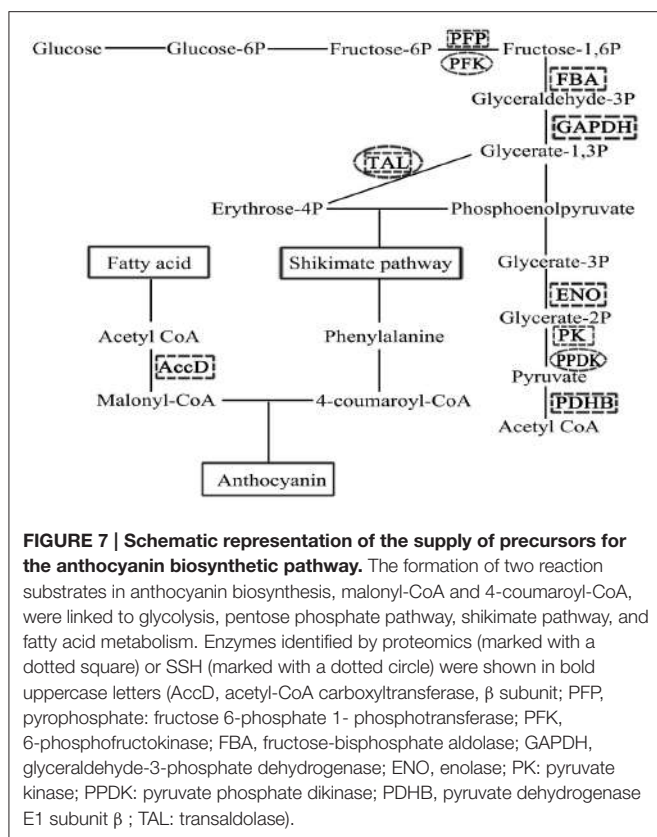
last step of the phenylpropanoid pathway leading to either lignins or flavonoids (Dixon et al., 2002), was induced by ALA treatment. UFGT is the last enzyme in anthocyanin biosynthetic pathway and has widely been considered as the key enzyme determining apple coloration (Li et al., 2002; Kim et al., 2003). Ju et al. (1995) found that anthocyanin biosynthesis in apple peel was most strongly correlated with UFGT activity. Here, the expression levels of UFGT (No. 50 in **Table 1** and UN007 in **Table 2**) were up-regulated at both transcript and protein level under ALA treatment. These results indicate that up-regulation of biosynthetic genes contributes greatly to ALA-promoted anthocyanin accumulation. Except up-regulation of anthocyanin biosynthetic genes, ALA also repressed cinnamoyl-CoA reductase (No. 52 in **Table 1**) at protein level in the lignin biosynthetic pathway. Ludwig et al. (2013) reported that there was a competition between lignin and anthocyanin biosynthetic pathways for their common precursors. These results indicate that ALA helps divert the metabolic flux from lignin to anthocyanin pathway, which also contribute to the anthocyanin accumulation. Our results add new evidence supporting the positive regulation of ALA on anthocyanin accumulation.

ALA, as a potential plant growth regulator, is known to be effective in improving plant tolerance to various stresses (Akram and Ashraf, 2013). In this study, ALA alters the expression of numerous genes at mRNA and protein levels associated with various biological processes in apple skin. One of the outstanding abundant classes is protein and genes involved in stress response, indicating the positive role of ALA in defense response of apple skin to stresses. Anthocyanin itself, is a secondary metabolite which shows antioxidant activity (Alessio et al., 2011), and plays essential roles in ameliorating environmental stresses, such as UV-B radiation, drought, and cold temperatures (Chalker-Scott, 1999). In the red-fleshed apples, a recent study suggested that anthocyanin was both associated with the red coloration and the stress tolerance (Wang et al., 2015). Here, the effects of ALA on apple skin included anthocyanin accumulation as well as a stress response. Thus, it is reasonable to speculate that ALA might promote anthocyanins accumulation, participating in stress resistance of apple skin.

Another more abundant functional class in ALA treatment is related to primary metabolites involved in the metabolism of amino acid, sugar, and fatty acid. Li et al. (2014) found that the differences between anthocyanin concentrations in the pear peel of green "Anjou" and its bud mutation "Red Anjou" were accompanied with up-regulated of sorbitol metabolism and altered amino acid metabolism in the peel of "Red Anjou." It is demonstrated that the manipulation of primary metabolism can change the production of secondary metabolites (Henkes et al., 2001; Dauwe et al., 2007). In this study, change of primary metabolism in apple skin under ALA treatment indicates that they may be crucial at the initial stage of ALA-induced anthocyanin accumulation. Therefore, we attempted to capture the potential links between primary metabolism and anthocyanin accumulation in ALA treatment (**Figure 7**). The first key step of the anthocyanin biosynthesis, catalyzed by chalcone synthase, involves two reaction substrates malonyl-CoA

and 4-coumaroyl-CoA (Winkel-Shirley, 2001). In plants, the formation of malonyl-CoA from the carboxylation of acetyl-CoA in fatty acid chain elongation pathway is catalyzed by acetyl-CoA carboxylase, which is an ATP-dependent biotinylated protein complex (Sasaki and Nagano, 2014). The β subunit of this protein (No. 36 in **Table 1**) was identified here, and it appears positively regulated by ALA. Another substrate 4-coumaroyl-CoA is converted by phenylalanine. The formation of phenylalanine in shikimate pathway is connected to two intermediate metabolites, phosphoenolpyruvate of glycolysis pathway and erythrose 4-phosphate of the pentose phosphate pathway in carbohydrate metabolism (Tzin and Galili, 2010). Here, we found that genes related to glycolysis, such as pyrophosphate: fructose 6-phosphate 1-phosphotransferase (No. 24), glyceraldehyde-3-phosphate dehydrogenase (No. 16 and 27), enolase (No. 20), fructose-bisphosphate aldolase (No. 19), pyruvate kinase (No. 29), and pyruvate dehydrogenase E1 subunit β (No. 12) were regulated and at protein level (**Table 1**) while 6-phosphofructokinase (UN092) and pyruvate phosphate dikinase (UN016) was up-regulated at mRNA level (**Table 2**) under ALA treatment. Moreover, plastidial and cytosolic enolase, respectively, have specific functions in metabolism (Voll et al., 2009). In the present study, the subcellular locations of enolase was predicted using an online tool Plant-mPLoc (<http://www.csbio.sjtu.edu.cn/bioinf/plant/>. Chou and Shen, 2010), suggesting that glycolytic enzyme is a cytosolic protein. This data supported the suggestion that, cytosolic enolase plays a central role to modulate the synthesis of aromatic amino acids and secondary phenylpropanoid compounds, even in the absence of a complete glycolysis pathway in the plastids (Voll et al., 2009; Eremina et al., 2015; Negri et al., 2015). Therefore, our results suggest that carbon flux into anthocyanin biosynthesis is activated by ALA during fruit coloration period. Transaldolase links the pentose phosphate pathway to glycosis and it was up-regulated by ALA at both protein and mRNA levels (No. 10, 13, 26 in **Table 1** and UN088 in **Table 2**). The high expression level of this gene could result in an accumulation of erythrose 4-phosphate. These results together indicate that the promotion of ALA-induced anthocyanin synthesis may also be associated with an ALA-enhanced supply of precursors from primary metabolism to secondary metabolism.

It is well-documented that the expression of genes related to stress responses, primary and secondary metabolism, cell wall metabolism, and hormonal metabolism contribute to fruit ripening process (Shi et al., 2014; Kumar et al., 2015). Previous studies have suggested that ALA enhanced fruit maturation with a promotion of many ripening-related biological events (Watanabe et al., 2006). However, to date, there is little evidence elucidating the molecular mechanism how ALA regulates fruit ripening. In this study, about 85% of changed proteins and 38% of up-regulated mRNA in ALA-treated apple skin have a secondary function associated with fruit ripening (**Figure 3C** and **Table 2**). This result is not surprising because most fruits accumulate anthocyanin only in their ripening phase (Jaakola et al., 2002; Whale and Singh, 2007; Negri et al., 2008; Bureau et al., 2009). Our results demonstrate that ALA regulates the expression of ripening-related genes and therefore



provide more evidence on the regulation of fruit ripening by ALA.

Our results suggest a role of ALA in the modulation of apple skin physiology by regulating fruit ripening-related processes. Transcription factors play important roles in controlling the switch to the ripening phase in fruits (Giovannoni, 2007; Karlova et al., 2014). Since studies on *ripening inhibitor* (*Rin*) mutation in tomato revealed SEPALLATA (SEP) subfamily of MADS-box genes play a key role in the developmental control of fruit ripening (Vrebalov et al., 2002), there is evidence that members of *SEP-like* orthologous gene families are involved in fruit development in other species, such as strawberry (Seymour et al., 2011), and banana (Elitzur et al., 2010). In fact, some MADS box TF from the AP1/SQUA class have been implicated in controlling of anthocyanin biosynthesis. *IbMADS10* expression was correlated with red pigmentation in sweet potato, and ectopic expression resulted in anthocyanin accumulation in transgenic sweet potato calli and transgenic *Arabidopsis* (Lalusin et al., 2006). *VmTDR4* expression was linked with color development and anthocyanin-related gene expression in bilberry (*Vaccinium myrtillus*), while silencing of this gene reduced anthocyanin levels (Jaakola et al., 2010). Meanwhile, *SEP-like* genes have also been reported to be associated with the accumulation of anthocyanin in pear (Wu et al., 2013). In strawberry, suppression of *SEP1/2-like FaMADS9* resulted in delayed ripening with respect to anthocyanin accumulation. Therefore, *SEP-like* gene regulated fruit ripening process including skin color change.

Here, we identified an ALA-responsive gene, *MdMADS1* (UN038 in Table 2), which belongs to the SEP subgroup (Sung and An, 1997). In apple, fruits of the *MdMADS1* antisense lines do not ripen in terms of both developmentally controlled ripening characters, such as starch degradation and background color change of fruit skin (Ireland et al., 2013). However, the authors did not investigate anthocyanin biosynthesis and accumulation in the transgenic fruits, and the exact relationship between *MdMADS1* and fruit coloration remains unknown. Our SSH result showed that ALA up-regulated the expression of *MdMADS1*, and this regulation was further confirmed by real-time quantitative PCR. Furthermore, under ALA treatment, the expression of *MdMADS1* was significantly positively correlated with that of anthocyanin biosynthetic genes, including *MdCHS*, *MdDFR*, *MdLDOX*, and *MdUFGT*. These results indicate that *MdMADS1* may play an important role in ALA-promoted anthocyanin accumulation. To prove the role of *MdMADS1*, we transformed and successfully obtained transgenic fruit calli. Overexpression of *MdMADS1* led to more anthocyanin accumulation. The six anthocyanin biosynthetic genes were up-regulated in overexpression transgenic calli and down-regulated in RNAi transgenic calli. Anthocyanin accumulated in overexpression and RNAi transgenic calli treated by ALA was higher not only than their corresponding control but also than that in transgenic calli without ALA. These results indicate that *MdMADS1* involves in ALA-induced anthocyanin accumulation, but the latter is not completely dependent on the former.

In apple fruit, *MdMADS1* is a master regulator that controls fruit ripening process including the initiation of ethylene biosynthesis (Ireland et al., 2013; Schaffer et al., 2013). The central role of ethylene in apple fruit ripening has been well-studies (Dandekar et al., 2004; Schaffer et al., 2007). Of these, ethylene appeared to be a key factor regulating anthocyanin biosynthesis and color development in apple fruit (Whale and Singh, 2007). In the present study, we also identified 1-aminocyclopropane-1-carboxylate oxidase 1 (ACO1, No. 34 in Table 1 and UN095 in Table 2) at protein and mRNA levels, a key enzyme in ethylene biosynthesis, and ethylene receptor 2 (ERS2, No. 35 in Table 1) at protein level, an ethylene signal transduction gene, suggesting that *MdMADS1* might regulate ALA-induced anthocyanin accumulation by its regulation of ethylene metabolism and action. However, the role of ethylene in apple cultivar "Fuji" fruit may be quiet limited, because the ethylene production in "Fuji" fruit was significant lower than that in other cultivars (Harada et al., 2000; Tatsuki et al., 2007). In addition, the skin color change in *MdMADS1* antisense fruits was not completely compensated for by exogenous ethylene (Ireland et al., 2013), suggesting a non-ethylene-dependent pathway exists in *MdMADS1*-regulated fruit coloration. In this study, the function of *MdMADS1* was tested in fruit calli, proving that the regulation of *MdMADS1* on anthocyanin biosynthesis is at least partly independent of fruit ripening process. Our data firstly reveal a positive regulation role of *MdMADS1* in anthocyanin biosynthesis. Further study is needed to reveal the mechanisms behind ripening-related and non-ripening-related anthocyanin accumulation mediated by *MdMADS1*. Except *MdMADS1*, ALA promotes anthocyanin

accumulation has been linked to regulatory genes *MYB*, *bHLH*, and *WD40* (Xie et al., 2013). Therefore, the interaction between the *MdMADS1* and *MYB*–*bHLH*–*WD40* complexes need further study.

CONCLUSION

In summary, the integrated proteomics and SSH techniques, in this study, provide us a comprehensive understanding of biological events that are relevant to ALA-improved fruit coloration. Based on the results, we identified a positive regulator, *MdMADS1*, and verified its role in ALA-induced anthocyanin accumulation by further functional characterization. In apple fruits, the expression of *MdMADS1* was induced by ALA, which was significantly positively correlated to that of anthocyanin biosynthetic genes under ALA treatment. In fruit calli, overexpressed *MdMADS1* enhanced anthocyanin content, and the accumulation was further enhanced by ALA treatment. However, silenced *MdMADS1* cannot completely repress anthocyanin accumulation in ALA-treated calli. The results indicate synergistic or additive responses between ALA and *MdMADS1* exists for regulation of apple skin anthocyanin accumulation. In addition, verification in apple calli, a non-fruit test system, suggested the regulation of *MdMADS1* on anthocyanin biosynthesis is partially independent of fruit ripening process. Our results contribute to the understanding of ALA-stimulated fruit coloration and expand the existing information on transcription regulation of anthocyanin accumulation in fruit. Further study is needed to elucidate

how *MdMADS1* regulates the genes encoding anthocyanin biosynthetic pathway enzymes.

AUTHOR CONTRIBUTIONS

XF, YA conceived and designed research. XF, JZ, MS carried out all the experiments. XF, YA analyzed the data. YA, LW wrote the manuscript. All authors read and approved the manuscript.

FUNDING

This research was supported by the Natural Science Foundation of Jiangsu Province, China (BK20140702), the National Natural Science Foundation of China (31401820), and the Fundamental Research Funds for the Central Universities (KJQN201538). The funders had no role in study design, data collection and analysis, decision to publish, or preparation of the manuscript.

ACKNOWLEDGMENTS

We thank Dr. Meixiang Zhang from Nanjing Agricultural University for his valuable comments and suggestions that help improve the manuscript.

SUPPLEMENTARY MATERIAL

The Supplementary Material for this article can be found online at: <http://journal.frontiersin.org/article/10.3389/fpls.2016.01615/full#supplementary-material>

REFERENCES

- Aguilar, M., Osuna, D., Caballero, J. L., and Munoz, J. (1997). Isolation of a cDNA encoding a metallothionein-like protein (Accession No. U81041) from strawberry fruit. *Plant Physiol.* 113, 663.
- Akram, N. A., and Ashraf, M. (2013). Regulation in plant stress tolerance by a potential plant growth regulator, 5-aminolevulinic acid. *J. Plant Growth Regul.* 32, 663–679. doi: 10.1007/s00344-013-9325-9
- Alessio, F., Cecilia, B., Martina, D. F., Francesco, F., and Massimiliano, T. (2011). Stress-induced flavonoid biosynthesis and the antioxidant machinery of plants. *Plant Signal. Behav.* 6, 709–711. doi: 10.4161/psb.6.5.15069
- An, X. H., Tian, Y., Chen, K. Q., Liu, X. J., Liu, D. D., Xie, X. B., et al. (2015). *MdMYB9* and *MdMYB12* are involved in the regulation of the JA-induced biosynthesis of anthocyanin and proanthocyanidin in apples. *Plant Cell Physiol.* 56, 650–662. doi: 10.1093/pcp/pcu205
- An, X. H., Tian, Y., Chen, K. Q., Wang, X. F., and Hao, Y. J. (2012). The apple WD40 protein MdTTG1 interacts with bHLH but not MYB proteins to regulate anthocyanin accumulation. *J. Plant Physiol.* 169, 710–717. doi: 10.1016/j.jplph.2012.01.015
- Arcondéguy, T., Lacazette, E., Millevoi, S., Prats, H., and Touriol, C. (2013). VEGF-A mRNA processing, stability and translation: a paradigm for intricate regulation of gene expression at the post-transcriptional level. *Nucleic Acids Res.* 41, 7997–8010. doi: 10.1093/nar/gkt539
- Bae, R. N., Kim, K. W., Kim, T. C., and Lee, S. K. (2006). Anatomical observations of anthocyanin rich cells in apple skins. *HortScience* 41, 733–736.
- Bradford, M. M. (1976). A rapid and sensitive method for the quantitation of microgram quantities of protein utilizing the principle of protein-dye binding. *Anal. Biochem.* 72, 248–254. doi: 10.1016/0003-2697(76)90527-3
- Bregoli, A. M., Scaramagli, S., Costa, G., Sabatini, E., Ziosi, V., Biondi, S., et al. (2002). Peach (*Prunus persica*) fruit ripening: aminoethoxyvinylglycine (AVG)
- and exogenous polyamines affect ethylene emission and flesh firmness. *Physiol. Plant.* 114, 472–481. doi: 10.1034/j.1399-3054.2002.1140317.x
- Bureau, S., Renard, C. M. G. C., Reich, M., Ginies, C., and Audergon, J. M. (2009). Change in anthocyanin concentrations in red apricot fruits during ripening. *LWT Food Sci. Technol.* 42, 372–377. doi: 10.1016/j.lwt.2008.03.010
- Burns, J. K., Hartmond, U., and Kender, W. J. (1999). Acetolactate synthase inhibitors increase ethylene production and cause fruit drop in citrus. *HortScience* 34, 908–910.
- Cao, Y., Tang, X., Giovannoni, J., Xiao, F., and Liu, Y. (2012). Functional characterization of a tomato COBRA-like gene functioning in fruit development and ripening. *BMC Plant Biol.* 12:211. doi: 10.1186/1471-2229-12-211
- Chalker-Scott, L. (1999). Environmental significance of anthocyanins in plant stress responses. *Photochem. Photobiol.* 70, 1–9. doi: 10.1111/j.1751-1097.1999.tb01944.x
- Chou, K. C., and Shen, H. B. (2010). Plant-mPLoc: a top-down strategy to augment the power for predicting plant protein subcellular localization. *PLoS ONE* 5:e11335. doi: 10.1371/journal.pone.0011335
- D'Ambrosio, C., Arena, S., Rocco, M., Verrillo, F., Novi, G., Viscosi, V., et al. (2013). Proteomic analysis of apricot fruit during ripening. *J. Proteomics* 78, 39–57. doi: 10.1016/j.jprot.2012.11.008
- Dandekar, A. M., Teo, G., Deflippi, B. G., Uratsu, S. L., Passey, A. J., Kader, A. A., et al. (2004). Effect of down-regulation of ethylene biosynthesis on fruit flavor complex in apple fruit. *Transgenic Res.* 13, 373–384. doi: 10.1023/B:TRAG.0000040037.90435.45
- Dauwe, R., Morreel, K., Goeminne, G., Gielen, B., Rohde, A., Beeumen, J. V., et al. (2007). Molecular phenotyping of lignin-modified tobacco reveals associated changes in cell-wall metabolism, primary metabolism, stress metabolism and photorespiration. *Plant J.* 52, 263–285. doi: 10.1111/j.1365-313X.2007.03233.x

- Deytieux, C., Geny, L., Lapaillerie, D., Claverol, S., Bonneau, M., and Donèche, B. (2007). Proteome analysis of grape skins during ripening. *J. Exp. Bot.* 58, 1851–1862. doi: 10.1093/jxb/erm049
- Dixon, R. A., Achnina, L., Kota, P., Liu, C. J., Reddy, M. S. S., and Wang, L. J. (2002). The phenylpropanoid pathway and plant defence - a genomics perspective. *Mol. Plant Pathol.* 3, 371–390. doi: 10.1046/j.1364-3703.2002.00131.x
- Elitzur, T., Vrebalov, J., Giovannoni, J. J., Goldschmidt, E. E., and Friedman, H. (2010). The regulation of MADS-box gene expression during ripening of banana and their regulatory interaction with ethylene. *J. Exp. Bot.* 61, 1523–1535. doi: 10.1093/jxb/erq017
- Eremina, M., Rozhon, W., Yang, S., and Poppenberger, B. (2015). ENO2 activity is required for the development and reproductive success of plants, and is feedback-repressed by AtMBP-1. *Plant J.* 81, 895–906. doi: 10.1111/tpj.12775
- Feng, F., Li, M., Ma, F., and Cheng, L. (2013). Phenylpropanoid metabolites and expression of key genes involved in anthocyanin biosynthesis in the shaded peel of apple fruit in response to sun exposure. *Plant Physiol. Biochem.* 69, 54–61. doi: 10.1016/j.plaphy.2013.04.020
- Feng, S., Li, M. F., Wu, F., Li, W. L., and Li, S. P., (2015). 5-Aminolevulinic acid affects fruit coloration, growth, and nutrition quality of *Litchi chinensis* Sonn. cv. Feizixiao in Hainan, tropical China. *Sci. Hortic.* 193, 188–194. doi: 10.1016/j.scienta.2015.07.010
- Fraige, K., González-Fernández, R., Carrilho, E., and Jorrín-Novo, J. V. (2014). Metabolite and proteome changes during the ripening of Syrah and Cabernet Sauvignon grape varieties cultured in a nontraditional wine region in Brazil. *J. Proteomics* 113, 206–225. doi: 10.1016/j.jprot.2014.09.021
- Gallego, P. P., Whotton, L., Picton, S., Grierson, D., and Gray, J. E., (1995). A role for glutamate decarboxylase during tomato ripening: the characterisation of a cDNA encoding a putative glutamate decarboxylase with a calmodulin-binding site. *Plant Mol. Biol.* 27, 1143–1151. doi: 10.1007/BF00020887
- Gao, J. J., Feng, X. X., Duan, C. H., Jian-Hua, L. I., Shi, Z. X., Gao, F. Y., et al. (2013). Effects of 5-aminolevulinic acid (ALA) on leaf photosynthesis and fruit quality of apples. *J. Fruit Sci.* 30, 944–951. doi: 10.13925/j.cnki.gxb.2013.06.015
- Giovannoni, J. J. (2007). Fruit ripening mutants yield insights into ripening control. *Curr. Opin. Plant Biol.* 10, 283–289. doi: 10.1016/j.pbi.2007.04.008
- Giribaldi, M., Perugini, I., Sauvage, F. X., and Schubert, A. (2007). Analysis of protein changes during grape berry ripening by 2-DE and MALDI-TOF. *Proteomics* 7, 3154–3170. doi: 10.1002/pmic.200600974
- Guo, L., Cai, Z. X., Zhang, B. B., Xu, J. L., Song, H. F., and Ma, R. J. (2013). The mechanism analysis of anthocyanin accumulation in peach accelerated by ALA. *Acta Hortic. Sin.* 40, 1043–1050. doi: 10.16420/j.issn.0513-353x.2013.06.004
- Han, Y. P., Vimolmangkang, S., Soria-Guerra, R. E., Rosales-Mendoza, S., Zheng, D. M., Lygin, A. V., et al. (2010). Ectopic expression of apple *F3'H* genes contributes to anthocyanin accumulation in the arabidopsis *t7* mutant grown under nitrogen stress. *Plant Physiol.* 153, 806–820. doi: 10.1104/pp.109.152801
- Harada, T., Sunako, T., Wakasa, Y., Soejima, J., Satoh, T., and Niizeki, M. (2000). An allele of the 1-aminocyclopropane-1-carboxylate synthase gene (*Md-ACS1*) accounts for the low level of ethylene production in climacteric fruits of some apple cultivars. *Theor. App. Genet.* 101, 742–746. doi: 10.1007/s001220051539
- Henkes, S., Sonnewald, U., Badur, R., Flachmann, R., and Stitt, M. (2001). A small decrease of plastid transketolase activity in antisense tobacco transformants has dramatic effects on photosynthesis and phenylpropanoid metabolism. *Plant Cell* 13, 535–551. doi: 10.1101/tpc.13.3.535
- Huerta-Ocampo, J. Á., Osuna-Castro, J. A., Lino-López, G. J., Barrera-Pacheco, A., Mendoza-Hernández, G., De León-Rodríguez, A., et al. (2012). Proteomic analysis of differentially accumulated proteins during ripening and in response to 1-MCP in papaya fruit. *J. Proteomics* 75, 2160–2169. doi: 10.1016/j.jprot.2012.01.015
- Ireland, H. S., Yao, J. L., Tomes, S., Sutherland, P. W., Nieuwenhuizen, N., Gunaseelan, K., et al. (2013). Apple *SEPALLATA1/2-like* genes control fruit flesh development and ripening. *Plant J.* 73, 1044–1056. doi: 10.1111/tpj.12094
- Jaakola, L., Määttä, K., Pirttilä, A. M., Törönen, R., Kärenlampi, S., and Hohtola, A. (2002). Expression of genes involved in anthocyanin biosynthesis in relation to anthocyanin, proanthocyanidin, and flavonol levels during bilberry fruit development. *Plant Physiol.* 130, 729–739. doi: 10.1104/pp.006957
- Jaakola, L., Pirttilä, A. M., Halonen, M., and Hohtola, A. (2001). Isolation of high quality RNA from bilberry (*Vaccinium myrtillus* L.) fruit. *Mol. Biotechnol.* 19, 201–203. doi: 10.1385/MB:19:2:201
- Jaakola, L., Poole, M., Jones, M. O., Kämäräinen-Karppinen, T., Koskimäki, J. J., Hohtola, A., et al. (2010). A SQUAMOSA MADS box gene involved in the regulation of anthocyanin accumulation in bilberry fruits. *Plant Physiol.* 153, 1619–1629. doi: 10.1104/pp.110.158279
- Janssen, B. J., Thodey, K., Schaffer, R. J., Alba, R., Balakrishnan, L., Bishop, R., et al. (2008). Global gene expression analysis of apple fruit development from the floral bud to ripe fruit. *BMC Plant Biol.* 8:16. doi: 10.1186/1471-2229-8-16
- Ju, Z. G. (1998). Fruit bagging, a useful method for studying anthocyanin synthesis and gene expression in apples. *Sci. Hortic.* 77, 155–164. doi: 10.1016/S0304-4238(98)00161-7
- Ju, Z. G., and Curry, E. A. (2000). Evidence that α -farnesene biosynthesis during fruit ripening is mediated by ethylene regulated gene expression in apples. *Postharvest Biol. Technol.* 19, 9–16. doi: 10.1016/S0925-5214(00)00078-8
- Ju, Z. G., Liu, C. L., and Yuan, Y. B. (1995). Activities of chalcone synthase and UDPGal:flavonoid 3-O-glycosyltransferase in relation to anthocyanin synthesis in apple. *Sci. Hortic.* 63, 175–185. doi: 10.1016/0304-4238(95)00807-6
- Karlová, R., Chapman, N., David, K., Angenent, G. C., Seymour, G. B., and de Maagd, R. A. (2014). Transcriptional control of fleshy fruit development and ripening. *J. Exp. Bot.* 65, 4527–4541. doi: 10.1093/jxb/eru316
- Kim, S. H., Lee, J. R., Hong, S. T., Yoo, Y. K., An, G., and Kim, S. R. (2003). Molecular cloning and analysis of anthocyanin biosynthesis genes preferentially expressed in apple skin. *Plant Sci.* 165, 403–413. doi: 10.1016/S0168-9452(03)00201-2
- Kumar, V., Irfan, M., Ghosh, S., Chakraborty, N., Chakraborty, S., and Datta, A. (2015). Fruit ripening mutants reveal cell metabolism and redox state during ripening. *Protoplasma* 253, 1–14. doi: 10.1007/s00709-015-0836-z
- Kushad, M. M., Richardson, D. G., and Ferro, A. J. (1985). 5'-Methylthioadenosine nucleosidase and 5-methylthioribose kinase activities and ethylene production during tomato fruit development and ripening. *Plant Physiol.* 79, 525–529. doi: 10.1104/pp.79.2.525
- Lalusin, A. G., Nishita, K., Kim, S. H., Ohta, M., and Fujimura, T. (2006). A new MADS-box gene (*lbdMADS10*) from sweet potato (*Ipomoea batatas* (L.) Lam) is involved in the accumulation of anthocyanin. *Mol. Genet. Genomics* 275, 44–54. doi: 10.1007/s00438-005-0080-x
- Lan, P., Li, W., and Schmidt, W. (2012). Complementary proteome and transcriptome profiling in phosphate-deficient *Arabidopsis* roots reveals multiple levels of gene regulation. *Mol. Cell. Proteomics* 11, 1156–1166. doi: 10.1074/mcp.M112.020461
- Law, R. D., and Plaxton, W. C. (1997). Regulatory phosphorylation of banana fruit phosphoenolpyruvate carboxylase by a copurifying phosphoehpyruvate carboxylase kinase. *Eur. J. Biochem.* 247, 642–651. doi: 10.1111/j.1432-1033.1997.00642.x
- Li, J., and Yuan, R. (2008). NAA and ethylene regulate expression of genes related to ethylene biosynthesis, perception, and cell wall degradation during fruit abscission and ripening in 'Delicious' apples. *J. Plant Growth Regul.* 27, 283–295. doi: 10.1007/s00344-008-9055-6
- Li, P., Zhang, Y., Einhorn, T. C., and Cheng, L. (2014). Comparison of phenolic metabolism and primary metabolism between green 'Anjou' pear and its bud mutation, red 'Anjou'. *Physiol. Plant.* 150, 339–354. doi: 10.1111/plp.12105
- Li, Y. Y., Mao, K., Zhao, C., Zhao, X. Y., Zhang, H. L., Shu, H. R., et al. (2012). MdCOP1 ubiquitin E3 ligases interact with MdMYB1 to regulate light-induced anthocyanin biosynthesis and red fruit coloration in apple. *Plant Physiol.* 160, 1011–1022. doi: 10.1104/pp.112.199703
- Li, Z., Sugaya, S., Gemma, H., and Iwahori, S. (2002). Flavonoid biosynthesis and accumulation and related enzyme activities in the sin of 'Fuji' and 'Ooirin' apples during their development. *J. Jpn. Soc. Hortic. Sci.* 71, 317–321. doi: 10.2503/jjshs.71.317
- Liu, J. H., Zhang, J., Xu, B. Y., Zhang, J. B., Jia, C. H., Wang, J. S., et al. (2012). Expression analysis of banana *MaECHII* during fruit ripening with different treatments. *Afr. J. Biotechnol.* 11, 12951–12957. doi: 10.5897/AJB12.763
- Liu, X., Hu, X. M., Jin, L. F., Shi, C. Y., Liu, Y. Z., and Peng, S. A. (2014). Identification and transcript analysis of two glutamate decarboxylase genes, *CsGAD1* and *CsGAD2*, reveal the strong relationship between *CsGAD1* and citrate utilization in citrus fruit. *Mol. Biol. Rep.* 41, 6253–6262. doi: 10.1007/s11033-014-3506-x

- Livak, K. J., and Schmittgen, T. D. (2001). Analysis of relative gene expression data using real-time quantitative PCR and the $2^{-\Delta\Delta C_T}$ method. *Methods* 25, 402–408. doi: 10.1006/meth.2001.1262
- Ludwig, R., Su-Ying, Y., Stephanie, H., Thomas, H., Rosario, B. P., Mathieu, F., et al. (2013). Metabolic interaction between anthocyanin and lignin biosynthesis is associated with peroxidase FaPRX27 in strawberry fruit. *Plant Physiol.* 163, 43–60. doi: 10.1104/pp.113.222778
- Majeran, W., Yang, C., Qi, S., and Wijk, K. J. V. (2005). Functional differentiation of bundle sheath and mesophyll maize chloroplasts determined by comparative proteomics. *Plant Cell* 17, 3111–3140. doi: 10.1105/tpc.105.035519
- Marondedze, C., Gehring, C., and Thomas, L. (2014). Dynamic changes in the date palm fruit proteome during development and ripening. *Hortic. Res.* 1, 14039. doi: 10.1038/hortres.2014.39
- Martínez-Esteso, M. J., Vilella-Antón, M. T., Pedreño, M. Á., Valero, M. L., and Bru-Martínez, R. (2013). iTRAQ-based protein profiling provides insights into the central metabolism changes driving grape berry development and ripening. *BMC Plant Biol.* 13:167. doi: 10.1186/1471-2229-13-167
- Meinholt, T., Richters, J. P., Damerow, L., and Blanke, M. M. (2010). Optical properties of reflection ground covers with potential for enhancing fruit colouration. *Biosys. Eng.* 107, 155–160. doi: 10.1016/j.biosystemseng.2010.07.006
- Minas, I. S., Tanou, G., Belghazi, M., Job, D., Manganaris, G. A., Molassiotis, A., et al. (2012). Physiological and proteomic approaches to address the active role of ozone in kiwifruit post-harvest ripening. *J. Exp. Bot.* 63, 2449–2464. doi: 10.1093/jxb/err418
- Murooka, Y., and Tanaka, T. (2014). “5-Aminolevulinic acid (5-ALA) – a multifunctional amino acid as a plant growth stimulator and stress tolerance factor,” in *Plant Adaptation to Environmental Change: Significance of Amino Acids and their Derivatives*, eds N. A. Anjum, S. S. Gill, and R. Gill (Wallingford: CABI Publishing), 18–34.
- Negri, A. S., Prinsi, B., Failla, O., Scienza, A., and Espen, L. (2015). Proteomic and metabolic traits of grape exocarp to explain different anthocyanin concentrations of the cultivars. *Front. Plant Sci.* 6:603. doi: 10.3389/fpls.2015.00603
- Negri, A. S., Prinsi, B., Rossini, M., Failla, O., Scienza, A., Cocucci, M., et al. (2008). Proteome changes in the skin of the grape cultivar Barbera among different stages of ripening. *BMC Genomics* 9:378. doi: 10.1186/1471-2164-9-378
- Nogueira, S. B., Labate, C. A., Gozzo, F. C., Pilau, E. J., Lajolo, F. M., and Oliveira do Nascimento, J. R. O. (2012). Proteomic analysis of papaya fruit ripening using 2DE-DIGE. *J. Proteomics* 75, 1428–1439. doi: 10.1016/j.jprot.2011.11.015
- Perez, M. H., Rodriguez, B. L., Shintani, T. T., Watanabe, K., Miyanari, S., and Harrigan, R. C. (2013). 5-Aminolevulinic acid (5-ALA): analysis of preclinical and safety literature. *Food Nutr. Sci.* 4, 1009–1013. doi: 10.4236/fns.2013.410131
- Prinsi, B., Negri, A. S., Fedeli, C., Morgutti, S., Negrini, N., Cocucci, M., et al. (2011). Peach fruit ripening: a proteomic comparative analysis of the mesocarp of two cultivars with different flesh firmness at two ripening stages. *Phytochemical* 72, 1251–1262. doi: 10.1016/j.phytochem.2011.01.012
- Qin, G., Wang, Y., Cao, B., Wang, W., and Tian, S. (2012). Unraveling the regulatory network of the MADS box transcription factor RIN in fruit ripening. *Plant J.* 70, 243–255. doi: 10.1111/j.1365-313X.2011.04861.x
- Sasaki, Y., and Nagano, Y. (2014). Plant acetyl-CoA carboxylase: structure, biosynthesis, regulation, and gene manipulation for plant breeding. *Biosci. Biotechnol. Biochem.* 68, 1175–1184. doi: 10.1271/bbb.68.1175
- Schaffer, R. J., Friel, E. N., Souleyre, E. J. F., Bolitho, K., Thodey, K., Ledger, S., et al. (2007). A genomics approach reveals that aroma production in apple is controlled by ethylene predominantly at the final step in each biosynthetic pathway. *Plant Physiol.* 144, 1899–1912. doi: 10.1104/pp.106.093765
- Schaffer, R. J., Ireland, H. S., Ross, J. J., Ling, T. J., and David, K. M. (2013). SEPALLATA1/2-suppressed mature apples have low ethylene, high auxin and reduced transcription of ripening-related genes. *Aob Plants* 5:pls047. doi: 10.1093/aobpla/pls047
- Scherp, P., Ku, G., Coleman, L., and Kheterpal, I. (2011). Gel-based and gel-free proteomic technologies. *Methods Mol. Biol.* 702, 163–190. doi: 10.1007/978-1-61737-960-4_13
- Seymour, G. B., Ryder, C. D., Cevik, V., Hammond, J. P., Popovich, A., King, G. J., et al. (2011). A SEPALLATA gene is involved in the development and ripening of strawberry (*Fragaria × ananassa* Duch.) fruit, a non-climacteric tissue. *J. Exp. Bot.* 62, 1179–1188. doi: 10.1093/jxb/erq360
- Shi, Y., Jiang, L., Zhang, L., Kang, R., and Yu, Z. (2014). Dynamic changes in proteins during apple (*Malus × domestica*) fruit ripening and storage. *Hortic. Res.* 1:6. doi: 10.1038/hortres.2014.6
- Sunchung, P., Nobuko, S., Larson, M. D., Randy, B., and Steven, V. N. (2006). Identification of genes with potential roles in apple fruit development and biochemistry through large-scale statistical analysis of expressed sequence tags. *Plant Physiol.* 141, 811–824. doi: 10.1104/pp.106.080994
- Sung, S. K., and An, G. H. (1997). Molecular cloning and characterization of a MADS-box cDNA clone of the Fuji apple. *Plant Cell Physiol.* 38, 484–489. doi: 10.1093/oxfordjournals.pcp.a029193
- Takos, A. M., Jaffé, F. W., Jacob, S. R., Bogs, J., Robinson, S. P., and Walker, A. R. (2006). Light-induced expression of a MYB gene regulates anthocyanin biosynthesis in red apples. *Plant Physiol.* 142, 1216–1232. doi: 10.1104/pp.106.088104
- Tatsuki, M., Endo, A., and Ohkawa, H. (2007). Influence of time from harvest to 1-MCP treatment on apple fruit quality and expression of genes for ethylene biosynthesis enzymes and ethylene receptors. *Postharvest Biol. Technol.* 43, 28–35. doi: 10.1016/j.postharvbio.2006.08.010
- Turner, W. L., and Plaxton, W. C. (2003). Purification and characterization of pyrophosphate- and ATP-dependent phosphofructokinases from banana fruit. *Planta* 217, 113–121. doi: 10.1007/s00425-002-0962-7
- Tzin, V., and Galili, G. (2010). New insights into the shikimate and aromatic amino acids biosynthesis pathways in plants. *Mol. Plant* 3, 956–972. doi: 10.1093/mp/ssq048
- Ubi, B. E., Honda, C., Bessho, H., Kondo, S., Wada, M., Kobayashi, S., et al. (2006). Expression analysis of anthocyanin biosynthetic genes in apple skin: effect of UV-B and temperature. *Plant Sci.* 170, 571–578. doi: 10.1016/j.plantsci.2005.10.009
- Voll, L. M., Hajirezaei, M. R., Czogalla-Peter, C., Lein, W., Stitt, M., Sonnewald, U., et al. (2009). Antisense inhibition of enolase strongly limits the metabolism of aromatic amino acids, but has only minor effects on respiration in leaves of transgenic tobacco plants. *New Phytol.* 184, 607–618. doi: 10.1111/j.1469-8137.2009.02998.x
- Vrebalov, J., Ruezinsky, D., Padmanabhan, V., White, R., Medrano, D., Drake, R., et al. (2002). A MADS-box gene necessary for fruit ripening at the tomato *ripening-inhibitor* (*Rin*) locus. *Science* 296, 343–346. doi: 10.1126/science.1068181
- Wang, N., Zheng, Y., Duan, N., Zhang, Z., Ji, X., Jiang, S., et al. (2015). Comparative transcriptomes analysis of red- and white-fleshed apples in an F1 population of *malus sieversii* f. *niedzwetzkyana* crossed with *M. domestica* ‘Fuji’. *PLoS ONE* 10:e0133468. doi: 10.1371/journal.pone.0133468
- Wang, S. H., You, Z. Y., Ye, L. P., Che, J., Qian, Q., Nanjo, Y., et al. (2014). Quantitative proteomic and transcriptomic analyses of molecular mechanisms associated with low silk production in silkworm *Bombyx mori*. *J. Proteome Res.* 13, 735–751. doi: 10.1021/pr4008333
- Watanabe, K., Nishihara, E., Watanabe, S., Tanaka, T., Takahashi, K., and Takeuchi, Y. (2006). Enhancement of growth and fruit maturity in 2-year-old grapevines cv. Delaware by 5-aminolevulinic acid. *Plant Growth Regul.* 49, 35–42. doi: 10.1007/s10725-006-0024-4
- Weiss, J., and Egea-Cortines, M. (2009). Transcriptomic analysis of cold response in tomato fruits identifies dehydrin as a marker of cold stress. *J. Appl. Genet.* 50, 311–319. doi: 10.1007/BF03195689
- Whale, S. K., and Singh, Z. (2007). Endogenous ethylene and color development in the skin of ‘Pink lady’ apple. *J. Am. Soc. Hort. Sci.* 132, 20–28.
- Winkel-Shirley, B. (2001). Flavonoid biosynthesis. A colorful model for genetics, biochemistry, cell biology, and biotechnology. *Plant Physiol.* 126, 485–493. doi: 10.1104/pp.126.2.485
- Wong, J. H., Kiss, F., Wu, M. X., and Buchanan, B. B. (1990). Pyrophosphate fructose-6-P 1-phototransferase from tomato fruit: evidence for change during ripening. *Plant Physiol.* 94, 499–506. doi: 10.1104/pp.94.2.499
- Wu, J., Xu, Z., Zhang, Y., Chai, L., Yi, H., and Deng, X. (2014). An integrative analysis of the transcriptome and proteome of the pulp of a spontaneous late-ripening sweet orange mutant and its wild type improves our understanding of fruit ripening in citrus. *J. Exp. Bot.* 65, 1651–1671. doi: 10.1093/jxb/eru044
- Wu, J., Zhao, G., Yang, Y. N., Le, W. Q., Khan, M. A., Zhang, S. L., et al. (2013). Identification of differentially expressed genes related to coloration in red/green mutant pear (*Pyrus communis* L.). *Tree Genet. Genomes* 9, 75–83. doi: 10.1007/s11295-012-0534-3

- Xiao, C. C., Zhang, S. L., Hu, H. J., Tian, R., Wu, J., Yang, Z. J., et al. (2012). Effects of bagging and exogenous 5-aminolevulinic acid treatment on coloration of 'Yunhongli 2'. *J. Nanjing Agricult. Univ.* 35, 25–29. doi: 10.7685/j.issn.1000-2030.2012.06.005
- Xie, L., Wang, Z. H., Cheng, X. H., Gao, J. J., Zhang, Z. P., and Wang, L. J. (2013). 5-Aminolevulinic acid promotes anthocyanin accumulation in Fuji apples. *Plant Growth Regul.* 69, 295–303. doi: 10.1007/s10725-012-9772-5
- Xie, X. B., Li, S., Zhang, R. F., Zhao, J., Chen, Y. C., Zhao, Q., et al. (2012). The bHLH transcription factor MdbHLH3 promotes anthocyanin accumulation and fruit colouration in response to low temperature in apples. *Plant Cell Environ.* 35, 1884–1897. doi: 10.1111/j.1365-3040.2012.02523.x
- Yin, X., Sakata, K., Nanjo, Y., and Komatsu, S. (2014). Analysis of initial changes in the proteins of soybean root tip under flooding stress using gel-free and gel-based proteomic techniques. *J. Proteomics* 106, 1–16. doi: 10.1016/j.jprot.2014.04.004
- Yuan, H., Chen, L., Palith, G., Sullivan, A., Murr, D. P., and Novotna, Z. (2006). Immunohistochemical localization of phospholipase D in strawberry (*Fragaria ananassa* Duch.) fruits. *Sci. Hortic.* 109, 35–42. doi: 10.1016/j.scienta.2006.02.023
- Zhang, L. Y., Feng, X. X., Gao, J. J., An, Y. Y., Tian, F., Li, J., et al. (2015). Effects of rhizosphere-applied 5-aminolevulinic acid(ALA) solutions on leaf physiological characteristics and fruit quality of apples. *Jiangsu J. Agric. Sci.* 31, 158–165. doi: 10.3969/j.issn.1000-4440.2015.01.025
- Zhang, Z., Jiang, S., Wang, N., Li, M., Ji, X., Sun, S., et al. (2015). Identification of differentially expressed genes associated with apple fruit ripening and softening by suppression subtractive hybridization. *PLoS ONE* 10:e0146061. doi: 10.1371/journal.pone.0146061
- Zheng, Q., Song, J., Campbell-Palmer, L., Thompson, K., Li, L., Walker, B., et al. (2013). A proteomic investigation of apple fruit during ripening and in response to ethylene treatment. *J. Proteomics* 93, 276–294. doi: 10.1016/j.jprot.2013.02.006
- Zheng, Y., Zhao, L., Gao, J., and Fei, Z. (2011). iAssembler: a package for *de novo* assembly of Roche-454/Sanger transcriptome sequences. *BMC Bioinform.* 12:453. doi: 10.1186/1471-2105-12-453
- Zhou, H., Kui, L. W., Wang, H. L., Gu, C., Dare, A. P., Espley, R. V., et al. (2015). Molecular genetics of blood-fleshed peach reveals activation of anthocyanin biosynthesis by NAC transcription factors. *Plant J.* 82, 105–121. doi: 10.1111/tpj.12792

Conflict of Interest Statement: The authors declare that the research was conducted in the absence of any commercial or financial relationships that could be construed as a potential conflict of interest.

Copyright © 2016 Feng, An, Zheng, Sun and Wang. This is an open-access article distributed under the terms of the Creative Commons Attribution License (CC BY). The use, distribution or reproduction in other forums is permitted, provided the original author(s) or licensor are credited and that the original publication in this journal is cited, in accordance with accepted academic practice. No use, distribution or reproduction is permitted which does not comply with these terms.



Comparative Physiological and Proteomic Analysis Reveal Distinct Regulation of Peach Skin Quality Traits by Altitude

Evangelos Karagiannis¹, Georgia Tanou¹, Martina Samiotaki², Michail Michailidis¹, Grigoris Diamantidis³, Ioannis S. Minas^{4,5} and Athanassios Molassiotis^{1*}

¹ Laboratory of Pomology, Department of Agriculture, Aristotle University of Thessaloniki, Thessaloniki, Greece, ² Biomedical Sciences Research Center "Alexander Fleming", Vari, Greece, ³ Laboratory of Agricultural Chemistry, Department of Agriculture, Aristotle University of Thessaloniki, Thessaloniki, Greece, ⁴ Department of Horticulture and Landscape Architecture, Colorado State University, Fort Collins, CO, USA, ⁵ Western Colorado Research Center at Orchard Mesa, Colorado State University, Grand Junction, CO, USA

OPEN ACCESS

Edited by:

Michel Genard,
Institut National de la Recherche
Agronomique, France

Reviewed by:

Panagiotis Kalaitzis,
Mediterranean Agronomic Institute of
Chania, Greece
Youssef Rouphael,
University of Naples Federico II, Italy

*Correspondence:

Athanassios Molassiotis
amolasio@agro.auth.gr

Specialty section:

This article was submitted to
Crop Science and Horticulture,
a section of the journal
Frontiers in Plant Science

Received: 05 August 2016

Accepted: 26 October 2016

Published: 10 November 2016

Citation:

Karagiannis E, Tanou G, Samiotaki M, Michailidis M, Diamantidis G, Minas IS and Molassiotis A (2016) Comparative Physiological and Proteomic Analysis Reveal Distinct Regulation of Peach Skin Quality Traits by Altitude. *Front. Plant Sci.* 7:1689.
doi: 10.3389/fpls.2016.01689

The role of environment in fruit physiology has been established; however, knowledge regarding the effect of altitude in fruit quality traits is still lacking. Here, skin tissue quality characters were analyzed in peach fruit (cv. June Gold), harvested in 16 orchards located in low (71.5 m mean), or high (495 m mean) altitudes sites. Data indicated that soluble solids concentration and fruit firmness at commercial harvest stage were unaffected by altitude. Peach grown at high-altitude environment displayed higher levels of pigmentation and specific antioxidant-related activity in their skin at the commercial harvest stage. Skin extracts from distinct developmental stages and growing altitudes exhibited different antioxidant ability against DNA strand-scission. The effects of altitude on skin tissue were further studied using a proteomic approach. Protein expression analysis of the mature fruits depicted altered expression of 42 proteins that are mainly involved in the metabolic pathways of defense, primary metabolism, destination/storage and energy. The majority of these proteins were up-regulated at the low-altitude region. High-altitude environment increased the accumulation of several proteins, including chaperone ClpC, chaperone ClpB, pyruvate dehydrogenase E1, TCP domain class transcription factor, and lipoxygenase. We also discuss the altitude-affected protein variations, taking into account their potential role in peach ripening process. This study provides the first characterization of the peach skin proteome and helps to improve our understanding of peach's response to altitude.

Keywords: antioxidants, peach [*Prunus persica* (L.) Batsch] fruit, proteins, elevation, ripening

INTRODUCTION

During the ripening of peach fruit [*Prunus persica* (L.) Batsch], coordinated genetic and biochemical events occur that result in changes to texture, flavor, aroma, and color in both exocarp (skin) and mesocarp (flesh) tissues. Despite significant progress in illuminating the regulation of peach mesocarp ripening (Prinsi et al., 2011; Reig et al., 2015; Desnoues et al., 2016; Tadiello et al., 2016), knowledge regarding the metabolic shifts that underlie skin ripening is still lacking. Skin

is of particular interest as this tissue is metabolically active during development and ripening, since it plays a central role in the synthesis of many compounds of interest (e.g., anthocyanins and aroma volatiles) (Tuan et al., 2015). The skin also constitutes a physical barrier between the external environment and the inner tissues, and its integrity is a key factor in preventing damage by physical injuries and pathogen attacks (Deytieux et al., 2007; Pilati et al., 2014).

Environmental factors, such as night/day temperature and wavelengths of ambient light or even a combination between all these parameters, can uncouple the processes of peach ripening (Reig et al., 2015). The majority of these factors are firmly associated with altitude; thus, altitude is one of the most crucial parameters that are involved in the final quality of fruits (Ziogas et al., 2010). Despite the fact that studies on the impact of environment in fruit skin biology will broaden our knowledge in fruit ripening, the role of environmental stimuli, such as altitude is yet to be understood (Leida et al., 2012).

Given the complexity of the ripening process, the use of post genomic tools that allow the global evaluation of the molecular processes triggered within the fruit is particularly important (Molassiotis et al., 2013). Metabolic studies on peach fruit ripening showed that amino acid levels decreased, coupled with the elevation of transcripts involved with amino acid and organic acid catabolism during ripening stage, consistent with the mobilization of amino acids to support respiration (Lombardo et al., 2011). Microarray transcriptome profiling identified several putative peach ripening-related genes belonging to several families including MADS-box, AUX/IAA, bZIP, bHLH, Myb (Trainotti et al., 2006), ethylene biosynthesis/signaling (ACS1, ACO1/ETR1, ETR2), and cell wall metabolism (PG and EXP2) (Ziliotto et al., 2008; Wang et al., 2013). Recently, it was also proposed that CTG134 gene, a precursor of a peptide hormone of the RGF/GLV, regulates ethylene-auxin cross-talk during peach fruit ripening (Tadiello et al., 2016). Given that the proteome is closer to the fruit phenotype than is the genome or the transcriptome along with the fact that it is more directly responsive to environmental stimuli (Chan, 2012), proteomic analysis provides a comprehensive view of fruit's adaptation to different environments. Almost all past proteomic studies of peach fruit were focused on mesocarp tissue (Lara et al., 2009; Nilo et al., 2010, 2012; Hu et al., 2011; Prinsi et al., 2011; Zhang et al., 2011; Giraldo et al., 2012); whereas research concerning skin proteome as an isolated component during peach ripening have not been reported yet.

On the basis of the evidence summarized above, we hypothesized that the altitude would significantly influence the ripening behavior of the peach fruit skin tissue. Thus, the first step of the present work was designed to characterize the impact of altitude on peach skin physiology. We show that high altitude regulates the pigmentation and the antioxidant dynamic of skin tissue. At the second step of analysis, two-dimensional gel electrophoresis (2-DE-PAGE) together with liquid chromatography-tandem mass spectrometry (LC-MS/MS), were employed to study the changes in protein profiles between low and high altitude orchards. The physiological and

biochemical implications of these skin proteins were discussed in the context of peach fruit ripening syndrome.

MATERIALS AND METHODS

Fruit Material, Sampling Strategy, and Quality Traits

In order to investigate the effect of altitude in peach fruit quality, skin tissue samples of the cultivar (cv) "June Gold" were collected at commercial harvest from 16 independently managed orchards at 2012 year in two regions with significant difference in altitude. The first group of 8 orchards was located at Meliki (Imathia, North Greece) at about 71.5 m (mean) altitude (defined as low altitude), and the second group of 8 orchards located at Velvedos (Kozani, North Greece) at about 495.7 m (mean) altitude (defined as high altitude). During the ripening period, the climate data (day/night temperature and relative humidity) of the two altitude regions were recorded (**Supplementary Figure S1**). All orchards consisted of 6–8-year old trees, planted at 5 × 5 m spacing between rows and along the row, grafted onto GF-677 rootstock, trained in open vase and subjected to standard cultural practices for peach production. Fruit samples were harvested and analyzed immediately after harvest and subsequently skin and flesh tissues were frozen with liquid nitrogen and stored at –80°C for further analysis.

Peach fruit were harvested from each orchard at the commercial mature pre-climacteric stage, based on ground color and fruit firmness and divided into 8 lots (orchards) of 40 fruits for each growing altitude. Harvest quality evaluation included subjunctive and objective analysis of skin color, and objective analysis of fruit firmness, soluble solids concentration (SSC), and titratable acidity (TA). Skin foreground (darkest red) and background color on two opposite sides of each fruit were measured objectively using a colorimeter (Konica Minolta CR200 Chroma Meter, Konica Minolta Sensing, Inc., Osaka, Japan) and the CIE (Commission Internationale de l'Eclairage) parameters (L^* , a^* , b^*), as previously described (Goulas et al., 2015). The percentage of red-blushed surface was subjectively estimated as the percentage of red overcolor on the total peach surface. Fruit firmness (kg), titratable acidity (TA, malic acid, %) and soluble solids content (SSC, %) of the peaches were measured according to procedure described in detail elsewhere (Minas et al., 2016). Furthermore, skin samples from two selected orchards (7 years old trees with GF-677 as rootstock) from low and one from high altitude region (situated 50 and 550 m above sea level; herein named as low- and high-altitude reference orchards, respectively) were used for both DNA nicking and proteomic analysis.

Anthocyanins and Carotenoids (β -Carotene Equivalent) Determinations

Peach outer pericarp (skin) anthocyanins at commercial harvest stage were extracted with 80% ethanol + 1% HCl, as described by Giusti and Wrolstad (2005). The content of anthocyanins was determined by the pH differential method (Wolfe et al., 2003) and results were expressed as $\mu\text{g g}^{-1}$ fresh weight (FW). β -Carotene extracts were prepared using 1 or 2.5 g (skin or flesh) by adding

hexan: Acetone: Ethanol (50:25:25 v/v) and incubation for 24 h at 5°C in darkness. β-Carotene concentration was calculated in both flesh and skin tissues through the absorbance at 450 nm (Kuti, 2004).

Total Phenols, Flavonoids, and Total Antioxidants Assays

Flesh and skin tissues at commercial harvest stage were extracted following conditions previously described (Asami et al., 2003). Total phenols content was determined by the reaction of the extract with the Folin-Ciocalteu reagent (Asami et al., 2003) and results were expressed as µg gallic acid equivalent (GAE) g⁻¹ FW. Total flavonoids concentration was assayed in skin tissues as reported by Cvek et al. (2007), using catechin as standard and results expressed as µg catechin g⁻¹ FW. Total antioxidant activity was determined in flesh and skin tissues using three different methodologies. The ferric reducing antioxidant power (FRAP) assay was performed according to Benzie and Strain (1996). The antioxidant potential of the extracts was determined from a standard curve using trolox as equivalent and expressed as µg Trolox g⁻¹ FW. The 2,2'-azino-bis-3-ethylbenzthiazoline-6-sulphonic acid (ABTS) free radical scavenging activity of sample was evaluated as reported by Re et al. (1999). Aqueous solution of trolox was used for the calibration curve and the results were expressed as µg Trolox g⁻¹ FW. The 1,1-diphenyl-2-picrylhydrazyl (DPPH) assay was determined according to Brand-Williams et al. (1995). An aqueous solution of Trolox was used for the calibration curve and the results were expressed as µg Trolox g⁻¹ FW.

DNA Protection Assay

The ability of skin extracts to protect the plasmid DNA from the destructive effects of hydroxyl radicals (•OH) was assessed by the DNA nicking assay described by Hu and Kitts (2001). For evaluating •OH-induced oxidative breakage generated by Fenton's reagent, samples from a reference low- and high-altitude orchards (with 50 and 550 m altitude, respectively) were collected at four distinct developmental stages (S2, green; S3, yellow-green; S4I, commercial harvest/pre-climacteric phase; S4II, tree-ripe/climacteric phase) based on the double sigmoidal fruit growth curve (data not shown). The reaction mixture contained 0.5 µg of supercoiled pBR322 plasmid DNA, 12 µL of Fenton's reagent (16.2 mM H₂O₂, 3.6 mM ascorbic acid and 36 mM FeCl₃) followed by the addition of skin phenolic extracts (100 µM GAE) and the final volume of the mixture was brought up to 20 µL using double-distilled water. The reaction mixtures were allowed to incubate for 30 min at 37°C. Agarose gel electrophoresis and ethidium bromide staining was conducted according to Ziogas et al. (2010). The supercoiled (SC), open circular (NC; after a single-strand break), and linear (NL; after double-strand break) forms of plasmid DNA were visualized using UV transilluminator system. The Image J software (National Institutes of Health, NIH) was used to quantify DNA strand breaks compared to the intensity of the supercoiled DNA. The assay was run in triplicate and averaged.

Two-Dimensional Gel Electrophoresis, Protein Visualization, and Image Analysis

Skin tissue samples from reference low- and high-altitude orchards (with 50 and 550 m altitude, respectively) at the commercial harvest stage were ground in liquid nitrogen with a pestle and mortar and soluble skin proteins were extracted through a phenol-based extraction protocol. Total proteins were extracted from 4 g of each homogenized sample with 5 mL extraction buffer containing 100 mM Tris-HCl pH 8.8, 20 mM DTT, 1 mM PMSF, 0.5% Triton X-100, 5 mM EDTA, 30% saccharose, and Complete Mini protease inhibitor cocktail tablet (Roche Molecular Biochemicals) (Tanou et al., 2009). An equal volume of phenol-Tris saturated was added and the protein extracts were stirred for 20 min at 4°C and centrifuged at 15000 g for 10 min at 4°C. Following the phenolic phase collection, a 5:1 cold 0.1 M ammonium acetate (dissolved in methanol) was added and the samples kept at -20°C overnight. After centrifugation (10000 g, 10 min, 4°C), the precipitated protein pellet was washed one time with ice-cold ammonium acetate, three times with ice-cold 70% acetone and subsequently was dried at a Thermoblock (Thermo Block 780). The proteins were resolubilized in rehydration buffer containing 42% Urea (w/v), 15.2% Thiourea (w/v), 4% CHAPS (w/v), 0.5% Triton X-100 (v/v), 0.3% DTT (w/v), and 0.5% ampholyte (v/v). Protein concentrations were measured according to Bradford (1976), using a Bio-Rad protein assay kit (Kit II, cat. n. 500-0002). Bovine serum albumin (Sigma) was used as a standard.

Samples' aliquots containing 50 µg proteins were loaded onto 11 cm pH 3-10 non-linear IPG strips, and isoelectric focusing was performed on a PROTEAN IEF Cell system (BIO-RAD) for a total of 35000 Vh at 20°C. Subsequently, the strips were equilibrated with 1.11% (w/v) DTT and afterwards with 4% (w/v) iodoacetamide in equilibration buffer containing Urea (36%), SDS (2%), 1.5 M Tris-HCl pH 8.8 (3.3%), and Glycerol (30%). Following equilibration, the strips were loaded on 12.5% Tris-HCl 1.0 mm Criterion™ PreCast (BIO-RAD) gels on a Criterion Dodeca™ Cell (BIO-RAD) device. Following the procedure of silver nitrate staining (Tanou et al., 2010), 2DE-gels were scanned with Bio-Rad GS-800 Calibrated Densitometer equipped with PDQuest Advanced 2-D Gel Analysis Software. Statistical analysis was done by one-way analysis of variance significance ($P \leq 0.05$) and individual means were compared using student's *t*-test (significance level 95%). The statistical significant differences further combined by the quantitative 1.5 fold change of spot volume (Supplementary Table S3). At least three biological replicates were performed for each treatment.

LC-MS/MS Analysis

Selected gel spots, with differential intensity, were subjected to tryptic in-gel digestion and analyzed by LC-MS/MS using a LTQ Orbitrap XL Mass spectrometer (Thermo Fisher Scientific, Bremen, Germany) coupled online with a nanoLC Ultimate 3000 chromatography system (Dionex, Sunnyvale, CA), as described in detail by Ainalidou et al. (2016). Raw files were searched against the Uniprot *Prunus persica* protein database (downloaded 21/1/2014) containing 28650 protein sequences using the

SequestHT software. Protein identification required minimal XCorr values of 2.0, and 2.5 for charge states of doubly, and triply precursor ions. To validate protein identification with one single peptide (spot 8033 at **Supplementary Table S3**) additional information are provided in **Supplementary Figure S3**.

Bioinformatics Analysis

To obtain additional protein information for subsequent functional validation, all of the differentially expressed proteins were subjected to a global protein network analysis using STRING tool (version 10) (<http://string.embl.de/>) (Szklarczyk et al., 2011). This tool was applied to predict protein—protein interactions based on both physical and functional associations by querying the list of proteins through multiple resources, including (a) experimentally confirmed interactions, (b) pathway knowledge from curate databases, (c) automated text-mining based on Medline/PubMed abstract and full-text articles, (d) predicted interactions using genomic information and co-expression analysis, and (e) interactions that were observed in one organism and then transferred to others (Szklarczyk et al., 2011). Since protein identification was based upon different organisms listed in the National Center for Biotechnology Information (NCBI) Viridiplantae database, all identified peach proteins were blasted against the *Arabidopsis thaliana* TAIR10 (The *Arabidopsis* Information Resource) protein database (<http://www.arabidopsis.org/>) with the intention of obtaining annotated protein entries for PPI tools. Results with the highest score and lowest E value were considered as relevant for each identified peach protein (**Supplementary Table S2**).

Statistical Analysis

For the physiological data, Student's *t*-test (using three replicates) at 5% level of significance was prepared by using the statistical package SPSS 12.0 (SPSS Inc., Chicago, USA). Pearson's correlation coefficients and principal component analysis (PCA) were performed to obtain an overview of correlation among fruit quality traits and protein function categories.

RESULTS AND DISCUSSION

The Phenotype of Peach Skin is Remarkably Affected by Altitude

Peach fruit, particularly skin tissue, undergo a broad metabolic reprogramming and definitive specialization during fruit ripening that involves internal signals refined by environmental cues (Frett et al., 2014). Nonetheless, no previous work has determined the impact of environmental factors in peach skin biology. Herein, we characterize the relationship between altitude and peach fruit quality and physiology using various parameters. Peach sampled at commercial harvest stage from sixteen orchards located at two environmental conditions had similar firmness (**Figure 1B**), SSC (**Figure 1C**), and TA (**Figure 1D**), which are considered suitable indicators of the peach ripening status (Iglesias and Echeverría, 2009). This indicates that at this stage both environmental-based types of peach fruit were at the same physiological status and the various quality differences can be mainly attributed to the environment

without alterations owing to adequate ripening stage. From the presented phenotypical data it was clear that peach fruit altered their physiognomy in response to the two different regions (**Figure 1A**). The first physiological response was the modulation of skin color parameters, such as lightness (*L**) and redness (*a**) (**Figures 1E,G**). In support, the percentage (%) of red-blushed surface of peach skin was almost doubled (84.5%) in the high altitude environment (**Figure 1E**), which agrees with the notion that the red coloration in other fruit species is stimulated by the growing altitude (Espley et al., 2007).

High-Altitude Environment Induce Antioxidant Activity and Pigmentation in Peach Fruit Skin

Previous studies indicated that the fruit skin pigmentation is linked with the biosynthesis of health promoting bioactive substances (Butelli et al., 2008). In the present study, the total antioxidant activity, assessed with three different assays (FRAP, ABTS, and DPPH assays) (**Figures 2A–C**) together with the total phenols content (**Figure 2D**), were not significantly differed in the flesh tissue between the low and high altitude areas. The same trend was also described by Montelevecchi et al. (2012) in various peach cultivars grown at difference landraces. However, the antioxidant capacity (evaluated by FRAP and ABTS assays) and the total phenols content were induced in skin tissue by the high altitude (**Figures 2A,B,D**). Another interesting finding in this work is the activation of pigments biosynthesis by high altitude in the skin tissue, as evidenced by the accumulation of carotenoids (β -carotene equivalent) (**Figure 2F**), total flavonoids (**Figure 2E**) and particularly anthocyanins (**Figure 2G**), suggesting that environmental factors at a higher altitude, such as low temperature (**Supplementary Figure S1**), favored pigments biogenesis in peach fruit, as already proposed in apple (Espley et al., 2007; Lin-Wang et al., 2011). All these differences between the two growing regions could be a result of specific modifications at ambient light, UV radiation, day length, temperature difference between day and night, or even a combination between all these parameters that affect fruit physiology. Thus, further research is needed to unravel the specific function of these climatic factors in peach fruit quality.

Interaction between Fruit Development Stage and Altitude Provides Different Perspectives on Peach Skin-Derived DNA Oxidation Properties

The substantial differences in antioxidant behavior observed in fruit skin of the two altitudes at harvest (**Figures 2A,B**) prompted us to study the relative protective effect of skin phenolic extracts at different developmental stages and altitudes on DNA strand cleavage by \bullet OH (**Figure 3**). DNA nicking in-gel assay (**Figure 3A**) and quantitative analysis (**Figure 3B**) of intact and oxidized DNA showed that no differences exist in the ability of skin extracts from the two altitudes to protect DNA from oxidation at yellow green (YG) and tree ripe (TR) stages. Low altitude-derived skin extracts in the green stage (G) had lower ability to protect DNA from breakage (**Figure 3B**), as visualized

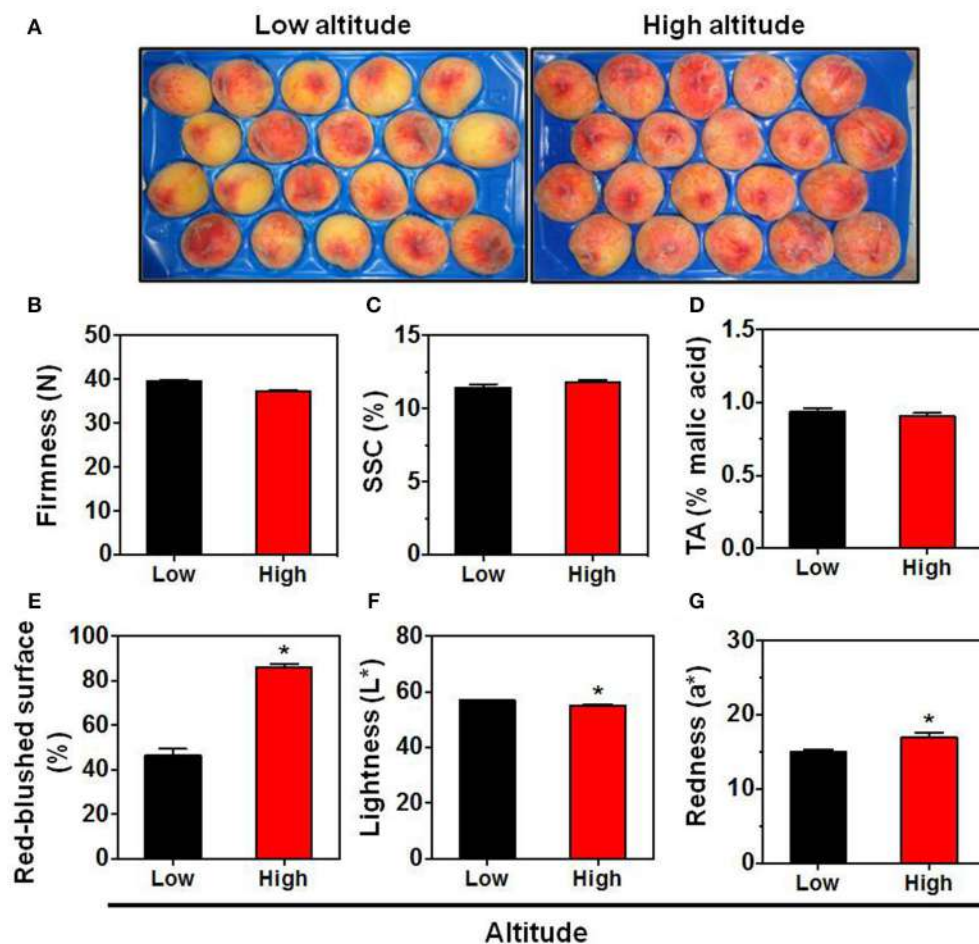


FIGURE 1 | Phenotype (A), firmness (B), soluble solids concentration (SSC) (C), titratable acidity (TA) (D), red overcolor coverage (E), skin lightness (L^*) (F), and skin redness (a^*) (G) of “June Gold” peaches. Fruit were collected at commercial harvest stage from 16 independently orchards that located in two regions with low altitude (8 orchards; mean 71.5 m) and high altitude (mean 495.7 m). For each orchard, the fruit were divided into 8 replicates, each with 5 fruit. The values shown are the mean \pm SD. Bars with asterisk are significantly different at $P = 0.05$ (Student’s t -test).

by the accumulation of open circular (NC) and linear (NL) forms, compared with the corresponding samples from the high altitude (Figure 3A). On the other hand, it was observed that commercial harvest (CH) stage-extracted phenols from low altitude exhibited relative higher protection against \bullet OH-induced DNA damage (Figures 3A,B), providing proof that the ripening stage and the altitude had a significant role in the production of phytochemicals responsible for DNA protection. It is noteworthy that there was no strict correlation between the ability of phenolic extracts to inhibit DNA damage (Figures 3A,B) and the phenols content (Figure 2D), an observation that was also noted in olive fruit by Ziogas et al. (2010).

Identification of Peach Skin Proteins Affected by Low- and High-Altitude Environment

To analyze the cellular basis underpinning the phenotypes observed in peach fruit that cultivated in the different

environments (Figure 1A), a proteomic analysis of “June Gold” peach skin samples at commercial harvest stage was performed. Through 2-DE analysis, 850 spots were detected, 38 of which were modified under the different environmental conditions based on the Student’s t -test and further validated by the 1.5 fold threshold change (Supplementary Table S1). Those spots were excised; trypsin digested, and analyzed by nano-LC-MS/MS. Representative spots are magnified and labeled in Figures 4A,B. LC/MS-MS analysis identified 42 proteins that were sorted into eight functional classes according to Bevan et al. (1998). The basic information of the identified proteins are listed in Table 1 (detailed information are provided at Supplementary Table S3), such as protein name, score, molecular weight, pI, unique peptides. Identified proteins in more than one protein spots suggest that a small number of different spots expressed or undergo post-translation modifications. Such proteins were adenine nucleotide hydrolase (two protein spots), agglutinin (two protein spots), and phosphomannomutase (two protein spots). The accumulation of many proteins has been changed

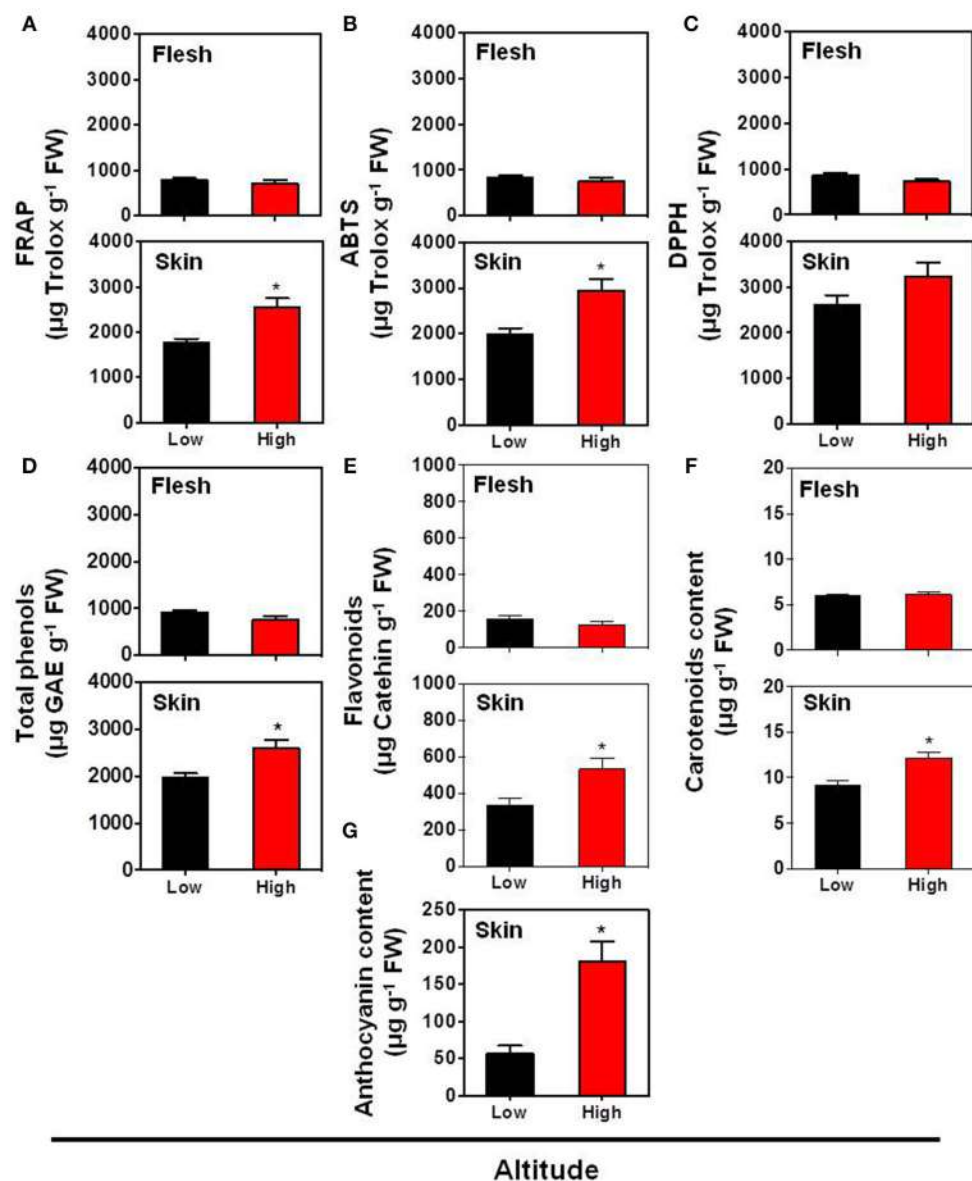


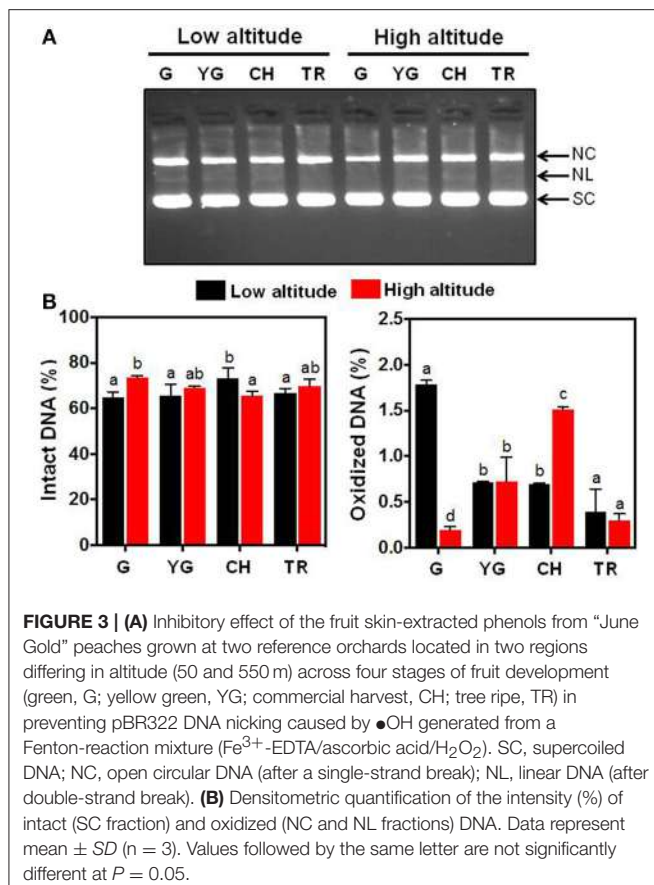
FIGURE 2 | Impact of altitude on the antioxidant capacity according to FRAP assay (A), ABTS assay (B), DPPH assay (C), as well as on the contents of total phenols (D), flavonoids (E), carotenoid (F), and anthocyanin (G) in the skin and flesh tissues of “June Gold” peaches. Additional experimental details as described in Figure 1. The values shown are the mean \pm SD. Bars with asterisk are significantly different at $P = 0.05$ (Student’s *t*-test). Data are means of values obtained from eight biological replicates, each with 5 fruits.

(increased or decreased) in response to different altitudes (Table 1). Differently expressed proteins belonged to different metabolic pathways, including 11 proteins associated with defense, followed by main/primary metabolism (9 proteins), destination and storage (8 proteins), energy (5 proteins), secondary metabolism (5 proteins), signal transduction (2 proteins), H^+ transporters (1 protein), and one protein with unknown biological function (Figure 5). The identified proteins were detected in nine (9) different parts of the cell, including chloroplast (50.0%), cytoplasm (21.4%), mitochondrion (7.1%), cytosol (7.1%), cell wall (4.8%), vacuole (2.4%), nucleus

(2.4%), endoplasmic reticulum (2.4%), and peroxisome (2.4%) (Supplementary Figure S2).

Characterization of Quality Traits and Protein Changes by Principal Component Analysis

Principal component analysis has been previously used to monitor the quality characteristic of peach fruit (Cantín et al., 2010). In this work, PCA was applied in order to determine the possible relationships between quality and proteomic data



in response to different environmental conditions (Figure 6). It is evident that the altitude affected several parameters that were studied in the current experiment. Particularly, three groups of variables (Group 1; total phenols, FRAP, ABTS, flavonoids, Group 2; proteins related to sugars/amino acids metabolism and secondary metabolism, Group 3; proteins involved in energy and detoxification) that displayed correlation coefficients above 0.99 were presented by the first part of each group based on Pearson's correlation coefficient (Supplementary Table S4). PCA analysis of low and high altitude was demonstrated by two interpretable factors that described about 79.1% of the total variation in the samples (61.3% for PC1 and 17.8% for PC2) (Figure 6). PC1 was more closely linked to the most of the protein functions as well as to color and to antioxidant-related traits; the first two were positively connected while the third negatively. PC2 was strongly associated with proteins that involved in the metabolism of lipids and sterols showing higher value inversely to hydroxycinnamic acids. Altitude was distributed on PC1, in which the negative values were represented by an increase in antioxidant-related parameters at high altitude. On the other hand, low altitude was positively associated with the induction of specific protein categories, such as signal, transporters and stress response, as well as with fruit color features, such as Hue angle and lightness (Figure 6). To our knowledge this is the first study that relates proteomic features of peach fruit tissue with its quality characteristics and response to altitude.

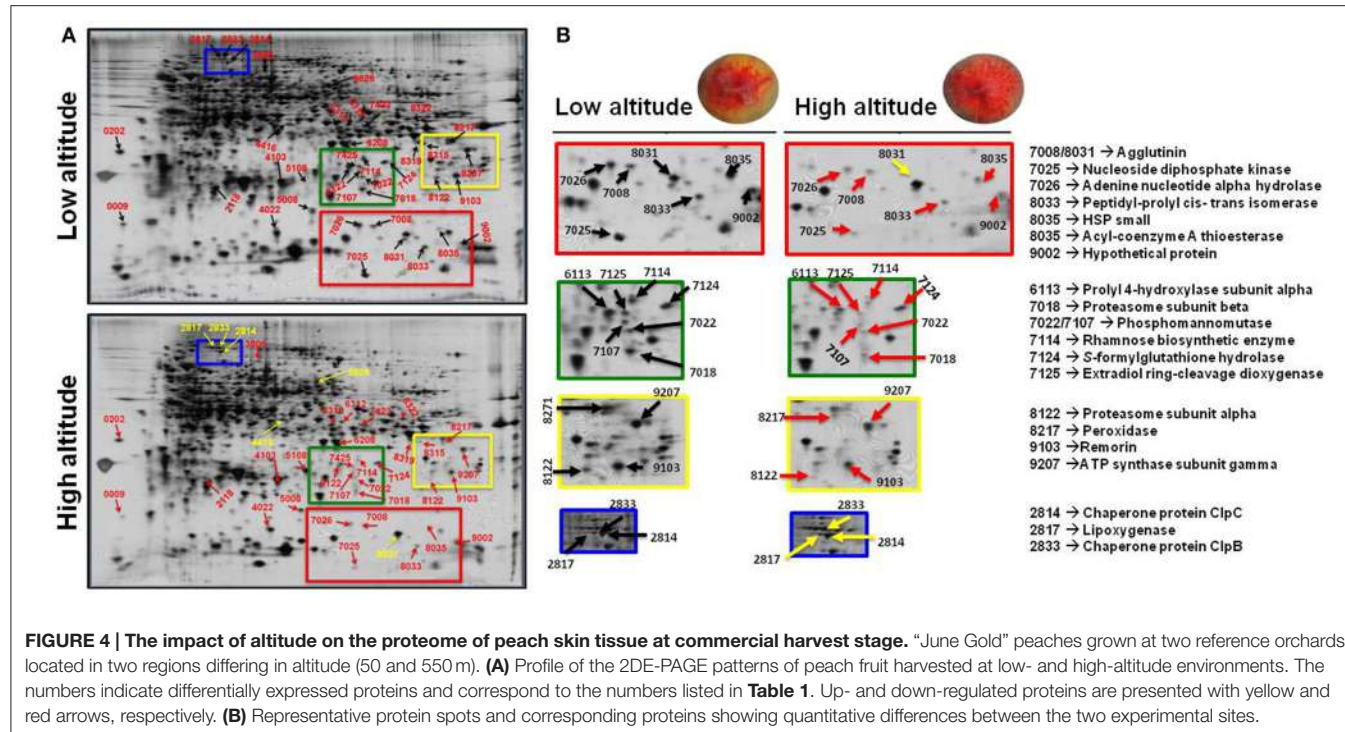
Global Protein Network Analysis

STRING tool (version 10) (Szklarczyk et al., 2011) was used in order to obtain additional protein information for subsequent functional validation of the identified proteins. The software is directed to a database of known and predicted protein—protein interactions, which could be direct (physical) or indirect (functional) associations. The database retrieved such information from four major sources, including genomic information, previous experiments, co-expression, and existing knowledge (<http://string.embl.de/>). Interestingly, using this tool in an unbiased manner (without any additional inputs except only for protein identification number or gene symbol), the data analysis depicted that plenty of protein—protein interactions occurred in our study model as presented at Figure 7.

The Physiological Function of Altitude-Affected Skin Proteins in Peach Fruit Ripening Behavior

Fruit cells employ a suite of complex mechanisms to activate acclimation processes in response to environmental factors that can be functionally categorized based on their recognition and signaling events (Molassiotis et al., 2013). An important point of the current proteomic analysis was the wide-spread up-regulation of protein abundance in response to low-altitude environment. Indeed, it was observed that 32 proteins were up-regulated at the low altitude region (Table 1), indicating that peach fruit is able to adapt the proteomic dynamic to environmental conditions, thus leading to phenotypic changes (Figure 1A). The oxidative stress is one of the major signaling pathways utilized by skin tissue to transduce extracellular stimuli into intracellular responses at the onset of fruit ripening (Pilati et al., 2014). The accumulation of glutathione-ascorbate cycle-associated enzymes, such as ascorbate peroxidase, peroxidase, and glutathione in peach grown at low altitude orchard could be associated with the elevated level of ROS, justifying the role of oxidative stress in peach fruit ripening (Prinsi et al., 2011; Nilo et al., 2012).

The fact that the antioxidant proteins were down-regulated at high altitude environment led us to hypothesize that this growing environment resulted in minimal requirement of such proteins. Antioxidant-defense proteins might be down-regulated due to the general induction of the non-enzymatic antioxidants (Figures 2A–D) and the stimulation of pigments (Figures 2E–G) that possess anti-oxidative activity (Butelli et al., 2008). Consistent with this, proteins involved in defense, such as plastid-lipid associated protein (fibrillin family protein), adenine nucleotide alpha hydrolase, annexin, agglutinin, and S-formylglutathione hydrolase were exclusively up-regulated at low altitude (Table 1), thus emphasizing the relevance of skin tissue as a physical barrier exerting an important part in peach fruit protection. The accumulation of plastid-lipid associated protein seems to be a ripening regulatory mechanism at low altitude grown fruits, as this protein is involved in carotenoid storage into fruit chromoplasts and induced upon high light (Rey et al., 2000), as obviously occurs at low altitude. The up-regulation of annexin (Table 1) in low altitude-grown peach fruits is in agreement with



the observation that this protein act as sensor for heat-stress responses in plant cells (Wang et al., 2015). Alternatively, annexin could serve as a signal to regulate ripening or to be involved in exocytosis of cell wall-degrading enzymes, acting to sequester Ca^{2+} released from the degrading cell wall matrix, as previously proposed in strawberry and kiwifruit (Bianco et al., 2009; Tanou et al., 2015). Particularly relevant is also the up-regulation of S-formylglutathione hydrolase (FGH) in fruit challenged by low altitude (**Table 1**). FGH catalyzes the glutathione-dependent formaldehyde oxidation to formic acid which is then converted to carbonic acid or enters one-carbon cycle. Formaldehyde is a toxic compound produced in one-carbon cycle metabolism and can also arise from methanol oxidation during pectin demethylation (Gharechahi et al., 2015). Therefore, FGH might be involved in the acclimation of oxidative stress situation during peach ripening at low altitude conditions.

Fruit have developed effective acclimation mechanisms to cope with environmental conditions encountered at almost every stage of their development (Molassiotis et al., 2013). Peach fruit grown during the summer at low altitudes require more energy to adapt in high temperature (Reig et al., 2015). We observed that the abundance of various energy-related proteins was increased at low altitude environment. In particular, the up-regulation of fructose bisphosphate aldolase, pyruvate dehydrogenase and 6-phosphogluconolactonase at low altitude area (**Table 1**) suggested that the interaction among these proteins exerts a positive effect on the glycolytic, TCA cycle and pentose-phosphate pathways, inducing energy generation in fruit cell (Tanou et al., 2015). In addition to these energy-related enzymes, several electron transfer-associated proteins were increased

at low-altitude environment. More specifically, the increased accumulation of NADH dehydrogenase (ubiquinone) and electron transfer flavoprotein subunit beta—a specific electron acceptor for dehydrogenases—along with the up-regulation of ATP synthase subunit gamma (**Table 1**) suggests that it would promote respiration burst and catabolic metabolism, such as redox regulation and energy accumulation in peach fruit.

Evidence defines the deep changes in sugar metabolism as a regulatory system for peach fruit ripening (Prinsi et al., 2011; Nilo et al., 2012; Desnoues et al., 2016). Among the over-expressed proteins at low altitude, the phosphomannomutase (PMM) was identified (**Table 1**). PMM catalyzes the interconversion between mannose-6-phosphate and mannose-1-phosphate that required for the synthesis of GDP-mannose, an intermediate in the biosynthesis of major cell wall polysaccharides (Mabeau and Kloareg, 1987) and also in ascorbate biosynthesis (Qian et al., 2007). An increase in the synthesis of precursors of cell wall polysaccharides, which are known to directly involved in fruit ripening (Tanou et al., 2015), might provide a mechanism to increase the buffering capacity of skin cell wall. Also, an induction in ascorbate synthesis is consistent with the need for the action of ascorbate-glutathione cycle at low altitude-exposed peach, as discussed above. Meanwhile, the induction of rhamnose biosynthetic enzyme at low altitude (**Table 1**) probably indicates that the skin tissue during ripening exhibits a loss in its capacity to convert the newly synthesized polyuronides to a more tightly bound form compared to high-altitude environment.

Two proteins were identified in skin as heat shock proteins (HSPs), i.e., a HSP20 and a small HSP (18.5 kDa class I heat shock protein). The induction of these HSPs (also called “molecular

TABLE 1 | List of peach (cv. "June Gold") skin proteins at commercial harvest stage identified by LC-MS/MS in fruits cultivated in the low- and high-altitude reference orchards.

Spot No. ^a	Protein name	Acc. No. ^b	U/D ^c	Functional categories ^d	Coverage ^e (%)	Score ^f	MW [kDa] ^g	Calc. pI ^h	Unique Peptides No. ⁱ
9	Elicitor-responsive protein	M5X0Z3	D	10.99-Signal Transduction/Others	15.43	16.80	19.1	4.27	2
202	Plastid-lipid associated protein PAP/fibrillin family protein isoform	M5WMK2	D	11.05-Disease/Defense/Stress responses	10.20	7.49	37.8	4.81	3
2118	GDSL esterase/lipase CPRD49 isoform	M5XRT2	D	01.06-Metabolism/Lipid and sterol	20.31	11.37	28.6	5.45	4
2814	Chaperone protein ClpC	M5WCY0	U	06.01-Protein destination and storage/Folding and stability	13.90	58.80	102.0	6.73	11
2817	Lipoxygenase	M5X5W8	U	01.06-Metabolism/Lipid and sterol	27.50	53.67	89.8	5.62	15
2833	Chaperone protein ClpB	M5WSD5	U	06.01-Protein destination and storage/Folding and stability	6.83	19.34	110.3	6.51	7
3806	NADH dehydrogenase [ubiquinone] iron-sulfur protein	M5WWP9	D	02.20-Energy/Electron-transport	25.41	68.07	85.8	6.83	15
4022	Adenine nucleotide alpha hydrolase	M5VKC1	D	11.05-Disease/Defense/Stress responses	20.11	7.31	19.3	6.29	3
4103	Ascorbate peroxidase	M5VZU3	D	11.06-Disease/Defense/Detoxification	65.20	71.83	27.3	6.16	10
4416	Pyruvate dehydrogenase E1 component subunit alpha	M5XCJ6	U	02.30-Energy/Photosynthesis	22.45	30.41	47.6	7.02	7
5008	Glutathione peroxidase	M5WAJ5	D	11.06-Disease/Defense/Detoxification	8.86	5.76	25.9	9.09	2
5108	6-phosphogluconolactonase	M5X1U6	D	02.07-Energy/Pentose phosphate	6.71	12.43	34.1	8.75	2
6113	Prolyl 4-hydroxylase subunit alpha	M5XS77	D	20.99-Secondary metabolism/Others	7.07	7.60	33.0	6.71	2
6208	Annexin	M5W098	D	11.05-Disease/Defense/Stress responses	18.99	17.88	35.9	6.64	5
6310	HSP20	M5XEL2	D	06.01-Protein destination and storage/Folding and stability	9.12	10.76	33.8	6.46	3
6312	Sinapyl alcohol dehydrogenase	M5WBG4	D	20.1-Secondary metabolism/Phenylpropanoids/Phenolics	36.74	100.43	38.9	6.76	11
6626	TCP domain class transcription factor	M5X5S1	U	06.01-Protein destination and storage/Folding and stability	28.22	86.43	59.2	6.49	13
7008	Agglutinin	M5WR60	D	11.02-Disease/Defense /Defense-related	54.09	35.22	17.9	6.34	6
7018	Proteasome subunit beta	M5XCF1	D	06.13-Protein destination and storage/Proteolysis	51.47	90.69	29.1	5.85	8
7018	Glutathione S-transferase	M5WTZ4	D	11.06-Disease/Defense/Detoxification	41.12	30.88	24.7	6.30	6
7022	Phosphomannomutase	M4QFW7	D	01.05-Metabolism/Sugars and polysaccharides	21.05	50.55	28.1	6.80	5
7025	Nucleoside diphosphate kinase	M5X104	D	01.03-Metabolism/Nucleotides	70.95	101.37	16.5	6.95	8
7026	Adenine nucleotide alpha hydrolase	M5W0J9	D	11.05-Disease /Defense/Stress responses	40.74	15.02	17.8	6.68	5
7107	Phosphomannomutase	M4QFW7	D	01.05-Metabolism/Sugars and polysaccharides	16.19	32.05	28.1	6.80	4
7114	Rhamnose biosynthetic enzyme	M5WBB7	D	01.05-Metabolism/Sugars and polysaccharides	24.08	30.62	33.4	6.57	6
7114	Electron transfer flavoprotein subunit beta	M5XZZ7	D	02.20-Energy/Electron-transport	17.13	29.74	27.5	6.61	6
7124	S-formylglutathione hydrolase	M5W9G4	D	11.06-Disease /Defense/Detoxification	32.06	47.28	32.2	7.08	7
7125	Extradiol ring-cleavage dioxygenase	M5WGS1	D	20.99-Secondary metabolism/Others	31.02	29.07	30.1	6.86	7
7423	Cinnamyl alcohol dehydrogenase	M5WB20	D	20.1-Secondary metabolism/Phenylpropanoids/Phenolics	49.30	61.70	38.4	6.93	12

(Continued)

TABLE 1 | Continued

Spot No. ^a	Protein name	Acc. No. ^b	U/D ^c	Functional categories ^d	Coverage ^e (%)	Score ^f	MW [kDa] ^g	Calc. pI ^h	Unique Peptides No. ⁱ
8031	Agglutinin	M5WNR2	U	11.02-Disease/Defense/Defense-related	69.62	142.10	17.9	7.49	7
8033	Peptidyl-prolyl cis-trans isomerase	M5W6L5	D	06.01-Protein destination and storage/Folding and stability	8.09	2.19	18.2	8.47	1
8035	HSP small	M5WDA5	D	06.01-Protein destination and storage/Folding and stability	33.54	34.49	18.1	8.32	3
8035	Acyl-coenzyme A thioesterase	M5WHT9	D	20.1-Secondary metabolism/Phenylpropanoids/Phenolics	23.13	22.41	17.1	8.09	4
8122	Proteasome subunit alpha	M5VQX2	D	06.13-Protein destination and storage/Proteolysis	32.93	17.84	27.1	7.96	7
8217	Peroxidase	M5W030	D	11.06-Disease/Defense/Detoxification	30.09	67.22	35.6	7.96	8
8217	Uricase	M5WGE6	D	01.99-Metabolism/Others	20.52	44.60	34.8	8.06	6
8315	c-1-tetrahydrofolate synthase	M5VKQ0	D	01.01-Metabolism/Amino acid	14.72	15.51	31.8	7.55	6
8319	Fructose-bisphosphate aldolase	M5W2H9	D	02.30-Energy/Photosynthesis	18.16	28.53	38.4	7.36	6
8322	Class I glutamine amidotransferase	M5WGA9	D	01.01-Metabolism/Amino acid	26.24	75.61	47.2	8.68	13
9002	Hypothetical protein	M5W0H8	D	13 Unclassified	33.13	38.04	18.1	8.29	4
9103	Remorin	M5XKT5	D	10.04-Signal transduction	45.18	56.89	21.8	8.02	10
9207	ATP synthase subunit gamma	M5WB68	D	07.22-Transporters/Transport ATPases	37.77	114.33	35.2	9.04	10

^aSpot No, protein spot number on the reference gel maps presented in **Figure 4A**; ^bAcc. No, Uniprot accession number; ^cU/D, (U; up-regulated protein, D; down-regulated) protein for comparison purposes, low altitude samples served as control; ^dFunctional category, proteins ontologically classified into functional categories proposed by of Bevan et al. (1998); ^eCoverage, percentage of sequence coverage obtained with identified peptides with SEQUEST software for the orthologous protein; ^fScore, SEQUEST score; the sum of all peptide Xcorr values above the specified score threshold; ^gMW, molecular weight; ^hCalc. pl, theoretical isoelectric point; ⁱUni. Pept. No, Number of unique identified peptides.

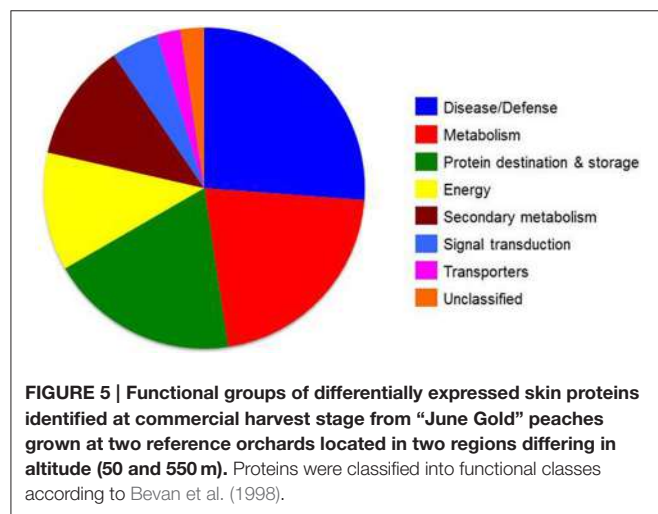


FIGURE 5 | Functional groups of differentially expressed skin proteins identified at commercial harvest stage from “June Gold” peaches grown at two reference orchards located in two regions differing in altitude (50 and 550 m). Proteins were classified into functional classes according to Bevan et al. (1998).

chaperones”) along with the up-regulation of peptidyl-prolyl cis-trans isomerase (**Table 1**), that also act as chaperone (Ou et al., 2001), is interesting because it was suggested that chaperones act as shields protecting proteins against oxidative damage, notably during peach fruit ripening (Nilo et al., 2010). In addition, it is thought that chaperones closely interact with misfolded or damaged proteins to assist their refolding upon environmental stress (Magi et al., 2004). Protein degradation plays an important role in maintaining cellular process by removing misfolded or

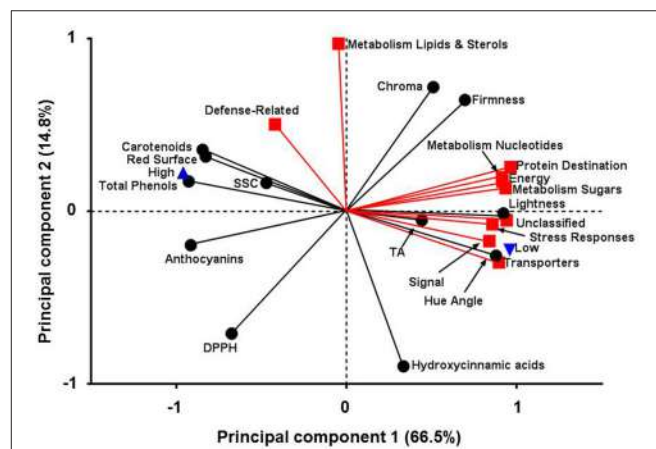
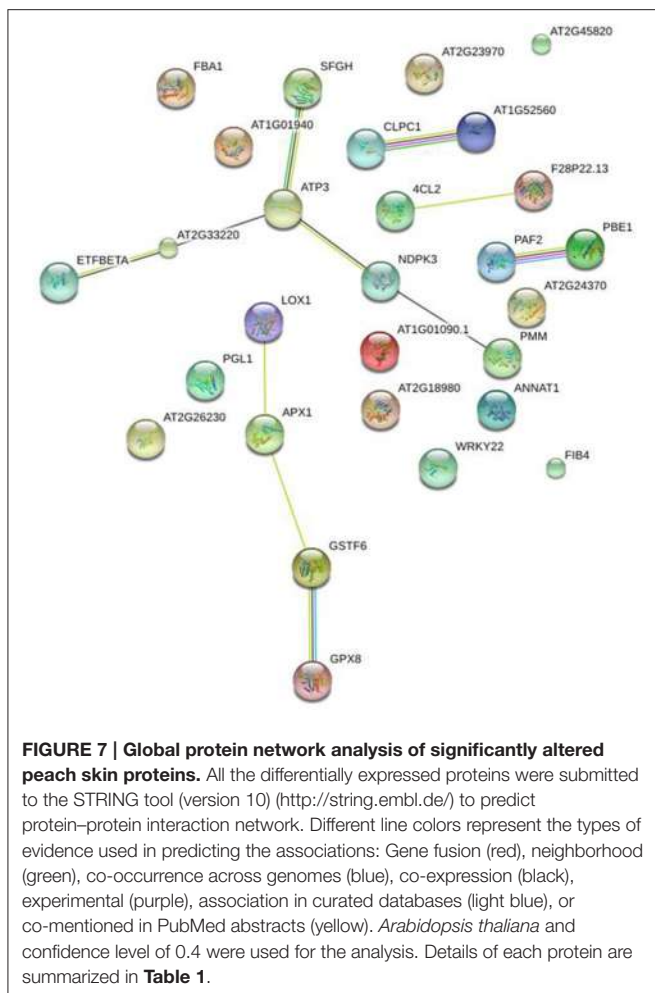


FIGURE 6 | Principal components analysis for fruit quality attributes and protein function categories in peach fruit cultivated in different altitude. First principal component (66.5%) on x-axis and second principal component (14.8%) on y-axis.

damaged proteins and controlling the level of certain regulatory. Two proteins (proteasome subunit alpha and proteasome subunit beta) involved in ubiquitin proteasome system were identified in this study, which were both largely induced by low altitude (**Table 1**). Plant cells use the proteasome pathway to effectively alter their proteome so as to ensure developmental plasticity and environmental adaptation (Stone and Callis, 2007). There



is evidence for involvement of the ubiquitin pathway in stress responses and fruit ripening (Molassiotis et al., 2013). Proteasome-related proteins probably regulate hormone signal transduction pathways, such as ethylene, abscisic acid (ABA) and gibberellins (GA) (Stone and Callis, 2007), thus altering the overall ripening profile.

Several other proteins were identified as low altitude-responsive proteins, including cinnamyl alcohol dehydrogenase (CAD), sinapyl alcohol dehydrogenase (SAD), and remorin (**Table 1**). Both CAD and SAD catalyze the monolignol biosynthesis and contribute to lignin formation. Thus, it seems likely that the up-regulation of CAD and SAD along with an increased accumulation in peroxidase may function to fruit skin against disease and herbivory. Lignin pathway is induced during stress and pathogen attack and/or defense (Dixon and Paiva, 1995) functions to enhance tissue rigidity, decreases digestibility and produce anti-microbial compounds in peach fruit at the ripe stage (Dardick et al., 2010). On the other hand, remorin belongs to a superfamily of plant-specific plasma membrane/lipid raft-associated filamentous proteins; this led to the suggestion that remorin may be associated with membrane skeletons, i.e., in superstructures that help to determine cell integrity and/or to act as scaffolds for signaling in defense or development

(Bariola et al., 2004). Recently, an increase in remorin was also observed in kiwifruit experience ripening (Tanou et al., 2015; Ainalidou et al., 2016; Minas et al., 2016). Based on these results, we propose that remorin may play a more general role in macromolecular trafficking during fruit ripening. It should be noted that several of the presently detected peach skin proteins have not been previously identified in other fruit studies. For example, we observed a strong up-regulation of extradiol ring-cleavage dioxygenase at high altitude (**Table 1**). Dioxygenases catalyze the incorporation of both atoms of molecular oxygen into substrates using a variety of reaction mechanisms. Cleavage of aromatic rings is one of the most important functions of dioxygenases, which play key roles in the degradation of aromatic compounds. Further studies are necessary to clarify the physiological meaning of these proteins in fruit developmental process.

The current proteomic analysis revealed that the abundance of six proteins was increased in response to high altitude (**Table 1**); these features strongly candidate these proteins as key elements in fruit ripening at high altitude and encourage further studies to identify their downstream function. Among these proteins that up-regulated at the higher altitude, two proteins act as chaperones (chaperone ClpC and chaperone ClpB) and their up-regulation has been suggested to regulate fruit biology (Minas et al., 2012), as these proteins play pivotal role in the degradation of damaged or misfolded peptides occurring during climacteric fruit ripening (Faurobert et al., 2007). Pyruvate dehydrogenase E1 is the first component of pyruvate dehydrogenase complex (PDC). Pyruvate dehydrogenase links the glycolytic pathway to the citric acid cycle, which releases energy via NADH. In this study, pyruvate dehydrogenase E1 component subunit alpha was up-regulated at high altitude (**Table 1**). Given that no direct evidence has been reported that this enzyme is regulated by environmental factors in plants, we suggest that the up-regulated pyruvate dehydrogenase was beneficial for peach fruit by releasing energy during ripening, as recently suggested in harvested banana fruit (Li et al., 2015). An interesting finding in this work is the activation of TCP domain class transcription factor by high altitude (**Table 1**). Because TCP transcription factors can integrate hormonal, environmental and developmental signals to modulate numerous biological processes (Li, 2015), it is possible that high altitude environmental, through manipulation of TCP transcription factor, could globally regulate development programs, thereby enabling peach skin to achieve maximum fitness under these conditions. Finally, the increased abundance of lipoxygenase (**Table 1**), which is involved in the synthesis of oxylipins, could be associated to membrane galactolipid peroxidation and aromatic volatiles (Pilati et al., 2014), confirming that LOX could serve as biomarker of skin physiological status.

CONCLUSION

This work gives, for the first time, insights to the peach skin proteome during fruit ripening at different growing

environments and focus on some interesting traits of this tissue, which is significantly related with the esthetic appearance of the fruit and consumer acceptance. In this view, we observed the high altitude-related induction of the pigments and antioxidant potential. These phenotypical and physiological variations were accompanied by a general depression in proteins of defense, energy, and primary metabolism, such as glutathione-ascorbate-associated proteins, heat shock proteins, plastid-lipid associated protein, S-formylglutathione hydrolase, NADH dehydrogenase, and phosphomannomutase. However, the complex and extensive interactions of various environment factors make it difficult to define the effect of single factor on peach skin physiology. Further studies from long-term field observations are needed to deeper understand peach skin metabolism and its regulation by the environment during fruit ripening. Collectively, these findings provide the basis to understand the regulation of peach skin biology that help breeding programs aimed at improving peach quality traits.

AUTHOR CONTRIBUTIONS

AM, IM, and GT designed the research. EK, GT, MS, IM, MM, and AM performed experiments and analyzed data. EK, GT, MS, GD, IM, MM, and AM wrote and edited the manuscript. All authors have read and approved the final manuscript.

REFERENCES

- Ainalidou, A., Tanou, G., Belghazi, M., Samiotaki, M., Diamantidis, G., Molassiotis, A., et al. (2016). Integrated analysis of metabolites and proteins reveal aspects of the tissue-specific function of synthetic cytokinin in kiwifruit development and ripening. *J. Proteom.* 143, 318–333. doi: 10.1016/j.jprot.2016.02.013
- Asami, D. K., Hong, Y.-J., Barrett, D. M., and Mitchell, A. E. (2003). Processing-induced changes in total phenolics and procyandins in clingstone peaches. *J. Sci. Food Agric.* 83, 56–63. doi: 10.1002/jsfa.1275
- Bariola, P. A., Retelska, D., Stasiak, A., Kammerer, R. A., Fleming, A., Hijri, M., et al. (2004). Remorins form a novel family of coiled coil-forming oligomeric and filamentous proteins associated with apical, vascular and embryonic tissues in plants. *Plant Mol. Biol.* 55, 579–594. doi: 10.1007/s11103-004-1520-4
- Benzie, I. F., and Strain, J. J. (1996). The ferric reducing ability of plasma (FRAP) as a measure of “antioxidant power”: the FRAP assay. *Anal. Biochem.* 239, 70–76. doi: 10.1006/abio.1996.0292
- Bevan, M., Bancroft, I., Bent, E., Love, K., Goodman, H., Dean, C., et al. (1998). Analysis of 1.9 Mb of contiguous sequence from chromosome 4 of *Arabidopsis thaliana*. *Nature* 391, 485–488. doi: 10.1038/35140
- Bianco, L., Lopez, L., Scalzone, A. G., Di Carli, M., Desiderio, A., Benvenuto, E., et al. (2009). Strawberry proteome characterization and its regulation during fruit ripening and in different genotypes. *J. Proteomics* 72, 586–607. doi: 10.1016/j.jprot.2008.11.019
- Bradford, M. M. (1976). A rapid and sensitive method for the quantitation of microgram quantities of protein utilizing the principle of protein-dye binding. *Anal. Biochem.* 72, 248–254.
- Brand-Williams, W., Cuvelier, M. E., and Berset, C. (1995). Use of a free radical method to evaluate antioxidant activity. *LWT Food Sci. Technol.* 28, 25–30. doi: 10.1016/S0023-6438(95)80008-5
- Butelli, E., Titta, L., Giorgio, M., Mock, H. P., Matros, A., Peterek, S., et al. (2008). Enrichment of tomato fruit with health-promoting anthocyanins by expression of select transcription factors. *Nat. Biotechnol.* 26, 1301–1308. doi: 10.1038/nbt.1506
- Cantín, C. M., Gogorcena, Y., and Moreno, M. Á. (2010). Phenotypic diversity and relationships of fruit quality traits in peach and nectarine [*Prunus persica* (L.) Batsch] breeding progenies. *Euphytica* 171, 211. doi: 10.1007/s10681-009-0023-4
- Chan, Z. (2012). Proteomic responses of fruits to environmental stresses. *Front. Plant Sci.* 3:311. doi: 10.3389/fpls.2012.00311
- Cvek, J., Medić-Sarić, M., Jasprica, I., Zubci, S., Vitali, D., Mornar, A., et al. (2007). Optimisation of an extraction procedure and chemical characterisation of Croatian propolis tinctures. *Phytochem. Anal.* 18, 451–459. doi: 10.1002/pca.1001
- Dardick, C. D., Callahan, A. M., Chiozzotto, R., Schaffer, R. J., Piagnani, M. C., and Scorza, R. (2010). Stone formation in peach fruit exhibits spatial coordination of the lignin and flavonoid pathways and similarity to *Arabidopsis thaliana*. *BMC Biol.* 8:13. doi: 10.1186/1741-7007-8-13
- Desnoues, E., Baldazzi, V., Génard, M., Mauroux, J.-B., Lambert, P., Confolent, C., et al. (2016). Dynamic QTLs for sugars and enzyme activities provide an overview of genetic control of sugar metabolism during peach fruit development. *J. Exp. Bot.* 67, 3419–3431. doi: 10.1093/jxb/erw169
- Deytieux, C., Geny, L., Lapaillerie, D., Claverol, S., Bonneau, M., and Donèche, B. (2007). Proteome analysis of grape skins during ripening. *J. Exp. Bot.* 58, 1851–1862. doi: 10.1093/jxb/erm049
- Dixon, R. A., and Paiva, N. L. (1995). Stress-induced phenylpropanoid metabolism. *Plant Cell* 7, 1085–1097. doi: 10.1105/tpc.7.7.1085
- Espley, R. V., Hellens, R. P., Putterill, J., Stevenson, D. E., Kutty-Amma, S., and Allan, A. C. (2007). Red colouration in apple fruit is due to the activity of the MYB transcription factor, MdMYB10. *Plant J.* 49, 414–427. doi: 10.1111/j.1365-313X.2006.02964.x
- Faurobert, M., Mihr, C., Bertin, N., Pawłowski, T., Negroni, L., Sommerer, N., et al. (2007). Major proteome variations associated with cherry tomato

ACKNOWLEDGMENTS

This work was partially supported by the Project “BIOTYPOS” (Synergasia) of the Greek General Secretariat for Research and Technology (GSRT). Authors would like also to acknowledge open access publication support by Colorado State University Libraries Open Access Research and Scholarship (OARS) Fund and the Department of Horticulture and Landscape Architecture.

SUPPLEMENTARY MATERIAL

The Supplementary Material for this article can be found online at: <http://journal.frontiersin.org/article/10.3389/fpls.2016.01689/full#supplementary-material>

Supplementary Figure S1 | Daily climate record (low/high temperature and relative humidity) in two altitude regions.

Supplementary Figure S2 | Subcellular localization of the identified peach skin fruit proteins.

Supplementary Figure S3 | Mascot results for peptidyl-prolyl cis-trans isomerase (protein spot 8033) identifications based on one peptide sequences.

Supplementary Table S1 | Quantitative data for peach skin proteins spot volumes from 2DE-gels.

Supplementary Table S2 | Identified peach skin proteins blasted against the TAIR database and their STRING 9.0 ID.

Supplementary Table S3 | Identification data of peach skin proteins.

Supplementary Table S4 | Pearson's correlation coefficients calculated between fruit quality trait and proteomic characteristics.

- pericarp development and ripening. *Plant Physiol.* 143, 1327–1346. doi: 10.1104/pp.106.092817
- Frett, T. J., Reighard, G. L., Okie, W. R., and Gasic, K. (2014). Mapping quantitative trait loci associated with blush in peach [*Prunus persica* (L.) Batsch]. *Tree Genet. Genomes* 10, 367–381. doi: 10.1007/s11295-013-0692-y
- Gharechahi, J., Hajirezaei, M. R., and Salekdeh, G. H. (2015). Comparative proteomic analysis of tobacco expressing cyanobacterial flavodoxin and its wild type under drought stress. *J. Plant Physiol.* 175, 48–58. doi: 10.1016/j.jplph.2014.11.001
- Giraldo, E., Díaz, A., Corral, J. M., and García, A. (2012). Applicability of 2-DE to assess differences in the protein profile between cold storage and not cold storage in nectarine fruits. *J. Proteomics* 75, 5774–5782. doi: 10.1016/j.jprot.2012.08.005
- Giusti, M. M., and Wrolstad, R. E. (2005). “Characterization and measurement of anthocyanins by UV-visible spectroscopy,” in *Handbook of Food Analytical Chemistry*, ed R. E. Wrolstad (New York, NY: John Wiley & Sons), 19–31. doi: 10.1002/0471709085.ch18
- Goulas, V., Minas, I. S., Kourdoulas, P. M., Lazaridou, A., Molassiotis, A. N., Gerothanassis, I. P., et al. (2015). ¹H NMR metabolic fingerprinting to probe temporal postharvest changes on qualitative attributes and phytochemical profile of sweet cherry fruit. *Front. Plant Sci.* 6:959. doi: 10.3389/fpls.2015.00959
- Hu, C., and Kitts, D. D. (2001). Evaluation of antioxidant activity of epigallocatechin gallate in biphasic model systems *in vitro*. *Mol. Cell. Biochem.* 218, 147–155. doi: 10.1023/A:1007220928446
- Hu, H., Liu, Y., Shi, G.-L., Liu, Y.-P., Wu, R.-J., Yang, A.-Z., et al. (2011). Proteomic analysis of peach endocarp and mesocarp during early fruit development. *Physiol. Plant.* 142, 390–406. doi: 10.1111/j.1399-3054.2011.01479.x
- Iglesias, I., and Echeverría, G. (2009). Differential effect of cultivar and harvest date on nectarine colour, quality and consumer acceptance. *Sci. Hortic.* 120, 41–50. doi: 10.1016/j.scientia.2008.09.011
- Kuti, J. O. (2004). Antioxidant compounds from four *Opuntia cactus* pear fruit varieties. *Food Chem.* 85, 527–533. doi: 10.1016/S0308-8146(03)00184-5
- Lara, M. V., Borsani, J., Budde, C. O., Lauxmann, M. A., Lombardo, V. A., Murray, R., et al. (2009). Biochemical and proteomic analysis of “Dixiland” peach fruit (*Prunus persica*) upon heat treatment. *J. Exp. Bot.* 60, 4315–4333. doi: 10.1093/jxb/erp267
- Leida, C., Conesa, A., Llácer, G., Badenes, M. L., and Ríos, G. (2012). Histone modifications and expression of DAM6 gene in peach are modulated during bud dormancy release in a cultivar-dependent manner. *New Phytol.* 193, 67–80. doi: 10.1111/j.1469-8137.2011.03863.x
- Li, S. (2015). The *Arabidopsis thaliana* TCP transcription factors: a broadening horizon beyond development. *Plant Signal. Behav.* 10:e1044192. doi: 10.1080/15592324.2015.1044192
- Li, T., Yun, Z., Zhang, D., Yang, C., Zhu, H., Jiang, Y., et al. (2015). Proteomic analysis of differentially expressed proteins involved in ethylene-induced chilling tolerance in harvested banana fruit. *Front. Plant Sci.* 6:845. doi: 10.3389/fpls.2015.00845
- Lin-Wang, K., Micheletti, D., Palmer, J., Volz, R., Lozano, L., Espley, R., et al. (2011). High temperature reduces apple fruit colour via modulation of the anthocyanin regulatory complex. *Plant Cell Environ.* 34, 1176–1190. doi: 10.1111/j.1365-3040.2011.02316.x
- Lombardo, V. A., Osorio, S., Borsani, J., Lauxmann, M. A., Bustamante, C. A., Budde, C. O., et al. (2011). Metabolic profiling during peach fruit development and ripening reveals the metabolic networks that underpin each developmental stage. *Plant Physiol.* 157, 1696–1710. doi: 10.1104/pp.111.186064
- Mabeau, S., and Kloareg, B. (1987). Isolation and analysis of the cell walls of brown algae: *Fucus spiralis*, *F. ceranoides*, *F. vesiculosus*, *F. serratus*, *bifurcaria bifurcata* and *laminaria digitata*. *J. Exp. Bot.* 38, 1573–1580. doi: 10.1093/jxb/38.9.1573
- Magi, B., Ettorre, A., Liberatori, S., Bini, L., Andreassi, M., Frosali, S., et al. (2004). Selectivity of protein carbonylation in the apoptotic response to oxidative stress associated with photodynamic therapy: a cell biochemical and proteomic investigation. *Cell Death Differ.* 11, 842–852. doi: 10.1038/sj.cdd.4401427
- Minas, I. S., Tanou, G., Belghazi, M., Job, D., Manganaris, G. A., Molassiotis, A., et al. (2012). Physiological and proteomic approaches to address the active role of ozone in kiwifruit post-harvest ripening. *J. Exp. Bot.* 63, 2449–2464. doi: 10.1093/jxb/err418
- Minas, I. S., Tanou, G., Karagiannis, E., Belghazi, M., and Molassiotis, A. (2016). Coupling of physiological and proteomic analysis to understand the ethylene- and chilling-induced kiwifruit ripening syndrome. *Front. Plant Sci.* 7:120. doi: 10.3389/fpls.2016.00120
- Molassiotis, A., Tanou, G., Filippou, P., and Fotopoulos, V. (2013). Proteomics in the fruit tree science arena: new insights into fruit defense, development, and ripening. *Proteomics* 13, 1871–1884. doi: 10.1002/pmic.201200428
- Montevecchi, G., Vasile Simone, G., Masino, F., Bignami, C., and Antonelli, A. (2012). Physical and chemical characterization of Pescavivona, a Sicilian white flesh peach cultivar [*Prunus persica* (L.) Batsch]. *Food Res. Int.* 45, 123–131. doi: 10.1016/j.foodres.2011.10.019
- Nilo, P., R., Campos-Vargas, R., and Orellana, A. (2012). Assessment of *Prunus persica* fruit softening using a proteomics approach. *J. Proteomics* 75, 1618–1638. doi: 10.1016/j.jprot.2011.11.037
- Nilo, R., Saffie, C., Lilley, K., Baeza-Yates, R., Cambiazo, V., Campos-Vargas, R., et al. (2010). Proteomic analysis of peach fruit mesocarp softening and chilling injury using difference gel electrophoresis (DIGE). *BMC Genomics* 11:43. doi: 10.1186/1471-2164-11-43
- Ou, W. B., Luo, W., Park, Y. D., and Zhou, H. M. (2001). Chaperone-like activity of peptidyl-prolyl cis-trans isomerase during creatine kinase refolding. *Protein Sci.* 10, 2346–2353. doi: 10.1101/ps.23301
- Pilati, S., Brazzale, D., Guella, G., Milli, A., Ruberti, C., Biasioli, F., et al. (2014). The onset of grapevine berry ripening is characterized by ROS accumulation and lipoxygenase-mediated membrane peroxidation in the skin. *BMC Plant Biol.* 14:87. doi: 10.1186/1471-2229-14-87
- Prinsi, B., Negri, A. S., Fedeli, C., Morgutti, S., Negrini, N., Cocucci, M., et al. (2011). Peach fruit ripening: a proteomic comparative analysis of the mesocarp of two cultivars with different flesh firmness at two ripening stages. *Phytochemistry* 72, 1251–1262. doi: 10.1016/j.phytochem.2011.01.012
- Qian, W., Yu, C., Qin, H., Liu, X., Zhang, A., Johansen, I. E., et al. (2007). Molecular and functional analysis of phosphomannomutase (PMM) from higher plants and genetic evidence for the involvement of PMM in ascorbic acid biosynthesis in *Arabidopsis* and *Nicotiana benthamiana*. *Plant J.* 49, 399–413. doi: 10.1111/j.1365-313X.2006.02967.x
- Re, R., Pellegrini, N., Proteggente, A., Pannala, A., Yang, M., and Rice-Evans, C. (1999). Antioxidant activity applying an improved ABTS radical cation decolorization assay. *Free Radic. Biol. Med.* 26, 1231–1237. doi: 10.1016/S0891-5849(98)00315-3
- Reig, G., Alegre, S., Gatus, F., and Iglesias, I. (2015). Adaptability of peach cultivars [*Prunus persica* (L.) Batsch] to the climatic conditions of the Ebro Valley, with special focus on fruit quality. *Sci. Hortic.* 190, 149–160. doi: 10.1016/j.scientia.2015.04.019
- Rey, P., Gillet, B., Römer, S., Eymery, F., Massimino, J., Peltier, G., et al. (2000). Over-expression of a pepper plastid lipid-associated protein in tobacco leads to changes in plastid ultrastructure and plant development upon stress. *Plant J.* 21, 483–494. doi: 10.1046/j.1365-313X.2000.00699.x
- Stone, S. L., and Callis, J. (2007). Ubiquitin ligases mediate growth and development by promoting protein death. *Curr. Opin. Plant Biol.* 10, 624–632. doi: 10.1016/j.pbi.2007.07.010
- Szklarczyk, D., Franceschini, A., Kuhn, M., Simonovic, M., Roth, A., Minguez, P., et al. (2011). The STRING database in 2011: functional interaction networks of proteins, globally integrated and scored. *Nucleic Acids Res.* 39, 561–568. doi: 10.1093/nar/gkq973
- Tadiello, A., Ziosi, V., Negri, A. S., Noferini, M., Fiori, G., Busatto, N., et al. (2016). On the role of ethylene, auxin and a GOLVEN-like peptide hormone in the regulation of peach ripening. *BMC Plant Biol.* 16:44. doi: 10.1186/s12870-016-0730-7
- Tanou, G., Job, C., Belghazi, M., Molassiotis, A., Diamantidis, G., and Job, D. (2010). Proteomic signatures uncover hydrogen peroxide and nitric oxide cross-talk signaling network in Citrus plants. *J. Proteome Res.* 9, 5994–6006. doi: 10.1021/pr100782h
- Tanou, G., Job, C., Rajjou, L., Arc, E., Belghazi, M., Diamantidis, G., et al. (2009). Proteomics reveals the overlapping roles of hydrogen peroxide and nitric oxide in the acclimation of citrus plants to salinity. *Plant J.* 60, 795–804. doi: 10.1111/j.1365-313X.2009.04000.x
- Tanou, G., Minas, I. S., Karagiannis, E., Tsikou, D., Audebert, S., Papadopoulou, K. K., et al. (2015). The impact of sodium nitroprusside and ozone in kiwifruit ripening physiology: a combined gene and protein expression profiling approach. *Ann. Bot.* 116, 649–662. doi: 10.1093/aob/mcv107649-662

- Trainotti, L., Bonghi, C., Ziliotto, F., Zanin, D., Rasori, A., Casadoro, G., et al. (2006). The use of microarray μ PEACH1.0 to investigate transcriptome changes during transition from pre-climacteric to climacteric phase in peach fruit. *Plant Sci.* 170, 606–613. doi: 10.1016/j.plantsci.2005.10.015
- Tuan, P. A., Bai, S., Yaegaki, H., Tamura, T., Hihara, S., Moriguchi, T., et al. (2015). The crucial role of PpMYB10.1 in anthocyanin accumulation in peach and relationships between its allelic type and skin color phenotype. *BMC Plant Biol.* 15:280. doi: 10.1186/s12870-015-0664-5
- Wang, L., Zhao, S., Gu, C., Zhou, Y., Zhou, H., Ma, J., et al. (2013). Deep RNA-Seq uncovers the peach transcriptome landscape. *Plant Mol. Biol.* 83, 365–377. doi: 10.1007/s11103-013-0093-5
- Wang, X., Ma, X., Wang, H., Li, B., Clark, G., Guo, Y., et al. (2015). Proteomic study of microsomal proteins reveals a key role for *Arabidopsis* annexin 1 in mediating heat stress-induced increase in intracellular calcium levels. *Mol. Cell. Proteomics* 14, 686–694. doi: 10.1074/mcp.M114.042697
- Wolfe, K., Wu, X., and Liu, R. H. (2003). Antioxidant activity of apple peels. *J. Agric. Food Chem.* 51, 609–614. doi: 10.1021/jf020782a
- Zhang, L., Yu, Z., Jiang, L., Jiang, J., Luo, H., and Fu, L. (2011). Effect of post-harvest heat treatment on proteome change of peach fruit during ripening. *J. Proteomics* 74, 1135–1149. doi: 10.1016/j.jprot.2011.04.012
- Ziliotto, F., Begheldo, M., Rasori, A., Bonghi, C., and Tonutti, B. (2008). Transcriptome profiling of ripening nectarine (*Prunus persica* L. Batsch) fruit treated with 1-MCP. *J. Exp. Bot.* 59, 2781–2791. doi: 10.1093/jxb/ern136
- Ziogas, V., Tanou, G., Molassiotis, A., Diamantidis, G., and Vasilakakis, M. (2010). Antioxidant and free radical-scavenging activities of phenolic extracts of olive fruits. *Food Chem.* 120, 1097–1103. doi: 10.1016/j.foodchem.2009.11.058

Conflict of Interest Statement: The authors declare that the research was conducted in the absence of any commercial or financial relationships that could be construed as a potential conflict of interest.

Copyright © 2016 Karagiannis, Tanou, Samiotaki, Michailidis, Diamantidis, Minas and Molassiotis. This is an open-access article distributed under the terms of the Creative Commons Attribution License (CC BY). The use, distribution or reproduction in other forums is permitted, provided the original author(s) or licensor are credited and that the original publication in this journal is cited, in accordance with accepted academic practice. No use, distribution or reproduction is permitted which does not comply with these terms.



A FERONIA-Like Receptor Kinase Regulates Strawberry (*Fragaria × ananassa*) Fruit Ripening and Quality Formation

Meiru Jia, Ning Ding, Qing Zhang, Sinian Xing, Lingzhi Wei, Yaoyao Zhao, Ping Du, Wenwen Mao, Jizheng Li, Bingbing Li* and Wensuo Jia*

College of Horticulture, China Agricultural University, Beijing, China

OPEN ACCESS

Edited by:

Maarten Hertog,
KU Leuven, Belgium

Reviewed by:

Benedetto Ruperti,
University of Padua, Italy
Shaohua Zeng,
South China Institute of Botany (CAS),
China

*Correspondence:

Bingbing Li
libingbing@cau.edu.cn
Wensuo Jia
jiaws@cau.edu.cn

Specialty section:

This article was submitted to
Crop Science and Horticulture,
a section of the journal
Frontiers in Plant Science

Received: 11 March 2017

Accepted: 07 June 2017

Published: 28 June 2017

Citation:

Jia M, Ding N, Zhang Q, Xing S, Wei L, Zhao Y, Du P, Mao W, Li J, Li B and Jia W (2017) A FERONIA-Like Receptor Kinase Regulates Strawberry (*Fragaria × ananassa*) Fruit Ripening and Quality Formation. *Front. Plant Sci.* 8:1099. doi: 10.3389/fpls.2017.01099

Ripening of fleshy fruits is controlled by a series of intricate signaling processes. Here, we report a FERONIA/FER-like receptor kinase, *FaMRLK47*, that regulates both strawberry (*Fragaria × ananassa*) fruit ripening and quality formation. Overexpression and RNAi-mediated downregulation of *FaMRLK47* delayed and accelerated fruit ripening, respectively. We showed that *FaMRLK47* physically interacts with *FaABI1*, a negative regulator of abscisic acid (ABA) signaling, and demonstrated that *FaMRLK47* regulates fruit ripening by modulating ABA signaling, a major pathway governing strawberry fruit ripening. In accordance with these findings, overexpression and RNAi-mediated downregulation of *FaMRLK47* caused a decrease and increase, respectively, in the ABA-induced expression of a series of ripening-related genes. Additionally, overexpression and RNAi-mediated downregulation of *FaMRLK47* resulted in an increase and decrease in sucrose content, respectively, as compared with control fruits, and respectively promoted and inhibited the expression of genes in the sucrose biosynthesis pathway (*FaSS* and *FaSPS*). Collectively, this study demonstrates that *FaMRLK47* is an important regulator of strawberry fruit ripening and quality formation, and sheds light on the signaling mechanisms underlying strawberry fruit development and ripening.

Keywords: **FaABI1, FaMRLK47, FERONIA, fruit quality formation, strawberry (*Fragaria × ananassa*)**

INTRODUCTION

Fleshy fruits are physiologically classified as climacteric or non-climacteric. Climacteric fruits show a sharp increase in respiration during the ripening process, while non-climacteric fruits do not (Nitsch, 1953; Coombe, 1976; Brady, 1987). Most basic studies of fruit development and ripening have focused on climacteric fruits, such as the model plant *Solanum lycopersicum* (tomato). *Fragaria × ananassa* (strawberry) is a typical non-climacteric fruit. Studies of strawberry fruit development and ripening are likely to provide insight into the regulatory mechanisms underlying non-climacteric fruit development and ripening.

The ripening of fleshy fruits is a complex process involving dramatic changes in physiological and biochemical metabolism, which trigger changes in color, texture, flavor, and aroma

(Giovannoni, 2001; Seymour et al., 2013). In the past decades, studies of fruit ripening have mainly focused on these metabolic changes, particularly regarding their interactions with phytohormones. Ethylene has long been known to be the critical signal controlling ripening of climacteric fruits (Nitsch, 1953; Coombe, 1976; Brady, 1987; Klee and Giovannoni, 2011). Early studies suggested that auxin (IAA) is a key regulator of strawberry fruit growth and ripening (Veluthambi and Poovaiah, 1984; Given et al., 1988). Whereas overexpression of *FaNCED1*, which encodes a key enzyme in the abscisic acid (ABA) biosynthesis pathway, promoted strawberry fruit ripening, knock-down of this gene delayed it Jia et al. (2011). Furthermore, manipulating the expression of an ABA receptor, FaPYR1, and of its downstream signal members, ABI1 and SnRK2.6, affected the accumulation of anthocyanins and other fruit qualities (Chai et al., 2011; Jia et al., 2013a; Han et al., 2015). These studies suggested that ABA is an important signal controlling strawberry fruit ripening. Besides IAA and ABA, there is evidence that ethylene (White, 2002; Trainotti et al., 2005; Villarreal et al., 2010) and jasmonic acid (Concha et al., 2013) also regulate strawberry fruit ripening and quality formation. Collectively, it appears that strawberry fruit development and ripening are regulated by the synergistic effects of multiple phytohormones. We recently showed that sucrose also regulates anthocyanin accumulation in strawberry fruit (Jia et al., 2013b).

While the senescence-associated, deteriorative aspects of ripening have historically been emphasized, it is now commonly accepted that ripening is a complex process determined by a series of signaling events (Brady, 1987; Fischer and Bennett, 1991; Giovannoni, 2001). At the cellular level, the process spanning fruit set to ripening can be categorized into three major stages: cell division, cell differentiation and expansion, and cell degradation (Nitsch, 1953; Giovannoni, 2001; Seymour et al., 2013). Regulation of the cell wall's physical properties is essential for plant growth and development, and a cell wall signaling pathway that reports on the status of the cell wall has long since been predicted to exist (Wolf et al., 2012). Recently, plasmalemma-anchored receptor-like kinases (RLKs) have attracted much attention due to their roles in sensing cell wall integrity (Humphrey et al., 2007; Cheung and Wu, 2011; Boisson-Dernier et al., 2011; Lindner et al., 2012). RLKs constitute a gene subfamily of over 600 members in *Arabidopsis* (Shiu and Bleecker, 2001a,b, 2003). Malectin is a membrane-anchored protein of the endoplasmic reticulum that recognizes and binds to Glc2-N-glycan, thereby regulating the production and secretion of *N*-glycosylated proteins (Schallus et al., 2008, 2010; Takeda et al., 2014). Interestingly, a group of RLKs harbors an extracellular sequence with a unique domain that is similar to malectin (Schulze-Muth et al., 1996; Boisson-Dernier et al., 2011; Lindner et al., 2012). The first malectin domain-containing RLK, CrRLK1, was identified in *Catharanthus roseus*. The *Arabidopsis thaliana* genome contains 17 CrRLK1-like RLK genes (Schulze-Muth et al., 1996), several of which have been functionally identified. FERONIA (FER) belongs to the CrRLK1-like subfamily and was first identified for its role in fertilization (Huck et al., 2003). FER directly interacts with guanine nucleotide exchange factors (RopGEFs), which

activate downstream components that mediate the production of reactive oxygen species (ROS) at the entrance point of the female gametophyte, thereby inducing pollen tube rupture and sperm release (Duan et al., 2014; Ngo et al., 2014; Kessler et al., 2015). Furthermore, FER is a pivotal mediator of cross-talk between phytohormones, including ABA, brassinosteroids (BRs), and ethylene (Yu et al., 2012). The mechanism by which FER modulates ABA signaling was revealed in a study by Yu et al. (2012), which found that ROP11, a downstream component of FER signaling, physically interacts with ABI2, a key signal in the ABA signaling pathway. As described above, IAA, ABA, BR, and ethylene are all critical regulators of strawberry fruit development and ripening. Although *Arabidopsis* is intrinsically different from strawberry with respect to fruit development and ripening, the convergent roles of FER in phytohormone signaling prompted us to examine whether FER-like kinase is involved in strawberry fruit development and ripening. Besides FER, a few of the other malectin domain-containing RLKs have also been functionally characterized in *Arabidopsis*. Theseus1 (THE1), which was identified in a screen for suppressors that attenuated the short hypocotyl phenotype of dark-grown seedlings, functions as a cell wall integrity sensor that mediates the disruption of cellulose synthesis (Hematy et al., 2007; Hematy and Hofte, 2008; Boisson-Dernier et al., 2011). Anxur1 (ANX1) and Anxur2 (ANX2), two close relatives of FER, were also found to be pollen-specific and to regulate pollen tube rupture and sperm release (Boisson-Dernier et al., 2009). As a redundant homolog of THE1, HERCULES 1 (HERK1) was demonstrated to regulate plant growth and development (Guo et al., 2009a,b).

Malectin domain-containing RLKs (MRLKs) have been proposed to sense cell wall integrity and FER, a member of the malectin domain-containing RLK family, has been implicated in phytohormone cross-talk (Duan et al., 2010; Huang et al., 2013; Chen et al., 2016). We identified 62 MRLK members in strawberry, which we named *FaMRLK1* to *FaMRLK62* based on their chromosome location (Zhang et al., 2016). In this study, we found that *FaMRLK47*, the homolog of FER, is a negative regulator of strawberry fruit development and ripening. Overexpression and RNAi-mediated downregulation of *FaMRLK47* delayed and accelerated fruit ripening, respectively. *FaMRLK47* physically interacts with FaABI1, and regulates fruit ripening by modulating ABA signaling, which results in changes in fruit ripening and qualities, such as sugar content and pigment accumulation. These findings provide insights into the molecular basis for the regulation of strawberry fruit development and ripening.

MATERIALS AND METHODS

Plant Materials and Growth Conditions

Strawberry plants (*Fragaria × ananassa* 'Benihoppe') were grown on soil supplemented with nutrient soil, organic fertilizer, and vermiculite (7:2:1; v/v/v) in the greenhouse. The controlled condition of greenhouse was 12/12-h photoperiod at $450 \mu\text{mol m}^{-2} \text{s}^{-1}$ and 70% humidity, under day/night temperature of 25°C/15°C.

Gene Isolation and Sequence Analysis

The cDNA sequences of full-length RLKs were obtained from the TAIR website¹ and NCBI². To identify *CrRLK1-like RLK* (*CrRLK1L*) genes in strawberry, the coding sequence of *FERONIA* (*At3g51550*) was used as query to BLAST the strawberry genome. Phylogenetic trees were constructed using the Neighbor-Joining (NJ) method in MEGA 4.0.2 software, with 1000 bootstrap replicates to evaluate the reliability of different phylogenetic groups. The deduced amino acid sequences of FaMRLKs were aligned using ClustalX 2.0.12 with default settings. The alignments were edited and marked using GeneDoc.

To isolate *FaMRLK47* and *FaMRLK50*, total RNA was extracted from strawberry fruit using an E.Z.N.A.[®] Total RNA Kit (OMEGA). The cDNA was synthesized from 1 µg of total RNA using M-MLV Reverse Transcriptase (Promega) according to the manufacturer's instruction. Full-length *FaMRLK47* and *FaMRLK50* were cloned by RT-PCR from cDNA using Q5 High-Fidelity DNA Polymerase (New England Biolabs) under the following conditions: 94°C/30 s for 1 cycle, 94°C/30 s, 56°C/25 s, and 72°C/5 min for 35 cycles, and a final extension of 72°C/5 min. The amplified fragments were subcloned into the pMD19-T vector and transformed into *Escherichia coli* DH5α. Then the selected positive colonies were sequenced by Invitrogen to confirm the full-length sequence. The Primer sequences and GenBank accession numbers are shown in Supplementary Table S1.

Quantitative Reverse Transcriptase PCR (RT-qPCR)

Quantitative reverse transcriptase PCR (RT-qPCR) was performed using SYBR Premix Ex TaqTM (TaKaRa) in a ABI7500 Real-Time PCR System. Primers used for RT-qPCR were designed using Primer3 Plus³. Three biological replicates were set up, and each sample was analyzed at least in triplicate. *FaACTIN* was used as an internal control and the $2^{-\Delta\Delta CT}$ method (where ΔCT represents the difference between the cycle threshold values of the target and reference genes) was used to calculate the relative transcript levels (Schmittgen and Livak, 2008).

Plant Material and Treatments

The process from fruit set to ripening was classified into six stages as follows: small green fruit (abbreviated as SG), large green fruit (LG), white fruit (W), initially reddening (IR), and fully reddening (FR). For each stage, five fruits were combined as an individual sample. After fruits were frozen in liquid nitrogen, seeds (achenes) were removed with a needle, and the receptacles were used to analyze gene expression. The expression of FaMRLKs was assessed by RT-qPCR analysis, using the primer sequences shown in Supplementary Table S2.

For phytohormone treatment, fruit disks (10 mm in diameter and 1 mm in thickness) were prepared and combined from 20 fruits in the large green stage. For each treatment, disk

samples (5 g per sample) were equilibrated for 30 min in equilibration buffer (Archbold, 1988; 10 mM MgCl₂, 5 mM CaCl₂, 200 mM mannitol, 10 mM EDTA, 5 mM vitamin C, and 50 mM MES-Tris, pH 5.5) and then shaken for 6 h at 25°C in equilibration buffer containing 100 µM ABA or 200 µM IAA under darkness. After a 6-h incubation, the samples were washed with deionized water, frozen immediately in liquid nitrogen, and kept at -80°C until use. For temperature treatment, the fruit was split longitudinally into two even parts; one half was subjected to high (40°C, 8 h) or low (4°C, 24 h) temperature treatment, and the other (the control) was incubated for the same period at 25°C. After treatment, the fruits without seeds were frozen in liquid nitrogen and stored at -80°C until use. Each individual analysis was conducted in triplicate. Primers of ripening-related genes used for the RT-qPCR analysis are presented in Supplementary Table S3.

Transfection of Strawberry by Agroinfiltration and ABA Treatment

To construct vectors for overexpression of *FaMRLK47* and *FaMRLK50* (abbreviated hereafter as *FaMRLK47-OE* and *FaMRLK50-OE*), full-length *FaMRLK47* and *FaMRLK50* were cloned into the plant expression vector pCambia1304 using the *XbaI* and *SacI* restriction sites. To construct vectors for downregulating *FaMRLK47* (abbreviated hereafter as *FaMRLK47-RNAi*), the plant expression vector pFGC5941 was used. pCambia1304, pFGC5941, *FaMRLK47-OE*, *FaMRLK47-RNAi*, and *FaMRLK50-OE* were transformed individually into *Agrobacterium tumefaciens* strain EHA105 (Lazo et al., 1991). The transformed strains were grown at 28°C in Luria-Bertani liquid medium containing 10 mM MES and 20 µM acetosyringone with appropriate antibiotics. When the culture reached an optical density at 600 nm of approximately 0.8, *A. tumefaciens* cells were harvested, resuspended in infection buffer [10 mM MgCl₂, 10 mM MES (pH 5.6), and 200 mM acetosyringone], and shaken for 2 h at room temperature before being used for infiltration. Pairs of fruits at 18 DPA (day past anthesis) and with similar phenotypes were selected and, for each pair of fruits, one was transfected with *FaMRLK47-OE*, *FaMRLK50-OE*, or *FaMRLK47-RNAi* and the other (the control) was transfected with pCambia1304, pCambia1304 empty vector, or pFGC5941, respectively. For transfection, *A. tumefaciens* suspension was evenly injected into the fruits with a syringe until the whole fruit became hygrophanous (Jia et al., 2013a), and for each gene, 25 pairs of fruit were injected. To examine the expression of ripening-related genes, *FaMRLK47-OE* and *FaMRLK50-OE* transformed fruits were collected 12 days after infiltration and *FaMRLK47-RNAi* fruit was collected 8 days after infiltration. After removing seeds, fruit samples were frozen in liquid nitrogen and kept at -80°C until used. To investigate the effect of *FaMRLK47-OE* or *FaMRLK47-RNAi* on ABA signaling in fruits, detached fruits were transfected with the *FaMRLK47-OE*, *FaMRLK47-RNAi*, or empty pCambia1304 vector, and then incubated at 22°C and 100% humidity. Three days after the transfection and incubation, fruits were treated with 100 µM ABA for 6 h and expression of the selected genes was analyzed as described above.

¹www.arabidopsis.org

²<https://www.ncbi.nlm.nih.gov/>

³<http://www.primer3plus.com/cgi-bin/dev/primer3plus.cgi>

Determination of Fruit Ripening-Associated Physiological Parameters and ABA Content

Flesh firmness was measured after removing fruit skin on opposite sides of the fruit using a GY-4 fruit hardness tester (Zhejiang Top Instrument). The contents of anthocyanins, flavonoid, and total phenol in the fruit were evaluated using described methods (Fuleki and Francis, 1968; Lees and Francis, 1971). The soluble sugar content was examined as described by Jia et al. (2011). The total titratable acidity calculated, expressed as percent malic acid, was measured using the acid–base titration method (Kafkas et al., 2007). Volatile organic components were analyzed by headspace solid-phase microextraction and gas chromatography–mass spectrometry as described by Dong et al. (2013). ABA content was measured by an indirect enzyme-linked immunosorbent assay (ELISA) (Zhang et al., 2009). The ELISA procedures were performed according to the instructions provided by the manufacturer (China Agricultural University, Beijing, China) and the assay plates were read by the Thermo Electron (Labsystems) Multiskan MK3 (PIONEER, Co., Beijing).

Yeast Two-Hybrid Assays

Yeast two-hybrid assays were performed using the Matchmaker GAL4-based Two-Hybrid System 3 (Clontech), according to the manufacturer's instructions. The coding sequence of the FaMRLK47 kinase domain (540–892 aa) was fused in-frame with the GAL4 DNA-binding domain (BD) in the pGBKT7 vector to generate the FaMRLK47-BD plasmid. The full-length cDNA sequences of *FaABI1* were inserted into the pGADT7 vector. Four different combinations, pGADT7/pGBKT7, *FaABI1*-AD/pGBKT7, pGADT7/FaMRLK47-BD, and *FaABI1*-AD/FaMRLK47-BD were respectively transformed into AH109 strains using the lithium acetate method. After transfection, strains were streaked on -Leu/-Trp medium and further selected on minimal -Leu/-Trp/-His/-Ade medium, and then treated with 20 µg/mL X-Gal for interaction validation. Combinations of pGADT7/pGBKT7, *FaABI1*-AD/pGBKT7, and pGADT7/FaMRLK47-BD were used as negative controls. The primers used for yeast two-hybrid assays are provided in Supplementary Table S4.

Bimolecular Fluorescence Complementation (BiFC) and Subcellular Localization Assays

For the bimolecular fluorescence complementation (BiFC) assay, the full-length cDNA sequence of *FaMRLK47* or *FaABI1* was cloned into pCambia1300-YFP^{n/c} to generate the interaction vectors *FaMRLK47*-YFP^c or *FaABI1*-YFPⁿ. *FaMRLK47*-YFP^c or *FaABI1*-YFPⁿ plasmids were further transformed into *A. tumefaciens* strain EHA105, and cultured at 28°C. To examine the *in vivo* interaction, *FaMRLK47*-YFP^c and *FaABI1*-YFPⁿ were co-expressed in tobacco leaves (*Nicotiana tabacum*) by *Agrobacterium*-mediated infiltration (Schütze et al., 2009). The negative control was performed by co-expressing *FaMRLK47*-YFP^c and empty pCambia1300-YFPⁿ vector in

tobacco leaves. Chimeric fluorescence was examined by confocal microscopy (Olympus Fluoview FV1000). For YFP and bright field imaging, excitation wavelengths of 488 and 543 nm were used, respectively.

For subcellular localization of FaMRLK47, full-length cDNA sequences were amplified by PCR using the forward primer 5'-TTAATTAAATGAAGTGTTCCTTTCTATATT TGGTTC-3' and the reverse primer 5'-GGCGCGCCAACGT CCCTTTGGGTTCATGATTGTGAG-3'. The PCR fragments were inserted into pMDC83 using *Asc*1 and *Pac*1 and the constructs were then introduced into *A. tumefaciens* strain EHA105 and transformed into tobacco leaves as described by Schütze et al. (2009). Transfected plants were grown in darkness for 24 h and in light for 48 h at 24°C. After 3 days, fluorescence was observed using a confocal laser-scanning microscope (Olympus Fluoview FV1000). The primers used for BiFC and localization are shown in Supplementary Table S5.

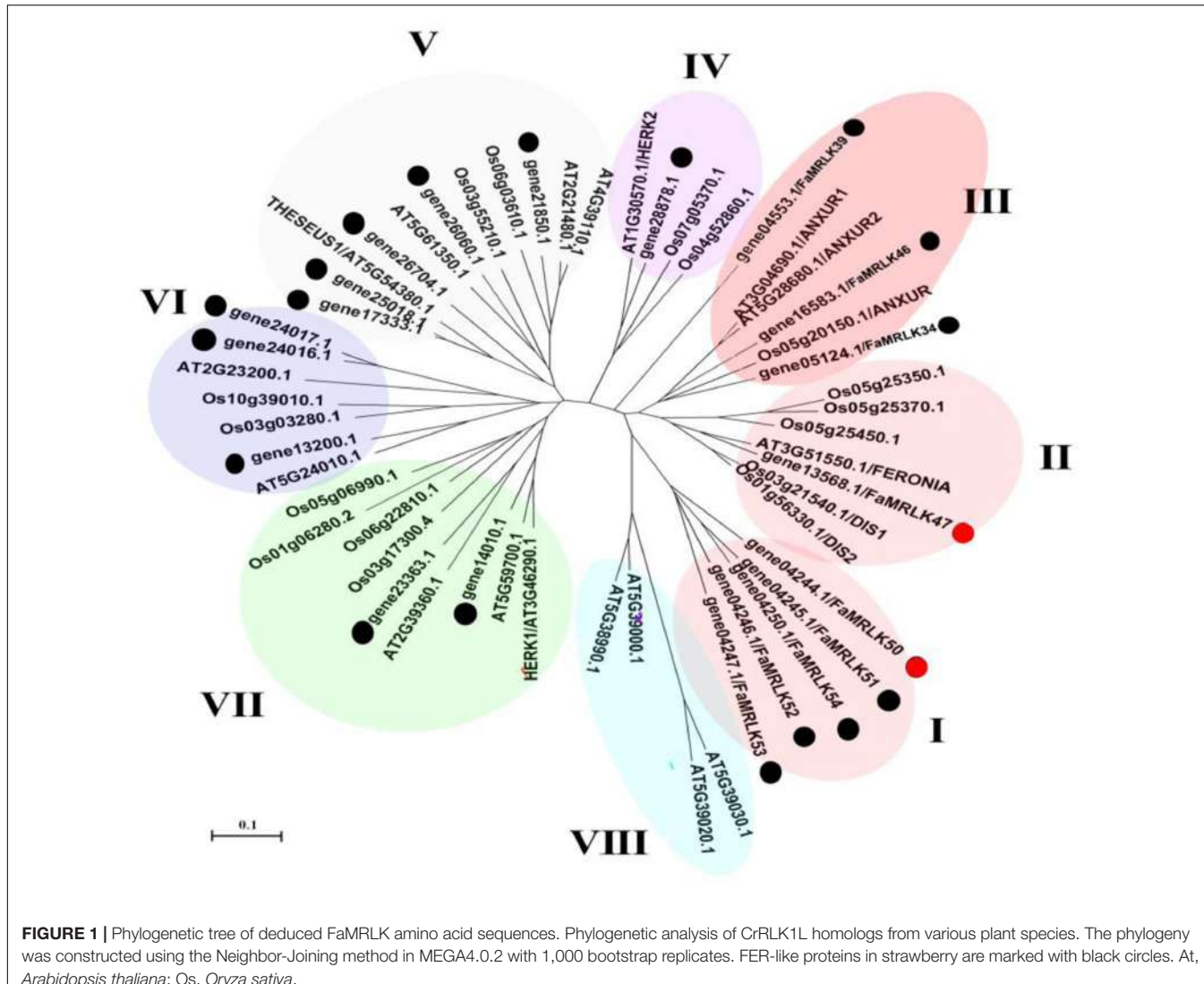
Statistical Analysis

Samples were analyzed in triplicate, and the data were noted as the mean ± SD. Data were analyzed using Student's *t*-test implemented in SAS software (version 8.1, United States), and the least significant difference at a 0.05 level of probability was used to explore the effect of P input on parameters. A *P*-value of ≤ 0.05 was considered to indicate a significant difference, and a *P*-value of ≤ 0.01 was considered to indicate a highly significant difference.

RESULTS

Genome-Wide Identification of *FER*-Like Genes

The FERONIA-like genes belong to a family of CrRLK1-like RLKs (CrRLK1Ls), which in turn belong to a super-family of malectin domain-containing RLKs. In a previous study (Zhang et al., 2016), we conducted a genome-wide screen of woodland strawberry, *Fragaria vesca*, for 'Malectin domain-containing RLKs' (accordingly designated as MRLKs) and identified 62 members (named FvMRLK1–62). In the present study, a screen of the *F. vesca* genome revealed a CrRLK1L family consisting of 20 members. Phylogenetic analysis of CrRLK1L homologs from various plant species revealed eight clades, with FERONIA, NAXURs, HERKs, and THESEUSSs being distributed in different clades (Figure 1 and Supplementary Figure S1). Notably, FERONIA was located in Clade II and only one member of the FaCrRLK1L family, i.e., FaMRLK47, was located in this clade. FaMRLK47 showed a relatively high level of amino acid sequence identity (72.33%) with FERONIA, and can thus be viewed as a homolog of FER. Interestingly, clade I, which contains five members (FaMRLK50–54), was found to consist exclusively of proteins from the strawberry genome. Furthermore, members of clades I, II, and III exhibited relatively high levels of amino acid sequence identity with FERONIA (FER hereafter), and can thus be considered FEL-like receptor kinases. FaCrRLK1Ls and FER exhibited between 42.45 and 48.03% amino acid sequence identity for



clade I proteins and between 38.02 and 50.66% for clade III proteins.

Expression Profile of the *FER*-Like Receptor Kinases during Strawberry Fruit Development and Ripening

Strawberry fruit development, from fruit set to ripening, can be divided into several substages, i.e., the small green fruit (SG), middle green fruit (MG), large green fruit (LG), white fruit (W), initially reddening fruit (IR), and fully reddening fruit (FR) substages (Figure 2A). Given that FaMRLK47 is a homolog of FER and the only FaMRLK member in clade II (Figure 1), we focused on this protein in the present study. As the members of clade I only existed in the strawberry genome and members of clade II exhibited relatively high levels of amino acid sequence identity with FERONIA, we also evaluated their expression in relation to strawberry fruit development and ripening (Figure 2B). Whereas *FaMRLK34*, *FaMRLK39*, and

FaMRLK6 transcripts were not detected in strawberry fruit, the relative levels of the other six members differed, all tending to decrease from the SG to W substages. Notably, *FaMRLK47* expression was higher than that of other members from clade I and II. Furthermore, while the expression levels of *FaMRLK47* started to drop during the MG substage, those of all other members examined started to decline during the SG substage, which suggests that *FaMRLK47* is more tightly associated with the onset of fruit ripening.

Expression of the *FER*-Like Receptor Kinases in Response to Internal and Environmental Signals Involved in the Regulation of Strawberry Fruit Development and Ripening

Strawberry fruit development and ripening are regulated by both internal and external factors, including IAA, ABA, and temperature (Giovannoni, 2001; Seymour et al., 2013). While the

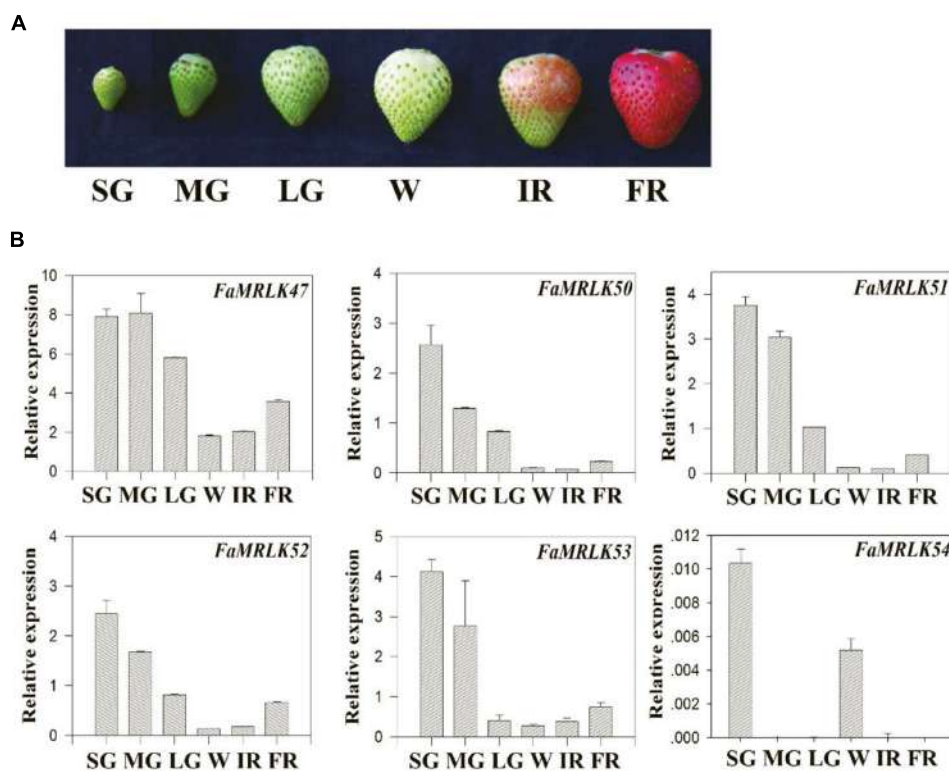


FIGURE 2 | Temporospatial pattern of *FaMRLK* expression in strawberry fruits. **(A)** Phenotypes of strawberry fruit at different developmental stages: small green (SG), middle green (MG), large green (LG), white (W), initial reddening (IR), and fully reddening (FR). **(B)** Quantitative reverse transcriptase PCR (RT-qPCR) analysis of the expression of various *FaMRLK* genes at the indicated developmental stages. Labels below bars denote the corresponding developmental stages, as in **(A)**. *FaACTIN* was used as an internal control. Values are means \pm SD of three biological replicates.

application of IAA delays strawberry fruit ripening, application of ABA promotes it Given et al. (1988) and Jia et al. (2011, 2013a). In our previous studies, we found that ripening of strawberry fruit was stimulated by high temperatures and delayed by low temperatures (Han et al., 2015). We therefore studied the expression profiles of the *FER*-like *FaMRLKs* in response to IAA, ABA, and low/high temperature treatment. While the transcription of all of these genes was sensitive to IAA, ABA, and temperature treatments, their responses differed. *FaMRLK47*, *FaMRLK50*, and *FaMRLK53* expression were inhibited by ABA treatment, whereas *FaMRLK51* and *FaMRLK52* expression were upregulated by ABA treatment. *FaMRLK47*, *FaMRLK50*, *FaMRLK52*, and *FaMRLK53* expression were also sensitive to temperature stress; however, while *FaMRLK47* expression was promoted by both low and high temperature treatment, *FaMRLK52* expression was inhibited and promoted, respectively, by low and high temperature treatments (Figure 3).

Manipulating *FaMRLK47* Expression Caused Changes in the Progress of Fruit Development and Ripening

To investigate a potential role of *FaMRLK47* in the regulation of strawberry fruit development and ripening, we transiently manipulated its expression in strawberry fruits.

As a representative member of the *FaMRLK* family that specifically exists in the strawberry genome, *FaMRLK50* was also investigated. Since *FaMRLK47* and *FaMRLK50* transcript levels dramatically decreased from the SG to LG substages, we first sought to examine the function of *FaMRLK47* and *FaMRLK50* by transiently overexpressing these two genes in strawberry plants. As shown in Figure 4A, overexpression of *FaMRLK47* and *FaMRLK50* resulted in a great increase in their transcript levels in fruits. While overexpression of *FaMRLK50* did not affect fruit development and ripening, overexpression of *FaMRLK47* delayed fruit ripening, as reflected by pigment accumulation. Conversely, RNAi-mediated downregulation of *FaMRLK47* accelerated fruit ripening (Figures 4A,B). Collectively, these experiments indicate that *FaMRLK47* is an important regulator of strawberry fruit development and ripening.

To further explore the *FaMRLK47*-mediated mechanisms underlying the regulation of strawberry fruit development and ripening, we examined the effects of *FaMRLK47* overexpression and downregulation on the expression of a series of ripening-related genes (Figure 4C). Most of these ripening-related genes are important structure genes and transcription factors that are involved in the formation of fruit qualities such as color, texture, aroma, and sugar (Jia et al., 2011, 2013a; Seymour et al., 2011; Lin-Wang et al., 2014; Han et al., 2015). Given that fruit ripening is highly affected by ABA, we also

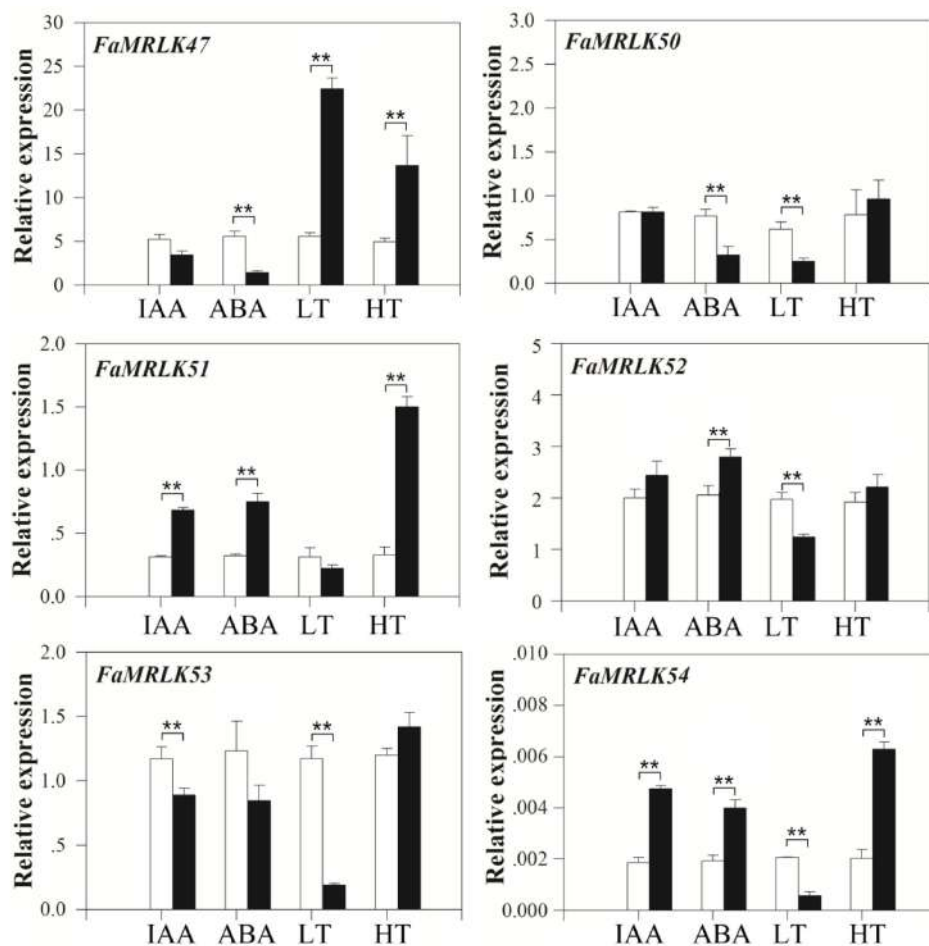
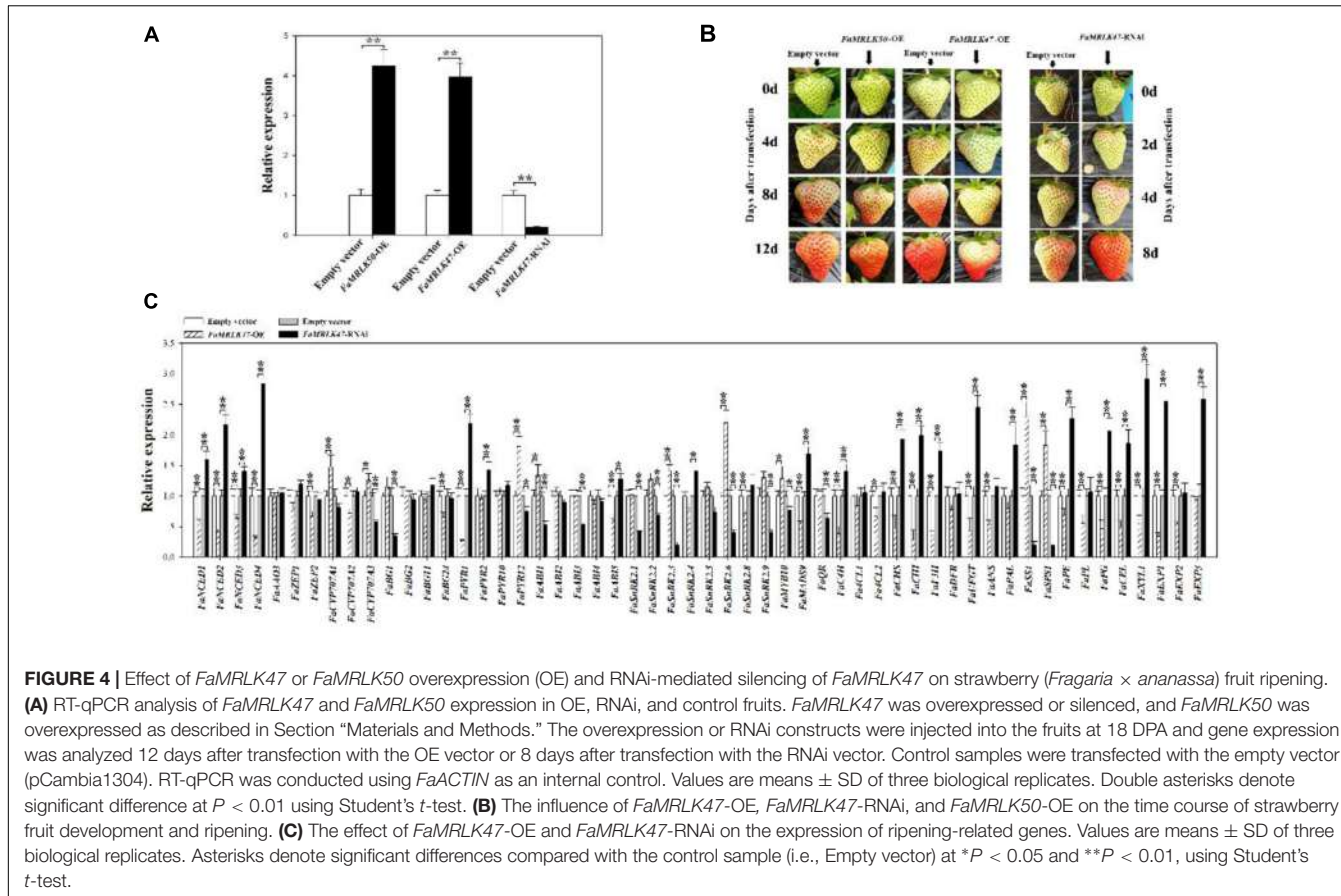


FIGURE 3 | Quantitative reverse transcriptase PCR analysis of *FaMRLK* expression in response to IAA, ABA, low temperature (LT), and high temperature (HT) treatments in fruits at the LG stage. RT-qPCR was conducted using *FaACTIN* as an internal control. Values are means \pm SD of three biological replicates. Asterisks denote significant differences compared with the control sample (i.e., the 0 concentration for hormone treatment and 25°C for temperature treatment) at $*P < 0.05$ and $^{**}P < 0.01$, according to Student's *t*-test. White bars indicate control samples; black bars indicate treated samples.

detected the expression of genes involved in ABA biosynthesis, metabolism, and signal transduction. As shown in **Figure 4C**, manipulating *FaMRLK47* expression altered the expression patterns of both ripening-related and ABA-related genes, which implied that *FaMRLK47* is an important regulator of diverse processes in fruit ripening, including fruit quality formation, ABA production, and signal transduction. Further detection of the ripening-related physiological parameters demonstrated that overexpression and downregulation of *FaMRLK47* resulted in a decrease and increase, respectively, in most of the fruit quality parameters that were expected to increase and decrease during fruit development and ripening (**Table 1**). Moreover, the ABA content showed a decline in *FaMRLK47*-OE fruit (**Figure 5A**). Comprehensive analysis of the changing patterns of gene expression and physiological parameters showed that *FaMRLK47* mainly plays a role in the regulation of anthocyanins accumulation, flavonoid metabolism and fruit softness, and *FaCHS*, *FaCHI*, *FaUFGT*, *FaPAL*, *FaPE*, *FaPG*, *FaXYL1*, and

FaEXP1 might function as the important downstream structure genes of *FaMRLK47* in these processes. In addition, as shown in **Figure 4C**, *FaNCED1-4*, *FaCYP707A*, *FaPYL1/12*, *FaABI1/5*, and *FaSnRK2.3/2.6* might participate in *FaMRLK47*-mediated ABA production and signal transduction.

Interestingly, in contrast to the changes in expression profiles of other ripening-related genes following *FaMRLK47* manipulation, overexpression and downregulation of *FaMRLK47* respectively promoted and inhibited the expression of *FaSS* and *FaSPS1*, two key genes in the sucrose biosynthesis pathway (**Figure 4C**). Further analysis of sugar metabolism showed that, while RNAi-mediated downregulation of *FaMRLK47* expression resulted in a dramatic increase in the major sugar components of the fruit, i.e., sucrose, fructose and glucose, overexpression of *FaMRLK47* caused a significant decrease in sucrose and fructose content (**Figure 5B**). Additionally, overexpression and RNAi-mediated downregulation of *FaMRLK47* resulted in a significant decrease and increase in starch content, respectively.



Collectively, these results suggest that *FaMRLK47* is an important regulator of sugar metabolism.

FaMYB10 was reported to be an important positive regulator of anthocyanin accumulation, whereas *FaMADS9* was shown to regulate fruit development and ripening (Seymour et al., 2011; Lin-Wang et al., 2014). In this study, we also monitored the expression of *FaMYB10* and *FaMADS9* (Figure 4C), and found that the expression of *FaMADS9* was repressed in *FaMRLK47*-OE fruit and upregulated in *FaMRLK47*-RNAi fruit. Although *FaMYB10* expression was not expected to be altered by changes in *FaMRLK47* expression, overexpression of *FaMRLK47* resulted in an increase in *FaMYB10* expression, and downregulation of *FaMRLK47* resulted in a decrease in *FaMYB10* expression. These results imply that *FaMRLK47* and *FaMYB10* are regulatory proteins with diverse functions in fruit ripening. Furthermore, their regulatory mechanisms are more complex than previously expected.

Manipulation of *FaMRLK47* Expression Modifies the Expression of ABA-Induced Genes in Fruit

In *Arabidopsis*, *FER* is involved in ABA signaling (Yu et al., 2012). As *FaMRLK47* shares 74% amino acid sequence identity with *FER*, which is known to modulate ABA signaling (Yu et al., 2012), we were interested in establishing whether *FaMRLK47*

was associated with ABA signaling in strawberry fruit. To investigate a possible role for *FaMRLK47* in the modification of the fruit's response to ABA treatment, we overexpressed and downregulated *FaMRLK47* in strawberry fruit for a short time (72 h), and then examined the expression of a series of ripening-related genes following ABA treatment. As shown in Figure 6, overexpression of *FaMRLK47* resulted in a great decrease in the ability of ABA to induce the expression of these genes in comparison with control fruits, and conversely, RNAi-mediated downregulation of *FaMRLK47* resulted in a great increase in the ability of ABA to induce the expression of these genes. These results indicate that *FaMRLK47* functions as a negative regulator of the ABA signaling cascade.

FaMRLK47 Physically Interacts with ABI1

Given that *FaMRLK47* is capable of modifying ABA signaling, we examined whether *FaMRLK47* could physically interact with important signal proteins in the ABA signaling pathway. As *FaABI1* is a key signaling protein in the ABA signaling pathway and negative regulator of strawberry fruit development and ripening (Jia et al., 2013a), we examined the interaction between *FaMRLK47* and *FaABI1*. Yeast two-hybrid analysis showed that by co-transformed of *FaMRLK47* and *FaABI1* into AH109, the transformed strain grew well on auxotrophic medium (SD-Ade-Leu-Trp-His), which indicated that *FaMRLK47* interacts with *FaABI1* (Figure 7A). To test whether *FaMRLK47*

TABLE 1 | Effects of *FaMRLK47-OE* and *FaMRLK47-RNAi* on major fruit ripening-related parameters.

Parameters	OE-C	OE	RNAi-C	RNAi	Notes
Firmness (kg.cm^{-2})	3.15 ± 0.776	7.375 ± 1.563**	6.435 ± 0.172	2.335 ± 0.168**	Cell wall metabolism-related parameter
Flavonoid content ($\mu\text{g.g}^{-1}$.fresh wt)	2.309 ± 0.035	3.516 ± 0.102**	3.968 ± 0.106	2.774 ± 0.037**	Pigment
Anthocyanin content (mg.g^{-1} .fresh wt)	0.78 ± 0.006	0.07 ± 0.003**	0.106 ± 0.008	0.652 ± 0.006**	metabolism-related compounds
Total phenol content ($\mu\text{g.g}^{-1}$.fresh wt)	7.382 ± 0.054	5.74 ± 0.069**	6.885 ± 0.075	9.65 ± 0.105**	
Total titratable acid content (%)	2.488 ± 0.036	3.104 ± 0.123**	4.115 ± 0.0562	1.788 ± 0.065**	Acid metabolism-related parameter
Acetic acid, methyl ester	4.24 ± 0.015	4.27 ± 0.008	3.765 ± 0.122	4.826 ± 0.365	Aroma metabolism-related compounds (expressed as percentage of the total volatiles)
Acetic acid, 1-methylethyl ester	0.155 ± 0.078	0.425 ± 0.098**	0.388 ± 0.006	0.000 ± 0.000**	
Silanediol, dimethyl	0.63 ± 0.011	0.85 ± 0.024	0.664 ± 0.115	0.365 ± 0.018**	
Butanoic acid, methyl ester	1.245 ± 0.163	1.01 ± 0.102	0.998 ± 0.086	0.906 ± 0.102	
2-Pentenal (E)	0.095 ± 0.002	0.125 ± 0.007**	0.88 ± 0.076	0.105 ± 0.008**	
Butanoic acid, 3-methyl-, methyl ester	0.13 ± 0.004	0.56 ± 0.012**	0.000 ± 0.000	0.105 ± 0.053**	
Hexanal	17.27 ± 2.931	18.95 ± 1.281*	15.535 ± 3.096	16.778 ± 1.055	
2-Hexenal (E)	0.88 ± 0.024	1.48 ± 0.099**	0.955 ± 0.076	0.35 ± 0.006**	
1-Butanol, 2-methyl-, acetate	0.08 ± 0.005	0.84 ± 0.016**	0.000 ± 0.000	0.000 ± 0.000	
Hexanoic acid, methyl ester	1.62 ± 0.605	4.055 ± 0.142**	2.455 ± 0.205	1.218 ± 0.08	
2-Heptenal (Z)	0.08 ± 0.095	0.23 ± 0.014**	0.000 ± 0.000	0.000 ± 0.000	
Hexanoic acid	2.01 ± 0.042	1.035 ± 0.077*	0.000 ± 0.000	0.785 ± 0.006**	
Octanal	0.135 ± 0.063	0.255 ± 0.007*	0.000 ± 0.000	0.000 ± 0.000	
3(2H)-Furanone, 4-methoxy-2, 5-dimethyl	2.99 ± 0.159	0.445 ± 0.017**	0.694 ± 0.022	4.519 ± 0.03**	
Hexanoic acid, 2-oxo-, methyl ester	0.6 ± 0.004	0.46 ± 0.028**	0.236 ± 0.052	0.382 ± 0.105	
1-Octanol	0.205 ± 0.049	0.24 ± 0.042	0.198 ± 0.006	0.000 ± 0.000**	
1,6-Octadien-3-ol, 3,7-dimethyl	0.96 ± 0.035	0.99 ± 0.117	0.78 ± 0.006	0.422 ± 0.078**	
Nonanal	0.215 ± 0.064	0.36 ± 0.042*	0.215 ± 0.09	0.382 ± 0.078	
Phenol,2,4-bis(1,1-dimethylethyl)	0.19 ± 0.042	0.275 ± 0.021*	0.384 ± 0.008	0.096 ± 0.002**	
Dodecanoic acid, ethyl ester	0.075 ± 0.007	0.115 ± 0.021**	0.215 ± 0.065	0.302 ± 0.096	

The *FaMRLK47-OE* or *FaMRLK47-RNAi* construct was transfected into fruits at 18 DPA. Fruits were detached and analyzed 12 or 8 days after transfection. Values are means ± SD of two samples (each sample includes five fruits). Asterisks denote significant differences compared with the control sample (i.e., OE-C or RNAi-C) at $P < 0.01$, using Student's t-test.

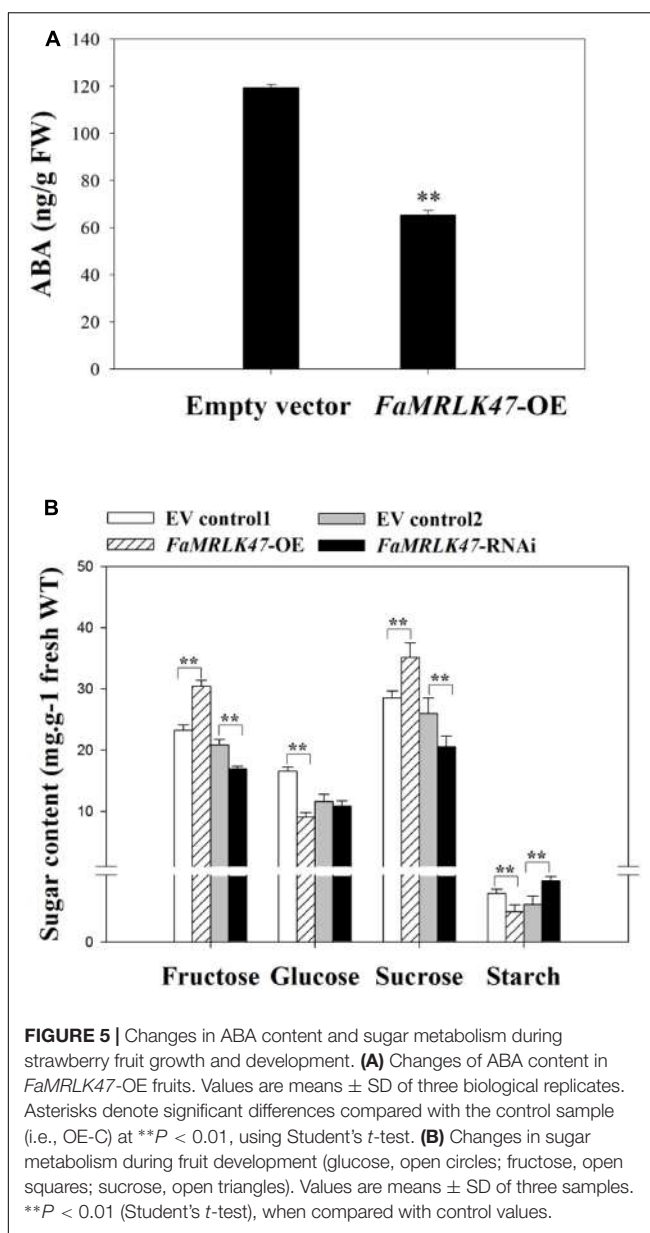
could interact with ABI1 in living plant cells, we first observed the localization of FaMRLK47 in tobacco leaf cells by fusing it with eGFP. We found that FaMRLK47 localized to the membrane in tobacco leaf cells (Figure 7B). Furthermore, we co-transformed the BiFC vectors *FaMRLK47-YFP^c* and *FaABI1-YFPⁿ* into tobacco leaves, using co-transformation of *FaMRLK47-YFP^c* and *pCambia1300-YFPⁿ* as a control. The results showed that, while fluorescence was not observed in the control transformed leaves, strong fluorescence appeared when *FaABI1-YFPⁿ* was combined with *FaMRLK47-YFP^c* (Figure 7C), indicating that *FaABI1* and *FaMRLK47* indeed physically interact.

DISCUSSION

Ripening is a complex process, which involves dramatic changes in physiological and biochemical metabolism, with cell wall degradation considered to be the most important event (Fischer and Bennett, 1991; Giovannoni, 2001). Cell enlargement necessitates an increase in the surface of cell walls, and cell wall extension has been assumed to take place as a result of the loosening of intercrossing cellulose fibrils (Fischer and Bennett, 1991). Cell wall loosening and subsequent

material deposition and rigidification must be tightly regulated, so that cell wall integrity and plant organ development can be coordinately maintained (Humphrey et al., 2007). Therefore, deciphering the mechanisms that sense and regulate cell wall integrity is of particular importance for understanding the process of strawberry fruit development and ripening.

Receptor like protein kinases (RLKs) are important candidate sensors of cell wall integrity and cell wall metabolism. Amongst the members of the RLK family, malectin domain-containing RLKs have attracted particular interest due to the presence of an extracellular sequence of the type thought to recognize and bind to oligosaccharides (Schulze-Muth et al., 1996; Schallus et al., 2008). In *Arabidopsis*, the malectin domain-containing RLKs are proposed to be encoded by a gene subfamily, named the *CrRLK1L* family, which has 17 members (Lindner et al., 2012). Numerous studies have aimed to identify the ligands of these RLKs, particularly the oligosaccharide-like ligands (Liu et al., 2009; Wolf et al., 2012; Engelsdorf and Hamann, 2014; Haruta et al., 2014; Kessler et al., 2015). While the malectin domain implies the existence of oligosaccharide-like ligands, one cannot exclude the possibility that the malectin domain functions to anchor the protein kinase to cell walls. Therefore, one would expect cell wall degradation to affect



the behavior of these RLKs. In support of this notion, the present study indicated that the expression of all malectin domain-containing RLKs dramatically decreased during fruit development and ripening (Figure 2), implying that malectin domain-containing RLKs are tightly associated with strawberry fruit development and ripening. Direct evidence for this came from the finding that manipulation of *FaMRLK47* expression altered the progression of fruit ripening.

FaMRLK47 shares 74% amino acid sequence identity with FER, a malectin domain-containing RLK from *Arabidopsis*. *FER* belongs to the *CrRLK1L* gene family, which consists of 17 members (Lindner et al., 2012). While little is known about most members of the *CrRLK1* family, a few members have been functionally identified. *FER* was identified for its role

in controlling pollen tube growth and fertilization (Escobar-Restrepo et al., 2007). Aside from *FER*, several other related members, such as *THESEUS1*, *HERCULES*, and *ANXURs*, have also been functionally identified (Hematy and Hofte, 2008; Miyazaki et al., 2009; Cheung and Wu, 2011). Intriguingly, studies suggest that all of these members are essentially associated with the sensing of cell wall integrity and thereby play important roles in regulating cell growth (Humphrey et al., 2007; Hematy and Hofte, 2008; Cheung and Wu, 2011; Lindner et al., 2012; Li and Zhang, 2014). Given that *FaMRLK47* shares a relatively high level of amino acid sequence identity with *FER* and that *FER*-related protein kinases have been suggested to be important regulators of cell growth, it is possible that *FaMRLK47* regulates early fruit growth in addition to the onset of fruit ripening. This assumption is consistent with the pattern of *FaMRLK47* expression, i.e., the transcript levels of *FaMRLK47* remain high throughout the early stages of fruit growth and decline dramatically during veraison.

It has been reported that ABA is an important regulator of strawberry fruit ripening (Jia et al., 2011; Han et al., 2015). In *Arabidopsis*, *FER*-mediated ABA signaling is based on a physical interaction between *FER* and guanine exchange factors (GEFs) (Yu et al., 2012). Specifically, *FER* physically interacts with GEFs, which results in activation of the GTPase *ROP11*. *ROP11*, in turn, physically interacts with *ABI2*, a critical signal downstream of the ABA receptor, thereby suppressing the ABA response. Recent reports also revealed that *FER* interacts directly with both *ABI1* and *ABI2* (Chen et al., 2016), but until now, the biological function of the interaction between *FER* and *ABI1* was unknown. In this study, we showed that *FaMRLK47* interacts directly with *FaABI1* (Figure 7). Moreover, we found that *FaMRLK47* changes the sensitivity of ripening-related genes to ABA treatment (Figure 6). These results imply that *FaMRLK47* suppresses ABA-induced gene expression by interacting with *FaABI1*. In *Arabidopsis*, *FER* has been shown to control pollen tube growth and fertilization (Huck et al., 2003). Future studies should examine whether *FaMRLK47* also controls pollen tube growth and fertilization in strawberry.

Fruit quality is primarily determined by the composition of organic constituents, including sugars, organic acids, pigments, and volatile compounds. Fruit ripening is tightly associated with fruit quality formation. The present study not only shows that *FaMRLK47* plays a crucial role in regulating fruit ripening progression, but also that it plays a role in modifying fruit quality, as evidenced by its function in regulating sugar (especially sucrose) metabolism. As shown in Figure 5, RNAi-mediated downregulation of *FaMRLK47* resulted in a large decrease in sucrose and fructose content, and overexpression of *FaMRLK47* appeared to increase the content of sucrose, fructose, glucose, and starch. In *Arabidopsis*, *FER* was reported to regulate starch content via a physical interaction with glyceraldehyde-3-phosphate dehydrogenase (Yang et al., 2015). A recent study in rice showed that *DRUS1/2*, the ortholog *FERONIA* in rice, influences sugar utilization or conversion (Pu et al., 2017). In the present study, we found that *FaMRLK47* is an important regulator of sucrose and starch metabolism, indicating that *FER*-like protein kinases have somewhat similar

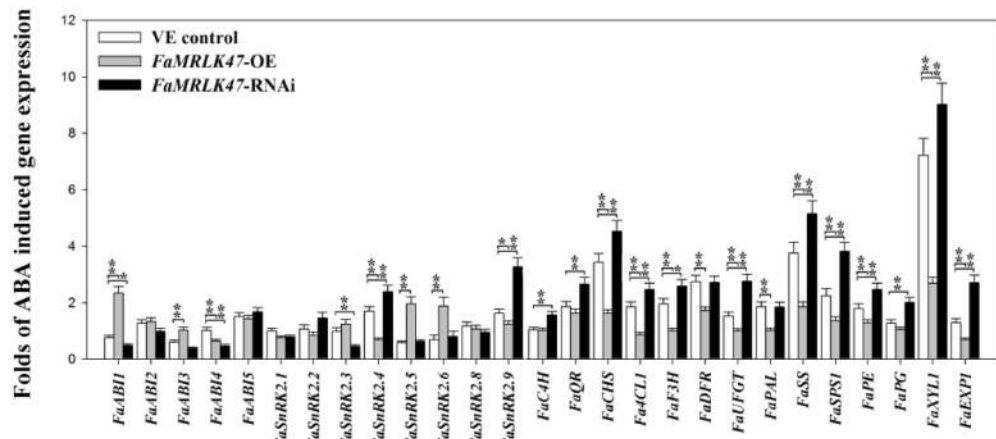


FIGURE 6 | Effect of *FaMRLK47*-OE and *FaMRLK47*-RNAi on the sensitivity of ripening-related genes to ABA. Quantification of the sensitivity of ripening-related gene expression to ABA, with gene expression being expressed as a ratio of ABA treatment/non-treatment control. *FaMRLK47*-OE and *FaMRLK47*-RNAi samples were treated with or without ABA as described in Section “Materials and Methods.” Values are means \pm SD of three replicates. ** $P < 0.01$ and * $P < 0.05$ (Student’s *t*-test), when compared with control values.

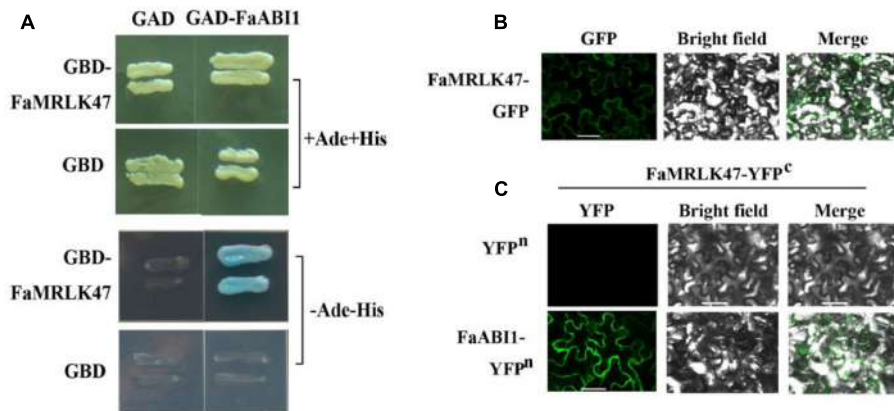


FIGURE 7 | Subcellular localization of FaMRLK47 and physical interaction between FaMRLK47 and FaABI1. **(A)** Yeast two-hybrid analysis of the physical interaction between FaMRLK47 and FaABI1. Protein interactions were examined using combinations of prey and bait vectors. All tests were conducted on media containing adenine (+Ade+His; /-Leu/-Trp/+His/+Ade) or lacking adenine (-Ade-His; /-Leu/-Trp/-His/-Ade). Interactions were determined based on cell growth and were confirmed by an α -Gal assay on medium lacking adenine (/Leu/-Trp/-His/-Ade). **(B)** Subcellular localization of FaMRLK47. pMDC83-FaMRLK47 was transformed into tobacco (*Nicotiana tabacum*) cells, and fluorescence was observed by confocal microscopy as described in Section “Materials and Methods.” Bars = 50 μ m. **(C)** BiFC analysis of the physical interaction between FaMRLK47 and FaABI1. FaMRLK47 and FaABI1 were fused with the C and N terminus of yellow fluorescent protein (YFP; designated as YFPc and YFPn, respectively). Different combinations of the fused constructs were co-transformed into tobacco (*Nicotiana tabacum*) cells, and the cells were visualized using confocal microscopy as described in Section “Materials and Methods.” YFP and bright field were excited at 488 and 543 nm, respectively. Bars = 50 μ m.

roles in different species. Given that FaMRLK47 functions in sucrose metabolism and that FER functions in starch metabolism (Yang et al., 2015), the FER-like protein kinases appear to regulate sugar metabolism via different mechanisms. The mechanism by which FaMRLK47 regulates sucrose metabolism merits further investigation.

The involvement of FaMRLK47 in the regulation of strawberry fruit development and ripening indicates that FER-related protein kinases are versatile regulators of plant growth and development. Consistent with this, it has been suggested that *Arabidopsis* FER proteins are involved in a variety of important

processes, such as root hair elongation (Duan et al., 2010; Huang et al., 2013), ethylene biosynthesis (Mao et al., 2015), starch accumulation (Yang et al., 2015), seed development (Yu et al., 2014), pathogen resistance (Keinath et al., 2010; Kessler et al., 2010), and vegetative growth (Guo et al., 2009a,b; Deslauriers and Larsen, 2010). A recent study showed that FER was transcriptionally downregulated by ethylene during post-harvest ripening and senescence of apple fruit (Zermiani et al., 2015), implying that FER also affects the ripening of climacteric fruits. Ethylene and ABA were demonstrated to be the main regulators of climacteric and non-climacteric fruit ripening, and

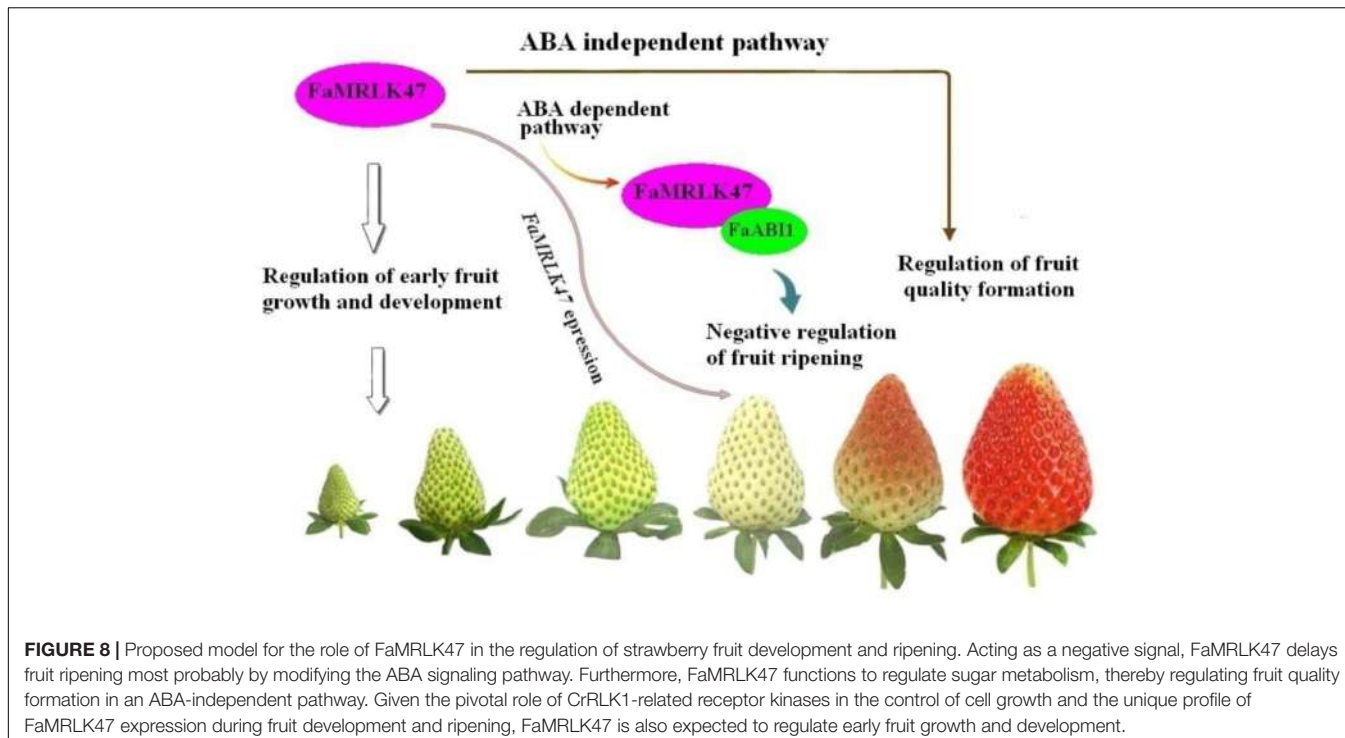


FIGURE 8 | Proposed model for the role of FaMRLK47 in the regulation of strawberry fruit development and ripening. Acting as a negative signal, FaMRLK47 delays fruit ripening most probably by modifying the ABA signaling pathway. Furthermore, FaMRLK47 functions to regulate sugar metabolism, thereby regulating fruit quality formation in an ABA-independent pathway. Given the pivotal role of CrRLK1-related receptor kinases in the control of cell growth and the unique profile of FaMRLK47 expression during fruit development and ripening, FaMRLK47 is also expected to regulate early fruit growth and development.

the results of both the Zermiani study and our study suggest that FER functions in the cross-talk between ethylene and ABA. The diverse signaling mechanisms of FER in fruit ripening need to be further explored.

While the results of the present study suggest that FaMRLK47 is a critical regulator of strawberry fruit development and ripening, it should be noted that FaMRLK47 may regulate different biological processes, such as early fruit growth and development, onset of fruit ripening, and fruit quality formation. It will be of great significance to establish how these different biological processes are mediated by the same signal, FaMRLK47. ABA has been demonstrated to promote sugar accumulation in strawberry fruits (Jia et al., 2011). Given that overexpression of FaMRLK47 suppresses the ABA response, the upregulation of *FaSS* and *FaSPS1* and the increase in sucrose content observed in FaMRLK47 overexpression lines clearly do not occur via the ABA signaling pathway.

In summary, the present study demonstrates that FaMRLK47 plays important roles not only in the regulation of strawberry ripening, but also in the regulation of fruit quality formation. Evidence for this is mainly derived from the following observations: (1) Overexpression and RNAi-mediated downregulation of *FaMRLK47* delayed and accelerated fruit ripening, respectively; (2) FaMRLK47 function is associated with ABA signaling, which is a major mechanism regulating strawberry fruit ripening. Specifically, FaMRLK47 physically interacts with ABI1, a key signal in the ABA signaling pathway, and manipulation of *FaMRLK47* expression modulated ABA-induced expression of ripening-related genes; (3) Manipulation of *FaMRLK47* expression modulated sucrose content and the expression of genes encoding key enzymes in

sucrose metabolism. As sucrose metabolism affects strawberry fruit quality formation, FaMRLK47 is a regulator of strawberry fruit quality formation. We propose that FaMRLK47 influences fruit ripening and quality via two distinct pathways, the ABA-dependent pathway and ABA-independent pathway (Figure 8). Thus, this study provides insight into the molecular mechanisms underlying the regulation of strawberry fruit development and ripening.

AUTHOR CONTRIBUTIONS

MJ performed most of the experiments; ND, QZ, SX, and LW provided assistance with some of the experiments; YZ, PD, WM, and JL provided technical assistance; BL designed the experiments and analyzed the data; WJ conceived the project, supervised the experiments, and complemented the writing.

ACKNOWLEDGMENTS

This work was supported by the National Natural Science Foundation of China (Grant No. 31471851, 31672133, 31572104), Fok Ying-Tong Education Foundation, China (Grant No. 151027) and the 111 Project (Grant No. B17043).

SUPPLEMENTARY MATERIAL

The Supplementary Material for this article can be found online at: <http://journal.frontiersin.org/article/10.3389/fpls.2017.01099/full#supplementary-material>

REFERENCES

- Archbold, D. D. (1988). Abscisic acid facilitates sucrose import by strawberry fruit explants and cortex disks in vitro. *Hortscience* 23, 880–881.
- Boisson-Dernier, A., Kessler, S. A., and Grossniklaus, U. (2011). The walls have ears: the role of plant CrRLK1Ls in sensing and transducing extracellular signals. *J. Exp. Bot.* 62, 1581–1591. doi: 10.1093/jxb/erq445
- Boisson-Dernier, A., Roy, S., Kritsas, K., Grobeij, M. A., Jaciubek, M., Schroeder, J. I., et al. (2009). Disruption of the pollen-expressed FERONIA homologs ANXUR1 and ANXUR2 triggers pollen tube discharge. *Development* 136, 3279–3288. doi: 10.1242/dev.040071
- Brady, C. J. (1987). Fruit ripening. *Annu. Rev. Plant Physiol.* 38, 155–178. doi: 10.1146/annurev.pp.38.060187.001103
- Chai, Y. M., Jia, H. F., Li, C. L., Dong, Q. H., and Shen, Y. Y. (2011). FaPYR1 is involved in strawberry fruit ripening. *J. Exp. Bot.* 62, 5079–5089. doi: 10.1093/jxb/err207
- Chen, J., Yu, F., Liu, Y., Du, C. Q., Li, X. S., Zhu, S., et al. (2016). FERONIA interacts with ABI2-type phosphatases to facilitate signaling cross-talk between abscisic acid and RALF peptide in Arabidopsis. *Proc. Natl. Acad. Sci. U.S.A.* 113, E5519–E5527. doi: 10.1073/pnas.1608449113
- Cheung, A. Y., and Wu, H. M. (2011). THESEUS 1, FERONIA and relatives: a family of cell wall-sensing receptor kinases? *Curr. Opin. Plant Biol.* 14, 632–641. doi: 10.1016/j.pbi.2011.09.001
- Concha, C. M., Figueroa, N. E., Poblete, L. A., Oñate, F. A., Schwab, W., and Figueroa, C. R. (2013). Methyl jasmonate treatment induces changes in fruit ripening by modifying the expression of several ripening genes in *Fragaria chiloensis* fruit. *Plant Physiol. Biochem.* 70, 433–444. doi: 10.1016/j.plaphy.2013.06.008
- Coombe, B. G. (1976). The development of fleshy fruits. *Annu. Rev. Plant Physiol.* 27, 207–228. doi: 10.1146/annurev.pp.27.060176.001231
- Deslauriers, S. D., and Larsen, P. B. (2010). FERONIA is a key modulator of brassinosteroid and ethylene responsiveness in Arabidopsis hypocotyls. *Mol. Plant* 3, 626–640. doi: 10.1093/mp/ssq015
- Dong, J., Zhang, Y., Tang, X., Jinb, W., and Hana, Z. (2013). Differences in volatile ester composition between *Fragaria × ananassa* and *F. vesca* and implications for strawberry aroma patterns. *Sci. Hortic.* 150, 47–53.
- Duan, Q., Kita, D., Johnson, E. A., Aggarwal, M., Gates, L., Wu, H. M., et al. (2014). Reactive oxygen species mediate pollen tube rupture to release sperm for fertilization in Arabidopsis. *Nat. Commun.* 5, 3129. doi: 10.1038/ncomms4129
- Duan, Q., Kita, D., Li, C., Cheung, A. Y., and Wu, H. M. (2010). FERONIA receptor-like kinase regulates RHO GTPase signaling of root hair development. *Proc. Natl. Acad. Sci. U.S.A.* 107, 17821–17826. doi: 10.1073/pnas.1005366107
- Engelsdorf, T., and Hamann, T. (2014). An update on receptor-like kinase involvement in the maintenance of plant cell wall integrity. *Ann. Bot.* 114, 1339–1347. doi: 10.1093/aob/mcu043
- Escobar-Restrepo, J. M., Huck, N., Kessler, S., Gagliardini, V., Gheyselinck, J., Yang, W. C., et al. (2007). The FERONIA receptor-like kinase mediates male-female interactions during pollen tube reception. *Science* 317, 656–660. doi: 10.1126/science.1143562
- Fischer, R. L., and Bennett, A. B. (1991). Role of cell wall hydrolases in fruit ripening. *Annu. Rev. Plant Physiol. Plant Mol. Biol.* 42, 675–703. doi: 10.1146/annurev.pp.42.060191.003331
- Fuleki, T., and Francis, F. J. (1968). Quantitative methods for anthocyanins. *J. Food Sci.* 33, 266–274. doi: 10.1111/j.1365-2621.1968.tb01365.x
- Giovannoni, J. (2001). Molecular biology of fruit maturation and ripening. *Annu. Rev. Plant Biol.* 52, 725–749.
- Given, N. K., Venis, M. A., and Gierson, D. (1988). Hormonal regulation of ripening in the strawberry, a non-climacteric fruit. *Planta* 174, 402–406. doi: 10.1007/BF00959527
- Guo, H., Li, L., Ye, H., Yu, X., Algreen, A., and Yin, Y. (2009a). Three related receptor-like kinases are required for optimal cell elongation in *Arabidopsis thaliana*. *Proc. Natl. Acad. Sci. U.S.A.* 106, 7648–7653. doi: 10.1073/pnas.0812346106
- Guo, H., Ye, H., Li, L., and Yin, Y. (2009b). A family of receptor-like kinases are regulated by BES1 and involved in plant growth in *Arabidopsis thaliana*. *Plant Signal. Behav.* 4, 784–786. doi: 10.1073/pnas.0812346106
- Han, Y., Dang, R. H., Li, J. X., Jiang, J. Z., Zhang, N., Jia, M. R., et al. (2015). SUCROSE NONFERMENTING1-RELATED PROTEIN KINASE2.6, an Ortholog of OPEN STOMATA1, is a negative regulator of strawberry fruit development and ripening. *Plant Physiol.* 167, 915–931. doi: 10.1104/pp.114.251314
- Haruta, M., Sabat, G., Stecker, K., Minkoff, B. B., and Sussman, M. R. (2014). A peptide hormone and its receptor protein kinase regulate plant cell expansion. *Science* 343, 408–411. doi: 10.1126/science.1244454
- Hematy, K., and Hofte, H. (2008). Novel receptor kinases involved in growth regulation. *Curr. Opin. Plant Biol.* 11, 321–328. doi: 10.1016/j.pbi.2008.02.008
- Hematy, K., Sado, P. E., Van, T. A., Rochange, S., Desnos, T., Balzergue, S., et al. (2007). A receptor-like kinase mediates the response of *Arabidopsis* cells to the inhibition of cellulose synthesis. *Curr. Biol.* 17, 922–931. doi: 10.1016/j.cub.2007.05.018
- Huang, G. Q., Li, E., Ge, F. R., Li, S., Wang, Q., Zhang, C. Q., et al. (2013). Arabidopsis RopGEF4 and RopGEF10 are important for FERONIA-mediated developmental but not environmental regulation of root hair growth. *New Phytol.* 200, 1089–1101. doi: 10.1111/nph.12432
- Huck, N., Moore, J. M., Federer, M., and Grossniklaus, U. (2003). The Arabidopsis mutant feronia disrupts the female gametophytic control of pollen tube reception. *Development* 130, 2149–2159. doi: 10.12410/f.1012937.188152
- Humphrey, T. V., Bonetta, D. T., and Goring, D. R. (2007). Sentinels at the wall; cell wall receptors and sensors. *New Phytol.* 176, 7–21. doi: 10.1111/j.1469-8137.2007.02192.x
- Jia, H. F., Chai, Y. M., Li, C. L., Lu, D., Luo, J. J., Qin, L., et al. (2011). Abscisic acid plays an important role in the regulation of strawberry fruit ripening. *Plant Physiol.* 157, 188–199. doi: 10.1104/pp.111.177311
- Jia, H. F., Dong, L., Sun, J. H., Li, C. L., Qin, L., and Shen, Y. Y. (2013a). Type 2C protein phosphatase ABI1 is a negative regulator of strawberry fruit ripening. *J. Exp. Bot.* 64, 1677–1687. doi: 10.1093/jxb/ert028
- Jia, H. F., Wang, Y. H., Sun, M. Z., Li, B. B., Han, Y., Zhao, Y. X., et al. (2013b). Sucrose functions as a signal involved in the regulation of strawberry fruit development and ripening. *New Phytol.* 198, 453–465. doi: 10.1111/nph.12176
- Kafkas, E., Koşar, M., Paydaş, S., Kafkas, S., and Başer, K. H. C. (2007). Quality characteristics of strawberry genotypes at different maturation stages. *Food Chem.* 100, 1229–1236. doi: 10.1016/j.foodchem.2005.12.005
- Keinath, N. F., Kierszniewska, S., Lorek, J., Bourdais, G., Kessler, S. A., Shimosato-Asano, H., et al. (2010). PAMP (pathogen-associated molecular pattern)-induced changes in plasma membrane compartmentalization reveal novel components of plant immunity. *J. Biol. Chem.* 285, 39140–39149. doi: 10.1074/jbc.M110.160531
- Kessler, S. A., Lindner, H., Jones, D. S., and Grossniklaus, U. (2015). Functional analysis of related CrRLK1L receptor-like kinases in pollen tube reception. *EMBO Rep.* 16, 107–115. doi: 10.15252/embr.201438801
- Kessler, S. A., Shimosato-Asano, H., Keinath, N. F., Wuest, S. E., Ingram, G., Panstruga, R., et al. (2010). Conserved molecular components for pollen tube reception and fungal invasion. *Science* 30, 968–971. doi: 10.1126/science.1195211
- Klee, H. J., and Giovannoni, J. J. (2011). Genetics and control of tomato fruit ripening and quality attributes. *Annu. Rev. Genet.* 45, 41–59. doi: 10.1146/annurev-genet-110410-132507
- Lazo, G. R., Stein, P. A., and Ludwig, R. A. (1991). A DNA transformation-competent *Arabidopsis* genomic library in *Agrobacterium*. *Nat. Biotechnol.* 9, 963–967. doi: 10.1038/nbt1091-963
- Lees, D. H., and Francis, F. J. (1971). Quantitative methods for anthocyanins. *J. Food Sci.* 36, 1056–1060. doi: 10.1111/j.1365-2621.1971.tb03345.x
- Li, S., and Zhang, Y. (2014). To grow or not to grow: FERONIA has her say. *Mol. Plant* 7, 1261–1263. doi: 10.1093/mp/ssu031
- Lindner, H., Muller, L. M., Boisson-Dernier, A., and Grossniklaus, U. (2012). CrRLK1L receptor-like kinases: not just another brick in the wall. *Curr. Opin. Plant Biol.* 15, 659–669. doi: 10.1016/j.pbi.2012.07.003
- Lin-Wang, K., McGhie, T. K., Wang, M., Liu, Y., Warren, B., Storey, R., et al. (2014). Engineering the anthocyanin regulatory complex of strawberry (*Fragaria vesca*). *Front. Plant Sci.* 5:651. doi: 10.3389/fpls.2014.00651
- Liu, Y., Palma, A. S., and Feizi, T. (2009). Carbohydrate microarrays: key developments in glycobiology. *Biol. Chem.* 390, 647–656. doi: 10.1515/BC.2009.071

- Mao, D., Yu, F., Li, J., Van de Poel, B., Tan, D., Li, J., et al. (2015). FERONIA receptor kinase interacts with S-adenosylmethionine synthetase and suppresses S-adenosylmethionine production and ethylene biosynthesis in *Arabidopsis*. *Plant Cell Environ.* 38, 2566–2574. doi: 10.1111/pce.12570
- Miyazaki, S., Murata, T., Sakurai-Ozato, N., Kubo, M., Demura, T., Fukuda, H., et al. (2009). ANXUR1 and 2, sister genes to FERONIA/SIRENE, are male factors for coordinated fertilization. *Curr. Biol.* 19, 1327–1331. doi: 10.1016/j.cub.2009.06.064
- Ngo, Q. A., Vogler, H., Litviev, D. S., Nestorova, A., and Grossniklaus, U. (2014). A calcium dialog mediated by the FERONIA signal transduction pathway controls plant sperm delivery. *Dev. Cell* 29, 491–500. doi: 10.1016/j.devcel.2014.04.008
- Nitsch, J. P. (1953). The physiology of fruit growth. *Annu. Rev. Plant Physiol.* 4, 199–236. doi: 10.1146/annurev.pp.04.060153.001215
- Pu, C. X., Han, Y. F., Zhu, S., Song, F. Y., Zhao, Y., Wang, C. Y., et al. (2017). The rice receptor-like kinases DWARF AND RUNTISH SPIKELET1 and 2 repress cell death and affect sugar utilization during reproductive development. *Plant Cell* 29, 70–89. doi: 10.1105/tpc.16.00218
- Schallus, T., Feher, K., Sternberg, U., Rybin, V., and Muhle-Goll, C. (2010). Analysis of the specific interactions between the lectin domain of malectin and diglucosides. *Glycobiology* 20, 1010–1020. doi: 10.1093/glycob/cwq059
- Schallus, T., Jaeckh, C., Feher, K., Palma, A. S., Liu, Y., Simpson, J. C., et al. (2008). Malectin: a novel carbohydrate-binding protein of the endoplasmic reticulum and a candidate player in the early steps of protein N-glycosylation. *Mol. Biol. Cell* 19, 3404–3414.
- Schmittgen, T. D., and Livak, K. J. (2008). Analyzing real-time PCR data by the comparative CT method. *Nat. Protoc.* 3, 1101–1108. doi: 10.1038/nprot.2008.73
- Schulze-Muth, P., Irmiger, S., Schroder, G., and Schroder, J. (1996). Novel type of receptor-like protein kinase from a higher plant (*Catharanthus roseus*). cDNA, gene, intramolecular autophosphorylation, and identification of a threonine important for auto- and substrate phosphorylation. *J. Biol. Chem.* 271, 26684–26689. doi: 10.1074/jbc.271.43.26684
- Schütze, K., Harter, K., and Chaban, C. (2009). Bimolecular fluorescence complementation (BiFC) to study protein-protein interactions in living plant cells. *Methods Mol. Biol.* 479, 189–202. doi: 10.1007/978-1-59745-289-2_12
- Seymour, G. B., Østergaard, L., Chapman, N. H., Knapp, S., and Martin, C. (2013). Fruit development and ripening. *Annu. Rev. Plant. Physiol.* 64, 219–241.
- Seymour, G. B., Ryder, C. D., Cevik, V., Hammond, J. P., Popovich, A., King, G. J., et al. (2011). A SEPALLATA gene is involved in the development and ripening of strawberry (*Fragaria × ananassa* Duch.) fruit, a non-climacteric tissue. *J. Exp. Bot.* 62, 1179–1188. doi: 10.1093/jxb/erq360
- Shiu, S. H., and Bleecker, A. B. (2001a). Plant receptor-like kinase gene family: diversity, function, and signaling. *Sci STKE* 2001:re22. doi: 10.1126/stke.2001.113.re22
- Shiu, S. H., and Bleecker, A. B. (2001b). Receptor-like kinases from *Arabidopsis* form a monophyletic gene family related to animal receptor kinases. *Proc. Natl. Acad. Sci. U.S.A.* 98, 10763–10768. doi: 10.1073/pnas.181141598
- Shiu, S. H., and Bleecker, A. B. (2003). Expansion of the receptor-like kinase/Pelle gene family and receptor-like proteins in *Arabidopsis*. *Plant Physiol.* 132, 530–543. doi: 10.1104/pp.103.021964
- Takeda, K., Qin, S. Y., Matsumoto, N., and Yamamoto, K. (2014). Association of malectin with ribophorin I is crucial for attenuation of misfolded glycoprotein secretion. *Biochem. Biophys. Res. Commun.* 454, 436–440. doi: 10.1016/j.bbrc.2014.10.102
- Trainotti, L., Pavanello, A., and Casadoro, G. (2005). Different ethylene receptors show an increased expression during the ripening of strawberries: does such an increment imply a role for ethylene in the ripening of these non-climacteric fruits? *J. Exp. Bot.* 56, 2037–2046. doi: 10.1093/jxb/eri202
- Veluthambi, K., and Poovaiah, B. W. (1984). Auxin-regulated polypeptide changes at different stages of strawberry fruit development. *Plant Physiol.* 75, 349–353. doi: 10.1104/pp.75.2.349
- Villarreal, N. M., Bustamante, C. A., Civello, P. M., and Martínez, G. A. (2010). Effect of ethylene and 1-MCP treatments on strawberry fruit ripening. *J. Sci. Food Agric.* 90, 683–689. doi: 10.1002/jsfa.3868
- White, P. J. (2002). Recent advances in fruit development and ripening: an overview. *J. Exp. Bot.* 53, 1995–2000. doi: 10.1093/jxb/erf105
- Wolf, S., Hématy, K., and Höfte, H. (2012). Growth control and cell wall signaling in plants. *Annu. Rev. Plant Physiol.* 63, 381–407. doi: 10.1146/annurev-aplant-042811-105449
- Yang, T., Wang, L., Li, C., Liu, Y., Zhu, S., Qi, Y., et al. (2015). Receptor protein kinase FERONIA controls leaf starch accumulation by interacting with glyceraldehyde-3-phosphate dehydrogenase. *Biochem. Biophys. Res. Commun.* 465, 77–82. doi: 10.1016/j.bbrc.2015.07.132
- Yu, F., Li, J., Huang, Y., Liu, L., Li, D., Chen, L., et al. (2014). FERONIA receptor kinase controls seed size in *Arabidopsis thaliana*. *Mol. Plant* 7, 920–922. doi: 10.1093/mp/ssu010
- Yu, F., Qian, L., Nibau, C., Duan, Q., Kita, D., Levasseur, K., et al. (2012). FERONIA receptor kinase pathway suppresses abscisic acid signaling in *Arabidopsis* by activating ABI2 phosphatase. *Proc. Natl. Acad. Sci. U.S.A.* 109, 14693–14698. doi: 10.1073/pnas.1212547109
- Zermiani, M., Zonin, E., Nonis, A., Begheldo, M., Ceccato, L., Vezzaro, A., et al. (2015). Ethylene negatively regulates transcript abundance of ROP-GAP rheostat-encoding genes and affects apoplastic reactive oxygen species homeostasis in epicarps of cold stored apple fruits. *J. Exp. Bot.* 66, 7255–7270. doi: 10.1093/jxb/erv422
- Zhang, M., Yuan, B., and Leng, P. (2009). The role of ABA in triggering ethylene biosynthesis and ripening of tomato fruit. *J. Exp. Bot.* 60, 1579–1588. doi: 10.1093/jxb/erp026
- Zhang, Q., Jia, M. R., Xing, Y., Qin, L., Li, B. B., and Jia, W. S. (2016). Genome-wide identification and expression analysis of MRLK family genes associated with strawberry (*Fragaria vesca*) fruit ripening and abiotic stress responses. *PLoS ONE* 11:e0163647. doi: 10.1371/journal.pone.0163647

Conflict of Interest Statement: The authors declare that the research was conducted in the absence of any commercial or financial relationships that could be construed as a potential conflict of interest.

Copyright © 2017 Jia, Ding, Zhang, Xing, Wei, Zhao, Du, Mao, Li, Li and Jia. This is an open-access article distributed under the terms of the Creative Commons Attribution License (CC BY). The use, distribution or reproduction in other forums is permitted, provided the original author(s) or licensor are credited and that the original publication in this journal is cited, in accordance with accepted academic practice. No use, distribution or reproduction is permitted which does not comply with these terms.



Exploring Blueberry Aroma Complexity by Chromatographic and Direct-Injection Spectrometric Techniques

Brian Farneti^{1*}, Iuliia Khomenko^{2,3}, Marcella Grisenti¹, Matteo Ajelli¹, Emanuela Betta², Alberto Alarcon Algarra², Luca Cappellin², Eugenio Aprea², Flavia Gasperi², Franco Biasioli² and Lara Giongo¹

¹ Genomics and Biology of Fruit Crop Department, Fondazione Edmund Mach, Trento, Italy, ² Food Quality and Nutrition Department, Fondazione Edmund Mach, Trento, Italy, ³ Institut für Ionenphysik und Angewandte Physik, Leopold-Franzens Universität Innsbruck, Innsbruck, Austria

OPEN ACCESS

Edited by:

Maarten Hertog,
KU Leuven, Belgium

Reviewed by:

Isabel Lara,
University of Lleida, Spain
Nikos Tzortzakis,
Cyprus University of Technology,
Cyprus

*Correspondence:

Brian Farneti
brian.farneti@fmach.it

Specialty section:

This article was submitted to
Crop Science and Horticulture,
a section of the journal
Frontiers in Plant Science

Received: 03 March 2017

Accepted: 05 April 2017

Published: 26 April 2017

Citation:

Farneti B, Khomenko I, Grisenti M, Ajelli M, Betta E, Algarra AA, Cappellin L, Aprea E, Gasperi F, Biasioli F and Giongo L (2017) Exploring Blueberry Aroma Complexity by Chromatographic and Direct-Injection Spectrometric Techniques. *Front. Plant Sci.* 8:617.
doi: 10.3389/fpls.2017.00617

Blueberry (*Vaccinium* spp.) fruit consumption has increased over the last 5 years, becoming the second most important soft fruit species after strawberry. Despite the possible economic and sensory impact, the blueberry volatile organic compound (VOC) composition has been poorly investigated. Thus, the great impact of the aroma on fruit marketability stimulates the need to step forward in the understanding of this quality trait. Beside the strong effect of ripening, blueberry aroma profile also varies due to the broad genetic differences among *Vaccinium* species that have been differently introgressed in modern commercial cultivars through breeding activity. In the present study, divided into two different activities, the complexity of blueberry aroma was explored by an exhaustive untargeted VOC analysis, performed by two complementary methods: SPME-GC-MS (solid phase microextraction- gas chromatography-mass spectrometry) and PTR-ToF-MS (proton transfer reaction-time of flight-mass spectrometry). The first experiment was aimed at determining the VOC modifications during blueberry ripening for five commercially representative cultivars ("Biloxi," "Brigitta Blue," "Centurion," "Chandler," and "Ozark Blue") harvested at four ripening stages (green, pink, ripe, and over-ripe) to outline VOCs dynamic during fruit development. The objective of the second experiment was to confirm the analytical capability of PTR-ToF-MS to profile blueberry genotypes and to identify the most characterizing VOCs. In this case, 11 accessions belonging to different *Vaccinium* species were employed: *V. corymbosum* L. ("Brigitta," "Chandler," "Liberty," and "Ozark Blue"), *V. virgatum* Aiton ("Centurion," "Powder Blue," and "Sky Blue"), *V. myrtillus* L. (three wild genotypes of different mountain locations), and one accession of *V. cylindraceum* Smith. This comprehensive characterization of blueberry aroma allowed the identification of a wide pull of VOCs, for the most aldehydes, alcohols, terpenoids, and esters that can be used as putative biomarkers to rapidly evaluate the blueberry aroma variations related to ripening and/or senescence as well as to genetic background differences. Moreover, the obtained results demonstrated the complementarity between chromatographic and direct-injection mass spectrometric techniques to study the blueberry aroma.

Keywords: *Vaccinium* spp., PTR-ToF-MS, SPME-GC-MS, VOCs, flavor, ripening, breeding

INTRODUCTION

The quality of fruits has to be considered as a central trait to address consumer appreciation and optimize the whole production chain management (Costa et al., 2000; Mowat and Collins, 2000; Benner and Geerts, 2003; Klee, 2010). In order to satisfy consumer's demands more effort has to be devoted to improve and optimize quality upon delivery to consumers. Quality of a fresh product can be defined by the achievement of four principal quality elements: appearance, flavor, texture, and nutritional properties (Costa et al., 2011). Defining and quantifying these quality components, in relation with distinct segments of the production chain, needs comprehensive investigations and a tight synergy of analytical approaches with a particular focus on rapid and non-invasive methods.

For many years most breeding efforts have been primarily devoted to improve and maintain the external quality of fruits, with little attention to other intrinsic characteristics. Selection for yield, fruit size, color, and shelf life traits might have had unintended negative consequences on sensory quality and nutritional effects (Goff and Klee, 2006; Farneti et al., 2015a, 2017; Tieman et al., 2017). Fruit flavor, in particular, depends upon taste (balance between sweetness and sourness or acidity, and low or no astringency) and aroma (concentration of VOCs). Although taste and aroma are well-integrated in their contribution to the overall flavor, aroma is often considered playing a dominant role (Folta and Klee, 2016). Although a single fruit synthesizes several 100 volatiles, only a small subset generates the "flavor fingerprint" that helps animals and humans to recognize appropriate and avoid dangerous food (Goff and Klee, 2006). Since aroma involves the perception of a myriad of VOCs, their assessment would be crucial to guarantee the selection and marketability of high-quality fruits. Another aspect to take into account is the interaction of volatile compounds may have with taste in fruits as recently evidenced in apple sweetness perception (Aprea et al., 2017). In the near future, the main breeding goal will be to produce fruits and vegetables that consumers actively seek, while maintaining industry-mandated qualities. High priority should thus be given to replacing poor flavor cultivars with more favorable ones, exploiting the variability already available in nature (Folta and Klee, 2016).

The extraordinary nutraceutical properties (Norberto et al., 2013) and the unique flavor (Gilbert et al., 2014, 2015), are the chief quality traits that are swiftly enhancing blueberry (*Vaccinium* spp.) consumption. Worldwide blueberry production has indeed increased over the last decade (Brazelton, 2011; Payne, 2014; Clarke, 2016), becoming the second most important soft fruit species after strawberry. Despite the economic and nutraceutical importance of blueberry, there has been little mention in the literature, over last 10 years, of the VOC composition of this fruit and of its possible impact on consumer preferences.

Blueberry aroma depends on the interaction of dozens of VOCs (Du et al., 2011; Gilbert et al., 2013; Beaulieu et al., 2014; Gilbert et al., 2015) synthesized by the fruit during ripening. Among them only a minor set of chemical compounds, for the most aldehydes, alcohols, ketones, terpenoids, and esters can

be distinctly perceived at the sensorial level (Du and Rouseff, 2014; Gilbert et al., 2015). Despite the strong effect of ripening, the blueberry aroma profiling also varies due to the broad genetic differences among the *Vaccinium* species. For instance lowbush blueberry (*V. angustifolium* L.), bilberry (*V. myrtillus* L.), and other wild species are mostly characterized by a high production of esters (i.e., methyl acetate, ethyl acetate, or methyl butanoate) while highbush (*V. corymbosum* L.) and rabbiteye blueberry (*V. virgatum* Aiton) profiles are mostly characterized by a high concentration of "green compounds" such as (E)-2-hexenal, hexanal, and (Z)-3-hexenol and terpene alcohols such as linalool, nerol, and geraniol (von Sydow and Anjou, 1969; von Sydow et al., 1970; Hall et al., 1979; Horvat et al., 1983, 1996).

Aroma characterization of different species has always represented a main analytical issue, especially because wide sample sets are needed to cover the expected biological variability. Traditionally, flavor attributes of horticultural products are assessed by sensory panels. However, this procedure is time consuming, and expensive. Therefore, in practical contexts, high resolution and rapid screening techniques are needed as analytical support for sensory analysis. These analytical tools have to deal with important issues such as the need of separating and quantifying VOCs in complex gas mixtures and the simultaneous detection of concentrations which may span a large range, from trace levels (i.e., part per trillion) to parts per million (Biasioli et al., 2011).

Given these experimental constraints, the ideal methodology for VOCs monitoring should be highly selective, with high sensitivity and dynamic range, and with high time resolution. The benchmark analytical method for VOCs identification and quantification is currently gas chromatography-mass spectrometry (GC-MS), often coupled with solid-phase microextraction (e.g., SPME fibers) to lower the detection limits. Although valuable and, in many cases, indispensable, gas chromatographic headspace analyses have several disadvantages such as low time resolution, laborious sample preparation and long operation time particularly when a concentrate headspace VOC content is needed to improve the detection limit (Dewulf et al., 2002). Moreover, the application of thermal desorption units, such as SPME fibers, precludes a feasible quantitative analysis of multicomponent mixtures, since the competition for active sites on the fiber and the relative proportions of the adsorbed compounds depend on their ratio in the sample VOC headspace (Górecki et al., 1999). Overcoming such limits means employing techniques without chromatographic separation. This might be the reason why total aromatic volatile concentrations, collected and concentrated from blueberry fruit extracts using a SPME technique, were not strongly correlated with sensory scores for flavor, overall eating quality or to any other sensory characteristic (Saftner et al., 2008; Gilbert et al., 2015). Thus, volatile concentration, at least when analyzed on the headspace of intact fruit by SPME technique, might not be a good indicator of blueberry taste or overall eating quality.

Different methods have been recently proposed, such as arrays of solid-state gas sensors (E-Noses), and direct injection mass spectrometry (DI-MS; Biasioli et al., 2011). Besides its technological performances (e.g., sensitivity and selectivity), the

greatest difficulty arising in DI-MS technologies, due to the lack of chromatographic separation, is the need to identify compounds that generate the observed peaks, since the latter can be the results of overlapping signals from the mix of different VOCs present in the sample. Among DI-MS techniques, Proton Transfer Reaction-Mass Spectrometry (PTR-MS) has the advantage of a very low detection limit and high sensitivity. (Blake et al., 2009). Significant improvements have been made by coupling PTR-MS technology with Time-of-Flight mass spectrometry (ToF-MS). PTR-ToF-MS instruments can generate entire mass spectra of complex trace gas mixtures in short response times with high mass resolution and with virtually no upper mass limit (Jordan et al., 2009).

In the present study the complexity of blueberry aroma was explored by an exhaustive untargeted VOC analysis, done by SPME-GC-MS and PTR-ToF-MS analysis. The aim of this investigation was to acquire a detailed and comprehensive characterization of the blueberry aroma according to different ripening stages and genetic differences, as well as to investigate the potential of PTR-ToF-MS as a rapid and reliable technique to address issues related to blueberry quality.

MATERIALS AND METHODS

Plant Materials

In this investigation, blueberry accessions were chosen from the experimental field of FEM Research and Innovation Center at Pergine (Trento), located in the north of Italy (Trentino Alto Adige region). At the time of the analysis, plants were in the full production phase, between 7 and 10 years old. The bushes were grown in trenches lined with permeable tissue, adjusted with a pit-bark mix. The crop's frame was 2.5 m between rows and 1 m along the row. An automatic fertigation system was used to guarantee water supply and soil acidification at pH 4.5 (by adding nitric acid 52% with an automatic dispenser), while water conductivity was periodically monitored at 1300 μS with a conductivimeter (Crison Instrument Mod. CM35). Bushes were maintained following standard pruning and surface bark mulching renewal. In the plot, each of the accessions was represented by five plants.

For the first experiment, aimed at determining the VOCs modifications during fruit ripening, we employed five blueberry cultivars, namely "Biloxi," "Brigitta Blue," "Centurion," "Chandler," and "Ozark Blue."

For the second experiment, aimed at testing the analytical capacity of PTR-ToF-MS to profile blueberry genotypes based on VOCs, we employed eleven accessions of four different *Vaccinium* species: *V. corymbosum* L. ("Brigitta Blue," "Chandler," "Liberty," and "Ozark Blue"), *V. virgatum* Aiton ("Centurion," "Powder Blue," and "Sky Blue"), *V. myrtillus* L. (three genotypes of different mountain locations), and one accession of *V. cylindraceum* Smith.

Fruit Maturity Assessment

Blueberry fruits, free from external damages or irregularities, were harvested from multiple plants and sorted into the established ripening stages [green (G), pink (P), ripe (R), and

overripe (Or)] analytically determined using Minolta colorimeter and non-destructive compression test using FirmTech firmness tester (BioWorks, Wamengo, KS, USA). Ten homogeneous berries, for each ripening stage, were selected for fruit maturity assessment. Texture was profiled by a texture analyzer (Zwick Roell, Italy), which profiled a mechanical force displacement using a 5 kg loading cell and a cylindrical flat head probe with a diameter of 4 mm entering into the berry flesh from the sagittal side (for more details see Giongo et al., 2013). On the force displacement profile, seven parameters were considered: maximum force, final force, area, maximum deformation, minimum deformation, maximum force strain, and gradient (or Young's module, also known as the elasticity module). Total soluble solid (TSS, °Bx), pH, and titratable acidity (TA, meq/100 g FW) were assessed on homogeneous berries with a DBR35 refractometer (XS Instruments, 199 Poncarale, Brescia, Italy), pH Meter, and Compact Titrator (Crison Instruments S.A., Alella, Barcelona, 200 Spain), respectively.

VOC Analysis by SPME-GC-MS

Three replicates of 1.0 g of powdered frozen samples, conserved at -80°C , were immediately inserted into 20 ml glass vials equipped with PTFE/silicone septa (Agilent, Cernusco sul Naviglio, Italy) and mixed with 1.0 ml of deionized water, 400 mg of sodium chloride, 5 mg of ascorbic acid, and 5 mg of citric acid (for more details see Aprea et al., 2011). Samples were then preserved at 4°C till the analysis.

The vials were equilibrated at 40°C for 10 min with constant stirring. Solid-phase microextraction fiber (DVB/CAR/PDMS, Supelco, Bellefonte, PA, USA) was exposed for 30 min in the vial headspace. The compounds adsorbed by HS-SPME were analyzed with a GC interfaced with a mass detector operating in electron ionization (EI) mode (internal ionization source; 70 eV) with a scan range of m/z 33–350 (GC Clarus 500, PerkinElmer, Norwalk CT, USA). Separation was carried out in an HP-INNOWax fused silica capillary column (30 m, 0.32-mm ID, 0.5- μm film thickness; Agilent Technologies, Palo Alto, CA, USA). The initial GC oven temperature was 40°C rising to 220°C at $4^{\circ}\text{C min}^{-1}$, the temperature of 220°C was maintained for 1 min, then increased at $10^{\circ}\text{C min}^{-1}$ until it reached 250°C , which was maintained for 1 min. The carrier gas was helium at a constant column flow rate of 1.5 ml min^{-1} . Samples were analyzed in triplicates. Semiquantitative data were expressed as microgram per liter equivalent of 2-octanol. Compound identification was based on mass spectra matching with the standard NIST/EPA/NIH (NIST 14) and Wiley 7th Mass Spectral Libraries, and linear retention indices (LRI) compared with the literature. LRI were calculated under the same chromatographic conditions after injection of a C7–C30 n-alkane series (Supelco).

VOC Analysis by PTR-ToF-MS

Measurements of blueberry VOCs with a PTR-ToF-MS 8000 apparatus (Ionicon Analytik GmbH, Innsbruck, Austria) were performed in three sample replicates prepared as for SPME-GC-MS analysis (without adding the internal standard). The conditions in the drift tube were the following ones: 110°C drift tube temperature, 2.30 mbar drift pressure, 550 V drift voltage.

This leads to an E/N ratio of about 140 Townsend (Td), with E corresponding to the electric field strength and N to the gas number density ($1 \text{ Td} = 1017 \text{ Vcm}^2$). The sampling time per channel of ToF acquisition was 0.1 ns, amounting to 350,000 channels for a mass spectrum ranging up to $m/z = 400$. Every single spectrum is the sum of about 28,600 acquisitions, resulting in a time resolution of 1 s. Sampling was performed in 60 cycles resulting in an analysis time of 60 s/sample. Each measurement was conducted automatically after 20 min of sample incubation at 40°C by using an adapted GC autosampler (MPS Multipurpose Sampler, GERSTEL) and it lasted for about 2 min (Capozzi et al., 2017). During each measurement a sample headspace was withdrawn through PTR-MS inlet with 40 sccm flow. For prevention of low pressure inside the vial, zero air was flushed continuously through it.

The analysis of PTR-ToF-MS spectral data proceeded as follows. Count losses due to the ion detector dead time were corrected off-line via a methodology based on Poisson statistics (Titzmann et al., 2010). To reach a good mass accuracy (up to 0.001 Th), internal calibration was performed according to a procedure described by Cappellin et al. (2011). Noise reduction, baseline removal and peak intensity extraction were performed according to Cappellin et al. (2011), using modified Gaussians to fit the peaks. Absolute headspace VOC concentrations expressed in ppbv (parts per billion by volume) were calculated from peak intensities according to Cappellin et al. (2012b).

Statistical Analysis

The detection of the array of masses with PTR-ToF-MS was reduced by applying noise and correlation coefficient thresholds. The first removed peaks not significantly different from blank samples (Farneti et al., 2015b); the latter excluded peaks having over 99% correlation, which correspond for the most to isotopes of monoisotopic masses (Farneti et al., 2017).

R.3.2.2 internal statistical functions and the external packages “mixOmics” and “clValid” were used for the multivariate statistical methods [Principal Component Analysis (PCA), Partial Least Squares (PLS), Self Organizing Tree Algorithm (SOTA)] employed in the whole work.

Visualization of significant VOCs correlations ($P < 0.01$; $R > 0.60$) was conducted by the generation of a PLS regression Network with Cytoscape (version 3.2.1; Cline et al., 2007).

RESULTS

Fruit Ripening Assessment

Fruits were non-destructively sorted into four ripening classes based on color. The homogeneity of each fruit batch was successively confirmed by destructive quality assessments such as texture, pH, titratable acidity, and soluble solid content, on randomly picked fruits.

Principal component analysis based on fruit textural proprieties (Supplementary Figure 1), beyond a distinct separation of *Vaccinium* cultivars, revealed a clear separation of the four harvest ripening stages, mostly explained by the variability of the first principal component (PC1: 95.6%). More ripe fruits were characterized by a greater deformation due to the

applied forces while more unripe fruit had a higher resistance to the forces (F_Min and F_Max) that resulted also in a greater area under the deformation curve.

As expected, textural differences between ripe and over ripe fruits were not as discernible as for the more unripe (green and pink) ones. However, differences between these two classes were magnified by the results of pH, treatable acidity (TA), and total soluble solids (TSS; Supplementary Figure 2). Overripe fruits of each cultivar were indeed characterized by higher pH and TSS-values and lower TA.

Chemical Composition of Blueberry Aroma Assessed by SPME-GC-MS

The gas chromatographic analysis by SPME-GC-MS assessed on five *Vaccinium* cultivars (“Biloxi,” “Brigitta Blue,” “Centurion,” “Chandler,” and “Ozark Blue”) harvested at different ripening stages (green, pink, ripe, over ripe) allowed the detection of 106 VOCs, among which only six were not identified (reported as “Unknown”; Table 1). Esters, 25 in total, were the most represented chemical class. Other classes of compounds are aldehydes (18 compounds), alcohols (16), monoterpenes (14), ketones (7), acids (4), hydrocarbons (4), sesquiterpenes (3), lactones (1), and norisoprenoids (1).

Based on VOC relative concentration, aldehydes were the most abundant class (in terms of total chromatographic area) since they covered almost 50% of the overall *Vaccinium* volatile profile (Figure 1). The highest fraction of aldehydes was composed by C6 aldehydes such as (E)-2-hexenal, hexanal, (Z)-3-hexenal, hexadienal, or heptenal. These compounds, predominantly detected in unripe fruits, decreased during fruit ripening with slight variability between cultivars. Remarkably, some isomers of these aldehydes, such as (Z)-3-hexenal and (E)-2-hexenal, did not show the same evolution during fruit ripening. For instance, while (Z)-3-hexenal concentration decreased exponentially during ripening, (E)-2-hexenal concentration reached the utmost level at the pink stage and it lasted till the full ripe stage. Hexanal, the third aldehyde based on average concentration levels, after (E)-2-hexenal and (Z)-3-hexenal, revealed a production trend similar to (E)-2-hexenal one.

Over 35% of the blueberry chromatographic profile was determined by alcoholic compounds (Figure 1). Nevertheless, this result should be discreetly considered since the largest fraction of these compounds was covered by ethanol. Besides ethanol, (Z)-3-hexenol and (Z)-2-hexenol were the most abundant alcohols. These alcohols, synthesized from their corresponding aldehydes [(Z)-3-hexenal and (Z)-2-hexenal], revealed an opposite evolution during fruit ripening. (Z)-3-hexenol was mostly synthesized by green blueberry and it suddenly decreased during fruit ripening. (Z)-2-hexenol amount, instead, increased linearly during fruit ripening and it reached significantly different end-levels at the overripe stage, according to the genotype. Likewise, hexanol was synthesized during fruit ripening and it reached different concentration that were genotype specific; for instance fruits of “Brigitta Blue,” differently from the other four cultivars considered in this study, were

TABLE 1 | Volatile compounds detected by SPME-GC-MS in blueberry fruits at different ripening stages.

Name	ID	SOTA ^a	Formula	RT	KI Calc	KI Nist	Min ^b	Max ^b	Mean ^b
ACIDS									
Hexanoic acid	Ac_1	8	C ₆ H ₁₂ O ₂	33.27	2,044	1,846	0.1	6.9	0.6
Octanoic acid	Ac_2	8	C ₈ H ₁₆ O ₂	38.25	2,222	2,060	0.0	3.0	0.4
Nonanoic acid	Ac_3	3	C ₉ H ₁₈ O ₂	40.40	2,299	2,171	1.5	8.4	3.4
Decanoic acid	Ac_4	8	C ₁₀ H ₂₀ O ₂	42.77	2,384	2,276	1.2	4.9	2.9
ALCOHOLS									
Ethanol	Al_1	1	C ₂ H ₆ O	2.36	937	932	569.6	809.2	675.2
3-Methyl-1-butanol	Al_2	1	C ₅ H ₁₂ O	9.21	1,223	1,209	0.0	2.8	0.5
Pentanol	Al_3	2	C ₅ H ₁₂ O	10.57	1,264	1,250	1.9	12.1	6.0
2-Heptanol	Al_4	1	C ₇ H ₁₆ O	12.88	1,332	1,320	0.0	1.6	0.1
Hexanol	Al_5	8	C ₆ H ₁₄ O	13.92	1,363	1,355	3.0	272.3	26.4
(E)-3-hexen-1-ol	Al_6	4	C ₆ H ₁₂ O	14.26	1,373	1,367	0.0	2.5	0.6
(Z)-3-hexen-1-ol	Al_7	1	C ₆ H ₁₂ O	14.90	1,392	1,382	1.1	147.1	34.4
(Z)-2-hexen-1-ol	Al_8	6	C ₆ H ₁₂ O	15.63	1,415	1,416	2.8	119.8	30.5
1-Octen-3-ol	Al_9	6	C ₈ H ₁₆ O	17.05	1,460	1,450	1.8	5.3	3.4
1-Heptanol	Al_10	8	C ₇ H ₁₆ O	17.17	1,464	1,453	0.5	11.2	1.2
2-Ethyl-1-hexanol	Al_11	1	C ₈ H ₁₈ O	18.26	1,498	1,491	0.4	1.1	0.6
1-Octanol	Al_12	8	C ₈ H ₁₈ O	20.30	1,566	1,557	1.1	28.2	3.0
HO-trienol	Al_13	1	C ₁₀ H ₁₆ O	21.86	1,619	1,613	0.0	8.1	1.1
1-Nonanol	Al_14	8	C ₉ H ₂₀ O	23.26	1,667	1,660	0.5	4.7	1.1
Benzyl alcohol	Al_15	8	C ₇ H ₈ O	29.01	1,879	1,870	0.0	3.9	0.4
Phenetyl alcohol	Al_16	8	C ₈ H ₁₀ O	29.85	1,912	1,906	0.0	1.5	0.1
ALDEHYDES									
2-Methyl butanal+3-methyl butanal	Ad_1	1	C ₅ H ₁₀ O	3.03	984	914	1.8	17.3	8.5
Hexanal	Ad_2	6	C ₆ H ₁₂ O	5.33	1,097	1,083	44.7	287.2	134.4
(E)-2-pentenal	Ad_3	1	C ₅ H ₈ O	6.66	1,142	1,127	0.5	11.1	3.4
(Z)-3-hexenal	Ad_4	1	C ₆ H ₁₀ O	7.68	1,175	1,141	1.6	508.7	176.3
Heptanal	Ad_5	8	C ₇ H ₁₄ O	8.39	1,198	1,184	2.8	15.0	4.7
(Z)-2-hexenal	Ad_6	1	C ₆ H ₁₀ O	8.91	1,214	1,189	6.2	45.9	25.8
(E)-2-hexenal	Ad_7	5	C ₆ H ₁₀ O	9.42	1,229	1,216	201.8	1206.9	632.4
Octanal	Ad_8	3	C ₈ H ₁₆ O	11.74	1,298	1,289	2.5	7.3	4.6
(E)-2-heptenal	Ad_9	1	C ₇ H ₁₂ O	12.80	1,330	1,323	3.9	17.8	10.7
2-Nonenal	Ad_10	3	C ₉ H ₁₆ O	15.13	1,399	1,537	4.3	14.2	8.1
(E,Z)-2,4-hexadienal	Ad_11	1	C ₆ H ₈ O	15.30	1,404	1,391	0.5	8.1	3.6
(E,E)-2,4-hexadienal	Ad_12	1	C ₆ H ₈ O	15.39	1,407	1,395	3.3	40.3	17.8
(E)-2-octenal	Ad_13	3	C ₈ H ₁₄ O	16.17	1,432	1,429	6.5	13.6	9.7
(E,E)-2,4-heptadienal	Ad_14	1	C ₇ H ₁₀ O	17.37	1,470	1,495	0.2	2.2	0.9
Decanal	Ad_15	8	C ₁₀ H ₂₀ O	18.40	1,503	1,498	1.0	4.2	2.3
Benzaldehyde	Ad_16	1	C ₇ H ₆ O	19.04	1,524	1,520	0.6	2.8	1.2
(E)-2-nonenal	Ad_17	7	C ₉ H ₁₆ O	19.44	1,538	1,534	0.6	3.4	1.5
3-Ethyl benzaldehyde	Ad_18	8	C ₉ H ₁₀ O	24.37	1,706	1,698	0.0	0.9	0.2
ESTERS									
Methyl acetate	E_1	8	C ₃ H ₆ O ₂	1.40	829	828	0.0	2.9	0.2
Ethyl acetate	E_2	8	C ₄ H ₈ O ₂	1.83	897	888	0.9	45.4	5.4
Ethyl propanoate	E_3	8	C ₅ H ₁₀ O ₂	2.68	960	953	0.0	0.3	0.0
Ethyl isobutyrate	E_4	8	C ₆ H ₁₂ O ₂	2.80	968	961	0.0	0.3	0.0
Methyl-2-methyl butanoate	E_5	8	C ₆ H ₁₂ O ₂	3.64	1,018	1,009	0.0	2.3	0.1
Methyl isovalerate	E_6	8	C ₆ H ₁₂ O ₂	3.85	1,028	1,018	0.0	20.0	1.9
Ethyl butyrate	E_7	8	C ₆ H ₁₂ O ₂	4.28	1,048	1,035	0.0	0.3	0.0
Ethyl-2-methyl butanoate	E_8	8	C ₇ H ₁₄ O ₂	4.60	1,063	1,051	0.0	8.9	0.7
Ethyl isovalerate	E_9	8	C ₇ H ₁₄ O ₂	4.99	1,081	1,068	0.0	76.1	8.0

(Continued)

TABLE 1 | Continued

Name	ID	SOTA ^a	Formula	RT	KI Calc	KI Nist	Min ^b	Max ^b	Mean ^b
Ethyl (2E)-2-butenoate	E_10	8	C ₆ H ₁₀ O ₂	7.78	1,178	1,160	0.0	3.3	0.3
Ethyl hexanoate	E_11	3	C ₈ H ₁₆ O ₂	10.01	1,247	1,233	0.0	0.2	0.0
Hexyl acetate	E_12	8	C ₈ H ₁₆ O ₂	11.27	1,284	1,272	0.0	3.4	0.4
(Z)-3-hexenyl acetate	E_13	1	C ₈ H ₁₄ O ₂	12.75	1,328	1,315	0.0	195.0	22.9
2-Hexenyl acetate	E_14	7	C ₈ H ₁₄ O ₂	13.33	1,345	1,352	0.0	18.5	2.5
Methyl 3-hydroxy-3-methylbutanoate	E_15	8	C ₆ H ₁₂ O ₃	14.44	1,379	1,363	0.0	3.7	0.2
Ethyl-3-hydroxy-3-methylbutanoate	E_16	1	C ₇ H ₁₄ O ₃	15.65	1,416	1,404	0.0	1.1	0.1
Ethyl-2-hydroxy-3-methylbutanoate	E_17	8	C ₇ H ₁₄ O ₃	16.15	1,432	1,422	0.0	4.9	0.4
(E,Z)-ethyl 2,4-hexadienoate	E_18	1	C ₁₀ H ₁₈ O ₂	16.90	1,455		0.0	0.3	0.0
(Z)-3-hexenyl butanoate	E_19	1	C ₁₀ H ₁₈ O ₂	17.29	1,468	1,454	0.0	13.2	1.2
(E,E)-ethyl 2,4-hexadienoate	E_20	2	C ₁₀ H ₁₂ O ₂	18.00	1,490	1,501	0.0	6.1	0.8
(Z,Z)-ethyl 2,4-hexadienoate	E_21	2	C ₈ H ₁₂ O ₂	18.70	1,513		0.0	1.2	0.2
Ethyl furan-2-carboxylate	E_22	1	C ₇ H ₈ O ₃	22.16	1,629	1,618	0.0	0.3	0.0
Ethyl benzoate	E_23	2	C ₉ H ₁₀ O ₂	23.26	1,667	1,658	0.0	0.5	0.1
Ethyl phenyl acetate	E_24	1	C ₉ H ₁₀ O ₂	26.63	1,789	1,783	0.0	0.1	0.0
2-Ethyl hexyl salicylate	E_25	8	C ₁₅ H ₂₂ O ₃	38.86	2,244		0.0	16.5	2.0
HYDROCARBONS									
Octane	H_1	7	C ₈ H ₁₈	1.23	802	800	0.2	23.5	5.2
Ethyl benzene	H_2	8	C ₈ H ₁₀	6.48	1,136	1,125	0.6	8.2	3.5
p-Xylene	H_3	8	C ₈ H ₁₀	6.71	1,143	1,127	0.0	1.3	0.5
m-Xylene	H_4	8	C ₈ H ₁₀	6.90	1,150	1,132	0.0	2.9	1.2
Ketones									
2-Heptanone	K_1	1	C ₇ H ₁₄ O	8.27	1,195	1,182	0.0	140.9	16.7
2-Octanone	K_2	2	C ₈ H ₁₆ O	11.59	1,294	1,287	3.4	4.5	3.8
1-Octen-3-one	K_3	3	C ₈ H ₁₄ O	12.16	1,311	1,300	0.9	4.1	2.3
6-Methyl-5-hepten-2-one	K_4	4	C ₈ H ₁₄ O	13.34	1,346	1,338	14.4	52.1	30.0
2-Nonanone	K_5	1	C ₉ H ₁₈ O	14.96	1,394	1,390	0.0	11.6	2.7
2-Undecanone	K_6	1	C ₁₁ H ₂₂ O	21.38	1,602	1,598	0.0	7.6	2.3
Acetophenone	K_7	3	C ₈ H ₈ O	22.76	1,650	1,647	0.1	2.4	0.5
LACTONES									
Butyrolactone	L_1	7	C ₄ H ₆ O ₂	22.05	1,625	1,632	0.6	2.0	1.0
MONOTERPENES									
β-Myrcene	M_1	7	C ₁₀ H ₁₆	7.68	1,175	1,161	0.0	8.7	1.6
Limonene	M_2	7	C ₁₀ H ₁₆	8.60	1,205	1,200	0.3	35.2	8.7
1,8-Cineole	M_3	1	C ₁₀ H ₁₈ O	8.83	1,212	1,213	4.0	222.4	63.6
(E)-β-ocimene	M_4	7	C ₁₀ H ₁₆	10.54	1,262	1,250	0.0	2.5	1.0
α-Terpinolene	M_5	7	C ₁₀ H ₁₆	11.41	1,288	1,283	0.5	8.0	2.9
Linalool oxide A	M_6	1	C ₁₀ H ₁₈ O ₂	16.55	1,444	1,452	0.1	5.9	1.6
Linalool oxide B	M_7	1	C ₁₀ H ₁₈ O ₂	17.46	1,473	1,444	0.0	14.3	2.9
Linalool	M_8	6	C ₁₀ H ₁₈ O	20.03	1,557	1,547	11.6	193.2	105.7
4-Terpineol	M_9	1	C ₁₀ H ₁₈ O	21.41	1,603	1,602	0.0	14.1	1.0
α-Terpineol	M_10	7	C ₁₀ H ₁₈ O	24.18	1,699	1,697	2.0	17.0	9.8
Nerol	M_11	8	C ₁₀ H ₁₈ O	27.08	1,806	1,797	0.0	1.5	0.3
Geraniol	M_12	7	C ₁₀ H ₁₈ O	28.36	1,855	1,847	0.3	7.2	1.9
Geranyl acetone	M_13	6	C ₁₃ H ₂₂ O	28.34	1,854	1,859	1.6	28.1	9.3
Eugenol	M_14	8	C ₁₀ H ₁₂ O ₂	36.07	2,144	2,169	0.0	2.4	0.1
NORISOPRENOIDS									
β-Damascenone	N_1	2	C ₁₃ H ₁₈ O	27.43	1,819	1,823	0.0	0.3	0.1
SESQUITERPENES									
δ-Elemene	S_1	8	C ₁₅ H ₂₄	17.32	1,469	1,470	0.0	2.4	0.1

(Continued)

TABLE 1 | Continued

Name	ID	SOTA ^a	Formula	RT	KI Calc	KI Nist	Min ^b	Max ^b	Mean ^b
(E)-caryophyllene	S_2	1	C ₁₅ H ₂₄	21.02	1,590	1,595	0.0	8.3	1.2
Caryophyllene oxide	S_3	1	C ₁₅ H ₂₄ O	31.31	1,970	1,989	0.0	1.5	0.3
UNIDENTIFIED COMPOUNDS									
Unknown 1	U_1	2	#	7.98	1,185		0.0	6.5	0.6
Unknown 2	U_2	7	#	10.18	1,252		0.0	84.2	18.4
Unknown 3	U_3	8	#	12.27	1,314		0.0	0.4	0.0
Unknown 4	U_4	7	#	12.57	1,323		0.0	40.6	4.7
Unknown 5	U_5	6	#	19.18	1,529		0.3	2.3	1.1
Unknown 6	U_6	1	#	31.36	1,972		0.2	8.6	2.7

^aSOTA (self-organizing tree algorithm) clusters based on **Figure 2**.

^bμg/Kg of 2-octanol.

#MS detection spectra showed in **Supplementary Figure 3**.

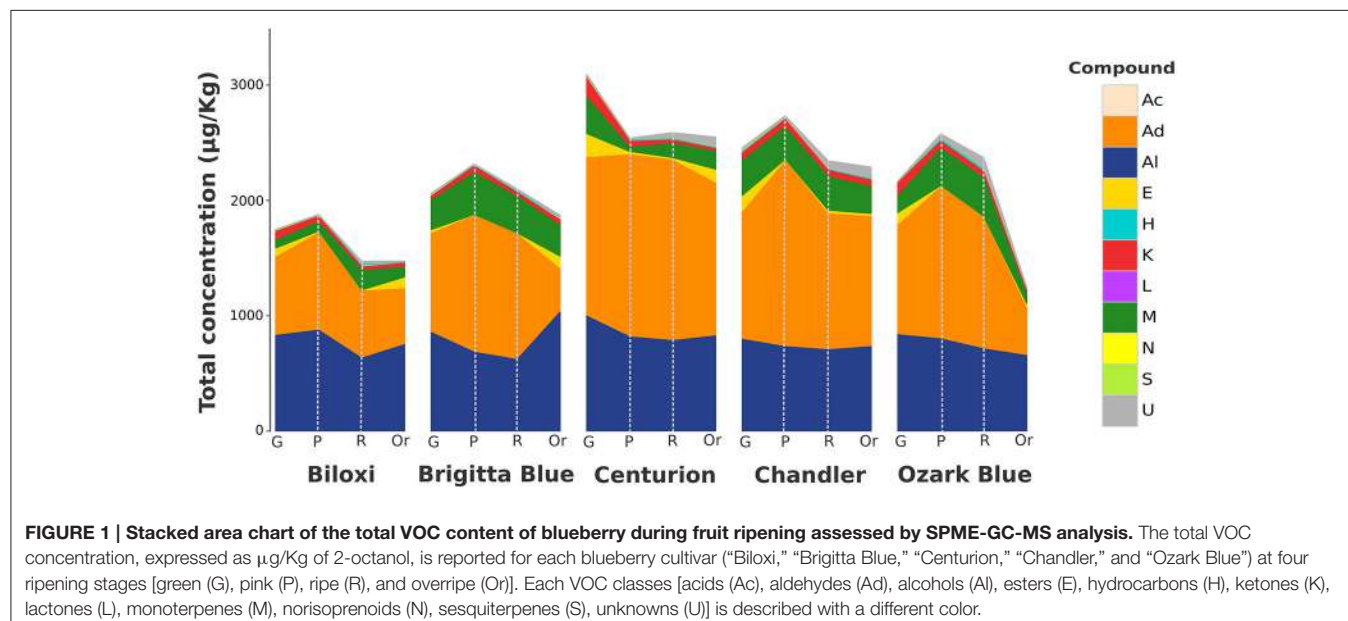


FIGURE 1 | Stacked area chart of the total VOC content of blueberry during fruit ripening assessed by SPME-GC-MS analysis. The total VOC concentration, expressed as μg/Kg of 2-octanol, is reported for each blueberry cultivar ("Biloxi," "Brigitte Blue," "Centurion," "Chandler," and "Ozark Blue") at four ripening stages [green (G), pink (P), ripe (R), and overripe (Or)]. Each VOC classes [acids (Ac), aldehydes (Ad), alcohols (Al), esters (E), hydrocarbons (H), ketones (K), lactones (L), monoterpenes (M), norisoprenoids (N), sesquiterpenes (S), unknowns (U)] is described with a different color.

characterized by an extremely high amount of hexanol in the overripe stage.

Another important fraction of the blueberry volatile profile was composed by monoterpenes (**Figure 1**), being 1,8-cineole and linalool two main elements of this chemical family: 1,8-cineole was mostly synthesized in green fruit and it rapidly reduced during fruit ripening; linalool was mostly produced in fruit at pink stage and preserved during the last phases of fruit ripening with different end-level amount according to the cultivar. A production course similar to the one of linalool was found also for geranyl acetone. Most of the other terpenes detected in blueberry, such as limonene, α-terpinolene, or α-terpineol, were mostly synthesized between the pink and ripe stage.

Esters, although been present at lower average amount compared to the aforementioned compounds (**Figure 1**), had an important role to fully characterized the blueberry aroma,

mostly at the overripe maturity stage. Most of the esters, such as ethyl acetate, methyl isoalate, or ethyl isoalate were largely synthesized in overripe fruit, while, contrariwise, only few esters, for instance (Z)-3-hexenyl acetate, were detectable at high concentration in green fruit.

Seven ketones were detected in blueberry fruit. 2-heptanone and 6-methyl-5-hepten-2-one were the two molecules with the higher chromatographic area. 2-heptanone, as well as 2-undecanone and 2-nonanone, were mostly detected in green fruit, with significant amount differences among cultivars. Their content decreased till trace levels during fruit ripening. 6-methyl-5-hepten-2-one was instead detectable in blueberry in all ripening stages without any distinct course related to fruit ripening.

Four hydrocarbons (octane, ethyl benzene, p-xylene, and m-xylene) were identified and, even if present in all ripening stages, they were mostly expressed in the ripe and overripe stages.

The remaining fraction of the blueberry aroma profile was composed by four volatile acids (hexanoic acid, octanoic acid, nonanoic acid, and decanoic acid), three sesquiterpenes (δ -elemene, (E)-caryophyllene and caryophyllene oxide), one norisoprenoid (β -damascenone), and one lactone (butyrolactone). Apart from caryophyllene, for the most produced only in green fruits, all these compounds were stable during all ripening phases except for the overripe fruits of “Brigitta Blue” that were characterized by an increased level of hexanoic acid and octanoic acid content.

Effect of Ripening and Genetic Differences on the Blueberry Aroma Profile

Principal component analysis (PCA) was carried out to describe relations among blueberry cultivars, ripening stages, and VOCs

(**Figure 2A**). Sixty-five percent of the total variability was accounted for the first three principal components. Differences related to fruit ripening stages were mostly explainable by the first principal component (PC1: 40%), while differences between cultivars were better defined using the second component (PC2: 15%). Moreover, the variability described by the second principal component was essential to distinguish fruit belonging to the “ripe” or “overripe” classes. Overripe blueberries were indeed differentiated from ripe ones by more negative values of PC2, without any significant variations of PC1. This variability concurred with an increased concentration of compounds already present at significant levels in ripe fruits (such as ethyl benzene, xilene, hexanol, or 1-octen-3-ol), and, mostly, with the synthesis of compounds not detectable (or detectable only at trace levels) in ripe fruits that were for the most esters (i.e., ethyl

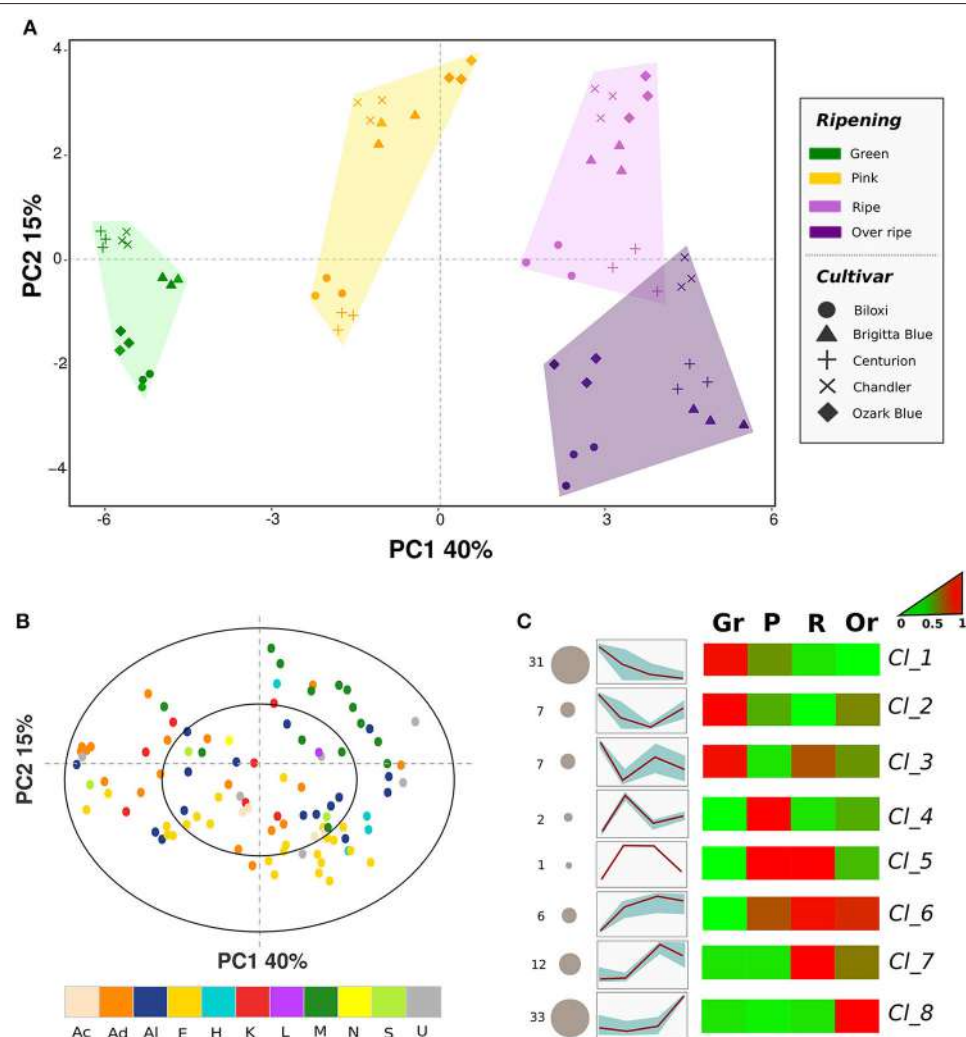


FIGURE 2 | Multivariate analysis of the blueberry VOC profile assessed by SPME-GC-MS. Plot (A) depicts the VOC profile distribution of five blueberry cultivars at four ripening stages over the PCA score plot defined by the first two principal components. Plot (B) shows the projection of the VOCs identified by SPME-GC-MS analysis. Each compound is reported using different color according to the chemical class [acids (Ac), aldehydes (Ad), alcohols (Al), esters (E), hydrocarbons (H), ketones (K), lactones (L), monoterpene (M), norisoprenoids (N), sesquiterpenes (S), unknowns (U)]. Plot (C) reports the sorting of all compounds into eight significant clusters defined by SOTA (Self-organizing tree algorithm) analysis. Several additional information are reported next to each SOTA cluster: the number of compounds (number plus size of circle), heatmap and plot of compound fold changes among time series (normalized data to 0–1 range). Details about each SOTA cluster are reported into **Supplementary Table 1**.

acetate, methyl 3-methylbutanoate, or ethyl 3-methylbutanoate; loading plot **Figure 2B**). In addition, overripe fruits were characterized by a lower concentration of monoterpenes (i.e., limonene, linalool, α -terpineol, and β -myrcene) that were fully synthesized in ripe fruit.

PCA analysis indicates that VOC emission of fruit at green maturity stages was characterized by high levels of aldehydes (i.e., 3-hexenal, 2-hexenal, 2-pentenal, or 2-heptenal) and of alcohols derived by these aldehydes, for instance (Z)-3-hexen-1-ol and 3-methyl butanol. The aromatic profile of unripe fruit was completed by some hexenyl esters (i.e., 3-hexenyl acetate, 3-hexenyl butanoate), one aromatic ester (ethyl benzoate), several ketones (i.e., 2-heptenone and 2-nonalone), one monoterpene (1,8-cineole), and by the sesquiterpenes (E)-caryophyllene and caryophyllene oxide.

The aromatic profile of fruit harvested at the pink ripening stage was mostly defined by both the aforementioned compounds (for the most aldehydes) detected in greens stage blueberries, which concentrations decreased at this ripening stage. Moreover, some monoterpenes, such as linalool, linalool oxide, 4-terpineol and geranyl acetate were produced at this ripening stage.

All VOCs detected in this study, beyond the biochemical classification, were grouped based on their concentration fold changes disclosed during the entire ripening process. All compounds were significantly sorted into eight clusters defined by SOTA (Self-organizing tree algorithm) analysis (**Figure 2C, Table 1**). Indeed, SOTA algorithm allowed a clustering based on relative fold changes of a compound among time series. The two groups with the higher number of VOCs were “cluster_1” and “cluster_8” respectively represented by 31 and 33 compounds. VOCs belonging to “cluster_1” were mostly produced by green blueberries and they were suddenly reduced during fruit ripening. Oppositely, compounds of “cluster_8” were exclusively synthesized in the last ripening step in overripe fruits. All left compounds were divided into the remaining six clusters (from “cluster_2” to “cluster_7”), which showed different dynamics patterns of VOCs concentration fold changes from green to overripe.

Direct Injection VOC Profiling by PTR-ToF-MS

Fruit samples analyzed by PTR-ToF-MS were prepared similarly to the ones used for SPME-GC-MS analysis in order to compare these two methodologies. The PTR-ToF-MS setting adopted in this study allowed the detection of the full VOC spectra in 1 s. Only the first 30 s of the full measurement (120 s) were analyzed and averaged, in order to avoid possible measurement inaccuracies caused by an excessive dilution of the sample headspace. The whole VOC spectra, assessed in triplicate for samples, were reduced from 293 to 105 masses, applying noise, and correlation coefficient thresholds (**Table 2**).

PCA analysis (**Figure 3A**) was carried out to describe the blueberry VOC profile regarding cultivars (“Biloxi,” “Brigitta Blue,” “Centurion,” “Chandler,” and “Ozark Blue”) and ripening stages (green, pink, ripe, overripe). Seventy-two percent of

the total variation was accounted for the first three principal components. Similarly to SPME-GC-MS analysis, differences between fruit sampled at different ripening stages were mostly explainable by the first principal component (PC1: 43%), while the second component (PC2: 18%) mostly defined differences between cultivars. Furthermore, PC2 variability allowed the separation of overripe fruit from ripe ones: overripe fruits, besides the cultivar “Chandler,” were all displaced into the PCA quadrant determined by positive values of PC1 and negative ones of PC2. Based on the loading plot (**Figure 3B**), this discrimination was mostly explainable by masses related to alcohols such as *m/z* 29.040 and 47.049 (ethanol), *m/z* 34.037 (methanol isotope; the nominal mass of methanol, *m/z* 33.030, was not considered in this study because in some samples its concentration was above the maximum threshold of accuracy), acetone (*m/z* 59.048), acetaldehyde (*m/z* 45.033), formaldehyde (*m/z* 31.019), and several masses tentatively associated to esters such as *m/z* 61.028, 75.044, 89.060, 103.076, 117.092, 131.107.

The aroma profile of unripe fruits, especially of the green ones, was mostly defined by negative values of PC1 that means a higher concentration of masses related to aldehydes, such as *m/z* 99.080, 81.070, 69.070, or 43.019, esters with “green” fragrances such as hexadienal and hexenyl acetate (*m/z* 97.06 and 143.108), butyrolactone (*m/z* 87.044), and sulfuric compounds (*m/z* 63.026 and 93.037, tentatively identified as dimethyl sulfide and 2-(methylthio)ethanol).

Almost one third of the PTR-ToF-MS masses was not strongly correlated ($R < 0.5$) with any of the three principal components. These masses, indeed, were detectable only at low concentrations (average level lower than 2 ppbv) and/or they did not vary significantly between cultivars and ripening stages such as for *m/z* 107.08 (ethyl benzene and/or xylene) and *m/z* 95.086 ((E)-2-heptenal).

As for SPME-GC-MS analysis, all 105 masses detected by PTR-ToF-MS were grouped into eight significant SOTA clusters based on their concentration fold changes during the entire ripening process (**Figure 3C, Table 2**). As formerly revealed by the PCA analysis, “cluster_1” grouped a set of 36 masses that did not significantly vary between cultivars and ripening stages. “Clusters_2, _3, and _4” sorted VOCs that were mostly produced by unripe fruits and they diminished during fruit ripening. Each of the three clusters was characterized by a different depletion slope of VOCs concentration. The remaining VOCs, that were mostly produced during fruit ripening, were arranged into the remaining four clusters, namely “cluster_5, _6, _7, and _8.”

“Cluster_5” was composed by seven VOCs masses whose concentration was highest in fruits assessed at the pink ripe stage. This concentration remained stable, or it slightly diminished, during the last ripening phases (ripe and overripe). The main masses grouped into this cluster were: *m/z* 47.013 (formic acid); *m/z* 83.086 (hexenols and/or hexenal fragment); *m/z* 101.09 (hexenal); *m/z* 127.113 (6-methyl-5-heptenone and terpenes such as myrcene and limonene); *m/z* 155.144 (terpenes such as linalool, geraniol, or cineole).

“Cluster_6” gathered five VOCs masses characterized by a constant and almost linear concentration increment during fruit ripening. Some of these masses were *m/z* 61.028 (acetic acid

TABLE 2 | Volatile compounds detected by PTR-ToF-MS in blueberry fruits at different ripening stages.

m/z	Formula	SOTA ^a	Tentative identification	Min ^b	Max ^b	Mean ^b
28.008		1	n.i.	0.6	0.7	0.6
29.040	C ₂ H ₅ ⁺	8	Ethanol fragment	1.9	64.8	2.4
30.995		1	n.i.	1.0	1.2	1.0
31.019	CH ₃ O ⁺	8	Formaldehyde	2.8	14.2	5.2
33.994	O[18]O ⁺	1	n.i.	4.7	5.1	4.9
34.037	[13]CH ₄ OH ⁺	8	Methanol	3.4	92.7	17.8
39.023	C ₃ H ₃ ⁺	3	Common fragment	5.2	29.8	12.2
41.039	C ₃ H ₅ ⁺	3	Common fragment	12.3	56.3	21.9
43.018	C ₂ H ₃ O ⁺	3	Common fragment	26.1	129.8	50.3
43.054	C ₃ H ₇ ⁺	3	Common fragment	3.3	23.0	8.8
45.033	C ₂ H ₄ OH ⁺	8	Acetaldehyde	59.8	1358.0	176.1
45.992	NO ₂ ⁺	1	n.i.	1.2	1.6	1.4
47.013	CH ₃ O ₂ ⁺	5	Formic acid	7.2	18.3	10.2
47.024		1	n.i.	4.4	5.2	4.7
47.049	C ₂ H ₆ OH ⁺	8	Ethanol	2.3	295.5	4.5
49.012	CH ₄ SH ⁺	2	Methanethiol	0.2	0.8	0.4
51.023		6	n.i.	0.2	0.9	0.4
51.043	CH ₃ OH ⁺ H ₃ O ⁺	8	Methanol cluster	4.7	132.4	25.0
53.039	C ₄ H ₅ ⁺	3	n.i.	1.5	8.9	3.9
55.018		2	n.i.	0.2	1.8	0.7
55.054	C ₄ H ₇ ⁺	2	Common fragment	21.4	193.8	81.5
55.934		1	n.i.	1.1	1.2	1.2
57.033	C ₃ H ₄ OH ⁺	5	Common fragment	48.1	779.2	231.2
57.070	C ₄ H ₉ ⁺	3	1-Octanol*, high alcohol fragment	0.1	5.1	3.6
59.049	C ₃ H ₆ OH ⁺	7	Acetone	26.6	880.1	37.6
61.028	C ₂ H ₄ O ₂ H ⁺	6	Acetic acid, common ester fragment	10.2	52.5	19.0
63.026	C ₂ H ₆ SH ⁺	4	Dimethyl sulfide, Ethanethiol	0.8	42.7	1.6
63.043	C ₂ H ₄ O ⁺ H ₃ O ⁺	8	Ethanol cluster	0.2	3.5	0.4
65.022		4	n.i.	0.2	2.1	0.3
65.039	C ₅ H ₅ ⁺	3	n.i.	0.1	0.4	0.1
67.054	C ₅ H ₇ ⁺	3	n.i.	0.9	4.2	1.8
69.034	C ₄ H ₆ OH ⁺	2	Furan	0.3	1.1	0.6
69.070	C ₅ H ₉ ⁺	3	Aldehyde fragment	3.8	22.4	8.7
70.039		3	n.i.	0.0	0.3	0.1
71.049	C ₄ H ₆ OH ⁺	2	Butenal	1.6	6.6	3.6
71.086	C ₅ H ₁₁ ⁺	4	3-Methyl-1-butanol*, 2-Methyl-1-butanol*, Pentanol*	1.1	10.8	2.7
73.028	C ₃ H ₄ O ₂ H ⁺	1	n.i.	0.8	1.0	0.9
73.048		1	n.i.	0.7	1.2	1.0
73.065	C ₄ H ₈ OH ⁺	2	Butanale, Isobutyraldehyde	2.5	7.2	4.3
75.027	C ₃ H ₆ SH ⁺	1	Allyl mercaptan, 3-mercaptopropanol	1.1	1.7	1.4
75.044	C ₃ H ₆ O ₂ H ⁺	8	Methyl acetate*	0.9	45.4	1.2
78.047	C ₆ H ₆ ⁺	1	n.i.	2.4	2.6	2.5
79.055	C ₆ H ₇ ⁺	3	Benzene	4.0	11.6	7.9
80.060	C ₅ [13]CH ₇ ⁺	3	n.i.	0.4	2.0	0.8
81.070	C ₆ H ₉ ⁺	4	Fragment of aldehydes (hexenals); fragment of terpenes (linalool)	19.1	1497.7	283.8
83.049	C ₅ H ₆ OH ⁺	2	Methylfuran	0.5	2.9	1.3
83.086	C ₆ H ₁₁ ⁺	5	(E)-3-hexen-1-ol*, (Z)-3-hexen-1-ol*, (Z)-2-hexen-1-ol*, Hexanal*, 2-Hexanone	14.3	123.0	49.9
85.065	C ₅ H ₈ OH ⁺	4	3-Penten-2-one	2.2	17.5	6.7
85.100	C ₆ H ₁₃ ⁺	6	Hexanol*	0.3	1.2	0.4
87.044	C ₄ H ₆ O ₂ H ⁺	3	Butyrolactone*	0.8	4.5	1.1
87.080	C ₅ H ₁₀ OH ⁺	3	2-Methyl butanal*, 3-Methyl butanal*	1.0	4.6	1.8
89.060	C ₄ H ₈ O ₂ H ⁺	8	Ethyl acetate*	0.8	11.2	1.2

(Continued)

TABLE 2 | Continued

m/z	Formula	SOTA^a	Tentative identification	Min^b	Max^b	Mean^b
90.949		1	n.i.	1.8	1.9	1.9
91.057	C ₇ H ₇ ⁺	1	Benzyl fragment*	0.9	1.5	1.1
93.037	C ₃ H ₈ OSH ⁺	1	2-(Methylthio)ethanol	1.4	1.7	1.5
93.070	C ₇ H ₉ ⁺	6	Monoterpene fragment	0.5	2.1	0.8
94.041		1	n.i.	0.4	0.5	0.4
95.022		1	n.i.	0.4	0.6	0.5
95.049	C ₆ H ₆ OH ⁺	1	Phenol	1.6	2.2	1.9
95.086	C ₇ H ₁₁ ⁺	1	(E)-2-heptenal*, Monoterpene fragment	1.1	4.2	2.2
97.065	C ₆ H ₈ OH ⁺	4	(E,Z)-2,4-hexadienal*, (E,E)-2,4-hexadienal*	0.4	3.1	1.2
97.102	C ₇ H ₁₃ ⁺	3	Heptanal*, fragment	0.5	2.5	0.6
99.080	C ₆ H ₁₀ OH ⁺	3	(Z)-3-hexenal*, (I _Z)-2-hexenal*, (E)-2-hexenal*	17.9	433.9	145.8
101.064	C ₅ H ₈ O ₂ H ⁺	3	2,3-Pantanedione	0.3	0.8	0.4
101.095	C ₆ H ₁₂ OH ⁺	5	Hexanal*	2.1	16.9	6.3
103.076	C ₅ H ₁₀ O ₂ H ⁺	8	Ethyl propanoate*	0.5	8.0	0.6
105.071	C ₈ H ₉ ⁺	6	Phenethyl alcohol*, Styrene	0.1	0.4	0.2
105.938		1	n.i.	0.2	0.2	0.2
107.050	C ₇ H ₆ OH ⁺	2	Benzaldehyde*	0.2	0.5	0.3
107.086	C ₈ H ₁₀ H ⁺	1	Ethyl benzene*, p-Xylene*, m-Xylene*	3.7	15.6	9.6
107.953		1	n.i.	0.3	0.3	0.3
108.957		1	n.i.	0.7	0.8	0.7
109.102	C ₈ H ₁₃ ⁺	5	n.i.	2.1	7.7	3.3
111.081	C ₇ H ₁₀ OH ⁺	3	(E,E)-2,4-heptadienal*	0.3	1.1	0.6
111.118	C ₈ H ₁₅ ⁺	1	(E)-2-Octenal*, Octanal*, 1-Octen-3-ol	0.3	0.5	0.4
113.027		2	n.i.	0.1	0.2	0.2
113.060	C ₆ H ₈ O ₂ H ⁺	4	Sorbic acid	0.2	2.0	0.4
113.097	C ₇ H ₁₂ OH ⁺	1	(E)-2-heptenal*	0.3	1.2	0.6
115.077	C ₆ H ₁₀ O ₂ H ⁺	2	Ethyl (2E)-2-butenoate*	0.2	0.6	0.3
115.113	C ₇ H ₁₄ OH ⁺	4	2-Heptanone*, Heptanal	0.2	24.2	1.3
117.092	C ₆ H ₁₂ O ₂ H ⁺	8	Ethyl isobutanoate*, Methyl-2-methyl butanoate*, Methyl isovalerate*, Ethyl butyrate*, Hexanoic acid*	0.9	17.6	1.2
119.088	C ₉ H ₁₁ ⁺	1	3-Phenylpropanol	0.5	0.6	0.5
121.066	C ₈ H ₈ OH ⁺	2	Acetophenone*, Phenylacetaldehyde	0.6	1.6	0.9
121.103	C ₉ H ₁₃ ⁺	1	1,3,5-Trimethylbenzene	0.2	0.3	0.3
123.118	C ₉ H ₁₅ ⁺	1	2-Nonenal*, (E)-2-nonenal*	0.3	0.4	0.3
125.097	C ₈ H ₁₂ OH ⁺	3	6-Methyl-3,5-heptadien-2-one	0.2	0.6	0.3
126.903		1	n.i.	0.3	0.3	0.3
127.113	C ₈ H ₁₄ OH ⁺	5	1-Octen-3-one*, 6-Methyl-5-hepten-2-one*, (E)-2-octenal*, β -Myrcene*, Limonene*, (E)- β -Ocimene*, α -Terpinolene*	0.8	3.0	1.4
129.128	C ₈ H ₁₆ OH ⁺	1	2-Octanone*, Octanal*, 1-Octen-3-ol	0.2	0.5	0.3
131.107	C ₇ H ₁₄ O ₂ H ⁺	8	Ethyl-2-methyl butanoate*, Ethyl isovalerate*	0.2	6.0	0.3
133.102	C ₁₀ H ₁₃ ⁺	1	Thymol	0.1	0.4	0.2
135.118	C ₁₀ H ₁₅ ⁺	7	HO-trienol*	0.3	3.6	0.7
137.134	C ₁₀ H ₁₇ ⁺	3	1,8-cineole*, Linalool*, 4-Terpineol*, α -Terpineol*, Nerol*, Geraniol*	1.6	13.2	5.8
139.076	C ₈ H ₁₀ O ₂ H ⁺	1	5,5-Dimethyl-2-cyclohexen-1,4-dione	0.1	0.3	0.2
139.115	C ₉ H ₁₄ OH ⁺	2	n.i.	0.2	0.4	0.3
141.129	C ₉ H ₁₆ OH ⁺	1	2-Nonenal*, (E)-2-nonenal*, Ethyl sorbate	0.2	0.3	0.3
143.108	C ₈ H ₁₄ O ₂ H ⁺	3	(Z)-3-hexenyl acetate*, 2-Hexenyl acetate*	0.2	0.6	0.3
143.145	C ₉ H ₁₈ OH ⁺	3	2-Nonanone*, Nonanal	0.1	0.8	0.4
144.914		1	n.i.	0.1	0.2	0.2
145.124	C ₈ H ₁₆ O ₂ H ⁺	1	Ethyl hexanoate*, Hexyl acetate*, Octanoic acid*	0.5	0.8	0.7
153.129	C ₁₀ H ₁₆ OH ⁺	7	HO-trienol*, 2,4-Decadienal	0.3	6.0	0.9

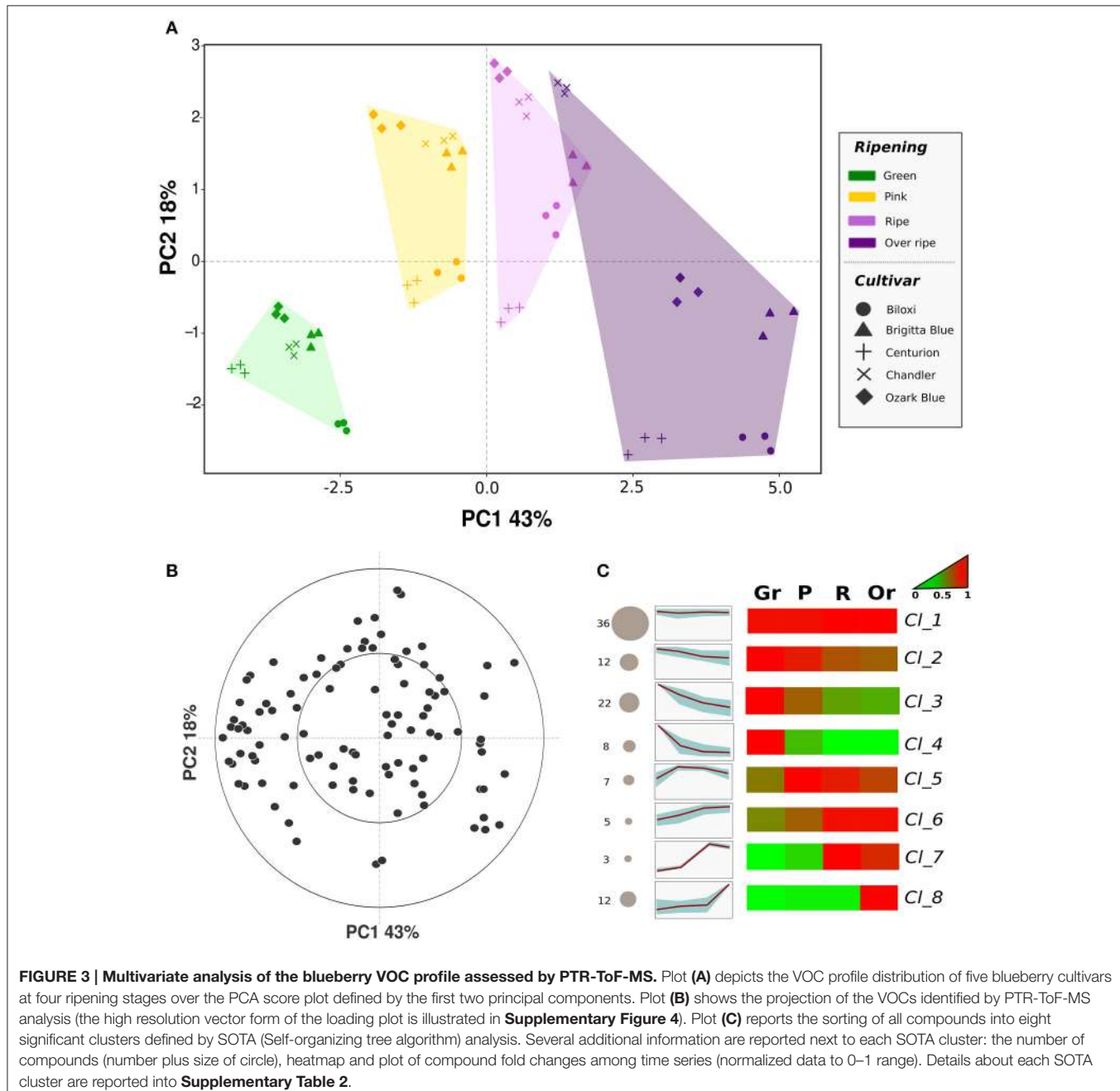
(Continued)

TABLE 2 | Continued

m/z	Formula	SOTA^a	Tentative identification	Min^b	Max^b	Mean^b
155.144	C ₁₀ H ₁₈ OH ⁺	5	1,8-Cineole*, Linalool*, 4-Terpineol*, α Terpineol*, Nerol*, Geraniol*	0.2	0.5	0.4
159.140	C ₉ H ₁₈ O ₂ H ⁺	1	Nonanoic acid*	0.7	1.6	1.2
173.156	C ₁₀ H ₂₀ O ₂ H ⁺	1	Decanoic acid*	0.4	0.8	0.7
177.166	C ₁₃ H ₂₁ ⁺	1	Geranyl acetone*	0.2	0.4	0.3

^aSOTA (self-organizing tree algorithm) clusters based on **Figure 3**.^bppb_v.

*Compound detected also by SPME-GC-MS analysis.



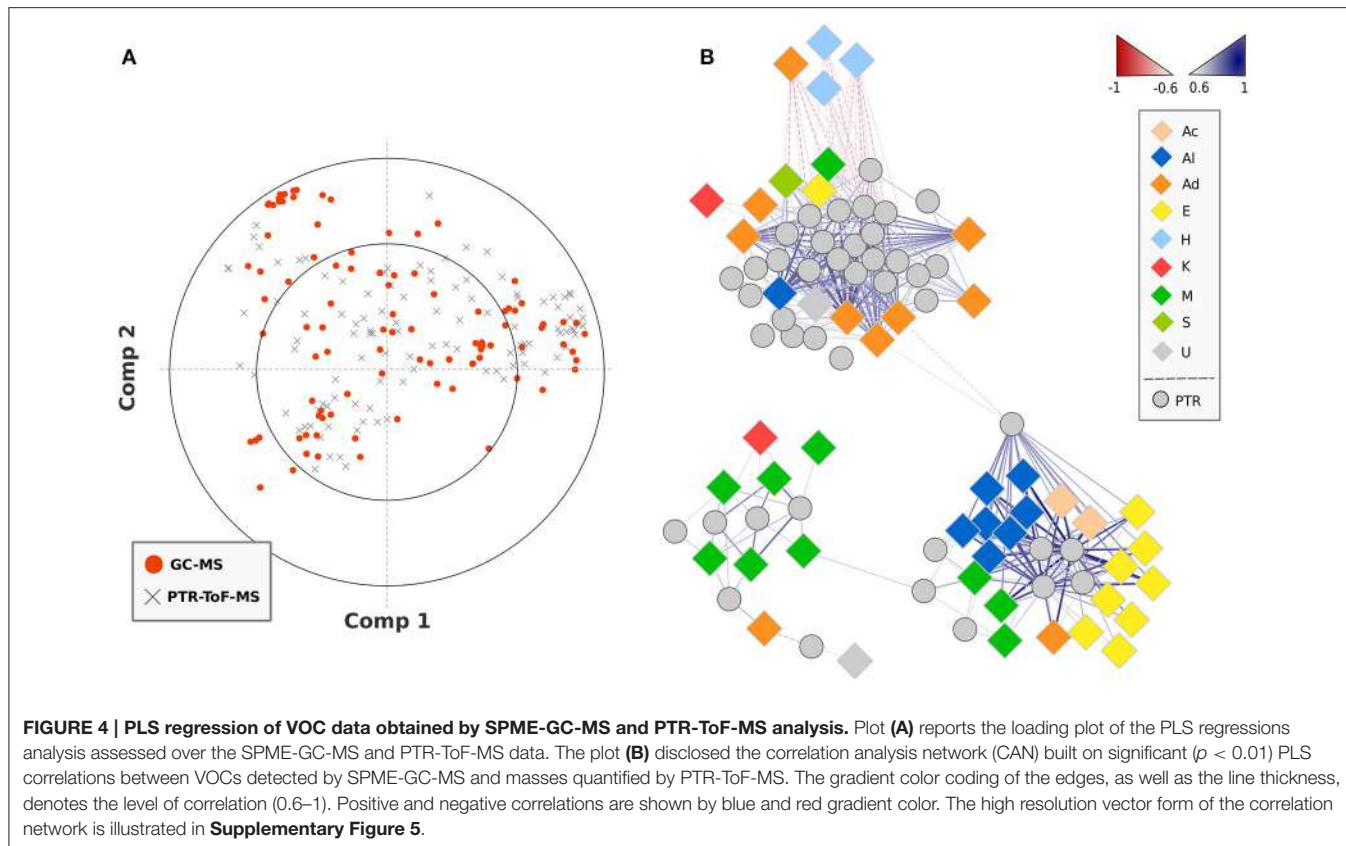


FIGURE 4 | PLS regression of VOC data obtained by SPME-GC-MS and PTR-ToF-MS analysis. Plot (A) reports the loading plot of the PLS regressions analysis assessed over the SPME-GC-MS and PTR-ToF-MS data. The plot (B) disclosed the correlation analysis network (CAN) built on significant ($p < 0.01$) PLS correlations between VOCs detected by SPME-GC-MS and masses quantified by PTR-ToF-MS. The gradient color coding of the edges, as well as the line thickness, denotes the level of correlation (0.6–1). Positive and negative correlations are shown by blue and red gradient color. The high resolution vector form of the correlation network is illustrated in **Supplementary Figure 5**.

and common ester fragment), m/z 85.100 (hexanol), m/z 93.07 (monoterpene fragment), and m/z 105.071 (phenethyl alcohol).

“Cluster_7” was only composed by three VOC masses namely m/z 59.049 (acetone), m/z 135.118 and 153.129 (HO-trienol). These VOCs were mostly produced by fruit analyzed at ripe stage.

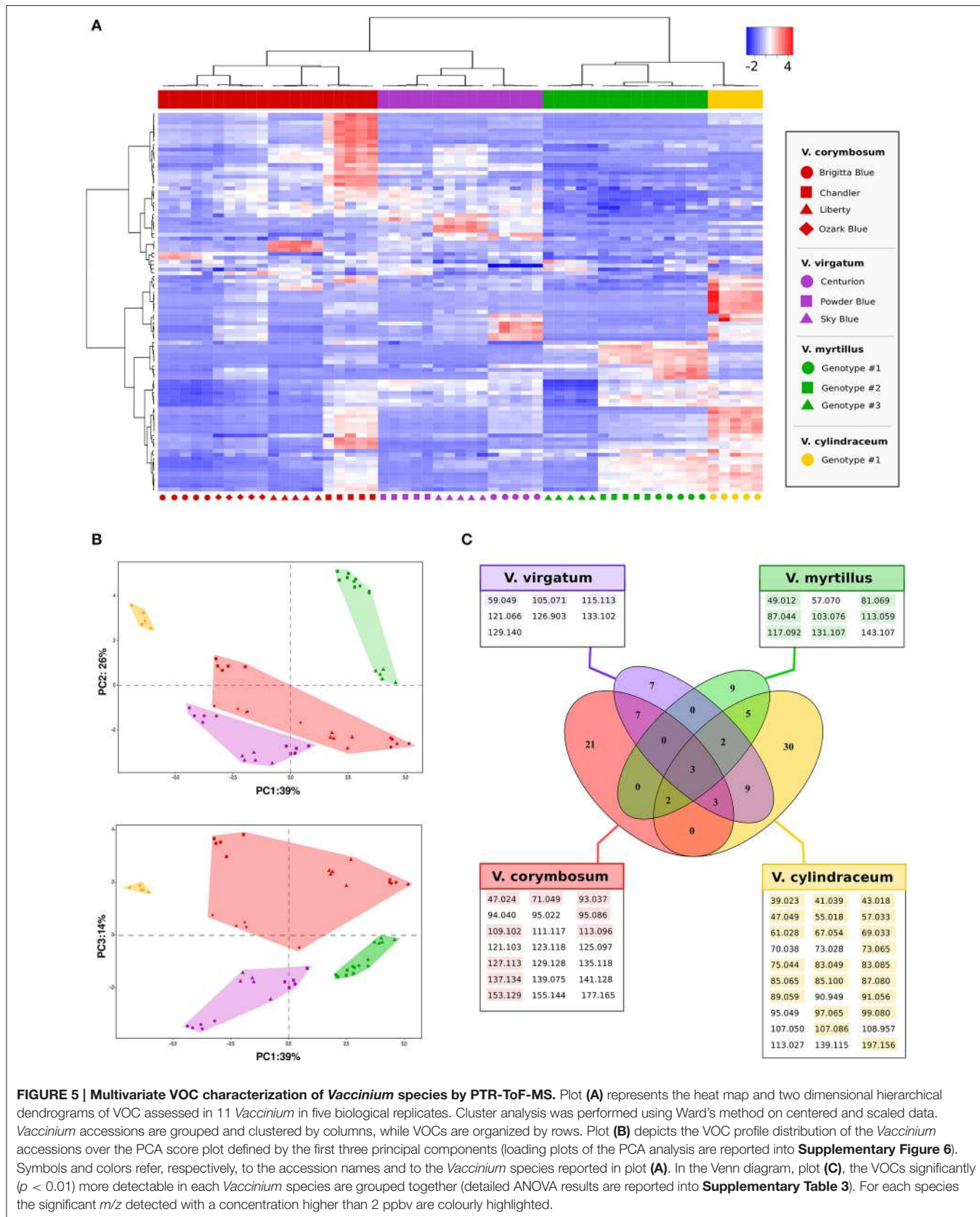
“Cluster_8,” lastly, counted 12 VOC masses whose concentration stood at low basal levels till the ripe stage and it greatly rose in overripe fruit. Among these compounds there were masses related to ethanol (m/z 29.040, 47.049, and 63.043), to methanol (m/z 34.037 and 51.043) and to ester compounds (m/z 75.044, 89.060, 103.076, 117.092, and 131.107).

A PLS regression network was created combining VOC data obtained by SPME-GC-MS and PTR-ToF-MS analysis (Figure 4). Based on the obtained regressions, graphically reported in the loading plot of Figure 4A, the network was built on significant ($p < 0.01$) correlations between VOCs detected by SPME-GC-MS and masses quantified by PTR-ToF-MS only taking into account correlation values >0.6 or <-0.6 . The gradient color coding of the edges (blue and red gradient color), as well as the line thickness, denotes the level of correlation (0.6–1). Most of the PTR-ToF-MS peaks considered in this study were putatively identified (Table 2) based on PLS regression analysis, *in silico* fragmentation of the compounds previously detected by SPME-GC-MS, and fragmentation analysis of commercial standards. Indeed, lots of incorrect attributions would be obtained by merely considering the SPLS results. For instance m/z 89.06 was highly correlated ($R > 0.9$) with at least eight

VOCs detected by SPME-GC-MS, such as the esters methyl-2-methylbutanoate or 3 methyl-3-hydroxy-3-methylbutanoate and the alcohols 1-octanol or 1-nonanol, even though all these molecules were differently fragmented during protonization. Therefore, ethyl acetate resulted to be the only detected compound by SPME-GC-MS highly correlated with m/z 89.060 and with an accurate chemical fragmentation.

VOCs Characterization of Vaccinium Species by PTR-ToF-MS

In addition to the previous study, PTR-ToF-MS methodology was applied to identify the VOCs profiles of different blueberry species assessed at the full ripe stage. In detail, we analyzed four cultivars of *V. corymbosum* L. (“Brigitta Blue,” “Chandler,” “Liberty,” and “Ozark Blue”), three cultivars of *V. virgatum* Aiton (“Centurion,” “Powder Blue,” and “Sky Blue”), three ecotypes of *V. myrtillus* L. propagated from different mountain locations of Trentino, and one accession of *V. cylindraceum* Smith. The entire volatile profiles assessed for these 11 accessions, in five biological replicates, were organized and depicted by the heat map showed in Figure 5A, using a data-set reduced to 98 masses by applying noise and correlation coefficient thresholds (all data are “centered” and “scaled”). The vertical dendrogram of the heat map shows the grouping of PTR-ToF-MS masses based on their relative abundance. On the same heat map all blueberry accessions were organized by a hierarchical clustering, based on VOCs relative content. The hierarchical clustering revealed a



significant grouping of the *Vaccinium* accessions based on their taxonomic differences, since each of the four species was grouped into a clearly separate cluster.

This separation was also confirmed by the PCA analysis done on Log-transformed data (**Figure 5B**). Seventy-nine percent of the total variability among aroma profile was accounted for the first three principal components (PC1: 39%; PC2: 26%; PC3: 14%). Based on these PCA results, all cultivars were properly and distinctly distributed based on their aromatic profile confirming the defined clusterization among *Vaccinium* species and low variability among biological replicates. For instance, the aromatic profile of *V. myrtillus* L. and *V. cylindraceum* Smith accessions were significantly distinct mostly based on PC1 and PC3-values. According to the PCA loading plot (**Supplementary Figure 4**) this separation was mostly explainable by a higher concentration of most of detected compounds (negative values of PC1). *V. corymbosum* L. and *V. virgatum* Aiton, instead, mostly differed according to PC3-values. However, the variability among these last two species was broad, with cultivars characterized by an intense VOC profile, such as "Chandler" or "Centurion," and others with reduced VOC concentrations, such as "Brigitta Blue."

All these indicative differences in aroma composition detected by PTR-ToF-MS are summarized into the Venn diagram (**Figure 5C**) where the VOCs significantly ($p < 0.01$) more detectable in each *Vaccinium* species are grouped together (**Supplementary Table 1**). Among the four species assessed in this study, *V. cylindraceum* L. was the most aromatic one. Its aroma profile was defined by 30 masses that were measured at significantly higher concentration such as some alcohols (m/z 47.049 and 85.100), ester fragments (i.e., m/z 61.028, 75.044, and 89.059), aldehydes (m/z 83.085, 97.065, and 99.080), and aromatic hydrocarbon compounds (m/z 95.049 and 107.086). The *V. myrtillus* L. ecotypes were characterized by a less intense VOC profile than *V. cylindraceum* L. This profile, on average levels, was defined by an increased amount of m/z 81.070 (C6 aldehyde and terpene fragment) and some ester related masses (i.e., m/z 103.076, 117.092, 131.107, and 143.108). The four cultivars of *V. corymbosum* L. differed from the other accessions for 21 masses. However, these VOCs were detectable at lower concentration, since only nine of them revealed at concentration higher than 2 ppbv, such as some terpene related masses (i.e., m/z 93.037, 127.113, or 137.135). Lastly, the VOCs profile of the cultivars of *V. virgatum* Aiton revealed several masses detected at the same level of *V. corymbosum* L. (13 masses) and *V. cylindraceum* Smith (11 masses), and 7 masses significantly more produced with only three of them with concentration higher than 2 ppbv (m/z 59.049, 105.071, and 115.113).

DISCUSSION

With an increased consumption of fresh blueberries in the last decade, a whole new generation of cultivars has to be released and bred, at least in part, for improved fruit quality, shelf life stability, and extension of the fresh-market harvest season (Gilbert et al., 2014). Although flavor is a complex trait, relatively

simple measurements are commonly used in an attempt to quantify flavor differences, such as titratable acidity, TTS, and firmness. Nevertheless, identification of VOCs that correspond to the fruity, intense, sweet, and characteristic blueberry flavors could help breeders to select for cultivars with a more desirable flavor. This is an essential first step in growing demand for fruits and vegetables rather than merely maintaining existing markets (Folta and Klee, 2016).

However, flavor phenotyping is expensive, subject to environmental variation, not amenable to high-throughput assays, and beyond the means of most breeding programs. Given the importance of aroma to define the complexity of flavor and consumer preferences, the development of techniques to rapidly, accurately, and comprehensively assess VOCs is crucial. This strategy may prevent the unintended negative consequences of breeding on other quality traits of blueberry, as it already happened in several important fruit species, such as strawberry, apple, peach, and tomato (Goff and Klee, 2006; Klee, 2010; Rambla et al., 2014; Folta and Klee, 2016; Farneti et al., 2017) where the breeding pressure led to an evident aroma decline.

Volatile compounds, as the majority of secondary plant metabolites, are detectable in blueberry fruits with high variability according to genetic and environmental differences (Gilbert et al., 2015) and, above all, to the biological ripening stage of the fruit at the time of analysis (Gilbert et al., 2013). In this survey, the environmental variable effect was fully reduced by using plants grown in the same experimental field with identical agronomic practices. The two main variance factors introduced in this experimental design were the genetic variability (five cultivars of *V. corymbosum* L. and *V. virgatum* Aiton; 11 accessions of *V. corymbosum* L., *V. virgatum* Aiton, *V. cylindraceum* Smith, and *V. myrtillus* L.) and the harvest ripening stages (green, pink, ripe, and overripe), that were analytically defined based on color, pH, titratable acidity, TSS, and texture.

This comprehensive characterization of blueberry aroma, assessed by chromatographic (SPME-GC-MS) and direct injection (PTR-ToF-MS) spectrometric techniques, allowed the identification of most compounds that may affect blueberry quality. To date, this is the most detailed characterization of blueberry aroma with 106 compounds, detected and tentatively identified by gas-chromatographic analysis. Moreover, PTR-ToF-MS analysis resulted to be complementary to SPME-GC-MS since, over the 105 significant masses detected, several compounds, in this study, were only detected and quantified by PTR-ToF-MS analysis such as methanol, ethanol, acetaldehyde, acetone, acetic acid, or some sulfuric compounds ($C_2H_6SH^+$, m/z 63.026).

All VOCs detected in this study with both chromatographic and direct injection techniques, beyond the biochemical classification, were grouped based on their concentration fold changes during the entire ripening process. This physiological classification straightly unravels how complex the blueberry VOCs profile can be, and that should not be simplified as the interaction of <10 compounds (i.e., linalool, trans-2-hexenol, trans-2-hexenal, or hexanal; (Parliment and Kolor, 1975; Hirvi

and Honkanen, 1983; Du et al., 2011). Based on the SOTA classification, indeed, all compounds can be broadly gathered into three main groups: (i) VOCs that do not significantly vary between cultivars and ripening stages and that are detectable only at low concentrations; (ii) VOCs that are mostly synthesized by unripe (green) blueberries and that are reduced during fruit ripening; (iii) VOCs that are exclusively synthesized in the last ripening steps (ripe and/or overripe). The last two groups, in addition, can be further divided into sub-clusters characterized by different depletion/production slopes of VOCs concentrations. Most of the compounds that are commonly considered being responsible for blueberry aroma are synthesized by the fruit in the ripe stage, such as linalool and majority of monoterpenes, (Z)-2-hexen-1-ol, and hexanal, or they are mostly detected in fruits at the pink stage of ripening, such as (E)-2-hexenal. (E)-2-hexenol has been linked to green-viney, sweet, and pungent characters, while (E)-2-hexenal has been described as fresh, leafy green, floral, sweet, and pungent (Hongsoongnern and Chambers, 2008). Linalool has often been cited as characteristic of blueberry aroma and mostly it is associated with a floral, fruity, citrus flavor (Parliment and Kolor, 1975; Hirvi and Honkanen, 1983; Du et al., 2011). This enhanced synthesis of terpenes during fruit ripening suggests the feasible upregulation of genes involved into the mevalonate and methylerythritol pathways and of specific terpene synthases, such as linalool synthase (Nagegowda, 2010).

However, it is not necessarily the total amount of the volatiles synthesized in each fruit that is important to flavor, but the presence of specific volatiles, sometimes even in small amounts, with low odor thresholds (Tieman et al., 2012; Folta and Klee, 2016). Esters, although being present in lower average concentration compared to the aforementioned compounds, were important to fully decipher the blueberry aroma, especially for their “sweet” and “fruity” fragrances (Du and Rouseff, 2014). A large fraction of these esters, such as ethyl acetate, methyl isovalerate, ethyl isovalerate, methyl 2-methylbutanoate, are exclusively synthesized in the last phase of ripening and magnified in overripe fruit (SOTA cluster_8 for both PTR-ToF-MS and SPME-GC-MS data). To date esters are not considered as important as aldehydes or terpenes to fully decipher the blueberry aroma, mostly because the majority of studies aimed to correlate sensory consumer perception and VOCs did not consider fruits at foremost ripening stage such as over ripe fruit or fruit after a long storage period. In our opinion these VOCs, mostly synthesized at the full ripening stage of the fruit, have to be considered crucial to fully decipher the aroma profile due to their ecological/evolutionary role to attract eaters. This is a common “ecological-strategy” of climacteric fruit, such as apple, melon, tomato, peach, in which the VOCs synthesis coincides with the ripening and the evolution of attractive quality attributes such as the sugar/acid ratio (Goff and Klee, 2006). On the other hand compounds that are present in green fruit, and that are drastically reduced during ripening (i.e., 1,8-cineole, (Z)-3-hexenal, (E,E)-2,4-hexadienal, (Z)-3-hexenyl acetate, or (E)-caryophyllene) may be considered as “not attractive” or even as “repellent” and so they might not be so important to enhance the final fruit quality perceived by consumer. Notably, the content evolution

of 1,8-cineole during fruit ripening reveals a totally contrasting behavior than most of blueberry terpenes, especially linalool. The extremely high concentration assessed in unripe blueberries suggests the upregulation of genes involved in the conversion of geranyl diphosphate into 1,8-cineole, such as terpineol synthase and 1,8-cineole synthase (Piechulla et al., 2016).

VOCs are not only responsible for the blueberry flavor, they also interact in the ecological network between plant/fruit and the environment and respond to stress conditions (e.g., herbivore or pathogen attack). Furthermore, it is important to know the dynamics of VOCs production not only for quality issues but also to predict the resistance of the fruit to abiotic and biotic stress. Several insects, for instance, are attracted by VOCs emitted by fruit such as *Drosophila suzukii* (Scheidler et al., 2015) or *Rhagoletis mendax* (Lugemwa et al., 1989). Identification of these compounds, often present at trace concentrations, would be an essential component of elucidating the mechanisms of oviposition site selection by these insects and also a helpful tool for breeding activities focused on the development on more resistant accessions.

The obtained results demonstrated the complementarity between chromatographic and direct-injection spectrometric techniques to study the blueberry aroma. The use of PTR-ToF-MS as an MS-e-noses resulted particularly suited to generating reliable blueberry VOCs fingerprints mainly due to a reduced compound fragmentation and precise concentration estimation. The application of PTR-MS has recently been demonstrated as a powerful phenotyping tool for fruit aroma assessment in both genetic and quality-related studies. These investigations require a detailed characterization of the aroma profile of a large fruit number; thus, fast techniques such as PTR-MS are particularly suited for this application. PTR-MS was indeed successfully applied to discriminate the aroma variability in tomato (Farneti et al., 2012, 2013), apple (Cappellin et al., 2012b; Farneti et al., 2015b, 2017), strawberry (Granitto et al., 2007), raspberry (Aprea et al., 2009), pepper (Taiti et al., 2015). Therefore, headspace VOCs fingerprint by PTR-MS provides a potential tool for discriminating blueberry fruit not only based on genetic differences but also based on origin and maturity stages.

On the other side, a weak aspect of this technology is still represented by compound identification. PTR-ToF-MS separates many blueberry isobaric compounds; however, isomers are still not distinguishable, because only the empirical formula of a compound can be determined from accurate mass data. When the formula has been identified, the step toward compound identification might not be trivial. Fragmentation, complex peak structure, and/or the presence of isomeric compounds may still make the chemical identification unpractical, especially in complex matrices. In particular, the link between PTR-ToF-MS peaks and SPME-GC-MS data of the same sample, as already pointed out by Cappellin et al. (2012a), is generally not obvious, meaning that a one-to-one relation is in general not expected, because of the presence of residual fragmentation and isobaric compounds (PTR-ToF-MS data) and of the semiquantitative analysis allowed by SPME fiber. In this study, most of the PTR-ToF-MS peaks detected in blueberry fruit were putatively identified based on PLS regression analysis. Unlike traditional

multiple regression models, PLS is not limited to uncorrelated variables and one of its advantages is that it can handle noisy, collinear, and missing variables. However, the *in silico* fragmentation of the compounds previously detected by SPME-GC-MS, and the fragmentation analysis of commercial standards were crucial to get rid of all incorrect attribution based only upon PLS correlations.

In our opinion the road map for flavor improvement of blueberry fruit is still at an early stage. A better understanding of the mechanisms controlling the synthesis of aroma volatiles in blueberry could provide us the ability to manipulate blueberry fruit to optimize flavor at the time of consumption. Understanding properties of enzymes involved in the production of aroma volatiles may lead to genetic and environmental manipulations to improve blueberry flavor following shipping and marketing. Nevertheless, results of this comprehensive characterization revealed the complexity of blueberry aroma profile and allowed the identification of the most affecting VOCs that can be used as putative biomarkers to rapidly evaluate the aroma variations related to ripening and/or senescence as well as to genetic background differences.

AUTHOR CONTRIBUTIONS

BF designed the research, analyzed and interpreted data, and wrote the manuscript. IK helped with measurements, processed, and analyzed PTR-ToF-MS data. MG and MA assessed the fruit quality analysis and sampled the blueberries. EB processed and analyzed SPME-GC-MS data. AA helped with samples and measurement preparation. LC and EA revised the manuscript and checked the data. FG guided the SPME-GC-MS analysis and edited the manuscript. FB guided the PTR-ToF-MS analysis and edited the manuscript. LG coordinated the work design,

contributed to data interpretation, and edited the manuscript. All authors approved the manuscript.

FUNDING

This work was financially supported by the AdP of the PAT (Provincia Autonoma di Trento) and by the project AppleBerry (L6/99 of the PAT).

SUPPLEMENTARY MATERIAL

The Supplementary Material for this article can be found online at: <http://journal.frontiersin.org/article/10.3389/fpls.2017.00617/full#supplementary-material>

Supplementary Figure 1 | PCA analysis based on textural proprieties of blueberry fruits harvested at different ripening stages.

Supplementary Figure 2 | Bar plot of differences in pH, titratable acidity, and total soluble solids content between blueberry fruits, of five cultivars, assessed at ripe, and overripe maturity stages.

Supplementary Figure 3 | MS detection spectra of unknown compounds detected by SPME-GC-MS analysis.

Supplementary Figure 4 | High resolution vector form of the loading plot reported in Figure 4B.

Supplementary Figure 5 | High resolution vector form of the PLS correlation network reported in Figure 4.

Supplementary Figure 6 | Loading plots of the PCA analysis reported in Figure 5.

Supplementary Table 1 | Volatile compounds identified by SPME-GC-MS sorted based on SOTA clustering.

Supplementary Table 2 | Volatile compounds identified by PTR-ToF-MS sorted based on SOTA clustering.

Supplementary Table 3 | ANOVA table of VOC differences between Vaccinium species assessed by PTR-ToF-MS.

REFERENCES

- Aprea, E., Biasioli, F., Carlin, S., Endrizzi, I., and Gasperi, F. (2009). Investigation of volatile compounds in two raspberry cultivars by two headspace techniques: solid-phase microextraction/gas chromatography-mass spectrometry (SPME/GC-MS) and proton-transfer reaction-mass spectrometry (PTR-MS). *J. Agric. Food Chem.* 57, 4011–4018. doi: 10.1021/jf803998c
- Aprea, E., Charles, M., Endrizzi, I., Corollaro, M. L., Betta, E., Biasioli, F., et al. (2017). Sweet taste in apple: the role of sorbitol, individual sugars, organic acids and volatile compounds. *Sci. Rep.* 7:44950. doi: 10.1038/srep44950
- Aprea, E., Gika, H., Carlin, S., Theodoridis, G., Vrhovsek, U., and Mattivi, F. (2011). Metabolite profiling on apple volatile content based on solid phase microextraction and gas-chromatography time of flight mass spectrometry. *J. Chromatogr. A* 1218, 4517–4524. doi: 10.1016/j.chroma.2011.05.019
- Beaulieu, J. C., Stein-Chisholm, R. E., and Boykin, D. L. (2014). Qualitative analysis of volatiles in rabbiteye blueberry cultivars at various maturities using rapid solid-phase microextraction. *J. Am. Soc. Hortic. Sci.* 139, 167–171. Available online at: <http://journal.ashpublications.org/content/139/2/167.full.pdf+html>
- Benner, M., and Geerts, R. F. R. (2003). A chain information model for structured knowledge management: towards effective and efficient food product improvement. *Trends Food Sci. Technol.* 14, 469–477. doi: 10.1016/S0924-2244(03)00154-7
- Biasioli, F., Yeretzian, C., Märk, T. D., Dewulf, J., and Van Langenhove, H. (2011). Direct-injection mass spectrometry adds the time dimension to (B)VOC analysis. *Trends Anal. Chem.* 30, 1003–1017. doi: 10.1016/j.trac.2011.04.005
- Blake, R. S., Monks, P. S., and Ellis, A. M. (2009). Proton-transfer reaction mass spectrometry. *Chem. Rev.* 109, 861–896. doi: 10.1021/cr800364q
- Brazelton, C. (2011). *World Blueberry Acreage & Production Report*. U.S. Highbush Blueberry Council, 1–51.
- Capozzi, V., Yener, S., Khomenko, I., Farneti, B., Cappellin, L., Gasperi, F., et al. (2017). PTR-ToF-MS coupled with an automated sampling system and tailored data analysis for food studies: bioprocess monitoring, screening and nose-space analysis. *J. Vis. Exp.* e54075. doi: 10.3791/54075
- Cappellin, L., Aprea, E., Granitto, P., Wehrens, R., Soukoulis, C., Viola, R., et al. (2012a). Linking GC-MS and PTR-TOF-MS fingerprints of food samples. *Chemometr. Intell. Lab.* 118, 301–307. doi: 10.1016/j.chemolab.2012.05.008
- Cappellin, L., Biasioli, F., Granitto, P. M., Schuhfried, E., Soukoulis, C., Costa, F., et al. (2011). On data analysis in PTR-TOF-MS: from raw spectra to data mining. *Sens. Actuators B* 155, 183–190. doi: 10.1016/j.snb.2010.11.044
- Cappellin, L., Soukoulis, C., Aprea, E., Granitto, P., Dallabetta, N., Costa, F., et al. (2012b). PTR-ToF-MS and data mining methods: a new tool for fruit metabolomics. *Metabolomics* 8, 761–770. doi: 10.1007/s11306-012-0405-9
- Clarke, S. (2016). *Blueberries in the European Union*. Agriculture and Agri-Food Canada. Available online at: <http://www.agr.gc.ca/resources/prod/Internet-Internet/MISB-DGSIM/ATS-SEA/PDF/6719-eng.pdf>.

- Cline, M. S., Smoot, M., Cerami, E., Kuchinsky, A., Landys, N., Workman, C., et al. (2007). Integration of biological networks and gene expression data using Cytoscape. *Nat. Protoc.* 2, 2366–2382. doi: 10.1038/nprot.2007.324
- Costa, A. I., Dekker, M., and Jongen, W. M. (2000). Quality function deployment in the food industry: a review. *Trends Food Sci. Technol.* 11, 306–314. doi: 10.1016/S0924-2244(01)00002-4
- Costa, F., Cappellin, L., Longhi, S., Guerra, W., Magnago, P., Porro, D., et al. (2011). Assessment of apple (*Malus x domestica* Borkh.) fruit texture by a combined acoustic-mechanical profiling strategy. *Postharvest Biol. Technol.* 61, 21–28. doi: 10.1016/j.postharvbio.2011.02.006
- Dewulf, J., Van Langenhove, H., and Wittmann, G. (2002). Analysis of volatile organic compounds using gas chromatography. *Trends Anal. Chem.* 21, 637–646. doi: 10.1016/S0165-9936(02)00804-X
- Du, X., Plotto, A., Song, M., Olmstead, J., Rouse, R., and States, U. (2011). Volatile composition of four southern highbush blueberry cultivars and effect of growing location and harvest date. *J. Agric. Food Chem.* 59, 8347–8357. doi: 10.1021/jf201184m
- Du, X., and Rouseff, R. (2014). Aroma active volatiles in four southern highbush blueberry cultivars determined by gas chromatography-olfactometry (GC-O) and gas chromatography-mass spectrometry (GC-MS). *J. Agric. Food Chem.* 62, 4537–4543. doi: 10.1021/jf50315t
- Farneti, B., Alarcón, A. A., Cristescu, S. M., Costa, G., Harren, F. J. M., Holthuyzen, N. T. E., et al. (2013). Aroma volatile release kinetics of tomato genotypes measured by PTR-MS following artificial chewing. *Food Res. Int.* 54, 1579–1588. doi: 10.1016/j.foodres.2013.09.015
- Farneti, B., Cristescu, S. M., Costa, G., Harren, F. J. M., and Woltering, E. J. (2012). Rapid tomato volatile profiling by using proton-transfer reaction mass spectrometry (PTR-MS). *J. Food Sci.* 77, C551–C559. doi: 10.1111/j.1750-3841.2012.02679.x
- Farneti, B., Di Guardo, M., Khomenko, I., Cappellin, L., Biasioli, F., Velasco, R., et al. (2017). Genome-wide association study unravels the genetic control of the apple volatilome and its interplay with fruit texture. *J. Exp. Bot.* doi: 10.1093/jxb/erx018. [Epub ahead of print].
- Farneti, B., Khomenko, I., Cappellin, L., Ting, V., Romano, A., Biasioli, F., et al. (2015b). Comprehensive VOC profiling of an apple germplasm collection by PTR-ToF-MS. *Metabolomics* 11, 838–850. doi: 10.1007/s11306-014-0744-9
- Farneti, B., Masuero, D., Costa, F., Magnago, P., Malnoy, M., Costa, G., et al. (2015a). Is there room for improving the nutraceutical composition of apple? *J. Agric. Food Chem.* 63, 2750–2759. doi: 10.1021/acs.jafc.5b00291
- Folta, K. M., and Klee, H. J. (2016). Sensory sacrifices when we mass-produce mass produce. *Hort. Res.* 3:16032. doi: 10.1038/hortres.2016.32
- Gilbert, J. L., Guthart, M. J., Gezan, S. A., De Carvalho, M. P., Schwieterman, M. L., Colquhoun, T. A., et al. (2015). Identifying breeding priorities for blueberry flavor using biochemical, sensory, and genotype by environment analyses. *PLoS ONE* 10:e0138494. doi: 10.1371/journal.pone.0138494
- Gilbert, J. L., Schwieterman, M. L., Colquhoun, T. A., Clark, D. G., and Olmstead, J. W. (2013). Potential for increasing southern highbush blueberry flavor acceptance by breeding for major volatile components. *HortScience* 48, 835–843. Available online at: <http://hortsci.ashpublications.org/content/48/7/835.full.pdf+html>
- Gilbert, J. L., Olmstead, J. W., Colquhoun, T. A., Levin, L. A., Clark, D. G., and Moskowitz, H. R. (2014). Consumer-assisted selection of blueberry fruit quality traits. *HortScience* 49, 864–873. Available online at: <http://hortsci.ashpublications.org/content/49/7/864.full.pdf+html>
- Giongo, L., Poncetta, P., Loretti, P., and Costa, F. (2013). Texture profiling of blueberries (*Vaccinium* spp.) during fruit development, ripening and storage. *Postharvest Biol. Technol.* 76, 34–39. doi: 10.1016/j.postharvbio.2012.09.004
- Goff, S. A., and Klee, H. J. (2006). Plant volatile compounds: sensory cues for health and nutritional value? *Science* 311, 815–819. doi: 10.1126/science.1112614
- Górecki, T., Yu, X., and Pawliszyn, J. (1999). Theory of analyte extraction by selected porous polymer SPME fibres. *Analyst* 124, 643–649. doi: 10.1039/a808487d
- Granitto, P., Biasioli, F., Aprea, E., Mott, D., Furlanello, C., Mark, T., et al. (2007). Rapid and non-destructive identification of strawberry cultivars by direct PTR-MS headspace analysis and data mining techniques. *Sens. Actuators B* 121, 379–385. doi: 10.1016/j.snb.2006.03.047
- Hall, I. V., Forsyth, F. R., and Lightfoot, H. J. (1979). Volatiles from developing fruit of *Vaccinium angustifolium*. *Can. Inst. Food Sci. Technol. J.* 3, 1–3. doi: 10.1016/S0008-3860(70)74243-8
- Hirvi, T., and Honkanen, E. (1983). The aroma of blueberries. *J. Sci. Food Agric.* 34, 992–996. doi: 10.1002/jsfa.2740340916
- Hongsognern, P., and Chambers, I. V. E. (2008). A lexicon for green odor or flavor and characteristics of chemicals associated with green. *J. Sens. Stud.* 23, 205–211. doi: 10.1111/j.1745-459X.2007.00150.x
- Horvat, R. J., Schlitzbauer, W. S., Chortyk, O. T., Nottingham, S. F., and Payne, J. A. (1996). Comparison of volatile compounds from rabbit-eye blueberry (*Vaccinium ashei*) and deerberry (*V. stamineum*) during maturation. *J. Essent. Oil Res.* 8, 645–648. doi: 10.1080/10412905.1996.9701033
- Horvat, R. J., Senter, S. D., and Dekazos, E. D. (1983). GLC-MS analysis of volatile constituents in Rabbit-eye blueberries. *J. Food Sci.* 48, 278–279. doi: 10.1111/j.1365-2621.1983.tb14849.x
- Jordan, A., Haidacher, S., Hanel, G., Hartungen, E., Märk, L., Seehauser, H., et al. (2009). A high resolution and high sensitivity proton-transfer-reaction time-of-flight mass spectrometer (PTR-TOF-MS). *Int. J. Mass Spectrom.* 286, 122–128. doi: 10.1016/j.ijms.2009.07.005
- Klee, H. J. (2010). Improving the flavor of fresh fruits: genomics, biochemistry, and biotechnology. *New Phytol.* 187, 44–56. doi: 10.1111/j.1469-8137.2010.03281.x
- Lugemwa, F. N., Lwande, W., Bentley, M. D., Mendel, M. J., and Alford, A. R. (1989). Volatiles of wild blueberry, *Vaccinium angustifolium*: possible attractants for the blueberry maggot fruit fly, *Rhagoletis mendax*. *J. Agric. Food Chem.* 37, 232–233. doi: 10.1021/jf00085a053
- Mowat, A., and Collins, R. (2000). Consumer behaviour and fruit quality: supply chain management in an emerging industry. *Supply Chain Manage.* 5, 45–54. doi: 10.1108/1359540010312963
- Nagegowda, D. A. (2010). Plant volatile terpenoid metabolism: biosynthetic genes, transcriptional regulation and subcellular compartmentation. *FEBS Lett.* 584, 2965–2973 doi: 10.1016/j.febslet.2010.05.045
- Norberto, S., Silva, S., Meireles, M., Faria, A., Pintado, M., and Calhau, C. (2013). Blueberry anthocyanins in health promotion: a metabolic overview. *J. Funct. Foods* 5, 1518–1528. doi: 10.1016/j.jff.2013.08.015
- Parliment, T. H., and Kolor, M. G. (1975). Identification of the major volatile components of blueberry. *J. Food Sci.* 40, 762–763. doi: 10.1111/j.1365-2621.1975.tb00550.x
- Payne, T. J. (2014). North American Highbush Blueberry Market Situation. US highbush blueberry council. Available online at: <http://www.blueberrymtech.org/publications/market-situation2014.pdf>
- Piechulla, B., Bartelt, R., Brosemann, A., Effmert, U., Bouwmeester, H., Hippauf, F., et al. (2016). The α-terpineol to 1,8-cineole cyclization reaction of tobacco terpene synthases. *Plant Physiol.* 172, 2120–2131. doi: 10.1104/pp.16.01378
- Rambla, J. L., Tikunov, Y. M., Monforte, A. J., Bovy, A. G., and Granell, A. (2014). The expanded tomato fruit volatile landscape. *J. Exp. Bot.* 65, 4613–4623. doi: 10.1093/jxb/eru128
- Saftner, R., Polashock, J., Ehlenfeldt, M., and Vinyard, B. (2008). Instrumental and sensory quality characteristics of blueberry fruit from twelve cultivars. *Postharvest Biol. Technol.* 49, 19–26. doi: 10.1016/j.postharvbio.2008.01.008
- Scheidler, N. H., Liu, C., Hamby, K. A., Zalom, F. G., and Syed, Z. (2015). Volatile codes: correlation of olfactory signals and reception in *Drosophila*-yeast chemical communication. *Sci. Rep.* 5:14059. doi: 10.1038/srep14059
- Taiti, C., Costa, C., Menesatti, P., Comparini, D., Bazihizina, N., Azzarello, E., et al. (2015). Class-modelling approach to PTR-TOFMS data: a peppers case study. *J. Sci. Food Agric.* 95, 1757–1763. doi: 10.1002/jsfa.6761
- Tieman, D., Bliss, P., McIntyre, L. M., Blandon-Ubeda, A., Bies, D., Odabasi, A. Z., et al. (2012). The chemical interactions underlying tomato flavor preferences. *Curr. Biol.* 22, 1035–1039. doi: 10.1016/j.cub.2012.04.016
- Tieman, D., Zhu, G., Resende, M. F. R., et al. (2017). A chemical genetic roadmap to improved tomato flavor. *Science* 355, 391–394. doi: 10.1126/science.aal1556

- Titzmann, T., Graus, M., Müller, M., Hansel, A., and Ostermann, A. (2010). Improved peak analysis of signals based on counting systems: illustrated for proton-transfer-reaction time-of-flight mass spectrometry. *Int. J. Mass Spectrom.* 295, 72–77. doi: 10.1016/j.ijms.2010.07.009
- von Sydow, E., Andersson, J., Anjou, K., and Karlsson, G. (1970). The aroma of bilberries (*Vaccinium myrtillus* L.). II. Evaluation of the press juice by sensory methods and by gas chromatography and mass spectrometry. *Lebensm. Wiss. Technol.* 3, 11–17.
- von Sydow, E., and Anjou, K. (1969). The aroma of bilberries (*Vaccinium myrtillus* L.). I. Identification of volatile compounds. *Lebensm. Wiss. Technol.* 2, 78–81.

Conflict of Interest Statement: The authors declare that the research was conducted in the absence of any commercial or financial relationships that could be construed as a potential conflict of interest.

Copyright © 2017 Farneti, Khomenko, Grisenti, Ajelli, Betta, Algarra, Cappellin, Aprea, Gasperi, Biasioli and Giongo. This is an open-access article distributed under the terms of the Creative Commons Attribution License (CC BY). The use, distribution or reproduction in other forums is permitted, provided the original author(s) or licensor are credited and that the original publication in this journal is cited, in accordance with accepted academic practice. No use, distribution or reproduction is permitted which does not comply with these terms.



Insights into the Sesquiterpenoid Pathway by Metabolic Profiling and *De novo* Transcriptome Assembly of Stem-Chicory (*Cichorium intybus* Cultigroup “Catalogna”)

Julio Testone¹, Giovanni Mele¹, Elisabetta Di Giacomo¹, Maria Gonnella², Massimiliano Renna^{2,3}, Gian Carlo Tenore⁴, Chiara Nicolodi¹, Giovanna Frugis¹, Maria Adelaide Iannelli¹, Giuseppe Arnesi⁵, Alessandro Schiappa⁵ and Donato Giannino^{1*}

¹ Institute of Agricultural Biology and Biotechnology, National Research Council, Rome, Italy, ² Institute of Sciences of Food Production, National Research Council, Bari, Italy, ³ Department of Agricultural and Environmental Science, University of Bari, Bari, Italy, ⁴ Department of Pharmacy, University of Naples Federico II, Naples, Italy, ⁵ Enza Zaden Italia, Tarquinia, Italy

OPEN ACCESS

Edited by:

Luis A. J. Mur,
Aberystwyth University, UK

Reviewed by:

Paola Leonetti,
National Research Council, Italy
Benedetto Ruperti,
University of Padova, Italy

*Correspondence:

Donato Giannino
donato.giannino@ibba.cnr.it

Specialty section:

This article was submitted to
Crop Science and Horticulture,
a section of the journal
Frontiers in Plant Science

Received: 23 August 2016

Accepted: 24 October 2016

Published: 08 November 2016

Citation:

Testone G, Mele G, Di Giacomo E, Gonnella M, Renna M, Tenore GC, Nicolodi C, Frugis G, Iannelli MA, Arnesi G, Schiappa A and Giannino D (2016) Insights into the Sesquiterpenoid Pathway by Metabolic Profiling and *De novo* Transcriptome Assembly of Stem-Chicory (*Cichorium intybus* Cultigroup “Catalogna”). *Front. Plant Sci.* 7:1676.
doi: 10.3389/fpls.2016.01676

Stem-chicory of the “Catalogna” group is a vegetable consumed for bitter-flavored stems. Type and levels of bitter sesquiterpene lactones (STLs) participate in conferring bitterness in vegetables. The content of lactucin—and lactucopocrin-like STLs was higher in “Molfettese” than “Galatina” landrace stalks, regardless of the cultivation sites, consistently with bitterness scores and gustative differences. The “Galatina” transcriptome assembly resulted in 58,872 unigenes, 77% of which were annotated, paving the way to molecular investigation of the STL pathway. Comparative transcriptome analysis allowed the identification of 69,352 SNPs and of 1640 differentially expressed genes that maintained the pattern independently of the site. Enrichment analyses revealed that 4 out of 29 unigenes were up-regulated in “Molfettese” vs “Galatina” within the sesquiterpenoid pathway. The expression of two germacrene A -synthase (GAS) and one -oxidase (GAO) genes of the costunolide branch correlated positively with the contents of lactucin-like molecules, supporting that STL biosynthesis regulation occurs at the transcriptional level. Finally, 46 genes encoding transcription factors (TFs) maintained a differential expression pattern between the two varieties regardless of the growth site; correlation analyses among TFs, GAS, GAO gene expressions and STLs contents suggest that one *MYB* and one *bHLH* may act in the pathway.

Keywords: *Cichorium intybus*, stem-chicory landraces, transcriptome, sesquiterpene lactones, bitterness

INTRODUCTION

Chicory (*Cichorium intybus* L.) is cultivated worldwide to produce food, coffee surrogates, forages pharmaceuticals, and healthcare compounds (Street et al., 2013). Genetic diversity analysis supported the three-cluster structure of *C. intybus* cultivated germplasm (Kiers et al., 2000; Raulier et al., 2016): witloof, root and leaf chicory groups. The latter embraces “Radicchio,” “Sugarloaf” and “Catalogna” sub-groups. Several “Catalogna” cultivars/landraces are cultivated in Italy for both

leaves and stems. These latter are appreciated for the bitter and crispy taste. Botanically, they bear a receptacle made of outer whorls of leaves (runcinate-pinnatifid type, large mid-rib) and an inner bulk of inflorescence stems (syn. flower stalks, turions). These stalks (cut at various lengths) are mostly eaten raw (sliced into curly and crunchy strips, a.k.a. "puntarelle") or cooked. Stem vegetables are novel products moving from a niche to a global market, showing potential use in the minimally or fully processed food chain (Renna et al., 2014).

The *C. intybus* species has a large ($2n = 2x = 18$; size 1405 Mbp) and complex genome (De Simone et al., 1997; Berardes et al., 2013). Culti-groups are mostly allogamous due to different mechanisms of self-incompatibility (Eenink, 1981, 1982; Varotto et al., 1995) and natural hybrids widely occur (Kiaer et al., 2009; Bai et al., 2012). Consistently, the "Catalogna" sub-group shows a high genetic variation at both inter- and intra- population levels (Raulier et al., 2016). So far, the *C. intybus* genetic toolbox includes a linkage consensus map (Cadalet et al., 2010), BAC libraries (Gonthier et al., 2010), EST databases (The Compositae Genome Project, 2000; Legrand et al., 2007; Dauchot et al., 2009), and transcriptomes (Hodgins et al., 2014). An increasing number of tools for molecular marker assisted breeding is predicted for the improvement of a wide range of chicory products.

Sesquiterpene lactones (STL) are secondary metabolites typical of *Asteraceae* spp., concentrated in the latex (Sessa et al., 2000) and active in defense against pathogens (Peña-Espinoza et al., 2015). From a nutritional standpoint, STL have both beneficial (e.g., anti-cancer, anti-leukemic) and allergenic properties (Chadwick et al., 2013), they contribute to the bitter taste of chicory food (Price et al., 1990; van Beek et al., 1990) and the contents vary significantly among culti-groups (Ferioli et al., 2015; Graziani et al., 2015). Bitterness is crucial for vegetable quality as high levels can cause rejection (D'Antuono et al., 2016), though the acceptance varies with consumers' use and culture (Drewnowski and Gomez-Carneros, 2000). Chemically, STL are C-15 terpenoids based on a guaiane skeleton bearing lactone rings (Cordell, 1976; Chadwick et al., 2013). The most abundant STLs of chicory leaves are lactucin, 8-deoxylactucin, lactucopicrin and the respective 11(S), 13-dihydroderivatives (Ferioli et al., 2015); glycosyl- and oxalyl- conjugate forms also occur (Kisiel and Zielinska, 2001; Graziani et al., 2015). As for STL biosynthesis, the enzymes germacrene A-synthase, -oxidase and costunolide synthase act upstream the pathway to convert farnesyl diphosphate into costunolide, this latter being the common precursor of STLs (de Kraker et al., 2002). The enzymes and respective genes (GAS, *germacrene A synthase*; GAO, *germacrene A oxidase*; COS, *costunolide synthase*) were characterized in several *Asteraceae* species (Nguyen et al., 2010;

Cankar et al., 2011; Ikezawa et al., 2011; Liu et al., 2011; Ramirez et al., 2013; Eljounaidi et al., 2014, 2015). Terpene synthase genes of the STL pathway have been identified in model plants (Kitaoka et al., 2015; Tholl, 2015) and crops, such as tomato (Falara et al., 2011) and grapevine (Schwab and Wust, 2015). However, to date, enzymes and genes leading to the Lc- and Lp-compounds have not been identified yet.

A major aim of this work was to characterize the factors that contribute to bitterness at the metabolic and genetic levels by comparing "Galatina" (Gal) and "Molfettese" (Mol) landraces. The STL quantification revealed a higher content of lactucins and lactucopicrins in the latter compared to the former, independently of the growing sites. Due to the lack of comprehensive genomic information on *C. intybus*, a reference Gal transcriptome for the "Catalogna" group was created. Digital gene expression (DGE) targeted to stems at the commercial maturity revealed those differentially expressed genes (DEGs), which maintained the patterns in Mol and Gal landraces irrespective of the cultivation area. Focusing on transcriptomic differences of the STL pathway, the Mol genotype was enriched of upregulated genes—two *germacrene A-synthase* and one *oxidase* (GAS and GAO)—acting upstream the route. The GAS and GAO transcription levels correlated positively with the contents of 11(S), 13-dihydrolactucin and 11(s), 13-dihydro-8-deoxylactucin, supporting that STL biosynthesis regulation occurs at the transcriptional level. Consequently, the GAS and GAO higher expression levels of Mol vs. Gal may account for higher contents of STLs, supporting that these genes may be good expression markers for bitterness selection. Correlation analyses among the expression levels of GAS, GAO, and transcription factor (TF) genes and STLs contents pointed at MYB and bHLH as the best TF candidates in the STL biosynthesis regulation.

MATERIALS AND METHODS

Plant Materials and Sampling

The "Galatina" (Gal) and "Molfettese" (Mol) landraces of stem chicory (*Cichorium intybus* L. "Catalogna" group) were previously described, including botanical classification, phenotypical traits, site coordinates, and cultivation parameters (D'Acunzo et al., 2016). In the current work, the landraces were grown both on local private farms in Apulia (Molfetta, southern Italy) and in the Enza Zaden fields (Tarquinia, Viterbo, Lazio, Italy). Plants were sown in August 2012 in both locations and transplanted after 30 days. Plant density was 8.3 plants/m² and similar growing techniques were applied in both growing areas. As for Lazio, harvesting was on the 08/01/2013 and 28/01/2013 for Mol and Gal, respectively; the average temperatures 1 week before harvesting were $9.0 \pm 0.9^\circ\text{C}$ and $6.9 \pm 1.4^\circ\text{C}$ and the average temperature during the 1–28/1/2013 period was $8.2 \pm 2.2^\circ\text{C}$ (www.idrografico.roma.it/annali). As for Apulia, harvesting occurred on the 14/01/2013 and 25/01/2013 for Mol and Gal, respectively; the average temperatures 1 week before harvesting were $9.4 \pm 0.1^\circ\text{C}$ and $9.5 \pm 0.3^\circ\text{C}$, and the average temperature of the 1–25/1/2013 lapse was $9.7 \pm 0.2^\circ\text{C}$ (www.agrometeopuglia.it). Harvested plants were brought to laboratories, selected for comparable weights (Lazio: $905 \pm$

Abbreviations: COS, costunolide synthase; DEGs, differentially expressed genes; DGE, digital gene expression; DHdLc, 11(s), 13-dihydro-8-deoxylactucin; DHdLp, 11(s), 13-dihydrolactucopicrin; DHlc, 1,3-dihydrolactucin; dLc, 8-deoxylactucin; Gal, 'Galatina'; GAO, germacrene A-oxidase; GAS, germacrene A-synthase; GO, gene ontology; Lc, lactucin; Lp, lactucopicrin; Mol, Molfettese'; PCA, principal component analysis; RPKM, reads per kilobases per million; SNPs, single nucleotide polymorphisms; SSR, simple sequence repeats; STL, sesquiterpene lactones; STP, sesquiterpenoid and triterpenoid pathway; TFs, transcription factors.

230gr and 850 ± 201 gr for Gal and Mol; Apulia: 820 ± 162 gr and 940 ± 128 gr for Gal and Mol; non-significant differences were scored by ANOVA) and processed. In the experiments of STL lactones quantification, transcriptional and allelic variation analyses, marketable stems were removed from rosettes ($n = 15$) of each landrace. A replicate batch consisted of 10 homogeneous stems (mean length 11.5 ± 1.5 cm, mean diameter of the median section: 2.7 ± 0.3 cm). These were immediately frozen in liquid nitrogen and stored at -80°C for RNA isolation or they were lyophilized at -50°C for 72 h (laboratory freeze dryer with stoppering tray dryer, FreeZone[®], Labconco Corp., Kansas City, MO, USA) and stored at -20°C for HPLC analyses. Three biological replicates were used in all the experiments.

Sesquiterpene Lactones Quantification

In order to quantify the total amount of STL (free and bound fractions), the samples were prepared by adopting both cellulase hydrolytic treatment (Tamaki et al., 1995) and ultrasound assisted extraction (UAE). As regards the enzymatic procedure, the lyophilized sample (2 g) was added to 50 mL of methanol/water solution (80:20, v/v) plus 2% of formic acid and 3 mL of santonin solution (101.7 $\mu\text{g/mL}$) as internal standard, and shaken (1000 g/min, for 15 min, at 80°C ; F80 Digit, Falc Instruments s.r.l., Italy). The supernatant was collected and the pellet underwent two additional extractions as described above. The final extract (about 150 mL) was dried under vacuum, re-dissolved in methanol/dichloromethane (1:7, v/v) solution, and loaded onto a solid phase extraction (SPE) column. The elution was carried out with 6 mL of a dichloromethane/ethyl acetate (3:2 v/v) solution; the eluted fractions were pooled and then vacuum-dried. The eluted fraction was re-dissolved in 1 mL of a cellulase enzyme solution (10 mg of cellulase/mL of water) and then incubated at 37°C for 2 h with stirring. The solvent was evaporated and then made up to 500 μL . As for the ultrasound assisted extraction, the same protocol as described above was adopted. Differently, the SPE eluted fraction was sonicated at 50 KHz for 30 min (37°C) by using an ultrasound bath (Labsonic LBS1-3, Falc Instruments s.r.l., Italy). The purified samples were added with methanol (4 mL) and the STL identification was performed by an HPLC apparatus Finnigan (Thermo Electron Corporation, San Jose, California), equipped with quaternary pump, DAD detector, and a C18 Kinetex column (250 \times 4.60 mm, 5 μm). The mobile phases A and B were, respectively, methanol/water 14:86 and 64:36 (v/v). The gradients were 0–20 min, 100–58% A; 20–30 min, 58% A; 30–45 min, 58–0% A; 45–50 min, 0% A; 50–52 min, 0–100% A; 52–62 min, 100% A. The flow was at 0.5 mL/min and the injection volume was 80 μL . STL peaks were monitored at 260 nm. Following an identical preliminary extraction protocol, UAE lead to equivalent amounts of STL as compared to the cellulase treatment (Table S1).

RNA Isolation and Sequencing

For transcriptome reference assembly, Gal plants at the transplant ($n = 5$, 3–4 true leaves) and commercial maturation ($n = 5$) stages were used; distinct tissues (apices, stems, leaves and roots) were sampled and ground in liquid nitrogen. 500 mg of each tissues was used to isolate total RNA by TRIzol reagent

(Invitrogen) followed by an additional purification step using RNAeasy separation columns (RNAeasy kit, Qiagen); yields were estimated by electrophoretic and spectrophotometric analyses (NanoDrop ND-1000; Thermo Scientific Inc.), and RNA integrity number (RIN > 7) was verified using BioAnalyzer 2100 (Agilent Technologies Inc). cDNA libraries were prepared using TruSeq RNA-seq sample preparation kit (Illumina) and sequenced in 100 bp paired-end mode using an Illumina HiSeq2000 (IGA Technology Services, Udine, Italy).

As for NGS transcriptional analyses and SNP mining, size-comparable stems ($n = 10$) at harvesting time were sampled from Gal ($n = 5$) and Mol ($n = 5$) grown in each location. Total RNA was isolated, quantified and controlled for yield and integrity as described above. Illumina Truseq cDNA libraries were prepared and sequenced in 50 bp single-end on Illumina HiSeq2000 platform. For a given genotype, three biological replicates for each growing area were generated. RNAseq data sets have been stored in the National Center for Biotechnology Information database (NCBI, www.ncbi.nlm.nih.gov) under the BioProject accession number PRJNA328202.

Transcriptome Assembly

Paired-end Illumina raw reads were filtered to remove adapter contaminations and low-quality reads using Trimmomatic v0.32 (Bolger et al., 2014). The high-quality reads were assembled by using both a one-step (*de novo*) and two-steps (EST-based backbone construction followed by a *de novo* assembly) approaches. In the one-step approach the cleaned reads were assembled using Trinity (Grabherr et al., 2011) with default parameters. In the two-steps approach, a collection of 53,973 *Cichorium intybus* EST was retrieved from the NCBI database. To create a unigene dataset, the EST were cleaned (trimming of vector tag, low quality stretches and repetitive element) and assembled using the EGassembler pipeline (Masoudi-Nejad et al., 2006) with the default parameters. The pipeline produced 26,085 unigenes (7199 contigs and 18,886 singletons). The filtered reads were mapped on the resulting unigenes by using Bowtie2 (Langmead and Salzberg, 2012). The unmapped reads were recovered and used in iterative contig extension processes using SeqMan Pro (DNASTAR, Madison, WI). The reads that did not extend contig lengths were *de novo* assembled Velvet/Oasis programs (Zerbino and Birney, 2008; Schulz et al., 2012) with a *k-mer* size of 25. Redundancy between one—and two-steps output was removed by TGICL-CAP3 (Pertea et al., 2003) using overlapping stretches 200 bp-long and minimal identity of 97%. The genes/isoforms clustering was performed using cd-hit-est from the CD-HIT package (Li and Godzik, 2006) with sequence identity threshold of 97%. The longest transcripts were selected as representative for each cluster.

Functional Annotation

Transcripts were annotated using BlastX (cut-off *E*-value of 10–5) mining the following databases: Nr, NCBI non-redundant database (January 12, 2015); TAIR, The Arabidopsis Information Resource (TAIR10); SwissProt and TrEMBL, the manually annotated and reviewed and the automatically annotated and not reviewed sections of the UniProt Knowledgebase (UniProtKB),

respectively (release 2014_02); KOG, euKaryotic Ortholog Groups (Koonin et al., 2004). Blast2GO (Conesa et al., 2005) was used to obtain Gene Ontology (GO) and KEGG (Kanehisa and Goto, 2000) annotations based on BLASTx hits against the Nr database. WEGO (Ye et al., 2006) was used for GO functional classification. To improve the pathway annotation, unigenes were also submitted to the online KEGG Automatic Annotation Server (Moriya et al., 2007). Deduced protein sequences were analyzed with InterProScan 5.1–44.0 (Jones et al., 2014) against 15 integrated databases (Phobius, TMHMM, Pfam, ProDom, Gene3d, Panther, SuperFamily, Coils, SMART, PrositeProfiles, PRINTS, SignalP, PIRSF, TIGRFAMs, HAMAP) and protein signatures were collected.

Polymorphisms Calling

BWA (Li and Durbin, 2009), Picard tools (<http://picard.sourceforge.net>), SAMtools (Li et al., 2009) and the BCFtools utilities were used to align the reads of Gal and Mol to the reference transcriptome, mark duplicated reads, compute the genotype likelihoods and call the variable positions, respectively. In order to provide a set of reliable SNPs useful in robust genotyping assays, the following filtering criteria were imposed: (a) quality score (“QUAL”) ≥ 30 (99.9% base call accuracy); (b) at least 10 high-quality reads (“DP4”) supporting the nucleotide differences; (c) SNP within homopolymer stretches of length ≥ 5 bp were excluded; (d) genotype quality score (“GQ”) ≥ 50 . The MISA perl script (<http://pgrc.ipk-gatersleben.de/misa>) was used for identification of potential simple sequence repeats (SSRs). Units with one to six nucleotides and a minimum repetition of twelve units for mono-nucleotides, six for di-nucleotides, five for tri-, tetra-, penta- and hexa-nucleotides were considered in the analysis.

Gene Expression Analyses

The raw single-end reads were trimmed as described above. For a given genotype, the cleaned reads were mapped on the reference assembly using BWA (Li and Durbin, 2009) and SAMtool pipeline, and read count for each transcript was scored in each replicate. The digital gene expression (DGE) levels were calculated and expressed as RPKM (reads *per* kilobases of transcript sequence *per* million of mapped reads) values.

Real Time Quantitative PCR (qPCR)

Total RNA derived from a pool ($n = 5$) of stems was isolated by the RNeasy Plant Mini Kit (Qiagen), DNase treated (RQ1, Promega), and 1 μ g was reverse-transcribed at 55°C by SuperscriptIII (Life Technologies). The cDNA (100 ng) was amplified by Eco Real-Time PCR System (Illumina) using 1x Quantimix easy master mix (Biotoools) and 0.3 μ M of each primer in a 10 μ l final volume. The triplicate reaction conditions were as follows: 95°C for 10 min, 45 cycles at 95°C for 15 s, 60°C for 15 s, and 72°C for 40 s. Primer specificity was checked by melting curve analysis and by agarose gel electrophoresis. Three technical replicates and three independent biological experiments were performed for each sample. The expression levels of the target unigenes were normalized with the reference genes ACT (Maroufi et al., 2010) by the Q-Gene program (Muller

et al., 2002). Primers were designed using Primer3 software (Untergasser et al., 2012) and they are listed in Table S2.

Statistical Analyses

The analysis of variance (ANOVA) was applied to STL content variation in landraces grown in Apulia and Lazio cultivation sites, followed by Duncan Multiple Range Test. All procedures, General Linear Model and means separation, were carried out by Statistical Analysis System program (SAS software, Version 9.1, Cary, NC, USA). The principal component analysis (PCA) allowed a visual overview about spatial distribution and grouping among genotypes and growing sites; it was based on mean centered and standardized data (unit variance scaled) and results were shown as bi-plots of scores (treatments) and loadings (variables) plots (XLStat Pro, Addinsoft, Paris, France). Differential expression analysis was performed using the Bioconductor edgeR package (Robinson et al., 2010). All samples were normalized by trimmed mean of M values (TMM). Unigenes with at least 1 read per million in at least 3 samples were retained and a false discovery rate (FDR) value ≤ 0.05 and an absolute value of \log_2 fold change ratio ($\log_2\text{FC}$) ≥ 1 were set as the thresholds for the significance of the gene expression difference. The hypergeometric test (Pang et al., 2013) was used for GO and KEGG enrichment analyses of differentially expressed genes with the whole transcriptome set as background. The significant GO and KEGG terms were identified after multiple testing adjustments with an FDR ≤ 0.05 . Correlations analyses were performed in R 3.2.2 (R Core Team, 2015) with the *rccor* function of the *Hmisc* package (Harrell, 2016), whilst *corrplot* function (Wei, 2013) was used to produce the correlation matrix.

RESULTS

Stems of “Molfette” Contain More STL than “Galatina” Independently of Cultivation Area

The major STLs lactucin (Lc), 8-deoxylactucin (dLc), lactucopicrin (Lp) and the respective dihydro-derivatives, 1,3-dihydrolactucin (DHLc), 11(s), 13-dihydro-8-deoxylactucin (DHdLc), 11(s), 13-dihydrolactucopicrin (DHdLp) were quantified in stems of Mol and Gal landraces. Overall, the total STL content was significantly higher in Mol than Gal stems (84.9 ± 5.0 vs. 55.4 ± 3.0 mg kg $^{-1}$ dry matter) as well as that of total lactucin-like forms (LcTOT, 66.2 ± 6.7 vs. 37.7 ± 4.5) independently of the growth site (Table 1, values in the “Both” line). The total lactucopicrin-like compounds showed comparable levels in both landraces (LpTOT, 18.6 ± 2.0 vs. 17.7 ± 2.5). The mean contents of DHLc and DHdLc were 2-fold higher in Mol than Gal (26.6 ± 2.8 vs. 11.1 ± 1.4 and 29.7 ± 2.8 vs. 12.2 ± 1.5 , respectively). Vice versa, the Lc and dLc contents were slightly but significantly higher in Gal than Mol (6.4 ± 0.8 vs. 5.1 ± 0.8 and 8.0 ± 0.9 vs. 4.9 ± 2.5). Finally, the Lp amount was higher in Mol than Gal stems, whilst that of DHdLp was comparable in the two genotypes. The environment change *per se* did not cause any significant variation of all compounds

TABLE 1 | The sesquiterpene lactone (STL) content in stems of “Galatina” and “Molfettese” landraces.

Genotype	Site ²	STLs content (mg kg ⁻¹ dry matter) ¹								
		Lc	DHLc	dLc	DHdLc	LcTOT	DHLP	Lp	LpTOT	TOTAL
“Galatina”	A	5.9 ± 0.9ab	10.3 ± 1.5c	7.3 ± 0.9	11.3 ± 1.5c	34.7 ± 4.6b	5.4 ± 1.4	10.8 ± 1.5b	16.2 ± 2.9b	50.9 ± 7.4b
	L	6.9 ± 0.3a	12.0 ± 0.8c	8.7 ± 0.4	13.1 ± 0.9c	40.6 ± 2.2b	6.5 ± 0.3	12.7 ± 0.7ab	19.2 ± 0.9a	59.9 ± 3.1b
	Both	6.4 ± 0.8	11.1 ± 1.4	8.0 ± 0.9	12.2 ± 1.5	37.7 ± 4.5	5.9 ± 1.1	11.8 ± 1.5	17.7 ± 2.5	55.4 ± 3.0
“Molfettese”	A	5.6 ± 0.9ab	28.6 ± 1.8a	5.3 ± 3.8	31.9 ± 2.1a	71.3 ± 4.3a	5.3 ± 0.7	14.7 ± 1.0a	20.0 ± 1.7a	91.3 ± 5.8a
	L	4.7 ± 0.4b	24.5 ± 2.1b	4.4 ± 0.6	27.5 ± 1.0b	61.2 ± 4.0a	4.5 ± 0.6	12.8 ± 0.9ab	17.3 ± 1.4b	78.5 ± 5.5a
	Both	5.1 ± 0.8	26.6 ± 2.8	4.9 ± 2.5	29.7 ± 2.8	66.2 ± 6.7	4.9 ± 0.7	13.7 ± 1.3	18.6 ± 2.0	84.9 ± 5.0
SIGNIFICANCE³										
Genotype	*	***	*	***	***	ns	*	ns	***	
Environment	ns	ns	ns	ns	ns	ns	ns	ns	ns	
Gen. × Env.	*	*	ns	**	*	ns	*	*	*	*

¹Lc, lactucin; DHLc, 11(S), 13-dihydrolactucin; dLc, 8-deoxylactucin; DHdLc, 11(S), 13-dihydro-8-deoxylactucin; Lp, lactucopicrin; DHLP, 11(s), 13-dihydrolactucopicrin; LcTOT, total lactucin-like STLs; LpTOT, total lactucopicrin-like STLs.

²Cultivation site: A, Apulia; L, Lazio; Both, data from both growing sites were merged for a given genotype and mean values ± s.d. reported.

³ns, non-significant. *, **, *** = significant at P < 0.05, 0.01, and 0.001, respectively. Genotype significance refers to both-site data; different letters within the same column indicate statistically significant differences in genotype X environment interactions.

in both landraces (Table 1, values in the “A” and “L” lines). However, genotype-environment interactions were observed for the content of DHdLc, which decreased in Mol and was unvaried in Gal, and for Lc and Lp, which differed between Mol and Gal, only in one of the two sites (Lazio for Lc and Apulia for Lp). The principal component analysis (PCA, Figure 1) of STL data produced the two principal components PC1 and PC2 explaining, respectively, 80.67 and 19.30% of the total variance. The PCA fully separated Gal from Mol genotypes, respectively, located on the left and right side of PC1. Negative values of PC1 correlated with DHLP, Lc and dLc whilst the positive ones showed high correlation with the other compounds. Referring to PC2, Gal from Lazio (L) and Mol from Apulia (A) were in the upper quadrants, mainly positively correlated to the highest content of DHLP in Gal/L and of Lp and total STL in Mol/A (Table 1).

Transcriptome Assembly

Cichorium intybus RNA-seq libraries were prepared from the apical tips, stems, leaves and roots sampled at transplant and harvest stages of the Gal landrace (Table 2). The Illumina HiSeq2000 sequencing yielded approximately 164 million raw (100 bp) paired-end reads. The reads were processed to remove low-quality and adapter sequences, and ca. 97.7% of them (Table 2) were used as common dataset to follow two workflows, named “one-step” and “two-step” assembly strategies (Table 3 and Figure S1). In the former, the high-quality reads were assembled *de novo* by Trinity (Grabherr et al., 2011) into 80,303 contigs with a N50 and mean lengths of 1472 and 1,130.9 bp, respectively. The two-step strategy first included a template-based assembly and then a *de novo* one. Briefly, a non-redundant set of 26,085 unique sequences was generated by EGassembler pipeline (Masoudi-Nejad et al., 2006) using all the *C. intybus* public ESTs available at current date. Subsequently, the filtered reads were mapped on the unigenes EST set of 26,085 resulting

into 11,153 read-supported EST fragments. These were used as input for iterative contig extension process using SeqMan Pro (DNAStar) which could raise the unigene mean length from ca. 760 to 1248 bp. Finally, the unmapped reads were retrieved by Bowtie2 (Langmead and Salzberg, 2012) and *de novo* assembled by Velvet/Oasis (Zerbino and Birney, 2008; Schulz et al., 2012) into 35,091 contigs. The output from both one- and two-step approaches were merged to obtain the final reference assembly consisting of 79,716 transcripts (N50 = 1545 bp and average contig length = 1230 bp) clustered into 58,872 isoform groups (unigenes). The unigenes set had a N50 and mean lengths of 1574 and 1220 bp, respectively (Table 3).

Annotation and Function Classification

In order to widen the information on the newly assembled transcriptome, sequence similarity searches were performed against eight databases (see Material and Methods, and Table 4). The BlastX analyses showed that 38,931 unigenes (66.1%) had significant (*E*-value $\leq 10^{-5}$) matches in the Nr database, 38,978 (66.2%) in the TrEMBL, 36,281 (61.6%) in the Tair, and 26,233 (44.6%) in the SwissProt databases. GO, KEGG and KOG databases allowed functional classification of unigenes. An overview of the unigene annotations are in Table S3. Over 109,900 GO annotations were assigned to 23,501 unigenes (39.9%), and 7947 of them fell in the three ontology groups (Table 4, Figure 2A, and Figure S2). The “metabolic” and “cellular processes” were the most abundant categories (13,025 and 12,146 unigenes) within the “biological process;” “cell” and “cell part” top ranked ($>10,500$ unigenes) in the “cellular component,” while “binding” and “catalytic activity” included the highest unigene numbers (14,198 and 11,628) in the “molecular function” ontology. As for KEGG (Table 4 and Figure 2B), 7393 unigenes (12.6%) were mapped into 5 main categories and 130 metabolic maps. Most of the unigenes fell into the “metabolism” cluster (10,634; 82.7% of the mapped unigenes) followed by

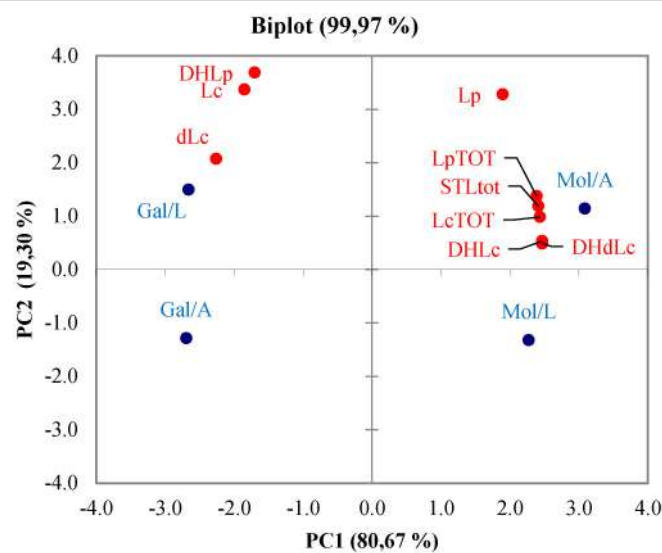


FIGURE 1 | Principal component analysis biplot showing the spatial distribution of the sesquiterpene lactones content in Mol and Gal puntarelle types cultivated in Lazio (L) and Apulia (A). Lc, lactucin; DHLC, 11(S), 13-dihydro-lactucin; dLc, 8-deoxylactucin; DHdLc, 11(S), 13-dihydro-8-deoxylactucin; LcTOT, total of lactucin-like STLs; Lp, lactucopirin; DHLP, 11(s), 13-dihydro-lactucopirin; LpTOT, total of lactucopirin-like STLs; STLs, total STL content.

TABLE 2 | *C. intybus* RNA sequencing datasets.

Reference assembly		
Genotype		"Galatina"
Tissue		Apex, stem, leaf, root
Stages		Transplant and harvest
Site		Apulia
Read types		2 × 100 bp
Raw reads		164,768,038
Cleaned reads		160,952,538
Retained reads		97.7%
RNA-SEQUENCING ^a		
Genotype	"Galatina"	"Molfettese"
Tissue	Edible stem	Edible stem
Stages	Harvest	Harvest
Growth site		
Apulia		
Replicates	3	3
Read types	1 × 50 bp	1 × 50 bp
Raw reads	19,469,829	18,953,475
Cleaned reads	19,424,671	18,864,361
Retained reads	99.8%	99.5%
Lazio		
Replicates	3	3
Read types	1 × 50 bp	1 × 50 bp
Raw reads	30,296,567	23,953,335
Cleaned reads	30,176,328	23,872,902
Retained reads	99.6%	99.7%

^aMean values for each group of triplicates.

the genetic information processing, "environmental information processing," "cellular processes" and "organismal systems" (11.9, 2.9, 1.5, and 0.9%, respectively). Within the "metabolisms,"

TABLE 3 | Features of assembled transcriptome.

	One-step	Two-step	
	<i>de novo</i> (Trinity)	EST-based	<i>de novo</i> (Velvet)
Contig number	80,303	11,153	35,091
Overall alignment rate (%)	93.1	23.5	64.4
Transcriptome size (Mb)	90.9	13.9	42.7
Contig N50 length (bp)	1472	1452	1314
Contig mean length (bp)	1,130.9	1,247.5	1,216.3
MERGED ^a			
Contig number ^b	79,716		
Overall alignment rate (%)	95.7		
Transcriptome size (Mb)	98.1		
Contig N50 length (bp)	1545		
Contig mean length (bp)	1230		
Unigene number ^c	58,872		
Unigene N50 length (bp)	1574		
Unigenes mean length (bp)	1220		

^aOne-step and two-step assembly strategies (described in the text) produced the merged transcriptome.

^bRedundancy minimized by TGCL/CAP3 pipeline.

^cThe longest transcripts were selected as representative for each cluster.

those of "carbohydrate" (2416; 18.8%), "nucleotide" (1718; 13.4%) and "cofactors and vitamins" (1648; 12.8%) contained the highest number of unigenes. Based on the KOG database (**Table 4** and **Figure 2C**), 11,650 unigenes (19.8%) belonged to 25 functional categories and the "general functional prediction only" (2309 unigenes; 17.6%), "post-translational modification, protein turnover, chaperones" (1341; 10.2%), and "signal transduction mechanisms" (1226; 9.4%), were the largest ones. InterProScan was used for structural annotation of the deduced products. The

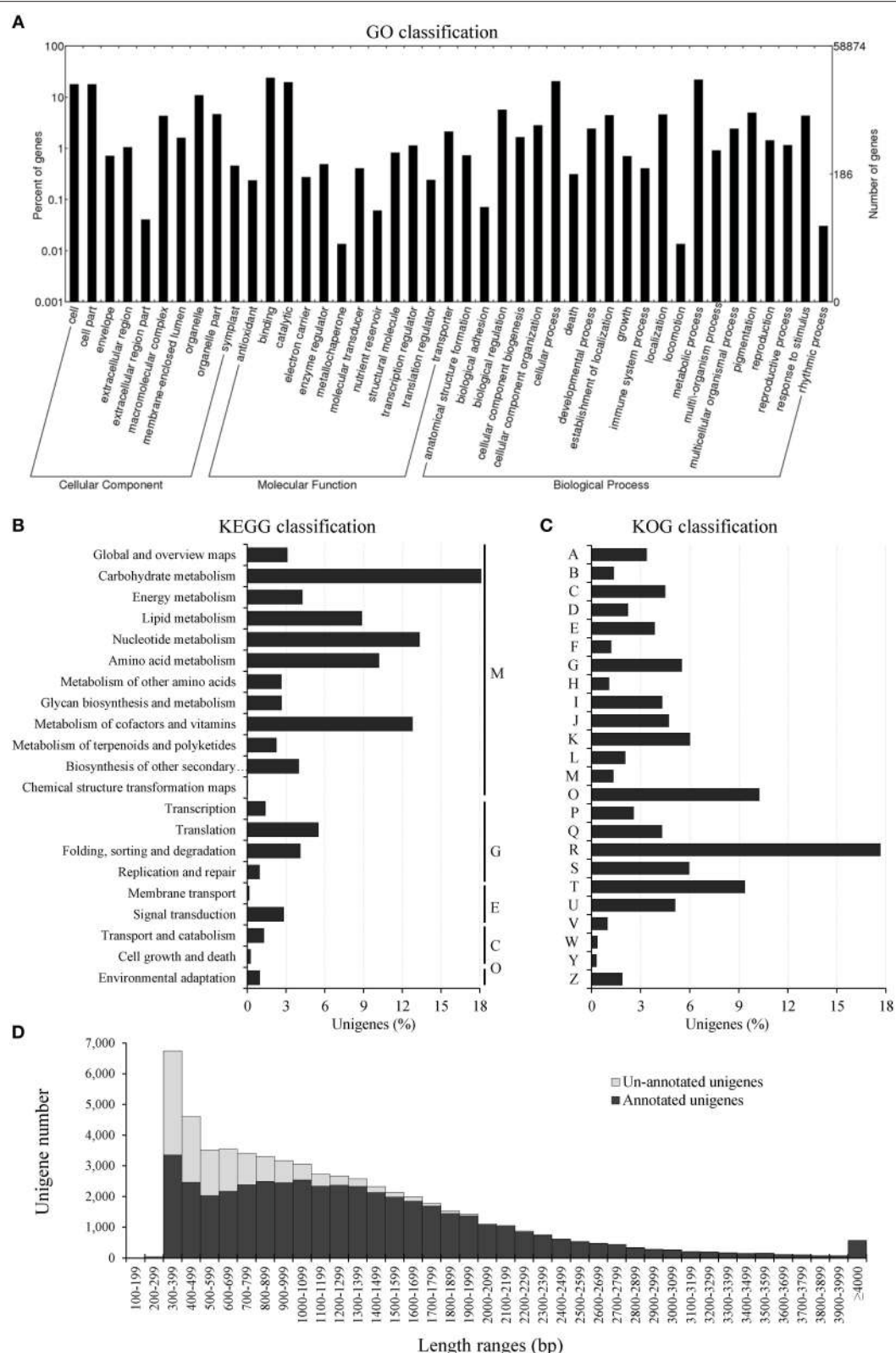


FIGURE 2 | Annotation of *Chichorium intybus* unigenes. (A) GO classification. The GO terms were classified into three ontologies: biological process, cellular component, and molecular function. **(B)** KEGG classification. The histogram represents the unigene distribution into five major KEGG metabolic categories. M, metabolism; G, genetic information processing; E, environmental information processing; C, cellular processes; O, organismal systems. **(C)** Unigene functional (Continued)

FIGURE 2 | Continued

classification into EuKaryotic Orthologous Groups (KOG). A, RNA processing and modification; B, Chromatin structure and dynamics; C, Energy production and conversion; D, Cell cycle control, cell division, chromosome partitioning; E, Amino acid transport and metabolism; F, Nucleotide transport and metabolism; G, Carbohydrate transport and metabolism; H, Coenzyme transport and metabolism; I, Lipid transport and metabolism; J, Translation, ribosomal structure and biogenesis; K, Transcription; L, Replication, recombination and repair; M, Cell wall/membrane/envelope biogenesis; N, Cell motility; O, Post-translational modification, protein turnover, chaperones; P, Inorganic ion transport and metabolism; Q, Secondary metabolites biosynthesis, transport and catabolism; R, General function prediction only; S, Function unknown; T, Signal transduction mechanisms; U, Intracellular trafficking, secretion, and vesicular transport; V, Defense mechanisms; Y, Nuclear structure; Z, Cytoskeleton. (D) Comparison of unigene length between annotated and non-annotated unigenes. The percentage of non-annotated transcripts (light gray bars) was high in the small-sized unigene category and progressively dropped along with the transcript length increase.

TABLE 4 | Number and percentage of annotated unigenes against public databases.

Database ^a	Unigenes n.	Unigenes %
Nr	38,931	66.1
TrEMBL	38,978	66.2
Tair	36,281	61.6
InterPro	31,514	53.5
SwissProt	26,233	44.6
GO	23,501	39.9
KEGG	7393	12.6
KOG	11,650	19.8
Total	45,570	77.4

^aNr, NCBI non-redundant database; TAIR, The Arabidopsis Information Resource; SwissProt is the manually annotated and reviewed section of the UniProt Knowledgebase (UniProtKB); TrEMBL, databases of UniProtKB automatically annotated and not reviewed; KOG, euKaryotic Ortholog Groups; InterPro, protein families database; GO, Gene Ontology; KEGG, Kyoto Encyclopedia of Genes and Genomes; Total, unigenes annotated in at least one database.

analysis used 15 databases and assigned 237,796 annotations to 31,516 unigenes (53.5%, in **Table 4**). The Interpro accessions (IPR, Table S4) were 20,642; 8935 putative proteins could be grouped into 2596 families, while 16,354 showed known domains, 1850 harbored repeats and 3308 hosted functional sites. Finally, the total unigenes of the *C. intybus* Gal transcriptome with at least one annotation signature were 45,572 (77.4%, in **Table 4**) and showed average length of 1372 bp; non-annotated unigenes were 13,302 (22.6%) and mostly of short size (ca. 700 bp; **Figure 2D**).

Digital Gene Expression and Functional Classification of Differentially Expressed Genes

Taken that Mol contained more STL than Gal, we first performed DGE profiling on the two genotypes within the same environment (inter-landrace comparison); subsequently, we selected the genes that maintained the relative expression pattern (independently of the area) for further characterization. 12,274 DEGs were identified (sum of up- and down- regulated unigenes bracketed in **Figure 3**); 6346 and 2294 DEGs were specific for Apulia and Lazio shires, respectively. Moreover, 1640 DEGs (961 down- plus 679 up-regulated unigenes, bolded in **Figure 3**) maintained the relative expression pattern independently from the cultivation zone, while 177 unigenes showed opposite

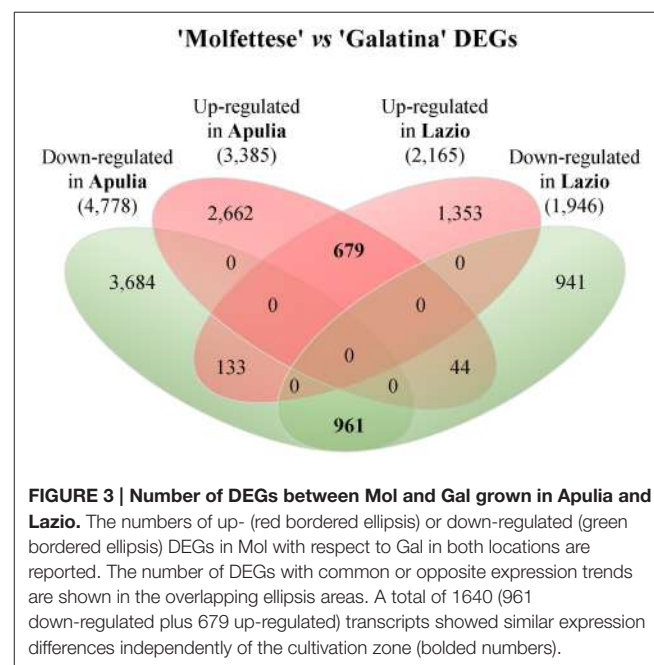


FIGURE 3 | Number of DEGs between Mol and Gal grown in Apulia and Lazio. The numbers of up- (red bordered ellipsis) or down-regulated (green bordered ellipsis) DEGs in Mol with respect to Gal in both locations are reported. The number of DEGs with common or opposite expression trends are shown in the overlapping ellipsis areas. A total of 1640 (961 down-regulated plus 679 up-regulated) transcripts showed similar expression differences independently of the cultivation zone (bolded numbers).

trends from one site to the other. The transcriptome variation within a given genotype following cultivation site change is reported in Figure S3. KEGG (**Table 5**) and GO (Tables S5, S6) enrichment analyses were performed to functionally classify the 1640 DEGs. The former revealed that Mol up- and down-regulated genes were significantly over-represented in 9 and 4 pathways, respectively. Four up-regulated DEGs fell in the sesquiterpenoid and triterpenoid biosynthesis (**Table 6**).

Dissections of Putative Genes Related to Sesquiterpenoid and Triterpenoid Pathway

Sesquiterpene lactones (STL) precursors belong to the sesquiterpenoid and triterpenoid pathway (STP); therefore, the latter was further characterized by identifying 29 unigenes putatively encoding 16 distinct enzymes (**Table 6** and Figure S4). Four unigenes were below the transcription threshold (RPKM 0–0.1), 13 showed a low expression (RPKM 0.1–3), 1 was moderately (RPKM 3–8) and 11 were highly (RPKM >8) expressed in the stems of both landraces (**Table 6**). DGE patterns were checked by qPCR assays (Figure S5) performed on 15 unigenes of the STP, and a significant positive correlation was found (**Figure 4**). Consequently, the DEG analysis (Table S7)

TABLE 5 | KEGG pathway enrichment of differentially expressed genes in Mol vs. Gal.

Map	Description	Count ^a	Size ^b	FDR ^c	Rich factor ^d
UP-REGULATED					
map00945	Stilbenoid, diarylheptanoid, and gingerol biosynthesis	4	18	6.83E-04	0.22
map01220	Degradation of aromatic compounds	1	6	2.40E-01	0.17
map00909	Sesquiterpenoid and triterpenoid biosynthesis	4	29	2.66E-03	0.14
map00941	Flavonoid biosynthesis	4	36	5.27E-03	0.11
map00940	Phenylpropanoid biosynthesis	19	258	2.01E-08	0.07
map00520	Amino sugar and nucleotide sugar metabolism	11	225	1.00E-03	0.05
map00360	Phenylalanine metabolism	12	248	6.83E-04	0.05
map00270	Cysteine and methionine metabolism	6	144	4.42E-02	0.04
map00500	Starch and sucrose metabolism	24	618	1.35E-05	0.04
DOWN-REGULATED					
map03440	Homologous recombination	3	28	2.88E-02	0.11
map00061	Fatty acid biosynthesis	5	68	1.77E-02	0.07
map03022	Basal transcription factors	4	58	2.88E-02	0.07
map00640	Propanoate metabolism	4	63	2.88E-02	0.06

^aDEGs number in the pathway; total up- and down-regulated genes were 97 and 72, respectively.

^bTotal number of genes referring to the specific pathway; the total gene number with KEGG annotation was 7393.

^cFalse discovery rate, the table includes pathways with values ≤ 0.05 .

^dRatio between the number of DEGs and genes annotated in a given pathway; higher rich factor values mean higher enrichment degree.

identified 4 unigenes (gray-shaded in **Table 6**) which maintained a significantly higher expression in Mol than Gal regardless of growth sites. These genes were the *germacrene A synthase* (GAS; Ci_contig62597 and Ci_contig62598), *germacrene A oxidase* (GAO; Ci_contig7113) and β -*amyrin synthase* (LUP4; Ci_contig3360). GAS and GAO are two key enzymes in the synthesis of germacrene-type STLs and act consecutively in the upstream steps that generate the costunolide (**Figure 5**). Within the STL branch, 8 sequences were found in the Gal transcriptome, consisting of 6 GAS transcripts (Table S7), 1 GAO and 1 *costunolide synthase* (COS) mRNAs. The GAS, GAO, and COS proteins shared significant identities with several Asteraceae orthologues (Table S7); the sequence variability among the 6 GAS ranged from 53.1 to 88.6% (Figure S6). The Asteraceae GAS phylogenetic tree (**Figure 6A**) placed Ci_contig62598 and Ci_contig7229 products in the clades of *C. intybus* short and long variants, respectively. The Ci_contig62597 derived protein belonged to the *L. sativa* LTC2 group, while the Ci_contig29105 and Ci_contig73080 formed a clade *per se*, sharing 88.6% sequence identity (Figure S6). The Asteraceae GAO phylogenetic tree (**Figure 6B**) assigned the Ci_contig7113 product in the branch of *C. intybus* GAO with which shared 100% identity (not shown).

Correlation Analyses among GAS, GAO, Putative Transcription Factors, and STLs

We approached the search for transcription factor genes (TFs) involved in the STL pathway. Globally, 2680 gene deduced products could be ascribed to 57 TF families according to PlantTFDB rules (Jin et al., 2014) and ca. 55% belonged to bHLH (258 proteins), WRKY (188), ERF (161), C2H2 (150), NAC (150), MYB (137), MYB-related (111), C3H (117),

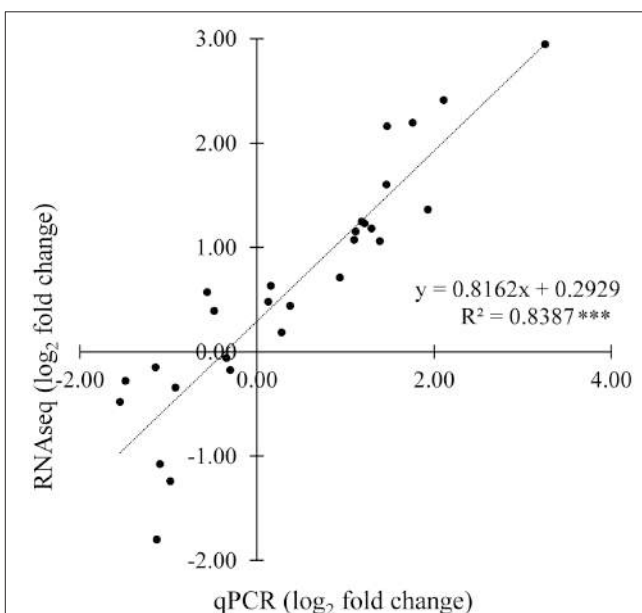
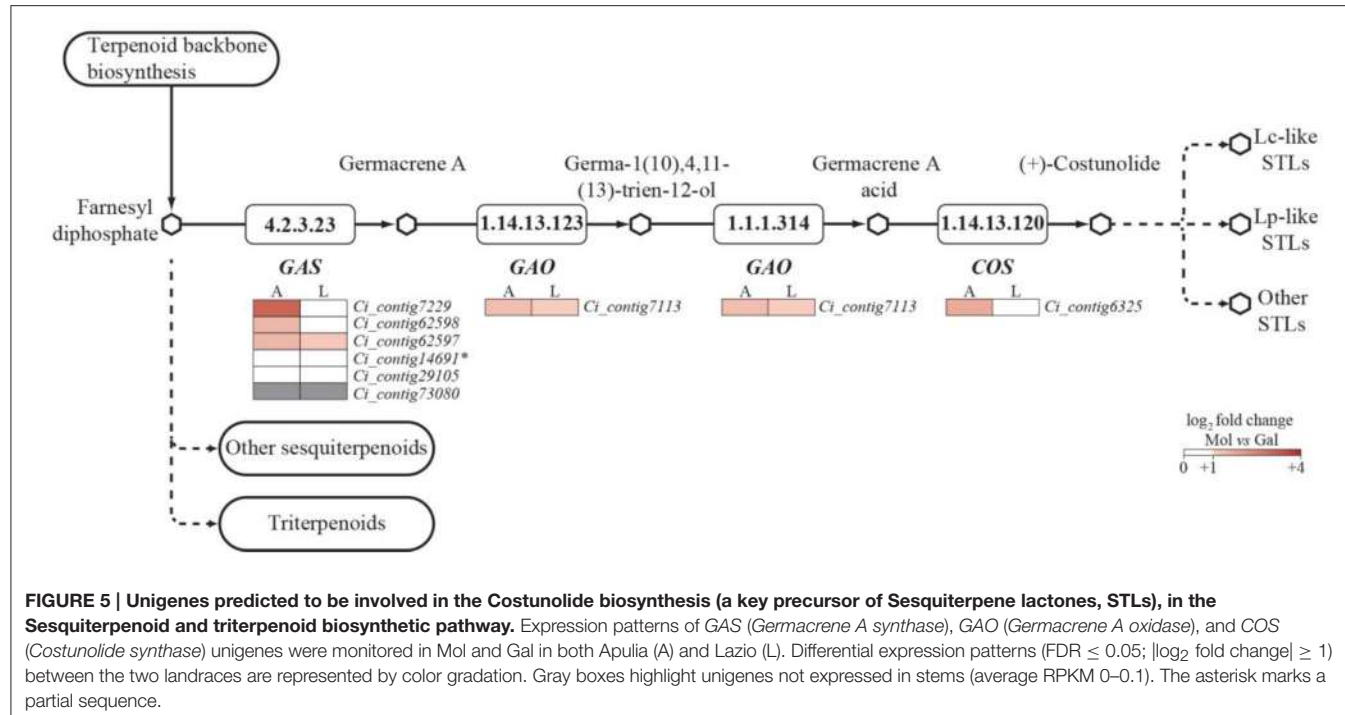


FIGURE 4 | Correlation of differential expression ratios (\log_2 fold change) obtained from RNAseq and quantitative PCR (qPCR) analyses.

Fourteen genes belonging to the sesquiterpenoid and triterpenoid pathway (Table S2) were arbitrarily chosen and their expression was monitored in Mol and Gal landraces in Apulia and Lazio areas. For a given unigene, RNAseq fold change refers to the ratios of RPKM values of Mol to Gal, whilst qPCR fold change is the relative expression of Mol normalized to those of Gal. R^2 , coefficient of determination; ***, significant correlation at $P < 0.001$.

bZIP (96) and Dof (96) families (**Figure 7A**). Moreover, 46 TF genes maintained differential expressions in Mol vs. Gal independently of growth sites; most of DEGs fell into ERF



(9), WRKY (6), C2H2 (5), FAR1 (4), NAC (4) and bHLH (4) groups (Figure 7B). Correlation analysis was carried out using the STL contents and the expression levels of GAS (Ci_contig62597, Ci_contig62598), GAO (Ci_contig7113) and the 46 TFs genes. A correlogram was built (Figure 7C) using 8 out of the 46 TF (see Table S2), which were selected by the criteria of transcript completeness and an absolute r value equal or greater than 0.75. Notably, the transcription of the biosynthesis genes GAS (Ci_contig62597, Ci_contig62598) and GAO (Ci_contig7113) showed very strong ($r > 0.8$) positive correlation between them and strong ($0.7 \leq r \leq 0.8$) correlation with total STL amounts (Figure 7C). As for TF, GAS and GAO, very strong positive correlations occurred between the expression of ERF (Ci_contig18477, Ci_contig48177) and MYB (Ci_contig49541) genes and both GAS and GAO. Conversely, strong ($-0.8 \leq r \leq -0.7$) and very strong ($r < -0.8$) negative correlations characterized the transcription of bHLH (Ci_contig48487) vs. that of GAS and GAO, while strong negative correlation of MIKC (Ci_contig17846) and ERF (Ci_contig18404) occurred just vs. GAO.

Genotype Differentiation by Gene Polymorphisms Mining

Polymorphism identification from transcriptome sequences is useful to score gene functional variations in species without a sequenced genome. Consequently, SSR and SNP were mined and a specific focus was on the STL pathway genes. Overall, 11,672 putative SSRs were found in 9826 unigenes and 1525 of them contained more than one microsatellite (Table S8). Excluded mononucleotides, the di- and tri-nucleotide repeats

were the most abundant (respectively 52.8 and 42.4% out of 6946 SSR); the AG/CT and ATC/ATG were the most frequent motifs (Table 7). The mapping of Mol reads vs. the Gal reference transcriptome scored 67,265 SNPs in 15,248 unigenes and ca. 68% were heterozygous (Table S9); the nucleotide substitutions (Figure S7) included 61.8% transition (C/T vs. A/G, 32.8 vs. 29%) and 38.2% transversion events (A/T was the most frequent). The average SNP frequency occurred at 1/1068 bp, with a mean of 4.4 per unigene. Eleven out of the 29 unigenes of the sesquiterpenoid pathway (Table S9) bore SNPs between Gal and Mol landraces and 5 genes included homozygous SNPs. Referring to DEGs, β -amyrin synthase (LUP4; Ci_contig3360) showed 7 SNPs, while GAS (Ci_contig62598) contained one heterozygous SNP, which produced a synonym substitution (Tyrosin).

DISCUSSION

In this work, the combination of a *de novo* transcriptome assembly, transcript and metabolite profiling was used to achieve insights in the genetic pathway of sesquiterpenes and, more generally, valuable genetic tools using two stem-chicory “Catalogna” landraces.

As for total STL extraction procedure, cellulase treatment, and ultrasound assisted extraction were compared. Sonication can disrupt cell walls causing the release of cell contents (Toma et al., 2001) and it was effective as much as cellulose hydrolysis for yielding both free and bound fractions in chicory stems (Table S1). The metabolic characterization pointed that total STL content of stems was ca. 50-fold lower than that reported for

“Catalogna” leaves (GEVES)¹. Typically, STL have been either undetected or found in traces in stalks (Chou and Mullin, 1993; Douglas et al., 2004; Eljounaidi et al., 2015). Mol stems contained more total STL than those of Gal and differences were ascribed mostly to the genotype diversity and poorly to the environment changes; genotype-environment (GxE) interactions affected the contents of Lc, DHLc, DHdLc, and Lp variation (Table 1 and Table S1). Genotype effects were also observed in chicory forage, because cultivars with higher STL than others maintained the characteristics regardless of the growth sites (Foster et al., 2006). Chicory studies also report STL content variation with organ developmental stage, cultivation and geo-localisation that account for GxE effects (Peters et al., 1997; Foster et al., 2006; Ramirez et al., 2013; Chen et al., 2014). The higher content of DHLc, DHdLc and Lp in Mol vs. Gal may account for bitterness differences. The conversion of STL amounts into bitterness degrees (van Beek et al., 1990) indicates that Mol has higher scores than Gal (Table S10) and that the difference was mostly due to total Lc-like compounds. Simple gustative tests further assessed that Mol stems were more bitter than Gal ones ($\chi^2 = 56.89$; $p < 0.001$; Table S11). Consistently, the contents of Lc-like compounds showed positive correlation with bitterness in leaves of *C. intybus* sugarloaf, witloof and radicchio (Price et al., 1990; Peters and van Amerongen, 1998; Poli et al., 2002) and DHLc contents strongly correlated with root bitterness (Hance et al., 2007). Lp is one of the most bitter among chicory STLs (van Beek et al., 1990) and Lp-like molecules are strongly related to bitterness in other Asteraceae species, such as lettuce (*L. sativa*) and endive (*C. endive*) leaves (Seo et al., 2009; D’Antuono et al., 2016). Finally, a recent survey on endives proposes that bitterness depends on the balance between STL and phenolic contents and that the different compounds within these two categories can affect the trait both individually and in a complex manner (D’Antuono et al., 2016). Known that total phenolic contents are comparable in Gal and Mol stems (Renna et al., 2014), analytic studies are envisaged in addressing bitterness in these novel products.

Comparative analysis of Gal and Mol transcriptomes scored that ca. 2.8% unigenes (1640 out of 58,872 total unigenes) maintained differential expression pattern between the two genotypes in both Apulia and Lazio sites. This suggested that environment minimally or equally affected this gene pool, which may represent a source of transcriptional markers. Within this pool, four up-regulated DEGs (Table 5) fell in the sesquiterpenoid (2 GAS and 1 GAO) and triterpenoid (β -amyrin synthase) biosynthesis (Table S7). The diversity in the functional amino acid stretches among the 6 GAS deduced proteins (Figure S6) suggests that they may have diversified catalytic functions with substrate specificity. The two GAS enzymes encoded by the up-regulated DEGs are similar but not identical, and ascribed to the *C. intybus* short form (Figure 6 and Figure

¹GEVES Groupe d’Etudes et de Contrôle des Variétés et des Semences. The International Chicory Database, [Online]. European Cooperative Programme for Plant Genetic Resources. Available online at: <http://ecpgr.cgn.wur.nl/LVintro/chicory/download.htm> [Accessed 2010].

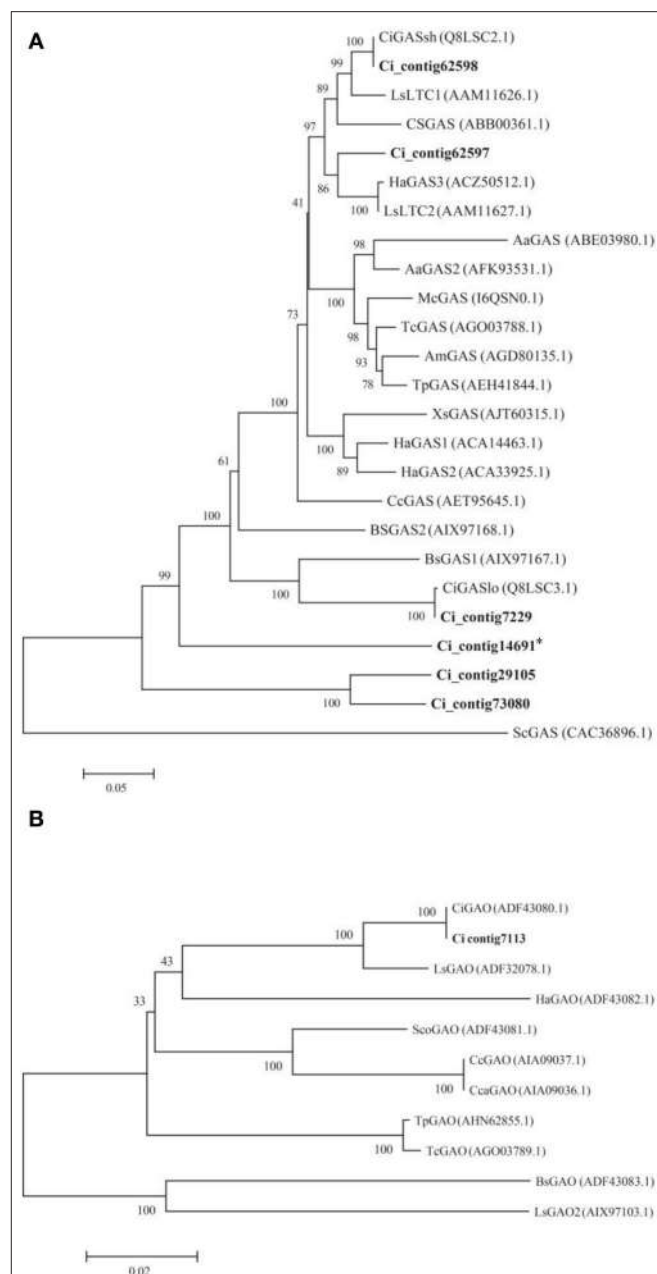


FIGURE 6 | Phylogenetic analysis of *C. intybus* GAS and GAO deduced proteins. The trees were inferred with the neighbor-joining method. Bootstrap values (at the branching points) are given for major nodes and are based on 1000 replicates. The length of the lines indicates the relative distances between nodes. Putative proteins identified from *C. intybus* assembled transcriptome are in bold. GenBank accession numbers are shown in parentheses. **(A)** Phylogenetic tree of GAS proteins from Asteraceae species. Asterisk indicate a partial deduced product. **(B)** Phylogenetic tree of GAO proteins from Asteraceae species. Aa, *Artemisia annua*; Am, *Achillea millefolium*; Bs, *Barnadesia spinosa*; Cc, *Cynara cardunculus* var. *scolymus*; Cca, *Cynara cardunculus* var. *altilis*; Ci, *Cichorium intybus*; Cs, *Crepidiastrum sonchifolium*; Ha, *Helianthus annuus*; Ls, *Lactuca sativa*; Mc, *Matricaria chamomilla* var. *recutita*; Sc, *Solidago canadensis*; Sco, *Saussurea costus*; Tc, *Tanacetum cinerariifolium*; Tp, *Tanacetum parthenium*; Xs, *Xanthium strumarium*.

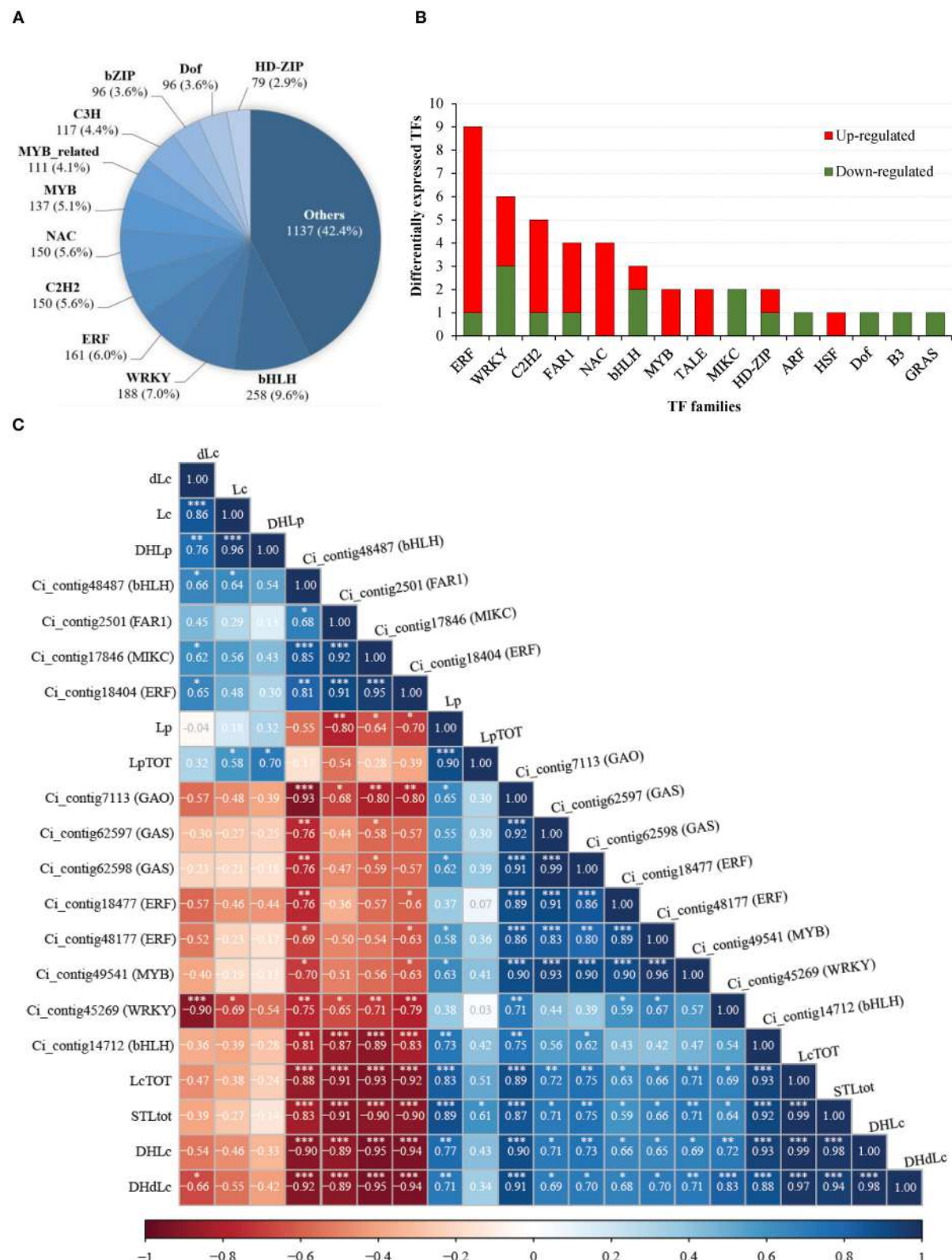


FIGURE 7 | Analysis of transcription factors (TFs) in *C. intybus* 'Catalogna' landraces. (A) Categorization of predicted TFs into families. The numbers below each TF family (bold) indicate the number of unigenes within the group. Family relative abundance (percentage) with respect to the total predicted TFs is in parenthesis. **(B)** Analysis of differentially expressed (FDR ≤ 0.05; |log2FC| ≥ 1) TFs in Mol vs. Gal independently by the cultivation area. Red and green bars refer to (Continued)

FIGURE 7 | Continued

up- and down-regulated TFs in Mol, respectively. **(C)** Correlogram representing Pearson's correlation coefficient (r) between content of STLs and gene expression abundances of both biosynthesis genes and putative TFs. Heat map is used to indicate the strength of correlation between the variables with ordering determined by hierarchical clustering. Red and blue indicate negative and positive correlations, respectively. Pearson's correlation coefficient values were reported into the colored squares. *; **; *** = significant at $P \leq 0.05$, 0.01, and 0.001, respectively. Lc, lactucin; DHLC, 11(S), 13-dihydro-lactucin; dLc, 8-deoxylactucin; DHdLc, 11(S), 13-dihydro-8-deoxylactucin; Lp, lactucopicrin; DHLp, 11(s), 13-dihydro-lactucopicrin; STLtot, total STL content; LcTOT, total lactucin-like STL; LpTOT, total lactucopicrin-like STLs.

TABLE 6 | Unigenes annotated in the sesquiterpenoid and triterpenoid pathway and DGE analysis.

EC number	Enzyme name	Unigenes	Size (bp)	DGE (RPKM) ^a				ER ^b
				Gal/A	Mol/A	Gal/L	Mol/L	
1.14.13.120	Costunolide synthase	Ci_contig6325	2002	25.2 ± 2.8	81.6 ± 2.3	13.5 ± 2.0	18.9 ± 2.7	H
1.1.1.216	Farnesol dehydrogenase	Ci_contig486	4166	15.4 ± 7.1	4.3 ± 4.1	23.0 ± 3.5	25.7 ± 5.3	H
		Ci_contig52488	1358	15.5 ± 1.7	7.4 ± 1.1	10.4 ± 0.7	9.4 ± 1.8	H
1.1.1.314; 1.14.13.123	Germacrene A oxidase	Ci_contig7113	2486	10.0 ± 0.3	23.8 ± 0.8	7.1 ± 0.6	15.0 ± 1.0	H
1.14.13.121	Premnaspriodene oxygenase	Ci_contig66434	1768	9.5 ± 7.5	7.0 ± 0.3	5.1 ± 0.6	4.9 ± 0.7	M
1.14.13.132	Squalene monooxygenase	Ci_contig52838	1825	46.9 ± 15.6	36.7 ± 3.1	48.3 ± 1.3	44.1 ± 6.7	H
		Ci_contig5712	2100	1.4 ± 0.3	1.6 ± 0.3	1.9 ± 0.0	1.5 ± 0.2	L
		Ci_contig34699	1322	34.3 ± 11.1	26.1 ± 2.4	44.7 ± 0.5	37.4 ± 5.9	H
2.5.1.21	Farnesyl-diphosphate farnesyltransferase	Ci_contig7389	1867	67.3 ± 5.8	82.1 ± 3.4	59 ± 3.3	59.4 ± 5.2	H
4.2.3.104; 4.2.3.57	α-humulene/β-caryophyllene synthase	Ci_contig56955	1382	0.1 ± 0.0	0.1 ± 0.1	0.1 ± 0.1	0.1 ± 0.1	L
4.2.3.23	Germacrene-A synthase	Ci_contig7229	3523	6.1 ± 1.3	46.7 ± 5.4	5.4 ± 0.3	8.4 ± 1.0	H
		Ci_contig14691	1850	0.1 ± 0.1	0.2 ± 0.1	0.1 ± 0.1	0.2 ± 0.1	L
		Ci_contig29105	1817	0.2 ± 0.1	0.1 ± 0.1	0.2 ± 0.1	0.0 ± 0.0	L
		Ci_contig62598	1827	28.8 ± 1.5	75.0 ± 14.0	12.2 ± 2.4	27.0 ± 2.1	H
		Ci_contig62597	1926	9.7 ± 1.3	22.6 ± 2.7	3.7 ± 0.7	8.4 ± 0.2	H
		Ci_contig73080	1937	0.0 ± 0.0	0.1 ± 0.0	0.2 ± 0.2	0.0 ± 0.1	N
4.2.3.39	Epi-cedrol synthase	Ci_contig41698	614	0.3 ± 0.1	0.1 ± 0.0	0.1 ± 0.0	0.1 ± 0.0	L
4.2.3.46	α-farnesene synthase	Ci_contig7791	1820	0.2 ± 0.1	0.0 ± 0.0	0.0 ± 0.0	0.1 ± 0.1	N
4.2.3.47	β-farnesene synthase	Ci_contig23130	677	0.1 ± 0.1	0.0 ± 0.0	0.1 ± 0.1	0.2 ± 0.1	N
		Ci_contig65366	1038	0.9 ± 0.0	0.8 ± 0.3	1.0 ± 0.1	1.4 ± 0.4	L
		Ci_contig65368	1550	0.5 ± 0.2	0.2 ± 0.1	0.6 ± 0.1	0.3 ± 0.1	L
		Ci_contig46748	321	0.2 ± 0.2	0.1 ± 0.1	0.0 ± 0.1	0.2 ± 0.2	L
4.2.3.48	(3S, 6E)-nerolidol synthase	Ci_contig10001	1595	0.8 ± 0.4	3.6 ± 2.4	0.4 ± 0.1	0.3 ± 0.1	L
4.2.3.57	β-caryophyllene synthase	Ci_contig10438	1552	0.5 ± 0.1	1.9 ± 0.7	0.5 ± 0.2	0.7 ± 0.2	L
4.2.3.75	(-)germacrene D synthase	Ci_contig41699	366	0.2 ± 0.2	0.0 ± 0.0	0.0 ± 0.1	0.0 ± 0.0	N
5.4.99.38	Camelliol C synthase	Ci_contig77181	3492	1.2 ± 0.1	1.6 ± 0.3	1.6 ± 0.1	2.1 ± 0.3	L
5.4.99.39	β-amyrin synthase	Ci_contig3360	2648	4.0 ± 0.3	23.1 ± 6.1	7.9 ± 1.9	16.2 ± 3.3	H
		Ci_contig34609	1169	1.0 ± 0.4	1.3 ± 1.0	1.5 ± 0.3	1.6 ± 0.3	L
		Ci_contig70336	2468	0.5 ± 0.2	0.6 ± 0.3	1.1 ± 0.3	4.2 ± 1.2	L

^aDGE, digital gene expression; mean ± standard deviation was based on 3 replicates per growing site, per genotype; bolded values indicate significant differences ($FDR \leq 0.05$; $|log_2 fold change| \geq 1$), gray shaded contigs indicate those genes with differential expression maintained in both planting sites.

^bER, expression range. H, high (RPKM > 8); M, moderate (RPKM 1–8); L, low (RPKM 0.1–1) expression. N, below the expression threshold (RPKM 0–0.1).

S6). Both GAS genes (Ci_contig62597 and Ci_contig62598) are 2-fold more expressed in Mol than Gal. Similarly, the GAO gene transcription is twice higher in Mol than Gal and the deduced protein corresponds to that of *C. intybus* available in public databases. Significant positive correlation occurred between GAS and GAO transcriptions and the contents of Lc-like (DHLC, DHdLc). These results corroborate the finding that

terpene accumulation goes in parallel with the expressions of respective synthase genes (Nagegowda, 2010) and are consistent with the correlation of artichoke GAS and GAO transcription levels with the cyanopicrin-STL abundance (Eljounaidi et al., 2015). Regarding the COS gene (costunolide is a down-stream precursor of STL), it is worth noting that the expression was more abundant in Mol than Gal in Apulia; the trend was

TABLE 7 | Summary of putative SSR identified in the 'Galatina' unigenes: sizes, frequencies and major types.

Unit repeat type	Number of repetitions							Total	Major type (%)
	5	6	7	8	9	10	>10		
Di-nucleotide	0	1090	681	477	422	384	614	3668	AG/CT (62.9%)
Tri-nucleotide	1681	803	382	108	40	37	33	3084	ATC/ATG (24.3%)
Tetra-nucleotide	81	15	0	0	0	0	1	97	AAAT/ATTT (24.7%)
Penta-nucleotide	11	1	0	1	1	0	0	14	ACATG/ATGTC (21.4%)
Hexa-nucleotide	48	16	6	1	2	2	8	83	AAAAAG/CTTTT (6.0%)

maintained in Lazio, but not at significant level (Table 6 and Figure S5).

The STL genetic pathway *per se* needs investigation in plants, namely, the biosynthesis genes downstream the COS (leading to Lc- and Lp-like compounds) have been unknown as well as the routes of catabolism and transport. Moreover, the knowledge on the TFs involved in sesqui- and triterpenoids biosynthesis is still fragmentary (Yamada and Sato, 2013). In this work, 46 TF genes conserved the differential expression between the two genotypes. Among these, some showed strong positive (*MYB*, *Ci_contig49541*) and negative (*bHLH*, *Ci_contig48487*) correlations with both the biosynthesis genes (GAS and GAO) and total STLs (three-way relationship). Given that MYB factors and bHLH members control sesquiterpenes synthesis in plants acting on terpene synthase genes (Hong et al., 2012; Reeves et al., 2012; Lu et al., 2013), it is proposed that the above-mentioned genes may represent TF that regulate the stem-chicory STL pathway. However, some TF showed significant strong correlations in two-way relationships. For instance, the *Ci_contig18404* (ERF) showed a very strong negative correlation ($r < -0.8$) with GAO and total STLs, but not with GAS. Similarly, the *Ci_contig45269* (WRKY) had a strong positive correlation with GAO but not with GAS or total STL. Consequently, these TFs might take part in STL metabolism of *C. intybus* through specific routes or indirectly, consistently with their role in regulating STL biosynthesis in other species (Yamada and Sato, 2013). Moreover, the future availability of GAS and GAO genomic sequences will allow prediction of motifs targeted by these candidate genes and pave the way for functional study experiments.

Cichorium intybus genome is esteemed ca. 1400 MB (De Simone et al., 1997), hence transcriptome sequencing was convenient to widen resources aimed to gene discovery, expression profiling, and diversity analysis and to marker production for breeding. There have been two Illumina-based transcriptomes of *C. intybus*, which derived from seedlings (Hodgins et al., 2014). The 'Galatina' reference transcriptome enriches the number of those within the leafy group—"Catalogna," Witloof (Hodgins et al., 2014) and Radicchio—and widens the investigation spectrum because it is based on several mature and young vegetative tissues. In the absence of a genome sequence, it is recommended that the transcriptome construction of non-model species is achieved through the joining of reference-guided and *de novo* transcriptome assemblies (Ockendon et al., 2016) and/or the

combinatorial use of different assemblers (Nakasugi et al., 2014). The assembly used in this work employed the one- and two-step strategies (Figure S1), which produced ca. 58,000 unigenes comparably to other *C. intybus* transcriptomes (Hodgins et al., 2014) but with nearly doubled length (1230 vs. 635–684 bp). Moreover, the Gal transcriptome contained 77.4% of annotated unigenes of average length of 1372 bp, consistently with features of other *Asteraceae* transcriptomes (Wang et al., 2013; Jung et al., 2014; Peng et al., 2014). The Gal transcriptome provided over 11,000 putative SSR markers; more than 15,000 unigenes differed between Gal and Mol for over 20,000 homozygous SNPs. The SSR and SNP validation by wide screening on different populations was beyond the scope of this work. However, the filtering criteria for polymorphism mining (Kumar et al., 2012) provide info to create SNP or SSR markers targeting alleles with variants in coding sequences. These marker types are useful to detect a causative mutation (Field and Wills, 1996) and are highly transferable across species (Varshney et al., 2005). The SNP frequency was 1/1068 bp suggesting that the two landraces are related. The polymorphisms events are expected to increase by screening a higher number of "Catalogna" landraces. As for SNPs in the STL pathway genes and the respective putative biological function, only a synonymous substitution was found in the *Ci_contig62598* (GAS) differentiating Gal and Mol unigenes. This implies that no protein mutation occurs that might explain the STL content differences. These latter are more likely due to a diversified gene expression regulation (e.g., residing in gene promoter regions). Nonetheless, the heterozygous SNP provides a tool for genetic mapping of this key gene in the stem-chicory populations.

Finally, the landrace comparative approach and data mining of transcriptome and metabolic variations were efficient to discover genes involved in STL pathway as a precious source to comprehend regulation of bitter taste in this vegetables and support plant breeding for product quality.

AUTHOR CONTRIBUTIONS

DG was responsible for research costs and guided the work design and manuscript writing. GT carried out transcriptome assembly, differential gene expression analysis, polymorphism mining, qPCR validation, statistics and writing. GM contributed to transcriptome assembly and software usage. MG and MR

performed statistical analysis on sesquiterpenes contents and gustative test. MG, GA and AS produced plant materials. GCT carried out the sesquiterpenes quantification. CN, GF, ED, MI performed sampling, phenotyping and nucleic acid extractions. All the authors reviewed, edited and approved the manuscript.

FUNDING

This work was supported by a dedicated grant from the Italian Ministry of Economy and Finance to the National Research Council for the project “Innovazione e Sviluppo del Mezzogiorno-Conoscenze Integrate per Sostenibilità ed Innovazione del Made in Italy Agroalimentare” Law 191/2009 (www.mezzogiorno.cnr.it). CNR solutions n. 73

REFERENCES

- Bai, C., Alverson, W., Follansbee, A., and Waller, D. (2012). New reports of nuclear DNA content for 407 vascular plant taxa from the United States. *Ann. Bot.* 110, 1623–1629. doi: 10.1093/aob/mcs222
- Berardes, E., Benko-Iseppon, A., Vasconcelos, S., Carvalho, R., and Brasileiro-Vidal, A. (2013). Intra- and interspecific chromosome polymorphisms in cultivated *Cichorium* L. species (Asteraceae). *Genet Mol. Biol.* 36, 357–363. doi: 10.1590/S1415-47572013005000025
- Bolger, A. M., Lohse, M., and Usadel, B. (2014). Trimmomatic: a flexible trimmer for Illumina sequence data. *Bioinformatics* 30, 2114–2120. doi: 10.1093/bioinformatics/btu170
- Cadalen, T., Morchen, M., Blassiau, C., Clabaut, A., Scheer, I., Hilbert, J. L., et al. (2010). Development of SSR markers and construction of a consensus genetic map for chicory (*Cichorium intybus* L.). *Mol. Breed.* 25, 699–722. doi: 10.1007/s11032-009-9369-5
- Cankar, K., van Houwelingen, A., Bosch, D., Sonke, T., Bouwmeester, H., and Beekwilder, J. (2011). A chicory cytochrome P450 mono-oxygenase CYP71AV8 for the oxidation of (+)-valencene. *FEBS Lett.* 585, 178–182. doi: 10.1016/j.febslet.2010.11.040
- Chadwick, M., Trewhin, H., Gawthrop, F., and Wagstaff, C. (2013). Sesquiterpenoids lactones: benefits to plants and people. *Int. J. Mol. Sci.* 14, 12780–12805. doi: 10.3390/ijms140612780
- Chen, Y., Wu, Y. G., Xu, Y., Zhang, J. F., Song, X. Q., Zhu, G. P., et al. (2014). Dynamic accumulation of sesquiterpenes in essential oil of *Pogostemon cablin*. *Rev. Bras. Farmacogn.* 24, 626–634. doi: 10.1016/j.bjph.2014.11.001
- Chou, J.-C., and Mullin, C. (1993). Phenologic and tissue distribution of sesquiterpene lactones in cultivated sunflower (*Helianthus annuus* L.). *J. Plant Physiol.* 142, 657–663. doi: 10.1016/S0176-1617(11)80898-9
- Conesa, A., Gotz, S., García-Gómez, J. M., Terol, J., Talon, M., and Robles, M. (2005). Blast2GO: a universal tool for annotation, visualization and analysis in functional genomics research. *Bioinformatics* 21, 3674–3676. doi: 10.1093/bioinformatics/bti610
- Cordell, G. A. (1976). Biosynthesis of sesquiterpenes. *Chem. Rev.* 76, 425–460. doi: 10.1021/cr60302a002
- D’Acunzo, F., Giannino, D., Longo, V., Ciardi, M., Testone, G., Mele, G., et al. (2016). Influence of cultivation sites on sterol, nitrate, total phenolic contents and antioxidant activity in endive and stem chicory edible products. *Int. J. Food Sci. Nutr.* doi: 10.1080/09637486.2016.1221386. [Epub ahead of print].
- D’Antuono, L. F., Ferioli, F., and Manco, M. A. (2016). The impact of sesquiterpene lactones and phenolics on sensory attributes: an investigation of a curly endive and escarole germplasm collection. *Food Chem.* 199, 238–245. doi: 10.1016/j.foodchem.2015.12.002
- Dauchot, N., Mingeot, D., Purnelle, B., Muys, C., Watillon, B., Boutry, M., et al. (2009). Construction of 12 EST libraries and characterization of a 12,226 EST dataset for chicory (*Cichorium intybus*) root, leaves and nodules in the context of carbohydrate metabolism investigation. *BMC Plant Biol.* 9:14. doi: 10.1186/1471-2229-9-14
- de Kraker, J. W., Franssen, M. C., Joerink, M., de Groot, A., and Bouwmeester, H. J. (2002). Biosynthesis of costunolide, dihydrocostunolide, and leucodin. Demonstration of cytochrome p450-catalyzed formation of the lactone ring present in sesquiterpene lactones of chicory. *Plant Physiol.* 129, 257–268. doi: 10.1104/pp.010957
- De Simone, M., Morgante, M., Lucchin, M., Parrini, P., and Marocco, A. (1997). A first linkage map of *Cichorium intybus* L. using a one-way pseudo-testcross and PCR-derived markers. *Mol. Breed.* 3, 415–425. doi: 10.1023/A:1009616801404
- Douglas, J. A., Smallfield, B. M., Burgess, E. J., Perry, N. B., Anderson, R. E., Douglas, M. H., et al. (2004). Sesquiterpene lactones in *Artemisia montana*: a rapid analytical method and the effects of flower maturity and simulated mechanical harvesting on quality and yield. *Planta Med.* 70, 166–170. doi: 10.1055/s-2004-815495
- Drewnowski, A., and Gomez-Carneros, C. (2000). Bitter taste, phytonutrients, and the consumer: a review. *Am. J. Clin. Nutr.* 72, 1424–1435.
- Eenink, A. (1981). Compatibility and incompatibility in witloof-chicory (*Cichorium intybus* L.). 2. The incompatibility system. *Euphytica* 30, 77–85. doi: 10.1007/BF00033662
- Eenink, A. (1982). Compatibility and incompatibility in witloof-chicory (*Cichorium intybus* L.). 3. Gametic competition after mixed pollinations and double pollinations. *Euphytica* 31, 773–786. doi: 10.1007/BF00039217
- Eljounaidi, K., Cankar, K., Comino, C., Moglia, A., Hehn, A., Bourgaud, F., et al. (2014). Cytochrome P450s from *Cynara cardunculus* L. CYP71AV9 and CYP71BL5, catalyze distinct hydroxylations in the sesquiterpene lactone biosynthetic pathway. *Plant Sci.* 223, 59–68. doi: 10.1016/j.plantsci.2014.03.007
- Eljounaidi, K., Comino, C., Moglia, A., Cankar, K., Genre, A., Hehn, A., et al. (2015). Accumulation of cynaropicrin in globe artichoke and localization of enzymes involved in its biosynthesis. *Plant Sci.* 239, 128–136. doi: 10.1016/j.plantsci.2015.07.020
- Falara, V., Akhtar, T. A., Nguyen, T. T., Spyropoulou, E. A., Bleeker, P. M., Schauvinhold, I., et al. (2011). The tomato terpene synthase gene family. *Plant Physiol.* 157, 770–789. doi: 10.1104/pp.111.179648
- Ferioli, F., Manco, M. A., and D’Antuono, F. (2015). Variation of sesquiterpene lactones and phenolics in chicory and endive germplasm. *J. Food Compos. Anal.* 39, 77–86. doi: 10.1016/j.jfca.2014.11.014
- Field, D., and Wills, C. (1996). Long, polymorphic microsatellites in simple organisms. *Proc. Biol. Sci.* 263, 209–215. doi: 10.1098/rspb.1996.0033
- Foster, J. G., Clapham, W. M., Belesky, D. P., Labreveux, M., Hall, M. H., and Sanderson, M. A. (2006). Influence of cultivation site on sesquiterpene lactone composition of forage chicory (*Cichorium intybus* L.). *J. Agric. Food Chem.* 54, 1772–1778. doi: 10.1021/jf052546g
- Gonthier, L., Bellec, A., Blassiau, C., Prat, E., Helmstetter, N., Rambaud, C., et al. (2010). Construction and characterization of two BAC libraries representing a deep-coverage of the genome of chicory (*Cichorium intybus* L., Asteraceae). *BMC Res. Notes* 3:225. doi: 10.1186/1756-0500-3-225

and n.74 of 29/3/2011 and pp. 1–26 of the annexed executive project.

ACKNOWLEDGMENTS

We thank R. Bollini (IBBA-CNR) for critical reading and suggestions, T. Biancari (ENZA ZADEN ITALIA) for agronomical support and the native English speaker Carla Ticconi for language editing.

SUPPLEMENTARY MATERIAL

The Supplementary Material for this article can be found online at: <http://journal.frontiersin.org/article/10.3389/fpls.2016.01676/full#supplementary-material>

- Grabherr, M. G., Haas, B. J., Yassour, M., Levin, J. Z., Thompson, D. A., Amit, I., et al. (2011). Full-length transcriptome assembly from RNA-Seq data without a reference genome. *Nat. Biotechnol.* 29, 644–652. doi: 10.1038/nbt.1883
- Graziani, G., Ferracane, R., Sambo, P., Santagata, S., Nicoletto, C., and Fogliano, V. (2015). Profiling chicory sesquiterpene lactones by high resolution mass spectrometry. *Food Res. Int.* 67, 193–198. doi: 10.1016/j.foodres.2014.11.021
- Hance, P., Martin, Y., Vasseur, J., Hilbert, J. L., and Tronin, F. (2007). Quantification of chicory root bitterness by an ELISA for 11b, 13-dihydrodactacin. *Food Chem.* 105, 742–748. doi: 10.1016/j.foodchem.2007.01.029
- Harrell, F. E. J. (2016). *Hmisc: Harrell Miscellaneous*. R package version 3.17-2 [Online]. Available online at: <http://CRAN.R-project.org/package=Hmisc> [Accessed].
- Hodgins, K. A., Lai, Z., Oliveira, L. O., Still, D. W., Scascitelli, M., Barker, M. S., et al. (2014). Genomics of *Compositae* crops: reference transcriptome assemblies and evidence of hybridization with wild relatives. *Mol. Ecol. Resour.* 14, 166–177. doi: 10.1111/1755-0998.12163
- Hong, G. J., Xue, X. Y., Mao, Y. B., Wang, L. J., and Chen, X. Y. (2012). Arabidopsis MYC2 interacts with DELLA proteins in regulating sesquiterpene synthase gene expression. *Plant Cell* 24, 2635–2648. doi: 10.1105/tpc.112.098749
- Ikezawa, N., Göpfert, J. C., Nguyen, D. T., Kim, S. U., O'Maille, P. E., Spring, O., et al. (2011). Lettuce costunolide synthase (CYP71BL2) and its homolog (CYP71BL1) from sunflower catalyze distinct regio- and stereoselective hydroxylations in sesquiterpene lactone metabolism. *J. Biol. Chem.* 286, 21601–21611. doi: 10.1074/jbc.M110.216804
- Jin, J., Zhang, H., Kong, L., Gao, G., and Luo, J. (2014). PlantTFDB 3.0: a portal for the functional and evolutionary study of plant transcription factors. *Nucleic Acids Res.* 42, D1182–D1187. doi: 10.1093/nar/gkt1016
- Jones, P., Binns, D., Chang, H. Y., Fraser, M., Li, W., McAnulla, C., et al. (2014). InterProScan 5: genome-scale protein function classification. *Bioinformatics* 30, 1236–1240. doi: 10.1093/bioinformatics/btu031
- Jung, W. Y., Lee, S. S., Kim, C. W., Kim, H. S., Min, S. R., Moon, J. S., et al. (2014). RNA-seq analysis and de novo transcriptome assembly of Jerusalem artichoke (*Helianthus tuberosus* Linne). *PLoS ONE* 9:e111982. doi: 10.1371/journal.pone.0111982
- Kanehisa, M., and Goto, S. (2000). KEGG: kyoto encyclopedia of genes and genomes. *Nucleic Acids Res.* 28, 27–30. doi: 10.1093/nar/28.1.27
- Kiaer, L., Felber, F., Flavell, A., Guadagnuolo, R., Guiatti, D., Hauser, T., et al. (2009). Spontaneous gene flow and population structure in wild and cultivated chicory, *Cichorium intybus* L. *Genet. Resour. Crop Evol.* 56, 405–419. doi: 10.1007/s10722-008-9375-1
- Kiers, A. M., Mes, T. H., van der Meijden, R., and Bachmann, K. (2000). A search for diagnostic AFLP markers in *Cichorium* species with emphasis on endive and chicory cultivar groups. *Genome Biol.* 43, 470–476. doi: 10.1139/g00-024
- Kisiel, W., and Zielinska, K. (2001). Guainolides from *Cichorium intybus* and structure revision of *Cichorium* sesquiterpene lactones. *Phytochemistry* 57, 523–527. doi: 10.1016/S0031-9422(01)00072-3
- Kitaoka, N., Lu, X., Yang, B., and Peters, R. J. (2015). The application of synthetic biology to elucidation of plant mono-, sesqui-, and diterpenoid metabolism. *Mol. Plant* 8, 6–16. doi: 10.1016/j.molp.2014.12.002
- Koonin, E. V., Fedorova, N. D., Jackson, J. D., Jacobs, A. R., Krylov, D. M., Makarova, K. S., et al. (2004). A comprehensive evolutionary classification of proteins encoded in complete eukaryotic genomes. *Genome Biol.* 5:R7. doi: 10.1186/gb-2004-5-2-r7
- Kumar, S., Banks, T. W., and Cloutier, S. (2012). SNP Discovery through next-generation sequencing and its applications. *Int. J. Plant Genomics* 2012:831460. doi: 10.1155/2012/831460
- Langmead, B., and Salzberg, S. L. (2012). Fast gapped-read alignment with Bowtie 2. *Nat. Methods* 9, 357–359. doi: 10.1038/nmeth.1923
- Legrand, S., Hendriks, T., Hilbert, J. L., and Quillet, M. C. (2007). Characterization of expressed sequence tags obtained by SSH during somatic embryogenesis in *Cichorium intybus* L. *BMC Plant Biol.* 7:27. doi: 10.1186/1471-2229-7-27
- Li, H., and Durbin, R. (2009). Fast and accurate short read alignment with burrows-wheeler transform. *Bioinformatics* 25, 1754–1760. doi: 10.1093/bioinformatics/btp324
- Li, H., Handsaker, B., Wysoker, A., Fennell, T., Ruan, J., Homer, N., et al. (2009). The Sequence Alignment/Map format and SAMtools. *Bioinformatics* 25, 2078–2079. doi: 10.1093/bioinformatics/btp352
- Li, W., and Godzik, A. (2006). Cd-hit: a fast program for clustering and comparing large sets of protein or nucleotide sequences. *Bioinformatics* 22, 1658–1659. doi: 10.1093/bioinformatics/btl158
- Liu, Q., Majdi, M., Cankar, K., Goedbloed, M., Charnikhova, T., Verstappen, F. W., et al. (2011). Reconstitution of the costunolide biosynthetic pathway in yeast and *Nicotiana benthamiana*. *PLoS ONE* 6:e23255. doi: 10.1371/journal.pone.0023255
- Lu, X., Zhang, L., Zhang, F., Jiang, W., Shen, Q., Zhang, L., et al. (2013). AaORA, a trichome-specific AP2/ERF transcription factor of *Artemisia annua*, is a positive regulator in the artemisinin biosynthetic pathway and in disease resistance to *Botrytis cinerea*. *New Phytol.* 198, 1191–1202. doi: 10.1111/nph.12207
- Maroufi, A., Van Bockstaele, E., and De Loose, M. (2010). Validation of reference genes for gene expression analysis in chicory (*Cichorium intybus*) using quantitative real-time PCR. *BMC Mol. Biol.* 11:15. doi: 10.1186/1471-2199-11-15
- Masoudi-Nejad, A., Tonomura, K., Kawashima, S., Moriya, Y., Suzuki, M., Itoh, M., et al. (2006). EGASsembler: online bioinformatics service for large-scale processing, clustering and assembling ESTs and genomic DNA fragments. *Nucleic Acids Res.* 34, W459–W462. doi: 10.1093/nar/gkl066
- Moriya, Y., Itoh, M., Okuda, S., Yoshizawa, A. C., and Kanehisa, M. (2007). KAAS: an automatic genome annotation and pathway reconstruction server. *Nucleic Acids Res.* 35, W182–W185. doi: 10.1093/nar/gkm321
- Muller, P. Y., Janovjak, H., Miserez, A. R., and Dobbie, Z. (2002). Processing of gene expression data generated by quantitative real-time RT-PCR. *Biotechniques* 32, 1372–1374, 1376, 1378–1379.
- Nagegowda, D. A. (2010). Plant volatile terpenoid metabolism: biosynthetic genes, transcriptional regulation and subcellular compartmentation. *FEBS Lett.* 584, 2965–2973. doi: 10.1016/j.febslet.2010.05.045
- Nakasugi, K., Crowhurst, R., Bally, J., and Waterhouse, P. (2014). Combining transcriptome assemblies from multiple *de novo* assemblers in the allo-tetraploid plant *Nicotiana benthamiana*. *PLoS ONE* 9:e91776. doi: 10.1371/journal.pone.0091776
- Nguyen, D. T., Göpfert, J. C., Ikezawa, N., Macnevin, G., Kathiresan, M., Conrad, J., et al. (2010). Biochemical conservation and evolution of germacrene A oxidase in Asteraceae. *J. Biol. Chem.* 285, 16588–16598. doi: 10.1074/jbc.M110.211757
- Ockendon, N. F., O'Connell, L. A., Bush, S. J., Monzon-Sandoval, J., Barnes, H., Szekely, T., et al. (2016). Optimization of next-generation sequencing transcriptome annotation for species lacking sequenced genomes. *Mol. Ecol. Resour.* 16, 446–458. doi: 10.1111/1755-0998.12465
- Pang, T., Ye, C. Y., Xia, X., and Yin, W. (2013). *De novo* sequencing and transcriptome analysis of the desert shrub, *Ammopiptanthus mongolicus*, during cold acclimation using Illumina/Solexa. *BMC Genomics* 14:488. doi: 10.1186/1471-2164-14-488
- Peña-Espinoza, M., Boas, U., Williams, A. R., Thamsborg, S. M., Simonsen, H. T., and Enemark, H. L. (2015). Sesquiterpene lactone containing extracts from two cultivars of forage chicory (*Cichorium intybus*) show distinctive chemical profiles and *in vitro* activity against *Ostertagia ostertagi*. *Int. J. Parasitol. Drugs Drug Resist.* 5, 191–200. doi: 10.1016/j.ijpdrr.2015.10.002
- Peng, Y., Gao, X., Li, R., and Cao, G. (2014). Transcriptome sequencing and *de novo* analysis of *Youngia japonica* using the illumina platform. *PLoS ONE* 9:e90636. doi: 10.1371/journal.pone.0090636
- Perteia, G., Huang, X., Liang, F., Antonescu, V., Sultana, R., Karamycheva, S., et al. (2003). TIGR Gene Indices clustering tools (TGICL): a software system for fast clustering of large EST datasets. *Bioinformatics* 19, 651–652. doi: 10.1093/bioinformatics/btg034
- Peters, A. M., Haagsma, N., and van Amerongen, A. (1997). A pilot study on the effects of cultivation conditions of chicory (*Cichorium intybus* L.) roots on the levels of sesquiterpene lactones in chicons. *Z. Fur Lebensm.* 205, 143–147. doi: 10.1007/s002170050142
- Peters, A. M., and van Amerongen, A. (1998). Relationship between levels of sesquiterpene lactones in chicory and sensory evaluation. *J. Amer. Soc. Hort. Sci.* 123, 326–329.
- Poli, F., Sacchetti, G., Tosi, B., Fogagnolo, M., Chillemi, G., Lazzarin, R., et al. (2002). Variation in the content of the main guainolides and sugars in *Cichorium intybus* var. "Rosso di Chioggia" selections during cultivation. *Food Chem.* 76, 139–147. doi: 10.1016/S0308-8146(01)00254-0

- Price, K. R., Dupont, M. S., Shepherd, R., Chan, H. W. S., and Fenwick, G. R. (1990). Relationship between the chemical and sensory properties of exotic salad crops—coloured lettuce (*Lactuca sativa*) and chicory (*Cichorium intybus*). *J. Sci. Food Agric.* 53, 185–192. doi: 10.1002/jsfa.2740530206
- Ramirez, A. M., Saillard, N., Yang, T., Franssen, M. C., Bouwmeester, H. J., and Jongasma, M. A. (2013). Biosynthesis of sesquiterpene lactones in *pyrethrum* (*Tanacetum cinerariifolium*). *PLoS ONE* 8:e65030. doi: 10.1371/journal.pone.0065030
- Raulier, P., Maudoux, O., Notte, C., Draye, X., and Bertin, P. (2016). Exploration of genetic diversity within *Cichorium endivia* and *Cichorium intybus* with focus on the gene pool of industrial chicory. *Genet. Resour. Crop Evol.* 63, 243–259. doi: 10.1007/s10722-015-0244-4
- R Core Team (2015). *R: A Language and Environment for Statistical Computing*. R Foundation for Statistical Computing, Vienna, Austria. [Online]. Vienna: R Foundation for Statistical Computing. Available online at: <http://www.R-project.org/>. [Accessed].
- Reeves, P. H., Ellis, C. M., Ploense, S. E., Wu, M. F., Yadav, V., Tholl, D., et al. (2012). A regulatory network for coordinated flower maturation. *PLoS Genet.* 8:e1002506. doi: 10.1371/journal.pgen.1002506
- Renna, M., Gonnella, M., Giannino, D., and Santamaría, P. (2014). Quality evaluation of cook-chilled chicory stems (*Cichorium intybus* L., Catalogna group) by conventional and sous vide cooking methods. *J. Sci. Food Agric.* 94, 656–665. doi: 10.1002/jsfa.6302
- Robinson, M. D., McCarthy, D. J., and Smyth, G. K. (2010). edgeR: a Bioconductor package for differential expression analysis of digital gene expression data. *Bioinformatics* 26, 139–140. doi: 10.1093/bioinformatics/btp616
- Schulz, M. H., Zerbino, D. R., Vingron, M., and Birney, E. (2012). Oases: robust *de novo* RNA-seq assembly across the dynamic range of expression levels. *Bioinformatics* 28, 1086–1092. doi: 10.1093/bioinformatics/bts094
- Schwab, W., and Wust, M. (2015). Understanding the constitutive and induced biosynthesis of mono- and sesquiterpenes in Grapes (*Vitis vinifera*): a key to unlocking the biochemical secrets of unique grape aroma profiles. *J. Agric. Food Chem.* 63, 10591–10603. doi: 10.1021/acs.jafc.5b04398
- Seo, M. W., Yang, D. S., Kays, S. J., Lee, G. P., and Park, K. W. (2009). Sesquiterpene lactones and bitterness in korean leaf lettuce cultivars. *Hort. Sci.* 44, 246–249.
- Sessa, R. A., Bennett, M. H., Lewis, M. J., Mansfield, J. W., and Beale, M. H. (2000). Metabolite profiling of sesquiterpene lactones from *Lactuca* species. Major latex components are novel oxalate and sulfate conjugates of lactucin and its derivatives. *J. Biol. Chem.* 275, 26877–26884. doi: 10.1074/jbc.M000244200
- Street, R. A., Sidana, J., and Prinsloo, G. (2013). *Cichorium intybus*: traditional uses, phytochemistry, pharmacology, and toxicology. *Evid. Based Complement. Alternat. Med.* 2013:579319. doi: 10.1155/2013/579319
- Tamaki, H., Robinson, R. W., Anderson, J. L., and Stoewsand, G. S. (1995). Sesquiterpene lactones in virus-resistant lettuce. *J. Agric. Food Chem.* 43, 6–8. doi: 10.1021/jf00049a002
- The Compositae Genome Project (2000). Available online at: <http://compgenomics.ucdavis.edu/> [Accessed].
- Tholl, D. (2015). Biosynthesis and biological functions of terpenoids in plants. *Adv. Biochem. Eng. Biotechnol.* 148, 63–106. doi: 10.1007/10_2014_295
- Toma, M., Vinatoru, M., Paniwnyk, L., and Mason, T. J. (2001). Investigation of the effects of ultrasound on vegetal tissues during solvent extraction. *Ultrason. Sonochim.* 8, 137–142. doi: 10.1016/S1350-4177(00)00033-X
- Untergasser, A., Cutcutache, I., Koressaar, T., Ye, J., Faircloth, B. C., Remm, M., et al. (2012). Primer3-new capabilities and interfaces. *Nucleic Acids Res.* 40, e115. doi: 10.1093/nar/gks596
- van Beek, T., Maas, P., King, B., Leclercq, E., Voragen, A., and de Groot, A. A. (1990). Bitter sesquiterpene lactones from chicory roots. *J. Agric. Food Chem.* 38, 1035–1038. doi: 10.1021/jf00094a026
- Varotto, S., Pizzoli, L., Lucchin, M., and Parrini, P. (1995). The incompatibility system in Italian red chicory (*Cichorium intybus* L.). *Plant Breed.* 114, 535–538. doi: 10.1111/j.1439-0523.1995.tb00851.x
- Varshney, R. K., Graner, A., and Sorrells, M. E. (2005). Genic microsatellite markers in plants: features and applications. *Trends Biotechnol.* 23, 48–55. doi: 10.1016/j.tibtech.2004.11.005
- Wang, H., Jiang, J., Chen, S., Qi, X., Peng, H., Li, P., et al. (2013). Next-generation sequencing of the *Chrysanthemum nankingense* (Asteraceae) transcriptome permits large-scale unigene assembly and SSR marker discovery. *PLoS ONE* 8:e62293. doi: 10.1371/journal.pone.0062293
- Wei, T. (2013). *Corrplot: Visualization of a Correlation Matrix*. [Online]. Available online at: <http://CRAN.R-project.org/package=corrplot> [Accessed].
- Yamada, Y., and Sato, F. (2013). Transcription factors in alkaloid biosynthesis. *Int. Rev. Cell Mol. Biol.* 305, 339–382. doi: 10.1016/B978-0-12-407695-2.00008-1
- Ye, J., Fang, L., Zheng, H., Zhang, Y., Chen, J., Zhang, Z., et al. (2006). WEGO: a web tool for plotting GO annotations. *Nucleic Acids Res.* 34, W293–W297. doi: 10.1093/nar/gkl031
- Zerbino, D. R., and Birney, E. (2008). Velvet: algorithms for *de novo* short read assembly using de Bruijn graphs. *Genome Res.* 18, 821–829. doi: 10.1101/gr.074492.107
- Conflict of Interest Statement:** The authors declare that the research was conducted in the absence of any commercial or financial relationships that could be construed as a potential conflict of interest.
- Copyright © 2016 Testone, Mele, Di Giacomo, Gonnella, Renna, Tenore, Nicolodi, Frugis, Iannelli, Arnesi, Schiappa and Giannino. This is an open-access article distributed under the terms of the Creative Commons Attribution License (CC BY). The use, distribution or reproduction in other forums is permitted, provided the original author(s) or licensor are credited and that the original publication in this journal is cited, in accordance with accepted academic practice. No use, distribution or reproduction is permitted which does not comply with these terms.*



Corrigendum: Insights into the Sesquiterpenoid Pathway by Metabolic Profiling and *De novo* Transcriptome Assembly of Stem-Chicory (*Cichorium intybus* Cultigroup “Catalogna”)

Giulio Testone¹, Giovanni Mele¹, Elisabetta Di Giacomo¹, Maria Gonnella², Massimiliano Renna^{2,3}, Gian Carlo Tenore⁴, Chiara Nicolodi¹, Giovanna Frugis¹, Maria A. Iannelli¹, Giuseppe Arnesi⁵, Alessandro Schiappa⁵ and Donato Giannino^{1*}

OPEN ACCESS

Edited and reviewed by:

Luis A. J. Mur,
Aberystwyth University, UK

*Correspondence:

Donato Giannino
donato.giannino@ibba.cnr.it

Specialty section:

This article was submitted to
Crop Science and Horticulture,
a section of the journal
Frontiers in Plant Science

Received: 01 February 2017

Accepted: 20 March 2017

Published: 07 April 2017

Citation:

Testone G, Mele G, Di Giacomo E, Gonnella M, Renna M, Tenore GC, Nicolodi C, Frugis G, Iannelli MA, Arnesi G, Schiappa A and Giannino D (2017) Corrigendum: Insights into the Sesquiterpenoid Pathway by Metabolic Profiling and *De novo* Transcriptome Assembly of Stem-Chicory (*Cichorium intybus* Cultigroup “Catalogna”). *Front. Plant Sci.* 8:478. doi: 10.3389/fpls.2017.00478

¹ Institute of Agricultural Biology and Biotechnology (IBBA), CNR - Monterotondo Scalo, Rome, Italy, ² Institute of Sciences of Food Production (ISPA), CNR, Bari, Italy, ³ Department of Agricultural and Environmental Science (DISAAT), University of Bari, Bari, Italy, ⁴ Department of Pharmacy, University of Naples Federico II, Naples, Italy, ⁵ Enza Zaden Italia, Tarquinia, Italy

Keywords: *Cichorium intybus*, stem-chicory landraces, transcriptome, sesquiterpene lactones, bitterness

A corrigendum on

Insights into the Sesquiterpenoid Pathway by Metabolic Profiling and *De novo* Transcriptome Assembly of Stem-Chicory (*Cichorium intybus* Cultigroup “Catalogna”) by Testone, G., Mele, G., Di Giacomo, E., Gonnella, M., Renna, M., Tenore, G. C., et al. (2016). *Front. Plant Sci.* 7:1676. doi: 10.3389/fpls.2016.01676

There were these typing errors: “Mbp” (incorrect) instead of “cM” (correct) and “Berardes” (incorrect) instead of “Bernardes” (correct).

In the Introduction, the sentence “The *C. intybus* species has a large (2n = 2x = 18; size 1405 Mbp) and complex genome (De Simone et al., 1997; Berardes et al., 2013).”

In the Discussion, the sentence (5th indent) “*Cichorium intybus* genome is esteemed ca.1400 MB (De Simone et al., 1997),”

were respectively corrected as follows:

“The *C. intybus* species has a large (2n = 2x = 18; size 1405 cM) and complex genome (De Simone et al., 1997; Bernardes et al., 2013).”

“*Cichorium intybus* genome is esteemed ca.1400 cM (De Simone et al., 1997).”

In the References section, the surname “Berardes” was replaced with “Bernardes.”

The authors apologize for these errors and state that these do not change the scientific conclusions of the article in any way.

REFERENCES

- De Simone, M., Morgante, M., Lucchin, M., Parrini, P., and Marocco, A. (1997). A first linkage map of *Cichorium intybus* L. using a one-way pseudo-testcross and PCR-derived markers. *Mol. Breed.* 3, 415–425. doi: 10.1023/A:1009616801404
- Bernardes, E., Benko-Iseppon, A., Vasconcelos, S., Carvalho, R., and Brasileiro-Vidal, A. (2013). Intra- and interspecific chromosome polymorphisms in cultivated *Cichorium* L. species (Asteraceae). *Genet Mol Biol.* 36, 357–363. doi: 10.1590/S1415-47572013005000025

Conflict of Interest Statement: The authors declare that the research was conducted in the absence of any commercial or financial relationships that could be construed as a potential conflict of interest.

Copyright © 2017 Testone, Mele, Di Giacomo, Gonnella, Renna, Tenore, Nicolodi, Frugis, Iannelli, Arnesi, Schiappa and Giannino. This is an open-access article distributed under the terms of the Creative Commons Attribution License (CC BY). The use, distribution or reproduction in other forums is permitted, provided the original author(s) or licensor are credited and that the original publication in this journal is cited, in accordance with accepted academic practice. No use, distribution or reproduction is permitted which does not comply with these terms.



Mechanisms of Selenium Enrichment and Measurement in Brassicaceous Vegetables, and Their Application to Human Health

Melanie Wiesner-Reinhold^{1*}, Monika Schreiner¹, Susanne Baldermann^{1,2}, Dietmar Schwarz³, Franziska S. Hanschen¹, Anna P. Kipp⁴, Daryl D. Rowan⁵, Kerry L. Bentley-Hewitt⁵ and Marian J. McKenzie⁵

¹ Plant Quality and Food Security, Leibniz Institute of Vegetable and Ornamental Crops, Grossbeeren, Germany, ² Food Chemistry, Institute of Nutritional Science, University of Potsdam, Nuthetal, Germany, ³ Functional Plant Biology, Leibniz Institute of Vegetable and Ornamental Crop, Grossbeeren, Germany, ⁴ Department of Molecular Nutritional Physiology, Institute of Nutrition, Friedrich Schiller University Jena, Jena, Germany, ⁵ Food Innovation, The New Zealand Institute for Plant & Food Research Limited, Palmerston North, New Zealand

OPEN ACCESS

Edited by:

Nadia Bertin,
Plantes et Système de cultures
Horticoles (INRA), France

Reviewed by:

Daniel A. Jacobo-Velázquez,
Tecnológico de Monterrey, Mexico
Karl Kunert,
University of Pretoria, South Africa

*Correspondence:

Melanie Wiesner-Reinhold
wiesner@igz.ve

Specialty section:

This article was submitted to
Crop Science and Horticulture,
a section of the journal
Frontiers in Plant Science

Received: 13 March 2017

Accepted: 21 July 2017

Published: 03 August 2017

Citation:

Wiesner-Reinhold M, Schreiner M,
Baldermann S, Schwarz D,
Hanschen FS, Kipp AP, Rowan DD,
Bentley-Hewitt KL and McKenzie MJ
(2017) Mechanisms of Selenium
Enrichment and Measurement in
Brassicaceous Vegetables, and Their
Application to Human Health.
Front. Plant Sci. 8:1365.
doi: 10.3389/fpls.2017.01365

Selenium (Se) is an essential micronutrient for human health. Se deficiency affects hundreds of millions of people worldwide, particularly in developing countries, and there is increasing awareness that suboptimal supply of Se can also negatively affect human health. Selenium enters the diet primarily through the ingestion of plant and animal products. Although, plants are not dependent on Se they take it up from the soil through the sulphur (S) uptake and assimilation pathways. Therefore, geographic differences in the availability of soil Se and agricultural practices have a profound influence on the Se content of many foods, and there are increasing efforts to biofortify crop plants with Se. Plants from the Brassicales are of particular interest as they accumulate and synthesize Se into forms with additional health benefits, such as methylselenocysteine (MeSeCys). The Brassicaceae are also well-known to produce the glucosinolates; S-containing compounds with demonstrated human health value. Furthermore, the recent discovery of the selenoglucosinolates in the Brassicaceae raises questions regarding their potential bioefficacy. In this review we focus on Se uptake and metabolism in the Brassicaceae in the context of human health, particularly cancer prevention and immunity. We investigate the close relationship between Se and S metabolism in this plant family, with particular emphasis on the selenoglucosinolates, and consider the methodologies available for identifying and quantifying further novel Se-containing compounds in plants. Finally, we summarize the research of multiple groups investigating biofortification of the Brassicaceae and discuss which approaches might be most successful for supplying Se deficient populations in the future.

Keywords: *Brassica vegetables, selenium, biofortification, glucosinolates, human health, immune system, cancer, analytical methods*

INTRODUCTION

Awareness of malnutrition, e.g., deficiencies in iron, iodine, vitamin A, and zinc, in the developing world is high, but micronutrient deficiency is rarely discussed in developed countries. This reduced awareness is surprising, especially since micronutrient deficiency or suboptimal supply of the essential micronutrient selenium (Se) is seen in several developed countries such as New Zealand to

(Thomson, 2004; Curtin et al., 2006), Australia (Oldfield, 2002) as well as in Europe, e.g., United Kingdom (Lyons et al., 2003), Germany (Hartfiel et al., 2010), and Finland (Alfthan et al., 2015), and is estimated affect about one billion persons worldwide (Haug et al., 2007). Micronutrient deficiency is usually regarded as having minor effects in developed countries where the diet is more diverse and the food comes from a range of sources rather than being limited to local produce. Therefore, Se deficiency in developed countries, such as New Zealand, is not as extreme as in the Se deficient areas of China and Tibet where local populations have suffered Se deficiency related disease that can be highly debilitating and sometimes fatal (Chen et al., 1980; Moreno-Reyes et al., 1998). However, there is increasing awareness that suboptimal amounts of Se can also be damaging to human health, in particular when coupled with malnutrition. Micronutrient deficiency may likely occur also in developed countries in the future, due to the consumption of fast-foods and the associated intake of so called “empty calories.”

As Se is an essential micronutrient, under-supply has direct and indirect consequences for human health. Direct disorders include a destabilized immune system, hypothyroidism and cardiomyopathy (Whanger, 2004; Rayman, 2012). Pathologic symptoms are developed as a consequence of a daily Se intake $<10 \text{ } \mu\text{g day}^{-1}$. Indirectly, Se deficiency results in loss of protective anti-cancerogenic effects through reduced expression of antioxidant selenoproteins and reduced availability of several seleno-compounds (Whanger, 2004). The dietary reference Se intake is $55 \text{ } \mu\text{g d}^{-1}$ for adult humans in the USA, according to the National Institutes of Health¹, whereas in Europe the recommended daily intake is $70 \text{ } \mu\text{g d}^{-1}$ according to the European Food Safety Authority (EFSA Panel on Dietetic Products, Nutrition and Allergies (NDA), 2014).

Consequently, agricultural and horticultural food production systems should develop to improve access to more Se nutritious food. One promising approach is to promote the production and consumption of Se-biofortified plant-based food. It is remarkable that about 10% of the world's vegetable production is generated from Brassicales species (Augustine et al., 2014) including the most economically important family Brassicaceae. Brassicales species are able to accumulate Se (White, 2016) and, furthermore, are characterized by a certain group of secondary plant metabolites—the glucosinolates—found almost exclusively in the order Brassicales (Verkerk et al., 2009). Certain individual glucosinolates are known to confer health-promoting effects, mainly due to the anti-carcinogenic and antidiabetogenic properties of their hydrolysis products (e.g., Lippmann et al., 2014; Guzmán-Pérez et al., 2016). In contrast to other plant species, Brassicales species demonstrate the ability to synthesize not only seleno-amino acids and selenoproteins but also selenoglucosinolates. Moreover, synthetic breakdown products of selenoglucosinolates are reported to be distinctly more protective in cancer prevention compared to their S-containing analogs (Sharma et al., 2008; Emmert et al., 2010). It also seems likely that the antioxidant selenoproteins may be of benefit in counteracting diseases of oxidative stress

such as cancer (Rayman et al., 2008). Previously several novel selenoglucosinolates have been identified from *Brassica* species (Matich et al., 2012, 2015; McKenzie et al., 2015b), and it was demonstrated that ingestion of Se-enriched broccoli, which contains these seleno-compounds alongside others, may have also a beneficial role in the human immune response (Bentley-Hewitt et al., 2014).

The focus of this review is to highlight the human health benefits implicit in the presence of unique Se-containing metabolites produced by *Brassica* species. This is an important and novel set of circumstances not present in other plant families—or contained in other reviews. The selenoglucosinolates in particular have not previously been reviewed in any depth, nor have their potential roles in human health. The review also highlights the latest methodology specific to the identification of Se containing compounds. Therefore, we aim to provide not only an up-to-date overview of previous and current research on Se metabolism in the Brassicales and its association with human health, but also provide new insight and motivation to further investigation.

SELENIUM IN BRASSICALES

In recent years several reviews have been published on the importance of Se in higher plants, such as Terry et al. (2000), Pilon-Smits (2005), Zhu et al. (2009), Pilon-Smits and Quinn (2010), Feng et al. (2013), El-Ramady et al. (2015), Malagoli et al. (2015), Winkel et al. (2015), White (2016), and Schiavon and Pilon-Smits (2017). The review of El-Ramady et al. (2015) gives an overview regarding Se physiology and biology in higher plants and describes many aspects of Se fertilization, whereas Winkel et al. (2015) deals with Se uptake and pathways, but also with Se sources and distribution in water, air and soil. The groups round Terry and Pilon-Smits have established the critical nature of the selenocysteine methyltransferase (SMT) gene in the biosynthesis of methylselenocysteine (MeSeCys) and the role Se plays throughout the plants' wider ecosystem. White's (2016) latest review provides an excellent overview of Se uptake, translocation and metabolism in plants in general concluding in the demand to breed crops with greater Se concentrations in their edible tissue.

Selenium Uptake

As in most plant genera, the Brassicales take up Se primarily as the selenate anion (SeO_4^{2-}), the predominant form occurring in alkaline and well-oxidized soils, as the selenite anion (SeO_3^{2-}) existing in well-drained mineral soils, and also as selenocysteine (SeCys) and selenomethionine (SeMet; Ajwa et al., 1998).

Generally, the amount of Se taken up is related directly to the amount present in the soil (Brown and Shrift, 1982; Zhao et al., 2005) or the nutrient solution the plants grow on (Bañuelos, 1996). However, this is not always the case; for example in the *Brassica* vegetable rutabaga (*Brassica napus* L.) there was a poor correlation between Se uptake and Se soil content grown on a landfill (Arthur et al., 1992). Also, after two plantings of canola (*B. napus*), 80% of the Se remained in soils (Ajwa et al., 1998).

¹<https://ods.od.nih.gov/factsheets/Selenium-HealthProfessional/>

Se uptake has been shown to be greater when supplied in nutrient solution. While some experiments report data related to Se uptake from natural soils, most data originate from experiments in the context of biofortification (see Section Selenium Biofortification). The amount of Se taken up varies between species of Brassicales (**Table 1**). Concentrations may reach up to 2,000 µg/g dry weight (DW) (Ximenez-Embus et al., 2004; Manion et al., 2014). Significant genetic effects on Se concentration in Brassicales have been observed for leaves of rapid-cycling *B. oleracea* L. (Kopsell and Randle, 2001), broccoli florets [*B. oleracea* L. Italica Group (Bañuelos et al., 2003; Farnham et al., 2007; Ramos et al., 2011)], sprouts of cauliflower (*B. oleracea* L. Botrytis Group), kale (*B. oleracea* L. acephala Group), cabbage (*B. oleracea* Capitata Group) and Chinese cabbage [*B. rapa* L. (Ávila et al., 2014)], as well as shoots of Indian mustard [*B. juncea* (L.) Czern (Bañuelos et al., 1997)]. Comparing different *Brassica* species cultivated on natural soils with a comparable Se concentration of about 0.32 mg kg⁻¹ the order of precedence in uptake (in µg g⁻¹ DW) was Brussels sprouts (*B. oleracea* Gemnifera Group) (0.247), broccoli (0.129), savoy cabbage (*B. oleracea* Savoy Cabbage Group) (0.104), cauliflower (0.102), red cabbage (0.091), white cabbage (0.085), kale (0.046), kohlrabi (*B. oleracea* var. *gongylodes* L.) (0.037), and finally turnip (*B. rapa* var. *rapa* L.) (0.029; De Temmerman et al., 2014). This demonstrates the wide range of Se uptake within the Brassicales. As an example of the potential differences within a single species, cultivars of Indian mustard originating from different countries were compared under the same growing conditions. The amount of Se taken up doubled between the cultivar with the lowest and the highest Se concentrations independent of the supply form (soil or hydroponics) and the plant tissue (root or shoot; Bañuelos et al., 1997).

The form in which Se is provided is also important, with selenate being taken up two-fold faster than selenite in Indian mustard (De Souza et al., 1998). The order of preference when Indian mustard was supplied over an 8-day period with different Se forms at 20 µM was dimethylselenopropionate (DMSeP) > SeMet > selenate > SeCys > selenite (Terry et al., 2000).

Although abiotic effects seem to be less influential than genetic effects, Se uptake also depends on environmental conditions and on the interaction with other nutrients supplied (see Section Promotion of Selenogluconolate Formation by Targeted Supply of N and S). In rapid-cycling *B. oleracea*, Se accumulation was clearly temperature-dependent (Chang and Randle, 2006), with Se concentrations increasing linearly with increasing temperature from 10 to 30°C in the leaves, ranging from 1.73 to 2.54 mg g⁻¹ DW. Conversely, Se content decreased linearly with increasing temperature in the roots and ranged from 2.87 to 2.17 mg Se g⁻¹ DW. Within environmental conditions, the microbiome also seems to be important for Se uptake. Inoculation of bacterial isolates into the rhizosphere of axenic plants (*B. juncea*) led to increased Se accumulation in shoots and roots following supply with 20 µmol selenate (De Souza et al., 1999). Depending on the strain selected, the tissue Se concentration increased up to three-fold in shoots and five-fold in roots. The influence of environmental factors has not yet been fully explored. However, knowledge in this area will

become a crucial topic when Se-biofortification in crops is investigated.

Selenate enters root cells through sulphate transporters in their plasma membranes (Terry et al., 2000; White et al., 2004). sulphate transporters are encoded by a small family of genes; e.g., 14 in the genome of *Arabidopsis thaliana* L., and a similar number in other Brassicaceae species (Buchner et al., 2004; Hawkesford et al., 2005). A detailed overview of the sulphate transporters identified in *Arabidopsis* and their function are given in White (2016). Briefly, all sulphate transporters can be placed into one of four groups based on their protein sequences and distinct functional characteristics (Hawkesford, 2003; Hawkesford et al., 2005; Gigolashvili and Kopriva, 2014). Group 1 contains high-affinity sulphate transporters (HAST) that are thought to catalyse most selenate influx to cells (Hawkesford et al., 2005), sulphate transporters from group 2 are thought to catalyse selenate uptake into cells within the stele. Further, group 3 transporter AtSULTR3;5 appears to modulate the activity of a group 2 transporter, but does not catalyse transport itself (White, 2016). In contrast to group 1 transporters, sulphate transporters of group 4 (AtSULTR4;1 and AtSULTR4;2) might be responsible for catalysing the selenate efflux from the vacuoles (Gigolashvili and Kopriva, 2014). However, while these transporters are well-characterized in *Arabidopsis*, transporters and their mode of action need to be more fully investigated in brassicaceous vegetables.

For selenite uptake, P transporters are activated as well (Winkel et al., 2015). The involvement of the phosphate transport system in the movement of selenite throughout a plant has been reported based on the observation that increasing P concentration reduced selenite uptake rates in different plant species (Broyer et al., 1972; Hopper and Parker, 1999), however, this has not yet been found in Brassicales.

Selenium Mobilization and Distribution

Selenate and selenite transport processes in all plants are energy-dependent (Hawkesford et al., 1993; Sors et al., 2005; Li et al., 2008). Selenate is rapidly translocated from the root to the shoot, whereas only ~10% of selenite is translocated in this way (De Souza et al., 1998). After uptake, Se is distributed within the plant to the different organs. The sites of accumulation depend on the species, its phase of development, and its physiological conditions. Overall, it follows: seeds > flowers > leaves > roots > stems (Terry et al., 2000; Quinn et al., 2011). A portion of the Se transported into the plant is volatilized as dimethyl selenide. Se-volatilisation rates of Indian mustard pre-treated for 7 d with 20 µg selenate amounted to 7 µg (g d)⁻¹ DW and were two- to three-fold higher from plants pre-treated with 20 µg selenite (De Souza et al., 1999). A clear correlation was found between Se-volatilization rates and total Se concentrations.

Selenium—a Non-essential Element for Plants That Has Beneficial or Toxic Effects

Unlike in animals and some green algae (Araie and Shiraiwa, 2016), Se is considered a non-essential element for the healthy growth of crops (Zhang and Gladyshev, 2009). Brassicales as well as many other plant species exposed to high concentrations of Se

TABLE 1 | Methods of Se enrichment in brassicaceous crops and resulting Se and MeSeCys content.

Crop	Tissues analyzed	Se application method	Total Se in tissue μg g ⁻¹ DW	MeSeCys content μg g ⁻¹ DW	References
Broccoli <i>Brassica oleracea</i> L. var. Italica Group	Florets	Hydroponic, mature plants, 20 μM selenite	1,200	<1.5 μmol	Lyi et al., 2005
	Florets	Soil fertilization, mature plants, 5 cultivars, 100 mL 1.5 mM Na ₂ SeO ₄ 2x per week, 3 weeks	<558	<137	Ávila et al., 2013)
	Florets	Soil fertilization, mature plants, up to 5.2 mM selenate, every 2 days for 12 days (10 mL per plant for first 8 days, 20 mL per plant for last 4 days)	<879	nd ^a	Lee et al., 2005
	Florets Leaves	Greenhouse soil—non-saline irrigation, 250 μg Se L ⁻¹	<51 <31	nd ^a	Bañuelos et al., 2003
	Florets Leaves	Soil fertilization with increasing amounts dried Se-enriched <i>S. pinnata</i> (~700 μg Se g ⁻¹ DW), 23 weeks	<3.5 <3.5	7.4% soluble Se-compounds	Bañuelos et al., 2015)
	Florets	Soil enriched with <i>S. pinnata</i> (see Bañuelos et al., 2015) after 3 years	<8.0	5.0% soluble Se-compounds	Bañuelos et al., 2016
	Florets	Soil in pots enriched with up to 100 μM Na ₂ SeO ₄ for up to 8 weeks	nd ^a	<3.4 μmol	Mahn, 2017
	Florets	Three field trials, SC, USA	<0.085	nd ^a	Farnham et al., 2007
	Sprouts	Hydroponic, sprouts, up to 100 μM Na ₂ SeO ₄ or Na ₂ SeO ₃ (1 week)	<263 (selenate) <185 (selenite)	<157 <167	Ávila et al., 2013
	Sprouts	Hydroponic, sprouts, 50 μM Na ₂ SeO ₃ (1 week)	~180	~90	Ávila et al., 2014
	Sprouts	Hydroponic, 10 μg mL ⁻¹ selenite for 7 days	32 FW	94.3% of 0.2M HCl plant extract	Sugihara et al., 2004
	Sprouts	Hydroponic, 3 cultivars, 100 μmol L ⁻¹ Na ₂ SeO ₄ or Na ₂ SeO ₃ for 5 days	~85 (selenate) ~75 (selenite)	nd ^a	Tian et al., 2016
	Sprouts	Hydroponic, selenate 127/ 635/1270 μmol L ⁻¹	max. 100/120/245		Arscott and Goldman, 2012
	Leaves	Greenhouse soil non-saline irrigation, 250 μg Se L ⁻¹	<31		Bañuelos et al., 2003
	Leaves	Hydroponic, 20 IM Na ₂ SeO ₄	<1,798		Ramos et al., 2011
	Head and upper stem	Foliar spray selenate, up to 20 mg Se plant ⁻¹ once, 3 month old plants ~2 mg Se plant ⁻¹ , once, mature plants	55 5	nd ^a nd ^a	Hsu et al., 2011
	Head, leaves, stem and roots in four cultivars	Foliar spray Na ₂ SeO ₄ , up to 50 g Se ha ⁻¹ , once, mature plants	Up to 1,000 in head tissue, less in leaves, stems and roots	Up to 0.1 in head tissue	Sindelarova et al., 2015
	Shoot root	Weekly sand fertilization, young plants, 40 μM selenate for 6 weeks	420.7	nd ^a	Hsu et al., 2011
	Shoots	Hydroponic, seedlings, 38 broccoli accessions, 20 μM selenate for 2 weeks	<1,789	<0.8 FM	Ramos et al., 2011
	Stalks, roots Leaves, florets	Field trial, irrigated with drainage water 150 μg Se L ⁻¹	< 2.9 < 2.6 < 3.7 < 4.5		Bañuelos, 2002

(Continued)

TABLE 1 | Continued

Crop	Tissues analyzed	Se application method	Total Se in tissue μg g ⁻¹ DW	MeSeCys content μg g ⁻¹ DW	References
Brussels Sprouts <i>B. oleracea</i> gemmifera Group	Sprouts	Hydroponic, sprouts, 50 μM Na ₂ SeO ₄ , 1 week	~50	~50	Ávila et al., 2014
Cabbage <i>B. oleracea</i> var. <i>capitata</i>	Sprouts	Hydroponic, 50 μM Na ₂ SeO ₄ , 1 week	~180	~70	Ávila et al., 2014
	Leaves roots	Peat fertilization, up to 158 mg kg ⁻¹ peat as selenite:selenate (1:9), up to 6 months	1,606.793	nd ^a	Funes-Collado et al., 2013
	Leaves	Hydroponic: 2 mg L ⁻¹ Na ₂ SeO ₄	120 max. 988 152 max. 531	nd ^a	Kopsell and Randle, 2001
Rapid cycling cabbage <i>B. oleracea</i> var. <i>capitata</i>	Shoots	Hydroponic, up to 9.0 mg L ⁻¹ selenate, 31 days	<732; < 1,740	nd ^a	Charron et al., 2001
	Leaf Stem root	Hydroponic, up to 9.0 mg L ⁻¹ selenate, young plants, 22 days	<1,916, <1,165 <1,636	nd ^a	Kopsell and Randle, 1999
	Leaf (seedlings)	Hydroponic, up to 1.5 mg L ⁻¹ Na ₂ SeO ₄ , 30 days	<375	nd ^a	Toler et al., 2007
Cauliflower <i>B. oleracea</i> var. <i>botrytis</i>	Sprouts	Hydroponic, sprouts, 50 μM Na ₂ SeO ₄ , 1 week	~200	~90	Ávila et al., 2014
	Edible portion	Clay loam soil fertilization, up to 2.5 mg kg ⁻¹ soil as selenate	~30	nd ^a	Dhillon and Dhillon, 2009
Kale <i>Brassica oleracea</i> var. <i>sabellica</i> L.	Sprouts	Hydroponic, 50 μM Na ₂ SeO ₄ , 1 week	~180	~100	Ávila et al., 2014
	Seedlings	Hydroponic, up to 45 μg mL ⁻¹ Na ₂ SeO ₃ < 15 days	<386	<24	Maneetong et al., 2013
Turnip <i>B. rapa</i> ssp. <i>rapa</i>	Edible portion	Soil fertilization, up to 2.5 mg kg ⁻¹ soil as selenite	~60	nd ^a	Dhillon and Dhillon, 2009
	Sprouts	Hydroponic, 10 μg mL ⁻¹ selenite for 8 days	37 (FW)	94.5% of 0.2M HCl plant extract	Sugihara et al., 2004
Indian Mustard <i>Brassica juncea</i> (L.) Czern	Shoots/roots	0.3-strength Hoagland solution + 4 mg L ⁻¹ Na ₂ SeO ₄ Pot trial (soil/compost 7/3) 2 mg Se kg ⁻¹ substrate	<1,092/< 470 <769/< 332	0.006–0.215	Bañuelos et al., 1997
	Mature shoots	Se contaminated soils (5 μg g ⁻¹)	<60	nd ^a	Bañuelos et al., 2005
	Shoots roots	Hydroponics, max 15 mg L ⁻¹ Se, wild mustard	<1,300;<554	nd ^a	Bañuelos et al., 1990; Bañuelos, 1996
	Seeds	Plants grown on naturally Se-rich soil (6.5 mg Se kg ⁻¹ soil)	110 FW	nd ^a	Jaiswal et al., 2012
	Seeds	Sandy loam soil, three times weekly with 20 μM SeO ₄ ²⁻	<2.2	29% aqueous Se species	Bañuelos et al., 2012
	Leaves/stem	Soil loaden with 1.1 mg kg ⁻¹ total Se	<70/<48		Bañuelos et al., 2000
	Shoot	Plants grown on naturally Se-rich soil (4.0 mg Se kg ⁻¹ soil), to 10 weeks old	~150	nd ^a	Van Huysen et al., 2004
	Seedlings	Hydroponic, up to 500 μM selenate, 1 week 150 μM selenite, 1 week	<200~400	5 FM nd ^a	Leduc et al., 2006
	Shoot /root Shoot /root	Hydroponic, seedlings, up to 5 mg L ⁻¹ Na ₂ SeO ₄ or Na ₂ SeO ₃ , 2 weeks	2,081/3,411 58/605 (selenite)	nd ^a	Ximenez-Embun et al., 2004
	Shoot/roots	Hydroponic, 4 week old plants, up to 50 μM selenate for 8 days.	<1,800/<960	nd ^a	Pilon-Smits et al., 1999

(Continued)

TABLE 1 | Continued

Crop	Tissues analyzed	Se application method	Total Se in tissue μg g ⁻¹ DW	MeSeCys content μg g ⁻¹ DW	References
White mustard <i>Sinapis alba</i> L.	Shoot/root	Hydroponic, 5 week old plants, 20 μM Se as selenate, or selenite, 1 week.	~500/~175 ~175/~35	nd ^a	Van Huysen et al., 2003
	Shoot/root	Hydroponic solution 20 μM Se as selenite, 1 week	~130/~145	nd ^a	De Souza et al., 1999
	Leaves/roots	Greenhouse, grown on seleniferous soil 1 mg kg ⁻¹	~125/~20	nd ^a	Cappa and Pilon-Smits, 2014
	Seeds	Sandy loam soil, three times weekly with 20 μM SeO ₄ ²⁻	<1.3	17% aqueous Se species	Bañuelos et al., 2012
	Leaves Stem Roots	Soil fertilization, up to 1.5 mg kg ⁻¹ , selenate and different organic forms	<284 <55 <88	nd ^a	Ajwa et al., 1998
	Leaves Stem Roots	Field trial, irrigated with drainage water 150 μg Se L ⁻¹	<6.2 <4.3 <3.1	nd ^a	Bañuelos, 2002
	Leaves/stem	Soil loaden with 1.1 mg kg ⁻¹ total Se	<80/< 30		Bañuelos et al., 2000
	Roots	Soil, 2 mg kg ⁻¹ total Se (SeO ₄ ²⁻)	<315		Bañuelos et al., 1996
	Seeds	Sandy loam soil, three times weekly with 20 μM SeO ₄ ²⁻	< 1.7	20% aqueous Se species	Bañuelos et al., 2012
	Edible portion	Soil fertilization, up to 2.5 mg kg ⁻¹ soil as selenate	~40	nd ^a	Dhillon and Dhillon, 2009
Radish <i>Raphanus sativus</i>	Edible portion	Soils, containing 0.39 mg Se kg ⁻¹	~0.018		De Temmerman et al., 2014
	Seedlings	Hydroponic, selenite or selenium nanoparticles (1 mg L ⁻¹) for 40 days	207 144	47–72 Se species, 25–47 Se species	Palomo-Siguero et al., 2015
	Sprouts	Hydroponic, 10 μg mL ⁻¹ selenite for 8 days	21 μg g ⁻¹ FM	96.5% of 0.2M HCl plant extract	Sugihara et al., 2004
Ethiopian kale <i>B. carinata</i> A.Braun	Shoot/root	0.3-strength Hoagland solution + 4 mg L ⁻¹ Na ₂ SeO ₄ Pot trial (soil/compost 7/3) 2 mg Se kg ⁻¹ substrate	695/225 543/201	nd ^a	Bañuelos et al., 1997
	Shoot	Hydroponic, up to 4 mg Se L ⁻¹ as selenate, harvested at 28 d	Up to 2,550	nd ^a	Manion et al., 2014

^and, not determined.

in their root environment exhibit symptoms of injury. Visible and often initial symptoms are stunting of growth, root shortening, chlorosis, withering, and drying of leaves accompanied by decreased protein synthesis and ending in premature death of the plant (Terry et al., 2000). Toxicity thresholds are very different depending on the species and the environment.

In contrast, several authors report beneficial effects of increased Se content in the Brassicales, where low-dose Se supplementation has been shown to increase growth in *Stanleya* (Cappa et al., 2015), broccoli, radish (*Raphanus raphanistrum* ssp. *sativus* (L.) Domin), and turnip. This beneficial effect has been suggested to be due to Se-induced mimicry of S-deficiency resulting in increased S uptake by S transporters (Boldrin et al., 2016), increased anti-oxidant activity (Hartikainen et al., 2000; Proietti et al., 2013), and decreased lipid peroxidation (Xue et al., 2001; Abd Allah et al., 2016). Further, benefit of increased Se content derives from herbivory protection from insects, as shown

in *S. pinnata*, *B. juncea* and *B. oleracea* Italica Group (Freeman et al., 2006a, 2007).

Based on their capacity for Se-uptake and tolerance plants are divided into three groups: Se non-accumulators, Se-indicators, and Se-accumulators (Brown and Shrift, 1982; Terry et al., 2000; White, 2016). The majority of plants are non-accumulating species, which cannot tolerate Se tissue concentrations of more than 10–100 μg g⁻¹ DW, and rapidly show signs of Se toxicity (Hartikainen et al., 2001) on exposure to higher concentrations of Se than this. This toxicity is due to the non-specific incorporation of seleno-amino acids into proteins, replacing Cys and Met and thus disrupting protein function, and causing toxicity to the plant (Van Hoewyk, 2013).

Several members of the Brassicaceae fall into the category of Se indicator plants (also known as Se secondary accumulator plants) and are able to tolerate Se concentrations up to 1,000 μg g⁻¹ DW in their tissues and can therefore colonize soils described as

seleniferous. These include broccoli (Lyi et al., 2005; Ramos et al., 2011; Ávila et al., 2013), Indian mustard (Bañuelos and Meek, 1989), kale (Maneetong et al., 2013), turnip, and headed cabbage (Sugihara et al., 2004; see **Table 1**).

Se-accumulator plants (also known as Se hyper-accumulators) are able to accumulate Se concentrations of $>1,000 \mu\text{g g}^{-1}$ DW in their tissues with no apparent ill-effects (Pickering et al., 2003; Broadley et al., 2006; Freeman et al., 2006b; El Mehdi and Pilon-Smits, 2012). Indeed, Se hyper-accumulators show a particularly strong growth effect which may exceed a two-fold increase in biomass production (El Mehdi and Pilon-Smits, 2012). They are also the only plants able to colonize highly-seleniferous soils. Hyperaccumulation among the Brassicaceae family is found for *Cardamine hupingshanesis* (Yuan et al., 2013) and species within the genus *Stanleya* and *Thelypodium*, such as *S. pinnata* and *T. laciniatum* Endl. (Death et al., 1940; Galeas et al., 2007; Cappa and Pilon-Smits, 2014; Winkel et al., 2015). Although stems and leaves of the wildflower princesplume (*S. pinnata*) are edible and have been used as cooked greens and as medicine, when crushed they may have an unpleasant odor, are bitter and basically disliked (Whiting, 1985). It is intriguing that these species are able to accumulate an element that is not essential for higher plants (Zhang and Gladyshev, 2009), and that they not only tolerate but even grow better at tissue Se levels that are lethal for other plant species (Winkel et al., 2015).

Metabolism of Specialized Selenocompounds in the Brassicaceae

Methyl Selenocysteine

Se-indicator or -accumulating Brassicaceae are able to take up and store excess Se due to the expression of an additional Se metabolism gene, SMT, which specifically methylates selenocysteine producing MeSeCys. MeSeCys is not incorporated into the plant's proteins, as SeCys or SeMet are, and therefore does not contribute to Se toxicity (Brown and Shrift, 1981). Instead it allows the safe storage of Se away from the plant's biosynthetic machinery. The SMT gene is inducible by selenate in broccoli (Lyi et al., 2005) and has been confirmed as the key to Se-tolerance in Se-accumulating plants (Neuhierl and Bock, 1996; Neuhierl et al., 1999). Its over-expression in non-Se accumulator species, such as tobacco and tomato, has been shown to convert such plants into Se-accumulators with up to 25% of the Se in these plants found as MeSeCys (McKenzie et al., 2009; Brummell et al., 2011).

MeSeCys content has been reported for many brassicaceous crops fertilized with Se (**Table 1**). Ávila et al. (2014) hydroponically fertilized sprouts from six different *Brassica* species with 50 mM selenate for 1 week and reported MeSeCys concentrations of up to $50\text{--}100 \mu\text{g g}^{-1}$ DW (**Table 1**). Sugihara et al. (2004) have also reported high quantities of Se as MeSeCys in broccoli, Chinese cabbage, radish, and turnip sprouts. There have been few reports of MeSeCys concentration in mature crop plants, though $108 \mu\text{g g}^{-1}$ DW (Ávila et al., 2013), $1.5 \mu\text{mol g}^{-1}$ DW (Lyi et al., 2005), and $3.4 \mu\text{mol g}^{-1}$ DW (Mahn, 2017) have been reported in broccoli florets. MeSeCys and its derivative γ -glutamyl methylselenocysteine, have been

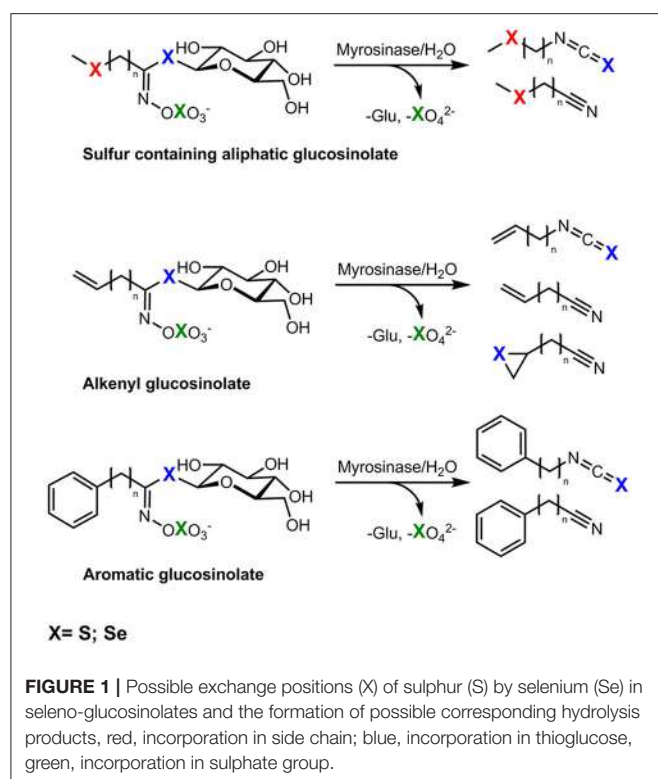
shown to have greater bioefficacy in preventing cancer cell proliferation than other Se-containing compounds (Whanger, 2002). These compounds are also believed to be responsible for the reported decreased rate of pre-cancerous cell production in rat models following ingestion of Se-enriched broccoli (Finley et al., 2001). Thus, the presence of MeSeCys is important when considering Se-metabolism in the Brassicales in the context of human health.

Selenoglucosinolates

Selenium *Brassica* accumulators contain glucosinolates, a group of secondary plant metabolites containing sulphur. Glucosinolates are β -D-thioglucoside-N-hydroxysulphates with a variable side chain. So far more than 130 glucosinolates have been reported (Agerbirk and Olsen, 2012). Due to their variable side chain glucosinolates can be classified into aliphatic, aromatic, or indole forms. The aliphatic glucosinolates can be subdivided into straight or branched chain aliphatics, alcohols or unsaturated alkenyl glucosinolates, as well into the sulphur containing aliphatic methylsulphonylalkyl (SII), methylsulphinylalkyl (SIV), or methylsulphonylalkyl glucosinolates (SVI; Hanschen et al., 2014). Thus, according to their structure, glucosinolates contain at least two, very often three, and sometimes four sulphur atoms that might be replaced by Se in plants grown in Se-rich soils. Upon cell disruption, glucosinolates are hydrolyzed by the endogenous plant enzyme myrosinase, resulting in the formation of volatile hydrolysis products such as nitriles and isothiocyanates (Kissen et al., 2009). Possible breakdown products are shown in **Figure 1**. Isothiocyanates are valued as pleiotropic agents that exert a multitude of cancer-preventive actions, among them chemopreventive phase-I enzyme inhibition and phase-II enzyme induction as well the induction of apoptosis and cell cycle arrest. Thus, these compounds are linked to the cancer-preventive effects of *Brassica* consumption (Veeranki et al., 2015).

As glucosinolates are precursors to cancer preventing substances and exchanging sulphur with Se might further enhance the bioactivity of glucosinolate hydrolysis products (Emmert et al., 2010), it is of great interest to study the effect of Se on glucosinolate production and the formation of selenoglucosinolates.

More than 40 years ago Stewart et al. (1974) reported a Se-containing sinigrin (2-propenyl glucosinolate) in horseradish (*Armoracia lapathifolia* Gilib.). In 1988, Kjær and Skrydstrup (1987) synthesized the first Se-containing glucosinolates by replacing the thioglucosidic S with Se in order to study their properties and their enzymatic hydrolysis. One year later, their group identified traces of selenogluconapin (Se-3-butetyl glucosinolate) and the corresponding isoselenocyanates in plants of *S. pinnata* after 3-weeks of Se fertilization with 100 ppm sodium selenite (Bertelsen et al., 1988), indicating incorporation of Se into the glucose moiety. However, the ratio of Se-glucosinolate to the normal glucosinolate did not exceed 1:50,000. Further, the authors did not detect significant Se incorporation in *Lepidium sativum* L., *A. lapathifolia* nor in *S. pinnata* grown at low Se-levels (Bertelsen et al., 1988).



Higher incorporation of Se into glucosinolates of *Brassica* species was reported by Matich and co-workers in 2012. Following treatment with sodium selenate (20 mL of 5 mM, twice weekly to the soil for 4 weeks) to forage rape (*cv. Maxima*), cauliflower (*cv. Liberty*), and broccoli (*cv. Triathlon*) the accumulation of methylselenoalkyl glucosinolates with up to 40% of the respective glucosinolate containing Se was reported (Matich et al., 2012). Further, they analyzed the respective volatile hydrolysis products and identified methylselenoalkyl nitriles and isothiocyanates indicating that Se was incorporated into the methylselenoalkyl side chain of the glucosinolate (Matich et al., 2012). For example, the main isothiocyanate, the 4-methylselenobutyl isothiocyanate was found in 3-times higher concentrations compared to the sulphur analog (Matich et al., 2012). In 2015, that group went on to study the distribution of Se-glucosinolates and their metabolites in these plants and reported that broccoli florets particularly accumulate methylselenoalkyl glucosinolates with up to $32.4 \mu\text{g g}^{-1}$ FW and about 50% of the glucosinolates present being selenised (Matich et al., 2015). Moreover, incorporation of Se into aromatic glucosinolates such as gluconasturtiin (2-phenylethyl glucosinolate) was observed. However, this was at very low rates (only 0.04% of the glucosinolate) and the authors observed no isoselenocyanate formation (Matich et al., 2015). Thus, Matich and coworkers concluded that selenoglucosinolate biosynthesis in *Brassica* via SeMet is the only efficient route (Matich et al., 2012, 2015).

Recently, Ouerdane et al. (2013) tentatively identified several selenoglucosinolates in seeds of *B. nigra*. As well as methylselenoalkyl glucosinolates such as glucoselenoerucin or glucoseleniberin [4-(methylseleno)butyl- and 3-(methylseleninyl)propyl glucosinolate], they reported the

detection of several non-typical glucosinolates. They postulated methylseleno-indole glucosinolates and glucosinolates acylated with methylselenoacetic acid or with methylselenosinapinic acid at position 6' of the thioglucose moiety. Typically, acylated glucosinolates are only found in seeds and not in other plant parts (Agerbirk and Olsen, 2012).

Promotion of Selenoglucosinolate Formation by Targeted Supply of N and S

The amounts of N- and S-containing compounds in plants, such as glucosinolates, can be highly variable and are strongly influenced by S and N supply (e.g., Kim et al., 2002; Li et al., 2007; Schonhof et al., 2007). Thus, *Brassica* species-specific N/S ratios distinctly stimulate the formation of glucosinolates (Fallovo et al., 2011). For example, N/S ratios between 7:1 and 10:1 promoted aliphatic alkyl and indole glucosinolates concentrations in broccoli florets (Schonhof et al., 2007), whereas high concentrations of aromatic glucosinolates occurred in turnip roots at N/S ratios <5 (Li et al., 2007). It seems that within these ranges of N/S the corresponding glucosinolate precursors of the amino acid-derived glucosinolates would be preferentially available for glucosinolate synthesis (and not for protein synthesis), such as Met for aliphatic glucosinolates and phenylalanine and tryptophan for aromatic and indole glucosinolates, respectively. Matich et al. (2015) suggested that SeMet is the decisive Se-precursor bottleneck or the major Se-precursor for the formation of selenoglucosinolates. Consequently, a targeted strategy for selenoglucosinolate production in *Brassica* plants could include the identification of a N/S/Se ratio and how to balance it for the promotion of selenoglucosinolate synthesis.

Selenium Biofortification

As Se is lacking in many diets, consumption of plants containing Se may be an effective way to increase dietary Se (McKenzie et al., 2015a). Furthermore, Se enrichment of the Brassicales produces Se-containing compounds with added bioefficacy, such as MeSeCys and potentially the selenoglucosinolates. To reach RDIs of $>55 \mu\text{g d}^{-1}$ as recommended for adult humans a 100 g serving of fresh *Brassica* food with a Se concentration of at least $5 \mu\text{g g}^{-1}$ DW is necessary. This can be achieved via biofortification; the idea of enhancing nutrients in food crops. Three methods of Se-biofortification have been used for the Brassicales; hydroponic culture, soil fertilization and foliar spraying, resulting in varying amounts of Se uptake (for references, see Table 1).

The highest reported Se concentration in the Brassicaceae have been recorded following hydroponic culture (Table 1), with Se concentrations of 1,200 and up to $1,800 \mu\text{g Se g}^{-1}$ DW reported in the florets and leaves of broccoli (Lyi et al., 2005; Ramos et al., 2011), up to $1,900 \mu\text{g Se g}^{-1}$ DW in rapid cycling cabbage leaves (Kopsell and Randle, 1999), and up to 1,800 and $2,000 \mu\text{g Se g}^{-1}$ DW in *B. juncea* shoots and seedlings, respectively (Bañuelos et al., 1990; Pilon-Smits et al., 1999; Ximenez-Embun et al., 2004). Presumably, the constant exposure of the plant's root system to the Se-enriched solution and the lack of Se-soil interactions act together to make hydroponic culture particularly efficient. The Se concentrations

achieved are dependent on the concentration of Se in the hydroponic solution and the length of time the plant is exposed, as well as the Se-accumulating capacity of the plant species, therefore direct comparisons between different experiments are difficult. However, broccoli, Indian mustard, and rapid-cycling *B. oleracea* appear to accumulate the highest Se contents following hydroponic culture ($1,800\text{--}1,900 \mu\text{g g}^{-1}$ DW in the shoot tissue, **Table 1**), taking them into the realm of the Se-hyper-accumulators. By comparison, the hydroponic culture of Brussels sprouts, cabbage, cauliflower, Chinese cabbage, kale, radish, and turnip for similar lengths of time and Se concentrations result in lower Se accumulation ($50\text{--}386 \mu\text{g g}^{-1}$ DW; **Table 1**).

Soil fertilization has also been used for Se enrichment, particularly for broccoli, resulting in a maximum reported content of $879 \mu\text{g g}^{-1}$ DW in the florets of mature, flowering plants fertilized with Se every second day for 12 days (Lee et al., 2005; **Table 1**). Recently, material from the Se-hyper-accumulator *S. pinnata* that had been grown on seleniferous soils was used to enrich the Se content of the soil broccoli plants were subsequently grown in. This resulted in a Se content of $3.5 \mu\text{g g}^{-1}$ DW in the leaves and floret material of the broccoli (Bañuelos et al., 2015). Indian mustard plants grown on naturally Se-rich soils have been shown to accumulate Se up to $150 \mu\text{g g}^{-1}$ DW in their shoot material (Van Huysen et al., 2003). Soil fertilization of other brassicaceous crops resulted in Se contents of $30\text{--}60 \mu\text{g g}^{-1}$ DW in cauliflower, radish and turnip (**Table 1**). Notably, when cabbage was grown on peat fertilized with Se at 158 mg kg^{-1} soil for 6 months Se accumulated to $1,600 \mu\text{g g}^{-1}$ DW in the leaves with no toxicity symptoms (Funes-Collado et al., 2013). This is a high concentration and presumably due to the length of time the plants were exposed to the Se treatment.

In order to develop a commercial regime for Se-enrichment of broccoli, Hsu et al. (2011) investigated foliar application of sodium selenate as a single dose to the leaves of plants growing in the field, resulting in head and upper stem tissue containing $5 \mu\text{g g}^{-1}$ DW Se. Recently, Palomo-Siguero et al. (2015) investigated the bioefficiency of Se supplied as Se-nanoparticles to the roots of radish plants hydroponically. There was no sign of Se toxicity in plants treated this way and the Se were incorporated into MeSeCys and SeMet. Se accumulation was 25% less when Se nanoparticles were used compared with selenite (**Table 1**). Nevertheless, this is the first report of Se being biotransformed from nanoparticles in plants.

Sodium selenate and sodium selenite are the most commonly used Se-sources for the enrichment of *Brassicas*. However, plants exposed to selenite have a much reduced Se content compared to those fertilized with selenate (Ximenez-Embun et al., 2004; Lyi et al., 2005). This is because selenate is taken up directly by high efficiency S transporters in the roots compared with the less efficient phosphate transporters used to take up selenite (see Section Selenium Uptake).

Transgenic approaches have also been used to successfully increase the Se and MeSeCys content of *Brassica* species. Over-expression of ATP-sulphurylase, the rate limiting step for Se uptake and assimilation, in *B. juncea* resulted in a two- to three-fold increase in Se content in the shoots (Pilon-Smits et al., 1999). A similar approach was used for SMT in *B. juncea*, resulting

in up to $4,000 \text{ Se } \mu\text{g g}^{-1}$ DW accumulating in seedlings, and $100 \mu\text{g Se g}^{-1}$ FW as MeSeCys; a four-fold increase compared with controls (Leduc et al., 2004). However, although effective, a transgenic approach to increasing Se content in crops is unlikely to be acceptable by consumers in the near future. Gene editing technologies such as CRISPR/Cas9, may offer an alternative, and ultimately more palatable method, though this technology is not so easily applied to the upregulation of genes as to down.

When producing vegetables with enhanced Se concentrations it is necessary to consider that toxic conditions might be reached in the diet of some consumer groups such as children or people with particularly high vegetable consumption. Therefore, it is important to produce plants with stable and defined Se contents so that food produced from these are safe and where advice on quantities for consumption can be relied upon. Careful consideration should be given to the amount of Se taken up by different Brassicales as well as reproducibility over the growing season. The amount of Se taken up can most effectively be controlled under hydroponic conditions. However, it is important to note that even using this method substantial differences have been noted for Se uptake in the same species (**Table 1**). Therefore, the amount of Se applied to a *Brassica* crop should be carefully determined in each case and over several growing seasons. Despite this, biofortification of crops through Se-enriched fertilizers has been conducted in Finland for the past two decades as the population was Se-deficient. Currently, the daily Se intake for the Finish population is considered to meet the Nordic and EU RDI (Alfthan et al., 2011). Thus, understanding mechanisms of Se-uptake into crop plants and how this is affected by environmental conditions is of great importance in producing biofortified plant foods.

INSTRUMENTAL APPROACHES FOR DETECTING, MEASURING, AND MONITORING SELENIUM AND ITS METABOLITES WITHIN BRASSICA SPECIES

Selenium readily substitutes for S in a non-specific manner in biological systems and is thus readily incorporated by living organisms into a variety of organic compounds which would normally contain sulphur. This process results in the biosynthesis of Se-containing amino acids, proteins and plant secondary metabolites such as glucosinolates. Biogenic production of methylselenol (MeSeH) from selenoamino acids may also result in the production of further Se-containing metabolites including selenosugars, selenosinapine, and selenourea derivatives as shown in mustard seeds (Ouerdane et al., 2013). We briefly summarize instrumental approaches for detecting, measuring, and monitoring Se and Se-containing metabolites.

Total and Inorganic Selenium

Inductively coupled plasma-optical emission spectrometry (ICP-OES) provides quantification by measuring the light emitted from excited ions and atoms at characteristic wavelengths. Excited ions and atoms are formed by reaction of the sample

in an inductively-coupled plasma (ICP) and detected by atomic emission. For Se, the detection limit is relatively high due to the poor emission intensity of Se compared to other elements. The primary detection wavelength is 196.026 nm with small interference with iron complicating the analysis of Se in iron rich samples (Ralston et al., 2008). ICP can be also coupled to mass analysers, typically a quadrupole mass spectrometer (MS) in ICP-MS. In addition, high resolution ICP-MS systems can be used to resolve Se-isotopes. Important in ICP-MS is the consideration of potential interferences and to minimize biases created by argon, germanium, and krypton isotopes. For example, the most abundant Se-isotope ^{80}Se cannot be used to measure trace Se concentrations because of the severe interference with argon-dimers, also m/z 80, that are also formed in the inductively-coupled plasma (Ralston et al., 2008; Pettine et al., 2015). Moreover, organic carbon and high sodium concentrations can non-specifically affect the Se-signal. Due to the high ionization potential of Se, the addition of organic carbon compounds such as methanol, ethanol, or propanol can enhance the ICP-MS signal for Se. Therefore, for the ICP-MS analysis of Se, it is essential to work with internal standards and use standardized approved methods. In order to reduce or eliminate polyatomic interference, devices equipped with additional collision/reaction cell (CRC) technology have been introduced. These devices allow the detection of the most abundant Se-isotopes by avoiding the interference with argon from the plasma.

Organic Selenium

In planta, Se is involved in biochemical pathways that are analogous to S, resulting in the potential production of a large number of Se-containing metabolites with widely different physical properties which make their analysis a complex task. Different strategies need to be applied to identify and quantify these chemically diverse Se-species. Most frequently

chromatographic separation methods are used for the physical separation of volatile or non-volatile Se-metabolites which are then detected, identified and measured by mass spectrometry (MS). The relatively large mass deficiency, coupled with a distinctive isotope pattern (Figure 2), and the high atomic mass relative to carbon and oxygen, greatly facilitates the detection, assignment of molecular formulae and identification of Se-containing compounds by high resolution mass spectrometry. The chromatographic methods include high performance liquid chromatography (HPLC or UHPLC), gas chromatography (GC), capillary electrophoresis (CE), and gel electrophoresis. For HPLC separations, reversed phase chromatography, ion pair chromatography, ion exchange chromatography, and size exclusion chromatography have all been employed (e.g., summarized in Lobinski et al., 2000; Uden, 2002). Among many others, anion exchange (Pedrero et al., 2007) and reversed phase column chromatography (McKenzie et al., 2009; Peñas et al., 2012) have been used for the separation of selenate, selenite, SeMet, SeMeCys, SeCys and other metabolites. More recently hydrophilic interaction liquid chromatography (HILIC) chromatography has been explored as method for analysis of amino acids and selenosugars (Aureli et al., 2012).

Selenoglucosinolates

Brassica glucosinolates may contain up to four S atoms. Substitution with Se is possible at any of these sites with the Se entering as SeMet leading to a methylselenide sidechain, as SeCys (proposed for the thioglucose moiety) or directly as selenate. To date mainly incorporation of Se via SeMet has been observed (Matich et al., 2012), but an incorporation via the SeCys into the glucose moiety was also observed (Bertelsen et al., 1988). Glucosinolates may be analyzed by HPLC or LC-MS either directly or after removal of the sulphate group. Se-glucosinolates have been successfully analyzed by

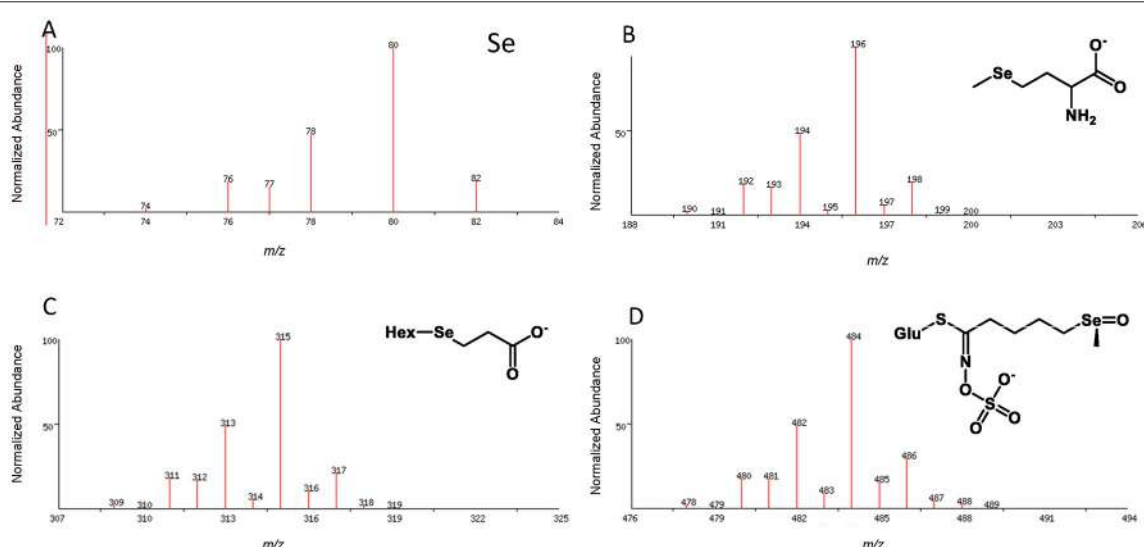


FIGURE 2 | Isotope pattern for elemental selenium (A) and as observed in the pseudomolecular ion ($M-H^-$) for organoselenium species, e.g., selenomethionine selenosugar derivative (B), Deamino-selenocysteine-selenosugar (C), Se-glucoraphanin (D); Hex, hexose; Glu, glucose.

LC-MS (Matich et al., 2012, 2015). The location of Se in selenoglucosinates may be determined by LC-MS/MS analysis using well-established negative ion fragmentations (**Figure 3**). The elemental composition of these fragment ions has been validated using tandem MS and ion trap analysis of the ^{32}S and ^{34}S isotope distributions in daughter ions derived from the glucosinolate M+2 (^{32}S and ^{34}S) pseudomolecular ion (Cataldi et al., 2010; **Figure 3**).

The increasing power of very high mass resolution LC-MS instruments to identify Se-containing metabolites in *Brassicas* has been demonstrated by Ouerdane et al. (2013). Selenosugars, selenosinapine, and selenourea derivatives have also been reported in seed of black mustard (*B. nigra*), grown on naturally Se-rich soil. These identifications are based on high resolution LC-MS, however, the exact structures of these compounds cannot be determined from the mass spectral data alone.

Selenium-containing Volatiles

Incorporation of Se into amino acids, glucosinolates, and other precursors, provides the potential for the formation of novel Se containing volatiles when these precursors are subjected to enzymatic action or non-biotic degradation. Se containing volatiles may arise via three biosynthetic pathways. Firstly direct substitution of Se for S in the amino acids cysteine, SeMeCys and Met leads to the production of dimethylselenide (Me_2Se), dimethyldiselenide (Me_2Se_2) and dimethylthioselenide (MeSSeMe) in transgenic tobacco (*Nicotiana benthamiana*; Matich et al., 2009), Se-enhanced green onions (*Allium fistulosum*; Shah et al., 2007) and *Brassicas* (Matich et al., 2012; Ouerdane et al., 2013). Enzymatic degradation of MeSeCys or SeMet may also result in the production of 2-(methylseleno)acetaldehyde, or the methylselenides so produced may react further with unsaturated aldehydes (2-alkenals) resulting from lipid oxidation (Matich et al., 2009). Thirdly, enzymatic hydrolysis of methylselenoalkyl-glucosinolates leads to methylselenoalkyl nitriles and methylselenoalkyl isothiocyanates (Matich et al., 2012, 2015).

Many Se-containing volatiles can be readily analyzed by standard GC-MS methods as used for their S-containing analogs. Gas chromatography has been used to separate Me_2Se and Me_2Se_2 and others (Kubachka et al., 2007) as well as Se-containing glucosinolate breakdown products (Matich et al.,

2012, 2015). However, selenoxides (e.g., dimethylselenoxide Me_2SeO analogous to dimethylsulphoxide Me_2SO) containing beta hydrogens ($\text{R}_2\text{CHC}(\text{SeO})\text{R}_2$) and selenones (analogous to sulphones such as dimethylsulphone Me_2SO_2) are thermally unstable above room temperatures and are not suitable for standard GC-MS analysis. For highly volatile selenides such as Me_2Se and Me_2Se_2 , headspace analysis using highly adsorbent graphite based SPME phases such as CarboxenTM or CarboxenTM-PDMS hybrid fibers (Matich et al., 2009) should be preferred. Further increases in sensitivity could be expected by the application of Stir Bar Sorptive Extraction SBSE (Twister) combined with cryofocusing of volatiles onto the GC column.

New Methods for Discovery of Selenometabolites

The finding and measurement of trace amounts of novel Se compounds in complex plant extracts can be difficult and tedious. Chromatographic separations coupled with ICP-MS reliably identify HPLC fractions containing Se but do not provide the molecular mass or information about the structure of the Se-containing molecules. This identification relies on the comparison of retention times with authentic reference compounds. Electrospray ionization mass spectrometry (ESI-MS) is very useful for the identification of Se-containing metabolites, however finding minor Se containing species in complex plant extracts is tedious and has disadvantages such as the oxidation of small Se-molecules and lower sensitivity engendered by the complex isotope distribution of Se. A robust approach, which should be also applied for the analysis of *Brassica* vegetables, is the combination of ICP-MS and ESI-MS. Such an approach has been used to investigate Se metabolites in kale (Chan et al., 2010).

Alternatively, bioinformatics approaches, based on the mass defect and Se isotopic ratios, may be used to identify Se-containing metabolites in complex plant extracts. Such strategies are susceptible to automation and the mass defect approach has been used to find Se-containing volatiles in Se-enriched green onions (*A. fistulosum*; Shah et al., 2007). The alternative would be to use the Se isotope pattern as a search requirement for the identification of putative Se-containing metabolites. Such an approach, based on relative isotope abundance and ultra-high resolution FT mass spectrometry, has been implemented to identify all S-containing metabolites in *Allium* species (Nakabayashi et al., 2013) but has not yet been applied to Se-containing metabolites. The application of such analytical approaches will help elucidate the principles that govern relationships between biological metabolites in brassicaceous vegetables and provide important tools for gaining deeper insight into Se metabolism in plants and humans.

SELENOGLUCOSINOLATES FOR HUMAN NUTRITION

Bioavailability and Metabolism of Selenoglucosinolates

Selenium is an essential micronutrient for humans, and is part of the 21st amino acid, SeCys, and therefore of selenoproteins.

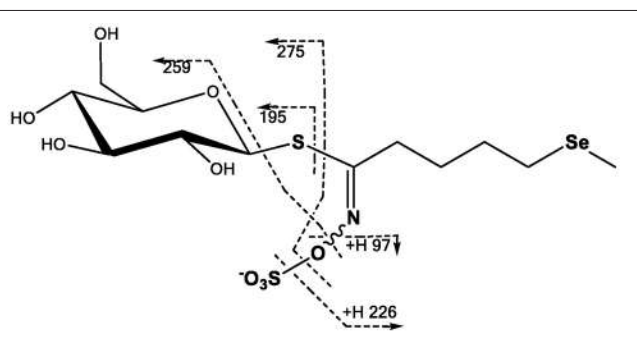


FIGURE 3 | Proposed MS/MS fragmentation pathway for glucoselenoerucin based on fragmentation analysis of glucosinolates (Cataldi et al., 2010; Lelario et al., 2012; Matich et al., 2012).

In most Se-dependent enzymes, SeCys is part of the active site, and Se often functions as a redox center in these enzymes. An detailed overview about the Se metabolism in humans is given by Roman et al. (2014). The bioavailability of Se strongly depends on the chemical form in the food. In plants a multitude of different species have been identified such as selenate, selenite, selenocystine, SeMet, selenohomocysteine, MeSeCys, γ -glutamyl-selenocystathionine, SeMet selenoxide, γ -glutamyl-MeSeCys, selenocysteineselenic acid, Se-propionylselenocysteine selenoxide, Se-methylselenomethionine, selenocystathionine, Me_2Se_2 , selenosinigrin, and other selenoglucosinolates, selenopeptides and selenowax (Navarro-Alarcon and Cabrera-Vique, 2008). In animal tissues selenocompounds are SeCys, SeMet, selenotrisulphides of cysteine, selenosugars, selenite, and selenate.

In humans, Se is mainly ingested and absorbed as SeMet, but also as selenate and selenite. The absorption efficiency of those compounds is supposed to range between 80 and 90% (Patterson et al., 1993; FAO/WHO, 2002). For all other Se-compounds, and especially for selenoglucosinolates, no studies on bioavailability have been systematically conducted so far. With regard to bioavailability, the limiting step is not the absorption of Se but rather its conversion into metabolically active forms. In general, the human body metabolizes the various Se forms into hydrogen selenide (H_2Se). H_2Se is the key metabolite formed from inorganic sodium selenite via selenodigitatathione through reduction by thiols and NADPH-dependent reductases and released from SeCys by a lyase-dependent reaction (Bjornstedt et al., 1992). H_2Se provides Se for the synthesis of selenoproteins (Ganther, 1999, **Figure 4**).

Also at this stage, it is unclear if and how selenoglucosinolates could be metabolized to release Se for selenoprotein synthesis. Alternatively, they could exert their effects only directly without modulating selenoprotein expression. In addition, their metabolism has not been studied yet.

It is also important to consider that many brassicaceous vegetables are processed by chopping, cooking or freezing. Such processing has been shown to severely influence the glucosinolate profile (Hanschen et al., 2014), and would also be expected to modulate the selenoglucosinolates within the vegetable matrix. To provide knowledge about the amount of their corresponding health-promoting breakdown products, the effect of various processing procedures on the degradation of selenoglucosinolates must be considered as well.

Chemo-Preventive Effects of Selenoglucosinolate Related Products

Selenium, often labeled as “antioxidant,” is actually not an antioxidant compound by itself, but rather an essential part of the catalytic center of selenoproteins, which are involved in protection against oxidative stress (Steinbrenner and Sies, 2009). Among the selenoproteins there are well-known redox-active selenoenzymes, such as glutathione peroxidase (GPx), thioredoxin reductase (TrxR), and methionine sulphoxide reductase B (MsrB). GPx isoenzymes reduce hydrogen peroxide (H_2O_2), organic hydroperoxides, and phospholipid hydroperoxides (only GPx4) using reduced glutathione as co-substrate (Papp et al., 2007; Brigelius-Flohe and Maiorino, 2013). TrxR isoenzymes reduce a wide variety of substrates, including

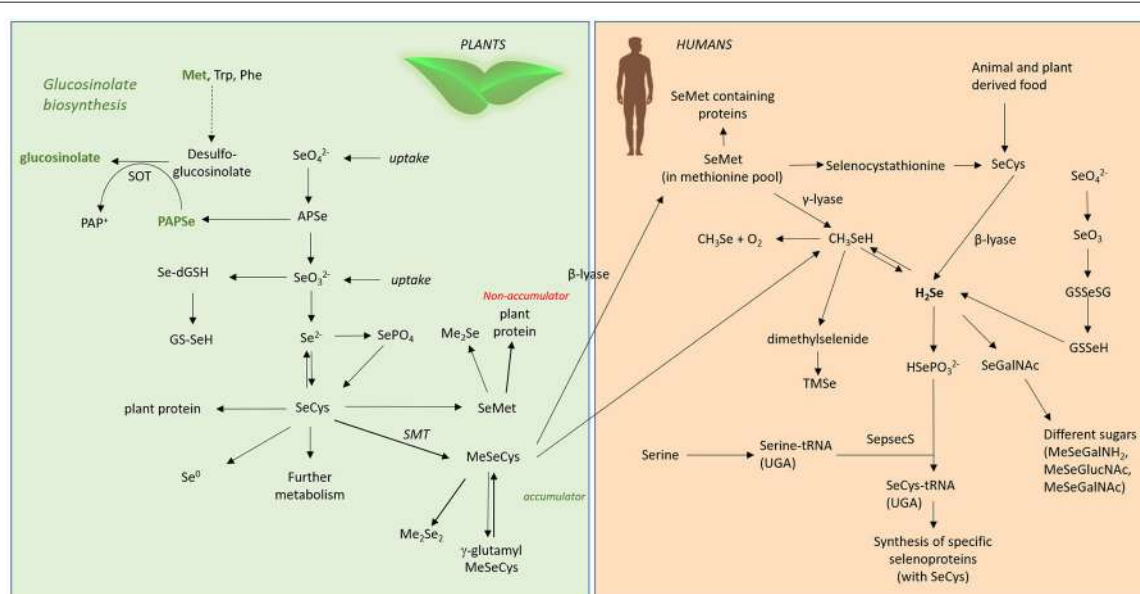


FIGURE 4 | Se metabolism in plants and humans. Met, methionine; Trp, tryptophane; Phe, phenylalanine; SOT, sulphotransferase; SeO_4^{2-} , selenate; SeO_3^{2-} , selenite; APSe, Adenosine-5'-phospho-selenate; Se-dGSH, seleno-diglutathione; GS-SeH, glutathioselenol; SePO_4 , selenophosphate; SeCys, selenocysteine; SMT, selenocysteinemethyltransferase; SeMet, selenomethionine; MeSeCys, methylselenocysteine; Me_2Se , dimethylselenide; Me_2Se_2 , dimethylselenide; γ -glutamyl-MeSeCys, γ -glutamyl-methylselenocysteine; H_2Se , hydrogen selenide; CH_3Se , methylselenyl; CH_3SeH , methylselenol; SeGalNAc, seleno-N-acetylgalactosamine; SepsecS, Sep (O-phosphoserine) tRNA:Sec (selenocysteine) tRNA synthase; HSePO_3^{2-} , selenophosphate; TMSe, trimethylselenonium.

oxidized thioredoxins, H₂O₂ and organic hydroperoxides (Bjornstedt et al., 1995), MsrB reduces free and protein-bound methionine sulphoxide to methionine (Moskovitz et al., 2002). Links between sulphur-containing isothiocyanates and selenoprotein production have been described in Barrera et al. (2012). Se in combination with isothiocyanates increased the expression of TrxR1 and GPx2 in colonic cell lines more strongly than Se or isothiocyanates alone (Barrera, 2010). In mice, the combination of the isothiocyanate sulphoraphane and a super-nutritional Se supply was most efficient in upregulating TrxR1 and glutathione-S-transferase activity in the colon (Krehl et al., 2012; see Section Selenoglucosinolates). A similar effect was observed in endothelial cells lines (Campbell et al., 2007) and in a colonic cell line (Wang et al., 2015).

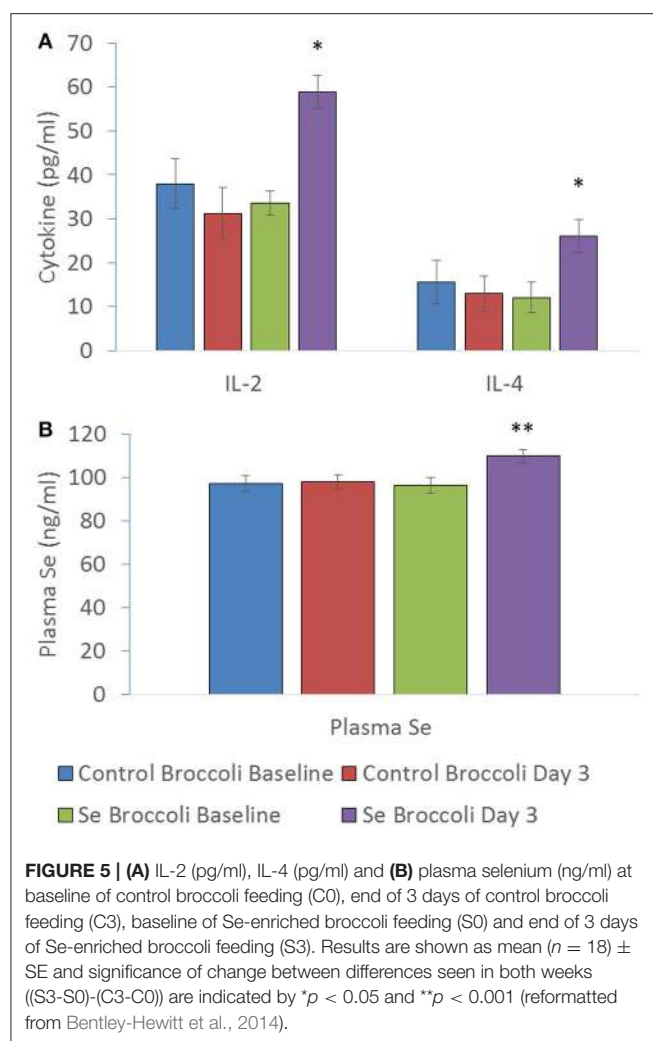
Any excess supply of Se results in increased metabolism, but marginal or no further increases in selenoprotein biosynthesis. Many of the metabolites including H₂Se and monomethylselenol are highly redox active and generate reactive oxygen species (ROS) upon reaction with and oxidation of thiols. These compounds are therefore termed as redox-active Se compounds (e.g., selenite, selenocystine, methylseleninic acid, MeSeCys that are known to exert oxidative stress; Spallholz, 1994). Such pro-oxidative properties reflect the opposite spectrum of a common consensus that Se is just an antioxidant (Jukes, 1983). Based on this, selenoglucosinolate related compounds were analyzed for their putative redox-modulatory properties: Preliminary studies focused on the effects of artificial phenylalkyl isoselenocyanates. In cell culture, these compounds were shown to be more cytotoxic compared to natural phenylalkyl isothiocyanates, to induce more apoptosis, and to inhibit cell proliferation of human melanoma cells more strongly (Sharma et al., 2008). Further, in a melanoma mouse model they reduced tumor size more efficiently than S-containing analogs (Sharma et al., 2008). The higher anticancer activity of isoselenocyanates was linked to their faster reaction with thiols such as glutathione and their more efficient modulation of the cellular redox status compared to isothiocyanates (Crampsie et al., 2012). Moreover, these artificial compounds effectively decrease Akt-3 signaling in mouse melanoma cells (Sharma et al., 2009) as well as in different xenograft models (Nguyen et al., 2011). Prostate apoptosis protein-4 can further enhance the antitumor activity of the phenylbutyl isoselenocyanate (ISC-4; Sharma et al., 2011) and a synergistic interaction of ISC-4 with the tumor therapeutic agent cetuximab was reported for colon cancer cells and a related xenograft model (Allen et al., 2013). The artificial 4-(methylsulphinyl)butyl isoselenocyanate (ISC-SFN) showed stronger induction of the redox-sensitive transcription factor Nrf2 compared to the corresponding isothiocyanate sulphoraphane (SFN; Emmert et al., 2010). Moreover, ISC-SFN was more cytotoxic to malignant cells but less toxic to non-cancer cells compared to SFN (Emmert et al., 2010). Recently, it was shown that derivatization of ISC-SFN with organofluorine substitutes can further enhance the selective toxicity toward tumor cells (Cierpial et al., 2016). Thus, selenoglucosinolates as possible precursors for related compounds studied in *in vitro* and xenograft models might have a relevant anti-cancer potential, which should be further analyzed in the future.

Selenoglucosinolate Related Compounds and Their Effects on the Immune System

Dietary Se plays an important role in inflammation and immunity. Selenium deficiency can lead to significant impairment of immune function and an increased susceptibility to infection and chronic disease (Calder and Kew, 2002). Our current knowledge suggests the effects of Se on the immune system are predominantly mediated through Se incorporation into selenoproteins (Huang et al., 2012). These selenoproteins can initiate or enhance immunity and some are involved in immune regulation.

Se enrichment of the diet is a subject of considerable debate. There is good evidence that supplementation between 100 and 200 µg day⁻¹ can be beneficial to immune function, e.g., enhanced cellular immune response and restored age-related decline in immune response in elderly patients (reviewed in Rayman et al., 2008). A study looking at Se supplementation in prawns showed increased phagocytic activity and increased respiratory burst, whilst also inducing a range of antioxidant selenoproteins (Chiu et al., 2010). This highlights the interesting paradox of Se regulating oxidation status (redox tone) in either direction e.g., reducing oxidation status or triggering oxidation. Selenylation of plant polysaccharides, known to be immune-stimulatory, were found to have enhanced immune activity *in vitro* (peripheral lymphocytes) and *in vivo* (chickens) compared to their un-selenated forms (Li et al., 2016), whilst Se-enriched *Lactobacillus brevis* induced interferon γ and interleukin 17 secretion and increased natural killer cell activity in mice compared to *L. brevis* alone (Yazdi et al., 2012). Both studies indicate the Se predominate effect may be immune enhancement rather than regulation.

Substantial evidence exists that both Se and *Brassica* compounds, mainly isothiocyanates, impact the immune response through mechanisms predominantly involving oxidation status (redox tone). There does appear to be some opposing effects of Se and isothiocyanates. The former is more commonly related to immune enhancing effects (Hoffmann and Berry, 2008) whilst the latter is linked to downregulation of immune signals (Wagner et al., 2013). Research investigating the effects of Se-enriched broccoli on immune response produced by peripheral blood mononuclear cells challenged *ex vivo* indicated that the overriding effect was immune-stimulatory (Bentley-Hewitt et al., 2014). This study involved participants consuming one serving of control broccoli or Se-enriched broccoli (200 µg Se) for 3 days with a wash-out period between dietary interventions. Plasma Se significantly increased from a baseline of 96 ± 4 ng ml⁻¹ to 110 ± 3 ng ml⁻¹ after Se-enriched broccoli consumption, along with cytokines interleukin-2 and interleukin-4 production from participants' peripheral blood mononuclear cells when stimulated with phorbol 12-myristate 13-acetate and ionomycin, whilst no increases were observed following consumption of control broccoli (**Figure 5**). Additionally Se-enriched radish sprouts were found to be immune-stimulatory in hens (Hossain et al., 2010). In contrast, a study testing Se-enriched sauerkraut extracts on a macrophage cell line *in vitro* showed anti-inflammatory effects (Peñas et al., 2012), highlighting a major discrepancy between *in vivo* and



in vitro studies. It appears that the anti-inflammatory effects of *Brassica* phytochemicals may predominate *in vitro*. This does not explain why Se supplementation of *Brassicas* in Peñas et al. (2012) have enhanced anti-inflammatory activity compared to the same *Brassica* extracts that were not supplemented with Se. However, it suggests that digestion, absorption, Se status, modification of the bioactive compounds by other cell types and/or the complexity of cellular cross talk *in vivo* may have a great influence on how immune cells respond to the bioactive compounds in Se-enriched *Brassicas*. The *in vitro* study by Peñas et al. (2012) includes an extraction procedure in an attempt to isolate the glucosinolate hydrolysis products for testing on a macrophage cell line. Therefore, it is possible that alternative seleno compounds that were removed in the process may drive the immuno-stimulatory effect *in vivo* e.g., seleno amino acids. To start to elucidate the reasons for the discrepancy between *in vitro* and *in vivo* results, one could use *in vitro* digestion of Se-enriched *Brassica* prior to exposure to cells *in vitro* and extract material to include seleno amino acids. Previous research, utilized *in vitro* digestion of Se-enriched broccoli before testing with colon cancer cells and found a reduction in H₂O₂ production,

however no inflammatory markers were measured (Tsai et al., 2013). At present, information into the effects of Se-enriched *Brassicas* on immune responses particularly human *in vivo* data is limited.

We still do not know the impact of all the Se-containing bioactives, which may be driving the immune response. Research should focus on whether naturally occurring selenoglucosinolate hydrolysis products and amino acids are more bioactive than the S-containing analogs. Additionally, research is required to ascertain whether modification to immune signals, such as increased levels of cytokines, results in a more robust immune response in humans.

CONCLUSION/FUTURE VIEW

Selenium deficiency or suboptimal Se intake is still regarded as a major health problem for about one billion people worldwide, while an even larger number may consume less Se than required for optimal protection against cancer, cardiovascular diseases, and severe infectious diseases (Haug et al., 2007). Furthermore, due to climate change and climate-soil-interactions, a global Se soil loss of about 8% is predicted by 2099 (Jones et al., 2017). These Se losses will have a higher impact on human health than predicted because Se losses for cropland and pasture are predicted to be 66 and 61%, respectively. These Se losses would be expected to increase global Se deficiency in humans further since the main Se sources for humans are plants and livestock grown on this land.

Due to their distinct biodiversity, *Brassica* vegetables are consumed regularly worldwide. Thus, Se-biofortification of *Brassica* crops is an important biotechnological tool that can be used to benefit of Se nutrition in humans. Furthermore, beside the general Se-metabolites, such as seleno-proteins and seleno aminoacids, which can be found in most plant species, *Brassicaceae* also contain specialized Se-containing compounds with health benefiting properties such as MeSeCys. Also, the recent discovery of significant amounts of the selenoglucosinolates in biofortified broccoli is encouraging as it opens a further avenue for the production of potentially health promoting compounds in this genera. However, so far no investigations have been conducted on the biosynthesis of selenoglucosinolates or on their bioefficacy in human health, which would be of particular interest due to the distinct protective potential of their potential hydrolysis products.

Increasing Se uptake by the *Brassicaceae* is best achieved via hydroponic means, where Se exposure can be carefully controlled and uptake maximized. For crops already grown using hydroponic or similar systems, such as drip lines, Se biofortification should be relatively easy to implement. However, alongside this it will be critical to consider issues relating to Se toxicity, as even *Brassicaceae* of the same species can have variable Se uptake rates. This means that a “one size fits all” approach cannot be implemented and biofortification regimes will have to be established for each crop and over the entire plant growth period in order to produce material with a known and stable Se content. Despite this, Se fertilization strategies have been successfully achieved in Finland to counter

Se deficiency and should be investigated by other countries where the malnutrition of Se effects the human health of their population.

Although, critical Se intake levels have already been determined with respect to Se undernourishment, we still need to understand the modes of action of individual Se-compounds in human metabolism before recommendations can be made for specific diseases. So far, no daily intake recommendation is established regarding the prevention of chronic diseases such as cancer or the maintenance of a well-regulated immune system. Moreover, further investigations are required to better understand the bioavailability and molecular effects of the selenoglucosinolates before determining their effective concentration for protection against chronic diseases. Achieving these goals will further establish the role Se plays in supporting human health, particularly through members of the Brassicales.

REFERENCES

- Abd Allah, E. F., Abeer, H., and Alqarawi, A. A. (2016). Mitigation of cadmium induced stress in tomato (*Solanum lycopersicum* L.) by selenium. *Pakistan J. Bot.* 48, 953–961.
- Agerbirk, N., and Olsen, C. E. (2012). Glucosinolate structures in evolution. *Phytochemistry* 77, 16–45. doi: 10.1016/j.phytochem.2012.02.005
- Ajwa, H. A., Banuelos, G. S., and Mayland, H. F. (1998). Selenium uptake by plants from soils amended with inorganic and organic materials. *J. Environ. Qual.* 27, 1218–1227. doi: 10.2134/jeq1998.00472425002700050029x
- Alfthan, G., Aspila, P., Ekholm, P., Eurola, M., Hartikainen, H., Hero, H., et al. (2011). “Nationwide supplementation of sodium selenate to commercial fertilizers: history and 25-year results from the Finnish Selenium Monitoring Programme,” in *Combating Micronutrient Deficiencies: Food Based Approaches*, eds. B. Thompson and L. Amoroso (Rome: Food and Agriculture Organization of the United Nations CAB International), 400.
- Alfthan, G., Eurola, M., Ekholm, P., Venäläinen, E.-R., Root, T., Korkkalainen, K., et al. (2015). Effects of nationwide addition of selenium to fertilizers on foods, and animal and human health in finland: from deficiency to optimal selenium status of the population. *J. Trace Elem. Med. Biol.* 31, 142–147. doi: 10.1016/j.jtemb.2014.04.009
- Allen, J. E., Gallant, J.-N., Dicker, D. T., Amin, S., Irby, R. B., Sharma, A. K., et al. (2013). The akt inhibitor isc-4 synergizes with cetuximab in 5-fu-resistant colon cancer. *PLoS ONE* 8:e59380. doi: 10.1371/annotation/aaa12360-0c90-42c3-bc43-d00022b68b81
- Araie, H., and Shiraiwa, Y. (2016). “Selenium in algae,” in *The Physiology of Microalgae*, eds M. A. Borowitzka, J. Beardall, and J. A. Raven (Heidelberg: Springer), 281–288.
- Arscott, S., and Goldman, I. (2012). Biomass effects and selenium accumulation in sprouts of three vegetable species grown in selenium-enriched conditions. *Hortscience* 47, 497–502.
- Arthur, M. A., Rubin, G., Woodbury, P. B., Schneider, R. E., and Weinstein, L. H. (1992). Uptake and accumulation of selenium by terrestrial plants growing on a coal fly-ash landfill 2. Forage and root crops. *Environ. Toxicol. Chem.* 11, 1289–1299. doi: 10.1002/etc.5620110909
- Augustine, R., Arya, G. C., Nambiar, D. M., Kumar, R., and Bisht, N. C. (2014). Translational genomics in *Brassica* crops: challenges, progress, and future prospects. *Plant Biotechnol. Rep.* 8, 65–81. doi: 10.1007/s11816-013-0298-8
- Aureli, F., Ouerdane, L., Bierla, K., Szpunar, J., Prakash, N. T., and Cubadda, F. (2012). Identification of selenosugars and other low-molecular weight selenium metabolites in high-selenium cereal crops. *Metalomics* 4, 968–978. doi: 10.1039/c2mt20085f
- Ávila, F. W., Faquin, V., Yang, Y., Ramos, S. J., Guilherme, L. R. G., Thannhauser, T. W., et al. (2013). Assessment of the anticancer compounds Se-methylselenocysteine and glucosinolates in Se-biofortified broccoli (*Brassica oleracea* L. var. *italica*) sprouts and florets. *J. Agric. Food Chem.* 61, 6216–6223. doi: 10.1021/jf4016834
- Ávila, F. W., Yang, Y., Faquin, V., Ramos, S. J., Guilherme, L. R. G., Thannhauser, T. W., et al. (2014). Impact of selenium supply on Se-methylselenocysteine and glucosinolate accumulation in selenium-biofortified *Brassica* sprouts. *Food Chem.* 165, 578–586. doi: 10.1016/j.foodchem.2014.05.134
- Bañuelos, G. S. (1996). Managing high levels of boron and selenium with trace element accumulator crops. *J. Environ. Sci. Health A Environ. Sci. Eng. Toxic Hazard. Subst. Control* 31, 1179–1196.
- Bañuelos, G. S. (2002). Irrigation of broccoli and canola with boron- and selenium-laden effluent. *J. Environ. Qual.* 31, 1802–1808.
- Bañuelos, G. S., Ajwa, H. A., Wu, L., Guo, X., Akohoue, S., and Zambrzuski, S. (1997). Selenium-induced growth reduction in *Brassica* land races considered for phytoremediation. *Ecotoxicol. Environ. Saf.* 36, 282–287.
- Bañuelos, G. S., and Meek, D. W. (1989). Selenium accumulation in selected vegetables. *J. Plant Nutr.* 12, 1255–1272.
- Bañuelos, G. S., Arroyo, I. S., Dangi, S. R., and Zambrano, M. C. (2016). Continued selenium biofortification of carrots and broccoli grown in soils once amended with se-enriched *S. pinnata*. *Front. Plant Sci.* 7:1251. doi: 10.3389/fpls.2016.01251
- Bañuelos, G. S., Arroyo, I., Pickering, I. J., Yang, S. I., and Freeman, J. L. (2015). Selenium biofortification of broccoli and carrots grown in soil amended with Se-enriched hyperaccumulator *Stanleya pinnata*. *Food Chem.* 166, 603–608. doi: 10.1016/j.foodchem.2014.06.071
- Bañuelos, G. S., Meek, D. W., and Hoffman, G. J. (1990). The influence of selenium, salinity, and boron on se uptake in wild mustard. *Plant Soil* 127, 201–206.
- Bañuelos, G. S., Pasakdee, S., and Finley, J. W. (2003). Growth response and selenium and boron distribution in broccoli varieties irrigated with poor quality water. *J. Plant Nutr.* 26, 2537–2549. doi: 10.1081/PLN-120025477
- Bañuelos, G. S., Walse, S. S., Yang, S. I., Pickering, I. J., Fakra, S. C., Marcus, M. A., et al. (2012). Quantification, localization, and speciation of selenium in seeds of canola and two mustard species compared to seed-meals produced by hydraulic press. *Anal. Chem.* 84, 6024–6030. doi: 10.1021/ac300813e
- Bañuelos, G. S., Zambrzuski, S., and Mackey, B. (2000). Phytoextraction of selenium from soils irrigated with selenium-laden effluent. *Plant Soil* 224, 251–258. doi: 10.1023/A:1004881803469
- Bañuelos, G. S., Zayed, A., Terry, N., Wu, L., Akohoue, S., and Zambrzuski, S. (1996). Accumulation of selenium by different plant species grown under increasing sodium and calcium chloride salinity. *Plant Soil* 183, 49–59.
- Bañuelos, G., Terry, N., Leduc, D. L., Pilon-Smits, E. A., and Mackey, B. (2005). Field trial of transgenic indian mustard plants shows enhanced phytoremediation of selenium-contaminated sediment. *Environ. Sci. Technol.* 39, 1771–1777. doi: 10.1021/es049035f

AUTHOR CONTRIBUTIONS

MW: Corresponding author; MS, FSH, DS, MM: Section Selenium in Brassicales; SB and DR: Section Instrumental Approaches for Detecting, Measuring, and Monitoring Selenium and Its Metabolites within Brassica Species; AK, KBH, FSH, MW: Section Selenoglucosiolates for Human Nutrition.

ACKNOWLEDGMENTS

The authors thank Royal Society Te Aparangi for funding provided by the Catalyst Seeding Fund (Project number 16-PAF-003-CSG) as well as the German Federal Office for Agriculture and Food (Project number 03/14-15-NZL) allowing this review to be written. The authors declare that all appropriate permissions have been obtained from the copyright holders of any work that has been reproduced in the manuscript (Figures 3, 5).

- Barrera, L. N. (2010). *Effect of Isothiocyanates and Selenium on Antioxidant Enzyme Expression and DNA Methylation in Colon Cancer Cells In vitro*. Ph.D. thesis, University of East Anglia.
- Barrera, L. N., Cassidy, A., Johnson, I. T., Bao, Y., and Belshaw, N. J. (2012). Epigenetic and antioxidant effects of dietary isothiocyanates and selenium: potential implications for cancer chemoprevention. *Proc. Nutr. Soc.* 71, 237–245. doi: 10.1017/S002966511200016X
- Bentley-Hewitt, K. L., Chen, R. K. Y., Lill, R. E., Hedderley, D. I., Herath, T. D., Matich, A. J., et al. (2014). Consumption of selenium-enriched broccoli increases cytokine production in human peripheral blood mononuclear cells stimulated *ex vivo*, a preliminary human intervention study. *Mol. Nutr. Food Res.* 58, 2350–2357. doi: 10.1002/mnfr.201400438
- Bertelsen, F., Gissel-Nielsen, G., Kiir, A., and Skrydstrup, T. (1988). Selenogluconolates in nature: fact or myth? *Phytochemistry* 27, 3743–3749. doi: 10.1016/0031-9422(88)83010-3
- Bjornstedt, M., Hamberg, M., Kumar, S., Xue, J., and Holmgren, A. (1995). Human thioredoxin reductase directly reduces lipid hydroperoxides by NADPH and selenocystine strongly stimulates the reaction via catalytically generated selenols. *J. Biol. Chem.* 270, 11761–11764. doi: 10.1074/jbc.270.20.11761
- Bjornstedt, M., Kumar, S., and Holmgren, A. (1992). Selenodiglutathione is a highly efficient oxidant of reduced thioredoxin and a substrate for mammalian thioredoxin reductase. *J. Biol. Chem.* 267, 8030–8034.
- Boldrin, P. F., De Figueiredo, M. A., Yang, Y., Luo, H. M., Giri, S., Hart, J. J., et al. (2016). Selenium promotes sulfur accumulation and plant growth in wheat (*Triticum aestivum*). *Physiol. Plant.* 158, 80–91. doi: 10.1111/ppl.12465
- Brigelius-Flohe, R., and Maiorino, M. (2013). Glutathione peroxidases. *Biochim. Biophys. Acta* 1830, 3289–3303. doi: 10.1016/j.bbagen.2012.11.020
- Broadley, M. R., White, P. J., Bryson, R. J., Meacham, M. C., Bowen, H. C., Johnson, S. E., et al. (2006). Biofortification of uk food crops with selenium. *Proc. Nutr. Soc.* 65, 169–181. doi: 10.1079/PNS2006490
- Brown, T. A., and Shrift, A. (1981). Exclusion of selenium from proteins of selenium-tolerant *Astragalus* species. *Plant Physiol.* 67, 1051–1053. doi: 10.1104/pp.67.5.1051
- Brown, T. A., and Shrift, A. (1982). Selenium: toxicity and tolerance in higher plants. *Biol. Rev.* 57, 59–84. doi: 10.1111/j.1469-185X.1982.tb00364.x
- Broyer, T. C., Johnson, C. M., and Huston, R. P. (1972). Selenium and nutrition of *Astragalus*. *Plant Soil* 36, 635–649. doi: 10.1007/BF01373513
- Brummell, D. A., Watson, L. M., Pathirana, R., Joyce, N. I., West, P. J., Hunter, D. A., et al. (2011). Biofortification of tomato (*Solanum lycopersicum*) fruit with the anticancer compound methylselenocysteine using a selenocysteine methyltransferase from a selenium hyperaccumulator. *J. Agric. Food Chem.* 59, 10987–10994. doi: 10.1021/jf202583f
- Buchner, P., Stuiver, C. E., Westerman, S., Wirtz, M., Hell, R., Hawkesford, M. J., et al. (2004). Regulation of sulfate uptake and expression of sulfate transporter genes in *Brassica oleracea* as affected by atmospheric H(2)S and pedospheric sulfate nutrition. *Plant Physiol.* 136, 3396–3408. doi: 10.1104/pp.104.046441
- Calder, P. C., and Kew, S. (2002). The immune system: a target for functional foods? *Br. J. Nutr.* 88(Suppl. 2), S165–177. doi: 10.1079/BJN2002682
- Campbell, L., Howie, F., Arthur, J. R., Nicol, F., and Beckett, G. (2007). Selenium and sulforaphane modify the expression of selenoenzymes in the human endothelial cell line EA.hy926 and protect cells from oxidative damage. *Nutrition* 23, 138–144. doi: 10.1016/j.nut.2006.10.006
- Cappa, J. J., and Pilon-Smits, E. A. (2014). Evolutionary aspects of elemental hyperaccumulation. *Planta* 239, 267–275. doi: 10.1007/s00425-013-1983-0
- Cappa, J. J., Yetter, C., Fakra, S., Cappa, P. J., Detar, R., Landes, C., et al. (2015). Evolution of selenium hyperaccumulation in stanleya (brassicaceae) as inferred from phylogeny, physiology and x-ray microprobe analysis. *New Phytol.* 205, 583–595. doi: 10.1111/nph.13071
- Cataldi, T. R., Lelario, F., Orlando, D., and Bufo, S. A. (2010). Collision-induced dissociation of the A + 2 isotope ion facilitates glucosinolates structure elucidation by electrospray ionization-tandem mass spectrometry with a linear quadrupole ion trap. *Anal. Chem.* 82, 5686–5696. doi: 10.1021/ac100703w
- Chan, Q. L., Afton, S. E., and Caruso, J. A. (2010). Investigation of selenium metabolites in se-enriched kale, *Brassica oleracea* a, via HPLC-ICPMS and nanoESI-ITMS. *J. Anal. Atom. Spectrom.* 25, 186–192. doi: 10.1039/B914157J
- Chang, P., and Randle, W. M. (2006). Influence of temperature on selenium and sulphur accumulation in *Brassica oleracea* L. *J. Horticult. Sci. Biotechnol.* 81, 754–758. doi: 10.1080/14620316.2006.11512133
- Charron, C. S., Kopsell, D. A., Randle, W. M., and Sams, C. E. (2001). Sodium selenate fertilisation increases selenium accumulation and decreases glucosinolate concentration in rapid-cycling *Brassica oleracea*. *J. Sci. Food Agric.* 81, 962–966. doi: 10.1002/jsfa.906
- Chen, X., Yang, G., Chen, J., Chen, X., Wen, Z., and Ge, K. (1980). Studies on the relations of selenium and Keshan disease. *Biol. Trace Elem. Res.* 2, 91–107. doi: 10.1007/BF02798589
- Chiu, S.-T., Hsieh, S.-L., Yeh, S.-P., Jian, S.-J., Cheng, W., and Liu, C.-H. (2010). The increase of immunity and disease resistance of the giant freshwater prawn, *Macrobrachium rosenbergii* by feeding with selenium-enriched-diet. *Fish Shellfish Immunol.* 29, 623–629. doi: 10.1016/j.fsi.2010.06.012
- Cierpial, T., Luczak, J., Kwiatkowska, M., Kielbasinski, P., Mielczarek, L., Wiktor ska, K., et al. (2016). Organofluorine isoselenocyanate analogues of sulforaphane: Synthesis and anticancer activity. *ChemMedChem* 11, 2398–2409. doi: 10.1002/cmdc.201600442
- Crampsie, M. A., Pandey, M. K., Desai, D., Spallholz, J., Amin, S., and Sharma, A. K. (2012). Phenylalkyl isoselenocyanates vs phenylalkyl isothiocyanates: thiol reactivity and its implications. *Chem. Biol. Interact.* 200, 28–37. doi: 10.1016/j.cbi.2012.08.022
- Curtin, D., Hanson, R., Lindley, T., and Butler, R. (2006). Selenium concentration in wheat (*Triticum aestivum*) grain as influenced by method, rate, and timing of sodium selenate application. *N. Z. J. Crop Hortic. Sci.* 34, 329–339. doi: 10.1080/01140671.2006.9514423
- De Souza, M. P., Chu, D., Zhao, M., Zayed, A. M., Ruzin, S. E., Schichness, D., et al. (1999). Rhizosphere bacteria enhance selenium accumulation and volatilization by Indian mustard. *Plant Physiol.* 119, 565–573. doi: 10.1104/pp.119.2.565
- De Souza, M. P., Pilon-Smits, E. A., Lytle, C. M., Hwang, S., Tai, J., Honma, T. S. U., et al. (1998). Rate-limiting steps in selenium assimilation and volatilization by Indian mustard. *Plant Physiol.* 117, 1487–1494. doi: 10.1104/pp.117.4.1487
- De Temmerman, L., Waegeneers, N., Thiry, C., Du Laing, G., Tack, F., and Ruttens, A. (2014). Selenium content of Belgian cultivated soils and its uptake by field crops and vegetables. *Sci. Total Environ.* 468, 77–82. doi: 10.1016/j.scitotenv.2013.08.016
- Death, O. A., Gilbert, C. S., and Epson, H. F. (1940). The use of indicator plants in locating seleniferous areas in western United States. III. Further studies. *Am. J. Bot.* 27, 564–573. doi: 10.2307/2437092
- Dhillon, K. S., and Dhillon, S. K. (2009). Accumulation and distribution of selenium in some vegetable crops in selenate-se treated clay loam soil. *Front Agric. China* 3, 366–373. doi: 10.1007/s11703-009-0070-6
- EFSA Panel on Dietetic Products, Nutrition and Allergies (NDA) (2014). Scientific opinion on dietary reference values for selenium. *EFSA J.* 12:3846. doi: 10.2903/j.efsa.2014.3846
- El Mehdaoui, A. F., and Pilon-Smits, E. A. (2012). Ecological aspects of plant selenium hyperaccumulation. *Plant Biol.* 14, 1–10. doi: 10.1111/j.1438-8677.2011.00535.x
- El-Ramady, H., Abdalla, N., Taha, H. S., Alshaal, T., El-Henawy, A., Faizy, S. E. D. A., et al. (2015). Selenium and nano-selenium in plant nutrition. *Environ. Chem. Lett.* 14, 123–147. doi: 10.1007/s10311-015-0535-1
- Emmert, S. W., Desai, D., Amin, S., and Richie Jr, J. P. (2010). Enhanced Nrf2-dependent induction of glutathione in mouse embryonic fibroblasts by isoselenocyanate analog of sulforaphane. *Bioorg. Med. Chem. Lett.* 20, 2675–2679. doi: 10.1016/j.bmcl.2010.01.044
- Fallovo, C., Schreiner, M., Schwarz, D., Colla, G., and Krumbein, A. (2011). Phytochemical changes induced by different nitrogen supply forms and radiation levels in two leafy Brassica species. *J. Agric. Food Chem.* 59, 4198–4207. doi: 10.1021/jf1048904
- FAO/WHO (2002). "Selenium," in *Human Vitamin and Mineral Requirements*, eds World Health Organization and Food and Agriculture Organization of the United Nations (Rome: FAO), 235–255.
- Farnham, M. W., Hale, A. J., Grusak, M. A., and Finley, J. W. (2007). Genotypic and environmental effects on selenium concentration of broccoli heads grown without supplemental selenium fertilizer. *Plant Breed. Z. Pflanzenzucht.* 126, 195–200. doi: 10.1111/j.1439-0523.2007.01294.x

- Feng, R., Wei, C., and Tu, S. (2013). The roles of selenium in protecting plants against abiotic stresses. *Environ. Exp. Bot.* 87, 58–68. doi: 10.1016/j.envepb.2012.09.002
- Finley, J. W., Ip, C., Lisk, D. J., Davis, C. D., Hintze, K. J., and Whanger, P. D. (2001). Cancer-protective properties of high-selenium broccoli. *J. Agric. Food Chem.* 49, 2679–2683. doi: 10.1021/jf0014821
- Freeman, J. L., Lindblom, S. D., Quinn, C. F., Fakra, S., Marcus, M. A., and Pilon-Smits, E. A. (2007). Selenium accumulation protects plants from herbivory by *Orthoptera* via toxicity and deterrence. *New Phytol.* 175, 490–500. doi: 10.1111/j.1469-8137.2007.02119.x
- Freeman, J. L., Quinn, C. F., Marcus, M. A., Fakra, S., and Pilon-Smits, E. A. (2006a). Selenium-tolerant diamondback moth disarms hyperaccumulator plant defense. *Curr. Biol.* 16, 2181–2192. doi: 10.1016/j.cub.2006.09.015
- Freeman, J. L., Zhang, L. H., Marcus, M. A., Fakra, S., McGrath, S. P., and Pilon-Smits, E. A. (2006b). Spatial imaging, speciation, and quantification of selenium in the hyperaccumulator plants *Astragalus bisulcatus* and *Stanleya pinnata*. *Plant Physiol.* 142, 124–134. doi: 10.1104/pp.106.081158
- Funes-Collado, V., Morell-Garcia, A., Rubio, R., and Lopez-Sanchez, J. F. (2013). Selenium uptake by edible plants from enriched peat. *Sci. Horticult.* 164, 428–433. doi: 10.1016/j.scienta.2013.09.052
- Galeas, M. L., Zhang, L. H., Freeman, J. L., Wegner, M., and Pilon-Smits, E. A. (2007). Seasonal fluctuations of selenium and sulfur accumulation in selenium hyperaccumulators and related nonaccumulators. *New Phytol.* 173, 517–525. doi: 10.1111/j.1469-8137.2006.01943.x
- Ganther, H. E. (1999). Selenium metabolism, selenoproteins and mechanisms of cancer prevention: complexities with thioredoxin reductase. *Carcinogenesis* 20, 1657–1666. doi: 10.1093/carcin/20.9.1657
- Gigolashvili, T., and Kopriva, S. (2014). Transporters in plant sulfur metabolism. *Front. Plant Sci.* 5:442. doi: 10.3389/fpls.2014.00442
- Guzmán-Pérez, V., Bumke-Vogt, C., Schreiner, M., Mewis, I., Borchert, A., and Pfeiffer, A. F. (2016). Benzylglucosinolate derived isothiocyanate from *Tropaeolum majus* reduces gluconeogenic gene and protein expression in human cells. *PLoS ONE* 11:e0162397. doi: 10.1371/journal.pone.0162397
- Hanschen, F. S., Lamy, E., Schreiner, M., and Rohn, S. (2014). Reactivity and stability of glucosinolates and their breakdown products in foods. *Angewandte Chemie. International Ed.* 53, 11430–11450. doi: 10.1002/anie.201402639
- Hartfiel, W., Lux, H., Lux, J., and Gentges, K. (2010). Bedeutung von Selen. *Ernährung Medizin* 25, 129–133. doi: 10.1055/s-0030-1248863
- Hartikainen, H., Pietola, L., and Simojoki, A. (2001). Quantification of fine root responses to selenium toxicity. *Agric. Food Sci.* 10, 53–58.
- Hartikainen, H., Xue, T. L., and Piironen, V. (2000). Selenium as an anti-oxidant and pro-oxidant in ryegrass. *Plant Soil* 225, 193–200. doi: 10.1023/A:1026512921026
- Haug, A., Graham, R. D., Christophersen, O. A., and Lyons, G. H. (2007). How to use the world's scarce selenium resources efficiently to increase the selenium concentration in food. *Microb. Ecol. Health Dis.* 19, 209–228. doi: 10.1080/08910600701698986
- Hawkesford, M. J. (2003). Transporter gene families in plants: the sulphate transporter gene family — redundancy or specialization? *Physiol. Plant.* 117, 155–163. doi: 10.1034/j.1399-3054.2003.00034.x
- Hawkesford, M. J., Buchner, P., Howarth, J. R., and Lu, C. (2005). Understanding the regulation of sulfur nutrition - from sulfate transporter genes to the field. *Phyton* 45, 57–67.
- Hawkesford, M. J., Davidian, J.-C., and Grignon, C. (1993). Sulphate/proton cotransport in plasma-membrane vesicles isolated from roots of *Brassica napus* L.: increased transport in membranes isolated from sulphur-starved plants. *Planta* 190, 297–304. doi: 10.1007/BF00196957
- Hoffmann, P. R., and Berry, M. J. (2008). The influence of selenium on immune responses. *Mol. Nutr. Food Res.* 52, 1273–1280. doi: 10.1002/mnfr.200700330
- Hopper, J. L., and Parker, D. R. (1999). Plant availability of selenite and selenate as influenced by the competing ions phosphate and sulfate. *Plant Soil* 210, 199–207. doi: 10.1023/A:1004639906245
- Hossain, M. S., Afrose, S., Takeda, I., and Tsujii, H. (2010). Effect of selenium-enriched Japanese radish sprouts and *Rhodobacter capsulatus* on the cholesterol and immune response of laying hens. *Asian Austral. J. Anim.* 23, 630–639. doi: 10.5713/ajas.2010.90394
- Hsu, F., Wirtz, M., Heppel, S. C., Bogs, J., Kramer, U., Khan, M. S., et al. (2011). Generation of Se-fortified broccoli as functional food: impact of Se fertilization on S metabolism. *Plant Cell Environ.* 34, 192–207. doi: 10.1111/j.1365-3040.2010.02235.x
- Huang, Z., Rose, A. H., and Hoffmann, P. R. (2012). The role of selenium in inflammation and immunity: from molecular mechanisms to therapeutic opportunities. *Antioxid. Redox Signal.* 16, 705–743. doi: 10.1089/ars.2011.4145
- Jaiswal, S. K., Prakash, R., Acharya, R., Reddy, A. V. R., and Prakash, N. T. (2012). Selenium content in seed, oil and oil cake of se hyperaccumulated *Brassica juncea* (Indian mustard) cultivated in a seleniferous region of India. *Food Chem.* 134, 401–404. doi: 10.1016/j.foodchem.2012.02.140
- Jones, G. D., Droz, B., Greve, P., Gottschalk, P., Poffet, D., McGrath, S. P., et al. (2017). Selenium deficiency risk predicted to increase under future climate change. *Proc. Natl. Acad. Sci. U.S.A.* 114, 2848–2853. doi: 10.1073/pnas.1611576114
- Jukes, T. H. (1983). Selenium, an “essential poison”. *J. Appl. Biochem.* 5, 233–234.
- Kim, S.-J., Matsuo, T., Watanabe, M., and Watanabe, Y. (2002). Effect of nitrogen and sulphur application on the glucosinolate content in vegetable turnip rape (*Brassica rapa* L.). *Soil Sci. Plant Nutr.* 48, 43–49. doi: 10.1080/00380768.2002.10409169
- Kissen, R., Rossiter, J. T., and Bones, A. M. (2009). The ‘mustard oil bomb’: Not so easy to assemble?! Localization, expression and distribution of the components of the myrosinase enzyme system. *Phytochem. Rev.* 8, 69–86. doi: 10.1007/s11101-008-9109-1
- Kjær, A., and Skrydstrup, T. (1987). Selenoglucosinolates: SYNTHESIS and enzymatic hydrolysis. *Acta Chem. Scand.* 41b, 29–33. doi: 10.3891/acta.chem.scand.41b-0029
- Kopsell, D. A., and Randle, W. M. (1999). Selenium accumulation in a rapid-cycling *Brassica oleracea* population responds to increasing sodium selenate concentrations. *J. Plant Nutr.* 22, 927–937. doi: 10.1080/01904169909365683
- Kopsell, D. A., and Randle, W. M. (2001). Genetic variances and selection potential for selenium accumulation in a rapid-cycling *Brassica oleracea* population. *J. Am. Soc. Hort. Sci.* 126, 329–335.
- Krehl, S., Loewinger, M., Florian, S., Kipp, A. P., Banning, A., Wessjohann, L. A., et al. (2012). Glutathione peroxidase-2 and selenium decreased inflammation and tumors in a mouse model of inflammation-associated carcinogenesis whereas sulforaphane effects differed with selenium supply. *Carcinogenesis* 33, 620–628. doi: 10.1093/carcin/bgr288
- Kubachka, K. M., Meija, J., Leduc, D. L., Terry, N., and Caruso, J. A. (2007). Selenium volatiles as proxy to the metabolic pathways of selenium in genetically modified *Brassica juncea*. *Environ. Sci. Technol.* 41, 1863–1869. doi: 10.1021/es0613714
- Leduc, D. L., Abdelsamie, M., Montes-Bayon, M., Wu, C. P., Reisinger, S. J., and Terry, N. (2006). Overexpressing both atp sulfurylase and selenocysteine methyltransferase enhances selenium phytoremediation traits in indian mustard. *Environ. Pollut.* 144, 70–76. doi: 10.1016/j.envpol.2006.01.008
- Leduc, D. L., Tarun, A. S., Montes-Bayon, M., Meija, J., Malit, M. F., Wu, C. P., et al. (2004). Overexpression of selenocysteine methyltransferase in *Arabidopsis* and Indian mustard increases selenium tolerance and accumulation. *Plant Physiol.* 135, 377–383. doi: 10.1104/pp.103.026989
- Lee, J., Finley, J. W., and Harnly, J. A. (2005). Effect of selenium fertilizer on free amino acid composition of broccoli (*Brassica oleracea* cv. *Majestic*) determined by gas chromatography with flame ionization and mass selective detection. *J. Agric. Food Chem.* 53, 9105–9111. doi: 10.1021/jf051221x
- Lelario, F., Bianco, G., Bufo, S. A., and Cataldi, T. R. I. (2012). Establishing the occurrence of major and minor glucosinolates in Brassicaceae by LC-ESI-hybrid linear ion-trap and Fourier-transform ion cyclotron resonance mass spectrometry. *Phytochemistry* 73, 74–83. doi: 10.1016/j.phytochem.2011.09.010
- Li, H. F., McGrath, S. P., and Zhao, F. J. (2008). Selenium uptake, translocation and speciation in wheat supplied with selenate or selenite. *New Phytol.* 178, 92–102. doi: 10.1111/j.1469-8137.2007.02343.x
- Li, S., Schonhof, I., Krumbein, A., Li, L., Stützel, H., and Schreiner, M. (2007). Glucosinolate concentration in turnip (*Brassica rapa* ssp. *rapifera* L.) roots as

- affected by nitrogen and sulfur supply. *J. Agric. Food Chem.* 55, 8452–8457. doi: 10.1021/jf070816k
- Li, X., Hou, R., Yue, C., Liu, J., Gao, Z., Chen, J., et al. (2016). The selenylation modification of epimedium polysaccharide and isatis root polysaccharide and the immune-enhancing activity comparison of their modifiers. *Biol. Trace Elem. Res.* 171, 224–234. doi: 10.1007/s12011-015-0511-4
- Lippmann, D., Lehmann, C., Florian, S., Barknowitz, G., Haack, M., Mewis, I., et al. (2014). Glucosinolates from pak choi and broccoli induce enzymes and inhibit inflammation and colon cancer differently. *Food Funct.* 5, 1073–1081. doi: 10.1039/C3FO6067G
- Lobinski, R., Edmonds, J. S., Suzuki, K. T., and Uden, P. C. (2000). Species-selective determination of selenium compounds in biological materials (Technical Report). *Pure Appl. Chem.* 72, 447–461. doi: 10.1351/pac200072030447
- Lyi, S. M., Heller, L. I., Rutzke, M., Welch, R. M., Kochian, L. V., and Li, L. (2005). Molecular and biochemical characterization of the selenocysteine Se-methyltransferase gene and Se-methylselenocysteine synthesis in broccoli. *Plant Physiol.* 138, 409–420. doi: 10.1104/pp.104.056549
- Lyons, G., Stangoulis, J., and Graham, R. (2003). High-selenium wheat: biofortification for better health. *Nutr. Res. Rev.* 16, 45–60. doi: 10.1079/NRR200255
- Mahn, A. (2017). Modelling of the effect of selenium fertilization on the content of bioactive compounds in broccoli heads. *Food Chem.* 233, 492–499. doi: 10.1016/j.foodchem.2017.04.144
- Malagoli, M., Schiavon, M., Dall'acqua, S., and Pilon-Smits, E. A. (2015). Effects of selenium biofortification on crop nutritional quality. *Front. Plant Sci.* 6:280. doi: 10.3389/fpls.2015.00280
- Maneetong, S., Chookhampaeng, S., Chantriratikul, A., Chinrasri, O., Thosaikhamp, W., Sittipout, R., et al. (2013). Hydroponic cultivation of selenium-enriched kale (*Brassica oleracea* var. *alboglabra* L.) seedling and speciation of selenium with HPLC-ICPMS. *Microchem. J.* 108, 87–91. doi: 10.1016/j.microc.2013.01.003
- Manion, L. K., Kopsell, D. E., Kopsell, D. A., Sams, C. E., and Rhykerd, R. L. (2014). Selenium fertilization influences biomass, elemental accumulations, and phytochemical concentrations in watercress. *J. Plant Nutr.* 37, 327–342. doi: 10.1080/01904167.2013.789110
- Matich, A. J., McKenzie, M. J., Brummell, D. A., and Rowan, D. D. (2009). Organoselenides from *Nicotiana tabacum* genetically modified to accumulate selenium. *Phytochemistry* 70, 1098–1106. doi: 10.1016/j.phytochem.2009.06.001
- Matich, A. J., McKenzie, M. J., Lill, R. E., Brummell, D. A., McGhie, T. K., Chen, R. K., et al. (2012). Selenoglucosinolates and their metabolites produced in *Brassica* spp. fertilised with sodium selenate. *Phytochemistry* 75, 140–152. doi: 10.1016/j.phytochem.2011.11.021
- Matich, A. J., McKenzie, M. J., Lill, R. E., McGhie, T. K., Chen, R. K., and Rowan, D. D. (2015). Distribution of selenoglucosinolates and their metabolites in *Brassica* treated with sodium selenate. *J. Agric. Food Chem.* 63, 1896–1905. doi: 10.1021/jf505963c
- McKenzie, M. J., Hunter, D. A., Pathirana, R., Watson, L. M., Joyce, N. I., Matich, A. J., et al. (2009). Accumulation of an organic anticancer selenium compound in a transgenic *Solanaceae* species shows wider applicability of the selenocysteine methyltransferase transgene from selenium hyperaccumulators. *Transgenic Res.* 18, 407–424. doi: 10.1007/s11248-008-9233-0
- McKenzie, M. J., Lill, R. E., Trolove, S. N., and Brummell, D. A. (2015a). “Biofortification of fruit and vegetables with selenium,” in *Selenium: Chemistry, Analysis, Function and Effects*, ed V. E. Preedy (Cambridge, UK: Royal Society of Chemistry), 304–323.
- McKenzie, M. J., Matich, A. J., Chen, R. K.-Y., Lill, R. E., McGhie, T. K., and Rowan, D. D. (2015b). “Identification and distribution of selenium-containing glucosinolate analogues in tissues of three brassicaceae species,” in *Molecular Physiology and Ecophysiology of Sulfur*, eds L. J. De Kok, M. Hawkesford, H. Rennenberg, K. Saito, and E. Schnug. (Cham: Springer International Publishing), 239–246.
- Moreno-Reyes, R., Suetens, C., Mathieu, F., Begaux, F., Zhu, D., Rivera, M. T., et al. (1998). Kashin-Beck Osteoarthropathy in Rural Tibet in Relation to Selenium and Iodine Status. *N. Engl. J. Med.* 339, 1112–1120. doi: 10.1056/NEJM199810153391604
- Moskovitz, J., Singh, V. K., Requena, J., Wilkinson, B. J., Jayaswal, R. K., and Stadtman, E. R. (2002). Purification and characterization of methionine sulfoxide reductases from mouse and *Staphylococcus aureus* and their substrate stereospecificity. *Biochem. Biophys. Res. Commun.* 290, 62–65. doi: 10.1006/bbrc.2001.6171
- Nakabayashi, R., Sawada, Y., Yamada, Y., Suzuki, M., Hirai, M. Y., Sakurai, T., et al. (2013). Combination of liquid chromatography-fourier transform ion cyclotron resonance-mass spectrometry with ¹³C-labeling for chemical assignment of sulfur-containing metabolites in onion bulbs. *Anal. Chem.* 85, 1310–1315. doi: 10.1021/ac302733c
- Navarro-Alarcon, M., and Cabrera-Vique, C. (2008). Selenium in food and the human body: a review. *Sci. Tot. Environ.* 400, 115–141. doi: 10.1016/j.scitotenv.2008.06.024
- Neuhierl, B., and Bock, A. (1996). On the mechanism of selenium tolerance in selenium-accumulating plants - purification and characterization of a specific selenocysteine methyltransferase from cultured cells of *Astragalus bisulcatus*. *Eur. J. Biochem.* 239, 235–238. doi: 10.1111/j.1432-1033.1996.0235ux
- Neuhierl, B., Thanbichler, M., Lottspeich, F., and Bock, A. (1999). A family of S-methylmethionine-dependent thiol/selenol methyltransferases - role in selenium tolerance and evolutionary relation. *J. Biol. Chem.* 274, 5407–5414. doi: 10.1074/jbc.274.9.5407
- Nguyen, N., Sharma, A., Nguyen, N., Sharma, A. K., Desai, D., Huh, S. J., et al. (2011). Melanoma chemoprevention in skin reconstructs and mouse xenografts using isoselenocyanate-4. *Cancer Prev. Res.* 4, 248–258. doi: 10.1158/1940-6207.CAPR-10-0106
- Oldfield, J. (2002). *Selenium World Atlas, Updated Edn*. Grimbergen: Selenium-Tellurium Development Association (STDA).
- Ouerdane, L., Aureli, F., Flis, P., Bierla, K., Preud'homme, H., Cubadda, F., et al. (2013). Comprehensive speciation of low-molecular weight selenium metabolites in mustard seeds using hplc - electrospray linear trap/orbitrap tandem mass spectrometry. *Metallomics* 5, 1294–1304. doi: 10.1039/c3mt00113j
- Palomo-Siguero, M., Lopez-Heras, M. I., Camara, C., and Madrid, Y. (2015). Accumulation and biotransformation of chitosan-modified selenium nanoparticles in exposed radish (*Raphanus sativus*). *J. Anal. Atom. Spectrom.* 30, 1237–1244. doi: 10.1039/C4JA00407H
- Papp, L. V., Lu, J., Holmgren, A., and Khanna, K. K. (2007). From selenium to selenoproteins: synthesis, identity, and their role in human health. *Antioxid. Redox Signal.* 9, 775–806. doi: 10.1089/ars.2007.1528
- Patterson, B. H., Zech, L. A., Swanson, C. A., and Levander, O. A. (1993). Kinetic modeling of selenium in humans using stable-isotope tracers. *J. Trace Elem. Electrolytes Health Dis.* 7, 117–120.
- Pedrero, Z., Elvira, D., Camara, C., and Madrid, Y. (2007). Selenium transformation studies during broccoli (*Brassica oleracea*) growing process by liquid chromatography-inductively coupled plasma mass spectrometry (LC-ICP-MS). *Anal. Chim. Acta* 596, 251–256. doi: 10.1016/j.aca.2007.05.067
- Peñas, E., Martínez-Villaluenga, C., Frias, J., Sánchez-Martínez, M. J., Pérez-Corona, M. T., Madrid, Y., et al. (2012). Se improves indole glucosinolate hydrolysis products content, se-methylselenocysteine content, antioxidant capacity and potential anti-inflammatory properties of sauerkraut. *Food Chem.* 132, 907–914. doi: 10.1016/j.foodchem.2011.11.064
- Pettine, M., McDonald, T. J., Sohn, M., Anquandah, G. A. K., Zboril, R., and Sharma, V. K. (2015). A critical review of selenium analysis in natural water samples. *Trends Environ. Anal. Chem.* 5, 1–7. doi: 10.1016/j.teac.2015.01.001
- Pickering, I. J., Wright, C., Bubner, B., Ellis, D., Persans, M. W., Yu, E. Y., et al. (2003). Chemical form and distribution of selenium and sulfur in the selenium hyperaccumulator *Astragalus bisulcatus*. *Plant Physiol.* 131, 1460–1467. doi: 10.1104/pp.014787
- Pilon-Smits, E. A. (2005). Phytoremediation. *Annu. Rev. Plant Biol.* 56, 15–39. doi: 10.1146/annurev.arplant.56.032604.144214
- Pilon-Smits, E. A., and Quinn, C. F. (2010). “Selenium metabolism in plants,” in *Cell Biology of Metal and Nutrients*, eds R. Hell and R. Mendel (Berlin: Springer), 225–241.
- Pilon-Smits, E. A., Hwang, S. B., Lytle, C. M., Zhu, Y. L., Tai, J. C., Bravo, R. C., et al. (1999). Overexpression of atp sulfurylase in indian mustard leads to increased selenate uptake, reduction, and tolerance. *Plant Physiol.* 119, 123–132. doi: 10.1104/pp.119.1.123

- Proietti, P., Nasini, L., Del Buono, D., D'amato, R., Tedeschini, E., and Businelli, D. (2013). Selenium protects olive (*Olea europaea* L.) from drought stress. *Sci. Horticult.* 164, 165–171. doi: 10.1016/j.scienta.2013.09.034
- Quinn, C. F., Prins, C. N., Freeman, J. L., Gross, A. M., Hantzis, L. J., Reynolds, R. J., et al. (2011). Selenium accumulation in flowers and its effects on pollination. *New Phytol.* 192, 727–737. doi: 10.1111/j.1469-8137.2011.03832.x
- Ralston, N. V., Unrine, J., and Wallschläger, D. (2008). *Biogeochemistry and Analysis of Selenium and Its Species*. Washington, DC: North American Metals Council.
- Ramos, S. J., Yuan, Y., Faquin, V., Guilherme, L. R. G., and Li, L. (2011). Evaluation of genotypic variation of broccoli (*Brassica oleracea* var. *italic*) in response to selenium treatment. *J. Agric. Food Chem.* 59, 3657–3665. doi: 10.1021/jf104731f
- Rayman, M. P. (2012). Selenium and human health. *Lancet* 379, 1256–1268. doi: 10.1016/S0140-6736(11)61452-9
- Rayman, M. P., Infante, H. G., and Sargent, M. (2008). Food-chain selenium and human health: spotlight on speciation. *Br. J. Nutr.* 100, 238–253. doi: 10.1017/S0007114508922522
- Roman, M., Jitaru, P., and Barbante, C. (2014). Selenium biochemistry and its role for human health. *Metalomics* 6, 25–54. doi: 10.1039/C3MT00185G
- Schiavon, M., and Pilon-Smits, E. A. (2017). The fascinating facets of plant selenium accumulation - biochemistry, physiology, evolution and ecology. *New Phytol.* 213, 1582–1596. doi: 10.1111/nph.14378
- Schonhof, I., Blankenburg, D., Müller, S., and Krumbein, A. (2007). Sulfur and nitrogen supply influence growth, product appearance, and glucosinolate concentration of broccoli. *J. Plant Nutr. Soil Sci.* 170, 65–72. doi: 10.1002/jpln.200620639
- Shah, M., Meija, J., and Caruso, J. A. (2007). Relative mass defect filtering of high-resolution mass spectra for exploring minor selenium volatiles in selenium-enriched green onions. *Anal. Chem.* 79, 846–853. doi: 10.1021/ac060703k
- Sharma, A. K., Kline, C. L., Berg, A., Amin, S., and Irby, R. B. (2011). The akt inhibitor isc-4 activates prostate apoptosis response protein-4 and reduces colon tumor growth in a nude mouse model. *Clin. Cancer. Res.* 17, 4474–4483. doi: 10.1158/1078-0432.CCR-10-2370
- Sharma, A. K., Sharma, A., Desai, D., Madhunapantula, S. V., Huh, S. J., Robertson, G. P., et al. (2008). Synthesis and anticancer activity comparison of phenylalkyl isoselenocyanates with corresponding naturally occurring and synthetic isothiocyanates. *J. Med. Chem.* 51, 7820–7826. doi: 10.1021/jm800993r
- Sharma, A., Sharma, A. K., Madhunapantula, S. V., Desai, D., Huh, S. J., Mosca, P., et al. (2009). Targeting akt3 signaling in malignant melanoma using isoselenocyanates. *Clin. Cancer. Res.* 15, 1674–1685. doi: 10.1158/1078-0432.CCR-08-2214
- Sindelarova, K., Szakova, J., Tremlova, J., Mestek, O., Praus, L., Kana, A., et al. (2015). The response of broccoli (*Brassica oleracea* convar. *italic*) varieties on foliar application of selenium: Uptake, translocation, and speciation. *Food Addit. Contam. Part A Chem. Anal. Control Expo. Risk Assess.* 32, 2027–2038. doi: 10.1080/19440049.2015.1099744
- Sors, T. G., Ellis, D. R., and Salt, D. E. (2005). Selenium uptake, translocation, assimilation and metabolic fate in plants. *Photosynth. Res.* 86, 373–389. doi: 10.1007/s11120-005-5222-9
- Spallholz, J. E. (1994). On the nature of selenium toxicity and carcinostatic activity. *Free Radic. Biol. Med.* 17, 45–64. doi: 10.1016/0891-5849(94)90007-8
- Steinbrenner, H., and Sies, H. (2009). Protection against reactive oxygen species by selenoproteins. *Biochim. Biophys. Acta* 1790, 1478–1485. doi: 10.1016/j.bbagen.2009.02.014
- Stewart, J. M., Nigiam, S. N., and McConnel, W. B. (1974). Metabolism of $\text{Na}_2^{75}\text{SeO}_4$ in horseradish: formation of selenosinigrin. *Can. J. Biochem.* 52, 144–145. doi: 10.1139/o74-023
- Sugihara, S., Kondo, M., Chihara, Y., Yuji, M., Hattori, H., and Yoshida, M. (2004). Preparation of selenium-enriched sprouts and identification of their selenium species by high-performance liquid chromatography-inductively coupled plasma mass spectrometry. *Biosci. Biotechnol. Biochem.* 68, 193–199. doi: 10.1271/bbb.68.193
- Terry, N., Zayed, A. M., De Souza, M. P., and Tarun, A. S. (2000). Selenium in higher plants. *Annu. Rev. Plant Physiol. Plant Mol. Biol.* 51:401432. doi: 10.1146/annurev.arplant.51.1.401
- Thomson, C. D. (2004). Selenium and iodine intakes and status in New Zealand and Australia. *Br. J. Nutr.* 91, 661–672. doi: 10.1079/BJN20041110
- Tian, M., Xu, X., Liu, Y., Xie, L., and Pan, S. (2016). Effect of Se treatment on glucosinolate metabolism and health-promoting compounds in the broccoli sprouts of three cultivars. *Food Chem.* 190, 374–380. doi: 10.1016/j.foodchem.2015.05.098
- Toler, H. D., Charron, C. S., Sams, C. E., and Randle, W. R. (2007). Selenium increases sulfur uptake and regulates glucosinolate metabolism in rapid-cycling *Brassica oleracea*. *J. Am. Soc. Hort. Sci.* 132, 14–19.
- Tsai, C. F., Ou, B. R., Liang, Y. C., and Yeh, J. Y. (2013). Growth inhibition and antioxidative status induced by selenium-enriched broccoli extract and selenocompounds in DNA mismatch repair-deficient human colon cancer cells. *Food Chem.* 139, 267–273. doi: 10.1016/j.foodchem.2013.02.001
- Uden, P. C. (2002). Modern trends in the speciation of selenium by hyphenated techniques. *Anal. Bioanal. Chem.* 373, 422–431. doi: 10.1007/s00216-002-1405-9
- Van Hoewyk, D. (2013). A tale of two toxicities: malformed selenoproteins and oxidative stress both contribute to selenium stress in plants. *Ann. Bot.* 112, 965–972. doi: 10.1093/aob/mct163
- Van Huysen, T., Abdel-Ghany, S., Hale, K. L., Leduc, D., Terry, N., and Pilon-Smits, E. A. (2003). Overexpression of cystathione-gamma-synthase enhances selenium volatilization in *Brassica juncea*. *Planta* 218, 71–78. doi: 10.1007/s00425-003-1070-z
- Van Huysen, T., Terry, N., and Pilon-Smits, E. A. (2004). Exploring the selenium phytoremediation potential of transgenic indian mustard overexpressing atp sulfurylase or cystathione-gamma-synthase. *Int. J. Phytoremed.* 6, 111–118. doi: 10.1080/16226510490454786
- Veeranki, O., Bhattacharya, A., Tang, L., Marshall, J., and Zhang, Y. (2015). Cruciferous vegetables, isothiocyanates, and prevention of bladder cancer. *Curr. Pharmacol. Rep.* 1, 272–282. doi: 10.1007/s40495-015-0024-z
- Verkerk, R., Schreiner, M., Krumbein, A., Ciska, E., Holst, B., Rowland, I., et al. (2009). Glucosinolates in *Brassica* vegetables: the influence of the food supply chain on intake, bioavailability and human health. *Mol. Nutr. Food Res.* 53:S219. doi: 10.1002/mnfr.200800065
- Wagner, A. E., Terschluesen, A. M., and Rimbach, G. (2013). Health promoting effects of *Brassica*-derived phytochemicals: from chemopreventive and anti-inflammatory activities to epigenetic regulation. *Oxid. Med. Cell. Longev.* 2013:964539. doi: 10.1155/2013/964539
- Wang, Y., Dacosta, C., Wang, W., Zhou, Z., Liu, M., and Bao, Y. (2015). Synergy between sulforaphane and selenium in protection against oxidative damage in colonic CCD841 cells. *Nutr. Res.* 35, 610–617. doi: 10.1016/j.nutres.2015.05.011
- Whanger, P. (2004). Selenium and its relationship to cancer: an update. *Br. J. Nutr.* 91, 11–28. doi: 10.1079/BJN20031015
- Whanger, P. D. (2002). Selenocompounds in plants and animals and their biological significance. *J. Am. Coll. Nutr.* 21, 223–232. doi: 10.1080/07315724.2002.10719214
- White, P. J. (2016). Selenium accumulation by plants. *Ann. Bot.* 117, 217–235. doi: 10.1093/aob/mcv180
- White, P. J., Bowen, H. C., Parmaguru, P., Fritz, M., Spracklen, W. P., Spiby, R. E., et al. (2004). Interactions between selenium and sulphur nutrition in *Arabidopsis thaliana*. *J. Exp. Bot.* 55, 1927–1937. doi: 10.1093/jxb/erh192
- Whiting, A. F. (1985). *Havasupai Habitat: A. F. Whiting's Ethnography of a Traditional Indian Culture*. Tuscon: University of Arizona Press.
- Winkel, L. H. E., Vriens, B., Jones, G. D., Schneider, L. S., Pilon-Smits, E., and Banuelos, G. S. (2015). Selenium cycling across soil-plant-atmosphere interfaces: a critical review. *Nutrients* 7, 4199–4239. doi: 10.3390/nu7064199
- Ximenez-Embun, P., Alonso, I., Madrid-Albaran, Y., and Camara, C. (2004). Establishment of selenium uptake and species distribution in lupine, Indian mustard, and sunflower plants. *J. Agric. Food Chem.* 52, 832–838. doi: 10.1021/jf034835f
- Xue, T. L., Hartikainen, H., and Piironen, V. (2001). Antioxidative and growth-promoting effect of selenium on senescing lettuce. *Plant Soil* 237, 55–61. doi: 10.1023/A:1013369804867
- Yazdi, M., Mahdavi, M., Kheradmand, E., and Shahverdi, A. (2012). The preventive oral supplementation of a selenium nanoparticle-enriched probiotic increases the immune response and lifespan of 4T1 breast cancer bearing mice. *Arzneimittelforschung* 62, 525–531. doi: 10.1055/s-0032-1323700
- Yuan, L., Zhu, Y., Lin, Z. Q., Banuelos, G., Li, W., and Yin, X. (2013). A novel selenocystine-accumulating plant in selenium-mine drainage area in Enshi, China. *PLoS ONE* 8:e65615. doi: 10.1371/journal.pone.0065615

- Zhang, Y., and Gladyshev, V. N. (2009). Comparative genomics of trace elements: emerging dynamic view of trace element utilization and function. *Chem. Rev.* 109, 4828–4861. doi: 10.1021/cr800557s
- Zhao, C. Y., Ren, J. G., Xue, C. Z., and Lin, E. D. (2005). Study on the relationship between soil selenium and plant selenium uptake. *Plant Soil* 277, 197–206. doi: 10.1007/s11104-005-7011-9
- Zhu, Y. G., Pilon-Smits, E. A., Zhao, F. J., Williams, P. N., and Meharg, A. A. (2009). Selenium in higher plants: understanding mechanisms for biofortification and phytoremediation. *Trends Plant Sci.* 14, 436–442. doi: 10.1016/j.tplants.2009.06.006

Conflict of Interest Statement: The authors declare that the research was conducted in the absence of any commercial or financial relationships that could be construed as a potential conflict of interest.

Copyright © 2017 Wiesner-Reinhold, Schreiner, Baldermann, Schwarz, Hanschen, Kipp, Rowan, Bentley-Hewitt and McKenzie. This is an open-access article distributed under the terms of the Creative Commons Attribution License (CC BY). The use, distribution or reproduction in other forums is permitted, provided the original author(s) or licensor are credited and that the original publication in this journal is cited, in accordance with accepted academic practice. No use, distribution or reproduction is permitted which does not comply with these terms.



Agronomic Trait Variations and Ploidy Differentiation of Kiwiberies in Northwest China: Implication for Breeding

Ying Zhang¹, Caihong Zhong², Yifei Liu³, Qiong Zhang², Xiaorong Sun⁴ and Dawei Li^{2*}

¹ Xian Botanical Garden of Shaanxi Province, Botany Institution of Shaanxi Province, Xian, China, ² Key Laboratory of Plant Germplasm Enhancement and Specialty Agriculture, Wuhan Botanical Garden, Chinese Academy of Sciences, Wuhan, China, ³ South China Botanical Garden, Chinese Academy of Sciences, Guangzhou, China, ⁴ College of Horticulture, Shenyang Agricultural University, Shenyang, China

OPEN ACCESS

Edited by:

Nadia Bertin,
Plantes et Système de Cultures
Horticoles (INRA), France

Reviewed by:

Rosario Muleo,
University of Tuscia, Italy
Liwang Liu,
Nanjing Agricultural University, China

*Correspondence:

Dawei Li
david.lee1983@163.com

Specialty section:

This article was submitted to
Crop Science and Horticulture,
a section of the journal
Frontiers in Plant Science

Received: 22 October 2016

Accepted: 18 April 2017

Published: 11 May 2017

Citation:

Zhang Y, Zhong C, Liu Y, Zhang Q, Sun X and Li D (2017) Agronomic Trait Variations and Ploidy Differentiation of Kiwiberies in Northwest China: Implication for Breeding. *Front. Plant Sci.* 8:711. doi: 10.3389/fpls.2017.00711

Polyplloid plants often have higher biomass and superior crop qualities. Breeders therefore search for crop germplasm with higher ploidy levels; however, whether higher ploidy levels are associated with better performance remains unclear. *Actinidia arguta* and related species, whose commercialized fruit are referred to as kiwiberies, harbor a series of ploidy races in nature, offering an opportunity to determine the link between ploidy levels and agronomic traits. In the present study, we determined the ploidy levels of *A. arguta* var. *arguta*, *A. arguta* var. *giraldii*, and *A. melanandra* in 16 natural populations using flow cytometry, and examined 31 trait variations in fruits, leaves and flowers by field observations, microscopic examination and laboratory analyses. Our results showed that octaploid and decaploid *A. arguta* var. *giraldii* had larger dimension of leaves than tetraploid *A. arguta* var. *arguta* and *A. melanandra*, but their fruits were significantly smaller. In addition, *A. arguta* var. *giraldii* (8x and 10x) had higher contents of nutrients such as ascorbic acid and amino acids; however, some important agronomic traits, including the content of total sugar and total acid, were significantly lower in the octaploids and decaploids. Moreover, octaploids and decaploids did not result in greater ecological adaptability for the challenging environments and climates. In conclusion, the differentiation of ecological adaptability and traits among natural kiwiberies' cytotypes suggested that higher ploidy levels are not inevitably advantageous in plants. The findings of *A. arguta* and related taxa in geographical distribution and agronomic trait variations will facilitate their germplasm domestication.

Keywords: *Actinidia arguta*, kiwiberies, sympatric area, ploidy levels, morphological variation, fruit characters, taxonomy, breeding

INTRODUCTION

Polypliody, or whole genome duplication, has been an important feature of evolution and diversification in flowering plants (Otto and Whitton, 2000). Recent analysis basing on genomic data inferred all extant angiosperms have descended from polyploid species and undergone one or more chromosomal duplication events (Soltis et al., 2009). Plant polyploidization, is not the

sum of parental genotypes (Adams and Wendel, 2005) but rather represents rapid and substantial genome reorganization, gene fractionation, transcriptomic and epigenetic alterations, and sub- and neofunctionalization of duplicate genes (Renny-Byfield and Wendel, 2014). The genomic changes subsequently altered plant physiology, morphology, phenology, and/or ecology within only one or a few generations (Levin, 2002), in particular, improved agronomical traits in some polyploid crops (Dubcovsky and Dvorak, 2007; Leitch and Leitch, 2008).

The connections between ploidy and agronomical traits in crops, however, are more complicated than breeders thought. Polyploidization provide de facto evidence for crop improvement, for example, enhanced cold adaptability in wild tetraploid potatoes (Hijmans et al., 2007) and increased vigor or higher biomass in polyploid cotton (Wendel and Cronn, 2003), rice (Cheng et al., 2007), wheat (Uddin et al., 1992), and maize (Crow, 1998; Duvick, 2001). Other changes in crop quality, such as doubling the amount of soluble proteins in *Panicum virgatum* (Warner et al., 1987), increased amino acid content in sorghum (Luo et al., 1992), improved fruit quality in tomato (Kagan-Zur et al., 1991) and higher secondary metabolite levels in *Cymbopogon* (Lavania et al., 2012), have also been observed. But there are also several disadvantages of polyploidy, including the disrupting effects of nuclear and cell enlargement and the propensity of polyploid mitosis and meiosis to produce aneuploid cells and epigenetic instability, resulting in transgressive (non-additive) gene regulation (Comai, 2005). Similarly, the elevated ploidy level does not consistently increase body size (Lavania, 2013). Even in grain crops, induced autopolyploid significantly increases seed size, but this advantage is offset by the reduction in overall seed set (Dhawan and Lavania, 1996). Basing on the comparison between diploid and its progenies, increasing evidences fuelled speculations that genome duplications may lead to the “dead-ends” (Wagner, 1970). Here, we want to ask more: do organisms with higher ploidy levels or multi-polyploidization (e.g., octoploid or decaploid) really perform better than their ancestors; namely, “the more (chromosome), the better?”

An effective way to evaluate the connections between ploidy level and ecological adaption might be focused on naturally existing that contains a mix of cytotypes. Cytogeographical investigations, particularly in sympatric areas containing different species, have provided valuable information to interpret the ecological adaption and evolutionary patterns (e.g., mating, competition) of different cytotypes (Soltis et al., 2010; King et al., 2012; Sonnleitner et al., 2016). Kiwiberies (sometimes called baby kiwi or hardy kiwifruit), the fruit of *Actinidia arguta* (Sieb. and Zucc.) Planch. ex Miq. and the related species, *A. melanandra* Franch. and *A. hypoleuca* Nakai, are widely distributed in Asia and particularly diverse in ploidy levels (2x, 4x, 6x, 8x, etc.) (Ferguson and Seal, 2008). *Actinidia arguta* var. *arguta* is distributed throughout eastern Siberia, Korea, Japan, and much of China (Li J. et al., 2007), the closely related *A. hypoleuca* is native to Japan, and *A. arguta* var. *giraldii* (Diels) Vorosh. and *A. melanandra* are unique to China. In Japan, hexaploid and heptaploid *A. arguta* var. *arguta* are found

in northern, deep-snow regions and diploid *A. hypoleuca* in warm Pacific hill areas, whereas tetraploid plants of *A. arguta* var. *arguta* are widely distributed throughout Japan (Kataoka et al., 2010; Asakura and Hoshino, 2016), indicating potential ecological sorting among the ploidy races of *A. arguta* var. *arguta* and *A. hypoleuca*. Furthermore, complex ploidy variation (4x, 6x, 8x, and 10x) was detected in a population of *A. arguta* var. *arguta* in northwest China (Li et al., 2013). However, studies of other taxa, such as *A. melanandra* and *A. arguta* var. *giraldii*, are lacking. In particular, the ecological adaptation and mechanisms (e.g., niche separation or reproductive isolation, Fowler and Levin, 1984; Van Dijk and Bijlsma, 1994; Suda et al., 2007; Sonnleitner et al., 2016) responsible for the spatial separation or co-existence of these taxa remain far from explicit.

Breeding to take advantage of the diversity of *Actinidia* taxa is a pivotal strategy to broaden the genetic basis of present kiwifruit cultivars (Ferguson, 2007; Ferguson and Huang, 2007; Datson and Ferguson, 2011). The 54 species of *Actinidia* (Li J. et al., 2007; Li X. et al., 2007) characterizing by complex ploidy variation (Ferguson and Huang, 2007), are particularly diverse in fruit characteristics, such as size, shape, skin hairiness, flesh color, flavor, nutrient content, time of maturation, and storage life (Ferguson and Seal, 2008). Kiwiberies appear to be the most promising for further commercialization of kiwifruit (Boyd et al., 2002) because their fruit have edible skins, colorful flesh, good flavor, and functional health components (Matich et al., 2003; Nishiyama et al., 2005, 2008). Except for some elite breeding programmes (Boyd et al., 2002; Bieniek, 2012), there have been few studies concerning the morphological characteristics, fruit quality and sensory analyses of natural resources to explore new fruit characteristics for further breeding. In particular, it is not known whether the biological features, including fruit size, quality, or disease resistance, of some genotypes with higher ploidy levels, such as octaploids and decaploids, might be enhanced as a result of polyploid advantage (Adams and Wendel, 2005; Udall and Wendel, 2006). For example, an autotetraploid of *A. chinensis* var. *chinensis*, derived from chromosome doubling, had significantly larger fruit than its diploid parent (Wu et al., 2012, 2013), and hexaploids [*Actinidia chinensis* var. *deliciosa* (A. Chev.) A. Chev.] are more resistant to *Pseudomonas syringae* pv. *actinidiae* than diploids (*A. chinensis* var. *chinensis*) (Datson et al., 2013).

Actinidia arguta and related species, whose have considerable commercial potential, harbor abundant ploidy and morphological variation in nature, providing the opportunity to better understand the relationship between ploidy levels and adaptability or agronomic traits. In this study, we conducted a series of morphometric and cytological investigations on sympatric populations of *A. arguta* var. *arguta*, *A. arguta* var. *giraldii*, and *A. melanandra* to assess (1) ploidy variation, distribution patterns, and potential co-existence mechanisms; (2) morphological characteristics, fruit quality, and relationships with ploidy levels. Specifically, we discuss the classification and germplasm utilization (e.g., superior germplasm having fruit with higher nutritional advantages or red or purple flesh) of these taxa for future breeding.

MATERIALS AND METHODS

Study Site and Sample Investigation

The Qinling Mountain in China is the main sympatric areas of natural kiwiberies populations, including *A. arguta* var. *arguta*, *A. arguta* var. *giraldii*, and *A. melanandra* (Figure 1A). From 2010 to 2015, we collected 16 natural populations across a 700-km region of the Qinling Mountain ($33^{\circ}21'18.42''$ – $34^{\circ}40'2.9844.138$ N and $105^{\circ}44'6.32''$ – $111^{\circ}41'46.86''$ E; Figure 1B, Table 1). In total, 119 plants with 64 *A. arguta* var. *arguta*, 28 *A. arguta* var. *giraldii*, and 27 *A. melanandra* were systematically investigated over the 5-year period. To better understand the ecological adaptability of kiwiberies, the climate and environmental data were collected and analyzed from each sample site. The altitude, latitude and longitude were recorded by GPS; and the climate data (30 years, 1980–2010) were obtained

from China Meteorological Data Service Centre (<http://data.cma.cn/>) or Local Meteorological Bureau. Here, we calculate the mean value of 30 years climate data as follows: annual cumulative sunshine hours, extreme maximum and minimum temperature, and monthly maximum and minimum temperature, humidity and precipitation.

Kiwiberies plants were initially classified as *A. arguta* var. *arguta*, *A. arguta* var. *giraldii*, or *A. melanandra* following the taxonomic treatment of *Actinidia* (Li J. et al., 2007), and their phenotypic traits were preliminary recorded. In addition, the fruits were harvested and stored fresh in a refrigerator for trait assessment in Northwest A&F University, Yangling, China. Voucher specimens of the leaves were made and deposited in the Herbarium of Xian Botanical Garden (XBG) for microscopic examination using an Olympus BH-2 microscope coupled with a Nikon D800 camera (Tokyo, Japan). The dormant canes were

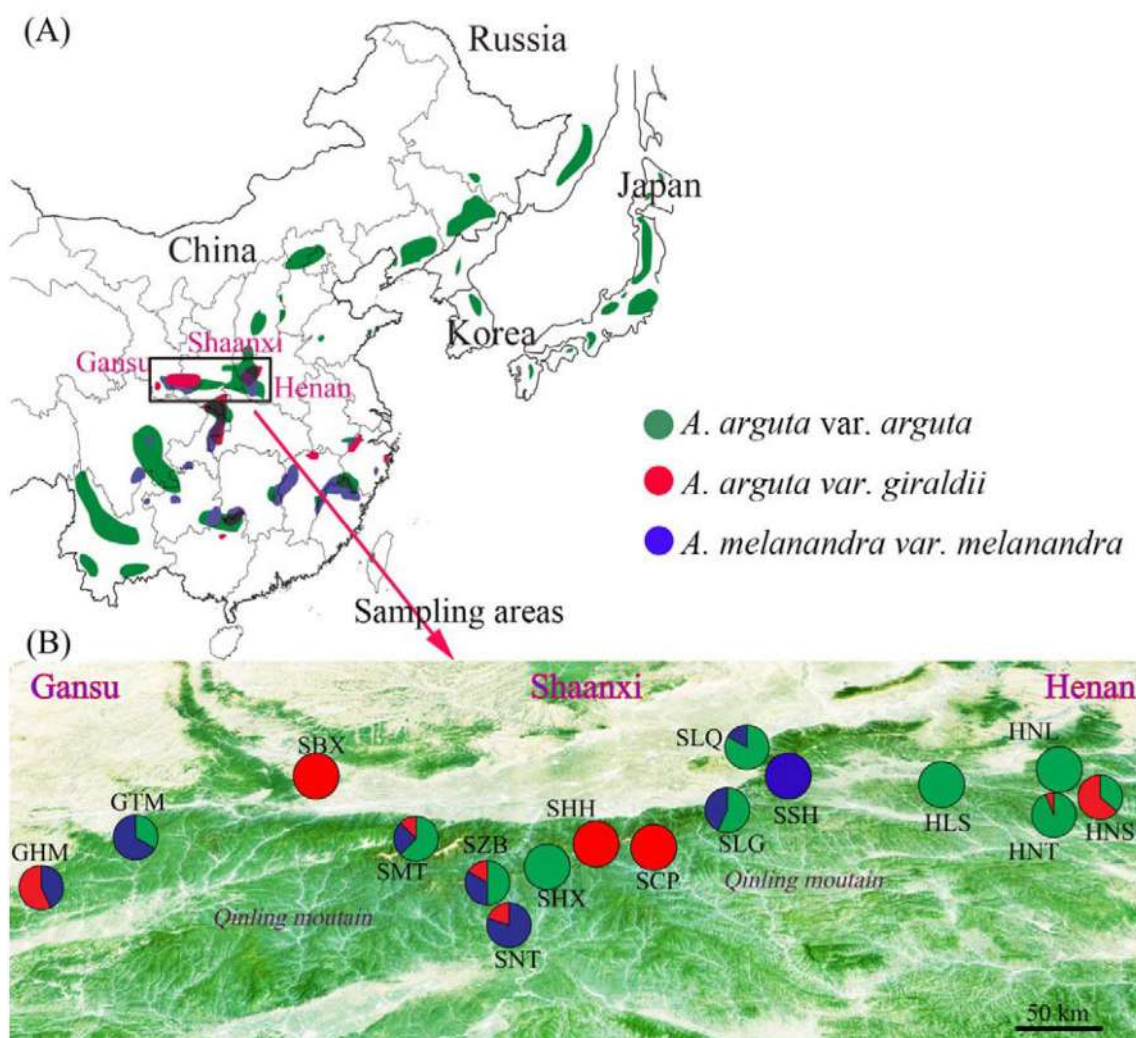


FIGURE 1 | (A) Overall geographic distribution of *Actinidia arguta* var. *arguta* (green spots), *A. arguta* var. *giraldii* (red spots), and *A. melanandra* (blue spots), and **(B)** the sympatric areas of three taxa sampled in the present study. The pie diagrams represent the proportion of *A. arguta* var. *arguta* (Green), *A. arguta* var. *giraldii* (red), and *A. melanandra* (blue) in each population. Population names and locations according to Table 1.

TABLE 1 | Ploidy and geographical distribution of *Actinidia arguta* var. *arguta*, *A. arguta* var. *giraldii* and *A. melanandra* in 16 populations from the Qinling Mountain, China.

Location	Population code	Taxon range (m)	Longitude and Latitude	Altitude	Number of ploidy races		
					4x	8x	10x
Laojielin, Luanchuan County, Henan Province	HNS	<i>A. arguta</i> var. <i>arguta</i> <i>A. arguta</i> var. <i>giraldii</i>	111°41'46.86" E, 33°41'45.02" N 111°39'30.51" E, 33°38'37.99" N	1148–1152 1005	4 1	7	
Taiping, Luanchuan County, Henan Province	HNT	<i>A. arguta</i> var. <i>arguta</i> <i>A. arguta</i> var. <i>giraldii</i>	111°39'30.51" E, 33°38'37.99" N	1005–1431	16		
Laojunshan, Luanchuan County, Henan Province	HNL	<i>A. arguta</i> var. <i>arguta</i>	111°38'12.24" E, 33°45'04.02" N	835–1111	13		
Shiziping, Lushi County, Henan Province	HLS	<i>A. arguta</i> var. <i>arguta</i>	110°51'10.89" E, 33°47'36.78" N	1140–1359	7		
Heilongkou, Shangluo County, Shaanxi Province	SSH	<i>A. melanandra</i>	109°38'59.01" E, 34°04'36.01" N	1371–1378	7		
Qingyu, Lantian County, Shaanxi Province	SLQ	<i>A. arguta</i> var. <i>arguta</i> <i>A. melanandra</i>	109°35'17.39" E, 34°13'34.48" N 1200	1185–1390	5 1		
Gepai, Lantian County, Shaanxi Province	SLG	<i>A. arguta</i> var. <i>arguta</i> <i>A. melanandra</i>	109°28'50.02" E, 33°53'09.01" N	1406–1410	8		
Peiyu, Changan County, Shaanxi Province	SCP	<i>A. arguta</i> var. <i>giraldii</i>	108°49'56.11" E, 33°52'38.03" N	1545–1587	3		
Hegou, Hu County, Shaanxi Province	SHH	<i>A. arguta</i> var. <i>giraldii</i>	108°26'54.45" E, 33°52'11.26" N	1215–1429	4	1	
Xiliu, Hu County, Shaanxi Province	SHX	<i>A. arguta</i> var. <i>arguta</i> <i>A. melanandra</i> <i>A. arguta</i> var. <i>giraldii</i>	108°23'33.56" E, 33°48'34.11" N 1500–1550 1550	1500–1672	2		
Tongche, Nongshan County, Shaanxi Province	SNT	<i>A. arguta</i> var. <i>arguta</i>	108°02'12.51" E, 33°21'18.42" N	601–696	3		
Bangfang, Zhouzhi County, Shaanxi Province	SZB	<i>A. melanandra</i> <i>A. arguta</i> var. <i>giraldii</i>	107°58'30.10" E, 33°46'03.67" N 1385	1424–1701	4		
Taibai, Mei County, Shaanxi Province	SMT	<i>A. arguta</i> var. <i>arguta</i> <i>A. melanandra</i> <i>A. arguta</i> var. <i>giraldii</i>	107°42'36.03" E, 34°05'06.47" N 1260–1300 1260–1300 1285	1260–1300	5		
Xigou, Baoji County, Shaanxi Province	SBX	<i>A. arguta</i> var. <i>giraldii</i>	107°04'28.71" E, 34°40'02.98" N	1232–1350	1	4	
Maiji, Tianshui County, Gansu Province	GTM	<i>A. arguta</i> var. <i>arguta</i> <i>A. melanandra</i>	106°06'48.05" E, 34°22'45.52" N 1603 1560–1606	1603	1	2	
Mayanhe, Hui County, Gansu Province	GHM	<i>A. melanandra</i> <i>A. arguta</i> var. <i>giraldii</i>	105°44'06.32" E, 34°05'29.13" N 1400–1520 1455–1481	1400–1520	3		
Total: 119 samples					91	17	11

pruned to graft onto rootstocks at the kiwifruit orchard at XBG for phenological investigations, and to sprout new leaves for ploidy analysis at Wuhan Botanical Garden.

Ploidy Examination

The ploidy level of each individual was determined by the flow cytometric measurement (FCM) using a flow cytometry system (Partec Cyflow Space, Germany). The new leaves of each sample were chopped and lysed in nuclear extraction buffer (solution A of High Resolution Kit, Partec, Germany) to extract the cells, followed by chromosome staining of 6-diamidino-2-phenylindole. FCM was based on a linear relationship between the fluorescence signals of the unknown sample and known internal standards. In the present study, individual DNA ploidy levels were calculated after comparing the position of the fluorescence peak of the unknown sample and the internal standard *Actinidia chinensis* var. *chinensis* "Hongyang" ($2n = 2x = 58$), whose chromosome number had previously been determined by counting. The detail experimental procedure followed the basic protocol of Li et al. (2010).

Trait Assessment

The organic size is an important aspect of polyploids that has been associated with crop yield. A total of 8 quantitative characters including leaf length and width, petiole length, flower diameter, fruit weight, length, greater, and less diameter were qualified in 119 samples at least 3 times. The measurement was carried out between 2011 and 2015 based on the following procedures. The second and third leaves on strong stems were chosen and over 30 leaves were measured in each sample using Vernier calipers (Table 2; Table S2). The diameters of 30 flowers per sample were also determined by Vernier calipers. Thirty-five fruits were randomly selected for size and average weight determination (Figure 2).

Qualitative characteristic analysis is an important feature for yield the performance of kiwiberies. Therefore, the content of soluble solids, ascorbic acid, total sugar, total acid, and total amino acids in all samples were measured according to the National Standard Methods of China. Total acid content, expressed as percentage of citric acid, was determined after titrating to pH 8.2 ± 0.1 using 0.1 M NaOH (SAC, 2008). Soluble

TABLE 2 | Dimensional variation of leaves, flowers, and fruit among *Actinidia arguta* var. *arguta*, *A. arguta* var. *giraldii*, and *A. melanandra*.

Taxon (ploidy levels)	Fruit				Flower		Leaf		
	Length (mm)	Greater diameter (mm)	Lesser diameter (mm)	Weight (g)	Diameter	Length (mm)	Width (mm)	Petiole length	
<i>A. arguta</i> var. <i>arguta</i> (4x)	27.44 ± 6.35a	18.68 ± 2.51b	17.09 ± 1.82b	4.85 ± 1.63b	19.30 ± 1.8a	97.17 ± 13.45b	56.22 ± 11.00b	44.74 ± 9.69b	
<i>A. arguta</i> var. <i>giraldii</i> (8x and 10x)	29.49 ± 6.24a	13.64 ± 1.99a	13.26 ± 1.57a	2.92 ± 1.27a	20.00 ± 1.2a	110.07 ± 13.67c	68.85 ± 15.17c	52.91 ± 12.80c	
<i>A. melanandra</i> (4x)	29.07 ± 4.00a	21.36 ± 3.10c	19.66 ± 2.831c	6.71 ± 1.52c	19.23 ± 1.6a	88.67 ± 14.35a	44.24 ± 9.65a	38.41 ± 11.21a	
P value	0.230 ^{ns}	0***	0***	0***	0.113 ^{ns}	0***	0***	0***	

Values are given as the mean ± s.d. Values in rows marked with different letters are significantly different at $p \leq 0.05$. (**P < 0.001; ns, not significant).

solids content was estimated as the mean of digital refractometer (Atago; Japan) readings taken of juice expressed from the 10 mm end caps removed from opposite ends of the fruits. Total sugar was determined by a direct titrimetric method using Fehling's reagent (SB/T 10203–1994). Ascorbic acid (vitamin C) content was estimated by titration using the colored oxidation/reduction indicator 2, 6-dichlorophenolindophenol (SAC, 1994). Total and amino acids were determined by the ninhydrin colorimetric method (Chinese standard GB/T 5009, 2003) using an automatic amino acid analyser (model 8800; Hitachi Ltd., Japan). Upon determining that, *A. arguta* var. *giraldii* had obviously higher content of total amino acids than *A. arguta* var. *arguta* and *A. melanandra*, the content of 17 amino acids were further measured. In addition, the fruit of 35 samples (14 samples of *A. arguta* var. *arguta*, 9 samples of *A. arguta* var. *giraldii* and 12 samples of *A. melanandra*) showed brilliant red-fleshed color, and their total anthocyanins were extracted by methanol/formic acid and analyzed by reversed-phase high-performance liquid chromatography (HPLC) followed the method described by Comeskey et al. (2009).

Statistics

Statistical calculations were performed using IBM® SPSS® Statistics 20 software (IBM SPSS Inc., Chicago, IL, USA). All data were assessed for normality and homogeneity of variance (Kolmogorov-Smirnov test) prior to further analysis to fulfill the requirements of statistical analysis of variance. Differences between the fruit, flower and leaf characters of *A. arguta* var. *arguta*, *A. arguta* var. *giraldii*, and *A. melanandra* were evaluated using one-way ANOVA at $p \leq 0.05$ and 0.01. When ANOVA was significant, the means were discriminated using Duncan's test. Correlations between ecological and climate factors vs. cytotypes' distribution and morphological/fruit quality characters vs. ploidy levels were estimated using Pearson's correlation analysis.

RESULTS

Cytotype Variation and Geographical Distribution

Three DNA ploidy levels (4x, 8x, and 10x) were detected: *A. arguta* var. *giraldii* at 8x and 10x, and *A. arguta* var. *arguta* and *A. melanandra* at 4x. The most frequent cytotype was 4x, accounting for 76.47% of the samples studied (Table 1).

Sympatric occurrence of *A. arguta* var. *arguta* (4x), *A. arguta* var. *giraldii* (8x and 10x) and *A. melanandra* (4x) was common in 16 sampled sites. In addition, all possible combination of cytotypes were found: 4x and 10x plants co-existed in the SZB, SMT and GHM populations; 4x and 8x plants in the HNS, HNT, and SHX populations; and 8x and 10x plants in the SHH and SBX populations.

The eco-geographical distribution of *A. arguta* var. *giraldii*, *A. arguta* var. *arguta*, and *A. melanandra* on multivariate vertical gradient, solar radiation, temperature, and precipitation are listed in Table S1 and depicted in Figure 1. Base on one-way ANOVA analysis, their eco-geographical distribution among three taxa had obvious difference of climate change, except for the maximum humidity (Figure 3). Of that, *A. arguta* var. *giraldii* (8x and 10x, 1,409 m asl) located at highest altitude, but it was not significantly different from *A. melanandra* (1,395 m). Furthermore, the individuals with higher ploidy levels (8x and 10x) did not show better adaptability for extreme temperature, higher solar radiation, lowest precipitation, and humidity. Similarity, Pearson correlation analysis demonstrated there was no significant relationship ($P < 0.01$) between ploidy levels and climate conditions (Table S3).

The Quantitative Traits of Kiwiberries' Fruits, Leaves, and Flowers

Dimensional variation of leaves, flowers, and fruits among *Actinidia arguta* var. *arguta*, *A. arguta* var. *giraldii*, and *A. melanandra* are listed in Table 2. Octaploid and decaploid *A. arguta* var. *giraldii* had larger leaves than tetraploid *A. arguta* var. *arguta* and *A. melanandra*. However, fruit sizes of tetraploid *A. melanandra* were larger than *A. arguta* var. *arguta* which were, in turn, larger than those of octaploid and decaploid *A. arguta* var. *giraldii*. There was no significant difference between the flower sizes ($P = 0.11 > 0.05$) and fruit length ($P = 0.23 > 0.05$) among the three taxa. Pearson's correlation analysis confirmed that, ploidy level of three taxa had a negative relationship with fruit size ($-0.67 < r < -0.53$; $P = 0 < 0.01$), but positively correlated with leaf size ($0.36 < r < 0.48$; $P = 0 < 0.01$) (Table S4).

Analysis of the traits related to flavor and nutrition are shown in Table 3. Obvious variations were detected among the three taxa. The total sugar content varied from 6.38 to 8.67 g/100 g F.W., while the total acid content varied from 0.89 to 1.17 g/100 g



FIGURE 2 | Natural kiwiberries (*A. arguta* and related species) collected from the Qinling Mountain, China. Fruits of (A–C) tetraploid *A. arguta* var. *arguta*, (G–I) tetraploid *A. melanandra*, (D,E) octaploid *A. arguta* var. *giraldii* (F) decaploid *A. arguta* var. *giraldii*, (J,K) elite germplasms selected from *A. arguta* var. *giraldii*.

F.W. The soluble solids content ranged from 12.85 to 13.88, which did not show significant difference ($P = 0.092 > 0.05$). The highest contents of soluble solids, total sugar, and total acid content were observed in fruit of *A. arguta* var. *arguta*, while the lowest were observed in *A. arguta* var. *giraldii*.

It is obvious that fruit of *A. arguta* var. *giraldii* contained more ascorbic acid and total amino acids than fruit from *A.*

arguta var. *arguta* and *A. melanandra*. Ascorbic acid of three taxa varied significantly from 0.05 to 0.09 g/100 g F.W. and the total amino acids varied from 0.93 to 1.63 g/100 g F.W. In particular, the contents of 17 amino acids in octaploid and decaploid *A. arguta* var. *giraldii* were generally higher than that in other two tetraploid taxa in present study (Table 3; Figure 4). Moreover, high standard deviations (e.g., total sugar in *A. arguta*

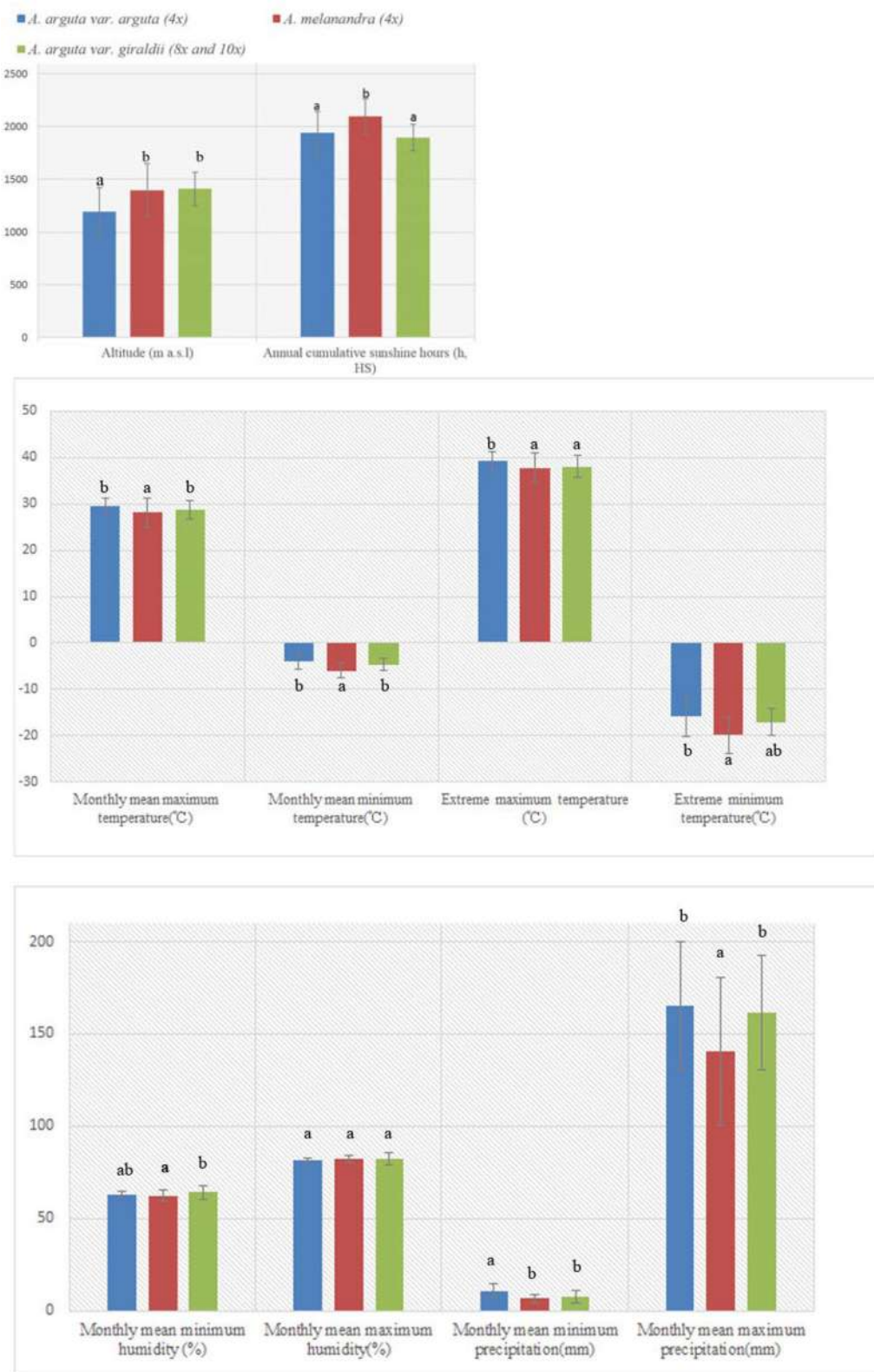


FIGURE 3 | The effect of climate and environment on *Actinidia arguta* var. *arguta*, *A. arguta* var. *giraldii* and *A. melanandra*.

TABLE 3 | Concentrations of total sugars, soluble solids, total anthocyanin, total acids, ascorbic acid, and amino acids in fruit of *Actinidia arguta* var. *arguta*, *A. arguta* var. *giraldii*, and *A. melanandra* collected from the Qinling Mountain, China (g/100 g fresh weight).

Species	Total sugar	Soluble solids content (%)	Total anthocyanin	Total acid	Ascorbic acid	Total amino acid
<i>A. arguta</i> var. <i>arguta</i>	8.66336 ± 1.5416b	13.88 ± 2.15a	1.61 ± 1.11	1.1683 ± 0.2754a	0.0518 ± 0.0186a	0.9298 ± 0.1958a
<i>A. arguta</i> var. <i>giraldii</i>	6.3786 ± 1.9987a	12.85 ± 1.91a	6.06 ± 2.18	0.8939 ± 0.1618a	0.0889 ± 0.0366b	1.6338 ± 0.3570b
<i>A. melanandra</i>	8.5785 ± 0.9452b	13.68 ± 2.01a	6.82 ± 2.67	1.0759 ± 0.2694b	0.07871 ± 0.016b	0.9522 ± 0.0959a
P-value	0***	0.092ns	0.02**	0***	0***	0***

Values are given as the mean ± s.d. Values in rows marked with different letters are significantly different at $p \leq 0.05$.

, *, at $P < 0.01, 0.001$, respectively; ns, not significant.

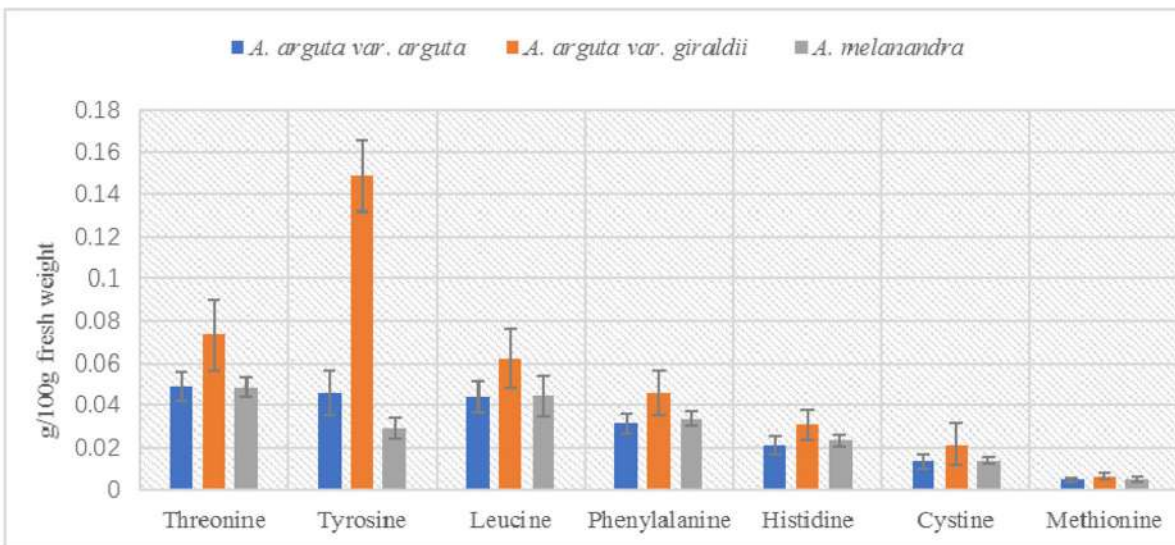
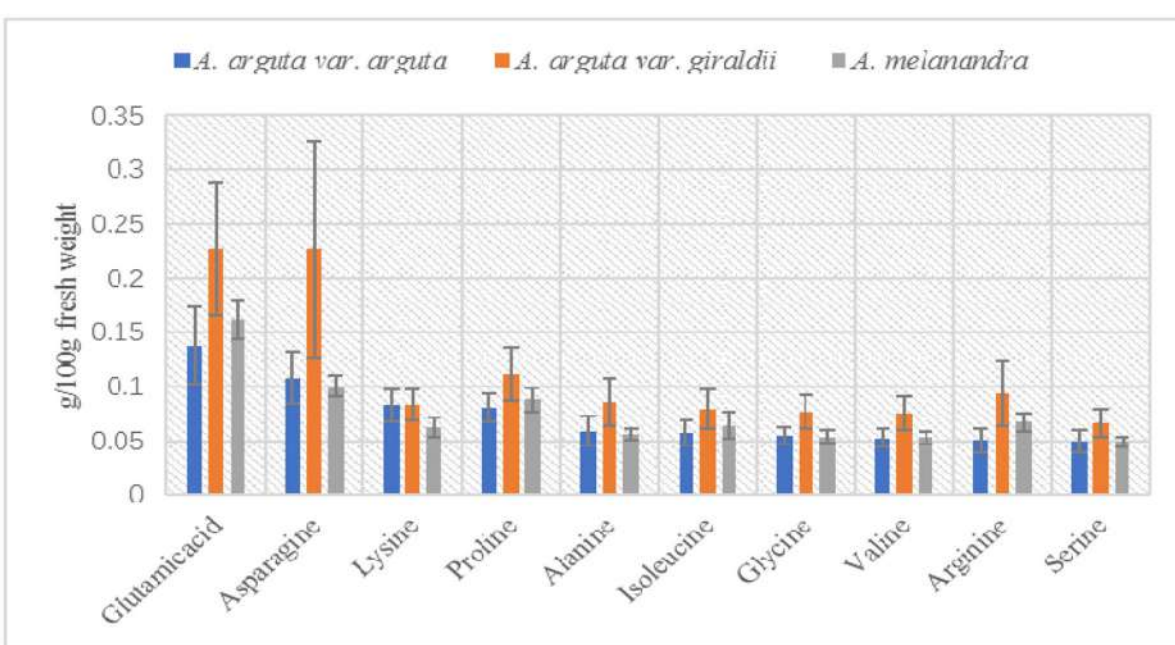


FIGURE 4 | The differentiation of 17 amino acids content among *Actinidia arguta* var. *arguta*, *A. arguta* var. *giraldii* and *A. melanandra*.

var. giraldii: 6.3786 ± 1.998 ; Table 3) within taxa indicate high intra-variability in natural kiwiberies.

Morphological and Phenological Variation

Fruit morphology of three taxa examined was highly variable both in the shape and color. *A. arguta* var. *arguta* predominantly had green fruit, whereas the fruits of *A. melanandra* and *A. arguta* var. *giraldii* were red or purple in color that differed in intensity (Figure 2). The average anthocyanins contents in *A. arguta* var. *giraldii* (6.11 mg/100 g F. W.) and *A. melanandra* (6.82 mg/100 g F. W.) are higher than *A. arguta* var. *arguta* (1.61 mg/100 g F. W.) in studied samples. Fruit shape of *A. arguta* var. *arguta* and *A. melanandra* (including ovoid, round, globose, oblong, and ellipsoidal) was more variable than *A. arguta* var. *giraldii*, whose fruit was similar in length but much leaner (Table 2).

Leaf shape and texture were similar in all three taxa. There was some micro-variation in the characteristics of the lower surface of the leaves (Figure S1). First, the lower surface of *A. melanandra* leaves were glaucous (Figure S1B), while this covering was almost completely absent from the leaves of both *A. arguta* var. *arguta* (Figure S1A) and *A. arguta* var. *giraldii* (Figures S1C,D). Secondly, the mid-vein on the lower surface of the leaves of *A. arguta* var. *giraldii* had a curly tomentum (Figures S1C,D), which was absent or very sparse on leaves of *A. arguta* var. *arguta* and *A. melanandra*.

There was no significant difference between the flower morphology of the three taxa (Figure S2). The flowers typically had white to light green petals, white filaments, and dark brown or black anthers. However, there were significant differences in phenology (Figure S3). *A. arguta* var. *arguta* (4x) and *A. melanandra* (4x) flowered in late April, partially overlapping from 2014 to 2016, whereas *A. arguta* var. *giraldii* (8x and 10x) flowered much later in mid-May. The ploidy races (8x and 10x) of *A. arguta* var. *giraldii* did not differ significantly in flowering time.

DISCUSSION

The Ploidy Variations, Distribution Patterns and Co-existent Mechanisms

High-throughput ploidy analyses based on flow cytometry have revolutionized the study of ploidy variations and cytogeography of *Actinidia* species (Ollitrault-Sammarelli et al., 1994; Yan et al., 1997; Li et al., 2010), the chromosomes of which are particularly small and numerous (e.g., decaploid, $2n = 10x = 290$). Octoploids and decaploids were initially discovered in natural *A. arguta* var. *giraldii* var. *giraldii*, which scattered in Qinling Mountains. Tetraploid *A. arguta* var. *giraldii* var. *arguta* and *A. melanandra* are the predominant ploidy races (76.47%), consistent with previous studies in Japan (Kataoka et al., 2010) and China (Li et al., 2013). Diploid kiwiberry (*A. hypoleuca*) was documented in Japan (Watanabe et al., 1990; Kataoka et al., 2010) that normally localized in relatively warm Pacific regions. Surprisingly, diploid species, as ancestors of polyploid races, were absented from the distributional areas of *A. arguta* var. *giraldii* and *A. melanandra*. The competitive exclusion could lead to their elimination from sympatric areas by polyploid

progenies, who frequently grow larger and faster, with higher yields and better resistance to disease (Fowler and Levin, 1984; Te Beest et al., 2012; Renny-Byfield and Wendel, 2014). To sum up, we cautiously concluded that natural kiwiberies (*A. arguta* var. *giraldii* and related species) has the ploidy levels as following: *A. hypoleuca* -2x, *A. melanandra* -4x, *A. arguta* var. *giraldii* var. *arguta* -4x, 6x, 7x, and 8x, *A. arguta* var. *giraldii* var. *giraldii* -8x and 10x.

The distributional pattern in sympatric areas of *A. arguta* var. *giraldii* var. *arguta*, *A. arguta* var. *giraldii* var. *giraldii*, and *A. melanandra* is characterized by a high frequency of mixed-ploidy populations (56.25%). The cytotype mixture was considered to be an evolutionarily unstable pattern, likely reflecting *in situ* formation or frequent cytotype immigration, consistent with the minority cytotype exclusion model (Levin, 1975), resulting in the elimination of the minority cytotypes (Baack, 2005; Zozomová-Lihová et al., 2015). Recent studies, however, have shown that mixed-cytotype populations are frequent and that balancing selection is commonly observed in these populations (Burton and Husband, 1999; Keeler, 2004; Kao, 2007; Castro et al., 2012; Duchoslav et al., 2016). Theoretical studies suggest that the long-term sympatric growth of cytotypes can only be maintained when different ploidy races have strong post- or prezygotic isolation mechanisms (Levin, 1975; Rodríguez, 1996). In the present study, no obvious niche differentiation was observed within the population to balance the spatial segregation of polyploidy species. However, over the three years studied, tetraploids consistently flowered much earlier than octaploids and decaploids (Figure S3). Divergence in flowering time is a by-product of natural selection, potentially resulting in reproductive isolation to maintain the co-existence of cytotypes (Van Dijk and Bijlsma, 1994; Petit et al., 1997); in the present study, the prezygotic isolation mechanism also played an important role in the co-existence of cytotypes in the 4x and 8x (HNA and HNT) and 4x and 10x populations (SZB and GHM).

The Plus, the Better? Higher Ploidy Level vs. Ecological Adaption and Agnomical Traits

Polyploids are deemed to be more resistant to extreme condition (Stebbins, 1985; Brochmann et al., 2004), such as higher altitude, cold, heat, or drought stress, which lead them more easier to invasion of new habitats (Te Beest et al., 2012). For example, a systematic investigation of the allopolyploid, autoploid, and diploid hybrid species along an elevation gradient from sea level to 4,500 m within British Columbia, Canada, provided evidence that polyploids were disproportionately present at high elevations (Vamosi and McEwen, 2012). Previous studies within *Actinidia* genus have shown that hexaploid *A. chinensis* var. *deliciosa* plants in China grow at higher altitudes than both tetraploid and diploid *A. chinensis* var. *chinensis* plants (Li et al., 2010) and hexaploid *A. arguta* var. *giraldii* var. *arguta* plants are geographically localized in the colder regions of Japan, whereas diploid plants of the closely related *A. hypoleuca* are located in warmer regions (Kataoka et al., 2010). In this study, *A. arguta*

var. giraldii var. *giraldii*, with higher ploidy levels ($8x$ and $10x$), were scattered in higher altitude than *A. arguta* var. *giraldii* var. *argute*, but the difference is no significant with tetraploid *A. melanandra*. In particular, the tetraploid *A. melanandra* could survived in more challenging climate, extreme temperature and few precipitation for instance (Figure 2). With diversified species, the tetraploid accounts for the highest proportion of ploidy races in natural kiwiberies, and successfully colonize different environments (Kataoka et al., 2010; Li et al., 2013). The adaptability of kiwiberies to harsh environments and climates, therefore, could not consistently enhance in response to the elevated ploidy levels.

The association between ploidy levels and morphological or quality characteristics is certainly complex in *Actinidia* genus. Studies on ploidy manipulation further confirmed that the fruit of colchicine-induced autotetraploids of *A. chinensis* were 50 to 60% larger than those of their diploid progenitors (Wu et al., 2012, 2013). A previous study on *A. arguta* var. *giraldii* and related species confirmed larger leaf and fruit sizes in the tetraploid and hexaploid fruit of *A. arguta* var. *giraldii* in Japan (Kataoka et al., 2010). In the present study, the leaf size was obviously larger in these individuals and positively correlated with higher ploidy levels ($8x$ and $10x$). Particularly, the nutritional ingredients of *A. arguta* var. *giraldii* var. *giraldii* ($8x$ and $10x$), including the amount of ascorbic acid and amino acids, were much higher than tetraploid *A. arguta* var. *giraldii* var. *arguta* and *A. melanandra*, implying that *A. arguta* var. *giraldii* var. *giraldii* could serve as a useful germplasm to attain rapid genetic improvement with respect to improved nutritional ingredients. However, the disadvantage of high ploidy races should be highlighted to scientists and breeders, as the fruit shape significantly varied after polyploidization of diploid *A. chinensis* (Wu et al., 2012). In addition, reduced flesh firmness and dry matter and less intense golden flesh color were observed in autotetraploid plants compared with parental diploid plants (Wu et al., 2013). In the present study, the fruit size of *A. arguta* var. *giraldii* var. *giraldii* decreased with the increasing ploidy level ($8x$ and $10x$), and some commercially important characteristics associated with fruit quality (e.g., total sugar and total acid content) was also poor on $8x$ and $10x$ plants. Therefore, the morphological and quality characteristics were not necessarily positively and linearly correlated with continuously increasing ploidy levels (Table S4). Thus, higher ploidy is not inevitably better in the *Actinidia* genus.

Conclusion and Breeding Implication

Studies of the natural resources of *A. arguta* var. *giraldii* and related species have enhanced our current understanding of ploidy variation, distributional pattern, and co-existence mechanisms of cytotypes. The establishment of a genetic diversity center of *A. arguta* var. *giraldii* and related species near Qinling Mountain, where species with abundant ploidy variations and diversified phenotypes presenting colorful fruit flesh, variable fruit shape, different fruit size, and nutritional compositions are

detected (Figure 2), would be advantageous. The relationship between ploidy levels and agronomic traits, such as the polyploid advantage on a higher content of ascorbic acid and amino acids, and the disadvantages regarding ecological adaptation, fruit size, and fruit flavor, will improve our knowledge of multi-polyploidization in plants.

Substantially, the present study of new genotypes, including higher nutrient content, edible skins, colorful fruit flesh (red, purple) and new flavors, is the first step in germplasm exploration, and we expect to extend the utility of such genetic material to ultimately improve traditional kiwifruit quality, which is characterized by brown hairy skin, green flesh and acid flavor. To achieve task, symmetrical large-scale surveys, and detailed evaluations (solid soluble content, dry matter, aroma, yield, etc.) of natural germplasms planted in kiwifruit orchards are needed. Similarly, whole genome re-sequencing of *A. arguta* var. *giraldii* var. *arguta*, *A. arguta* var. *giraldii* var. *giraldii*, and *A. melanandra* should be conducted, although there may be particular challenges for analyzing improvement traits, reflecting the high genomic heterozygosity and inadequacies of the analytic techniques used to examine polyploidy. We anticipate that these methodological challenges will be overcome by advances in genome sequencing technologies (Faino and Thomma, 2014). Finally, other powerful approaches (e.g., CRISPR-Cas system) (Kanchiswamy et al., 2015) for the examination of kiwifruit will improve association studies examining the genotype vs. phenotype, an essential prerequisite to targeted breeding efforts.

AUTHOR CONTRIBUTIONS

DL and YZ conceived and planned the study. YZ and CZ collected the materials and measured the traits of fruit, leaf and flower. XS provided materials and data of *A. arguta* var. *arguta* of North China. DL, YL, and QZ tested the ploidy levels. DL wrote the manuscript.

FUNDING

This research is funded by the National Natural Science Foundation of China (Project no. 31572092) and the Agricultural Public Relations Project of Shaanxi Technology Committee (Project no. 2014K01-07-02).

ACKNOWLEDGMENTS

We thank Ross Ferguson for critically reading and revising the article and Lv Haiyan for assay support.

SUPPLEMENTARY MATERIAL

The Supplementary Material for this article can be found online at: <http://journal.frontiersin.org/article/10.3389/fpls.2017.00711/full#supplementary-material>

REFERENCES

- Adams, K. L., and Wendel, J. F. (2005). Polyploidy and genome evolution in plants. *Curr. Opin. Plant Biol.* 8, 135–141. doi: 10.1016/j.pbi.2005.01.001
- Asakura, I., and Hoshino, Y. (2016). Distribution, ploidy levels, and fruit characteristics of three *Actinidia* species native to Hokkaido, Japan. *Horticul. J.* 85, 105–114. doi: 10.2503/hortj.MI-082
- Baack, E. J. (2005). Ecological factors influencing tetraploid establishment in snow buttercups (*Ranunculus adoneus*, Ranunculaceae): minority cytotype exclusion and barriers to triploid formation. *Am. J. Bot.* 92, 1827–1835. doi: 10.3732/ajb.92.11.1827
- Biernik, A. (2012). Yield, morphology and biological value of fruits of *Actinidia arguta* and *Actinidia purpurea* and some of their hybrid cultivars grown in north-eastern Poland. *Acta. Sci. Pol. Hortorum. Cultus* 11, 117–130.
- Boyd, L., McNeilage, M., Macrae, E., Ferguson, A., Beatson, R., Martin, P., et al. (2002). “Development and commercialization of ‘baby kiwi’(*Actinidia arguta* Planch.),” in *V International Symposium on Kiwifruit* (Wuhan).
- Brochmann, C., Brysting, A., Alsos, I., Borgen, L., Grundt, H., Scheen, A. C., et al. (2004). Polyploidy in arctic plants. *Biol. J. Linn. Soc.* 82, 521–536. doi: 10.1111/j.1095-8312.2004.00337.x
- Burton, T. L., and Husband, B. C. (1999). Population cytotype structure in the polyploid Galax urceolata (Diapensiaceae). *Heredity* 82, 381–390. doi: 10.1038/sj.hdy.6884910
- Castro, S., Loureiro, J., Procházka, T., and Münzbergová, Z. (2012). Cytotype distribution at a diploid–hexaploid contact zone in *Aster amellus* (Asteraceae). *Ann. Bot.* 110, 1047–1055. doi: 10.1093/aob/mcs177
- Cheng, S. H., Zhuang, J. Y., Fan, Y. Y., Du, J. H., and Cao, L. Y. (2007). Progress in research and development on hybrid rice: a super-domesticate in China. *Ann. Bot.* 100, 959–966. doi: 10.1093/aob/mcm121
- Chinese standard GB/T 5009. (2003). *Chinese Standard GB/T 5009.124-2003, 2004. Inspection of Grain and Oilseeds: Method for Determination of Amino Acids in Foods*. Beijing: Standards Press of China.
- Comai, L. (2005). The advantages and disadvantages of being polyploid. *Nat. Rev. Genet.* 6, 836–846. doi: 10.1038/nrg1711
- Comeskey, D. J., Montefiori, M., Edwards, P. J. B., and McGhie, T. K. (2009). Isolation and structural identification of the anthocyanin components of red kiwifruit. *Agric. Food Chem.* 57, 2035–2039. doi: 10.1021/jf803287d
- Crow, J. F. (1998). 90 years ago: the beginning of hybrid maize. *Genetics* 148, 923–928.
- Datson, P., and Ferguson, A. (2011). “*Actinidia*,” in *Wild Crop Relatives: Genomic and Breeding Resources*, ed C. Kole (Berlin; Heidelberg: Springer), 1–20.
- Datson, P., Nardozza, S., Manako, K., Herrick, J., Martinez-Sanchez, M., Curtis, C., et al. (2013). “Monitoring the *Actinidia* germplasm for resistance to *Pseudomonas syringae* pv. *Actinidiae*,” in *I International Symposium on Bacterial Canker of Kiwifruit* (Mt Maunganui).
- Dhawan, O., and Lavania, U. (1996). Enhancing the productivity of secondary metabolites via induced polyploidy: a review. *Euphytica* 87, 81–89. doi: 10.1007/BF00021879
- Dubcovsky, J., and Dvorak, J. (2007). Genome plasticity a key factor in the success of polyploid wheat under domestication. *Science* 316, 1862–1866. doi: 10.1126/science.1143986
- Duchoslav, M., Fialová, M., and Jandová, M. (2016). The ecological performance of tetra-, penta-and hexaploid geophyte *Allium oleraceum* in reciprocal transplant experiment may explain the occurrence of multiple-cytotype populations. *J. Plant Ecol.* rtw039. doi: 10.1093/jpe/rtw039
- Duvick, D. N. (2001). Biotechnology in the 1930s: the development of hybrid maize. *Nat. Rev. Genet.* 2, 69–74. doi: 10.1038/35047587
- Faino, L., and Thamma, B. P. (2014). Get your high-quality low-cost genome sequence. *Trends Plant Sci.* 19, 288–291. doi: 10.1016/j.tplants.2014.02.003
- Ferguson, A. (2007). The need for characterisation and evaluation of germplasm: kiwifruit as an example. *Euphytica* 154, 371–382. doi: 10.1007/s10681-006-9188-2
- Ferguson, A., and Huang, H. (2007). Genetic resources of kiwifruit: domestication and breeding. *Hortic. Rev.* 33, 1–121. doi: 10.1002/9780470168011.ch1
- Ferguson, A., and Seal, A. (2008). “Kiwifruit,” in *Temperate Fruit Crop Breeding*, ed J. F. Hancock (Springer), 235–264.
- Fowler, N. L., and Levin, D. A. (1984). Ecological constraints on the establishment of a novel polyploid in competition with its diploid progenitor. *Am. Nat.* 124, 703–711. doi: 10.1086/284307
- Hijmans, R. J., Gavrilenko, T., Stephenson, S., Bamberg, J., Salas, A., and Spooner, D. M. (2007). Geographical and environmental range expansion through polyploidy in wild potatoes (Solanum section Petota). *Glob. Ecol. Biogeogr.* 16, 485–495. doi: 10.1111/j.1466-8238.2007.00308.x
- Kagan-Zur, V., Yaron-Miron, D., and Mizrahi, Y. (1991). A study of triploid tomato fruit attributes. *J. Am. Chem. Soc.* 116, 228–231.
- Kanchiswamy, C. N., Sargent, D. J., Velasco, R., Maffei, M. E., and Malnoy, M. (2015). Looking forward to genetically edited fruit crops. *Trends Biotechnol.* 33, 62–64. doi: 10.1016/j.tibtech.2014.07.003
- Kao, R. H. (2007). Asexuality and the coexistence of cytotypes. *New Phytol.* 175, 764–772. doi: 10.1111/j.1469-8137.2007.02145.x
- Kataoka, I., Mizugami, T., Kim, J. G., Beppu, K., Fukuda, T., Sugahara, S., et al. (2010). Ploidy variation of hardy kiwifruit (*Actinidia arguta*) resources and geographic distribution in Japan. *Sci. Hortic.* 124, 409–414. doi: 10.1016/j.scienta.2010.01.016
- Keeler, K. H. (2004). Impact of intraspecific polyploidy in *Andropogon gerardii* (Poaceae) populations. *Am. Midl. Nat.* 152, 63–74. doi: 10.1674/0003-0031(2004)152[0063:IOPIIA]2.0.CO;2
- King, K., Seppälä, O., and Neiman, M. (2012). Is more better? Polyploidy and parasite resistance. *Biol. Lett.* 8, 598–600. doi: 10.1098/rsbl.2011.1152
- Lavania, U. C. (2013). Polyploidy, body size, and opportunities for genetic enhancement and fixation of heterozygosity in plants. *Nucleus* 56, 1–6. doi: 10.1007/s13237-013-0075-7
- Lavania, U. C., Srivastava, S., Lavania, S., Basu, S., Misra, N. K., and Mukai, Y. (2012). Autopolyploidy differentially influences body size in plants, but facilitates enhanced accumulation of secondary metabolites, causing increased cytosine methylation. *Plant J.* 71, 539–549. doi: 10.1111/j.1365-313X.2012.05006.x
- Leitch, A., and Leitch, I. (2008). Genomic plasticity and the diversity of polyploid plants. *Science* 320, 481–483. doi: 10.1126/science.1153585
- Levin, D. A. (1975). Minority cytotype exclusion in local plant populations. *Taxon* 24, 35–43. doi: 10.2307/1218997
- Levin, D. A. (2002). *The Role of Chromosomal Change in Plant Evolution*. New York, NY: Oxford University Press.
- Li, D., Liu, Y., Zhong, C., and Huang, H. (2010). Morphological and cytotype variation of wild kiwifruit (*Actinidia chinensis* complex) along an altitudinal and longitudinal gradient in central-west China. *Biol. J. Linn. Soc.* 164, 72–83. doi: 10.1111/j.1095-8339.2010.01073.x
- Li, J., Li, X., and Soejarto, D. (2007). Actinidiaceae. *Flora China* 12, 334–360.
- Li, X., Li, J., and Soejarto, D. D. (2007). New synonyms in Actinidiaceae from China. *Acta Phytotax Sin.* 45, 633–660. doi: 10.1360/aps06061
- Li, Z. Z., Man, Y. P., Lan, X. Y., and Wang, Y. C. (2013). Ploidy and phenotype variation of a natural *Actinidia arguta* population in the east of Daba Mountain located in a region of Shaanxi. *Sci. Hortic.* 161, 259–265. doi: 10.1016/j.scienta.2013.07.008
- Luo, Y., Yen, X., Zhang, G., and Liang, G. (1992). Agronomic traits and chromosome behavior of autotetraploid sorghums. *Plant Breed.* 109, 46–53. doi: 10.1111/j.1439-0523.1992.tb00149.x
- Matich, A. J., Young, H., Allen, J. M., Wang, M. Y., Fielder, S., McNeilage, M. A., et al. (2003). *Actinidia arguta*: volatile compounds in fruit and flowers. *Phytochemistry* 63, 285–301. doi: 10.1016/S0031-9422(03)00142-0
- Nishiyama, I., Fukuda, T., and Oota, T. (2005). Genotypic differences in chlorophyll, lutein, and β-carotene contents in the fruits of *Actinidia* species. *J. Agr. Food Chem.* 53, 6403–6407. doi: 10.1021/jf050785y
- Nishiyama, I., Fukuda, T., Shimohashi, A., and Oota, T. (2008). Sugar and organic acid composition in the fruit juice of different *Actinidia* varieties. *Food Sci. Technol. Res.* 14, 67–73. doi: 10.3136/fstr.14.67
- Ollitrault-Sammarelli, F., Legave, J., Michaux-Ferrière, N., and Hirsch, A. M. (1994). Use of flow cytometry for rapid determination of ploidy level in the genus *Actinidia*. *Sci. Hortic.* 57, 303–313. doi: 10.1016/S0304-4238(94)90113-9
- Otto, S. P., and Whitton, J. (2000). Polyploid incidence and evolution. *Annu. Rev. Genet.* 34, 401–437. doi: 10.1146/annurev.genet.34.1.401
- Petit, C., Lesbros, P., Ge, X., and Thompson, J. D. (1997). Variation in flowering phenology and selfing rate across a contact zone between

- diploid and tetraploid *Arrhenatherum elatius* (Poaceae). *Heredity* 79, 31–40. doi: 10.1038/hdy.1997.120
- Renny-Byfield, S., and Wendel, J. F. (2014). Doubling down on genomes: polyploidy and crop plants. *Am. J. Bot.* 101, 1711–1725. doi: 10.3732/ajb.1400119
- Rodriguez, D. J. (1996). Model for the establishment of polyploidy in plants: viable but infertile hybrids, iteroparity, and demographic stochasticity. *J. Theor. Biol.* 3, 189–196. doi: 10.1006/jtbi.1996.0095
- SAC (1994). *Determination of Vitamin C in Vegetables and Fruits (2. 6-dichloro-indophenol titration)*. Beijing: Standards Press of China.
- SAC (2008). *Determination of Total Acid in Foods*. Vol. GB/T 12456-2008, Standardization Administration of the People's Republic of China. Beijing: Standards Press of China.
- Soltis, D. E., Albert, V. A., Leebens-Mack, J., Bell, C. D., Paterson, A. H., Zheng, C., et al. (2009). Polyploidy and angiosperm diversification. *Am. J. Bot.* 96, 336–348. doi: 10.3732/ajb.0800079
- Soltis, D. E., Buggs, R., Doyle, J. J., and Soltis, P. S. (2010). What we still don't know about polyploidy. *Taxon* 59, 1387–1403. doi: 10.2307/20774036
- Sonnleitner, M., Hülber, K., Flatscher, R., García, P. E., Winkler, M., Suda, J., et al. (2016). Ecological differentiation of diploid and polyploid cytotypes of *Senecio carniolicus* sensu lato (Asteraceae) is stronger in areas of sympatry. *Ann. Bot.* 117, 269–276. doi: 10.1093/aob/mcv176
- Stebbins, G. L. (1985). Polyploidy, hybridization, and the invasion of new habitats. *Ann. Mo. Bot. Gard.* 72, 824–832. doi: 10.2307/2399224
- Suda, J., Weiss-Schneeweiss, H., Tribsch, A., Schneeweiss, G. M., Trávníček, P., and Schönswetter, P. (2007). Complex distribution patterns of di-, tetra-, and hexaploid cytotypes in the European high mountain plant *Senecio carniolicus* (Asteraceae). *Am. J. Bot.* 94, 1391–1401. doi: 10.3732/ajb.94.8.1391
- Te Beest, M., Le Roux, J. J., Richardson, D. M., Brysting, A. K., Suda, J., Kuběsová, M., et al. (2012). The more the better? The role of polyploidy in facilitating plant invasions. *Ann. Bot.* 109, 19–45. doi: 10.1093/aob/mcr277
- Udall, J. A., and Wendel, J. F. (2006). Polyploidy and crop improvement. *Crop Sci.* 46, 3–14. doi: 10.2135/cropsci2006.07.0489tpg
- Uddin, M., Ellison, F., O'Brien, L., and Latter, B. (1992). Heterosis in F1 hybrids derived from crosses of adapted Australian wheats. *Crop Pasture Sci.* 43, 907–919. doi: 10.1071/AR9920907
- Vamosi, J. C., and McEwen, J. R. (2012). Origin, elevation, and evolutionary success of hybrids and polyploids in British Columbia, Canada. *Botany* 91, 182–188. doi: 10.1139/cjb-2012-0177
- Van Dijk, P., and Bijlsma, R. (1994). Simulations of flowering time displacement between two cytotypes that form inviable hybrids. *Heredity* 72, 522–535. doi: 10.1038/hdy.1994.70
- Wagner, W. (1970). Biosystematics and evolutionary noise. *Taxon* 19, 146–151.
- Warner, D. A., Ku, M. S., and Edwards, G. E. (1987). Photosynthesis, leaf anatomy, and cellular constituents in the polyploid C4 grass *Panicum virgatum*. *Plant Physiol.* 84, 461–466. doi: 10.1104/pp.84.2.461
- Watanabe, K., Takahashi, B., and Shirato, K. (1990). Chromosome numbers in kiwifruit (*Actinidia deliciosa*) and related species. *J. Jpn. Soc. Food Sci.* 58, 835–840. doi: 10.2503/jjshs.58.835
- Wendel, J. F., and Cronn, R. C. (2003). Polyploidy and the evolutionary history of cotton. *Adv Agron.* 78, 139–186. doi: 10.1016/S0065-2113(02)78004-8
- Wu, J. H., Ferguson, A. R., Murray, B. G., Duffy, A. M., Jia, Y., Cheng, C., et al. (2013). Fruit quality in induced polyploids of *Actinidia chinensis*. *HortScience* 48, 701–707.
- Wu, J. H., Ferguson, A. R., Murray, B. G., Jia, Y., Datson, P. M., and Zhang, J. (2012). Induced polyploidy dramatically increases the size and alters the shape of fruit in *Actinidia chinensis*. *Ann. Bot.* 109, 169–179. doi: 10.1093/aob/mcr256
- Yan, G., Yao, J., Ferguson, A., McNeilage, M., Seal, A., and Murray, B. (1997). New reports of chromosome numbers in Actinidia (Actinidiaceae). *New Zeal. J. Bot.* 35, 181–186. doi: 10.1080/0028825X.1997.10414154
- Zozomová-Lihová, J., Malánová-Krásná, I., Vít, P., Urfus, T., Senko, D., Svitok, M., et al. (2015). Cytotype distribution patterns, ecological differentiation, and genetic structure in a diploid-tetraploid contact zone of *Cardamine amara*. *Am. J. Bot.* 102, 1380–1395. doi: 10.3732/ajb.1500052

Conflict of Interest Statement: The authors declare that the research was conducted in the absence of any commercial or financial relationships that could be construed as a potential conflict of interest.

Copyright © 2017 Zhang, Zhong, Liu, Zhang, Sun and Li. This is an open-access article distributed under the terms of the Creative Commons Attribution License (CC BY). The use, distribution or reproduction in other forums is permitted, provided the original author(s) or licensor are credited and that the original publication in this journal is cited, in accordance with accepted academic practice. No use, distribution or reproduction is permitted which does not comply with these terms.



Grape Composition under Abiotic Constraints: Water Stress and Salinity

José M. Mirás-Avalos* and Diego S. Intrigliolo

Departamento de Riego, Centro de Edafología y Biología Aplicada del Segura, Consejo Superior de Investigaciones Científicas, Murcia, Spain

Water stress and increasing soil salt concentration represent the most common abiotic constraints that exert a negative impact on Mediterranean vineyards performance. However, several studies have proven that deficit irrigation strategies are able to improve grape composition. In contrast, irrigation with saline waters negatively affected yield and grape composition, although the magnitude of these effects depended on the cultivar, rootstock, phenological stage when water was applied, as well as on the salt concentration in the irrigation water. In this context, agronomic practices that minimize these effects on berry composition and, consequently, on wine quality must be achieved. In this paper, we briefly reviewed the main findings obtained regarding the effects of deficit irrigation strategies, as well as irrigation with saline water, on the berry composition of both red and white cultivars, as well as on the final wine. A meta-analysis was performed using published data for red and white varieties; a general liner model accounting for the effects of cultivar, rootstock, and midday stem water potential was able to explain up to 90% of the variability in the dataset, depending on the selected variable. In both red and white cultivars, berry weight, must titratable acidity and pH were fairly well simulated, whereas the goodness-of-fit for wine attributes was better for white cultivars.

OPEN ACCESS

Edited by:

Nadia Bertin,
Plantes et Système de cultures
Horticoles (INRA), France

Reviewed by:

Claudio Lovisolo,
University of Turin, Italy
Jose Carlos Herrera,
University of Natural Resources
and Life Sciences, Vienna, Austria

***Correspondence:**

José M. Mirás-Avalos
jmmiras@cebas.csic.es

Specialty section:

This article was submitted to
Crop Science and Horticulture,
a section of the journal
Frontiers in Plant Science

Received: 17 February 2017

Accepted: 08 May 2017

Published: 30 May 2017

Citation:

Mirás-Avalos JM and Intrigliolo DS (2017) Grape Composition under Abiotic Constraints: Water Stress and Salinity. *Front. Plant Sci.* 8:851.
doi: 10.3389/fpls.2017.00851

INTRODUCTION

Grape quality is a complex concept that mainly refers to berry chemical composition, including sugars, acids, phenolics, and other aroma compounds (Lund and Bohlmann, 2006). The composition and concentration of these chemical compounds change during berry development and can be affected by many factors, either environmental, endogenous, or management practices (Jackson and Lombard, 1993; Dai et al., 2011). In this context, climate change will pose relevant constraints to grape and wine production in the coming years (Santos et al., 2012). Increasing temperatures, lower rainfall amounts, and heat waves are expected to become more frequent over the course of this century (IPCC, 2014). However, the most imminent challenges that grape, wine, and raisin industries must face, especially in arid and semi-arid regions, are increasing drought and salinity due to higher evaporation and declining water availability (Schultz and Stoll, 2010).

The effects of water stress on grapevine (*Vitis vinifera* L.) metabolism, vegetative development, productive performance, and berry composition have been widely studied for many combinations of rootstocks, cultivars, and climate conditions (e.g., Acevedo-Opazo et al., 2010; Intrigliolo et al., 2016). However, the extents to which berry secondary metabolites and wine composition are affected by water stress have seldom been assessed.

Salinity effects on vine performance and berry composition have been studied mainly in Australia (e.g., Stevens et al., 2011; Walker et al., 2014) but research in other areas is scarce. Reported results suggest that cultivar, rootstock, salt concentration, and time of exposure to saline conditions are relevant factors for the final berry and wine composition.

This review summarizes the main findings on the effects of water and salinity stresses on berry and wine composition, both in red and white cultivars.

WATER STRESS

Water is critical for viticulture sustainability because grape production, quality, and economic viability largely depend on water availability (Medrano et al., 2015). A great effort has been devoted to assess the influence of grapevine water status on berry composition, mainly on red varieties under semi-arid conditions, accounting for total soluble solids (TSS), titratable acidity, and pH, although some other traits such as malic and tartaric acid concentrations, phenolics, anthocyanins, and tannins have been considered in some studies (e.g., Peyrot des Gachons et al., 2005; Bindon et al., 2008; van Leeuwen et al., 2009). However, detailed assessments of aroma precursors (Savoi et al., 2016), individual anthocyanins (Bindon et al., 2008, 2011; Santesteban et al., 2011; Cook et al., 2015; Hochberg et al., 2015), or phenolics (Ojeda et al., 2002; Ollé et al., 2011) have rarely been undertaken.

Reported results suggest that many factors including genotypes, climate, soil, and vineyard management can influence vine response to water stress, as reviewed by Medrano et al. (2015) and confirmed by the meta-analysis reported by Lavoie-Lamoureux et al. (2017). In water-limited areas, deficit irrigation practices can be a useful tool for manipulating berry composition to enhance and modulate the season-to-season variability in red wine composition (Intrigliolo et al., 2012), leading to changes in wine sensory properties (Chapman et al., 2005). However, the intensity of water stress and its period of occurrence over the grapevine growing cycle are of paramount importance. Apart from the variability in the response due to genotypes, environment, experimental setup, management practices among others, water stress imposed at pre-veraison stages induces major metabolic modifications in the berry that can be maintained even after re-watering (Shellie, 2014; Keller et al., 2016). In contrast, post-veraison water deficit effects are more variable, preventing a generalization of its positive or negative influences (Girona et al., 2009; Intrigliolo and Castel, 2010; Munitz et al., 2017).

In general, a moderate water stress reduces berry weight and titratable acidity but increases TSS, total anthocyanins, and phenolics concentrations in red grapes (Romero et al., 2010), improving berry quality. However, when a certain threshold of water stress is surpassed, these beneficial effects are no longer observed. This response seems to depend on the combination rootstock/cultivar as well as on soil and climate conditions. Water potential is the main indicator of vine water status and some authors established relations between this indicator and berry compositional traits (Salón et al., 2005; van Leeuwen et al., 2009; Romero et al., 2010; Shellie and Bowen, 2014);

however, these relationships differ amongst cultivars, region, year, soil types, and management practices. Usually, higher levels of water stress are reported to reduce berry weight and malic acid concentrations while increasing anthocyanins and sugar contents up to a threshold where they are negatively affected. However, these responses depend on other factors such as crop load, vineyard age, fertilization, soil type, berry maturation stage at harvest, and canopy development, amongst others. Furthermore, few studies have accounted for the effects that water stress might exert on berry skin and seeds (Ojeda et al., 2002; Roby and Matthews, 2004; Buccetti et al., 2011; Merli et al., 2015), even though this issue is relevant to discern between the effects of dilution of components or to what extent water stress is affecting compound synthesis and metabolism. Ojeda et al. (2002) imposed three levels of water deficit to Shiraz grapevines and observed that the concentration of phenolic compounds increased in berry skins due to berry size reduction; however, timing of stress occurrence and its severity could lead to negative effects on phenolic compound concentrations. Ollé et al. (2011) observed that water deficits affected differently the anthocyanin composition of Shiraz berries and suggested a differential regulation of the genes involved in the last steps of the anthocyanin biosynthesis pathway. In this sense, Hochberg et al. (2015) found that water stress modified polyphenol metabolism of Shiraz and Cabernet Sauvignon depending on the phenological stage, inducing the accumulation of stress-related metabolites such as proline and ascorbate. Cook et al. (2015) reported that sustained deficit irrigation increased the concentrations of di-hydroxylated anthocyanins while regulated deficit irrigation increased those of tri-hydroxylated anthocyanins. It has been shown that grapevine responds to drought by modulating several secondary metabolic pathways, altering the abundance of some transcripts and metabolites involved in phenyl propanoid, isoprenoid, carotenoid, amino acid, and fatty acid metabolism, as observed for Cabernet Sauvignon and Chardonnay (Deluc et al., 2009) and Sauvignon vert (Savoi et al., 2016). This might affect flavor and quality characteristics of grapes and wines.

In this context, we attempted a meta-analysis using published data from irrigation studies in field-grown red and white grapevine varieties from several wine regions worldwide (Supplementary Table 1). A search under the terms “grapevine,” “water stress,” and “berry composition” was carried out in the Web of Knowledge database. This yielded 184 references. Those works referred to potted vines and those not including leaf (Ψ_1) or stem (Ψ_{stem}) water potential measurements were discarded. When only one of these measurements was present, we used the relationships reported by Intrigliolo and Castel (2006) to obtain the values for the missing one. In the end, 48 works have been used (Supplementary Table 1).

Data retrieval from publications was carried out similarly to that described in Lavoie-Lamoureux et al. (2017). The following information was associated to the data in the database, when available: cultivar, country, year, treatment, rootstock, and developmental stage in which water stress was imposed (pre- or post-veraison).

Data were analyzed using the IBM SPSS Statistics for Windows, version 23.0 (IBM Corp., Armonk, NY, United States).

Data on berry size and composition (and wine attributes, when available) were used as dependent variables, while Ψ_{stem} was considered as a covariate and cultivar, rootstock, and timing when water stress was imposed as fixed factors. Moreover, Pearson's coefficient of correlation was used to assess the relationships among vine water status (as determined by predawn, leaf, and stem water potentials) and berry size and composition.

The final database contained 420 data points (298 for red and 122 for white varieties) obtained from 48 references published between 1979 and 2017 (Supplementary Table 1). Twenty different *Vitis vinifera* cultivars were represented (11 red and 9 white). The number of data retrieved per publication varied between 2 and 28, averaging 10.5. Merlot and Tempranillo were the most represented varieties (79 and 78 data, respectively) among the red ones. In the case of white cultivars, Sauvignon blanc showed the highest number of data with 48.

For red varieties, cultivar, timing, and Ψ_{stem} intervened significantly on the model; whereas for white varieties the factors were cultivar, rootstock, and Ψ_{stem} (Table 1). No significant interactions among factors were detected. Overall, the models explained between 2 and 99.4% of the variation in the data distribution, depending on the variable considered (Supplementary Table 2).

The different measurements for assessing vine water status (predawn, leaf, and stem water potentials) considered in the current study were significantly related to several grape and wine compositional attributes. In the case of red varieties, midday stem water potential measured before veraison (Ψ_{stempre}) was significantly and positively correlated to berry weight and must titratable acidity, whereas it was negatively correlated to must TSS, malic acid concentration and wine pH, tartaric acid, anthocyanins, and total phenolic index (TPI) (Table 2). The other measurements of water status were significantly correlated with a lower number of attributes; for instance, Ψ_{stem} was positively correlated with berry weight and must titratable acidity and negatively correlated to TSS (Table 2). However, Ψ_{stem} is the most widely used measurement for assessing vine water status and thus we used it for depicting the relationships between berry traits and water stress.

In the case of red varieties, berry weight tended to decline with increasing Ψ_{stem} ; however, the slope of this decrease depended on the cultivar (Supplementary Figure 1). This suggests that genetics may play a relevant role on the response of grapevines to water stress and those cultivars with small berries, such as Cabernet Sauvignon, suffer less important reductions when they are grown within a given interval of Ψ_{stem} . In contrast, cultivars with large berries, such as Bobal or Merlot, seem to be more sensitive to little variations in grapevine water status.

The dataset did not show a clear relation between Ψ_{stem} and TSS in the berries (Supplementary Figure 1). Nevertheless, a certain degree of water stress (up to -1.3 MPa) was beneficial for sugar accumulation in the berry. When this threshold was surpassed, the concentration of TSS decreased. Similarly, no clear trend was observed for titratable acidity and anthocyanins (Supplementary Figure 1). However, Merlot berries showed a

TABLE 1 | Factors included in the first univariate general linear model performed on the red and white varieties databases.

Factors	p-value
Red varieties	
Cultivar	<0.001
Rootstock	ns
Timing	<0.05
Ψ_{stem}	<0.05
Cultivar × rootstock	ns
Cultivar × timing	ns
Cultivar × Ψ_{stem}	ns
Rootstock × timing	ns
Rootstock × Ψ_{stem}	ns
Timing × Ψ_{stem}	ns
Cultivar × rootstock × timing	ns
Cultivar × rootstock × Ψ_{stem}	ns
Cultivar × timing × Ψ_{stem}	ns
Rootstock × timing × Ψ_{stem}	ns
Cultivar × rootstock × timing × Ψ_{stem}	ns
White varieties	
Cultivar	<0.001
Rootstock	<0.01
Timing	ns
Ψ_{stem}	<0.01
Cultivar × rootstock	ns
Cultivar × timing	ns
Cultivar × Ψ_{stem}	ns
Rootstock × timing	ns
Rootstock × Ψ_{stem}	ns
Timing × Ψ_{stem}	ns
Cultivar × rootstock × timing	ns
Cultivar × rootstock × Ψ_{stem}	ns
Cultivar × timing × Ψ_{stem}	ns
Rootstock × timing × Ψ_{stem}	ns
Cultivar × rootstock × timing × Ψ_{stem}	ns

Non-significant factors were not included in the final model. ns, non-significant.

steep increase in the concentration of anthocyanins when Ψ_{stem} varied from -0.5 to -1.5 MPa.

Winemaking was not usually involved in the experimental design and a low amount of data was available for performing this meta-analysis. The lack of significant relations may have been caused by the variability in winemaking procedures in the different studies (yeast strain, fermentation temperature, and time, etc.). However, lower pre-veraison midday stem water potentials were significantly correlated with higher values of anthocyanins and TPI in wines (Table 2).

In the case of white varieties, data availability is much lower and, usually, studies are referred to cool climates. In this case, a significant but slight trend to lower berry weights with increasing water stress was observed (Supplementary Table 3). Cultivar seems to have a strong effect since Albariño berries remained almost unaffected whereas Sauvignon Blanc or Riesling berries were strongly reduced in terms of weight when Ψ_{stem} became more negative (Supplementary Figure 2). It must be noticed,

TABLE 2 | Pearson's correlation coefficients (*r*) among different modalities of vine water status assessment and berry size and compositional traits for red cultivars.

		Ψ_{pd}	$\Psi_{stempre}$	$\Psi_{stempost}$	Ψ_{stem}
Berry weight	<i>r</i>	0.284	0.567	0.326	0.406
	Significance	0.000	0.000	0.000	0.000
	<i>n</i>	255	107	119	255
Total soluble solids	<i>r</i>	-0.199	-0.419	-0.453	-0.234
	Significance	0.001	0.000	0.000	0.000
	<i>n</i>	286	126	138	286
pH	<i>r</i>	-0.161	-0.218	0.002	-0.090
	Significance	0.024	0.055	0.989	0.208
	<i>n</i>	196	78	90	196
Titratable acidity	<i>r</i>	0.171	0.200	0.166	0.162
	Significance	0.005	0.040	0.072	0.008
	<i>n</i>	266	106	118	266
Malic acid	<i>r</i>	0.065	0.384	0.137	0.086
	Significance	0.536	0.040	0.479	0.411
	<i>n</i>	94	29	29	94
Tartaric acid	<i>r</i>	0.052	-0.128	0.187	0.082
	Significance	0.641	0.507	0.332	0.458
	<i>n</i>	84	29	29	84
Anthocyanins	<i>r</i>	-0.029	-0.027	0.413	-0.021
	Significance	0.796	0.914	0.079	0.852
	<i>n</i>	81	19	19	81
Total phenolics index	<i>r</i>	0.145	-0.276	0.254	0.140
	Significance	0.269	0.173	0.211	0.285
	<i>n</i>	60	26	26	60
Wine alcohol	<i>r</i>	-0.213	-0.140	-0.273	-0.189
	Significance	0.055	0.402	0.097	0.088
	<i>n</i>	82	38	38	82
Wine titratable acidity	<i>r</i>	0.168	0.313	0.172	0.187
	Significance	0.164	0.081	0.347	0.121
	<i>n</i>	70	32	32	70
Wine pH	<i>r</i>	0.003	-0.680	0.229	-0.101
	Significance	0.977	0.000	0.208	0.408
	<i>n</i>	70	32	32	70
Wine malic acid	<i>r</i>	-0.004	-0.144	-0.128	-0.046
	Significance	0.973	0.430	0.485	0.707
	<i>n</i>	70	32	32	70
Wine tartaric acid	<i>r</i>	0.050	-0.619	-0.156	-0.126
	Significance	0.720	0.001	0.445	0.364
	<i>n</i>	54	26	26	54
Wine anthocyanins	<i>r</i>	0.049	-0.434	-0.047	0.046
	Significance	0.676	0.013	0.800	0.693
	<i>n</i>	76	32	32	76
Wine total phenolics index	<i>r</i>	-0.061	-0.623	-0.265	-0.068
	Significance	0.604	0.000	0.143	0.562
	<i>n</i>	76	32	32	76

Significant correlations are shown in bold. Ψ_{pd} , pre-dawn leaf water potential; $\Psi_{stempre}$, pre-veraison midday stem water potential; $\Psi_{stempost}$, post-veraison midday stem water potential; Ψ_{stem} , midday stem water potential. Significance indicates the p-value for each correlation. *n*, number of data points.

however, that the levels of water stress experienced by the different cultivars were not the same.

In white cultivars, TSS seemed to be unaffected by water stress when the whole dataset was accounted for (Supplementary Figure 2). However, Riesling, Godello, Albariño, or Treixadura tended to show high TSS values with increasing water stress. In

contrast, Muscat and Sauvignon Blanc showed similar TSS for various levels of Ψ_{stem} . Although slight, a significant reduction in titratable acidity with increasing water stress was detected (Supplementary Figure 2). This relation was more marked in Godello and Riesling. Since these data come from experiments performed in cool climates, severe water restriction has rarely

been achieved and Ψ_{stem} varied within narrow ranges. Only for Sauvignon Blanc and Muscat, Ψ_{stem} reached values close to -1.5 MPa or even more negative. Similarly to red cultivars, winemaking has rarely been carried out. Nevertheless, a trend to higher alcohol contents with increasing Ψ_{stem} was observed (data not shown). In addition, more negative Ψ_{stem} values led to lower titratable acidities (Supplementary Figure 2).

Water stress or deficit irrigation strategies effects on wine volatiles have seldom been assessed; likely because winemaking practices can modulate wine composition to a great extent (Ilc et al., 2016). Recently, Talaverano et al. (2017) reported that higher alcohols such as 2-methyl-1-butanol and 2,3-butanediol, as well as C6 compounds such as 1-hexanol increased in Tempranillo wines under water stress conditions in Western Spain; in contrast, 2-phenylethyl acetate concentration was significantly decreased by water deficit. Despite the fact that other 16 compounds did not present significant differences caused by vine water status, changes in 2-phenylethyl acetate might have consequences on wine sensory perception because this compound provides floral and sweet notes, whereas 2-methyl-1-butanol, 2,3-butanediol, and 1-hexanol provide malt, burned and creamy notes to wines. In this line of work, Mendez-Costabel et al. (2014) reported that moderate water stress would reduce 3-isobutyl-2-methoxypyrazine concentration, and thus the intensity of green aromas, without altering that of C6 compounds in Merlot grapes and wines. Finally, Ou et al. (2010) observed that deficit irrigation affected the concentrations of terpene alcohols and norisoprenoids in wines, whereas it had not consistent influence on ester concentrations.

SALINE STRESS

Continued rates of water extraction for agriculture, declining rainfall trends and increased portioning of water for ecosystem servicing have led to unsustainable levels of water consumption in many parts of the world (Hamilton et al., 2007). This has focused the attention on the use of alternative water sources such as municipal and winery wastewaters for irrigation instead of scarce water sources (Laurenson et al., 2012). However, wastewater may contain constituents of potential concern such as heavy metals, pathogens, and a high biological oxygen demand (Mosse et al., 2011). Furthermore, the salt content of these recycled waters, and the concentrations of specific salt ions (Na^+ , K^+), is of paramount importance in relation to soil structure, vine performance, and berry and wine composition (Laurenson et al., 2012; Mosse et al., 2013; Netzer et al., 2014). In certain areas, such as the Mediterranean, water reuse can be considered as a cost-effective solution for agriculture since it reduces the need to develop new water resources and provides an adaptive solution to climate change along with an increase in the social and environmental value of water (Costa et al., 2016). Although wastewater use might mitigate drought stress, the short and mid-term detrimental effects of salt stress must be quantified, as pointed out by several authors (Laurenson et al., 2012; Costa et al., 2016).

Rising salinization of soil could pose a serious threat to grape growing because most irrigated vineyards, especially those deficit-irrigated, are at risk due to dissolved salts in irrigation water (Keller, 2010). The deleterious effects of salinity on plant growth are caused by an osmotic effect in which the increase in soluble salt concentration of the soil solution imposes an osmotic drought on the plant and a toxic effect in which the tissue concentrations of the micronutrient chloride and the beneficial element sodium increase to toxic levels (Marschner, 1986).

Salinity damage has been a concern for a long time in Australian vineyards (e.g., Hickinbotham and Williams, 1933; Walker et al., 2014); however, studies in other areas are scarce. Usually, tolerance of grapevines to salinity is measured by yield performance and by the capacity for salt exclusion, necessary to prevent salt damage to leaves and to minimize Cl^- and Na^+ accumulation in grape juice and wine (Teakle and Tyerman, 2010). Nevertheless, the effects of salinity on berry or juice composition seem to depend on the combination of cultivar and rootstock and on the salt concentration in the irrigation water, as well as on its time of application over the growing season.

In a 6-year study on Colombard vines grafted onto Ramsey rootstock, Stevens et al. (2011) observed that saline irrigation applied at different stages over the growing cycle increased Na^+ concentration in juice over the first four seasons but in the last two seasons this concentration only increased in some of the treatments. In contrast, Cl^- concentration in juice increased over the 6 years independently of the treatment. Interestingly, saline irrigation caused small variations in juice Brix, titratable acidity, pH, and malate concentration. Recently, Degaris et al. (2016) proved that ion partitioning in grapevines and thus Cl^- , Na^+ , and K^+ in berries and juice depends on the type of deficit irrigation applied in two red cultivars (Shiraz and Grenache). Partial root-zone drying reduced the concentration of these ions in the fruit of both cultivars when compared with a fully irrigated control and a deficit irrigated treatment.

The negative effects that salinity might provoke in grape composition can be reduced by the selection of a tolerant rootstock able to exclude salts. In a long-term trial, Walker et al. (2014) observed that Chardonnay and Shiraz vines showed a low yield and a high concentration of both chloride and sodium in grape juice ($>500 \text{ mg/L}$) when they were own-rooted. However, Chardonnay on C5 and Shiraz on C7 rootstocks had the lowest concentration of grape juice chloride and sodium ($<50 \text{ mg/L}$). Moreover, TSS in juice was significantly reduced when Chardonnay vines were own-rooted in comparison with those grafted on rootstocks. These authors noted also significant differences in pH and titratable acidity as a function of rootstock in both cultivars. Finally, Walker et al. (2014) highlighted the different responses between cultivars; Shiraz vines had been less affected by prolonged exposure to salinity when compared with Chardonnay vines. An interesting feature of this study was that significant correlations between juice chloride and sodium concentrations and those found in trunk wood were detected. Previously, Walker et al. (2000) had observed that, under salinity conditions, rootstock would influence color density and anthocyanin concentration in the berries, detecting significant

differences among rootstocks for wine titratable acidity and wine score.

From the sensory point of view, salinity derived attributes ("brackish," "seawater like," "soapy") are considered negative and had been correlated with high concentrations of Na, K, and Cl in wines (Mira de Orduña, 2010). In a study carried out on 4000 wines across 3 years, Kaufmann (1996) found a significant correlation between high chloride levels and arid producing regions. Average chloride levels of 0.69 mM across all European red and white wines analyzed contrasted with the 3.78 mM average for wines produced in the United States, Mexico, Argentina, and Australia.

SUMMARY, CONCLUSIONS, AND IMPLICATIONS

Under the current scenario of global change, the constraints that water scarcity and salinity might induce on grape composition are becoming increasingly important worldwide. These stresses may endanger viticulture sustainability in the medium term by reducing yields and grape composition. Despite the huge amount of work aiming at assessing the effects of water status on vine yield and grape composition, no clear relationships could be established between Ψ_{stem} and berry size and composition. This is due to the large number of factors involved in grape composition development, indicating that water status might not be its main driver. The dataset analyzed in the current study proved that cultivar, timing of exposure to water restrictions and rootstock have a great influence on must and wine composition. Nevertheless, other factors, such as climate, leaf surface/yield ratio, training systems, amongst others, might interact with the

ones that we focused on in the current study and should be taken into account for future research.

Water restrictions can be worsened by increasing salinity levels in soils and irrigation waters, especially in Mediterranean climates. Previous research proved that rootstocks possess different sensitivities to salinity levels in the soil and might reduce the concentration of saline ions in the fruit. Moreover, it seems that cultivars present also a different sensitivity to chloride and sodium.

AUTHOR CONTRIBUTIONS

Both JM-A and DI devised the structure and decided on the content of the paper, JM-A conducted the literature survey, and then JM-A wrote the manuscript. DI contributed to a general revision of the manuscript.

FUNDING

This research has been performed within the framework of the Spanish Ministry of Economy, Industry and Competitiveness MINECO (FEDER co-financing) Project AGL2014-54201-C4-4-R.

SUPPLEMENTARY MATERIAL

The Supplementary Material for this article can be found online at: <http://journal.frontiersin.org/article/10.3389/fpls.2017.00851/full#supplementary-material>

REFERENCES

- Acevedo-Opazo, C., Ortega-Farias, S., and Fuentes, S. (2010). Effects of grapevine (*Vitis vinifera* L.) water status on water consumption, vegetative growth and grape quality: an irrigation scheduling application to achieve regulated deficit irrigation. *Agric. Water Manage.* 97, 956–964. doi: 10.1016/j.agwat.2010.01.025
- Balint, G., and Reynolds, A. G. (2013). Effects of different irrigation strategies on vine physiology, yield, grape composition and sensory profile of Sauvignon blanc (*Vitis vinifera* L.) in a cool climate area. *J. Int. Sci. Vigne Vin* 47, 159–181. doi: 10.20870/oenone.2013.47.3.1547
- Balint, G., and Reynolds, A. G. (2017). Irrigation level and time of imposition impact vine physiology, yield components, fruit composition and wine quality of Ontario Chardonnay. *Sci. Hortic.* 214, 252–272. doi: 10.1016/j.scienta.2016.11.052
- Bindon, K., Dry, P., and Loveys, B. (2008). Influence of partial rootzone drying on the composition and accumulation of anthocyanins in grape berries (*Vitis vinifera* c. Cabernet Sauvignon). *Aust. J. Grape Wine Res.* 14, 91–103. doi: 10.1111/j.1755-0238.2008.00009.x
- Bindon, K., Myburgh, P., Oberholster, A., Roux, K., and Du Toit, C. (2011). Response of grape and wine phenolic composition in *Vitis vinifera* L. cv. Merlot to variation in grapevine water status. *S. Afr. J. Enol. Vitic.* 32, 71–88.
- Bucchetti, B., Matthews, M. A., Falginella, L., Peterlunger, E., and Castellarin, S. D. (2011). Effect of water deficit on Merlot grape tannins and anthocyanins across four seasons. *Sci. Hortic.* 128, 297–305. doi: 10.1016/j.scienta.2011.02.003
- Chapman, D. W., Roby, G., Ebeler, S. E., Guinard, J. X., and Matthews, M. A. (2005). Sensory attributes of Cabernet Sauvignon wines made from vines with different water status. *Aust. J. Grape Wine Res.* 11, 339–347. doi: 10.1111/j.1755-0238.2005.tb00033.x
- Chaves, M. M., Santos, T. P., Souza, C. R., Ortúñoz, M. F., Rodrigues, M. L., Lopes, C. M., et al. (2007). Deficit irrigation in grapevine improves water-use efficiency while controlling vigour and production quality. *Ann. Appl. Biol.* 150, 237–252. doi: 10.1111/j.1744-7348.2006.00123.x
- Choné, X. (2003). Terroir effect on the aromatic potential of Sauvignon Blanc. *Progrès Agric. Vitic.* 120, 63–68.
- Cook, M. G., Zhang, Y., Nelson, C. J., Gambetta, G., Kennedy, J. A., and Kurtural, S. K. (2015). Anthocyanin composition of Merlot is ameliorated by light microclimate and irrigation in Central California. *Am. J. Enol. Vitic.* 66, 266–278. doi: 10.5344/ajev.2015.15006
- Coombe, B. G., and Monk, P. R. (1979). Proline and abscisic acid content of the juice of ripe Riesling grape berries: effect of irrigation during harvest. *Am. J. Enol. Vitic.* 30, 64–67.
- Costa, J. M., Vaz, M., Escalona, J., Egipio, R., Lopes, C., Medrano, H., et al. (2016). Modern viticulture in southern Europe: vulnerabilities and strategies for adaptation to water scarcity. *Agric. Water Manage.* 164, 5–18. doi: 10.1016/j.agwat.2015.08.021
- Dai, Z. W., Ollat, N., Gomès, E., Decroocq, S., Tandonnet, J. P., Bordenave, L., et al. (2011). Ecophysiological, genetic, and molecular causes of variation in grape berry weight and composition: a review. *Am. J. Enol. Vitic.* 62, 413–425. doi: 10.5344/ajev.2011.10116
- De la Hera, M. L., Romero, P., Gómez-Plaza, E., and Martínez, A. (2007). Is partial root-zone drying an effective irrigation technique to improve water use efficiency and fruit quality in field-grown wine grapes under semiarid

- conditions? *Agric. Water Manage.* 87, 261–274. doi: 10.1016/j.agwat.2006.08.001
- Derigas, K. A., Walker, R. R., Loveys, B. R., and Tyerman, S. D. (2016). Comparative effects of deficit and partial root-zone drying irrigation techniques using moderately saline water on ion partitioning in Shiraz and Grenache grapevines. *Aus. J. Grape Wine Res.* 22, 296–306. doi: 10.1111/ajgrwr.12220
- Deluc, L. G., Quilici, D. R., Decendit, A., Grimplet, J., Wheatley, M. D., Schaluch, K. A., et al. (2009). Water deficit alters differentially metabolic pathways affecting important flavor and quality traits in grape berries of Cabernet Sauvignon and Chardonnay. *BMC Genomics* 10:212. doi: 10.1186/1471-2164-10-212
- Döring, J., Frisch, M., Tittmann, S., Stoll, M., and Kauer, R. (2015). Growth, yield and fruit quality of grapevines under organic and biodynamic management. *PLoS ONE* 10:e0138445. doi: 10.1371/journal.pone.0138445
- dos Santos, T. P., Lopes, C. M., Rodrigues, M. L., de Souza, C. R., Ricardo-da-Silva, J. M., Maroco, J. P., et al. (2007). Effects of deficit irrigation strategies on cluster microclimate for improving fruit composition of Moscatel field-grown grapevines. *Sci. Hortic.* 112, 321–330. doi: 10.1016/j.scientia.2007.01.006
- El-Ansary, D. O., Nakayama, S., Hirano, K., and Okamoto, G. (2005). Response of Muscat of Alexandria table grapes to post-veraison regulated deficit irrigation in Japan. *Vitis* 44, 5–9.
- El-Ansary, D. O., and Okamoto, G. (2007). Vine water relations and quality of 'Muscat of Alexandria' table grapes subjected to partial root-zone drying and regulated deficit irrigation. *J. Jpn. Soc. Hort. Sci.* 76, 13–19. doi: 10.2503/jjhs.76.13
- Girona, J., Marsal, J., Mata, M., Del Campo, J., and Basile, B. (2009). Phenological sensitivity of Berry growth and composition of Tempranillo grapevines (*Vitis vinifera* L.) to water stress. *Aus. J. Grape Wine Res.* 15, 268–277. doi: 10.1111/j.1755-0238.2009.00059.x
- Girona, J., Mata, M., del Campo, J., Arbonés, A., Bartra, E., and Marsal, J. (2006). The use of midday leaf water potential for scheduling deficit irrigation in vineyards. *Irrig. Sci.* 24, 115–127. doi: 10.1007/s00271-005-0015-7
- Gouveia, J., Lopes, C. M., Pedroso, V., Martins, S., Rodrigues, P., and Alves, I. (2012). Effect of irrigation on soil water depletion, vegetative growth, yield and berry composition of the grapevine variety Touriga Nacional. *Ciência Téc. Vitiv.* 27, 115–122.
- Greven, M., Green, S., Neal, S., Clothier, B., Neal, M., Dryden, G., et al. (2005). Regulated deficit irrigation (RDI) to save water and improve Sauvignon Blanc quality? *Water Sci. Technol.* 51, 9–17.
- Hamilton, A. J., Stagnitti, F., Xiong, X., Kreidl, S. L., Benke, K. K., and Maher, P. (2007). Wastewater irrigation: the state of play. *Vadose Zone J.* 6, 823–840. doi: 10.2136/vzj2007.0026
- Hickinbotham, A. R., and Williams, R. A. (1933). Soluble salts in non-irrigated vineyards. *South Aus. J. Agric.* 36, 217–223.
- Hochberg, U., Degu, A., Cramer, G. R., Rachmilevitch, S., and Fait, A. (2015). Cultivar specific metabolic changes in grapevines berry skins in relation to deficit irrigation and hydraulic behavior. *Plant Physiol. Biochem.* 88, 42–52. doi: 10.1016/j.plaphy.2015.01.006
- Ilc, T., Werck-Reichart, D., and Navrot, N. (2016). Meta-analysis of the core aroma components of grape and wine aroma. *Front. Plant Sci.* 7:1472. doi: 10.3389/fpls.2016.01472
- Intrigliolo, D. S., and Castel, J. R. (2006). Vine and soil-based measures of water status in a Tempranillo vineyard. *Vitis* 45, 157–163.
- Intrigliolo, D. S., and Castel, J. R. (2008). Effects of irrigation on the performance of grapevine cv. Tempranillo in Requena, Spain. *Am. J. Enol. Vitic.* 59, 30–38.
- Intrigliolo, D. S., and Castel, J. R. (2009). Response of *Vitis vinifera* cv. 'Tempranillo' to partial rootzone drying in the field: water relations, growth, yield and fruit and wine quality. *Agric. Water Manage.* 96, 282–292. doi: 10.1016/j.agwat.2008.08.001
- Intrigliolo, D. S., and Castel, J. R. (2010). Response of grapevine cv. 'Tempranillo' to timing and amount of irrigation: water relations, vine growth, yield and berry and wine composition. *Irrig. Sci.* 28, 113–125. doi: 10.1007/s00271-009-0164-1
- Intrigliolo, D. S., and Castel, J. R. (2011). Interactive effects of deficit irrigation and shoot and cluster thinning on grapevine cv. Tempranillo. Water relations, vine performance and berry and wine composition. *Irrig. Sci.* 29, 443–454. doi: 10.1007/s00721-010-0252-2
- Intrigliolo, D. S., Lizama, V., García-Esparza, M. J., Abrisqueta, I., and Álvarez, I. (2016). Effects of post-veraison irrigation regime on Cabernet Sauvignon grapevines in Valencia, Spain: yield and grape composition. *Agric. Water Manage.* 170, 110–119. doi: 10.1016/j.agwat.2015.10.020
- Intrigliolo, D. S., Pérez, D., Risco, D., Yeyes, A., and Castel, J. R. (2012). Yield components and grape composition responses to seasonal water deficits in Tempranillo grapevines. *Irrig. Sci.* 30, 339–349. doi: 10.1007/s00271-012-0354-0
- IPCC (2014). "Climate Change 2014: Synthesis Report," in *Contribution of Working Groups I, II and III to the Fifth Assessment Report of the Intergovernmental Panel on Climate Change*, eds Core Writing Team, R. K. Pachauri, and L. A. Meyer (Geneva: IPCC), 151.
- Jackson, D. I., and Lombard, P. B. (1993). Environmental and management practices affecting grape composition and wine quality—A review. *Am. J. Enol. Vitic.* 44, 409–430.
- Junquera, P., Lissarrague, J. R., Jiménez, L., Linares, R., and Baeza, P. (2012). Long-term effects of different irrigation strategies on yield components, vine vigour, and grape composition in cv. Cabernet-Sauvignon (*Vitis vinifera* L.). *Irrig. Sci.* 30, 351–361. doi: 10.1007/s00271-012-0348-y
- Kaufmann, A. (1996). Chloride in wine. *Dtsch. Lebensmitt. Rundsch.* 92, 205–209.
- Keller, M. (2010). Managing grapevines to optimize fruit development in a challenging environment: a climate change primer for viticulturists. *Aus. J. Grape Wine Res.* 16, 56–59. doi: 10.1111/j.1755-0238.2009.00077.x
- Keller, M., Romero, P., Gohil, H., Smithyman, R. P., Riley, W. R., Casassa, L. F., et al. (2016). Deficit irrigation alters grapevine growth, physiology, and fruit microclimate. *Am. J. Enol. Vitic.* 67, 426–435. doi: 10.5344/ajev.2016.16032
- Keller, M., Smithyman, R. P., and Mills, L. J. (2008). Interactive effects of deficit irrigation and crop load on Cabernet Sauvignon in an arid climate. *Am. J. Enol. Vitic.* 59, 221–234.
- Kounduras, S., Marinou, V., Gkoulioti, A., Koyseridis, Y., and van Leeuwen, C. (2006). Influence of vineyard location and vine water status on fruit maturation of nonirrigated cv. Agiorgitiko (*Vitis vinifera* L.). Effects on wine phenolic and aroma components. *J. Agric. Food Chem.* 54, 5077–5086. doi: 10.1021/jf0605446
- Lanari, V., Palliotti, A., Sabbatini, P., Howell, G. S., and Silvestroni, O. (2014). Optimizing deficit irrigation strategies to manage vine performance and fruit composition of field-grown 'Sangiovese' (*Vitis vinifera* L.) grapevines. *Sci. Hortic.* 179, 239–247. doi: 10.1016/j.scientia.2014.09.032
- Laurenson, S., Bolan, N. S., Smith, E., and McCarthy, M. (2012). Review: use of recycled wastewater for irrigating grapevines. *Aus. J. Grape Wine Res.* 18, 1–10. doi: 10.1111/j.1755-0238.2011.00170.x
- Lavoie-Lamoureux, A., Sacco, D., Rissé, P. A., and Lovisolo, C. (2017). Factors influencing stomatal conductance in response to water availability in grapevine: a meta-analysis. *Physiol. Plant.* 159, 468–482. doi: 10.1111/ppl.12530
- Lund, S. T., and Bohlmann, J. (2006). The molecular basis for wine grape quality—a volatile subject. *Science* 311, 804–805. doi: 10.1126/science.1118962
- Marschner, H. (1986). *Mineral Nutrition of Higher Plants*. London: Academic Press.
- Medrano, H., Tomás, M., Martorell, S., Escalona, J. M., Pou, A., Fuentes, S., et al. (2015). Improving water use efficiency of vineyards in semi-arid regions. A review. *Agron. Sustain. Dev.* 35, 499–517. doi: 10.1007/s13593-014-0280-z
- Mendez-Costabel, M. P., Wilkinson, K. L., Bastian, S. E. P., Jordans, C., McCarthy, M., Ford, C. M., et al. (2014). Effect of increased irrigation and additional nitrogen fertilization on the concentration of green aroma compounds in *Vitis vinifera* L. Merlot fruit and wine. *Aust. J. Grape Wine Res.* 20, 80–90. doi: 10.1111/ajgw.12062
- Merli, M. C., Gatti, M., Galbignani, M., Bernizzoni, F., and Magnanini, E. (2015). Comparison of whole-canopy water use efficiency and vine performance of cv. Sangiovese (*Vitis vinifera* L.) vines subjected to a post-veraison water deficit. *Sci. Hortic.* 185, 113–120. doi: 10.1016/j.scientia.2015.01.019
- Mira de Orduña, R. (2010). Climate change associated effects on grape and wine quality and production. *Food Res. Int.* 43, 1844–1855. doi: 10.1016/j.foodres.2010.05.001
- Mirás-Avalos, J. M., Trigo-Córdoba, E., Bouzas-Cid, Y., and Orriols-Fernández, I. (2016). Irrigation effects on the performance of grapevine (*Vitis vinifera* L.) cv. 'Albariño' under the humid climate of Galicia. *OENO One* 50, 183–194. doi: 10.20870/oeno-one.2016.50.4.63
- Mosse, K. P. M., Lee, J., Leachman, B. T., Parikh, S. J., Cavagnaro, T. R., Patti, A. F., et al. (2013). Irrigation of an established vineyard with winery cleaning agent solution (simulated winery wastewater): vine growth, berry quality, and soil chemistry. *Agric. Water Manage.* 123, 93–102. doi: 10.1016/j.agwat.2013.02.008

- Mosse, K. P. M., Patti, A. F., Christen, E. W., and Cavagnaro, T. R. (2011). Review: winery wastewater quality and treatment options in Australia. *Aus. J. Grape Wine Res.* 17, 111–122. doi: 10.1111/j.1755-0238.2011.00132.x
- Munitz, S., Netzer, Y., and Schwartz, A. (2017). Sustained and regulated deficit irrigation of field-grown Merlot grapevines. *Aus. J. Grape Wine Res.* 23, 87–94. doi: 10.1111/ajgw.12241
- Myburgh, P. A. (2005). Water status, vegetative growth and yield responses of *Vitis vinifera* L. cvs. Sauvignon blanc and Chenin blanc to timing of irrigation during berry ripening in the Coastal Region of South Africa. *S. Afr. J. Enol. Vitic.* 26, 59–67.
- Myburgh, P. A. (2006). Juice and wine quality responses of *Vitis vinifera* L. cvs. Sauvignon blanc and Chenin blanc to timing of irrigation during berry ripening in the Coastal Region of South Africa. *S. Afr. J. Enol. Vitic.* 27, 1–7.
- Myburgh, P. A. (2011a). Response of *Vitis vinifera* L. cv. Merlot to low frequency drip irrigation and partial root zone drying in the Western Cape Coastal Region—Part I. Soil and plant water status. *S. Afr. J. Enol. Vitic.* 32, 89–103.
- Myburgh, P. A. (2011b). Response of *Vitis vinifera* L. cv. Merlot to low frequency drip irrigation and partial root zone drying in the Western Cape Coastal Region – Part II. Vegetative growth, yield and quality. *S. Afr. J. Enol. Vitic.* 32, 104–116.
- Naor, A., Bravdo, B., and Hepner, Y. (1993). Effect of post-véraison irrigation level on Sauvignon Blanc yield, juice quality and water relations. *S. Afr. J. Enol. Vitic.* 14, 19–25.
- Netzer, Y., Shenker, M., and Schwartz, A. (2014). Effects of irrigation using treated wastewater on table grape vineyards: dynamics of sodium accumulation in soil and plant. *Irrig. Sci.* 32, 283–294. doi: 10.1007/s00271-014-0430-8
- Ojeda, H., Andary, C., Kraeva, E., Carboneau, A., and Deloire, A. (2002). Influence of pre- and postveraison water deficit on synthesis and concentration of skin phenolic compounds during berry growth of *Vitis vinifera* cv. Shiraz. *Am. J. Enol. Vitic.* 53, 261–267.
- Ollé, D., Guiraud, J. L., Souquet, J. M., Terrier, N., Ageorges, A., Cheynier, V., et al. (2011). Effect of pre- and post-veraison water deficit on proanthocyanidins and anthocyanin accumulation during Shiraz berry development. *Aus. J. Grape Wine Res.* 17, 90–100. doi: 10.1111/j.1755-0238.2010.00121.x
- Ou, C., Du, X., Shellie, K., Ross, C., and Qian, M. (2010). Volatile compounds and sensory attributes of wine from cv. Merlot (*Vitis vinifera* L.) grown under differential levels of water deficit with or without a kaolin-based, foliar reflectant particle film. *J. Agric. Food Chem.* 58, 12890–12898. doi: 10.1021/jf102587x
- Peyrot des Gachons, C., van Leeuwen, C., Tominaga, T., Soyer, J. P., Gaudillère, J. P., et al. (2005). Influence of water and nitrogen deficit on fruit ripening and aroma potential of *Vitis vinifera* L. cv. Sauvignon blanc in field conditions. *J. Sci. Food Agric.* 85, 73–85. doi: 10.1002/jsfa.1919
- Reynolds, A. G., Lowrey, W. D., Tomek, L., Hakimi, J., and de Savigny, C. (2007). Influence of irrigation on vine performance, fruit composition, and wine quality of Chardonnay in a cool, humid climate. *Am. J. Enol. Vitic.* 58, 217–228.
- Roby, G., and Matthews, M. A. (2004). Relative proportions of seed, skin and flesh, in ripe berries from Cabernet Sauvignon grapevines grown in a vineyard either well irrigated or under water deficit. *Aus. J. Grape Wine Res.* 10, 74–82. doi: 10.1111/j.1755-0238.2004.tb00009.x
- Romero, P., Fernández-Fernández, J. I., and Martínez-Cutillas, A. (2010). Physiological thresholds for efficient regulated deficit-irrigation management in winegrapes grown under semiarid conditions. *Am. J. Enol. Vitic.* 61, 300–312.
- Romero, P., Gil-Muñoz, R., del Amor, F. M., Valdés, E., Fernández, J. I., and Martínez-Cutillas, A. (2013). Regulated deficit irrigation based upon optimum water status improves phenolic composition in Monastrell grapes and wines. *Agric. Water Manage.* 121, 85–101. doi: 10.1016/j.agwat.2013.01.007
- Salón, J. L., Chirivella, C., and Castel, J. R. (2005). Response of cv. Bobal to timing of deficit irrigation in Requena, Spain: water relations, yield, and wine quality. *Am. J. Enol. Vitic.* 56, 1–8.
- Santesteban, L. G., Miranda, C., and Royo, J. B. (2011). Regulated deficit irrigation effects on growth, yield, grape quality and individual anthocyanin composition in *Vitis vinifera* L. cv. ‘Tempranillo’. *Agric. Water Manage.* 98, 1171–1179. doi: 10.1016/j.agwat.2011.02.011
- Santos, J. A., Malheiro, A. C., Pinto, J. G., and Jones, G. V. (2012). Macroclimate and viticultural zoning in Europe: observed trends and atmospheric forecasting. *Clim. Res.* 51, 89–103. doi: 10.3354/cr01056
- Savoi, S., Wong, D. C. J., Arapitas, P., Miculan, M., Buchetti Peterlunger, E., Fait, A., et al. (2016). Transcriptome and metabolite profiling reveals that prolonged drought modulates the phenylpropanoid and terpenoid pathway in white grapes (*Vitis vinifera* L.). *BMC Plant Biol.* 16:67. doi: 10.1186/s12870-016-0760-1
- Schultz, H. R., and Stoll, M. (2010). Some critical issues in environmental physiology of grapevines: future challenges and current limitations. *Aus. J. Grape Wine Res.* 16, 4–24. doi: 10.1111/j.1755-0238.2009.0074.x
- Shellie, K. C. (2010). Water deficit effect on ratio of seed to berry fresh weight and berry weight uniformity in winegrape cv. Merlot. *Am. J. Enol. Vitic.* 61, 414–418.
- Shellie, K. C. (2014). Water productivity, yield, and berry composition in sustained versus regulated deficit irrigation of Merlot grapevines. *Am. J. Enol. Vitic.* 65, 197–205. doi: 10.5344/ajev.2014.13112
- Shellie, K. C., and Bowen, P. (2014). Isohydrodynamic behavior in deficit-irrigated Cabernet Sauvignon and Malbec and its relationship between yield and berry composition. *Irrig. Sci.* 32, 87–97. doi: 10.1007/s00271-013-0416-y
- Stevens, R. M., Harvey, G., and Partington, D. L. (2011). Irrigation of grapevines with saline water at different growth stages: effects on leaf, wood and juice composition. *Aus. J. Grape Wine Res.* 17, 239–248. doi: 10.1111/j.1755-0238.2011.00145.x
- Talaverano, I., Valdés, E., Moreno, D., Gamero, E., Mancha, L., and Vilanova, M. (2017). The combined effect of water status and crop level on Tempranillo wine volatiles. *J. Sci. Food Agric.* 97, 1533–1542. doi: 10.1002/jsfa.7898
- Teakle, N. L., and Tyerman, S. D. (2010). Mechanisms of Cl⁻ transport contributing to salt tolerance. *Plant Cell Environ.* 33, 566–589. doi: 10.1111/j.1365-3040.2009.02060.x
- Trégoat, O., van Leeuwen, C., Choné, X., and Gaudillère, J. P. (2002). Étude du régime hydrique et de la nutrition azotée de la vigne pour des indicateurs physiologiques: influence sur le comportement de la vigne et la maturation du raisin (*Vitis vinifera* L. cv. Merlot, 2000, Bordeaux). *J. Int. Sci. Vigne Vin* 36, 133–142.
- Trigo-Córdoba, E., Bouzas-Cid, Y., Orriols-Fernández, I., and Mirás-Avalos, J. M. (2015). Effects of deficit irrigation on the performance of grapevine (*Vitis vinifera* L.) cv. ‘Godello’ and ‘Treixadura’ in Ribeiro, NW Spain. *Agric. Water Manage.* 161, 20–30. doi: 10.1016/j.agwat.2015.07.011
- van Leeuwen, C., Trégoat, O., Choné, X., Bois, B., Pernet, D., and Gaudillère, J.-P. (2009). Vine water status is a key factor in grape ripening and vintage quality for red Bordeaux wine. How can it be assessed for vineyard management purposes? *J. Int. Sci. Vigne Vin* 43, 121–134. doi: 10.20870/oeno-one.2009.43.3.798
- Walker, R. R., Blackmore, D. H., Clingeleffer, P. R., and Emanuelli, D. (2014). Rootstock type determines tolerance of Chardonnay and Shiraz to long-term saline irrigation. *Aus. J. Grape Wine Res.* 20, 496–506. doi: 10.1111/ajgw.12094
- Walker, R. R., Read, P. E., and Blackmore, D. H. (2000). Rootstock and salinity effects on rates of berry maturation, ion accumulation and colour development in Shiraz grapes. *Aus. J. Grape Wine Res.* 6, 227–239. doi: 10.1111/j.1755-0238.2000.tb00183.x
- Williams, L. E. (2012). Interaction of applied water amounts and leaf removal in the fruiting zone on grapevine water relations and productivity of Merlot. *Irrig. Sci.* 30, 363–375. doi: 10.1007/s00271-012-0355-z

Conflict of Interest Statement: The authors declare that the research was conducted in the absence of any commercial or financial relationships that could be construed as a potential conflict of interest.

Copyright © 2017 Mirás-Avalos and Intrigliolo. This is an open-access article distributed under the terms of the Creative Commons Attribution License (CC BY). The use, distribution or reproduction in other forums is permitted, provided the original author(s) or licensor are credited and that the original publication in this journal is cited, in accordance with accepted academic practice. No use, distribution or reproduction is permitted which does not comply with these terms.



The Role of Polyphenoloxidase, Peroxidase, and β -Glucosidase in Phenolics Accumulation in *Olea europaea* L. Fruits under Different Water Regimes

Marco Cirilli^{1†}, Giovanni Caruso², Clizia Gennai², Stefania Urbani³, Eleonora Frioni¹, Maurizio Ruzzi⁴, Maurizio Servili³, Riccardo Gucci², Elia Poerio⁴ and Rosario Muleo^{1,5*}

¹ Laboratorio di Ecofisiologia Molecolare delle Piante Arboree, Dipartimento di Scienze Agrarie e Forestali, Università degli Studi della Tuscia, Viterbo, Italy, ² Dipartimento di Scienze Agrarie, Alimentari e Agro-ambientali, Università di Pisa, Pisa, Italy,

³ Dipartimento di Scienze Agrarie, Alimentari ed Ambientali, Università degli studi di Perugia, Perugia, Italy, ⁴ Dipartimento per la Innovazione nei Sistemi Biologici, Agro-alimentari e Forestali, Università degli Studi della Tuscia, Viterbo, Italy, ⁵ Tree and Timber Institute, National Research Council of Italy, Sesto Fiorentino, Italy

OPEN ACCESS

Edited by:

Nadia Bertin,
Plantes et Système de Cultures
Horticoles (INRA), France

Reviewed by:

Ana Maria Gomez-Caravaca,
University of Granada, Spain
Panagiotis Kalaitzis,
Mediterranean Agronomic Institute
of Chania, Greece

*Correspondence:

Rosario Muleo
muleo@unitus.it

†Present address:

Marco Cirilli,
Department of Agricultural
and Environmental Sciences,
University of Milan, Milan, Italy

Specialty section:

This article was submitted to
Crop Science and Horticulture,
a section of the journal
Frontiers in Plant Science

Received: 20 February 2017

Accepted: 19 April 2017

Published: 09 May 2017

Citation:

Cirilli M, Caruso G, Gennai C,
Urbani S, Frioni E, Ruzzi M,
Servili M, Gucci R, Poerio E and
Muleo RM (2017) The Role of Polyphenoloxidase, Peroxidase,
and β -Glucosidase in Phenolics
Accumulation in *Olea europaea* L.
Fruits under Different Water Regimes.
Front. Plant Sci. 8:717.
doi: 10.3389/fpls.2017.00717

Olive fruits and oils contain an array of compounds that contribute to their sensory and nutritional properties. Phenolic compounds in virgin oil and olive-derived products have been proven to be highly beneficial for human health, eliciting increasing attention from the food industry and consumers. Although phenolic compounds in olive fruit and oil have been extensively investigated, allowing the identification of the main classes of metabolites and their accumulation patterns, knowledge of the molecular and biochemical mechanisms regulating phenolic metabolism remains scarce. We focused on the role of polyphenoloxidase (PPO), peroxidase (PRX) and β -glucosidase (β -GLU) gene families and their enzyme activities in the accumulation of phenolic compounds during olive fruit development (35–146 days after full bloom), under either full irrigation (FI) or rain-fed (RF) conditions. The irrigation regime affected yield, maturation index, mesocarp oil content, fruit size, and pulp-to-pit ratio. Accumulation of fruit phenolics was higher in RF drupes than in FI ones. Members of each gene family were developmentally regulated, affected by water regime, and their transcript levels were correlated with the respective enzyme activities. During the early phase of drupe growth (35–43 days after full bloom), phenolic composition appeared to be linked to β -GLU and PRX activities, probably through their effects on oleuropein catabolism. Interestingly, a higher β -GLU activity was measured in immature RF drupes, as well as a higher content of the oleuropein derivate 3,4-DHPEA-EDA and verbascoside. Activity of PPO enzymes was slightly affected by the water status of trees during ripening (from 120 days after full bloom), but was not correlated with phenolics content. Overall, the main changes in phenolics content appeared soon after the supply of irrigation water and remained thereafter almost unchanged until maturity, despite fruit growth and the progressive decrease in pre-dawn leaf water potential. We suggest that enzymes involved in phenolic catabolism in the olive fruit have a differential sensitivity to soil water availability depending on fruit developmental stage.

Keywords: enzyme activities, phenols, secoiridoids, catabolism, olive, oleuropein, relative transcript level, water deficit

INTRODUCTION

Over the last 20 years, the world consumption of olive oil has increased by 54% (International Olive Council [IOC], 2016), mostly due to a growing consumption in countries outside of the Mediterranean region. An increasing body of evidence suggests that the beneficial effects of VOO arise not only from its balanced fatty acid composition, but also from the presence of bio-active minor components such as tocopherols and phenolic compounds. Olive phenolic compounds have antioxidant properties and affect organoleptic properties of the olive fruit and oil.

The phenolics composition of olive fruits and derived VOOs is affected by many factors, namely cultivar, fruit development, climate conditions, and cultural practices (Ryan and Robards, 1998; Servili et al., 2007a; Tura et al., 2008). Several studies have focused on changes in the phenolics composition and content during fruit development until ripening (Amiot et al., 1986; Ryan et al., 1999; Alagna et al., 2012; Talhaoui et al., 2015). Secoiridoids, which include oleuropein, ligstroside, and their aglycon derivates *p*-HPEA-EA (ligstroside aglycon) and 3,4-DHPEA-EA (oleuropein aglycon isomer), dialdehydic forms of elenolic acid (3,4-DHPEA-EDA and *p*-HPEA-EDA), phenylethanoids such as tyrosol (*p*-HPEA) and hydroxytyrosol (3,4-DHPEA), and verbascoside (a phenylpropanoid) are the main phenols in olive fruit, whereas flavonoids (rutin, luteolin, and cyanidin) represent only a minor fraction (Servili et al., 2004). The total phenol content is highest in immature drupes and gradually decreases during fruit development, although the rate of change varies depending on cultivar and environmental conditions (Monteleone et al., 1995; Romani et al., 1999; Rotondi et al., 2004; Talhaoui et al., 2015). Oleuropein and its derivative 3,4-DHPEA-EDA are the main bisphenols in olive mesocarp (Amiot et al., 1986; Alagna et al., 2012). During fruit growth, oleuropein progressively decreases concomitantly with the increase of 3,4-DHPEA-EDA. Some cultivars are also able to synthesize demethyloleuropein, which increases during ripening (Sivakumar et al., 2007; Alagna et al., 2012). Other secoiridoids, such as ligstroside (*p*-HPEA-EDA), hydroxytyrosol (3,4-DHPEA), and tyrosol (*p*-HPEA) follow the same decreasing trend as oleuropein during fruit maturation and ripening (Servili et al., 1999, 2004; Morelló et al., 2004), whereas the verbascoside content does not follow an unequivocal pattern (Amiot et al., 1986; Ryan et al., 2002; Alagna et al., 2012). Despite this knowledge, molecular and biochemical mechanisms regulating the accumulation of specific phenolic metabolites in the olive fruit are still far from being clear. Candidate genes involved in the biosynthesis of secoiridoids, phenylpropanoids, and flavonoids have recently been identified in *Olea europaea* (Alagna et al., 2009; Iaria et al., 2016). Nevertheless, several steps in the secoiridoid biosynthetic pathways remain unknown, as well as the general role of specific enzymatic classes, including the polyphenoloxidase (PPO), peroxidase (PRX), and β -glycosidase (β -GLU) families. The quantity and localization of in different fruit tissues affect the phenolic composition and oil quality of VOO during extraction (Luaces et al., 2007; Servili et al., 2007a). Endogenous glycosidase and esterase activities were hypothesized

to play a pivotal role in the regulation of oleuropein hydrolysis (Amiot et al., 1989; Gutierrez-Rosales et al., 2010, 2012). Recently, several members of the β -glucosidase family have been found in proteomic and transcriptomic studies (Corrado et al., 2012; Bianco et al., 2013). An olive β -glucosidase (Oe β -GLU) able to deglycosilate oleuropein with high affinity has recently been isolated and functionally characterized (Koudounas et al., 2015).

Water availability represents the main limiting factor for growth and yield of crops of the Mediterranean region. A wide array of physiological responses, signals and genes are triggered in response to drought (Shao et al., 2008; Krasensky and Jonak, 2012). When the water stress signal reaches a threshold value, it determines morphological and physiological changes, including the production of reactive oxygen species (ROS) that act as an alarm to induce plant survival responses (Cruz de Carvalho, 2008). As phenolic compounds have strong antioxidant properties, a role in the protection against ROS during water stress adaptation has been long suggested (Ramakrishna and Ravishankar, 2011). Olive trees are typically adapted to long periods of high temperatures and drought during the summer (Lavee et al., 1991). Soil water availability dramatically affects the concentration of phenolic compounds during fruit development (Servili et al., 2007b; Caruso et al., 2014). In Greek cultivars, severe water stress induced an increase in total phenol content, mainly due to a rise in oleuropein content (Petridis et al., 2012). A positive relationship between total phenol content and antioxidant activity has also been detected, suggesting that phenols could play a relevant role in the protection against the effects of drought (Petridis et al., 2012). The effect of three different irrigation water regimes on analytical parameters of olive oil was evaluated in cultivars 'Leccino' and 'Frantoio' (Servili et al., 2007b; Caruso et al., 2014). Full irrigation (FI) decreased the concentration of total phenol and *o*-diphenol in VOOs, with wide differences in the concentration of the aglycone derivate of oleuropein. In olive trees of cultivar 'Arbequina' subjected to four irrigation management approaches, at different stages of fruit development, the highest content of total phenols, hydroxytyrosol acetate, 3,4-DHPEA-EDA, *p*-HPEA-EDA, 3,4-DHPEA-EA, *o*-diphenols, tyrosyl elenolate (*p*-HPEA-EA), and total secoiridoids was detected in trees stressed from the end of fruit drop to the end of July (Del Campo and García, 2013). Fruit ripening and irrigation treatments have been also found to induce considerable variation in the concentrations of secoiridoid derivatives of hydroxytyrosol and tyrosol in VOO of cultivars 'Cornicabra' (Gümez-Rico et al., 2006), 'Souri' (Dag et al., 2008), and 'Cipressino' (Martinelli et al., 2013). Similar results were found in trees of cultivar 'Leccino,' where the highest content of phenolic compounds was detected in rain-fed (RF) trees, although the transcript level of the PAL gene did not differ among the water regimes (Martinelli et al., 2012).

Since there are no reports providing molecular evidence concerning the role of gene families involved in the oxidative catabolism of phenolic compounds in olive fruit, we set up a field experiment to provide insight about the role of PPOs, PRXs, and β -GLUs in the accumulation of phenolic compounds in olive fruits during their development and ripening. We used an integrated approach at the molecular, biochemical, and metabolic

levels to investigate the role of the above enzymes on phenolic metabolism in fruits when the water status was manipulated by imposing either FI or RF conditions to field-grown olive trees ('Frantoio').

MATERIALS AND METHODS

Plant Material and Site Characteristics

Experiments were conducted in a fully productive, irrigated olive ('Frantoio') orchard located at Venturina, Italy, in 2011. Olive trees had been planted at a spacing of 5 m × 3.9 m in April 2003. The soil was a deep (1.5 m), sandy-loam (ISSS classification), consisting of 60% sand, 15% clay, and 25% silt. The climate at the study site was sub-humid Mediterranean (Caruso et al., 2013), with an annual mean temperature and annual rainfall of 15°C and 635 mm, respectively (means of 21 years, 1990–2010). Climatic conditions over the study period were monitored using an iMETOS IMT 300 weather station (Pessl Instruments GmbH, Weiz, Austria). Reference annual evapotranspiration (ET_0), calculated according to the Penman-Monteith equation, was 840 mm. The year 2011 was hot and dry with annual and summer (21 June–22 September) precipitations of 197 and 18 mm, respectively (Supplementary Figure S1). Cultural practices and monitoring of phenological parameters were performed as previously reported (Caruso et al., 2013). In 2011, full bloom, estimated as when 70% of inflorescences showed at least 50% of flowers open, occurred on 24 May. Three blocks, each consisting of two irrigation treatments (three plots per treatment) randomly distributed, were used for the trial. Each of the six plots included 12 trees arranged in three rows of four trees. Only the inner trees of the central row were used for monitoring the tree water status, and only four of the six trees per treatment were used for measurements and sampling.

Irrigation and Tree Water Status

Subsurface drip irrigation lines (2.3 L h⁻¹ pressure-compensated drippers spaced at 0.6 m), placed at a depth of 0.35–0.40 m and 0.8 m distance from the tree row, were used to supply 100% (FI) or 2% (RF) of water requirements calculated from reference evapotranspiration using a crop coefficient of 0.55 (Caruso et al., 2013). RF trees received a total of 33 m³ ha⁻¹ irrigation on three dates [93, 94, and 113 days after full bloom (DAFB)], to avoid tree damage due to extreme water stress. Therefore, the RF condition was partially alleviated by three complementary irrigations because of the particularly dry year. The irrigation period lasted from 1st July to 26th September, and FI trees received water 4–5 days a week (3–7 h per day); the volume applied was 734 m³ ha⁻¹, corresponding to 1431 L per tree. Irrigation volumes were calculated on the basis of the effective evapotranspiration, and tree water status was determined by measuring pre-dawn leaf water potential (PLWP) during the dry season at 7–10 days intervals. Leaves were excised with a razor blade, immediately put in the chamber cylinder (Tecnogas, Pisa, Italy), which was then pressurized with nitrogen gas at a maximum rate of 0.02 MPa s⁻¹ (Caruso et al., 2013). Fertigation was used to supply mineral nutrients in spring, before irrigation

treatments were put into action. Each tree received a total of approx. 90 g of N, P₂O₅, and K₂O.

Fruit Growth and Production

Five fruits per tree in the south-east sector of the canopy were identified prior to the beginning of irrigation and their volume measured non-destructively by water displacement using a graduated cylinder. Fruits were sampled for enzymatic studies and determination of phenolic compounds at 35, 43, 63, 77, 93, 115, 136, and 146 DAFB and immediately frozen in liquid nitrogen. Frozen samples were finely ground in liquid nitrogen using a mortar and pestle and preserved at -80°C until biochemical and molecular analyses was carried out. The number of fruits sampled at each date was adjusted to account for fruit growth and obtain sufficient material for further analysis. In particular, 20 (35 DAFB), 15 (43, 63, and 77 DAFB), and 10 (93, 115, 136, and 146 DAFB) fruits were sampled from each of the four trees per treatment. Immediately before harvest, which occurred 146 DAFB, 50 fruits were randomly sampled from around the canopy of each tree to measure average fruit weight. The same fruits were also scored based on the color of the exocarp and mesocarp using a 0–7 arbitrary scale to determine the maturation index (MI) according to standard methodology (Caruso et al., 2013). Each tree was harvested individually by hand. The total number of fruits per tree was calculated by dividing the crop yield by the average fruit weight. At harvest (146 DAFB), five fruits per tree, similar to those used for enzyme assays and phenolic concentrations, were destructively sampled and their fresh weight (FW) determined. The mesocarp was separated from the endocarp using a sharp blade, the FW of both tissues was measured, and then the dry weight (DW) was determined after oven drying at 70°C to constant weight. The oil content of the fruit mesocarp of five fruits per tree, previously sampled for fresh and dry weight determinations, was also measured at harvest by nuclear magnetic resonance using an Oxford MQC-23 analyser (Oxford Analytical Instruments Ltd., Oxford, UK) as previously reported by Caruso et al. (2013).

High-Performance Liquid Chromatography (HPLC) Analysis of Phenolic Compounds

Fruit samples were frozen in liquid nitrogen and stored at -80°C, and successively used for phenolic determination. The phenols were extracted from the olive pulp according to the procedure described by Servili et al. (2012) modified as follows: 5 g of frozen olive pulp was homogenized with 100 mL of 80% methanol containing 20 mg L⁻¹ butylated hydroxytoluene (BHT); the extraction was performed in triplicate. After methanol removal, the aqueous extract was used for extraction by solid-phase separation (SPE) of phenols. The SPE procedure was applied by loading a 1000 mg Bond Elute Jr-C18 cartridge (Agilent Technologies, Santa Clara, CA, USA) with 1 mL of sample, using 50 mL of methanol as the eluting solvent. After solvent removal under vacuum at 30°C, the phenolic extract was recovered and then dissolved in methanol (1 mL) and filtered through a polyvinylidene fluoride (PVDF) syringe filter

(0.2 μm). The HPLC analyses of the phenolic extracts were conducted according to the method of Selvaggini et al. (2006) with a reversed-phase column using an Agilent Technologies system Model 1100 (Agilent Technologies, Santa Clara, CA, USA) that was composed of a vacuum degasser, a quaternary pump, an autosampler, a thermostatted column compartment, a diode array detector (DAD), and a fluorescence detector (FLD). The C18 column used in this study was a Spherisorb ODS-1 250 mm \times 4.6 mm with a particle size of 5 μm (Waters, Milford, MA, USA); the injected sample volume was 20 μL . The mobile phase was composed of 0.2% acetic acid (pH 3.1) in water (solvent A)/methanol (solvent B) at a flow rate of 1 mL min^{-1} , and the gradient was changed as follows: 95% A/5% B for 2 min, 75% A/25% B over 8 min, 60% A/40% B over 10 min, 50% A/50% B over 16 min, and 0% A/100% B over 14 min; this composition was maintained for 10 min, then returned to the initial conditions and equilibration over 13 min; the total running time was 73 min. Lignans were detected by an FLD operated at an excitation wavelength of 280 nm and emission at 339 nm, while the other compounds were detected by DAD at 278 nm.

HPLC Analysis of VOO Phenolic Compounds

The extraction of VOO phenolic compounds was performed as reported by Montedoro et al. (1992). The HPLC analyses of the phenolic extracts were conducted according to the method of Selvaggini et al. (2014); for the detection of phenolic compounds, a DAD was employed with the wavelength set at 278 nm.

Enzyme Extraction and Activities

Two hundred milligrams of fruit pulp frozen powder was suspended in 1 mL of an extraction buffer consisting of 50 mM potassium phosphate, 1 mM EDTA, 1 mM PMSF, and 1% (w/v) PEG4000, pH 6.2. The suspension was shaken at 2000 rpm for 1 h at 4°C, and the supernatant was recovered by centrifugation (12000 rpm for 15 min at 4°C). The pellet was re-extracted, and the two supernatants were combined, filtered through a 0.45 μm filter (Sartorius, Italy), and used for enzyme activity assays.

Polyphenoloxidase activity was measured at 25°C, according to the method of Zouari-Mechichi et al. (2006), by monitoring oxidation of 2,6-dimethoxyphenol (2,6-DMP) spectrophotometrically ($\epsilon_{469\text{nm}} = 27.5 \text{ mM}^{-1} \text{ cm}^{-1}$); the reaction mixture (1 mL final volume) consisted of 5 mM 2,6-DMP in McIlvaine buffer at pH 6.0. PRX activity was measured at 25°C, according to the method of Makkar et al. (2001), by monitoring oxidation of 2,2'-azino-bis(3-ethylbenzothiazoline-6-sulfonic acid) (ABTS) spectrophotometrically ($\epsilon_{420} = 36.0 \text{ mM}^{-1} \text{ cm}^{-1}$); the reaction mixture (1 mL final volume) consisted of 5 mM ABTS and 0.2 mM H₂O₂ in McIlvaine buffer at pH 3.0.

β -glycosidase activity was measured at 25°C, according to Romero-Segura et al. (2009), by monitoring formation of *p*-nitrophenol spectrophotometrically ($\epsilon_{405} = 0.553 \text{ mM}^{-1} \text{ cm}^{-1}$) due to hydrolysis of *p*-nitrophenyl- β -D-glucopyranoside (*p*-NPG). The reaction mixture (1 mL final volume) consisted of 5 mM *p*-NPG in McIlvaine buffer at pH 6.0. All enzyme activities were expressed as IU per g (FW) fruit tissue.

Identification of Putative Genes Coding for Enzymes of Phenols Degradation

Sequences of transcripts coding for *PPO*, *PRX*, and β -*GLU* genes were identified by a tBLASTn approach, implemented in BioLign 4.0¹, using amino acid sequences of enzymes already characterized in other plant species, including *Arabidopsis thaliana*, *Malus domestica* Borkh., *Vitis vinifera* L., and *Populus trichocarpa*. A search for *O. europaea* orthologous genes was performed by exploring olive fruit² (Alagna et al., 2009) and flower EST databases (Alagna et al., 2016). Identified transcripts were annotated by BLAST against the NCBI-nr database and used as a query to retrieve genomic sequences of each gene from an advanced genome assembly of cultivar 'Leccino' (Olea Genome Project). Genomic sequences were aligned with EST clusters to reconstruct the full-length ORF tentative consensus.³ Specific primers were designed by using Primer3 software³ (Supplementary Table S1).

Amino Acid Sequence Comparisons and Phylogenetic Analysis

The full predicted amino acid sequences of candidate genes were used to reconstruct the phylogeny with their homologs from others species. Alignments were performed using the ClustalW2 algorithm⁴ with default parameters and GeneDoc software. Gene models for multiple alignment analysis were obtained from the Phytozome V11.0 database⁵ (Supplementary Table S2). A rooted tree was reconstructed using the neighbor-joining method in MEGA6 software (Tamura et al., 2013). Tree nodes were evaluated by bootstrap analysis of 1500 replicates (pairwise deletion, uniform rates, and Poisson correction options). Intracellular localization was inferred for each protein by the TargetP1.1 server⁶.

Real-Time Quantitative PCR Expression Analysis

Total RNA was extracted from fruit tissues, following the guidelines of a modified protocol of Doyle and Doyle (1990). Samples were DNase treated using an RNeasy Plant Mini Kit (Qiagen, Cat. No. 74904, Italy), following the manufacturer's instructions. RNA purity was evaluated by agarose gel electrophoresis and quantified using a QUBIT® 2.0 Fluorometer (Invitrogen, Cat. No. Q32866, Italy). First-strand cDNA was synthesized using Ready-To-GO™ RT-PCR Beads (GE Healthcare™ Illustra™, Cat. No. 27-9267-01, Italy), following the manufacturer's guidelines. Real-time PCR analysis was conducted using the thermal cycler LC480II® (Roche, Italy). Each reaction (20 μL) contained 10 μL of LightCycler 480 SYBR Green I Master (Roche, Cat. No. 04 707 516 001, Italy), 0.5 μM of each primer, 1 μL of cDNA, and 7 μL of PCR-grade water.

¹<http://biolign.software.informer.com/4.0/>

²<http://140.164.45.140/oleaestdb/search.php>

³<http://www.Primer3.com>

⁴<http://www.ebi.ac.uk/Tools/msa/clustalw2/>

⁵<https://phytozome.jgi.doe.gov/pz/portal.html>

⁶<http://www.cbs.dtu.dk/services>

The PCR reaction was conducted using the following conditions: 95°C for 10 min; 45 cycles at 94°C for 20 s, 59°C for 30 s, and 72°C for 30 s; followed by a melting cycle from 65–95°C. Real-time quantitative PCR was performed using three biological replicates, with three technical replicates for each sample. Data were expressed with the 2^{ΔC_p} method (Kubista et al., 2006) using the geometric means of the *elongation factor-1 alpha* (*OeEF1- α* , no. AM946404.1) and actin genes as endogenous reference genes for the normalization of transcript abundance. After PCR amplification, all products were sequenced to confirm their identity.

RESULTS

Water Status and Yield Components

The PLWP of the FI trees was usually maintained at approx. -1 MPa by irrigation. The PLWP dropped below -1 MPa three times and temporarily reached -1.43 MPa at 99 DAFB during the irrigation period due to pump failure (Figure 1A). The PLWP of RF trees decreased progressively with increasing seasonal drought and reached very low values of -3.70 and -3.99 MPa at 109 and 142 DAFB (Figure 1A). Fruits from FI trees grew according to an almost linear pattern (Figure 1B). The size of FI fruits was greater than that of RF ones starting from 87 DAFB until harvest, when fruit volume of RF fruits was only 70% that of FI fruits (Figure 1B). Fruit yield of FI trees was higher (227%) and significantly different from that of RF trees (Table 1). The number of fruits of FI trees was higher, but not significantly different, than that of RF trees, and this difference disappeared if the number of fruits per tree was expressed on a trunk cross-sectional area basis (Table 1). Significant differences in fruit FW were found between the two irrigation regimes; the maturation index (pigmentation of skin and pulp) was delayed in FI trees (Table 1). The oil yield of the RF treatment was 41% of that of FI trees.

Trees subjected to substantial water deficit (RF) had fruit measurements significantly lower than those for FI trees for all fruit parameters, except the endocarp DW (Table 2). The mesocarp, endocarp, and whole fruit FW of FI trees was 182, 130, and 162% of those of the RF trees. The meso-to-endocarp ratio, the FW to DW ratio, and the mesocarp moisture were significantly higher (136, 126, and 130%, respectively) in fruits from FI trees compared with fruits from RF trees (Table 2).

Phenolic Composition in Fruit and VOO

Total phenols content (TPC), calculated as the sum of phenolic fractions on a mesocarp FW basis [mg (g FW)^{-1}], showed a decreasing trend during fruit development, independently of the irrigation regime (Figure 2A). At maturity (146 DAFB), TPC was significantly higher in drupes of the RF trees than in those of the FI trees [24.7 vs. $14.8 \text{ mg (g FW)}^{-1}$, respectively] (Supplementary Table S3). Differences in TPC between the two treatments were already evident at early stages of drupe development (43–65 DAFB) and were thereafter maintained without major changes until fruit maturity. Notably, the TPC content was higher in mature RF drupes on a DW basis (Table 3). As for individual fractions 3,4-DHPEA-EDA, verbascoside, and

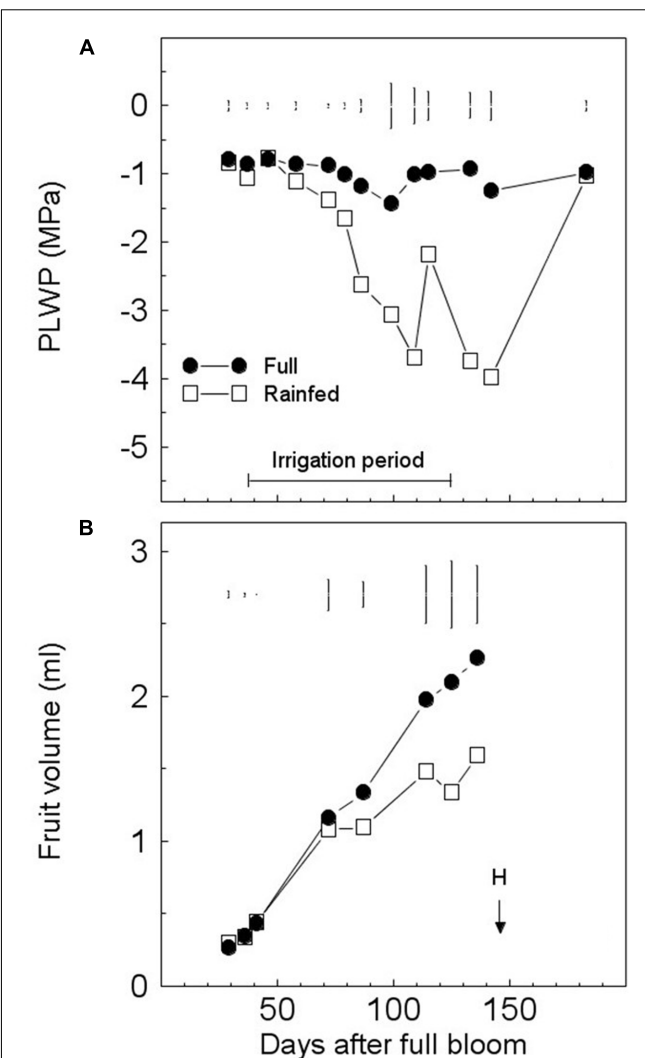


FIGURE 1 | Seasonal variations in pre-dawn leaf water potential (PLWP) (A) and fruit growth of olive trees ('Frantoio') (B) under full (FI) or rain-fed irrigation (RF). Symbols are means of six (tree water status) or four (fruit growth) trees per treatment. Vertical bars represent least significant differences (LSD) between irrigation treatments after analysis of variance (ANOVA) ($p < 0.05$). H, harvest date.

oleuropein contributed the most to the difference between mature fruits of FI and RF trees (Table 3). 3,4-DHPEA-EDA and verbascoside increased from 35 to 63 DAFB, but both tended to decrease later (Figures 2C,D and Supplementary Table S3). The oleuropein content was higher at the beginning of drupe development (from 35 to 43 DAFB) [60% of phenol fraction: $41.5 \text{ mg (g FW)}^{-1}$] and after that strongly decreased, reaching a plateau at about 77 DAFB, under both water regimes (Figure 2B and Supplementary Table S3). The simple phenols 3,4-DHPEA and *p*-HPEA accounted for less than 3% of the phenol fraction analyzed (Figures 2E,F and Supplementary Table S3). Their content was higher at the early stage of fruit development and then declined sharply, apparently unaffected by water

management. 3,4-DHPEA-EDA reached maximum content at 63 DAFB. Also, the lignans (+)-1-acetoxipinoresinol and (+)-1-pinoresinol, accounting for less than 1.5% of the phenol fraction, were unaffected by water status (Supplementary Table S4).

The phenolic compounds concentration in VOO was also markedly affected by the soil water availability. The differences in TPC content were similarly significant in VOO, with contents in oils extracted from RF drupes more than twofold higher than those of oils extracted from FI drupes (Table 3). The 3,4-DHPEA-EDA, p-HPEA-EDA, and the sum of phenolic fractions in VOO obtained from RF trees were significantly higher (438, 257, and 223%, respectively) than those from the FI trees.

Changes in Enzyme Activities during Fruit Development

Polyphenoloxidase activity remained low throughout fruit development until the onset of fruit ripening (from 43 to 115 DAFB), without significant changes between FI and RF trees (Figure 3A). PPO activity increased during ripening (from 136 to 146 DAFB), with higher values in FI trees (Figure 3A). In both FI and RF trees, the levels of PRX activity progressively decreased during the first 93 days of ripening before increasing in the following 50 days. In fruits from FI trees, the PRX activity at day 146 was twofold higher than that in fruits from RF trees (Figure 3B). A peak of β -GLU activity was detected at about 50 DAFB in fruits from both FI and RF treatments, then this activity declined to become almost undetectable after the pit-hardening stage (Figure 3C).

Identification of Transcripts Putatively Involved in Phenols Catabolism

A number of transcripts coding for PPO, PRX, and β -GLU enzymes and putatively expressed in fruit tissues have been identified.

Four full-length transcripts coding for PPO genes were arbitrarily named *OePPO1-like*, *2-like*, *3-like*, and *4-like*, after identification in a flower and fruit library (Supplementary Table S2). The isoforms were encoded by a single exon, as also reported in other plant species (Tran et al., 2012). Conceptual translation of the four putative PPO sequences allowed identification of the conserved tyrosinase domain (Supplementary Figure S2), composed of the copper-binding sub-domains CuA and CuB and characterized by six conserved histidine residues that bond the two copper ions of the active site (Tran et al., 2012). Moreover, two domains with unknown function, DWL (Pfam12142) and KFDW (Pfam12143), previously identified in *P. trichocarpa* PPOs, were also present (Supplementary Figure S2). A chloroplast localization signal was identified in all four olive PPO genes, as also predicted in other species (Supplementary Table S5). Phylogenetic analysis grouped *OePPO1-like*, *2-like*, and *4-like* in a clade comprising several PPO members of *Mimulus guttatus*, while *OePPO3-like* seemed to be phylogenetically distant (Supplementary Figure S3). Class III peroxidases are heme-containing glycoproteins encoded by a multigene family (Hiraga et al., 2001). At least 61 members of class III peroxidase gene family were identified in a draft assembly of *O. europaea* cv. 'Leccino' genome (data not shown), 5 of which resulted the most represented in RNA-seq libraries from olive fruit tissues. Active site residues of identified OePRXs contained the catalytic distal Arg38, His42 hydrogen-bonded to Asn70 (Supplementary Figure S4) (Smith and Veitch, 1998). Furthermore, we identified other conserved amino acid residues, such as Pro139, which putatively accepts a hydrogen bond from reducing substrates, and His170, which is coordinated to heme Fe³⁺ and hydrogen-bonded to Asp247. In OePRX42, the His70 was replaced by Ser70, and this substitution also occurred in other plant PRXs, such as *A. thaliana* PRX1 (Tognolli et al., 2002). Predicted side chain ligands to the distal and the proximal Ca²⁺ ions were also identified (Supplementary

TABLE 1 | Yield, yield components, yield efficiency (fruit yield/TCSA), and maturation index (MI) of olive trees ('Frantoio') subjected to full irrigation (FI) or rain-fed (RF) conditions.

Irrigation	Fruit yield (g/tree)	Fruit yield/TCSA (g/dm ⁻²)	Fruits/tree	Oil yield (g/tree)	Fruit FW (g)	MI	Oil in mesocarp (%/DW)
FI	8070b	3437	3255	1960b	2.5b	3.2a	68.3b
RF	3559a	2074	2311	792a	1.5a	4.0b	58.4a
LSD	3339	1580	1454	985	0.2	0.4	2.0

Values are means of four trees per treatment ($n = 4$). Different letters indicate least significant differences (LSD) between irrigation treatments after analysis of variance (ANOVA) within each year ($p < 0.05$). TCSA, trunk cross-sectional area; FW, fresh weight; DW, dry weight.

TABLE 2 | Fresh weight and dry weight of fruit, mesocarp, and endocarp, meso-to-endocarp ratio, fruit FW/DW ratio, and mesocarp moisture of fruits sampled from olive trees ('Frantoio') subjected to FI or RF conditions.

Irrigation	Fruit FW (g)	Fruit DW (g)	Mesocarp FW (g)	Endocarp FW (g)	Mesocarp DW (g)	Endocarp DW (g)	Mesocarp to endocarp ratio (FW)	FW/DW fruit	Mesocarp moisture (%)
FI	2.60b	1.42b	1.78b	0.82b	0.90b	0.52	2.16b	1.84b	49.0b
RF	1.61a	1.10a	0.98a	0.63b	0.61b	0.49	1.59a	1.46b	37.6a
LSD	0.28	0.13	0.18	0.14	0.08	0.08	0.36	0.27	7.73

Values are means of four trees per treatment ($n = 4$). Different letters indicate LSD between irrigation treatments ANOVA ($p < 0.05$).

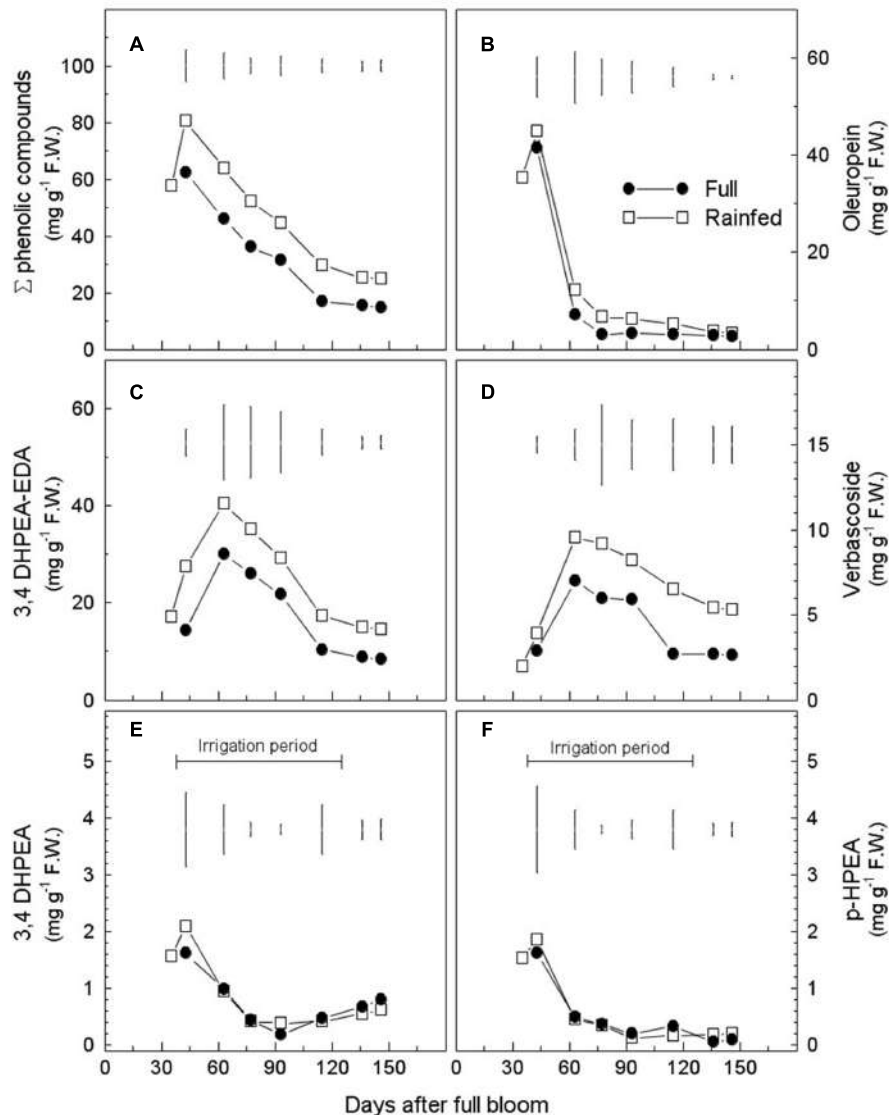


FIGURE 2 | Seasonal variations in phenolic compounds [$\text{mg} (\text{g FW})^{-1}$] in mesocarp of fruits from fully irrigated (FI) and rain-fed (RF) olive trees during fruit development. Total phenol content is shown in (A), oleuropein in (B), 3,4-DHPEA-EDA in (C), verbascoside in (D), 3,4-DHPEA in (E) and *p*-HPEA in (F). Values are means of three trees for each irrigation treatment. Vertical bars represent LSD between irrigation treatments ANOVA ($p < 0.05$).

Figure S4). OePRXs contained eight conserved cysteine residues putatively involved in disulfide bridges and a buried salt bridge motif present in all class III PRXs (Welinder, 1992). Putative OePRXs were predicted as secretory proteins (Supplementary Table S6). Moreover, as in other species, OePRXs had several N-linked glycans in the sequence motif Asn-X-Ser/Thr (Veitch, 2004). Phylogenetic analysis confirmed the similarity of the identified olive PRXs with other class III PRXs (Supplementary Figure S5).

Amino acid alignments of the four identified members of the olive glycoside hydrolase (GH) family 1 highlight the presence of the two glutamate residues embedded in

the highly conserved motifs TF/LNEP (acid/base catalyst) and I/VTENG (nucleophile), except for Oe β -GLU46-like characterized by the motifs TVNEA/IHENG (Supplementary Figure S6). The analysis with TargetP v1.0 predicted that Oe β -GLU11 and 46-like are localized in extra-cellular space, while the localization of both Oe β -GLU12-like isoforms is uncertain (Supplementary Table S7). Phylogenetic analyses were performed to gain information about their putative substrates (Supplementary Figure S7). Oe β -GLU12-like1 and Oe β -GLU12-like2, both belonging to the GH1 subgroup 12, cluster in a well-differentiated clade composed of the recently characterized Oe β -GLU, and RsSG and RsRG enzymes of *Rauvolfia serpentina*,

TABLE 3 | Phenolic compounds in mesocarp of fruits [mg (g DW)⁻¹] sampled at harvest (146 DAFB) and oils (mg kg⁻¹) obtained from fruits sampled at the same date from olive trees subjected to FI or RF conditions.

Irrigation	p-HPEA	3,4-DHPEAz	Oleuropein	Verbascoside	3-4 DHPEA-EDA	Sum of phenolic fractions
Fruit						
FI	0.16	1.54	4.93	5.16	15.91a	28.47a
RF	0.34	0.99	5.40	8.57	23.56b	39.94b
LSD	0.40	0.58	1.22	4.24	4.36	7.88
Olive oil						
FI	13.6	2.0	28.3a	35.7a	80.4ab	167.5a
RF	10.7	3.9	124.2	92.0b	133.3b	373.3b
LSD	5.1	3.0	8.8	12.77	40.81	59.1

Values are means of three trees for each irrigation treatment. Different letters indicate LSD between irrigation treatments ANOVA ($p < 0.05$).

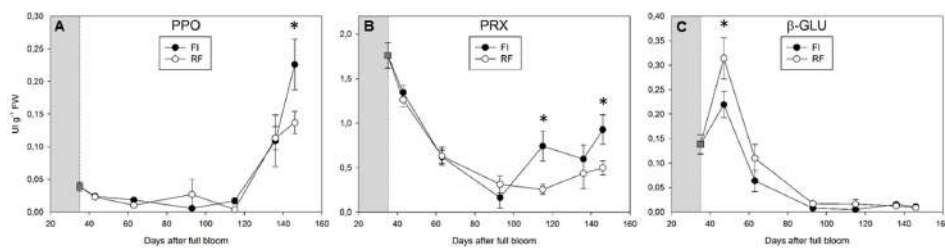


FIGURE 3 | Polyphenoloxidase (PPO) (A), peroxidase (PRX) (B), and β -glucosidase (β -GLU) (C) activity detected in olive fruit of FI and RF trees. Dashed line indicates the beginning of treatment. Symbols and bars indicate the average and SD of four biological and two technical replications. Asterisks (*) indicate a significant statistical difference between FI and RF treatments at $p < 0.01$ (Student's *t*-test).

involved in monoterpenoid indole alkaloids biosynthesis (Warzecha et al., 2000; Gerasimenko et al., 2002). It is unclear whether the two olive *Oeβ-GLU12* isoforms are different alleles of the same isoform, since *Oeβ-GLU* is encoded by a single locus in olive cultivar 'Koroneiki' (Koudounas et al., 2015). *Oeβ-GLU46* belongs to a large subgroup composed of glucosidases putatively involved in the phenylpropanoids pathway and lignin biosynthesis. Consistent with this hypothesis, *Oeβ-GLU46* is predicted to be targeted to the extracellular space (Supplementary Table S7). *Oeβ-GLU11* belongs to the *AtGLU11* subgroup, the members of which seem to work on different substrates, such as hydroxyisourate for the biosynthesis of the allantoin precursor in *Glycine max* (Raychaudhuri and Tipton, 2002).

Relative Gene Expression

The expression of *OePPO* genes was differently modulated along the stages of drupe development and appeared to be affected by plant water status. *OePPO1* expression was high during young fruit development, decreased after 43 DAFB, and strongly increased again at the two late sampling dates (136 and 146 DAFB) (Figure 4A). This expression pattern may suggest that *OePPO1* is the main enzymatic isoform active during ripening. Moreover, *OePPO1* was expressed twofold more in drupes of FI trees. By contrast, *OePPO2* showed the highest peak of transcripts during the pit-hardening phase (from 77 to 93 DAFB), with the maximum expression value in FI trees reached earlier than that in RF trees (Figure 4B). *OePPO3* and *OePPO4* were expressed at lower levels, although the former was up-regulated from 77 to

115 DAFB in fruits of FI trees and only at 93 DAFB in fruits of RF trees, whereas the latter gene was downregulated from 63 DAFB until the harvest of fruits (Figures 4C,D).

Among the *Oeβ-GLU* genes analyzed, *Oeβ-GLU12.1* transcripts showed the highest magnitude and were essentially expressed early in drupe development (from 43 to 63 DAFB) (Figure 4E). The other isoform, *Oeβ-GLU12.2*, showed two peaks, one at the beginning of drupe growth (35 DAFB) and the other near ripening (146 DAFB) (Figure 4F). Both *Oeβ-GLU12* genes showed higher transcript levels in FI trees. *Oeβ-GLU11* showed higher expression in young fruit that then increased again at ripening, more in FI drupes (Figure 4G). *Oeβ-GLU46* expression did not seem to be affected by either fruit development or water availability (Figure 4H).

Transcript levels of all *OePRX* genes were higher during the earlier stages of fruit development and then sharply decreased. At ripening, *OePRX17* and *OePRX72* were barely detectable (Figures 5A,E), while *OePRX64* and *OePRX55* increased again, more in FI fruit (Figures 5B,D). *OePRX42* showed an expression pattern similar to that of *OePRX17*, although the reduction of transcript levels during fruit development was less drastic (Figure 5C).

DISCUSSION

We confirmed the general decrease in phenolics content during olive fruit development reported in previous work (Alagna et al., 2012) but, interestingly, each metabolite showed a specific pattern

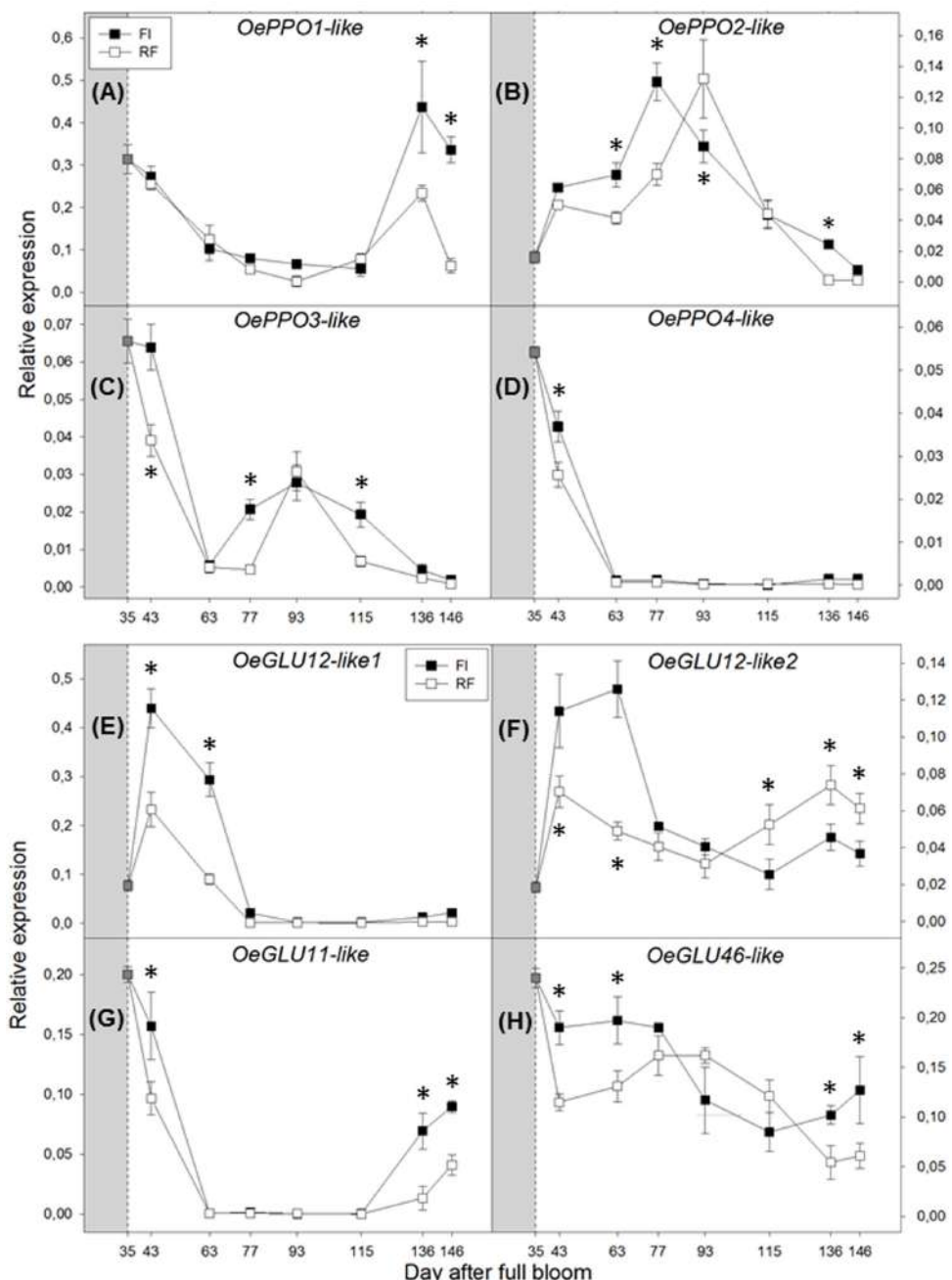


FIGURE 4 | Real-time quantitative PCR analysis of *OePPO1-like* (A), *OePPO2-like* (B), *OePPO3-like* (C), *OePPO4-like* (D), *OeGLU12-like1* (E), *OeGLU12-like2* (F), *OeGLU46-like* (G), and *OeGLU11-like* (H), in FI and RF trees. Dashed line indicates the beginning of treatment. Symbols indicate the average of four biological replications, and bars show \pm SD. Asterisks (*) indicate a significant statistical difference between FI and RF treatments at $p < 0.01$ (Student's *t*-test).

(Figure 2). An inverse relationship between oleuropein content and its derivative 3,4-DHPEA-EDA appeared evident during early stages of fruit development. The up-regulation of both identified *Oeβ-GLU12-like* isoforms, showing a high similarity with *Oeβ-GLU* (involved in oleuropein deglycosylation), and the peak of β-GLU activity further supported their predominant role in the oleuropein catabolic processes occurring during early

stages of fruit development and contributing to the composition of olive phenolics (Figures 3C, 4E,F). These results agree with those reported by Gutierrez-Rosales et al. (2010), who hypothesized that 3,4-DHPEA-EDA was formed via oleuropein by β-GLU activity. Transcription levels of *OeGLU12-like1* and *like2* were higher in FI trees, unlike enzyme activity and 3,4-DHPEA-EDA content, which were both higher in RF trees.

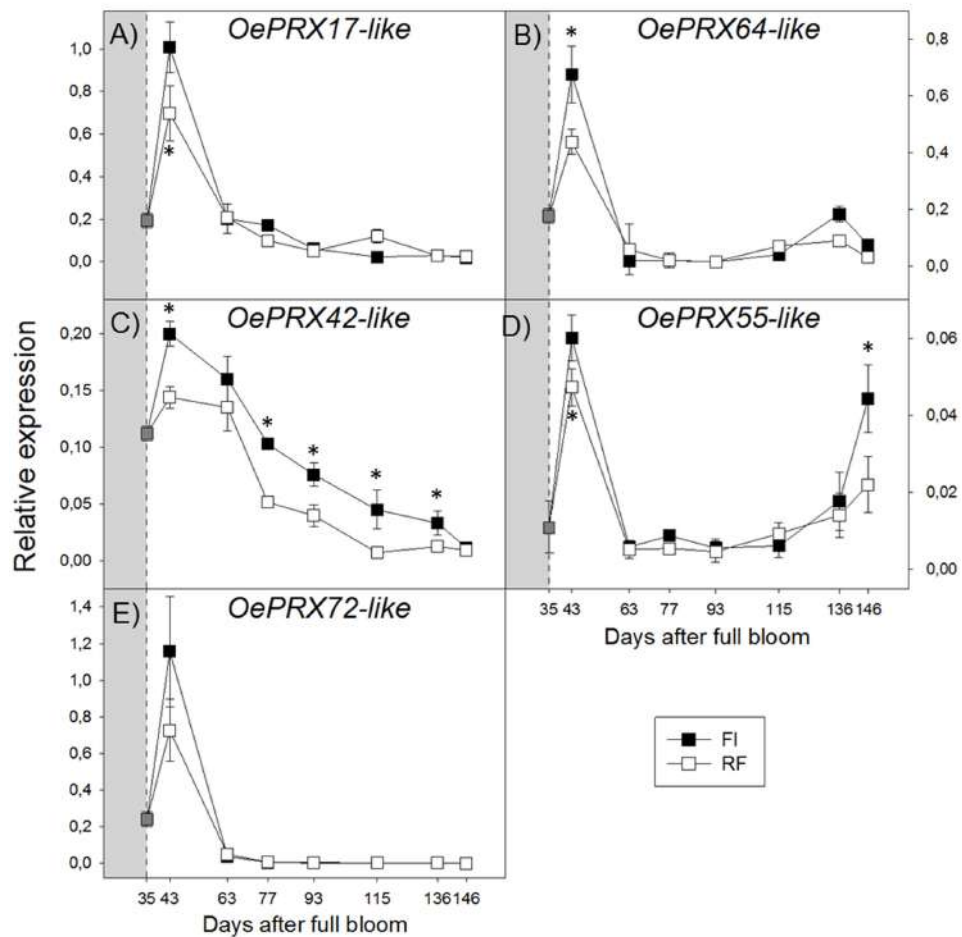


FIGURE 5 | Real-time quantitative PCR analysis of *OePRX17-like* (A), *OePRX64-like* (B), *OePRX42-like* (C), *OePRX55-like* (D), and *OePRX72-like* (E), in FI and RF trees. Dashed line indicates the beginning of treatment. Symbols indicate the average of four biological replications, and bars show \pm SD. Asterisks (*) indicate a significant statistical difference between FI and RF treatments at $p < 0.01$ (Student's *t*-test).

Although a positive effect of water deficit on GLU activity could be hypothesized, the identification of putative esterase enzyme(s) regulating 3,4-DHPEA-EDA biosynthesis will help to better elucidate this pathway and the effect of water availability.

The expression of olive PPO genes was affected by olive fruit developmental stages as well as plant water status (Figure 4). *OePPO1* seems to be the main isoform during early fruit development and maturation (after 115 DAFB), whereas *OePPO2* was mainly expressed during the pit-hardening period (from 77 to 93 DAFB). A relationship between the expression of olive PPO genes and PPO activity appeared evident during fruit ripening (Figures 3A, 4), and a close relationship between drupe PPO activity and fruit developmental stage has already been observed in cultivar 'Zard' accompanied by differential expression of isoenzymes (Ebrahimzadeh et al., 2003). Significant changes in kinetic behavior of PPO were observed also during fruit maturation in cultivar 'Picual,' and it was suggested that the assayed activity may be the result of the expression of different genes (Ortega-García et al., 2008). Transcript levels of

OePPO1 and PPO activity were higher in irrigated trees during advanced stages of fruit maturation, but gene expression and activity were not correlated with phenolic amount or specific metabolites, which remained stable during ripening. This agrees with the findings of Ortega-García et al. (2008), who showed that the increase in PPO activity during fruit ripening of cultivar 'Picual' did not parallel the variation in oleuropein concentration. Therefore, in intact olive drupes, PPO activity apparently plays a minor role in secoiridoid metabolism.

Peroxidases (Class III) oxidize phenolics as preferential substrates at the expense of peroxides. The highest levels of *OePRX* transcripts were detected from 35 to 43 DAFB. *OePRX* transcripts accumulation decreased sharply after the first stage of growth (Supplementary Figure S2). However, levels of *OePRX64* and *OePRX55* increased again in ripe fruits. In most cases, the expression levels were higher in FI trees than in RF trees, and we generally found a good correlation between PRX transcript accumulation and PRX activity: the highest enzyme activity was detected early during fruit development (35 DAFB), subsequently

it decreased and then increased again at maturation (**Figure 3B**). High levels of PRX activity have been found in olive seed, and the effect of this enzymatic activity on the VOO phenolic profile has been proved (Luaces et al., 2007). A PRX enzyme that binds specifically to pectic polysaccharides has been purified from black ripened olives ('Douro') (Saraiva et al., 2007), and more recently Tzika et al. (2009) have reported the partial purification of a PRX enzyme from 'Koroneiki' olive fruits that seems to be active toward some olive fruit phenols but inactive toward oleuropein. Contribution of PRX to the oxidation of phenols is generally limited by the availability of H_2O_2 , which usually increases under stress conditions or tissue damage (Sharma et al., 2012). The expression pattern and activity of several PRX isoforms was well correlated with phenol content in immature fruits but seemed to be unaffected by water availability, since the levels of PRX activity were similar between FI and RF treatments. Considering that a direct involvement of PRXs in oleuropein oxidation has yet to be demonstrated, such activity does not appear to play a pivotal role in explaining the different phenolics contents found in immature drupes.

Water availability is one of the major factors affecting olive yield and quality of both table olives and olive oils, particularly in areas where long periods of summer drought occurs during fruit growth and development. It has been shown that water availability affects the content of olive phenolics in fruit and oil and that the increase in irrigation volumes is negatively correlated with secoiridoids content (Patumi et al., 1999, 2002; Tovar et al., 2001, 2002; Gümez-Rico et al., 2006; Servili et al., 2007b; Caruso et al., 2014). In our study, fruits and oils from RF trees had consistently higher phenolic contents than those from FI trees. The ratio of phenolic content between FI and RF trees was 71 and 45% in the mesocarp (DW basis) and VOO, respectively, indicating that the RF conditions probably increased the fraction of phenols transferring into VOO during extraction. Nonetheless, there are many intriguing issues that remain to be clarified. For example, differences in fruit phenolic contents arose soon after the beginning of irrigation (35–43 DAFB), when drupe size was not significantly different between FI and RF trees, and thereafter remained almost unchanged until maturity, despite the progressive decrease in PLWP and fruit enlargement. Therefore, we hypothesize that phenolic catabolism is particularly sensitive to water availability during early stages of drupe development, affecting oleuropein catabolism through the regulation of glucosidase activity. As already reported in other species, the timing of water deficit, and its intensity and duration, is crucial for assimilate partitioning between primary and secondary pathways (Ni et al., 2009; Ripoll et al., 2014). In olive fruits, moderate water deficit starting 63 DAFB had no effects on cell division, but reduced mesocarp cell expansion, FW, and, only slightly and later in the mature stage of development, DW, suggesting that different cellular processes are involved depending on

the stage of fruit development (Gucci et al., 2009, 2011). Analogously, we hypothesize that a cross-talk is active between fruit development and cell water status for regulating the expression of genes and activity of enzymes playing a role in phenolic catabolism, but further studies are needed to clarify this point.

CONCLUSION

We have provided integrated evidence concerning the regulation and role of GLU, PRX, and PPO in the accumulation of phenolic compounds in olive fruits, suggesting a key role for β -GLU in oleuropein catabolism. Moreover, we provide the first detailed study on the effect of water availability on phenolics metabolism during fruit growth and ripening, suggesting that fruit response may vary depending on the developmental stage and the timing of water deficit. Knowledge of the genetic and physiological mechanisms underlying plant responses to the frequent succession of severe drought periods becomes a crucial factor, especially in optimizing irrigation management to achieve a balanced trade-off between olive oil yield and quality, and the saving of water resources.

AUTHOR CONTRIBUTIONS

RG, MS, MR, EP, MC, and RM developed the concept of the paper, wrote the paper, GC and CG performed eco-physiological analysis, collected and analysed meteorological data, MC and EF carried out qRT-PCR analyses and bioinformatic analyses, SU performed HPLC-polyphenolic analysis and quantification, and EF, EP, and MR performed enzymatic activities. All authors discussed and commented the manuscript.

FUNDING

This research was supported by the Project OLEA – Genomics and Breeding of Olive (D.M.27011/7643/10), funded from 'Ministero delle politiche agricole, alimentari e forestali,' Italy. The grant from 'Donazione Anna Maria Catalano – ONLUS,' Italy, also provided partial financial support. The funders had no role in study design, data collection and analysis, decision to publish, or preparation of the manuscript.

SUPPLEMENTARY MATERIAL

The Supplementary Material for this article can be found online at: <http://journal.frontiersin.org/article/10.3389/fpls.2017.00717/full#supplementary-material>

REFERENCES

- Alagna, F., Cirilli, M., Galla, G., Carbone, F., Daddiego, L., Facella, P., et al. (2016). Transcript analysis and regulative events during flower development in olive (*Olea europaea* L.). *PLoS ONE* 11:e0152943. doi: 10.1371/journal.pone.0152943
- Alagna, F., D'Agostino, N., Torchia, L., Servili, M., Rao, R., Pietrella, M., et al. (2009). Comparative 454 pyrosequencing of transcripts from two olive genotypes during fruit development. *BMC Genom.* 10:399. doi: 10.1186/1471-2164-10-399
- Alagna, F., Mariotti, R., Panara, F., Caporali, S., Urbani, S., Veneziani, G., et al. (2012). Olive phenolic compounds: metabolic and transcriptional profiling during fruit development. *BMC Plant Biol.* 12:162. doi: 10.1186/1471-2229-12-162
- Amiot, M. J., Fleuriel, A., and Macheix, J. J. (1986). Importance and evolution of phenolic compounds in olive during growth and maturation. *J. Agric. Food Chem.* 34, 823–826. doi: 10.1021/jf00071a014
- Amiot, M. J., Fleuriel, A., and Macheix, J. J. (1989). Accumulation of oleuropein derivates during olive maturation. *Phytochemistry* 28, 67–69. doi: 10.1016/0031-9422(89)85009-5
- Bianco, L., Alagna, F., Baldoni, L., Finnie, C., Svensson, B., and Perrotta, G. (2013). Proteome regulation during *Olea europaea* fruit development. *PLoS ONE* 8:e53563. doi: 10.1371/journal.pone.0053563
- Caruso, G., Gucci, R., Urbani, S., Esposto, S., Taticchi, A., Di Maio, I., et al. (2014). Effect of different irrigation volumes during fruit development on quality of virgin olive oil of cv. *Frantoio*. *Agric. Water Manag.* 134, 94–103. doi: 10.1016/j.agwat.2013.12.003
- Caruso, G., Rapoport, H. F., and Gucci, R. (2013). Long-term evaluation of yield components of young olive trees during the onset of fruit production under different irrigation regimes. *Irrigation Sci.* 31, 37–47. doi: 10.1007/s00271-011-0286-0
- Corrado, G., Alagna, F., Rocco, M., Renzone, G., Varricchio, P., Coppola, V., et al. (2012). Molecular interactions between the olive and the fruit fly *Bactrocera oleae*. *BMC Plant Biol.* 12:86. doi: 10.1186/1471-2229-12-86
- Cruz de Carvalho, M. H. (2008). Drought stress and reactive oxygen species. *Plant Signal. Behav.* 3, 156–165. doi: 10.4161/psb.3.3.5536
- Dag, A., Ben-Gal, A., Yermiyahu, U., Basheer, L., Nir, Y., and Kerem, Z. (2008). The effect of irrigation level and harvest mechanization on virgin olive oil quality in a traditional rain-fed 'Souri' olive orchard converted to irrigation. *J. Sci. Food Agric.* 88, 1524–1528. doi: 10.1002/jsfa.3243
- Del Campo, M. G., and Garcia, J. M. (2013). Summer deficit-irrigation strategies in a hedgerow olive cv. Arbequina orchard: effect on oil quality. *J. Agric. Food Chem.* 61, 8899–8905. doi: 10.1021/jf402107t
- Doyle, J. J., and Doyle, J. L. (1990). Isolation of plant DNA from fresh tissue. *Focus* 12, 13–15.
- Ebrahimzadeh, H., Motamed, N., Rastgar-Jazt, F., Montasser-Kouhsai, S., and Shokrap, E. H. (2003). Oxidative enzyme activities and soluble protein content in leaves and fruits of olives during ripening. *J. Food Biochem.* 27, 181–196. doi: 10.1111/j.1745-4514.2003.tb00276.x
- Gerasimenko, I., Sheludko, Y., Ma, X., and Stöckigt, J. (2002). Heterologous expression of a *Rauvolfia* cDNA encoding strictosidine glucosidase, a biosynthetic key to over 2000 monoterpenoid indole alkaloids. *Eur. J. Biochem.* 269, 2204–2213. doi: 10.1046/j.1432-1033.2002.02878.x
- Gucci, R., Caruso, G., Rapoport, H. F., and Lodolini, E. M. (2011). Irrigation differently affects endocarp and mesocarp growth during olive fruit development. *Acta Hortic.* 889, 297–302. doi: 10.17660/ActaHortic.2011.889.35
- Gucci, R., Lodolini, E. M., and Rapoport, H. F. (2009). Water deficit-induced changes in mesocarp cellular processes and the relationship between mesocarp and endocarp during olive fruit. *Tree Physiol.* 29, 1575–1585. doi: 10.1093/treephys/tpp086
- Gutierrez-Rosales, F., Romero, M. P., Casanovas, M., Motilva, M. J., and Minguez-Mosquera, M. (2010). Metabolites involved in oleuropein accumulation and degradation in fruits of *Olea europaea* L.: Hojiblanca and Arbequina varieties. *J. Agric. Food Chem.* 58, 12924–12933. doi: 10.1021/jf103083u
- Gutierrez-Rosales, F., Romero, M. P., Casanovas, M., Motilva, M. J., and Minguez-Mosquera, M. (2012). β -Glucosidase involvement in the formation and transformation of oleuropein during the growth and development of olive fruits (*Olea europaea* L. cv. Arbequina) grown under different farming practices. *J. Agric. Food Chem.* 60, 4348–4358. doi: 10.1021/jf205209y
- Gümez-Rico, A., Salvador, M. D., La Greca, M., and Fregapane, G. (2006). Phenolic and volatile compounds of extra virgin olive oil (*Olea europaea* L. cv. Cornicabra) with regard to fruit ripening and irrigation management. *J. Agric. Food Chem.* 54, 7130–7136. doi: 10.1021/jf060798r
- Hiraga, S., Sasaki, K., Ito, H., Ohashi, Y., and Matsui, H. (2001). A large family of class III plant peroxidases. *Plant Cell Physiol.* 42, 462–468. doi: 10.1093/pcp/pce061
- Iaria, D. L., Chiappetta, A., and Muzzalupo, I. (2016). A De novo transcriptomic approach to identify flavonoids and anthocyanins "Switch-Off" in olive (*Olea europaea* L.) drupes at different stages of maturation. *Front. Plant Sci.* 6:1246. doi: 10.3389/fpls.2015.01246
- International Olive Council [IOC] (2016). *Market Newsletter. No 108 – September 2016*. Available at: <http://www.internationaloliveoil.org/news/view/686-year-2016-news/762-marketnewsletter-september-2016>
- Koudounas, K., Banilas, G., Michaelidis, C., Demoliou, C., Rigas, S., and Hatzopoulos, P. (2015). A defence-related *Olea europaea* β -glucosidase hydrolyses and activates oleuropein into a potent protein cross-linking agent. *J. Exp. Bot.* 66, 2093–2106. doi: 10.1093/jxb/erv002
- Krasensky, J., and Jonak, C. (2012). Drought, salt, and temperature stress-induced metabolic rearrangements and regulatory networks. *J. Exp. Bot.* 63, 1593–1608. doi: 10.1093/jxb/err460
- Kubista, M., Andrade, J. M., Bengtsson, M., Forootan, A., Jonák, J., Lind, K., et al. (2006). The real-time polymerase chain reaction. *Mol. Aspects Med.* 27, 95–125. doi: 10.1016/j.mam.2005.12.007
- Lavee, H., Imeson, A. C., Pariente, S., and Benyamin, Y. (1991). The response of soils to simulated rainfall along a climatological gradient in an arid and semi-arid region. *Catena Suppl.* 19, 19–37.
- Luaces, P., Romero, C., Gutierrez, F., Sanz, C., and Pérez, A. G. (2007). Contribution of olive seed to the phenolic profile and related quality parameters of virgin olive oil. *J. Sci. Food Agric.* 87, 2721–2727. doi: 10.1002/jsfa.3049
- Makkar, R. S., Tsuneda, A., Tokuyasu, K., and Mori, Y. (2001). *Lentinula edodes* produces a multicomponent protein complex containing manganese (II)-dependent peroxidase, laccase and β -glucosidase. *FEMS Microbiol. Lett.* 200, 175–179. doi: 10.1016/s0378-1097(01)00159-8
- Martinelli, F., Basile, B., Morelli, G., d'Andria, R., and Tonutti, P. (2012). Effects of irrigation on fruit ripening behavior and metabolic changes in olive. *Sci. Hortic.* 144, 201–207. doi: 10.1016/j.scienta.2012.07.012
- Martinelli, F., Remorini, D., Saia, S., Massai, R., and Tonutti, P. (2013). Metabolic profiling of ripe olive fruit in response to moderate water stress. *Sci. Hortic.* 159, 52–58. doi: 10.1016/j.scienta.2013.04.039
- Montedoro, G., Servili, M., Baldioli, M., and Minati, E. (1992). Simple and hydrolyzable compounds in virgin olive oil. 1. Their extraction, separation and quantitative and semiquantitative evaluation by HPLC. *J. Agric. Food Chem.* 40, 1571–1576. doi: 10.1021/jf00021a019
- Monteleone, E., Caporale, G., Lencioni, L., Favati, F., and Bertuccoli, M. (1995). Optimization of virgin olive oil quality in relation to fruit ripening and storage. *Dev. Food Sci.* 37, 397–418. doi: 10.1016/S0167-4501(06)80168-8
- Morelló, J. R., Romero, M. P., and Motilva, M. J. (2004). Effect of the maturation process of the olive fruit on the phenolic fraction of drupes and oils from arbequina, farga, and morrut cultivars. *J. Agric. Food Chem.* 52, 6002–6009. doi: 10.1021/jf035300p
- Ni, F. T., Chu, L. Y., Shao, H. B., and Liu, Z. H. (2009). Gene expression and regulation of higher plants under soil water stress. *Curr. Genomics* 10, 269–280. doi: 10.2174/138920209788488535
- Ortega-García, F., Blanco, S., Peinado, M. A., and Peragün, J. (2008). Polyphenol oxidase and its relationship with oleuropein concentration in fruits and leaves of olive (*Olea europaea*) cv. 'Picual' trees during fruit ripening. *Tree Physiol.* 28, 45–54. doi: 10.1093/treephys/28.1.45
- Patumi, M., d'Andria, R., Fontanazza, G., Morelli, G., and Giorio, P., Sorrentino, G. (1999). Yield and oil quality of intensively trained trees cultivars of olive (*Olea europaea* L.) under irrigation regimes. *J. Hortic. Sci. Biotechnol.* 74, 729–737. doi: 10.1080/14620316.1999.11511180
- Patumi, M., d'Andria, R., Marsilio, V., Fontanazza, G., Morelli, G., and Lanza, B. (2002). Olive and olive oil quality after intensive monocone olive growing (*Olea europaea* L. cv. Kalamata) in different irrigation regimes. *Food Chem.* 77, 27–34. doi: 10.1016/S0308-8146(01)00317-X

- Petridis, A., Therios, I., and Samouris, G. (2012). Genotypic variation of total phenol and oleuropein concentration and antioxidant activity of 11 Greek olive cultivars (*Olea europaea* L.). *Hortscience* 47, 339–342.
- Ramakrishna, A., and Ravishankar, G. A. (2011). Influence of abiotic stress signals on secondary metabolites in plants. *Plant Signal Behav.* 6, 1720–1731. doi: 10.4161/psb.6.11.17613
- Raychaudhuri, A., and Tipton, P. A. (2002). Cloning and expression of the gene for soybean hydroxysourate hydrolase. Localization and implications for function and mechanism. *Plant Physiol.* 130, 2061–2068. doi: 10.1104/pp.011049
- Ripoll, J., Urban, L., Staudt, M., Lopez-Lauri, F., Bidel, L. P., and Bertin, N. (2014). Water shortage and quality of fleshy fruit making the most of the unavoidable. *J. Exp. Bot.* 65, 4097–4117. doi: 10.1093/jxb/eru197
- Romani, A., Mulinacci, N., Pinelli, P., Vincieri, F. F., and Cimato, A. (1999). Polyphenolic content of five Tuscan cultivars of *Olea europaea* L. *J. Agric. Food Chem.* 47, 964–967. doi: 10.1021/jf980264t
- Romero-Segura, C., Sanz, C., and Perez, A. G. (2009). Purification and characterization of an olive fruit β -Glucosidase involved in the biosynthesis of virgin olive oil phenolics. *J. Agric. Food Chem.* 57, 7983–7988. doi: 10.1021/jf901293c
- Rotondi, A., Bendini, A., Mari, L. M., Lercker, G., and Toschi, T. G. (2004). Effect of olive ripening degree on the oxidative stability and organoleptic properties of Cv. Nostrana di Brisighella extra virgin olive oil. *J. Agric. Food Chem.* 52, 3649–3654. doi: 10.1021/jf049845a
- Ryan, D., Antolovich, M., Herlt, T., Prenzler, P. D., Lavee, S., and Robards, K. (2002). Identification of phenolic compounds in tissues of the novel olive cultivar Hardy's Mammoth. *J. Agric. Food Chem.* 50, 6716–6724. doi: 10.1021/jf025736p
- Ryan, D., and Robards, K. (1998). Phenolic compounds in olives. *Analyst* 123, 31–44. doi: 10.1039/a708920a
- Ryan, D., Robards, K., and Lavee, S. (1999). Change in phenolic content of olive during maturation. *Int. J. Food Sci. Technol.* 34, 265–274. doi: 10.1046/j.1365-2621.1999.00261.x
- Saraiva, J., Nunes, C., and Coimbra, M. (2007). Purification and characterization of olive (*Olea europaea* L.) peroxidase – Evidence for the occurrence of a pectin binding peroxidase. *Food Chem.* 101, 1571–1579. doi: 10.1016/j.foodchem.2006.04.012
- Selvaggini, R., Esposto, S., Taticchi, A., Urbani, S., Veneziani, G., Di Maio, I., et al. (2014). Optimization of the temperature and oxygen concentration conditions in the malaxation during the oil mechanical extraction process of four Italian olive cultivars. *J. Agric. Food Chem.* 62, 3813–3822. doi: 10.1021/jf405753c
- Selvaggini, R., Servili, M., Urbani, S., Esposto, S., Taticchi, A., and Montedoro, G. F. (2006). Evaluation of phenolic compounds in virgin olive oil by direct injection in high performance liquid chromatography with fluorometric detection. *J. Agric. Food Chem.* 54, 2832–2838. doi: 10.1021/jf0527596
- Servili, M., Baldioli, M., Selvaggini, R., Macchioni, A., and Montedoro, J. F. (1999). Phenolic compounds of olive fruit: one-and two-dimensional Nuclear Magnetic Resonance characterization of nüzenide and its distribution in the constitutive parts of fruit. *J. Agric. Food Chem.* 47, 12–18. doi: 10.1021/jf9806210
- Servili, M., Esposto, S., Lodolini, E., Selvaggini, R., Taticchi, A., Urbani, S., et al. (2007a). Irrigation effects on quality, phenolic composition, and selected volatiles of virgin olive oils cv. Leccino. *J. Agric. Food Chem.* 55, 6609–6618.
- Servili, M., Selvaggini, R., Esposto, S., Taticchi, A., Montedoro, G. F., and Morozzi, G. (2004). Health and sensory properties of virgin olive oil hydrophilic phenols: agronomic and technological aspects of production that affect their occurrence in the oil. *J. Chromatogr. A* 1054, 113–127. doi: 10.1016/S0021-9673(04)01423-2
- Servili, M., Taticchi, A., Esposto, S., Sordini, B., and Urbani, S. (2012). “Technological aspects of olive oil production,” in *Olive Germplasm—The Olive Cultivation, Table Olive and Olive Oil Industry in Italy*, ed. I. Mazzalupo (Rijeka: Intech).
- Servili, M., Taticchi, A., Esposto, S., Urbani, S., Selvaggini, R., and Montedoro, G. F. (2007b). Effect of olive stoning on the volatile and phenolic composition of virgin olive oil. *J. Agric. Food Chem.* 55, 7028–7035.
- Shao, H. B., Chu, L. Y., Jaleel, C. A., and Zhao, C. X. (2008). Water-deficit stress-induced anatomical changes in higher plants. *C. R. Biol.* 331, 215–225. doi: 10.1016/j.crvi.2008.01.002
- Sharma, P., Bhushan Jha, A., Shanker Dubey, R., and Pessarakli, M. (2012). Reactive oxygen species, oxidative damage, and antioxidative defense mechanism in plants under stressful conditions. *J. Bot.* 2012, 26. doi: 10.1155/2012/217037
- Sivakumar, G., Briccoli Bati, C., and Uccella, N. (2007). Demethyloleuropein and beta-glucosidase activity in olive fruits. *Biotechnol. J.* 2, 381–385. doi: 10.1002/biot.200600118
- Smith, A. T., and Veitch, N. C. (1998). Substrate binding and catalysis in heme peroxidases. *Curr. Opin. Chem. Biol.* 2, 269–278. doi: 10.1016/S1367-5931(98)80069-0
- Talhaoui, N., Gómez-Caravaca, A. M., Leon, L., de la Rosa, R., Fernandez-Gutierrez, A., and Segura-Carretero, A. (2015). Pattern of variation of fruit traits and phenol content in olive fruits from six different cultivars. *J. Agric. Food Chem.* 63, 10466–10476. doi: 10.1021/acs.jafc.5b04315
- Tamura, K., Stecher, G., Peterson, D., Filipski, A., and Kumar, S. (2013). MEGA6: Molecular Evolutionary Genetics Analysis Version 6.0. *Mol. Biol. Evol.* 30, 2725–2729. doi: 10.1093/molbev/mst197
- Tognoli, M., Penel, C., Greppin, H., and Simon, P. (2002). Analysis and expression of the class III peroxidase large gene family in *Arabidopsis thaliana*. *Gene* 288, 129–138. doi: 10.1016/S0378-1119(02)00465-1
- Toval, M. J., Motilva, M. J., and Romero, M. P. (2001). Changes in the phenolic composition of virgin olive oil from young trees (*Olea europaea* L. cv. Arbequina) grown under linear irrigation strategies. *J. Agric. Food Chem.* 49, 5502–5508. doi: 10.1021/jf0102416
- Toval, M. J., Romero, M. P., Girona, J., and Motilva, M. J. (2002). L-Phenylalanine ammonia-lyase activity and concentration of phenolics in developing olive (*Olea europaea* L. cv Arbequina) fruit grown under different irrigation regimes. *J. Sci. Food Agric.* 82, 892–898. doi: 10.1002/jsfa.1122
- Tran, L. T., Taylor, J. S., and Constabel, C. P. (2012). The polyphenol oxidase gene family in land plants: lineage-specific duplication and expansion. *BMC Genomics* 13:395. doi: 10.1186/1471-2164-13-395
- Tura, D., Failla, O., Bassi, D., Pedo, S., and Serraiocco, A. (2008). Cultivar influence on virgin olive (*Olea europaea* L.) oil flavor based on aromatic compounds and sensorial profile. *Sci. Hortic.* 118, 139–148. doi: 10.1016/j.scienta.2008.05.030
- Tzika, E. D., Sotirodhis, T. G., Papadimitriou, V., and Xenakis, A. (2009). Partial purification and characterization of peroxidase from olives (*Olea europaea* cv. Koroneiki). *Eur. Food Res. Technol.* 228, 487–495. doi: 10.1007/s00217-008-0956-1
- Veitch, N. C. (2004). Horseradish peroxidase: a modern view of a classic enzyme. *Phytochemistry* 65, 249–259. doi: 10.1016/j.phytochem.2003.10.022
- Warzecha, H., Gerasimenko, I., Kutchan, T. M., and Stöckigt, J. (2000). Molecular cloning and functional bacterial expression of a plant glucosidase specifically involved in alkaloid biosynthesis. *Phytochemistry* 54, 657–666. doi: 10.1016/S0031-9422(00)00175-8
- Welinder, K. G. (1992). “Plant peroxidases: structure-function relationships,” in *Plant Peroxidases 1980–1990: Topics and Detailed Literature on Molecular, Biochemical, and Physiological Aspects*, eds C. Penel, T. Gaspar, and H. Greppin (Geneva: University of Geneva), 1–24.
- Zouari-Mechichi, H., Mechichi, T., Dhouib, A., Sami Sayadi, S., Angel, T., and Martinez, A. T. (2006). Laccase purification and characterization from *Trametes trogii* isolated in Tunisia: decolorization of textile dyes by the purified enzyme. *Enzyme Microb. Technol.* 39, 141–148. doi: 10.1016/j.enzmicro.2005.11.027
- Conflict of Interest Statement:** The authors declare that the research was conducted in the absence of any commercial or financial relationships that could be construed as a potential conflict of interest.
- Copyright © 2017 Cirilli, Caruso, Gennai, Urbani, Frioni, Ruzzi, Servili, Gucci, Poerio and Muleo. This is an open-access article distributed under the terms of the Creative Commons Attribution License (CC BY). The use, distribution or reproduction in other forums is permitted, provided the original author(s) or licensor are credited and that the original publication in this journal is cited, in accordance with accepted academic practice. No use, distribution or reproduction is permitted which does not comply with these terms.



Evaluating Spatially Resolved Influence of Soil and Tree Water Status on Quality of European Plum Grown in Semi-humid Climate

Jana Kähnner^{1*}, Alon Ben-Gal², Robin Gebbers¹, Aviva Peeters², Werner B. Herppich¹ and Manuela Zude-Sasse^{1*}

¹ Horticultural Engineering, Leibniz Institute for Agricultural Engineering and Bioeconomy (ATB), Potsdam, Germany, ² Institute of Soil, Water, and Environmental Sciences, Agricultural Research Organization, Gilat Research Center, Gilat, Israel

OPEN ACCESS

Edited by:

Nadia Bertin,
Plantes et Système de Cultures
Horticoles (INRA), France

Reviewed by:

Mark Andrew Skewes,
South Australian Research and
Development Institute, Australia
Rhuanito Soranz Ferrarezi,
University of Florida, United States

*Correspondence:

Jana Kähnner
jkaethner@atb-potsdam.de
Manuela Zude-Sasse
zude@atb-potsdam.de

Specialty section:

This article was submitted to
Crop Science and Horticulture,
a section of the journal
Frontiers in Plant Science

Received: 21 March 2017

Accepted: 31 May 2017

Published: 20 June 2017

Citation:

Kähnner J, Ben-Gal A, Gebbers R,
Peeters A, Herppich WB and
Zude-Sasse M (2017) Evaluating
Spatially Resolved Influence of Soil
and Tree Water Status on Quality of
European Plum Grown in Semi-humid
Climate. *Front. Plant Sci.* 8:1053.
doi: 10.3389/fpls.2017.01053

In orchards, the variations of fruit quality and its determinants are crucial for resource effective measures. In the present study, a drip-irrigated plum production (*Prunus domestica* L. "Tophit plus"/Wavit) located in a semi-humid climate was studied. Analysis of the apparent electrical conductivity (ECa) of soil showed spatial patterns of sand lenses in the orchard. Water status of sample trees was measured instantaneously by means of leaf water potential, Ψ_{leaf} [MPa], and for all trees by thermal imaging of canopies and calculation of the crop water stress index (CWSI). Methods for determining CWSI were evaluated. A CWSI approach calculating canopy and reference temperatures from the histogram of pixels from each image itself was found to suit the experimental conditions. Soil ECa showed no correlation with specific leaf area ratio and cumulative water use efficiency (WUEc) derived from the crop load. The fruit quality, however, was influenced by physiological drought stress in trees with high crop load and, resulting (too) high WUEc, when fruit driven water demand was not met. As indicated by analysis of variance, neither ECa nor the instantaneous CWSI could be used as predictors of fruit quality, while the interaction of CWSI and WUEc did succeed in indicating significant differences. Consequently, both WUEc and CWSI should be integrated in irrigation scheduling for positive impact on fruit quality.

Keywords: fruit quality, precision horticulture, plum, spatial variability, tree water status

INTRODUCTION

Following the concept of precision agriculture, correlation of spatial variation of soil and yield data has been analyzed in field crops, vegetable production, vineyards, and orchards. Spatial patterns of fruit yield are typically explained in one of two approaches. The first analyzes the spatial correlation between soil properties influencing the water supply as one main growth factor and yield as the

Abbreviations: ρ , density of dry air [kg m^{-3}]; t, time course, diurnal variation [h], Ψ_{leaf} , leaf water potential [MPa]; Ψ_π , osmotic potential [MPa]; u, wind speed [m s^{-1}]; T, temperature [$^\circ\text{C}$]; T_K , absolute temperature [K]; T_w , temperature of wet reference [$^\circ\text{C}$]; T_d , temperature of dry reference [$^\circ\text{C}$]; T_c , current canopy temperature [$^\circ\text{C}$]; T_{air} , air temperature [$^\circ\text{C}$]; CWSI, crop water stress index [0; 1]; ECa, soil apparent electrical conductivity [mS m^{-1}]; VPD, water vapor pressure deficit [kPa]; WUE_i, instantaneous water use efficiency [$\mu\text{Mol mMol}^{-1}$]; WUE_c, cumulative water use efficiency [g/].

target variable. This is consistent with findings in precision viticulture, where soil maps have provided a basis for delineating management zones (Williams and Araujo, 2002). The second approach is more driven by the endogenous growth factors of the plant. It uses the correlation of plant data such as canopy volume representing the growth capacity, tree water status, and fruit quality at harvest (Zaman and Schumann, 2006). This latter approach may be more appropriate for orchards where fruit quality is crucial for marketing. However, the analysis of spatially-resolved soil and plant data and its influence on fruit quality has rarely been studied.

The most common method for soil mapping is to analyze the apparent electrical conductivity (ECa) of the soil (Bramley and Hamilton, 2004). Soil ECa measurements can be performed at field capacity to gain information regarding texture of the soil, while measurements in dry periods may better indicate soil water distribution. Mapping of electrical properties in orchard soils appears not without its challenges as commercial rolling systems often fail to measure close to the trees. Manually performed readings, most often with equidistant Wenner array, have been used with more success in covering the entire orchard soil (Halvorson and Rhoades, 1976; Gebbers et al., 2009). Experimental-scale ECa mapping, concomitantly performed with fruit yield analyses, confirmed a correlation between soil patterns and yield in various fruit crops including apples (Türker et al., 2011; Aggelopoulou et al., 2013), olives (Fountas et al., 2011; Agam et al., 2014), and citrus (Zaman and Schumann, 2006; Peeters et al., 2015). However, while patterns of soil properties are generally stable over time (Mann et al., 2011), spatial patterns of variables measured on trees are more likely to vary (Aggelopoulou et al., 2013). Furthermore, in orchards, soil water status is frequently influenced by irrigation causing intentionally reduced impact of a-priori patterns of soil properties on vegetative and generative plant growth. As a result, the effect of soil patterns on the quality of fruit might be reduced.

Using a physiological approach, the spatial variability of yield and quality have been found to be highly correlated with the canopy volume in citrus production (Zaman and Schumann, 2006; Zude et al., 2008). From a physiological point of view, it may be assumed that canopy volume, yield, and fruit quality are influenced by the exogenous water supply and the endogenous crop load (Palmer, 1992; Naor et al., 2001, 2006; Bustan et al., 2016). Strong interaction between water status of soil and trees has been pointed out in arid and semi-arid conditions (Naor et al., 2006; Ben-Gal et al., 2009; Gómez-del-Campo, 2013; Bustan et al., 2016), but also more ambiguous effects of crop load on tree water status have been reported for crops including peach, apple, and olive (Berman and DeJong, 1996; Bellvert et al., 2016; Bustan et al., 2016). The ultimate objective of orchard management of course would be to optimize not only the fruit quality, but also the cumulative water use efficiency (WUEc) in terms of yield per liter of totally applied irrigation and precipitation water (Viets, 1962).

The measurement of both, soil water status and plant water status, is challenged by the fact that any individual proximal sensor represents only a small volume of interest; a tree or part

of a tree or a small volume of soil. Consequently, measuring the spatial distribution of water status in fruit trees has been approached by means of remote sensing, often via thermal imaging. Thermal images of canopies provide a measure of instantaneous tree water status interpreted by means of the crop water stress index (CWSI; Jones, 1992). The CWSI is a surface-temperature based index between 1 and 0, with 1 representing the temperature of non-transpiring dry leaves and 0 equivalent to that of fully transpiring wet leaves (Jackson et al., 1981; Sammis et al., 1988; Maes and Steppe, 2012). While application of thermal imaging is easily applied in the laboratory, the technique has also been developed for field studies, particularly in the semi-arid and arid sub-tropics (Jones, 1992; Cohen et al., 2005; Hellebrand et al., 2006). Thermal imaging of canopies has been applied by means of unmanned aerial systems (Berni et al., 2009; González-Dugo et al., 2013) and frequently tractor-mounted cameras providing either top or side views. The method has further been refined to measure CWSI and guide irrigation protocols in olives in Israel (Ben-Gal et al., 2009). In peach orchards located in a semi-arid environment, the CWSI was found to successfully differentiate between irrigation treatments (Bellvert et al., 2016). In differently irrigated apple trees under a hail net, CWSI values ranged between 0.08 and 0.55. Values >0.3 were considered as stressed trees under the given conditions (Nagy, 2015). The development and use of CWSI has focused on sub-tropical, arid, and semi-arid climates and has not yet been sufficiently studied under semi-humid conditions, where improving fruit quality, instead of providing for canopy transpiration, may be the most significant driver of irrigation water management. It is questionable if instantaneous methods for measuring water status, such as the thermal based CWSI, can support optimization of fruit quality on one hand and WUEc on the other side.

Consequently, this study aimed (i) to select a feasible method for utilization of thermal imaging in a semi-humid climate, (ii) to spatially characterize the soil ECa and instantaneous water status of fruit trees in an orchard, and (iii) to analyze the interaction of tree water status and quality of fruit.

MATERIALS AND METHODS

Site Description and Plant Material

The experiment was carried out in a 0.37 ha commercial *Prunus domestica* L. (plum) orchard located in the "Werder fruit production" area in Brandenburg, Germany ($52^{\circ} 28' 1.56''$ N, $12^{\circ} 57' 28.8''$ E). The soil is typical for fruit production in temperate climate of Europe and Asia formed by glacial and post-glacial deposits after the last ice age about 10,000 years ago with typically small scale variability. The cultivar was "Tophit plus" with "Jojo" serving as a pollinator. One hundred and four 7 year old "Tophit plus" trees, located every 4 m in 4 rows spaced 5 m apart, were considered. On average, trees were 2.10 m tall and insertion height of the first branch varied between 0.46 and 0.96 m above the soil. Mean soil texture was 45% sand, 29% silt, and 26% clay with a mean pH of 7.72. Plum trees were irrigated using a drip system with one line per row and two emitters every 0.5 m. The irrigation laterals and drippers were mounted 50 cm above the ground to facilitate mechanical weed control. Independent of

precipitation, trees were irrigated twice a week for 1.5 h with flow rate of 0.96 L h^{-1} .

Meteorological Readings

Global radiation, wind speed, air temperature, air pressure, precipitation, and relative humidity were measured at 24 min intervals by a weather station (UNIKLIMA vario, Toss, Germany) positioned 100 m from the experimental orchard. Canopy temperature and relative humidity (Modul DLTi, UP GmbH, Germany) were recorded in 18 trees every 5 min. Water vapor pressure deficit (VPD) of the air was calculated according to the Goff–Gratch-equation (Jones, 1992; von Willert et al., 1995) from hourly averages of air temperature, relative humidity, and air pressure.

Soil Properties

A resistivity meter (4-point light hp, LGM, Germany) was used to map the EC_a of the soil at the experimental site on 16th August 2012 and 2nd August 2013. The four electrodes were arranged in a Wenner array with the tree trunk in the center to obtain EC_a values representing 25 cm depth (Telford et al., 1990). Full details are given in Käthner and Zude-Sasse (2015). Soil water matric potential (pf-meter 80, ecoTech Umwelt-Messsysteme GmbH, Germany) was measured at 15, 35, and 45 cm depths. In addition, the gravimetric soil water content (GWC) was ascertained by drying soil samples at 105°C for 48 h with $n = 26$ in 2012 and $n = 6$ in 2013.

Leaf Water Status

Three mature leaves were randomly detached from the north-eastern side of each tree and rapidly transported to the laboratory. Here, projected surface area [cm^2] was measured for each leaf with a portable area meter (CI-203, CID Bio-Science, Inc., USA). Leaf dry mass [g] was consequently obtained after oven drying at 65°C for 24 h and specific leaf area (SLA) was calculated as the ratio of leaf area and dry mass.

In the orchard, leaf water potential (Ψ_{leaf}) was measured with a Scholander bomb (Plant Water Status Console 3000, Soilmoisture Equipment Corp., USA) on three shaded leaves from the lower part of the canopy on the east side of the tree. In 2012, 44 trees were analyzed predawn and midday over 4 days (19th June–27th June). In 2013, 67 trees were sampled over 5 days (19th July–2nd August). Following determination of Ψ_{leaf} , the leaves were rapidly packed in plastic bags, transported to the laboratory, frozen at -30°C . After thawing, centrifuged tissue sap was analyzed for osmotic content (c_{osmol}) with a water vapor osmometer (Vapro 5520, Wescor Inc., USA). The osmotic potential (Ψ_{π}) of tissue sap was calculated according to the van't Hoff's equation (von Willert et al., 1995).

Crop Water Stress Index

Thermal images of the canopies were taken with an uncooled infrared thermal camera (ThermaCAM model SC 500, FLIR Systems, Inc., USA) with resolution of 320×240 pixel and spectral sensitivity range from 7.5 to $13.0 \mu\text{m}$ in the temperature range of -50 to 60°C on 15th August 2012 and 25th July 2013. The camera was mounted on a tractor with $z = 3.3 \text{ m}$ above

ground and pointed to the top of the canopies. Images were acquired with an opening angle (β) of 45° resulting in the length (l) of the imaged area (Equation 1).

$$l = 2 \cdot z \cdot \tan\left(\frac{\beta}{2}\right) \quad (1)$$

For extraction of temperature values, the raw thermal images were obtained in the FLIR systems' proprietary format and converted to text file format for the processing with MATLAB® (R2010B, MathWorks, USA). Crop water stress index (CWSI_J) was calculated (Equation 2) according to Jones (1992) ranging from 0 to 1:

$$\text{CWSI}_J = \frac{T_c - T_{\text{wref}}}{T_{\text{dref}} - T_{\text{wref}}} \quad (2)$$

where T_c is actual canopy temperature, T_w is temperature of a fully transpiring leaf with open stomata obtained from a wet paper leaf analog, and T_d is temperature of a non-transpiring leaf. When using references T_{dref} was obtained from a dry and T_{wref} from paper leaf analog (Jones, 2004). For this purpose, green paper leaves were cut to the formerly measured mean leaf area of 6 cm^2 , mounted on a 2 m stick, and manually placed in the center of the canopy in each tree.

In addition, CWSI was also calculated according to three alternative methods. Irmak et al. (2000) calculated the CWSI_I (Equation 3) setting non-transpiring leaf temperature at 5°C higher than air temperature ($T_d + 5$) and T_w as the minimum temperature found in the canopy.

$$\text{CWSI}_I = \frac{T_c - T_{\text{wmin}}}{T_d + 5 - T_{\text{wmin}}} \quad (3)$$

As described by work groups of Jones (1999) and Ben-Gal et al. (2009), T_w and T_d was obtained analytically (Appendix in Supplementary Material) to calculate CWSI_{JB} (Equation 4).

$$\text{CWSI}_{JB} = \frac{T_c - T_{\text{wana}}}{T_{\text{dana}} - T_{\text{wana}}} \quad (4)$$

CWSI_R was determined according to the work of Rud et al. (2015). Likely the most suitable for automated readings, this method calculates (Equation 5) the canopy temperature (T_{chisto}) and reference temperatures of dry (T_{dhisto}) and wet (T_{whisto}) leaves from the histogram of pixels from each image itself.

$$\text{CWSI}_R = \frac{T_{\text{chisto}} - T_{\text{whisto}}}{T_{\text{dhisto}} - T_{\text{whisto}}} \quad (5)$$

In the CWSI_R approach, before processing histograms, extreme values above air temperature representing Fresnel reflection from the sun were removed from the further analysis. In the histogram of pixels, thresholds were determined for separating temperatures of soil, grass, and canopy. Dry reference, T_{dhisto} , was defined as the minimum temperature of soil visible as a peak with high values in the histogram. Wet reference, T_{whisto} , was taken as the minimum temperature of canopy. Since the canopy and grass partly coincided, pixels were spatially compared

considering equal values as grass and varying values as canopy. This threshold was found with Wiener filter to enhance the contrast (Honig and Goldstein, 2002; Chen et al., 2006). After removing the soil and grass data, the $T_{d,histo}$ and mean canopy temperature ($T_{c,histo}$) were extracted and averaged for each tree.

Water Use Efficiency

On the day of CWSI measurement, a portable porometer (CIRAS-1, PP Systems, Hitchin, UK) was used to monitor the diurnal course ($n = 3$) of CO_2 exchange and transpiration. The instantaneous water use efficiency (WUE_i) was calculated as ratio of these parameters (von Willert et al., 1995) in $\mu\text{Mol CO}_2 \text{ m}^{-2} \text{ s}^{-1}/\text{mMol H}_2\text{O m}^{-2} \text{ s}^{-1}$.

The WUE_c (Equation 6) of the production system represents the ratio of yield (y) and water volume supplied to the plants [g L^{-1}],

$$\text{WUE}_c = y/(i + pp) \quad (6)$$

with i = irrigation water, pp = precipitation from the start of vegetation period until harvest time.

In 2012, the accounted period lasted from 17th April to 30th August during which 182 mm of irrigation and 273 mm rain with a total of 455 mm water were supplied. In 2013, irrigation water was given from 22nd April to 9th September accounting for 168 mm of irrigation water and 248 mm of rain was recorded summing up to 416 mm water supply.

Fruit Quality

Soluble solids content [%] of fruit was analyzed using a digital refractometer (DR 301-95, A. Krüss Optronic, Germany). Dry matter content of fruit [%] was calculated as the ratio of fruit dry mass and fruit fresh mass. Fruit flesh firmness [N cm^{-2}] was analyzed as maximum force measured with a convex plunger at a velocity of 200 cm min^{-1} (TA-XT Plus Texture Analyzer, Stable Micro Systems, UK). Fruit size measured as height [mm], fresh mass [g], and yield as number of fruits per tree and fresh mass per tree, was measured at harvest. In 2012, the analysis of fruit quality was carried out on all fruit of every tree, while in 2013, 3 fruits per tree were analyzed.

Data Analysis

Statistical analyses were carried out using the statistical package for MATLAB® (R2014b, MathWorks, U.S.). Multi-way analysis of variance (ANOVA) was used for testing the effects of multiple factors on the plant variables. Therefore, the ECa data were grouped in 8 classes (Käthner and Zude-Sasse, 2015), while CWSI and WUE_c were grouped according to the results of hotspot analysis.

Descriptive statistics of spatially resolved data was carried out using hotspot analysis according to Peeters et al. (2015), who used ArcGIS (ESRI, Redlands, CA, USA). In the present study, the algorithm was adapted for using the free spatial Matlab toolbox (Spatial Filtering, Max Planck Institute for Biochemistry, Germany). The method is based on the general (G) statistic for testing the effect of spatial autocorrelation (Getis and Ord, 1992) of the variables. Thereby a locally weighted mean around each observation is separately compared with the mean of the

whole data (Anttila and Kairesalo, 2010). The outputs of the statistic are the z-score and the p -value, which indicate whether an observed pattern of clusters is statistically significant. Spatial clusters with statistically significant positive z-score are called hot spots, whereas the clusters with statistically significant negative z-score are called cold spots (Getis and Ord, 1992; Ferstl, 2007).

RESULTS

Soil, Meteorological Conditions, and Thermal Imaging

The ECa of soil at 25 cm depth indicated small-scale variability (Figure 1). The values of soil ECa reached a maximum of 24 mS m^{-1} with a pattern of reduced values pointing to a sand lens visible in the center-eastern part of the experimental field (Figure 1) and neighboring area. Another sandy area was located in the south-west of the orchard. Values of soil ECa measured in 2013, increased compared to those obtained in 2012. This may be due to wetter soils, which was caused by the relatively high precipitation occurring in July and August 2013. This assumption is further supported by the close correlations found between the gravimetric soil water content and ECa with $R = 0.45$ and $R = 0.68$ in 2012 and 2013, respectively (Table 1). In contrast, correlation coefficients of soil matric potential (pF) and soil ECa were only $R = 0.15$ and $R = 0.44$ in 2012 and 2013, respectively (Table 1). Repeated analyses showed similar pattern in different years with $R = 0.88$ considering 2011 and 2012 and $R = 0.71$ for years 2012 and 2013.

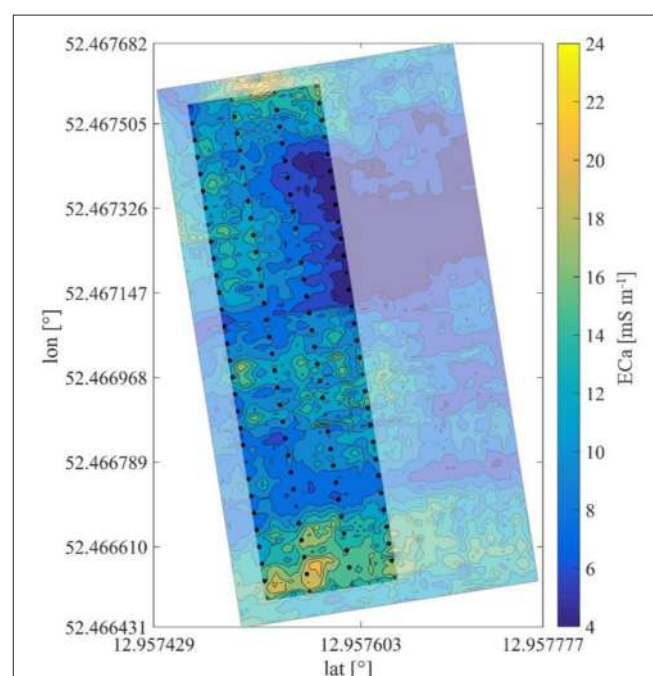


FIGURE 1 | Plum orchard in north orientation with trees marked, showing apparent electrical conductivity of soil in false color.

In 2012, during the acquisition of thermal images on 15th August from 13:40 until 16:19 (Figure 2), the mean global radiation was 641.1 W m^{-2} . August was the warmest month of the year with a mean maximum temperature of 25.6°C . The maximum air temperature on the day of measurement was 25.4°C . The diurnal increase of air temperature coincided with increasing VPD. The mean wind speed was 0.9 m s^{-1} . In 2013, mean global radiation of 306.8 W m^{-2} , maximum air temperature of 25.4°C , and wind speed of 1.2 m s^{-1} were measured.

Compared to the free air temperature recorded by the automatic weather station, maximum temperature measured within the tree canopy occurred with a 3 h-delay. Maximum instantaneous water use efficiency was calculated just before noon and then declined during the rest of the day. In general, it ranged from 4.42 to $1.28 \mu\text{Mol CO}_2 \text{ m}^{-2} \text{ s}^{-1}/\text{mMol H}_2\text{O m}^{-2} \text{ s}^{-1}$ (Figure 2). Inside the canopy, the VPD increased midday reaching a maximum in the afternoon at 17:00.

The instantaneous Ψ_{leaf} at midday varied between -0.40 and -2.14 MPa and Ψ_{π} between -1.93 and -2.56 MPa . At predawn,

Ψ_{leaf} varied between -0.12 and -1.48 MPa and Ψ_{π} between -1.50 and -2.46 MPa .

Thermal images were acquired on partially cloudy days and wet and dry leaf-references were moved with the camera for each tree record within the orchard. With our camera set-up, $1 = 2.734 \text{ m}$ and thus one pixel corresponded to 8.543 mm in width. This resolution was, thus, high enough to differentiate leaves, and to select the pixels that represent the wet and dry leaf-references (Table 2). In 2012, Vaseline® covered leaves were additionally used as dry leaf-references; however, the fingerprints of the application procedure remained visible on thermal images thus producing artifacts (data not shown).

The reference temperatures calculated with the analytical method (Ben-Gal et al., 2009) were always lower ($T_{\text{w,ana}}$ 12–15 and $T_{\text{d,ana}}$ 17) compared to those measured on paper references or obtained from the histogram of images (T_{whisto} 16–21°C

TABLE 1 | Summary of soil properties measured in plum orchard.

Variable	n	Mean	Minimum	Maximum	SD	Skewness
2012						
ECa [mS m^{-1}]	104	7.09	1.67	24.38	5.77	0.90
pF units [0;7]	19	1.63	0.04	2.10	0.44	-2.58
Water content [%]	26	7.61	4.43	9.63	1.37	-0.57
2013						
ECa [mS m^{-1}]	180	32.43	8.89	83.89	13.69	0.75
pF-units [0;7]	19	1.70	0.01	3.30	0.98	-0.51
Water content [%]	6	18.58	9.14	31.13	4.07	0.25

TABLE 2 | Ranges of wet (T_{w}) and dry (T_{d}) reference temperatures obtained according to work groups of Jones and Ben-Gal (Ben-Gal et al., 2009) using weather data (CWSI_{JB}), Jones (Jones, 1992) using dry and wet paper leaves (CWSI_{J}), and Rud (Rud et al., 2015) using both references from the histogram of image (CWSI_{R}).

Variable	n	CWSI_{JB}	CWSI_{J}	CWSI_{R}
T_{w}		12.07–15.03	19.98	16.10–20.80
T_{d}		16.95–17.06	24.93	21.00–24.00
Ψ_{leaf}	11	R F	-0.65 4800***	-0.12 3671***
Ψ_{π}	11	R F	-0.57 872***	0.33 911***

Correlation coefficients (R) and F-values, asterisks (**) denoting significance at $p < 0.001$ considering leaf water potential (Ψ_{leaf}), osmotic potential (Ψ_{π}), and crop water stress indexes are given of the same measuring day.

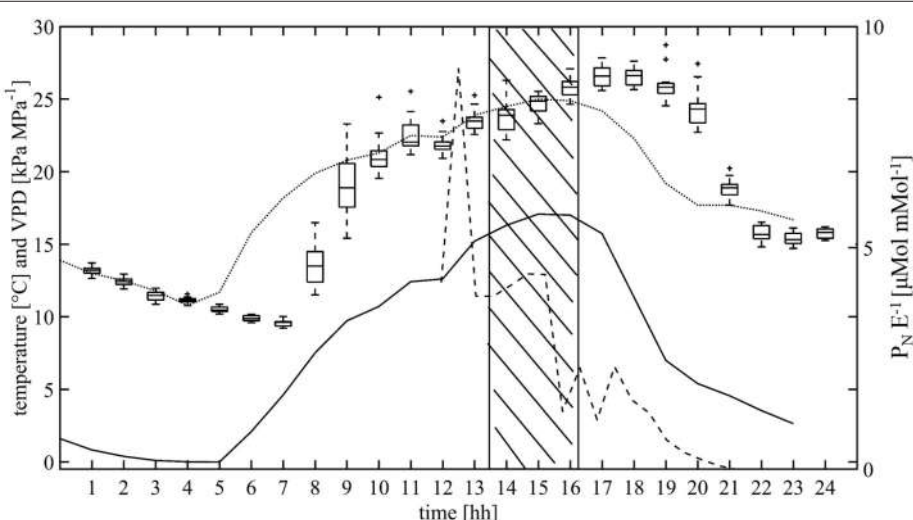


FIGURE 2 | Air temperature (dotted line), water vapor pressure deficit (VPD; solid line) and instantaneous water use efficiency (WUE_i as $P_N E^{-1}$, dashed line) measured in the orchard on 15th August 2012. In addition, the variation ($n = 18$) and diurnal course of tree canopy temperature is shown as boxplot. The dashed area indicates the period used for analyzing the CWSI.

and Td_{histo} 21–25°C). Furthermore, the correlations between leaf water potential (ψ_{leaf}) or osmotic potential (ψ_π) and the different crop water stress indexes were analyzed using data that were all obtained on the same day. Of all tested approaches, correlation coefficients for both ψ_{leaf} and ψ_π were highest for CWSI_{JB}, i.e., when the dry and wet temperatures were calculated analytically. In contrast, correlation between CWSI_J and ψ_{leaf} was low, showing enhanced variability caused by the appearance of clouds (Table 2). The use of air temperature plus 5° as Td and minimum temperature in the image as Tw for calculating CWSI_I (Irmak et al., 2000) resulted in a bias with overestimated values and also tremendously high variability due to clouds and, therefore, data were not used further. The CWSI_R ranged from 0.15 to 0.88, while the CWSI_J and CWSI_{JB} ranged from 0.03 to 0.78 and from 0.47 to 0.51, respectively. For CWSI_{JB} correlation with ψ_{leaf} was high, while the automated analysis of CWSI_R resulted in slightly reduced, but significant ($p < 0.001$) correlation coefficient of $R = 0.52$ (Table 2). However, the latter approach provided the advantage of feasible analysis of Td and Tw based on the individual images taken in the varying environment. Consequently, all further analyses were based on CWSI_R.

Hotspot Analyses

Hotspot analysis of ECa revealed one cold spot representing extreme low conductivity and 5 hot spots showing soil of high conductivity. Around the cold spot with critical z -value of < -1.65 (90% confidence level) a sand lens with an extension of $\sim 20 \times 25$ m was found (Figure 1), while at the hot spots with critical value > 1.65 (90% confidence level) water logging was observed after heavy rain fall indicating soil with lower particle size (Figure 3). The soil ECa was correlated with the number of leaves per tree. Consistently, spatial variability of canopy VPD within the orchard was found in the x-direction, which pointed to an influence of geographical position in the orchard ($R_x = 0.31$, $R_y = 0.03$, $R_z = 0.20$). This is the same direction as found for extreme values of soil ECa.

The CWSI_R ranged from 0.15 to 0.88. The hotspot analysis of CWSI_R revealed 5 cold spots occurring at z -values < -1.65 representing trees with no water shortage. The 3 hot spots appeared at critical value > 1.65 referring to high CWSI_R. Here, the hot spots refer to unfavorable conditions with enhanced water deficit. The hot spots appeared on the east side of the orchard, within and adjacent to the position of the central sand lens (Figure 3). The cold spots were found in the western positions of the orchard.

The comparison of spots considering soil ECa and CWSI_R pointed to no correlation. Also, no correlation was found between canopy size dimension and CWSI_R considering the canopy length parallel to the row ($R = 0.010$), canopy width perpendicular to the row ($R = 0.015$), and volume calculated from length, width, and distance between first branch and last shoot ($R = 0.001$).

Tree Water Status and Fruit Quality

In 2012, the average leaf number per tree was 2,362. The SLA ranged from 32.00 to 59.76 cm² g⁻¹ and showed no

correlation with soil ECa. The fruit size was correlated with soil ECa at $R = 0.223$ considering the hot and cold spots. However, other fruit quality variables did not correlate with soil properties.

No correlation between leaf water potential and fruit quality was found in the few trees measured. CWSI_R was correlated with SLA, but no significant difference was found for the number of leaves or fruit quality (Table 3). WUEc obviously depends primarily on the degree of crop load, because the water supply was kept uniform in the orchard. Mean WUEc was 2.362 g L⁻¹ in 2012 and 2.521 g L⁻¹ in 2013. In 2012, WUEc seemed only slightly, if at all, affected by soil ECa ($R = 0.133$), while in 2013, the correlation increased ($R = 0.274$).

The WUEc showed a correlation of $R = -0.367$, $R = 0.183$, and $R = -0.270$ with the fruit size, dry matter, and fruit flesh firmness, respectively, in 2012 (Table 3). Particularly, larger fruit size was correlated with low WUEc, and consequently with decreased crop load (Figure 4). Correlation between the above parameters seemed to be stronger in 2013. However, the reduce sample size in 2013 hampered the statistical comparison of the influence of slight drought stress on fruit quality in the different years.

WUEc showed no correlation with CWSI_R with $R = 0.071$ and $R = 0.093$ in 2012 and 2013, respectively. However, fruit quality was strongly affected considering the interaction of both variables (Table 4). Grouping according to WUEc and the instantaneous values of CWSI_R resulted in highly significant differences for fruit size and dry matter.

DISCUSSION

Spatial Patterns in the Orchard

Shortly before harvest, the spatial patterns of soil ECa appeared closely related to soil water content with decreased ECa values at the positions of a sand lens found in the experimental orchard. This finding is consistent with earlier investigations carried out in areas with arid conditions (McCutcheon et al., 2006). The low correlation between soil matric potential and soil apparent electrical conductivity could be expected because previous chemical analyses of soils (Käthner and Zude-Sasse, 2015) at 10 spots of the same experimental site indicated only marginal <5% variations of phosphorus and potassium content, salinity, and pH. Increased, but still <10% variation was found for magnesium, calcium, sodium, and chloride contents. Nevertheless, the analyses of the variations of soil ECa during fruit development may provide data and information for the evaluation of spatial distribution pattern of water, which could potentially affect the quality of the mature fruit.

The ψ_{leaf} measured predawn showed high variability and minimum value of -1.48 MPa indicating at least slight drought stress in some trees. Based on the measurements of weather and tree canopy microclimate, stable environmental conditions (Bellvert et al., 2014) during thermal imaging between 13:40 and 16:19 can be assumed for both years. Only the variation of radiation due to changing cloud cover could have slightly impaired thermal imaging due to the different dynamics of surface and air (ambient) temperatures (Agam et al., 2013).

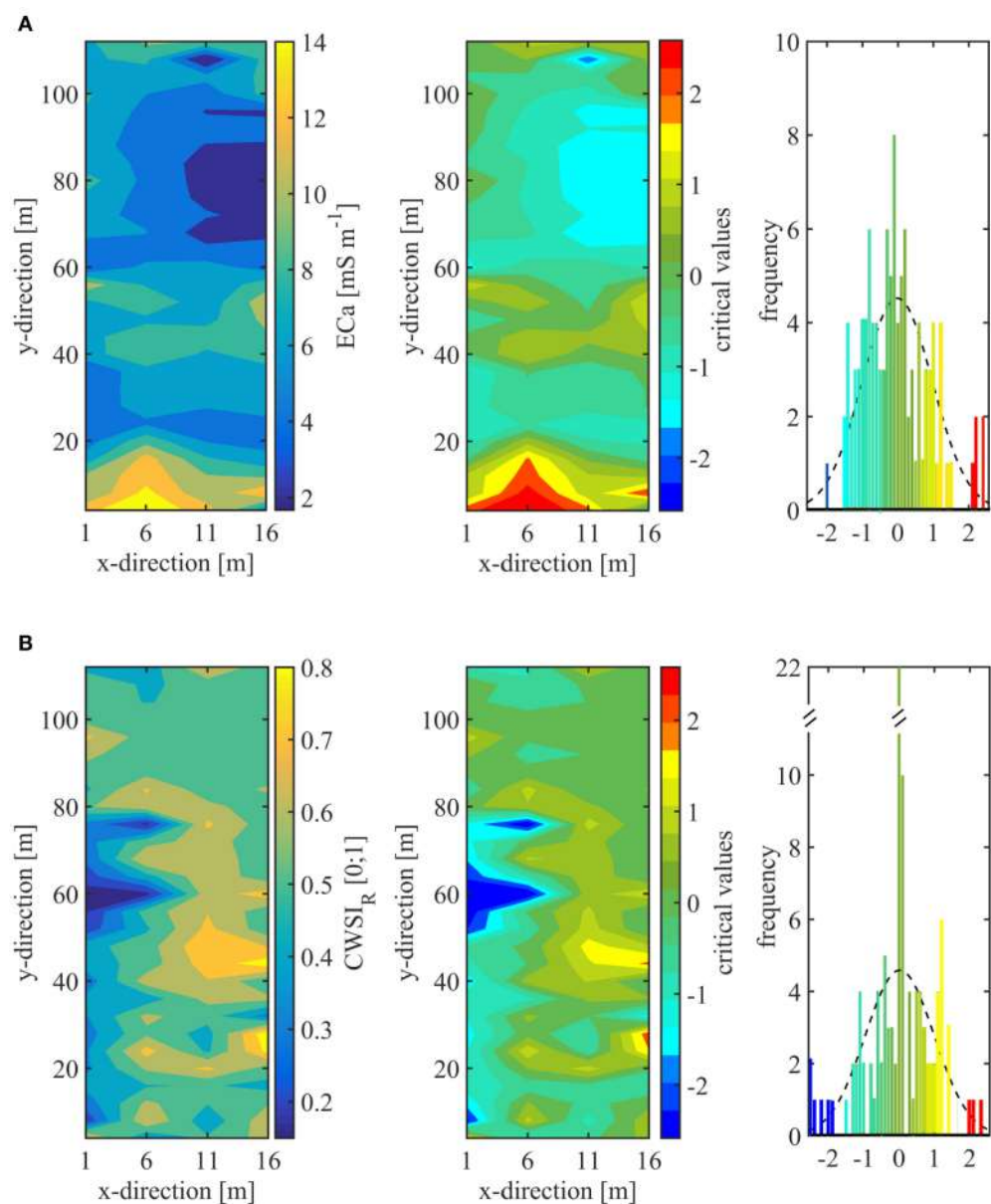


FIGURE 3 | False color maps providing the spatial distribution of **(A)** soil apparent electrical conductivity (ECa) and **(B)** instantaneous tree water status measured as crop water stress index (CWSI_R) in the experimental plum orchard. Given are raw data (left), critical values by hotspot analysis (middle), and histograms of critical values (right).

TABLE 3 | Mean values and *p*-level of plant variables grouped according to low (cold spot), random, and high (hot spot) crop water stress index (CWSI_R) and cumulative water use efficiency (WUEc) considering mean values of all fruits and leaves of each tree.

Variable	CWSI _R cold spot	CWSI _R random	CWSI _R hot spot	<i>p</i>	WUEc cold spot	WUEc random	WUEc hot spot	<i>p</i>
# Leaves per tree	1973	2341	2734	0.589	2181	2399	2266	0.568
Specific leaf area [cm ² g ⁻¹]	na	47.07	49.27	0.023	49.05	49.29	48.48	0.730
Fruit size [mm]	58.22	55.04	54.67	0.670	59.82	54.79	52.34	<0.001
Firmness [N cm ⁻²]	3.59	2.70	2.80	0.635	3.29	2.75	2.23	0.109
Dry matter [%]	33.97	32.37	32.08	0.393	32.30	32.27	32.96	0.031

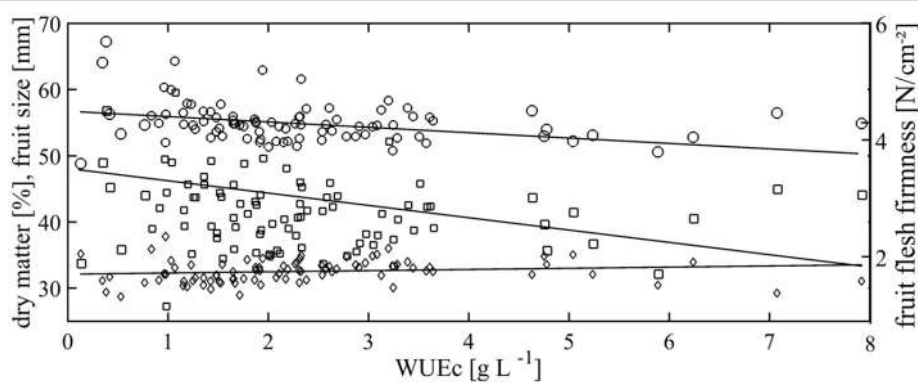


FIGURE 4 | Regression analyses of data (means per tree; $n = 88$) of fruit dry matter (diamonds, $y = 5.903x_1 + 34.67$), fruit size (circles, $y = -80.17x_2 + 24.29$), fruit flesh firmness (squares, $y = -0.129x_3 + 3.017$), and cumulative water use efficiency (WUEc). Increased symbol size represents cold and hot spots.

TABLE 4 | Interaction of cumulative water use efficiency (WUEc) \times crop water stress index ($CWSI_R$) and its effect on fruit quality analyzed by 2 factorial ANOVA considering all data and data excluding hot and cold spots.

Variable of fruit quality	$WUEc \times CWSI_R$ of all data		$WUEc \times CWSI_R$ without spots	
	F	p	F	p
Fruit size [mm]	1.94	<0.0001	1.89	<0.0001
Dry matter [%]	1.91	<0.0001	1.82	<0.0003
Firmness [N cm ⁻²]	1.16	0.2178	0.5	0.9977

On the other hand, the analysis of the instantaneous WUEi, performed at the same time, revealed diurnal changes in a value range reported in other investigations on plum trees under similar conditions (Flores et al., 1985). Consequently, consistent sets of thermal readings may have been obtained on each measurement day.

The influence of clouds indeed appeared as a perturbing factor in the present study, especially when using dry and wet paper as references for obtaining Tw and Td. The use of air temperature plus 5 K for setting Td with low difference of Td and Tw resulted in high bias of CWSI_I. The analytical analysis of Td and Tw, as well as the automated approach resulted in significant correlation of CWSI and Ψ_{leaf} . Calculating Td and Tw analytically (Jones, 1999; Ben-Gal et al., 2009) had the disadvantage that weather data were needed. However, this method provided some insurance against artifacts. In the approach of intrinsic analysis of thermal images to calculate CWSI_R (Rud et al., 2015), references are directly obtained from the images, which is presumably the most feasible approach for an application of thermal imaging in a real world orchard avoiding the need for additional measurements. The approach appeared to be appropriate for the semi-humid summer rain region with cloudy conditions of the current study. The correlation coefficient of $R = -0.52$ considering Ψ_{leaf} and CWSI_R was at least encouraging to estimate the water stress of the plum trees.

Hotspot analysis (Getis and Ord, 1992) was applied to identify geographically located trees that differ from the mean. The spots found in the ECa data set point to significantly different clusters of trees appearing in the orchard. This small scale variability of soil ECa is typical for postglacial deposits which are common sources of soils in fruit production regions in temperate areas of Europe and Asia.

The CWSI_R varied between 0.15 and 0.88 presumably indicating a range of unstressed to stressed trees in the orchard. As for the ECa patterns, the appearance of significant clusters considering instantaneous CWSI_R points to a possible impact of tree water status on plant growth. However, we can certainly make no a-priori assumption on stable CWSI patterns, since crop load, stage of fruit development, and vegetative growth are all expected to influence water demand. This said, neither ECa nor crop load in the current study showed a correlation with CWSI_R.

Potential of Irrigation Adjustment for Improving Fruit Quality

Bellvert and co-authors identified an influence of the fruit development stage on the correlation coefficient of leaf water potential and CWSI in peach and nectarine (Bellvert et al., 2016) with increased correlation shortly before harvest, which is developmental stage 3. In olive fruits, less severe but equally directed correlation was found (Martin-Virtedor et al., 2011). In the current study, CWSI_R was similarly measured in stage 3 of plum fruit development corresponding to the second peak of fruit growth rate with high water demands.

In plum production, fruit size is of highest economic importance. In the present study, no effect of instantaneous tree water status as indicated by CWSI_R on fruit size was found. However, at high crop load, fruit size was reduced and water required to produce high quality (large enough) fruits may have been deficient. While the instantaneous canopy transpiration based CWSI_R alone did not indicate this level of potential water deficit, cumulative data of WUEc was correlated with fruit quality.

The reducing effect of crop load on Ψ_{leaf} or stem water potential has been pointed out previously (Naor et al., 2001;

Marsal et al., 2010), particularly under very high crop load (Sadras and Trentacoste, 2011). An impact on the fruit size is consequent. WUEc, by definition, was dependent of crop load, since, as said, the water supply was uniform in the orchard. However, the variability of soil ECa might point to differences in effective water supply, which would be worthwhile to consider in future studies for calculating the effective WUEc.

Considering the spatial variability measured in the present study, the factor combination of the cumulative WUEc and instantaneous CWSI_R resulted in highly significant interaction with fruit quality. The effects of WUEc and CWSI outweighed the effect of soil ECa on the fruit quality. However, these findings certainly need additional experimentation and confirmation before development as a practical management tool.

CONCLUSIONS

Spatially resolved soil analysis is commonly applied in precision horticultural applications. In the present study, analysis of histograms of thermal images in a plum orchard located in a temperate climate characterized by cloud cover and semi-humid conditions was additionally confirmed as a feasible method for spatial quantification of water status.

Different spatial clusters of apparent electrical conductivity of soil and instantaneous CWSI were found, but none was correlated with fruit quality in the evenly irrigated orchard. While the WUEc showed an effect on fruit size, only combined analysis of instantaneous water status and WUEc yielded a close correlation with various fruit quality parameters. In practice, i.e., in model-based regulated deficit irrigation of orchards with frequently present small scale variability of soil and varying crop load, the coupled CWSI and WUEc, together with the stage of fruit development, is expected to be an effective driver.

REFERENCES

- Agam, N., Cohen, Y., Alchanatis, V., and Ben-Gal, A. (2013). How sensitive is the CWSI to changes in solar radiation? *Int. J. Remote Sens.* 34, 6109–6120. doi: 10.1080/01431161.2013.793873
- Agam, N., Segal, E., Peeters, A., Levi, A., Dag, A., Yermiyahu, U., et al. (2014). Spatial distribution of water status in irrigated olive orchards by thermal imaging. *Precis. Agric.* 15, 346–359. doi: 10.1007/s11119-013-9331-8
- Aggelopoulos, K., Castrignanò, A., Gemtos, T., and De Benedetto, D. (2013). Delineation of management zones in an apple orchard in Greece using a multivariate approach. *Comput. Electron. Agric.* 90, 119–130. doi: 10.1016/j.compag.2012.09.009
- Anttila, S., and Kairesalo, T. (2010). Mean and variance estimations with different pixel sizes: case study in a small water quality monitoring area in southern Finland. *Boreal Environ. Res.* 15, 335–346.
- Bellvert, J., Marsal, J., Girona, J., Gonzalez-Dugo, V., Fereres, E., Ustin, S. L., et al. (2016). Airborne thermal imagery to detect the seasonal evolution of crop water status in peach, nectarine and saturn peach orchards. *Remote Sens.* 8, 1–17. doi: 10.3390/rs8010039
- Bellvert, J., Zarco-Tejada, P. J., Girona, J., and Fereres, E. (2014). Mapping crop water stress index in a Pinot-noir vineyard: comparing ground measurements with thermal remote sensing imagery from an unmanned aerial vehicle. *Precis. Agric.* 15, 361–376. doi: 10.1007/s11119-013-9334-5
- Ben-Gal, A., Agam, N., Alchanatis, V., Cohen, Y., Zipori, I., Presnov, E., et al. (2009). Evaluating water stress in irrigated olives: correlation of soil water status, tree water status, and thermal imagery. *Irrig. Sci.* 27, 367–376. doi: 10.1007/s00271-009-0150-7
- Berman, M. E., and DeJong, T. M. (1996). Water stress and crop load effects on fruit fresh and dry weights in peach (*Prunus persica*). *Tree Physiol.* 16, 859–864. doi: 10.1093/treephys/16.10.859
- Berni, J. A. J., Zarco-Tejada, P. J., Sepulcre-Cantó, G., Fereres, E., and Villalobos, F. (2009). Mapping canopy conductance and CWSI in olive orchards using high resolution thermal remote sensing imagery. *Remote Sens. Environ.* 113, 2380–2388. doi: 10.1016/j.rse.2009.06.018
- Bramley, R. G. V., and Hamilton, R. P. (2004). Understanding variability in winegrape production systems. *Aust. J. Grape Wine Res.* 10, 32–45. doi: 10.1111/j.1755-0238.2004.tb00006.x
- Bustan, A., Dag, A., Yermiyahu, U., Erel, R., Presnov, E., Agam, N., et al. (2016). Fruit load governs transpiration of olive trees. *Tree Physiol.* 36, 380–391. doi: 10.1093/treephys/tpv138
- Chen, J., Benesty, J., Huang, Y., and Doclo, S. (2006). New insights into the noise reduction Wiener filter. *IEEE Trans. Audio Speech Lang. Process.* 14, 1218–1234. doi: 10.1109/TSA.2005.860851
- Cohen, Y., Alchanatis, V., Meron, M., Saranga, Y., and Tsipris, J. (2005). Estimation of leaf water potential by thermal imagery and spatial analysis. *J. Exp. Bot.* 56, 1843–1852. doi: 10.1093/jxb/eri174
- Ferstl, R. (2007). Spatial filtering with EViews and MATLAB. *Aust. J. Stat.* 36, 17–26.
- Flores, J. A., Lakso, A. N., and Moon, J. W. (1985). The effect of water stress and vapor pressure gradient on stomatal conductance, water use

AUTHOR CONTRIBUTIONS

AB as an expert in irrigation of fruit trees in arid and semi-arid conditions contributed on the methodology of thermal imaging, including experimental set-up and CWSI analysis. He also added to the structuring and wording of the manuscript. AP as an expert in geospatial information systems introduced and supported the spatial descriptive statistical analysis. JK carried out the experiments and all statistical data analyses. She prepared the figures and tables and made a recent literature search and proposed the text. MZ as a horticulturist provided the objectives of the experiments, supervised the methodology, added the red line in the manuscript and supported the writing. RG as an expert in soil science supported the measurements of apparent soil electrical conductivity and data analysis. WH as a plant physiologist with focus on produce quality and particularly plant water status supported the analysis of tree water status.

ACKNOWLEDGMENTS

Research has been carried out in the framework of the 3D-Mosaic project (FP7, ICT-AGRI, 2810ERA095), targeting the Advanced Monitoring of Tree Crops for Optimized Management and the USER-PA project (FP7, ICT-AGRI, 2812ERA038) USability of Environmentally sound and Reliable techniques in Precision Agriculture.

SUPPLEMENTARY MATERIAL

The Supplementary Material for this article can be found online at: <http://journal.frontiersin.org/article/10.3389/fpls.2017.01053/full#supplementary-material>

- efficiency, and photosynthesis of fruit crops. *Acta Hortic.* 171, 207–218. doi: 10.17660/ActaHortic.1985.171.18
- Fountas, S., Aggelopoulou, K., Bouloulis, C., Nanos, G. D., Wulfsohn, D., Gemtos, T. A., et al. (2011). Site-specific management in an olive tree plantation. *Precis. Agric.* 12, 179–195. doi: 10.1007/s11119-010-9167-4
- Gebbers, R., Lück, E., Dabas, M., and Domsch, H. (2009). Comparison of instruments for geoelectrical soil mapping at the field scale. *Near Surf. Geophys.* 88, 179–190. doi: 10.3997/1873-0604.2009011
- Getis, A., and Ord, J. K. (1992). The analysis of spatial association by use of distance statistics. *Geogr. Anal.* 24, 189–206. doi: 10.1111/j.1538-4632.1992.tb00261.x
- Gómez-del-Campo, M. (2013). Summer deficit irrigation in a hedgerow olive orchard cv. Arbequina: relationship between soil and tree water status, and growth and yield components. *Span. J. Agric. Res.* 11, 547–557. doi: 10.5424/sjar/2013112-3360
- González-Dugo, V., Zarco-Tejada, P., Nicolás, E., Nortes, P. A., Alarcón, J. J., Intrigliolo, D. S., et al. (2013). Using high resolution UAV thermal imagery to assess the variability in the water status of five fruit tree species within a commercial orchard. *Precis. Agric.* 14, 660–678. doi: 10.1007/s11119-013-9322-9
- Halvorson, A. D., and Rhoades, J. D. (1976). Field mapping soil conductivity to delineate dryland saline seeps with four-electrode technique. *Soil Sci. Soc. Am. J.* 40, 571–575. doi: 10.2136/sssaj1976.03615995004000040032x
- Hellebrand, H. J., Beuche, H., and Linke, M. (2006). “Thermal imaging a promising high-tec method in agriculture and horticulture,” in *Physical Methods in Agriculture*, eds J. Blahovek and M. Kutlick (Prague: Springer), 411–427.
- Honig, M. L., and Goldstein, J. S. (2002). Adaptive reduced-rank interference suppression based on the multistage wiener filter. *IEEE Trans. Commun.* 50, 986–994. doi: 10.1109/TCOMM.2002.1010618
- Irmak, S., Haman, D., and Bastug, R. (2000). Determination of crop water stress index for irrigation timing and yield estimation of corn. *Agron. J.* 92, 1221–1227. doi: 10.2134/agronj2000.9261221x
- Jackson, R. D., Idso, R. J., Reginato, P., and Printer, J. (1981). Canopy temperature as a crop water stress indicator. *Water Resour. Res.* 1133–1138. doi: 10.1029/WR017i004p01133
- Jones, H. (1992). *Plants and Microclimate, a Quantitative Approach to Environmental Plant Physiology*, 2nd and 3rd Edn. Melbourne: Cambridge University Press.
- Jones, H. G. (1999). Use of thermography for quantitative studies of spatial and temporal of stomatal conductance over leaf surfaces. *Plant Cell Environ.* 22, 1043–1055. doi: 10.1046/j.1365-3040.1999.00468.x
- Jones, H. G. (2004). Irrigation scheduling: advantages and pitfalls of plant-based methods. *J. Exp. Bot.* 55, 2427–2436. doi: 10.1093/jxb/erh213
- Käthner, J., and Zude-Sasse, M. (2015). Interaction of 3D soil electrical conductivity and generative growth in *Prunus domestica* L. *Eur. J. Hortic. Sci.* 80, 231–239. doi: 10.17660/eJHS.2015/80.5.5
- Maes, W. H., and Steppe, K. (2012). Estimating evapotranspiration and drought stress with ground-based thermal remote sensing in agriculture: a review. *J. Exp. Bot.* 13, 4671–4712. doi: 10.1093/jxb/ers165
- Mann, K. K., Schumann, A. W., and Obreza, T. A. (2011). Delineating productivity zones in a citrus grove using citrus production, tree growth and temporally stable soil data. *Precis. Agric.* 12, 457–472. doi: 10.1007/s11119-010-9189-y
- Marsal, J., Behboudian, M. H., Mata, M., Basile, B., Del Campo, J., Girona, J., et al. (2010). Fruit thinning in ‘Conference’ pear grown under deficit irrigation to optimise yield and to improve tree water status. *J. Hortic. Sci. Biotechnol.* 85, 125–130. doi: 10.1080/14620316.2010.11512642
- Martin-Vertedor, A. I., and Pérez-Rodrigue J M Prieto-Losada H Fereres-Castiel, E. (2011). Interactive responses to water deficits and crop load in olive (*Olea europaea* L., cv. Morisca). *Agric. Water Manage.* 98, 941–949. doi: 10.1016/j.agwat.2011.01.002
- McCutcheon, M. C., Farahani, H. J., Stednick, J. D., Buchleiter, G. W., and Green, T. R. (2006). Effect of soil water on apparent soil electrical conductivity and texture relationships in a dryland field. *Biosyst. Eng.* 94, 19–32. doi: 10.1016/j.biosystemseng.2006.01.002
- Nagy, A. (2015). Thermographic evaluation of water stress in an apple orchard. *J. Multidisc. Eng. Sci. Technol.* 2, 2210–2215.
- Naor, A., Gal, Y., and Peres, M. (2006). The inherent variability of water stress indicators in apple, nectarine and pear orchards, and the validity of a leaf-selection procedure for water potential measurements. *Irrig. Sci.* 24, 129–135. doi: 10.1007/s00271-005-0016-6
- Naor, A., Hupert, H., Greenblat, Y., Peres, M., Kaufman, A., and Klein, I. (2001). The response of nectarine fruit size and midday stem water potential to irrigation level in stage III and crop load. *J. Am. Soc. Hortic. Sci.* 126, 140–143.
- Palmer, J. W. (1992). Effects of varying crop-load on photosynthesis, dry matter production and partitioning of Crispin/M.27 apple trees. *Tree Physiol.* 11, 19–33 doi: 10.1093/treephys/11.1.19
- Peeters, A., Zude, M., Käthner, J., Ünlü, M., Kanber, R., Hetzroni, A., et al. (2015). Getis-Ord’s hot-and cold-spot statistics as a basis for multivariate spatial clustering of orchard tree data. *Comput. Electron. Agric.* 111, 140–150. doi: 10.1016/j.compag.2014.12.011
- Rud, R., Cohen, Y., Alchanatis, V., Beiersdorf, I., Klose, R., Presnov, E., et al. (2015). Characterization of salinity-induced effects in olive trees based on thermal imagery. *Precision Agric.* 15, 511–518. doi: 10.3920/978-90-8686-814-8_63
- Sadras, V. O., and Trentacoste, E. R. (2011). Phenotypic plasticity of stem water potential correlates with crop load in horticultural trees. *Tree Physiol.* 31, 494–499. doi: 10.1093/treephys/tpv043
- Sammis, T. W., Riley, W. R., and Lugg, D. G. (1988). Crop water stress index of pecans. *Appl. Eng. Agric.* 1, 39–45. doi: 10.13031/2013.26577
- Telford, W. M., Geldart, L. P., and Sheriff, R. E. (1990). *Applied Geophysics*. Cambridge: Cambridge University Press.
- Türker, U., Talebpour, B., and Yegül, U. (2011). Determination of the relationship between apparent soil electrical conductivity with pomological properties and yield in different apple varieties. *Žemdirbyste* 98, 307–314.
- Viets, F. G., Jr. (1962). Fertilizers and the efficient use of water. *Adv. Agron.* 14, 223–264. doi: 10.1016/S0065-2113(08)60439-3
- von Willert, D., Herppich, W. B., Matyssek, R. (1995). *Experimentelle Pflanzenökologie: Grundlagen und Anwendungen*. Stuttgart: Thieme.
- Williams, L. E., and Araujo, F. J. (2002). Correlations among predawn leaf, midday leaf, and midday stem water potential and their correlations with other measures of soil and plant water status in *Vitis vinifera*. *J. Am. Soc. Hortic. Sci.* 127, 448–454.
- Zaman, Q., and Schumann, A. W. (2006). Nutrient management zones for citrus based on variation in soil properties and tree performance. *Precis. Agric.* 7, 45–63. doi: 10.1007/s11119-005-6789-z
- Zude, M., Pflanz, M., Kaprielian, C., and Aivazian, B. L. (2008). NIRS as a tool for precision horticulture in the citrus industry. *J. Biosyst. Eng.* 99, 455–454 doi: 10.1016/j.biosystemseng.2007.10.016

Conflict of Interest Statement: The authors declare that the research was conducted in the absence of any commercial or financial relationships that could be construed as a potential conflict of interest.

Copyright © 2017 Käthner, Ben-Gal, Gebbers, Peeters, Herppich and Zude-Sasse. This is an open-access article distributed under the terms of the Creative Commons Attribution License (CC BY). The use, distribution or reproduction in other forums is permitted, provided the original author(s) or licensor are credited and that the original publication in this journal is cited, in accordance with accepted academic practice. No use, distribution or reproduction is permitted which does not comply with these terms.



Vegetable Grafting: The Implications of a Growing Agronomic Imperative for Vegetable Fruit Quality and Nutritive Value

Marios C. Kyriacou¹, Youssef Rousphael², Giuseppe Colla³, Rita Zrenner⁴ and Dietmar Schwarz^{4*}

¹ Department of Vegetable Crops, Agricultural Research Institute, Nicosia, Cyprus, ² Department of Agricultural Sciences, University of Naples Federico II, Naples, Italy, ³ Department of Agricultural and Forestry Sciences, University of Tuscia, Viterbo, Italy, ⁴ Leibniz Institute of Vegetable and Ornamental Crops, Großbeeren, Germany

OPEN ACCESS

Edited by:

Nadia Bertin,
Plantes et Système de Cultures
Horticoles (INRA), France

Reviewed by:

Yuksel Tuzel,
Ege University, Turkey
Georgia Ntatsi,
Agricultural University of Athens,
Greece

***Correspondence:**

Dietmar Schwarz
schwarz@igzev.de

Specialty section:

This article was submitted to
Crop Science and Horticulture,
a section of the journal
Frontiers in Plant Science

Received: 03 March 2017

Accepted: 20 April 2017

Published: 12 May 2017

Citation:

Kyriacou MC, Rousphael Y, Colla G, Zrenner R and Schwarz D (2017) Vegetable Grafting: The Implications of a Growing Agronomic Imperative for Vegetable Fruit Quality and Nutritive Value.

Front. Plant Sci. 8:741.
doi: 10.3389/fpls.2017.00741

Grafting has become an imperative for intensive vegetable production since chlorofluorocarbon-based soil fumigants were banned from use on grounds of environmental protection. Compelled by this development, research into rootstock-scion interaction has broadened the potential applications of grafting in the vegetable industry beyond aspects of soil phytopathology. Grafting has been increasingly tapped for cultivation under adverse environs posing abiotic and biotic stresses to vegetable crops, thus enabling expansion of commercial production onto otherwise under-exploited land. Vigorous rootstocks have been employed not only in the open field but also under protected cultivation where increase in productivity improves distribution of infrastructural and energy costs. Applications of grafting have expanded mainly in two families: the Cucurbitaceae and the Solanaceae, both of which comprise major vegetable crops. As the main drives behind the expansion of vegetable grafting have been the resistance to soilborne pathogens, tolerance to abiotic stresses and increase in yields, rootstock selection and breeding have accordingly conformed to the prevailing demand for improving productivity, arguably at the expense of fruit quality. It is, however, compelling to assess the qualitative implications of this growing agronomic practice for human nutrition. Problems of impaired vegetable fruit quality have not infrequently been associated with the practice of grafting. Accordingly, the aim of the current review is to reassess how the practice of grafting and the prevalence of particular types of commercial rootstocks influence vegetable fruit quality and, partly, storability. Physical, sensorial and bioactive aspects of quality are examined with respect to grafting for watermelon, melon, cucumber, tomato, eggplant, and pepper. The physiological mechanisms at play which mediate rootstock effects on scion performance are discussed in interpreting the implications of grafting for the configuration of vegetable fruit physicochemical quality and nutritive value.

Keywords: carotenoids, Cucurbitaceae, flavor, functional compounds, physiological mechanism, mRNA transport, rootstock, Solanaceae

INTRODUCTION

Retail cost for fresh horticultural products reflects capital investment in developing suitable plant stock, in fostering its cultivation, and in product storage and handling along the food supply chain. Although a multifaceted concept drawing on various implicated stakeholders, quality is ultimately what captures the expectations to be met at the retail customer's end of the agroindustry spectrum. The perception of quality is dependent on intrinsic traits of horticultural commodities, shaped by genotypic, cultural and ecophysiological effects, and on extrinsic traits formulated by the socio-economic and marketing environment (Schreiner et al., 2013). Multidisciplinary studies have highlighted that quality is more important to consumers than price when the latter varies within the anticipated range (Harker et al., 2003). Although consonance of quality with the cost of purchase influences consumer behavior, quality is that which largely commands recurring customers. In regulatory context, the issue of quality is addressed chiefly by crop-specific class standards based on limited key visual and organoleptic characteristics (Commission Implementing Regulation (EU) No 543/2011, 2011). Quality standards thus tend to define class criteria for minimum acceptability and provide practical, effective, mostly non-destructive means for standardization procedures. They fail, however, to address complex compositional aspects of quality pertaining to flavor, particularly the volatile aroma fraction, or to nutritional and bioactive value which consumers are becoming increasingly conscious of Schreiner et al. (2013).

Plant breeding on the other hand, has aimed preeminently at improving yield, endowing plant stock with disease resistance, at providing resilience to mechanical injury and improving overall postharvest performance, and to a lesser extent at improving sensory quality traits (Bai and Lindhout, 2007). However, the configuration of important sensory traits, such as volatile aroma components, seems mediated by ethylene-dependent biosynthetic pathways linked also to shelf-life performance (Pech et al., 2008), and to textural changes associated with cell wall matrix solubilization events (Dos-Santos et al., 2013). Hence breeding for shelf-life may elicit adverse pleiotropic effects on desirable sensory attributes (Causse et al., 2002). This is particularly critical in fruits characterized by autocatalytic climacteric ripening, as aptly exemplified by the distinct sensory profile of odorous climacteric vs. inodorous non-climacteric melons (Verzera et al., 2011). Collecting desirable traits while avoiding undesirable combinatorial effects complicates breeding efforts. In this respect, grafting may provide expedient means of selecting independently for rootstock and scion traits, provided the compatibility of the graft combination.

Driven initially by its efficiency as an alternative to the banned use of chlorofluorocarbon-based soil fumigants, the grafting of annual fruit crops has grown across crops and beyond applications restricted to addressing soilborne disease problems (Rouphael et al., 2010). Grafting has

been increasingly tapped for cultivation under adverse environments posing abiotic and biotic stresses to vegetable crops, thus enabling expansion of commercial production onto otherwise under-exploited land. The ability of tapping wild genetic resources for exploiting traits of root physiological tolerance to stress independently to scion characteristics has facilitated the application of grafting for the cultivation of annual fruit crops under marginal conditions of salinity, nutrient stress, water stress, organic pollutants, and alkalinity (Savvas et al., 2010; Schwarz et al., 2010; Borgognone et al., 2013). Moreover, the economic implications of the significant yield increase imparted by select vigorous commercial rootstocks has encouraged their use under protected cultivation where increase in productivity improves distribution of infrastructural and energy costs (Colla et al., 2011). Provided the anatomical and physiological compatibility of the graft combinations, rootstock effects on plant performance under soil biotic and abiotic stress conditions clearly outweigh those of the scion. Moreover, there is evidence of rootstock mediation in the configuration of scion fruit quality characteristics, widely reported in a range of crops but confounded with frequent rootstock–scion interaction which cannot always be explained in the context of narrow rootstock–scion specificity (Rouphael et al., 2010).

As the main drives behind the expansion of vegetable grafting have been the resistance to soilborne pathogens (Louws et al., 2010), tolerance to abiotic stresses (Schwarz et al., 2010; Kumar et al., 2015; Rouphael et al., 2016) and increase in yields (Lee et al., 2010), rootstock selection and breeding have accordingly conformed to the prevailing demand for improving productivity, arguably at the expense of fruit quality. Thus, grafting has not been employed as a method for improving vegetable fruit quality. Quite the contrary, often yield and quality are contradictory traits (Klee and Tieman, 2013). Considering the rapid expansion of the vegetable grafting industry, understanding the implications of grafting for fruit quality is imperative, and equally pressing is the unraveling of the mechanisms involved. Possible factors engaged in rootstock mediation of quality include changes in water and nutrient uptake efficiency, indirect effects on ripening behavior resulting from altered crop load and source-sink balance, and even an epigenetic component to the grafting process involving transfer of genetic material from rootstock to scion (Savvas et al., 2010; Soteriou et al., 2014; Avramidou et al., 2015). Previous reviews on the grafting of annual fruit crops that have covered aspects relating to fruit quality were published by Davis et al. (2008a, only Cucurbitaceae), Flores et al. (2010 only tomato), and Rouphael et al. (2010). The current review aims at providing an updated critical review of scientific advances addressing grafting effects on the fruit quality of annual crops; moreover, it discusses methodological postulates and mechanisms possibly mediating these effects. Current knowledge has been compiled in a crop specific approach where fruit quality attributes and rootstocks employed are discussed in a uniform and integrated context.

THE CONFIGURATION OF FRUIT QUALITY IN GRAFTED VEGETABLES

Cucurbitaceae

Watermelon [*Citrullus lanatus* (Thunb.) Matsum. and Nakai]

The adoption of grafting as a means to secure watermelon crop stand and productivity, mainly against conditions of biotic stress, by far exceeds that of any other open cultivated annual fruit crop (FAO, 2012). The use of rootstocks resistant to soilborne diseases has become a prerequisite for watermelon production, especially in areas where intensive cultivation is practiced and scarcity of arable land precludes the application of broad rotation schemes. While most studies assessing rootstock–scion interaction had initially laid emphasis on aspects of disease resistance and agronomic performance, a plethora of works has been produced that examine the implications of grafting for watermelon fruit quality, involving mainly interspecific hybrids [*Cucurbita maxima* (Duchesne) × *C. moschata* (Duchesne ex Poir)] and gourd [*Lagenaria siceraria* (Molina Standl.] rootstocks.

Morphometric characteristics

Although a trait prominently delineated by genotype, watermelon fruit weight might be influenced by environmental conditions and cultural practices, including grafting, that affect overall field performance (Alexopoulos et al., 2007; Cushman and Huan, 2008; Proietti et al., 2008; Soteriou and Kyriacou, 2014). Vigorous interspecific and *L. siceraria* rootstocks can improve yields significantly, which in genotypically large-fruited scions usually translates into a tendency for higher unit fruit weight, while in small-fruited cultivars it tends to increase the number of fruits per plant (Colla et al., 2006a; Alexopoulos et al., 2007; Cushman and Huan, 2008; Proietti et al., 2008; Soteriou and Kyriacou, 2014). Decrease in fruit weight against non-grafted control is usually an indicator of rootstock–scion incompatibility, while in compatible grafts maximum reported fruit weight increase approximates 55% (Yetisir and Sari, 2003; Yetisir et al., 2003; Huitrón et al., 2007; Cushman and Huan, 2008; Soteriou and Kyriacou, 2014).

Secondary morphological characteristics of watermelon fruit that may appeal to consumers' perception of quality include shape, expressed as the ratio of longitudinal to equatorial diameter, and rind thickness. Fruit shape constitutes a trait predominantly governed by scion genotype and little affected by environmental or cultural factors; hence the effect of grafting thereupon has been circumstantial and mostly non-significant or minimal (Colla et al., 2006a; Alan et al., 2007; Roushafel et al., 2008; Soteriou and Kyriacou, 2014; Fredes et al., 2017). On the other hand, rind thickness is a morphological trait more responsive to grafting, and to cultural practice at large, as it relates to watermelon harvest maturity (Soteriou et al., 2014; Kyriacou et al., 2016). On commercial *C. maxima* × *C. moschata* and *L. siceraria* rootstocks, especially on landraces of the latter, thickening of watermelon rind is often observed (Yetisir et al., 2003; Alexopoulos et al., 2007; Proietti et al., 2008;

Kyriacou and Soteriou, 2015). However, this has not been a ubiquitous effect across the above rootstocks, or with less common rootstocks such as *C. moschata*, *Sicyos angulatus* L., *C. lanatus* var. *citroides* (L. H. Bailey) Mansf. and *C. pepo* L. which were only sporadically effective in this respect (Davis and Perkins-Veazie, 2005; Alan et al., 2007; Huitrón et al., 2008; Soteriou and Kyriacou, 2014; Fredes et al., 2017). Rootstock effect on watermelon rind thickness is in general limited and studies involving multiple rootstock–scion combinations have demonstrated the predominance of the relative effect of the scion cultivar on this attribute (Kyriacou and Soteriou, 2015). Thinning of the rind is known to characterize watermelon maturation, but also its postharvest life (Corey and Schlimme, 1988); therefore, potential rootstock effect should be examined under conditions that account carefully for the effect of harvest maturity (Soteriou et al., 2014). In any case, thickening of the rind can improve the postharvest performance of watermelon fruit and may also provide a tool for increasing the source of important bioactive compounds concentrated in the rind, such as citrulline, which constitute potential by-products of the fresh-cut industry (Tarazona-Díaz et al., 2011).

Colourimetric attributes

Among the physical characteristics of watermelon fruit that strongly influence consumer preference, is the intensity of red coloration of the pulp. Change in the intensity of red hue, expressed as increase in colourimetric CIELAB component a^* , marks the development of watermelon pulp color during ripening; moreover, a widening of hue angle (h°), signifying transition from red to orange-yellow is characteristic of watermelon over-ripening and senescence (Brown and Summers, 1985; López-Galarza et al., 2004; Soteriou et al., 2014). Watermelon pulp color is directly dependent upon lycopene synthesis and its accumulation in chromoplasts, while cultivar differences in pulp color correlate highly with differences in lycopene content (Perkins-Veazie and Collins, 2006; Kyriacou and Soteriou, 2015). Grafting therefore may affect pulp color to the extent it affects lycopene content (Davis and Perkins-Veazie, 2005). Watermelon scions grafted on interspecific *Cucurbita* hybrid rootstocks may incur delayed pulp color development, compared to non-grafted control, expressed as a delayed peak in colourimetric component a^* synchronous to the peak in lycopene content (Soteriou et al., 2014).

Textural characteristics

Pulp firmness constitutes one of the most important sensory traits of watermelon fruit subject to wide genotypic variation, with pronounced firmness observed usually in seedless, triploid cultivars (Leskovar et al., 2004; Soteriou and Kyriacou, 2015). Notwithstanding the genotypic effect of the scion, rootstock effects on watermelon pulp firmness can be significant hence the choice of rootstock instrumental for improving fruit quality and postharvest life (Yetisir et al., 2003; Cushman and Huan, 2008; Bruton et al., 2009; Kyriacou and Soteriou, 2015). Interspecific *Cucurbita* hybrid rootstocks most consistently increase watermelon pulp firmness in both diploid and triploid scions (Bruton et al., 2009; Huitrón et al., 2009; Soteriou et al., 2014;

Soteriou and Kyriacou, 2015). The effect of grafting, however, might render the pulp of certain cultivars, especially mini triploids that are genotypically inclined to outstanding firmness, undesirably hard (Soteriou and Kyriacou, 2015). Among less commonly used rootstocks, the parents of interspecific hybrids *C. maxima* and *C. moschata*, *C. ficifolia* Bouché, and citron melon (*C. lanatus* var. *citroides*) have been reported to elicit firmer watermelon pulp (Cushman and Huan, 2008; Bruton et al., 2009), whereas cushaw squash (*C. argyrosperma* C. Huber) pumpkin had the opposite effect (Davis and Perkins-Veazie, 2005). Gourd rootstocks *L. siceraria* usually have no effect on pulp firmness although erratic cultivar-specific effects, both positive and negative, have been reported (Yetisir et al., 2003; Cushman and Huan, 2008; Bruton et al., 2009; Özdemir et al., 2016). Morphological abnormalities scarcely associated with watermelon grafting include yellow bands in the pulp bordering the rind, hollow heart, excessively hard and discolored pith, and overall poor texture (Lee, 1994; Yamasaki et al., 1994; Davis et al., 2008b; Soteriou and Kyriacou, 2014). However, most reports on commercially available *C. maxima* × *C. moschata* and *L. siceraria* rootstocks do not make reference to such defects which may reflect rootstock-scion incompatibility and adverse environmental conditions or cultural practices.

Sweetness and acidity

The most valued singular quality trait of watermelon is undoubtedly sweetness, sensorially triggered mostly but not entirely by soluble mono- and di-saccharides, since other juice solutes including organic acids, soluble pectins and amino acids, phenolic compounds and minerals influence sweet sensation (Kader, 2008; Magwaza and Opara, 2015). The soluble solids content (SSC) – containing sugars and acids, together with small amounts of dissolved vitamins, fructans, proteins, pigments, phenolics, and minerals – is the most important quality measure used to indicate sweetness of watermelon as well as other fruits (Magwaza and Opara, 2015). It is in general not highly compromised by grafting on most commercial *C. maxima* × *C. moschata* rootstocks (Colla et al., 2006a; Proietti et al., 2008; Huitrón et al., 2009; Soteriou and Kyriacou, 2014; Kyriacou et al., 2016). Scion response to *L. siceraria* rootstocks appears more erratic and rootstock-specific with most graft combinations not demonstrating a significant effect on SSC but exceptions of SSC reduction, especially on landraces, or SSC increase are not infrequent (Yetisir and Sari, 2003; Alan et al., 2007; Alexopoulos et al., 2007; Cushman and Huan, 2008; Çandır et al., 2013). Effects on watermelon sweetness have occasionally been demonstrated by more marginal or experimental rootstocks, such as reduction of SSC by *C. argyrosperma* and *C. pepo* (Davis and Perkins-Veazie, 2005), and increase by *C. lanatus* var. *citroides* (Fredes et al., 2017).

Sweetness depends mostly on the total concentration of soluble carbohydrates, which in most fruits constitutes the largest fraction of the SSC, but also on the relative proportions of the three main sugars, glucose, fructose, and sucrose, which contribute differentially to sweetness and combine to yield what is termed sweetness index (Elmstrom and Davis, 1981;

Brown and Summers, 1985; Kader, 2008). Among cucurbit genotypes, variation in sugar content and sweetness index has been associated mostly with their ability to accumulate sucrose at the expense of fructose and glucose during ripening, owing to the activity of sucrose phosphate synthase and sucrose synthase and the decline in activity of soluble acid invertase (Stepansky et al., 1999; Yativ et al., 2010). In watermelon, fructose and glucose are the main sugars supplying the demands of the ovary during initial fruit development, due to the high activities of neutral and acid invertases (Lanchun et al., 2010). Sucrose is the main soluble carbohydrate accumulating in watermelon fruit during ripening at the expense of reducing sugars (Brown and Summers, 1985; Chisholm and Picha, 1986; López-Galarza et al., 2004; Soteriou et al., 2014), although less common genotypes accumulating reducing-sugars throughout ripening have been reported (Yativ et al., 2010). Lower accumulation of hexoses at the onset of fruit development and reduced sucrose accumulation during ripening have been implicated in moderate reduction of watermelon total sugar content in response to the use of *C. maxima* × *C. moschata* and *L. siceraria* rootstocks (Miguel et al., 2004; Liu et al., 2006; Kyriacou and Soteriou, 2015; Fredes et al., 2017). However, other studies involving the same rootstock types have revealed no significant effects on glucose, fructose, sucrose, or total sugars content (Colla et al., 2006a; Proietti et al., 2008; Soteriou et al., 2014). Disparity of results regarding the effect of grafting on non-structural carbohydrates in many cases reflects differential ripening events, notwithstanding the possible effects of cultural practice and climatic conditions particularly on flowering and fruit setting. Grafting may affect the earliness of flowering and thereby affect the time to commercial maturity (Satoh, 1996; Sakata et al., 2007), however, the delay in maturation relates mainly to retarded post-anthesis ripening events as a result of increased crop load on grafted plants (Soteriou et al., 2014; Kyriacou and Soteriou, 2015; Soteriou and Kyriacou, 2015).

Acidity balances sweetness in the taste profile of most fruits, although effectively the ratio between SSC and titratable acidity (TA) is considered crucial in terms of consumer acceptability mostly for sour fruits. Acidity in watermelon fruit is very low, with a pH range of 5.5–5.8 and acid concentration in its juice 0.7–1.2 g/l predominantly in malate form (Kyriacou and Soteriou, 2012; Çandır et al., 2013; Soteriou et al., 2014; Fredes et al., 2017). Grafting on *C. maxima* × *C. moschata* has been found to increase the TA and reduce the pH of the pulp (Colla et al., 2006a; Proietti et al., 2008; Soteriou et al., 2014). Increase in watermelon acidity has been elicited by grafting not only on hybrid rootstocks but also on *C. lanatus* var. *citroides* and on certain *L. siceraria* rootstocks, expressed mostly in higher malic acid levels in the juice (Çandır et al., 2013; Fredes et al., 2017). The TA of watermelon pulp declines linearly with ripening; grafting, however, sustains higher TA throughout the ripening period in comparison to non-grafted plants, which verifies that this is less mediated by maturity than the effect of grafting on sugars (Soteriou et al., 2014), moreover it predisposes the fruit for improved postharvest performance (Kyriacou and Soteriou, 2015).

Aroma profile

Alcohol and aldehyde characteristics of the Cucurbitaceae family constitute the main aroma volatiles in watermelon fruit, with the former usually in higher concentrations (Beaulieu and Lea, 2006; Saftner et al., 2007). The most abundant alcohols identified in the aroma profile of mini watermelons include (*Z*)-3-Nonen-1-ol (fresh melon), (*Z,Z*)-3,6-Nonadien-1-ol (pumpkin, cucumber), hexanol (flower, green), nonanol (herbaceous) and (*Z*)-6-Nonen-1-ol (pumpkin-like, green melon) (Yajima et al., 1985; Dima et al., 2014). Among identified aldehydes most abundant were (*Z*)-2-nonenal (honeydew melon, fruity), hexanal (green), (*E,Z*)-2,6-nonadienal (cucumber, green), nonanal (melon, orange peel), (*Z*)-6-nonenal (honeydew melon, fruity), 6-methyl-5-hepten-2-one (flower) and (*E*)-6-nonenal (earthy) (Dima et al., 2014). Although significant rootstock-specific effects on watermelon volatile profile have been identified, the effect of grafting on watermelon aroma profile remains at large a scarcely charted territory (Petropoulos et al., 2014; Fredes et al., 2017). Grafting midi-watermelon cultivars (≈ 6 kg) on *C. maxima* \times *C. moschata* and *L. siceraria* rootstocks was found to increase fruit content in several aroma volatiles, including (*E*)-2-nonenal (fat, cucumber) and (*Z,Z*)-3,6-nonadien-1-ol (green, cucumber) (Petropoulos et al., 2014). Fredes et al. (2017) identified differential effects among *C. maxima* \times *C. moschata* rootstocks in the levels of (*Z*)-6-nonenal and (*E,Z*)-2,6-nonadienal, associated with melon-like and cucumber-like aromas, respectively. A critical and consistent finding across *C. maxima* \times *C. moschata* rootstocks, but not on *C. lanatus* var. *citroides*, is the increased level of (*Z*)-6-nonen-1-ol, which confers undesirable pumpkin-like odor in fruits from grafted plants. However, the identification of higher levels of lycopene degradation products, such as 6-methyl-5-heten-2-one and geranylacetone in the volatile profile of fruit from non-grafted plants, characterized by earlier peak in lycopene content (Soteriou et al., 2014), suggests differential harvest maturity between treatments may be implicated in these findings (Lewinsohn et al., 2005). Available work is far from providing conclusive evidence on the effect of grafting on watermelon aroma profile. Future work needs to take carefully into consideration the evolution of aroma profile during ripening so that the potential effects of grafting are discerned from those of harvest maturity. Analysis of volatiles performed using a GC-MS-olfactory approach combined with extensively trained sensory panels would provide a more resilient basis for further investigation into rootstock-mediated effects on watermelon aroma profile (Saftner et al., 2007).

Functional compounds

Notwithstanding wide genotypic variation, watermelon is a lycopene-rich food source with higher lycopene concentration in its pulp than that of tomato (Perkins-Veazie et al., 2001; Fish and Davis, 2003; Soteriou et al., 2014). Grafting, particularly on *C. maxima* \times *C. moschata* rootstocks, has been reported to raise lycopene levels significantly in watermelon fruit (Perkins-Veazie et al., 2007; Proietti et al., 2008; Soteriou et al., 2014; Kyriacou and Soteriou, 2015). Increase was also reported on selected *L. siceraria* genotypes (Çandır et al., 2013) and on *C. argyrosperma* and *C. pepo* but limited to seedless scions

(Davis and Perkins-Veazie, 2005). Decrease in lycopene levels associated with certain rootstock-scion combinations involving *L. siceraria* and *C. argyrosperma* (Davis and Perkins-Veazie, 2005; Çandır et al., 2013), or absence of effect (Bruton et al., 2009; Soteriou and Kyriacou, 2014) have been more infrequently reported. Conflicting reports may be explained in the light of recent work demonstrating that lycopene content is affected more by maturity and less by grafting, as the peak in lycopene content appears about 1 week earlier in fruit from non-grafted than from grafted plants (Soteriou et al., 2014). Ripening-dependent accumulation of lycopene may derive from the inhibition of β -carotene synthesis or from an alternative ripening-specific pathway, such as the 1-deoxy-D-xylulose-5-phosphate (DOXP) pathway (Bramley, 2002; Schofield et al., 2008). It is also not known whether the progressive transition in pulp color from red to orange-yellow, which signifies over-ripening, derives from the conversion of accumulated lycopene to β -carotene, or from a senescence-related degradation of lycopene (Ronen et al., 2000; Schofield et al., 2008). The implications of grafting for both of the above processes remain uninvestigated. In addition, lycopene synthesis events are carried over to the postharvest period where they appear temperature-controlled and linked to changes in pulp color (Perkins-Veazie and Collins, 2006). Lycopene content peaked 7 days postharvest at 25°C and was further increased by grafting on *C. maxima* \times *C. moschata* rootstocks (Kyriacou and Soteriou, 2015). Depending upon maturity at the time of harvest, postharvest lycopene synthesis may appear as a continuation of the ripening-dependent pattern observed preharvest.

A non-essential amino acid found in abundance in watermelon and other cucurbits is citrulline (Rimando and Perkins-Veazie, 2005). It is a metabolic intermediate in the nitric oxide cycle, active in biological functions such as vasodilation and muscle relaxation which derive from the dissipation of NO during conversion of citrulline to arginine (Nissinen et al., 2003). Earlier indications that grafting could increase amino acid content of watermelon fruit, particularly citrulline (Davis et al., 2008c) have been confirmed by more recent work. Grafting onto *C. maxima* \times *C. moschata* rootstock resulted in higher citrulline content in the pulp throughout fruit ripening (Soteriou et al., 2014). Grafting improves the performance of watermelon under deficit irrigation (Proietti et al., 2008), while the accumulation of citrulline in watermelon vegetative tissues under drought conditions has been proposed to contribute to oxidative stress tolerance based on its novel hydroxyl radical scavenging activity (Akashi et al., 2001). Citrulline accumulation in watermelon rind and pulp, possibly relates to an osmotic role during cell expansion as it constitutes a potentially significant fraction of the non-carbohydrate soluble solids in the fruit (Curis et al., 2005; Davis et al., 2011; Tarazona-Díaz et al., 2011; Soteriou et al., 2014).

Melon (*Cucumis melo* L.)

Melon constitutes an annual fruit species of complex quality configuration owing to the diverse ripening patterns and associated aroma profiles of its botanical varieties. These are discerned into two major groups: the climacteric short shelf-life

odorous varieties *cantalupensis* and *reticulata* (e.g., charentais and muskmelon) characterized by intense aroma, as opposed to the non-climacteric, long shelf-life, non-aromatic *inodorus* varieties, such as honeydew and canary melons (Pech et al., 2008; Allwood et al., 2014). Cantaloupes are among the most widely produced melon varieties but the range of specialty melon types cultivated commercially includes many others, such as Galia, Ananas, Persian, Honeydew, Piel de Sapo, Casaba, Crenshaw, Canary, and Asian melons (Strang et al., 2007). Melon grafting as a phytoprotective measure targets Fusarium and Monosporascus wilts by exploiting mainly resistant same-species (*C. melo*) genotypes, interspecific (*C. maxima* × *C. moschata*) pumpkin hybrids and white gourd [*Benincasa hispida* (Thunb.) Cogn.]; whereas grafting on resistant *Cucumis metuliferus* E. Mey. ex Naudin and *C. melo* subsp. *Agrestis* (Naudin) Pangalo rootstocks emerges as a growing practice against Meloidogyne root knot nematodes (Trionfetti-Nisini et al., 2002; Fita et al., 2007; Davis et al., 2008a; Louws et al., 2010; Guan et al., 2014). Graft incompatibility and deterioration in the fruit quality of grafted plants are common problems, particularly with *Cucurbita* hybrid rootstocks, further complicated by pronounced rootstock interaction with the wide range of melon scion genotypes (Traka-Mavrona et al., 2000; Roush et al., 2010; Soteriou et al., 2016).

Morphometric characteristics

Whereas compatible *C. melo* and *Cucurbita* hybrid rootstocks generally tend to have no effect on melon fruit weight, there is also widespread rootstock–scion interaction in the responses of different melon types to grafting. For instance, the fruit weight of muskmelon (cv. Proteo) was not influenced by either *C. melo* (cvs. Energia and Sting) or *Cucurbita* hybrid rootstocks (cvs. Polifemo, AS10, RS841, P360, and Elsi) (Condurso et al., 2012). However, the same scion (cv. Proteo) grown hydroponically on other *C. melo* (cvs. Dinero and Jador) and hybrid rootstocks (cvs. P360 and PS1313), incurred a limited mean increase of 6.8% in fruit weight (Colla et al., 2010a). In the case of *inodorus* honeydew melon (cv. Incas), fruit weight was not influenced by grafting onto *C. melo* (cvs. Belimo, Energia, Griffin, Sting, and ES liscio) and *Cucurbita* hybrid rootstocks (cvs. AS10, P360, ES99-13, and Elsi), although it was increased moderately when grafted onto hybrids 'RS841' and 'Polifemo' (Crinò et al., 2007; Verzera et al., 2014). Commercial hybrid rootstocks 'TZ148', 'N101', 'Carnivor', and '30900' also had no effect on the fruit weight of an Ananas type (cv. Raymond) and two Galia type (cvs. Elario and Polynica) melons (Soteriou et al., 2016), as was also the case with cantaloupe (cv. Athena) grafted on interspecific hybrids 'Strong Tosa' and 'Tetsukabuto' (Zhao et al., 2011). By contrast, Schultheis et al. (2015) identified a general trend for reduction of fruit weight as a result of grafting in field trials of muskmelon, honeydew and specialty melons, tested, however, only on hybrid rootstock cv. Carnivor. Traka-Mavrona et al. (2000) found grafting had no effect on fruit weight of three *inodorus* melons (cvs. Thraki, Peplo, and Lefko Amynteou), and a cantaloupe (cv. Kokkini Banana) using two hybrids ('TZ-148' and 'Mamouth') and one pumpkin (*C. maxima*) landrace ('Kalkabaki') as rootstocks under protected and open field cultivation. Similarly, grafting galia (cv. Arava)

and honeydew (cv. Honey Yellow) melons onto nematode-resistant *C. metuliferus* had no effect on fruit weight under organic or conventional production systems (Guan et al., 2014). Exceptional increase (29%) in fruit weight was reported for cantaloupe (cv. Cyrano) when grafted on hybrid 'P360' and grown under greenhouse salinity treatments (Colla et al., 2006b). Decrease in fruit weight of muskmelon cv. Proteo resulted from grafting onto *B. hispida*, whereas *C. metuliferus*, *C. zeyheri* Sond., *C. moschata*, *C. maxima*, and *C. maxima* × *C. moschata* hybrids had no such effect on muskmelon cultivars Proteo and Supermarket (Trionfetti-Nisini et al., 2002). Finally, Park et al. (2013) examined four *C. melo* accessions and a Shintoza hybrid as rootstocks and found that none of these had an effect on the fruit weight of muskmelon ('Earl's elite') and honeydew ('Homerunstar') except a *C. melo* accession ('K134069') which produced fruits of greater weight and size than the non-grafted control.

Other morphological traits of relevance to melon quality include fruit shape, exocarp and pulp thickness. Reports on melon grafting do not present significant rootstock effects on these variables which rather seem strongly delineated by the scion genotype. In the case of honeydew, muskmelon, cantaloupe and Piel de Sapo melons these traits were not affected by grafting on *Cucurbita* hybrid, *C. melo*, *C. maxima* and *C. melo* subsp. *agrestis* rootstocks (Traka-Mavrona et al., 2000; Fita et al., 2007; Colla et al., 2010a; Verzera et al., 2014). Similar results on fruit shape were obtained with Ananas and Galia type melons (Soteriou et al., 2016), and with cantaloupe grafted on hybrid rootstocks (Colla et al., 2006b), notwithstanding a limited increase in rind thickness.

Textural characteristics

Fruit texture is an essential characteristic for the organoleptic assessment of melon fruit and one often reported to deteriorate as a result of grafting (Roush et al., 2010). Grafting honeydew melon onto *Cucurbita* hybrids and *C. melo* rootstocks had no effect on fruit dry matter content and pulp firmness (Crinò et al., 2007). On the contrary, Colla et al. (2006b) found that pulp firmness values recorded for cantaloupe grafted on hybrid rootstock were significantly higher (19–32%) than those observed for non-grafted plants, and the same effect was observed with muskmelon grafted either on *C. melo* or *Cucurbita* hybrid rootstocks (Colla et al., 2010a), despite that grafting resulted in lower pulp dry matter content in both these studies. By contrast, flesh firmness of Galia melon was consistently reduced by grafting on four different hybrid rootstocks and a similar tendency was evidenced with Ananas melon; however, these results were obtained from graft combinations that demonstrated incompatibility problems, variably causing plant decline, with loss of pulp firmness being one of the quality indices proposed for prognostication of incompatibility (Soteriou et al., 2016). Galia melon grafted onto interspecific hybrid rootstocks and onto *C. metuliferus* incurred reduced overall sensory rating but not reduced flesh firmness compared to non-grafted controls (Guan et al., 2015), although the same scion grafted on *C. metuliferus* and grown organically in nematode infested soil incurred a reduction in pulp firmness (Guan et al., 2014).

Grafting interacted with scion cultivar in respect to firmness but a general trend for loss of firmness was identified in two annual field trials involving numerous cultivars of muskmelon, honeydew and specialty melon scions, although assessment of firmness across the various melon types was hampered by the difficulty of harvesting melons of the same maturity (Schultheis et al., 2015). Grafting cantaloupe on two interspecific hybrid rootstocks reduced flesh firmness compared to non-grafted and self-grafted control, with differences minimized after prolonged postharvest storage (Zhao et al., 2011). Finally, no effect on flesh firmness was reported when Piel de Sapo-type melon was grafted on either Monosporascus-resistant *C. melo* subsp. *agrestis* or the widely used but less compatible interspecific hybrid RS841 (Fita et al., 2007). From the findings above it is evident that, unlike the case of grafted watermelon (Kyriacou and Soteriou, 2015; Kyriacou et al., 2016), melon grafting, whether on same or different species rootstocks, unequivocally does not increase flesh firmness; it either has no effect or it results in loss of textural quality, depending largely on rootstock–scion compatibility and to a lesser extent on cultural conditions.

Sweetness and acidity

Fruit sweetness is a major sensory feature of melon quality (Yamaguchi et al., 1977; Liu et al., 2010), which stems mainly from soluble carbohydrates but is commonly quantitated on the basis of the SSC derived from the temperature-compensated refractive index of the fruit juice. Understanding rootstock-mediated effects on melon sweetness is critical for safeguarding sensorial acceptability of melon fruit produced on grafted plants. Available reports describing these effects manifest widespread rootstock–scion interaction attesting the importance of selecting appropriate graft combinations. For instance, grafting cantaloupe (cv. Cyrano) on hybrid ‘P360’ under greenhouse conditions reduced the fruit SSC by an absolute 1.6% when compared to the non-grafted control; however, the SSC (10.9%) remained highly acceptable (Colla et al., 2006b). Similar findings were reported for muskmelon (cv. Proteo) grafted on hybrid rootstock (‘P360’) in open field cultivation, though both grafted (8.3%) and non-grafted (7.5%) plants exhibited quite low fruit SSC (Colla et al., 2010b). However, evaluating the same scion (‘Proteo’) on hybrid rootstocks ‘P360’ and ‘PGM96-05,’ revealed no effect on SSC though grafting both ‘Proteo’ and ‘Supermarket’ muskmelons on *B. hispida* and *C. metuliferus* did reduce their SSC (Trionfetti-Nisini et al., 2002). Crinò et al. (2007) found no effect on the SSC of honeydew melon (cv. Incas) by grafting on four hybrids and four *C. melo* rootstocks, as also verified by Verzera et al. (2014) using the same scion on three hybrids and two *C. melo* rootstocks, but not with hybrid rootstock ‘AS10’ which increased the SSC from 15.5 to 16.3%. Galia melon ‘Arava’ grafted onto hybrids ‘Strong Tosa’ and ‘Carnivor’ incurred reduced overall acceptability, flavor rating and SSC compared to non-grafted controls, but not when grafted onto *C. metuliferus* (Guan et al., 2014, 2015). Moreover, honeydew scion (‘Honey Yellow’) on the same rootstocks did not differ in sensory properties and SSC in comparison with either non-grafted or self-grafted controls (Guan et al., 2014, 2015). The SSC of Piel de Sapo melon was slightly reduced when grafted on

Monosporascus-resistant rootstock *C. melo* subsp. *agrestis* (‘Pat 81’) and also on hybrid ‘RS 841,’ but not to an extent that might significantly affect marketability (Fita et al., 2007). Although decrease in the SSC is not an infrequent response to grafting, with potential implications on, the increment of decrease in none of the reported studies seemed decisive for overall quality and marketability.

Besides the case of hybrid ‘AS10’ above, few are the cases of rootstocks reported of causing increase in melon SSC. One such is the absolute increase of 1.2% obtained in the mean SSC (10.4%) of greenhouse grown Galia melon grafted onto hybrid rootstocks ‘TZ148,’ ‘N101,’ ‘Carnivor,’ and ‘30900’ (Soteriou et al., 2016). Most often, grafting on compatible rootstocks has no effect on the fruit SSC. Out of four hybrid rootstocks onto which Ananas melon was grafted only one (‘30900’) had an effect on the SSC causing an absolute reduction by 1.12% relative to the non-grafted control (Soteriou et al., 2016). Field trials of muskmelon, honeydew and specialty melon types (Persian, Tuscan, Canary, Galia, Piel de Sapo) grafted on hybrid rootstock ‘Carnivor’ vs. self-grafted and non-grafted controls generally showed no effect on the SSC although limited grafting × scion interaction was evident (Schultheis et al., 2015). Traka-Mavrona et al. (2000) also found grafting had no effect on the fruit SSC of three inodorous melon and one cantaloupe cultivars tested on two hybrids and one pumpkin landrace rootstocks under protected and open field cultivation. Finally, in a study closely observing fruit harvest maturity based on the date of fruit setting, Park et al. (2013) reported that grafting both muskmelon (‘Earl’s elite’) and honeydew melon (‘Homerunstar’) onto four *C. melo* accessions and one Shintoza type *Cucurbita* hybrid had no effect on the scions’ fruit SSC, and they repudiated categorically claims of reduced fruit quality as a result of grafting, provided compatible rootstocks.

Further to the effect of grafting on SSC, the concentrations of soluble sugars are also critical as they dictate their relative contribution to the sweetness index (SI) of fruits (Elmstrom and Davis, 1981). According to Liu et al. (2010), accumulation patterns for hexoses, sucrose and oligosaccharides were similar during muskmelon ripening from non-grafted and grafted plants, despite differences in sugar levels between rootstocks. Moreover, during the period of fast sugar accumulation (32–48 days after anthesis) muskmelons from grafted plants maintained higher starch content than the non-grafted control, and the starch fraction was higher in the lower sugar content rootstock and lower in the non-grafted control. It was further postulated that the marked increase in mesocarp starch content may derive from competition by the vigorous rootstocks for the soluble sugars translocated to sink fruit which the rate of sucrose decomposition was unable to satisfy. Differential rootstock-mediated patterns of soluble sugars’ accumulation were depicted in a recent study by Soteriou et al. (2016), wherein total soluble sugars in the pulp of both Galia and Ananas melons were not differentiated between four hybrid rootstocks and the non-grafted control; however, grafting Galia generally increased fruit sucrose levels at the expense of fructose and glucose whereas the opposite was observed with Ananas melon (Soteriou et al., 2016).

Like most cucurbits, melon is a fruit of very low acidity, usually below 0.2% in citrate equivalents, which nevertheless affects the sweet-to-sour balance in sensory perception (Crinò et al., 2007; Colla et al., 2010b; Verzera et al., 2014; Guan et al., 2015). Grafting honeydew melon and cantaloupe on hybrid rootstocks had a minimal effect on fruit TA which was inconsequential to fruit sensory quality (Colla et al., 2006b; Verzera et al., 2014). Similarly, no effect was found on the TA of muskmelon and Galia melon by grafting on either *Cucurbita* hybrid or *C. melo* rootstock (Crinò et al., 2007; Colla et al., 2010b; Zhao et al., 2011; Guan et al., 2015).

Aroma profile

The production of volatile compounds in melon is associated with ethylene-dependent pathways (Obando-Ulloa et al., 2008; Pech et al., 2008) and with textural changes related to cell wall matrix solubilization events (Dos-Santos et al., 2013). Hence, the climacteric (*cantalupensis* and *reticulatus*) and the non-climacteric (*inodorus*) types demonstrate distinct volatile profiles, with C9 aliphatic aldehydes being the key aroma and flavor descriptors for inodorous honeydew melons (Verzera et al., 2014), as opposed to the mainly ester-based (ethyl butanoate, methyl 2-methylbutanoate and ethyl 2-methylpropanoate) descriptors for fruity and sweet aroma notes of *cantalupensis* and *reticulatus* muskmelon cultivars (Kourkoutas et al., 2006; Beaulieu and Lea, 2007). Grafting seems to affect the aroma profile of both muskmelon and honeydew type melons. Grafting muskmelon on interspecific *Cucurbita* hybrids and on *C. melo* rootstocks generally elicited higher levels of non-key alcohol and aldehyde volatile compounds responsible for green and fresh notes, such as flower-green (1-hexanol), fruity (2-methyl-1-butanol), fatty-green (1-octanol), ethereal (ethanol), green [(E)-2-butenal], and fresh-lemon-green (octanal) aromas (Condurso et al., 2012). Ester-based aromas characteristic of muskmelon were generally higher in non-grafted control, such as cantaloupe-like, green fruity, melon (ethyl 2-methylbutanoate) and sweet-fruit (ethyl butanoate) aromas (Chuan-qiang et al., 2011; Condurso et al., 2012). However, significant exceptions to this motif were found among both *Cucurbita* spp. and *C. melo* rootstocks, rendering screening for optimum rootstock-scion combinations essential. In fact, some commercial *Cucurbita* hybrids (e.g., 'RS-841') and *C. melo* (e.g., 'Energia') rootstocks can be successfully used for controlling soilborne pathogens without any significant effect on the fruit aroma (Condurso et al., 2012). Similarly, Verzera et al. (2014) examined the effect of four inter-specific hybrids and two melon genotypes on the fruit aroma and sensory quality of honeydew melon cv. Incas (*C. melo* L. subsp. *melo* var. *inodorus* H. Jacq.). Prevalent volatiles in both grafted and non-grafted *inodorus* melon were mainly aldehydes and alcohols such as nonanal (melon, orange peel), (Z)-6-nonenal and (E)-2-nonenal (honeydew melon fruity), (E,Z)-2,6-nonadienal, 1-nonal (herbaceous), (Z)-3-nonen-1-ol (melon, green, floral) and (Z,Z)-3,6-nonadien-1-ol (pumpkin, cucumber). Fruits from plants grafted on three of the interspecific hybrids (cvs. RS-841, P-360, Polifemo) and one *C. melo* rootstock ('Energia') had similar aroma profiles to the control, however, particular rootstocks from either type (e.g., 'AS10' and 'Sting') were found to decrease the amounts of key aroma compounds.

Grafting was generally found to reduce the intensity of honeydew melon and herbaceous aroma descriptors and increase those related to fruity aroma and flavor. It is important to emphasize that selection is possible of resistant interspecific hybrid rootstocks (e.g., 'RS-841') that increase yield and fruit weight of both honeydew cv. Incas and muskmelon cv. Proteo scions, without having a detrimental effect on sensory characteristics, including the aroma profile (Condurso et al., 2012; Verzera et al., 2014).

Functional compounds

Melon is a rich source of α -, ζ -, and especially β -carotene but also of lutein, cryptoxanthin, phytoene, and the violaxanthin cycle carotenoids, however, little is known on the effect of grafting on these components (Laur and Tian, 2011). The fruit carotenoid profile of odorous melon, was either non-differentiated, or highly improved particularly with regards to the α - and β -carotene components in response to grafting on *C. maxima* \times *C. moschata* hybrid rootstocks vis-à-vis the non-grafted control; whereas grafting on *C. melo* rootstocks resulted in significantly reduced β -carotene levels, which inadvertently emphasized ζ -carotene content, while lutein was increased with grafting on both types of rootstocks (Condurso et al., 2012). Carotenoid content is largely responsible for melon pulp color; hence the effects of grafting on these traits are expectedly associated. Colla et al. (2006b) reported that grafting cantaloupe (cv. Cyrano) on hybrid rootstock 'P360' influenced pulp colourimetric values positively, resulting in brighter (higher L*) and more intense orange hue (higher a*/b* ratio), probably reflecting higher α - and β -carotene concentrations in the pulp (Condurso et al., 2012). Intriguingly, increased levels of both chlorophylls and β -carotene were obtained in the leaves of Galia type cvs. Arava and Resisto grafted on interspecific rootstocks 'Shintoza,' 'Kamel,' and particularly on 'RS841' (Romero et al., 1997).

Cucumber (*Cucumis sativus* L.)

Cucumber constitutes an annual vegetable species mostly grown under protected cultivation. The use of rootstocks resistant or tolerant to soilborne diseases, foliar pathogens, arthropods, and weeds has become instrumental for cucumber production, especially under intensive farming practices with limited crop rotations (Lee et al., 2010; Louws et al., 2010). Several rootstocks (*C. maxima* \times *C. moschata*, *C. ficifolia*, *C. moschata*, *C. argyrosperma*, *L. siceraria*, *B. hispida*, *Luffa cylindrica* (L.) M. Roem., *Momordica charantia* L., *S. angulatus*, *Citrullus* spp.) have been used for cucurbit grafting; most enhance scion growth and productivity under unfavorable soil and environmental conditions, but some lack tolerance to specific stresses and others can have a detrimental effect on vegetable fruit quality (Rouphael et al., 2010, 2012). The most popular rootstocks for cucumbers belong to the genus *Cucurbita*. In particular, the interspecific cross *C. maxima* \times *C. moschata* has been exploited as a favorable source of rootstocks, currently the most common commercial rootstocks for cucumber (Lee et al., 2010). Less frequent is the use of single non-hybrid *Cucurbita* species as rootstocks, such as accessions of *C. argyrosperma*, *C. ficifolia*, *C. maxima*, *C. moschata*, and *C. pepo*. Fruit quality deterioration in grafted

plants, reported chiefly as decrease in sweetness and acidity, is a common problem particularly with *Cucurbita* hybrids which are frequently implicated in scion × rootstock interactions, further compounded by crop management practices (Davis et al., 2008b; Rousphael et al., 2010).

Morphometric characteristics

It is well established that vigorous *Cucurbita* interspecific hybrids can improve cucumber yields significantly (Davis et al., 2008b). More frequently, the effect on yield is related to the variation in fruit size, as grafted plants are characterized by a vigorous root system (high root length and density) able to enhance photosynthetic rate as well as water and nutrient uptake efficiency (particularly N, P, Ca, and Mg) and, consequently, crop productivity (Rousphael et al., 2010). Several authors have demonstrated a significant increase in fruit weight when cucumber plants were grafted onto *Cucurbita* interspecific hybrids ('RS841', 'Strong Tosa', 'PS1313', and 'P360') and *Cucumis pustulatus* Naudin ex Hook.f. compared to non-grafted control (Colla et al., 2012, 2013; Goreta Ban et al., 2014; Liu et al., 2015). However, in some cases increased cucumber yield has been attained mainly by an increase in the number of fruits per plant rather than an increase in mean fruit size (Huang et al., 2009).

Other morphological traits that constitute primary criteria for making purchasing decisions are the fruit shape index and the colouration of the skin (Rousphael et al., 2010). Reports on cucumber grafting demonstrated that the effect of rootstocks on fruit shape has been mostly non-significant or minimal (Lee et al., 1999; Colla et al., 2013). Regarding color, Colla et al. (2012) reported that lightest colouration, expressed as an increase in colourimetric CIELAB component L*, was observed on the skin of cucumber cv. Akito grafted onto the commercial rootstock 'PS1313' (*C. maxima* × *C. moschata*) compared to fruit from plants grown on their own roots.

Textural characteristics

Fruit firmness constitutes also an important physical property influencing consumer acceptability (Rousphael et al., 2010). Hwang et al. (1992) demonstrated that cucumber from plants grafted onto *S. angulatus* 'Andong' rootstock tended to be firmer than those grafted onto figleaf gourd (*C. ficifolia* 'Heukjong'). On the contrary, Morishita (2001) reported that 'Kema' and 'Kifujin New Type' cucumber plants grafted onto the bloomless rootstock 'Big Ben Kitora' carried fruits of softer flesh than those grown on their own roots. Nevertheless, more popular rootstocks such as *C. moschata* or *C. maxima* × *C. moschata* had no effect on fruit firmness when compared to non-grafted plants (Sakata et al., 2007; Colla et al., 2013). The variation in fruit firmness induced by rootstocks may be attributed to several mechanisms such as the uptake and translocation of calcium, modulated water relations and nutritional status, increased synthesis of endogenous hormones as well as variation in cell morphology and turgor (Rousphael et al., 2010).

Sweetness and acidity

It has been reported that changes in grafted vegetable aroma and taste appear to be not only scion but also rootstock-dependent attesting the importance of selecting appropriate graft

combinations (Rousphael et al., 2010). For instance, grafting cucumber onto 'Heukjong' figleaf gourd (*C. ficifolia*) reduced the fruit SSC and fructose concentration when compared to the non-grafted control; whereas the SSC remained high when 'Andong' (*S. angulatus*) was used as rootstock (Lee et al., 1999). Moreover, Huang et al. (2009) observed a lower accumulation of SSC in plants grafted onto figleaf gourd and grown under unstressed conditions compared to self-grafted control. However, under saline conditions of 60 mM NaCl the SSC and TA incurred significant increase in both grafted and self-grafted plants. Similarly, the SSC of 'Akito' cucumber increased when grafted onto the interspecific hybrid 'PS1313', whereas an opposite trend was recorded for the TA (Colla et al., 2013).

Aroma profile

Besides taste, the effect of grafting on aroma was also quantitated in cucumber. In a recent study, Guler et al. (2013) demonstrated that grafting affected the aroma profile of both the peel and flesh of cucumber cv. Cengelköy in response to the use of a bottle gourd rootstock. Thus, grafting caused a substantial increase in the alcohol content [(Z)-6-Nonenol, (E,Z)-2,6-nonadienol, 1-nonanol, and (Z,Z)-3,6-nonadienol], a decrease in the aldehyde content [(E,Z)-2,6-nonadienal] with no significant influence on ketones, terpenes and hydrocarbons in both cucumber peel and flesh tissues. The authors concluded that the bottle gourd '33-41' could be considered a promising rootstock for improving major volatile components identified in cucumber.

Solanaceae

Tomato (*Solanum lycopersicum* L.)

Nowadays tomato production under protected environment is resorting to the use of grafted plants. Reservations against their use relate to their higher price being considered non-affordable by growers, the use of speciality cultivars or particular problems associated with disease outbreaks, such as the novel tobamoviruses (Luria et al., 2017). However, the number of commercial rootstocks offered by breeding companies has burst and their widespread use is becoming highly visible. Not only rootstocks from the species *Solanum lycopersicum* L. are available but also interspecific hybrids, such as *S. lycopersicum* × *Solanum habrochaites* S. Knapp & D.M. Spooner, and rootstocks from other species, such as *Solanum torvum* L. or *Solanum melongena* L. Therefore, growers often follow breeders' recommendation and use same-company scions and rootstocks. Even in the field, the application of grafted plants has started, e.g., as a means to protect the scion from invasive weeds, such as broomrape. Compared to the Cucurbitaceae representatives, the effect of rootstocks on fruit quality traits seems less intense and reports on reduced quality are mainly related to reduced sweetness. The effects of grafting on most tomato quality characteristics have been variable, strongly influenced by the rootstock–scion combination. Moreover, the effect of the grafting combination interacts with other factors, such as climate, cultural practice, duration and intensity of stress, water and nutrient disposability and not to least with the sampling strategy (Riga, 2015; see chapter 'Methodological approaches').

Morphometric characteristics

Grafting tomato often results in significant increase in fruit weight and consequently in fruit diameter and size compared with non- or self-grafted plants (Passam et al., 2005; Moncada et al., 2013; Riga, 2015). This was reported for many different rootstock–scion combinations resulting in total yield increase. However, yield gain may be also attributed to an increase in the number of fruits rather than an increase in mean fruit weight (Savvas et al., 2011). The effect of grafting on fruit weight and size depends on grafting combinations (Khah et al., 2006; Leonardi and Giuffrida, 2006; Schwarz et al., 2013). Larger fruit size seems to be attained when vigorous rootstocks are used, such as ‘Maxifort’ (Krumbein and Schwarz, 2013; Schwarz et al., 2013), ‘Beaufort’ (Romano et al., 2000; Pogonyi et al., 2005; Turhan et al., 2011), ‘Heman’ (*S. habrochaites*), ‘Joint’, ‘P1614,’ and ‘RS1427’ (Romano et al., 2000), or ‘Star Fighter’ (Theodoropoulou et al., 2007). This phenomenon is particularly recognized when scions have smaller fruit sizes, e.g., cherry tomato with less than 40 g (Schwarz et al., 2013). In some cases, grafting may reduce fruit size when less vigorous rootstocks are used, such as ‘Brigeor’ (Schwarz et al., 2013), ‘Energy,’ ‘Firefly,’ ‘Linea9243,’ ‘Nico’ (Romano et al., 2000). Based on the same reasons, fruit size of two different scion cultivars was significantly reduced when a salt tolerant goji berry (*Lycium chinense* Mill.) served as rootstock (Huang et al., 2015).

Fruit shape has seldom been assessed in grafted tomato despite indications of its differentiation once the fruit size is affected (Schwarz et al., 2013). Increase in shape index, measured as the ratio of fruit diameter to maximal height, was reported as corresponding to increase in fruit size (Turhan et al., 2011). However, rootstock ‘Beaufort’ raised the fruit shape index, compared to non-grafted tomato, irrespective of the scion cultivar (‘Yeni Talya,’ ‘Swanson,’ ‘Beril’), while rootstock ‘Arnold’ only increased it in combination with the scion ‘Yeni Talya.’ This indicates a similar dependence of fruit shape to rootstock vigor as already mentioned for the fruit size.

Fruit color was in certain cases affected by grafting (Di Gioia et al., 2010; Brajović et al., 2012) but in others not (Krumbein and Schwarz, 2013; Schwarz et al., 2013). As in the case of watermelon (see chapter ‘Watermelon’), changes pertained particularly to color component a^* (redness) which is associated with lycopene content. Thus, also for tomato, an effect of grafting on color seems to be significant if a rootstock influences the fruit lycopene content (Miskovic et al., 2016). However, color as well as texture assessment, are often presented with the difficulty of obtaining sufficient and uniform fruit samples in terms of development and harvest maturity to constitute a representative sample. Failure to control sampling procedures effectively may lead to misleading or inconsistent results (see also chapter ‘Methodological approaches’).

Physiological defects

Although physiological disorders related to grafted plants have not received much attention in the literature, they are not uncommon. Blossom end-rot (BER), the most typical tomato disorder (Ho and White, 2005), was invariably reduced in tomato grafted on rootstocks ‘Brigeor,’ ‘Maxifort,’ and LA1777

(*S. habrochaites*), and under different environmental conditions shaped by factors such as salinity, potassium nutrition, sub-optimal temperature, and light conditions (Fan et al., 2011; Krumbein and Schwarz, 2013; Schwarz et al., 2013; Ntatsi et al., 2014). Moreover, reduction in BER incidence with grafting was pronounced under stress conditions in comparison to both non- and self-grafted scions. Decrease in BER was mainly related to the rootstock genotype; e.g., the BER incidence in ‘Classy,’ a medium round type tomato of ~70 g, was more diminished when grafted on the rootstock ‘Brigeor’ compared to ‘Maxifort’ or self-grafted plants. The BER reduction was also influenced by rootstock–scion interaction; e.g., it was decreased to a greater extent when cherry tomato ‘Piccolino’ was used as a scion. Under certain conditions, the use of a rootstock may raise the BER incidence. This was the case in an experiment where two cultivation systems were compared during summer: hydroponics vs. soil (Takasu et al., 1996); the improved nutrient and water uptake facilitated by grafting did not cope sufficiently with the very fast fruit growth under high radiation conditions. Also, BER increased in trials involving rootstock ‘Edkawi,’ or eggplant rootstocks (e.g., ‘EG203,’ ‘VFR Takii’) (Oda et al., 1996; Poudel and Lee, 2009; Fan et al., 2011). Here possible reasons are justified by the characteristics of the rootstocks selected. Rootstock ‘Edkawi,’ although known as salinity-tolerant, as well as eggplant rootstocks, lower the uptake and transport of Ca ions into the fruits compared with self-grafted tomato. Results indicate that the incidence of BER is reduced by grafting when Ca uptake and transport into the fruits is improved (Fan et al., 2011; Savvas et al., 2017). Increased fruit Ca concentration may lead to strengthening of cell walls and cellular integrity and improvement of fruit firmness (Dorais, 2007; Schwarz et al., 2013).

Textural characteristics

Attributes of texture are seldom considered in grafted tomato. Cultivar Jack grown under Mediterranean conditions as a scion grafted onto nine rootstocks typified rootstock effects: e.g., ‘Alligator’ tended to reduce, ‘Maxifort’ did not affect and ‘King Kong’ enhanced firmness (Riga, 2015). Other reports corroborate these findings although loss of firmness seems as the predominant effect. Thus, fruits of the cultivars ‘Classy’ and ‘ASVEG10’ obtained from plants grafted onto ‘Brigeor’ or ‘Maxifort’ and grown under potassium deficiency but also fruits from plants grafted on eggplant rootstock were less firm and scored higher maximum deformation than fruits from self-grafted tomato (Poudel and Lee, 2009; Schwarz et al., 2013). The reasons are not clear but K^+/Ca^{2+} interaction was not implicated in the differences in fruit firmness. Independently, it could be clearly demonstrated that fruit Ca content was increased by grafting (Khah et al., 2006; Fan et al., 2011; Savvas et al., 2017). However, as in the case of Khah et al. (2006) it did not affect fruit firmness. While Riga (2015) did not find differences in fruit firmness between non- and self-grafted ‘Jack’ tomato, Rahmatian et al. (2014) found significantly lower firmness in fruits from self-grafted compared to non-grafted ‘Synda’ tomato. However, the use of a rootstock (cv. King Kong) independently of simple or double grafting did not affect firmness.

Sweetness and acidity

Results concerning the variation in taste of grafted tomato fruit, comprising sugars (glucose, fructose), SSC as a non-specific sweetness parameter, and TA are also very contradictory and seem to be affected by the same parameters as mentioned above. In several experiments, the use of a rootstock did not change fruit taste attributes (Matsuzoe et al., 1996; Khah et al., 2006; Savvas et al., 2011; Barrett et al., 2012). However, decrease and increase in the main components of taste were also observed, as explained below, and based on these findings grafting appears not to constitute a reliable tool for improving tomato fruit taste. This conclusion was confirmed by the results of one of the rare consumer sensory tests performed during a 2-year cultivation of the heirloom tomato 'Brandywine' as non-, self-grafted and grafted onto 'Survivor' and 'Multifort.' While in the first year the rootstock 'Survivor' scored significantly lower than the non-grafted 'Brandywine' in appearance, acceptability, and flavor, no differences were observed between these treatments in the second year (Barrett et al., 2012).

The main sugars in mature tomato are glucose and fructose in equal shares and the total sugar concentration ranges from about 20 to 100 g·kg⁻¹ fresh mass, depending on cultivar and growing conditions. Improvement of fruit sweetness related to grafting is rather seldomly reported. Such cases described were with tomato grafted onto 'Fanny,' 'King Kong,' 'LA1777' (*S. habrochaites*), or onto scarlet eggplant rootstocks (e.g., 'EG 203'), whereby the enhanced SSC content was associated with the effect of water deficiency which lowered plant growth and yield and decreased fruit water content (Oda et al., 1996; Fernández-García et al., 2004a,b; Poudel and Lee, 2009; Ntatsi et al., 2014; Rahmatian et al., 2014). The same association occurred when grafted plants grew under saline or drought conditions or when using a drought tolerant cultivar as a rootstock (Flores et al., 2010; Sánchez-Rodríguez et al., 2012a) or when grafting onto a medicinal plant (*L. chinense*; Huang et al., 2015). However, in many grafting combinations, rootstocks reportedly decreased SSC and sugar concentration in the scion fruits (Poganyi et al., 2005; Qaryouti et al., 2007; Turhan et al., 2011; Barrett et al., 2012; Nicoletto et al., 2013a,b; Schwarz et al., 2013; Gajc-Wolska et al., 2015; Kumar et al., 2015; Riga, 2015). Nevertheless, the decline caused by grafting is very low compared to the potential increase procured by employing a selected scion that might at least double the fruit sugar concentration. The decline in sugars incurred with grafting is reported to account for approximately not more than 16% (Riga, 2015), which does not exceed the range of maximum decline proposed for consumer acceptability (Kader, 1999; Maynard et al., 2002). The reasons for a lower carbohydrate content in grafted tomato may stem indirectly through rootstock effect on scion vigor, timing of flowering, fruit load, yield and, ultimately, fruit maturation, as fruit sugar concentration is highly dependent on fruit maturity at harvest (Rouphael et al., 2010; Soteriou and Kyriacou, 2015). In this respect, grafting may be considered a high-input production method, with a prevalent tendency for increasing crop load and potentially suppressing fruit sugar content (Davis et al., 2008b; Soteriou and Kyriacou, 2015). Moreover, vigorous rootstocks may act as additional sinks for

assimilates and thus, reduce assimilate flow to the fruits (Xu et al., 2006; Martínez-Ballesta et al., 2010). Alternatively, water uptake-efficient rootstocks may increase fruit water content even if sufficient assimilates are available, thus, leading to a reduced fruit sugar concentration (Turhan et al., 2011; Krumbein and Schwarz, 2013). Fruits of grafted scions are often larger than fruits of the same non- or self-grafted scion, and though the fruit sugar/acid ratio might remain unaffected, a decline in soluble carbohydrates may be incurred as a dilution effect (Tieman et al., 2017).

While sugars may decrease in grafted tomato, acid content expressed as TA is on the contrary enhanced (Turhan et al., 2011; Sánchez-Rodríguez et al., 2012a; Nicoletto et al., 2013a,b; Schwarz et al., 2013; Krumbein and Schwarz, 2013; Huang et al., 2015; Kumar et al., 2015; Riga et al., 2016). Total organic acids in tomato fruit are usually in the range of 0.2 to 1.7 g·kg⁻¹ fresh mass, with citric and malic acid being the main components of sourness. Grafting accounts for an increase in TA up to 15% reported under a range of different environmental conditions which indicates a direct rootstock effect. Comparing fruits from 'Classy' and 'Piccolino' self-grafted or grafted onto 'Maxifort' and 'Brigeor' resulted under different experimental conditions almost always in the highest TA produced by 'Maxifort' followed by 'Brigeor' and self-grafted. Independent of the presence or absence of water stress, tomato fruits from the drought sensitive cultivar Josefina grafted onto the drought tolerant cv. Zarina had always higher TA contents, particularly citric acid, compared with non-, self-grafted or the reciprocal grafting combination (Sánchez-Rodríguez et al., 2012a).

The mechanisms involved in grafting-elicited increase of fruit TA have not been thoroughly investigated; however, organic acids constitute a direct substrate for respiratory demands and their increased *de novo* synthesis in developing fruits might be a plausible mechanism for coping with the sugar deficit incurred on the heavy crop load supported by vigorous rootstocks. Moreover, the capability of a vigorous root system to enhance the uptake of nutrients, such as K, could be another reason (Ruiz and Romero, 1999; Leonardi and Giuffrida, 2006; Albacete et al., 2009). Potassium is positively related to the acid concentration in tomato fruits, and plays a role in maintaining electroneutrality of acids in the fruit. However, K transport depends not only on the rootstock but also on growing conditions, such as the current K concentration in the root zone, and on climatic factors (Albacete et al., 2009). Interestingly, differences in K concentration were found not to be significant between fruits of self-grafted and grafted plants, but increase in fruit TA was significant (Schwarz et al., 2013). To complicate matters further, an exceptional report demonstrated that when cv. Lemance was grafted onto 'Beaufort,' fruit organic acid concentration was lower compared with fruits from non-grafted plants (Poganyi et al., 2005). Therefore, the enhanced TA in fruits of grafted tomato warrants further investigation (Leonardi and Giuffrida, 2006).

Aroma profile

Odor-active volatiles contribute to tomato flavor (Krumbein and Auerswald, 1998) but their influence on sensory properties

awaits further treatise. Six major volatiles which contribute to tomato flavor were evaluated by a consumer panel in Florida (USA): 2-butylacetate, *cis*-3-hexen-1-ol, 3-methyl-1-butanol, 2-methylbutanal, 1-octen-3-one, *trans,trans*-2,4-decadienal (Tieman et al., 2012; Zhang B. et al., 2016). Krumbein and Schwarz (2013) found that for two different scion cultivars, 'Piccolino' – a cherry, and 'Classy' – a round type, grafting on rootstocks 'Brigeor' and 'Maxifort' induced a general enhancement of three aroma volatiles: methyl salicylate, guaiacol and eugenol, with oily, sweet and spicy odors, respectively; but the concentrations of three other aroma volatiles with almond-like odor (benzaldehyde), violet-like odor (β -ionone) and tomato-like flavor (geranylacetone) were decreased by grafting. The variation of the carotenoid content in tomato (see below) affects the carotenoid-derived volatiles responsible for tomato flavor, such as the violet-like odor (β -ionone) and the tomato-like flavor (geranylacetone) (Krumbein and Schwarz, 2013). However, the actual sensory contribution of these volatiles to changes in tomato flavor was not assessed, which remains critical particularly under the light of the findings of Tieman et al. (2012).

Functional compounds

Carotenoid content of tomato fruit, mainly lycopene and β -carotene, can be influenced by grafting, but it is subject to significant rootstock–scion interaction which indicates that graft combination plays an important role. Moreover, as Riga et al. (2016) demonstrated, the comparison of the grafting combination to either the non-grafted or self-grafted scion is very important. According to several authors, lycopene concentration in tomato fruits tends to decrease with grafting (Helyes et al., 2009; Brajović et al., 2012; Nicoletto et al., 2013b); e.g., most out of 15 rootstocks investigated, including 'Maxifort,' 'Beaufort,' and 'King Kong,' decreased the fruit lycopene concentration of tomato scion 'Jeremy' and 'Jack' (Miskovic et al., 2009; Riga et al., 2016). Similar results have been reported for tomato scion 'Cecilia' grafted onto 'Beaufort' and 'Heman' (Mohammed et al., 2009), for scion 'Macarena' grafted onto 'Maxifort' (Gajc-Wolska et al., 2010), as well as for 'Classy' grafted onto 'Brigeor' (Krumbein and Schwarz, 2013; Schwarz et al., 2013). Though in the latter experiments total carotenoids were diminished due to lycopene decrease, under specific conditions of grafting the lycopene/carotenoid content may increase. When eggplant rootstock 'Madonna' was used, tomato lycopene concentration increased (Miskovic et al., 2016). In another experiment, nutritional stress caused by low potassium in the nutrient solution was applied to 'Classy' grafted onto 'Maxifort' resulting in enhanced β -carotene (Schwarz et al., 2013), as well as in another grafting combination ('Amati' grafted onto 'Robusta' or 'Body') under non-stressed conditions (Brajović et al., 2012). The mechanisms for these opposite responses remain unclear. In other studies, authors did not find any grafting effect on carotenoids (Khah et al., 2006; Vinkovic-Vrcek et al., 2011) of 'Big Red' tomato grafted onto 'Heman' and 'Primavera' (*S. lycopersicum*) under open-field and greenhouse conditions and of 'Tamaris' grafted onto 'Heman,' 'Efiato,' and 'Maxifort' always comparing with fruits from non-grafted cultivars.

Tomato fruit contains significant amounts of ascorbic acid, and several studies showed that fruit content strongly reduced by grafting both in greenhouse and field studies (Fernández-García et al., 2004a,b; Arvanitoyannis et al., 2005; Di Gioia et al., 2010; Vinkovic-Vrcek et al., 2011; Djidonou et al., 2016; Riga et al., 2016). Fruit vitamin C content was reduced in soil cultivation of different tomato scions grafted onto 'Heman,' 'Spirit,' 'Arnold,' 'Beaufort' (Qaryouti et al., 2007; Turhan et al., 2011) and in hydroponics using 'Maxifort,' 'Interpro,' or 'King Kong' rootstocks (Riga et al., 2016). The lower ascorbic acid content could be explained by the higher plant/shoot biomass in grafted plants compared with non-grafted ones or by the fact that grafted plants were initially subjected to stress following the grafting operation. Ascorbic acid is known to control cell differentiation (Arrigoni, 1994) and to promote callus division and growth (Tabata et al., 2001). The decreased total vitamin C content of the fruits from grafted plants could therefore be a resultant of redistribution or accumulation of vitamin C in other parts of grafted plants (Wadano et al., 1999). Alternatively, changes in ascorbic acid content can be influenced by the choice of rootstock, as shown for tomato grafted onto 'King Kong,' 'Beaufort,' or 'Maxifort' rootstocks, which exhibited higher ascorbic acid content compared to the same plants self-grafted or grafted onto 'Arnold' and 'Brigeor' rootstock, respectively (Turhan et al., 2011; Schwarz et al., 2013; Rahmatian et al., 2014). A similar increase in Vitamin C was analyzed when tomato were grafted on *L. chinense* (Huang et al., 2015).

Abundant flavonoids in tomato fruits are the hydroxycinnamic acids and their derivatives (Gómez-Romero et al., 2010; Sánchez-Rodríguez et al., 2012b; Riga et al., 2016), as well as naringenin, chalcone and rutin (quercetin-3-O-rutinoside) (Slimestad et al., 2008; Sánchez-Rodríguez et al., 2012b), which are natural antioxidants. The choice of cultivar (Steward et al., 2000) as well as abiotic and agronomic factors are major contributing factors to the total content of phenolics in tomato (Tomas-Barberan and Espin, 2001). Under water stress the combination with a drought tolerant rootstock (cv. Zarina) resulted in the highest value in total flavonoids, hydroxycinnamic acids and rutin compared with not or self-grafted 'Zarina.' Nicoletto et al. (2013b) found also a higher phenolic acid content for another grafting combination with 'Profitto' grafted onto 'Beaufort' compared with non-grafted plants, but this was not observed with rootstock 'Big Power.' However, Vinkovic-Vrcek et al. (2011) reported that grafting significantly reduced the total phenolic content of tomato cv. Tamaris grafted onto 'Heman,' 'Efiato,' and 'Maxifort,' while no significant differences were found among these rootstocks. Comparing nine different mainly commercial rootstocks, Riga et al. (2016) confirmed that the reduction or increase in flavonoids clearly depends on the selection of the rootstock when the same scion cultivar was used. Thus, relative to tomato from non-grafted 'Jack,' soluble and total phenolics were reduced when grafted onto 'King Kong' but increased when grafted onto 'Brigeor.' The trigger for the rootstock to affect flavonoid concentration remains unclear. Although as indicated by the drought experiment, rootstocks better adapted to stress conditions responsible for

higher flavonoid production may improve total flavonoids in the whole plant (Sánchez-Rodríguez et al., 2012b).

Among other functional compounds, serotonin concentration in fruits was found lower after grafting 'Jack' onto different commercial rootstocks independent of the cultivars selected (Riga et al., 2016).

Eggplant (*Solanum melongena* L.)

Eggplant and its relatives constitute an important source of rootstocks for the production of not only eggplant itself but also of tomato. By far the most common rootstock for eggplant is *S. torvum* (Lee et al., 2010). However, numerous other rootstock species and interspecific hybrids have also been tested as rootstocks for eggplant, including *S. incanum*, *S. incanum* × *S. melongena*, *S. melongena* × *S. aethiopicum*, *S. macrocarpon*, *S. sisymbriifolium*, *S. torvum* × *S. sanitwongsei*, *S. integrifolium* syn., *S. aethiopicum* gr. *Aculeatum* × *S. melongena*, *S. lycopersicum*, *S. lycopersicum* × *S. lycopersicum*, *S. habrochaites*, *S. lycopersicum* × *S. habrochaites* and *S. melongena* (Lee et al., 2010; Gisbert et al., 2011a,b; Khah, 2011; Moncada et al., 2013; Marsic et al., 2014; Sabatino et al., 2016). Current reports on the changes conferred by grafting on eggplant fruit quality provide conflicting information. This could be attributed in part to the environment in which experiments were ran (greenhouse vs. open-field), possible rootstock–scion interaction underscoring graft combinations, and differences stemming from failure to standardize fruit harvest maturity (Rouphael et al., 2010; Kyriacou et al., 2016).

Morphometric characteristics

Based on recent studies, the effect of grafting on eggplant mean fruit weight tends to be non-significant, compared to non- and self-grafted plants. For instance, when cultivar Black Beauty was cultivated non-grafted, self-grafted or grafted onto *S. torvum*, *S. incanum* × *S. melongena* and *S. melongena* × *S. aethiopicum* similar mean fruit weights were observed (Gisbert et al., 2011b). Similar findings were also recorded when *S. melongena* landraces 'Bianca,' 'Sciaccia,' 'Marsala,' and 'Sicilia' were grafted onto *S. torvum* under open field conditions (Sabatino et al., 2016). Khah (2011) also confirmed these results when eggplant cv. Rima was cultivated non-grafted, self-grafted, or grafted onto two hybrid tomato rootstocks, 'Heman' and 'Primavera' under both greenhouse and open-field conditions. Exceptional increase (29%) in fruit weight was reported for eggplant 'Black Bell' when grafted onto *S. torvum* and grown in a soilless system (Cassaniti et al., 2011).

Eggplant fruit shape is highly heritable and subject to strong genetic control (Gisbert et al., 2011b). Several studies revealed that the effect of grafting on shape index has been circumstantial and mostly non-significant or minimal (4%) when the following rootstocks were used: *S. incanum*, *S. incanum* × *S. melongena* and *S. torvum* (Cassaniti et al., 2011; Gisbert et al., 2011a,b). Information on fruit physical properties of grafted eggplants, such as peel color, is conflicting but generally considered as having a negative effect (Moncada et al., 2013). For instance, the calyx of 'Brigah' fruits from non-grafted plants exhibited higher values of lightness (L*) and more vivid color saturation

(chroma) in comparison to those from plants grafted onto *S. torvum*; however, in other similar works such differences between fruits of grafted and non-grafted plants were not observed (Cassaniti et al., 2011; Gisbert et al., 2011b). The most likely source of this disparity could be the difficulty of standardizing sampling practices based on optimal harvest maturity for eggplant.

Textural characteristics

Negative effects on eggplant fruit textural properties amounting to loss of firmness were reported when the *S. melongena* cultivars Black Bell and Tsakoniki were grafted onto *S. torvum* and *S. sisymbriifolium* rootstocks, respectively (Arvanitoyannis et al., 2005; Cassaniti et al., 2011). The greater fruit external and pulp internal firmness of non-grafted plants observed by Arvanitoyannis et al. (2005) could be attributed to the fact that the pest and disease pressures were more pronounced in this treatment. Therefore, it is likely that restriction of water uptake efficiency in non-grafted plants resulted fruits with lower water content and tougher texture.

Sweetness and acidity

Information on taste compounds of eggplant fruits in relation to grafting remains conflicting and conclusive trends may be difficult to deduce currently, however, the reporting of positive effects is the one mostly absent. For example, according to Lee et al. (2010) *S. torvum* rootstock had no effect on eggplant fruit sugar content. Moreover, only non-significant differences in the SSC, in TA, and in juice pH were recorded among fruits from non-grafted, self-grafted and plants grafted onto *S. habrochaites* and *S. lycopersicum* rootstocks (Khah, 2011). In line with the previous work, Arvanitoyannis et al. (2005) observed that grafted plants yielded less sweet fruits with lower ratings of sensory acceptability than non-grafted plants. The reduced fruit sugar concentration in the fruits of grafted plants may be attributed to several mechanisms, including (i) the reduction of assimilate flow to the reproductive organs since vigorous rootstocks may act as additional sinks for assimilates, and (ii) the increased water uptake by rootstocks which could reduce fruit dry matter content and consequently sugar content (Martínez-Ballesta et al., 2010; Rouphael et al., 2010).

Functional compounds

Eggplant is among the most important vegetables in terms of oxygen radicals scavenging capacity, which is a quality trait associated with its high content of phenolic antioxidants (Cao et al., 1996). Gisbert et al. (2011b) observed a higher total phenolic content only in fruits of eggplant 'Cristal' grafted onto *S. macrocarpon* rootstock. Furthermore, Sabatino et al. (2016) showed that grafting eggplant onto *S. torvum* increased total polyphenol fruit content in three out of four Sicilian landraces grown under open-field conditions, whereas an opposite trend was observed by Moncada et al. (2013), wherein the total phenolic content was greater in the non-grafted plants. Moreover, changes in fruit phenolic contents and other important flavonoids, notably anthocyanins, can be highly influenced by the rootstock–scion combination which is often subject to significant

interaction (Marsic et al., 2014). However, the latter study also highlighted the importance of environmental parameters such as solar radiation in the same respect, as fruits from the same landrace/rootstock combination behaved differently in two growing seasons, with the first season being characterized by lower solar radiation compared to second. The higher vigor of grafted plants may have a negative effect on the concentration of anthocyanins, therefore grafted plants should be properly pruned under low solar conditions to improve light interception since the accumulation of anthocyanins in eggplant fruit epidermis is strongly dependent on light exposure (Awad et al., 2001).

Pepper (*Capsicum annuum* L.)

Pepper is currently the least grafted among the solanaceous crops, especially compared to tomato and eggplant, presumably because the commercial rootstocks currently available provide modest benefits (Lee et al., 2010). Accordingly, an urgent need exists for developing new rootstocks that can augment efforts to meet growing demands for fresh sweet pepper. The most popular rootstocks currently used are intraspecific hybrids or cultivars of *C. annuum*, however, accessions of the cultivated *Capsicum* species, including *C. baccatum* L., *C. chacoense* Hunz., *C. chinense* Jacq., and *C. frutescens* L. and their interspecific hybrids *C. annuum* × *C. chinense*, have also been tested as rootstocks for pepper (Lee et al., 2010). As might be expected, the main reason for grafting pepper has been the resistance to soilborne pathogens and nematodes but also to abiotic stresses (Schwarz et al., 2010; Penella et al., 2016), and very limited work has yet been conducted to address the implications of grafting for pepper fruit quality.

Morphometric characteristics

Several reports in the scientific literature indicated strong rootstock specificity in the responses of pepper to grafting (Rouphael et al., 2010). For instance, Doñas-Uclés et al. (2014) demonstrated an increase in fruit weight when cv. Palermo was grafted onto the *C. annuum* rootstock 'Tesor,' whereas the use of rootstocks 'Oscos' and 'AR40' incurred a minimal increase in fruit weight. Similarly, Leal-Fernández et al. (2013) showed that the mean fruit weight was higher when sweet pepper 'Triple star' was grafted onto chili pepper rootstock 'AR96029,' in comparison to non-grafted plants. In the case of F1 hybrids 'Edo' and 'Lux,' fruit weight was not influenced by grafting onto *C. annuum* rootstocks of the cultivars Snooker, Tresor, RX360, DRO8801, and 97.9001 (Colla et al., 2008). By contrast Gisbert et al. (2010) identified a general trend for reduction of fruit weight in greenhouse trials of grafted pepper (cvs. Almuden and Coyote), based, however, only on two hybrid rootstocks, 'Charlot' and 'Foc.' Decrease in fruit weight against non-grafted control is usually an indicator of rootstock–scion incompatibility.

Moreover, absence of defects in particular blossom end rot (BER) is another important quality consideration for peppers. This physiological disorder of the pepper fruit could be ascribed to a local shortage of Ca and is manifested as a leathery brown patch at the blossom-end of the fruit. However, to date there is no information in the international literature on whether the incidence of BER is reduced by grafting. The incidence of

BER in grafted pepper plants could be influenced positively by rootstocks able to improve uptake and translocation of Ca to the fruits, thus strengthening cell walls and cellular integrity, or could be exacerbated by vigorous rootstocks of high nitrogen-uptake efficiency that may encourage fast growth whose demands in calcium might be difficult to meet. Therefore, research in this field is currently a prime necessity.

Sweetness and acidity

The SSC and TA of pepper fruit is in general not highly compromised by grafting on most commercial *C. annuum* rootstocks (Colla et al., 2008; López-Marín et al., 2013). In the former, two studies neither SSC nor TA were affected when pepper plants, cultivated under greenhouse conditions, were grafted onto the following *Capsicum* rootstocks: 'Snooker,' 'Tresor,' 'RX360,' 'DRO8801,' '97.90001,' 'Atlante,' 'Creonte,' and 'Terrano' (Colla et al., 2008; López-Marín et al., 2013). Contrarily, positive effects were observed in the TA and SSC of 'Herminio' grafted onto 'Atlante' under both full and deficit irrigation conditions (López-Marín et al., 2017). The contradictory results pertaining to these taste compounds could relate to differential environments and cultural practices, as well as to possible rootstock–scion interaction.

Functional compounds

Pepper fruit carotenoid content, in particular lycopene and β-carotene which is a precursor of vitamin A, can be affected by grafting and is strongly dependent on the choice of rootstock. For instance, red cultivar Fascinato and yellow cultivar Jeanette when grafted onto the rootstock 'Terrano' incurred increase in fruit antioxidant capacity and β-carotene content, but not in lycopene content (Chávez-Mendoza et al., 2013). Polyphenols, which constitute a large family of secondary metabolites that act as major antioxidants in the neutralization of free radicals, are abundant in pepper (Colla et al., 2013). Two studies conducted by Spanish researchers showed that grafting effects on the levels of total phenolics in pepper were non-significant (Chávez-Mendoza et al., 2013; López-Marín et al., 2013; Sánchez-Torres et al., 2016).

Pepper fruit contains significant amounts of ascorbic acid, however, currently available studies have presented conflicting results concerning the variation in vitamin C content in response to grafting (Gisbert et al., 2010; Chávez-Mendoza et al., 2013; López-Marín et al., 2013; Sánchez-Torres et al., 2016). For example, Chávez-Mendoza et al. (2013) observed a significant enhancement of ascorbic acid in grafted pepper plants; but the same effect was not confirmed by López-Marín et al. (2013). The former authors concluded that variation in vitamin C depends on both scion–rootstock combinations and growing conditions, such as plant shading. Nevertheless, other authors reported that grafting had no effect on pepper content in ascorbic acid, such as Gisbert et al. (2010) and Sánchez-Torres et al. (2016) who found no differences when two commercial pepper hybrid cultivars (Almuden and Coyote) were grafted onto two rootstocks ('Foc' and 'Charlot'). In light of the above studies, it might be inferred that high genotypic dependence of this quality trait in pepper scions likely confounds more limited rootstock effects.

METHODOLOGICAL APPROACHES AND POSTULATES IN ASSESSING GRAFTING EFFECTS

Homeografting vs. Heterografting

In attempting to discern the effects of various rootstocks on the fruit quality of annual crops, an implicit postulate is whether the observed responses stem not entirely from the rootstock but partly from the grafting process itself. In a number of studies, focused mainly on melon, this postulate has been addressed by using homeografts, i.e., self-grafted controls, apart from non-grafted controls. In a study assessing melon transplant growth for 10 days in a hydroponic system, Aloni et al. (2011) found that self-grafting reduced salinity-induced oxidative stress and improved the growth of homeografts compared to both non-grafted control and heterografts on interspecific hybrid TZ148; spanning, however, only a brief vegetative period this could be considered a transient post-transplanting effect. At 30 days after planting, Edelstein et al. (2011) found no difference in shoot and root dry weights between self-grafted and non-grafted treatments of either Galia melon or pumpkin. Additionally, Galia homeografts yielded no differences against non-grafted control in instrumental measurements of quality (SSC and firmness) but only sporadic differences in sensory evaluation, whereas in the case of honeydew melon self-grafting and non-grafting showed no differences in any respect of quality (Guan et al., 2014, 2015); moreover, differences in yield parameters of either scion type were not identified, as was also the case with a wide range of homeografts and non-grafted melon cultivars tested by Schultheis et al. (2015). Notwithstanding the above findings, it cannot be precluded that the grafting process in itself affects plant physiological responses to the growth environment; for instance, improved growth of homeografted melon under salinity stress (Orsini et al., 2013), and improved water relations and xylem water transport efficiency (Agele and Cohen, 2009). Nevertheless, the potential effects of homegrafting seem to pertain chiefly to the early vegetative stages of grafted transplants, as there is no convincing evidence of a lasting effect expressed at the reproductive stage on the quality characteristics of the fruit, which are unequivocally rootstock-mediated. Further to the numerous reports on rootstock mediation of fruit quality discussed in the context of the current review, the effect of heterografting was recently highlighted by high throughput sequencing which revealed that 787 and 3485 genes, associated with primary and secondary metabolism, hormone signaling, transcription factor regulation, transport, and responses to stimuli, were differentially expressed in watermelon when grafted onto bottle gourd and squash rootstocks, respectively, as opposed to self-grafted watermelon (Liu et al., 2016).

Confounding Harvest Maturity with Rootstock Effects on Quality

Quality is configured in the course of post-anthesis ontogeny and ripening, hence harvesting at optimum maturity is particularly critical for non-climacteric annual fruits (e.g., watermelon, honeydew melon, cucumber, eggplant, and bell pepper), the

quality of which is configured while on the plant and steadily deteriorates postharvest at a temperature-dependent rate; whereas the quality of climacteric fruits (e.g., muskmelon and tomato), provided they are harvested physiologically mature, will improve postharvest with the onset of the climacteric and ethylene-induced changes in physicochemical composition (Kader, 1999, 2008). Harvest maturity is a major parameter of quality configuration in annual fruit crops which owed to be standardized before sound conclusions can be drawn on the effects of grafting thereon. Most studies reporting rootstock-mediated effects on fruit quality have relied on an implicit assumption of synchronous ripening behavior in grafted and non-grafted plants, and either did not explicitly monitor harvest maturity or have implicitly relied on crop-specific empirical maturity indices, such as skin color development, formation of abscission layer, or axillary tendril wilting and ground spot formation, which may provide only limited standardization of maturity (Reid, 2002); however, satisfactory standardization must rely principally on the age of the fruit monitored in days post-anthesis (Kyriacou et al., 1996, 2016). The simultaneous harvest of grafted and non-grafted plants is inherently problematic as it overlooks the potential effect of grafting on fruit ripening behavior and may yield misleading results regarding rootstock effects on quality (Davis et al., 2008a). This may partly explain contradictory reports on rootstock-mediated effects on quality and widespread rootstock-scion interaction. The significant effect of vigorous commercial rootstocks, especially of interspecific hybrids, on the yield characteristics of grafted plants indicates that grafting may mediate source-sink relations in the course of ripening. Recent work has demonstrated that grafting watermelon on vigorous rootstocks can increase crop load and retard ripening events responsible for physicochemical changes in fruit composition (Soteriou et al., 2014; Kyriacou et al., 2016). In this case, the apparent effect of grafting on key quality traits, such as the concentration of non-structural carbohydrates and the SSC, was found insignificant and differences between grafted and non-grafted treatments were sourced to the interaction of grafting with maturity due to asynchronous ripening. The synthesis of key pigments responsible for fruit color development, such as lycopene, is also highly dependent on the stage of maturity. Monitoring pigment levels and colourimetric values during the course of fruit ripening has revealed significant grafting × maturity interaction which, in the absence of standardized sampling, might be taken as mere grafting effect (Soteriou et al., 2014). Further complications in interpreting grafting effects might be compiled by recurrent harvests from the same plants and from non-discriminate data analysis on fruits sampled from different orders of fruit clusters.

BIOLOGICAL MECHANISMS AFFECTING QUALITY IN GRAFTED ANNUAL FRUIT CROPS

The interactions between rootstock and scion are highly complex, but increasing investigations in this field have recently shed considerable light on the biological mechanisms involved

(Goldschmidt, 2014; Wang et al., 2016). It is widely accepted that metabolic substances could be transferred from one grafting partner to the other, including signaling molecules that may cause large biological effects. Hormonal signaling is implicated in graft union formation, rootstock–scion communication, growth, yield, and potentially flowering and fruit quality (Aloni et al., 2010). Specific studies have documented that grafting also enables long-distance movement of RNA through the phloem (Lucas et al., 2001), the functional importance of which, however, needs to be determined individually. For example, long-distance movement of mutant mRNA from the rootstock to the wild-type tomato scions caused obvious change in leaf morphology, suggesting that translocated RNAs were functional (Kim et al., 2001). Many other phloem-mobile mRNAs have been identified (Harada, 2010), and recent work with grafted grapevines suggests that genomic-scale mRNA exchange across graft junctions is widespread in grafted fruit and vegetable species (Yang et al., 2015). From the different mRNA patterns, it might be concluded that the profile of mobile mRNAs has specific genotype- and environment-dependent characteristics able to modulate plant performance (Yang et al., 2015). But what determines that an mRNA is selected for long-distance movement? Current knowledge is increasing regarding RNA motifs that trigger mobility, the extent of mRNA transport, and the potential for post-transport translation of mRNAs into functional proteins. Long-distance transport of gibberellic acid insensitive-RNA via the phloem altered leaf morphology and raised the question whether RNA delivery may be regulated by sequence motifs conserved between plant families (Haywood et al., 2005). Further studies indicated that coding sequences, 3' untranslated regions, and also the structure of the RNA might be factors to target for RNA long-distance movement (Huang and Yu, 2009). A recent study exploring the motifs triggering mobility of mRNA demonstrated that tRNA-derived sequences with specific structures are sufficient to mediate mRNA transport and seem necessary for the mobility of a large number of endogenous transcripts that can move through graft junctions (Zhang W.N. et al., 2016). However, it must be considered that the great number of mobile mRNAs identified by combining interspecific grafting with high throughput RNA sequencing, indicate that a postulated tissue-specific gene expression profile might not be predictive for the actual plant body part in which a transcript exerts its function (Thieme et al., 2015).

Furthermore, it also has to be taken into account that grafting itself induces differential gene expression. For example, transcriptomic analysis of grapevine scions demonstrated extensive transcriptional re-programming after heterografting onto two different genotypes (Cookson and Ollat, 2013). While the choice of rootstock genotype had little effect on gene expression in the shoot apex, it was concluded that homegrafting and heterografting was the major factor regulating gene expression (Cookson and Ollat, 2013). Besides, heterografting with non-self rootstocks induced genes involved in stress responses at the graft interface when compared with homegrafted controls (Cookson et al., 2014). Genome-wide investigation using high-throughput sequencing and comparative analysis of grafting-responsive mRNA in watermelon grafted onto bottle gourd and squash

rootstocks identified genes associated with primary and secondary metabolism, hormone signaling, transcription factors, transporters, and response to stimuli, which provide an excellent resource to further elucidate the molecular mechanisms underlying grafting-induced physiological processes (Liu et al., 2016). In addition to protein-encoding mRNAs, various non-coding small RNAs have been shown to move long distances via phloem sap in grafts. Some specifically accumulate in response to nutrient deprivation (Buhtz et al., 2010) with potential signaling role in long distance regulation of gene expression (Pant et al., 2008). Furthermore, it was reported that transgene derived small RNAs from endogenous inverted repeat loci are mobile through the graft union with direct epigenetic modification in recipient cells (Molnar et al., 2010). However, it also has to be considered that grafting itself induces differential expression of microRNAs, as aptly demonstrated by high-throughput sequencing in watermelon grafted onto different rootstocks (Liu et al., 2013). This leads to the suggestion that microRNAs playing an important role in diverse biological and metabolic processes might regulate plant development and adaptation to stress by grafting-induced alterations (Liu et al., 2013).

Despite the mobility of RNA, the transport of various macromolecules through the phloem has received increasing interest following the discovery that FLOWERING LOCUS T protein moves from leaves to the shoot apical meristem where it induces flowering (Corbesier et al., 2007). Paultre et al. (2016) further addressed movement of proteins through the phloem and showed that many proteins in companion cells can get swept away by the translocation stream without resembling a specific protein signal (Paultre et al., 2016). These data reveal that proteins are lost constitutively to the translocation stream, making the identification of unique systemic phloem signals a difficult challenge for the future. However, movement of proteins across graft unions is not restricted to the phloem path as it was demonstrated in transgrafting pathogen resistant, genetically engineered rootstocks with wild type scions. Rootstocks expressing transgenic polygalacturonase inhibiting protein (PGIP) as components of the defense against invasion with pathogens, onto which non-expressing scions were grafted, do not export the respective encoding nucleic acid rather than the PGIP protein itself via the xylem system (Aguero et al., 2005). Furthermore, the PGIP protein in the wild-type scion tissue grafted onto PGIP-expressing genetically engineered rootstocks reduced pathogen damage in scion tissues (Haroldsen et al., 2012). Thus, defense factors in roots can be made available to scions via grafting, improving the vigor, quality, and pathogen resistance of the food-producing scion and its crop (Guan et al., 2012).

It has long been questioned whether grafting might stimulate heritable changes in the scion. Studies have documented that grafting enables the exchanges of DNA molecules between the grafting partners, thus providing a molecular basis for grafting-induced genetic variation (Stegemann and Bock, 2009). By grafting sexually incompatible species, it was further shown that complete chloroplast genomes can travel across the graft junction from one species into another (Stegemann et al., 2012). Additionally, it has been demonstrated that upon grafting entire

nuclear genomes can be transferred between plant cells (Fuentes et al., 2014). Although these alterations are localized to the contact zone between scion and rootstock it indicates that the changes may become heritable via lateral shoot formation from the graft site. Hence, it demonstrates that large DNA pieces or entire plastid genomes can travel into the scion as a prerequisite of graft hybridization (Liu et al., 2010). Heritable changes in the scion might also be the result of epigenetic effects associated with grafting. Wu and co-workers demonstrated that in solanaceous plants heterografting causes extensive alteration of DNA methylation patterns in a locus-specific manner, especially in the scions (Wu et al., 2013). They further detected that altered methylation patterns could be inherited to sexual progenies with some sites showing additional alterations or revisions. Such putatively heritable changes in the DNA methylation pattern of solanaceous scion genomes were extended to the Cucurbitaceae. Using methylation-sensitive amplified polymorphism markers, global DNA methylation changes in scions of cucumber, melon and watermelon heterografted onto pumpkin rootstocks were observed (Avramidou et al., 2015). The differential epigenetic marking in different rootstock-scion combinations will enable the development of epi-molecular markers for generation and selection of superior quality grafted vegetables in the future (Avramidou et al., 2015).

CONCLUDING REMARKS AND THE CHALLENGES AHEAD

Regarded primarily as a phytoprotective measure and as a means to alleviate abiotic plant stress, the grafting of annual fruit crops carries significant, crop-specific implications for fruit quality and nutritive value. The positive effects of vigorous interspecific rootstocks on scion performance are often reflected on fruit size, particularly in crops such as watermelon, cucumber, and tomato, whereas fruit shape constitutes a trait predominantly governed by the scion genotype. Similarly, grafting effect on exocarp and mesocarp thickness is limited and inferior to that of the scion genotype, moreover it interacts with fruit maturity. Variation in the epidermal and pulp colouration of annual fruits, determined by changes in pigment concentrations, can be influenced by grafting directly and indirectly through its interaction with fruit ripening behavior; such an interaction is common for watermelon while colouration effects on tomato, melon and pepper appear strongly rootstock-specific.

Fruit texture can be highly affected by grafting as manifested most consistently in the case of watermelon grafted on interspecific cucurbit rootstocks which generally increase pulp firmness; whereas loss of firmness in melon can reflect latent rootstock-scion incompatibility. Arguably the most important sensorial attribute is fruit sweetness, elicited by soluble carbohydrates whose concentration is liable to the effects of grafting. Rootstock-mediated changes in sweetness may also encompass changes in melon starch content and in the relative proportions of hexoses to sucrose. Decrease in sugars is not an infrequent response to grafting, but the increments of reported

decrease are in general not highly critical for overall quality and marketability. Nevertheless, additional work is warranted across fruit crops to elucidate widespread rootstock-scion interactions regarding sugar content. While advances have been made with regards to grafting effects on fruit aroma profile and the levels of secondary bioactive phytochemicals, these areas remain largely uncharted, underscored by conflicting reports and warranting further research before grafting may constitute a reliable tool for improving fruit sensorial and nutritional quality.

Disparate results on critical quality attributes such as sugar content and aroma profile often reflect a wider effect of grafting on flowering behavior and post-anthesis ripening events partly mediated by changes in crop load. Further complications can be compounded by sampling practices such as recurrent harvests from the same plants and non-standardization of harvest maturity. From a physiological standpoint, the grafting process in itself may modulate plant responses to the growth environment, but these effects of homeografting appear concerted mainly in the early vegetative stages following graft union formation; unlike heterografting whose effects may pervade the reproductive stage configuring fruit quality characteristics. Hormonal signaling, however, is implicated in graft union formation, rootstock-scion communication, growth, yield, and potentially flowering and fruit quality. Moreover, the long-distance phloem transport of genomic-scale mRNA across graft unions is widespread in grafted fruit and vegetable species. Yet, additional knowledge is required on RNA motifs that trigger mobility, the extent of mRNA transport, and the potential for its post-transport translation into functional and tissue-specific proteins. The identification of systemic phloem signals, including noncoding microRNAs and proteins with diverse roles in post-grafting biological and metabolic processes, will prove valuable in understanding grafting effects on fruit quality. Ultimately, the identification of inheritable locus-specific alterations in scion DNA methylation patterns may enable the development of epi-molecular markers for generation and selection of superior quality grafted vegetables in the future.

AUTHOR CONTRIBUTIONS

The review invitation was addressed to DS. Authors' contributed as follows: Introduction and conclusion – all authors; Watermelon and melon – MK; Cucumber, eggplant, and pepper – YR and GC; Tomato – DS; Methodological approaches and postulates – MK; and Biological mechanisms affecting quality – RZ.

FUNDING

The work of DS was supported by the German Federal Ministry of Food, Agriculture and Consumer Protection, the Brandenburg State Ministry of Infrastructure and Agriculture and the Thuringia State Ministry for Agriculture, Nature and Environment Protection.

REFERENCES

- Agele, S., and Cohen, S. (2009). Effect of genotype and graft type on the hydraulic characteristics and water relations of grafted melon. *J. Plant Interact.* 4, 59–66. doi: 10.1080/17429140802311671
- Aguero, C. B., Uratsu, S. L., Greve, C., Powell, A. L. T., Labavitch, J. M., Meredith, C. P., et al. (2005). Evaluation of tolerance to Pierce's disease and *Botrytis* in transgenic plants of *Vitis vinifera* L. expressing the pear PGIP gene. *Mol. Plant Pathol.* 6, 43–51. doi: 10.1111/j.1364-3703.2004.00262.x
- Akashi, K., Miyake, C., and Yokota, A. (2001). Citrulline, a novel compatible solute in drought-tolerant wild watermelon leaves, is an efficient hydroxyl radical scavenger. *FEBS Lett.* 508, 438–442. doi: 10.1016/s0014-5793(01)03123-4
- Alan, O., Ozdemir, N., and Gunen, Y. (2007). Effect of grafting on watermelon plant growth, yield and quality. *J. Agron.* 6, 362–365. doi: 10.3923/ja.2007.362.365
- Albacete, A., Martínez-Andújar, C., Ghanem, M. E., Acosta, M., Sánchez-Bravo, J., Asins, M. J., et al. (2009). Rootstock-mediated changes in xylem ionic and hormonal status are correlated with delayed leaf senescence, and increased leaf area and crop productivity in salinized tomato. *Plant Cell Environ.* 32, 928–938. doi: 10.1111/j.1365-3040.2009.01973.x
- Alexopoulos, A. A., Kondylis, A., and Passam, H. C. (2007). Fruit yield and quality of watermelon in relation to grafting. *J. Food Agric. Environ.* 5, 178–179.
- Allwood, J. W., Cheung, W., Xu, Y., Mumm, R., De Vos, R. C. H., Deborde, C., et al. (2014). Metabolomics in melon: a new opportunity for aroma analysis. *Phytochemistry* 99, 61–72. doi: 10.1016/j.phytochem.2013.12.010
- Aloni, B., Cohen, R., Karni, L., Aktas, H., and Edelstein, M. (2010). Hormonal signaling in rootstock-scion interactions. *Sci. Hortic.* 127, 119–126. doi: 10.1016/j.scientia.2010.09.003
- Aloni, B., Karni, L., Deventurero, G., Cohen, R., Katzir, N., Edelstein, M., et al. (2011). The use of plant grafting and plant growth regulators for enhancing abiotic stress tolerance in vegetable transplants. *Acta Hortic.* 898, 255–264. doi: 10.17660/actahortic.2011.898.31
- Arrigoni, O. (1994). Ascorbate system in plant development. *J. Bioenerg. Biomemb.* 26, 407–419. doi: 10.1007/bf00762782
- Arvanitoyannis, I. S., Khah, E. M., Christakou, E. C., and Bletsos, F. A. (2005). Effect of grafting and modified atmosphere packaging on eggplant quality parameters during storage. *Intern. J. Food Sci. Techn.* 40, 311–322. doi: 10.1111/j.1365-2621.2004.00919.x
- Avramidou, E., Kapazoglou, A., Aravanopoulos, F. A., Xanthopoulou, A., Ganopoulos, I., Tsaballa, A., et al. (2015). Global DNA methylation changes in Cucurbitaceae inter-species grafting. *Crop Breed. Appl. Biotechnol.* 15, 112–116. doi: 10.1590/1984-70332015v15n2n20
- Awad, M. A., de Jager, A., van der Plas, L. H. W., and van der Krol, A. R. (2001). Flavonoid and chlorogenic acid changes in skin 'Elstar' and 'Jonagold' apples during development and ripening. *Sci. Hortic.* 90, 69–83. doi: 10.1016/s0304-4238(00)00255-7
- Bai, Y., and Lindhout, P. (2007). Domestication and breeding of tomatoes: what have we gained and what can we gain in the future? *Ann. Bot.* 100, 1085–1094. doi: 10.1093/aob/mcm150
- Barrett, C. E., Zhao, X., Sims, C. A., Brecht, J. K., Dreyer, E. Q., and Gao, Z. F. (2012). Fruit Composition and sensory attributes of organic Heirloom tomatoes as affected by grafting. *HortTechnology* 22, 804–809.
- Beaulieu, J. C., and Lea, J. M. (2006). Characterization and semiquantitative analysis of volatiles in seedless watermelon varieties using solid-phase microextraction. *J. Agric. Food Chem.* 54, 7789–7793. doi: 10.1021/jf060663l
- Beaulieu, J. C., and Lea, J. M. (2007). Quality changes in cantaloupe during growth, maturation, and in stored fresh-cut cubes prepared from fruit harvested at various maturities. *J. Am. Soc. Hortic. Sci.* 132, 720–728.
- Borgognone, D., Colla, G., Rousphael, Y., Cardarelli, M., Rea, E., and Schwarz, D. (2013). Effect of nitrogen form and nutrient solution pH on growth and mineral composition of self-grafted and grafted tomatoes. *Sci. Hortic.* 149, 61–69. doi: 10.1016/j.scientia.2012.02.012
- Brajović, B., Kastelic, D., Šircelj, H., and Maršić, N. K. (2012). The effect of scion/rootstock combination and ripening stage on the composition of carotenoids and some carpometric characteristics of tomato fruit. *Eur. J. Hortic. Sci.* 77, 261–271. doi: 10.1093/jxb/erf059
- Bramley, P. M. (2002). Regulation of carotenoids formation during tomato fruit ripening and development. *J. Exper. Bot.* 53, 2107–2113. doi: 10.1093/jxb/erf059
- Brown, A. C., and Summers, W. L. (1985). Carbohydrate accumulation and color development in watermelon. *J. Am. Soc. Hortic. Sci.* 110, 683–687. doi: 10.2174/1874256400903010015
- Bruton, B. D., Fish, W. W., Roberts, W., and Popham, T. W. (2009). The influence of rootstock selection on fruit quality attributes of watermelon. *Open Food Sci. J.* 3, 15–34. doi: 10.2174/1874256400903010015
- Buhtz, A., Pieritz, J., Springer, F., and Kehr, J. (2010). Phloem small RNAs, nutrient stress responses, and systemic mobility. *BMC Plant Biol.* 10:64. doi: 10.1186/1471-2229-10-64
- Çandır, E., Yetişir, H., Karaca, F., and Üstün, D. (2013). Phytochemical characteristics of grafted watermelon on different bottle gourds (*Lagenaria siceraria*) collected from the Mediterranean region of Turkey. *Turkish J. Agric. For.* 37, 443–456. doi: 10.3909/tar-1207-21
- Cao, G. H., Sofic, E., and Prior, R. L. (1996). Antioxidant capacity of tea and common vegetables. *J. Agric. Food Chem.* 44, 3426–3431. doi: 10.1021/jf9602535
- Cassaniti, C., Giuffrida, F., Scuderi, D., and Leonardi, C. (2011). Effect of rootstock and nutrient solution concentration on eggplant grown in a soilless system. *J. Food Agric. Environ.* 9, 252–256.
- Causse, M., Saliba Colombani, V., Lecomte, L., Duffé, P., Rousselle, P., and Buret, M. (2002). QTL analysis of fruit quality in fresh market tomato: a few chromosome regions control the variation of sensory and instrumental traits. *J. Exp. Bot.* 53, 2089–2098. doi: 10.1093/jxb/erf058
- Chávez-Mendoza, C., Sánchez, E., Carvajal-Millán, E., Muñoz-Márquez, E., and Guevara-Aguilar, A. (2013). Characterization of the nutraceutical quality and antioxidant activity in bell pepper in response to grafting. *Molecules* 18, 15689–15703. doi: 10.3390/molecules181215689
- Chisholm, D. N., and Picha, D. H. (1986). Effect of storage temperature on sugar and organic acid contents of watermelon. *HortScience* 21, 1031–1033.
- Chuan-qiang, X., Yu-xue, H., and Lin, Y. (2011). Effects of grafting on four characteristic ester aromas contents and related enzyme activities in muskmelon fruit. *North. Hortic.* 16, 41–44.
- Colla, G., Rousphael, Y., Cardarelli, M., and Rea, E. (2006a). Effect of salinity on yield, fruit quality, leaf gas exchange, and mineral composition of grafted watermelon plants. *HortScience* 41, 622–627.
- Colla, G., Rousphael, Y., Cardarelli, M., Massa, D., Salerno, A., and Rea, E. (2006b). Yield, fruit quality and mineral composition of grafted melon plants grown under saline conditions. *J. Hortic. Sci. Biotechnol.* 81, 146–152. doi: 10.1080/14620316.2006.11512041
- Colla, G., Rousphael, Y., Cardarelli, M., Temperini, O., Rea, E., Salerno, A., et al. (2008). Influence of grafting on yield and fruit quality of pepper (*Capsicum annuum* L.) grown under greenhouse conditions. *Acta Hortic.* 782, 359–363. doi: 10.17660/actahortic.2008.782.45
- Colla, G., Rousphael, Y., Jawad, R., Kumar, P., Rea, E., and Cardarelli, M. (2013). The effectiveness of grafting to improve NaCl and CaCl₂ tolerance in cucumber. *Sci. Hortic.* 164, 380–391. doi: 10.1016/j.scientia.2013.09.023
- Colla, G., Rousphael, Y., Leonardi, C., and Bie, Z. (2010a). Role of grafting in vegetable crops grown under saline conditions. *Sci. Hortic.* 127, 147–155. doi: 10.1016/j.scientia.2010.08.004
- Colla, G., Suárez, C. M. C., Cardarelli, M., and Rousphael, Y. (2010b). Improving nitrogen use efficiency in melon by grafting. *HortScience* 45, 559–565.
- Colla, G., Rousphael, Y., Mirabelli, C., and Cardarelli, M. (2011). Nitrogen-use efficiency traits of mini-watermelon in response to grafting and nitrogen-fertilization doses. *J. Plant Nutr. Soil Sci.* 174, 933–941. doi: 10.1002/jpln.201000325
- Colla, G., Rousphael, Y., Rea, E., and Cardarelli, M. (2012). Grafting cucumber plants enhance tolerance to sodium chloride and sulfate salinization. *Sci. Hortic.* 135, 177–185. doi: 10.1016/j.scientia.2011.11.023
- Commission Implementing Regulation (EU) No 543/2011 (2011). Commission Implementing Regulation (EU) No 543/2011 of 7 June 2011 laying down detailed rules for the application of Council Regulation (EC) No 1234/2007 in respect of the fruit and vegetables and processed fruit and vegetables sectors. *Off. J. Eur. Union* L 157, 1–163.
- Condurso, C., Verzera, A., Dima, G., Tripodi, G., Crinò, P., Paratore, A., et al. (2012). Effects of different rootstocks on aroma volatile compounds and carotenoid content of melon fruits. *Sci. Hortic.* 148, 9–16. doi: 10.1016/j.scientia.2012.09.015

- Cookson, S. J., Moreno, M. J. C., Hevin, C., Mendome, L. Z. N., Delrot, S., Magnin, N., et al. (2014). Heterografting with nonself rootstocks induces genes involved in stress responses at the graft interface when compared with autografted controls. *J. Exp. Bot.* 65, 2473–2481. doi: 10.1093/jxb/eru145
- Cookson, S. J., and Ollat, N. (2013). Grafting with rootstocks induces extensive transcriptional re-programming in the shoot apical meristem of grapevine. *BMC Plant Biol.* 13:147. doi: 10.1186/1471-2229-13-147
- Corbesier, L., Vincent, C., Jang, S. H., Fornara, F., Fan, Q. Z., Searle, I., et al. (2007). FT protein movement contributes to long-distance signaling in floral induction of *Arabidopsis*. *Science* 316, 1030–1033. doi: 10.1126/science.1141752
- Corey, K. A., and Schlimme, D. V. (1988). Relationship of rind gloss and grounds pot colour to flesh quality of watermelon fruits during maturation. *Sci. Hortic.* 34, 211–218. doi: 10.1016/0304-4238(88)90094-5
- Crinò, P., Lo Bianco, C., Rousphæl, Y., Colla, G., Saccardo, F., and Paratore, A. (2007). Evaluation of rootstock resistance to *Fusarium* wilt and gummy stem blight and effect on yield and quality of a grafted 'Inodorus' melon. *HortScience* 42, 521–525.
- Curis, E., Nicolis, I., Moinard, C., Osowska, S., Zerrouk, N., Bénazeth, S., et al. (2005). Almost all about citrulline in mammals. *Amino Acids* 29, 177–205. doi: 10.1007/s00726-005-0235-4
- Cushman, K. E., and Huan, J. (2008). Performance of four triploid watermelon cultivars grafted onto five rootstock genotypes: yield and fruit quality under commercial growing conditions. *Acta Hortic.* 782, 335–337. doi: 10.17660/actahortic.2008.782.42
- Davis, A. R., and Perkins-Veazie, P. (2005). Rootstock effects on plant vigor and watermelon fruit quality. *Cucurbit Gen. Coop. Rep.* 2, 39–42.
- Davis, A. R., Perkins-Veazie, P., Hassell, R., Levi, A., King, S. R., and Zhang, X. (2008a). Grafting effects on vegetable quality. *HortScience* 43, 1670–1672.
- Davis, A. R., Perkins-Veazie, P., Sakata, Y., Lopez-Galarza, S., Maroto, J. V., Lee, S. G., et al. (2008b). Cucurbit grafting. *Crit. Rev. Plant Sci.* 27, 50–74. doi: 10.1080/07352680802053940
- Davis, A. R., Webber, C. L., Perkins-Veazie, P., Russo, V., Lopez Galarza, S., and Sakata, Y. (2008c). "A review of production systems on watermelon quality," in *Proceedings of the IXth EUCARPIA Meeting on Genetics and Breeding of Cucurbitaceae*, ed. M. Pitrat (Avignon: INRA).
- Davis, A. R., Webber, C. L., and Fish, W. W. (2011). L-Citrulline levels in watermelon cultigen tested in two environments. *HortScience* 46, 1572–1575.
- Di Gioia, F., Serio, F., Buttarro, D., Ayala, O., and Santamaría, P. (2010). Vegetative growth, yield, and fruit quality of 'Cuore di Bue', an heirloom tomato, as influenced by rootstock. *J. Hortic. Sci. Biotechnol.* 85, 477–482. doi: 10.1080/14620316.2010.11512701
- Dima, G., Tripodi, G., Condurso, C., and Verzera, A. (2014). Volatile constituents of mini-watermelon fruits. *J. Essent. Oil Res.* 26, 323–327. doi: 10.1080/10421905.2014.933449
- Djidonou, D., Simonne, A. H., Koch, K. E., Brecht, J. K., and Zhao, X. (2016). Nutritional quality of field-grown tomato fruit as affected by grafting with interspecific hybrid rootstocks. *HortScience* 51, 1618–1624. doi: 10.21273/hortsci11275-16
- Doñas-Uclés, F., Jiménez-Luna, M. M., Gongora-Corral, J. A., Pérez-Madrid, D., Verde-Fernandez, D., and Camacho-Ferre, F. (2014). Influence of three rootstocks on yield and commercial quality of 'Italian sweet' pepper. *Ciènc. Agrotecnol.* 38, 538–545. doi: 10.1590/s1413-70542014000600002
- Dorais, M. (2007). Effect of cultural management on tomato fruit health qualities. *Acta Hortic.* 744, 279–293. doi: 10.17660/actahortic.2007.744.29
- Dos-Santos, N., Bueso, M. C., and Fernández-Trujillo, J. P. (2013). Aroma volatiles as biomarkers of textural differences at harvest in non-climacteric near-isogenic lines of melon. *Food Res. Int.* 54, 1801–1812. doi: 10.1016/j.foodres.2013.09.031
- Edelstein, M., Plaut, Z., and Ben-Hur, M. (2011). Sodium and chloride exclusion and retention by non-grafted and grafted melon and *Cucurbita* plants. *J. Exper. Bot.* 62, 177–184. doi: 10.1093/jxb/erq255
- Elmstrom, G. W., and Davis, P. L. (1981). Sugars in developing and mature fruits of several watermelon cultivars. *J. Amer. Soc. Hort. Sci.* 106, 330–333.
- Fan, M., Bie, Z., Krumbein, A., and Schwarz, D. (2011). Salinity stress in tomatoes can be alleviated by grafting and potassium depending on the rootstock and K-concentration employed. *Sci. Hortic.* 130, 615–623. doi: 10.1016/j.scienta.2011.08.018
- FAO (2012). *Food and Agricultural Organization*. Available at: www.fao.org [accessed December 12, 2016].
- Fernández-García, N., Martínez, V., and Carvajal, M. (2004a). Effect of salinity on growth, mineral composition, and water relations of grafted tomato plants. *J. Plant Nutr. Soil Sci.* 167, 616–622. doi: 10.1002/jpln.200420416
- Fernández-García, N., Martínez, V., Cerda, A., and Carvajal, M. (2004b). Fruit quality of grafted tomato plants grown under saline conditions. *J. Hortic. Sci. Biotechnol.* 79, 995–1001. doi: 10.1080/14620316.2004.11511880
- Fish, W. W., and Davis, A. R. (2003). The effects of frozen storage conditions on lycopene stability in watermelon tissue. *J. Agric. Food Chem.* 51, 3582–3585. doi: 10.1021/jf030022f
- Fita, A., Pico, B., Roig, C., and Nuez, F. (2007). Performance of *Cucumis melo* ssp. *agrestis* as a rootstock for melon. *J. Hortic. Sci. Biotechnol.* 82, 184–190. doi: 10.1080/14620316.2007.11512218
- Flores, F. B., Sanchez-Bel, P., Estan, M. T., Martinez-Rodriguez, M. M., Moyano, E., Morales, B., et al. (2010). The effectiveness of grafting to improve tomato fruit quality. *Sci. Hortic.* 125, 211–217. doi: 10.1016/j.scienta.2010.03.026
- Frederes, A., Roselló, S., Beltrán, J., Cebolla-Cornejo, J., Pérez-de-Castro, A., Gisbert, C., et al. (2017). Fruit quality assessment of watermelons grafted onto citron melon rootstock. *J. Sci. Food Agric.* 97, 1646–1655. doi: 10.1002/jsfa.7915
- Fuentes, I., Stegemann, S., Golczyk, H., Karcher, D., and Bock, R. (2014). Horizontal genome transfer as an asexual path to the formation of new species. *Nature* 511, 232–235. doi: 10.1038/nature13291
- Gajc-Wolska, J., Kowalczyk, K., Marcinkowska, M., Radzanowska, J., and Bujalski, D. (2015). Influence of growth conditions and grafting on the yield, chemical composition and sensory quality of tomato fruit in greenhouse cultivation. *J. Elementol.* 20, 73–81. doi: 10.5601/jelem.2014.19.4.565
- Gajc-Wolska, J., Łyszkowska, M., and Zielony, T. (2010). The influence of grafting and biostimulators on the yield and fruit quality of greenhouse tomato cv. (*Lycopersicon esculentum* Mill.) grown in the field. *Veg. Crops Res. Bull.* 72, 63–70. doi: 10.2478/v10032.010-0006-y
- Gisbert, C., Prohens, J., and Nuez, F. (2011a). Performance of eggplant grafted onto cultivated and wild materials and hybrids of eggplant and tomato. *Intern. J. Plant Prod.* 5, 367–380.
- Gisbert, C., Prohens, J., Raigón, M. D., Stommel, J., and Nuez, F. (2011b). Eggplant relatives as sources of variation for developing new rootstocks: effects of grafting on yield and fruit apparent quality and composition. *Sci. Hortic.* 128, 14–22. doi: 10.1016/j.scienta.2010.12.007
- Gisbert, C., Sánchez-Torres, P., Dolores Raigón, M., and Nuez, F. (2010). *Phytophthora capsici* resistance evaluation in pepper hybrids: agronomic performance and fruit quality of pepper grafted plants. *J. Food Agric. Environ.* 8, 116–121.
- Goldschmidt, E. E. (2014). Plant grafting: new mechanisms, evolutionary implications. *Front. Plant Sci.* 5:725. doi: 10.3389/fpls.2014.00727
- Gómez-Romero, M., Segura-Carretero, A., and Fernández-Gutiérrez, A. (2010). Metabolite profiling and quantification of phenolic compounds in methanol extracts of tomato fruit. *Phytochemistry* 71, 1848–1864. doi: 10.1016/j.phytochem.2010.08.002
- Goreta Ban, S., Zanic, K., Dumiciv, G., Raspuđic, E., Vučetić Selak, G., and Ban, D. (2014). Growth and yield of grafted cucumbers in soil infested with root-knot nematodes. *Chilean J. Agric. Res.* 74, 29–34. doi: 10.4067/s0718-58392014000100005
- Guan, W., Zhao, X., Dickson, D. W., Mendes, M. L., and Thies, J. (2014). Root-knot nematode resistance, yield, and fruit quality of specialty melons grafted onto *Cucumis metulifer*. *HortScience* 49, 1046–1051.
- Guan, W. J., Zhao, X., Hassell, R., and Thies, J. (2012). Defense mechanisms involved in disease resistance of grafted vegetables. *HortScience* 47, 164–170.
- Guan, W., Zhao, X., Hubler, J. H., Huber, J. D., and Sims, A. C. (2015). Instrumental and sensory analyses of quality attributes of grafted specialty melons. *J. Sci. Food. Agric.* 95, 2989–2995. doi: 10.1002/jsfa.7050
- Guler, Z., Karaca, F., and Yetisir, H. (2013). Volatile compounds in the peel and slesh of cucumber (*Cucumis sativus* L.) grafted onto bottle gourd (*Lagenaria siceraria*) rootstocks. *J. Hortic. Sci. Biotechnol.* 88, 123–128. doi: 10.1080/14620316.2013.11512945
- Harada, T. (2010). Grafting and RNA transport via phloem tissue in horticultural plants. *Sci. Hortic.* 125, 545–550. doi: 10.1016/j.scienta.2010.05.013

- Harker, F. R., Gunson, F. A., and Jaeger, S. R. (2003). The case for fruit quality: an interpretive review of consumer attitudes, and preferences for apples. *Postharvest Biol. Technol.* 28, 333–347. doi: 10.1016/s0925-5214(02)00215-6
- Haroldsen, V. M., Szczerba, M. W., Aktas, H., Lopez-Baltazar, J., Odias, M. J., Chi-Ham, C. L., et al. (2012). Mobility of transgenic nucleic acids and proteins within grafted rootstocks for agricultural improvement. *Front. Plant Sci.* 3:39. doi: 10.3389/fpls.2012.00039
- Haywood, V., Yu, T. S., Huang, N. C., and Lucas, W. J. (2005). Phloem long-distance trafficking of Gibberellin acid-insensitive RNA regulates leaf development. *Plant J.* 42, 49–68. doi: 10.1111/j.1365-313x.2005.02351.x
- Helyes, L., Lugasi, A., Pogonyi, A., and Pek, Z. (2009). Effect of variety and grafting on lycopene content of tomato (*Lycopersicon lycopersicum* L. Karsten) fruit. *Acta Aliment.* 38, 27–34. doi: 10.17660/actahortic.2006.712.62
- Ho, L., and White, P. J. (2005). A cellular hypothesis for the induction of blossom-end rot in tomato fruit. *Ann. Bot.* 95, 571–581. doi: 10.1093/aob/mci065
- Huang, N. C., and Yu, T. S. (2009). The sequences of Arabidopsis GA-INSENSITIVE RNA constitute the motifs that are necessary and sufficient for RNA long-distance trafficking. *Plant J.* 59, 921–929. doi: 10.1111/j.1365-313x.2009.03918.x
- Huang, W., Liao, S., Lv, H., Khaldun, A. B. M., and Wang, Y. (2015). Characterization of the growth and fruit quality of tomato grafted on a woody medicinal plant, *Lycium chinense*. *Sci. Hortic.* 197, 447–453. doi: 10.1016/j.scienta.2015.10.005
- Huang, Y., Tang, R., Cao, Q., and Bie, Z. (2009). Improving the fruit yield and quality of cucumber by grafting onto the salt tolerant rootstock under NaCl stress. *Sci. Hortic.* 122, 26–31. doi: 10.1016/j.scienta.2009.04.004
- Huitrón, M. V., Diaz, M., Díanez, F., and Camacho, F. (2007). The effect of various rootstocks on triploid watermelon yield and quality. *J. Food Agric. Environ.* 5, 344–348.
- Huitrón, M. V., Ricárdez, M., Díanez, F., and Camacho, F. (2009). Influence of grafted watermelon plant density on yield and quality in soil infested with melon necrotic spot virus. *HortScience* 44, 1838–1841.
- Huitrón, M. V., Rodriguez, N., Diaz, M., and Camacho, F. (2008). Effect of different rootstocks on the production and quality of watermelon cv. Reina de Corazones. *Acta Hortic.* 797, 437–442. doi: 10.17660/actahortic.2008.797.63
- Hwang, J. M., Lee, W. H., and Hwang, G. S. (1992). Yield performance test of cucumber (*Cucumis sativus* L.) grafted with the rootstocks, *Sicyos angulatus* L. grown in the farm plastic house. *Korean J. Hortic. Sci. Technol.* 10, 34–35.
- Kader, A. A. (1999). Fruit maturity, ripening and quality relationships. *Acta Hortic.* 485, 203–208. doi: 10.17660/actahortic.1999.485.27
- Kader, A. A. (2008). Flavor quality of fruits and vegetables - Perspective. *J. Sci. Food Agric.* 88, 1863–1868. doi: 10.1002/jsfa.3293
- Khah, E. M. (2011). Effect of grafting on growth, performance and yield of aubergine (*Solanum melongena* L.) in greenhouse and open-field. *Intern. J. Plant Prod.* 5, 359–366.
- Khah, E. M., Kakava, E., Mavromatis, A., Chachalis, D., and Goulas, C. (2006). Effect of grafting on growth and yield of tomato (*Lycopersicon esculentum* Mill.) in greenhouse and open-field. *J. Appl. Hortic.* 8, 3–7.
- Kim, M., Canio, W., Kessler, S., and Sinha, N. (2001). Developmental changes due to long-distance movement of a homeobox fusion transcript in tomato. *Science* 293, 287–289. doi: 10.1126/science.1059805
- Klee, H. J., and Tieman, D. M. (2013). Genetic challenges of flavor improvement in tomato. *Trends Gen.* 29, 257–262. doi: 10.1016/j.tig.2012.12.003
- Kourkoutas, D., Elmore, J. S., and Mottram, D. S. (2006). Comparison of the volatile compositions and flavor properties of cantaloupe, Galia and honeydew muskmelons. *Food Chem.* 97, 95–102. doi: 10.1016/j.foodchem.2005.03.026
- Krumbein, A., and Auerswald, H. (1998). Characterization of aroma volatiles in tomatoes by sensory analyses. *Food* 42, 395–399. doi: 10.1002/(sici)1521-3803(199812)42:06<395::aid-food395<3.3.co;2-z
- Krumbein, A., and Schwarz, D. (2013). Grafting: A possibility to enhance health-promoting and flavour compounds in tomato fruits of shaded plants? *Sci. Hortic.* 149, 97–107. doi: 10.1016/j.scienta.2012.09.003
- Kumar, P., Lucini, L., Roushphal, Y., Cardarelli, M., Kalunke, R. M., and Colla, G. (2015). Insight into the role of grafting and arbuscular mycorrhiza on cadmium stress tolerance in tomato. *Front. Plant Sci.* 6:477. doi: 10.3389/fpls.2015.00477
- Kyriacou, M. C., Polking, G. F., Hannapel, D. J., and Gladon, R. J. (1996). Activity of 5-aminolevulinic acid dehydratase declines during tomato fruit development and ripening. *J. Am. Soc. Hortic. Sci.* 121, 91–95.
- Kyriacou, M. C., and Soteriou, G. A. (2012). Postharvest change in compositional, visual and textural quality of grafted watermelon cultivars. *Acta Hortic.* 934, 985–992. doi: 10.17660/actahortic.2012.934.131
- Kyriacou, M. C., and Soteriou, G. A. (2015). Quality and postharvest behavior of watermelon fruit in response to grafting on inter-specific cucurbit rootstocks. *J. Food Qual.* 38, 21–29. doi: 10.1111/jfq.12124
- Kyriacou, M. C., Soteriou, G. A., Roushphal, Y., Siomos, A. S., and Gerasopoulos, D. (2016). Configuration of watermelon fruit quality in response to rootstock-mediated harvest maturity and postharvest storage. *J. Sci. Food Agric.* 96, 2400–2409. doi: 10.1002/jsfa.7356
- Lanchun, N., Jifang, C., Xueying, Z., and Bao, D. (2010). Changes in carbohydrates and carbohydrate metabolizing enzymes during watermelon fruit set. *Acta Hortic. ISHS* 871, 313–318. doi: 10.17660/actahortic.2010.871.42
- Laur, L. M., and Tian, L. (2011). Provitamin A and vitamin C contents in selected California-grown cantaloupe and honeydew melons and imported melons. *J. Food Comp. Anal.* 24, 194–201. doi: 10.1016/j.jfca.2010.07.009
- Leal-Fernández, C., Godoy-hernández, H., Núñezcolin, C. A., Anaya-López, J. A., Villalobos-Reyes, S., and Castellanos, J. Z. (2013). Morphological response and fruit yield of sweet pepper (*Capsicum annuum* L.) grafted onto different commercial rootstocks. *Biol. Agric. Hortic.* 29, 1–11. doi: 10.1080/01448765.2012.746063
- Lee, J. M. (1994). Cultivation of grafted vegetables, I. Current status, grafting methods, and benefits. *HortScience* 29, 235–239.
- Lee, J. M., Bang, H. J., and Ham, H. S. (1999). Quality of cucumber fruit as affected by rootstock. *Acta Hortic.* 483, 117–123. doi: 10.17660/actahortic.1999.483.12
- Lee, J. M., Kubota, C., Tsao, S. J., Biel, Z., Hoyos Echevaria, P., Morra, L., et al. (2010). Current status of vegetable grafting: diffusion, grafting techniques, automation. *Sci. Hortic.* 127, 93–105. doi: 10.1016/j.scienta.2010.08.003
- Leonardi, C., and Giuffrida, F. (2006). Variation of plant growth and macronutrient uptake in grafted tomatoes and eggplants on three different rootstocks. *Eur. J. Hortic. Sci.* 71, 97–101.
- Leskovar, D. I., Bang, H., Crosby, K. M., Maness, N., Franco, J. A., and Perkins-Veazie, P. (2004). Lycopene, carbohydrates, ascorbic acid and yield components of diploid and triploid watermelon cultivars are affected by deficit irrigation. *J. Hortic. Sci. Biotechnol.* 79, 75–81. doi: 10.1080/14620316.2004.11511739
- Lewinsohn, E., Sitrit, Y., Bar, E., Azulay, Y., Meir, A., Zamir, D., et al. (2005). Carotenoid pigmentation affects the volatile composition of tomato and watermelon fruits, as revealed by comparative genetic analyses. *J. Agric. Food Chem.* 53, 3142–3148. doi: 10.1021/jf047927
- Liu, B., Ren, J., Zhang, Y., An, J., Chen, M., Chen, H., et al. (2015). A new grafted rootstock against root-knot nematode for cucumber, melon, and watermelon. *Agron. Sustain. Dev.* 35, 251–259. doi: 10.1007/s13593-014-0234-5
- Liu, H. Y., Zhu, Z. J., Diao, M., and Guo, Z. P. (2006). Characteristic of the sugar metabolism in leaves and fruits of grafted watermelon during fruit development. *Plant Phys. Commun.* 42, 835–840.
- Liu, N., Yang, J. H., Fu, X. X., Zhang, L., Tang, K., Guy, K. M., et al. (2016). Genome-wide identification and comparative analysis of grafting-responsive mRNA in watermelon grafted onto bottle gourd and squash rootstocks by high-throughput sequencing. *Mol. Genet. Genomics* 291, 621–633. doi: 10.1007/s00438-015-1132-5
- Liu, N., Yang, J. H., Guo, S. G., Xu, Y., and Zhang, M. F. (2013). Genome-wide identification and comparative analysis of conserved and novel MicroRNAs in grafted watermelon by high-throughput sequencing. *PLoS ONE* 8:e57359. doi: 10.1371/journal.pone.0057359
- Liu, Y. S., Wang, Q. L., and Li, B. Y. (2010). New insights into plant graft hybridization. *Heredity* 104, 1–2. doi: 10.1038/hdy.2009.115
- López-Marín, J., Gálvez, A., del Amor, F. M., Albacete, A., Fernandez, J. A., Egea-Gilabert, C., et al. (2017). Selecting vegetative/generative/dwarfing rootstocks for improving fruit yield and quality in water stressed sweet peppers. *Sci. Hortic.* 214, 9–17. doi: 10.1016/j.scienta.2016.11.012
- López-Marín, J., González, A., Pérez-Alfocea, F., Egea-Gilabert, C., and Fernandez, J. A. (2013). Grafting is an efficient alternative to shading screens to alleviate thermal stress in greenhouse-grown sweet pepper. *Sci. Hortic.* 149, 39–46. doi: 10.1016/j.scienta.2012.02.034
- López-Galarza, S., San Batista, A., Perez, D. M., Miquel, A., Baixauli, C., Pascual, B., et al. (2004). Effects of grafting and cytokinin – induced fruit setting on colour and sugar – content traits in glasshouse – grown triploid watermelon.

- J. Hortic. Sci. Biotechnol.* 79, 971–976. doi: 10.1080/14620316.2004.11511875
- Louws, F. J., Rivard, C. L., and Kubota, C. (2010). Grafting fruiting vegetables to manage soilborne pathogens, foliar pathogens, arthropods and weeds. *Sci. Hortic.* 127, 127–146. doi: 10.1016/j.scientia.2010.09.023
- Lucas, W. J., Yoo, B. C., and Kragler, F. (2001). RNA as a long-distance information macromolecule in plants. *Nat. Rev. Mol. Cell Biol.* 2, 849–857. doi: 10.1038/35099096
- Luria, N., Smith, E., Reingold, V., Bekelman, I., Lapidot, M., Levin, I., et al. (2017). A new Israeli *Tobamovirus* isolate infects tomato plants harboring Tm-22 resistance genes. *PLoS ONE* 12:e0170429. doi: 10.1371/journal.pone.0170429
- Magwaza, L. S., and Opara, U. L. (2015). Analytical methods for determination of sugars and sweetness of horticultural products – A review. *Sci. Hortic.* 184, 179–192. doi: 10.1016/j.scientia.2015.01.001
- Marsic, N. K., Mikulik-Petkovsek, M., and Stampar, F. (2014). Grafting influences phenolic profile and carpometric traits of fruits of greenhouse-grown eggplant (*Solanum melongena* L.). *J. Agric. Food Chem.* 62, 10504–10514. doi: 10.1021/jf503338m
- Martínez-Ballesta, M. C., Alcaraz-Lopez, C., Murias, B., and Carvajal, M. (2010). Physiological aspects of rootstock–scion interactions. *Sci. Hortic.* 127, 112–118. doi: 10.1016/j.scientia.2010.08.002
- Matsuzoe, N., Hiromi, A., Hanada, K., Ali, M., Okubo, H., and Fujieda, K. (1996). Fruit quality of tomato plants grafted on *Solanum* rootstocks. *J. Jpn. Soc. Hortic. Sci.* 65, 73–80. doi: 10.2503/jjshs.65.73
- Maynard, D. N., Dunlap, A. M., and Sidoti, B. J. (2002). Sweetness in diploid and triploid watermelon fruit. *Cucurbit Genet. Coop. Rep.* 25, 32–35.
- Miguel, A., Maroto, J. V., San Bautista, A., Baixaupi, C., Cebolla, V., Pascual, B., et al. (2004). The grafting of triploid watermelon is an advantageous alternative to oil fumigation. *Sci. Hortic.* 103, 9–17. doi: 10.1016/j.scientia.2004.04.007
- Miskovic, A., Ilic, O., Bacanovic, J., Vujasinovic, V., and Kukiae, B. (2016). Effect of eggplant rootstock on yield and quality parameters of grafted tomato. *Acta Sci. Polon. Hortic. Cul.* 15, 149–159.
- Miskovic, A., Ilin, Z., and Markovic, V. (2009). Effect of different rootstock type on quality and yield of tomato fruits. *Acta Hortic.* 807, 619–624. doi: 10.17660/actahortic.2009.807.92
- Mohammed, S. T. M., Humidan, M., Boras, M., and Abdalla, O. A. (2009). Effect of grafting tomatoon different rootstocks on growth and productivity under glasshouse conditions. *Asian J. Agric. Res.* 3, 47–54. doi: 10.3923/ajar.2009.47.54
- Molnar, A., Melnyk, C. W., Bassett, A., Hardcastle, T. J., Dunn, R., and Baulcombe, D. C. (2010). Small silencing RNAs in plants are mobile and direct epigenetic modification in recipient cells. *Science* 328, 872–875. doi: 10.1126/science.1187959
- Moncada, A., Miceli, A., Vetrano, F., Mineo, V., Planeta, D., and D'Anna, F. (2013). Effect of grafting on yield and quality of eggplant (*Solanum melongena* L.). *Sci. Hortic.* 149, 108–114. doi: 10.1016/j.scientia.2012.06.015
- Morishita, M. (2001). Origin and characteristics of the local cucumber variety 'Kema' in the Osaka district. *Bull. Osaka Prefectural Agric. For. Res. Center* 37, 27–34.
- Nicoletto, C., Tosini, F., and Sambo, P. (2013a). Effect of grafting and ripening conditions on some qualitative traits of 'Cuore di bue' tomato fruits. *J. Sci. Food Agric.* 93, 1397–1403. doi: 10.1002/jsfa.5906
- Nicoletto, C., Tosini, F., and Sambo, P. (2013b). Effect of grafting on biochemical and nutritional traits of 'Cuore di bue' tomatoes harvested at different ripening stages. *Acta Agric. Scand. B* 63, 114–122. doi: 10.1080/09064710.2012.729606
- Nissinen, R., Paimela, L., Julkunen, H., Tienari, P. J., Leirisalo-Repo, M., Palosuo, T., et al. (2003). Peptidylarginine deiminase, the arginine to citrulline converting enzyme, is frequently recognized by sera of patients with rheumatoid arthritis, systemic lupus erythematosus and primary Sjögren syndrome. *Scand. J. Rheumatol.* 32, 337–342. doi: 10.1080/03009740410004990
- Ntatsi, G., Savvas, D., Huntenburg, K., Druege, U., and Schwarz, D. (2014). A study on ABA involvement in the response of tomato to suboptimal root temperature using reciprocal grafts with *notabilis*, a null mutant in the ABA-biosynthesis gene *LeNCED1*. *Environ. Exp. Bot.* 97, 11–21. doi: 10.1016/j.envexpbot.2013.09.011
- Obando-Ulloa, M., Moreno, E., Garcia-Mas, J., Nicolai, B., Lammertyn, J., Monforte, A. J., et al. (2008). Climacteric or non-climacteric behavior in melon fruit: 1. Aroma volatiles. *Postharvest Biol. Technol.* 49, 27–37. doi: 10.1016/j.postharvbio.2007.11.004
- Oda, M., Nagata, M., Tsuji, K., and Sasaki, H. S. O. (1996). Effects of scarlet eggplant rootstock on growth, yield, and sugar content of grafted tomato fruits. *J. Jpn. Soc. Hortic. Sci.* 65, 531–536. doi: 10.2503/jjshs.65.531
- Orsini, F., Sanoubar, R., Oztekin, G. B., Kappel, N., Tepecik, M., Quacquarelli, C., et al. (2013). Improved stomatal regulation and ion partitioning boost salt tolerance in grafted melon. *Funct. Plant Biol.* 40, 628–636. doi: 10.1071/FP12350
- Özdemir, A., Çandır, E., Yetişir, H., Aras, V., Arslan, Ö., Baltacı, Ö., et al. (2016). Effects of rootstocks on storage and shelf life of grafted watermelons. *J. Appl. Bot. Food Qual.* 9, 191–201. doi: 10.5073/JABFQ.2016.089.024
- Pant, B. D., Buhtz, A., Kehr, J., and Scheible, W. R. (2008). MicroRNA399 is a long-distance signal for the regulation of plant phosphate homeostasis. *Plant J.* 53, 731–738. doi: 10.1111/j.1365-313x.2007.03363.x
- Park, D. K., Son, S. H., Kim, S., Lee, W. M., Lee, H. J., Choi, H. S., et al. (2013). Selection of melon genotypes with resistance to *Fusarium* wilt and *Monosporascus* root rot for rootstocks. *Plant Breed. Biotechnol.* 1, 277–282. doi: 10.9787/pbb.2013.1.3.277
- Passam, H. C., Stylianoy, M., and Kotsiras, A. (2005). Performance of eggplant grafted on tomato and eggplant rootstocks. *Eur. J. Hortic. Sci.* 70, 130–134.
- Paultre, D. S. G., Gustin, M. P., Molnar, A., and Oparka, K. J. (2016). Lost in transit: long-distance trafficking and phloem unloading of protein signals in *Arabidopsis* homografts. *Plant Cell* 28, 2016–2025. doi: 10.1105/tpc.16.00249
- Pech, J. C., Bouzayen, M., and Latché, A. (2008). Climacteric fruit ripening: ethylene-dependent and independent regulation of ripening pathways in melon fruit. *Plant Sci.* 175, 114–120. doi: 10.1016/j.plantsci.2008.01.003
- Penella, C., Landi, M., Giudi, L., Nebauer, S. G., Pellegrini, E., San Bautista, A., et al. (2016). Salt tolerant rootstock increases yield of pepper under salinity through maintenance of photosynthetic performance and sinks strength. *J. Plant Physiol.* 193, 1–11. doi: 10.1016/j.jplph.2016.02.007
- Perkins-Veazie, P., and Collins, J. K. (2006). Carotenoid changes of intact watermelons after storage. *J. Agric. Food Chem.* 54, 5868–5874. doi: 10.1021/jf0532664
- Perkins-Veazie, P., Collins, J. K., Pair, S. D., and Roberts, W. (2001). Lycopene content differs among red-fleshed watermelon cultivars. *J. Sci. Food Agric.* 81, 983–987. doi: 10.1002/jsfa.880
- Perkins-Veazie, P., Zhang, X., Lu, G., and Huan, J. (2007). Grafting increases lycopene in seedless watermelon. *HortScience* 42, 959.
- Petropoulos, S. A., Olympios, C., Ropokis, A., Vlachou, G., Ntatsi, G., Paraskevopoulos, A., et al. (2014). Fruit volatiles, quality, and yield of watermelon as affected by grafting. *J. Agric. Sci. Technol.* 16, 873–885.
- Pogonyi, Á., PéK, Z., Helyes, L., and Lugasi, A. (2005). Effect of grafting on the tomato's yield, quality and main fruit components in spring forcing. *Acta Aliment.* 34, 453–462. doi: 10.1556/aalim.34.2005.4.12
- Poudel, S. R., and Lee, W. S. (2009). Response of eggplant (*Solanum melongena* L.) as rootstock for tomato (*Solanum lycopersicum* L.). *Hortic. NCHU* 34, 39–52.
- Proietti, S., Roushelin, Y., Colla, G., Cardarelli, M., De Agazio, M., Zacchini, M., et al. (2008). Fruit quality of mini-watermelon as affected by grafting and irrigation regimes. *J. Sci. Food Agric.* 88, 1107–1114. doi: 10.1002/jsfa.3207
- Qaryouti, M. M., Qawasmi, W., Hamdan, H., and Edwan, M. (2007). Tomato fruit yield and quality as affected by grafting and growing system. *Acta Hortic.* 741, 199–206. doi: 10.17660/actahortic.2007.741.22
- Rahmatian, A., Delshad, M., and Salehi, R. (2014). Effect of grafting on growth, yield and fruit quality of single and double stemmed tomato plants grown hydroponically. *Hortic. Environ. Biotechnol.* 55, 115–119. doi: 10.1007/s13580-014-0167-6
- Reid, M. S. (2002). "Maturation and maturity indices" in *Postharvest Technology of Horticultural Crops*, 3rd Edn, ed. A. A. Kader (Oakland, CA: University of California).
- Riga, P. (2015). Effect of rootstock on growth, fruit production and quality of tomato plants grown under low temperature and light conditions. *Hortic. Environ. Biotechnol.* 56, 626–638. doi: 10.1007/s13580-015-0042-0
- Riga, P., Benedicto, L., García-Flores, L., Villano, D., Medina, S., and Gil-Izquierdo, A. (2016). Rootstock effect on serotonin and nutritional quality of tomatoes produced under low temperature and light conditions. *J. Food Compost. Anal.* 46, 59–59. doi: 10.1016/j.jfca.2015.11.003
- Rimando, A., and Perkins-Veazie, P. (2005). Determination of citrulline in watermelon rind. *J. Chromatogr. A* 1078, 196–200. doi: 10.1016/j.chroma.2005.05.009

- Romano, D., Paratore, A., and Vindigni, G. (2000). "Caratteristiche dei frutti di pomodoro in rapporto a diversi portinnesi," in *Proceedings of the Workshop on 'Applicazione di Tecnologie Innovative per il Miglioramento dell'Orticoltura Meridionale'*, Rome: Consiglio Nazionale delle Ricerche, 113–114.
- Romero, L., Belakbir, A., Ragala, L., and Ruiz, M. (1997). Response of plant yield and leaf pigments to saline conditions: effectiveness of different rootstocks in melon plants (*Cucumis melo* L.). *Soil Sci. Plant Nutr.* 43, 855–862. doi: 10.1080/00380768.1997.10414652
- Ronen, G., Carmel, G. L., Zamir, D., and Hirschberg, J. (2000). An alternative pathway to beta-carotene formation in plant chromoplasts discovered by map-based cloning of Beta and old-gold color mutations in tomato. *Proc. Natl. Acad. Sci. U.S.A.* 97, 11102–11107. doi: 10.1073/pnas.190177497
- Rouphael, Y., Cardarelli, M., and Colla, G. (2008). Yield, mineral composition, water relations, and water use efficiency of grafted mini-watermelon plants under deficit irrigation. *HortScience* 43, 730–736.
- Rouphael, Y., Cardarelli, M., Rea, E., and Colla, G. (2012). Improving melon and cucumber photosynthetic activity, mineral composition, and growth performance under salinity stress by grafting onto *Cucurbita* hybrid rootstocks. *Photosynthetica* 50, 180–188. doi: 10.1007/s11099-012-0002-1
- Rouphael, Y., Rea, E., Cardarelli, M., Bitterlich, M., Schwarz, D., and Colla, G. (2016). Can adverse effects of acidity and aluminum toxicity be alleviated by appropriate rootstock selection in cucumber? *Front. Plant Sci.* 7:1283. doi: 10.3389/fpls.2016.01283
- Rouphael, Y., Schwarz, D., Krumbein, A., and Colla, G. (2010). Impact of grafting on product quality of fruit vegetables. *Sci. Hortic.* 127, 172–179. doi: 10.1016/j.scientia.2010.09.001
- Ruiz, J. M., and Romero, L. (1999). Nitrogen efficiency and metabolism in grafted melon plants. *Sci. Hortic.* 81, 113–123. doi: 10.1016/s0304-4238(98)00200-3
- Sabatino, L., Iapichino, G., Maggio, A., D'anna, E., Bruno, M., and D'Anna, F. (2016). Grafting affects yield and phenolic profile of *Solanum melongena* L. landraces. *J. Integr. Agric.* 15, 1017–1024. doi: 10.1016/s2095-3119(15)61323-5
- Saftner, R., Luo, Y., McEvoy, J., Abbott, J. A., and Vinyard, B. (2007). Quality characteristics of fresh-cut watermelon slices from non-treated and 1-methylcyclopentene- and/or ethylene-treated whole fruit. *Postharvest Biol. Technol.* 44, 71–79. doi: 10.1016/j.postharvbio.2006.11.002
- Sakata, Y., Ohara, T., and Sugiyama, M. (2007). The history and present state of grafting of cucurbitaceous vegetables in Japan. *Acta Hortic.* 731, 159–170. doi: 10.17660/actahortic.2007.731.22
- Sánchez-Rodríguez, E., Leyva, R., Constan-Aguilar, C., Romero, L., and Ruiz, J. M. (2012a). Grafting under water stress in tomato cherry: improving the fruit yield and quality. *Ann. Appl. Biol.* 161, 302–312. doi: 10.1111/j.1744-7348.2012.00574.x
- Sánchez-Rodríguez, E., Ruiz, J. M., Ferreres, F., and Moreno, D. A. (2012b). Phenolic profiles of cherry tomatoes as influenced by hydric stress and rootstock technique. *Food Chem.* 134, 775–782. doi: 10.1016/j.foodchem.2012.02.180
- Sánchez-Torres, P., Raigón, M. D., Gammoudi, N., and Gisbert, C. (2016). Effects of grafting combinations on the nutritional composition of pepper fruit. *Fruits* 71, 249–256. doi: 10.1051/fruits/2016014
- Satoh, S. (1996). Inhibition of flowering of cucumber grafted on rooted squash rootstocks. *Physiol. Plantarum.* 97, 440–444. doi: 10.1034/j.1399-3054.1996.970304.x
- Savvas, D., Colla, G., Rouphael, Y., and Schwarz, D. (2010). Amelioration of heavy metal and nutrient stress in fruit vegetables by grafting. *Sci. Hortic.* 127, 156–161. doi: 10.1016/j.scientia.2010.09.011
- Savvas, D., Öztekin, G. B., Tepecik, M., Ropokis, A., Tüzel, Y., Ntatsi, G., et al. (2017). Impact of grafting and rootstock on nutrient-to-water uptake ratios during the first month after planting of hydroponically grown tomato. *J. Hortic. Sci. Biotechnol.* 92, 294–302. doi: 10.1080/14620316.2016.1265903
- Savvas, D., Savva, A., Ntatsi, G., Ropokis, A., Karapanos, I., Krumbein, A., et al. (2011). Effects of three commercial rootstocks on mineral nutrition, fruit yield, and quality of salinized tomato. *J. Plant Nutr. Soil Sci.* 174, 154–162. doi: 10.1002/jpln.201000099
- Schofield, A., Vasantha Rupasinghe, H. P., and Gopinadhan, P. (2008). "Isoprenoid Biosynthesis in fruits and vegetables," in *Postharvest Biology and Technology of Fruits, Vegetables and Flowers*, eds G. Paliyath, D. P. Murr, A. K. Handa, and S. Lurie (Ames: Wiley-Blackwell Publishing).
- Schreiner, M., Korn, M., Stenger, M., Holzgreve, L., and Altmann, M. (2013). Current understanding and use of quality characteristics of horticulture products. *Sci. Hortic.* 163, 63–69. doi: 10.1016/j.scientia.2013.09.027
- Schlutheis, J., Thompson, W., and Hassel, R. (2015). Specialty melon yield and quality response to grafting in trials conducted in the Southeastern United States. *Acta Hortic.* 1086, 269–278. doi: 10.17660/actahortic.2015.1086.34
- Schwarz, D., Öztekin, G. B., Tüzel, Y., Brückner, B., and Krumbein, A. (2013). Rootstocks can enhance tomato growth and quality characteristics at low potassium supply. *Sci. Hortic.* 149, 70–79. doi: 10.1016/j.scientia.2012.06.013
- Schwarz, D., Rouphael, Y., Colla, G., and Venema, J. H. (2010). Grafting as a tool to improve tolerance of vegetables to abiotic stresses: thermal stress, water stress and organic pollutants. *Sci. Hortic.* 127, 162–171. doi: 10.1016/j.scientia.2010.09.016
- Slimestad, R., Fossen, T., and Verhuel, M. J. (2008). The flavonoids of tomatoes. *J. Agric. Food Chem.* 56, 2436–2441. doi: 10.1021/jf073434n
- Soteriou, G. A., and Kyriacou, M. C. (2014). Rootstock mediated effects on watermelon field performance and fruit quality characteristics. *Intern. J. Vegetable Sci.* 21, 344–362. doi: 10.1080/19315260.2014.881454
- Soteriou, G. A., and Kyriacou, M. C. (2015). Rootstock-mediated effects on watermelon field performance and fruit quality characteristics. *Int. J. Vegetable Sci.* 21, 344–362. doi: 10.1080/19315260.2014.881454
- Soteriou, G. A., Kyriacou, M. C., Siomos, A. S., and Gerasopoulos, D. (2014). Evolution of watermelon fruit physicochemical and phytochemical composition during ripening as affected by grafting. *Food Chem.* 165, 282–289. doi: 10.1016/j.foodchem.2014.04.120
- Soteriou, G. A., Papayiannis, L. C., and Kyriacou, M. C. (2016). Indexing melon physiological decline to fruit quality and vine morphometric parameters. *Sci. Hortic.* 203, 207–215. doi: 10.1016/j.scientia.2016.03.032
- Stegemann, S., and Bock, R. (2009). Exchange of genetic material between cells in plant tissue grafts. *Science* 324, 649–651. doi: 10.1126/science.1170397
- Stegemann, S., Keuthe, M., Greiner, S., and Bock, R. (2012). Horizontal transfer of chloroplast genomes between plant species. *Proc. Natl. Acad. Sci. U.S.A.* 109, 2434–2438. doi: 10.1073/pnas.1114076109
- Stepansky, A., Kovalski, I., Schaffer, A. A., and Peri-Treves, R. (1999). Variation in sugar levels and invertase activity in mature fruit representing a broad spectrum of *Cucumis melo* genotypes. *Genet. Res. Crop Evol.* 46, 53–62. doi: 10.1023/A:1008636732481
- Steward, A. J., Bozonnet, S., Mullen, W., Jenkins, G. I., Lean, M. E. J., and Crozier, A. (2000). Occurrence of flavonols in tomatoes and tomato-based products. *J. Agric. Food Chem.* 48, 2663–2669. doi: 10.1021/jf000070p
- Strang, J., Bale, K., Snyder, J., Carpenter, D., and Smigell, C. (2007). *Specialty Melon Variety Evaluations (Kentucky)*. Lexington, KY: University of Kentucky.
- Tabata, K., Oba, K., Suzuki, K., and Esaka, M. (2001). Generation and properties of ascorbic acid-deficient transgenic tobacco cells expressing antisense RNA for L-galactono-1,4-lactone dehydrogenase. *Plant J.* 27, 139–148. doi: 10.1046/j.1365-313x.2001.01074.x
- Takasu, E., Wu, D. L., and Imai, H. (1996). Effects of grafting on blossom end rot incidence in summer tomato production. *TVIS Newsletter* 1, 22–23.
- Tarazona-Díaz, M. P., Viegas, J., Moldao-Martins, M., and Aguayo, E. (2011). Bioactive compounds from flesh and by-product of fresh-cut watermelon cultivars. *J. Sci. Food Agric.* 91, 805–812. doi: 10.1002/jsfa.4250
- Theodoropoulou, A., Giotsis, C., Hunt, J., Gilroy, J., Toufexi, E., Liopatas-Tsakalidis, A., et al. (2007). "Effect of variety choice and use of resistant rootstock on crop yield and quality parameters of tomato plants grown in organic, low input and conventional production systems/growth media," in *Proceedings of the 3rd QLIF Congress: Improving Sustainability in Organic and Low Input Food Production System*, eds U. Niggli, C. Leifert, T. Alföldi, L. Lück, and H. Willer (Stuttgart: University of Hohenheim), 177–180.
- Thieme, C. J., Rojas-Triana, M., Stecyk, E., Schudoma, C., Zhang, W. N., Yang, L., et al. (2015). Endogenous *Arabidopsis* messenger RNAs transported to distant tissues. *Nat. Plants* 1:15025. doi: 10.1038/nplants.2015.25
- Tieman, D., Bliss, P., McIntyre, L. M., Blandon-Ubeda, A., Bies, D., Odabasi, A. Z., et al. (2012). The chemical interactions underlying tomato flavor preferences. *Curr. Biol.* 22, 1035–1039. doi: 10.1016/j.cub.2012.04.016
- Tieman, D., Zhu, G., Resende, M. F. Jr, Lin, T., Nguyen, C., Bies, D., et al. (2017). A chemical genetic roadmap to improved tomato flavor. *Science* 355, 391–394. doi: 10.1126/science.aal1556

- Tomas-Barberan, F. A., and Espin, J. C. (2001). Phenolic compounds and related enzymes as determinants of quality in fruits and vegetables. *J. Sci. Food Agric.* 81, 853–876. doi: 10.1002/jsfa.885
- Traka-Mavrona, E., Koutsika-Sotiriou, M., and Prita, T. (2000). Response of squash (*Cucurbita* spp.) as rootstock for melon (*Cucumis melo* L.). *Sci. Hortic.* 83, 353–362. doi: 10.1016/s0304-4238(99)00088-6
- Trionfetti-Nisini, P., Colla, G., Granati, E., Temperini, O., Crinò, P., and Saccardo, F. (2002). Rootstock resistance to *Fusarium* wilt and effect on fruit yield and quality of two muskmelon cultivars. *Sci. Hortic.* 93, 281–288. doi: 10.1016/s0304-4238(01)00335-1
- Turhan, A., Ozmen, N., Serbeci, M. S., and Seniz, V. (2011). Effects of grafting on different rootstocks on tomato fruit yield and quality. *Hortic. Sci.* 38, 142–149. doi: 10.1007/s00122-015-2462-8
- Verzera, A., Dima, G., Tripodi, G., Condurso, C., Crinò, P., and Romano, D. (2014). Aroma and sensory quality of honeydew melon fruits (*Cucumis melo* L. subsp. *Melo* var. *inodorus* H. Jacq.) in relation to different rootstocks. *Sci. Hortic.* 169, 118–124. doi: 10.1016/j.scientia.2014.02.008
- Verzera, A., Dima, G., Tripodi, G., Ziino, M., Lanza, C. M., and Mazzaglia, A. (2011). Fast quantitative determination of aroma volatile constituents in melon fruits by headspace solid-phase microextraction and gas chromatography-mass spectrometry. *Food Anal. Meth.* 4, 141–149. doi: 10.1007/s12161-010-9159
- Vinkovic-Vrcak, I., Samobor, V., Bojic, M., Medic-Saric, M., Vukobratovic, M., Erhardt, R., et al. (2011). The effect of grafting on the antioxidant properties of tomato (*Solanum lycopersicum* L.). *Spanish J. Agric. Res.* 9, 844–851. doi: 10.5424/sjar/20110903.414-10
- Wadano, A., Azeta, M., Itotani, S., Kanda, A., Iwaki, T., Taira, T., et al. (1999). Change of ascorbic acid level after grafting of tomato seedlings. *Z. Naturforsch.* 54, 830–833. doi: 10.1515/znc-1999-9-1032
- Wang, J., Jiang, L., and Wu, R. (2016). Plant grafting: how genetic exchange promotes vascular reconnection. *New Phytol.* 214, 56–65. doi: 10.1111/nph.14383
- Wu, R., Wang, X. R., Lin, Y., Ma, Y. Q., Liu, G., Yu, X. M., et al. (2013). Inter-species grafting caused extensive and heritable alterations of DNA methylation in Solanaceae plants. *PLoS ONE* 8:e61995. doi: 10.1371/journal.pone.0061995
- Xu, C. Q., Li, T. L., and Qui, H. Y. (2006). Effects of grafting on development, carbohydrate content, and sucrose metabolizing enzymes activities of muskmelon fruit. *Acta Hortic.* 33, 773–778.
- Yajima, I., Sakakibara, H., Ide, J., Yanai, T., and Hayashi, K. (1985). Volatile flavor components of watermelon (*Citrullus vulgaris*). *Agric. Biol. Chem.* 49, 3145–3150. doi: 10.1271/bbb1961.49.3145
- Yamaguchi, M., Hughes, D. L., Yabumoto, K., and Jennings, W. G. (1977). Quality of cantaloupe muskmelons: variability and attributes. *Sci. Hortic.* 6, 59–70. doi: 10.1016/0304-4238(77)90079-6
- Yamasaki, A., Yamashita, M., and Furuya, S. (1994). Mineral concentrations and cytokinin activity in the xylem exudate of grafted watermelons as affected by rootstocks and crop load. *J. Jpn. Soc. Hortic. Sci.* 62, 817–826. doi: 10.2503/jjshs.62.817
- Yang, Y. Z., Mao, L. Y., Jittayasothon, Y., Kang, Y. M., Jiao, C., Fei, Z. J., et al. (2015). Messenger RNA exchange between scions and rootstocks in grafted grapevines. *BMC Plant Biol.* 15:251. doi: 10.1186/s12870-015-0626-y
- Yativ, M., Hanany, I., and Wolf, S. (2010). Sucrose accumulation in watermelon fruits: genetic variation and biochemical analysis. *J. Plant Physiol.* 167, 589–596. doi: 10.1016/j.jplph.2009.11.009
- Yetisir, H., and Sari, N. (2003). Effect of different rootstock on plant growth, yield and quality of watermelon. *Austr. J. Exp. Agric.* 43, 1269–1274. doi: 10.1071/ea02095
- Yetisir, H., Sari, N., and Yncel, S. (2003). Rootstock resistance to *Fusarium* wilt and effect on watermelon fruit yield and quality. *Phytoparasitica* 31, 163–169. doi: 10.1007/bf02980786
- Zhang, B., Tieman, D., Jiao, C., Xu, Y., Chen, K., Fei, Z., et al. (2016). Chilling-induced tomato flavor loss is associated with altered volatile synthesis and transient changes in DNA methylation. *Proc. Nat. Acad. Sci. U.S.A.* 113, 12580–12585. doi: 10.1073/pnas.1613910113
- Zhang, W. N., Thieme, C. J., Kollwig, G., Apelt, F., Yang, L., Winter, N., et al. (2016). tRNA-related sequences trigger systemic mRNA transport in plants. *Plant Cell* 28, 1237–1249. doi: 10.1105/tpc.15.01056
- Zhao, X., Guo, Y., Huber, D. J., and Lee, J. (2011). Grafting effects on postharvest ripening and quality of 1-methylcyclopropene-treated muskmelon fruit. *Sci. Hortic.* 130, 581–587. doi: 10.1016/j.scientia.2011.08.010

Conflict of Interest Statement: The authors declare that the research was conducted in the absence of any commercial or financial relationships that could be construed as a potential conflict of interest.

Copyright © 2017 Kyriacou, Rouphael, Colla, Zrenner and Schwarz. This is an open-access article distributed under the terms of the Creative Commons Attribution License (CC BY). The use, distribution or reproduction in other forums is permitted, provided the original author(s) or licensor are credited and that the original publication in this journal is cited, in accordance with accepted academic practice. No use, distribution or reproduction is permitted which does not comply with these terms.



Assuring Potato Tuber Quality during Storage: A Future Perspective

M. C. Alamar, Roberta Tosetti, Sandra Landahl, Antonio Bermejo and Leon A. Terry*

Plant Science Laboratory, Cranfield University, Bedfordshire, United Kingdom

Potatoes represent an important staple food crop across the planet. Yet, to maintain tuber quality and extend availability, there is a necessity to store tubers for long periods often using industrial-scale facilities. In this context, preserving potato quality is pivotal for the seed, fresh and processing sectors. The industry has always innovated and invested in improved post-harvest storage. However, the pace of technological change has and will continue to increase. For instance, more stringent legislation and changing consumer attitudes have driven renewed interest in creating alternative or complementary post-harvest treatments to traditional chemically reliant sprout suppression and disease control. Herein, the current knowledge on biochemical factors governing dormancy, the use of chlorpropham (CIPC) as well as existing and chemical alternatives, and the effects of pre- and post-harvest factors to assure potato tuber quality is reviewed. Additionally, the role of genomics as a future approach to potato quality improvement is discussed. Critically, and through a more industry targeted research, a better mechanistic understanding of how the pre-harvest environment influences tuber quality and the factors which govern dormancy transition should lead to a paradigm shift in how sustainable storage can be achieved.

OPEN ACCESS

Edited by:

Maarten Hertog,
KU Leuven, Belgium

Reviewed by:

George A. Manganaris,
Cyprus University of Technology,
Cyprus

María Serrano,
Universidad Miguel Hernández
de Elche, Spain

Domingos Almeida,
Universidade de Lisboa, Portugal

***Correspondence:**

Leon A. Terry
l.a.terry@cranfield.ac.uk

Specialty section:

This article was submitted to
Plant Breeding,
a section of the journal
Frontiers in Plant Science

Received: 26 May 2017

Accepted: 14 November 2017

Published: 28 November 2017

Citation:

Alamar MC, Tosetti R, Landahl S, Bermejo A and Terry LA (2017)
Assuring Potato Tuber Quality during Storage: A Future Perspective.
Front. Plant Sci. 8:2034.
doi: 10.3389/fpls.2017.02034

Keywords: *Solanum tuberosum*, dormancy, sprouting, reducing sugars, phytohormones

INTRODUCTION

Potato tubers (*Solanum tuberosum*) have been cultivated for more than 6000 years. Currently, potato is the fourth most important crop produced worldwide with an annual production of ca. 382 MT. Europe and Asia are the biggest producers with a share of 40.7% each, followed by America and Africa (12.6 and 4.5%, respectively) (FAOSTAT, 2014¹). Potatoes provide an excellent source of nutrients and vitamins, but year-round availability depends on industrial-scale storage, especially in countries which rely on an annual crop. In the United Kingdom, approximately half of the total harvested tubers are stored for up to 11 months (Dale, 2014). Sub-optimal handling, poor tuber quality, and deficient post-harvest storage can lead to significant amounts of waste. The United Kingdom recorded overall losses of 17% (770,000 tons) in 2012, where premature sprouting and rotting during storage was the main cause of wastage (Terry et al., 2011; Pritchard et al., 2012). The United Kingdom outlined a strategy for a more sustained and secure food system in its Food Standard Agency (FSA) Strategic Plan 2015–2020, which aims, among several targets, to reduce waste (Food Standards Agency [FSA], 2015). This strategy is aligned with consumers' requirements of improved nutritional value and sensory attributes, and with new regulation demanding the reduction of agrochemical usage (Lacy and Huffman, 2016).

¹<http://www.fao.org/faostat/>

Current challenges in the potato industry include the preservation of tuber quality throughout storage, restriction of isopropyl-*N*-(3-chlorophenyl) carbamate (chlorpropham or CIPC) residues (mainly for ware potatoes destined for processing), control of sweetening processes, and ensuring tuber marketability (visual appearance is the main factor driving consumers purchase of fresh potatoes; Terry et al., 2013).

FACTORS GOVERNING DORMANCY

Dormancy break in potato tubers is a physiological phenomenon that is regulated by both exogenous (environmental factors) and endogenous signals (Sonnewald and Sonnewald, 2014). The relative concentration of several biochemical compounds such as plant growth regulators [*viz.* abscisic acid (ABA), auxins, cytokinins (CKs), gibberellins (GAs), ethylene, and strigolactones (SLs)] and other compounds (*viz.* carbohydrates and organic acids) are believed to orchestrate the onset and further development of dormancy break (Sonnewald, 2001; Viola et al., 2007; Pasare et al., 2013).

Endogenous ethylene is required at the earliest stage of dormancy initiation (endodormancy induction) (Suttle, 1998); however, its role during dormancy and sprouting is still unclear. Exogenous ethylene ($10 \mu\text{L L}^{-1}$) has been reported to break endodormancy following short-term treatments (Foukaraki et al., 2014), but also to inhibit sprout growth and promote ecodormancy when supplied continuously – either starting immediately after harvest or at first indication of sprouting (Foukaraki et al., 2016a). However, work carried out on cv. Russet Burbank minitubers showed that ethylene was not involved in hormone-induced dormancy break (Suttle, 2009). These findings support the suggestion that the effect of ethylene depends on the physiological state of potato tubers.

The role of ABA is better understood. It is well known that a sustained synthesis and action of ABA is required for dormancy induction and maintenance (Suttle, 2004; Mani et al., 2014). That said, although ABA levels decrease as endodormancy weakens, there is no evidence of an ABA threshold concentration for dormancy release (Biemelt et al., 2000; Destefano-Beltrán et al., 2006; Suttle et al., 2012; Ordaz-Ortiz et al., 2015). It is also known that there is cross-talk between ABA and other phytohormones (Chang et al., 2013), as well as with sugar metabolic pathways, which facilitates the onset of dormancy break and further sprouting (Brady, 2013). Nevertheless, the increase in ABA as a result of exogenous ethylene application has been postulated to delay dormancy break (Foukaraki et al., 2016b). Concomitant to the ABA decline, there is an increase in sucrose contents, which is considered a prerequisite for bud outgrowth (Viola et al., 2007; Sonnewald and Sonnewald, 2014). In this context, auxins are essential for their role in vascular development. Auxins favor the symplastic reconnection of the apical bud region – a discrete cell domain which remains symplastically isolated throughout tuberisation. This reconnection is, therefore, essential for sucrose to reach the

meristematic apical bud. High sucrose levels promote trehalose-6-phosphate accumulation (T6P) which supports sprouting probably decreasing sensitivity to ABA (Debast et al., 2011; Tsai and Gazzarrini, 2014).

It has also been demonstrated that, CKs and GAs are required for the reactivation of meristematic activity and sprout growth (Hartmann et al., 2011). Just prior to dormancy break, an increase in both cytokinin concentration and sensitivity have been reported as key factors for meristematic reactivation (Suttle, 2004). Furthermore, CKs coordinated with auxins stimulate sprout elongation (Aksanova et al., 2013). Sensitivity to GAs, which is negatively affected by SLs, increases throughout post-harvest storage and is possibly responsible for sprout vigor (Roumeliotis et al., 2012). SLs may be related to paradormancy establishment instead of eco- and endodormancy since they are key as regulators of lateral bud development (Pasare et al., 2013).

Optimum length of dormancy differs depending on cultivars and final usage of potato tubers. Thus, longer dormancy and delayed sprouting (at a desired time) would be best for ware potatoes storage, while accelerated sprouting would be preferable for seed potatoes. As reviewed by Eshel and Teper-Bamnolker (2012), sprouting has been induced in seed potatoes by the application of “Rinditie” (commercial mixture of ethylene chlorhydrin, ethylene dichloride, and carbon tetrachloride), bromoethane, carbon disulphide, and GAs (Sonnewald and Sonnewald, 2014).

USE OF CIPC DURING POTATO STORAGE

Suppression of sprout growth in potato tubers represents a crucial step to manage potato quality during storage. Sprouting can be inhibited by the application of chemical sprout suppressants and by controlling environmental conditions, e.g., cold storage, tuned humidity and regulated gas composition conditions. Due to its high efficacy, CIPC is the world's most utilized sprout suppressant chemical; it inhibits meristematic cell division, delaying sprout development. Nevertheless, concerns about CIPC usage have increased following studies which described toxic and carcinogenic properties of CIPC and its metabolites (Balaji et al., 2006; El-Awady Aml et al., 2014). However, evidence on the apparent toxicity of CIPC is sparse.

The use of CIPC is covered by the Code of Practice for using plant protection products (DEFRA, 2006). To deal with the continuous updates and concerns over exceedances in CIPC regulation, the United Kingdom assembled in 2008 the Potato Industry CIPC Stewardship Group (PICSG), which is supported by the potato industry and CIPC-related companies. From July 2017, new legislation came into force establishing that CIPC applications (36 g ton^{-1} for processing potatoes and 24 g ton^{-1} for fresh market tubers) must be done through ‘active recirculation’ of storage air by fans to optimize CIPC application (AHDB, 2017). Thus, increasing legislation constraints are driving the potato industry to seek alternative novel technologies which are able to extend post-harvest storage while maintaining tuber quality. Industry aims to

provide high quality potatoes with contained costs for storage management; for this reason, it is pivotal to have sprout suppression technologies which can be exploited in the long-term.

SPROUT CONTROL DURING POST-HARVEST – PHYSICAL AND CHEMICAL ALTERNATIVES TO CIPC

Premature sprouting is one of the major causes of loss during post-harvest storage of ware potatoes, since it reduces the number of marketable tubers and fresh weight due to water loss from sprout surfaces, and the remobilisation of starch (Sonnewald and Sonnewald, 2014). The sprout suppressant CIPC is, in general, commercially applied as a thermal hotfog (single or multiple treatments) during prolonged potato storage (Blenkinsop et al., 2002). However, legislative bodies are constraining its use. Alternatives (or supplements) to traditional sprout control include hydrogen peroxide plus (HPP) (Al-Mughrabi, 2010; Mani et al., 2014), 1,4-dimethylnaphthalene (1,4-DMN) (de Weerd et al., 2010), UV-C (Cools et al., 2014), essential oils and ethylene. Continuous exogenous ethylene supplementation has been commercially approved as a sprout suppressant in United Kingdom by the Chemicals Regulation Directorate (CRD) (Briddon, 2006); yet, the way in which ethylene inhibits sprout growth has not been completely clarified. It is known that ethylene supplementation can increase the content of reducing sugars in tubers (Daniels-Lake et al., 2005), which negatively affects processed potato quality. Nevertheless, late ethylene supplementation (at eye movement stage) was efficacious at delaying tuber sprouting, and more effective preventing accumulation of reducing sugars when compared to early supplementation (applied after curing and from the beginning of storage) (Foukaraki et al., 2014). Therefore, late ethylene supplementation may reduce storage costs whilst providing high quality tubers. The ethylene-induced increase in ABA levels may explain this delay of dormancy break (Foukaraki et al., 2016b).

Low temperature conditions is a worldwide used storage technology, which delays tuber sprouting. Besides low temperature, other physical methods such as gamma radiation have been shown to be effective in controlling sprout growth (Rezaee et al., 2013); yet its use is subject to strict legislation. Short wave ultraviolet radiation has been likewise suggested as an alternative or complementary method for sprout control (Pristijono et al., 2016). Thus, moderate UV-C doses ($5\text{--}20\text{ kJ m}^{-2}$) have been found to suppress sprout length and sprout incidence in a range of potato cultivars when applied at first indication of sprouting (Cools et al., 2014). The direct deleterious effect on the meristematic tissue, combined with potential changes in tuber biochemistry have been postulated as mechanisms by which gamma and UV-C radiation control sprouting.

The use of alternative chemical sprout suppressants during post-harvest aim at damaging the meristematic tissue to cease or disrupt cell proliferation; for example, local necrosis of

the bud meristem was found after the application of mint essential oils (Teper-Bamnolker et al., 2010). Previously, Eshel et al. (2008) had shown the potential of mint oil vapor to be used at large scale to control sprouting in four commercial potatoes cultivars. Repeated applications of Talent®, trade name for a monoterpane (carvone) derived from caraway seed, can inhibit sprout growth for up to a year; however, the number of applications required may make this solution uncompetitive when compared to CIPC (Npcs Board of Consultants and Engineers, 2007). Additionally, both, HPP and 1,4-DMN have been successfully applied as a fog to control sprouting. Afek et al. (2000) achieved complete sprout suppression (6 months at $10 \pm 1^\circ\text{C}$) when potatoes were treated with HPP for 10 h; whereas the use of 1,4-DMN (at a rate of $20\text{ }\mu\text{L L}^{-1}$) needs more investigation to elucidate whether it is environmentally safe (Oteef, 2008).

EFFECT OF PRE-HARVEST FACTORS AND STORAGE CONDITIONS ON TUBER QUALITY

The quality of potatoes is established in the field and can only be preserved during post-harvest. Abiotic factors influencing tuber maturity, cultivar- and season-variability have great impact on final quality. Driskill et al. (2007) reported that the processing quality (fry color) of younger tubers (late planting) was better than that of tubers planted earlier. High nutrient demand on soil for good tuber quality requires high organic matter and nitrogen input (Nesbitt and Adl, 2014). Sustainable agricultural practices such as balanced fertilizer regimes improved not only tuber yield but also marketing quality of potato (e.g., tuber size; Tan et al., 2016). Vine desiccation (diquat, comm. Reglone®) is another factor which strongly impacts quality; it triggers both maturation of the tuber periderm and stolon release, and in seed potato production it can also control tuber size. To manage all these variables a multifactorial approach is recommended to mitigate side effects which may affect quality (De Meulenaer et al., 2008).

After harvest, tuber quality management aims to delay dormancy break and limit weight loss and sweetening of potatoes. Senescent sweetening is a natural process that occurs as a result of tuber aging; it is irreversible and involves cellular breakdown. Following cellular breakdown, structural and non-structural carbohydrates are depolymerized by hydrolytic enzymes. To delay this process, correct storage conditions are crucial. Cold storage is commonly used to control sprouting, yet temperature management depends on the intended market: tubers for the fresh market can be stored at temperatures below 7°C while tubers destined for the processing market need higher temperature ($8\text{--}13^\circ\text{C}$) to preserve frying quality. Quality loss is also caused by ‘cold-induced sweetening’ when sucrose hydrolysis leads to reducing sugars accumulation; although it can be partially reversed by temperature reconditioning (Driskill et al., 2007). Cold-induced sweetening, however, does not only depend on post-harvest storage conditions but also on potato variety (Elmore et al., 2016) and growing location

(Muttucumaru et al., 2017). Low levels of reducing sugars are preferred in processing potatoes since when tubers are cooked at high temperatures ($>120^{\circ}\text{C}$) the Maillard reaction can occur. During the Maillard reaction, reducing sugars are responsible for the browning (non-enzymatic reactions) of the product (French fries, crisps) and, as a side effect acrylamide may also accumulate. As recently reviewed by Muttucumaru et al. (2017), the principal pathway for acrylamide formation is the deamination and decarboxylation of free asparagine under high temperatures and its reaction with reducing sugars. Potato is one of the major contributors to dietary acrylamide (Group 2A, ‘probably carcinogenic to humans’) intake in the European Union (Borda and Alexe, 2011). The European Commission issued ‘indicative’ levels (not regulatory or safety thresholds) of acrylamide in food in 2011, which were revised downward for many products in 2013 (e.g., crisps = $100\text{ }\mu\text{g kg}^{-1}$ and French fries = $600\text{ }\mu\text{g kg}^{-1}$). In this context, FoodDrinkEurope (2013) created a ‘Toolbox’ which compiles different strategies from the food industry to reduce acrylamide formation by modifying food processing.

As previously mentioned, continuous ethylene supplementation is currently used as a sprout suppressant during storage; yet, it can induce sucrose hydrolysis (ethylene-induced sweetening). A recent study has shown that this type of sweetening can be prevented with a single application (24 h) of 1-methylcyclopropene (1-MCP) prior to early and late ethylene supplementation (Foukaraki et al., 2016a). The impact of CO_2 , another storage extension gas, on frying quality is less clear. Studies on processing potato varieties showed negative effects on fry color when ethylene and CO_2 were applied together. Despite this, cultivar, gas concentration and timing, and seasonality strongly affect responses of tubers to CO_2 treatment (Daniels-Lake, 2013).

THE ROLE OF GENOMICS IN POTATO QUALITY IMPROVEMENT

Breeding programs aim to develop new cultivars with improved features (productivity, pathogens- and stress-resistance). Due to the complex genetic heterogeneity of modern potato cultivars, conventional potato breeding requires approximately 10 years for the phenotypic selection cycle: from crossing to variety release (Slater et al., 2014). The increasing knowledge about the geno-phenotypic relationships and the availability of new technologies has allowed for the development of ‘precision breeding.’ Precision breeding increases the efficiency in selection of targeted traits through genetics techniques (e.g., marker assisted selection, MAS) and shorten the selection cycle (Gebhardt, 2013). These have been used to identify disease resistance genes in wild relatives and to cross them into commercial potatoes (Gebhardt et al., 2014). The knockout of the vacuolar invertase gene, *Vinv*, in potato tubers resulted in cold induced-sweetening inhibition and high quality processed tubers (Clasen et al., 2016). Other simple traits have been identified for tuber shape, tissue colors, and eye depth (Slater et al., 2014). Despite these advances, the majority of commercially

interesting traits are complex. Post-harvest traits such as tuber yield, starch content, crisp color, or bruising susceptibility are regulated by multiple genetic and environmental factors (Gebhardt, 2013). The complexity of these traits requires a deeper knowledge of geno-phenotypic interactions and more powerful technologies.

The release of the potato genome (Potato Genome Sequencing Consortium, 2011), improved gene annotations and linkage maps led to the development of new genetic resources (e.g., single nucleotide polymorphisms arrays, SNPs arrays; genome-wide association studies, GWAS). These new technologies have been exploited to analyze the regulation of complex traits and QTL (quantitative traits loci). The Illumina Infinium 8303 SNPs Potato Array (Hamilton et al., 2011; Douches et al., 2014) allowed improved understanding of genetic control for several complex traits such as tuber dormancy and starch metabolism (Schreiber et al., 2014; Sharma et al., 2014). GWAS was proved beneficial when clarifying other quality traits of potato tubers [i.e., maturity and ‘after baking darkening’ (Björn et al., 2008; Ramakrishnan et al., 2015)]. Precision breeding has decreased breeding costs, reducing field-related expenses, and simplified the selection of interesting relatives. Furthermore, continuous progress of new genetic technologies has allowed the costs of genotyping to be cut, and the quicker screening of large populations to be more accessible. Other ‘omics’ technologies, such as transcriptomics, proteomics, and metabolomics, can be coupled with genomics and may improve the identification of quality candidate traits (Gebhardt, 2013).

Gene editing technologies are greatly increasing due to the generation of transgenic-free genetically modified organisms; additionally, gene editing allows targeted mutation with high specificity and precision in selected loci (Georges and Ray, 2017). This is achieved by inducing breaks in the genome and utilizing DNA repair pathways to modify target genes (Curtin et al., 2012). Double-strands breaks (DBS) are induced by endonuclease enzymes (like transcription activator-like effector nucleases (TALEN), and CRISPR-associated (Cas) endonucleases). Following DBS, the DNA repair pathways may inactivate a gene (knockout) through a non-homologous end joining (NHEJ) pathway, or replace-insert a gene through homologous recombination (HR) pathway (Symington and Gautier, 2011). Gene editing with insertion is often achieved by combining the action of *Agrobacterium tumefaciens* with plant viruses. This combination showed very promising results when *Agrobacterium* was coupled with DNA virus *Geminivirus* replicon (GVR), which allows a larger carrying capacity compared to RNA viruses. Potato plants modified with this technique exhibited reduced herbicide susceptibility (Butler et al., 2016).

CONCLUSION

In order to assure future potato tuber quality, industry and academic communities have to work together while considering consumers preferences. Deploying molecular and

improved phenotyping techniques to increase the knowledge of mechanisms which mediate physiological responses during pre-harvest production, post-harvest storage and processing (*viz.* acrylamide formation) will improve tuber quality. These combined efforts will benefit the development of new cultivars with improved features and provide guidelines for more sustainable agricultural techniques and storage strategies. At the same time, alternative pre- and post-harvest technologies have to be embraced and further implemented by the potato industry. Through a more industry targeted research, the

combination of genomics, pre- and post-harvest technologies will aid the preservation, enhancement, and viability of future tuber quality.

AUTHOR CONTRIBUTIONS

MA: Paper writing (35%). RT: Paper writing (35%). SL: Paper writing (10%). AB: paper writing (10%). LT: Overall supervision (10%).

REFERENCES

- Afek, U., Orenstein, J., and Nuriel, E. (2000). Using HPP (hydrogen peroxide plus) to inhibit potato sprouting during storage. *Am. J. Potato Res.* 77, 63–65. doi: 10.1007/BF02853663
- AHDB (2017). Be CIPC Compliant 2017. Available at: <http://www.cipccompliant.co.uk>
- Aksanova, N. P., Sergeeva, L. I., Konstantinova, T. N., Golyanovskaya, S. A., Kolachevskaya, O. O., and Romanov, G. A. (2013). Regulation of potato tuber dormancy and sprouting. *Russ. J. Plant Physiol.* 60, 301–312. doi: 10.1134/S1021443713030023
- Al-Mughrabi, K. (2010). Post harvest treatment with hydrogen peroxide suppresses silver scurf (*Helminthosporium solani*), dry rot (*Fusarium sambucinum*), and soft rot (*Erwinia carotovora* subsp. *carotovora*) of stored potatoes. *Am. J. Plant Sci. Biotechnol.* 4, 74–81.
- Balaji, V., Chandra, S., Goswami, D. A., Das, S. K., Mandal, T. K., Chakraborty, A. K., et al. (2006). Toxicokinetics, metabolism, and microsomal studies of chlorpropham in rats. *Toxicol. Environ. Chem.* 88, 527–539. doi: 10.1080/02772240600741528
- Biemelt, S., Hajirezaei, M., Hentschel, E., and Sonnewald, U. (2000). Comparative analysis of abscisic acid content and starch degradation during storage of tubers harvested from different potato varieties. *Potato Res.* 43, 371–382. doi: 10.1007/BF02360541
- Björn, B., Paulo, M. J., Mank, R. A., Van Eck, H. J., and Van Eeuwijk, F. A. (2008). Association mapping of quality traits in potato (*Solanum tuberosum* L.). *Euphytica* 161, 47–60. doi: 10.1534/g3.114.012377
- Blenkinsop, R. W., Copp, L. J., Yada, R. Y., and Marangoni, A. G. (2002). Changes in compositional parameters of tubers of potato (*Solanum tuberosum*) during low-temperature storage and their relationship to chip processing quality. *J. Agric. Food Chem.* 50, 4545–4553. doi: 10.1021/jf0255984
- Borda, D., and Alexe, P. (2011). Acrylamide levels in food. *Romanian J Food D. Sci.* 1, 3–15.
- Brady, S. M. (2013). When the time is ripe. *eLife* 2:e00958. doi: 10.7554/eLife.00958
- Briddon, A. (2006). *The Use of Ethylene for Sprout Control*. Oxford: British Potato Council.
- Butler, N. M., Baltes, N. J., Voytas, D. F., and Douches, D. S. (2016). Geminivirus-mediated genome editing in potato (*Solanum tuberosum* L.) using sequence-specific nucleases. *Front. Plant Sci.* 7:1045. doi: 10.3389/fpls.2016.01045
- Chang, K. N., Zhong, S., Weirauch, M. T., Hon, G., Pelizzola, M., Li, H., et al. (2013). Temporal transcriptional response to ethylene gas drives growth hormone cross-regulation in *Arabidopsis*. *eLife* 2:e00675. doi: 10.7554/eLife.00675
- Clasen, B. M., Stoddard, T. J., Luo, S., Demorest, Z. L., Li, J., Cedrone, F., et al. (2016). Improving cold storage and processing traits in potato through targeted gene knockout. *Plant Biotechnol. J.* 14, 169–176. doi: 10.1111/pbi.12370
- Cools, K., Alamar, M. C., and Terry, L. A. (2014). Controlling sprouting in potato tubers using ultraviolet-C irradiance. *Postharvest Biol. Technol.* 98, 106–114. doi: 10.1016/j.postharvbio.2014.07.005
- Curtin, S. J., Voytas, D. F., and Stupar, R. M. (2012). Genome engineering of crops with designer nucleases. *Plant Genome* 5, 42–50. doi: 10.3835/plantgenome2012.06.0008
- Dale, F. (2014). *Breeding for Storage*. Available at: https://potatoes.ahdb.org.uk/sites/default/files/publication_upload/Breeding%20for%20storage%20-%20Finlay%20Dale.pdf
- Daniels-Lake, B. J. (2013). The combined effect of CO₂ and ethylene sprout inhibitor on the fry colour of stored potatoes (*Solanum tuberosum* L.). *Potato Res.* 56, 115–126. doi: 10.1007/s11540-013-9234-0
- Daniels-Lake, B. J., Prange, R. K., Nowak, J., Asiedu, S. K., and Walsh, J. R. (2005). Sprout development and processing quality changes in potato tubers stored under ethylene: 1. Effects of ethylene concentration. *Am. J. Potato Res.* 82, 389–397. doi: 10.1007/BF02871969
- De Meulenaer, B., De Wilde, T., Mestdagh, F., Govaert, Y., Ooghe, W., Fraselle, S., et al. (2008). Comparison of potato varieties between seasons and their potential for acrylamide formation. *J. Sci. Food Agric.* 88, 313–318. doi: 10.1002/jsfa.3091
- de Weerd, J. W., Thornton, M. J., and Shafii, B. (2010). Sprout suppression residue levels of 1,4-dimethylnaphthalene (1,4DMN) in potato cultivars. *Am. J. Potato Res.* 87, 434–445. doi: 10.1007/s12230-010-9146-3
- Debast, S., Nunes-Nesi, A., Hajirezaei, M. R., Hofmann, J., Sonnewald, U., Fernie, A. R., et al. (2011). Altering trehalose-6-phosphate content in transgenic potato tubers affects tuber growth and alters responsiveness to hormones during sprouting. *Plant Physiol.* 156, 1754–1771. doi: 10.1104/pp.111.179903
- DEFRA (2006). *Pesticides - Code of Practice for Using Plant Protection Products*. London: Department for Environment, Food and Rural Affairs.
- Destefano-Beltrán, L., Knauber, D., Huckle, L., and Suttle, J. C. (2006). Effects of postharvest storage and dormancy status on ABA content, metabolism, and expression of genes involved in ABA biosynthesis and metabolism in potato tuber tissues. *Plant Mol. Biol.* 61, 687–697. doi: 10.1007/s11103-006-0042-7
- Douches, D., Hirsch, C. N., Manrique-Carpintero, N. C., Massa, A. N., Coombs, J., Hardigan, D., et al. (2014). The contribution of the Solanaceae coordinated agricultural project to potato breeding. *Potato Res.* 57, 215–224. doi: 10.1007/s11540-014-9267-z
- Driskill, E. P., Knowles, L. O., and Knowles, N. R. (2007). Temperature-induced changes in potato processing quality during storage are modulated by tuber maturity. *Am. J. Potato Res.* 84, 367–383. doi: 10.1007/BF02987183
- El-Awady Aml, A., Moghazy, A. M., Gouda, A. E. A., and Elshatoury, R. S. A. (2014). Inhibition of sprout growth and increase storability of processing potato by antisprouting agent. *Trends Hortic. Res.* 4, 31–40. doi: 10.3923/thr.2014.31.40
- Elmore, J. E., Briddon, A., Dodson, A. T., Muttucumaru, N., Halford, N. G., and Mottram, D. S. (2016). Acrylamide in potato crisps prepared from 20 UK-grown varieties: effects of variety and tuber storage time. *Food Chem.* 182, 1–8. doi: 10.1016/j.foodchem.2015.02
- Eshel, D., Orenstein, J., Tsror, L., and Hazanovsky, M. (2008). Environmentally friendly method for the control of sprouting and tuber-borne diseases in stored potato. *Acta Hortic.* 830, 363–368. doi: 10.17660/ActaHortic.2009.830.51
- Eshel, D., and Teper-Bamnolker, P. (2012). Can loss of apical dominance in potato tuber serve as a marker of physiological age? *Plant Signal. Behav.* 7, 1158–1162. doi: 10.4161/psb.21324
- FoodDrinkEurope (2013). *Annual Report 2013*. Available at: http://www.fooddrinkeurope.eu/uploads/publications_documents/FoodDrinkEurope_Annual_Report_2013.pdf
- Food Standards Agency [FSA] (2015). *Food We Can Trust - Strategic Plan 2015–2020*. Available at: https://www.food.gov.uk/sites/default/files/FSA%20strategy%20document%202015-2020_April%202015_interactive%20%282%29.pdf
- Foukaraki, S. G., Cools, K., Chope, G. A., and Terry, L. A. (2014). Effect of the transition between ethylene and air storage on the post-harvest quality in six UK-grown potato cultivars. *J. Hortic. Sci. Biotechnol.* 89, 599–606. doi: 10.1080/14620316.2014.11513126

- Foukaraki, S. G., Cools, K., Chope, G. A., and Terry, L. A. (2016a). Impact of ethylene and 1-MCP on sprouting and sugar accumulation in stored potatoes. *Postharvest Biol. Tec.* 114, 95–103. doi: 10.1016/j.postharvbio.2015.11.013
- Foukaraki, S. G., Cools, K., and Terry, L. A. (2016b). Differential effect of ethylene supplementation and inhibition on abscisic acid metabolism of potato (*Solanum tuberosum* L.) tubers during storage. *Postharvest Biol. Tec.* 112, 87–94. doi: 10.1016/j.postharvbio.2015.10.002
- Gebhardt, C. (2013). Bridging the gap between genome analysis and precision breeding in potato. *Trends Genet.* 29, 248–256. doi: 10.1016/j.tig.2012.11.006
- Gebhardt, C., Urbany, C., and Stich, B. (2014). “Dissection of potato complex traits by linkage and association genetics as basis for developing molecular diagnostics in breeding programs,” in *Genomics of Plant Genetic Resources*, eds R. Tuberosa, A. Graner, and E. Frison (Dordrecht: Springer), 47–85.
- Georges, F., and Ray, H. (2017). Genome editing of crops: a renewed opportunity for food security. *GM Crops Food* 8, 1–12. doi: 10.1080/21645698.2016.1270489
- Hamilton, J. P., Hansey, C. N., Whitty, B. R., Stofel, K., Massa, A. N., Van Deynze, A., et al. (2011). Single nucleotide polymorphism discovery in elite North American potato germplasm. *BMC Genomics* 12:302. doi: 10.1186/1471-2164-12-302
- Hartmann, A., Senning, M., Hedden, P., Sonnewald, U., and Sonnewald, S. (2011). Reactivation of meristem activity and sprout growth in potato tubers require both cytokinin and gibberellin. *Plant Physiol.* 155, 776–796. doi: 10.1104/pp.110.168252
- Lacy, K., and Huffman, W. E. (2016). Consumer demand for potato products and willingness-to-pay for low-acrylamide, sulfite-free fresh potatoes and dices: evidence from lab auctions. *J. Agric. Resour. Econ.* 41, 116–37.
- Mani, F., Bettaiib, T., Doudech, N., and Hannachi, C. (2014). Physiological mechanisms for potato dormancy release and sprouting: a review. *Afr. Crop Sci. J.* 22, 155–174.
- Muttucumar, N., Powers, S. J., Elmore, J. S., Dodson, A., Briddon, A., Mottram, D. S., et al. (2017). Acrylamide-forming potential of potatoes grown at different locations, and the ratio of free asparagine to reducing sugars at which free asparagine becomes a limiting factor for acrylamide formation. *Food Chem.* 220, 76–86. doi: 10.1016/j.foodchem.2016.09.199
- Nesbitt, J. E., and Adl, S. M. (2014). Differences in soil quality indicators between organic and sustainably managed potato fields in Eastern Canada. *Ecol. Indic.* 37, 119–130. doi: 10.1016/j.ecolind.2013.10.002
- Npc Board of Consultants and Engineers (2007). *Potato and Potato Products Cultivation, Seed Production, Manuring, Harvesting, Organic Farming, Storage and Processing*. Delhi: NIIR Project Consultancy Services.
- Ordaz-Ortiz, J. J., Foukaraki, S. G., and Terry, L. A. (2015). Assessing temporal flux of plant hormones in stored processing potatoes using high definition accurate mass spectrometry. *Hortic. Res.* 2:15002. doi: 10.1038/hortres.2015.2
- Oteef, M. D. Y. (2008). *Analysis of the Potato Sprout Inhibitor 1, 4-Dimethylnaphthalene: HPLC Method Development and Applications*. Ph.D. thesis, University of Glasgow, Glasgow.
- Pasare, S. A., Ducreux, L. J., Morris, W. L., Campbell, R., Sharma, S. K., Roumeliotis, E., et al. (2013). The role of the potato (*Solanum tuberosum*) CCD8 gene in stolon and tuber development. *New Phytol.* 198, 1108–1120. doi: 10.1111/nph.12217
- Potato Genome Sequencing Consortium (2011). Genome sequence and analysis of the tuber crop potato. *Nature* 475, 189–195. doi: 10.1038/nature10158
- Pristijono, P., Scarlett, C. J., Bowyer, M. C., Vuong, Q. V., Stathopoulos, C. E., et al. (2016). “Effect of UV-C irradiation on sprouting of potatoes in storage,” in *Proceedings of the 8th International Postharvest Symposium*, Murcia.
- Pritchard, S., Lee, J., Tao, C. W., Burgess, P., Allchurch, E., Campbell, A., et al. (2012). WRAP. Reducing Supply Chain and Consumer Potato Waste (RBC820-004). Available at: <http://www.wrap.org.uk/sites/files/wrap/Amcor%20project%20report%20final%2C%202003%20Jan%202012.pdf>
- Ramakrishnan, A. P., Ritland, C. E., Sevillano, R. H. B., and Riseman, A. (2015). Review of potato molecular markers to enhance trait selection. *Am. J. Potato Res.* 92, 455–472. doi: 10.1007/s12230-015-9455-7
- Rezaee, M., Almassi, M., Minaei, S., and Paknejad, F. (2013). Impact of post-harvest radiation treatment timing on shelf life and quality characteristics of potatoes. *J. Food Sci. Technol.* 50, 339–345. doi: 10.1007/s13197-011-0337-9
- Roumeliotis, E., Kloosterman, B., Oortwijn, M., Kohlen, W., Bouwmeester, H. J., Visser, R. G., et al. (2012). The effects of auxin and strigolactones on tuber initiation and stolon architecture in potato. *J. Exp. Bot.* 63, 4539–4547. doi: 10.1093/jxb/ers132
- Schreiber, L., Nader-Nieto, A. C., Schönhalz, E. M., Walkemeier, B., and Gebhardt, C. (2014). SNPs in genes functional in starch-sugar interconversion associate with natural variation of tuber starch and sugar content of potato (*Solanum tuberosum* L.). *G3* 4, 1797–1811. doi: 10.1534/g3.114.012377
- Sharma, R., Bhardwaj, V., Dalamu, D., Kaushik, S. K., Singh, B. P., Sharma, S., et al. (2014). Identification of elite potato genotypes possessing multiple disease resistance genes through molecular approaches. *Sci. Hortic.* 179, 204–211. doi: 10.1016/j.scientia.2014.09.018
- Slater, A. T., Cogan, N. O., Hayes, B. J., Schultz, L., Dale, M. F. B., Bryan, G. J., et al. (2014). Improving breeding efficiency in potato using molecular and quantitative genetics. *Theor. Appl. Genet.* 127, 2279–2292. doi: 10.1007/s00122-014-2386-8
- Sonnewald, S., and Sonnewald, U. (2014). Regulation of potato tuber sprouting. *Planta* 239, 27–38. doi: 10.1007/s00425-013-1968-z
- Sonnewald, U. (2001). Control of potato tuber sprouting. *Trends Plant Sci.* 6, 333–335. doi: 10.1016/S1360-1385(01)02020-9
- Suttle, J. C. (1998). Involvement of ethylene in potato microtuber dormancy. *Plant Physiol.* 118, 843–848. doi: 10.1104/pp.118.3.843
- Suttle, J. C. (2004). Physiological regulation of potato tuber dormancy. *Am. J. Potato Res.* 81:253. doi: 10.1007/BF02871767
- Suttle, J. C. (2009). Ethylene is not involved in hormone-and bromoethane-induced dormancy break in Russet Burbank minitubers. *Am. J. Potato Res.* 86, 278–285. doi: 10.1007/s12230-009-9081-3
- Suttle, J. C., Abrams, S. R., De Stefano-Beltrán, L., and Huckle, L. L. (2012). Chemical inhibition of potato ABA-8'-hydroxylase activity alters *in vitro* and *in vivo* ABA metabolism and endogenous ABA levels but does not affect potato microtuber dormancy duration. *J. Exp. Bot.* 63, 5717–5725. doi: 10.1093/jxb/ers146
- Symington, L. S., and Gautier, J. (2011). Double-strand break end resection and repair pathway choice. *Annu. Rev. Genet.* 45, 247–271. doi: 10.1146/annurevgenet-110410-132435
- Tan, B., Huang, Z., Yin, Z., Min, X., Liu, Y. G., Wu, X., et al. (2016). Preparation and thermal properties of shape-stabilized composite phase change materials based on polyethylene glycol and porous carbon prepared from potato. *RSC Adv.* 6, 15821–15830. doi: 10.1039/C5RA25685B
- Teper-Bamnolker, P., Dudai, N., Fischer, R., Belausov, E., Zemach, H., Shoseyov, O., et al. (2010). Mint essential oil can induce or inhibit potato sprouting by differential alteration of apical meristem. *Planta* 232, 179–186. doi: 10.1007/s00425-010-1154-5
- Terry, L. A., Medina, A., Foukaraki, S., and Whitehead, P. (2013). *Review of Factors Affecting Fruit and Vegetable Demand. Defra - FO0438*. Available at: http://www.WRAPNI.org.uk/sites/files/wrap/Resource_Map_Fruit_and_Veg_final_6_june_2011.fc479c40.10854.pdf
- Terry, L. A., Mena, C., Williams, A., Jenney, N., and Whitehead, P. (2011). *Fruit and Vegetables Resource Maps - RSC-008*. Available at: http://www.WRAPNI.org.uk/sites/files/wrap/Resource_Map_Fruit_and_Veg_final_6_june_2011.fc479c40.10854.pdf
- Tsai, A. Y. L., and Gazzarrini, S. (2014). Trehalose-6-phosphate and SnRK1 kinases in plant development and signalling: the emerging picture. *Front. Plant Sci.* 5:119. doi: 10.3389/fpls.2014.00119
- Viola, R., Pelloux, J., van der Ploeg, A., Gillespie, T., Marquis, N., Roberts, A. G., et al. (2007). Symplastic connection is required for bud outgrowth following dormancy in potato (*Solanum tuberosum* L.) tubers. *Plant Cell Environ.* 30, 973–983. doi: 10.1111/j.1365-3040.2007.01692.x
- Conflict of Interest Statement:** The authors declare that the research was conducted in the absence of any commercial or financial relationships that could be construed as a potential conflict of interest.
- Copyright © 2017 Alamar, Tosetti, Landahl, Bermejo and Terry. This is an open-access article distributed under the terms of the Creative Commons Attribution License (CC BY). The use, distribution or reproduction in other forums is permitted, provided the original author(s) or licensor are credited and that the original publication in this journal is cited, in accordance with accepted academic practice. No use, distribution or reproduction is permitted which does not comply with these terms.



Combined Effects of Irrigation Regime, Genotype, and Harvest Stage Determine Tomato Fruit Quality and Aptitude for Processing into Puree

Alexandre Arbex de Castro Vilas Boas¹, David Page², Robert Giovinazzo³, Nadia Bertin¹ and Anne-Laure Fanciullino^{1*}

¹ UR 1115 Plantes et Systèmes de cultures Horticoles, Institut National de la Recherche Agronomique, Centre PACA, Avignon, France, ² UMR 408 Sécurité et Qualité des Produits d'Origine Végétale, INRA, Centre PACA, Université d'Avignon, Avignon, France, ³ Société Nationale Interprofessionnelle de la Tomate, Avignon, France

OPEN ACCESS

Edited by:

Marcello Mastorilli,
CREA, Italy

Reviewed by:

Youssef Roushail,
University of Naples Federico II, Italy
Ep Heuvelink,
Wageningen University & Research,
Netherlands

*Correspondence:

Anne-Laure Fanciullino
anne-laure.fanciullino@inra.fr

Specialty section:

This article was submitted to
Crop Science and Horticulture,
a section of the journal
Frontiers in Plant Science

Received: 01 June 2017

Accepted: 20 September 2017

Published: 05 October 2017

Citation:

Arbex de Castro Vilas Boas A,
Page D, Giovinazzo R, Bertin N and
Fanciullino A-L (2017) Combined
Effects of Irrigation Regime, Genotype,
and Harvest Stage Determine Tomato
Fruit Quality and Aptitude for
Processing into Puree.
Front. Plant Sci. 8:1725.
doi: 10.3389/fpls.2017.01725

Industry tomatoes are produced under a range of climatic conditions and practices which significantly impact on main quality traits of harvested fruits. However, the quality of tomato intended for processing is currently addressed on delivery through color and Brix only, whereas other traits are overlooked. Very few works provided an integrated view of the management of tomato puree quality throughout the chain. To gain insights into pre- and post-harvest interactions, four genotypes, two water regimes, three maturity stages, and two processes were investigated. Field and glasshouse experiments were conducted near Avignon, France, from May to August 2016. Two irrigation regimes were applied: control plants were irrigated in order to match 100% of evapotranspiration (ETP); water deficit (WD) plants were irrigated as control plants until anthesis of the first flowers, then irrigation was reduced to 60 and 50% ETP in field, and glasshouse respectively. Fruits were collected at three stages during ripening. Their color, fresh weight, dry matter content, and metabolite contents were determined before processing. Pericarp cell size was evaluated in glasshouse only. Two laboratory-scaled processing methods were applied before structural and biochemical analyses of the purees. Results outlined interactive effects between crop and process management. WD hardly reduced yield, but increased dry matter content in the field, in contrast to the glasshouse. The puree viscosity strongly depended on the genotype and the maturity stage, but it was disconnected from fruit dry matter content or Brix. The process impact on puree viscosity strongly depended on water supply during fruit production. Moreover, the lycopene content of fresh fruit may influence puree viscosity. This work opens new perspectives for managing puree quality in the field showing that it was possible to reduce water supply without affecting yield and to improve puree quality.

Keywords: quality, *Solanum lycopersicum*, deficit irrigation, pre- and post-harvest links, antioxidants, thermal processing, consistency

INTRODUCTION

There is much interest in improving fruit and vegetable quality through sustainable means in order to meet future food needs and tackle environmental challenges. While about 800 million people are undernourished globally (Welch and Graham, 1999; McGuire, 2015), up to one third of food is never consumed (FAO, 2011), especially fruits and vegetables, which are naturally rich in major phytonutrients. Food losses occur throughout the supply chain: during harvest, during post-harvest handling and storage, during processing and at distribution and consumer levels. Therefore, processing fruits and vegetables represent a strategic approach to meet nutritional needs of the growing population, considering their availability all along the year, and provided that organoleptic and nutritional properties are preserved during processes. Processing tomato is a major crop that represents the principal source of important phytonutrients such as β -carotene and lycopene (Dorais et al., 2008). The most part is consumed as tomato puree, paste, or sauce (Mirondo and Barringer, 2015).

In addition, a major environmental concern in agriculture is the use of fresh water for irrigation (Postel et al., 1996). Water resources are under threat due to the increase in water demand for agriculture, and the gap between water availability and demand is exacerbated by global climate changes (Afzal et al., 2016). Processing tomato, an intensive production in terms of water use, is highly concerned with this issue (Rinaldi et al., 2007). For example, in Italy, the blue water footprint (ratio of the volume of irrigation to the crop yield) of this production has been estimated at 60 m³ per ton (Aldaya and Hoekstra, 2010). In line with this, considerable efforts have been made for increasing water use efficiency of tomato crop (Stikic et al., 2003; Costa et al., 2007; Rinaldi et al., 2007; Patanè and Cosentino, 2010; Patanè et al., 2016). These works underlined that water deficit (WD) is one of the main limiting factors affecting the yield of processing tomato (Costa et al., 2007; Patanè and Cosentino, 2010). The yield reduction depends on water deficit intensity and duration as well as on its timing during tomato development (Rinaldi et al., 2007; Patanè and Cosentino, 2010). WD reduces the weight of individual fruits more than the number of fruits per plant (Casa and Rouphael, 2014). Because mild WD decreases fruit water accumulation more than dry mass accumulation, the decrease in yield may in fact turn out positive for processing. Indeed, tomato process includes a phase of dehydration/concentration, and reducing water content of raw material makes the process more efficient. In addition, many other traits related to fruit quality (soluble solid content and titratable acidity) and to fruit nutritional value (vitamin C and carotenoids) are affected by WD depending on climatic conditions, cultivars, or fruit developmental stages (Garcia and Barrett, 2006; Patanè and Cosentino, 2010; Anthon et al., 2011; Patanè et al., 2011; Barbagallo et al., 2013). Several works have analyzed the effect of one specific pre-harvest factor on quality traits of both fresh fruits and processed purees. According to Patanè and Cosentino (2010) WD decreased Bostwick consistency of purees. Large variations in paste quality traits (color, consistency, soluble solid content, pH and titratable acidity) were found among cultivars and among maturity stages (Garcia and Barrett, 2006). Delayed harvesting

caused a rise in pH and a loss of citric acid (Anthon et al., 2011). Therefore, considering production management as a levy to monitor the quality of processed fruits may lead to innovative strategies to improve puree quality.

High viscosity, fresh flavor and retention of natural color are important quality traits of ketchup and tomato puree (Chong et al., 2009). Interestingly, color shift during processes results from putative modifications of lycopene storage structures (more easily extractable) rather than from variations in lycopene content (Svelander et al., 2010; Page et al., 2012; Makroo et al., 2017). Concerning viscosity, dehydration during processing has a major influence. Relationships between dry matter content and viscosity on one hand, and between dry matter content and soluble solid content (SSC, in °Brix) on the other hand, are well-known from manufacturers since puree price is based on °Brix. However, SSC is not the only factor affecting rheology (Barrett et al., 1998). Processing parameters such as breaking temperature and dynamic sieving modify the water soluble/insoluble solid content ratio, particle sizes and pectin state, which, in turn, affect the puree rheology (Sanchez et al., 2002; Moelants et al., 2014). Those physicochemical variables depend on the biological structures of fruit tissues and their reactivity to the process. For example, breaking temperature is currently used to modulate the consistency of tomato products: a high temperature treatment, immediately after fruit crushing (hot break, HB: 90°C) produces much more viscous purees than cold break (CB) treatment, where fruits are first crushed and then macerated at moderate temperature (70°C; Moelants et al., 2014).

The quality of tomato puree is built throughout the food chain. Yet, very few works have simultaneously analyzed factors affecting fruit quality during the growing season and those that operate during processing. Currently, in industry, the quality of processed fruits is assessed through the color and Brix index only, whereas other physical, structural and biochemical traits are overlooked. In order to better understand variations in puree quality, insights into pre- and post-harvest interactions should be gained. To fulfill this objective, we investigated major traits of fruit quality in response to water supply, genotypes and ripening stages, and we assessed their impact on puree quality obtained from HB and CB processes. The response to WD under different climatic conditions was assessed by conducting both field and glasshouse experiments.

MATERIALS AND METHODS

Two experiments were conducted concurrently in spring and summer 2016, the first in the field according to commercial practices and the second in a glasshouse under controlled climatic conditions. In both experiments, four industry-type (determinate) cultivars of *Solanum lycopersicum*, namely "H1015," "H1311," "Miceno," and "Terradou," were selected on the basis of a previous study (not published), based on the contrasted purees obtained: from low ("Terradou") to medium ("H1015" and "Miceno"), or high ("H1311") lycopene content

Abbreviations: Bw, Bostwick; ETP, evapotranspiration; PG, polygalacturonase; PME, pectin methyl-esterase; SSC, soluble solid content; WD, water deficit.

and from low ("Terradou") to medium ("H1015" and "Miceno") or high viscosity ("H1311"). Those four genotypes were studied under two levels of irrigation, control and water deficit (WD). All seeds were germinated under standard glasshouse conditions (25°C day, 15°C night) near Avignon, France, in April 2016.

Open-Field Experiment

Two blocks of 1,800 plants each (450 plants per cultivar) were designed in an experimental field near Avignon (43°54'N 4°52'E), France. Each block was 7 m wide and 90 m long and surrounded by border plants. The four genotypes and the two irrigation regimes were randomly distributed within the two blocks. All plants were grown under identical field conditions: 900 plants per genotype were transplanted in May 2016 at a density of 3.3 plants m⁻², fertilizers (86 kg.ha⁻¹ of N, 33 kg.ha⁻¹ of P, and 198 kg.ha⁻¹ of K) were supplied before transplanting and insects and diseases were controlled according to current practices. The water irrigation was supplied by a drip irrigation system. Irrigation was scheduled daily to compensate the evapotranspiration loss from tomato crop (ETP). ETP was determined daily using reference evapotranspiration estimated from the Penman-Monteith equation (Monteith, 1965) and taking into account crop coefficient (Kc) and precipitations. The variations of Kc during the season are given in Supplementary Figure 1. Daily variations in air temperature, rainfall and solar radiation are reported in Supplementary Figure 2. Water was first supplied every day in order to fully fit 100% of ETP. Forty-five days after sowing, two levels of irrigation were applied: (1) water deficit (60% replacement of ETP) and (2) well-watered to match 100% replacement of ETP (Supplementary Figure 3). To mimic current production practices, irrigation was stopped 1 week before harvest. The soil water potential was recorded hourly using Watermark (Campbell Scientific, Antony, France) soil moisture sensors (six per water regime), which were installed at 25 and 50 cm depths. The records showed reduced soil humidity at 25 cm depth when compared to the control (Figure 1). Control plants experienced higher soil water potentials than plants under WD at 25 cm depth (Figure 1A). Under well-watered condition, 50% of the data (between the upper and the lower quartile) ranged from -38 to -13 kPa, while under WD 50% of the data ranged from -57 to -27 kPa. At 50 cm depth, soil water potentials remained similar between the two irrigation treatments (Figure 1B).

Three independent samples of 15 fruits from each treatment, genotype, and block were harvested at 40 (light orange), 47 (orange red), and 55 (red ripe) days after anthesis (DAA) for quality analyses and processing.

Glasshouse Experiment

Eighteen plants per genotype were grown in 4 L pots filled with compost (substrate 460, Klasmann, Champétry, France) at a density of 1.8 plant.m⁻² under glasshouse conditions near Avignon (43°54'N 4°52'E), France. Day-night temperature controls were set at 25–15°C and the air humidity ranged between 30 and 95%. Solar radiation inside the glasshouse varied from 7.3 to 26.2 MJ m⁻² day⁻¹ (Supplementary Figure 4).

Flowers were pollinated three times a week using an electrical bee. Plants were supplied daily with a nutrient solution (Liquoplant Rose, Plantin, Courthézon, France). This solution was diluted between 4‰ (NO₃⁻, 1.7 mM; NH₄⁺, 1.3 mM; P₂O₅, 0.5 mM; K₂O, 2.2 mM; MgO, 0.9 mM, and FeEDTA, 15 µM) and 8‰ (NO₃⁻, 3.4 mM; NH₄⁺, 2.6 mM; P₂O₅, 1 mM; K₂O, 4.4 mM; MgO, 1.8 mM, and FeEDTA, 30 µM) according to the plant developmental stage, which corresponded to an average electro conductivity of 1.8 dS m⁻¹. First, all plants were irrigated in order to match 100% replacement of ETP. ETP was determined daily using reference evapotranspiration estimated from the Penman-Monteith equation (Monteith, 1965) and taking into account Kc. Soil relative humidity and drainage were maintained around 70% (maximum water retention capacity of the substrate) and 15%, respectively. After 30 days (corresponding to the anthesis of the first flowers), a water deficit treatment was applied to half of the plants. The irrigation was reduced to 50% of ETP for plants under WD, while maintained at 100% of ETP for control plants from 30 to 120 days after planting (until end of fruit ripening; Supplementary Figure 3). The drip irrigation system was scheduled to irrigate every 0.25 mm. Soil relative humidity was measured weekly between 9 and 10 a.m. (solar time) in all pots using water content sensors (WCM-control, Grodan, Roermond, The Netherlands). Figures 1C–F shows changes in soil relative humidity during the treatment. A 25–60% reduction in soil relative humidity was monitored in all pots following WD treatment (gray lines). The electro-conductivity of both limited-water and well-watered pots ranged between 1 and 2 dS m⁻¹ until 90 days after planting and between 2 and 3 thereafter.

For fruit quality analyses and processing, four independent samples of 15 fruits were harvested from 9 plants at three stages: 40, 47, and 55 DAA.

Plant and Fresh Fruit Physiological Measurements

During the WD treatment, from June to August 2016, leaf and stem water potentials, leaf conductance and fruit growth were monitored on control and WD plants. Measurements of leaf conductance were conducted between 9 and 10 a.m. (solar time) using an AP4 porometer (Delta-T Devices Ltd, Cambridge, England), while measurements of water potentials were performed between 12 and 13 p.m. (solar time) using a pressure chamber (Scholander et al., 1965). Every week, 12 newly mature leaves from six individuals were marked for each treatment, genotype, and block. Half of the marked leaves were used for leaf conductance (g_s) and midday leaf water potential ($\psi_{Lmidday}$) measurements, while six other leaves were covered with aluminum foil and plastic bags to allow leaf and stem water potentials to equilibrate at least 2 h before stem water potential measurements ($\psi_{Smidday}$). At least three mature leaves from three individuals per treatment, per genotype, and per block were sampled at the end of the experiment for specific leaf area (SLA) determination.

Fruit growth was measured weekly with a digital caliper between 9 and 10 a.m. (solar time). Three fruits from three different trusses were monitored on three plants per treatment,

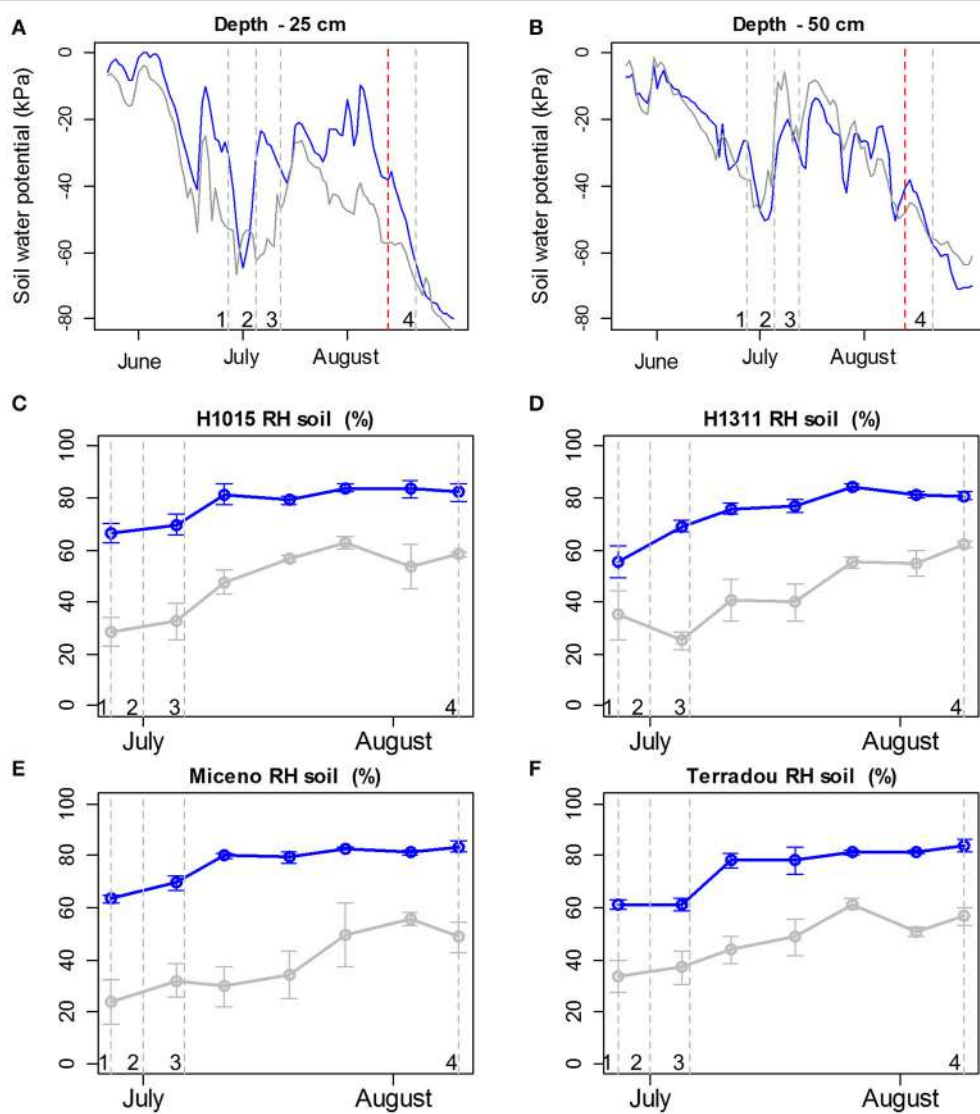


FIGURE 1 | Variations in soil humidity under field (**A,B**) and glasshouse (**C–F**) conditions. (**A,B**) Soil water potentials determined with 6 Watermark sensors installed at 25 (**A**) and 50 (**B**) cm depths under the well-watered regime (blue lines) and the water deficit regime (gray lines). (**C–F**) soil relative humidity (RH) determined weekly in 9 pots for the 4 cultivars (“H1015,” “H1311,” “Miceno,” and “Terradou”) and the 2 water regimes: well-watered (blue lines) and water deficit (gray lines). Note that a RH of 80% corresponds to the maximum of soil water retention. Mean values are reported \pm SE. On (**A–F**), vertical gray lines with number 1, 2, 3, and 4 indicate anthesis of the first, second, third truss, and the harvest of those trusses respectively. The vertical red line on (**A,B**) indicates the end of irrigation.

per genotype, and per block. Flowers were labeled at anthesis at three different dates, so that fruits at three stages around maturity (light orange, orange red, and red ripe) could be collected on the same day in August. Consequently, all harvested fruits underwent similar environmental conditions from anthesis to harvest (**Figure 1**).

At the end of the experiment in August, at least four plants per treatment, per genotype, and per block were collected for fresh and dry yield determination.

Fresh Fruit Quality

Fruit color, dry matter, starch, soluble sugar, organic acid, and carotenoid contents were analyzed in both experiments.

The color was measured with a Minolta CR.400 calibrated with a standard background. At least three fruits from the three or four samples were tested three times at equidistant points along the equatorial plane. The dry matter content was determined by weighting 3 g of fruit pericarp pieces before and after drying at 85°C. For biochemical analyses, pieces of fruit pericarp were immediately frozen and kept at -80°C. Soluble sugars, starch and organic acids were extracted according to the method described by Gomez et al. (2002) and analyzed by HPLC (Waters 410, Part WAT070390, Milford, U.S.A.). Carotenoids were extracted according to the method described by Sérino et al. (2009) modified by Page et al. (2012) for quantification against internal standard (apo_8'carotenal) after

HPLC separation on a C30-column (Develosil® C30-UG-3, Nomura chemical CO., Seto, Japan) with a UV-visible detector (SPD-M20A; Shimadzu, Kyoto, Japan). The pericarp cell number was measured after tissue dissociation according to a method adapted from Bünger-Kibler and Bangerth (1983). Cells were counted using a microscope equipped with a camera (QImaging, Surrey, Canada) and Qcapture Pro 6.0 software (QImaging, Surrey, Canada; Bertin et al., 2002).

Tomato Processing and Quality

Purees were prepared by either hot break (HB) or cold break (CB) treatment according to a laboratory scaled method described by Page et al. (2012). Fruits were cut into large pieces (around 2 cm³), mixed altogether, and split into two identical batches of 400 g each. For HB, one batch was first heated until boiling temperature in a microwave oven (900 w, full power, 0.9 s g⁻¹ of tomato), then chopped for 30 s in a Waring® blender. For CB, the other batch was first chopped at room temperature for 30 s in the same Waring® blender and then heated for the same duration and conditions than for HB. Both purees were then passed through a hand-held potato masher with a 2 mm grid to remove skins and seeds, stored into a 500 ml glass jar with sealed lid, sterilized for 15 min at 100°C in a laboratory scaled autoclave, and stored at 4°C before analysis. The grinding step at room temperature in CB process allowed for the reaction of fruit intrinsic enzymes (especially polygalacturonase and pectin-methyl esterase) on cell walls, and therefore leads to lower consistency of purees compared to HB ones (Anthon et al., 2002). Consequently, the enzymatic potential of fruits was indirectly estimated as the difference in puree consistency between HB and CB processes, in our standardized conditions. The color of the purees was measured with a Minolta CR.400 using a specific cuvette for measurement of liquid or paste color and calibrated against a white background. Color results were expressed in the CIE L * a * b * color space. Color coordinates were used to calculate the hue angle (H°), which identifies the color at a 360° angle (McGuire, 1992). The dry matter content was determined by weighting around 3 g of fruit puree before and after drying for 3 days at 85°C. The soluble solid content (SSC) was measured by refractometry with an ATAGO PR-1000 digital refractometer with automatic temperature compensation at 25°C and results were expressed in degree Brix, according to AOAC (2002). Rheological behavior of the puree was assessed through two characteristic measurements: (1) consistency was measured using a Bostwick consistometer (CSC Scientific Company, Fairfaix, USA) and according to manufacturer's manual, results were expressed as arbitrary Bostwick unit (Bw). The lower the Bostwick value, the higher the puree consistency; (2) the viscosity was calculated from a steady state measurement performed on an Anton Paar MCR 301 viscosimeter (Graz, Austria), with a double ribbon impeller (with an inner radius of 11 mm, a pitch of 45 mm, a length of 45 mm, and an outer stationary cup with an outer radius of 14.46 mm). A flow curve was registered between 0.1 and 100 s⁻¹, 50 points and 5 s per point. Flow properties were described by the Herschel-Bulkley model (Espinosa et al., 2011).

Data Analysis

Data were analyzed using R statistical software (<http://www.R-project.org>). Physiological traits, data of yield, and quality traits were analyzed by analysis of variance (the agricolae R package and aov function; De Mendiburu, 2014). Heteroscedasticity and normality tests were performed before model evaluation. Regarding field experiment, when the ANOVA F-test showed no significant difference in means between the blocks, data from block 1 and 2 were pooled. **Tables 1, 2** synthesize results from univariate ANOVAs. Multiple comparison of means was performed using the Least Significant Differences (LSD) test ($\alpha = 0.05$). When heteroscedasticity was detected, we used the Kruskal-Wallis non-parametric test followed by multiple comparisons of means through a t-student test on the ranks ($\alpha = 0.05$).

The Factomine R package and the plot PCA function were used to perform PCA analysis. Data from field were composed of 15 variables of fruit and puree quality and 48 observations (4 cultivars \times 3 stages \times 2 blocks \times 2 irrigation levels). Data (means of 3 biological replicates) were centered and scaled by variables. Data from glasshouse are presented in Supplementary Figure 5. Eigen values and contribution of variables to each dimension are reported in Supplementary Tables 1, 2 for field and glasshouse, respectively.

Pearson correlation was performed to investigate links between fresh fruit and puree quality traits. The coorplot package was used to draw the correlation matrix of the quality traits (Wei et al., 2016). The GGMselect, GeneNet, and igraph packages (Schaefer et al., 2013; Csardi and Nepusz, 2014; Bouvier et al., 2016) were used to build a partial correlation network on fruit and puree quality traits based on the residues of the linear regressions (elimination of the genotype and treatment effects). Correlation matrix and partial correlation network were performed independently for field and glasshouse experiments.

RESULTS

Yield and Fruit Composition Were Not Much Affected by Water Deficit, Despite Significant Plant Responses

Univariate ANOVAs were performed on plant traits to analyze the effects of WD, genotype and WD \times genotype interactions in the field and glasshouse experiment, separately (**Table 1**). In field, no block effect was found. This factor was omitted in **Table 1**. None of the WD \times genotype interactions were significant, except for individual leaf dry weight measured in field (**Table 1**). During the decline in soil humidity in the WD treatment, physiological traits were highly affected by WD ($p \leq 0.001$). A 50% reduction in stomatal conductance (g_s) was observed for all cultivars in both open-field and glasshouse experiments (not shown). Accordingly, significant reductions in individual leaf area (from -22 to -40% according to the genotype) and individual leaf dry weight (from -14 to -39%) were observed under WD treatment in field. These reductions did not result in significant changes in specific leaf area (**Table 1**). In glasshouse,

TABLE 1 | Results of univariate analyses of variance (ANOVAs) for the plant traits measured under field and glasshouse conditions.

Factors	WD		Genotype		Interaction (WD × Genotype)		R ² (%)
	p-value	SSx/SStotal%	p-value	SSx/SStotal%	p-value	SSx/SStotal%	
FIELD							
Stomatal conductance gs	<2e-16***	55.65	0.14	2.68	0.96	0.14	58.47
Individual leaf dry weight	6.82e-10***	50.79	0.00371**	12.27	0.04935*	6.62	69.68
Individual leaf area	<2e-16***	76.61	0.26302	1.69	0.40959	1.20	79.51
Specific leaf area	0.3428	1.62	0.0342*	16.75	0.1278	10.59	28.96
Total fruit biomass (g FW per plant)	0.865	0.03	5.19e-06***	38.03	0.608	2.01	40.07
Total fruit biomass (g DW per plant)	0.000315***	12.02	6.1e-08***	41.52	0.583241	1.60	55.14
Total fruits (number per plant)	0.298	1.15	1.41e-06***	40.97	0.987	0.14	42.27
Individual fruit fresh weight	0.174	1.88	5.15e-07***	42.75	0.368	3.20	47.83
GLASSHOUSE							
Leaf water potential ψ_L	<2e-16***	52.72	5.95e-07***	4.63	0.352	0.46	57.81
Stem water potential ψ_S	<2e-16***	28.79	0.00351**	3.08	0.39672	0.66	32.53
Stomatal conductance gs	<2e-16***	33.88	0.0453*	1.72	0.822	0.19	35.79
Total plant biomass (g FW per plant)	0.000543***	16.27	0.371852	3.91	0.784159	1.31	21.49
Total plant biomass (g DW per plant)	0.441	0.83	0.126	8.19	0.573	2.77	11.79
Total fruit biomass (g FW per plant)	1.23e-10***	44.74	0.135	4.39	0.415	2.20	51.33
Total fruit biomass (g DW per plant)	3.2e-09***	38.01	0.0255*	8.01	0.4095	2.36	48.39
Total fruits (number per plant)	1.02e-06***	27.85	0.0447*	8.12	0.371	3.04	39.01
Individual fruit fresh weight	1.95e-09***	33.14	5.91e-06***	22.58	0.743	0.85	56.57

R² (%) Proportion of total variance explained by the model. SS, Sum of squares; SSx/SStotal %, the proportion of the explained variance. Significance codes: 0 **** 0.001 *** 0.01 **.

all cultivars experienced variations in water status. Differences of midday leaf and stem water potentials ($\psi_{L\text{midday}}$ and $\psi_{S\text{midday}}$) between control and WD plants were significant ($p \leq 0.001$). The highest variations were registered for $\psi_{L\text{midday}}$, which ranged from -0.7 to -0.5 MPa for control plants and from -1.0 to -0.6 MPa for WD plants. In the glasshouse, the total plant fresh biomass was reduced under WD treatment (up to -44% for “Miceno”).

Interestingly, under field-grown conditions, WD did not impact the fresh yield, expressed as total fruit biomass per plant, and yield-related traits (number of fruits and individual fruit fresh weight; **Table 1**), but it slightly increased the dry yield (up to $+27\%$ for “H1015”). We further analyzed the interactions between genotype, irrigation t and growing condition (**Figures 2, 3**). Overall in field under well-watered conditions, all cultivars reached almost similar fresh yields (on average 2,636 g plant⁻¹ or 87 t ha⁻¹), but different dry yields (**Figures 2A,C**, blue bars). The dry yield was the highest for “Terradou” and the lowest for “H1015” ($+46\%$ comparing “Terradou” to “H1015”). Under WD, “Terradou” reached the highest fresh and dry yields (**Figures 2A,C**, gray bars). The fruit dry matter content was higher under WD than under control condition, and the difference was significant for “H1015” and “Miceno” ($+27\%$ for “H1015” and $+26\%$ for “Miceno,” **Figure 3E**).

Under glasshouse conditions, the fresh and dry yields were similar for all cultivars, except “Terradou” which outperformed under WD (**Figures 2B,D**). In the glasshouse, WD significantly decreased the fresh and dry yields of

all cultivars (from -34 to -44% for fresh yield and from -25 to -47% for dry yield **Figures 2,B,D**). This reduction resulted from a decrease in both the number of fruits per plant and the individual fruit fresh weight (**Figures 3B,D**). Under WD, the dry matter content of fruit pericarp did not significantly change in glasshouse (**Figure 3F**).

Comparing field and glasshouse experiments, fresh and dry yields of control plants were significantly higher in the glasshouse whatever the cultivar (up to $+50\%$ of fresh yield; **Figures 2A,B**). Overall, the mean fresh mass of individual fruit was lower in the glasshouse than in the field, but the number of fruits per plant was higher, especially under well-watered conditions (-22% , and $+101\%$, respectively) (**Figures 3A,C**). On the other hand the fruit dry matter content was higher in the field than in the glasshouse, especially under WD ($+22\%$; **Figures 3E,F**). The genotype effect was higher in field than in glasshouse (between 38 and 43% of the variance associated to genotype in field, **Table 1**).

In field, the low impact of WD on yield prompted us to calculate water use efficiency as the ratio between total fresh yield and total water used for irrigation (kg m⁻³). In field, the water use efficiency ranged from 25 to 29 kg m⁻³ (depending on cultivars) for control plants and from 33 to 41 kg m⁻³ for WD plants. “Terradou” presented the highest values under both water treatments. In the glasshouse, the water use efficiency ranged from 32 to 39 and from 38 to 50 kg m⁻³ for control and WD plants, respectively. The highest value was reached by “H1015”

TABLE 2 | Results of univariate analyses of variance (ANOVAs) for the quality traits measured under field and glasshouse conditions.

Factors	WD	Genotype		Stage	Interaction (WD × Genotype)		Interaction (WD × Stage)		Interaction (Genotype × Stage)		Interaction (WD × Genotype × Stage)		R^2		
		p-value	SSx/ SStotal %	p-value	SSx/ SStotal %	p-value	SSx/ SStotal %	p-value	SSx/ SStotal %	p-value	SSx/ SStotal %	p-value			
FIELD															
Brix Fresh Fruit	0.45581	0.15	0.45581	2.35	1.594e-07***	56.13	0.64208	1.48	0.57835	0.98	0.045-05*	13.45	0.52889	4.56	79.10
Starch	0.1858229	1.50	0.0001169***	26.03	0.0003225***	18.55	0.2854716	3.25	0.5404158	1.02	0.0018167*	24.45	0.3486161	5.75	80.56
Glucose	0.612931	0.30	0.000515***	28.86	0.021832*	10.23	0.49786	2.78	0.256552	3.27	0.051573-	16.94	0.213701	10.37	72.75
Fructose	0.7798865	0.09	0.0004726***	29.67	0.0136013*	11.89	0.5626139	2.41	0.3888617	2.27	0.0687178	15.81	0.2269084	10.22	72.38
Citric	0.65117	0.42	0.1284-	12.59	0.3449	4.47	0.8127	1.91	0.8508	0.65	0.2421	17.32	0.3436	14.38	51.76
Malic	0.56157	0.73	0.03647*	21.10	0.21523	6.92	0.74182	2.65	0.9773	0.10	0.4821	11.98	0.8321	5.81	49.29
Hue Fresh Fruit	0.96733	0.00	0.7357	0.37	1.909e-14***	89.00	0.643	0.49	0.912	0.05	0.539	1.48	0.451	1.72	93.10
Lycopene	0.2719442	0.85	4.95e-08***	56.71	0.0009003***	12.79	0.9728094	0.15	0.9099104	0.13	0.0406639*	10.68	0.6972749	2.58	83.89
Brix CB	0.069902-	1.50	2.737e-11***	74.70	0.0011186**	7.52	0.478907	1.06	0.410176	0.77	0.262013	3.45	0.8645551	1.03	90.02
Hue CB	0.8297	0.02	3.839e-07***	33.64	5.163e-09***	46.87	0.5709	1.03	0.9863	0.01	0.2021	4.68	0.7433	1.74	87.99
Viscosity CB	0.0283*	4.60	0.0512-	7.55	5.739e-08***	61.00	0.782	0.91	0.2575	2.42	0.8863	1.96	0.9506	1.31	79.75
Brix HB	0.12391	1.23	1.926e-10**	71.87	0.01665*	4.63	0.40413	1.47	0.12056	2.23	0.30448	3.70	0.3727	3.29	88.42
Hue HB	0.6248	0.12	1.425e-06***	28.44	7.613e-10***	56.24	0.61	0.91	0.8623	0.15	0.7556	1.74	0.9766	0.56	88.17
Viscosity HB	1.266e-06***	5.63	8.655e-15***	51.50	9.928e-13***	29.64	0.84965	0.11	0.02576*	1.17	3.026e-05**	7.51	0.25536	1.15	96.71
GLASSHOUSE															
Brix Fresh Fruit	0.05954-	2.88	8.08e-05***	19.60	0.28507	2.01	0.31688	2.82	0.95269	0.08	0.56471	3.83	0.02538*	12.18	43.39
Starch	0.97117	0.00	0.5116	2.26	0.0183*	8.23	0.2386	4.20	0.2652	2.63	0.2636	7.65	0.5288	5.02	29.98
Glucose	0.14498	1.51	2.931e-07***	29.19	0.6562	0.59	0.52881	1.55	0.26001	1.91	0.07321-	8.46	0.11715	7.40	50.61
Fructose	0.06437-	1.87	1.246e-11***	42.14	0.57975	0.58	0.3772	1.66	0.16636	1.95	0.02459*	8.25	0.09310-	6.02	62.46
Citric	0.40156	0.36	1.639e-13***	49.78	0.23954	1.46	0.41953	1.43	0.02681*	3.81	0.1827	4.58	0.42107	3.05	64.47
Malic	0.421699	0.48	1.165e-05***	22.63	0.746217	0.44	0.228504	3.28	0.214946	2.33	0.74837	2.56	0.004073*	15.70	47.41
Hue Fresh Fruit	0.023877	2.74	0.000181***	11.69	6.856e-12***	38.65	0.90874	0.28	0.249043	1.46	0.291466	3.86	0.237691	4.24	62.92
Lycopene	0.03946*	1.53	<2e-16***	63.96	0.33174	0.78	0.21975	1.57	0.34003	0.76	0.07845-	4.14	0.36543	2.31	75.03
Brix HB	3.023e-05***	14.06	1.278e-05***	21.41	0.01586*	6.23	0.60554	1.31	0.869	0.20	0.71807	2.61	0.62031	3.14	48.97
Hue HB	0.0311284*	1.70	2.761e-12***	30.22	3.275e-12***	27.51	0.0007376***	6.66	0.4668811	0.54	0.0430425*	4.87	0.1988222	3.12	74.64
Viscosity HB	0.010617*	2.44	3.327e-13***	33.90	3.258e-12***	27.75	0.428888	1.00	0.720723	0.23	0.001505**	8.62	0.966472	0.48	74.43

R^2 (%) Proportion of total variance explained by the model. SS, Sum of squares; SS/SStotal %, the proportion of the explained variance. Significance codes: 0 ***n, 0.001 **n, 0.01 *n, 0.05 n.

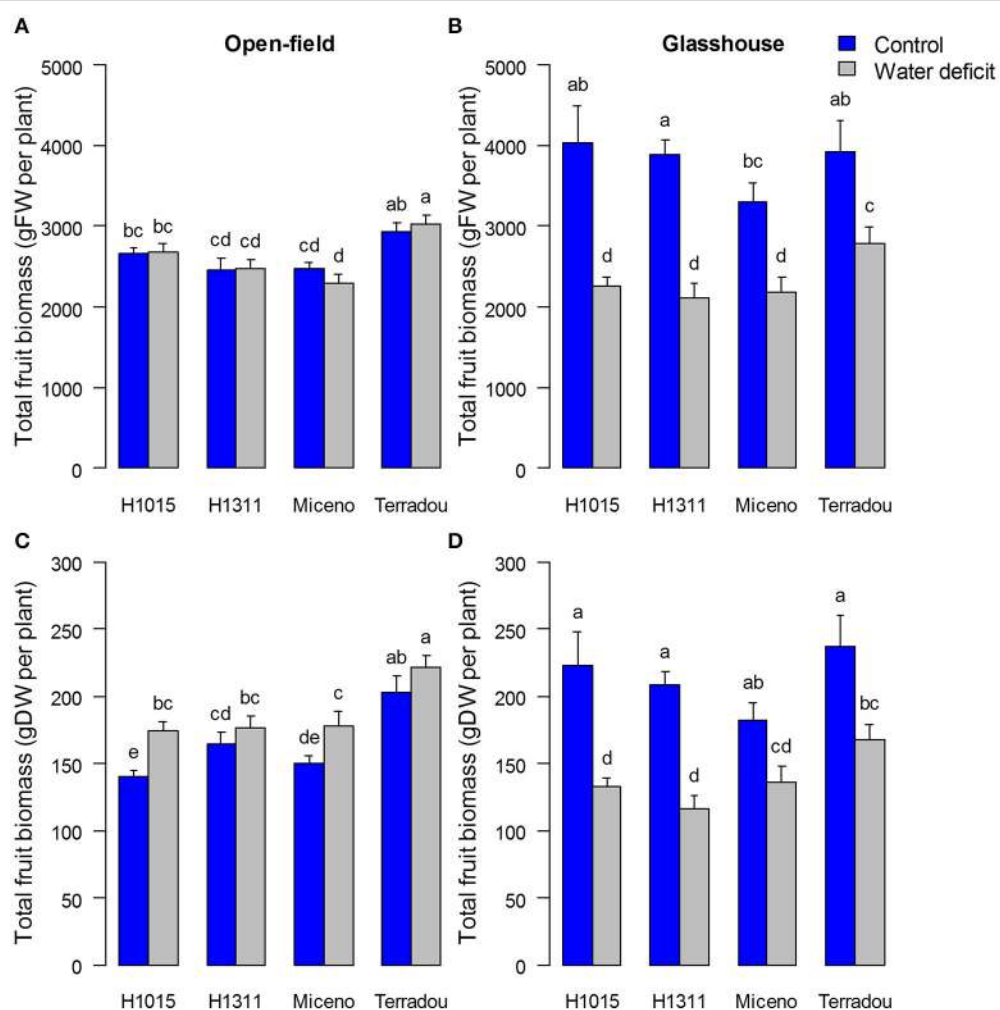


FIGURE 2 | Impact of water deficit and cultivar on fresh (**A,B**) and dry (**C,D**) yield expressed as total fruit biomass (g) per plant under field (**A,C**) and glasshouse (**B,D**) conditions. Note that the color code is blue for well-watered plants and gray for plants under water deficit. Values are means of $n \geq 8 \pm \text{SE}$. Bars marked by different letters indicate significant different values (Kruskal-Wallis test, $\alpha = 0.05$).

under control, whereas “Terradou” showed the highest efficiency under WD.

Table 2 synthetizes the effects of WD, genotype and maturity stage on quality traits analyzed by univariate ANOVAs. Fruit composition in soluble sugars, organic acids, and carotenoids was determined on a dry weight basis. None of the tests involving WD (including interactions) was significant except for Lycopene and citric acid under glasshouse conditions (Table 2). Fruit composition was mainly controlled by the genotype (between 26 and 57% of the variance associated to genotype in field and between 23 and 64% in glasshouse).

Genotype and Maturity Stage Controlled Puree Quality While WD Improved Rheological Properties

Tomatoes from field and glasshouse experiment were processed through CB and HB methods and puree quality was assessed

based on viscosity and color parameters. In all tests, genotype and maturity stage effects were significant. The genotype effect was higher than the maturity stage effect, except for the Hue angle and the viscosity of CB purees from field (Table 2). A highly significant genotype \times stage interaction was found for the viscosity of HB purees (Table 2). We further analyzed the interactions between genotype, maturity stage and irrigation treatment in field, and their effects on puree rheological properties (Figure 4). Cultivar “H1311” produced the most viscous purees in all situations (Figure 4). With regard to the maturity stage impact, viscosity slightly declined or was stable when fruits were harvested between 40 and 47 DAA and then sharply increased for fruits harvested between 47 and 55 DAA (up to +100%, Figure 4C). Interestingly, WD led to significant higher puree viscosity and consistency (Figures 4A,B). Within the WD group, the viscosity of “H1311” purees was 22.3, 44.36, and 49.62% higher than the viscosity of purees from “Miceno,” “H1015,” and “Terradou,” respectively. The ranking of genotypes

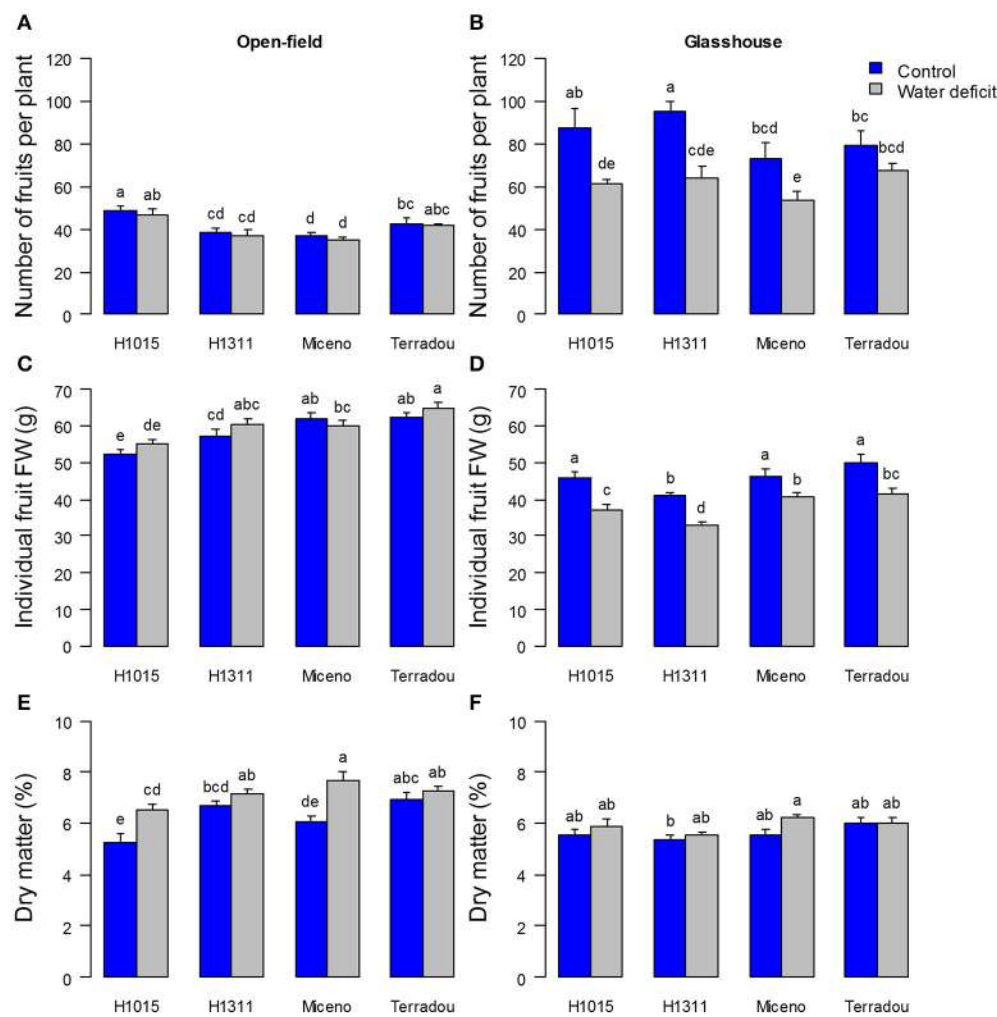


FIGURE 3 | Changes in yield-related traits determined for the four cultivars under field (**A,C,E**) and glasshouse (**B,D,F**) conditions and under the two water regimes (control in blue and water deficit in gray): number of fruits per plant (**A,B**), individual fruit fresh weight (FW) (**C,D**) and dry matter content of fruit pericarp collected at 55 DAA (**E,F**). For (**A–D**), mean \pm SE, $n \geq 8$. For (**E,F**), mean \pm SE, $n \geq 4$. Bars marked by different letters indicate significant different values (Kruskal-Wallis test, $\alpha = 0.05$).

was similar in the control group and consistent patterns of viscosity and Bw consistency were obtained. Another major finding of our study was that WD significantly influenced the fruit reactivity, assessed through the difference in consistency between HB and CB purees. For all genotypes, the reactivity was remarkably lower for purees produced from WD tomatoes than for purees from control tomatoes (Figure 4D). At 55 DAA, the losses in consistency ranged from -48% for "H1311" to -75% for "Terradou."

The responses of puree viscosity to genotype, maturity stage and WD treatment were similar when fruits were produced under glasshouse conditions, but they differed in absolute values. Interestingly, purees from the glasshouse production were always less viscous when compared to the field production whatever the cultivar, the water regime or the maturity stage. The puree made from WD fruits produced in open-field showed 69.45% increase in viscosity and 21.67% decrease in Bw, while purees made from

control fruits showed 68.46% increase in viscosity and 23.40% decrease in Bw, when compared to the glasshouse.

Regarding the color parameters under field-grown conditions, Hue angle values were significantly affected by genotype and maturity stage only. The hot break purees from "H1311" ripe fruits presented the lowest values (Figure 5), which was consistent with the lowest Hue angle of fresh fruits among cultivars. As expected, Hue angle values significantly varied according to the maturity stage.

Correlation between Fresh Fruit and Puree Quality Traits

To understand the links between crop and process management, a PCA analysis was performed on fruit and puree quality traits under field conditions (Figure 6 and Supplementary Table 1), and under glasshouse conditions (Supplementary Figure 5 and Supplementary Table 2). The first and the second dimensions

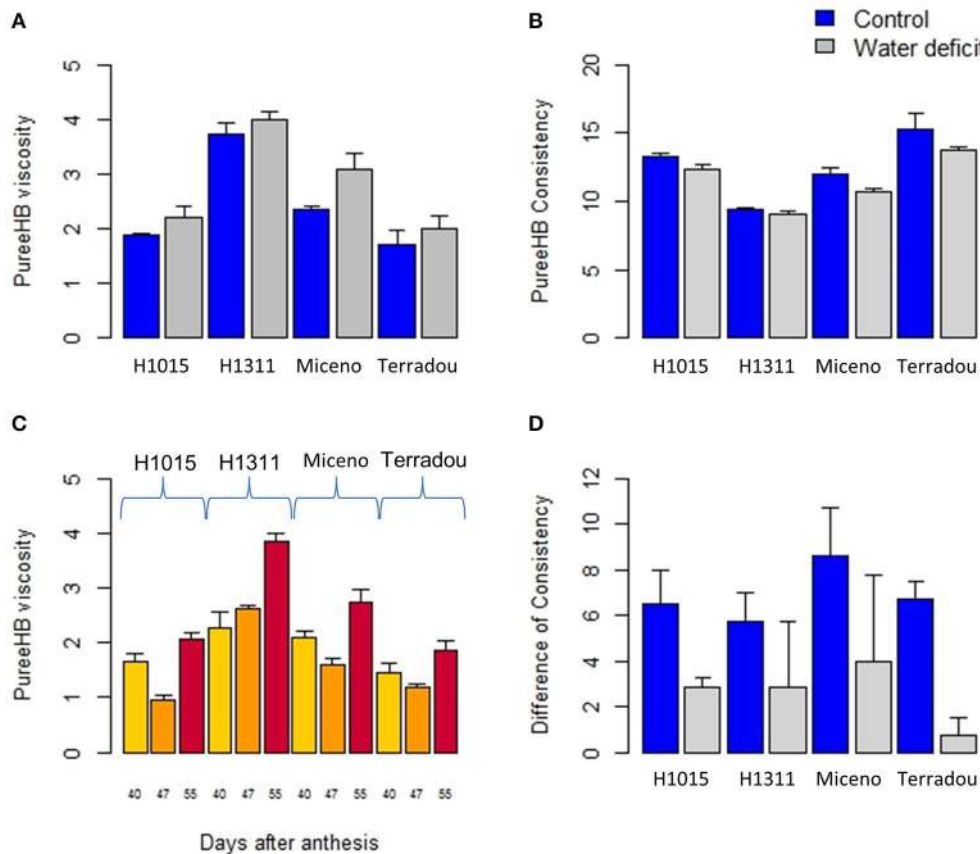


FIGURE 4 | Impact of water deficit (**A,B,D**), genotype (**A–D**) and maturity stage (**C**) on the rheology of puree, under field-grown conditions. (**A,B**) Changes in Hot break puree viscosity and Bostwick value, all fruits were collected at 55 DAA. (**C**) Variations in Hot break puree viscosity obtained with fruit when fruits were collected [40, 47, and 55 days after anthesis] (**C**). (**D**) Difference of consistency (measured by Bostwick device) between Cold break and Hold break purees obtained from fruits collected at 55 DAA. Values are mean \pm SE, $n \geq 2$.

(Dim.) explained 54% of the total variance (Figure 6). The quality traits are plotted on the first two dimensions in (Figure 6A) while (Figures 6B–D) shows the projection of the observations and the centers of gravity for water treatments, genotypes, and maturity stages, respectively. Dim. 1 positively correlated with Hue HB, Hue CB, Hue fresh fruits, fructose, starch, and glucose and negatively correlated with lycopene, viscosity HB and viscosity CB (Figure 6A, and Supplementary Table 1). Fewer traits were well represented on Dim. 2: Brix HB, Brix CB, and Brix fresh fruits correlated with the positive values of Dim. 2 (Figure 6A, and Supplementary Table 1). The dry matter content of the pericarp was poorly represented on Dim. 1, 2, and 3. Citric and malic acids were poorly represented on Dim. 1 and 2, but contributed to Dim. 3 (Figure 6A, and Supplementary Table 1). The projection of individuals (Figures 6B–D) confirmed the effects of genotypes and maturity stages on fruit and puree quality (Figure 6). Cultivars were separated on Dim. 1 and 2 whereas Dim. 1 explained differences among maturity stages. As mentioned, some traits were poorly represented on the first two dimensions. Consequently, Pearson correlation correlations between fresh fruit and puree quality traits were analyzed further.

Figure 7 summarizes data obtained under field (Figure 7A) and glasshouse (Figure 7B) conditions. Significant correlations are indicated by a color code: red for negative significant correlation and blue for positive significant correlation. Of the 120 pairs of traits, there were 32 significant correlations ($P < 0.01$) under field conditions (vs. 18 significant correlations among 105 pairs of traits under glasshouse conditions). As expected, color of CB and HB purees, determined by Hue angle values, positively and negatively correlated with, respectively, Hue values and lycopene contents of fresh fruits (Figure 7A). Brix of CB and HB purees positively correlated with Brix of fresh fruits. Some correlations were also found among fruit traits, such as individual sugars, individual acids, and sugar-acid balance or among puree traits such as CB and HB viscosities. Surprisingly, no correlation was found between puree viscosity and fruit dry matter content, starch, or Brix. It was also interesting to note that viscosity of HB purees positively correlated with lycopene contents of fresh fruits. There was a concordance between field and glasshouse experiments. However, the positive correlations between Hue angle of HB purees and Hue angle of fresh fruits or between Brix of purees and Brix of fresh fruits were not significant under

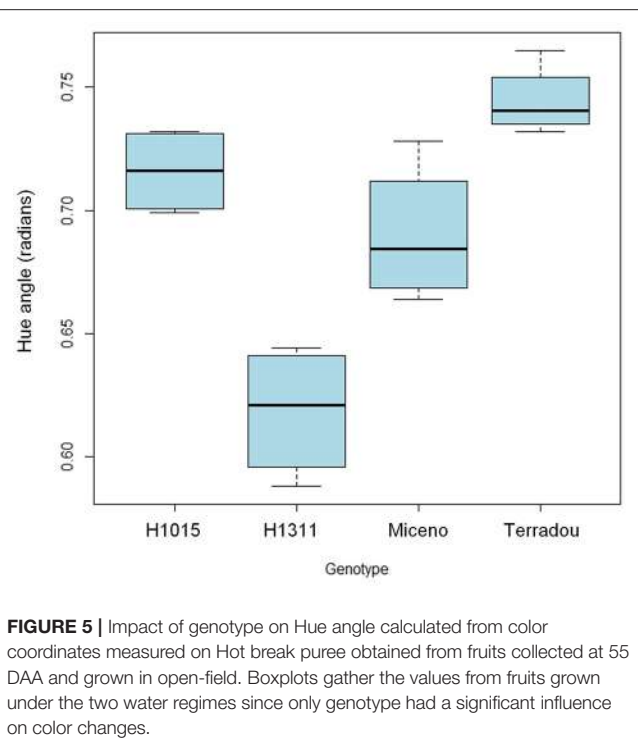


FIGURE 5 | Impact of genotype on Hue angle calculated from color coordinates measured on Hot break puree obtained from fruits collected at 55 DAA and grown in open-field. Boxplots gather the values from fruits grown under the two water regimes since only genotype had a significant influence on color changes.

glasshouse conditions (**Figure 7B**). On the other hand, a positive correlation was observed between the average pericarp cell size and the Hue angle of the puree.

A partial correlation network was built on fruit and puree quality traits, based on the residues of the linear regression (elimination of the genotype and treatment effects) to determine traits that were functionally related (**Figures 8A,B**). Partial correlation analysis was performed independently for the field (**Figure 8A**) and the glasshouse (**Figure 8B**) experiments. Correlations among fruit and puree quality traits were confirmed for color and Brix (**Figure 8A**). However, puree viscosity was not related to any trait of fruit quality (**Figure 8A**). Under glasshouse conditions, puree quality was unrelated to fresh fruit traits (**Figure 8B**).

DISCUSSION

The quality of tomatoes intended for processing is currently addressed on delivery through color and Brix, whereas other traits are overlooked. In the field, irrigation is currently stopped 1 week before harvest in order to increase the fruit dry matter content. During processing, part of the water is removed and the matrix is submitted to thermal treatments in order to control more or less empirically the final puree viscosity. Yet very few works provided an integrated view of the management of tomato puree quality from field to can. For this purpose insights into interactions between factors that drive fruit quality during the growing season and those that operate during processing should be gained. In this work we investigated fruit quality in response to

water supply, genotypes and ripening stages, and we assessed their impact on puree quality obtained from HB and CB processes.

Moderate Effects of WD on Fruit Yield and Quality Are Observed in Glasshouse Conditions Only Irrespective of the Genotype

Water availability is one of the main factor impacting plant growth and consequently harvestable yield (Boyer, 1982; Tardieu et al., 2011; Katerji et al., 2013; Ripoll et al., 2014). For all genotypes, under glasshouse conditions, the effect of WD, as reflected by changes in water status and stomatal conductance, resulted in reductions in total plant biomass, fruit setting, and fruit fresh mass. The reduction of plant growth observed under WD is likely to originate from a sink, hydromechanical limitation rather than a source, photosynthetic limitation since growth is generally more affected by drought than carbon assimilation (Muller et al., 2011). Nonetheless, carbon supply could also represent a significant growth limitation in the fruit, where carbon-rich osmotica are required for sustaining expansive growth (Pantin et al., 2013). In addition, impairment of carbon supply may have been determinant for fruit set (D'Aoust et al., 1999). Under field conditions, WD reduced leaf area and total plant biomass, did not impact the total fresh yield, but slightly increased the total dry yield, and in average, increased the water use efficiency by 20% compared to control condition. The average total fresh yield obtained in this study corresponded to total yields commonly observed in France under well-watered conditions (80 t ha^{-1} , <http://www.sonito.fr>). Total fresh and dry yields were genotype-dependent. These results are in agreement with previous works on the effects of moderate deficit irrigation on processing tomato. According to Patanè et al. (2011) a deficit irrigation at 50% ETc from flowering does not significantly reduce the total or marketable yields, but increases water use efficiency by about 40%. Similarly, Stikic et al. (2003) have shown that partial root drying (PRD) induces a significant reduction of total plant biomass without affecting fruit diameter and fresh mass. Accordingly, water use efficiency at crop level is increased by PRD treatment (Stikic et al., 2003).

Under glasshouse conditions, the effect of WD on yield was higher than the effect measured in field. In addition, substantially higher yields were achieved in glasshouse than in field. It may result from lower plant density and temperatures in glasshouse (Poorter et al., 2016). In glasshouse, inter-cultivar variations in total yields were observed under WD only. This suggests that the ranking of genotypes resulted from differential adaptation to WD in glasshouse and to abiotic factors other than WD in field (density or temperature).

In contrast to the negative effect on plant growth and fruit fresh mass, moderate water deficit has been reported to improve fruit quality of tomato (Pernice et al., 2010; Patanè et al., 2011; Barbagallo et al., 2013; Ripoll et al., 2016). The increase in fruit dry matter content in response to WD is well-known (Ripoll et al.,

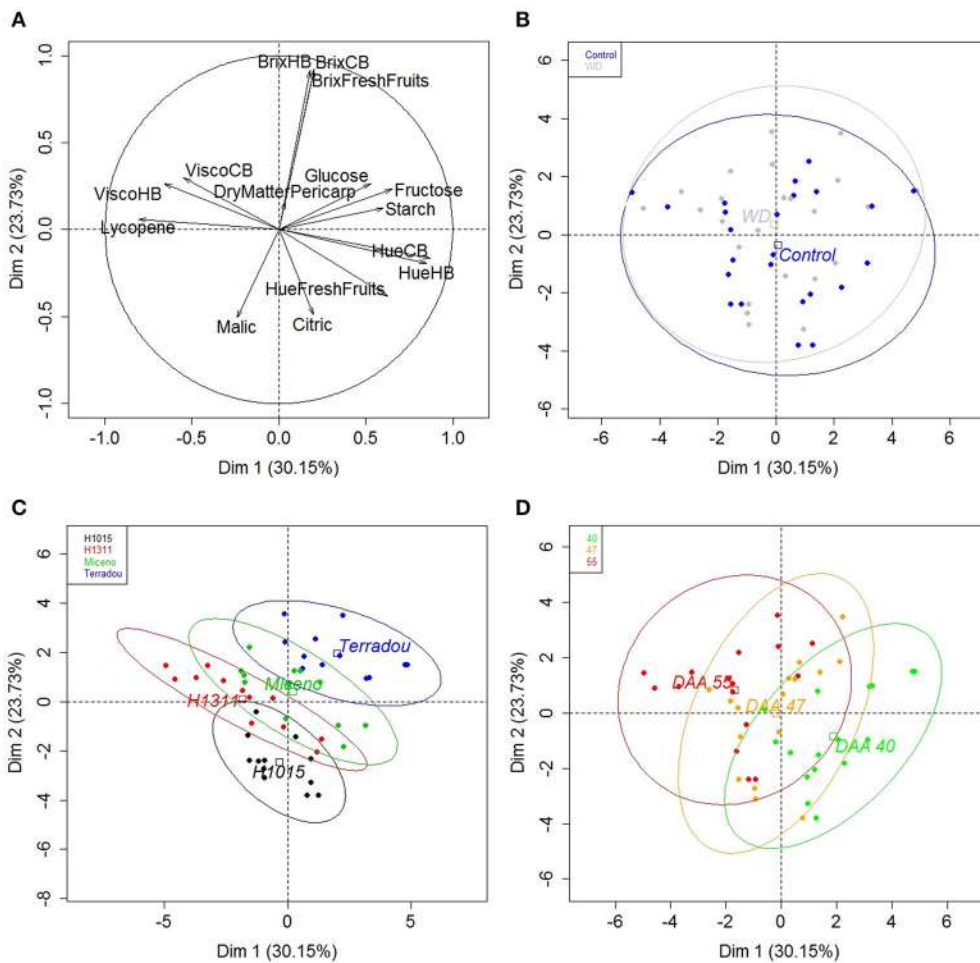


FIGURE 6 | PCA results of fruit quality traits ($^{\circ}$ Brix of fresh fruits, dry matter content of pericarp, Hue angle of fresh fruits, starch, glucose, fructose, citric and malic acids, and lycopene determined on dry weight basis) and puree quality traits ($^{\circ}$ Brix, Hue angle, and viscosity of purees obtained after CB and HB processes) in field according to dimension 1 and 2 (53.88% of the total variance). The proportions of explained variability are indicated for each axis. **(A)** Projection of the quality traits taken into account; **(B–D)** Projection of individuals. Each point corresponds to the mean of three replicates. **(B)** Centers of gravity for water treatments, **(C)** Centers of gravity for genotypes, and **(D)** Centers of gravity for maturity stages.

2014). However, whatever the genotype, we did not observe any change in sugar, acid, and lycopene contents, expressed on a dry weight basis, in response to WD. Ripoll et al. (2016) have already underlined that beneficial effects of moderate WD on fruit sugar, acid and carotenoid contents, reported on a fresh weight basis, mainly results from a dehydration effect, which is confirmed by our study. In addition, effects of WD on fruit dry matter composition strongly depend on genotype and stress intensity (Ripoll et al., 2016). In our study, the ranking of genotype in terms of fruit composition was not modified by the WD applied from flowering to harvest.

Water Deficit Improves Puree Rheological Properties

Consistency constitutes one of the main quality traits of tomato purees, which are considered as suspensions of insoluble

particles (pulp) into an aqueous solution (serum) (Moelants et al., 2014). In tomato, fruit dry matter encompasses soluble (mainly sugars and acids) and insoluble (such as pectins and other polysaccharides) solids (Foolad, 2007). Insoluble solids are thought to determine puree viscosity (Davies et al., 1981). However, the precise role of the physicochemical properties of these solids remains unrevealed. Pectin composition and degradation were stressed out as major parameters, while some authors put solid particle size and shape on first stage (Sanchez et al., 2002; Lin H. et al., 2005; Moelants et al., 2014). All those parameters are regulated during fruit maturation and genetic control (Sanchez et al., 2002; Foolad, 2007; Anthon et al., 2011). Our results are in agreement since cultivar and maturity stage had major impacts on puree viscosity (Figure 5). Interestingly, the WD applied in our experiment improved puree viscosity of all cultivars, despite no change in fruit composition (on a dry weight basis) and no correlation between fruit dry matter

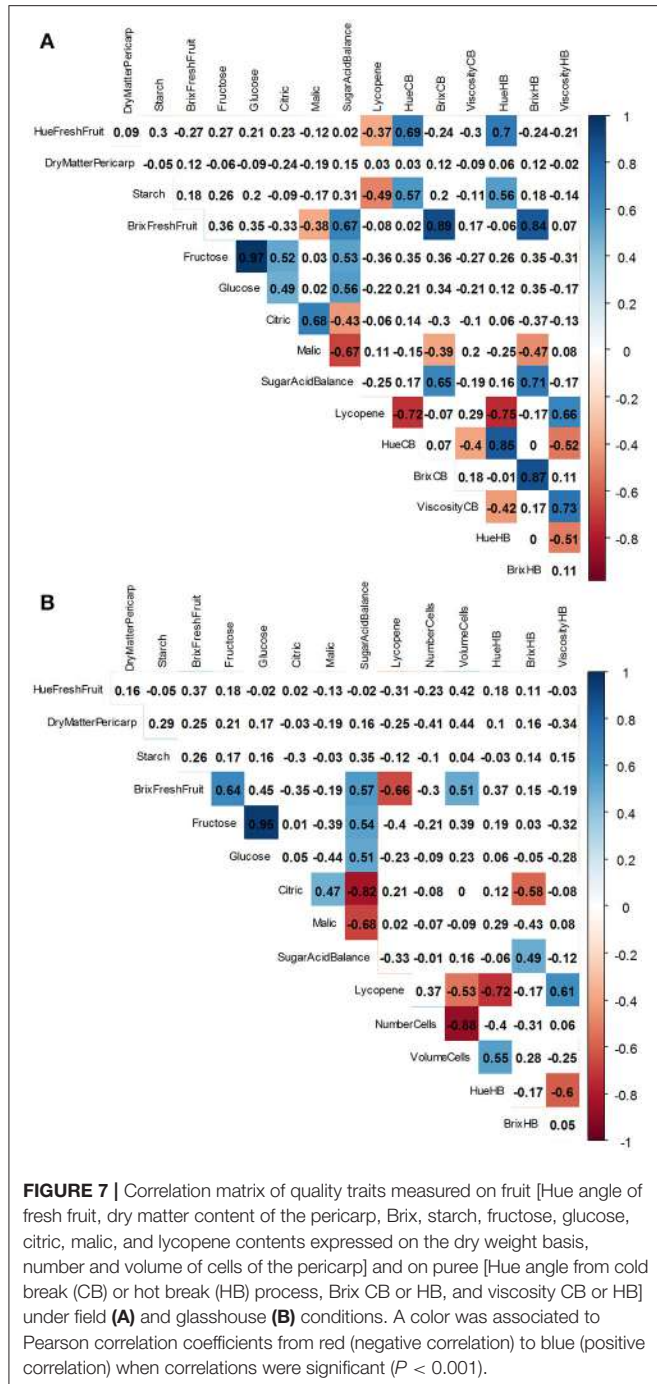


FIGURE 7 | Correlation matrix of quality traits measured on fruit [Hue angle of fresh fruit, dry matter content of the pericarp, Brix, starch, fructose, glucose, citric, malic, and lycopene contents expressed on the dry weight basis, number and volume of cells of the pericarp] and on puree [Hue angle from cold break (CB) or hot break (HB) process, Brix CB or HB, and viscosity CB or HB] under field (**A**) and glasshouse (**B**) conditions. A color was associated to Pearson correlation coefficients from red (negative correlation) to blue (positive correlation) when correlations were significant ($P < 0.001$).

content and puree viscosity. We propose that the effect of WD on puree rheology was driven by changes in pectin composition, and by changes in particle size and shape. Indeed, transcriptome analysis have revealed that plant response to drought includes differential cell wall synthesis and remodeling (Tenhaken, 2014). In addition, we found that WD decreased the loss of viscosity between HB and CB purees which suggests that the activity of pectin-degrading enzymes in fruits, produced under WD, was modified. The difference in rheology after HB and CB treatments is attributed to temperature effects on endogenous pectinolytic

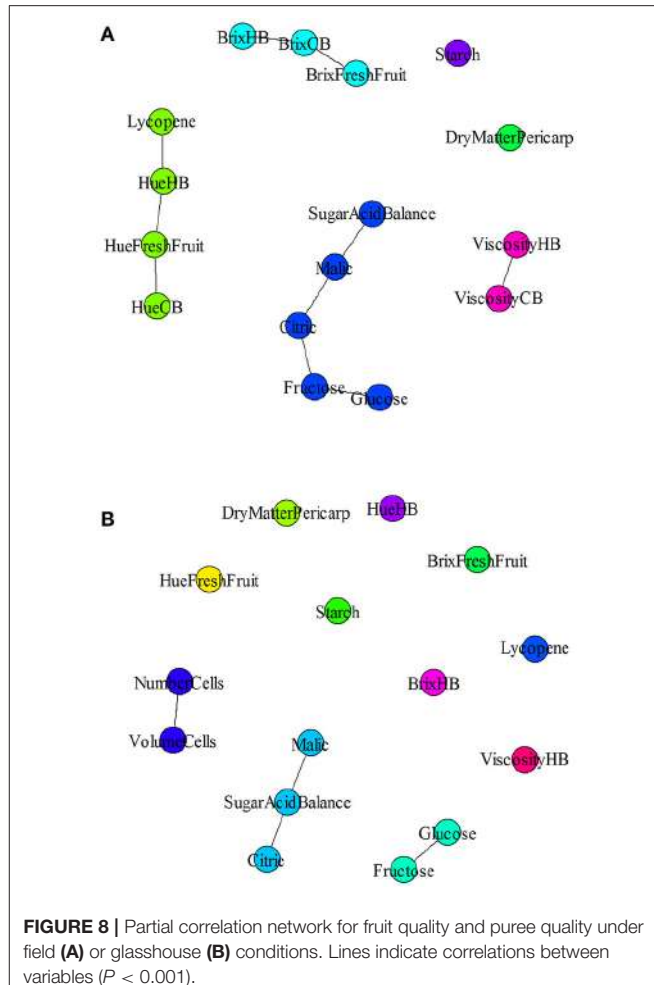


FIGURE 8 | Partial correlation network for fruit quality and puree quality under field (**A**) or glasshouse (**B**) conditions. Lines indicate correlations between variables ($P < 0.001$).

enzymes, namely polygalacturonase (PG) and pectin methyl-esterase (PME) involved in fruit softening (Anthon et al., 2002; Moelants et al., 2014). The involvement of these enzymes has been confirmed by HB/CB processing of genetically modified tomatoes (Errington et al., 1998), but the exact relationship between PG, PME and rheology remained partially obscure. Indeed CB treatment leads to different biochemical and physical properties of water soluble pectins when compared to HB (Lin H. et al., 2005; Lin H. J. et al., 2005). The proportion of water insoluble solids is not significantly different between CB and HB purees (Sanchez et al., 2002), but particle size and shape are also impacted by the breaking temperature (Errington et al., 1998). It has been shown in other plant species, that pectin-degrading enzymes can be down-regulated by water stress (Le Gall et al., 2015). Thus, the activity of pectin-degrading enzymes in response to WD should be analyzed in further details to disentangle the effect of pectinolytic enzymes from the effect of particles.

Fruit Lycopene Content Rather Than Dry Matter Content Controls Puree Quality

Lycopene is the main pigment of red tomato cultivars (Fraser et al., 1994). It is well-established that color parameters measured

with a chromameter provide a robust evaluation of lycopene contents determined by HPLC (Arias et al., 2000). So the strong correlations between fruit lycopene, fruit color parameters, and puree color parameters were not surprising. On the contrary the correlation between lycopene content of fresh fruits and puree viscosity is new.

Several studies reported relations between puree viscosity and fruit dry matter or soluble solid contents (Davies et al., 1981). However, such correlation was not observed in our study. Moelants et al. (2014) have reviewed relationships between food structure and rheological properties of plant-tissue-based food suspensions. Besides the importance of particle concentration already mentioned, particle size and particle morphology also appear to be key structural parameters controlling the rheological properties (Moelants et al., 2014), and especially, particle size distribution (Leverrier et al., 2016). Lycopene is known to be included in membrane-shaped structures of chromoplasts (Egea et al., 2010). The correlation between lycopene content of fresh fruit and the puree viscosity prompts us to suggest that lycopene content improves puree rheological properties by enhancing the proportion of small particles of lycopene.

Our study demonstrated that challenging tomato producers to reduce water withdrawal could be eased by a better integration of the manufacturing requirements. Previous studies indicated that tomato fruit growth and quality were weakly impacted by moderate WD in glasshouse production, and our study confirmed that this result could be transposed in field production. A reduction of water supply from 100 to 60% of the ETP, increased the water use efficiency by 20% on average and may enhanced the dry yield depending on genotype. This result holds out some progress margin for the industry that spends most of its energy in water removal from raw material. We also found that WD modified the reactivity of tomato fruits to process.

REFERENCES

- Afzal, M., Battilani, A., Solimando, D., and Ragab, R. (2016). Improving water resources management using different irrigation strategies and water qualities: field and modelling study. *Agric. Water Manage.* 176, 40–54. doi: 10.1016/j.agwat.2016.05.005
- Aldaya, M. M., and Hoekstra, A. Y. (2010). The water needed for Italians to eat pasta and pizza. *Agric. Syst.* 103, 351–360. doi: 10.1016/j.agsy.2010.03.004
- Anthon, G. E., LeStrange, M., and Barrett, D. M. (2011). Changes in pH, acids, sugars and other quality parameters during extended vine holding of ripe processing tomatoes. *J. Sci. Food Agric.* 91, 1175–1181. doi: 10.1002/jsfa.4312
- Anthon, G. E., Sekine, Y., Watanabe, N., and Barrett, D. M. (2002). Thermal inactivation of pectin methylesterase, polygalacturonase, and peroxidase in tomato juice. *J. Agric. Food Chem.* 50, 6153–6159. doi: 10.1021/jf020462r
- AOAC (2002). *Official Methods of Analysis of AOAC International*, 17th Edn. Gaithersburg, MD: AOAC International.
- Arias, R., Lee, T. C., Logendra, L., and Janes, H. (2000). Correlation of lycopene measured by HPLC with the L*, a*, b* color readings of a hydroponic tomato and the relationship of maturity with color and lycopene content. *J. Agric. Food Chem.* 48, 1697–1702. doi: 10.1021/jf990974e
- Barbagallo, R. N., Di Silvestro, I., and Patanè, C. (2013). Yield, physicochemical traits, antioxidant pattern, polyphenol oxidase activity and total visual quality of field-grown processing tomato cv. Brigade as affected by water stress in Mediterranean climate. *J. Sci. Food Agric.* 93, 1449–1457. doi: 10.1002/jsfa.5913
- Barrett, D. M., Garcia, E., and Wayne, J. E. (1998). Textural modification of processing tomatoes. *Crit. Rev. Food Sci. Nutr.* 38, 173–258. doi: 10.1080/10408699891274192
- Bertin, N., Gautier, H., and Roche, C. (2002). Number of cells in tomato fruit depending on fruit position and source-sink balance during plant development. *Plant Growth Regul.* 36, 105–112. doi: 10.1023/A:1015075821976
- Bouvier, A., Giraud, C., Huet, S., and Bouvier, M. A. (2016). Package 'GGMselect'.
- Boyer, J. S. (1982). Plant productivity and environment. *Science* 218, 443–448. doi: 10.1126/science.218.4571.443
- Bünger-Kibler, S., and Bangerth, F. (1983). Relationship between cell number, cell size and fruit size of seeded fruits of tomato and those induced parthenocarpically by the application of plant growth regulators. *Plant Growth Regul.* 1, 143–154.
- Casa, R., and Rouphael, Y. (2014). Effects of partial root-zone drying irrigation on yield, fruit quality, and water-use efficiency in processing tomato. *J. Hortic. Sci. Biotechnol.* 89, 389–396. doi: 10.1080/14620316.2014.11513097
- Chong, H. H., Simsek, S., and Reuhs, B. L. (2009). Analysis of cell-wall pectin from hot and cold break tomato preparations. *Food Res. Int.* 42, 770–772. doi: 10.1016/j.foodres.2009.02.025
- Costa, J. M., Ortu-o, M. F., and Chaves, M. M. (2007). Deficit irrigation as a strategy to save water: physiology and potential application to horticulture. *J. Integr. Plant Biol.* 49, 1421–1434. doi: 10.1111/j.1672-9072.2007.00556.x
- Csardi, G., and Nepusz, T. (2014). *The Igraph Software Package for Complex Network Research*. R Package Version 0.6. 6. Available online at: <http://cran.r-project.org/web/packages/igraph/>

As a whole, the strong impact of genotype on puree's viscosity and the lack of correlation between puree viscosity and fruit soluble solid content or dry matter content, open interesting perspectives to better understand the links between crop and process management. Yield or fruit dry matter content matter a lot, but yet the condition of fruit production and their ability to produce high quality and stable industrial products should be considered as well.

AUTHOR CONTRIBUTIONS

DP, NB, and AF: Planned and designed the research. AA, DP, RG, and AF: Performed experiments. AA, DP, NB, and AF: Analyzed the data and wrote the manuscript.

FUNDING

AA was supported by a grant from CAPES and from the Brazilian Ministry of Education. This work was also supported by the Société Nationale Interprofessionnelle de la Tomate (SONITO) and the Structure Fédérative de Recherche Tersys.

ACKNOWLEDGMENTS

We thank Marielle Bogé, Béatrice Brunel, Julie Duboue, Caroline Garcia, Guillaume Garcia, Patrice Reiling, and Sylvie Sérino for their technical assistance.

SUPPLEMENTARY MATERIAL

The Supplementary Material for this article can be found online at: <https://www.frontiersin.org/articles/10.3389/fpls.2017.01725/full#supplementary-material>

- D'Aoust, M. A., Yelle, S., and Nguyen-Quoc, B. (1999). Antisense inhibition of tomato fruit sucrose synthase decreases fruit setting and the sucrose unloading capacity of young fruit. *Plant Cell* 11, 2407–2418. doi: 10.1105/tpc.11.12.2407
- Davies, J. N., Hobson, G. E., and McGlasson, W. B. (1981). The constituents of tomato fruit — the influence of environment, nutrition, and genotype. *Crit. Rev. Food Sci. Nutr.* 15, 205–280. doi: 10.1080/10408398109527317
- De Mendiburu, F. (2014). *Agricolae: Statistical Procedures for Agricultural Research*. R package version 1, 1–6. Available online at: <http://CRAN.R-project.org/package=agricolae>
- Dorais, M., Ehret, D. L., and Papadopoulos, A. P. (2008). Tomato (*Solanum lycopersicum*) health components: from the seed to the consumer. *Phytochem. Rev.* 7, 231–250. doi: 10.1007/s11101-007-9085-x
- Egea, I., Barsan, C., Bian, W., Purgatto, E., Latché, A., Chervin, C., et al. (2010). Chromoplast differentiation: current status and perspectives. *Plant Cell Physiol.* 51, 1601–1611. doi: 10.1093/pcp/pcq136
- Errington, N., Tucker, G. A., and Mitchell, J. R. (1998). Effect of genetic down-regulation of polygalacturonase and pectin esterase activity on rheology and composition of tomato juice. *J. Sci. Food Agric.* 76, 515–519. doi: 10.1002/(SICI)1097-0010(199804)76:4<515::AID-JSFA979>3.0.CO;2-X
- Espinosa, L., To, N., Symoneaux, R., Renard, C., Biau, N., and Cuvelier, G. (2011). “Effect of processing on rheological, structural and sensory properties of apple puree,” in *11th International Congress on Engineering and Food*, eds G. Saravacos, P. Taoukis, M. Krokida, V. Karathanos, H. Lazarides, N. Stoforos, C. Tzia, and S. Yanniotis (Amsterdam: Elsevier Science Bv), 513–520. doi: 10.1016/j.profoo.2011.09.078
- FAO (2011). *Global Food Losses and Food Waste – Extent, Causes and Prevention*.
- Foolad, M. R. (2007). Genome mapping and molecular breeding of tomato. *Int. J. Plant Genomics* 2007:64358. doi: 10.1155/2007/64358
- Fraser, P. D., Truesdale, M. R., Bird, C. R., Schuch, W., and Bramley, P. M. (1994). Carotenoid biosynthesis during tomato fruit development (evidence for tissue-specific gene expression). *Plant Physiol.* 105, 405–413. doi: 10.1104/pp.105.1.405
- Garcia, E., and Barrett, D. M. (2006). Evaluation of processing tomatoes from two consecutive growing seasons: quality attributes, peelability and yield. *J. Food Process. Preserv.* 30, 20–36. doi: 10.1111/j.1745-4549.2005.0044.x
- Gomez, L., Rubio, E., and Auge, M. (2002). A new procedure for extraction and measurement of soluble sugars in ligneous plants. *J. Sci. Food Agric.* 82, 360–369. doi: 10.1002/jsfa.1046
- Katerji, N., Campi, P., and Mastrorilli, M. (2013). Productivity, evapotranspiration, and water use efficiency of corn and tomato crops simulated by AquaCrop under contrasting water stress conditions in the Mediterranean region. *Agric. Water Manage.* 130, 14–26. doi: 10.1016/j.agwat.2013.08.005
- Le Gall, H., Philippe, F., Domon, J. M., Gillet, F., Pelloux, J., and Rayon, C. (2015). Cell wall metabolism in response to abiotic stress. *Plants* 4, 112–166. doi: 10.3390/plants4010112
- Leverrier, C., Almeida, G., Espinosa-Mu noz, L., and Cuvelier, G. (2016). Influence of particle size and concentration on rheological behaviour of reconstituted apple purees. *Food Biophys.* 11, 235–247. doi: 10.1007/s11483-016-9434-7
- Lin, H., Qin, X., Aizawa, K., Inakuma, T., Yamauchi, R., and Kato, K. (2005). Chemical properties of water-soluble pectins in hot-and cold-break tomato pastes. *Food Chem.* 93, 409–415. doi: 10.1016/j.foodchem.2004.12.009
- Lin, H., Aizawa, K., Inakuma, T., Yamauchi, R., and Kato, K. (2005). Physical properties of water-soluble pectins in hot- and cold-break tomato pastes. *Food Chem.* 93, 403–408. doi: 10.1016/j.foodchem.2004.09.036
- Makroo, H. A., Rastogi, N. K., and Srivastava, B. (2017). Enzyme inactivation of tomato juice by ohmic heating and its effects on physico-chemical characteristics of concentrated tomato paste. *J. Food Process. Eng.* 40:e12464. doi: 10.1111/jfpe.12464
- McGuire, R. G. (1992). Reporting of objective color measurements. *HortScience* 27, 1254–1255.
- McGuire, S. (2015). FAO, IFAD, and WFP. The state of food insecurity in the World 2015: Meeting the 2015 international hunger targets: taking stock of uneven progress. Rome: FAO, 2015. *Adv. Nutr.* 6, 623–624. doi: 10.3945/an.115.009936
- Mirondo, R., and Barringer, S. (2015). Improvement of flavor and viscosity in hot and cold break tomato juice and sauce by peel removal. *J. Food Sci.* 80, S171–S179. doi: 10.1111/1750-3841.12725
- Moelants, K. R. N., Cardinaels, R., Van Buggenhout, S., Van Loey, A. M., Moldenaers, P., and Hendrickx, M. E. (2014). A review on the relationships between processing, food structure, and rheological properties of plant-tissue-based food suspensions. *Compr. Rev. Food. Sci. Food Saf.* 13, 241–260. doi: 10.1111/1541-4337.12059
- Monteith, J. L. (1965). Evaporation and environment. *Symp. Soc. Exp. Biol.* 19, 205–234.
- Muller, B., Pantin, F., Génard, M., Turc, O., Freixes, S., Piques, M., et al. (2011). Water deficits uncouple growth from photosynthesis, increase C content, and modify the relationships between C and growth in sink organs. *J. Exp. Bot.* 62, 1715–1729. doi: 10.1093/jxb/erq438
- Page, D., Van Stratum, E., Degrou, A., and Renard, C. (2012). Kinetics of temperature increase during tomato processing modulate the bioaccessibility of lycopene. *Food Chem.* 135, 2462–2469. doi: 10.1016/j.foodchem.2012.06.028
- Pantin, F., Fanciullino, A. L., Massonet, C., Dauzat, M., Simonneau, T., and Muller, B. (2013). Buffering growth variations against water deficits through timely carbon usage. *Front. Plant Sci.* 4:483. doi: 10.3389/fpls.2013.00483
- Patanè, C., and Cosentino, S. (2010). Effects of soil water deficit on yield and quality of processing tomato under a Mediterranean climate. *Agric. Water Manage.* 97, 131–138. doi: 10.1016/j.agwat.2009.08.021
- Patanè, C., Scordia, D., Testa, G., and Cosentino, S. L. (2016). Physiological screening for drought tolerance in Mediterranean long-storage tomato. *Plant Sci.* 249, 25–34. doi: 10.1016/j.plantsci.2016.05.006
- Patanè, C., Tringali, S., and Sortino, O. (2011). Effects of deficit irrigation on biomass, yield, water productivity and fruit quality of processing tomato under semi-arid Mediterranean climate conditions. *Sci. Hortic.* 129, 590–596. doi: 10.1016/j.scientia.2011.04.030
- Pernice, R., Parisi, M., Giordano, I., Pentangelo, A., Graziani, G., Gallo, M., et al. (2010). Antioxidants profile of small tomato fruits: effect of irrigation and industrial process. *Sci. Hortic.* 126, 156–163. doi: 10.1016/j.scientia.2010.06.021
- Poorter, H., Fiorani, F., Pieruschka, R., Wojciechowski, T., Putten, W. H., Kleyer, M., et al. (2016). Pampered inside, pestered outside? Differences and similarities between plants growing in controlled conditions and in the field. *New Phytol.* 212, 838–855. doi: 10.1111/nph.14243
- Postel, S. L., Daily, G. C., and Ehrlich, P. R. (1996). Human appropriation of renewable fresh water. *Science* 271:785. doi: 10.1126/science.271.5250.785
- Rinaldi, M., Ventrella, D., and Gagliano, C. (2007). Comparison of nitrogen and irrigation strategies in tomato using CROPGRO model. A case study from Southern Italy. *Agric. Water Manage.* 87, 91–105. doi: 10.1016/j.agwat.2006.06.006
- Ripoll, J., Urban, L., Brunel, B., and Bertin, N. (2016). Water deficit effects on tomato quality depend on fruit developmental stage and genotype. *J. Plant Physiol.* 190, 26–35. doi: 10.1016/j.jplph.2015.10.006
- Ripoll, J., Urban, L., Staudt, M., Lopez-Lauri, F., Bidel, L. P., and Bertin, N. (2014). Water shortage and quality of fleshy fruits—making the most of the unavoidable. *J. Exp. Bot.* 65, 4097–4117. doi: 10.1093/jxb/eru197
- Sanchez, M. C., Valencia, C., Gallegos, C., Ciruelos, A., and Latorre, A. (2002). Influence of processing on the rheological properties of tomato paste. *J. Sci. Food Agric.* 82, 990–997. doi: 10.1002/jsfa.1141
- Schaefer, J., Opgen-Rhein, R., and Strimmer, K. (2013). *GeneNet: Modeling and Inferring Gene Networks*. R package version 1.2. 5. Available online at: <http://CRAN.R-project.org/package=GeneNet>
- Scholander, P. F., Bradstreet, E. D., Hemmingsen, E. A., Hammel, H. T. (1965). Sap pressure in vascular plants. *Science* 148, 339–346. doi: 10.1126/science.148.3668.339
- Sérino, S., Gomez, L., Costagliola, G., and Gautier, H. (2009). HPLC assay of tomato carotenoids: validation of a rapid microextraction technique. *J. Agric. Food Chem.* 57, 8753–8760. doi: 10.1021/jf902113n
- Stikic, R., Popovic, S., Srdic, M., Savic, D., Jovanovic, Z., Prokic, L., et al. (2003). Partial root drying (PRD): a new technique for growing plants that saves water and improves the quality of fruit. *Bulg. J. Plant Physiol.* 29, 164–171.
- Svelander, C. A., Tiback, E. A., Ahgne, L. M., Langton, M. I., Svanberg, U. S., and Alminger, M. A. (2010). Processing of tomato: impact on *in vitro* bioaccessibility of lycopene and textural properties. *J. Sci. Food Agric.* 90, 1665–1672. doi: 10.1002/jsfa.4000

- Tardieu, F., Granier, C., and Muller, B. (2011). Water deficit and growth. Co-ordinating processes without an orchestrator? *Curr. Opin. Plant Biol.* 14, 283–289. doi: 10.1016/j.pbi.2011.02.002
- Tenhaken, R. (2014). Cell wall remodeling under abiotic stress. *Front. Plant Sci.* 5:771. doi: 10.3389/fpls.2014.00771
- Wei, T., Simko, V., and Wei, M. T. (2016). Package ‘corrplot’. *Statistician* 56, 316–324.
- Welch, R. M., and Graham, R. D. (1999). A new paradigm for world agriculture: meeting human needs - Productive, sustainable, nutritious. *Field Crops Res.* 60, 1–10. doi: 10.1016/S0378-4290(98)00129-4

Conflict of Interest Statement: The authors declare that the research was conducted in the absence of any commercial or financial relationships that could be construed as a potential conflict of interest.

Copyright © 2017 Arbex de Castro Vilas Boas, Page, Giovinazzo, Bertin and Fanciullino. This is an open-access article distributed under the terms of the Creative Commons Attribution License (CC BY). The use, distribution or reproduction in other forums is permitted, provided the original author(s) or licensor are credited and that the original publication in this journal is cited, in accordance with accepted academic practice. No use, distribution or reproduction is permitted which does not comply with these terms.



Firmness at Harvest Impacts Postharvest Fruit Softening and Internal Browning Development in Mechanically Damaged and Non-damaged Highbush Blueberries (*Vaccinium corymbosum* L.)

Claudia Moggia^{1,2*}, Jordi Graell², Isabel Lara², Guillermina González¹ and Gustavo A. Lobos^{1*}

OPEN ACCESS

Edited by:

Maarten Hertog,
KU Leuven, Belgium

Reviewed by:

Fisun G. Çelikel,
Ondokuz Mayıs University, Turkey

Rosario Muleo,
University of Tuscia, Italy

*Correspondence:

Claudia Moggia
cmoggia@utalca.cl
Gustavo A. Lobos
globosp@utalca.cl

Specialty section:

This article was submitted to
Crop Science and Horticulture,
a section of the journal
Frontiers in Plant Science

Received: 19 December 2016

Accepted: 27 March 2017

Published: 11 April 2017

Citation:

Moggia C, Graell J, Lara I, González G and Lobos GA (2017)
Firmness at Harvest Impacts
Postharvest Fruit Softening and Internal Browning Development in Mechanically Damaged and Non-damaged Highbush Blueberries (*Vaccinium corymbosum* L.). *Front. Plant Sci.* 8:535.
doi: 10.3389/fpls.2017.00535

Fresh blueberries are very susceptible to mechanical damage, which limits postharvest life and firmness. Softening and susceptibility of cultivars "Duke" and "Brigitta" to developing internal browning (IB) after mechanical impact and subsequent storage was evaluated during a 2-year study (2011/2012, 2012/2013). On each season fruit were carefully hand-picked, segregated into soft (<1.60 N), medium (1.61–1.80 N), and firm (1.81–2.00 N) categories, and then either were dropped (32 cm) onto a hard plastic surface or remained non-dropped. All fruit were kept under refrigerated storage (0°C and 85–88% relative humidity) to assess firmness loss and IB after 7, 14, 21, 28, and 35 days. In general, regardless of cultivar or season, high variability in fruit firmness was observed within each commercial harvest, and significant differences in IB and softening rates were found. "Duke" exhibited high softening rates, as well as high and significant r^2 between firmness and IB, but little differences for dropped vs. non-dropped fruit. "Brigitta," having lesser firmness rates, exhibited almost no relationships between firmness and IB (especially for non-dropped fruit), but marked differences between dropping treatments. Firmness loss and IB development were related to firmness at harvest, soft and firm fruit being the most and least damaged, respectively. Soft fruit were characterized by greater IB development during storage along with high soluble solids/acid ratio, which could be used together with firmness to estimate harvest date and storage potential of fruit. Results of this work suggest that the differences in fruit quality traits at harvest could be related to the time that fruit stay on the plant after turning blue, soft fruit being more advanced in maturity. Finally, the observed differences between segregated categories reinforce the importance of analyzing fruit condition for each sorted group separately.

Keywords: blueberry, bruising, soluble solids, acidity, maturity, firmness segregation, storage

INTRODUCTION

Blueberry production has increased rapidly around the world over the last two decades (Lobos and Hancock, 2015). Chile is the second largest global producer, as well as the first exporter of fresh blueberries to the Northern Hemisphere (USA, Canada, Europe, and Asia). Most of the Chilean fruit is sent by boat, with transit periods of 20–50 days depending on destination. Blueberries are highly perishable, so fruit quality upon arrival to the final markets has major relevance to ensure economic returns (Beaudry et al., 1998; Retamales et al., 2014).

Several quality (dust, contaminants, size, bloom, russet/scars, attached stems, flower remains, and color) and condition (decay, mold, wounds, dehydration, firmness, and shriveling) traits are evaluated by inspection companies at destination markets. Among them, and regardless of season, dehydration and softening are the most common defects causing shipment rejections (Moggia et al., 2016b).

At present, due to low availability and high costs of labor for hand picking, farmers are being forced to invest in the mechanization of this critical production phase (Takeda et al., 2008; Xu et al., 2015). Mechanical harvesting of blueberries has the advantages of increasing capacity and efficiency as well as of reducing labor costs, but there are discrepancies as to their real contribution for the fresh fruit market. In general, machine harvest leads to the reduction of the acceptable amount of fruit that can be exported as a result of softening and excessive bruising; nevertheless, promising results have been reported on the use of a particular shaker, this being a viable alternative during critical periods (Lobos et al., 2014b). Fruit can also develop bruising during transport from the field to the packing-house, or when being processed on the packing-lines (Xu et al., 2015).

Blueberries are especially susceptible to mechanical damage, with injured berries resulting in loss of firmness that leads to reduced fruit quality and shelf-life (Xu et al., 2015). Bruises develop in the flesh of the damaged fruit as internal browning (IB) areas, resulting from tissue breakage and oxidation of phenolic compounds (Studman, 1997; Opara and Pathare, 2014). In order to relate the effect of mechanical damage with bruise damage, as done on large fruits and vegetables with instrumented spheres, a blueberry impact-recording device (BIRD) has been developed (Yu et al., 2011, 2014). Recently, Xu et al. (2015) measured the mechanical impacts on packing lines with the BIRD, showing that most of them occurred at the transfer points and that the highest impacts were recorded in one of the final handling steps, when the sensor dropped into the hopper above the clamshell filler.

Unfortunately, blueberry bruising can be expected to continue occurring, not only because of the use of mechanical/semi-mechanical harvest, or of differences between packing-line designs (e.g., number and height of transfer points, presence/absence of cushion materials), but also because of the lack of enough processing facilities during harvest peaks. Because of this, operators are forced to increase the speed at the sorting/packing lines, increasing the risk that fruit develop softening and IB during postharvest.

By simulating mechanical impact damage (as for other fruit species such as apples), the resistance of blueberries to IB has

been evaluated by dropping fruit from different heights onto diverse surfaces; damage is rated on an internal bruise severity scale (affected area) after a period of cold storage (Brown et al., 1996; Yu et al., 2014). When berries were dropped from 15 to 30 cm onto hard surfaces, Brown et al. (1996) concluded that fruit developed IB on up to 50% of fruit area, and firmness declined significantly in samples having 25% or more damaged area. Yu et al. (2014) also reported a genotype effect, soft-textured cultivars being more susceptible than firm-textured ones when dropped on a hard plastic surface. However, all reported studies omit the high variability in firmness that occurs within a commercial clamshell, and hence the question arises whether results obtained for a given cultivar may be reproducible when variations in maturity stage, environmental conditions, and management procedures affect the proportions of soft, medium and firm fruit on a particular picking.

To the best of our knowledge, there are no previous reports on the implications of firmness segregation at harvest for the development of IB and softening of blueberries maintained under refrigerated conditions. Thus, the objective of this study was to understand how initial firmness and a single mechanical impact could affect the evolution of these traits during postharvest. For this, during two seasons, “Duke” and “Brigitta” fruit were segregated into soft, medium and firm categories at harvest, evaluating firmness loss and IB development of dropped (32 cm) and non-dropped fruit during 35 days under cold storage.

MATERIALS AND METHODS

Plant Materials

During two consecutive seasons [2011/2012 (Y1) and 2012/2013 (Y2)], highbush blueberry (*Vaccinium corymbosum* L.) fruit of cultivars “Duke” and “Brigitta” (6- and 4-year-old, correspondingly) were collected at the peak of the commercial harvest from Chilean orchards located in Longaví (36°00'S; 71°35'W) and Santa Bárbara (37°29'S; 72°19'W), respectively. Both cultivars were planted on raised beds, at 3 m × 1 m in a loam soil. Each bed had two drip irrigation lines (2.4 L h⁻¹ each 50 cm); irrigation frequency and timing were determined according to tensiometers established on each block at 30 and 50 cm depth. Pruning (May to July) was oriented to contribute for light entrance and air circulation, assuring a balance between canes of different ages and a stable production over time; pruning consisted in removing canes either unproductive or causing excessive shade on the plant. Fertigation was applied according to soil/foliar analysis and yield estimations; main nutrients were N (90–120 and 10–25 kg ha⁻¹ for “Duke” and “Brigitta,” correspondingly), K₂O (25–30 kg ha⁻¹), and P₂O₅ (150–180 kg ha⁻¹). Environmental conditions are summarized in Supplementary Table S1.

In order to mimic the marketable characteristics of exported fresh fruit, all fruit were harvested upon commercial criterion, which is based on 100% blue color (“Duke” December 5, 2011 and December 3, 2012; “Brigitta” December 29, 2011 and January 3, 2013). Berries were hand-picked by qualified workers belonging to each orchard. To avoid potential differences in

sorting and packaging facilities, and to reduce IB damage, fruit were harvested directly into plastic clamshells (125 g). Fruit were immediately transported to the laboratory facilities at Universidad de Talca ($35^{\circ}24' S$; $71^{\circ}38' W$), for further analysis and treatment establishment.

Experimental Set-up and Measurements

Upon arrival to the research facilities, fruit were initially characterized in terms of firmness and IB, and then subjected to firmness segregation, impact damage simulation, and finally stored under refrigerated conditions as described below.

Firmness and IB at Harvest

In order to assess firmness and IB variability on commercial fruit coming from the field, a sample of 200 fruit were evaluated on each cultivar and season prior to firmness segregation. Firmness (N) was assessed using a compression device (FirmTech 2, BioWorks, KS, USA) with the force thresholds set between 200 g (maximum) and 15 g (minimum) (Ehlenfeldt and Martin, 2002; Saftner et al., 2008). IB was assessed by slicing fruit equatorially and then rating flesh browning on each individual fruit, according to the extent of the bruised area, as 0 (0–5%), 1 (6–25%), 2 (26–50%), 3 (51–75%), or 4 (>75%) (Figure 1).

Firmness Segregation and Initial Condition on Each Category

Using the same equipment as for firmness assessments, fruit were assigned to one of three firmness categories: soft (<1.60 N), medium (1.60–1.80 N), and firm (1.81–2.00 N). For each season, this segregation represented 50 clamshells (125 g) per cultivar and category, from which each replicate was withdrawn. Then, for each firmness group, the following traits were assessed as initial condition: (i) firmness on five replicates of 20 fruit each; (ii) total soluble solids (TSS, %) using a digital refractometer (Pocket PAL-1, Atago, Tokyo, Japan), from juice obtained from five replicates of five berries each; (iii) titratable acidity (TA, % citric acid equivalents) from five replicates; each one consisted of 10 mL of blueberry juice diluted to 100 mL with distilled water and titrated with 0.1 mol L⁻¹ NaOH to an end-point pH of 8.2; (iv) TSS/TA ratio; and (v) IB on slices of five replicates of 20 fruit each.

Impact Damage Simulation

In order to study the evolution of IB and softening originated by impact damage, half of the fruit within each firmness category

group were dropped from 32 cm onto a 30 cm × 30 cm of a hard plastic surface (6.4 mm-thick plexiglass), while the other half remained non-dropped. Dropping height was selected based on previous findings (data not published), as well as reports on extensive bruising resulting from 15–30 cm drop heights onto hard surfaces (Brown et al., 1996; Xu et al., 2015). For each cultivar, both dropped (32 cm) and non-dropped (0 cm) fruit were placed within clamshells into cardboard boxes, and then stored during 35 days at 0°C and 85–88% relative humidity (RH).

Firmness and IB Evolution during Postharvest

For each cultivar, firmness category group, and dropping treatment, firmness and IB evaluations were undertaken in samples (five replicates of 20 fruit each) from clamshells removed from cold storage after 7, 14, 21, 28, and 35 days. After each storage removal, fruit were acclimated to room temperature (18°C) for 3 h prior to perform measurements. Individual fruit were first assessed for firmness and then cut transversally for IB rating.

Statistical Analysis

Firmness and IB condition of commercial fruit at harvest (before firmness segregation) was described for each cultivar and season, through box and whisker plots. Quality traits of fruit segregated at harvest were analyzed considering a completely randomized design with factorial arrangement, considering three firmness categories (soft, medium, and firm) × two seasons (Y1 and Y2). Data of parametric variables were subjected to analysis of variance (ANOVA), and significance of the differences was determined by Tukey's test ($p \leq 0.05$). IB data was subjected to non-parametric ANOVA with aligned rank for non-parametric analysis of multifactor designs (Oliver-Rodríguez and Wang, 2013) and mean separation by Tukey's test ($p \leq 0.05$) for ranked data.

For the postharvest study, in order to determine the relationships between firmness and IB during storage, data were subjected to regression analysis (r^2) and models were fitted for each cultivar, season, firmness category, and drop heights. Additionally, statistical comparisons of slopes and intercepts between models for dropped vs. non-dropped fruit and, between firmness categories of each dropping treatment (soft vs. medium; medium vs. firm, and soft vs. firm) were performed. Data were transformed to obtain linearized models between firmness (x) and IB (y). The best-fitted model was 1/x for both cultivars.



FIGURE 1 | Scale used for assessing internal browning (IB) severity in blueberry fruit. Categories were assigned based on the extent of bruised equatorial area: 0 (0–5%), 1 (6–25%), 2 (26–50%), 3 (51–75%), and 4 (>75%).

Analyses were executed using commercial statistical software Statgraphics Centurion XVI (v.16.0.09, Statpoint, VA, USA) and R 3.0.0 (R Development Core Team, 2008).

RESULTS

Fruit Condition at Harvest

Firmness and IB before Fruit Segregation

When commercial fruit sample was assessed for firmness at harvest, both cultivars displayed a wide range of values (**Figure 2A**). “Duke” firmness showed similar mean values during seasons 2011/2012 (Y1) and 2012/2013 (Y2) (1.55 and 1.60 N, respectively), whereas higher disparity was found on “Brigitta” (1.52 and 1.92 N, correspondingly). Yet, comparison by Kolmogorov-Smirnov test ($p \leq 0.05$) evidenced significant differences in frequency distribution between years for both varieties (data not shown). Additionally, on both cultivars, fruit harvested on Y1 had greater variability (largest and smallest data values, wider quartile distributions, greater number of outliers) than berries picked on Y2. For “Duke,” 55 and 50% of fruit were below 1.6 N (upper threshold of the soft firmness category) for Y1 and Y2, respectively. For “Brigitta” these values reached 60 and 15% for Y1 and Y2, correspondingly. If a threshold of 1.4 N for very soft fruit is considered, 25% (Y1) and 10% (Y2) of “Duke” fruit were below that level, whereas values for “Brigitta” were 42 and 5% for Y1 and Y2, in that order (**Figure 2**).

Although not subjected to the dropping procedure, fruit displayed some IB at harvest (**Figure 2B**), with mean IB scores of 0.15–0.19 for “Duke,” and 0.10–0.01 for “Brigitta,” on Y1 and Y2, correspondingly. The most heterogeneous IB values were found for “Brigitta” fruit harvested on Y1. Yet, overall percentages of non-bruised fruit (category 0) at harvest were higher for “Brigitta” (90.0–92.5%) than for “Duke” (83.1–89.8%) (data not shown).

Fruit Quality after Firmness Segregation

Once samples were segregated by firmness, the ANOVA proved that fruit quality at harvest was influenced by initial firmness

(**Table 1**). On both cultivars, firmer fruit was related to higher TA but lower TSS/TA and IB; TSS were significant only on “Brigitta,” and higher on the softer group (<1.60 N). Differences between years occurred for TSS, TA, and TTS/TA for “Duke” and for TSS, TA, and IB on “Brigitta,” reinforcing the higher variability found on this last trait during Y1. Significant interactions occurred for TA on “Duke” (with differences between categories on Y1, but no differences on Y2) and for IB on “Brigitta” (with differences only on soft fruit between years, having Y1 higher IB than Y2) (Supplementary Figure S1).

Firmness and IB Evolution of Dropped and Non-dropped Fruit during Postharvest

In comparison to “Brigitta,” “Duke” berries showed lower firmness retention along time, irrespective of firmness category, dropping treatment or season (**Figure 3**). Between harvest and the end of storage, and for both seasons, firmness of “Duke” blueberries was reduced on average by 39.8, 33.6, and 38.6% (**Figures 3A,C,E**) for soft, medium, and firm fruit, respectively (data not shown), whereas firmness loss in “Brigitta” averaged 17.3, 24.4, and 23.8%, correspondingly (**Figures 3B,D,F**). When dropped and non-dropped fruit were compared, “Brigitta” fruit appeared to be more sensitive to initial firmness, since significant differences between damaged and non-damaged fruit were found for most of storage evaluations (medium on Y1; soft, medium, and firm on Y2). In contrast, for “Duke” samples consistent differences between dropped and non-dropped fruit along the whole storage period were observed on soft fruit harvested on Y1 uniquely. Additionally, the magnitude of the differences between dropped and non-dropped fruit, as well as between seasons, were higher for “Brigitta.”

In general, IB was higher after storage than at harvest, particularly for soft fruit (**Figure 4**), regardless of cultivar, year, or dropping treatment. “Duke” fruit exhibited relatively low IB values up to 21 days of storage, with the highest IB at 35 days for soft (Y1 and Y2) and medium firmness fruit

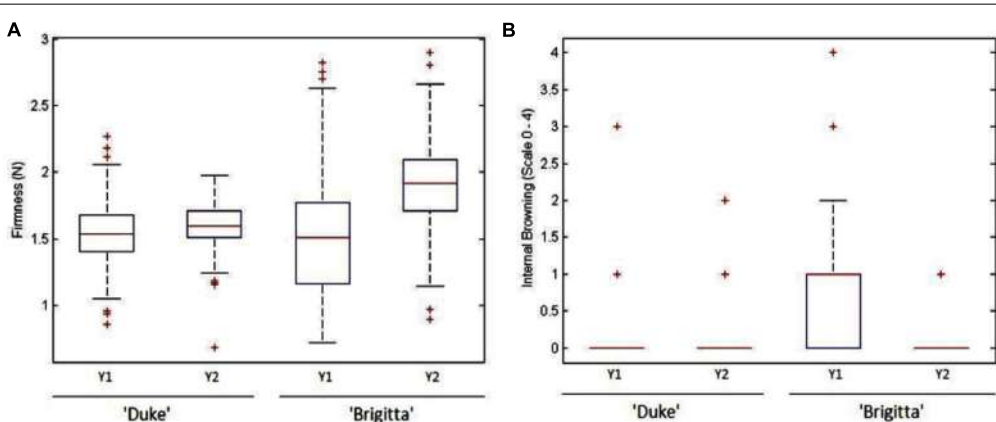


FIGURE 2 | Fruit firmness (**A**) and internal browning (**B**) variability at commercial harvest of “Duke” and “Brigitta” blueberries, during seasons 2011/2012 (Y1) and 2012/2013 (Y2). IB categories: 0 (0–5%), 1 (6–25%), 2 (26–50%), 3 (51–75%), and 4 (>75%). $n = 200$ per year and cultivar. On each box and whisker plot, “+” represent outliers.

TABLE 1 | Analysis of variance for fruit quality traits^a at harvest of “Duke” and “Brigitta” blueberries according to three-firmness category groups, during seasons 2011/2012 (Y1) and 2012/2013 (Y2).

Cultivar	Factor	TSS (%)	TA (% citric acid)	TSS/TA	IB (scale 0–4)
“Duke”	Firmness category (F)				
	Soft (<1.60 N)	11.2	0.59c	19.4a	0.38a
	Medium (1.60–1.80 N)	11.1	0.71b	17.5ab	0.44a
	Firm (1.81–2.00 N)	11.1	0.83a	15.1b	0.19b
	Year (Y)				
	Y1	12.4a	0.93a	13.7b	0.34
	Y2	9.9b	0.49b	20.9a	0.31
	Significance (<i>p</i> -value)				
	F	0.974 ^b	0.000	0.049	0.000
	Y	0.000	0.000	0.000	0.069
	F × Y	0.527	0.002	0.118	0.352
“Brigitta”	Firmness category (F)				
	Soft (<1.60 N)	15.2a	0.57b	28.4a	1.28a
	Medium (1.60–1.80 N)	13.5b	0.64ab	21.4b	0.26b
	Firm (1.81–2.00 N)	13.2b	0.75a	18.0b	0.19c
	Year (Y)				
	Y1	15.1a	0.74a	22.3	0.69a
	Y2	12.8b	0.57b	22.9	0.45b
	Significance (<i>p</i> -value)				
	F	0.008	0.030	0.002	0.000
	Y	0.000	0.007	0.692	0.000
	F × Y	0.243	0.329	0.844	0.000

For a given cultivar, or factor, and significance *p* ≤ 0.05, different letters within a column represent significant differences (Tukey's test, *p* ≤ 0.05).

^aTraits: total soluble solids (TSS), titratable acidity (TA), and internal browning (IB) damage categories: 0 (0–5%), 1 (6–25%), 2 (26–50%), 3 (51–75%), or 4 (>75%).

^bIn red, *p*-values lower than 0.05.

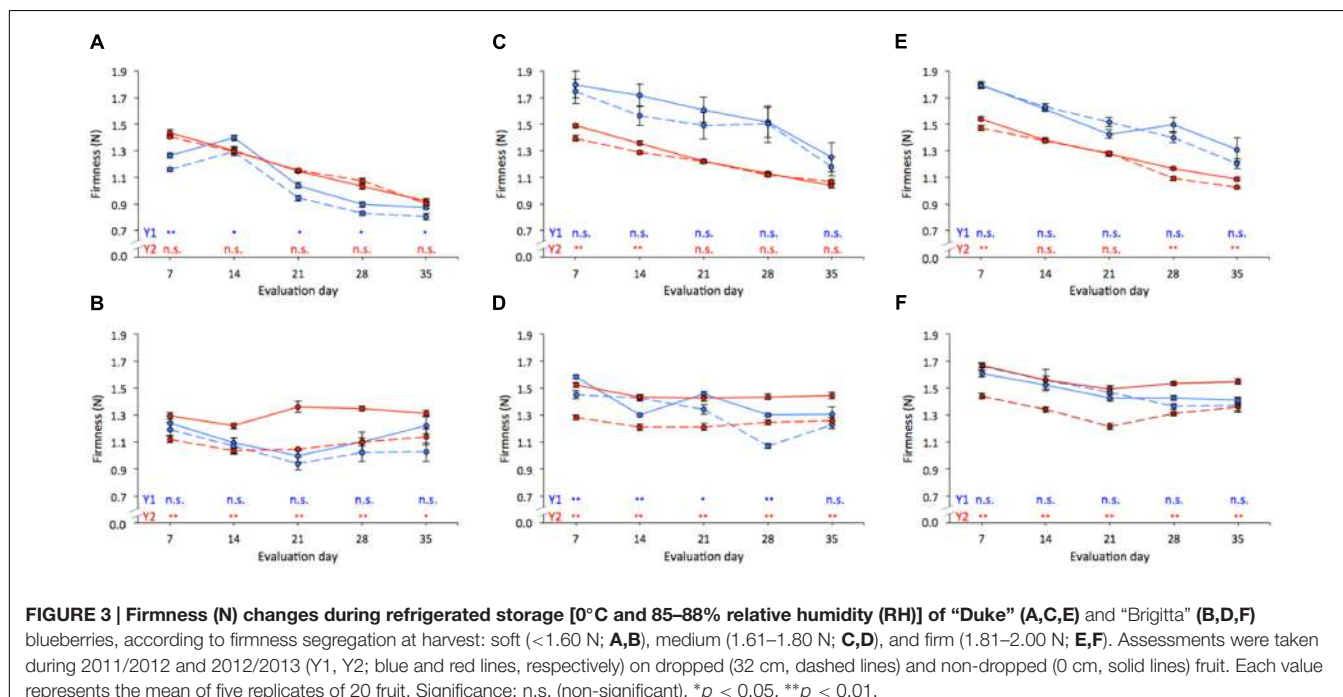


FIGURE 3 | Firmness (N) changes during refrigerated storage [0°C and 85–88% relative humidity (RH)] of “Duke” (A,C,E) and “Brigitta” (B,D,F) blueberries, according to firmness segregation at harvest: soft (<1.60 N; A,B), medium (1.61–1.80 N; C,D), and firm (1.81–2.00 N; E,F). Assessments were taken during 2011/2012 and 2012/2013 (Y1, Y2; blue and red lines, respectively) on dropped (32 cm, dashed lines) and non-dropped (0 cm, solid lines) fruit. Each value represents the mean of five replicates of 20 fruit. Significance: n.s. (non-significant), **p* < 0.05, ***p* < 0.01.

(Y2) (Figures 4A,C). Similarly to the evolution of firmness in postharvest (Figure 3), “Duke” fruit also developed less IB in response to dropping, given that no significant differences

between treatments were found at most of the evaluation dates. “Brigitta,” on the other hand, showed marked differences in IB development between dropped and non-dropped fruit for all

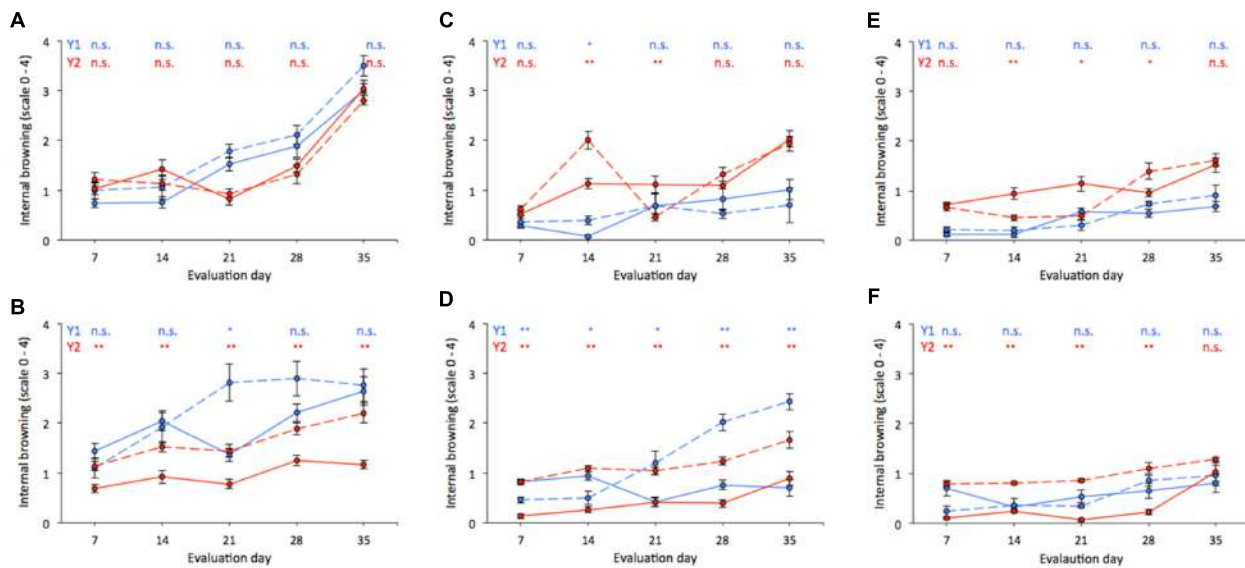


FIGURE 4 | Internal browning changes during refrigerated storage (0°C and 85–88% RH) of “Duke” (A,C,E) and “Brigitta” (B,D,F) blueberries, according to firmness segregation at harvest: soft (<1.60 N; A,B), medium (1.61–1.80 N; C,D), and firm (1.81–2.00 N; E,F). Assessments were taken during 2011/2012 and 2012/2013 (Y1, Y2; blue and red lines, respectively) on dropped (32 cm, dashed lines) and non-dropped (0 cm, solid lines) fruit. Each value represents the mean of five replicates of 20 fruit. IB scale: 0 (0–5%), 1 (6–25%), 2 (26–50%), 3 (51–75%), and 4 (>75%). Significance: n.s. (non-significant), * p < 0.05, ** p < 0.01.

firmness categories (Figures 4B,D,F). Compared to “Duke” and regardless of dropping treatment, “Brigitta” fruit developed lower IB within medium and firm categories (Figures 4B,D).

Relationship between IB and Firmness

For “Duke” samples, the regression analyses (r^2) between IB and firmness (Table 2 and Figure 5) revealed significant effects on dropped and non-dropped fruit for all three firmness categories and for both seasons. Although r^2 varied among comparisons, soft and firm fruit showed in general the highest values. In contrast, 9 out of the 12 models fitted for “Brigitta,” which included all non-dropped fruit of both years and dropped fruit of Y2, showed no significant associations. During Y1, the highest r^2 values for dropped fruit were found on soft and medium fruit of this cultivar (72.7 and 80.6, respectively). The comparisons of slopes and intercepts between dropping treatments (Table 2) showed that significant differences for “Duke” were found only between intercepts of firm fruit harvested in Y2. In contrast, equations developed for “Brigitta” differed in slopes (soft and medium fruit of Y1) and intercepts (medium fruit of Y1, all three categories on Y2) on five out of the six instances.

When firmness categories were contrasted within the same dropping treatment (Table 3), outcomes varied among seasons. On non-dropped fruit of Y1, three comparisons resulted on different intercepts (medium vs. firm on “Duke”; soft vs. medium, and soft vs. firm on “Brigitta”), but no differences were found between slopes. For the same treatment, differences on Y2 occurred amid slopes of “Duke” (medium vs. firm, and soft vs. firm) and intercepts of “Brigitta” (soft vs. medium). Within dropped fruit of Y1 no significant differences were

found for any comparison on “Duke,” whereas two cases were statistically significant for “Brigitta” (soft vs. medium differed on intercept and slope; medium vs. firm differed on slopes). On Y2, differences between intercepts of medium vs. firm, and soft vs. firm occurred for “Duke,” meanwhile for “Brigitta” the only significant difference happened between slopes of soft vs. firm fruit.

DISCUSSION

The analysis of fruit characteristics at harvest revealed two important aspects that have not been reported previously. The first one is that, regardless of cultivar or season, high variability in fruit firmness occurred within each commercial harvest. In comparison with other fruit species such as apple, for which very soft fruit (58–62 N) represent less than 0.5–0.8% (Herregods and Goffings, 1993; De Silva et al., 2000), a high percentage of “Duke” and “Brigitta” blueberries showed this characteristic (<1.4 N) in Y1 (25 and 42%, respectively) and Y2 (10 and 5%, respectively). The second one refers to the noticeable differences in quality traits found between firmness categories, which highlights the relevance of analyzing the development of softening and IB for each sorted group separately. These two aspects will be covered during the discussion.

Susceptibility of Blueberries to Develop IB

IB was detected at harvest in this study, even though fruit were carefully hand-picked and not subjected to sorting or packing. Gołacki et al. (2009) indicated that vibration forces, usually

TABLE 2 | Internal browning (IB) vs. firmness (F) regression analysis for non-dropped (0 cm) and dropped (32 cm) fruit.

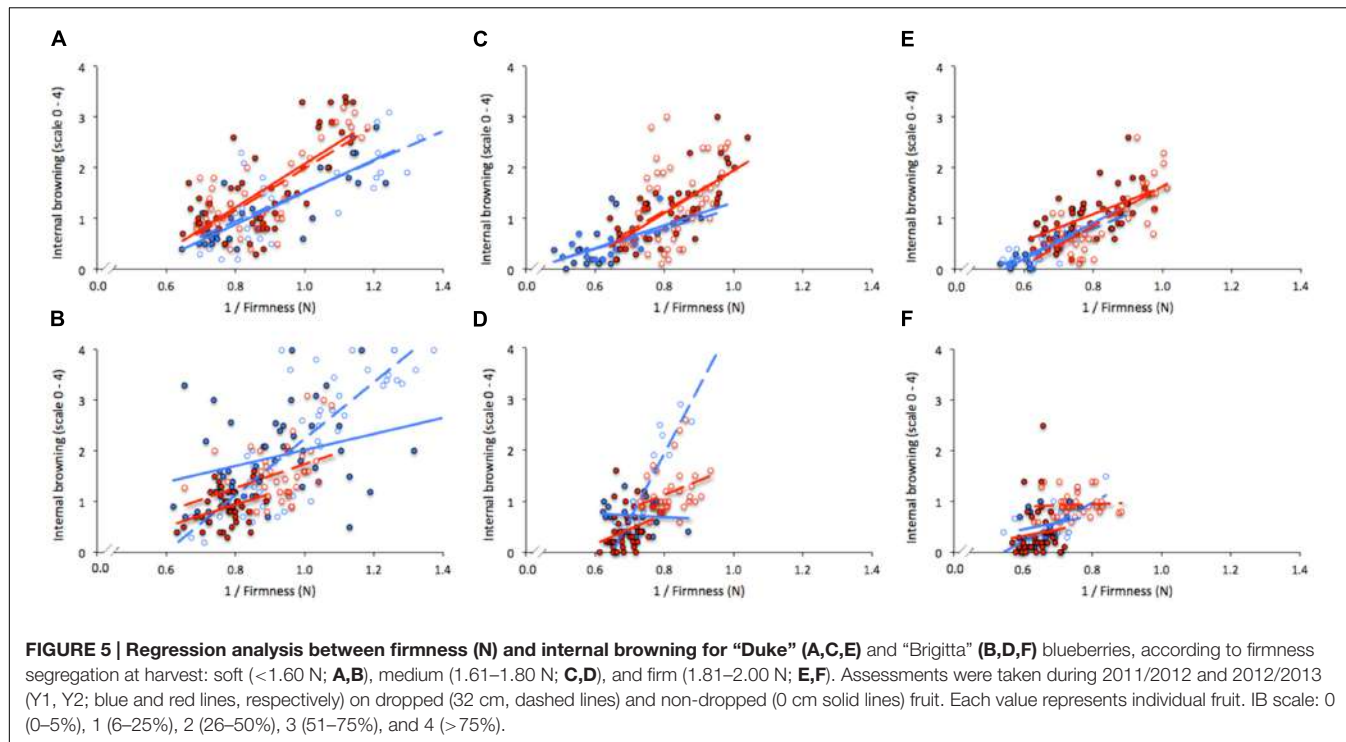
Cultivar	Year	Firmness category	Model			Model comparisons (p-values)	
			Equation	n ^a	r ^{2b}	Intercept	Slope
"Duke"	Y1	Soft (<1.60 N)	$IB_0 = -1.669 + 3.188 \times (1/F)$	30	69.2***	0.772 ^c	0.740
		Medium (1.60–1.80 N)	$IB_{32} = -1.429 + 2.966 \times (1/F)$	30	53.7***		
		Firm (1.81–2.00 N)	$IB_0 = -1.213 + 2.745 \times (1/F)$	16	25.7*	0.643	0.600
			$IB_{32} = -0.796 + 1.994 \times (1/F)$	16	34.3*		
			$IB_0 = -1.936 + 0.825 \times (1/F)$	18	72.1***	0.585	0.369
	Y2	Soft (<1.60 N)	$IB_0 = -2.233 + 4.311 \times (1/F)$	50	50.3***	0.528	0.864
		Medium (1.60–1.80 N)	$IB_{32} = -2.185 + 4.173 \times (1/F)$	50	58.0***		
		Firm (1.81–2.00 N)	$IB_0 = -2.256 + 4.203 \times (1/F)$	50	55.0***	0.747	0.834
			$IB_{32} = -2.013 + 3.953 \times (1/F)$	50	20.3*		
			$IB_0 = -1.039 + 2.656 \times (1/F)$	50	35.3***	0.002	0.118
"Brigitta"	Y1	Soft (<1.60 N)	$IB_0 = 0.439 + 1.584 \times (1/F)$	48	8.57 ^{n.s.}	0.814	0.000
		Medium (1.60–1.80 N)	$IB_{32} = -3.333 + 5.576 \times (1/F)$	48	72.7***		
		Firm (1.81–2.00 N)	$IB_0 = 0.963 - 0.340 \times (1/F)$	20	0.57 ^{n.s.}	0.016	0.000
			$IB_{32} = -8.393 + 12.921 \times (1/F)$	20	80.6***		
			$IB_0 = -0.359 + 1.354 \times (1/F)$	26	4.48 ^{n.s.}	0.507	0.219
	Y2	Soft (<1.60 N)	$IB_{32} = -2.060 + 3.798 \times (1/F)$	26	43.9**		
		Medium (1.60–1.80 N)	$IB_0 = -0.780 + 2.153 \times (1/F)$	40	12.4 ^{n.s.}	0.028	0.904
		Firm (1.81–2.00 N)	$IB_{32} = -0.597 + 2.338 \times (1/F)$	40	11.7 ^{n.s.}		
			$IB_0 = -1.580 + 2.910 \times (1/F)$	40	7.06 ^{n.s.}	0.012	0.947
			$IB_{32} = -1.081 + 2.763 \times (1/F)$	40	10.6 ^{n.s.}		

^aSample size.^bSignificance: n.s. (non-significant), *p < 0.05, **p < 0.01, ***p < 0.001.^cIn red, p-values lower than 0.05.Intercept and slope comparison between IB_0 and IB_{32} , of "Duke" and "Brigitta" blueberries according to three firmness category groups, during seasons 2011/2012 (Y1) and 2012/2013 (Y2).

occurring during transportation from the field, are difficult to avoid and may also cause damage. In addition to possible damage sources before harvest (e.g., due to wind or machinery), fruit samples used herein underwent a ~3-h trip from the field to the laboratory, and hence transportation may have impacted the basal IB found. Indeed, unless a packinghouse facility is available at the producing orchard, it is common that fruit travel 2–3 h until being processed. This observation highlights the importance of careful handling of the fruit throughout the whole production and distribution chain, and evidences high differences within a particular cultivar among seasons. In fact, variability in firmness and IB at harvest showed dissimilarities between cultivars, with "Duke" fruit being more homogeneous for both seasons, whereas "Brigitta" berries showed higher differences within and between years. The high IB values in Y1 at harvest for "Brigitta" were associated to softer fruit (**Figure 2**). Variations in ambient temperature between both seasons (Supplementary Table S1) may partially account for the differences in fruit condition between seasons and cultivars, especially for higher heterogeneity of "Brigitta" samples on Y1. Although there is not much information, it has been suggested that an ideal range of temperatures for northern highbush blueberries might range 20–25°C (Davies and Flore, 1986); values

above 30°C (also associated with high light intensity as in Chile) cause plant damage (Trehane, 2004; Lobos and Hancock, 2015), as well as lowered wax coverage of fruit, which tend to be smaller and softer (Mainland, 1989). With the exception of precipitation (Y1: 32.9 mm and Y2: 102 mm), Longaví does not usually register substantial differences in environmental conditions from early October (full bloom) to early December (harvest) (Supplementary Table S1). This might in part explain the lower variability between seasons observed for "Duke." On the other hand, different temperature patterns for each season were registered in Santa Bárbara in December. Even though more favorable temperatures occurred in Y1 (20–25°C), more temperature extremes took place (greater number of hours or days hotter than 27, 29, and 32°C), probably leading to early softening of fruit.

It is also highly likely that blueberries can be damaged on packing-lines. Xu et al. (2015) studied 11 commercial packing lines using the BIRD and found that the tested lines differed in their combinations and alignments, thus creating different points for potential impact damage. Yet, all the impacts occurred at transfer points, the highest drop heights being 35–36 cm. Additionally, the latter part of the packing line, where fruit drop into the hopper for loading clamshells, is another point for



potential damage due to the combination of hard contact surface (usually stainless steel) and high drop height (Xu et al., 2015), and especially when the first berries drop into the hopper, since they will impact directly onto the hard surface. As more fruit get into the line, ever more fruit-to-fruit impacts will take place, this being a source of impact that has not been fully incorporated in studies dealing with mechanical damage. Results obtained in the present study show that significant differences in IB development between “Duke” and “Brigitta” occurred with drop heights of 32 cm, evidencing a differential effect of season, cultivar, and firmness category.

In order to standardize sorting/packing-lines and to establish some basic recommendations to improve condition, it is critical to identify which fruit would be more prone to softening and IB during postharvest. Unfortunately, given that the main criterion for establishing harvest date of blueberries is skin color, and that high labor costs are associated to this operation (Brown et al., 1996; Takeda et al., 2008; Lobos et al., 2014b), growers wait for blue fruit to accumulate in the bush before starting commercial pickings. This practice results in fruit with similar external appearance but, as found in the present study, with important heterogeneity in maturity status, that will lead to a wide range of firmness levels at harvest, as well as in softening rates during postharvest. Previous works have proved that delaying harvest increases TSS and TSS/TA but reduces TA and firmness (Woodruff et al., 1960; Ballinger et al., 1963; Kushman and Ballinger, 1963; Lobos et al., 2014a), since TSS increase and acids decrease due to fruit respiration in the course of maturation (Famiani et al., 2005; Dai et al., 2009). In fact, when fruit showing no differences in skin color at harvest (determined either visually or instrumentally) were picked 2 or 6

days after turning 100% blue on the bush, important differences in fruit condition were demonstrated associated to these two maturity stages (Moggia et al., 2016a,b). In those previous studies, when similar percentages of green and pink fruit were reached early in the season, clusters with similar characteristics and canopy position were selected and labeled. Fruit development was followed until both maturity stages were reached: 100% blue and residing on the plant for a maximum of 2 days (ripe), and 100% blue and residing on the plant for 6 days (overripe). That methodology allowed the authors to conclude that, when these two maturity stages were selectively picked, important differences were found, “Duke” being more sensitive than “Brigitta” to this factor. The elapsed time between harvests was enough to increase TSS and TSS/TA of “Duke” samples, and to reduce fruit firmness in both cultivars. These findings reinforce the importance of the time that fruit stay on the plant after turning 100% blue for fruit heterogeneity. In the present study, segregation by firmness at harvest revealed similar trends for these traits, suggesting that fruit within the soft category had actually stayed longer in the plant after turning completely blue. Accordingly, when fruit were segregated based on firmness, berries assigned to the soft category displayed the highest IB, TSS, and TSS/TA values (Table 1). Given the variability found at harvest (box and whisker plots), these dissimilarities would be higher for Y1 “Brigitta” fruit, thus accounting for the greater differences found according to the dropping treatment between fruit within the soft and the medium categories. In fact, according to the Chilean blueberry industry, overall commercial defects (including softening, dehydration, and mechanical damage) differ between seasons, and the affected produce may account for 10–45% of the fresh fruit reaching final markets (Moggia et al., 2016b).

TABLE 3 | Intercept and slope comparisons of internal browning vs. firmness regression analysis, between firmness category groups for non-dropped (0 cm) and dropped (32 cm) "Duke" and "Brigitta" blueberries, during seasons 2011/2012 (Y1) and 2012/2013 (Y2).

Cultivar	Drop height (cm)	Firmness category	Model comparisons (<i>p</i> -values)			
			Y1		Y2	
			Intercept	Slope	Intercept	Slope
"Duke"	0	Soft vs. medium	0.273 ^a	0.746	0.304	0.902
		Medium vs. firm	0.035	0.572	0.779	0.045
		Soft vs. firm	0.840	0.783	0.152	0.066
	32	Soft vs. medium	0.911	0.517	0.908	0.851
		Medium vs. firm	0.164	0.492	0.007	0.702
		Soft vs. firm	0.576	0.877	0.001	0.870
"Brigitta"	0	Soft vs. medium	0.000	0.443	0.019	0.691
		Medium vs. firm	0.148	0.399	0.678	0.558
		Soft vs. firm	0.007	0.954	0.126	0.689
	32	Soft vs. medium	0.029	0.002	0.397	0.810
		Medium vs. firm	0.346	0.000	0.148	0.081
		Soft vs. firm	0.783	0.370	0.146	0.034

^aIn red, *p*-values lower than 0.05.

Bruising as Related to Firmness

Firmness is one of the characteristics most frequently measured to evaluate quality of fresh fruit (Timm et al., 1996). As for many other fruit species, firmer blueberries can more readily withstand harvest handling, and will therefore have longer storage potential (Hanson et al., 1993; Yu et al., 2014). Differences in firmness among highbush blueberry cultivars seem to be more dependent on physiological maturity at harvest than on genotypic differences (Beaudry et al., 1998; Lobos et al., 2014a); yet there is limited information on the relevance of firmness at harvest for postharvest quality of fruit within a particular cultivar. Wolfe et al. (1983) demonstrated that firmness separation of blueberries at harvest allows better control of postharvest decay, since soft, medium, and firm fruit show different susceptibility to rot, and fruit segregation enhanced disease control when combined with a hot water dip. Similarly, the present study demonstrates that softening and IB development are related to firmness at harvest of individual fruit, and that high IB can be expected in soft fruit of both cultivars after prolonged storage.

Since in this study the highest IB rates were always found for soft berries (<1.60 N), our findings strengthen the idea that mid-to-firm berries can better withstand a long trip to distant markets. Therefore, any strategy oriented to increase the percentage of these firmness classes into the clamshells will assure higher and more homogeneous quality upon arrival to final destination.

Dropping the fruit did not always lead to higher IB values, and this observation was more evident for "Duke" samples, in which high softening rates but small differences in IB between dropped and non-dropped fruit occurred (Figure 4). This finding agrees with the lack of differences between slopes and intercepts of the models fitted for fruit of this cultivar (0 vs. 32 cm drop heights) (Table 2); the only difference was found between intercepts of firm fruit, but not between slopes, which indicates similar rates of change in IB per firmness unit both for dropped and non-dropped fruit (Table 2 and Figure 5). Yet, significant

associations between firmness and IB, and generally higher *r*² coefficients, both for dropped and non-dropped fruit were obtained for "Duke" as compared to "Brigitta" samples (Table 2). On the other hand, the fact that "Brigitta" fruit did not show significant associations for most of the equations indicates a weak relationship between firmness and IB development for this cultivar, especially for samples harvested in Y2. However, higher IB levels in dropped than in non-dropped fruit, regardless of fruit firmness at harvest should be expected for this cultivar (Table 2 and Figure 5). The analyses undertaken for "Brigitta" samples corresponding to Y1 (more heterogeneous in initial condition, and significant *r*² values for dropped fruit uniquely) reveal that differences in slopes and intercepts occurred for all three firmness categories, with different rates of change between dropping treatments. When equations were compared between firmness categories within each dropping treatment (Table 3), variability between seasons became more evident, since significances were not the same in both years considered. Moreover, different slopes (meaning dissimilar rate of change in IB per firmness unit) were found on "Duke" 0 cm and "Brigitta" 32 cm, whereas different intercepts (indicating similar rates, but different damage threshold) occurred on "Duke" 32 cm and "Brigitta" 0 cm. Additionally, most of these differences were observed between soft and firm fruit, which emphasizes the negative effects on quality resulting from a high proportion of soft fruit on a particular picking.

According to these results, each cultivar would display a different pattern of IB development when subjected to mechanical damage. Therefore, and depending upon fruit condition at harvest (initial firmness), fruit might not necessarily exhibit severe IB symptoms but would probably show different softening patterns. Another important aspect to consider is that sectioning berries through the equator detects bruising caused by impacts occurring onto that area, but this procedure does not take into account damage at or near the calyx or stem ends, and it

would hence lead to an underestimation of the actual mechanical damage (Yu et al., 2014).

The present study demonstrated the different susceptibility to IB development and softening rates in blueberry fruit among different cultivars and firmness categories at harvest, and suggests that fruit displaying firmness lower than 1.6 N at harvest should be avoided if long-term storage is intended. Galletta et al. (1971) proposed that good keeping quality could be expected when TSS/TA ratios are <18, whereas intermediate keeping quality would result from higher TSS/TA values. Given that TSS/TA ratios at harvest of medium and firm fruit ranged from 15 to 21, and that soft fruit values ranged 19–29, it is suggested that this ratio could be used as an additional index to define harvest time and destination of the fruit (long- vs. short-term storage).

Overall, “Duke” fruit were characterized by high rates of firmness loss, as well as by a strong association between firmness and IB, but little differences were found between dropped and non-dropped fruit. “Brigitta” berries had slower softening rates, and displayed very weak relationships between firmness and IB (especially for non-dropped fruit), but marked differences between dropping treatments were found.

CONCLUSION

Results of this work suggest that the mean firmness value may be not adequate as an indicator of blueberry fruit condition at harvest, and that the differences in fruit quality traits associated to the initial firmness level might be related to the time that fruit stay on the plant after turning blue, softer fruit displaying more advanced maturity. This finding suggests that, during seasons in which adverse environmental events occur (probably associated to high temperatures close to harvest), the proportion and evolution of soft fruit during shipments would enhance rejections at destination markets. Future research should

REFERENCES

- Ballinger, W. E., Kushman, L. J., and Brooks, J. F. (1963). Influence of crop load and nitrogen applications upon yield and fruit qualities of ‘Wolcott’ blueberries. *Proc. Am. Soc. Hortic. Sci.* 42, 264–276.
- Beaudry, R. M., Moggia, C., Retamales, J. B., and Hancock, J. F. (1998). Quality of ‘Ivanhoe’ and ‘Bluecrop’ blueberry fruit transported by air and sea from Chile to North America. *HortScience* 33, 313–317.
- Brown, G. K., Schulte, N.-L., Timm, E. J., Beaudry, R. M., Peterson, D. L., Hancock, J. F., et al. (1996). Estimates of mechanization effects on fresh blueberry quality. *Appl. Eng. Agric.* 12, 21–26. doi: 10.13031/2013.25435
- Dai, Z. W., Vivin, P., Robert, T., Milin, S., Li, S. H., and Genard, M. (2009). Model-based analysis of sugar accumulation in response to source-sink ratio and water supply in grape (*Vitis vinifera*) berries. *Funct. Plant Biol.* 36, 527–540. doi: 10.1071/FP08284
- Davies, F. S., and Flore, J. A. (1986). Gas exchange and flooding stress of highbush and rabbiteye blueberry. *J. Am. Soc. Hortic. Sci.* 111, 565–571.
- De Silva, H. N., Hall, A. J., Cashmore, W. M., and Tustin, D. S. (2000). Variation of fruit size and growth within an apple tree and its influence on sampling methods for estimating the parameters of mid-season size distributions. *Ann. Bot.* 86, 493–501. doi: 10.1006/anbo.2000.1220
- Ehlenfeldt, M. K., and Martin, R. B. Jr. (2002). A survey of fruit firmness in highbush blueberry and species-introgressed blueberry cultivars. *HortScience* 37, 386–389.
- Famiani, F., Cultrera, N. G. M., Battistelli, A., Casulli, V., Proietti, P., Standardi, A., et al. (2005). Phosphoenolpyruvate carboxykinase and its potential role in the catabolism of organic acids in the flesh of soft fruit during ripening. *J. Exp. Bot.* 56, 2959–2969. doi: 10.1093/jxb/erj293
- Galletta, G. J., Ballinger, W. E., Monroe, R. J., and Kushman, L. J. (1971). Relationships between fruit acidity and soluble solids level of highbush blueberry clones and fruit keeping quality. *J. Am. Soc. Hortic. Sci.* 6, 758–762.
- Gofacki, K., Bobin, G., and Stropek, Z. (2009). Bruise resistance of apples (Melrose variety). *TEKA Kom. Mot. Roln. OL PAN* 9, 40–47.
- Hanson, E., Beggs, L., and Beaudry, R. M. (1993). Applying calcium chloride postharvest to improve highbush blueberry firmness. *HortScience* 28, 1033–1034.
- Herregods, M., and Goffings, G. (1993). Variability in maturity, quality and storage ability of Jonagold apples on a tree. *Acta Hortic.* 326, 59–64. doi: 10.17660/ActaHortic.1993.326.5
- Kushman, L. J., and Ballinger, W. E. (1963). Influence of season and harvest interval upon quality of Wolcott blueberries grown in eastern North Carolina. *Proc. Am. Soc. Hortic. Sci.* 83, 395–405.
- Lobos, G. A., Callow, P., and Hancock, J. F. (2014a). The effect of delaying harvest date on fruit quality and storage of late highbush blueberry cultivars (*Vaccinium corymbosum* L.). *Postharvest Biol. Technol.* 87, 133–139. doi: 10.1016/j.postharvbio.2013.08.001
- Lobos, G. A., and Hancock, J. F. (2015). Breeding blueberries for a changing global environment: a review. *Front. Plant Sci.* 6:782. doi: 10.3389/fpls.2015.00782

include a more detailed study on potential sources of fruit heterogeneity. Furthermore, more systematic measurements of changes throughout fruit development from early stages, as done for other species, could help in modeling softening and IB during postharvest. Finally, long-time studies are needed to quantify the real genotypic and environmental effects on softening and IB development in blueberries.

AUTHOR CONTRIBUTIONS

CM and GL contributed to the conception and design of the work. GG, CM, and GL performed acquisition, analysis, and interpretation of data for the work. CM, GL, JG, and IL collaborated to generate and validate the version to be published.

FUNDING

In Chile, this work was supported by the National Commission for Scientific and Technological Research CONICYT (FONDECYT 11130539) and the Universidad de Talca (research programs “Adaptation of Agriculture to Climate Change (A2C2)”, “Fondo Proyectos de Investigación” and “Núcleo Científico Multidisciplinario”). In Spain, this work was partially supported by “Fundación Carolina” and “Programa de Doctorado en Ciencia y Tecnología Agraria y Alimentaria”, Universitat de Lleida.

SUPPLEMENTARY MATERIAL

The Supplementary Material for this article can be found online at: <http://journal.frontiersin.org/article/10.3389/fpls.2017.00535/full#supplementary-material>

- Lobos, G. A., Moggia, C., Sánchez, C., and Retamales, J. B. (2014b). Postharvest effects of mechanized (Automotive or Shaker) vs. hand harvest on fruit quality of blueberries (*Vaccinium corymbosum* L.). *Acta Hortic.* 1017, 135–139. doi: 10.17660/ActaHortic.2014.1017.13
- Mainland, C. M. (1989). "Harvesting, sorting and packing quality blueberries," in *Proceedings of the 23rd Annual Open House, Southeastern Blueberry Council*, (Elizabethtown, KY: North Carolina State University).
- Moggia, C., González, C., Lobos, G. A., Bravo, C., Valdés, M., Lara, I., et al. (2016a). "Changes in quality and maturity of 'Duke' and 'Brigitta' blueberries during fruit development: postharvest implications," in *Proceedings of the ISHS VIII International Postharvest Symposium*, Cartagena.
- Moggia, C., Graell, J., Lara, I., Schmeda-Hirschmann, G., Thomas-Valdés, S., and Lobos, G. A. (2016b). Fruit characteristics and cuticle triterpenes as related to postharvest quality of highbush blueberries. *Sci. Hortic.* 211, 449–457. doi: 10.1016/j.scientia.2016.09.018
- Oliver-Rodríguez, J. C., and Wang, X. T. (2013). Non-parametric three-way mixed ANOVA with aligned rank tests. *Br. J. Math. Stat. Psychol.* 68, 23–42. doi: 10.1111/bmsp.12031
- Opara, U. L., and Pathare, B. (2014). Bruise damage measurement and analysis of fresh horticultural produce—a review. *Postharvest Biol. Technol.* 91, 9–24. doi: 10.1016/j.postharvbio.2013.12.009
- R Development Core Team (2008). *R: A Language and Environment for Statistical Computing*. Vienna: R Foundation for Statistical Computing.
- Retamales, J. B., Palma, M. J., Morales, Y. A., Lobos, G. A., Moggia, C., and Mena, C. A. (2014). Blueberry production in Chile: current status and future developments. *Rev. Bras. Frutic.* 36, 58–67. doi: 10.1590/0100-2945-446/13 01.008
- Studman, C. (1997). "Factors affecting the bruise susceptibility of fruit," in *Proceedings of the 2nd International Conference of Plant Biomechanics*, eds G. Jeronimidis and J. F. V. Vincent (Reading: University of Reading), 273–281.
- Takeda, F., Krewer, G., Andrews, E. L., Mullinix, B. Jr., and Petreson, D. L. (2008). Assessment of the V45 blueberry harvester on rabbiteye blueberry and southern highbush blueberry pruned to V-shaped canopy. *HortTechnology* 1, 130–138.
- Timm, E. J., Brown, G. K., Armstrong, P. R., Beaudry, R. M., and Shirazi, A. (1996). Portable instrument for measuring firmness of cherries and berries. *Appl. Eng. Agric.* 12, 71–77. doi: 10.13031/2013.25441
- Trehane, J. (2004). *Blueberries, Blueberries and Other Vacciniums*. Portland, OR: Timber Press.
- Wolfe, R., Abrams, M. L., and Probasco, W. F. (1983). Controlling postharvest decay of blueberries using firmness separation and hot water treatments. *Trans. ASAE* 26, 312–315. doi: 10.13031/2013.33927
- Woodruff, R. E., Dewey, D. H., and Sell, H. M. (1960). Chemical changes of Jersey and Rubel blueberry fruit associated with ripening and deterioration. *Proc. Am. Soc. Hortic. Sci.* 75, 387–401.
- Xu, R., Takeda, F., Krewer, G., and Li, C. (2015). Measure of mechanical impacts in commercial blueberry packing lines and potential damage to blueberry fruit. *Postharvest Biol. Technol.* 110, 103–130. doi: 10.1016/j.postharvbio.2015.07.013
- Yu, P., Li, C., Rains, G., and Hamrita, T. (2011). Development of the berry impact recording device sensing system: hardware design and calibration. *Comput. Electron. Agric.* 79, 103–111. doi: 10.1016/j.compag.2011.08.013
- Yu, P., Li, C., Takeda, F., and Krewer, G. (2014). Visual bruise assessment and analysis of mechanical impact measurement in southern highbush blueberries. *Appl. Eng. Agric.* 30, 29–37. doi: 10.13031/aea.30.10224

Conflict of Interest Statement: The authors declare that the research was conducted in the absence of any commercial or financial relationships that could be construed as a potential conflict of interest.

Copyright © 2017 Moggia, Graell, Lara, González and Lobos. This is an open-access article distributed under the terms of the Creative Commons Attribution License (CC BY). The use, distribution or reproduction in other forums is permitted, provided the original author(s) or licensor are credited and that the original publication in this journal is cited, in accordance with accepted academic practice. No use, distribution or reproduction is permitted which does not comply with these terms.



Population Modeling Approach to Optimize Crop Harvest Strategy. The Case of Field Tomato

Dinh T. Tran¹, Maarten L. A. T. M. Hertog^{2*}, Thi L. H. Tran¹, Nguyen T. Quyen¹, Bram Van de Poel³, Clara I. Mata² and Bart M. Nicolai^{2,4}

¹ Faculty of Food Science and Technology, Vietnam National University of Agriculture, Hanoi, Vietnam, ² KU Leuven, BIOSYST-MeBioS, Leuven, Belgium, ³ KU Leuven, BIOSYST, Crop Biotechnics, Leuven, Belgium, ⁴ Flanders Center of Postharvest Technology, Leuven, Belgium

OPEN ACCESS

Edited by:

Leo Marcelis,
Wageningen University and Research
Center, Netherlands

Reviewed by:

Simon Pearson,
University of Lincoln, UK
Oliver Körner,
Danish Technological Institute,
Denmark

*Correspondence:

Maarten L. A. T. M. Hertog
maarten.hertog@kuleuven.be

Specialty section:

This article was submitted to
Crop Science and Horticulture,
a section of the journal
Frontiers in Plant Science

Received: 16 February 2017

Accepted: 04 April 2017

Published: 20 April 2017

Citation:

Tran DT, Hertog MLATM, Tran TLH,
Quyen NT, Van de Poel B, Mata CI
and Nicolai BM (2017) Population
Modeling Approach to Optimize Crop
Harvest Strategy. The Case of Field
Tomato. *Front. Plant Sci.* 8:608.
doi: 10.3389/fpls.2017.00608

In this study, the aim is to develop a population model based approach to optimize fruit harvesting strategies with regard to fruit quality and its derived economic value. This approach was applied to the case of tomato fruit harvesting under Vietnamese conditions. Fruit growth and development of tomato (cv. "Savior") was monitored in terms of fruit size and color during both the Vietnamese winter and summer growing seasons. A kinetic tomato fruit growth model was applied to quantify biological fruit-to-fruit variation in terms of their physiological maturation. This model was successfully calibrated. Finally, the model was extended to translate the fruit-to-fruit variation at harvest into the economic value of the harvested crop. It can be concluded that a model based approach to the optimization of harvest date and harvest frequency with regard to economic value of the crop as such is feasible. This approach allows growers to optimize their harvesting strategy by harvesting the crop at more uniform maturity stages meeting the stringent retail demands for homogeneous high quality product. The total farm profit would still depend on the impact a change in harvesting strategy might have on related expenditures. This model based harvest optimisation approach can be easily transferred to other fruit and vegetable crops improving homogeneity of the postharvest product streams.

Keywords: tomato, biological age, fruit development, ripening, optimal harvest strategy, modeling

INTRODUCTION

Tomato, *Solanum lycopersicum* Mill, is a worldwide economic valuable and healthy crop with good nutritional properties (Kimura and Sinha, 2008). It continues to increase in importance for consumption as a fresh crop. During the past decades, the tomato production area in Vietnam has been increasingly expanding as tomato has become an important export crop. As a result, the farmer's income from tomato cultivation is four-fold higher than that from rice cultivation (Ta Thu Cuc, 2003).

Currently, there are two main types of tomato cultivars being cultivated in Vietnam: traditional heat sensitive cultivars and new heat tolerant cultivars (Ha, 2015). The latter are widely grown in the North of Vietnam where the farmer can grow them during both the winter and summer season. Among the heat tolerant cultivars, "Savior," a plum tomato, is favored for its high yield, good appearance and popularity among consumers.

Postharvest losses of tomato are still huge in Vietnam (Genova et al., 2006) as farmers are unable to define the optimal picking time that ensures a good postharvest life of fruit (Moneruzzaman et al., 2009). In contrast to European greenhouse production systems, where ripe fruit are harvested selectively, in the open field production systems as applied in Vietnam the crop is typically harvested at once. There, are several anecdotal reasons for this practice. Some farmers might lack knowledge about the best harvest practice and the consequences it will have on the marketing potential of their product. In some cases the labor cost can be higher than the profits growers can make due to market saturation. Also when the weather goes bad farmers decide to harvest the whole crop at once.

Growers mostly decide on picking date based on fruit color and the time after anthesis. However, the actual time required from anthesis to reach full maturity can vary due to genetic and environmental differences (Klee and Giovannoni, 2011). Moreover, the currently used color based classification of tomato is discrete and subjective and does not take into account the biological variation within a batch of fruit. By harvesting the whole crop at once, some fruit are harvested too early failing to properly ripen while others are harvested too late becoming susceptible to handling damage in the supply chain. Furthermore, no facilities are available to grade the fruit after harvest allowing the heterogeneous batches to reach the market. Hence, there is an urgent need to optimize the harvesting strategy for tomato fruit without going immediately into technological solutions.

The variation in postharvest storage behavior can often be interpreted as the expression of the same generic product behavior, only the choice of time zero from which moment the individual fruit are being observed is randomly determined by the moment of harvest (Hertog et al., 2007a). The biological (or physiological) age of the individual fruit is defined as the age of the product relative to an arbitrary reference point. The biological variation at harvest can thus be interpreted in terms of variation in the biological age of the harvested fruit.

So far, there have been few research groups using the biological age concept to classify the maturity of different fruit organs such as tomato (Hertog et al., 2004; Van de Poel et al., 2012, 2014), nectarines (Tijskens et al., 2007; Rizzolo et al., 2009), cucumber (Schouten et al., 2004), kiwifruit (Jordan and Loeffen, 2013), and apple (Tijskens et al., 2008, 2009). In this study, the aim is to bridge the gap between pre- and postharvest by using the biological age concept to optimize harvesting strategies that are at the root of postharvest biological variation. This approach is applied to the case of tomato (cv. "Savior") grown in Vietnam during both the winter and summer season to quantify the potential economic benefits of more dedicated harvesting strategies to the Vietnamese growers. To compare fruit quality of the harvested crop, market acceptance is used to translate fruit quality of the harvested crop into an equivalent economic value taking into account fruit-to-fruit variation. The economic value of the crop is thus defined as the maximum amount of money a specific actor, in this case a wholesaler, is willing to pay for the harvested crop. By focussing on saleable weight discarding overripe fruit, optimisation of growers' revenues will go hand in hand with reducing postharvest waste which is a major

worldwide concern (Gustavsson et al., 2011). The workflow applied in this study is outlined in **Figure 1**. The innovation of this approach lies in the integration of existing concepts bridging the gap from pre-harvest horticultural production via postharvest quality back to the economic impact for the growers taking into account biological variation.

MATERIALS AND METHODS

Plant Material

Tomato seedlings (cv. "Savior") were transplanted during the winter season 2014 and the summer season 2015 at the Fruit and Vegetables Research Institute, Hanoi, Vietnam ($21^{\circ}00'38.9''N$ $105^{\circ}55'39.2''E$). Plants were grown under cover with protection against birds, wind, rainfall, and excessive sunlight. Shortly

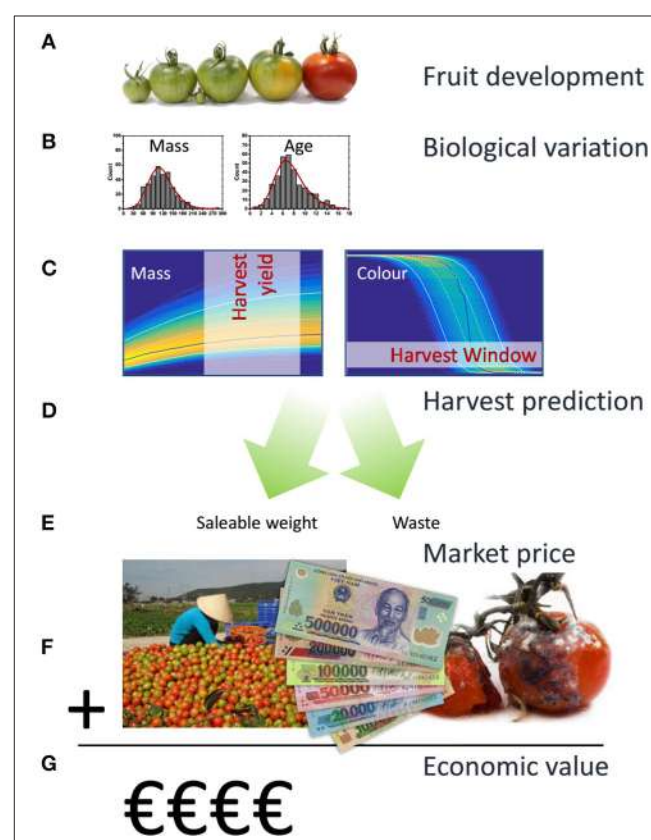


FIGURE 1 | Workflow applied in the current population model based approach. Tomato fruit development can, from an economic perspective, be characterized by fruit growth and fruit color as they largely define yield and quality. In a first step **(A)** existing kinetic models were used to describe both aspects for individual tomatoes. Biological variation between individual fruit was subsequently characterized in terms of variation in final fruit mass and biological age **(B)**. Using Monte Carlo simulations the population dynamics for a large batch of fruit was calculated **(C)** generating the expected density distributions for fruit mass and color over time. Applying various harvesting strategies **(D)** total yield in the various color classes, including overripe waste, was determined from the Monte Carlo results **(E)**. Using an independent surface response model describing wholesalers price as a function of the color composition of a batch of fruit **(F)**, the economic value of the harvested fruit was calculated **(G)**.

after anthesis flowers were labeled checking for new flowers three times at 5 d intervals. In total, 700 tomato flowers from 300 randomly chosen plants were labeled covering a wide range of fruit variation. From these labeled flowers 342 fruit grown in winter and 370 fruit grown in summer were successfully monitored for color and size on the plant. During fruit development measurements were taken at 3 d intervals while during fruit ripening measurements were taken at 2 d intervals.

Experimental Measurements

Fruit Mass

Fruit diameter was monitored on-plant using a caliper (Mitutoyo, Japan). Fruit mass was calculated from fruit diameter assuming a spherical fruit and an average fruit density of 873 kg.m⁻³ according to:

$$m = \frac{4}{3}\pi \left(\frac{D}{2}\right)^3 d$$

where m : fruit mass (kg); D : fruit diameter (m); d : fruit density (kg.m⁻³)

The constant value for fruit density was based on a preliminary experiment where both diameter and mass were measured on a range of harvested tomato fruit showing that the ratio between measured mass and volume calculated from the measured diameter could be considered constant over the whole fruit mass range (Figure S1)

Fruit Color

Fruit color was always measured on the same spot at the equator using a Minolta CM-2500d colorimeter (Minolta Camera Co., Ltd, Osaka, Japan) and expressed in the CIELAB color space L*, a*, and b*. The fruit color was expressed as hue angle (degree).

$$H = \arctan\left(\frac{b^*}{a^*}\right)$$

Model Development

Fruit Model

During fruit development, fruit mass of the green fruit is gradually increasing until some maximum fruit size is reached. Subsequently the fruit will start to ripen as mirrored by its color change. To describe these changes the modeling approach developed earlier in our group was adopted (Van de Poel et al., 2012) which is summarized below.

The change of fruit mass (M (kg)) in time was modeled using the following differential equation describing the Gompertz growth model (Winsor, 1932):

$$\begin{cases} \frac{d}{dt}M(t) = k_m M \ln\left(\frac{M_{\max}}{M}\right) \\ M(0) = M_{\max} \exp(-C) \end{cases} \quad (1)$$

with k_m (d⁻¹): the growth rate; M_{\max} (kg): the maximum fruit mass; C : a dimensionless displacement factor from the Gompertz function. The parameters k_m and C are assumed to be constant for a specific cultivar, while M_{\max} was assumed to be different for single every fruit.

Color change (measured as H in degree) was modeled using an exponential decay model implemented in its differential form.

$$\begin{cases} \frac{d}{dt}H(t) = -(H - H_{\min})k_h \\ H(0) = H_0 \end{cases} \quad (2)$$

with k_h (d⁻¹): the rate of color change; H_{\min} (degree): the minimum hue value; H_0 (degree): the initial hue value. The parameters k_h , H_{\min} , and H_0 were assumed to be constant for a specific cultivar.

Color change was modeled as being triggered once the fruit approaches its maximum mass by incorporating a biological switch for the rate constant k_h following:

$$k_h = \frac{k_h^{\max}}{(1 + ((M_{\max} - M)/M_{\max}))^s} \quad (3)$$

with k_h^{\max} (d⁻¹): the maximum rate of color change once fully triggered; s : (dimensionless) defining the steepness of the switch.

Biological Age

While the experimental time is counted relative to the first observed moment of anthesis, the individual fruits will all have a slightly shifted starting point as defined by their own biological age. This biological age of an individual fruit (t_{age} in d) can be calculated from the experimental time values (t_{exp} in d, relative to the day of harvest) by adding a fruit specific biological shift factor (Δt in d) following Equation 4.

$$t_{age} = t_{exp} + \Delta t \quad (4)$$

Model Calibration Using Time Series Based Data

The ODE based model was implemented and model parameters were estimated using OptiPa (Hertog et al., 2007b; www.optipa.be), a dedicated simulation and optimisation tool for ODE based models which was developed using Matlab (The MathWorks, Inc., Natick, MA, USA). The integrated model (Equations 1–4) was calibrated using the two dataset on fruit color and mass collected during the winter and summer season. Based on the data, common values for k_m , Ck_m , k_h^{\max} , H_{\min} , and H_0 and fruit specific values for M_{\max} , M_{\max} , M_{\max} and Δt were estimated. During the least square non-linear regression, the residual sum of squares was calculated by comparing the simulated values resulting from Equations 1–3 to the time corrected experimental values applying Equation 4. The dependent variables mass and color were both normalized (by subtracting their mean and dividing by their standard deviation) while calculating the combined residual sum of squares to give them equal weight during the model fitting. The ODE45 solver was selected for the numerical integration of the ODE based model.

Price Model

In order to judge market acceptance of batches of fruit of different homogeneity, fruit mixtures were presented to a panel of 30 wholesalers. To quantify acceptance, wholesalers were

asked to judge the quality in terms of a price per kg for each mixture. The wholesalers were presented either homogenous batches of a single ripening stage (Figure S2), or heterogeneous batches following a mixture design as indicated in **Table 1**. The mixtures were created to mimic normal harvested crop. This evaluation was performed for both winter and summer tomatoes in one session. The prices were normalized between 0 and 1 per wholesaler and per season. (**Table 1**), making it possible to compare the relative prices of the various tomato mixtures between wholesalers and seasons.

The dependency of the price on composition of the batch in term of different ripening stages was modeled by applying a mixture design. In a mixture experiment, the independent factors (the ripening stages) are proportions of different components of a blend together summing up to 100%. Under the assumption that the presence of extremely different maturity classes within a batch could potentially interact with each other in negatively affecting the overall price, only interaction terms were included for the most different maturity classes. (Equation 5):

$$Y = \alpha_1 RS_1 + \alpha_2 RS_2 + \alpha_3 RS_3 + \alpha_4 RS_4 + \alpha_5 RS_5 + \alpha_6 RS_6 \\ + \alpha_7 RS_1 RS_6 + \alpha_8 RS_2 RS_6 + \alpha_9 RS_1 RS_5 \quad (5)$$

where Y is the response variable (normalized price/kg); $\alpha_1 - \alpha_6$ are regression coefficients for the main linear effects, $\alpha_7 - \alpha_9$ refer to the interaction effects. $RS_1 - RS_6$ represent the independent variables being the percentage of fruit in the batch representing different ripening stages ranging from immature green (RS_1) to ripe red (RS_6). Note that the model, being a mixture design, does not include an intercept term due to the correlation between all the components (their sum equals 100%). The ripening classification based on Hue limits is given in Table S1. The

coefficients were estimated by least square non-linear regression. The significance of the overall model and of each coefficient was evaluated by analysis of variance (ANOVA). The statistical analysis were done using JMP® Pro 12, SAS Institute Inc., Cary, NC, 1989–2015.

Optimizing Harvest Strategy for Tomato

To find the optimal harvest strategy at which the maximum price was realized a Monte-Carlo analysis was performed using the OptiPa software. Starting from the fruit specific parameters M_{max} and Δt as derived from the calibration data a new virtual parameter set was generated representing a population of 10,000 tomatoes with the same distribution characteristics (average, variation, shape, and correlation) as the original parameter set (**Figure 2**). In combination with the other cultivar specific model parameters, these were used to simulate the fruit growth model 10,000 times generating detailed time varying distributions for both fruit color and fruit mass. The 10,000 Monte Carlo simulation were analyzed using custom Matlab scripts basically counting the number of fruit falling in the various ripening stages at any point in time during the simulation. Using these scripts, fruit meeting the harvest criteria were virtually harvested while the remaining fruit was allowed to continue to develop. The color distribution of the harvested fruit was translated into its equivalent economic value using the price model taking into account production volume based on the simulated fruit weight. Overripe fruit (defined as having a hue color $<54^\circ$) was considered waste and would not contribute to the overall production. Harvested volumes from the subsequent harvest dates were cumulated to obtain the total economic value generated. Different harvest strategies for tomato grown in both winter and summer were simulated to find the scenario

TABLE 1 | Mixture design for different ripening stages (RS) of tomato cv. "Savior" grown in winter and summer.

Mixture ¹	Mixing ratio						Normalized price/ kg ²	
	RS6	RS5	RS4	RS3	RS2	RS1	Winter	Summer
1	1	0	0	0	0	0	1.00 ± 0.02 ^a	1.00 ± 0.02 ^a
2	0	1	0	0	0	0	0.98 ± 0.05 ^a	0.97 ± 0.07 ^a
3	0	0	1	0	0	0	0.93 ± 0.08 ^a	0.73 ± 0.20 ^b
4	0	0	0	1	0	0	0.51 ± 0.26 ^{c,d}	0.61 ± 0.19 ^{b,c,d}
5	0	0	0	0	1	0	0.36 ± 0.21 ^e	0.30 ± 0.18 ^e
6	0	0	0	0	0	1	0 ^f	0 ^f
7	0.25	0.25	0.25	0.25	0	0	0.63 ± 0.19 ^{b,c}	0.62 ± 0.16 ^{b,c}
8	0.2	0.2	0.2	0.2	0.2	0	0.54 ± 0.20 ^{b,c,d}	0.52 ± 0.19 ^{c,d}
9	0	0.2	0.2	0.2	0.2	0.2	0.49 ± 0.21 ^{d,e}	0.47 ± 0.20 ^d
10	0.1	0.3	0.3	0.15	0.1	0.05	0.54 ± 0.18 ^{b,c,d}	0.50 ± 0.18 ^{c,d}
11	0.1	0.3	0.2	0.1	0.1	0.2	0.50 ± 0.16 ^{c,d,e}	0.50 ± 0.21 ^{c,d}
12	0.1	0.5	0.4	0	0	0	0.66 ± 0.14 ^b	0.62 ± 0.17 ^{b,c}
13	0.1	0.2	0.2	0.2	0.2	0.1	0.47 ± 0.16 ^{d,e}	0.48 ± 0.19 ^{c,d}

The mixtures were created to mimic normal harvested crop.

¹Tomatoes at different ripening stages were mixed at various ratios ranging from 0–1. RS1, mature green fruit; RS2, breaker fruit; RS3, light orange fruit; RS4, orange fruit; RS5, red fruit; RS6, red ripe fruit.

²Average normalized price values accompanied by standard deviation were assessed by 30 wholesalers for winter and summer tomato.

Within a column, results with the same letter were not significantly different in a one way Tukey multiple comparison test on a 95% confidence level.

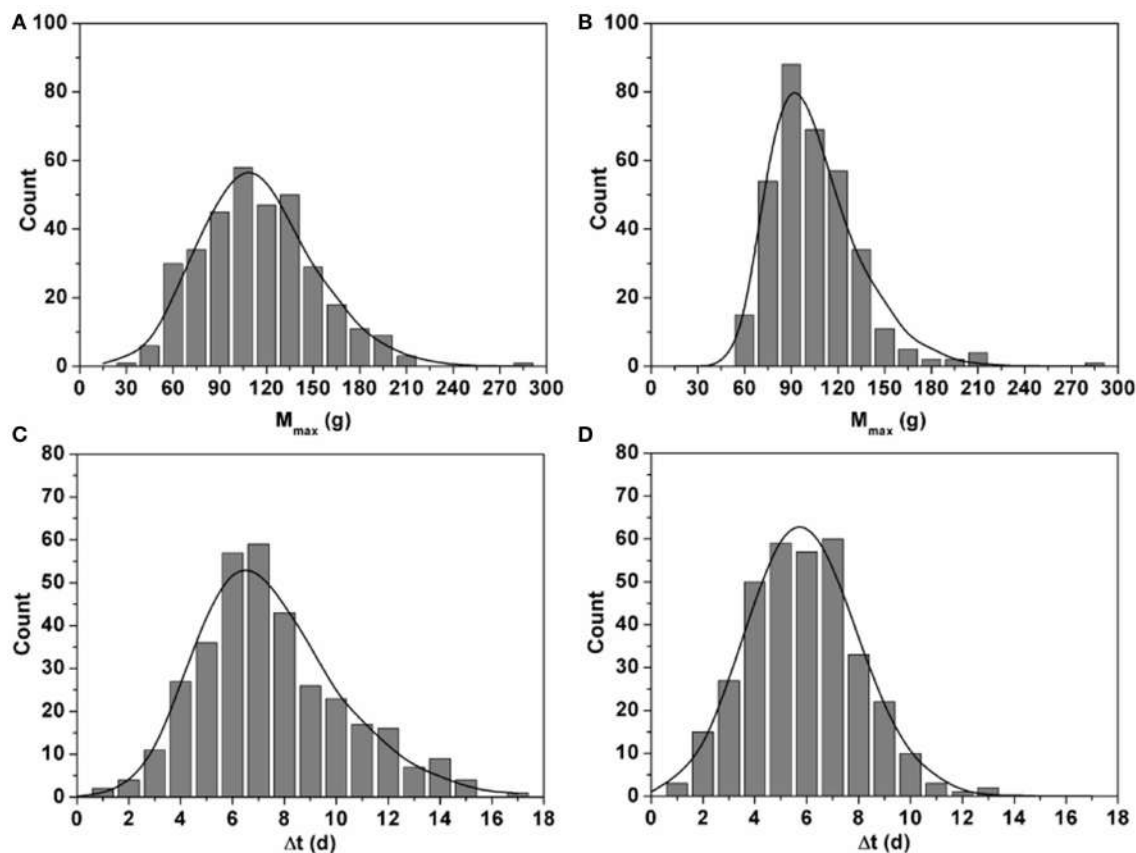


FIGURE 2 | Histograms showing the distributions of estimated M_{max} (g) (A,B) and Δt (d) (C,D) for the 342 fruit grown in winter (A,C) and the 370 fruit grown in summer (B,D). The curves represent the equivalent distributions based on 10,000 fruits generated during the Monte Carlo analysis. Comparing the two shows the agreement between the experimentally observed variation and the variation mimicked during the Monte Carlo simulations.

with the best return and the lowest postharvest waste. These strategies representing either a single harvest (all tomatoes in the field were harvested at once) or focused multiple harvests (only harvesting ripening stages RS4, RS5, and RS6 or only RS5 and RS6) combined with fixed harvest intervals (one, two, three or four day intervals) or flexible harvest intervals (dynamic harvest). The dynamic harvest regime consisted of multiple harvests of ripening stages RS5 and RS6 at varying time intervals as indicated in Figure 3.

RESULTS

Modeling Fruit Development

The typical change of mass and color during fruit development and ripening is illustrated by two exemplar fruits in Figure 4. All fruit followed an identical growth pattern. The development stage for “Savior” took about 52–55 d after anthesis. It was observed that different fruit reached a wide range of mass (from 50 to 110 g) despite their similar flowering time.

During the main part of fruit growth fruit color remained constant. Color change was only triggered once the fruit approached its final mass. While mass remained almost constant, color dropped from immature green (hue ranging from 104

to 106°) down to mature red (hue ranging from 50 to 55°). Moreover, the color data revealed a shift along the time axis between fruit, indicating the variation in biological age between the individual fruit.

Using both mass and color data from the time series obtained in winter and summer, the integrated model (Equation 1–4) was calibrated by estimating the various model parameters through non-linear regression analysis. The generic parameter estimates are given in Table 2. The variation in final fruit mass and time shift was captured by the fruit specific model parameters M_{max} and Δt which were estimated for every single fruit. The distribution of the fruit specific parameters is shown in Figure 2. The maximum fruit mass M_{max} for winter ranged from 25.5 to 275.2 g with a mean of 107.1 ± 36.9 g and for summer ranged from 48.9 to 275.7 g with a mean of 99.03 ± 28.39 g, representing the broad range of fruit mass encountered. The mean values of Δt for winter and summer were 7.01 ± 2.82 d and 5.39 ± 2.12 d, respectively.

Price Model Describing the Market Value of the Harvested Crop

To examine how the economic value changed as a function of the heterogeneity of the harvested crop representative fruit mixtures

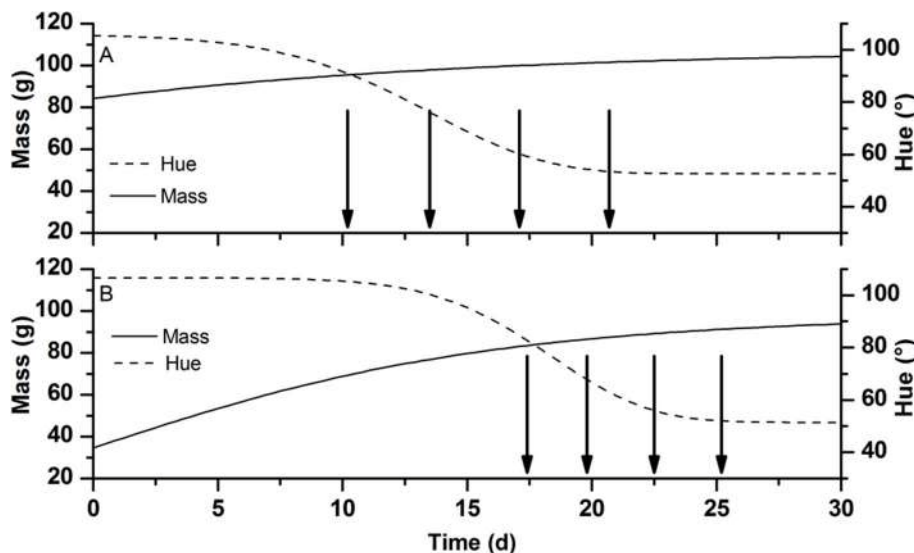


FIGURE 3 | Schematic representation showing dynamic harvest strategy for tomatoes at RS5 and RS6 grown (A) in winter and (B) in summer. The lines represent the typical change in mass in g (full line) and hue color in degree (broken line) of developing tomato fruit during the winter and summer season. Arrows indicate the planned moments of harvest. Time 0 is taken at an arbitrarily early data well before the colouration of the fruit skipping most of the fruit growth part to focus on the period near harvest.

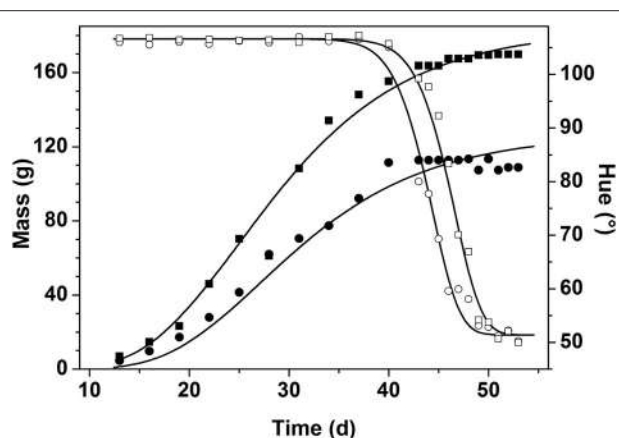


FIGURE 4 | Change of fruit mass in g (closed symbols) and hue color in degree (open symbols) during fruit development and ripening for two randomly chosen fruits from the first flowering period in winter. The symbols represent the measured data while the lines represent the model fit for the selected fruit.

were judged on their economic value by 30 wholesalers. Pure homogeneous batches of either RS1 (green) or RS6 (fully ripe) where positioned at the two extremes of the normalized price spectrum ranging from 0/kg to 1/kg (**Table 1**).

For both seasons a batch of tomato containing only RS6 (mixture N°1) or RS5 (mixture N°2) had the highest prices (0.99/kg and 0.98/kg respectively). For winter tomatoes, there was no significant difference in price given for a batch of only RS3 (N°4) and mixtures of equal percentage of RS6 to RS2 (N°8) or of RS1 to RS5 (N°9), and combination of all ripening stages (N°10, 11, 13). The price of a mixture containing 25% of each stage from

RS6 to RS3 (N°7), was not statistically significant from that of a mixture containing 10% RS6, 50% RS5, and 40% RS4 (N°12).

In order to investigate the dependence of price on the composition of the batch the linear regression model from Equation 5 was fitted to the data combined over all 30 wholesalers. The parameter estimates for winter and summer tomato are given in **Table 3**. The explained part was 0.64 and 0.63 for winter and summer tomatoes respectively (see **Figure 5** for the summer fruit results). When the responses of the wholesalers were analyzed per wholesaler, explained parts for the individual wholesalers ranged from 0.51 to 0.97 with an average explained part of 0.88 and 0.87 for respectively summer and winter fruit (see **Figure 5** for the summer fruit results).

Monte Carlo Evaluation of Harvesting Strategies

In order to evaluate the various harvest strategies taking into account fruit-to-fruit variation, a Monte Carlo approach was applied. **Figure 6** illustrates the situation in which a single harvest was applied. Considering a 30 d harvest window the highest economic value for winter tomatoes was observed for a harvest at 15 d while that for summer tomatoes was about 5 d later (19.8 d). The figure shows the realized economic value and the harvested and wasted biomass as function of time assuming all fruit was harvested during a single harvest. The normalized value increased with the increasing harvested mass. When the total harvested mass started to decrease, its economic value continued to increase for a little longer as the maturity of the diminishing amount of harvested fruit continued to increase. Only when the harvest was further delayed the economic value started to decrease as well. This coincided with an increasing amount

of waste accumulating as fruit became overripe. Eventually all tomatoes would be harvested overripe, reducing the value to zero.

To study the effect of harvest interval and the maturity classes targeted during harvest on economic return, multiple harvest strategies were simulated. In the Monte Carlo simulation tomatoes were harvested at either RS4, RS5, and RS6 or only at RS5 and RS6 applying harvest intervals ranging from 1 d to 4 d (**Figure 7**). In addition, one dynamic harvesting scenario was simulated following the harvest schedule from **Figure 3**. For both winter (**Figure 7A**) and summer (**Figure 7B**) tomato the optimal single harvest from **Figure 6** was taken as a reference. The additional harvest strategies all started earlier from the moment the first ripe fruit (RS6) would be on the vines (10.2 d for winter and 17.4 d for summer fruit). The different patterned parts of each bar represent the economic value generated per harvest day. The bottom part of each stack represents the first harvest day with subsequent layers referring to subsequent harvest days. The height of each bar represents the accumulated economic value over the whole harvest period for a given harvest strategy.

DISCUSSION

Fruit-to-Fruit Variation Was Accurately Captured by the Fruit Model While Revealing Seasonal Effects

The observed growth curves (**Figure 4**) can be understood in terms of the known underlying fruit development processes (Gillaspy et al., 1993). The high variation in final fruit mass (**Figure 2**) can be explained by the fact that fruit are exposed to different microclimate conditions and sink/source relations within the plant (Van de Poel et al., 2012) which is not related to the biological age of the fruit as such.

The changes in fruit color can be understood in terms of the breakdown of chlorophyll and the production of carotenoids, two processes that occur in parallel (Fraser et al., 1994). While the model assumes a single constant final color value for all fruit, small fruit to fruit variation does exist. Although one might expect some correlation between this final color and final fruit mass this was not the case (**Figure S3A**). Data in **Table 2** reveal that the generic parameters were estimated very accurately for both seasons as demonstrated by their small approximate standard deviations. When the generic parameters were compared between winter and summer tomatoes, some interesting trends were observed. While the growth parameters (C and k_m) of winter tomato were almost half of those of summer tomato, the rate of color change k_h^{\max} of the former (26.02 d^{-1}) was double the latter (14.83 d^{-1}), indicating that the high summer temperature stimulates the growth rate of tomato but slows down the color change and with that fruit ripening. At the end of ripening, they both have a similar value for H_{\min} , of about 52° . For s , the higher value obtained for winter (54.30) than for summer (33.39), implies that the color change of winter tomato is triggered more toward the end of the growth cycle as compared to the summer tomato which started to color earlier. Clearly, the Vietnamese growing season varies largely affecting the supposedly generic model

TABLE 2 | Parameter estimates for the calibration of the integrated model (Equations 1–4 fitted to the dataset of mass and color of tomato grown in winter ($n = 342$) and summer ($n = 370$).

Parameter	Winter ($R^2 = 98.9\%$)	Summer ($R^2 = 98.5\%$)
GROWTH MODEL PARAMETERS		
C	4.87 ± 0.03	$9.76 \pm 7.26 \cdot 10^{-4}$
$k_m (\text{d}^{-1})$	0.0702 ± 0.0003	$0.11 \pm 4.57 \cdot 10^{-5}$
COLOR CHANGE MODEL PARAMETERS		
$k_h^{\max} (\text{d}^{-1})$	26.02 ± 2.45	14.83 ± 0.55
$H_0 (\text{°})$	105.74 ± 0.04	106.63 ± 0.05
$H_{\min} (\text{°})$	52.55 ± 0.20	51.37 ± 0.07
BIOLOGICAL SWITCH PARAMETER		
s	54.30 ± 0.88	33.39 ± 0.30

The parameter estimates are accompanied by their standard errors.

C: A dimensionless displacement factor from the Gompertz function; $k_m (\text{d}^{-1})$: The growth rate; $k_h^{\max} (\text{d}^{-1})$: The maximum rate of color change once fully triggered; $H_{\min} (\text{°})$: The minimum hue value; $H_0 (\text{°})$: The initial hue value; s : (dimensionless) defining the steepness of the switch.

parameters thus contrasting the assumptions from Van de Poel et al. (2012). However, the Vietnamese growing practices and climate conditions are completely different from the Belgian situation where tomatoes are grown almost year round under well controlled conditions inside Venlo type glass greenhouses. In the end, by introducing season specific parameter values the model could be applied successfully. Further, research is needed to quantify the extent to which these parameters vary over the years and seasons.

Though the fruit model does not pretend to be a detailed description of the physiological reality it does contain elements inspired by the fruit's physiology. Especially the biological switch is an empirical approach to simplify the underlying climacteric regulation of fruit ripening. In real life this is about the plant hormone ethylene orchestrating a complex cascade of events turning on the various processes involved in fruit ripening (Lin et al., 2009). In spite of being descriptive in nature the model is fit to purpose and convenient to capture biological variation as observed through the fruit specific model parameters. The estimated values for Δt and M_{\max} showed no correlation, indicating two distinctly different sources of biological variation were involved (**Figure S3B**).

The Price Model Revealed Inconsistent Behavior between Individual Wholesalers

The common harvesting practice in some Vietnamese regions is that farmers harvest their whole crop at once resulting in a mix of various ripening stages. This indirectly causes economic losses as some fruit are harvested overripe while others are still too immature to gain full profits. At the same mixture composition, the averaged normalized prices of tomato grown in winter based on the evaluation by 30 wholesalers were either higher or at least equal to those of tomato grown in summer (**Table 1**). This indicates that within the fixed normalized range a shift has occurred toward higher prices. This can be explained by the fact that the winter tomatoes have better

TABLE 3 | Parameter estimates of the price mixture model fitted to the combined responses of 30 wholesalers.

Explanatory variables	Model parameters	Estimates	p-value
WINTER SEASON		R² = 64 %	
RS1	α_1	0.00 ± 0.03	1.00
RS2	α_2	0.35 ± 0.03	< 0.0001
RS3	α_3	0.47 ± 0.03	< 0.0001
RS4	α_4	0.81 ± 0.03	< 0.0001
RS5	α_5	0.84 ± 0.03	< 0.0001
RS6	α_6	0.94 ± 0.03	< 0.0001
RS6 × RS1	α_7	-3.21 ± 2.90	0.27
RS6 × RS2	α_8	-4.11 ± 0.88	< 0.0001
RS5 × RS1	α_9	-0.21 ± 0.88	0.81
SUMMER SEASON		R² = 63 %	
RS1	α_1	0.00 ± 0.03	0.98
RS2	α_2	0.29 ± 0.03	< 0.0001
RS3	α_3	0.57 ± 0.03	< 0.0001
RS4	α_4	0.62 ± 0.03	< 0.0001
RS5	α_5	0.85 ± 0.03	< 0.0001
RS6	α_6	0.95 ± 0.03	< 0.0001
RS6 × RS1	α_7	-2.33 ± 2.86	0.42
RS6 × RS2	α_8	-3.66 ± 0.86	< 0.0001
RS5 × RS1	α_9	-0.10 ± 0.87	0.90

The parameter estimates are accompanied by their standard error and p-values. p-values below 0.05 indicate estimates not significantly different from zero.

overall appearance and fruit weight therefore increasing the normalized price relative to its extremes. When the more green tomatoes were added to the mixtures, a lower wholesale price was obtained as Vietnamese consumers do not have the habit to buy green tomato. Similar trends were observed for summer tomato.

Concerning the dependence of price on the composition of the batch of fruit **Table 3** revealed that the parameter estimates for both seasons had similar magnitudes. They showed that the main factors had positive effect on the normalized price with the size of the effect increasing with maturity stage from about 0 (for RS1) to about 1 (for RS6). This range is a direct consequence of the normalization of the price data where the prices given by each wholesaler was rescaled between 0 and 1. Given the parameter estimate for RS1 was not significant mirrors the fact that the wholesalers were unanimously about RS1 representing the lowest economic value. When green fruit were added to the mixture, lower prices were obtained for the batch. This was due to the inherent lower prices paid for the more immature fruit as mimicked by the negative values obtained for the interaction terms. However, it was expected that the presence of more immature fruit stages would suppress the prices disproportionately. Although the coefficients for the various interaction terms were all estimated to be negative only one of them (RS6 × RS2) was statistically significant (**Table 3**). From a logical point of view one would expect that if the negative interaction term RS6 × RS2 is significant the presence of even more immature fruit should definitely have a

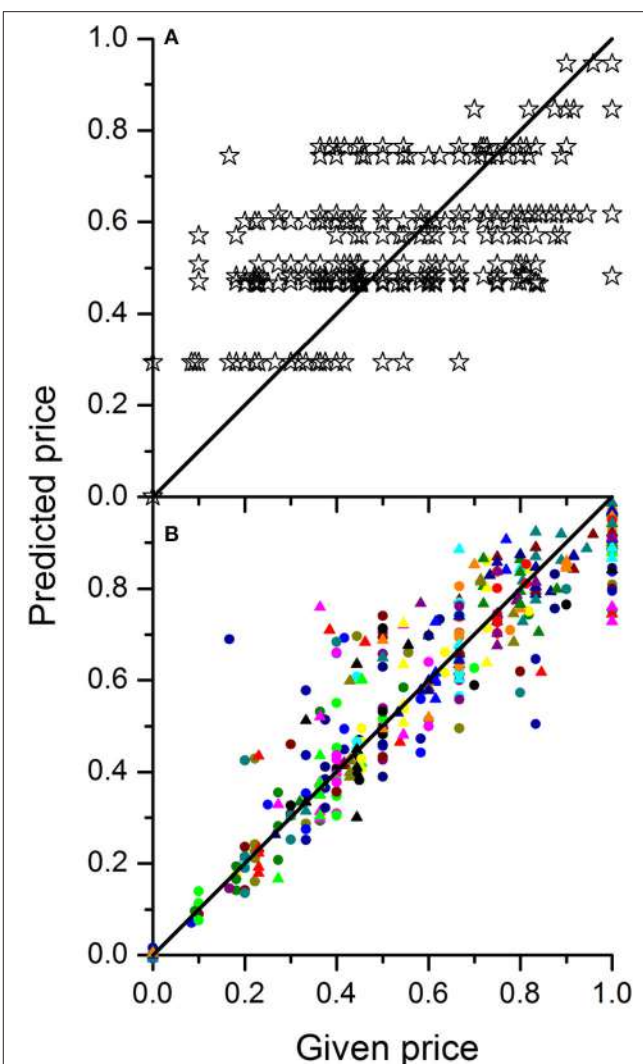


FIGURE 5 | Plots of predicted normalized price vs. the given normalized price for tomato grown in summer either based on the calibration of a single mixture model to the combined data of 30 wholesalers (A) or by calibrating one mixture model per wholesaler (B). The different colored symbols in B represent the 30 different wholesalers. In case of a perfect price model calibration, all points should sit on the diagonal line.

significant negative effect as well (thus resulting in a significant negative term for RS6 × RS1). However, this could not be confirmed through the current experimental data which might indicate a difference in opinion between the 30 wholesalers. Also the relative low explained part indicates inconsistencies in how the wholesalers judged the various mixtures. When the responses of the wholesalers were analyzed per wholesaler much better results were obtained indicating that the limited fit of the price model is not due to restrictions of the model structure applied, but merely due to a lack of agreement between individual wholesalers on the economic value of the fruit.

To predict the market price for a given mixture of fruit one could either use the overall mixture model calibrated on

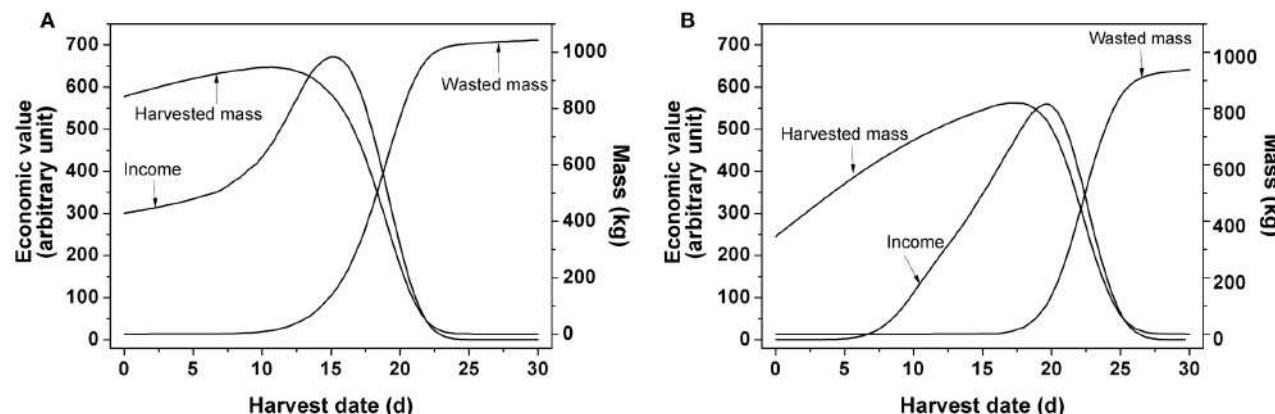


FIGURE 6 | Changes in economic value, harvested and wasted mass as function of time by single harvest for tomato grown (A) in winter and (B) in summer as extracted from the Monte Carlo analysis. Based on 10,000 simulated fruits a 30 d harvest window was considered. For each day counts were generated for the number of fruit falling in the various ripening classes while keeping track of the total harvested fruit mass. Overripe fruit was assigned to waste. Based on the resulting mixture of ripening classes the economic value of the unsorted fruit was calculated.

all wholesalers as one or make multiple predictions using the individually calibrated models averaging out the predicted prices afterwards. Both approaches would eventually lead to the same results although the latter approach would allow to provide insight in the market uncertainties depending on who one would sell to.

Model Based Evaluation of Various Harvesting Strategies Enables to Quantify the Economic Incentive for Growers to Move Away from Their Current Practice

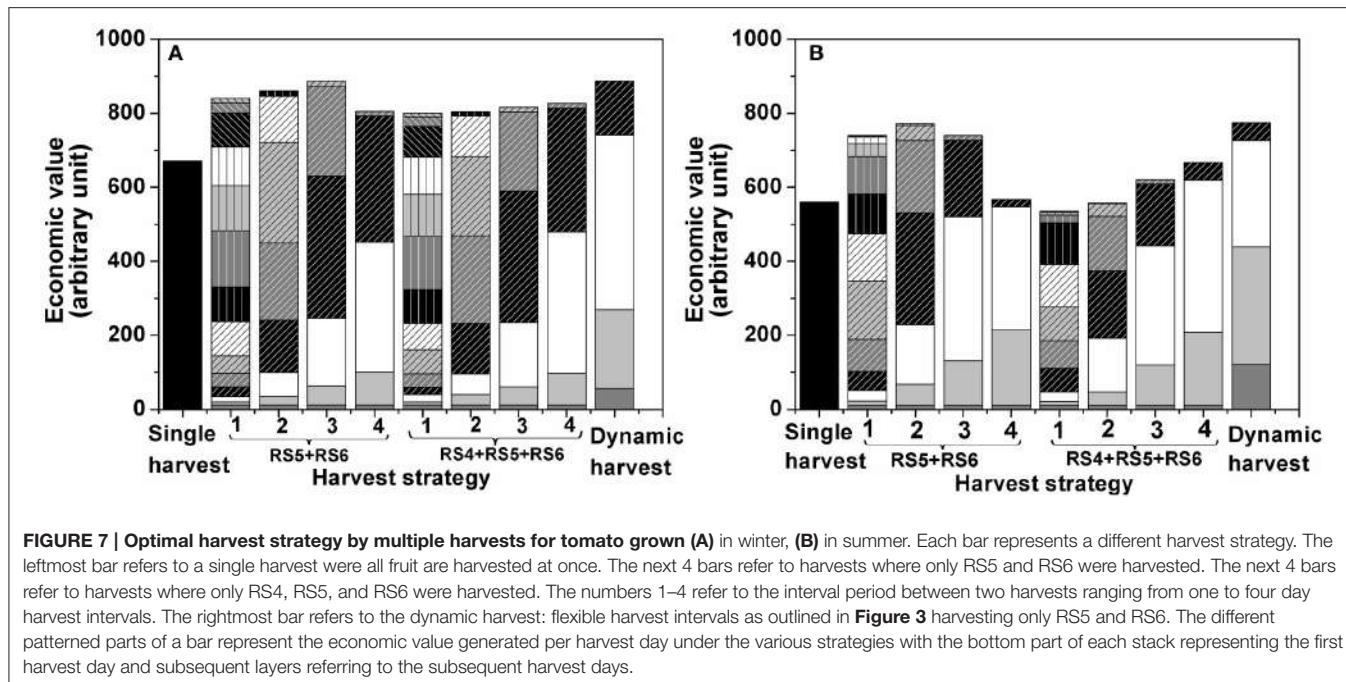
The Monte Carlo analysis from Figure 6 combined the model on fruit growth with the price model. Based on the simulation of fruit development of 10,000 individual fruit (with regard to mass and color), using the parameter distributions from Figure 2 as an input, the evolution of fruit color distribution and fruit mass was collated over time. Overripe fruit was assigned to waste while for the remaining batch of fruit the economic value was calculated using the price model with the parameters from Table 3. By applying a single harvest, the economic value of the crop depended on the level of heterogeneity of the harvested crop in relation to the amount of overripe fruit present. In addition, the maximum normalized economic value for winter tomato was higher than that for summer tomato because the fruit weight and the normalized price for the former were higher than for the latter (Figure 6).

Theoretically, maximum profit is obtained when only harvesting the most mature heaviest fruit (RS6). Of course, to prevent waste, fruit has to be harvested as often as needed, based on the time needed for the RS5 fruit to develop into RS6 before turning into waste. Depending on the season this might require 1 d or 2 d harvest intervals. By harvesting less frequently, workload can be reduced but one should at the same time prevent waste to accumulate as this would imply economic losses. As a first alternative to a single harvest, fruit harvest was simulated for a

narrow maturity range of RS5–RS6 varying the harvest interval from 1 d to 4 d (Figure 7). For the slower growing winter fruit the economic value increased with an increasing harvest interval. The 1 d intervals resulted in many small harvests while, in between two harvests, it did not allow enough time for the remaining fruit to ever develop into full ripe fruit of RS6. By increasing the harvest interval to 3 d more time is available for the fruit to continue to develop in heavier ripe fruit without turning into waste increasing the obtained market price and minimizing waste at harvest. Going from 3 d to 4 d interval economic value dropped because the harvest interval became too long. This enabled the fruit to become overripe and turn into waste.

By expanding the harvested maturity range to RS4–RS6, the effect of harvest interval was largely removed for the winter fruit. The reason for this being that winter fruit developed too slow to bridge the gap from RS3 to RS6, even during the 4 d intervals (Figure 7A).

Note that in both cases the economic value generated during the subsequent harvest days strongly depended on the harvest interval. Using 1 d intervals only small revenues were generated per harvest as only small amounts were harvested at once. By increasing the harvest interval, the early harvest blocks increased in size, but the latter ones were reduced. The reason for this being that during the early harvests the fruit was not yet developing at full speed (and therefore the first harvest could have been postponed) but during the latter harvests fruit is developing in average much faster and waste is being generated (shorter harvest intervals should have been applied to prevent waste). By adapting the timing of the harvest actions to the development of the crop overall revenue can be optimized. One example of such dynamic harvesting scenario is shown for winter fruit harvested at RS5 and RS6. It is clearly seen that the economic value generated during the dynamic harvest intervals was similar to that for 3 d harvest intervals while the labor cost was reduced due to less frequent harvests of the former than the latter.



The summer fruit was characterized by a faster fruit growth, affecting the outcome of the simulated harvesting strategies accordingly (**Figure 7B**). While the overall economic value remained lower as compared to the winter fruit, there was much more flexibility in improving the economic value by adapting the harvesting strategy. For the narrow maturity range (RS5 and RS6) the summer fruit showed an earlier decrease in economic value, starting from the 3 d harvest interval, as the fruit more rapidly turned into waste. For the wider maturity range (RS4, RS5, and RS6) the 1 d harvest interval resulted in a lower economic value as compared to the single harvest. This was due to the earlier start of the simulated harvesting season which, in combination with the frequent harvesting, resulted in an overrepresentation of relative small unripe fruit in all subsequent harvests as the fruit was not allowed to ripen properly. By increasing the harvest interval to 4 d revenues increased accordingly, in contrast to what was observed for the winter fruit. Similarly, a dynamic harvesting scenario was implemented for tomatoes harvested at RS5 and RS6. Even though the workload of the dynamic harvest was reduced by 30% compared to 2 d harvest interval (effectively 4 harvests under the dynamic scenario vs. 6 harvests under the 2 d harvest interval), it still generated the highest economic value compared to all fixed harvest intervals as it allowed the fruits fully develop and turn into good ripening stages with no mass going to waste (**Figure 7B**).

CONCLUSIONS

The current study developed a population based approach to optimize the harvest strategy for “Savior” tomato grown in either winter or summer in Vietnam. Using the data on mass and color obtained during fruit development and ripening, a kinetic fruit growth model was successfully calibrated which then was used to

quantify the population variation in terms of the physiological maturity of the tomatoes. While the applied model does not pretend to be a physiological model its level of detail seemed to be fit for the intended purpose of optimizing the postharvest economic value of the crop taking into account pre-harvest biological variation.

The calibrated growth model was successfully coupled to the wholesalers price model through a Monte Carlo approach to evaluate and optimize the harvest strategy with regard to economic value of the crop taking into account the omnipresent fruit-to-fruit variation. This study quantified an economic incentive for growers in developing countries to move away from their current single harvest strategy which will benefit the wider market by (i) spreading out fruit supply, (ii) increasing homogeneity of the fruit supplied to the market, and (iii) maximizing the profits for the growers and, above all, (iv) reducing post-harvest waste. It was shown that the potential sales value of a crop could be increased by undertaking multiple harvests assuming all other costs remain the same. The ideal situation was shown to depend on the rate of fruit development and ripening in relation to the choice of the targeted maturity range and the selected harvest interval. The total farm profit would still depend on other aspects such as different picking efficiencies at different crop densities, possible damage to the non-harvested crop or possible physiological effects on fruit development of the non-harvested crop by the reduced crop load, and the need for multiple transports. In a real application case the approach should be further detailed to align the timing of harvests with labor availability, market demands, available storage space, price uncertainty, etc. This work provides a first framework that allows the industry to design dynamic scenario's to start maximizing postharvest operations.

AUTHOR CONTRIBUTIONS

DT, MH, and BN designed the experiments; DT, TT, NQ, CM, and BV acquired the experimental data; DT, MH, and CM analyzed the experimental data, all authors contributed to the interpretation of the data, DT and MH drafted the manuscript with all authors being involved in the revision of the manuscript.

ACKNOWLEDGMENTS

The research was performed in the framework of the Bilateral Scientific Research Cooperation Projects FWO.106.2013.20

REFERENCES

- Fraser, P. D., Truesdale, M. R., Bird, C. R., Schuch, W., and Bramley, P. M. (1994). Carotenoid biosynthesis during tomato fruit development (Evidence for tissue-specific gene expression). *Plant Physiol.* 105, 405–413. doi: 10.1104/pp.105.1.405
- Genova, I. I. C., Weinberger, K., An, H. B., Dam, D. D., Loc, N. T. T., et al. (2006). *Postharvest Loss in The Supply Chain for Vegetables—The Case of Chili and Tomato in Viet Nam No. 18*, AVRDC Working Paper Series, Shanhua.
- Gillaspy, G., Ben-David, H., and Grussem, W. (1993). Fruits: a developmental perspective. *Plant Cell* 5, 1439–1451. doi: 10.1105/tpc.5.10.1439
- Gustavsson, J., Cederberg, C., Sonesson, U., van Otterdijk, R., and Meybeck, A. (2011). *Global Food Losses and Food Waste. Extent, Causes and Prevention*. FAO.
- Ha, T. M. (2015). Agronomic requirements of tomatoes and production methods in the Red River Delta of Vietnam. *J. Trop. Crop Sci.* 2, 33–38.
- Hertog, M. L. A. T. M., Lammertyn, J., De Ketelaere, B., Scheerlinck, N., and Nicolai, B. M. (2007a). Managing quality variance in the postharvest food chain. *Trends Food Sci. Technol.* 18, 320–332. doi: 10.1016/j.tifs.2007.02.007
- Hertog, M. L. A. T. M., Lammertyn, J., Desmet, M., Scheerlinck, N., and Nicolai, B. M. (2004). The impact of biological variation on postharvest behavior of tomato fruit. *Postharvest Biol. Technol.* 34, 271–284. doi: 10.1016/j.postharvbio.2004.05.014
- Hertog, M. L. A. T. M., Verlinden, B. E., Lammertyn, J., and Nicolai, B. M. (2007b). OptiPa, an essential primer to develop models in the postharvest area. *Comput. Electron. Agric.* 57, 99–106. doi: 10.1016/j.compag.2007.02.001
- Jordan, R. B., and Loeffen, M. P. F. (2013). A new method for modelling biological variation using quantile functions. *Postharvest Biol. Technol.* 86, 387–401. doi: 10.1016/j.postharvbio.2013.07.008
- Kimura, S., and Sinha, N. (2008). Tomato (*Solanum lycopersicum*): A model fruit-bearing crop. *Cold Spring Harb. Protoc.* 3:pdb.em105. doi: 10.1101/pdb.em105
- Klee, H. J., and Giovannoni, J. J. (2011). Genetics and control of tomato fruit ripening and quality attributes. *Annu. Rev. Genet.* 45, 41–59. doi: 10.1146/annurev-genet-110410-132507
- Lin, Z., Zhong, S., and Grierson, D. (2009). Recent advances in ethylene research. *J. Exp. Bot.* 60, 3311–3336. doi: 10.1093/jxb/erp204
- Moneruzzaman, K. M., Hossain, A. B. M. S., Sani, W., Saifuddin, M., and Alenazi, M. (2009). Effect of harvesting and storage conditions on the post harvest quality of tomato (*Lycopersicon esculentum* Mill) cv. Roma, V. F. *Aust. J. Crop Sci.* 3, 113–121.
- Rizzolo, A., Vanoli, M., Eccher Zerbini, P., Jacob, S., Torricelli, A., Spinelli, L., et al. (2009). Prediction ability of firmness decay models of nectarines based on the biological shift factor measured by time-resolved reflectance spectroscopy. *Postharvest Biol. Technol.* 54, 131–140. doi: 10.1016/j.postharvbio.2009.05.010
- Schouten, R. E., Jongbloed, G., Tijskens, L. M. M., and van Kooten, O. (2004). Batch variability and cultivar keeping quality of cucumber. *Postharvest Biol. Technol.* 32, 299–310. doi: 10.1016/j.postharvbio.2003.12.005
- Ta Thu Cuc (2003). *Kỹ thuật trồng cà chua [Tomato Planting Techniques]*. Nha xuát ban Nông nghiệp [Agriculture Publisher], 104 [in Vietnamese].
- Tijskens, L. M. M., Konopacki, P. J., Schouten, R. E., Hribar, J., and Simcic, M. (2008). Biological variance in the color of Granny Smith apples modeling the effect of senescence and chilling injury. *Postharvest Biol. Technol.* 50, 153–163. doi: 10.1016/j.postharvbio.2008.05.008
- Tijskens, L. M. M., Unuk, T., Tojko, S., Hribar, J., and Simcic, M. (2009). Biological variation in the development of Golden Delicious apples in the orchard. *J. Sci. Food. Agric.* 89, 2045–2051. doi: 10.1002/jsfa.3689
- Tijskens, L. M. M., Zerbini, P. E., Schouten, R. E., Vanoli, M., Jacob, S., Grassi, M., et al. (2007). Assessing harvest maturity in nectarines. *Postharvest Biol. Technol.* 45, 204–213. doi: 10.1016/j.postharvbio.2007.01.014
- Van de Poel, B., Bulens, I., Hertog, M. L. A. T. M., Nicolai, B. M., and Geeraerd, A. H. (2014). A transcriptomics-based kinetic model for ethylene biosynthesis in tomato (*Solanum lycopersicum*) fruit: development, validation and exploration of novel regulatory mechanisms. *New Phytol.* 202, 952–963. doi: 10.1111/nph.12685
- Van de Poel, B., Bulens, I., Hertog, M. L. A. T. M., Van Gastel, L., De Proft, M. P., Nicolai, B. M., et al. (2012). Model based classification of tomato fruit development and ripening related to physiological maturity. *Postharvest Biol. Technol.* 67, 59–67. doi: 10.1016/j.postharvbio.2011.12.005
- Winsor, C. P. (1932). The Gompertz curve as a growth curve. *Proc. Natl. Acad. Sci. U.S.A.* 18, 1–8. doi: 10.1073/pnas.18.1.1
- Conflict of Interest Statement:** The authors declare that the research was conducted in the absence of any commercial or financial relationships that could be construed as a potential conflict of interest.
- Copyright © 2017 Tran, Hertog, Tran, Quyen, Van de Poel, Mata and Nicolai. This is an open-access article distributed under the terms of the Creative Commons Attribution License (CC BY). The use, distribution or reproduction in other forums is permitted, provided the original author(s) or licensor are credited and that the original publication in this journal is cited, in accordance with accepted academic practice. No use, distribution or reproduction is permitted which does not comply with these terms.*

Advantages of publishing in Frontiers



OPEN ACCESS

Articles are free to read for greatest visibility and readership



FAST PUBLICATION

Around 90 days from submission to decision



HIGH QUALITY PEER-REVIEW

Rigorous, collaborative, and constructive peer-review



TRANSPARENT PEER-REVIEW

Editors and reviewers acknowledged by name on published articles



REPRODUCIBILITY OF RESEARCH

Support open data and methods to enhance research reproducibility



DIGITAL PUBLISHING

Articles designed for optimal readership across devices



FOLLOW US
@frontiersin



IMPACT METRICS
Advanced article metrics track visibility across digital media



EXTENSIVE PROMOTION
Marketing and promotion of impactful research



LOOP RESEARCH NETWORK
Our network increases your article's readership